



VOL. 499 JANUARY 19, 1990

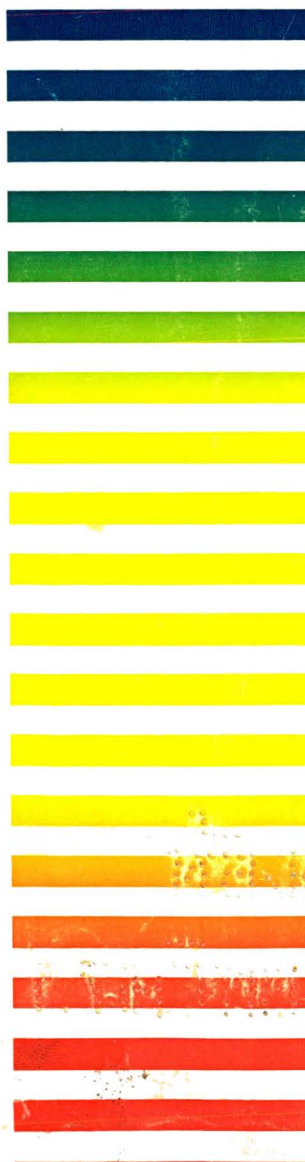
COMPLETE IN ONE ISSUE

**Csaba Horváth Honour Volume**

JOURNAL OF

# CHROMATOGRAPHY

INTERNATIONAL JOURNAL ON CHROMATOGRAPHY, ELECTROPHORESIS AND RELATED METHODS



**EDITORS**

- R. W. Giese (Boston, MA)
- J. K. Haken (Kensington, N.S.W.)
- K. Macek (Prague)
- L. R. Snyder (Orinda, CA)

EDITOR, SYMPOSIUM VOLUMES, E. Heftmann (Orinda, CA)

**EDITORIAL BOARD**

- D. W. Armstrong (Rolla, MO)
- W. A. Aue (Halifax)
- P. Boček (Brno)
- A. A. Boulton (Saskatoon)
- P. W. Carr (Minneapolis, MN)
- N. H. C. Cooke (San Ramon, CA)
- V. A. Davankov (Moscow)
- Z. Deyl (Prague)
- S. Dilli (Kensington, N.S.W.)
- H. Engelhardt (Saarbrücken)
- F. Erni (Basle)
- M. B. Evans (Hatfield)
- J. L. Glajch (N. Billerica, MA)
- G. A. Guiochon (Knoxville, TN)
- P. R. Haddad (Kensington, N.S.W.)
- I. M. Hais (Hradec Králové)
- W. S. Hancock (San Francisco, CA)
- S. Hjertén (Uppsala)
- Cs. Horváth (New Haven, CT)
- J. F. K. Huber (Vienna)
- K.-P. Hupe (Waldbronn)
- T. W. Hutchens (Houston, TX)
- J. Janák (Brno)
- P. Jandera (Pardubice)
- B. L. Karger (Boston, MA)
- E. sz. Kováts (Lausanne)
- A. J. P. Martin (Cambridge)
- L. W. McLaughlin (Chestnut Hill, MA)
- R. P. Patience (Sunbury-on-Thames)
- J. D. Pearson (Kalamazoo, MI)
- H. Poppe (Amsterdam)
- F. E. Regnier (West Lafayette, IN)
- P. G. Righetti (Milan)
- P. Schoenmakers (Eindhoven)
- G. Schomburg (Mülheim/Ruhr)
- P. Schwarzenbach (Dübendorf)
- H. E. Sjöcup (West Lafayette, IN)
- A. M. Sjöuffi (Marseille)
- D. J. Strydom (Boston, MA)
- K. K. Unger (Mainz)
- J. T. Watson (East Lansing, MI)
- B. D. Westerlund (Uppsala)

**EDITORS, BIOGRAPHY SECTION**

- Z. Deyl (Prague), J. Janák (Brno), V. Schwarz (Prague), K. Macek (Prague)

ELSEVIER

## JOURNAL OF CHROMATOGRAPHY

**Scope.** The *Journal of Chromatography* publishes papers on all aspects of chromatography, electrophoresis and related methods. Contributions consist mainly of research papers dealing with chromatographic theory, instrumental development and their applications. The section *Biomedical Applications*, which is under separate editorship, deals with the following aspects: developments in and applications of chromatographic and electrophoretic techniques related to clinical diagnosis or alterations during medical treatment; screening and profiling of body fluids or tissues with special reference to metabolic disorders; results from basic medical research with direct consequences in clinical practice; drug level monitoring and pharmacokinetic studies; clinical toxicology; analytical studies in occupational medicine.

**Submission of Papers.** Papers in English, French and German may be submitted, in three copies. Manuscripts should be submitted to: The Editor of *Journal of Chromatography*, P.O. Box 681, 1000 AR Amsterdam, The Netherlands, or to: The Editor of *Journal of Chromatography, Biomedical Applications*, P.O. Box 681, 1000 AR Amsterdam, The Netherlands. Review articles are invited or proposed by letter to the Editors. An outline of the proposed review should first be forwarded to the Editors for preliminary discussion prior to preparation. Submission of an article is understood to imply that the article is original and unpublished and is not being considered for publication elsewhere. For copyright regulations, see below.

**Subscription Orders.** Subscription orders should be sent to: Elsevier Science Publishers B.V., P.O. Box 211, 1000 AE Amsterdam, The Netherlands, Tel. 5803 911, Telex 18582 ESPA NL. The *Journal of Chromatography* and the *Biomedical Applications* section can be subscribed to separately.

**Publication.** The *Journal of Chromatography* (incl. *Biomedical Applications*) has 37 volumes in 1990. The subscription prices for 1990 are:

*J. Chromatogr.* (incl. *Cum. Indexes, Vols. 451-500*) + *Biomed. Appl.* (Vols. 498-534):

Dfl. 6734.00 plus Dfl. 1036.00 (p.p.h.) (total ca. US\$ 3564.25)

*J. Chromatogr.* (incl. *Cum. Indexes, Vols. 451-500*) only (Vols. 498-524):

Dfl. 5616.00 plus Dfl. 756.00 (p.p.h.) (total ca. US\$ 2923.00)

*Biomed. Appl.* only (Vols. 525-534):

Dfl. 2080.00 plus Dfl. 280.00 (p.p.h.) (total ca. US\$ 1082.50).

Our p.p.h. (postage, package and handling) charge includes surface delivery of all issues, except to subscribers in Argentina, Australia, Brasil, Canada, China, Hong Kong, India, Israel, Malaysia, Mexico, New Zealand, Pakistan, Singapore, South Africa, South Korea, Taiwan, Thailand and the U.S.A. who receive all issues by air delivery (S.A.L. — Surface Air Lifted) at no extra cost. For Japan, air delivery requires 50% additional charge; for all other countries airmail and S.A.L. charges are available upon request. Back volumes of the *Journal of Chromatography* (Vols. 1-497) are available at Dfl. 195.00 (plus postage). Claims for missing issues will be honoured, free of charge, within three months after publication of the issue. Customers in the U.S.A. and Canada wishing information on this and other Elsevier journals, please contact Journal Information Center, Elsevier Science Publishing Co. Inc., 655 Avenue of the Americas, New York, NY 10010. Tel. (212) 633-3750.

**Abstracts/Contents Lists** published in Analytical Abstracts, ASCA, Biochemical Abstracts, Biological Abstracts, Chemical Abstracts, Chemical Titles, Chromatography Abstracts, Clinical Chemistry Lookout, Current Contents/Physical, Chemical & Earth Sciences, Current Contents/Life Sciences, Deep-Sea Research/Part B: Oceanographic Literature Review, Excerpta Medica, Index Medicus, Mass Spectrometry Bulletin, PASCAL-CNRS, Pharmaceutical Abstracts, Referativnyi Zhurnal, Science Citation Index and Trends in Biotechnology.

**See inside back cover** for Publication Schedule, Information for Authors and information on Advertisements.

© ELSEVIER SCIENCE PUBLISHERS B.V. — 1990

0021-9673/90/\$03.50

All rights reserved. No part of this publication may be reproduced, stored in a retrieval system or transmitted in any form or by any means, electronic, mechanical, photocopying, recording or otherwise, without the prior written permission of the publisher, Elsevier Science Publishers B.V., P.O. Box 330, 1000 AH Amsterdam, The Netherlands.

Upon acceptance of an article by the journal, the author(s) will be asked to transfer copyright of the article to the publisher. The transfer will ensure the widest possible dissemination of information.

Submission of an article for publication entails the authors' irrevocable and exclusive authorization of the publisher to collect any sums or considerations for copying or reproduction payable by third parties (as mentioned in article 17 paragraph 2 of the Dutch Copyright Act of 1912 and the Royal Decree of June 20, 1974 (S. 351) pursuant to article 16 b of the Dutch Copyright Act of 1912) and/or to act in or out of Court in connection therewith.

**Special regulations for readers in the U.S.A.** This journal has been registered with the Copyright Clearance Center, Inc. Consent is given for copying of articles for personal or internal use, or for the personal use of specific clients. This consent is given on the condition that the copier pays through the Center the per-copy fee stated in the code on the first page of each article for copying beyond that permitted by Sections 107 or 108 of the U.S. Copyright Law. The appropriate fee should be forwarded with a copy of the first page of the article to the Copyright Clearance Center, Inc., 27 Congress Street, Salem, MA 01970, U.S.A. If no code appears in an article, the author has not given broad consent to copy and permission to copy must be obtained directly from the author. All articles published prior to 1980 may be copied for a per-copy fee of US\$ 2.25, also payable through the Center. This consent does not extend to other kinds of copying, such as for general distribution, resale, advertising and promotion purposes, or for creating new collective works. Special written permission must be obtained from the publisher for such copying.

No responsibility is assumed by the Publisher for any injury and/or damage to persons or property as a matter of products liability, negligence or otherwise, or from any use or operation of any methods, products, instructions or ideas contained in the materials herein. Because of rapid advances in the medical sciences, the Publisher recommends that independent verification of diagnoses and drug dosages should be made. Although all advertising material is expected to conform to ethical (medical) standards, inclusion in this publication does not constitute a guarantee or endorsement of the quality or value of such product or of the claims made of it by its manufacturer.

This issue is printed on acid-free paper.

Printed in The Netherlands

For contents see p. VII

JOURNAL OF CHROMATOGRAPHY  
VOL. 499 (1990)



# JOURNAL *of* CHROMATOGRAPHY

INTERNATIONAL JOURNAL ON CHROMATOGRAPHY,  
ELECTROPHORESIS AND RELATED METHODS

## EDITORS

R. W. GIESE (Boston, MA), J. K. HAKEN (Kensington, N.S.W.), K. MACEK (Prague),  
L. R. SNYDER (Orinda, CA)

## EDITOR, SYMPOSIUM VOLUMES

E. HEFTMANN (Orinda, CA)

## EDITORIAL BOARD

D. W. Armstrong (Rolla, MO), W. A. Aue (Halifax), P. Boček (Brno), A. A. Boulton (Saskatoon), P. W. Carr (Minneapolis, MN), N. H. C. Cooke (San Ramon, CA), V. A. Davankov (Moscow), Z. Deyl (Prague), S. Dilli (Kensington, N.S.W.), H. Engelhardt (Saarbrücken), F. Erni (Basle), M. B. Evans (Hatfield), J. L. Glajch (N. Billerica, MA), G. A. Guiochon (Knoxville, TN), P. R. Haddad (Kensington, N.S.W.), I. M. Hais (Hradec Králové), W. S. Hancock (San Francisco, CA), S. Hjertén (Uppsala), Cs. Horváth (New Haven, CT), J. F. K. Huber (Vienna), K.-P. Hupe (Waldbronn), T. W. Hutchens (Houston, TX), J. Janák (Brno), P. Jandera (Pardubice), B. L. Karger (Boston, MA), E. sz. Kováts (Lausanne), A. J. P. Martin (Cambridge), L. W. McLaughlin (Chestnut Hill, MA), R. P. Patience (Sunbury-on-Thames), J. D. Pearson (Kalamazoo, MI), H. Poppe (Amsterdam), F. E. Regnier (West Lafayette, IN), P. G. Righetti (Milan), P. Schoenmakers (Eindhoven), G. Schomburg (Mülheim/Ruhr), R. Schwarzenbach (Düben-dorf), R. E. Shoup (West Lafayette, IN), A. M. Siouffi (Marseille), D. J. Strydom (Boston, MA), K. K. Unger (Mainz), J. T. Watson (East Lansing, MI), B. D. Westerlund (Uppsala)

## EDITORS, BIBLIOGRAPHY SECTION

Z. Deyl (Prague), J. Janák (Brno), V. Schwarz (Prague), K. Macek (Prague)



ELSEVIER  
AMSTERDAM — OXFORD — NEW YORK — TOKYO

---

*J. Chromatogr.*, Vol. 499 (1990)

All rights reserved. No part of this publication may be reproduced, stored in a retrieval system or transmitted in any form or by any means, electronic, mechanical, photocopying, recording or otherwise, without the prior written permission of the publisher, Elsevier Science Publishers B.V., P.O. Box 330, 1000 AH Amsterdam, The Netherlands.

Upon acceptance of an article by the journal, the author(s) will be asked to transfer copyright of the article to the publisher. The transfer will ensure the widest possible dissemination of information.

Submission of an article for publication entails the authors' irrevocable and exclusive authorization of the publisher to collect any sums or considerations for copying or reproduction payable by third parties (as mentioned in article 17 paragraph 2 of the Dutch Copyright Act of 1912 and the Royal Decree of June 20, 1974 (S. 351) pursuant to article 16 b of the Dutch Copyright Act of 1912) and/or to act in or out of Court in connection therewith.

**Special regulations for readers in the U.S.A.** This journal has been registered with the Copyright Clearance Center, Inc. Consent is given for copying of articles for personal or internal use, or for the personal use of specific clients. This consent is given on the condition that the copier pays through the Center the per-copy fee stated in the code on the first page of each article for copying beyond that permitted by Sections 107 or 108 of the U.S. Copyright Law. The appropriate fee should be forwarded with a copy of the first page of the article to the Copyright Clearance Center, Inc., 27 Congress Street, Salem, MA 01970, U.S.A. If no code appears in an article, the author has not given broad consent to copy and permission to copy must be obtained directly from the author. All articles published prior to 1980 may be copied for a per-copy fee of US\$ 2.25, also payable through the Center. This consent does not extend to other kinds of copying, such as for general distribution, resale, advertising and promotion purposes, or for creating new collective works. Special written permission must be obtained from the publisher for such copying.

No responsibility is assumed by the Publisher for any injury and/or damage to persons or property as a matter of products liability, negligence or otherwise, or from any use or operation of any methods, products, instructions or ideas contained in the materials herein. Because of rapid advances in the medical sciences, the Publisher recommends that independent verification of diagnoses and drug dosages should be made.

Although all advertising material is expected to conform to ethical (medical) standards, inclusion in this publication does not constitute a guarantee or endorsement of the quality or value of such product or of the claims made of it by its manufacturer.

This issue is printed on acid-free paper.

SPECIAL VOLUME



**HONOUR VOLUME**

**on the occasion of the 60th birthday of**

**CSABA HORVÁTH**

*Editors*

**E. HEFTMANN**

(Orinda, CA, U.S.A.)

**L. R. SNYDER**

(Orinda, CA, U.S.A.)





## CONTENTS

## HONOUR VOLUME ON THE OCCASION OF THE 60TH BIRTHDAY OF Cs. HORVÁTH

Preface	
by L. R. Snyder . . . . .	1
Determination of competitive adsorption isotherms for modeling large-scale separations in liquid chromatography	
by J. M. Jacobson (Brisbane, CA, U.S.A.) and J. Frenz (South San Francisco, CA, U.S.A.) . . . . .	5
Quantitative comparison between the experimental band profiles of binary mixtures in overloaded elution chromatography and their profiles predicted by the semi-ideal model	
by A. M. Katti (Knoxville, TN, U.S.A.) and G. Guiochon (Knoxville and Oak Ridge, TN, U.S.A.) . . . . .	21
Scaling-up procedure from the range of milligrams to grams for the purification of amino acid derivatives in displacement chromatography	
by F. Cardinali, A. Ziggotti and G. C. Viscomi (Rome, Italy) . . . . .	37
Purification of monoclonal antibodies by complex-displacement chromatography on CM-cellulose	
by A. R. Torres and E. A. Peterson (Logan, UT, U.S.A.) . . . . .	47
Preparative-scale high-performance liquid chromatographic separation and purification of 3'-azido-3'-deoxythymidine-5'-phosphate	
by J. G. Turcotte, P. E. Pivarnik, S. S. Shirali, H. K. Singh and R. K. Sehgal (Kingston, RI, U.S.A.), D. Macbride (Wakefield, RI, U.S.A.) and N.-I. Jang and P. R. Brown (Kingston, RI, U.S.A.) . . . . .	55
Thermodynamic model for electrostatic-interaction chromatography of proteins	
by I. Mazsaroff (Cambridge, MA, U.S.A.) and L. Várady, G. A. Mouchawar and F. E. Regnier (W. Lafayette, IN, U.S.A.) . . . . .	63
Physicochemical studies of biologically active peptides by low-temperature reversed-phase high-performance liquid chromatography	
by D. E. Henderson and J. A. Mello (Hartford, CT, U.S.A.) . . . . .	79
Reversed-phase chromatographic behavior of proteins in different unfolded states	
by S. Lin and B. L. Karger (Boston, MA, U.S.A.) . . . . .	89
High-performance liquid chromatography of amino acids, peptides and proteins. XCV. Thermodynamic and kinetic investigations on rigid and soft affinity gels with varying particle and pore sizes: comparison of thermodynamic parameters and the adsorption behaviour of proteins evaluated from bath and frontal analysis experiments	
by F. B. Anspach, A. Johnston, H.-J. Wirth, K. K. Unger and M. T. W. Hearn (Clayton, Australia) . . . . .	103
Factors influencing the performance of peptide mapping by reversed-phase high-performance liquid chromatography	
by M. W. Dong (Norwalk, CT, U.S.A.) and A. D. Tran (Raritan, NJ, U.S.A.) . . . . .	125
Binary and ternary salt gradients in hydrophobic-interaction chromatography of proteins	
by Z. El Rassi, L. F. De Ocampo and M. D. Bacolod (Stillwater, OK, U.S.A.) . . . . .	141
High-performance adsorption chromatography of transfer ribonucleic acids and proteins on 2- $\mu$ m spherical beads of hydroxyapatite. Influence of sodium chloride and magnesium ions on the resolution	
by J. Lindeberg, T. Srichaiyo and S. Hjertén (Uppsala, Sweden) . . . . .	153

Unexpected elution behaviour of peptides with various reversed-phase columns by H. Engelhardt (Saarbrücken, F.R.G.), G. Appelt (Leipzig, G.D.R.) and E. Schweinheim (Saarbrücken, F.R.G.) . . . . .	165
Hydrophilic-interaction chromatography for the separation of peptides, nucleic acids and other polar compounds by A. J. Alpert (Baltimore, MD, U.S.A.) . . . . .	177
Investigation of some $\alpha$ -amylases by high-performance hydrophobic-interaction chromatography by L. Szepesy, L. Vida, M. Tóth and E. László (Budapest, Hungary) . . . . .	197
Analysis of glycoprotein-derived oligosaccharides by high-pH anion-exchange chromatography by L. J. Basa and M. W. Spellman (South San Francisco, CA, U.S.A.) . . . . .	205
Automated evaluation of tryptic digest from recombinant human growth hormone using ultraviolet spectra and numeric peak information by H.-J. P. Sievert (Avondale, PA, U.S.A.) and S.-L. Wu, R. Chloupek and W. S. Hancock (South San Francisco, CA, U.S.A.) . . . . .	221
Protein chromatography with pyridine- and alkyl-thioether-based agarose adsorbents by S. Oscarsson and J. Porath (Uppsala, Sweden) . . . . .	235
New latex-bonded pellicular anion exchangers with multi-phase selectivity for high-performance chromatographic separations by J. R. Stillian and C. A. Pohl (Sunnyvale, CA, U.S.A.) . . . . .	249
Micropellicular stationary phases for rapid protein analysis by high-performance liquid chromato- graphy by K. Kalghatgi (New Haven, CT, U.S.A.) . . . . .	267
Comparison of retention behavior on polymeric resins and an alkyl-bonded silica phase in reversed- phase high-performance liquid chromatography by S. Pedigo and L. D. Bowers (Minneapolis, MN, U.S.A.) . . . . .	279
Physical and chemical characterization of microporous zirconia by M. P. Rigney, E. F. Funkenbusch and P. W. Carr (Minneapolis, MN, U.S.A.) . . . . .	291
Effect of coverage density on the retention mechanism in reversed-phase high-performance liquid chromatography by B. Buszewski, Z. Suprynowicz and P. Staszczuk (Lublin, Poland) and K. Albert, B. Pfei- derer and E. Bayer (Tübingen, F.R.G.) . . . . .	305
Studies on the stability of <i>n</i> -alkyl-bonded silica gels under basic pH conditions by N. T. Miller and J. M. DiBussolo (Conshohocken, PA, U.S.A.) . . . . .	317
Mechanism of retention in high-performance liquid chromatography on porous graphitic carbon as revealed by principal component analysis of structural descriptors of solutes by R. Kaliszán and K. Ośmiałowski (Gdańsk, Poland) and B. J. Bassler and R. A. Hartwick (Piscataway, NJ, U.S.A.) . . . . .	333
Preparation of silicone-coated 5–25- $\mu$ m I.D. fused-silica capillary columns for open-tubular liquid chromatography by O. van Berkel-Geldof, J. C. Kraak and H. Poppe (Amsterdam, The Netherlands) . . . . .	345
Prediction of the high-performance liquid chromatographic retention behaviour of some benzodiaze- pine derivatives by thin-layer chromatography by K. Valko, S. Olajos and T. Cserhádi (Budapest, Hungary) . . . . .	361
Study of partition models in reversed-phase liquid chromatography based on measured mobile phase solute activity coefficients by W. J. Cheong and P. W. Carr (Minneapolis, MN, U.S.A.) . . . . .	373
Retention characteristics of several compound classes in reversed-phase liquid chromatography with $\beta$ -cyclodextrin as a mobile phase modifier by R. M. Mohseni and R. J. Hurtubise (Laramie, WY, U.S.A.) . . . . .	395

Reversed-phase ion-pair liquid chromatography of glucuronides. Retention and selectivity by M. Stefansson and D. Westerlund (Uppsala, Sweden) . . . . .	411
Basis of the rational selection of the hydrophobicity and concentration of the ion-pairing reagent in reversed-phase ion-pair high-performance liquid chromatography by A. Bartha and G. Vigh (College Station, TX, U.S.A.) and Z. Varga-Puchony (Veszprem, Hungary) . . . . .	423
Estimation of the reversed-phase liquid chromatographic lipophilicity parameter $\log k'_w$ using ET-30 solvatochromism by J. J. Michels and J. G. Dorsey (Gainesville, FL, U.S.A.) . . . . .	435
Strategies of mobile phase transfer from thin-layer to medium-pressure liquid chromatography with silica as the stationary phase by S. Nyiredy, K. Dallenbach-Toelke, G. C. Zogg and O. Sticher (Zürich, Switzerland) . . . . .	453
Investigation and improvement of the Horváth-Lin equation of state by P. Benedek and T. Jankó (Budapest, Hungary) . . . . .	463
Reversed-phase liquid chromatographic studies of non-ionic surfactants and related solutes by P. Varughese, M. E. Gangoda and R. K. Gilpin (Kent, OH, U.S.A.) . . . . .	469
Effect of alcohol chain length, concentration and polarity on separations in high-performance liquid chromatography using bonded cyclodextrin columns by I. Z. Atamna, G. M. Muschik and H. J. Issaq (Frederick, MD, U.S.A.) . . . . .	477
Optimization of selectivity, detectability and analysis time in high-performance liquid chroma- tography by S. Ahuja (Suffern, NY, U.S.A.) . . . . .	489
Strategy for peak tracking in liquid chromatography on the basis of a multivariate analysis of spectral data by J. K. Strasters, H. A. H. Billiet and L. de Galan (Delft, The Netherlands) and B. G. M. Vandeginste (Nijmegen, The Netherlands) . . . . .	499
Peak tracking and subsequent choice of optimization parameters for the separation of a mixture of local anaesthetics by high-performance liquid chromatography by J. K. Strasters, F. Coolsaet, A. Bartha, H. A. H. Billiet and L. de Galan (Delft, The Netherlands) . . . . .	523
Performance of micro-liquid chromatographic columns in an industrial environment: a case history by N. G. F. M. Lammers and J. H. M. van den Berg (Weesp, The Netherlands) and M. Verzele and C. Dewaele (Ghent, Belgium) . . . . .	541
Direct coupling of capillary liquid chromatography with conventional high-performance liquid chro- matography by T. Takeuchi, M. Asai, H. Haraguchi and D. Ishii (Nagoya, Japan) . . . . .	549
Appraisal of four pre-column derivatization methods for the high-performance liquid chromato- graphic determination of free amino acids in biological materials by P. FÜRST, L. Pollack, T. A. Graser, H. Godel and P. Stehle (Stuttgart, F.R.G.) . . . . .	557
Preparation of electrophoric derivatives of N7-(2-hydroxyethyl)guanine, an ethylene oxide DNA adduct by K. Allam, M. Saha and R. W. Giese (Boston, MA, U.S.A.) . . . . .	571
Application of 3-(2-furoyl)quinoline-2-carbaldehyde as a fluorogenic reagent for the analysis of pri- mary amines by liquid chromatography with laser-induced fluorescence detection by S. C. Beale, Y.-Z. Hsieh, D. Wiesler and M. Novotny (Bloomington, IN, U.S.A.) . . . . .	579
Chromatographic studies on the binding, action and metabolism of (-)-deprenyl by H. Kalász, L. Kerecsen, J. Knoll and J. Pucsok (Budapest, Hungary) . . . . .	589
Determination of fluoxetine and norfluoxetine by high-performance liquid chromatography by S. H. Y. Wong, S. S. Dellafera, R. Fernandes and H. Kranzler (Farmington, CT, U.S.A.) . . . . .	601

On-line high-performance liquid chromatography for the determination of cephalosporin C and by-products in complex fermentation broths by K. Holzhauser-Rieger, W. Zhou and K. Schügerl (Hannover, F.R.G.) . . . . .	609
Determination of D-myo-1,2,6-inositol trisphosphate by ion-pair reversed-phase liquid chromatography with post-column ligand exchange and fluorescence detection by H. Irth, M. Lamoree, G. J. de Jong, U. A. Th. Brinkman and R. W. Frei (Amsterdam, The Netherlands) and R. A. Kornfeldt and L. Persson (Perstorp, Sweden) . . . . .	617
Separation of carotenes on cyclodextrin-bonded phases by A. M. Stalcup, H. L. Jin and D. W. Armstrong (Rolla, MO, U.S.A.) and P. Mazur, F. Derguini and K. Nakanishi (New York, NY, U.S.A.) . . . . .	627
Comparative supercritical-fluid chromatographic properties of carbon dioxide and sulphur hexafluoride-ammonia mixtures with packed columns by J. L. Veuthey (Genève, Switzerland) and J. L. Janicot, M. Caude and R. Rosset (Paris, France) . . . . .	637
Use of high-performance liquid chromatography for the characterization of synthetic copolymers by G. Glöckner (Dresden, G.D.R.) and H. G. Barth (Wilmington, DE, U.S.A.) . . . . .	645
Effect of operating parameters on polymer molecular weight accuracy with time-delay, exponential-decay thermal field flow fractionation by J. J. Kirkland and W. W. Yau (Wilmington, DE, U.S.A.) . . . . .	655
Ion chromatography of transition metals on an iminodiacetic acid bonded stationary phase by G. Bonn and S. Reiffenstühl (Innsbruck, Austria) and P. Jandik (Milford, MA, U.S.A.) . . . . .	669
Calculation of column performance in nitrate removal from water supplies by anion exchange by R.-J. Leu, Y.-L. Hwang and F. G. Helfferich (University Park, PA, U.S.A.) . . . . .	677
Determination of inorganic anions by flow injection analysis and high-performance liquid chromatography combined with photolytic-electrochemical detection by L. Dou and I. S. Krull (Boston, MA, U.S.A.) . . . . .	685
Kinetics of cysteine oxidation in immobilized pH gradient gels by M. Chiari, C. Chiesa, P. G. Righetti and M. Corti (Milan, Italy) and T. Jain and R. Shorr (Malvern, PA, U.S.A.) . . . . .	699
Capillary electrophoresis with indirect amperometric detection by T. M. Olefirowicz and A. G. Ewing (University Park, PA, U.S.A.) . . . . .	713
High-efficiency liquid extractor for isolation of a desired material from complex organic mixtures by M. Brenner, C. Moirandat and R. Schlimme (Basle, Switzerland) . . . . .	721
Gas chromatographic study of the solution thermodynamics of organic solutes in tetraalkylammonium alkanesulfonate and perfluoroalkanesulfonate solvents by R. M. Pomaville and C. F. Poole (Detroit, MI, U.S.A.) . . . . .	749
<i>Author Index</i> . . . . .	761

\*\*\*\*\*  
 \*  
 \* In articles with more than one author, the name of the author to whom correspondence should be addressed is indicated in the \*  
 \* article heading by a 6-pointed asterisk (\*) \*  
 \*  
 \*\*\*\*\*

## PREFACE

The present volume of the *Journal of Chromatography* is dedicated to Professor Csaba Horváth, who celebrates his 60th birthday on January 25, 1990. Dr. Horváth was born in Hungary and received his graduate degree in chemical engineering from the Technical University of Budapest in 1952. He was on the faculty of the Department of Organic Chemical Technology until the end of 1956. At that time in the wake of the Hungarian revolution he left his country for Germany, where for the next four years he was employed at Farbwerke Hoechst AG in Frankfurt am Main-Höchst. His work involved scaling-up of processes and then research on applied surface chemistry, an experience that proved useful in his later work in chromatography.

In 1961 Dr. Horváth left industry and in 1963 received his Ph.D. in physical chemistry from the Johann Wolfgang Goethe University in Frankfurt am Main. His graduate research under the direction of the late István Halász was quite fruitful and indicative of the directions his future career would take. In the course of his doctoral research Csaba Horváth developed the first support-coated open-tubular columns<sup>1</sup> for gas chromatography, as well as surface-treated beads<sup>2</sup> that would later evolve into special column packings for high-performance liquid chromatography (HPLC). His next position was as a research fellow at the Harvard Medical School, and in 1964 he moved on to Yale University, where he has since remained. He currently holds the rank of professor, and he is also chairman of the Department of Chemical Engineering.

Since the late sixties Professor Horváth has established a vigorous research program in biochemical engineering at Yale. His interest was first focussed on enzyme technology and bioreactors, and later he devoted himself mainly to bioseparations and established a leading research group in this field. Over the years he has taught various courses in chemical engineering and supervised numerous doctoral theses. Many of his former students have become eminent biochemical engineers.

During the mid 1960s Dr. Horváth (in collaboration with the late Sandy Lipsky) pioneered the development of HPLC, and he was the first to construct and publish a complete system for carrying out separations by this technique<sup>3,4</sup>. Throughout the following two decades, Professor Horváth devoted most of his research efforts to a better understanding of both the fundamentals and the practice of HPLC. More than 200 technical publications and innumerable lectures during this period represent an inspiring example of dedication to science—I personally know of no one who has worked harder or accomplished more in this field.

Professor Horváth is associated with many specific innovations and new concepts that have collectively made an enormous impact on our use of chromatography. His introduction of pellicular packings for HPLC played a significant role in the early acceptance of this technique; he has also recently shown that similar particles with diameters of 1–5  $\mu\text{m}$  are unique in their ability to separate large biomolecules in times of a few seconds<sup>5</sup>. Dr. Horváth was among the first to recognize the exceptional promise of reversed-phase HPLC, aided by his further development of the solvophobic theory as a quantitative basis for understanding the physico-chemical basis of retention in these systems<sup>6,7</sup>, and for interpretation of the hydrophobic effect<sup>8</sup>. His early application of reversed-phase chromatography to the separation of biochemical mixtures stands as another landmark contribution. This theoretical work was later

extended to a unified treatment of HPLC retention based on concepts drawn from the field of physical-organic chemistry.

In the late 1970s Professor Horváth began work in another major area of HPLC: preparative separations, especially those based on displacement chromatography<sup>9-11</sup>. This was a classic example of the use of some early (almost forgotten) work to suggest a promising new line of research. At about the same time Professor Horváth extended his earlier work on small biomolecules to the use of HPLC for separating large biomolecules such as peptides, proteins and oligonucleotides. This work aimed at both a theoretical understanding of these separations and the development of new column packings designed specifically for large biomolecules. In due time his separate interests in preparative separations and analytical biotechnology merged, and today he is an acknowledged leader in the area of preparative and process chromatography of large biomolecules.

Professor Horváth is also famous for his interest in philology and his attention to appropriate names for new (or old) ideas. Despite the fact he learned English rather later in life upon arriving in the United States, he has mastered the language as have few other chromatographers. We are indebted to him for coining many new words such as "isocratic" which have become part of our language. His lectures are always a highlight of any meeting, as much for their humor and entertainment as for the novelty and importance of the results and ideas presented.

My own association with Csaba goes back to 1968, when, together with Barry Karger we embarked on writing a book on separation science<sup>12</sup> —a project that would stretch out over the next five years. I often recall this period with a smile, because of our many meetings enlivened by Csaba's remarkable wit and ability to express his thoughts in concise (and usually humorous) terms. Toward the end of our book-writing activities, Csaba and I became involved in another project that lasted for the balance of the 1970s. I was then at Technicon, and Csaba proposed that a great improvement could be effected in the way certain clinical testing was carried out —by making use of enzyme reagents that were immobilized on the inside of the tubing used in the Technicon analyzers<sup>13,14</sup>. He soon carried this concept from the laboratory to production, and eventually these enzyme-coated tubes became a major product line at Technicon. This work well illustrated Csaba's early involvement in applied biochemistry and biochemical engineering, an area that he would later combine so successfully with HPLC.

During the past two decades I have often been in touch with Csaba, as have many others. He is constantly traveling from one country to another, in order to touch base with chromatographers and biotechnologists in all parts of the world. The past two decades have brought him a wide recognition of his many contributions and given him the opportunity to exercise his talents on a vast stage. Among his many notable accomplishments, along this line I think first of his chairmanship of the "HPLC'84" Symposium in New York City. This was at the time the best attended HPLC meeting by far, with the most impressive collection of technical presentations. Another important contribution is a series of volumes he has edited under the title *High-Performance Liquid Chromatography —Advances and Perspectives*. He is also the founder of the New England Chromatography Council, an active group of local chromatographers, and was Chairman of the Chromatography Subdivision of the American Chemical Society in 1987.

He has served on the editorial boards of several journals, including the *Journal of Chromatography* since 1977. Dr. Horváth has received numerous awards and other honors, including the Dal Nogare Award (1978), the Commemorative Tswett Medal of the USSR Academy of Science (1979), the M.S. Tswett Award in Chromatography (1980), The Humboldt Award (1982), the American Chemical Society Award in Chromatography (1983), the Chromatography Award of the Eastern Analytical Symposium (1986), and honorary degrees from Yale (1986) and the University of Technical Sciences in Budapest (1986). He is also an honorary member of the Hungarian Chemical Society (1986).

Finally, I would like to acknowledge Csaba as both a personal and professional associate, one who over the years has exhibited all the characteristics of a good and loyal friend: sympathy, empathy, consistency, caring and sharing. It is encouraging to see that he has not slowed down after 60 years, and we all wish him well in the years to come.

Orinda, CA (U.S.A.)

L. R. SNYDER

- 1 I. Halász and Cs. Horváth, *Anal. Chem.*, 35 (1963) 499.
- 2 I. Halász and Cs. Horváth, *Anal. Chem.*, 36 (1964) 1178.
- 3 Cs. Horváth and S. R. Lipsky, *Nature (London)*, 211 (1966) 748.
- 4 Cs. Horváth, B. A. Preiss and S. R. Lipsky, *Anal. Chem.*, 39 (1967) 1422.
- 5 K. Kalghatgi and Cs. Horváth, *J. Chromatogr.*, 398 (1987) 335.
- 6 Cs. Horváth, W. Melander and I. Molnár, *J. Chromatogr.*, 125 (1976) 129.
- 7 Cs. Horváth and W. Melander, *J. Chromatogr. Sci.*, 15 (1977) 393.
- 8 W. Melander and Cs. Horváth, *Arch. Biochem. Biophys.*, 183 (1977) 200.
- 9 Cs. Horváth, A. Nahum and J. H. Frenz, *J. Chromatogr.*, 218 (1981) 365.
- 10 J. Frenz and Cs. Horváth, *AIChE J.*, 31 (1985) 400.
- 11 J. Frenz and Cs. Horváth, in Cs. Horváth (Editor), *High-Performance Liquid Chromatography — Advances and Perspectives*, Vol. 5, Academic Press, New York, 1988, pp. 212–314.
- 12 B. L. Karger, L. R. Snyder and Cs. Horváth, *An Introduction to Separation Science*, Wiley-Interscience, New York, 1973.
- 13 Cs. Horváth and B. A. Solomon, *Biotechnol. Bioeng.*, 14 (1972) 885.
- 14 L. P. Leon, S. Narayanan, R. Dellenbach and Cs. Horváth, *Clin. Chem.*, 22 (1976) 1017.





CHROM. 21 858

## DETERMINATION OF COMPETITIVE ADSORPTION ISOTHERMS FOR MODELING LARGE-SCALE SEPARATIONS IN LIQUID CHROMATOGRAPHY

JANA M. JACOBSON

*BioWest Research, P.O. Box 135, Brisbane, CA 94005 (U.S.A.)*

and

JOHN FRENZ\*

*Genentech, Inc., 460 Point San Bruno Blvd., South San Francisco, CA 94080 (U.S.A.)*

---

### SUMMARY

Preparative and process-scale high-performance liquid chromatography has assumed an increasingly important role in the production of highly purified substances, such as proteins expressed by recombinant DNA technology for use as human pharmaceuticals. The theory for modeling chromatographic separations is well-developed, but requires data on the competitive adsorption behavior of all mixture components for accurate predictions and process design. This paper describes two new methods for determining competitive adsorption isotherms from multi-component frontal chromatography experiments. The first new method reported here complements a method described previously that employed the theory of chromatography to estimate Langmuir isotherm parameters from the breakthrough volumes in frontal chromatography. The new method estimates Langmuir parameters from the experimentally determined compositions of the breakthrough zones, rather than from retention volumes, and so provides a check on the magnitudes of these parameters, but also yields values that may more accurately predict the concentrations of zones in a chromatogram than the Langmuir parameters estimated by other methods. The second method is based on both the mass balance and composition velocity approaches to analysis of the profile obtained in frontal chromatography. The method does not require measurement of concentrations in the profile, instead, concentrations are estimated according to the theory of chromatography from the breakthrough volumes of zones of different composition. The resulting method enables calculation of data points for mobile and stationary phase concentrations at equilibrium, yet it eliminates the need for a tandem rapid analytical high-performance liquid chromatographic unit to monitor effluent compositions.

---

### INTRODUCTION

Preparative chromatography has long been an essential tool for purification of compounds at the laboratory and production scales. Recently, large-scale high-

performance liquid chromatography (HPLC) has become an important process purification step, and is used in the production of biosynthetic human insulin<sup>1</sup>. Such proteins, produced by recombinant DNA technology, require extremely high purity for their intended use as human pharmaceuticals<sup>2</sup>. HPLC is one of the most important analytical techniques for verifying purity<sup>3</sup> and for isolating contaminants or variants of a protein<sup>4</sup>. The separation by HPLC can be relatively easy to scale-up<sup>5</sup>, and so has lately taken its place in the process stream as a purification step *par excellence*<sup>6</sup>. In order to support this extension of HPLC into large-scale applications, a growing body of theoretical work has been reported, to model the different modes of LC, to describe column behavior and to predict separation performance. Horváth has been a pioneer in this area, working on both theoretical and practical aspects of preparative HPLC<sup>6-23</sup>, measuring adsorption isotherms<sup>24,25</sup> and demonstrating the importance of theory in understanding the workings of large-scale HPLC that differs in certain respects from the more familiar analytical modes<sup>26-30</sup>.

Large-scale HPLC is most efficiently operated at relatively high concentrations, where manifestations of "column overloading" may be apparent<sup>31</sup>. These phenomena give rise to asymmetrical peak shapes<sup>32</sup>, displacement effects<sup>33</sup> and selectivity reversals<sup>19</sup> that may impede simple strategies for scale-up from the analytical separation. Therefore, mathematical modeling of the process can provide valuable insight into the physical processes occurring within the column and aid in design of the HPLC system. Since HPLC is a relatively expensive process, and a very high resolution step, an adequate understanding of the dynamics of the chromatographic process is essential to an efficient and effective installation. While modeling is not a substitute for experimentation with a variety of mobile and stationary phase systems in the development process, it can be important to rapidly gaining insight into, and optimizing the HPLC step in use<sup>34</sup>.

A key element in accurately modeling the chromatographic process is the data describing the equilibrium adsorption of each of the components in the system constituting the feed material and mobile phase components. No prediction of column performance can be made without first measuring or estimating adsorption isotherms for these components under the conditions of interest, and the accuracy of the prediction is strongly dependent on the accuracy of this data<sup>27</sup>. At elevated concentrations, such as employed in large-scale separations, interference<sup>35-37</sup> among components is important, and an adequate description of the way in which species mutually affect one another's adsorption properties also can improve the accuracy of the modeling effort. Little effort, however, has gone into determining multicomponent isotherms in chromatographic systems, until the work of Horváth cited above. This is due to the low efficiency of "classical" chromatographic columns, where the influence of such effects would be negligible compared to the large bandspreading forces, and to the *de facto* restriction of HPLC systems to low, analytical-scale concentrations, where interference effects are not manifest. Thus, the modern columns and equipment for large-scale HPLC need a higher level of sophistication in isotherm determination in order to represent column behavior that can differ substantially from that associated with separations in analytical modes of chromatography.

Jacobson *et al.*<sup>24,25</sup> have presented methods for measurement of single- and multicomponent isotherms in HPLC by frontal methods that are accurate and economical of both time and sample. Two of the methods developed by these workers

and reported in the chemical engineering literature<sup>25</sup>, describe techniques and instrumentation for rapidly measuring competitive adsorption isotherms of systems with, in principal, any number of components. These methods, described in the next section, differ in experimental complexity and in their restriction to Langmuir adsorption behavior. The first method utilizes a mass balance on the frontal chromatographic concentration profile, and so requires monitoring of the column effluent by a selective detector, such as the tandem HPLC analytical unit described in ref. 25. The second method did not require the selective detector, but was restricted to compounds whose adsorption behavior could individually be described by a Langmuir model. In this report, two additional means of determining competitive adsorption behavior are described and applied to the same data set as the earlier methods<sup>25</sup>. The first new method reported here employs the theory of chromatography<sup>36</sup> to obtain Langmuir adsorption parameters that best describe the concentration levels obtained within the frontal chromatogram. This complements the earlier method that was optimized to predict the breakthrough volumes of the steps in the chromatogram. The second new method employs a mass balance, but concentration values in the frontal chromatogram are not measured, rather they are estimated from the results of the compositions velocities method in ref. 25. This method has the advantage of yielding discrete surface concentration data points, without the need for an ancillary analytical HPLC. Incorporation of the mass balance approach in this method also relaxes the strict adherence to Langmuir adsorption behavior that is associated with the other simplified methods. This paper will also show how the two new methods, together with the earlier approaches, provide an arsenal of techniques for accurate data gathering for modeling column performance in large-scale HPLC.

## THEORY

### *The Langmuir isotherm*

The Langmuir adsorption isotherm<sup>38</sup> for a system of  $n$  components is commonly expressed as

$$q_i = \frac{a_i c_i}{1 + \sum_{j=1}^n b_j c_j} \quad (1)$$

where  $q_i$  is the surface concentration of component  $i$  in equilibrium with mobile phase concentration  $c_i$ , and  $a_i$  and  $b_i$  are parameters characteristic of species  $i$ . It has been shown<sup>39</sup> that eqn. 1 violates the Gibbs–Duhem isotherm, unless  $a_i/b_i$  is constant for all  $i$ , and so is thermodynamically inconsistent as an extension of single component isotherms. Alternative models have been proposed<sup>40</sup> but the resulting isotherms are more complex, require collection of more adsorption data in order to evaluate parameters, and do not satisfy the assumptions underlying the theory of chromatography<sup>36</sup>, an analytic approach to solution of the equations for ideal multicomponent chromatographic behavior. Thus the Langmuir model has retained broad popularity as a means of expressing adsorption data. The aim of this and the previous report<sup>25</sup> is essentially to put forward methods for conveniently and accurately evaluating the

parameters in eqn. 1 for multicomponent systems in order to improve the reliability of the Langmuir formalism in predictions of chromatographic behavior.

#### *The h-transformation*

The theory of multicomponent chromatography<sup>35-37</sup> is a comprehensive treatment of ideal column performance that has been shown to accurately model high-performance displacement chromatography in a reversed-phase system<sup>27</sup>. This theory underlies one approach to determination of isotherms described earlier<sup>25</sup>. Only the results of the treatment are described here, and the reader is directed to the original references for a full description of the approach.

The  $h$ -transformation, as developed by Helfferich<sup>35</sup> and Helfferich and Klein<sup>36</sup>, is a means for transforming the dependent variables,  $c_i$ , to natural variables, dubbed  $h_i$ , in order to simplify mathematical analysis of chromatographic performance. For compounds that obey the Langmuir isotherm, eqn. 1, the transformation is given by

$$\sum_{i=1}^n \frac{b_i c_i}{h(a_i/a_1) - 1} = 1 \quad (2)$$

Eqn. 2 is an  $n$ -th order polynomial with roots ordered as  $h_1 > h_2 > \dots > h_n$ . The transformation simplifies calculation of breakthrough volumes,  $V_i$ , that are given in reduced terms as

$$v_i = \frac{V_i}{V_0 - V_i} = h_{ia} h_{ib} \frac{P_i}{a_1 \varphi} \quad (3)$$

where

$$P_i = \prod_{j=i+1}^n h_{ja} \prod_{j=1}^{i-1} h_{jb} \prod_{j=1}^n a_j / a_1 \quad (4)$$

and  $\varphi = V_{sp}/V_0$  is the phase ratio in the column,  $V_{sp}$  is the volume of stationary phase in the column,  $V_0$  is the column dead volume and  $v_i$  is defined as the reduced front velocity<sup>36</sup>.  $h_{ia}$  and  $h_{ib}$  are the values of  $h_i$  ahead of and behind the composition change, respectively.

The reverse of the  $h$ -transformation is given by

$$c_i = \frac{\prod_{j=1}^n \frac{h_j a_i}{a_1} - 1}{b_i \left( \prod_{\substack{j=1 \\ j \neq i}}^n \frac{a_i}{a_j} - 1 \right)} \quad (5)$$

from which concentrations within a zone can be calculated from known values of  $h_i$ .

#### *Frontal chromatography*

Frontal chromatography can be operationally defined as that mode in which the

composition of the mobile phase flowing into the column is changed in a stepwise fashion and the breakthrough profile is monitored from the initial conditions until the final composition is reached. This technique can be used to very efficiently purify the least-retained component of a mixture<sup>21</sup>. Fig. 1 shows a general breakthrough profile obtained for a two-component mixture, in which the composition at the column inlet has been increased from  $c_{1a}, c_{2a}$  to  $c_{1b}, c_{2b}$ , where the subscripts 1 and 2 distinguish the two components of the feed, and a and b refer to the initial and final conditions, respectively. Fig. 1 shows that intercalated between the initial and final compositions is a band of intermediate composition, with concentrations  $c_{1m}, c_{2m}$ , where m indicates the middle, or “mezzanine” band. The breakthrough profile shown in Fig. 1 is typical of binary frontal chromatography, and in general, a frontal chromatogram of an  $n$  component mixture will contain  $n - 1$  zones of intermediate composition, each of them a mezzanine band<sup>36</sup>. The other characteristic feature of an  $n$ -component frontal chromatogram is that it contains  $n$  fronts between zones of changing composition, such as those labelled  $V_1$  and  $V_2$  in Fig. 1<sup>36</sup>.

#### Methods for isotherm determination

*The method of mass balance (MMB).* One way to determine points on the competitive adsorption isotherm is by a mass balance on the profile shown in Fig. 1, as has been described earlier<sup>25</sup>. When the experiment is performed so that all concentrations increase from the initial to the final conditions, and sharp fronts are obtained as in Fig. 1, the increase in the amount of component  $i$  bound to the surface is

$$\Delta q_i = q_{ib} - q_{ia} = [(V_2 - V_D)(c_{ib} - c_{ia}) - (V_2 - V_1)(c_{im} - c_{ia})]/V_{sp} \quad (6)$$

where  $V_D$  is the system dead volume,  $V_1$  and  $V_2$  are the breakthrough volumes of the fronts and  $V_{sp}$  is the volume of adsorbent in the column. Thus the complete adsorption

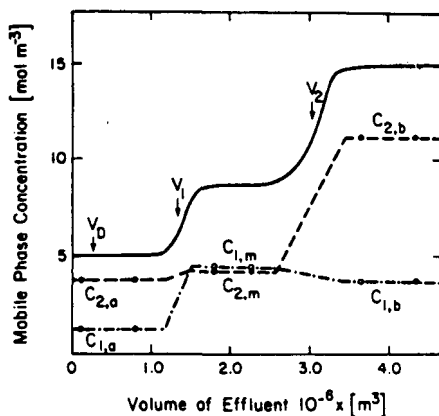


Fig. 1. Schematic of the profile obtained in a frontal chromatography experiment, in which the composition of the mobile phase pumped into the column is changed from  $c_{1a}, c_{2a}$  to  $c_{1b}, c_{2b}$ . The composition of the mezzanine zone in the column effluent is  $c_{1m}, c_{2m}$ .  $V_1$  and  $V_2$  are the breakthrough volumes of the boundaries of the mezzanine zone and  $V_D$  is the dead volume of the system. Reprinted with permission of the American Chemical Society from ref. 25.

isotherm over the concentration range of interest can be determined by several frontal chromatography experiments with different combinations of initial and final conditions spanning the concentration range of interest. Jacobson *et al.*<sup>25</sup> have implemented this approach on a microbore column scale, and described an apparatus for determining the mezzanine concentrations,  $c_{1m}$ ,  $c_{2m}$ , which must be measured along with the breakthrough volumes  $V_1$  and  $V_2$ . One advantage of the mass balance method for isotherm determination is that it is not restricted to compounds that exhibit Langmuir adsorption behavior, but in principal can be applied to any system for which frontal chromatographic data can be obtained.

*The method of composition velocities (MCV).* An alternative means of estimating competitive adsorption isotherms of substances that approximate Langmuir behavior was also advanced in ref. 25. This method, based on the theory of chromatography, requires that the breakthrough volumes in the frontal chromatogram be measured, *i.e.*,  $V_1$  and  $V_2$  in Fig. 1. These values can then be regressed to a model for chromatographic retention to determine isotherm parameters. The model used is that due to Helfferich and Klein<sup>36</sup>, which uses the  $h$ -transformation, eqn. 2, in order to simplify the mathematical description of the chromatographic process. For two components eqn. 2 becomes a quadratic equation with roots given by

$$h_i = \frac{Q_1}{2} \pm \sqrt{\frac{Q_1^2 - 4Q_2}{4}} \quad (7)$$

where

$$Q_1 = \frac{a_1}{a_2} + 1 + b_1c_1 + \frac{a_1}{a_2}b_2c_2 \quad (8)$$

and

$$Q_2 = \frac{a_1}{a_2}(b_1c_1 + b_2c_2 + 1) \quad (9)$$

and the roots are indexed as  $h_1 > h_2$ .

For two components, eqns. 3 and 4 become

$$v_1 = \frac{V_1}{V_0 - V_1} = \frac{h_{1a}h_{1b}}{a_1\phi} h_{2a} \frac{a_2}{a_1} \quad (10)$$

and

$$v_2 = \frac{V_2}{V_0 - V_2} = \frac{h_{2a}h_{2b}}{a_1\phi} h_{1b} \frac{a_2}{a_1} \quad (11)$$

A non-linear regression can be performed, as described previously, using eqns. 7–11 and values of  $V_i$  measured in several frontal chromatography experiments to obtain Langmuir adsorption parameters,  $a_i$  and  $b_i$ , for each of the components of the mixture.

The isotherms so obtained closely approximate the adsorption behavior as determined by the more involved mass balance approach<sup>25</sup>, at least for the system examined.

*The method of mezzanine concentrations (MMC).* The two new isotherm determination methods reported here are complements to the approaches developed earlier, viz., MMB and MCV. The first, termed the method of mezzanine concentrations (MMC), employs measured compositions of the mezzanine bands and correlation with the “reversed  $h$ -transformation”, given for two components by

$$c_{1m} = \frac{h_{1b}h_{2a} - 1}{b_1 \left( \frac{a_1}{a_2} - 1 \right)} \quad (12)$$

and

$$c_{2m} = \frac{h_{1b}h_{2a}(a_2/a_1)^2 - 1}{b_2 \left( \frac{a_2}{a_1} - 1 \right)} \quad (13)$$

Together with eqns. 7–9, eqns. 12 and 13 express mezzanine concentrations in terms of the Langmuir parameters  $a_i$  and  $b_i$  and the initial and final concentrations of the step change in concentration at the inlet of the column. This model therefore provides an alternative set of equations to which measured  $c_{im}$  values can be regressed in order to obtain values of  $a_i$  and  $b_i$  that are optimized for prediction of concentration values in the reversed  $h$ -transformation.

*The hybrid method of mass balance (HMMB).* The second method advanced here is a modification of the mass balance approach, in which the values of  $c_{im}$  in eqn. 6 are not measured, but estimated by eqns. 12 and 13 using the Langmuir parameters given by the regression of MCV. Thus in this method, only breakthrough volumes,  $V_i$ , are determined experimentally, obviating the need for the tandem HPLC experimental set-up employed in the rigorous mass balance approach<sup>25</sup>. This modification of the mass balance, which is a hybrid of MCV and MMB, is thus termed the hybrid method of mass balance (HMMB). While HMMB employs the mobile phase concentration values estimated by MCV, it yields discrete data points on the adsorption isotherm, like MMB, and the restriction to Langmuir adsorption behavior is relaxed, compared to MCV and MMC.

## RESULTS AND DISCUSSION

### *Comparison of the methods*

The two methods proposed here, together with those reported earlier<sup>25</sup> provide four distinct approaches for the determination of competitive adsorption isotherms from frontal chromatographic experiments. The approaches are all suited to measurements with columns and equipment developed for HPLC, and rapidly provide data of high precision with relatively small sample amounts. The four methods differ in certain important respects that are summarized in Table I. The mass balance method (MMB) requires measurement of both  $V_i$  and  $c_{im}$  for isotherm determination, while the

TABLE I

## COMPARISON OF FOUR METHODS FOR DETERMINING COMPETITIVE ADSORPTION ISOTHERMS

Y = Yes, N = no.

	<i>Method name abbreviation</i>			
	<i>MMB</i>	<i>MCV</i>	<i>MMC</i>	<i>HMMB</i>
Data required by each method				
Measured $V_i$	Y	Y	N	Y
Measured $c_{im}$	Y	N	Y	N
Estimated $c_{im}^a$	N	N	N	Y
Values determined by each method				
Isotherm data points <sup>b</sup>	Y	N	N	Y
Langmuir parameters	N <sup>c</sup>	Y	Y	N <sup>c</sup>
Restricted to Langmuir behavior	N	Y	Y	N <sup>d</sup>

<sup>a</sup>  $c_{im}$  estimated by Langmuir parameters from MCV and eqns. 12 and 13.

<sup>b</sup> Y indicates that discrete surface concentrations are determined for each mobile phase composition.

<sup>c</sup> Langmuir parameters can be determined by regression of isotherm data points to eqn. 1 in a subsequent analysis.

<sup>d</sup> Mezzanine concentrations are estimated by assuming Langmuir behavior, but the calculated isotherm can show departures from the Langmuir form.

methods of composition velocities (MCV) and hybrid mass balance (HMMB) require measurement only of  $V_i$ . The method of mezzanine compositions (MMC) employs only the measured mobile phase concentrations,  $c_{im}$ . In HMMB,  $c_{im}$  values are employed in the calculations, but these values are estimated from the results of the MCV technique. The four methods also differ in the values that are produced by the data manipulations. Both MMB and HMMB yield discrete isotherm data points, *i.e.*, values of surface concentrations,  $q_i$ , for each experimental value of mobile phase concentration,  $c_i$ . The MCV and MMC methods, on the other hand, yield parameters of the Langmuir equation,  $a_i$  and  $b_i$ , since these methods are regressions of measured data to models derived from the theory of chromatography that assumes Langmuir behavior. In the discussion below the results of the isotherm determinations by each new model are described and compared with the other methods.

#### *The method of mezzanine concentrations (MMC)*

The data employed in the regression of the mezzanine concentration values to eqns. 12 and 13, taken from refs. 25 and 41, are given in Table II. Each line in Table II represents one frontal chromatography experiment, in which the column equilibrated with the solution of composition  $c_{1a}$ ,  $c_{2a}$  was switched to  $c_{1b}$ ,  $c_{2b}$  and the effluent monitored with a fast analytical HPLC unit to determine the mezzanine composition  $c_{1m}$ ,  $c_{2m}$ . The data were collected over three regimes of compositions: the 3:1 regime in which initial and final concentrations of *p*-cresol and phenol were in a 3:1 molar ratio, the 1:1 or equimolar regime, and the 1:3 regime, in which the *p*-cresol to phenol molar ratios were 1:3. To determine the Langmuir parameters of the two components these data were regressed to the model for  $c_{im}$  given by eqns. 12 and 13 as outlined above.



TABLE II

CONCENTRATION DATA EMPLOYED IN REGRESSION FOR DETERMINATION OF LANGMUIR ISOTHERM PARAMETERS BY THE METHOD OF MEZZANINE CONCENTRATIONS

Concentrations in mol/l, component 1 = *p*-cresol, component 2 = phenol, a = ahead of the composition change, m = mezzanine composition, b = behind the composition change.

<i>Initial</i>		<i>Mezzanine</i>		<i>Final</i>	
$c_{1a}$	$c_{2a}$	$c_{1m}$	$c_{2m}$	$c_{1b}$	$c_{2b}$
0.0000	0.0000	0.0000	0.0015	0.0038	0.0013
0.0038	0.0013	0.0042	0.0046	0.0113	0.0038
0.0113	0.0038	0.0122	0.0073	0.0188	0.0063
0.0188	0.0063	0.0205	0.0102	0.0263	0.0088
0.0263	0.0088	0.0293	0.0148	0.0375	0.0125
0.0375	0.0125	0.0403	0.0188	0.0488	0.0163
0.0488	0.0163	0.0515	0.0223	0.0600	0.0200
0.0600	0.0200	0.0649	0.0272	0.0750	0.0250
0.0000	0.0000	0.0000	0.0021	0.0025	0.0025
0.0025	0.0025	0.0026	0.0080	0.0075	0.0075
0.0075	0.0075	0.0082	0.0133	0.0125	0.0125
0.0125	0.0125	0.0133	0.0185	0.0175	0.0175
0.0175	0.0175	0.0191	0.0265	0.0250	0.0250
0.0250	0.0250	0.0263	0.0342	0.0325	0.0325
0.0325	0.0325	0.0332	0.0404	0.0400	0.0400
0.0400	0.0400	0.0416	0.0489	0.0500	0.0500
0.0000	0.0000	0.0000	0.0037	0.0013	0.0038
0.0013	0.0038	0.0016	0.0111	0.0038	0.0113
0.0038	0.0113	0.0042	0.0186	0.0063	0.0188
0.0063	0.0188	0.0071	0.0268	0.0088	0.0263
0.0088	0.0263	0.0100	0.0389	0.0125	0.0375
0.0125	0.0375	0.0138	0.0493	0.0163	0.0488
0.0163	0.0488	0.0172	0.0583	0.0200	0.0600
0.0200	0.0600	0.0223	0.0713	0.0250	0.0750

The Langmuir isotherm parameters for *p*-cresol (component 1) and phenol (component 2) resulting from this regression (MMC) are listed in Table III, along with the corresponding parameters reported earlier for the mass balance (MMB) and composition velocity (MCV) methods. The three methods yield differing values of the

TABLE III

LANGMUIR PARAMETERS FOR *p*-CRESOL AND PHENOL DETERMINED BY THREE MULTICOMPONENT FRONTAL CHROMATOGRAPHIC METHODS

<i>Method</i>	<i>p-Cresol</i>		<i>Phenol</i>	
	<i>a</i>	<i>b</i> ( $M^{-1}$ )	<i>a</i>	<i>b</i> ( $M^{-1}$ )
MMB	32.0	24.2	11.0	11.6
MCV	23.1	13.2	10.3	10.8
MMC	33.0	14.9	9.34	7.97

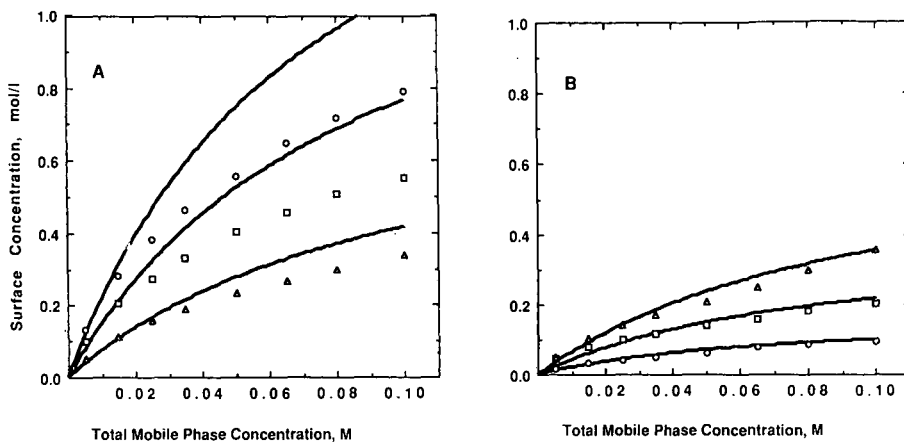


Fig. 2. Comparison of competitive adsorption isotherm of (A) *p*-cresol and (B) phenol determined by two different methods. The data points, from ref. 25, were obtained by the method of mass balance with *p*-cresol to phenol molar ratios of 3:1 (○), 1:1 (□) and 1:3 (△). The solid lines are the corresponding isotherms calculated by eqn. 1 using the MMC parameters from Table III.

four parameters. These differences demonstrate that even the relatively simple system examined here does not rigorously follow Langmuir adsorption behavior, since an ideal Langmuirian system would yield identical parameters by all three methods. The Langmuir model has been shown to be thermodynamically inconsistent<sup>39</sup>, so this result is unsurprising. As an empirical tool, however, the Langmuir isotherm provides an adequate representation of the adsorption behavior of many systems<sup>41</sup> and is the most convenient competitive isotherm that satisfies the assumptions underlying the theory of ideal multicomponent chromatography. Since the HPLC system does not rigorously adhere to the assumptions underlying the Langmuir model, selection of the appropriate method of determination of Langmuir parameters provides a means of optimizing the parameters to most accurately model the system of interest. Thus, the availability of several different means of determining isotherm parameters also enhances the utility of the Langmuir model.

The adsorption isotherms predicted by MMC deviate significantly from the adsorption data obtained by MMB, as seen in Fig. 2. The data obtained for each of the three regimes of concentration are shown together in Fig. 2. In all three regimes the MMC parameters greatly overestimate the amount of *p*-cresol adsorbed to the surface, while surface-bound phenol is accurately estimated. Examination of the Langmuir parameters in Table III shows that  $b_1$  for *p*-cresol is lower when determined by the MMC method than by MMB, while the  $a_1$  values are similar. Since  $b_1$  appears in the denominator of the compound Langmuir isotherm, eqn. 1, the result is an overestimation of the amount of *p*-cresol bound. The large deviation in Fig. 2A indicates that this approach is not an accurate method for determining the adsorption isotherm of individual species, at least for the system examined here. An analogous result has been obtained for modeling displacement chromatography in a reversed-phase system<sup>27</sup>. The Langmuir parameters obtained by frontal chromatography in that study yielded results that matched retention times well, but were less successful at predicting compositions of individual bands. Thus, a single set of parameters is inadequate to

describe all features of the chromatographic system. These results reiterate the finding that Langmuir models have limited scope in modeling the adsorption behavior even of simple systems such as *p*-cresol and phenol in reversed-phase chromatography, so the parameters must be optimized for the intended use.

MMC poorly predicts the adsorption isotherms of these compounds but, since it is a regression of a model for  $c_{im}$  data, it would be expected to accurately predict mobile phase concentration values. The Langmuir isotherm is a convenient means of empirically representing adsorption data so a judicious choice of the protocol for regression of the data can improve the accuracy of the predictions of a model based on this isotherm. Fig. 3A compares the mezzanine concentrations predicted by the Langmuir parameters of the MMB approach, with the experimentally measured mobile phase concentrations. The calculated concentrations in the ordinate were obtained with the MMB parameters of Table III and using eqns. 7–9, 12 and 13. The results of the same comparison using the MMC parameters are shown in Fig. 3B, and demonstrate that the MMC parameters, which are optimized for this calculation, perform slightly better for prediction of mezzanine concentrations, particularly at high concentrations. In calculations involving estimates of the concentrations in a band, therefore, the MMC approach may be the best choice for representing Langmuir parameters. In this way the choice of the approach to determining Langmuir parameters may compensate for part of the inaccuracy of this means of data representation in particular applications.

#### *The hybrid method of mass balance (HMMB)*

In the hybrid mass balance method of competitive isotherm determination, the mezzanine concentrations are estimated by the MCV approach, and used *in lieu* of measured concentrations in eqn. 6. This method is thus a hybrid of the MCV and MMB methods, since it is experimentally as simple as the MCV, yet it retains some of the stringency of the mass balance approach, which is not restricted to a particular isotherm model. Fig. 4 shows the mezzanine concentrations estimated using eqns. 7–9,

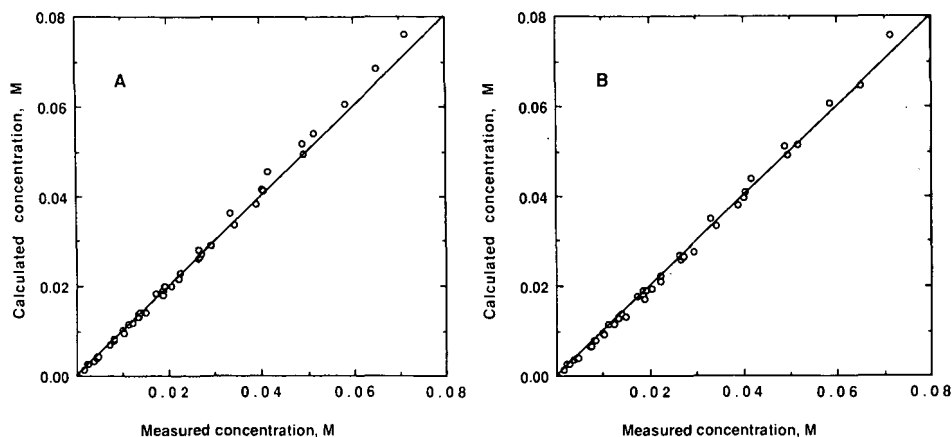


Fig. 3. Comparison of mobile phase concentrations in the mezzanine band,  $c_{1m}$  and  $c_{2m}$ , calculated by eqns. 7–9, 12 and 13 with the Langmuir isotherms parameters determined by (A) MMB and (B) MMC. The parameters were taken from Table III.

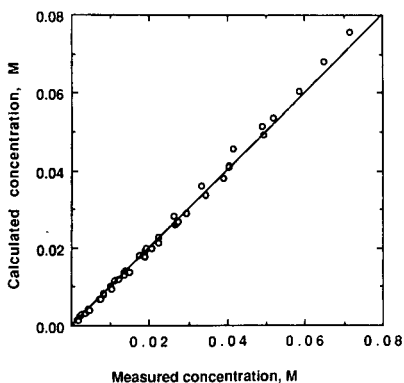


Fig. 4. Comparison of mezzanine concentrations calculated by eqns. 7–9, 12 and 13 with the Langmuir isotherm parameters determined by MCV. The parameters were taken from Table III.

12 and 13 with the MCV Langmuir parameters from Table III. The calculated HMMB and measured MMB concentrations using this approach agree well. When these estimated concentrations are used in Eqn. 1 along with the measured  $V_1$  and  $V_2$  breakthrough volumes given in Table I of ref. 25, a good fit to the measured isotherm points results, as shown in Fig. 5. At the upper limit of the range of concentrations for which the isotherms were determined the deviation between the two isotherms is greatest. According to eqn. 6, errors in determination of  $c_{im}$  in this range will result in a proportional error in  $\Delta q_i$ . Nevertheless, over most of the concentration range studied the fit to data points measured by MMB is excellent. Since it has been shown above that this chromatographic system deviates from the Langmuir model, an approach such as HMMB may be the most convenient for gathering accurate competitive adsorption data.

The hybrid approach employs MCV only to estimate mezzanine concentrations, so can be expected to more accurately estimate adsorption isotherms than MCV proper, which is forced to obey the Langmuir model. Fig. 6A shows the excellent

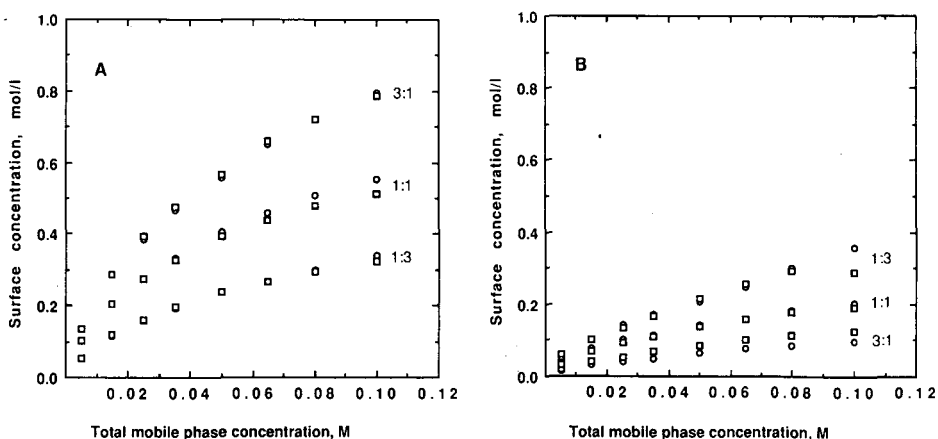


Fig. 5. Comparison of competitive adsorption isotherms of surface concentrations of (A) *p*-cresol and (B) phenol determined by MMB (○) and HMMB (□) for the three concentration regimes described in Fig. 2.

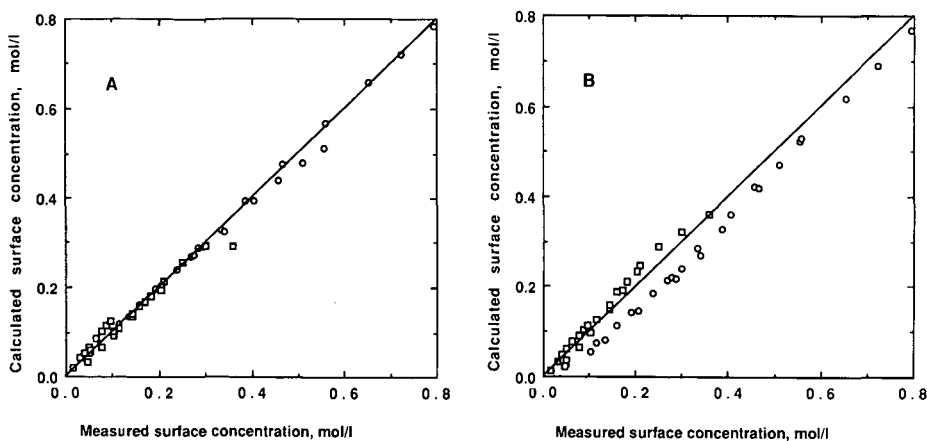


Fig. 6. Comparison of measured surface adsorption isotherm data from MMB with that calculated by (A) the hybrid mass balance method and (B) using eqn. 1 and the Langmuir parameters obtained by MCV. The measured surface concentrations are those determined by MMB for *p*-cresol ( $\circ$ ) and phenol ( $\square$ ) and shown in Fig. 2.

match between surface concentrations determined by MMB and calculated by HMMB. Fig. 6B shows the comparison between surface concentrations measured by MMB with those calculated using the MCV parameters from Table III and the Langmuir isotherm model, eqn. 1. Comparison of the two figures illustrates the significant improvement in representation of adsorption data afforded by the hybrid approach. Since the reversed-phase system employed here does not stringently adhere to the assumptions underlying the Langmuir model, the added flexibility provided by the hybrid mass balance approach improves the accuracy of isotherm determination.

## CONCLUSIONS

As noted previously, the Langmuir isotherm is not an exact representation of the adsorption behavior of this reversed-phase system, as evidenced by the deviation of adsorption parameters obtained by the four different approaches applied to the same set of data. One way to improve accuracy in the face of this deviation is by regression of measured data to a model for the variable of interest. This is the approach employed in the method of mezzanine concentrations advanced here. The Langmuir parameters then are optimized so that the best fit of calculated to measured concentration values in the frontal chromatogram are obtained. This method is shown here to improve the calculated concentration values, compared to other means of determining Langmuir parameters. The parameters obtained by MMC are tailored for this calculation, and poorly estimate other adsorption behavior, such as the amount of a component adsorbed to the surface. Nevertheless, this method is one way to improve the utility of the Langmuir model in predictions of column performance.

The second new method described here is an improvement on the method of concentration velocities (MCV) previously described. The new method, termed the hybrid mass balance method, requires the same experimental data as the MCV, but is more accurate for systems, such as that examined here, that deviate from strict

adherence to Langmuir adsorption. The method is a hybrid of the mass balance and concentration velocity procedures reported earlier, with nearly the accuracy of the former and the experimental simplicity of the latter approach.

With the increasing emphasis on large-scale HPLC, interest has grown in modeling of column performance, so that techniques for assessing adsorption behavior of systems of interest are required. The two new methods described here, building on the approaches reported earlier, provide the tools for such an assessment. Analysis of frontal chromatographic data with these methods can reveal the nature of competitive adsorption, the degree of adherence to Langmuir isotherm behavior, and provide optimal parameters to facilitate use of the Langmuir model in prediction of HPLC system performance.

#### ACKNOWLEDGEMENT

The authors gratefully acknowledge on this occasion our mentor, Csaba Horváth, for his profound role in the development of our personal and professional lives and in the genesis of this work and the studies behind it.

#### REFERENCES

- 1 E. P. Kroeff, R. A. Owens, E. L. Campbell, R. D. Johnson and H. I. Marks, *J. Chromatogr.*, 461 (1989) 45.
- 2 S. E. Builder and W. S. Hancock, *Chem. Eng. Prog.*, August (1988) 42.
- 3 W. S. Hancock, *Chromatogr. Forum*, 1 (1986) 57.
- 4 W. S. Hancock and J. T. Sparrow, in Cs. Horváth (Editor), *High Performance Liquid Chromatography—Advances and Perspectives*, Vol. 3, Academic Press, New York, 1983, p. 49.
- 5 G. B. Cox, P. E. Antle and L. R. Snyder, *J. Chromatogr.*, 444 (1988) 325.
- 6 A. L. Lee, A. Velayudhan and Cs. Horváth, in G. Durand, L. Bobichon and J. Florent (Editors), *Eighth International Biotechnology Symposium*, Société Française de Microbiologie, Paris, 1988, pp. 593–610.
- 7 Cs. Horváth, A. Nahum and J. Frenz, *J. Chromatogr.*, 218 (1981) 365.
- 8 H. Kalász and Cs. Horváth, *J. Chromatogr.*, 215 (1981) 295.
- 9 H. Kalász and Cs. Horváth, *J. Chromatogr.*, 239 (1982) 423.
- 10 Cs. Horváth, J. Frenz and Z. El Rassi, *J. Chromatogr.*, 255 (1983) 273.
- 11 Z. El Rassi and Cs. Horváth, *J. Chromatogr.*, 266 (1983) 319.
- 12 G. E. Veress, Cs. Horváth and E. Pungor, in H. Kalász (Editor), *New Approaches in Liquid Chromatography*, Akadémiai Kiadó, Budapest, 1984, pp. 45–56.
- 13 H. Kalász and Cs. Horváth, in H. Kalász (Editor), *New Approaches in Liquid Chromatography*, Akadémiai Kiadó, Budapest, 1984, pp. 57–68.
- 14 J. Frenz, Ph. van der Schrieck and Cs. Horváth, *J. Chromatogr.*, 330 (1985) 1.
- 15 Cs. Horváth, in F. Bruner (Editor), *The Science of Chromatography*, Elsevier, Amsterdam, 1985, pp. 179–203.
- 16 S. M. Cramer and Cs. Horváth, *Prep. Chromatogr.*, 1 (1988) 29.
- 17 S. M. Cramer, Z. El Rassi and Cs. Horváth, *J. Chromatogr.*, 394 (1987) 305.
- 18 J.-X. Huang and Cs. Horváth, *J. Chromatogr.*, 406 (1987) 275.
- 19 J.-X. Huang and Cs. Horváth, *J. Chromatogr.*, 406 (1987) 285.
- 20 A. W. Liao, Z. El Rassi, D. M. LeMaster and Cs. Horváth, *Chromatographia*, 24 (1987) 881.
- 21 A. L. Lee, A. W. Liao and Cs. Horváth, *J. Chromatogr.*, 443 (1988) 31.
- 22 G. Viscomi, S. Lande and Cs. Horváth, *J. Chromatogr.*, 440 (1988) 157.
- 23 A. W. Liao and Cs. Horváth, *Ann. NY Acad. Sci.* in press.
- 24 J. M. Jacobson, J. Frenz and Cs. Horváth, *J. Chromatogr.*, 316 (1984) 53.
- 25 J. M. Jacobson, J. Frenz and Cs. Horváth, *Ind. Eng. Chem. Res.*, 26 (1987) 43.
- 26 J. Frenz and Cs. Horváth, *J. Chromatogr.*, 282 (1983) 249.
- 27 J. Frenz and Cs. Horváth, *Am. Inst. Chem. Eng. J.*, 31 (1985) 400.

- 28 A. Velayudhan and Cs. Horváth, *J. Chromatogr.*, 367 (1986) 160.
- 29 A. Velayudhan and Cs. Horváth, *J. Chromatogr.*, 443 (1988) 13.
- 30 F. D. Antia and Cs. Horváth, *Ann. NY Acad. Sci.*, in press.
- 31 A. W. J. de Jong, J. C. Kraak, H. Poppe and F. Nooitgedacht, *J. Chromatogr.*, 193 (1980) 181.
- 32 J. R. Conder and C. L. Young, *Physicochemical Measurements by Gas Chromatography*, Wiley, New York, 1979.
- 33 A. Tiselius, *Ark. Kemi Mineral Geol.*, 16A (1943) 1.
- 34 S. Ghodbane and G. Guiochon, *J. Chromatogr.*, 444 (1988) 275.
- 35 F. G. Helfferich, *Ind. Eng. Chem. Fundam.*, 6 (1967) 362.
- 36 F. G. Helfferich and G. Klein, *Multicomponent Chromatography —Theory of Interference*, Marcel Dekker, New York, 1970.
- 37 F. G. Helfferich, *J. Chromatogr.*, 373 (1986) 45.
- 38 I. Langmuir, *J. Am. Chem. Soc.*, 38 (1916) 2221.
- 39 D. G. Broughton, *Ind. Eng. Chem.*, 40 (1948) 1506.
- 40 M. D. LeVan and T. Vermeulen, *J. Phys. Chem.*, 85 (1981) 3247.
- 41 J. M. Jacobson, *Ph.D. Dissertation*, Yale University, New Haven, CT, 1984.





CHROM. 21 857

QUANTITATIVE COMPARISON BETWEEN THE EXPERIMENTAL BAND PROFILES OF BINARY MIXTURES IN OVERLOADED ELUTION CHROMATOGRAPHY AND THEIR PROFILES PREDICTED BY THE SEMI-IDEAL MODEL<sup>a</sup>

A. M. KATTI

*Department of Chemical Engineering, University of Tennessee, Knoxville, TN 37996 (U.S.A.)*

and

G. GUIOCHON\*

*\*Department of Chemistry, University of Tennessee, Knoxville, TN 37996, and Division of Analytical Chemistry, Oak Ridge National Laboratory, Oak Ridge, TN 37817 (U.S.A.)*

---

SUMMARY

The experimental elution profiles of the components of a binary mixture were determined under conditions where the column is strongly overloaded and the two bands interfere markedly. These profiles were derived from the analysis of approximately 100 fractions collected during the elution of large samples of synthetic mixtures of two similar compounds having different compositions. The system investigated was the separation of 2-phenylethanol and 3-phenylpropanol on Vydac ODS silica eluted isocratically with methanol–water (50:50).

The results demonstrate the displacement and the “tag-along” effects previously predicted on the basis of theoretical investigations of the elution behavior of binary mixtures in non-linear chromatography. The displacement of the first band by the second takes place essentially when the concentration of the second eluted component is the larger. The tag-along effect of the second component is observed when the major component of the mixture is the first eluted.

Comparison between the experimental profiles and the profiles predicted by the semi-ideal model was performed using the competitive Langmuir isotherm model. For numerical calculations, the parameters of these isotherms were determined by measurement of the single-component isotherms of each of the two compounds by frontal analysis. The results of the comparison show that the competitive Langmuir isotherm gives only a fair approximation of the multi-component adsorption behavior of the two compounds studied. Competition between them for adsorption seems to be stronger than predicted by the competitive Langmuir model.

---

<sup>a</sup> Ezzel a tanulmányal Horváth Csaba Professor Urat köszöntjük 60. szüületésnapja alkalmából.

## INTRODUCTION

Recent investigations on the theory of non-linear chromatography have led to the prediction of the profiles of incompletely separated bands, such as those which are often observed in preparative liquid chromatography<sup>1,2</sup>. These predictions are based on simple assumptions and straightforward derivations, which gives them high credibility<sup>3</sup>. Comparison between these predictions and experimental results must be performed systematically, because a detailed understanding of the processes involved in preparative chromatography can only come from a fruitful combination of sound theory and carefully planned and executed experiments. This understanding is required in order to improve the methods used in the design and operation of preparative chromatographs in laboratories and in plants.

Few experimental results are available at this stage that could permit a proper investigation of the important new phenomena in overloaded elution chromatography predicted by the theoretical models, the displacement and the "tag-along" effects<sup>4</sup>. Both effects result from the competition of the components of a mixture for the stationary phase due to adsorption, exchange, complexation or reaction. The displacement effect results from stronger interaction of the more retained compound with the stationary phase. The higher the concentration of the second eluted component and the larger the separation factor of the two components, the stronger is the displacement effect. The tag-along effect results from the crowding of the stationary phase by the molecules of the less retained component in the front part of the mixed band between the two interfering components, when they are not completely resolved. This crowding increases with increasing relative concentration of the first component in the sample and with decreasing value of the separation factor. Accordingly, the tag-along effect is most prominent when the relative concentration of the second component is lower than that of the first and their separation factor is close to unity.

The displacement effect is more common since displacement chromatography is a well known process and an established technique of separation. Moreover, this effect proceeds from the same phenomenon, but under slightly different conditions (there is no way an isotachic train can develop under elution conditions, as a plateau does not form). This effect has been reported experimentally, on a qualitative basis, by Newburger and co-workers<sup>5,6</sup> and Hodges<sup>7</sup>, among others<sup>8</sup>. The tag-along effect has not yet been documented experimentally.

Comparison between the band profiles predicted by the theory of non-linear chromatography for a binary mixture and the experimental band profiles raises the difficult problem of determining the two individual profiles. Although some tests can be made under conditions when the elution bands are totally or nearly completely resolved, the most definitive experiments will obviously involve the investigation of bands which are incompletely separated. The use of the signal of conventional LC detectors is unsuitable. Although pairs of solutes can be found such that one of them absorbs at a UV wavelength where the other is transparent, there are several major drawbacks to this approach. First, this scheme permits the detection of only one component and not the other, which leaves half the problem unsolved. Second, the two compounds selected will necessarily have markedly different chemical structures. Their chromatographic separation is then a trivial problem. Moreover, few relevant

conclusions can be derived from the results regarding the competitive adsorption isotherms of chemically unrelated compounds. The important separation problems in both preparative and analytical chromatography are those which involve closely related compounds. Finally, the calibration of UV detectors under the conditions where they must be used is a difficult task, complicated by the need to avoid any response contribution due to the other component.

Accordingly, we have used a more direct approach. Bands are generated by injecting large samples of binary mixtures of various compositions, where a certain degree of band interference occurs. A large number of fractions are collected during the elution of these bands and they are analysed by liquid chromatography under conditions where total separation of these analytical samples occurs. From these quantitative analyses, the desired elution profiles of each component are calculated. The method is simple and powerful. This procedure is not very time consuming if an automatic fraction collector and an automatic sampling system are used, especially in overnight runs.

The second difficulty encountered in the systematic investigation of the validity of theoretical predictions is the prerequisite for a suitable set of equations to describe the equilibrium isotherms of the compounds used. The studies of phase equilibria made so far have focused on single-compound equilibria and they are of little interest in preparative chromatography. Of major concern, in contrast, is the competitive isotherm behavior of the two components of the mixtures considered. In practice, there is only one workable model available, the set of competitive Langmuir isotherms. The validity of this model has not been investigated systematically in order to determine its limitations. It has been shown that it cannot be used to model crossed isotherms<sup>9,10</sup>. The Langmuir model assumes ideal behavior of both the mobile phase and the adsorbed layer, whereas we know that molecular interactions are pervasive in condensed phases. Deviations between the predictions of the semi-ideal model and the experimental results are important to determine, as they will give important clues regarding the extent of the deviations between the actual adsorption behavior of the compounds investigated and the predictions of the competitive Langmuir model.

This paper presents the first results obtained in a long series of experiments and reports on the first experimental demonstration of the tag-along effect. Additionally, it reports on the degree of agreement observed between the theoretical predictions and the experimental profiles derived from the experiment. This leads to important conclusions regarding the validity of the competitive Langmuir isotherm model.

## THEORY

Band profiles in this paper are predicted by numerically solving the system of partial differential equations that describes the band migration in liquid chromatography<sup>2</sup>. This system of equations states the conservation of mass for each component of the mixture in a column slice. For a binary mixture, assuming plug flow and equilibrium for both components between the mobile and the stationary phases (ideal model) at all points along the column, the mass balance equations are written as follows for each component  $i$  in the mixture:

$$FdQ_i/dt + dC_i/dt + u_0dC_i/dz = 0 \quad (1)$$

A solution of this system of equations requires a relationship between the  $Q_i$  and the  $C_i$  values (*i.e.*, the composition of the stationary phase in equilibrium with the mobile phase). One of the simplest relationships that describes this equilibrium is the Langmuir competitive equilibrium isotherm:

$$Q_i = a_i C_i / (1 + \sum b_i C_i) \quad (2)$$

The parameters of these two equations are obtained by determining successively the single-component isotherms of each of the pure two components. This very simple procedure and the functional simplicity of eqn. 2 explain the great interest for the competitive Langmuir isotherm in practical applications of the theory of non-linear chromatography.

Given the concentration–time functionality at the entrance of the column (injection profile) and the values for the various parameters, the system of eqns. 1 and 2 can be solved numerically<sup>2,3</sup>. The band-broadening effects of the axial dispersion and the deviation of the system from thermodynamic equilibrium, which are the basic reasons for the finite column efficiency, can be accounted for by employing a finite difference algorithm for the calculations. The column is divided into a linear grid,  $nh$ , and the concentrations of the two compounds are calculated at each summit of the grid, at increasing times,  $t\tau$ . By using carefully chosen space ( $h$ ) and time ( $\tau$ ) increments<sup>11,12</sup>, we can obtain a solution where the column height equivalent to a theoretical plate (HETP) is based on the average variance of the two components eluting under linear conditions. Thus, the finite nature of the column efficiency is taken into account numerically<sup>13</sup>.

## EXPERIMENTAL

### *Equipment*

The modular liquid chromatograph used for the preparative separations was assembled from two Waters Assoc. (Milford, MA, U.S.A.) Model 510 pumps, a Valco (Houston, TX, U.S.A.) electrically actuated six-port valve fitted with a 100- $\mu$ l sample loop, a Kratos (Ramsey, NJ, U.S.A.) Spectroflow 757 variable-wavelength detector operated at 272 nm and a Gilson (Middleton, WI, U.S.A.) Model 232/401 automatic sample processor and injector with a Model 401 diluter operated in the fraction collection mode. The pumps were controlled and the detector signal was monitored via a Waters Assoc. system interface module using the Waters Assoc. Maxima 860 Dynamic Solutions (Ventura, CA, U.S.A.) software installed on an NEC APCIV Powermate 2 computer. The collected fractions were then diluted using the Model 232/401 sample processor in the dilution mode.

The modular chromatograph used for the analysis of the collected fractions was assembled by connecting the Model 510 pump outlet directly into the Model 232/401 sample processor in the autosampler operation mode, fitted with a 20- $\mu$ l loop. The column effluent was monitored at 254 nm with the Spectroflow 757 detector. Quantitative determinations of the unknown concentrations of the two components in each of the collected fractions was accomplished using the Maxima 860 software.

### *Columns and chemicals*

The 25 cm × 4.5 mm I.D. preparative column and the 5 cm × 4.5 mm I.D. analytical column were packed in our laboratory at 9000 p.s.i. with 10- $\mu$ m Vydac ODS stationary phase (The Separation Group, Hesperia, CA, U.S.A.), generously donated to us.

3-Phenylethanol and 2-phenylpropanol were purchased from Fluka (Ronkonkoma, NY, U.S.A.) and used without further purification. High-performance liquid chromatographic grade methanol and water (Burdick and Jackson, Baxter Chemical, Muskegon, MI, U.S.A.) were used.

### *Procedure*

The experiments were carried out by first injecting 100  $\mu$ l of the selected mixture at a concentration at which the preparative separation is incomplete. During the elution of the partially separated mixture, fractions are collected on a time basis, at a rate of one vial every 3 s (*i.e.*, the fractions collected were *ca.* 50  $\mu$ l for a mobile phase flow-rate of 1 ml/min). Then, a dilution was performed on each fraction by adding 300  $\mu$ l of solvent to each vial at a rate of *ca.* 3  $\mu$ l/s. Finally, the automatic sampler was employed to aspirate 100  $\mu$ l of the sample at a rate of 6  $\mu$ l/s, dispense these 100- $\mu$ l aliquots into the 20- $\mu$ l loop at the same rate and then inject the sample. After 5 min the run was complete. The apparatus rinsed the syringe needle with solvent and the whole process was repeated until the contents of each vial had been analyzed.

On switching the sampling valve from load to inject, the sampling system sent an electric signal to the interface box to initiate data acquisition. Chromatograms were obtained automatically and sequentially. The detector signal was acquired by the software, which opens a file for each fraction analyzed, acquires data for 5 min at a rate of 2 points/s, closes and stores the file and repeats this process for each sample. The peak area of the two components was obtained by running an analysis program on each of the stored files. The concentration of each component in each fraction was calculated from a linear calibration graph previously determined for the two compounds and adjusted according to the dilution factor.

All experiments were conducted at ambient temperature. The preparative column was operated at 1 ml/min with methanol–water (50:50) as the mobile phase and with detection at 272 nm. The analytical column was operated at 1 ml/min with methanol–water (35:65) as the mobile phase and with detection at 254 nm.

### *Detector calibration*

This is a most delicate problem, as the UV detector gives an optical absorbance profile of the eluent, whereas we are interested in the concentration profile. As the concentration of the solutes in the eluent is high when the column is overloaded, the detector response is not linear and thus the calibration is more difficult.

Depending on whether we are dealing with the single-component elution profiles or with those of binary mixtures, the problem is different. For the single-component band profiles, the use of a non-linear calibration graph is possible. For binary mixtures, it is not possible and fractions have to be collected and analyzed. Then a conventional linear calibration graph is employed in quantitation.

*Single component.* Conversion of the single-component overloaded chromatograms (*i.e.*, the elution profiles supplied by the detector response) into concentration

profiles of each of the corresponding compounds (2-phenylethanol and 3-phenylpropanol) was accomplished by using a non-linear concentration *versus* response calibration graph. This graph was derived from experimental absorbances measured for standard solutions having concentrations between 0 and 80 mg/ml of each compound studied. However, the curve fitting was done only over the concentration range required for prediction of the band profiles. The concentration *versus* absorbance data were fitted to a polynomial. In fitting the calibration data for 2-phenylethanol, oscillations were found when using a third- or a fifth-degree polynomial. These oscillations lead to artifactual humps on the concentration profiles. This problem was avoided by eliminating the odd power terms greater than 1 (ref. 14). The 3-phenylpropanol response calibration was fitted to a fifth-degree polynomial.

In practice, the experimental data for the calibration graphs were derived from the detector responses obtained for each concentration plateau recorded in frontal analysis during the determination of the equilibrium isotherm for each of the compounds studied<sup>15</sup>.

Fig. 1 shows the non-linear calibration graph at 272 nm of 2-phenylethanol and 3-phenylpropanol used for quantitation of the single-component band profiles. Note that 3-phenylpropanol absorbs more strongly than 2-phenylethanol.

*Binary mixtures.* The concentration of each component in each fraction was

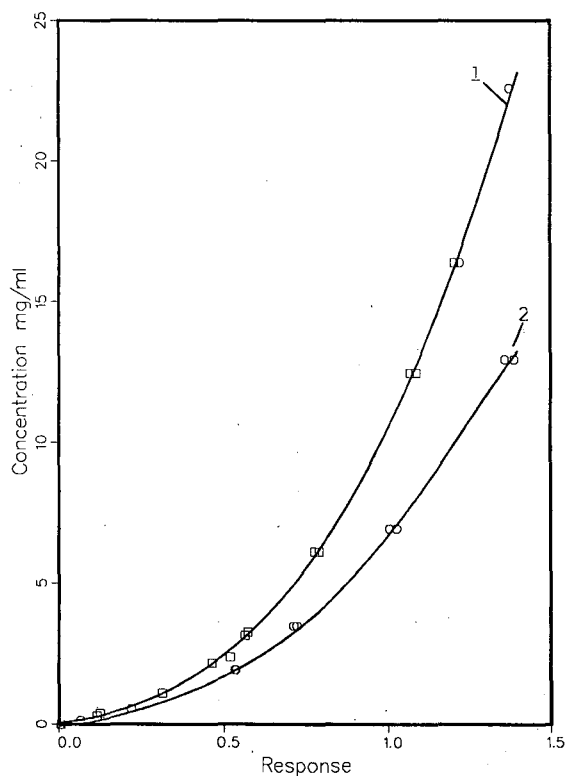


Fig. 1. Calibration graphs of the response (absorbance) of a UV spectrophotometric detector for (1, □) 2-phenylethanol and (2, ○) 3-phenylpropanol at 272 nm. Experimental points and polynomial curve fit.

determined by using standard analytical techniques. The fractions are small and dilute enough that their analysis can be carried out under linear conditions. Twelve standards were prepared and samples were injected in the same way as the fraction aliquots. The peak areas were calculated from the detector responses monitored at 254 nm, where the absorbance is much stronger than at 272 nm. A linear calibration graph of concentration *versus* peak area was determined by a least-squares fit of the data to the equation of a straight line for each of the two components. The standard deviation was 0.99991 and 0.99992 for the 2-phenylethanol and 3-phenylpropanol fits, respectively.

## RESULTS AND DISCUSSION

The retention times at infinite dilution for 2-phenylethanol and 3-phenylpropanol were measured on the preparative column by injection of several samples at decreasing concentrations. This procedure insures that the retention times obtained correspond to the slope of the tangent to the isotherm at the origin of coordinates. The dead time was measured from the solvent peak. The dead time was 3 min, which corresponded to a mobile phase volume of 3.0 ml and a column porosity of 0.755. In the methanol–water (50:50) mobile phase, the capacity factors of the two compounds were 0.68 and 1.25, respectively. The separation factor was 1.84.

The single-component isotherms of the two compounds were measured by frontal analysis<sup>16,17</sup>. The parameters were obtained by a least-squares fit of the data on the linearized equation ( $1/Q_i = 1/a_i C_i + a_i/b_i$ ) or by a non-linear least-squares fit. The values obtained were  $a_E = 1.9239$  ml/ml,  $b_E = 1.8092$  ml/mole,  $a_P = 3.554$  ml/ml and  $b_P = 3.479$  ml/mole, respectively (the subscripts E and P represent 2-phenylethanol and 3-phenylpropanol, respectively). The values of the phase ratio derived from the porosity (3.09) and from the ratio of the isotherm slope to the column capacity factor (2.84) were in good agreement.

The total column saturation capacity corresponding to monolayer coverage is 140 mg for the first and 150 mg for the second component. The saturation capacities differ by 7% (whereas the total number of carbon and oxygen atoms in their molecules differ by 10%), which suggests that Langmuirian behavior for the competitive isotherms is a possibility. However, we know that the Langmuir competitive isotherms are consistent with thermodynamics only if the column saturation capacity is the same for the two compounds (otherwise they do not satisfy the Gibbs–Duhem equation). Further, Cox *et al.*<sup>18</sup> have shown that the profiles of overloaded interfering bands depend on the ratio of the column saturation capacities of the two components.

For the calculation of the amount loaded onto the column in terms of the percentage of the column saturation capacity for monolayer coverage,

$$\text{Column saturation capacity} = 1/2 \sum a_i V_{sp}/b_i \quad (3)$$

an arbitrary average value of 145 mg was used in all the calculations. This equation gives an approximate value of the degree of column overloading.

Two experimental single-component overloaded elution chromatograms were measured by injecting successively amounts corresponding to 5% of the column saturation capacity for 2-phenylethanol and 3-phenylpropanol. The detector response profiles were converted into concentration profiles by using a polynomial fit to

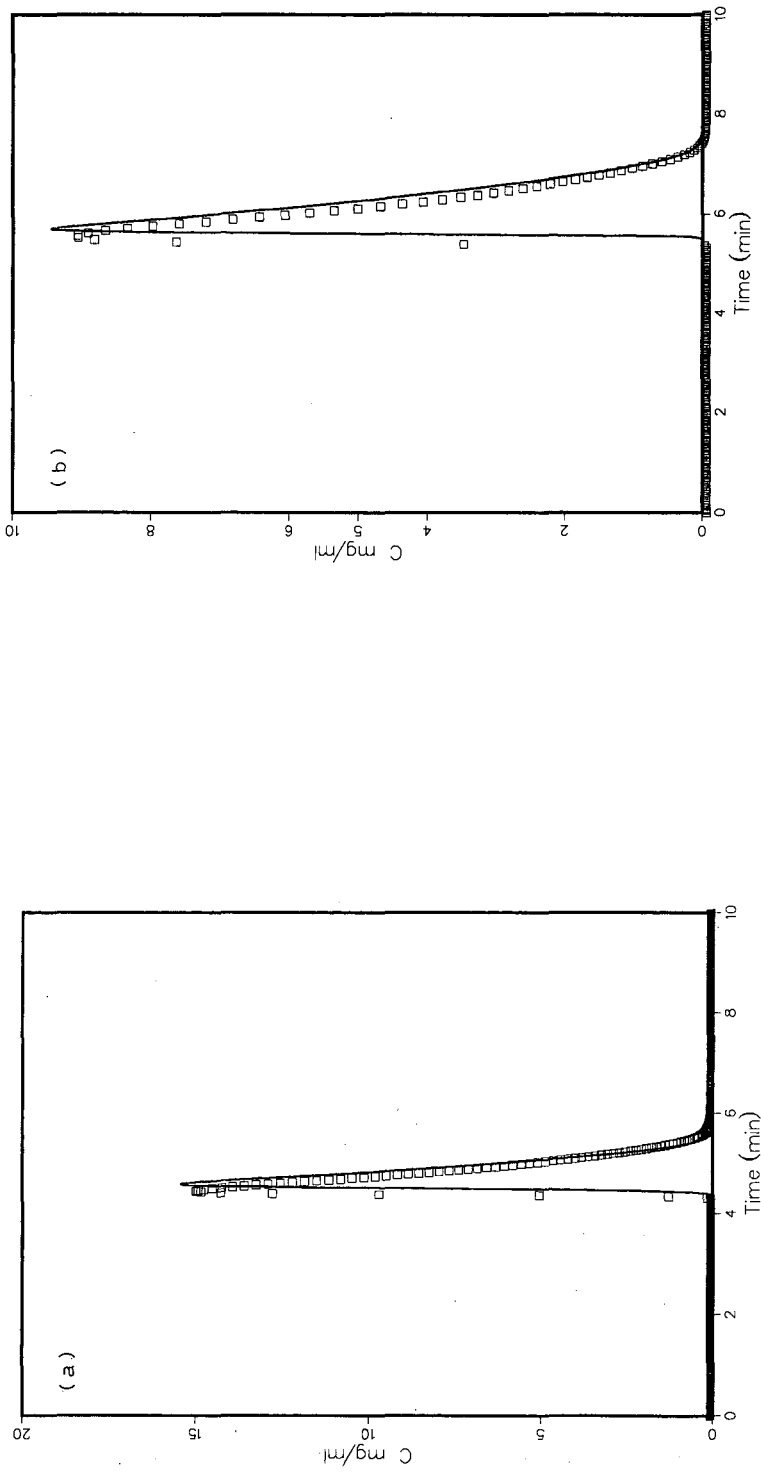


Fig. 2. Comparison of single-component overloaded elution profiles with the prediction of the semi-ideal model of chromatography using the single-component Langmuir equilibrium model. Symbols: concentration of each collected fraction. Solid line: profile calculated with the semi-ideal model program using the isotherm parameters determined by frontal analysis. Column, 25 cm long, packed with 10- $\mu$ m Vydac ODS silica; mobile phase, methanol-water (50:50); flow-rate, 1 ml/min; sample size, 5% of the column saturation capacity. (a) 2-Phenylethanol (7.1 mg); (b) 3-phenylpropanol (7.1 mg).



a non-linear calibration graph as described above. The symbols in Fig. 2a and b show the concentration–time profiles for 2-phenylethanol and 3-phenylpropanol, respectively, determined experimentally. The solid line represents the theoretical prediction based on the fit of the single-component adsorption isotherm data to the single-component Langmuir isotherm and calculated using the program for the single-compound semi-ideal model<sup>3</sup>. The excellent agreement suggests that the Langmuir expression is a good model for the equilibrium data. Additionally, the validity of the assumptions of the semi-ideal model is confirmed<sup>1,3</sup>. This model can give a very accurate quantitative prediction of the band profiles provided accurate isotherms are determined, which classical frontal analysis permits<sup>19</sup>.

For binary mixtures, the individual band profiles were determined by analysis of collected fractions. For the purpose of evaluation of this technique, a comparison was made with the profiles obtained for 2-phenylethanol by direct calibration of the detector. The results (Fig. 3) are in excellent agreement and demonstrate that the fraction collection system contributes very little to band broadening.

A comparison was made between experimental and theoretical profiles for 1:3 and 3:1 mixtures of 2-phenylethanol and 3-phenylpropanol. The theoretical profiles were calculated using the program for the two-component semi-ideal model<sup>2</sup>. The competitive Langmuir isotherms were derived from the parameters of the single-component Langmuir isotherms measured by frontal analysis (see Theory section). The experimental band profiles for the two-component mixtures were measured using the technique described above.

Fig. 4 shows the comparison between theory and experiment for the 1:3 mixture. The sample size used corresponds to 5% of the column saturation capacity for

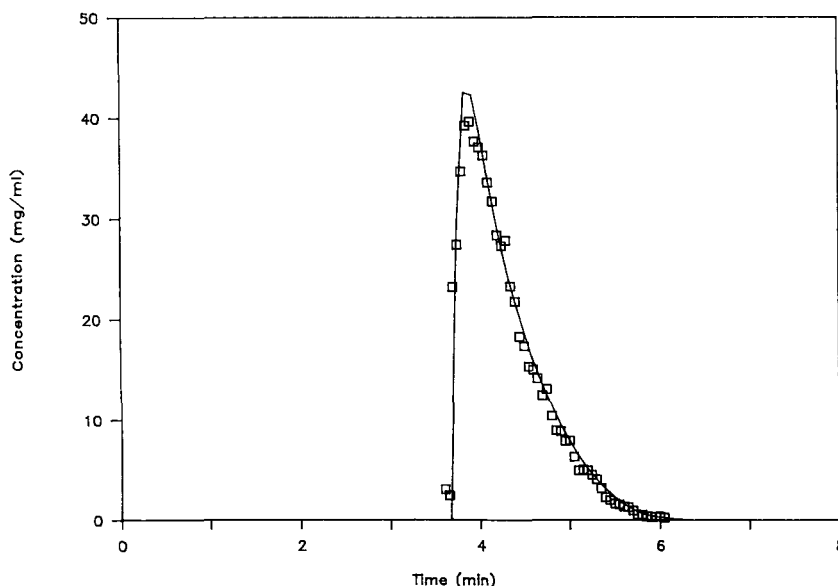


Fig. 3. Evaluation of the fraction collector. Solid line: concentration profile derived from the detector signal and a calibration graph. Symbols: composition of the collected fractions. Experimental conditions as in Fig. 2a, except amount injected (30 mg).

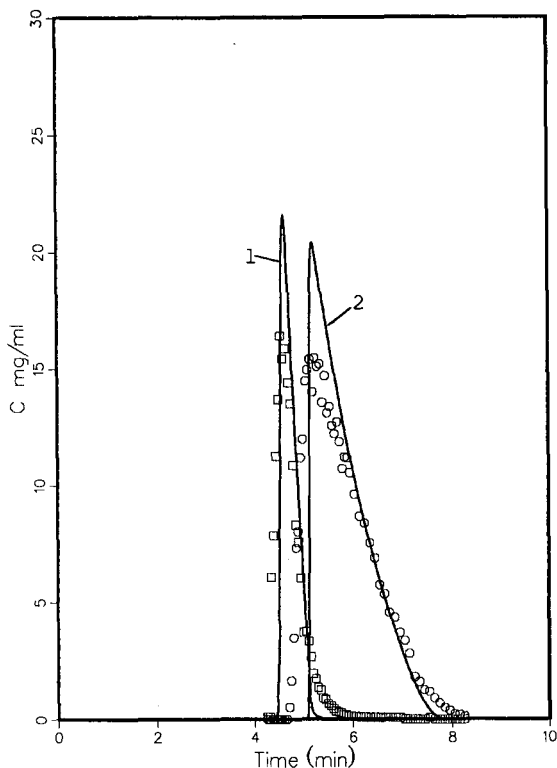


Fig. 4. Comparison of the experimental and theoretical band profiles of the two components for a 1:3 mixture of (1,  $\square$ ) 2-phenylethanol and (2,  $\circ$ ) 3-phenylpropanol using a competitive Langmuir adsorption isotherm (eqn. 2). Column as in Fig. 2. Sample sizes: 7.6 mg of 2-phenylethanol and 21.1 mg of 3-phenylpropanol. Symbols: experimental results. Solid lines: prediction of the semi-ideal model of chromatography using the competitive Langmuir isotherm (eqn. 2) with the coefficients derived from the single-component adsorption isotherms determined by frontal analysis.

component 1 and 15% of that for component 2. This is a significant degree of overloading, but the relative retention of the two components is high so partial resolution of the band is expected. The experimental profile shown includes the effect of extra-column and post-detector dead volume whereas the theoretical profile assumes no dispersion as the effluent elutes through these volumes. The experimental profiles demonstrate the displacement effect encountered in the elution of high concentration bands of a binary mixture.

The agreement observed in Fig. 4 between experimental results and theory is, however, of an approximate nature, within 10%. The rear boundary of the second component coincides with the predicted boundary, which is an important test of the applicability of the semi-ideal model. The rear boundary of the second component band profile should be identical with the band profile of the same amount of the second component when it is pure, a profile which is predicted by the single-component isotherm data. It appears that there is slightly more dispersion at the very end of the tail than predicted, probably the result of some additional and unavoidable diffusion in the tubing of the fraction collector.

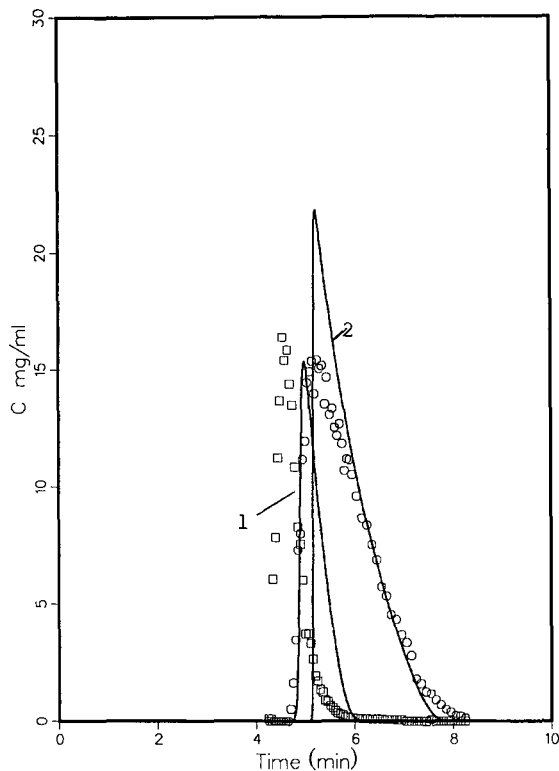


Fig. 5. Comparison of the experimental and theoretical band profiles calculated for the elution of the 1:3 mixture in Fig. 3, using a non-interacting (single-component) Langmuir isotherm model for each compound (solid lines). (1,  $\square$ ) 2-Phenylethanol; (2,  $\circ$ ) 3-phenylpropanol.

Fig. 5 shows a comparison of the experimental data for the mixture and the band profiles predicted as if the two components did not interact. The solid line represents the band profile predicted for two components having as their competitive isotherm their respective single-component isotherms (or, alternately, the profiles obtained when each component is injected alone). The symbols represent the experimental data which were also shown in Fig. 4. The presence of a displacement effect of the second component on the first is clearly seen in the experimental results, because the first component elutes faster in the experimental mixture than if the two bands were not interacting. The band obtained for the first component is taller and narrower than it would be if it were injected alone. In conclusion, Fig. 5 demonstrates that a non-interacting isotherm model (*i.e.*, two single-component isotherms) gives a poor representation of the chromatographic behavior of the two components of interfering bands. Together, Figs. 4 and 5 show the existence and potential importance of the displacement effect and the necessity for modelling accurately the competitive adsorption behavior in the chromatography of binary mixtures at high concentration.

Fig. 6 illustrates a comparison between theory and experiment for a 3:1 mixture for the same compounds. The experimental profiles are shown by the symbols and the predicted profiles are the solid lines. Here the major component of the mixture is eluted

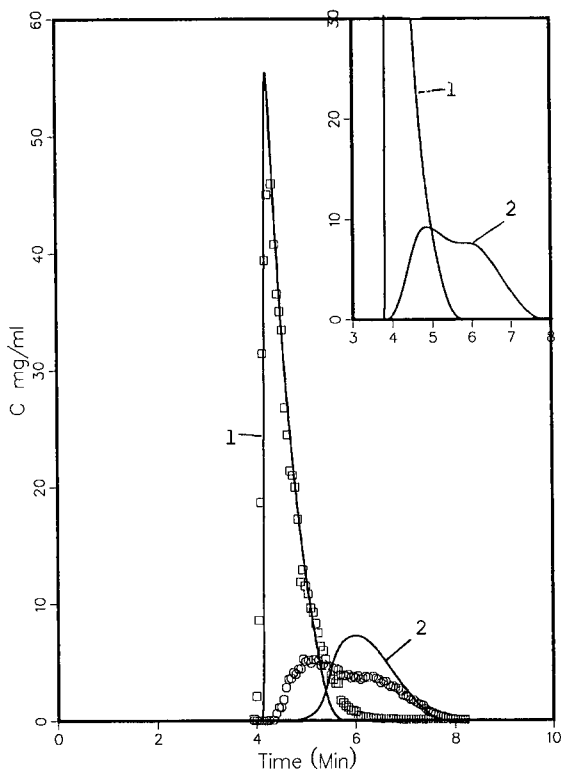


Fig. 6. Comparison of the experimental and theoretical band profiles of the two compounds for a 3:1 mixture of (1,  $\square$ ) 2-phenylethanol and (2,  $\circ$ ) 3-phenylpropanol, using a competitive Langmuir adsorption isotherm (eqn. 2). Main figure: same conditions as in Fig. 4, except sample composition (3:1) and size (30.1 mg of 2-phenylethanol and 10.2 mg of 3-phenylpropanol). Symbols: composition of the collected fractions. Solid lines: prediction of the semi-ideal model of chromatography using the competitive Langmuir isotherm (eqn. 2) with the coefficients derived from the single-component adsorption isotherms determined by frontal analysis. Inset: theoretical band profile calculated as for the main figure, but for twice the sample size.

first, not second. The column is loaded to 21% and 7% of the column saturation capacity for the first and second components, respectively. The tag-along effect predicted on the basis of computational results<sup>2,4</sup> is demonstrated for the first time. As observed previously<sup>4</sup>, this effect is a consequence of the first component being in large excess in the front of the zone where the two components coexist and thus covering a large fraction of the adsorption sites. As there is near equilibrium between the mobile and the stationary phases, adsorption of the second component follows according to eqn. 2. The second component must move faster than it would if it were alone, because fewer sites are available for adsorption of its molecules, and this gives rise to the profiles shown in Fig. 6. Experimentally, the bands overlap to a greater extent than predicted, which means that the exclusion of 2-phenylethanol molecules from the surface by 3-phenylpropanol molecules is not as strong as predicted by the competitive Langmuir isotherm.

The inset in Fig. 6 shows the calculated elution profiles of the two components of the same 3:1 mixture at twice the loading factor and at the same composition. This

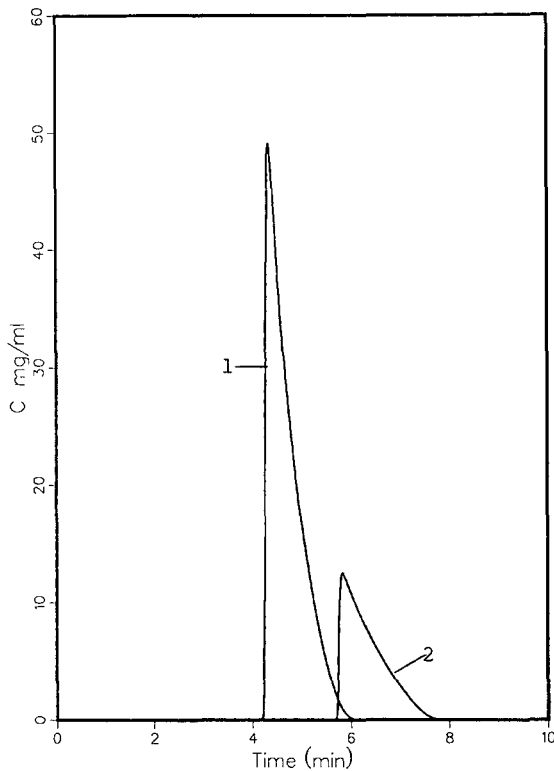


Fig. 7. Theoretical band profile calculated for the 3:1 mixture at the same loading as in Fig. 6, but using a non-interacting (single-component) Langmuir isotherm model (same as for Fig. 5).

permits a qualitative comparison of the second component profile with the experimental profile in the main part of Fig. 6. The inset shows that the semi-ideal model of chromatography can predict the strange shape of the elution profile of the later eluting component. This comparison suggests that the difficulty in predicting the interference profile observed experimentally is in the proper representation of the competitive adsorption isotherm and not in the assumptions made in the semi-ideal model.

The band profiles of the two components, predicted by the semi-ideal model in the assumption that they are not competing for access to the stationary phase, are shown in Fig. 7. Comparison of the band profiles in the interacting and non-interacting cases shows that there is no significant difference in the profiles predicted for the first component. The experimental profile is very slightly wider than the predicted profiles. In contrast, large deviations are predicted and seen for the front part of the profile of the second component. The profile front is no longer a sharp boundary; it is very flat and the plateau predicted by the theory of non-linear chromatography<sup>1</sup> can be observed in Fig. 6. The rear boundaries of the profiles predicted with and without interaction and of the profile determined experimentally for the second component coincide. Experiments are in progress<sup>19</sup> to determine whether the slope of this front is related to the column efficiency, as predicted by the semi-ideal model<sup>1</sup>.

## CONCLUSION

While the agreement between the experimental results and the calculations derived from the semi-ideal model of non-linear chromatography show excellent agreement for the single-component elution profiles under all the experimental conditions investigated, substantial differences are observed for the elution profiles of binary mixtures. The reason for this disagreement stems from the fact that, although the single-component Langmuir isotherm offers most often a very good description of the adsorption equilibrium of a pure compound in a chromatographic system, the competitive Langmuir isotherms offer only a first-order approximation to the adsorption behavior of the components of a binary mixture. Owing to the lack of a suitable set of equations describing the competitive equilibrium of the components of a mixture in a biphasic system, it is not yet possible to predict more accurately the individual component profiles of the interfering zones in overloaded elution chromatography of binary mixtures.

In the system investigated here, which seems fairly simple with its two homologous components, we note that the exclusion of the lower molecular weight component by the heavier one is less than predicted on the basis of the Langmuir model. This lower extent of competition results in the second component travelling faster than predicted in the presence of the first component. A more detailed understanding of the competitive adsorption behavior must wait until the competitive isotherms are determined experimentally<sup>20</sup>.

## ACKNOWLEDGEMENTS

This work was supported in part by Grant CHE-8715211 of the National Science Foundation and by the cooperative agreement between the University of Tennessee and the Oak Ridge National Laboratory. We acknowledge the loan of the Model 232/401 automatic sample processor and injector with diluter by Gilson (Middleton, NJ, U.S.A.) and fruitful discussions with Francis Verillon (Gilson, Villiers-le-Bel, France). 10- $\mu$ m Vydac ODS was generously supplied by the Separation Group (Hesperia, CA, U.S.A.).

## REFERENCES

- 1 S. Golshan-Shirazi and G. Guiochon, *J. Phys. Chem.*, 93 (1989) 4.
- 2 G. Guiochon and S. Ghodbane, *J. Phys. Chem.*, 92 (1988) 3682.
- 3 G. Guiochon, S. Golshan-Shirazi and A. Jaulmes, *Anal. Chem.*, 60 (1988) 1856.
- 4 S. Ghodbane and G. Guiochon, *J. Chromatogr.*, 440 (1988) 9.
- 5 J. Newburger, L. Liebes, H. Colin and G. Guiochon, *Sep. Sci. Technol.*, 22 (1987) 1933.
- 6 J. Newburger and G. Guiochon, paper presented at HPLC '88, Washington, DC, June 1988.
- 7 R. S. Hodges, *Chromatographia*, 24 (1989) 565.
- 8 G. Guiochon and A. M. Katti, *Chromatographia*, 22 (1987) 165.
- 9 J. X. Huang and G. Guiochon, *J. Colloid Interface Sci.*, 116 (1989).
- 10 B. Lin, Z. Ma, S. Golshan-Shirazi and G. Guiochon, *J. Chromatogr.*, 475 (1989) 1.
- 11 B. Lin and G. Guiochon, *Sep. Sci. Technol.*, 24 (1989) 32.
- 12 G. Guiochon, S. Ghodbane, S. Golshan-Shirazi, J. X. Huang, A. M. Katti, B. Lin and Z. Ma, *Talanta*, 32 (1989) 19.
- 13 B. Lin, Z. Ma and G. Guiochon, *J. Chromatogr.*, 484 (1989) 83.
- 14 E. Dose and G. Guiochon, *Anal. Chem.*, in press.

- 15 S. Golshan-Shirazi, S. Ghodbane and G. Guiochon, *Anal. Chem.*, 60 (1988) 2630.
- 16 D. H. James and C. S. G. Phillips, *J. Chem. Soc.*, (1954) 1066.
- 17 G. Schay and G. Szekeley, *Acta Chim. Acad. Sci. Hung.*, 5 (1954) 167.
- 18 G. B. Cox, L. R. Snyder and J. W. Dolan, presented at *the 13th International Symposium on Column Liquid Chromatography, Stockholm, Sweden, June 25-30, 1989.*
- 19 S. Golshan-Shirazi and G. Guiochon, *Anal. Chem.*, 60 (1988) 3634.
- 20 A. M. Katti and G. Guiochon, in preparation.





CHROM. 21 614

## SCALING-UP PROCEDURE FROM THE RANGE OF MILLIGRAMS TO GRAMS FOR THE PURIFICATION OF AMINO ACID DERIVATIVES IN DISPLACEMENT CHROMATOGRAPHY<sup>a</sup>

F. CARDINALI, A. ZIGGIOTTI and G. C. VISCOMI\*<sup>b</sup>  
*Enricerche, 00015 Monterotondo, Rome (Italy)*

---

### SUMMARY

A scaling up method in displacement chromatography was applied to the purification of the amino acid derivative N<sup>ε</sup>-9-fluorenoxycarbonyl-S-tritylcysteine [Fmoc-Cys(Trt)-OH]. Once the adsorption isotherm of the compound and some related impurities had been determined, the displacement chromatographic runs were carried out in the normal phase. The influence of parameters such as particle diameter of the stationary phase, carrier composition, nature of the displacer, concentration of the loaded sample and flow-rate is reported. The eluates were analysed directly at the outlet of the preparative columns with dedicated on-line detection equipment.

The results demonstrate that, once the proper conditions have been established, it is possible to purify in one run 100 mg and 38 g of feed mixture by proportionally increasing the amount of the stationary phase, using a larger column and maintaining the linear velocity and displacer concentration constant.

---

### INTRODUCTION

High-performance displacement chromatography has recently been proposed as a potentially useful technique for the preparative purification of natural and synthetic compounds<sup>1-5</sup>. Relative to the elution mode, displacement chromatography offers the advantages of a higher loading capacity, concentrated eluates and a low consumption of solvents as eluents.

In displacement chromatography, the column is first equilibrated with an eluent, the carrier, which has to be able to dissolve the feed components and the displacer at high concentrations and has to retain the bulk of the desired products on the stationary phase. After sample loading, an eluent containing a displacer, namely a compound that is strongly adsorbed on the stationary phase, is pumped so as to push the adsorbed feed components out of the column. The main feature of a compound to be considered

---

<sup>a</sup> Preliminary data were presented at the *2nd International Symposium on Preparative and Up-Scale Liquid Chromatography, Baden-Baden, February 1-3, 1988*. The majority of the papers presented at this symposium have been published in *J. Chromatogr.*, Vol. 450, No. 1 (1988).

<sup>b</sup> Present address: Peptide Synthesis Laboratory, SCLAVO SpA, 00015 Monterotondo, Rome, Italy.

as a displacer is that its adsorption isotherm overlies those of the feed components to be displaced.

The aim of this work was to show the feasibility of a scaling-up procedure from the range of milligrams to grams in displacement chromatography for preparative purifications. The choice of  $N^{\alpha}$ -9-fluorenoxycarbonyl-S-tritylcysteine [Fmoc-Cys(Trt)-OH] as a model for this study came from considerations that the retention time ( $t_R$ ) of the desired product falls between the  $t_{RS}$  of the impurities, that the presence of a polar carboxyl group makes its purification by normal-phase elution chromatography difficult because of tailing and that the compound cannot be purified by reversed-phase chromatography because it is not soluble in aqueous solvents at high concentrations.

As the concentrations of the eluted components in displacement chromatography are so high as to saturate completely common detectors, dedicated on-line detection equipment was set up to provide the information needed for the appropriate pooling of the fractions within the time of a displacement run. The proposed equipment carries out the following functions: picking up and appropriately diluting a small amount of the eluent, injecting it into a high-speed chromatographic system and analysing the corresponding chromatographic data. The entire sequence of the events is performed in less than 2 min and can be repeated any number of times.

## EXPERIMENTAL

### *Materials*

Fmoc-Cys(Trt)-OH was synthesized following the general procedure described by Kruse and Holden<sup>6</sup>.

Benzyltributylammonium chloride (BTBA), benzylhexadecylammonium chloride (BHDA), triphenylmethanol (Trt-OH), 9-fluorenylmethanol (Fmoc-OH) and trifluoroacetic acid (TFA) were supplied by Fluka (Buchs, Switzerland); TFA was distilled prior to use. Methanol, chloroform and acetonitrile [high-performance liquid chromatographic (HPLC) grade] were purchased from Merck (Darmstadt, F.R.G.).

Water was purified with a Milli-Q system (Millipore, Bedford, MA, U.S.A.). The aqueous eluents were filtered through a 0.45- $\mu\text{m}$  cellulose acetate filter and the organic solvents through a 0.5- $\mu\text{m}$  PTFE filter; all the eluents were degassed by helium purging prior to use.

### *Apparatus*

Displacement chromatographic runs in the milligram range were carried out on a LiChrocart RP-18 (10  $\mu\text{m}$ ) column (250  $\times$  4.0 mm I.D. (Merck). The HPLC equipment consisted of a Model M-45 pump (Waters Assoc., Milford, MA, U.S.A.), a Model 7010 injector (Rheodyne, Cotati, CA, U.S.A.) with a 3 ml loop, a PU 4025 UV detector (Pye Unicam, Cambridge, U.K.) and a Model 2210 recorder (LKB, Bromma, Sweden). The column effluent was collected with a Model 2070 Ultrarack II (LKB).

The displacement runs in the gram range were carried out on axial compression columns of I.D. 20, 40 and 80 mm (Jobin-Yvon, Longjumeau, France) and packed with LiChroprep Si 60 silica (25–40  $\mu\text{m}$ ) (Merck). The pump was a Model 590 programmable HPLC pump (Waters Assoc.) and the effluents were collected with a Model 2211 Superrack fraction collector (LKB).

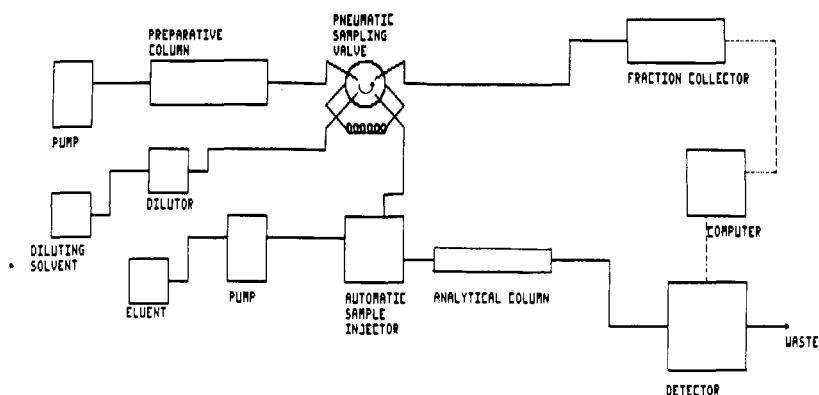


Fig. 1. Flow scheme of the on-line detection equipment used for displacement chromatographic monitoring.

The columns of I.D. 4, 20, 40, and 80 mm were equilibrated with the carrier for 20 min at a flow-rate of 0.4, 8, 32 and 128 ml/min, respectively. The same procedure, except the solvent that was methanol, was applied to regenerate the stationary phase after the displacement runs. Taking in account the steps of equilibration, elution and regeneration, the total chromatographic time for the displacement runs was about 230 min. The presence of the displacer agent in the fractions was monitored by thin-layer chromatography or spectrophotometry<sup>7</sup>.

The on-line detection equipment (Fig. 1) consisted of a Model 401 dilutor (Gilson, Villiers-le-Bel, France), a Model 7010 injector controlled by a Model 7163 solenoid valve (Rheodyne), an isocratic HPLC system composed of a Model M-45 pump, a Model 231 sample injector (Gilson), a 100 × 2.1 mm I.D. HS C-18 (3 μm) column (Perkin-Elmer, Norwalk, CT, U.S.A.), a PU 4025 UV detector and a Model 7700 Professional Computer with Chrom 3 software (Perkin-Elmer) for data handling. This apparatus differs slightly from that described previously<sup>8</sup> because it permits controlled dilution of the eluate so as not to overload the analytical column.

An appropriate programme on the Model 231 sample injector directly controls the run time, the dilution volume, the injection onto the analytical column and, indirectly, through some relays, the turning of the pneumatic valve, the change of the fractions of the collector and the start of the data acquisition on the computer.

The adsorption isotherms, calculated by frontal chromatography<sup>9</sup>, were obtained on equipment consisting of a Model 303 micro-pump (Gilson), a Model 7001 pneumatic actuator connected to two Model 7010 injectors with 1-ml loops and a solenoid valve (Rheodyne), a 51 × 2.1 mm I.D. stainless-steel column packed with LiChroprep Si 60 silica (25–40 μm), a Model 875 UV detector with a micro-cell (Jasco, Tokyo, Japan) and an Omniscribe Model D-2000 recorder (Houston Instruments, Austin, TX, U.S.A.). The column and the injection system were thermostated to the appropriate temperature in a Model 12B bath (Julabo, Seelbach, F.R.G.).

## RESULTS AND DISCUSSION

Fig. 2 shows the reversed-phase analytical chromatogram of crude material to be

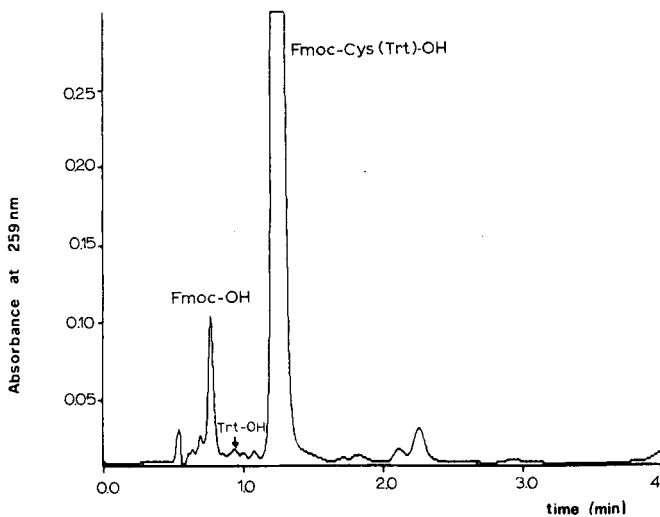


Fig. 2. Analytical chromatogram of crude Fmoc-Cys(Trt)-OH with isocratic elution. Column, Perkin-Elmer HS-3 C<sub>18</sub> (100 mm I.D.); eluent, 83% acetonitrile with 0.1% TFA; flow-rate, 1.7 ml/min; sample, 8  $\mu$ g of Fmoc-Cys(Trt)-OH mixture.

purified; 75% of the mixture was calculated to be Fmoc-Cys(Trt)-OH (retention time,  $t_R = 1.2$  min). The impurities at  $t_R$  0.75 and 0.87 min were Fmoc-OH and Trt-OH, respectively.

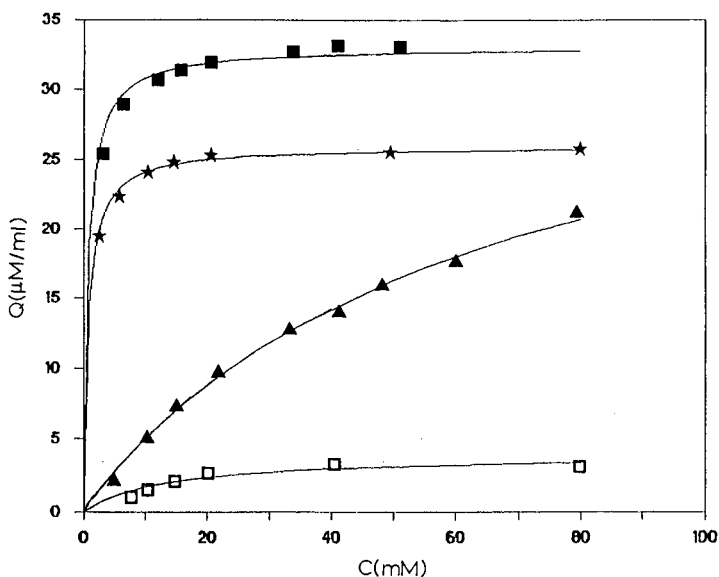


Fig. 3. Adsorption isotherms of (■) BTBA, (★) Fmoc-Cys(Trt)-OH, (▲) Fmoc-OH and (□) Trt-OH on a  $51 \times 2.1$  mm I.D. LiChroprep Si 60 (25–40  $\mu$ m) column with chloroform at 25°C.  $Q = \mu$ mol/ml of adsorbent in the column.

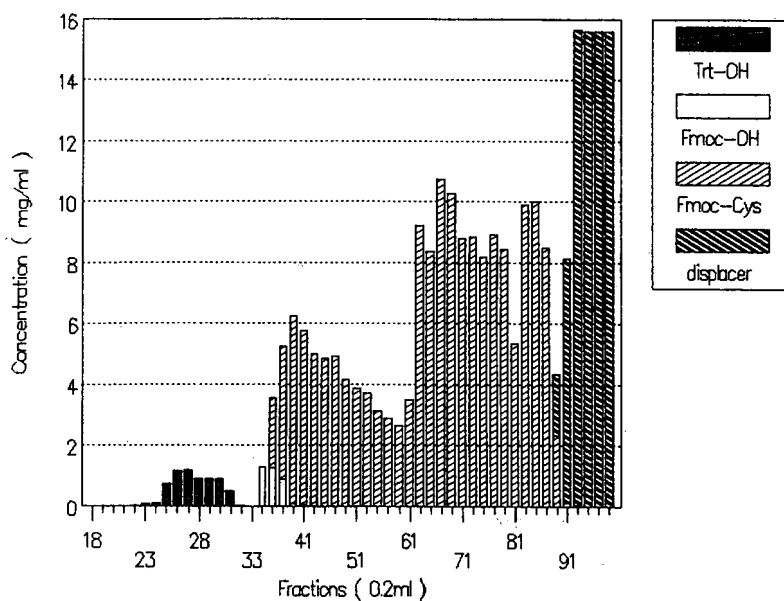


Fig. 4. Displacement chromatography of crude Fmoc-Cys(Trt)-OH. Column, 10  $\mu$ m LiChocart Si 60 (250  $\times$  4.0 mm I.D.); carrier, chloroform; displacer, 50 mM BTBA in chloroform; flow-rate, 0.1 ml/min; temperature, 23°C; feed, 100 mg of Fmoc-Cys(Trt)-OH mixture in 2 ml of chloroform.

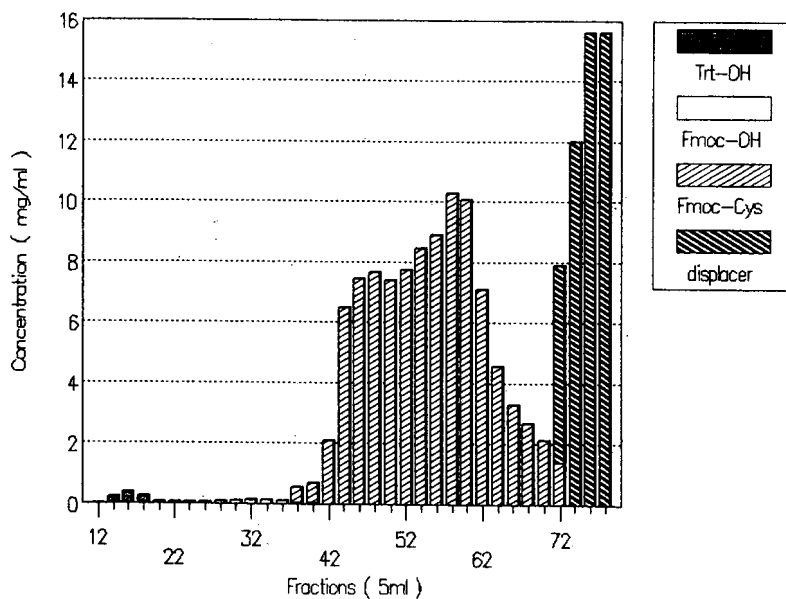


Fig. 5. Gram-scale displacement chromatography. Column, 25–40  $\mu$ m LiChorep Si 60 (230  $\times$  20 mm I.D.); carrier, displacer and temperature as in Fig. 4; flow-rate, 2 ml/min; feed, 1.5 g of Fmoc-Cys(Trt)-OH mixture in 30 ml of chloroform.

Based on the adsorption isotherms on silica of Fmoc-Cys(Trt)-OH, Fmoc-OH, Trt-OH and BTBA, measured in chloroform and shown in Fig. 3, BTBA was selected as the displacer compound for the Fmoc-Cys(Trt)-OH mixture. Chloroform was chosen as the carrier eluent because it dissolved large amounts of crude material and it did not elute Fmoc-Cys(Trt)-OH in normal-phase chromatography.

The histogram of displacement chromatography for the purification of 100 mg of Fmoc-Cys(Trt)-OH mixture on a  $250 \times 4.0$  mm I.D. LiChocart Si 60 column, constructed on the basis of the reversed-phase analysis of the fractions, is shown in Fig. 4. The displacement conditions are given in the caption. About 65 mg of pure Fmoc-Cys(Trt)-OH were recovered from the pool of fractions 39–87 with a collected volume of 9.8 ml. The chromatographic yield was 95%, calculated as the ratio of pure collected compound to the total amount present in the crude sample.

In the first step of the scaling-up procedure, a 20 mm I.D. column packed with 30 g of LiChroprep Si-60 silica ( $25\text{--}40 \mu\text{m}$ ) was employed. With respect to the chromatographic conditions in Fig. 4, 1.5 g of Fmoc-Cys(Trt)-OH mixture, dissolved in 30 ml of chloroform, was loaded to maintain a ratio of 50 mg of loaded sample per gram of stationary phase and a concentration of 50 mg/ml of injected sample. The flow-rate was increased to 2 ml/min to obtain the same breakthrough time of the displacer front.

Fig. 5 shows the relative histogram; 1.08 g of pure Fmoc-Cys(Trt)-OH was collected in 145 ml of eluate from fractions 42–70 with a recovery of 95%.

As under the last chromatographic conditions the separation efficiency and the yield were as good as those obtained on the analytical column, the diameter of the

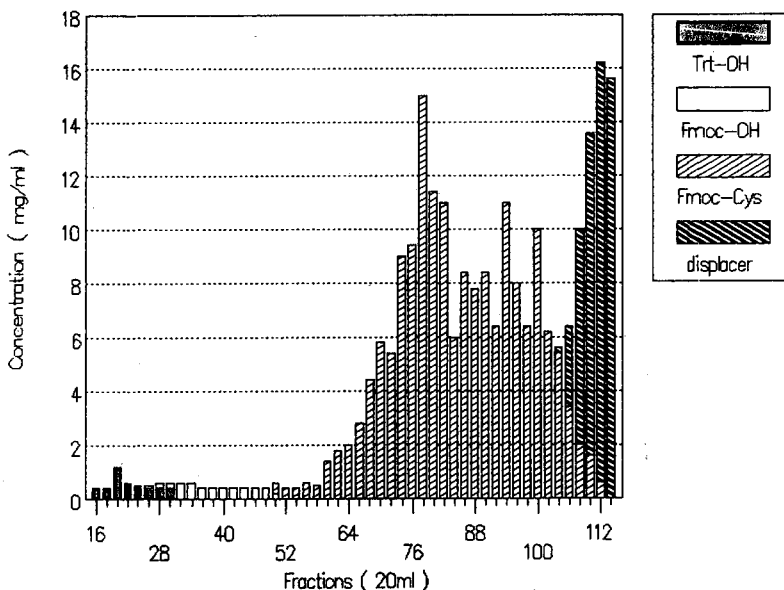


Fig. 6. Gram-scale displacement chromatography. Column,  $25\text{--}40 \mu\text{m}$  LiChroprep Si 60 ( $270 \times 40$  mm I.D.); carrier, displacer and temperature as in Fig. 4; flow-rate, 8 ml/min; feed, 9.5 g of Fmoc-Cys(Trt)-OH mixture in 190 ml of chloroform.

preparative column was increased further to 40 and 80 mm I.D. The two columns were packed with 200 and 800 g of LiChrorep Si-60 silica (25–40  $\mu\text{m}$ ), respectively, and, to maintain the same ratio of sample per gram of stationary phase, 9.5 and 38 g of Fmoc-Cys(Trt)-OH mixture, respectively, were injected. The flow-rate was increased 4- and 8-fold, respectively, all the other chromatographic parameters being maintained constant.

Figs. 6 and 7 show the relative displacement histograms. From the 40 mm I.D. column 6.42 g of pure material were obtained from fractions 50–102 (1040 ml of collected eluate, yield 92%), whereas from the 80 mm I.D. column 25.4 g were recovered in fractions 59–79 (2520 ml of collected eluate, yield 89%). After each displacement run, the stationary phase was washed with 3.7 ml of methanol per gram of stationary phase and no reduction in the column efficiency was detected after the regeneration cycles.

The influence of various operational parameters was investigated. Fig. 8 shows a displacement chromatogram obtained under the same conditions as in Fig. 5 except that the flow-rate was increased 3-fold. A 960-mg amount of pure material was recovered from fractions 40–60 with a yield of 86%.

The replacement of LiChrorep Si-60 (25–40  $\mu\text{m}$ ) silica with LiChrorep Si-60 (40–60  $\mu\text{m}$ ) silica or with Baker 30–60  $\mu\text{m}$  silica significantly increased the area of the overlapping zones, reducing the yield to 30%. When BTBA was replaced with BHDA, the breakthrough volume of the displacement train increased, but no appreciable differences in the recovery of the products were detected. An elution rather than a displacement mechanism was observed when chloroform, used as the carrier and the

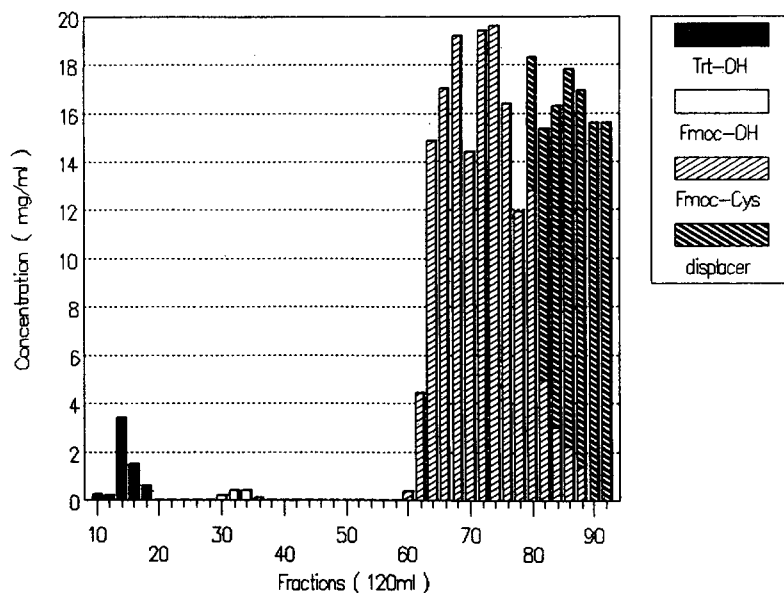


Fig. 7. Gram-scale displacement chromatography. Column, 25–40  $\mu\text{m}$  LiChrorep Si 60 (270  $\times$  80 mm I.D.); carrier, displacer and temperature as in Fig. 4; flow-rate, 32 ml/min; feed, 38 g of Fmoc-Cys(Trt)-OH mixture in 760 ml of chloroform.

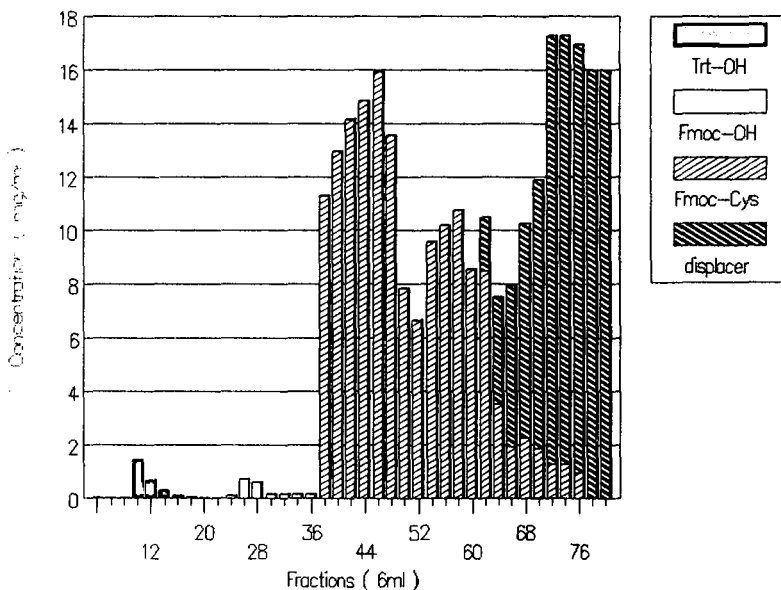


Fig. 8. Effect of flow-rate on the recovery. Conditions as in Fig. 5 except flow-rate, 6 ml/min.

solvent for the displacer solution, was replaced with ethyl acetate-chloroform-hexane (33:57:10, v/v/v), an eluent that under analytical conditions gave for a similar performance to chloroform with respect to the Fmoc-Cys(Trt)-OH mixture. A small reduction in the yield occurred when the concentration of the loaded sample was increased.

The reported separations demonstrate that a scaled-up purification of an amino acid, *i.e.*, Fmoc-Cys(Trt)-OH, can be carried out in the displacement mode from 100 mg up to 38 g simply by proportionally increasing the amount of the stationary phase and adjusting the flow-rate to the column and the particle diameter. Indeed, the advantageous performance of displacement chromatography, namely a high recovery (90%), a high sample loadings [50 mg of crude Fmoc-Cys(Trt)-OH per gram of silica], concentrated eluates (10–20 mg/ml) and low consumption of solvents as eluents and displacer washing (0.5 ml/mg of purified material), were maintained over the whole range of purified material.

The need to minimize the cost of the preparative columns prompted us to replace the expensive 10  $\mu\text{m}$  stationary phase with the less expensive 25–40  $\mu\text{m}$  material. This substitution did not have any significant effect on the displacement performance and also permitted the use of a reduced velocity in the run in Fig. 5 that was faster than that employed in Fig. 4. A further increase in the flow rate (Fig. 8) caused a decrease in the recovery from 97% to 86%<sup>10</sup>. However, as 86% might still be a satisfactory yield, it is a matter of optimization to decide whether the lower recovery could be justified by a reduction in the run time. Silica with particle diameters larger than 40  $\mu\text{m}$  did not seem to be usable because the recovery was drastically reduced.

The change in the elution mechanism observed when the chloroform was



replaced with ethyl acetate–chloroform–hexane could be explained by the fact that when the silica is equilibrated with a mixed eluent, the solvent with the highest polarity in the mixture is preferentially absorbed on the stationary phase<sup>11</sup>. During the displacement run this solvent is displaced out of the stationary phase by the injected sample and mainly by the displacer solution, so that close to the displacer front the eluent becomes richer in the more polar solvent, causing the elution of the products.

#### CONCLUSION

The major requirements in a scaling-up procedure in preparative chromatography are that, in order to save time and materials, the conditions for purification should be optimized in milligram-scale runs and that the same conditions should be applied to the gram or kilogram scales without any extra experiment to adjust the chromatographic parameters. In this work it has been demonstrated that these requirements are fulfilled by displacement chromatography; indeed, when parameters such as the composition of the carrier, nature of the displacer, stationary phase, amount of sample loaded per gram of stationary phase, concentration of the injected sample, linear velocity and regeneration procedure were maintained constant in all preparative experiments in runs in which from 100 mg to 38 g of crude mixture were loaded, similar performances were obtained.

#### ACKNOWLEDGEMENTS

The authors thank M. Pinori and B. Biancini, who kindly supplied the synthesized Fmoc-Cys(Trt)-OH mixture.

#### REFERENCES

- 1 Cs. Horváth, A. Nahum and J. H. Frenz, *J. Chromatogr.*, 218 (1981) 365.
- 2 H. Kalasz and Cs. Horváth, *J. Chromatogr.*, 215 (1981) 295.
- 3 Gy. Vigh, Z. Varga-Puchony, G. Szepesi and M. Gazdag, *J. Chromatogr.*, 386 (1987) 353.
- 4 K. Valco, P. Slegel and J. Bati, *J. Chromatogr.*, 386 (1987) 345.
- 5 G. C. Viscomi, S. Lande and Cs. Horváth, *J. Chromatogr.*, 440 (1988) 157.
- 6 C. H. Kruse and K. G. Holden, *J. Org. Chem.*, 50 (1985) 2792.
- 7 E. Papp and J. Inczedy, *Talanta*, 27 (1980) 49.
- 8 J. H. Frenz, Ph. van der Schriek and Cs. Horváth, *J. Chromatogr.*, 330 (1985) 1.
- 9 J. Jacobson, J. H. Frenz and Cs. Horváth, *J. Chromatogr.*, 316 (1984) 53.
- 10 Cs. Horváth, J. H. Frenz and Z. El Rassi, *J. Chromatogr.*, 255 (1983) 273.
- 11 L. R. Snyder and H. Poppe, *J. Chromatogr.*, 184 (1980) 363.



CHROMSYMP. 1643

## PURIFICATION OF MONOCLONAL ANTIBODIES BY COMPLEX-DISPLACEMENT CHROMATOGRAPHY ON CM-CELLULOSE<sup>a</sup>

ANTHONY R. TORRES\* and ELBERT A. PETERSON

*Bio-Fractionations, 1725 S. State Highway 89-91, Logan, UT 84321 (U.S.A.)*

---

### SUMMARY

A single high-capacity chromatographic procedure was used to purify a monoclonal antibody from ascites fluid. A new displacement procedure involving a displacer protein complex is described. The scale-up from 1 ml to 450 ml of ascites sample was easily accomplished with this complex-displacement system. A monoclonal antibody recovery of 79% was measured for the largest-scale purification.

---

### INTRODUCTION

There is an increasing demand for purified monoclonal antibodies. These highly specific antibodies<sup>1</sup> have found uses in many fields, including agriculture, biochemistry, medicine, immunology, microbiology, pharmaceuticals and virology. In addition, larger amounts (g to kg/year) are required, as diagnostic and therapeutic applications expand. At the present time, chromatographic methods offer the best means of purification and there are several methods which work well for small-scale purifications<sup>2-7</sup>. However, the purification of large amounts of monoclonal antibodies remains a challenge<sup>8</sup>. The use of displacement chromatography seems advantageous in monoclonal antibody purification, since high resolution, high capacity and high recovery are important for expensive proteins.

The advantages of displacement chromatography in the separation of small molecules were pointed out by Tiselius<sup>9</sup> as early as 1943 and this approach has been pursued by Porath and Li<sup>10</sup> as well as other investigators<sup>11</sup> for protein separations. However, because of the lack of suitable spacing displacers, separations of complex protein mixtures were inadequate and the method was not considered useful. The first successful application of protein displacement chromatography was published by Peterson<sup>12</sup> in 1978 with the description of carboxymethyl-dextran (CM-D) displacers, both as final displacers and spacing displacers for anion-exchange columns. It was subsequently shown by Torres and Peterson<sup>13</sup> that the chromatographic behavior of model proteins in such a system matched that observed with small molecules in established displacement systems. This was an important observation, as it showed that these CM-Ds were classical displacers as described by Tiselius in the theory of

---

<sup>a</sup> Patent pending.

displacement chromatography. The high resolution and high capacity of the CM-D displacement system were demonstrated with simple protein mixtures, such as the genetic variants of the very similar  $\beta$ -lactoglobulins A and B<sup>14</sup>. Chromatography was first performed on classical cellulosic ion exchangers and then on high-performance liquid chromatography (HPLC) columns under very similar conditions. The separations of 12.8 mg of the  $\beta$ -lactoglobulins A and B on a 150- $\mu$ l HPLC anion-exchange column was the first demonstration of a separation of proteins by ion-exchange displacement chromatography by this column technology<sup>15</sup>. Horváth's laboratory has more recently repeated the separation of these two proteins on an HPLC column, using a natural anionic carbohydrate, chondroitin sulfate as a final displacer<sup>16</sup>. Their separation was accomplished without adding spacing displacers and relied on protein protein displacement. Although protein protein displacement can be useful, as discussed in the early years<sup>17</sup>, spacing displacers will usually be necessary to separate proteins from complex biological mixtures.

The use of spacing CM-D displacers to isolate proteins from complex mixtures has been demonstrated with the separation of Gc-globulin from human serum<sup>18</sup>, alkaline phosphatase from *E. coli* periplasm<sup>19</sup>, and the resolution of an artificial mixture containing ovalbumin and other proteins<sup>20</sup>. The displacement separation of Gc-globulin represents a good model for a difficult separation, as serum contains well over a 100 proteins, and previous researchers have used up to 11 chromatographic steps to purify Gc-globulin<sup>21</sup>. The separation of *E. coli* alkaline phosphatase clearly shows that high-capacity separations can be achieved in displacement chromatography as the column was 80% saturated with protein sample before the displacer was applied.

In this paper, a new type of displacement chromatography is described. The same negatively charged CM-Ds used on anion-exchange columns were used as displacers with cation-exchange columns. However, the displacer in the latter case binds to the immobilized proteins and not the adsorbent. When an adequate amount of displacer has been bound to the protein, the protein is released from the column as a CM-D-protein complex. The single-step purification of mg to g amounts of a monoclonal antibody from mouse ascites fluid is described.

## EXPERIMENTAL

### Materials

Kontes (Vineland, NJ, U.S.A.) supplied the columns (5 cm  $\times$  2.5 cm I.D., 10 cm  $\times$  4.7 cm I.D., and 20 cm  $\times$  9 cm I.D.), column end-plates and mobile phase reservoirs. The smallest column (3 ml) was constructed from a 3-ml polypropylene syringe. The solutions, including the sample, for the last experiment (Fig. 4) were applied through a Kontes six-valve manifold and a Kontes Chromoflex LC pump. Flow-through pH and conductivity meters (Kontes) were used for selected experiments. Columns were packed with Whatman CM-52 (Clifton, NJ, U.S.A.). An Isco (Lincoln, NE, U.S.A.) UA-5 detector and recorder and an Isco Foxy fraction collector were used. Goat anti-mouse immunoglobulin G (IgG) (heavy and light chain) whole serum was obtained from Hyclone Lab. (Logan, UT, U.S.A.). The CM-D (reciprocal of the pellet volume, RPV = 25) was manufactured by Bio-Fractionations (Logan, UT, U.S.A.). An RPV of 25 indicates a high incorporation of carboxymethyl groups<sup>14</sup>.

### *Sample preparation*

Mouse ascites fluid containing an IgG<sub>2b</sub> monoclonal antibody (4.6 mg/ml) was centrifuged at 500 g for 15 min to remove particulate matter. The ascites fluid was then filtered through Whatman No. 2 filter paper and finally through a 0.45- $\mu$ m filter.

The ascites samples were diluted ten-fold with a 20 mM histidine · HCl, pH 5.7, buffer in order to decrease the normal saline to a level which would not interfere with the chromatographic process. For example, 1 l of 0.1 M histidine (free base) was added to a 500-ml ascites sample, then the mixture was adjusted to pH 5.7 with 1 M hydrochloric acid and diluted to 5 l with water.

### *Column chromatography*

A 20 mM histidine · HCl buffer (pH 5.7, column buffer) was used to equilibrate the ion-exchange columns. The CM-D was used as a 1.5% solution in the same buffer. All buffers, displacers, and salt solutions were filtered through sterile 0.22- $\mu$ m filters into sterile, autoclaved reservoirs for the last experiment (Fig. 4). This was done to decrease the chances of contaminating the purified antibody with endotoxin or bacteria. The flow-rate was set for 2–3 column volumes/h and fractions equal to *ca.* 1 column volume were collected. After each experiment, the column was washed with 1 column volume of 1.0 M sodium hydroxide, followed by several column volumes of water. The columns were equilibrated with 20 mM histidine · HCl (pH 5.7) when ready for reuse.

### *Gel electrophoresis*

The Pharmacia (Piscataway, NJ, U.S.A.) PhastSystem with 10–15% gels and sodium dodecyl sulfate (SDS) buffer strips and the standard method from the Phast-System manual were used to analyze the protein components. Samples were diluted with water to give an absorbance of *ca.* 1 at 280 nm. The diluted samples (10  $\mu$ l) were mixed with 2  $\mu$ l of 10% SDS and placed on a block at 95°C for 5 min. The microcentrifuge tubes were spun for 5 s in a microcentrifuge to move condensate to the bottom. The sample strip for application of 0.5  $\mu$ l of each sample was used. The gel was stained with Coomassie Brilliant Blue R 350 (Pharmacia) according to the standard method in the PhastSystem manual.

### *Protein quantitation*

The protein concentrations for the purified monoclonal antibodies were determined spectrophotometrically, using an extinction coefficient of 15 for a 1% solution at 280 nm with a 1-cm pathlength.

### *Nephelometry*

A Beckman (Brea, CA, U.S.A.) Auto ICS rate nephelometer was used to measure the amount of mouse IgG in the chromatographic fractions (circles in Fig. 3). A 1:16 dilution of goat anti-mouse IgG (heavy and light chain) whole serum (42  $\mu$ l) was used with 10  $\mu$ l of column fraction, following the Beckman instructions for manual operations. This instrument measures the rate of change of light scatter resulting from an immunoprecipitation reaction between antigen and antibody. Although this method can be used to determine concentrations, it was used in this project only to identify those fractions containing mouse IgG. The circles in Fig. 3 show the relative rate units

for each fraction. Background polyclonal antibodies present in ascites fluid could not be distinguished from the monoclonal antibody with this method as used.

#### *CM-D determination*

Small portions (50  $\mu$ l) of the column fractions (Fig. 3) were allowed to react with anthrone<sup>22</sup> and then read at 625 nm to provide a measure of the CM-D carbohydrate concentration.

#### RESULTS AND DISCUSSION

A cation-exchange column was selected, because immunoglobulins are among the proteins most tightly bound to this type of sorbent and provides the highest capacity for purifying this class of proteins. Instead of a classical displacement system with positive displacers competing with the sorbed proteins for column sites, the same negatively charged displacers (CM-Ds) were employed that are used with anion-exchange columns. Under these conditions, the displacer is not sorbed by the negatively charged sorbent but forms complexes with proteins immobilized on the sorbent. When sufficient amounts of displacer are bound to the protein, the complex is released from the column. It was found that contaminating proteins could be removed as protein-CM-D complexes without removing the antibody. Transferrin was the critical contaminant, since it was present in relatively large concentrations and is the most difficult protein to separate from monoclonal antibodies by ion exchange<sup>23</sup>. After washing the unbound displacer from the column with column buffer, the monoclonal antibody was eluted with phosphate-buffered saline.

Figs. 1-4 show the separation of 1 ml, 8 ml, 65 ml and 450 ml of ascites fluid by complex-displacement chromatography on 3-ml, 20-ml, 160-ml, and 1200-ml CM-cellulose columns, respectively. The results in these four experiments were very similar and demonstrate the ease of scale-up. The first large peak in the chromatogram contained several unbound proteins, mainly albumin. Some of these had little or no

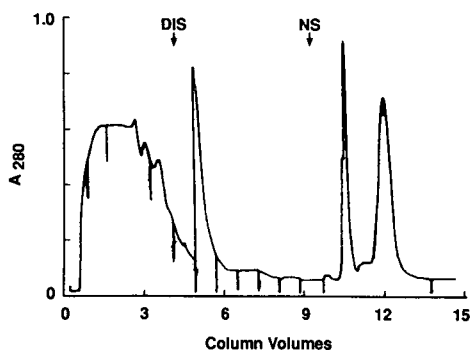


Fig. 1. Purification of a monoclonal antibody from 1 ml of ascites fluid. A 1-ml volume of ascites fluid was chromatographed on a 3-ml column of CM-cellulose. The column was equilibrated with 20 mM histidine · HCl (pH 5.7). The 1.5% displacer also contained 20 mM histidine · HCl (pH 5.7). The arrows show the application of the displacer and 0.15 M sodium chloride containing 10 mM sodium phosphate (pH 7.4). The column effluent was monitored at 280 nm at 2 a.u.f.s. DIS = Displacer; NS = phosphate buffered saline.

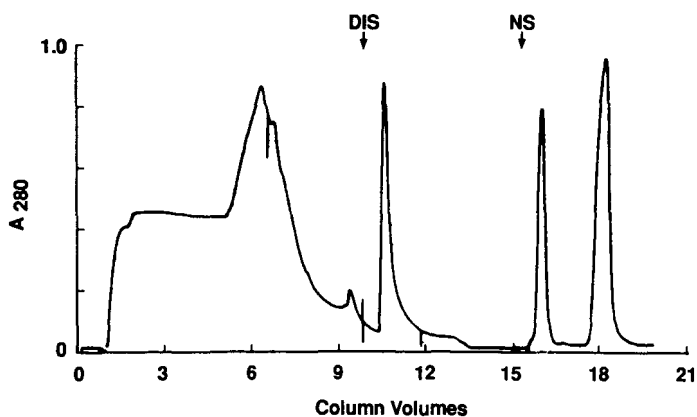


Fig. 2. Purification of a monoclonal antibody from 8 ml of ascites fluid. Conditions as for Fig. 1 except 8 ml of ascites fluid was chromatographed on a 20-ml column.

affinity for the sorbent under these conditions, but others were displaced by more tightly bound proteins that remained on the column.

The direct dilution of the normal saline (0.15 M sodium chloride) in ascites fluid with 9 volumes of 20 mM histidine · HCl (pH 5.7) allowed the binding of transferrin, the monoclonal antibody, and other proteins. It also obviated a dialysis or desalting step, which is often necessary before column chromatography. The samples were followed by column buffer (2–3 column volumes) and a 1.5% displacer (1–3.3 column volumes) in the same buffer. One column volume was found to be as effective as larger

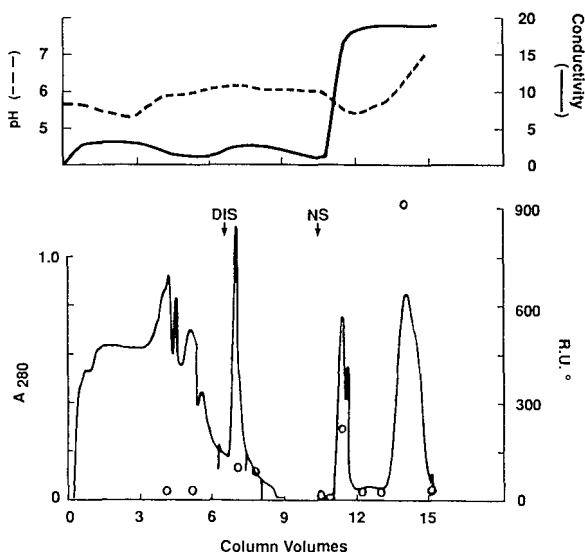


Fig. 3. Purification of a monoclonal antibody from 65 ml of ascites fluid. Conditions as for Fig. 1 except 65 ml of ascites fluid was separated on a 160-ml column. The circles show the rate units (R.U.) or relative IgG levels. Conductivity (in mS) and pH tracings are shown above.

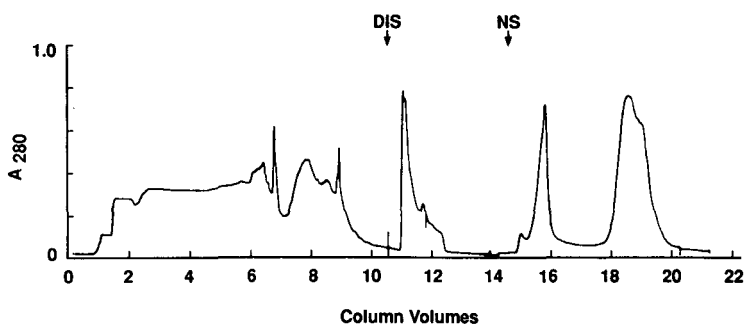


Fig. 4. Purification of a monoclonal antibody from 450 ml of ascites fluid. Conditions as for Fig. 1 except 450 ml of ascites fluid was separated on a 1200-ml column.

amounts. The displacer removed large amounts of transferrin and other proteins. The column was then washed with 2–3 column volumes of buffer to remove unbound displacer. This step was quite effective in removing displacer, as shown by a decrease in dextran concentrations from 7.1 mg/ml in fraction 8 to 0.035 mg/ml in fraction 12 (Fig. 3), as measured by the anthrone reaction. After this buffer wash, normal saline (0.15 *M* sodium chloride), containing 10 *mM* sodium phosphate (pH 7.4) was pumped into the column. The salt front eluted some transferrin and immunoglobulin. The last peak, containing the monoclonal antibody, was eluted when the effluent pH increased due to the phosphate buffer (Fig. 3). The pH increase followed about 2 column volumes behind the normal saline, as the dilute sodium phosphate buffer interacted with the sorbent and the remaining protein. This delayed pH increase was beneficial, as it allowed a more tightly bound transferrin (fraction 16, Fig. 4) to be separated from the monoclonal antibody. Transferrin is an iron-binding glycoprotein, which can contain one or more negatively charged sialic acids<sup>24</sup>. These negative charges as well as the amount of bound iron alter the isoelectric point and column affinity of transferrin.

Samples from the experiment shown in Fig. 4 were examined for purity by gel electrophoresis in Fig. 5. The gel photograph in Fig. 5 is representative of all the experiments. Lane 1 shows the proteins in the ascites fluid sample. Lanes 2 and 3 show the proteins present in the first peak (mainly albumin). Lane 4 contains the proteins in the second peak (fraction 12) after the displacer addition (mainly transferrin), lane 5 contains the proteins in the third peak (fraction 16) after the normal saline addition and the last three lanes show the purity of the monoclonal antibody from the last peak (fractions 18–20). A single chromatographic step thus resulted in a high-purity monoclonal antibody that was contained in normal saline with 10 *mM* sodium phosphate. A 79% antibody recovery was calculated from the ascites fluid used for Fig. 4: 1.63 g of purified monoclonal antibody from 2.07 g of sample.

The scale-up from 1 ml to 450 ml of ascites fluid was easily accomplished. Scale-up was limited by the amount of ascites fluid available and not by the chromatographic process. It should be possible to purify much larger amounts, if the mechanical stability of the sorbent in larger columns permits. Although there would be little advantage, this procedure should also work with HPLC cation-exchange columns.



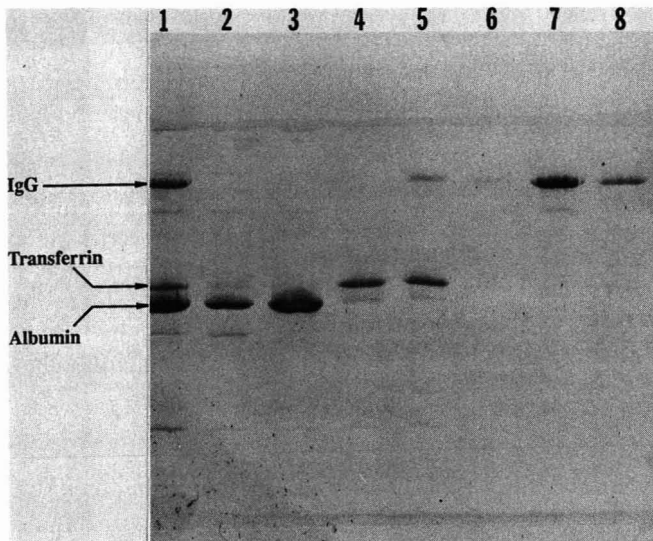


Fig. 5. Examination of column fraction by polyacrylamide gel electrophoresis. Fractions from Fig. 4 were subjected to electrophoresis in the presence of SDS on a 10–15% gel. Lane 1 shows the proteins in the ascites standard, lanes 2 and 3 show the proteins in the first peak (fractions 6 and 8) and lane 4 shows the proteins in the second peak (fraction 12) after the displacer addition (largely transferrin). Lane 5 shows the proteins in the peak (fraction 16) just after the addition of normal saline containing 10 mM sodium phosphate. Lanes 6–8 contain the purified monoclonal antibody (fractions 18–20).

The same chromatographic results have been observed for one IgG<sub>3</sub>, three IgG<sub>2a</sub>, and two IgG<sub>2b</sub> isotypes from ascites fluid. However, two IgG<sub>1</sub> monoclonal antibodies could not be separated by this system, as they did not bind to the CM-cellulose adsorbent. IgM immunoglobulins have not been examined.

An IgG<sub>2a</sub> monoclonal antibody against Pichinde virus (Arenavirus family) was assayed for viral recognition before and after purification. The purified monoclonal antibody was undistinguishable by an indirect immunofluorescent assay from the unchromatographed one and the titer did not change<sup>25</sup>. Another purified monoclonal antibody against *Actinobacillus seminis* has been successfully used in an Eliza assay<sup>26</sup>. These immunoassay results are an indication that this complex-displacement chromatographic method is a mild procedure.

Mouse serum was chromatographed with this complex-displacement system to obtain an estimate of the percentage of the full range of antibodies that might be separated by this system. The wide variation in isoelectric points (pI 5.8–8.2) in polyclonal antibodies<sup>27</sup> indicates the potential range of isoelectric points that might be encountered in monoclonal antibodies. The results were very similar to those obtained with ascites fluid, with four peaks appearing. There was a large amount of polyclonal antibody in the same location as the monoclonal antibody in the above experiments (fractions 18–20, Fig. 4). However, nephelometric assays also showed the presence of IgG in the first two peaks. Using the distribution of serum polyclonal antibodies as a guide, we estimate that 60–80% of monoclonal antibodies can be separated by this system as described. Changes in buffers and pH should make it possible to separate other polyclonal or monoclonal antibodies that do not bind to

the sorbent under present conditions. The observations on serum antibodies also indicate that the low nephelometer rate unit readings in the albumin and transferrin peaks (Fig. 3) may be due to contaminating polyclonal antibodies present in ascites fluid. The same data indicates that about 60–80% of the host polyclonal antibody is in the monoclonal antibody peak.

The ion-exchange complex-displacement system described in this manuscript offers another method for monoclonal antibody purification. It should be useful for many purifications since it is a mild single step procedure with good recoveries. Standard ion-exchange elution chromatography offers several advantages over Protein A affinity chromatography for bulk monoclonal antibody purifications<sup>28</sup>. These advantages include the ability to routinely sanitize the columns with sodium hydroxide, mild conditions, less expensive and the ability to remove host polyclonal antibodies.

#### ACKNOWLEDGEMENTS

We wish to thank Charles Rivers Biotech Services Inc., Wilmington, MA, U.S.A. for supplying the ascites fluid.

#### REFERENCES

- 1 G. Kohler and C. Milstein, *Nature (London)*, 256 (1975) 495.
- 2 P. L. Ey, S. J. Prowse and C. R. Jenkin, *Immunochemistry*, 15 (1978) 429.
- 3 B. Akerstrom and L. Bjorck, *J. Biol. Chem.*, 261 (1986) 10240.
- 4 W. E. Schwartz, F. M. Clark and I. B. Sabran, *LC · GC*, 4 (1986) 442.
- 5 H. Juarez-Silinas, S.C. Engelhorn, S. L. Bigbee, M. A. Lowry and L. H. Stanker, *BioTechniques*, 5 (1984) 164.
- 6 J. Porath, F. Maisano and M. Belew, *FEBS Lett.*, 185 (1985) 306.
- 7 M. Belew, N. Juntti, A. Larsson and J. Porath, *J. Immunol. Methods*, 102 (1987) 173.
- 8 D. R. Nau, *Biochromatogr.*, 4, No. 1 (1989) 4.
- 9 A. Tiselius, *Ark. Kemi, Mineral Geol.*, 16A, Vol. 8 (1943).
- 10 J. Porath and C. H. Li, *Biochim. Biophys. Acta*, 13 (1954) 268.
- 11 S. M. Partridge and R. C. Brimley, *Biochem. J.*, 51 (1952) 628.
- 12 E. A. Peterson, *Anal. Biochem.*, 90 (1978) 767.
- 13 A. R. Torres and E. A. Peterson, *J. Biochem. Biophys. Methods*, 1 (1979) 349.
- 14 E. A. Peterson and A. R. Torres, *Anal. Biochem.*, 130 (1983) 271.
- 15 A. R. Torres, B. E. Dunn, S. C. Edberg and E. A. Peterson, *J. Chromatogr.*, 316 (1984) 125.
- 16 A. W. Liao, Z. El Rassi, D. M. LeMaster and Cs. Horváth, *Chromatographia*, 24 (1987) 881.
- 17 R. W. Hartley, E. A. Peterson and H. A. Sober, *Biochemistry*, 1 (1962) 60.
- 18 A. R. Torres, G. G. Krueger and E. A. Peterson, *Anal. Biochem.*, 144 (1985) 469.
- 19 B. E. Dunn, S. E. Edberg and A. R. Torres, *Anal. Biochem.*, 168 (1988) 25.
- 20 A. R. Torres, S. C. Edberg and E. A. Peterson, *J. Chromatogr.*, 389 (1987) 177.
- 21 M. Imawari, K. Kida and DeW. S. Goodman, *J. Clin. Invest.*, 58 (1976) 514.
- 22 T. A. Scott and E. H. Melvin, *Anal. Chem.*, 25 (1953) 1656.
- 23 B. Malm, *J. Immunol. Methods*, 104 (1987) 103.
- 24 S. Petren and O. Vesterberg, *Biochim. Biophys. Acta*, 994 (1989) 161.
- 25 B. Barnett, presented at the VI International Conference on Comparative and Applied Virology, Banff, October 15–21, 1989.
- 26 M. Healey, ADVS Department, Utah State University, Logan, UT 84321, U.S.A., personal communications.
- 27 E. G. Young, in M. Florkin and E. H. Stotz (Editors), *Comprehensive Biochemistry*, Vol. 7, Elsevier, Amsterdam, New York, 1963, p. 25.
- 28 S. A. Duffy, B. J. Moellering, G. M. Prior, K. R. Doyle and C. P. Prior, *BioPharm*, 2 No. 6 (1989) 34.

CHROMSYMP. 1653

## PREPARATIVE-SCALE HIGH-PERFORMANCE LIQUID CHROMATOGRAPHIC SEPARATION AND PURIFICATION OF 3'-AZIDO-3'-DEOXYTHYMIDINE-5'-PHOSPHATE

JOSEPH G. TURCOTTE\*, PHILIP E. PIVARNIK, SHYAM S. SHIRALI, HARIBANSH K. SINGH and RAJ K. SEHGAL

*Department of Medicinal Chemistry, University of Rhode Island, Kingston, RI 02881 (U.S.A.)*

DIANE MACBRIDE

*Separations Technology, Inc., Wakefield, RI 02879 (U.S.A.)*

and

NAN-IN JANG and PHYLLIS R. BROWN\*

*Department of Chemistry, University of Rhode Island, Kingston, RI 02881 (U.S.A.)*

---

### SUMMARY

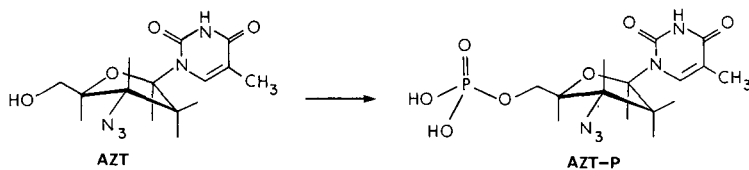
Crude 3'-azido-3'-deoxythymidine-5'-phosphate (AZT-P), obtained from direct phosphorylation of 3'-azido-3'-deoxythymidine (azidothymidine, AZT), was separated and purified by isocratic preparative high-performance liquid chromatography. The components in a 2.5-g load of crude AZT-P, obtained from work-up of the phosphorylation reaction, were separated in 50 min to give 1.8 g of 99.5% pure AZT-P. AZT-P was analyzed by high-performance liquid chromatography and by high-resolution nuclear magnetic resonance ( $^1\text{H}$ ,  $^{13}\text{C}$ ,  $^{31}\text{P}$ ) spectroscopy. The practical and rapid preparative chromatographic method is being applied to the purification of AZT-P and other antiretroviral dideoxynucleotides, used as intermediates in the synthesis of target-directed experimental drugs for the treatment of AIDS.

---

### INTRODUCTION

3'-Azido-3'-deoxythymidine (azidothymidine, AZT), an antiretroviral analogue of thymidine, is presently the principal drug used for the clinical treatment of acquired immunodeficiency syndrome (AIDS) and early AIDS-related complex (ARC). It is used therapeutically as a single agent or in combination with other anti-AIDS drugs. Since AZT exhibits hematologic toxicity and other undesirable side-effects, new target-directed derivatives of the drug are currently being synthesized<sup>1</sup>. For these syntheses, relatively large quantities of pure 3'-azido-3'-deoxythymidine-5'-phosphate (AZT-P) are required. Consequently, a reversed-phase high-performance liquid chromatographic (RP-HPLC) method was developed for the separation and purification of AZT-P on a preparative scale. Analytical HPLC methods have been reported (*e.g.* refs. 2–5) for the determination of the nucleoside AZT, its metabolically derived glucuronide, and other antiretroviral dideoxynucleosides in plasma, serum, and urine. However, little work is reported in the literature on the analysis of the nucleotide AZT-P, which is of interest in the monitoring of synthetic

reactions in the purification of starting materials for the synthesis of AZT derivatives, and as an intracellular metabolite of AZT itself.



## EXPERIMENTAL

### Materials

AZT was obtained from five different sources: by synthesis according to two independent routes<sup>6-9</sup>; as a gift from the U.S. National Cancer Institute; from commercial capsules of AZT (Zidovudine, Retrovir<sup>TM</sup>); and from Sigma (St. Louis, MO, U.S.A.). AZT-P was synthesized by phosphorylation of AZT with phosphorus oxychloride-trimethylphosphate according to known procedures<sup>9,10</sup>. Potassium dihydrogenphosphate, ammonium acetate, and the solvents absolute methanol, chloroform, and diethyl ether (HPLC grade) were purchased from Fisher (Fairlawn, NJ, U.S.A.).

All solvents used in sample preparation and for the mobile phases were prepared with doubly distilled, deionized water, filtered through 0.45- $\mu$ m Nylon-66 membrane filters (AllTech Assoc., Deerfield, IL, U.S.A.). Mobile phases, which were deaerated by helium, contained either KH<sub>2</sub>PO<sub>4</sub> or ammonium acetate at a concentration of 10 mM and were mixtures of buffer and methanol. The pH of the mobile phase was adjusted to 5.0 with phosphoric acid or potassium hydroxide (Fisher). A standard solution of AZT, which was prepared by dissolving AZT in the buffer solution at pH 6.0, was stored at -20°C. A solution of the reaction mixture, which contained AZT-P and trimethylphosphate, was diluted with the solvent and kept at 4°C.

Since residual trimethylphosphate, the solvent used in the AZT phosphorylation reaction<sup>9,10</sup>, was difficult to separate from the crude reaction mixture by distillation *in vacuo* at relatively low temperature (<30°C), the following preliminary procedure was developed to remove the compound prior to preparative HPLC. Typically, crude AZT-P (5 g, containing trimethylphosphate) was dissolved in chloroform (18 ml, HPLC grade). A column of silica gel (190 g, mesh 70-230, "flash" type, EM Science, Cherry Hill, NJ, U.S.A.) was prepared in anhydrous diethyl ether, and the chloroform solution of crude AZT-P was loaded onto the column. It then was eluted sequentially with diethyl ether (600 ml), chloroform (700 ml), and chloroform-methanol (95:5, 300 ml). The solvent was drained from the column, the silicagel was emptied into a 1000-ml flask and stirred with chloroform-methanol (1:1) (3  $\times$  250 ml), and then filtered through a sintered-glass funnel. The filtrate, upon evaporation of the solvent, gave a white solid (0.19 g, 0.21 g theoretical) which contained a slightly yellowish oily contaminant. The latter solidified upon cooling and addition of a small amount of hexane. Thin-layer chromatography (TLC); *R<sub>F</sub>* 0.60, ammonium hydroxide-*n*-propanol-water (20:20:3, v/v/v).

### Methods

The chromatograph used for analytical and methods development studies consisted of a Waters 6000A pump (Waters Division, Millipore, Milford, MA, U.S.A.), a Rheodyne 7125 injector (Rheodyne, Berkeley, CA, U.S.A.), and a Waters M440 absorbance detector at a fixed wavelength of 254 nm. The separations were performed on a Waters  $\mu$ Bondapak C<sub>18</sub> column (30 cm  $\times$  4.6 mm I.D., 10  $\mu$ m particle size) with a guard column (5 cm  $\times$  4.6 mm I.D.) containing Whatman C<sub>18</sub> pellicular packing (37–53- $\mu$ m particle size). AZT and AZT-P were isocratically eluted with a mobile phase of 0.01 M KH<sub>2</sub>PO<sub>4</sub>–methanol (85:15, v/v), or 0.01 M ammonium acetate–methanol (85:15, v/v) (pH 5.0). The flow-rate was 1 ml/min. Data were recorded on both a HP 3390A integrator (Hewlett-Packard, Avondale, PA, U.S.A.) and an Omniscribe recorder (Houston Instruments, Austin, TX, U.S.A.). All separations were achieved at ambient temperature.

For analytical HPLC studies on the starting material itself, AZT, the conditions were: Perkin-Elmer (Norwalk, CT) C<sub>18</sub> reversed-phase column (25 cm  $\times$  4.6 mm I.D., 10- $\mu$ m particle size); mobile phase 0.01 M ammonium acetate–methanol (85:15, v/v; pH 5); flow-rate, 1 ml/min; sensitivity, 0.2 a.u.f.s.; chart-speed, 5 mm/min; detector, 254 nm; sample (AZT) size, 0.03 mg.

The methods development system was the same as the analytical system, except that the detector was a Knauer variable-wavelength detector (254 nm) (Sonntek, Woodcliff Lake, NJ, U.S.A.) and the column was a SepTech methods-development column (20 cm  $\times$  4.6 mm I.D., Separations Technology, Wakefield, RI, U.S.A.), containing C<sub>18</sub> reversed-phase packing material (10–15- $\mu$ m particle size, YMC, Newark, NJ, U.S.A.). Aliquots of the crude product were injected and eluted isocratically with a mobile phase of 0.01 M ammonium acetate–methanol (85:15, v/v; pH 5). Loading studies on larger amounts of crude product were also performed. The flow-rate was 1.0 ml/min.

A SepTech ST/800A preparative chromatograph (Separations Technology) with a SepTech Annular Expansion (A/E) C<sub>18</sub> (YMC, 10–15- $\mu$ m particle size) preparative column (20 cm  $\times$  7.3 cm I.D.), and a Knauer variable-wavelength detector (fixed wavelength, 254 nm) were used. A sample of 30 ml (equivalent to 2.5 g of crude AZT-5'-P) was injected into the system with a 10-ml syringe (Hamilton, Reno, NV, U.S.A.) flushed immediately with 10 ml of the mobile phase. AZT-P was eluted isocratically within 50 min with a mobile phase of 0.01 M ammonium acetate–methanol (85:15, v/v) at pH 5.0. The flow-rate was 150 ml/min. Data were recorded on both a strip-chart recorder and a HP 3393A integrator. Ten fractions were collected.

An aliquot of each preparative HPLC fraction was subsequently characterized on the analytical system. The fractions that contained the product were pooled, evaporated to a small volume, and lyophilized, giving a white, amorphous solid (AZT-P; diammonium salt); TLC,  $R_f$  0.60, ammonium hydroxide–*n*-propanol–water (20:20:3, v/v/v); <sup>1</sup>NMR (300 MHz, <sup>2</sup>H<sub>2</sub>O)  $\delta$  1.90 (singlet, 3H, methyl), 2.48 (triplet, 2H, H-2'), 4.06 (broad singlet, 2H, H-5'), 4.19 (broad singlet, 1H, H-4'), 4.50 (multiplet, 1H, H-3'), 6.27 (triplet, 1H, H-1'), 7.78 (singlet, 1H, H-6); <sup>13</sup>C NMR (75.4 MHz, <sup>2</sup>H<sub>2</sub>O)  $\delta$  169.23 (C-4), 154.44 (C-2), 140.18 (C-6), 114.52 (C-5); 87.86 (C-1'), 86.10 (C-4'), 67.31 (C-5'), 63.60 (C-3'), 39.04 (C-2'), 14.33 (C-methyl); <sup>31</sup>P NMR (121.5 MHz, H<sub>2</sub>O)  $\delta$  0.28 (broad singlet).

## RESULTS AND DISCUSSION

AZT-P was synthesized in *ca.* 90% yield (crude) by direct phosphorylation (phosphorus oxychloride–trimethylphosphate)<sup>10,11</sup> from its dideoxynucleoside precursor, AZT. Analytical RP-HPLC of the starting material obtained by direct synthesis<sup>10</sup> and from commercial capsules (Retrovir) showed a broadening at the higher retention sides of the AZT peaks (retention time, 50 min) in each case, as well as a contaminant at a retention time of 5–6 min. That the contaminant is thymine was suggested by the retention time and by a chromatogram of a mixture with an authentic sample of thymine.

Optimal capacity factors ( $k'$ ) of AZT and AZT-P were obtained with a mobile phase of 0.01 M ammonium acetate–methanol (85:15, v/v) at pH 5.0. When the pH was 6.8 (the pH which has been used in HPLC assays for AZT has ranged from 2.2 to 7.1<sup>2–5</sup>), the AZT-P peak appeared as a triplet. This phenomenon has been observed in the HPLC of other nucleotides<sup>11</sup>. Therefore, a mobile phase, buffered to pH 5.0, was used for analytical, methods development, and preparative chromatography. AZT-P was eluted at 5.4 min and AZT at 13.8 min (Fig. 1); the  $k'$  values were 0.6 and 3.19, respectively. These  $k'$  values were adequate for the loading studies and the preparative separation. When the separation was scaled up to a methods-development column, good separation of AZT and AZT-P was obtained (Fig. 2). In a separate experiment, *ca.* 240  $\mu$ l of crude reaction mixture were loaded on the column, and 24 mg of AZT-P were isolated. To facilitate removal of the mobile phase from the isolated AZT-P, a more volatile buffer, ammonium acetate, was used instead of  $\text{KH}_2\text{PO}_4$ . To

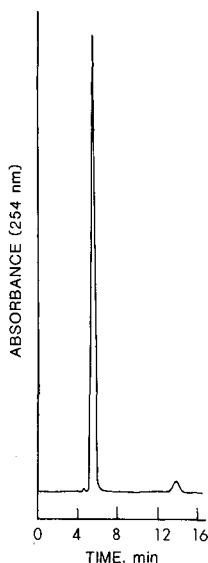


Fig. 1. Analytical RP-HPLC chromatogram of components in crude AZT phosphorylation reaction mixture. Conditions: Waters  $\mu$ Bondapak  $\text{C}_{18}$  column (30 cm x 4.6 mm I.D., 10- $\mu$ m particle size); mobile phase, 0.01 M  $\text{KH}_2\text{PO}_4$ –MeOH 5:15, v/v; pH 5.0; flow-rate, 1.0 ml/min; sensitivity, 0.05 a.u.f.s.; detector, Waters M440 absorbance detector; injection volume, 2  $\mu$ l; sample size, 1.7 ng.

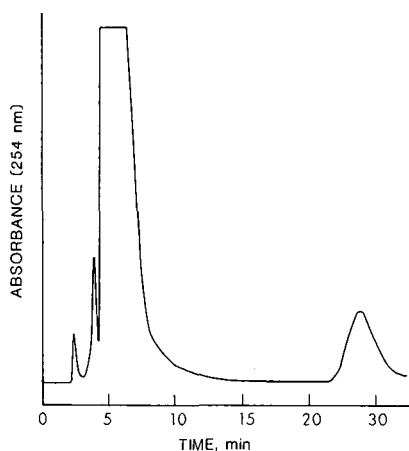


Fig. 2. Methods-development RP-HPLC chromatogram of separation of phosphorylation reaction mixture. Conditions: column, SepTech  $C_{18}$  (YMC) methods-development column (20 cm  $\times$  4.6 mm I.D., 10–15- $\mu$ m particle size); mobile phase, 0.01 M ammonium acetate–methanol (85:15, v/v), pH 5.0; flow-rate, 1.0 ml/min; sensitivity, 2.0 au.f.s.; detector, Waters M440 absorbance detector (254 nm); injection volume, 100  $\mu$ l; sample size, 10 mg).

prevent saturation of the detector a Knauer detector with a larger flow-cell was used instead of the Waters detector.

Impurities not seen in the analytical separation were observable when larger amounts of the crude reaction mixture were injected onto the column. These impurities were eluted prior to AZT-P. In the reaction mixture, unreacted AZT was also present. The scale-up factor for the preparative system was determined by the software from Separations Technology. A chromatogram of the crude product at a 2.5-g load (30 ml) is shown in Fig. 3. AZT, which has a longer retention time than AZT-P, was eluted at 40 min and did not interfere with recovery of the AZT-P. Ten fractions containing AZT-P were collected. These fractions were tested for the purity of the AZT-P with the analytical system; representative chromatograms are seen in Fig. 4. No AZT-P was recovered from fraction 1. Fraction 2 contained *ca.* 50% AZT-P and 50% impurities, including thymine. In fraction 3 the amount of impurities had de-

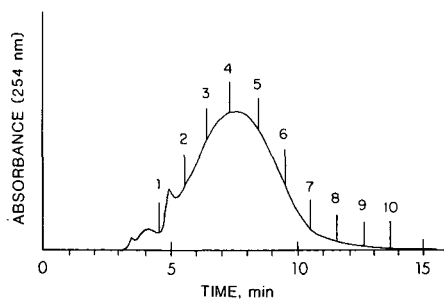


Fig. 3. Preparative RP-HPLC chromatogram showing the AZT-P and contaminants in the reaction mixture. Conditions: column, SepTech  $C_{18}$  (YMC) preparative column (20 cm  $\times$  7.3 cm I.D., 10–15- $\mu$ m particle size); mobile phase, 0.01 M ammonium acetate–methanol 85:15, v/v; pH 5.0; flow-rate, 150 ml/min; detector, Knauer variable-wavelength (254 nm); injection volume, 30 ml; sample size, 2.5 g of crude reaction mixture. Numbers indicate fractions taken for analytical RP-HPLC (see Fig. 4).

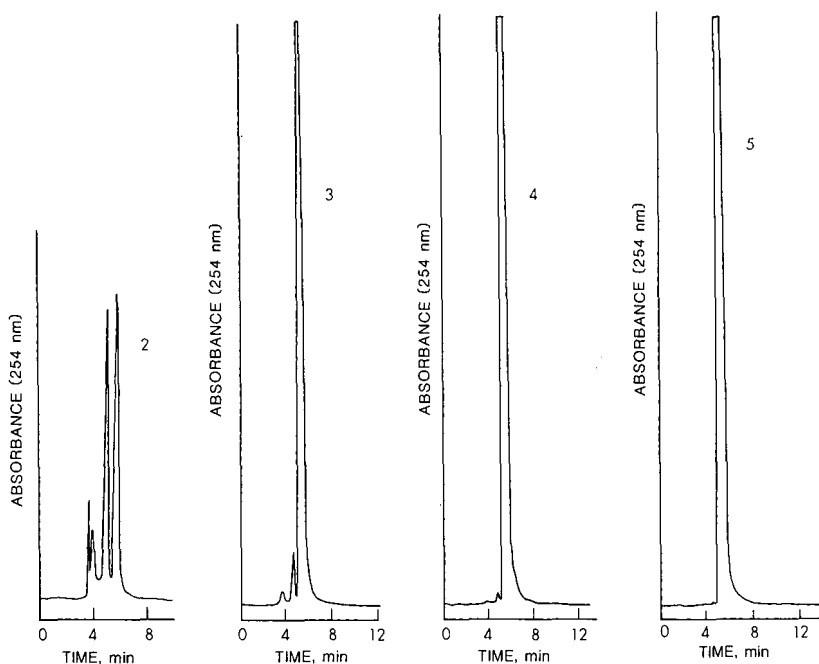


Fig. 4. Analytical RP-HPLC of aliquots of AZT-P-containing fractions (fractions 2–5) obtained from preparative RP-HPLC (Fig. 3). For chromatographic conditions, see Fig. 1.

creased to *ca.* 5%, and in fraction 4, only 0.7% of impurity was present. In fractions 5–10 the amount of impurity was negligible; relatively little AZT-P is present in fractions 8–10. In the pooled fractions 4–10, 1.81 g of AZT-P were obtained in 99.5% purity. When fractions 3–10 were pooled, 2.2 g of product (97.3% purity) were obtained. Four subsequent preparative HPLC runs gave comparable results.

The structure of the purified 3'-azido-3'-deoxythymidine-5'-phosphate was confirmed by  $^1\text{H}$ ,  $^{13}\text{C}$  and  $^{31}\text{P}$  NMR spectroscopy.

#### ACKNOWLEDGEMENTS

A gift of 3'-azido-3'-deoxythymidine from the Pharmaceutical Resources Branch, Developmental Therapeutics Program, Division of Cancer Treatment, U.S. National Cancer Institute, is gratefully acknowledged. This research was supported in part by grants from the American Foundation for AIDS Research (000464R) and from the U.S. National Institute of Allergy and Infectious Diseases (AI 25690), National Cooperative Drug Discovery Group for the Treatment of AIDS.

#### REFERENCES

- 1 J. G. Turcotte, H. K. Singh, S. S. Shirali, R. K. Sehgal and J. M. Steim; unpublished results.
- 2 J. D. Unadkat, S. S. Crosby, J. P. Wang and C. C. Hertel, *J. Chromatogr.*, 430 (1988) 420.



- 3 S. S. Good, D. J. Reynolds and P. de Miranda, *J. Chromatogr.*, 431 (1988) 123.
- 4 L. E. Mathes, G. Muschik, L. Demby, P. Pollas, D. W. Mellini, H. J. Issaq and R. Sams, *J. Chromatogr.*, 432 (1988) 346.
- 5 M. A. Hedaya and R. J. Sawchuk, *Clin. Chem.*, 34 (1988) 1565.
- 6 R. P. Glinski, M. S. Khan, R. L. Kalamas and M. B. Sporn, *J. Org. Chem.*, 38 (1973) 4299.
- 7 M. Imazawa and F. Eckstein, *J. Org. Chem.*, 43 (1978) 3042.
- 8 L. Vrang, H. Bazin, G. Remaud, J. Chattopadhyaya and B. Oberg, *Antiviral Res.*, 7 (1987) 139.
- 9 J. L. Rideout, D. W. Barry, S. N. Lehrman, *et al.*, *Eur. Pat. Appl.*, 86301896.6 (1986) 18.
- 10 V. E. Zaitseva, N. B. Dyatina, A. A. Kraevskii, N. V. Skaptsova, O. V. Turina, N. V. Gnucher, B. P. Gottikh and A. V. Azhaev, *Biorg. Khim.*, 10 (1984) 670.
- 11 C. Yi, J. L. Fasching and P. R. Brown, *J. Chromatogr.*, 352 (1986) 221.



CHROMSYMPO. 1671

## THERMODYNAMIC MODEL FOR ELECTROSTATIC-INTERACTION CHROMATOGRAPHY OF PROTEINS

ISTVÁN MAZSAROFF\*

*PerSeptive Biosystems, Inc., Cambridge, MA 02139 (U.S.A.)*

LÁSZLÓ VÁRADY

*Department of Biochemistry, Purdue University, W. Lafayette, IN 47907 (U.S.A.)*

GABRIEL A. MOUCHAWAR

*Department of Electrical Engineering, Purdue University, W. Lafayette, IN 47907 (U.S.A.)*

and

FRED E. REGNIER

*Department of Biochemistry, Purdue University, W. Lafayette, IN 47907 (U.S.A.)*

---

### SUMMARY

A thermodynamic model derived by Record *et al.* [M. T. Record, Jr., *Biopolymers*, 14 (1975) 2137 and M. T. Record, Jr., C. F. Anderson and T. M. Lohman, *Q. Rev. Biophys.*, 11 (1978) 103] from Wyman's linkage theory [J. Wyman, *Adv. Protein Chem.*, 19 (1964) 223] using Manning's condensation model [J. Manning, *J. Chem. Phys.*, 51 (1969) 924] was extended to electrostatic interaction chromatography. Mixed, electrostatic and hydrophobic interactions of a model protein, ovalbumin were characterized by ion and water release.

---

### INTRODUCTION

Retention properties of proteins on ion-exchange surfaces were explained qualitatively on the basis of the law of mass action by Boardman and Partridge<sup>1</sup> and applied to describe weak cation-exchange behavior by Arányi and Boross<sup>2</sup>. Barford *et al.*<sup>3</sup> have also developed an ion-exchange theory applying the mass action law. Based on the work of Boardman and Partridge, a stoichiometric displacement model was introduced<sup>4</sup>. Barford *et al.*<sup>3</sup> pointed out the possibility of a "mixed-mode" mechanism occurring during protein adsorption. Mixed electrostatic and hydrophobic interactions of proteins were investigated in detail by Kennedy *et al.*<sup>5</sup> and Horváth *et al.*<sup>6</sup>.

The importance of interactions of biopolymers with ions and ligands and their effects on macromolecular interactions was placed at the center of biothermodynamics as early as the late 1940s<sup>7</sup>. Wyman<sup>8,9</sup> developed a general thermodynamic approach to interpret the effects of ligands on the oxygenation of hemoglobin and the effects of ligands on hemoglobin dissociation. Tanford<sup>10</sup> extended Wyman's theory taking into account the Gibbs-Duhem relationship between solvent and ligand activities, *i.e.*, between solvation and ligand binding. Aune and Tanford<sup>11,12</sup> extended the binding analysis to cover cation and anion participation in a macromolecular equilibrium.

Record *et al.*<sup>13,14</sup> utilized the results of Wyman, Aune and Tanford and established a unified theoretical approach to interpret the effects of electrolyte ions and solvent on macromolecular equilibria involving biopolyelectrolytes in solution. This theory includes solubility equilibria, binding and aggregation equilibria and conformational transitions.

Record *et al.*<sup>14</sup> focused, in particular, on salt-dependent macromolecular equilibria in which the phenomenological association constant expressed in terms of macromolecular concentration, increases dramatically with decreasing electrolyte concentration. These authors offered evidence that the complexes are stabilized partly by the formation of ionic interactions and the concomitant release of low-molecular-weight ions previously associated with the charged groups on the biopolymers. Since ions are released in these ionic interactions, the equilibrium shifts to favour complex formation when the salt concentration is reduced. Consequently, ion release, or in other words, reduction in electrolyte activity, can be considered to drive these reactions<sup>15,16</sup>. Reduction in electrolyte activity is an "entropic" phenomenon in its nature. According to Record *et al.*<sup>14</sup>, there are at least five potential origins of the effect of an electrolyte (CA) on the phenomenological equilibrium quotient,  $K_{\text{obs}}$ .

$$\frac{d \ln K_{\text{obs}}}{d \ln a_{\pm}} = \Delta(n_{\text{C}} + n_{\text{A}^-} \frac{pm}{55.5} n_{\text{W}}) + \frac{d \ln \gamma_{\text{O}_{\text{M}_1} \gamma_{\text{O}_{\text{M}_2}}}{d \ln a_{\pm}} - \Delta n_{\text{L}} \frac{d \ln a_{\text{L}}}{d \ln a_{\pm}} \quad (1)$$

These are: (1) differential cation binding ( $\Delta n_{\text{C}} \neq 0$ ); (2) differential anion binding ( $\Delta n_{\text{A}} \neq 0$ ); (3) differential hydration ( $\Delta n_{\text{W}} \neq 0$ ) at high salt concentration,  $m$ ; (4) differential screening (Debye-Hückel) effects of electrolyte on macroion charges reflected in a variation of the macromolecular activity coefficient ratio with  $a_{\pm}$ , and (5) the effect of  $a_{\pm}$  on the ligand activity coefficient,  $\gamma_{\text{L}}$ .

In eqn. 1,  $a_{\pm} = (a_{\text{C}}^{p^+} a_{\text{A}}^{p^-})^{1/p}$ , the mean ionic activity of the salt;  $\Delta n_{\text{C}} = n_{\text{CM}_1} + n_{\text{CM}_2} - n_{\text{CM}_1\text{M}_2}$ , the number of moles of cations released at association of one mole of  $\text{M}_1$  and one mole of  $\text{M}_2$  macromolecules, and in the same way,  $\Delta n_{\text{A}}$ ,  $\Delta n_{\text{W}}$  and  $\Delta n_{\text{L}}$  are the number of moles of anions, water molecules and ligands released, the  $\gamma$  terms are the activity coefficients of the macromolecular reference states,  $a_{\text{L}}$  is the ligand activity and  $p$  is the valency of the ion.

It should be emphasized that eqn. 1 is completely general and independent of any molecular model for the macromolecular binding process. Interpretation of experimental values of the derivative ( $d \ln K_{\text{obs}}/d \ln a_{\pm}$ ) in terms of molecular quantities (number of cations, anions or water molecules released, number of ionic interactions, etc.) requires a molecular model. According to Record *et al.*<sup>14</sup>, the association of ions with charged biopolymers can be modeled as either (a) mass action binding of ions to discrete classes of identical non-interacting sites on a macroion of arbitrary structure and charge distribution<sup>7</sup>, or (b) condensation, the ionic strength-independent association of counterions with a linear polyeion<sup>17</sup> (see details in Appendix I).

Based on Manning's condensation model<sup>17</sup>, Record *et al.*<sup>14</sup> have derived a model from eqn. 1 to evaluate the stoichiometry of binding of cationic oligopeptides to nucleic acids (summary of their derivations are in Appendix II.).

The logarithm of the phenomenological equilibrium quotient derived by Record *et al.*<sup>14</sup> is

$$\ln K_{\text{obs}} = \ln K_T^0 - \zeta[1 - (2\xi)^{-1}] \ln m + \zeta\xi^{-1} \ln \delta\gamma_{\pm} \quad (2)$$

and

$$\left( \frac{d \ln K_{\text{obs}}}{d \ln m} \right)_{T, p, \text{pH}} = - \zeta \left[ \psi - \xi^{-1} \frac{d \ln \gamma_{\pm}}{d \ln m} \right] \quad (3)$$

A series of experiments shows good agreement with data predicted by eqn. 3 (ref. 15, 18–21). It should be stressed, however, that this model neglects possible co-ion release and change in hydration during association.

The stoichiometric displacement model considers a pure ion-exchange process, where co-ion release and change in hydration are neglected, and estimates the number of counterions released at protein binding by  $d \ln k'/d \ln m$ , ( $k'$  = capacity factor). The thermodynamic model provides the same parameter (*cf.* eqn. 3). Basis of this similarity, the retention equation of the stoichiometric displacement model, at least formally, can be traced to Wyman's linkage theory<sup>9</sup>.

In this paper, extension of this fundamental thermodynamic model to electrostatic interaction chromatography of proteins is studied. Using a stationary phase with known structure, polyethyleneimine (PEI), parameters of interaction of a large biopolymer, ovalbumin, were estimated at different mobile phase pH values.

#### EXPERIMENTAL

Ovalbumin (OVA), conalbumin (CON) and  $\beta$ -lactoglobulin A (B-LAC) were obtained from Calbiochem (La Jolla, CA, U.S.A.). Piperazine, 2,2-bis(hydroxymethyl)-2,2',2''-nitrilotriethanol (bis-tris) and 1,3-bis[tris(hydroxymethyl)methylamino]propane (bistrispropane) were obtained from Aldrich (Milwaukee, WI, U.S.A.), tris(hydroxymethyl)aminomethane (Tris) from Boehringer Mannheim (Indianapolis, IN, U.S.A.) and sodium chloride from Fisher Scientific (Fair Lawn, NJ, U.S.A.).

Experiments were carried out on a Model 1090 liquid chromatograph equipped with a filter-photometric detector ( $\lambda = 280 \text{ nm}$ ) from Hewlett-Packard (Palo Alto, CA, U.S.A.) and with a Rheodyne 7125 injection valve fitted with a 20- $\mu\text{l}$  loop (Cotati, CA, U.S.A.). Chromatograms were recorded by using a Linear Series 1200 recorder (Reno, NV, U.S.A.).

A 50  $\times$  4.6 mm I.D. column was packed with Synchronapak Q300 strong anion-exchange support (Synchrom, Lafayette, IN, U.S.A.).

The mobile phase contained 20 mM piperazine  $\cdot$  HCl at pH 4.8, 5.0 and 6.0, bis-tris  $\cdot$  HCl at pH 6.5, bistrispropane  $\cdot$  HCl at pH 7.0, Tris  $\cdot$  HCl at pH 8.0 and various amounts of sodium chloride in order to vary the protein retention factor from 1 to 10 in isocratic elutions. Calculation of  $k'$  was performed according to  $k' = (V_R - V_0)/V_0$ , where  $V_R$  is the retention volume of the solute and  $V_0$  is the hold-up volume which was determined according to the method described in ref. 22. Averages of three parallel determinations were used in the calculations, standard deviations of these measurements were always less than 2%. Mobile phase flow-rate was 1 ml/min and the temperature 25°C, in all cases.

A fourth order polynomial equation was fitted to the logarithm of retention

factor for ovalbumin *vs.* the logarithm of salt concentration. Linear regression analyses were used to fit eqn. 5 and 8 to retention data of ovalbumin.

## RESULTS AND DISCUSSION

### *Extension of thermodynamic model to electrostatic interaction chromatography*

As a first step, a quasi two-dimensional ion-exchange surface with  $N$  charges is considered instead of linear array charges on a polynucleotide. Therefore, in the equilibrium equation (eqn. A8) S represents the stationary phase and P is a symbol for peptides or proteins with  $\zeta$  number of charges in their binding sites. For the sake of simplicity, a possible release of co-ions bound to the charged groups of the protein binding site and change in the protein's hydration state are neglected. This means that the reference state equilibrium and, consequently, the expression for the apparent equilibrium quotient (eqns. A8, 2, 3) remain unchanged.

The  $k'$  is expressed by the equation<sup>22,23</sup>

$$k' = K_{\text{obs}} \varphi \quad (4)$$

where  $\varphi$  is a chromatographic phase ratio that is independent of salt concentration. From eqn. 2 and 3

$$\ln k' = \ln K_T^0 + \ln \varphi + \zeta \xi^{-1} \ln \delta \gamma_{\pm} - \zeta \psi \ln m \quad (5)$$

and

$$\left( \frac{d \ln k'}{d \ln m} \right)_{T, p, \text{pH}} = - \zeta \left[ \psi - \xi^{-1} \frac{d \ln \gamma_{\pm}}{d \ln m} \right] \quad (6)$$

Eqn. 5 is considered as the retention equation of electrostatic interaction chromatography of proteins. According to eqn. 6, the slope of the plot  $\ln k'$  *vs.*  $\ln m$  is a function of the number of protein charges interacting with the stationary phase,  $\zeta$ , the average charge spacing,  $b$  and the effect of mobile phase salt concentration on the mean ionic activity coefficient of the salt. For sodium chloride,  $d \ln \gamma_{\pm} / d \ln m$  is constant between 0.1 and 0.5  $M$  concentration ( $r = 0.9999$ ), and its value is  $-0.04$  (ref. 24). Below 0.1  $M$ , the absolute value of this slope decreases. Error arising from neglecting the second term in the right-hand side of eqn. 6 is expected to be approximately 3%.

### *Evaluation of the quaternized polyethyleneimine stationary phase*

Distance between two nitrogen atoms in PEI was estimated by using atomic distance and angle values of glycine and trimethylamine<sup>25</sup>. Based on the significant repulsion forces between charged amine groups, it was assumed that two neighbouring N atoms are in the *trans* position. Therefore, the charge spacing,  $b$ , is approximately 3.9 Å. According to Rounds<sup>26</sup>, the degree of quaternization of a well made quaternized PEI coating at maximum is 70%. At least 75–80% of tertiary amine groups left are ionized at pH 6.0 (ref. 27). At 65% quaternization of amine groups in PEI and 80% ionization of the residual tertiary amines, approximately 90% of the amino groups in

PEI are ionized. Therefore, the average charge spacing,  $b$ , is *ca.* 4.5 Å. Since PEI coatings can be several layers thick, the influence of layer thickness on the electrostatic potential must be considered. When the mobile phase salt concentration is over 0.1  $M$ , the electrostatic field of the amine groups below the surface of the PEI coating is mostly shielded by mobile phase ions and their effect can be ignored.

Using the estimated  $b$  value (4.5 Å), the model provides values for the other parameters:  $\zeta = 1.59$  and  $\psi = 0.686$ . Assuming the quaternized PEI chain has an average radius about 4 Å (ref. 25), the thickness  $\Delta x$  of cylindrical shells of volume  $V$  around the polyelectrolyte chain (see eqn. A5), in the case of sodium chloride as electrolyte, is 12 Å which is equivalent to about four water layers.

#### *Evaluation of elution data for ovalbumin*

Retention of ovalbumin as a function of mobile phase salt concentration was measured at pH 5, 6, 7 and 8 (Fig. 1). The isocratic elution profiles were always single peaks. Eqn. 6 was used to determine  $\zeta$  values (Table I). The slope of  $\ln k'$  vs.  $\ln m$  determined from polynomial equation, as a function of mobile phase salt concentration,  $m$ , is shown in Fig. 2. As expected, an increase in mobile phase pH increases the value of  $d \ln k' / d \ln m$ . The change in the derivative is most pronounced at pH 5 and decreases with increasing pH. The constant  $k'$  curves represent isoenergetic conditions. Increasing mobile phase pH and consequently the number of interacting charges decreases the free energy change of the interaction per unit  $\zeta$  ( $\approx d \ln k' / d \ln m$ ); moreover, the smaller the  $k'$ , the greater the change.

The isoenergetic curves are linear over 0.1  $M$  salt concentration. The slope of these straight lines is equal to

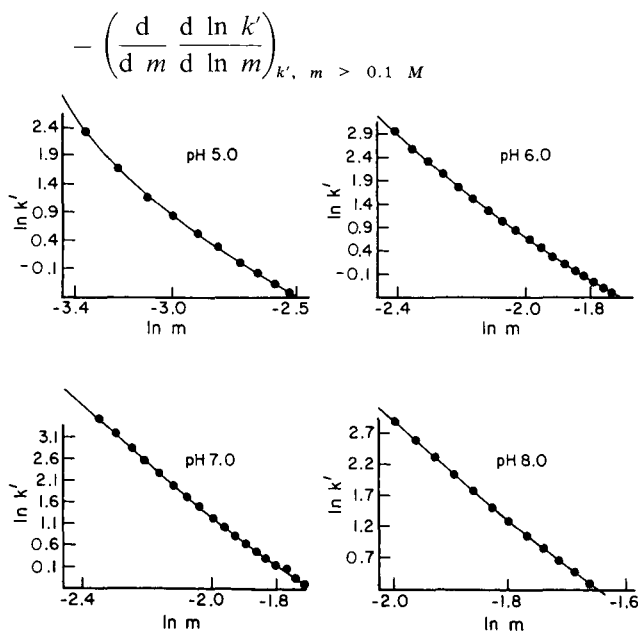


Fig. 1. Plot of  $\ln k'$  vs.  $\ln m$  for ovalbumin at pH 5, 6, 7, and 8. Solid lines represent the fit of a fourth order polynomial equation.

TABLE I  
 $\zeta$  VALUES OF OVALBUMIN DETERMINED BY EQN. 6

pH	$\zeta$	$r$
5	4.82	0.984
6	7.48	0.997
7	8.53	0.998
8	11.06	0.999

which is depending on the change of stoichiometry, and decreases with an increase in binding energy ( $\approx k'$ ) as it is shown in Fig. 3. According to this, it can be stated that this interaction is more sensitive to the change of  $\zeta$  at low  $k'$  values than at higher ones. Below 0.1 M salt concentration, the isoenergetic curves deviate from a straight line. Plots of  $(d \ln k'/d \ln m)_{\text{pH } 5}$  vs.  $m$  are non-linear and shifted to higher values. At higher salt concentrations ( $m > 0.05$  M), however, the plot is straight and deviation of  $[(d \ln k'/d \ln m)_{\text{pH } 5, \text{ obs}} - (d \ln k'/d \ln m)_{\text{pH } 5, \text{ lin}}]$  as a function of salt concentration approaches zero (Fig. 4). According to the thermodynamic model by Record *et al.*<sup>14</sup>,  $d \ln k'/d \ln m$  is constant. This prediction is more or less realized at the high salt concentration range (at pH 8). When decreasing mobile phase pH and concomitantly salt concentration required to elute OVA, the change in slope is more pronounced (Fig. 2). The slope of the isoenergetic curves at greater than 0.1 M salt concentration shows that the increase in  $d \ln k'/d \ln m$  as a consequence of an increase in the  $\zeta$  value (or in pH) is a linear function of the salt concentration required to elute OVA at constant free energy change.

If ovalbumin has a mixed (electrostatic and hydrophobic) interaction with the stationary phase, the contribution of hydrophobic interaction to the overall interaction would be greater when the contact area of the protein is more hydrophobic (in other words, contains less charges). The closer the mobile phase pH is to the

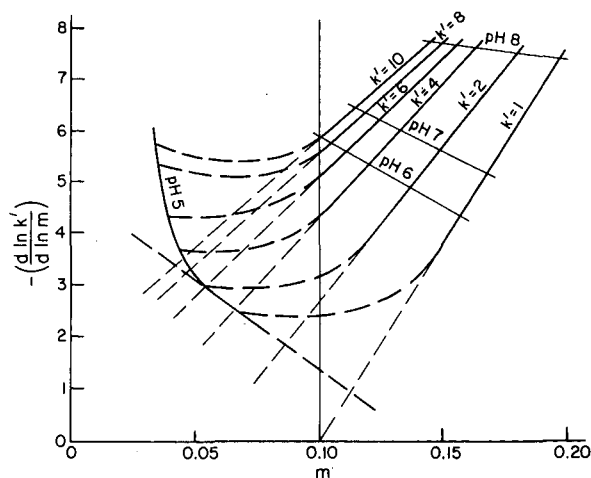


Fig. 2.  $(d \ln k'/d \ln m)$  vs.  $m$  for OVA at different pHs.



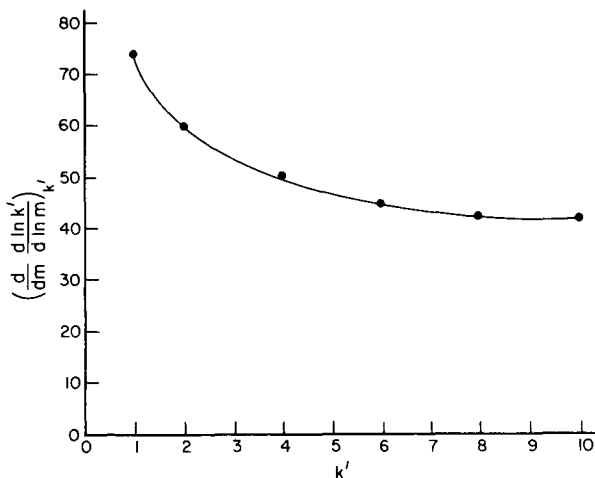


Fig. 3. Slope of the isoenergetic curves observed over 0.1 *M* salt concentration vs. retention factor.

isoenergetic point, the less charge there is on the protein surface. The isoelectric point of OVA is 4.7 (ref. 28); therefore, one would expect the binding site of OVA to be more hydrophobic at pH 5 than at higher pH values<sup>29</sup>. Thus, when evaluating the retention equation of OVA, both electrostatic and hydrophobic interaction should be considered<sup>30</sup>.

The first term on the right-hand side of eqn. 1 derived by Tanford<sup>10</sup>, considers hydrophobic interaction at high salt concentration. If we extend Tanford's equation to the low salt concentration range as proposed by Aune *et al.*<sup>31</sup>, the slope of the retention equation can be expressed as follows:

$$\left(\frac{d \ln k'}{d \ln m}\right) = -\zeta\psi + \Delta(n_C + n_A - \frac{mp}{55.5} n_W) \left(1 + \frac{\ln \gamma_{\pm}}{\ln m}\right) \quad (7)$$

The number of moles of water molecules released at binding of 1 mole protein can be determined from the slope of the plot ( $d \ln k'/d \ln m$ ) vs.  $m$  (Table II). According to eqn. 7,  $\zeta$  and  $(\Delta n_C + \Delta n_A)$  cannot be determined independently. Other authors should have faced the same problem earlier<sup>11,12,31</sup>. If we assume that there is no ion release due to hydrophobic interaction,  $\zeta$  can be estimated to be 6.92 at pH 5, 12.7 at pH 6, 13.4 at pH 7 and 12.9 at pH 8.  $\zeta$  values show a jump between pH 5 and 6, but remain constant between pH 6 and 8. Therefore, ion release as a consequence of hydrophobic interaction cannot be ignored.

If  $\zeta$  is set to be equal to that determined by eqn. 6, the total ion release due to hydrophobic interaction,  $\Delta n_i \approx (\Delta n_A + \Delta n_C)$  can be estimated as well (Table II). At pH 6, 7, and 8, plots of  $d \ln k'/d \ln m$  are quasi linear and the slope of the plot [ $d/d m (d \ln k'/d \ln m)$ ] decreases with increasing pH and concomitantly  $\zeta$  values (*i.e.*, the contribution of change in hydration due to hydrophobic interaction). At pH 5, however, the plot is non-linear. The straight line relating to the slope of hydrophobic interaction ( $d \ln k'/d \ln m$  vs.  $m$ ) at pH 5, was estimated using isoenergetic functions (Fig. 2). Parameters were determined fitting eqn. 7 to the estimated change in  $d \ln k'/d$

TABLE II  
PARAMETERS DETERMINED BY FITTING EQN. 7

$pH$	$\Delta n_w^a$	$\Delta n_i^b$
5 <sup>c</sup>	839	1.36
6	655	3.02
7	552	2.81
8	172	1.03

<sup>a</sup> Calculated for mid salt concentration value of measured range.

<sup>b</sup> Calculation based on  $\zeta = \zeta_{eqn.6}$ .

<sup>c</sup> Fit on  $(d \ln m'/d \ln m)_{pH 5, lin}$  vs.  $m$ .

In  $m$  as well (Table II). Non-linearity of the plot  $d \ln k'/d \ln m$  vs.  $m$  shows that the model does not take into account a phenomenon which has a significant role at low salt concentration. Change in  $\Delta n_i$  and  $\Delta n_w$  as a function of  $pH$  reflects to opposite effects on hydrophobic ion release. At low  $pH$ , close to protein isoelectric point, the binding site contains a relatively small amount of charges, *i.e.*, it is relatively hydrophobic (large  $-\Delta n_w$  value) and the salt concentration necessary to elute the protein is low. This means that the population of ions at hydrophobic binding sites is low (low  $-\Delta n_i$  value). When the mobile phase  $pH$  is increased and concomitantly salt concentration required for the elution of OVA also increases, the binding site of the protein contains an increasing number of charges, *i.e.*, its hydrophobicity decreases ( $-\Delta n_w$  and number of hydrophobic binding sites decrease) but the occupation level of remaining hydrophobic binding sites increases. Consequently,  $-\Delta n_i$  has a maximum.

The discrepancy between the model and measured data near the  $pI$  of a protein was found not only in the case of OVA but in that of conalbumin and  $\beta$ -lactoglobulin as well. Slopes ( $s$ ), intercepts ( $I$ ), correlation coefficients ( $r$ ) of linear regression analyses were  $s = -1.56$ ,  $I = -5.41$ ,  $r = 0.986$  for CON and  $s = -1.81$ ,  $I = -4.98$ ,  $r = 0.988$  for B-LAC, respectively. This deviation may originate from neglecting possible change in co-ion release, effect of the unshielded amino groups below the surface of the PEI coating, change in hydration of ions, and in the worst case, aggregation or a possible conformational change in protein structure.

Relatively weak interactions of electrolyte ions with charged groups or polar

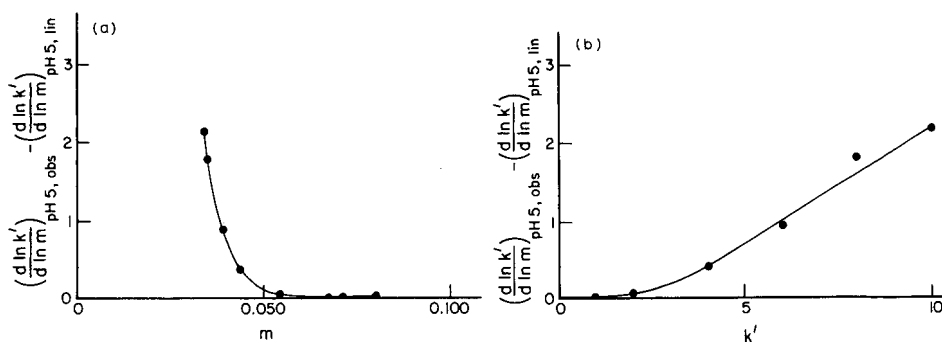


Fig. 4. Deviation of the change in the slope of  $\ln k'$  vs.  $\ln m$  at  $pH 5$  from straight line observed over  $50 \text{ mM}$ , as a function of (a) salt concentration and (b) retention factor.

residues on the surface of a protein are important in determining its conformation, biological activity, solubility, aggregation and chromatographic behavior. There have been many investigations of salt effects on macromolecular equilibria started by Hofmeister<sup>32</sup> about one hundred years ago. The most detailed information currently available on ion-protein interaction can be obtained by using halide NMR<sup>33</sup>. Thermodynamic modeling of macromolecular binding has been used extensively<sup>7,10,11,34</sup>. In the case of electrostatic interaction chromatography of proteins, co-ion release at protein binding can be considered as an additional energy term to the total free energy change<sup>12,34</sup>:

$$\exp\left(-\frac{\Delta G_c^0}{RT}\right) = K_c = (1 + k_c a_c)^{-\Delta q_c} \quad (8)$$

where  $k_c$  and  $a_c$  are the intrinsic binding constant and activity of co-ion, respectively, and  $\Delta q_c$  is the number of co-ions released. Considering the fact that the isocratic measurements of the plot  $\ln k'$  vs.  $\ln m$  are usually performed at relatively low and in a narrow salt concentration range, changes of activity coefficient of salt can be neglected. Furthermore<sup>14</sup>,

$$q_c = \zeta \theta_c \quad (9)$$

where  $\theta_c = k_c m / (1 + k_c m)$ .

Combining eqns. 8 and 9, the logarithm of the equilibrium quotient for ion-binding is

$$\ln K_c = -\zeta k_c m / (1 + k_c m) \ln (1 + k_c m) \quad (10)$$

In the case of a uni-univalent salt, interaction between a co-ion (with respect to the ion-exchange surface) and a protein charged group is relatively weak, *i.e.*,  $k_c m \ll 1$ , therefore, the additional term to the retention equation is

$$\ln K_c \approx -\zeta k_c m \ln (1 + k_c m) \quad (11)$$

or

$$\ln K_c \approx -\zeta (k_c m)^2$$

Eqn. 11 describes a convex curve which is the opposite curvature of the measured function. Therefore, based on the theory for site binding, co-ion release cannot be responsible for discrepancy observed at pH near  $pI$  of proteins.

The other possible explanation for the non-linear nature of the slope of  $(d \ln k' / d \ln m)$  vs.  $m$  is the effect of the unshielded amino groups below the surface of the PEI coating at low salt concentration in the eluent. In this case an apparent decrease of  $b$  number should be considered. Quantitative description of this effect needs further investigation.

At a pH near to  $pI$ , where the binding is relatively weak (low  $\zeta$  value), elution salt

concentration is below 0.1  $M$ . In this concentration region, the Debye–Hückel theory is valid, and the thickness of double layer around a charged group ( $1/\kappa$ ) varies steeply with ionic strength of the mobile phase, while above 0.1  $M$ , the change of  $1/\kappa$  is relatively small. Deviation observed may be originated from the assumption that the change in macromolecular hydration can be neglected. In the Debye–Hückel region, this assumption is, probably, not valid. To consider change in ionic hydration, a model is needed to describe the binding of proteins to an ion-exchange stationary phase. At present a satisfactory model has not been developed for *large* biomolecules.

According to Eisenman<sup>35</sup>, interaction of ionic species can be described as the sum of free energy change of electrostatic interaction and that of hydration.

$$\Delta G = \Delta G_{\text{e.s.}} + \Delta G_{\text{hydr.}} \quad (12)$$

In the case of electrostatic interaction of proteins and stationary phase, the influence of  $\Delta G_{\text{hydr.}}$  on the overall process is a function of the nature of the interacting ions (cosmotrop, chaotrop) and the salt concentration of the bulk (thickness of the hydration shells).

According to Manning<sup>36</sup>, though, the free energy of stabilization of the charged fraction due to the short-range effect accompanying dehydration, is expected to be fairly small compared to the non-specific long-range polyelectrolyte effect. Nevertheless, short-range effects due to dehydration of ions and polar groups may be the key to some of the most crucial problems in biology. If the affinity of a counterionic species for sites on the polyion contains a non-ionic component, the binding is more tight and localized resulting, probably, in an even greater change in ionic hydration. Since there is no quantitative description of this phenomenon available today, the possible contribution of dehydration of ions and polar groups cannot be evaluated.

At low salt concentration (below 0.1  $M$ ), the nature of the protein can be altered due to the unshielding effect of its charged groups<sup>37</sup>. The increased hydrophobicity of a protein due to the mobile phase pH set near to the  $pI$  and the alteration in protein structure at low salt concentration may result in protein aggregation.

Deviation of measured data from the model at the protein  $pI$  may be considered as a consequence of the combination of phenomena mentioned above. This founding warns us that care must be taken at designing a protein separation to obtain a desired purity and biological activity of the product.

## CONCLUSION

The model investigated in this paper is an applied form of Wyman's linkage theory which is completely general. Consequently, it is valid not only for association, precipitation and conformational changes of proteins but for any kind or surface mediated chromatography of proteins (electrostatic interaction, hydrophobic interaction, reversed-phase, bioaffinity, and metal–chelate interaction) as well. Gradient elution chromatography of proteins can be characterised with a general relationship:

$$K_{\text{obs}} \approx \exp \left\{ \left( \frac{\partial \Delta G}{\partial \mu_1} \right)_{T, p} \frac{\mu_1}{RT} \right\} \quad (13)$$

where  $\mu_1 = -RT \ln a_1$ , subscript 1 stands for ligand in general, and special solutions of eqn. 1 for different kind of interactions, provides expressions for  $(\partial \Delta G / \partial \mu_1)_{T,p}$ . Under practical separation conditions, the extended form of this thermodynamic model was successfully applied to the retention of a protein.

#### ACKNOWLEDGEMENT

The authors gratefully acknowledge professor Csaba Horváth for helpful discussions. Special thanks go to Dr. Steve Cook for computing assistance. We thank Dr. Noubar Afeyan for his suggestions during preparation of the manuscript. This work was supported by PerSeptive Biosystems and by grant GM 25431-12 from the National Institutes of Health. This is journal paper number 12,067 from Purdue Agricultural Experiment Station.

#### APPENDIX I

In the case of site binding, the association of a single ligand L with a class of  $N$  identical, independent sites on a macromolecule M is considered. Ignoring hydration effects and using the unligated macromolecule as the reference state, the binding polynomial<sup>18</sup> is

$$\Sigma_M = (1 + k_{L,M} a_L)^N \quad (\text{A1})$$

where  $a_L$  is activity of the ligand and  $k_{L,M}$  the intrinsic binding constant of L to a site on M. Applying Wyman's linkage theory<sup>9</sup>, the derivative of eqn. A1 is

$$\left( \frac{d \ln \Sigma_M}{d \ln a_L} \right)_{a_W, a_C, a_A} = n_{L,M} = \frac{N k_{L,M} a_L}{1 + k_{L,M} a_L} = N \theta_{L,M} \quad (\text{A2})$$

where  $\theta_{L,M} = n_{L,M}/N$  is the binding density.

According to Manning's condensation theory<sup>17</sup>, if the macromolecule can be modeled as a linear array of  $N$  univalent charges of average spacing  $b$ , then the extent of association of monovalent counterions with the polyion can be determined by a dimensionless charge density parameter,

$$\xi = e^2 / b D k T \quad (\text{A3})$$

where  $D$  is the bulk dielectric constant,  $k$  is the Boltzman factor and  $T$  is the absolute temperature.

Assuming that the interaction of bound and free ions with the solvent is the same, and the "bound" ions may translate freely within the volume  $V$  centered along the axis of the polyelectrolyte, charging the ionic groups of a polyelectrolyte against their mutual electrostatic repulsion and mixing free cations, bound cations and solvent molecules, were found to result in an equilibrium state where the number of associated counterions per fixed charge,  $\theta_D$ , has a value between 0 and 1. Furthermore,  $\theta_D$  does not tend to zero with  $m$  but remains positive<sup>38</sup>. For a 1:1 salt, at the free energy

minimum, in the limit  $m \rightarrow 0$ , the fraction of a counterion condensed on a infinite polyion per structural polyion charge is

$$\theta_D = 1 - \xi^{-1} \quad (\text{A4})$$

The quantity of  $\theta_D$  has been determined for native DNA using  $^{23}\text{Na}$  NMR, and it was found to be independent of sodium chloride concentration in the range of 0.005 to 0.5  $M$  (ref. 33). The volume of the region surrounding the polyelectrolyte within which cations are “bound”,  $V$ , is described by eqn. 6 (ref. 38):

$$V = 10^3 \nu v^{-1} Z^{-1} (1 - Z^{-1} \xi^{-1}) (\kappa b)^2 m^{-1} \quad (\text{A5})$$

where  $\nu$  is the number of  $Z$ -valent ions per formula salt, and  $\kappa$  is the Debye–Hückel parameter.  $V$  is independent of  $m$ , since the ratio  $\kappa^2/m$  is independent of  $m$ .

The thermodynamic binding parameter,  $\psi$ , contains two important quantities characterizing the interaction of the polyion with the counterions: the extent of condensation,  $\theta_D$ , and the screening effect of low-molecular-weight ions on the interactions of these residual polyelectrolyte charges, which is thermodynamically equivalent to the binding of an additional fraction  $(2\xi)^{-1}$  of a counterion per polyion structural charge<sup>15</sup>

$$\psi = \theta_D + (2\xi)^{-1} = 1 - (2\xi)^{-1} \quad (\text{A6})$$

## APPENDIX II

The equilibrium where a nucleic acid, S, consisting of  $N$  nucleotides interacts with an oligopeptide, P, with  $\xi$  positive charges in its binding site for S, and forms a complex, SP, is described as:



and the phenomenological equilibrium quotient,  $K_{\text{obs}}$ , is

$$K_{\text{obs}} = \frac{[\text{SP}]}{[\text{S}] [\text{P}]} \quad (\text{A8})$$

This equilibrium is established in a dilute aqueous solution of the oligopeptide which contains an excess of salt  $\text{C}_p + \text{A}_p^-$ . (Effect of pH on  $K_{\text{obs}}$  is not considered here.)  $K_{\text{obs}}$  is, in general, a function of the activities of the participant species, as a result of indirect effect of low-molecular-weight ions on the macromolecular activity coefficients. If the change in macromolecular hydration during association is negligible, the reference state equilibrium where the polypeptide is in hydrated but unligated form and the nucleic acid is hydrated and with its complement of condensed counterions is



where  $D$  is the counterion,

$$\Delta r^0 = r_s^0 - r_{SP}^0 \quad (\text{A10})$$

the number of moles of counterion released at the binding of 1 mole of oligopeptide, and

$$K^0 = \frac{[SP^0]}{[S^0][P^0]} a_D^{\Delta r} \quad (\text{A11a})$$

$$= K_T^0 \frac{\gamma_S^0 \gamma_P^0}{\gamma_{SP}^0} \quad (\text{A11b})$$

where  $K_T^0$  is the thermodynamic equilibrium constant and  $\gamma$  terms are the activity coefficients at the reference state. The phenomenological equilibrium ratio<sup>9,10,34</sup> is

$$K_{\text{obs}} = K^0 \Sigma_{SP}^0 / \Sigma_S^0 \Sigma_P^0 \quad (\text{A12})$$

where  $\Sigma$  terms are the binding polynomials<sup>34</sup> reflecting activity coefficient effects and interrelationships among “ligand” activities. Combining eqns. A11 and A12 leads to

$$\ln K_{\text{obs}} = \ln K_T^0 + \ln \frac{\gamma_S^0 \gamma_P^0}{\gamma_{SP}^0} + \ln \Sigma_{SP}^0 - \ln \Sigma_S^0 - \ln \Sigma_P^0 \quad (\text{A13})$$

where the binding polynomials

$$\Sigma_P^0 = 1 \quad (\text{A14})$$

$$\Sigma_S^0 = a_D r_S^0 \quad (\text{A15})$$

$$\Sigma_{SP}^0 = a_D r_{SP}^0 \quad (\text{A16})$$

From eqns. A9, and A13–A16, it follows that

$$\ln K_{\text{obs}} = \ln K_T^0 + \ln \frac{\gamma_P^0 \gamma_S^0}{\gamma_{SP}^0} - \Delta r^0 \ln a_D \quad (\text{A17})$$

According to the condensation model<sup>38</sup>

$$r_S^0 = N(1 - \xi_S^{-1}) \quad (\text{A18})$$

and

$$r_{SP}^0 = (N - \zeta)(1 - \xi^{-1}) \quad (\text{A19})$$

Assuming that  $\xi_s^{-1} = \xi_{sp}^{-1} = \xi^{-1}$ , then from eqns. A9, A18, and A19 it follows that

$$\Delta r^0 = \zeta (1 - \xi^{-1}) \quad (\text{A20})$$

Note that the following approximations are made to obtain the activity coefficients in eqn. A17: (a) only electrostatic contributions to the activity coefficients are considered; (b) since  $\ln \gamma$  is an excess electrostatic free energy, contributions to  $\ln \gamma$  from different regions on a macroion may be additive.

Extending this derivation further,

$$\ln \gamma_P^0 = \ln \gamma_{P^0, \text{site}} + \ln \gamma_{P^0, \text{remainder}} \quad (\text{A21})$$

Assuming that

$$\ln \gamma_{P^0, \text{site}} = \zeta \ln \gamma_D \quad (\text{A22})$$

and

$$\ln \gamma_{SP^0} = \frac{N - \zeta}{N} \ln \gamma_S^0 + \ln \gamma_{P^0, \text{remainder}} \quad (\text{A23})$$

and moreover, for the polynucleotide<sup>38</sup>

$$\ln \gamma_S^0 = \frac{NG_{el}}{RT} = -N\xi^{-1} \ln \kappa b = -0.5N\xi^{-1} \ln [D] - N\xi^{-1} \ln \delta \quad (\text{A24})$$

where  $G_{el}$  is the excess electrostatic free energy per mole of structural charges,  $\kappa$  is the Debye–Hückel screening parameter and  $\delta = 0.33b$  in aqueous solution near 25°C. Therefore,

$$\ln \frac{\gamma_P^0 \gamma_S^0}{\gamma_{SP^0}} = \zeta \xi^{-1} (0.5 \ln [D] + \ln \delta) + \zeta \ln \gamma_D \quad (\text{A25})$$

For uni-univalent electrolyte,  $[D]=[C] = m$ , and assuming that  $\gamma_D = \gamma_C = \gamma_{\pm}$

$$\ln K_{\text{obs}} = \ln K_T^0 - \zeta [1 - (2\xi)^{-1}] \ln m + \zeta \xi^{-1} \ln \delta \gamma_{\pm} \quad (\text{A26})$$

and

$$\left( \frac{d \ln K_{\text{obs}}}{d \ln m} \right)_{T, p, \text{pH}} = -\zeta \left[ \psi - \xi^{-1} \frac{d \ln \gamma_{\pm}}{d \ln m} \right] \quad (\text{A27})$$

NOTE ADDED IN PROOF

During the review of this paper, Melander *et al.*<sup>39</sup> have published an article in which they have also used Manning's condensation theory to treat retention data of



proteins obtained on different ion-exchange columns. This article has provided a different perspective of the phenomena involved in ion-exchange chromatography of proteins. The retention equation developed by Melander *et al.* which combines both electrostatic and hydrophobic theory has allowed a comprehensive analysis of retention data of proteins.

## REFERENCES

- 1 N. K. Boardman and S. M. Partridge, *Biochem. J.*, 59 (1955) 543.
- 2 P. Arányi and L. Boross, *J. Chromatogr.*, 89 (1974) 239.
- 3 R. A. Barford, B. J. Sliwinski and H. L. Rothbard, *J. Chromatogr.*, 185 (1979) 393.
- 4 W. Kopaciewicz, M. A. Rounds, J. Fausnaugh and F. E. Regnier, *J. Chromatogr.*, 266 (1983) 3.
- 5 L. A. Kennedy, W. Kopaciewicz and F. E. Regnier, *J. Chromatogr.*, 359 (1986) 73.
- 6 Cs. Horváth, W. R. Melander and Z. El Rassi, presented at the 9th International Symposium on Column Liquid Chromatography, Edinburgh, July 1-5, 1985.
- 7 G. Scatchard, *Ann. NY Acad. Sci.*, 51 (1949) 660.
- 8 J. Wyman, *Adv. Protein Chem.*, 4 (1948) 407.
- 9 J. Wyman, *Adv. Protein Chem.*, 19 (1964) 223.
- 10 C. Tanford, *J. Molec. Biol.*, 39 (1969) 539.
- 11 K. C. Aune and C. Tanford, *Biochemistry*, 8 (1969) 4579.
- 12 K. C. Aune and C. Tanford, *Biochemistry*, 8 (1969) 4586.
- 13 M. T. Record, Jr., *Biopolymers*, 14 (1975) 2137.
- 14 M. T. Record, Jr., C. F. Anderson and T. M. Lohman, *Q. Rev. Biophys.*, 11 (1978) 103.
- 15 M. T. Record, Jr., T. M. Lohman and P. L. DeHaseth, *J. Mol. Biol.*, 107 (1976) 145.
- 16 P. L. DeHaseth, T. M. Lohman and M. T. Record, *Biochemistry*, 16 (1977) 4783.
- 17 G. S. Manning, *J. Chem. Phys.*, 51 (1969) 924.
- 18 D. E. Jensen and P. H. Von Hippel, *J. Biol. Chem.*, 251 (1976) 7198.
- 19 D. E. Jensen, R. C. Kelly and P. H. Von Hippel, *J. Biol. Chem.*, 251 (1976) 7198.
- 20 A. Rezin and P. H. Von Hippel, *Biochemistry*, 16 (1977) 4769.
- 21 D. E. Draper and P. H. Von Hippel, *J. Molec. Biol.*, 122 (1978) 321.
- 22 I. Mazsaroff and F. E. Regnier, *J. Chromatogr.*, 442 (1988) 115.
- 23 A. Velayudhan and Cs. Horváth, *J. Chromatogr.*, 367 (1987) 160.
- 24 R. A. Robinson and R. H. Stokes, *Electrolyte Solutions*, Butterworths Scientific Publications, London, 1955, p. 477.
- 25 R. C. Weast (Editor), *Handbook of Chemistry and Physics*, CRC Press, Cleveland, OH, 58th ed., 1977-1978, p. F-218.
- 26 M. A. Rounds, personal communication.
- 27 A. Alpert and F. E. Regier, *J. Chromatogr.*, 158 (1979) 375.
- 28 P. G. Righetti and T. Caravaggio, *J. Chromatogr.*, 127 (1976) 1.
- 29 E. J. Cohn and J. T. Edsall, *Proteins, Amino Acids and Peptides as Ions and Dipolar Ions*, Reinhold, New York, 1943, Ch. 24.
- 30 W. R. Melander and Cs. Horváth, in Cs. Horváth (Editor), *High-Performance Liquid Chromatography—Advances and Perspectives*, Vol. 2, Academic Press, New York, 1980, p. 114.
- 31 K. C. Aune, L. C. Goldsmith and S. N. Timasheff, *Biochemistry*, 10 (1971) 1617.
- 32 F. Hofmeister, *Naunyn-Schmiedebergs Arch. Exp. Pathol. Pharmacol.*, 24 (1888) 247.
- 33 C. F. Anderson, M. T. Record, Jr. and P. A. Hart, *Biophys. Chem.*, 9 (1978) 301.
- 34 J. Schellman, *Biopolymers*, 14 (1975) 999.
- 35 G. Eisenman, in A. Klenzeller and A. Kotyk (Editors), *Membrane Transport and Metabolism*, Academic Press, New York, 1961, 163.
- 36 G. S. Manning, *Biophys. Chem.*, 7 (1977) 95.
- 37 A. J. Russel and A. R. Fersht, *Nature (London)*, 328 (1987) 496.
- 38 G. S. Manning, *Q. Rev. Biophys.*, 11 (1978) 179.
- 39 W. R. Melander, Z. El Rassi and Cs. Horváth, *J. Chromatogr.*, 469 (1989) 3.



CHROMSYMP. 1649

## PHYSICOCHEMICAL STUDIES OF BIOLOGICALLY ACTIVE PEPTIDES BY LOW-TEMPERATURE REVERSED-PHASE HIGH-PERFORMANCE LIQUID CHROMATOGRAPHY<sup>a</sup>

DAVID E. HENDERSON\* and JILL A. MELLO

*Department of Chemistry, Trinity College, Hartford, CT 06106 (U.S.A.)*

---

### SUMMARY

The high-performance liquid chromatographic separation of biologically active peptides containing 1-prolyl residues is demonstrated. Rapid isomer interconversion between *cis*- and *trans*-isomeric forms at the prolyl peptide bond is shown to produce classical secondary equilibrium effects in the peak shapes. By operating the column at temperatures in the range  $-15^{\circ}\text{C}$  to  $5^{\circ}\text{C}$  it is possible to obtain normal separations of the various isomeric forms. The use of low column temperatures makes physicochemical studies possible, *e.g.*, the effect of pH on isomer composition in free solution as reported here for morphiceptin.

---

### INTRODUCTION

Low-temperature high-performance liquid chromatography (HPLC) has proved to be an effective method for the study of physicochemical properties. Work to date has demonstrated this for both metal coordination complexes<sup>1</sup> and for rotational *cis*–*trans*-isomerism of the peptide bond in proline dipeptides<sup>2</sup>. For both of the above chemical systems, isomerization processes with moderate energy barriers result in impaired chromatographic performance at room temperature. For chemically reversible systems, the resultant chromatographic behavior is that of a classic secondary equilibrium system, as described by Horváth and co-workers<sup>3,4</sup>.

The specific isomerization addressed in this report arises in peptides and proteins containing proline residues. While the peptide bonds at the proline nitrogen are sufficiently rigid to prevent free rotation, the rate of isomerization is typically too fast to permit separation of the isomers by HPLC at room temperature<sup>5</sup>. The resulting chromatograms contain broad peaks that are highly flow-dependent. Subambient temperatures slow the rate of isomerization, enabling the separation of the pure rotational forms by HPLC<sup>2</sup>. This has allowed the use of HPLC for the analysis of isomer concentrations and for physicochemical studies of molecular conformation.

---

<sup>a</sup> This paper is dedicated to Csaba Horváth on his sixtieth birthday with deepest thanks for his introducing me to the areas of peptide separations and secondary equilibrium studies and for his friendship and many helpful suggestions.

The investigation reported here is part of a long-term project leading to the separation and characterization of pure isomers by physicochemical, spectroscopic and eventually biological methods. The ultimate goal is the elucidation of the structure function relationships of the isomeric forms of biologically active peptides. Low-temperature HPLC allows the analysis of isomeric composition as a function of solvent, temperature, pH, etc. and can provide information about the hydrophobic surface of isomeric forms. The information obtained by HPLC<sup>6</sup> provides an important adjunct to that obtainable from the traditional techniques used for this type of study, most importantly nuclear magnetic resonance (NMR) spectroscopy. The HPLC techniques are more accessible and cheaper than NMR.

A survey of commercially available bioactive peptides indicates the prevalence of peptides containing proline. This amino acid residue is found in peptides of virtually every class of biological activity. The peptides selected for this study were chosen so as to allow a survey of a number of important types of biological activity and to identify classes of peptides for which the active site might depend on one isomeric form of the proline residue. The peptides used in this study, along with their primary structures, are shown in Table I. In the course of this work, a number of important studies by others have come to light which indicate the significance of this type of analysis. The work of Castiglione-Morelli *et al.*<sup>7</sup> is particularly interesting in that their results correlate well with the findings of this study and demonstrate the potential of low-temperature HPLC as a route to understanding the activity of morphiceptin.

#### EXPERIMENTAL

The liquid chromatograph consisted of a Constametric-II pump (Laboratory Data Control, Riviera Beach, FL, U.S.A.), a Rheodyne 7126 valve with 10- $\mu$ l injector loop (Rheodyne, Berkeley, CA, U.S.A.), a Pecosphere-3  $\times$  3 C<sub>18</sub> 33  $\times$  4.6 mm I.D. (Perkin Elmer, Norwalk, CT, U.S.A.) and a  $\mu$ LC-10 detector (ISCO, Lincoln, NE, U.S.A.). The column was immersed in a constant temperature bath controlled by an Exatrol controller and cooled by a PBC-4 bath cooler (Neslab, Portsmouth, NH,

TABLE I  
BIOLOGICALLY ACTIVE PEPTIDES SEPARATED AT LOW TEMPERATURE

<i>Peptide</i>	<i>Sequence</i>
<i>Aliphatic peptides</i>	
Diprotin B	Val-Pro-Leu
Elastin chemotactic fragment	Val-Gly-Val-Ala-Pro-Gly
<i>Arginine peptides</i>	
Bradykinin	Arg-Pro-Pro-Ala-Phe-Ser-Pro-Phe-Arg
<i>Tyrosine peptides</i>	
Morphiceptin	Tyr-Pro-Phe-Pro-NH <sub>2</sub>
$\beta$ -Casomorphin	Tyr-Pro-Phe-Pro-Gly-Pro-Ile
<i>Arginine and tyrosine peptides</i>	
Proctolin	Arg-Tyr-Leu-Pro-Thr

U.S.A.). Chromatograms were recorded, using LabTech Notebook (Laboratory Technologies, Wilmington, MA, U.S.A.) with an AT & T 6300 Personal Computer and integrated, using Lotus 123 (Lotus Development, Cambridge, MA, U.S.A.). A Model 90 digital pH/temperature meter and a micro-electrode (Markson Science, Phoenix, AZ, U.S.A.) were used for pH measurements. The pH of THAM buffers was adjusted with phosphoric acid. All mobile phases were prepared from HPLC-grade solvents (Fisher Scientific, Pittsburgh, PA, U.S.A.), which were filtered and then degassed by helium purge. Flow-rates were 1.0 ml/min except where otherwise noted and the chromatograms were monitored at 210 nm.

Ion-pairing reagents were obtained from Eastman Kodak (Rochester, NY, U.S.A.) and from Aldrich (Milwaukee, WI, U.S.A.) Trizma base for buffer preparation and all peptides were obtained from Sigma (St. Louis, MO, U.S.A.). All peptide solutions contained 1 mg/ml of peptide dissolved in the mobile phase unless otherwise noted.

## RESULTS AND DISCUSSION

### *Isomer separations at low temperature*

HPLC separations of isomers of four classes of peptides were developed: aliphatic peptides, peptides with a tyrosine residue, peptides with an arginine residue and those with both arginine and tyrosine residues. Aliphatic peptides, Ala-Pro, Leu-Pro, Ala-Pro-Gly, Val-Pro-Leu, Phe-Ala-Pro and Val-Gly-Val-Ala-Pro-Gly, were initially studied using 0.05 M phosphate mobile phases with varying amounts of methanol. All of the peptides produced broad peaks, characteristic of

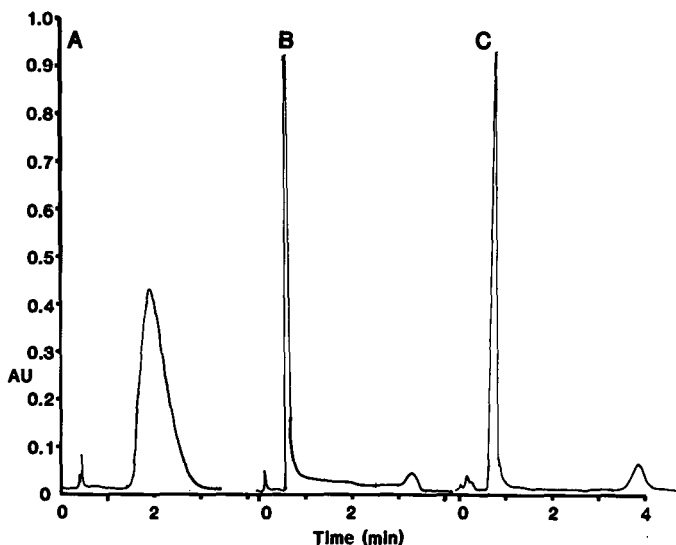


Fig. 1. Separation of Val-Pro-Leu isomers. (A) Room temperature; column Pecosphere  $3 \times 3$  C<sub>18</sub>  $33 \times 4.6$  mm I.D.; mobile phase methanol-0.05 M phosphate (pH 7.0) (15:85); flow-rate 2.0 ml/min; detection at 210 nm, 0.5 AUFS. (B) Column temperature  $-0.1^\circ\text{C}$ ; mobile phase methanol-phosphate buffer (pH 7.0) (20:80); flow-rate 2.0 ml/min; detector 1.0 AUFS. (C) Column temperature  $-11^\circ\text{C}$ ; flow-rate 1.8 ml/min; detector 1.0 AUFS.

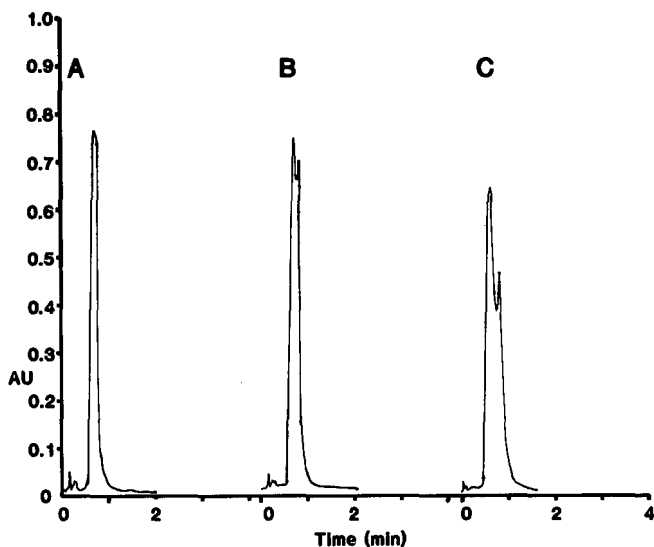


Fig. 2. Chromatograms of proctolin as a function of temperature. Column and detector as in Fig. 1; mobile phase acetonitrile-0.05 *M* phosphate buffer (pH 7.0)/0.02 *M* hexanesulfonic acid 20:80; flow-rate 2.0 ml/min; detector 1.0 AUFS. (A) Column temperature 0°C. (B) Column temperature - 5°C. (C) Column temperature, - 10.0°C.

secondary equilibria, at room temperature and two peaks, attributable to the *cis*- and *trans*-isomers, when the temperature was reduced to 0°C. This is typified by the chromatograms for Val-Pro-Leu shown in Fig. 1. The ability to obtain baseline separation depends on the rate of isomerization, flow-rate and retention time. At -10°C, baseline resolution is obtained even at a flow-rate of 1.0 ml/min (chromatogram not shown), which yields a retention time of about 6.5 min for the second isomer peak. At 0°C a retention time of 3.2 min still produces a noticeable region of sample interconversion between the two peaks, as shown in Fig. 1B.

Separation of polar peptides containing Tyr residues is typified by the separations shown in Fig. 2 for proctolin. This separation required the addition of an alkyl

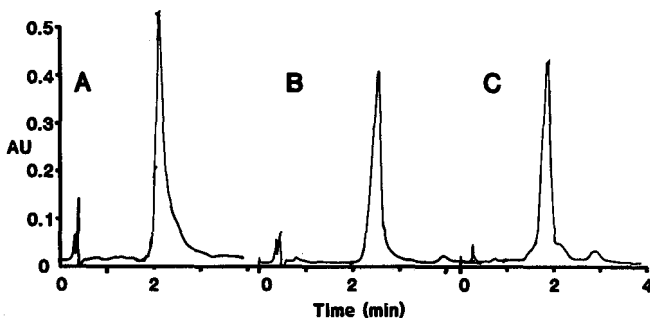


Fig. 3. Separation of bradykinin isomers as a function of temperature. Mobile phase acetonitrile-0.05 *M* THAM, 0.02 *M* octanesulfonic acid (pH 7.0) (30:70); flow-rate 1.0 ml/min; 0.5 AUFS; other conditions as in Fig. 1. (A) Column temperature 25°C. (B) Column temperature 0°C. (C) Column temperature - 10°C.

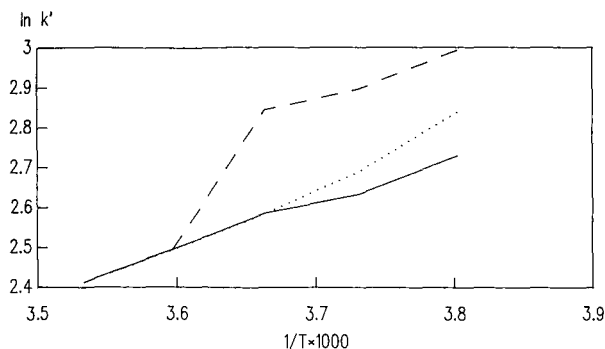


Fig. 4. Van 't Hoff plots for morphiceptin, showing variation of capacity factor ( $k'$ ) as a function of the reciprocal of absolute temperature. Mobile phase acetonitrile-0.05 M THAM, 0.02 M octanesulfonic acid (pH 7.0) (25:75); other conditions as in Fig. 1. — = Peak 1; ... = peak 2; --- = peak 3.

sulfonate to improve separation of the isomers. The use of acetonitrile instead of methanol as the non-polar component of the mobile phase improved most separations. However, the column became plugged due to salt precipitation when this system was used with phosphate buffers at sub-zero temperatures. The substitution of trishydroxymethane (THAM) for phosphate eliminated this problem.

The separation of peptides containing the Arg residue is demonstrated in Fig. 3 for bradykinin. This peptide contains three proline residues and could occur in eight possible isomeric forms. The chromatograms show the appearance of additional peaks as the column temperature is reduced. It is not clear whether the absence of eight peaks is due to inability to separate the isomers or to the absence of some isomers due to low stability.

The effect of temperature on the capacity factor ( $k'$ ) was studied for morphiceptin and  $\beta$ -casomorphin. A graph of  $\ln k'$  vs. reciprocal of temperature (Fig. 4) demonstrates the effect of reduced temperature on the resolution obtained for the three isomers of morphiceptin. Note that as the temperature increases no resolution of the isomers is observed due to rapid interconversion. Good separation was attained at  $-10.0^\circ\text{C}$  with a mobile phase of 0.05 M THAM (pH 7.0), 0.02 M octanesulfonic

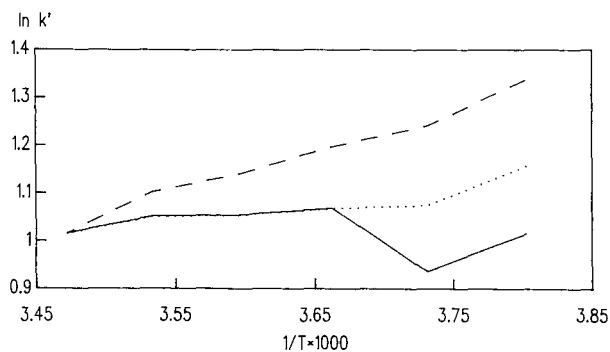


Fig. 5. Van 't Hoff plots for  $\beta$ -casomorphin. Conditions and lines as in Fig. 4.

TABLE II  
PERCENT ISOMER AS A FUNCTION OF SOLUTION pH FOR PHE-ALA-PRO

pH	% Isomer	
	Peak 1	Peak 2
3.08	46.9	53.1
4.01	32.6	67.4
5.01	28.8	71.2
5.95	28.5	71.5
6.98	27.2	72.8
7.94	23.7	76.3
8.90	20.9	79.1
9.94	20.4	79.6

acid-acetonitrile (75:25). The results of this study for  $\beta$ -casomorphin are shown in Fig. 5. Figs. 4 and 5 clearly demonstrate the variation in retention as a function of temperature for these two peptides. Such studies can also provide useful information about the hydrophobic character of the individual isomers.

#### Isomer composition vs. solution pH

Three peptides: Phe-Ala-Pro, bradykinin and morphiceptin, which had been separated most completely were chosen for a study of the effect of pH of the peptide sample on the amount of each isomer. These studies were conducted using the optimal mobile phase and temperature conditions. Eight peptide solutions, identical except for their pH were prepared, covering the pH range from 3.0 to 10.0. All peptide solutions contained *ca.* 0.5 mg/ml. Phe-Ala-Pro solutions were prepared in phosphate buffers, while the other two peptides were prepared with THAM.

*Phe-Ala-Pro.* Baseline separation of two peaks was obtained for Phe-Ala-Pro at 0°C with a mobile phase of 0.05 M phosphate (pH 7.0)-methanol (70:30). Excellent

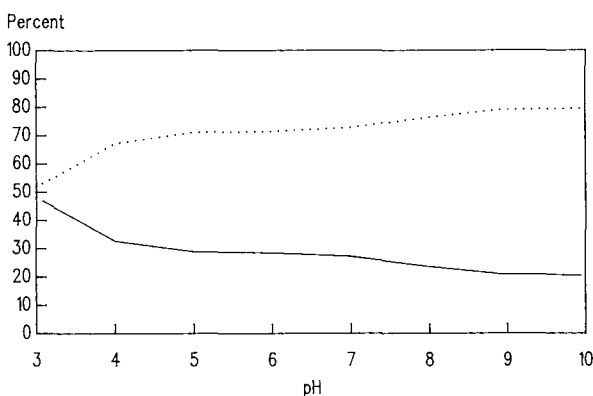


Fig. 6. Composition *cis*- and *trans*-isomers of Phe-Ala-Pro as a function of pH in 0.05 M phosphate solution at room temperature. Mobile phase, methanol-0.05 M phosphate (pH 7.0) (30:70); column temperature 0°C; flow-rate 1.0 ml/min; column and detector as in Fig. 1. Peak 1 is the *trans*-isomer (—), peak 2 the *cis*-isomer (· · ·).



TABLE III

## PERCENT ISOMER AS A FUNCTION OF SOLUTION pH FOR MORPHICEPTIN

Peak areas are based on the total area of the three peaks as 100%. A very small leading peak (retention time, 56 s) at low pH which could be the *cis-cis*-isomer is not included.

pH	% Isomer		
	Peak 1	Peak 2	Peak 3
3.06	31.8	47.4	20.8
3.87	32.5	44.6	22.9
5.06	38.5	42.3	19.2
6.02	37.4	45.9	16.7
6.98	35.5	50.0	14.5
7.95	23.3	65.7	11.0
8.92	21.7	67.8	10.6
9.98	20.5	70.2	9.3

separation was obtained for the eight peptide samples. The pH of each sample, covering a range of 3.08 to 9.94, is listed in Table II. A graph of percent isomer vs. pH for each Phe-Ala-Pro isomer is shown in Fig. 6. There is a significant shift in isomer composition from pH 3.08 to 9.94. Based on similar behavior for Ala-Pro previously reported, the first peak is assigned to the *trans*-isomer. It has been previously shown for similar aliphatic peptides that the *cis*-isomer predominates at high pH<sup>8</sup>.

*Morphiceptin*. The isomeric composition of morphiceptin solutions at various pH values are listed in Table III. A graph of percent isomer vs. pH, including all three peaks (Fig. 7) shows the trend of each peak over the entire pH range. Chromatograms for solutions of pH 3.87 and 6.98 are shown in Figs. 8 and 9, respectively. A significant change in the distribution of the area between the first two peaks is obvious from the chromatograms themselves.

The most significant change occurs at the interval between pH 6.98 and pH

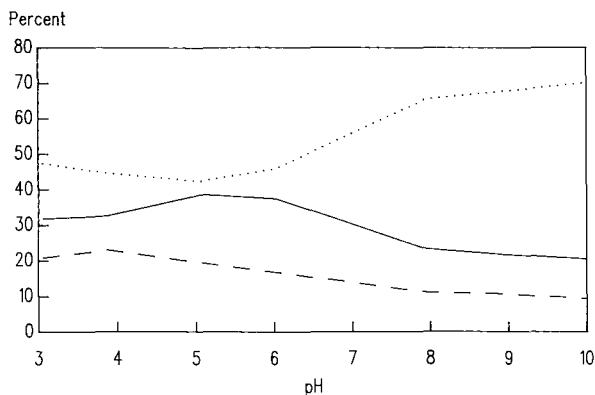


Fig. 7. Variation of morphiceptin isomers as a function of pH. Chromatographic conditions as in Fig. 8. Lines as in Fig. 4.

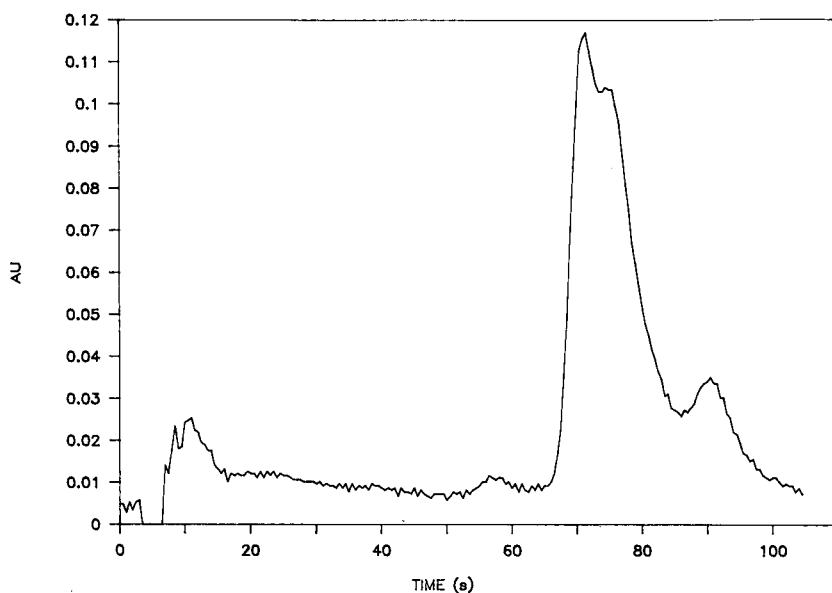


Fig. 8. Chromatogram of morphiceptin solution in 0.05 *M* THAM at pH 3.87. Column and detector as in Fig. 1. Mobile phase acetonitrile-0.05 *M* THAM, 0.02 *M* octanesulfonic acid (pH 7.0) (25:75); flow-rate 1.0 ml/min.

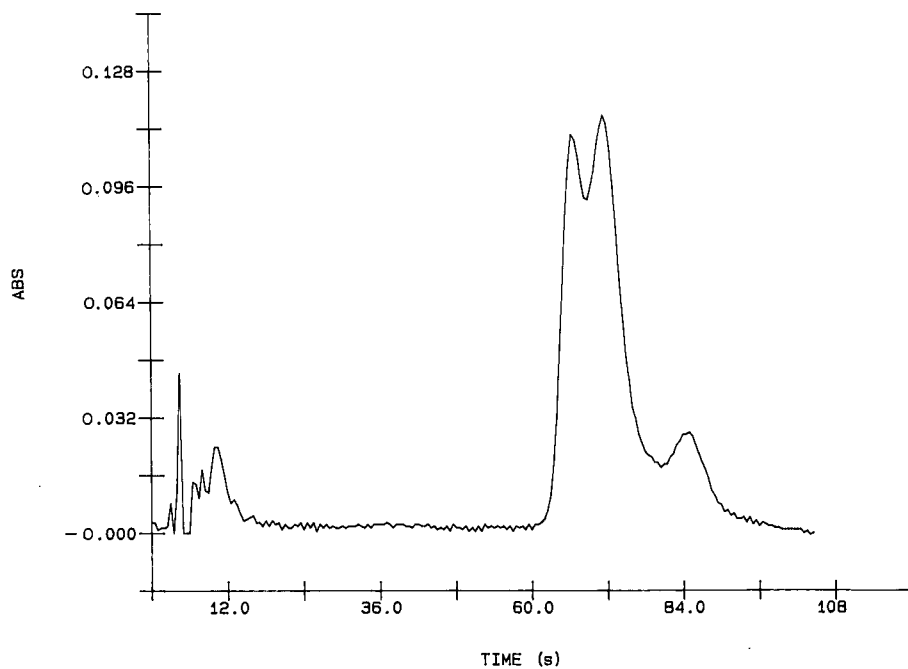


Fig. 9. Chromatogram of morphiceptin solution in 0.05 *M* THAM at pH 6.98. Chromatographic conditions as in Fig. 8.

7.95, as the first and second peak change by 12.2% and 15.7%, respectively. Thus, a large shift in the conformation of morphiceptin occurs at a biologically important pH range. Recent studies of morphiceptin and its analogues containing other amino acids to restrict conformational flexibility, indicate that the *cis-cis*-form is the biologically active form. This form is not quantitatively measured in the chromatograms, but the small first peak in Fig. 8 may be due to the *cis-cis*-isomer. The isomer ratios for the four peaks in Figs. 8 and 9 imply that the peaks can be assigned to the *cis-cis*-, *cis-trans*-, *trans-trans*- and *trans-cis*-isomers based on a comparison with NMR spectra. The first designation in each pair corresponds to the Tyr-Pro bond and the second to the Phe-Pro bond. The relative amounts of the four isomers reported in dimethyl sulfoxide solution were 7%, 23%, 56% and 14% for the *cis-cis*-, *cis-trans*-, *trans-trans*- and *trans-cis*-conformations respectively<sup>7</sup>. Further study of the peaks and isolation of individual peaks for spectroscopic study will be necessary to confirm the peak assignments.

#### CONCLUSIONS

There are broad implications of the present study for the entire area of protein and peptide separations. Secondary equilibrium effects due to conformational changes at proline residues can be expected in a large number of proteins and peptides, as the fractions of such molecules which contain at least one prolyl residue is large. The peak-broadening effects of these equilibria may represent a significant contribution to the overall band broadening observed for peptides and proteins. Several solutions to these separation problems are evident. The mobile phase can be selected to provide extreme conditions at which only a single conformation predominates. This will often result in separations which, while of higher efficiency for analytical purposes, have little relevance to the actual structure of the protein. A second alternative is to increase the temperature to accelerate attainment of equilibrium. Again, this approach will often destroy the biological activity and preclude the acquisition of conformational information. Finally, one can reduce temperature to preserve protein structure and attempt to deal with the multiple peaks produced. This approach produces the greatest amount of information about structural factors. The cost of this approach is a greater demand on the chromatographic column in terms of selectivity, particle diameters and pressure to cope with the high viscosity and slow diffusion rates at low temperatures. Clearly, the optimal approach will depend on the goals of the specific separation.

#### ACKNOWLEDGEMENTS

This work was supported by a grant from the Trinity College Faculty Research Committee.

#### REFERENCES

- 1 D. E. Henderson, S. J. Saltzman, P. C. Uden and Z. Cheng, *Polyhedron*, 7 (1988) 369.
- 2 D. E. Henderson and Cs. Horváth, *J. Chromatogr.*, 368 (1986) 203.
- 3 W. R. Melander, H.-J. Lin, J. Jacobson and Cs. Horváth, *J. Phys. Chem.*, 88 (1984) 4527.
- 4 J. Jacobson, W. R. Melander, G. Valsnys and Cs. Horváth, *J. Phys. Chem.*, 88 (1984) 4536.

- 5 W. R. Melander, J. Jacobson and Cs. Horváth, *J. Chromatogr.*, 234 (1982) 269.
- 6 T. Brauman, *J. Chromatogr.*, 373 (1986) 191.
- 7 M. A. Castiglione-Morelli, B. Hartrodt, K. Neubert, P. A. Temussi and E. Trivellone, *Biochem. Biophys. Res. Commun.*, 152 (1988) 512.
- 8 C. A. Evans and D. L. Rabenstein, *J. Am. Chem. Soc.*, 96 (1974) 7312.

CHROM. 21 987

## REVERSED-PHASE CHROMATOGRAPHIC BEHAVIOR OF PROTEINS IN DIFFERENT UNFOLDED STATES<sup>a</sup>

SHIWEN LIN and BARRY L. KARGER\*

*Barnett Institute of Chemical Analysis and Department of Chemistry, Northeastern University, Boston, MA 02115 (U.S.A.)*

---

### SUMMARY

A series of standard small globular proteins in different unfolded states was studied by gradient reversed-phase liquid chromatography. The retention parameters  $Z$  [slope of log capacity factor ( $k'$ ) vs. log molar concentration of organic modifier, 1-propanol, in the mobile phase] and  $I$  (the value of log  $k'$  at 1  $M$  1-propanol) were derived from gradient retention data. Each protein in four different conformational states, *i.e.*, folded, chromatographic surface-unfolded, urea-unfolded and disulfide-bridge reduced-unfolded, showed a variation of 10-fold in  $Z$  and up to  $10^{1.2}$ -fold in  $I$  values. For the different states of all the proteins studied, the order of  $Z$  and  $I$  values was as follows: folded  $\ll$  surface-unfolded  $<$  urea-unfolded  $<$  reduced-unfolded. The differences in the values of the coefficients suggest, in agreement with literature reports, that proteins with their disulfide bridges cleaved have the largest degree of unfolding. In addition, the  $Z$  and  $I$  values and solution refolding kinetics all suggest that chromatographic surface-unfolded proteins have a lower degree of unfolding than their urea-unfolded forms. It was also found that an additional chemical cross-link in lysozyme caused a significant decrease in the first-order rate constant of the surface-induced unfolding process.

---

### INTRODUCTION

Currently reversed-phase liquid chromatography (RPLC) plays an important role in the analysis of peptides and proteins. This significance has prompted numerous studies aimed at a better understanding of the retention process of these biopolymers in order to optimize separations<sup>1–4</sup>. Despite some differences between the RPLC behavior of proteins and low-molecular-weight molecules, recent experience indicates that linear solvent strength (LSS) gradient elution theory developed for simple organic molecules can also be used to characterize the retention behavior of proteins<sup>5</sup>.

The LSS model is based on the fact that the retention of solutes in RPLC can be

---

<sup>a</sup> Dedicated to Professor Csaba Horváth on the occasion of his 60th birthday. A dear and loyal friend and an outstanding scientist.

approximated by a logarithmic relation between the capacity factor ( $k'$ ) and volume fraction ( $\varphi$ ) of organic solvent in the mobile phase:

$$\log k' = \log k'_0 - S\varphi \quad (1)$$

where  $k'_0$  is the extrapolated capacity factor at zero volume fraction of the organic modifier. The slope  $S$ , which is dependent on the organic modifier and the specific solute, can be used to predict gradient retention time and band width<sup>6</sup>. For proteins, the plot of  $\log k'$  vs.  $\varphi$  is generally very steep yielding a large value of  $S$ . In addition, it has been found that the  $S$  value is in part related to the size and contact area of the protein molecule.

Based on ion-exchange chromatography, Geng and Regnier<sup>2</sup> have developed a displacement model for retention in RPLC which can be described by the following equation:

$$P_m + ZM_a \rightleftharpoons P_a + ZM_m \quad (2)$$

where  $P$  stands for protein,  $M$  for organic solvent,  $Z$  is the number of organic solvent molecules needed to displace the adsorbed protein from the surface, and subscripts  $m$ ,  $a$  represent mobile and adsorbed states, respectively. Based on this displacement model, retention can be written as

$$\log k' = \log I - Z \log [D_0] \quad (3)$$

where  $[D_0]$  is the molar concentration of the organic modifier and  $I$  the value of  $k'$  at  $[D_0] = 1 M$ .

Assuming a constant amount of organic solvent adsorbed (imbibed) to the bonded phase and a constant activity coefficient of the organic modifier in the mobile phase as  $D_0$  is varied,  $Z$  can be used as a measure of the contact area of the adsorbed protein. In addition,  $I$  represents a measure of the relative binding strength of individual proteins under a fixed mobile phase composition. From the relation of molar concentration  $[D_0]$  and volume fraction  $\varphi$ ,  $Z$  can be related to  $S$  by the expression<sup>7</sup>

$$Z = 2.3\varphi S \quad (4)$$

Determination of  $S$  and  $k'_0$  from the gradient retention data thus permits calculation of  $Z$  and  $I$ .

The stoichiometric parameters  $S$  and  $Z$  have been shown to be related to protein molecular weight in RPLC; however, different dependencies have been found as a function of the extent of denaturation under the mobile phase conditions. For example, Stadalius *et al.*<sup>8</sup> examined values of  $S$  vs. molecular weight (MW) from several studies and obtained a relationship of  $S \approx (\text{MW})^{0.44}$ . On the other hand, Geng and Regnier<sup>2</sup> found that  $Z$  was linearly dependent on the protein molecular weight, when a strong denaturing mobile phase [formic acid–isopropanol (60:40)] was used. Aguilar *et al.*<sup>9</sup> have also reported  $S$  values for peptides and found significant scatter in the  $S$  vs. molecular weight correlation. The variable dependence of  $S$  and  $Z$  on the

molecular weight of proteins implies different degrees of unfolding of proteins on the chromatographic surface.

It is well-known that proteins can alter conformation on chromatographic surfaces, resulting in changes in retention, sometimes with broad asymmetrical peaks<sup>10</sup>, or multiple peaks<sup>4,11,12</sup>. It is a general rule that water-soluble peptides and proteins adsorbed on hydrophobic surfaces elute later in an unfolded form than in a folded conformation. Moreover, the *S* and *Z* values for various states of unfolding of a protein could be significantly different<sup>7,13</sup>. It is now recognized that *Z* values of proteins in RPLC are determined in large part by the hydrophobic contact area or the number of the interaction sites established between the solute and the stationary phase during the adsorption process. The hydrophobic contact area is, in turn, dependent on the conformation of the protein on the chromatographic surface.

To date, no direct measurement of *Z* or *S* values for proteins in the native (or folded) conformation on a reversed-phase column has been reported. Previous work from this laboratory<sup>4,14</sup> has shown that on a short alkyl ( $C_4$ ) bonded silica gel column with 1-propanol as organic modifier and at low temperature (4°C), a number of proteins yielded two well-separated peaks corresponding to the folded and an unfolded conformation, respectively. The conversion of the folded conformation to an unfolded one allowed the measurement of the first-order unfolding kinetics of several proteins on the  $C_4$  bonded phase surface<sup>14</sup>.

This paper examines the behavior of proteins in various conformational states on a  $C_4$  reversed-phase column and correlates *Z* and  $\log I$  values to the extent of unfolding of the protein on the chromatographic surface. The values were derived from gradient elution data generated by varying gradient time. Multiple peaks corresponding to different conformational states of proteins were observed, and the parameters of these conformations were determined within the same gradient run. In addition, chemical cross-links were incorporated into the protein molecules, and the chromatographic behavior of these more rigid species was examined. Solution refolding and surface unfolding kinetics were also measured to provide further information on the changes of solute structure within the chromatographic column.

## EXPERIMENTAL

### *Equipment*

The chromatographic system consisted of two Altex 110A pumps with an Altex 420 system control programmer (Beckman, San Ramon, CA, U.S.A.), a fast-scan photodiode array detector (Hewlett Packard, Palo Alto, CA, U.S.A.) and a Model 7125 syringe loading sample injector containing a 20- $\mu$ l loop (Rheodyne, Cotati, CA, U.S.A.). The chromatograms were collected and stored in an HP 9000 workstation (Hewlett Packard) through HP 7996A operating software (Hewlett Packard).

The  $C_4$  reversed-phase packing material was made using standard bonding procedures<sup>14</sup>. Vydac silica (5.6  $\mu$ m, 300 Å, 64 m<sup>2</sup>/g) (Separations Group, Hesperia, CA, U.S.A.) was bonded with *n*-butyltrimethoxysilane (Petrarch Systems, Bristol, PA, U.S.A.). The  $C_4$  ligand density was determined by elemental analysis to be 7.1  $\mu$ mol/m<sup>2</sup>, assuming a bonding stoichiometry of two methoxy groups. The 10 cm  $\times$  4.6 mm I.D. column was slurry packed in 1-propanol–methanol (30:70, v/v) with methanol as driving solvent.

The column temperature was maintained within  $\pm 0.5^\circ\text{C}$  by immersing the injector, the column, and the tubing connecting the mobile phase mixer to the inlet of the column in a thermostated water bath (Neslab, Newington, NH, U.S.A.). Mobile phase A was either 0.5% 1-propanol in 10 mM  $\text{H}_3\text{PO}_4$ , pH 2.1, 2% 1-propanol in 10 mM  $\text{H}_3\text{PO}_4$  or 2% 1-propanol in 1 mM hydrochloric acid, pH 3.0 and mobile phase B was either 45% 1-propanol in 10 mM  $\text{H}_3\text{PO}_4$ , pH 2.1 or 45% 1-propanol in 1 mM hydrochloric acid, pH 3.0. The mobile phases were degassed with helium during all the experiments to remove oxygen dissolved in the solvent. Linear gradients from mobile phase A to B in various gradient times with a flow-rate of 1.0 ml/min were used for the measurement of  $S$ . For the determination of the refolding kinetics of ribonuclease A, the flow-rate was varied in the same proportion as the gradient time to maintain the gradient volume constant, see ref. 15.

### Reagents

All proteins used in this study were obtained from Sigma (St. Louis, MO, U.S.A.) in the highest available grade and used as received. The proteins and their biological origin are as follows: papain (papaya latex, type IV), lysozyme (chicken egg white, grade I),  $\alpha$ -chymotrypsinogen A (bovine pancreas, type II), myoglobin (horse skeletal muscle, type I) and ribonuclease A (bovine pancreas, type IIIA). Reagent-grade phosphoric acid, 1-propanol, and other reagents were obtained from J. T. Baker (Phillipsburg, NJ, U.S.A.).

### Preparation of protein samples

The urea-denatured protein samples were prepared as follows: 2.5 mg/ml protein solutions in 8 M urea were heated to  $90^\circ\text{C}$  for 2–5 min and cooled to  $5^\circ\text{C}$  before injection. The disulfide-bond reduced protein samples were prepared using a standard method from the literature<sup>16</sup>. In particular, a 5-mg/ml protein solution in 8 M urea was incubated overnight with 0.3 M mercaptoethanol at  $25^\circ\text{C}$ . Before injection, each of the solutions was diluted two-fold with water to obtain the reduced protein sample in a final concentration of 2.5 mg/ml.

Lys(7)–Lys(41) (intramolecular) cross-linked ribonuclease A was prepared using the method of Lin *et al.*<sup>17</sup>. Ribonuclease A (55 mg) was dissolved in 100 ml of 50 mM Tris–HCl buffer (pH 8.5). A 10-ml volume of 2,4-difluoro-1,3-dinitrobenzene in methanol–water (2:98) was added at a rate of 0.02 ml/min while the solution was stirred in the dark at room temperature. The solution was stirred for 20 h, and the reaction was quenched by adding hydrochloric acid to reach pH 2. The reaction mixture was then desalted and concentrated on an ultracentrifugation cell, Prep-10, (Amicon, Danvers, MA, U.S.A.) to a final concentration of about 2.5 mg/ml.

Glu(35)–Trp(108) cross-linked lysozyme was prepared by following the procedure of Imato *et al.*<sup>18</sup>. Lysozyme (20 mg/ml) was oxidized with  $\text{I}_2$  (0.6 mol  $\text{I}_2$  per mol of protein) for 7 h at room temperature. The reaction mixture was then applied to a 90 cm  $\times$  4 cm I.D. CM-Sephadex C-25 column, equilibrated with 0.05 M sodium borate–0.05 M sodium carbonate buffer, pH 10, and eluted with a ten-step gradient over 2 l of solution from 0.02 to 0.1 M sodium chloride in the same buffer. The last eluting component corresponding to the ester bond cross-linked lysozyme between the carboxyl group of Glu(35) and the indole C-2 of Trp(108) was collected and concentrated to roughly 2.5 mg/ml before use.



## RESULTS AND DISCUSSION

*Derivation of Z and log I from gradient data*

Operating under linear-solvent strength (LSS) conditions, the relationship between the instantaneous capacity factor  $k'$  and time  $t$  in a gradient elution can be expressed as:

$$\log k' = \log k'_0 - b(t/t_0) \quad (5)$$

where  $b$  is the gradient steepness parameter and  $t_0$  is the migration time of the unretained species through the column. The gradient retention time ( $t_g$ ) can be derived from eqn. 5 (see ref. 6) as:

$$t_g = (t_0/b)\log(2.3bk'_0 + 1) + t_0 + t_D \quad (6)$$

in which  $t_D$  is the gradient delay time, *i.e.*, the time needed for the mobile phase to travel from the mixer to the inlet of the column. The gradient steepness parameter  $b$  is related to important gradient and solute parameters as

$$b = \frac{t_0 \Delta\varphi S}{t_G} \quad (7)$$

where  $\Delta\varphi$  is the gradient range, *i.e.*, the difference in the volume fraction of the organic modifier from the start to the end of the gradient and  $t_G$  is the gradient time. By substituting eqn. 7 into eqn. 6 and assuming  $2.3bk'_0 \gg 1$ , we can obtain an expression of

$$\frac{t_g - t_0 - t_D}{t_G} = -\frac{1}{S\Delta\varphi} \log t_G + \frac{1}{S\Delta\varphi} \log(2.3S\Delta\varphi t_0 k'_0) \quad (8)$$

Since  $S$  is independent of  $t_G$ , a plot of  $(t_g - t_0 - t_D)/t_G$  vs.  $\log t_G$  will yield a straight line of slope  $1/S\Delta\varphi$ . The values of  $S$  and  $k'_0$  can then be determined from the slope and intercept of the plot. This method is similar to that based on two gradient runs<sup>19</sup>.

The solvent displacement stoichiometric parameter  $Z$  can be derived from the corresponding  $S$  value by the use of eqn. 4:

$$Z = 2.3\bar{\varphi}S \quad (9)$$

where

$$\bar{\varphi} = \varphi_0 + (t_g - t_0 - t_D - 0.3 \frac{t_G}{\Delta\varphi S}) \frac{\Delta\varphi}{t_G} \quad (10)$$

and  $\bar{\varphi}$  is the value of volume fraction of the organic solvent as the solute band passes the center of the column and  $\varphi_0$  is the volume fraction at the start of the gradient. For 1-propanol,  $[D_0] = 1 M$  at  $\varphi = 0.075$ . The binding strength,  $\log I$ , can then be determined by calculating  $\log k'$  at this volume fraction in eqn. 1 from corresponding  $S$  and  $\log k'_0$  values.

*Z and log I for folded and unfolded states*

The gradient elution chromatograms for four proteins, papain (PAPN), lysozyme (LYSO),  $\alpha$ -chymotrypsinogen A (CHTG), and myoglobin (MYOG) are shown in Fig. 1. As described before<sup>4,14</sup>, the first peak for PAPN, LYSO and CHTG are ascribed to the folded state of these proteins, and the second peak to an unfolded state. By lengthening the contact time of each protein with the stationary phase, the area of the second peak increased at the expense of the first peak.

It is interesting to note that the first eluted peak of PAPN, LYSO and CHTG could not be observed with the gradient of Fig. 1 using a C<sub>8</sub> bonded phase column of the ligand density of 4.6  $\mu\text{mol}/\text{m}^2$ . Evidently, the hydrophobicity of the C<sub>8</sub> phase was sufficient to unfold the proteins rapidly at 5°C. In addition, even on the C<sub>4</sub> bonded phase column, the first peak for CHTG could only be substantially seen when a less acidic (pH  $\geq$  3.0) mobile phase was used. Therefore, in Fig. 1, a mobile phase of pH 3 was used for CHTG to obtain a sufficient amount of the folded conformation. These results emphasize that both the stationary and the mobile phase contribute to the unfolding of proteins on the adsorbent surface.

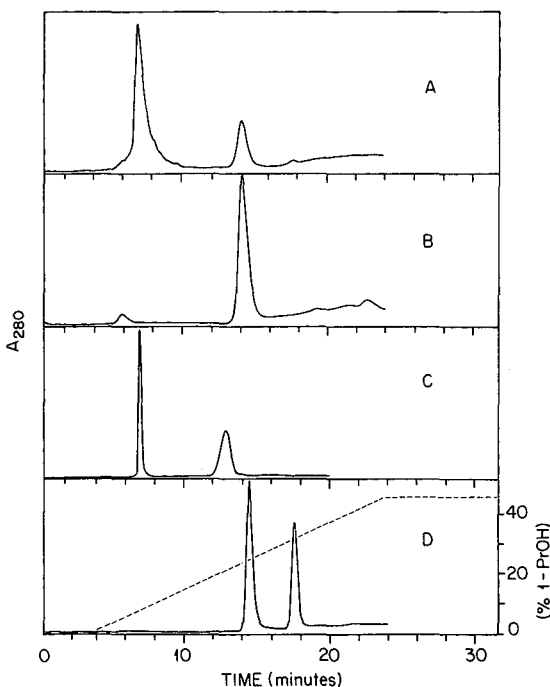


Fig. 1. Reversed-phase chromatographic behavior of (A) papain (PAPN), (B)  $\alpha$ -chymotrypsinogen A (CHTG), (C) lysozyme (LYSO) and (D) myoglobin (MYOG). Column: 10 cm  $\times$  4.6 mm I.D., C<sub>4</sub> bonded phase on Vydac silica (5.6  $\mu\text{m}$ , 300  $\text{\AA}$ ). Sample: 2.5 mg/ml protein in HPLC-grade water, 20  $\mu\text{l}$  injection. Mobile phase A: 0.5% 1-propanol in 10 mM H<sub>3</sub>PO<sub>4</sub>, pH 2.1 (LYSO), 2% 1-propanol in 10 mM H<sub>3</sub>PO<sub>4</sub>, pH 2.1 (PAPN, MYOG), 2% 1-propanol in 1 mM hydrochloric acid, pH 3.0 (CHTG). Mobile phase B: 45% 1-propanol in 10 mM H<sub>3</sub>PO<sub>4</sub>, pH 2.1 (LYSO, PAPN, MYOG), 45% 1-propanol in 1 mM HCl, pH 3.0 (CHTG). Gradient time: A to B in 20 min. Flow-rate: 1.0 ml/min. Column temperature: 5°C. 1-PrOH = 1-Propanol.

It is also to be noted that the first peak of MYOG was eluted at a time corresponding to the unfolded peaks of other proteins and the second peak was eluted even later. The on-line UV spectrum collected from the photodiode array detector identified the second peak as the prosthetic heme group ( $\lambda_{\max} = 400$  nm) released from myoglobin upon unfolding and the first peak as apomyoglobin (APMY) ( $\lambda_{\max} = 280$  nm). This result is consistent with that found by others<sup>12</sup>.

Plots of  $(t_g - t_0 - t_D)/t_G$  vs.  $\log t_G$  for each folded and unfolded state of the above proteins were linear ( $r^2 \geq 0.98$ ). The values of  $S$  and  $\log k'_0$  were derived from the slope and intercept of these plots, with the relative standard deviation of 10% ( $n = 6$ ). Care was also taken to avoid potential errors in accuracy<sup>19</sup>. From  $S$  and  $\log k'_0$ , the values of  $Z$  and  $\log I$  were determined as described previously. Table I presents these latter values along with  $S$  in order to compare with the results of other workers who reported this coefficient<sup>8,9</sup>.

Before proceeding, it is useful to note that while the displacement model has been shown to be applicable to RPLC<sup>2</sup>, it does require that the adsorbed amount of the organic modifier on the bonded phase be maintained approximately constant over the whole mobile composition range of interest. Since the range over which the different conformational states of the solutes elute is between roughly 5 and 25% (v/v)

TABLE I

Z, S AND LOG I VALUES OF PROTEINS IN DIFFERENT CONFORMATIONAL STATES

For chromatographic conditions, see Fig. 1.

Proteins and states	MW	Z	S	log I
Heme	618			
In water		10 ± 1 <sup>a</sup>	17 ± 1	2.3 ± 0.3
In urea		10 ± 1	17 ± 1	2.3 ± 0.3
RNase A	13 000			
Surface-unfolded		11 ± 1	36 ± 4	2.5 ± 0.7
Urea-unfolded		16 ± 2	38 ± 4	4.9 ± 0.4
Disulfide-reduced		21 ± 3	44 ± 4	7.0 ± 0.7
LYSO	14 300			
Folded		2.6 ± 0.1	25 ± 2	-0.6 ± 0.2
Surface-unfolded		20 ± 1	46 ± 3	4.9 ± 0.6
Disulfide-reduced		35 ± 3	57 ± 5	11.6 ± 1.2
APMY	17 000			
Surface-unfolded		22 ± 2	45 ± 4	6.5 ± 1.1
Urea-unfolded		34 ± 1	52 ± 5	11.2 ± 1.2
PAPN	21 000			
Folded		4.3 ± 0.1	26 ± 2	-0.3 ± 0.3
Surface-unfolded		23 ± 1	43 ± 2	6.1 ± 0.5
Urea-unfolded		33 ± 3	53 ± 5	10.7 ± 1.1
CHTG	25 000			
Folded		3.9 ± 0.3	34 ± 2	-1.3 ± 0.1
Surface-unfolded		27 ± 2	53 ± 5	7.9 ± 1.1
Urea-unfolded		38 ± 3	61 ± 5	9.6 ± 0.1

<sup>a</sup> ± Standard deviation ( $n = 6$ ).

propanol, some change in the amount of adsorbed or imbibed propanol may be expected. Consequently, the  $Z$  values for different conformational states should be viewed in a qualitative fashion, rather than as quantitative differences in contact area.

As can be seen from Table I, the prosthetic heme group has a much smaller  $Z$  value ( $Z = 10$ ) than the unfolded parent protein APMY ( $Z = 22$ ). This result is expected when the differences in the sizes of the two species are considered. On the other hand, compared to small peptides in the same molecular weight range (MW  $\approx 600$ )<sup>8</sup>, the  $Z$  (or  $S$ ) value for heme is still large. This is undoubtedly due to the relatively large contact area of the porphyrin moiety with the hydrophobic surface.

It is interesting to note that the  $S$  values for the unfolded conformation of PAPN, LYSO and CHTG are above 40 and are close to the values reported by others<sup>8</sup> for these particular proteins under more unfolding-favored conditions ( $C_8$ -bonded silica as stationary phase, and/or acetonitrile as organic solvent at room temperature). By using less destabilizing conditions ( $5^\circ\text{C}$ ,  $C_4$ -bonded stationary phase, 1-propanol), we were able to maintain both unfolded and folded conformations of these proteins in the chromatographic process.

Table I shows that the  $Z$  and  $\log I$  values for each of the folded proteins are much smaller than those for the corresponding unfolded species. Low  $Z$  values have also been found in hydrophobic interaction chromatography (HIC) of proteins under mild conditions<sup>13</sup>. The results demonstrate that proteins adsorbed in a folded conformation have less contact area with the hydrophobic surface than in the unfolded state. In the folded form, the proteins appear to act as weakly binding small molecules. When the protein unfolds on the surface, the contact area increases, leading to stronger binding and an increase in the values of each of the parameters.

It is also interesting to note in Table I that the  $I$  values for the folded proteins are only in the range of 0.05–0.5 and are  $10^{11}$ – $10^{12}$  times smaller than the  $I$  values for unfolded proteins. This substantial difference in binding strength for the two conformers emphasizes the important point that the chromatographic surface can act as a means of amplifying structural differences in macromolecules. Finally, it is seen that the  $I$  values for the folded proteins are even smaller than that of heme, a small molecule. The reason for this result, in spite of the larger  $S$  values for the folded proteins, is probably due to the quite hydrophobic porphyrin moiety of heme.

#### *Urea-unfolded and reduced-unfolded states*

In order to investigate further the relationship of  $Z$  and  $\log I$  to the conformation of the protein on the chromatographic surface, we next measured the appropriate values for urea-unfolded and disulfide-reduced proteins. Fig. 2 presents the chromatograms for the urea-unfolded proteins (PAPN, CHTG and MYOG) obtained under the same column conditions as in Fig. 1. The  $Z$  and  $\log I$  values are listed in Table I. (For urea-treated LYSO, a complex elution pattern was observed and measurements were not possible.) Note in Fig. 2 that the first peak corresponding to the folded form does not appear in the elution profile of the urea-treated PAPN and CHTG, and the second peak corresponding to the unfolded form is shifted to longer retention. Note also that the urea-unfolded APMY appeared as a broader peak with larger retention than the surface-unfolded APMY.

As can be seen from Table I, the  $Z$  values were larger for each of the urea-unfolded proteins (PAPN, CHTG and APMY) than for their surface-unfolded

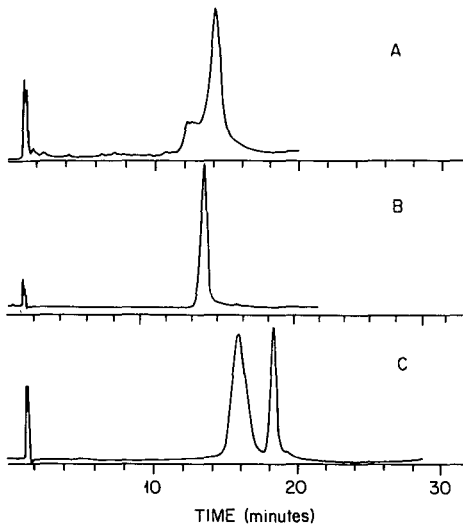


Fig. 2. Chromatographic behavior of urea-unfolded proteins. (A) PAPN; (B) CHTG; (C) MYOG. Conditions are same as in Fig. 1.

form. On the other hand, as expected, the values for heme did not change with the urea treatment. The above results suggest that the urea-treated proteins are more unfolded and adsorb on the chromatographic surface with a larger contact area than the surface-induced unfolded state of these proteins. It is important from the separation point of view to recognize that urea can alter the conformation and retention of proteins, although at times complex peak shape can be observed<sup>20</sup>.

The next step was to investigate the influence of disulfide bonds on the adsorption behavior of these globular proteins on the C<sub>4</sub> reversed-phase support. Upon reduction of the disulfide bridge(s), proteins can be completely unfolded to a random coil structure. For LYSO, the reduced species was eluted later in the gradient than the surface-unfolded species and with larger *Z* and log *I* values, see Fig. 3. The

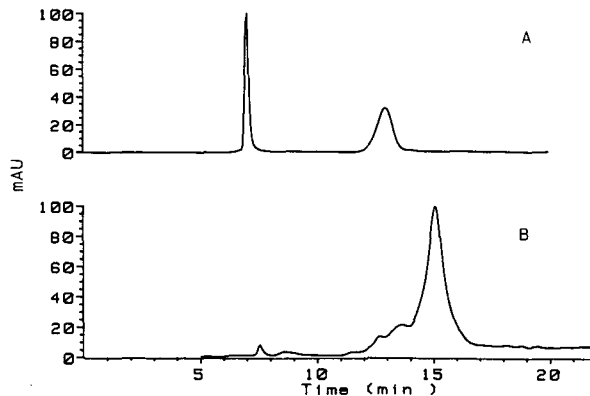


Fig. 3. Chromatographic behavior of (A) LYSO and (B) reduced LYSO. Conditions are same as in Fig. 1C.

longer retention of the reduced LYSO is in agreement with other published results<sup>21</sup>, in which it is suggested that the stronger interaction is due to the more exposed hydrophobic residues on the protein.

Ribonuclease A (RNase A) is another well-defined globular protein. Injection of urea-denatured and disulfide reduced RNase A yielded similar peak shapes to that of the unmodified RNase A shown previously<sup>15</sup>, although the retention for the former two species was longer (see Fig. 4). In agreement with earlier results<sup>10</sup>, the on-line absorbance ratio determined at 288 and 254 nm ( $A_{288}/A_{254}$ ) for the folded conformation of RNase A was close to unity whereas the ratio was less than one for an unfolded state. The  $A_{288}/A_{254}$  for each of the late eluted peak maxima of Fig. 4A-C, was found to be 0.55, 0.50 and 0.69, respectively. On the other hand, the  $A_{288}/A_{254}$  ratio measured at the maxima of each of the early eluting shoulders was 0.91, 0.88 and 0.71, respectively. These absorbance ratios suggest that the late eluted peak of each of the RNase A samples corresponds to an unfolded conformation<sup>10</sup>. The shoulder in the case of the urea-unfolded RNase A (see Fig. 4B), in analogy to the surface unfolded results, is assumed to be the refolded form.

It is known that unfolded RNase A can gradually refold in solution once the denaturant is removed or diluted<sup>22</sup>. In the present case, the denaturant urea was washed away from the adsorbed RNase A at the beginning of the chromatographic process and the conformational stress of the hydrophobic surface was released upon desorption. Therefore, favorable conditions existed for RNase A to refold in the mobile phase upon desorption. However, the shoulder in the case of reduced RNase A (see Fig. 4C) had an  $A_{288}/A_{254}$  ratio similar to that of the major peak. While not proven, it is possible that this shoulder may represent an intermediate in the refolding pathway of the reduced RNase A. More work is required to identify this band in Fig. 4C.

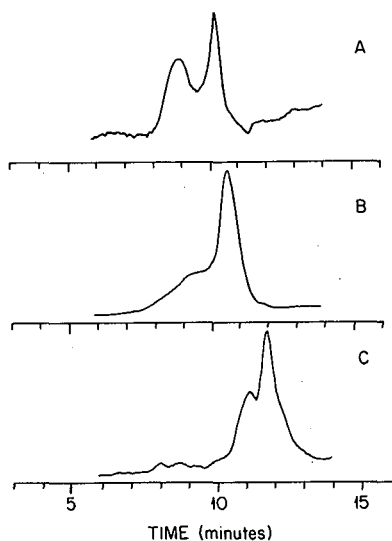


Fig. 4. Chromatographic behavior of (A) RNase A; (B) urea-unfolded RNase A; (C) reduced RNase A. Conditions are same as in Fig. 1C.

The results of  $Z$  and  $\log I$  reveal a similar pattern for RNase A as that of the other proteins studied. The urea-unfolded form had larger  $Z$  and  $\log I$  values than the surface-unfolded form, supporting the argument that urea unfolds the protein to a larger extent with a resultant larger contact area and stronger interaction with the stationary surface. The even larger  $Z$  and  $\log I$  values of the reduced-unfolded RNase A indicate that the reduced species is the most unfolded with the largest contact area. From the results with all the above studied proteins, the order of binding strength for different states can be summarized as: folded  $\ll$  surface-unfolded  $<$  urea-unfolded  $<$  reduced-unfolded.

#### *Effect of additional cross-link on surface unfolding*

In contrast to the reduction of the internal disulfide bridges, modification of proteins with additional cross-links would be expected to yield a more rigid structure with restricted conformation. Two well-characterized cross-linked proteins—dinitrophenyl cross-linked [Lys(7)–Lys(41)]RNase A and the ester bond cross-linked [Glu(35)–Trp(108)]LYSO—were used in this study. X-Ray crystallographic studies have shown that the dinitrophenyl cross-link in the 7–41 positions of RNase A is blocked in the enzymatic pocket<sup>23</sup>. Furthermore, the ester bond cross-link between the carboxyl of Glu(35) and the indole C-2 of Trp(108) in the 35–108 positions of LYSO is also buried in the cleft of this enzyme<sup>18</sup>. The three-dimensional structures of these cross-linked proteins are almost identical to their corresponding intact folded structures except for a very small movement of the two cross-linked residues.

The  $Z$  and  $\log I$  values for the cross-linked and unmodified LYSO and RNase A are listed in Table II. For LYSO, there is essentially no difference in the values for the two folded species. Evidently, the cross-link in the active site cleft does not influence the surface position of contact which is believed to be opposite the catalytic site<sup>24,25</sup>. However, in the unfolded state there is a small but meaningful difference in the two forms, with the species with the extra cross-link displaying a smaller  $Z$  and  $I$  value, as might be expected<sup>21</sup>. In agreement with these results, Perry and Witzel<sup>26</sup> have recently found that T<sub>4</sub>-lysozyme engineered with an additional disulfide bridge eluted earlier than its non-cross linked mutant on a C<sub>8</sub> reversed-phase column.

For RNase A, the unfolded forms of the two species reveal identical  $Z$  and  $I$  values. Only when the reduced forms are compared is a significant difference observed between the two species. Four disulfide bridges in RNase A were destroyed upon reduction, while the artificial Lys(7)–Lys(41) cross-link remained in the reduced (7–41) RNase A. This cross-link restricted the unfolding and reduced the contact area of (7–41)RNase A with the stationary phase, resulting in a smaller value of  $Z$  and  $I$ .

The results of Table II suggest that in certain cases it may not be possible to observe differences in folded forms of protein variants where disulfide scrambling takes place. Sometimes examining the surface-unfolded forms may be helpful (LYSO), but this is not always true (RNase A). Another sensitive approach is to determine the rate of surface unfolding or solution refolding upon desorption. Kinetic parameters can prove to be highly useful in characterizing variants as shown in the following sections.

#### *Surface unfolding kinetics of cross-linked LYSO*

In order to study the effect of a cross-link in protein molecules on the

TABLE II

Z, S AND I VALUES vs. NUMBER OF CROSS-LINKS OF PROTEINS

For chromatographic conditions, see Fig. 1.

Protein	Cross-links	Z	S	log I
Folded (35-108)LYSO	5	2.5 ± 0.1	22 ± 2	-0.3 ± 0.1
Folded LYSO	4	2.6 ± 0.1	25 ± 2	-0.6 ± 0.2
Unfolded (35-108)LYSO	5	16 ± 1	40 ± 4	4.6 ± 0.7
Unfolded LYSO	4	20 ± 1	45 ± 4	4.9 ± 0.6
(7-41)RNase A	5	10 ± 1	34 ± 2	2.6 ± 0.7
RNase A	4	11 ± 1	36 ± 2	2.5 ± 0.7
Reduced (7-41)RNase A	1	16 ± 1	39 ± 1	3.0 ± 1.1
Reduced RNase A	0	21 ± 3	44 ± 2	4.5 ± 0.7

surface-induced unfolding kinetics, we measured chromatographically the first-order unfolding rate constant of the cross-linked (35-108)LYSO as well as that of LYSO. As previously<sup>14</sup>, the area of the first peak, corresponding to the concentration of the folded conformation, decreased with contact time of the protein with the chromatographic surface. The area of the second peak correspondingly increased. By following the reduction in the area of the first peak with on-column incubation time, the first-order unfolding rate constant  $k_u$  could be determined<sup>14</sup>. At 20°C the first order unfolding rate constant was found to be  $9.1 \cdot 10^{-4} \text{ s}^{-1}$  for the cross-linked (35-108)LYSO and  $6.7 \cdot 10^{-3} \text{ s}^{-1}$  for unmodified LYSO. The significantly slower unfolding rate constant for the cross-linked LYSO variant corresponds to a higher activation energy of 1.2 kcal/mol. A solution study of (35-108)LYSO in 1-propanol-water (4.6 M or 35%) also showed that the cross-linked LYSO was more stable towards thermal unfolding<sup>23</sup>. Since the Glu(35)-Trp(108) cross-link spans the catalytic cleft of LYSO<sup>18,27</sup>, it is reasonable to conclude that the opening of this cleft is part of the unfolding process on the surface.

The assumption that the Glu(35)-Trp(108) region participates in the unfolding process is also in agreement with the results of chromatographic and surface spectroscopic studies. Using a series of lysozymes obtained from different biological species, it was shown, as already noted, that the protein adsorbed on a hydrophobic patch that is on the opposite side of the catalytic cleft<sup>24</sup>. The same conclusion was arrived at with computer modeling of the hydrophobic sites on the surface of LYSO<sup>25</sup>, and the on-column intrinsic fluorescence of LYSO on a C<sub>4</sub> reversed-phase surface also suggested the opening of the catalytic cleft<sup>28</sup>. The cross-linking of Glu(35) and Trp(108) restricted the opening of the cleft and therefore increased the activation energy of the unfolding process.

Based on these results, the kinetics of surface unfolding may be a useful tool for evaluating protein conformation resulting from cross-linking. In particular, it may be possible to differentiate in a sensitive manner species that have formed incorrect disulfide bridges. In combination with retention patterns<sup>7</sup>, the surface unfolding kinetics as determined by chromatography or by on-line intrinsic fluorescence of adsorbed species may represent a powerful analytical approach.



*Refolding kinetics of RNase A upon desorption*

As noted in Fig. 4, the shoulder for urea-denatured RNase A was lower than that of surface-unfolded RNase A. Since on-line spectroscopy revealed that in both cases the shoulder was due to refolding in the mobile phase upon desorption, the first-order rate constants in each case were measured as described previously<sup>15</sup>. At 20°C, the refolding rate constant  $k_r$  for the surface-unfolded RNase A and urea-unfolded RNase A were  $1.04 \cdot 10^{-2} \text{ s}^{-1}$  and  $4.33 \cdot 10^{-3} \text{ s}^{-1}$ , respectively, corresponding to a difference of 0.51 kcal/mol in the activation energy of the refolding process. The slower refolding of urea-unfolded RNase A may be a result of the more unfolded structure of this denatured protein on the chromatographic surface.

It might be argued that since urea-unfolded RNase A desorbed at a slightly higher concentration of 1-propanol in the gradient elution, the slower refolding could simply be the effect of the propanol. However, from the previous calibration of  $k_r$  vs. percentage propanol<sup>15</sup>, such a small difference in the concentration of 1-propanol at desorption (14.8% for urea-unfolded RNase A and 14.0% for the surface-unfolded RNase A) could not cause a 2-fold change in the refolding rate constant. It can be concluded that the solution kinetics upon desorption may be a function of the state of the molecule on the chromatographic surface.

## CONCLUSIONS

It has been demonstrated that a protein can exist on a chromatographic surface with different extents of unfolding. These states lead to changes in  $Z$  and  $\log I$  and hence retention patterns. Particularly striking were the large differences in  $I$  between the folded and unfolded state, indicating the amplifying nature of the support surface for structure variations. This amplification could also be observed in the kinetics of unfolding on the surface. Indeed, the measurement of the rate of unfolding of adsorbed species either by chromatography or intrinsic fluorescence in which precisions of rate constants of better than 10% relative standard deviation are possible<sup>29</sup> may represent in appropriate cases a significant method for characterization of protein variants. Finally, it needs to be recognized that sample pretreatment can have a significant effect on the ultimate chromatographic separation. This point should be kept in mind as separation procedures are being developed.

## ACKNOWLEDGEMENTS

The authors gratefully acknowledge the support of this work from NIH under grant GM 15847. The authors further thank Hewlett-Packard for the gift of the photodiode array detector. They also thank Drs. R. Rush, P. Oroszlan and R. Blanco for their helpful discussions. This is contribution No. 385 from the Barnett Institute of Chemical Analysis and Material Science.

## REFERENCES

- 1 L. R. Snyder and M. A. Stadalius, in Cs. Horváth (Editor), *High Performance Liquid Chromatography—Advances and Perspectives*, Vol. 4, Academic Press, New York, 1986, p. 195.
- 2 X. Geng and F. E. Regnier, *J. Chromatogr.*, 296 (1984) 15.
- 3 M. T. W. Hearn and M. I. Aguilar, *J. Chromatogr.*, 397 (1987) 47.

- 4 S. A. Cohen, K. P. Benedek, S. Dong, Y. Tapuhi and B. L. Karger, *Anal. Chem.*, 56 (1984) 217.
- 5 M. A. Stadalius, M. A. Quarry, T. H. Mourey and L. R. Snyder, *J. Chromatogr.*, 358 (1986) 17.
- 6 J. L. Glajch, M. A. Quarry, J. F. Vasta and L. R. Snyder, *Anal. Chem.*, 58 (1986) 280.
- 7 M. Kunitani, D. Johnson and L. R. Snyder, *J. Chromatogr.*, 371 (1986) 313.
- 8 M. A. Stadalius, H. S. Gold and L. R. Snyder, *J. Chromatogr.*, 296 (1984) 31.
- 9 M. I. Aguilar, A. N. Hodder and M. T. W. Hearn, *J. Chromatogr.*, 327 (1985) 115.
- 10 S. A. Cohen, K. Benedek, Y. Tapuhi, J. C. Ford and B. L. Karger, *Anal. Biochem.*, 144 (1985) 275.
- 11 M. T. W. Hearn, A. N. Hodder and M. I. Aguilar, *J. Chromatogr.*, 327 (1985) 47.
- 12 R. H. Ingraham, S. Y. M. Lau, A. K. Taneja and R. S. Hodges, *J. Chromatogr.*, 327 (1985) 77.
- 13 S.-L. Wu, A. Figueroa and B. L. Karger, *J. Chromatogr.*, 371 (1986) 3.
- 14 K. Benedek, S. Dong and B. L. Karger, *J. Chromatogr.*, 317 (1984) 227.
- 15 X. M. Lu, K. Benedek and B. L. Karger, *J. Chromatogr.*, 159 (1986) 19.
- 16 F. H. White, *Methods Enzymol.*, 11 (1967) 481.
- 17 S. H. Lin, Y. Konishi, M. E. Denton and H. A. Sheraga, *Biochemistry*, 23 (1984) 5504.
- 18 T. Imato, F. Hartdegen and J. A. Rupley, *J. Mol. Biol.*, 80 (1973) 637.
- 19 M. A. Quarry, R. L. Grob and L. R. Snyder, *Anal. Chem.*, 58 (1986) 907.
- 20 K. D. Nugent, W. G. Burton and L. R. Snyder, *J. Chromatogr.*, 443 (1988) 381.
- 21 A. S. Acharya, *J. Protein Chem.*, 5 (1986) 199.
- 22 L. N. Lin and J. F. Brandts, *Biochemistry*, 22 (1983) 553.
- 23 S. Segawa and M. Sugihara, *Biopolymers*, 23 (1984) 2489.
- 24 J. L. Fausnaugh and F. E. Regnier, *J. Chromatogr.*, 359 (1986) 131.
- 25 D. Horsley, J. Herron, V. Hlady and J. D. Andrade, in J. L. Brash and T. A. Horbett (Editors), *Proteins at Interfaces—Physicochemical and Biochemical Studies*, American Chemical Society, Washington, DC, 1987, p. 290.
- 26 J. L. Perry and R. Witzel, *Science (Washington, D.C.)*, 226 (1984) 555.
- 27 C. R. Beddell, C. C. F. Blake and S. J. Oatley, *J. Mol. Biol.*, 97 (1975) 643.
- 28 X. M. Lu, A. Figueroa and B. L. Karger, *J. Am. Chem. Soc.*, 110 (1988) 1978.
- 29 P. Oroszlan, R. Blanco, X.-M. Lu, D. Yarmush and B. L. Karger, *J. Chromatogr.*, 500 (1990) 481.

CHROMSYM. 1646

## HIGH-PERFORMANCE LIQUID CHROMATOGRAPHY OF AMINO ACIDS, PEPTIDES AND PROTEINS

### XCV<sup>a</sup>. THERMODYNAMIC AND KINETIC INVESTIGATIONS ON RIGID AND SOFT AFFINITY GELS WITH VARYING PARTICLE AND PORE SIZES: COMPARISON OF THERMODYNAMIC PARAMETERS AND THE ADSORPTION BEHAVIOUR OF PROTEINS EVALUATED FROM BATH AND FRONTAL ANALYSIS EXPERIMENTS<sup>b</sup>

F. B. ANSPACH, A. JOHNSTON, H.-J. WIRTH, K. K. UNGER<sup>c</sup> and M. T. W. HEARN\*

*Department of Biochemistry and Centre of Bioprocess Technology, Monash University, Clayton, Victoria 3168 (Australia)*

---

#### SUMMARY

The thermodynamic constants, associated with the interaction of three proteins with triazine dye affinity sorbents, have been derived from bath and frontal analysis experiments. In cases where mass-transfer restrictions are very high, calculation of the thermodynamic constants directly from frontal analysis experiments could not be achieved. In such cases, a portion of the adsorbate was always present in the effluent, a situation which has its effect as the split peak phenomenon. With Fractogel-based triazine dye affinity sorbents none of the test proteins applied in frontal analysis were adsorbed. A similar behaviour was observed for a Cellufine sorbent during the adsorption of human serum albumin and the Blue Sepharose CL6B sorbent during the adsorption of alcohol dehydrogenase, which displayed much slower apparent adsorption kinetics than observed in the bath experiments. These phenomena were shown to be associated with changes in the gel structure, caused in part by the column packing procedure.

Silica-based sorbents performed better in the adsorption of lysozyme in the column mode than soft-gel affinity sorbents, as was evident in the higher capacities and steeper breakthrough curves. At high protein concentrations (feedstock concentration >0.2 mg/ml) breakthrough curves obtained with small- and large-particle-size sorbents, but of constant pore size, were found to be identical. This finding demonstrates that the use of small-particle-size sorbents (*e.g.* particle diameter,

---

<sup>a</sup> For Part XCIV, see ref. 1.

<sup>b</sup> The authors wish to acknowledge the enormous enthusiasm, insight and scholarship which Csaba Horváth has brought to the field of chromatographic sciences. His example has stimulated them in numerous ways over the past decade to examine in greater detail more systematic methods to elucidate chromatographic processes and phenomena. For these reasons alone, this manuscript is dedicated to Csaba Horváth in celebration of his sixtieth birthday.

<sup>c</sup> On sabbatical leave from the Institut für Anorganische Chemie und Analytische Chemie, Johannes Gutenberg-Universität, 6500 Mainz, F.R.G.

$d_p \leq 5 \mu\text{m}$ ) for the preparative isolation of proteins may not be justified when operating in the overload mode.

With other higher-molecular-weight proteins and the silica-based sorbent systems examined, the small-particle-size sorbents ( $d_p = 5 \mu\text{m}$ ) displayed less symmetrical shapes of their breakthrough curves than the larger-particle-size and soft-gel sorbents. This behaviour was further exacerbated when non-porous glass or silica-based sorbents were utilized. These non-porous affinity sorbents displayed nearly rectangular breakthrough shapes at the onset of the adsorption process, but comparatively slow adsorption kinetics became evident as saturation was approached. This phenomenon has been attributed to surface rearrangement and/or reorientation of the adsorbed proteins, particularly with sorbents of high ligand densities.

---

## INTRODUCTION

The evaluation of thermodynamic data from continuously stirred bath experiments has been addressed in an associated publication<sup>2</sup>, including the description of a simple method for comparing apparent adsorption kinetics with different types of affinity sorbents. Such data have been found useful for the prediction of the capacity of affinity sorbents for the preparative chromatographic isolation of proteins. Furthermore, the observed adsorption kinetics in the bath experiments can be related to the breakthrough behaviour of sorbents. Collectively, guidelines, derived from bath experiments, provide a basis for the choice of sorbent for a particular chromatographic isolation procedure. For example, after the application of mathematical models which incorporate the kinetics during adsorption, we and others have shown that thermodynamic and kinetic data, obtained from bath experiments, can be used to predict the position and the shape of the breakthrough curve<sup>2-6</sup>.

The comparison of thermodynamic data derived from static bath and dynamic chromatographic experiments was thus of major interest in this investigation. Chromatographic data were obtained by the application of frontal analysis, a technique which lends itself to systematic acquisition of data over a very wide range of experimental and loading conditions. Furthermore, as has been discussed extensively by Jacobsen *et al.*<sup>7</sup> and Kasai *et al.*<sup>8</sup>, frontal analysis is an accurate method for quantitative description of the characteristics of the chromatographic adsorption of solutes, including proteins.

In this study, we extend our earlier investigations with a variety of affinity sorbents in the bath experiments to include the use of small-particle-size and non-porous silica-based sorbents (particle diameter,  $d_p \leq 5 \mu\text{m}$ ). We were interested to examine whether these sorbents displayed enhanced adsorption performances when used at the upper part of the equilibrium isotherm, or whether they would display the same characteristics shown by large-particle-size sorbents, when used in the overload mode, as reported for zonal chromatographic systems<sup>9</sup>.

## THEORY

According to Graves and Wu<sup>10</sup>, equilibrium isotherms can be measured by static (bath) methods, where discrete points on the isotherms are calculated on the basis of

the concentrations of the adsorbate in solution and the adsorbate in the sorbent. In order to follow the kinetics of adsorption in bath systems, protein concentrations must be monitored continuously by techniques similar to those described by Horstmann *et al.*<sup>11</sup> or by Anspach *et al.*<sup>2</sup>. The results of our previous and current studies clearly demonstrated that bath adsorption methods can display the characteristics of column affinity systems in a realistic way, allowing information about diffusion restrictions of the affinity sorbents to be enunciated. However, there are drawbacks with bath techniques, such as limitations of the type of stationary phases which can be subjected to investigation. Similar conclusions have been reached by Jacobsen *et al.*<sup>7</sup>. Furthermore, when soft gel sorbents are examined in column systems, the structure of the porous network may change as a consequence of the pressure on the bed leading to bed compression. This will influence the permeability and porosity of the gel and at the same time will affect the accessibility of the adsorbate to the immobilized ligands. When thermodynamic and kinetic parameters from bath experiments are employed to design fixed bed procedures, any change in these sorbent characteristics will lead to a significant decrease in separation efficiency, productivity and loadability.

The determination of thermodynamic parameters by means of zonal or frontal chromatographic methods has been described in numerous publications (for reviews see refs. 12–14). As discussed by Jacobsen *et al.*<sup>7</sup> frontal analysis appears to be the method of choice when proteins with relatively large diffusion restrictions are subjected to chromatographic separation. In particular, frontal analysis is particularly suited for adsorbate–ligand interactions when the dissociation constant,  $K_d$ , is in the range  $10^{-4}$ – $10^{-7}$  M, *e.g.* ion-exchange, hydrophobic interaction or reversed-phase, metal chelate and some forms of biomimetic and biospecific affinity chromatography. In frontal analysis ideally, after a step increase of the protein concentration at the column inlet, an equivalent step increase in protein concentration should develop at the column outlet when saturation of the column is achieved. Due to mass-transfer resistances (associated with film, pore and surface diffusion and surface reaction resistances) and dispersion effects (mediated by axial, molecular and Eddy diffusion and external dead-volume), the breakthrough front is established as a sigmoidal profile. When the system reaches equilibrium (column inlet concentration equals column outlet concentration), the breakthrough volume can be calculated. This volume at a particular protein concentration corresponds to one point on the equilibrium isotherm. As outlined in our previous publication<sup>2</sup>, the feed concentration,  $c$ , and solid-phase concentration,  $q$ , can be transformed, as required, to yield  $K_d$ , the accessible ligand concentration, and the effective capacity of the sorbent,  $q_m$ . Using Scatchard plot analysis, the heterogeneity of the affinity sorbents can additionally be recognised.

Using the approach developed by Nichol *et al.*<sup>15</sup>, which assumes a Langmuir-type isotherm, the equilibrium constant,  $K_a$ , and  $q_m$  can be determined without consideration of the shape of the equilibrium isotherm. In the absence of any competing ligand, the relationship between  $c$  and  $q_m$  can be simplified to

$$\frac{1}{V_e - V_0} = \frac{1}{V_0 q_m K_a} + \frac{c}{V_0 q_m} \quad (1)$$

where  $V_e$  is the breakthrough volume,  $V_0$  the elution volume of a non-retained

component with a molecular weight similar to that of the protein of interest,  $c$  is the concentration of the applied feed solution, and  $q_m$  is the capacity of the affinity sorbent. For the purposes of the present studies, experimental data were fitted to eqn. 1 by standard methods of numerical analysis.

## EXPERIMENTAL

### *Chromatographic supports*

The soft-gel chromatographic support Trisacryl GF 2000 was obtained from Reactifs IBF (Villeneuve la Garenne, France), Cellufine GC 700 Medium from Amicon (Danvers, MA, U.S.A.) and Sepharose CL6B and Blue Sepharose CL6B from Pharmacia LKB (Uppsala, Sweden).

The porous silica-based supports, Spherosil (Type: XOB030) were obtained from Rhône-Poulenc (Usine de Salindres, France); Nucleosil 300-2540, 4000-2540, 300-5, 1000-5, 4000-5 and Polygosil 300-2540 from Machery-Nagel (Düren, F.R.G.). Non-porous silica with a particle size of 1.5  $\mu\text{m}$  was made in our laboratories and is commercially available from E. Merck (Darmstadt, F.R.G.), under the tradename Monospher. Non-porous glass beads were a gift from Polters-Ballotini (Kirchheimbolanden, F.R.G.) and were size-fractionated as described in our previous publication<sup>2</sup>.

### *Chemicals*

3-Mercaptopropyltrimethoxysilane (MPS) was obtained from EGA (Steinheim, F.R.G.). Tris, hen egg white lysozyme (E.C. 3.2.1.17, dialysed and lyophilized) and alcohol dehydrogenase (ADH) (E.C. 1.1.1.1, crystallised and lyophilized) from baker's yeast were purchased from Sigma (Sydney, Australia). Cibacron Blue F3GA was obtained from Serva (Heidelberg, F.R.G.). Human serum albumin (HSA) (chromatographically isolated, containing 250 mg/ml protein, 85–130 mM sodium chloride and 40 mM sodium octanoate) was a gift from the Commonwealth Serum Laboratories (Melbourne, Australia).

### *Preparation of affinity sorbents*

Spherosil XOB030 and Nucleosil 300 were chemically modified with MPS as described in an earlier publication<sup>16</sup>. With silicas of larger pore sizes, such as Nucleosil 1000 and 4000, preliminary investigations established that 5 times the amount of MPS was needed compared to that calculated on the basis of specific surface area and hydroxyl group content. When lower quantities were employed the coverage with MPS was insufficient, and this resulted in low immobilization levels of reactive dyes and non-specific interactions of adsorbed proteins with free hydroxyl groups at the silica surface. Due to the higher silane concentration, the reaction time was reduced to 2 h, in order to avoid polymerization of the silane at the surface of the supports.

The immobilization of Cibacron Blue F3GA on MPS-activated silica and glass beads, and on soft-gel supports was performed as described in refs. 2 and 17.

### *Chromatographic setup for the frontal analysis experiments*

Frontal analysis experiments on soft affinity sorbents and on silica-based and non-porous glass affinity sorbents were performed using the Pharmacia LCC-500

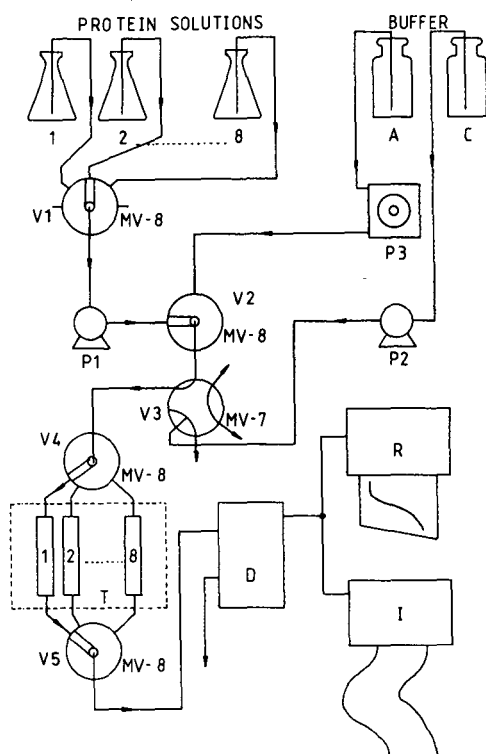


Fig. 1. Schematic diagram of the equipment design used for frontal analysis. Up to eight columns and eight protein concentrations can be investigated with a Pharmacia Fast Protein Liquid Chromatograph in this configuration, with the unit automatically performing under the control of the Pharmacia LCC-500. A: Regeneration buffer [50 mM Tris-HCl (pH 7.8) + 2.5 M KSCN]; C: equilibration buffer [50 mM Tris-HCl (pH 7.8)]; P1: pump for different protein concentrations; P2: pump for equilibration buffer; P3: pump for regeneration buffer; V1: valve for selection of different protein concentrations (eight inlets); V2: valve for the selection of either adsorbate or equilibration buffer; V3: valve for control of either equilibration, adsorption, or wash cycles; V4 and V5: valves for selection of up to eight different columns; D: detector (cell volume: 10  $\mu$ l, absorbance 280 nm); R: chart recorder; I: integrator (Shimadzu C-R3A); T: thermostat (e.g., at 35.5°C). MV-8 and MV-7 are eight- and seven-port valves, respectively.

system, connected with 4 MV-8 and 1 MV-7 motor valves as outlined in Fig. 1. This chromatographic system was controlled exclusively by the LCC-500. In a single frontal analysis experiment four columns could be tested automatically in a period of 24–48 h, depending on the adsorption capacity of the affinity sorbents. Eight protein solutions of increasing concentrations were applied in each set of experiments, in order to obtain, where possible, data encompassing every part of the isotherm. The dimensions of the affinity columns were 25–35 mm  $\times$  5 mm I.D., depending on the adsorption capacity of the affinity gel. Columns were packed by attaching a syringe to one end of each column and applying suction to transfer suspended affinity sorbent to the columns. In order to saturate the active sites on “virgin” chromatographic supports, which lead to non-specific and often irreversible interactions with adsorbed proteins, a solution of 0.2 mg/ml lysozyme was pumped through the columns prior to their experimental use. The columns were then placed in a water bath thermostated at

35.5°C and equilibrated with the regeneration buffer. It should be noted that although this procedure can be used in a practical context to mimic the well documented differences between new and regenerated sorbents, it is appreciated that presaturation of non-specific sites on a sorbent with a particular protein will mask contribution of these sites to the overall adsorption process and could even induce specific protein-protein interactions. Each experimental run was terminated when the test protein concentration at the column outlet was equal to the inlet concentration. The column was regenerated immediately after saturation until no further change in the UV absorption of the effluent was measurable. The regeneration buffer was then maintained in the column, and the next column was investigated via the multiway valves. Each column was equilibrated with the equilibration buffer prior to the adsorption studies with the proteins. After examination of the breakthrough volume of the columns, the valve controlling the protein concentration steps was switched to the next position until the highest concentration was accomplished. The UV absorption at the column outlet was digitalized by an integrator and the equilibrium capacity ( $q^*$ ) of a given adsorbate concentration ( $c^*$ ) was evaluated by numerical integration of the area beneath the breakthrough curve.  $V_e$  refers to that point of the breakthrough curve where 50% of the amount of adsorbate, as determined by the values of the initial and final condition of the breakthrough curve, was found in the effluent stream. Utilizing this procedure, breakthrough volumes and hence breakthrough times could also be calculated when the corresponding breakthrough curves were not symmetrical around the inflection point.  $V_0$  was determined as the retention volume of a non-retained contaminant of the protein applied to the column.

#### *Evaluation of thermodynamic data*

The equilibrium capacity,  $q^*$ , was plotted against the corresponding protein concentration,  $c^*$ , at the column inlet (see Fig. 2a and b). As described in a prior publication<sup>2</sup>, the shape of the isotherm can be utilized to evaluate the type of interaction.  $q_m$  and  $K_d$  were determined from a double reciprocal plot. In addition, the determination of  $K_a$  and of  $q_m$  was performed by the method of Nichol *et al.*<sup>15</sup>, utilizing eqn. 1.

## RESULTS

#### *Comparison of thermodynamic data*

*Adsorption behaviour of lysozyme.* Compared to the values obtained from the corresponding bath experiments<sup>2</sup>, affinity constants for lysozyme binding to Cibacron Blue F3GA were considerably lower than affinity constants for HSA, based on the same affinity sorbents and buffer conditions (see Table I). Because of the attenuated interaction of lysozyme with the Cibacron Blue F3GA sorbents in the absence of NaCl, most experiments with this protein were accomplished with at least 0.5 M NaCl added to the equilibration buffer. As a result,  $K_d$  values for the lysozyme Cibacron Blue F3GA interaction obtained in the presence of 0.5 M NaCl were at least one order of magnitude larger than in absence of salt, a result which conforms to  $K_d$  values determined with the bath experiments. The interaction of HSA with immobilised Cibacron Blue also decreased in the presence of 0.5 M NaCl, but the change in  $K_d$  values was far less significant than  $K_d$  values derived from the corresponding bath experiments.



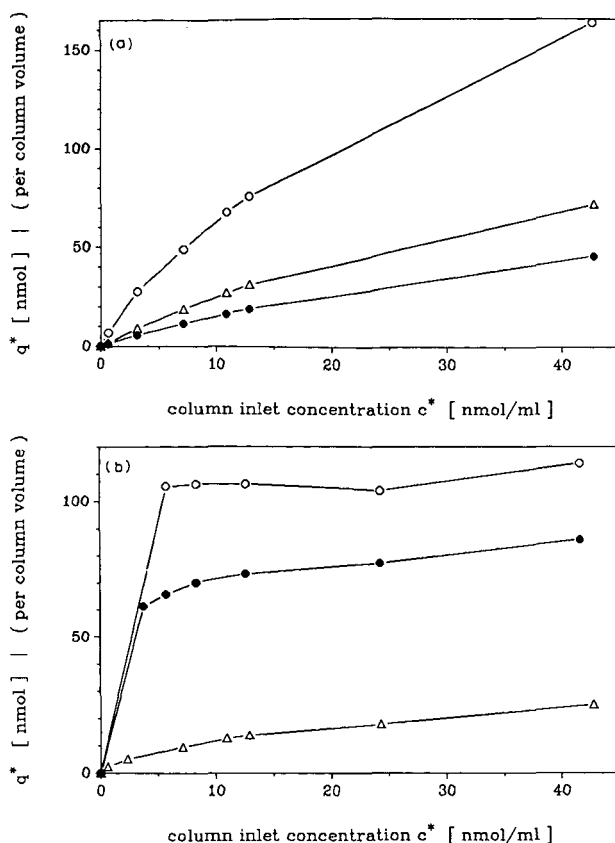


Fig. 2. Equilibrium isotherms for the adsorption of lysozyme on Cibacron Blue F3GA. (a) Adsorption of the protein on the soft-gel sorbents gives typical Langmuir-type isotherms.  $\circ$  = Cellufine GC 700;  $\triangle$  = Sepharose CL6B;  $\bullet$  = Trisacryl GF 2000. (b) Adsorption on silica-based affinity sorbents gives rectangular-shaped isotherms for some of the sorbents due to non-specific interactions with the silica surface.  $\circ$  = Nucleosil 1000-5;  $\bullet$  = Nucleosil 4000-5;  $\triangle$  = non-porous glass beads (20–40  $\mu\text{m}$ ).

The interaction behaviour of lysozyme with the dye affinity sorbents increased on Sepharose and Cellufine chromatographic sorbents with increasing protein concentration, resulting in non-linear Scatchard plots, as evident from Fig. 3. This behaviour was not displayed with the corresponding Trisacryl-based affinity sorbents. The participation of multimodal interactions, including “non-specific” binding effects between lysozyme and other (non-triazine dye) chemical groups accessible on the chromatographic supports as well as protein–protein interactions, must thus be taken into account. This “non-specific” binding behaviour may have its origin in processes that are mechanistically similar to those observed for the interaction between lysozyme and Sephadex G-100 sorbents<sup>15</sup>. When calculation of the thermodynamic parameters was accomplished from data obtained at low and high protein concentrations, affinity constants corresponding to a low and a high affinity binding site could be distinguished, as displayed in Table I. Furthermore, evaluation of the Scatchard plots in terms of a two-component binding model permitted the number of binding sites per

TABLE I  
THERMODYNAMIC CONSTANTS FROM FRONTAL ANALYSIS

	$q_m$ (mol/ml)	$K_d$ (M)
Trisacryl GF 2000		
Lysozyme <sup>a</sup>	$2.0 \cdot 10^{-7}$	$4.9 \cdot 10^{-5}$
HSA (without salt)	$9.7 \cdot 10^{-8}$	$5.5 \cdot 10^{-7}$
HSA (with 0.5 M NaCl)	$6.1 \cdot 10^{-8}$	$5.7 \cdot 10^{-7}$
Cellufine GC 700		
Lysozyme (low affinity) <sup>a</sup>	$4.0 \cdot 10^{-7}$	$3.6 \cdot 10^{-5}$
Lysozyme (high affinity) <sup>a</sup>	$1.6 \cdot 10^{-7}$	$1.0 \cdot 10^{-5}$
Sephacrose CL6B		
Lysozyme (low affinity) <sup>a</sup>	$1.4 \cdot 10^{-7}$	$6.4 \cdot 10^{-5}$
Lysozyme (high affinity) <sup>a</sup>	$7.0 \cdot 10^{-8}$	$2.7 \cdot 10^{-5}$
HSA (without salt) <sup>c</sup>	$2.4 \cdot 10^{-7}$	$6.5 \cdot 10^{-7}$
HSA (with 0.5 M NaCl)	$5.1 \cdot 10^{-8}$	$1.5 \cdot 10^{-6}$
Nucleosil 300-2540		
Lysozyme (A) <sup>b</sup> (0.5 M)	$1.1 \cdot 10^{-6}$	$4.7 \cdot 10^{-7}$
(B) <sup>b</sup> (0.8 M)	$1.5 \cdot 10^{-6}$	$5.4 \cdot 10^{-6}$
Polygosil 300-2540		
Lysozyme (B) <sup>b</sup> (0.8 M)	$4.8 \cdot 10^{-7}$	$4.7 \cdot 10^{-7}$
Nucleosil 4000-2540		
Lysozyme (A) <sup>b</sup> (0.5 M)	$8.5 \cdot 10^{-8}$	$1.5 \cdot 10^{-6}$
(B) <sup>b</sup> (0.5 M)	$2.5 \cdot 10^{-7}$	$1.1 \cdot 10^{-5}$
(B) <sup>b</sup> (0.8 M)	$2.2 \cdot 10^{-7}$	$1.2 \cdot 10^{-5}$
(B) <sup>b</sup> (1.2 M)	$2.1 \cdot 10^{-7}$	$1.7 \cdot 10^{-5}$
Nucleosil 300-5		
Lysozyme (C) <sup>b</sup> (1.0 M)	$9.1 \cdot 10^{-7}$	$2.4 \cdot 10^{-5}$
(B) <sup>b</sup> (0.8 M)	$9.0 \cdot 10^{-7}$	$5.5 \cdot 10^{-7}$
Nucleosil 1000-5		
Lysozyme (A) <sup>b</sup> (0.5 M)	$3.1 \cdot 10^{-7}$	$3.3 \cdot 10^{-7}$
(B) <sup>b</sup> (0.5 M)	$2.5 \cdot 10^{-7}$	$8.3 \cdot 10^{-6}$
(B) <sup>b</sup> (0.8 M)	$2.4 \cdot 10^{-7}$	$1.0 \cdot 10^{-5}$
(B) <sup>b</sup> (1.2 M)	$2.2 \cdot 10^{-7}$	$1.6 \cdot 10^{-5}$
Nucleosil 4000-5		
Lysozyme (A) <sup>b</sup> (0.5 M)	$2.2 \cdot 10^{-7}$	$2.2 \cdot 10^{-6}$
(B) <sup>b</sup> (0.5 M)	$1.7 \cdot 10^{-7}$	$1.6 \cdot 10^{-5}$
(B) <sup>b</sup> (0.8 M)	$1.7 \cdot 10^{-7}$	$1.8 \cdot 10^{-5}$
(B) <sup>b</sup> (1.2 M)	$1.5 \cdot 10^{-7}$	$2.4 \cdot 10^{-5}$
Glass beads fraction 2		
Lysozyme	$3.3 \cdot 10^{-8}$	$< 10^{-5}$
Glass beads fraction 3		
Lysozyme	$1.1 \cdot 10^{-8}$	$< 10^{-5}$
Glass beads fraction 4		
Lysozyme (low affinity)	$4.4 \cdot 10^{-9}$	$2.8 \cdot 10^{-5}$
Lysozyme (high affinity)	$3.8 \cdot 10^{-9}$	$2.3 \cdot 10^{-6}$
Non-porous silica, 1.5 $\mu$ m		
Lysozyme (C) <sup>b</sup>	$3.3 \cdot 10^{-7}$	$1.3 \cdot 10^{-6}$

<sup>a</sup> Adsorption of lysozyme on Cibacron Blue F3GA-immobilized soft-gel supports was always accomplished with 0.5 M NaCl in the adsorption buffer.

<sup>b</sup> Experiments with sorbents prepared from different MPS derivatisation reactions. The dye sorbents derived from these different batches are indicated with (A), (B), and (C).

<sup>c</sup> These data are results from previous investigations<sup>2</sup>.

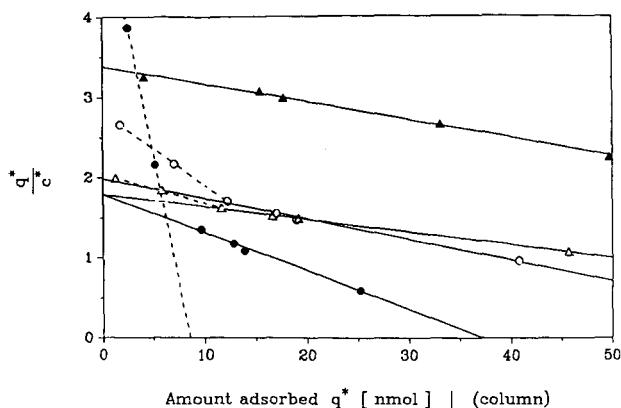


Fig. 3. Scatchard plot analysis of the adsorption of lysozyme on Cibacron Blue F3GA, immobilized on different chromatographic supports. Changes in the mechanism of the affinity interaction can be perceived by changes of the slope of the corresponding graph. (▲) Trisacryl GF 2000: specific adsorption of lysozyme on immobilized Cibacron Blue F3GA only. (Δ) Sepharose CL6B: at higher lysozyme concentrations protein interactions with low-affinity sites (Sepharose support) cause alteration in the slope of the graph. (○) Cellufine GC 700: deviation from affinity interaction is higher than for Sepharose CL6B. (●) Non-porous glass beads: interaction of lysozyme with the silica surface overrides affinity interaction at low protein concentration.

unit column (or area) of gel matrix to be determined. When determined in this way, the ligand densities associated with the high-affinity sites were (i) generally of lower value compared to those of the “non-specific” low-affinity sites, and (ii) of similar in magnitude to those calculated from the amount of triazine dye immobilised per ml of gel. Consequently, the high-affinity sites were attributed to the immobilized triazine dye ligand, whereas the low-affinity sites were attributed to binding sites on the chromatographic support itself. However, the values of the dissociation constants, associated with these non-specific interactions, were in the same range as those found for the interaction of the protein with the immobilized ligand.

In the column mode, Cibacron Blue F3GA immobilized on Fractogel HW 55, HW 65 and HW 75 sorbents exhibited very little binding with lysozyme and no binding with HSA. Furthermore, leakage of the triazine dyes was observed for all Fractogel sorbents during each chromatographic run. In contrast, when bath experiments were utilized with the same batch of dye immobilised Fractogel affinity gel only small amounts of triazine dye were released during the adsorption experiments. The origin of this anomalous leakage behaviour remains to be determined.

In the matrix systems we have examined, silica-based affinity sorbents prepared under different chemical derivatization conditions occasionally displayed higher affinity constants with lysozyme than the soft-gel sorbents, presumably due to non-specific polar interactions between hydroxyl groups at the silica surface and the basic protein. Associated studies revealed that these free hydroxyl groups were present largely as a result of unsatisfactory modification conditions. When the modification conditions described in the Experimental section were used, these ionic interactions could be minimized and dissociation constants for lysozyme binding to silica-based triazine dye affinity sorbents were in the same range as those obtained for soft-gel affinity sorbents. Furthermore, when adsorption studies were carried out over a range

of salt concentrations (0.8–1.2 M NaCl) during the frontal analysis experiments, the derived values of  $q_m$  and  $K_d$  were also similar (Table I). Association constants for the interaction of the protein with the silica-based sorbents decreased dramatically up to 0.5 M NaCl when this salt was added to the buffer, but subsequently did not change substantially in value when higher salt concentrations were utilized (*cf.* Table I). This salt-dependent effect was also reflected in changes in the capacity of the sorbents. These results indicate that for silica-based sorbents the interaction of Cibacron Blue F3GA with lysozyme is protein-specific in the presence of 0.5–1.2 M NaCl. When low protein concentrations were utilized, as for the studies with non-porous glass affinity sorbents (size fraction 4), both ionic and biomimetic affinity interactions could be distinguished by Scatchard analysis (Fig. 3). In these cases, the dissociation constant, which corresponded to the low-affinity sites, was found to be comparable to dissociation constants of the soft-gel affinity sorbents associated with specific protein dye interactions.

Based on data provided by the manufacturer on the physical properties of the porous silica supports, the theoretical capacity of silica affinity sorbents was estimated from the known molecular dimensions of the adsorbates. Analogously, the theoretical capacity of non-porous supports was estimated based on their geometric particle dimensions. As anticipated, the effective capacity was less than the theoretical capacity, because portion of the surface area was not accessible to proteins due to steric restrictions. When the estimated and measured capacities of the silica-based dye affinity sorbents were compared, the large-pore-size and non-porous silica sorbents tended to have improved accessibility for the adsorbate, as is evident from Table II. However, our experience with silica-based sorbents over several years has shown that batch-to-batch fluctuations of affinity sorbents from individual reactions with MPS can be significant and result in different capacities and dissociation constants for nominally the same affinity sorbent. The relatively low dissociation constant of the Nucleosil 300 sorbents—compared to the other silica-based sorbents—may be one reason why the capacity of these sorbents is higher. In addition, with non-porous glass beads (or other silicas), polymerization of the silane at the surface of the beads can lead to higher capacities than is theoretically possible on the basis of the geometric dimensions of the particle covered with a monolayer of MPS groups.

As is evident from the data used in Fig. 2a and b, the dissociation constant also influenced the shape of the equilibrium isotherms. For example, when the Cibacron Blue F3GA affinity sorbents were saturated with lysozyme by using very low lysozyme concentration in the feed stock, relatively low values of the dissociation constants and rectangular-shaped equilibrium isotherms were observed. Such isotherms have been previously described by Horváth and co-workers<sup>7,18</sup> and by Kopaciewicz *et al.*<sup>19</sup> for protein ligand binding on ion exchangers and have been attributed to very strong ionic interactions. The determination of thermodynamic constants from rectangular isotherms presents difficulties, because very low protein concentrations must be utilized to obtain data in the ascending part of the isotherm. At such concentrations (*e.g.* below 10  $\mu\text{g/ml}$ ), breakthrough times become unacceptably long (in some experiments > 24 h with 0.002 mg/ml protein solution) and, in addition, detector or baseline fluctuations can lead to significant errors in the numerically derived values of  $q_m$  and  $K_d$ . With protein concentrations between 0.01 and 1 mg/ml the evaluation of the dissociation constants from rectangular isotherms is again difficult because the

TABLE II  
COMPARISON OF CALCULATED AND EXPERIMENTAL CAPACITIES OF THE SORBENTS

	<i>Experimental capacity (mol/ml)</i>	<i>Calculated capacity (mol/ml)</i>	<i>Ratio of coverage (%)</i>
Nucleosil 300-2540 (A) <sup>a</sup>	$1.1 \cdot 10^{-6}$	$1.0 \cdot 10^{-5}$	11
(B) <sup>a</sup>	$1.5 \cdot 10^{-6}$	$1.0 \cdot 10^{-5}$	14
Polygosil 300-2540	$4.8 \cdot 10^{-7}$	$1.0 \cdot 10^{-5}$	5
Nucleosil 300-5 (A) <sup>a</sup>	$4.8 \cdot 10^{-7}$	$1.0 \cdot 10^{-5}$	5
(B) <sup>a</sup>	$9.0 \cdot 10^{-7}$	$1.0 \cdot 10^{-5}$	9
Nucleosil 1000-5	$3.1 \cdot 10^{-7}$	$3.1 \cdot 10^{-6}$	10
Nucleosil 4000-5	$2.2 \cdot 10^{-7}$	$1.0 \cdot 10^{-6}$	21
Nucleosil 4000-2540	$8.5 \cdot 10^{-8}$	$1.0 \cdot 10^{-6}$	8
Glass beads (20–40 $\mu\text{m}$ )	$5.5 \cdot 10^{-8}$	$1.1 \cdot 10^{-7}$	52
Glass beads (10–25 $\mu\text{m}$ )	$1.8 \cdot 10^{-8}$	$1.8 \cdot 10^{-7}$	10
Glass beads (5–10 $\mu\text{m}$ )	$3.3 \cdot 10^{-8}$	$4.2 \cdot 10^{-7}$	8
Non-porous silica (1.5 $\mu\text{m}$ )	$3.3 \cdot 10^{-7}$	$2.1 \cdot 10^{-6}$	16

<sup>a</sup> Experiments with sorbents prepared from different MPS derivatisation reactions. The dye affinity sorbents prepared from these batches are indicated by (A) and (B).

sorbents under these conditions may be nearly (or completely) saturated. In addition, small errors in the determination of the protein concentration or breakthrough volume will lead to significant fluctuations in the adsorption capacity. Such errors can result in the calculation of apparent negative dissociation constants, as was observed, for example, in our investigations with lysozyme adsorption on several dye affinity sorbents under low salt-binding conditions. Adsorption of lysozyme on Cibacron Blue F3GA, immobilized on soft-gel supports resulted in an adsorption behaviour reminiscent of Langmuir-type isotherms, as shown in Fig. 2b.

Calculation of thermodynamic constants from breakthrough curves, based solely on application of eqn. 1, will not provide information about the shape of the isotherm. As demonstrated in Fig. 4 for the adsorption of lysozyme on silica-based dye affinity sorbents, in each case with three different sorbents, linear dependencies between  $(V_e - V_0)^{-1}$  and column inlet concentration,  $c^*$ , were observed, *i.e.* the adsorption process is apparently characterized by eqn. 1. However, as demonstrated in associated studies, the interaction of lysozyme with the silica surface of Nucleosil 300-2540 and Nucleosil 1000-5 sorbent was initially dominant, due to the high affinity constant for the binding of the silica surface sites with the protein. As a consequence, data on the specific, biomimetic binding of the dye ligand with the protein were only available from the upper part of the equilibrium isotherm. Because of the limitations described above, regression analysis of the frontal analysis data corresponding to the adsorption of lysozyme to Cibacron Blue F3GA, immobilized on Nucleosil 300-2540, resulted in a negative value of the  $(V_e - V_0)^{-1}$  intercept at  $c^* = 0$ . The low dissociation constant corresponding to the specific adsorption with the Nucleosil 1000-5 sorbent is questionable, on the basis of the same argument.

*Adsorption behaviour of HSA and ADH.* Adsorption of HSA on the Trisacryl GF 2000 and Sepharose CL6B dye affinity sorbent in packed columns displayed almost the same accessible ligand concentrations as were found in the bath

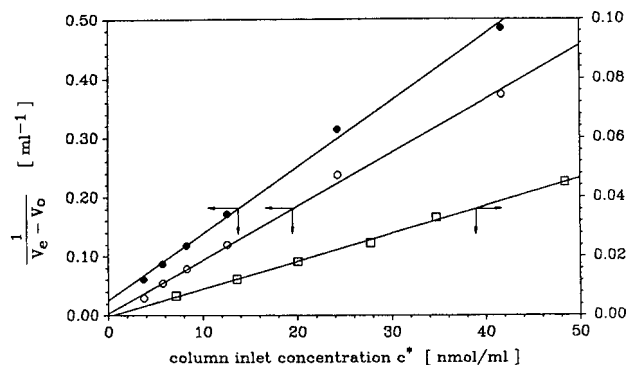


Fig. 4. Evaluation of thermodynamic constants from frontal analysis experiments by application of eqn. 1.  $\square$  = Nucleosil 300-2540;  $\circ$  = Nucleosil 1000-5;  $\bullet$  = Nucleosil 4000-5.

experiments<sup>2</sup> (*cf.* Table III). The value of the dissociation constants determined by these two methods differed by < 15%. This difference may simply reflect the specific experimental conditions, since the average adsorbate concentration range in the frontal analysis experiments was usually higher than in the bath experiments. Furthermore, we experienced more frequent data fluctuation in the equilibrium isotherm data in the column experiments than in the bath experiment. Due to very slow adsorption kinetics during the adsorption of HSA on the Cellufine GC 700 dye sorbent, no thermodynamic constants could be determined with this system. Since HSA could not be desorbed from the silica- and glass-based affinity sorbents, these sorbents were also excluded from frontal analysis experiments.

The adsorption of ADH on Blue Sepharose CL6B appears to be mainly controlled by mass-transfer restrictions, and this results in an early breakthrough of the protein, as shown in Fig. 5. This result was in contrast to the corresponding bath experiments where ADH was adsorbed on Blue Sepharose CL6B at a relatively rapid rate. Since the breakthrough volume, as calculated by numeric integration from the breakthrough curve, did not show a dependency on the increasing protein concentrations, as predicted by eqn. 1, calculation of thermodynamic data was not possible. One

TABLE III

COMPARISON OF THERMODYNAMIC CONSTANTS FROM FRONTAL ANALYSIS AND BATH EXPERIMENTS

	<i>Frontal analysis</i>		<i>Bath experiment</i>	
	$q_m$ (mol/ml)	$K_d$ (M)	$q_m$ (mol/ml)	$K_d$ (M)
Trisacryl GF 2000				
Lysozyme	$2.0 \cdot 10^{-7}$	$4.9 \cdot 10^{-5}$	$4.7 \cdot 10^{-6}$	$1.2 \cdot 10^{-3}$
HSA (without salt)	$9.7 \cdot 10^{-8}$	$5.5 \cdot 10^{-7}$	$7.8 \cdot 10^{-8}$	$1.0 \cdot 10^{-6}$
HSA (+ 0.5 M NaCl)	$6.1 \cdot 10^{-8}$	$5.7 \cdot 10^{-7}$	$6.4 \cdot 10^{-8}$	$2.1 \cdot 10^{-6}$
Sepharose CL6B				
HSA (without salt)	$2.4 \cdot 10^{-7}$	$6.5 \cdot 10^{-7}$	$4.9 \cdot 10^{-8}$	$5.2 \cdot 10^{-7}$
HSA (+ 0.5 M NaCl)	$5.1 \cdot 10^{-8}$	$1.5 \cdot 10^{-6}$	$6.8 \cdot 10^{-8}$	$7.3 \cdot 10^{-7}$

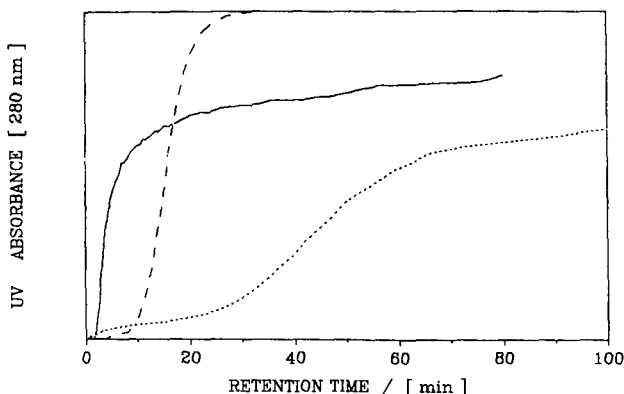


Fig. 5. Shape of the breakthrough curve and retention volumes during the adsorption of proteins on Blue Sepharose CL6B. Flow-rate, 0.3 ml/min. --- = Lysozyme (hen egg white, 0.05 mg/ml); ..... = serum albumin (human, 0.33 mg/ml); ——— = alcohol dehydrogenase (yeast, 0.02 mg/ml).

reason for this early breakthrough of ADH in the frontal analysis experiments with Blue Sepharose CL6B would appear to be a consequence of aggregation of ADH at the selected protein concentrations. The average concentration of the feed solution was higher in the frontal analysis experiments than in the corresponding bath experiments. In addition, deformation of the soft-gel sorbent, which has its origin in the mechanical properties of the gels, led to deformation of pore entrances and/or connectivity of the network of the sorbent. Evidence for the elastic deformation of Sepharose gels occurring during the packing procedure or as a consequence of the pressure associated with the flow-rate is well known. In the present studies, the bed volume decreased approximately 30% over the flow-rate range of 0.3–0.5 ml/min. Both effects result in an increase of diffusion restrictions and, consequently, slower adsorption kinetics.

Evaluation of the experimental data for all three proteins (lysozyme, HSA and ADH) as breakthrough curves obtained with the dye affinity sorbents in terms of the chromatographic model developed by Nichol *et al.*<sup>15</sup> or by double reciprocal plots, derived from equilibrium isotherms, resulted in values of the thermodynamic constants that were in close agreement for all affinity sorbents (*cf.* Table I). Deviations, which were never greater than 10% from predicted values with these different theoretical models, could be attributed to the sample rate of data acquisition by the detector integrator, which varied from 1 datapoint per 15 s to 1 datapoint per 120 s, depending on the capacity of the sorbent and the protein concentration used for the experiment.

#### *Comparison of breakthrough curves*

The capacity of affinity sorbents and the dissociation constant of the affinity complex are reflected in the retention volume of the breakthrough curve. Similarly, the kinetics during adsorption of the protein to the dye affinity sorbent are reflected in the shape of the breakthrough curve. As demonstrated in Fig. 6, normalised retention times for lysozyme shifted significantly when dye affinity sorbents with higher binding capacity, such as the Nucleosil 1000-5-derived sorbent, were employed under the same chromatographic conditions. Due to the relatively small capacity of the Sepharose and

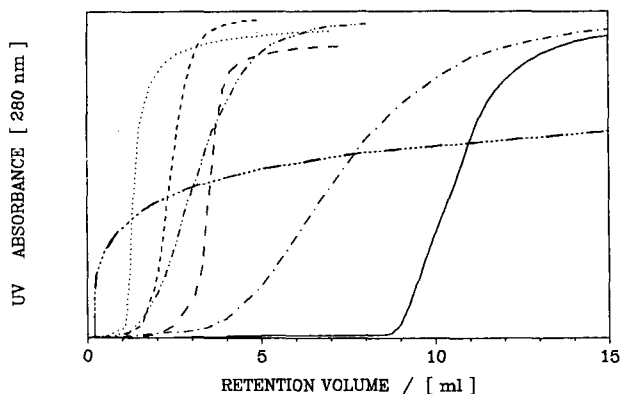


Fig. 6. Shape of the breakthrough curve and retention volume of various chromatographic sorbents with different pore sizes and particle sizes during the adsorption of lysozyme. Flow-rate, 0.5 ml/min; protein concentration, 0.10 mg/ml. — = Nucleosil 1000-5 (5  $\mu\text{m}$ ); --- = Nucleosil 4000-2540 (25-40  $\mu\text{m}$ ); - - - - = Sepharose CL6B (40-165  $\mu\text{m}$ ); - · - · - = Trisacryl GF 2000 (40-80  $\mu\text{m}$ ); - · - · - = Cellufine GC 700 (45-105  $\mu\text{m}$ ); · - · - · = Spherosil XOB030 (100-300  $\mu\text{m}$ ); · · · · · = non-porous glass beads (20-40  $\mu\text{m}$ ).

Trisacryl dye affinity sorbents for lysozyme, the solute breakthrough occurred relatively early in the chromatogram. In contrast, the Cellufine sorbent, which contained a higher Cibacron Blue F3GA density, was capable of adsorbing more lysozyme than the other soft-gel sorbents. However, the pore size of this sorbent is relatively small (pore diameter <40 nm), and this resulted in shallower breakthrough curves. Because of the small pore size of this matrix, the adsorption of HSA on the Cellufine GC 700 dye affinity sorbent was a very slow process, resulting in a shape of the breakthrough curve similar to that displayed in Fig. 6 for the adsorption of lysozyme on the Spherosil XOB030 dye affinity sorbent. These results suggest that the Cellufine GC 700-based affinity sorbent will be unsuitable for the high-capacity adsorption of proteins with molecular weights larger than 20 000.

Although silica gel affinity sorbents displayed lower dissociation constants when only partial modification of the silica surface was accomplished, the steepness of the breakthrough curve was largely dependent on the pore size. Breakthrough curves obtained with low lysozyme concentrations and the Nucleosil 4000 dye affinity sorbents with particle sizes of 5  $\mu\text{m}$  were steeper than the corresponding 25 to 40- $\mu\text{m}$ -diameter sorbents, as illustrated in Fig. 7. At higher protein concentrations, which corresponded to the plateau of the equilibrium isotherm, only minor differences could be observed in the shape of the breakthrough curve for both types of Nucleosil-based sorbents of different particle diameter. This behaviour is similar to that observed in zonal chromatography, where the number of theoretical plates per column volume decreases more dramatically with small particle sizes than with large particles, when the column is operated in the overload mode<sup>9</sup>. In particular, major differences occurred at the onset of the breakthrough curves when small-particle or non-porous dye affinity sorbents were employed, and this resulted in a rapid increase in the protein concentration at the column outlet. As saturation was approached, the shape of the breakthrough curves became similar for sorbents of different particle size.



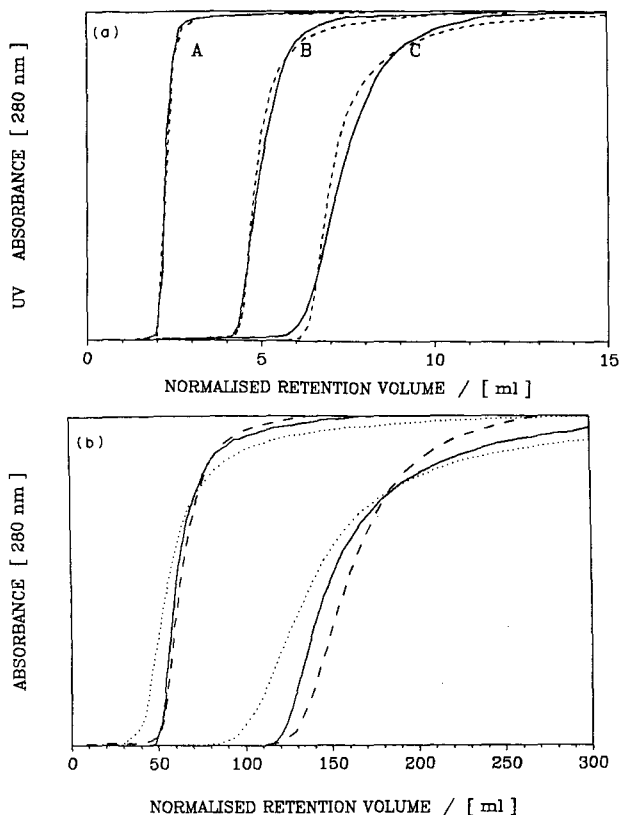


Fig. 7. Profile of breakthrough curves on silica-based affinity sorbents with different particle sizes but constant pore size during the adsorption of lysozyme in 50 mM Tris-HCl (pH 7.8)/0.8 M NaCl at a flow-rate of 0.5 ml/min. (a) ----- = Nucleosil 4000-5; ——— = Nucleosil 4000-2540; (protein concentration, A = 1.0 mg/ml, B = 0.2 mg/ml, C = 0.05 mg/ml). (b) ······· = Polygosil 300-2540; ----- = Nucleosil 300-2540; ——— = Nucleosil 300-5 (protein concentrations, 1.0 mg/ml and 0.2 mg/ml).

This adsorption behaviour resulted in rather asymmetrical curves when small-particle-size sorbents were utilized. During investigation of breakthrough curves at three different salt concentrations (0.5 M, 0.8 M, and 1.2 M NaCl) but under otherwise identical conditions, the normalised breakthrough curves for the 5- $\mu$ m particles crossed the breakthrough curves of the 25- to 40- $\mu$ m particles a second time near the saturation point, indicating that overall adsorption was slower, or at least of similar rate in this region of the breakthrough curve (*cf.* Fig. 7). The most shallow breakthrough curves and therefore the silica-based dye affinity sorbent which performed poorest in our tests, was the Polygosil 300-2540 dye sorbent. This sorbent is based on an irregularly shaped silica with characteristics claimed by the manufacturer to be otherwise identical with those described for the Nucleosil 300-2540 support.

As noted above, asymmetrical shapes of the breakthrough curves were evident with all small-sized silica affinity sorbents and were extremely marked when non-porous glass beads or silica beads were used (see Fig. 6). This type of breakthrough phenomenon might be based on secondary equilibrium effects,

associated with the rearrangement of already adsorbed proteins. Similar breakthrough shapes have been found for the adsorption of lysozyme on monoclonal antibodies immobilized on non-porous, activated silicas<sup>6</sup> and the adsorption of trypsin on non-porous benzamidine sorbents<sup>16</sup>.

## DISCUSSION

This study documents the further use of MPS for the chemical modification of microparticulate glasses and silicas. Under reaction conditions where the molar ratio of introduced silane to the silanol group content is maintained constant affinity sorbents with different levels of dye ligands are generated when silica particles of different pore sizes or non-porous glass and silica beads are used. For example, a 5-fold increase in the amount of MPS, based on the theoretical quantity required for the large-pore-size silicas Nucleosil 1000 or 4000 was needed to achieve comparable immobilization levels of Cibacron Blue F3GA to that obtained with small-pore-size silicas Nucleosil 300. A consequence of increasing the MPS concentration in the modification reaction with silicas is however increased polymer coverage by the silane. This has a subsequent effect on the protein adsorption capacity of the dye-affinity sorbent. Typical of these effects are the results obtained with the non-porous glass beads where the polymerization levels increased with increasing particle size, leading to higher immobilization levels of Cibacron Blue F3GA than would be theoretically possible, based on the geometric dimensions of the particle and its known silanol content. Although non-specific protein silanol or protein silane polymer interactions could not be suppressed completely, as demonstrated, *e.g.* in Fig. 3 by the Scatchard plots for non-porous glass affinity sorbents, interactions between the protein and polymerized silane molecules were found to be less important than interactions between the protein and hydroxyl groups at the silica surface. Furthermore, the polymerization of the silane at the silica surface also does not appear to influence the overall adsorption kinetics dramatically, because breakthrough curves for non-porous glass affinity sorbents and also for Nucleosil 4000-5 showed nearly rectangular profiles typical of very good adsorption characteristics. However, the capacities of the non-porous glass dye affinity sorbents were considerably lower than those of the porous silica and soft-gel affinity sorbents.

Dissociation constants for the affinity interactions of lysozyme with Cibacron Blue F3GA, immobilized on soft gel as well as silica sorbents, were generally one order of magnitude higher when 0.5 M NaCl was added to the equilibration buffer. This indicates that the adsorption mechanism in the absence of salt might be controlled mainly by ionic interactions of oppositely charged groups on the dye and protein molecules. Results reported by Chase<sup>3</sup> for the adsorption of lysozyme on Blue Sepharose CL6B in the absence of NaCl also demonstrated dissociation constants ( $K_d = 1.7 \cdot 10^{-6} M$ ) that were lower than ours for salt-free silica-based systems. Increasing the concentration of NaCl above 0.5 M did not significantly affect the dissociation constant and this suggests that specific biomimetic affinity interactions contribute to the adsorption under these conditions.

As is evident from Fig. 5 for the adsorption of lysozyme to Spherosil XOB030 and from Fig. 6, showing the adsorption of ADH on Blue Sepharose CL6B, breakthrough curves characteristic of unusual adsorption behaviour, typically

associated with the breakthrough of a portion of the selected protein solution at  $V_0$ , were observed. This behaviour was also observed for the adsorption of HSA on Cellufine GC 700 dye affinity sorbents and may be related to the split peak phenomenon in zonal chromatography. This phenomenon occurs when sorbents with high mass-transfer restrictions are employed for the separation of proteins under conditions of relatively high flow-rates<sup>20,21</sup>. Under these experimental conditions, two peaks can be observed for a single protein, the relative abundance of the two zones depending on the flow-rate. Using sorbents exhibiting a relatively high ratio ( $\lambda$ ) of protein size to pore size, a percentage of the adsorbate will not be able to enter the porous system nor will it be able to interact with the outer surface of the sorbent due to prior saturation of these external binding sites. A portion of the protein concentration will therefore pass through the column without interaction. This behaviour will be particularly important in protein particle system involving (i) long diffusion pathways of the adsorbate from the eluent stream to the outer surface of the sorbent, (ii) significant mass-transfer restrictions at pore entrances and (iii) significant film thickness of stagnant mobile phase surrounding each particle. When unusual shapes of the breakthrough curve were observed for the protein adsorption on the immobilised dye sorbents, these curves were invariably associated with long adsorption times and an almost horizontal progress of the adsorption curve. Due to the small but monotonously incremental changes in adsorption it is difficult to judge when the system had reached equilibrium. Even when this problem is overcome, as was achieved for the adsorption of ADH on Blue Sepharose, the determination of thermodynamic constants for some protein systems still remains problematical. For example, when human immunoglobulin G (IgG) was adsorbed on Cibacron Blue-immobilized Sepharose CL6B, the breakthrough volumes monotonously increased over the protein concentration range from 0.04–0.32 mg/ml. Instead of being anticipated by eqn. 1 for all human IgG concentrations, the calculated breakthrough volumes continued to change with increasing protein concentration when a particular protein concentration was exceeded. Although human IgG has a molecular weight similar to that of ADH, the adsorption of this protein may involve a different interaction mode<sup>22</sup>. The explanation for such specific behaviour may have its origin in the inability of all adsorbate molecules to interact with the dye affinity sorbent due to steric effects, some protein molecules being simply flushed through the column and therefore not being accounted for in the equilibrium equation.

Some dye affinity systems showing typical adsorption behaviour in the bath experiments<sup>2</sup>, such as the HSA/Cellufine GC 700 sorbent system or the ADH/Blue Sepharose sorbent system, also displayed very slow adsorption kinetics and early breakthrough of proteins occurred when they were used as packed columns. In case of the Fractogel dye sorbents, no noticeable adsorption occurred of any of the three proteins in the column mode. These unexpected results may have their origin in changes in the gel structure of these sorbents as a result of the operating conditions, such as the influence of flow-rate and attendant pressure on the bed. In the column systems the porous structure of the Fractogel dye sorbents is significantly deformed so that even lysozyme could not penetrate the porous system. These changes observed in the adsorption kinetics with column systems clearly illustrate a major limitation of the bath model. Although the thermodynamic constants from bath and column experiments with several protein dye sorbent systems corresponded very well, where changes

in the gel structure were not dominant or could not occur, for other dye affinity systems the data from the bath experiments did not agree with the column experiments. Consequently, comparative behaviour of the bath and column model can only be expected for sorbents having a rigid gel structure, such as silica-based sorbents, where no significant deformation of the porous network structure occurs. The nature of the dependency of pressure drop,  $\Delta p$ , upon flow-rate for a packed column may thus be an important parameter in comparing bath and column models of adsorption behaviour, *i.e.* whether the dependency is linear over a wide range of flow-rates or exhibits the asymptotic behaviour characteristic of many soft gels at higher flow-rates.

Sorbents based on small-particle-size supports generally showed steeper breakthrough curves and therefore better performance than the large-particle-size sorbents in the lower part of the breakthrough curve. With the non-porous dye sorbents based on either silica or glass beads, a nearly rectangular shape was observed. However, the shape of the breakthrough curve with these high-performance sorbents was never symmetrical around the inflection point and when compared to large-particle-size sorbents the adsorption process displayed considerably slower adsorption kinetics in the upper part of the curve than in the lower part (*cf.* Fig. 7). This adsorption phenomenon was also observed in our previous studies, when non-porous silica supports were employed as sorbents in frontal analysis experiments with immobilized ligands, such as benzamidine for the adsorption of trypsin<sup>16</sup> and with monoclonal antibodies against lysozyme<sup>6</sup>. The relatively slow adsorption kinetics for proteins displayed in the upper part of the breakthrough curves may be attributable to a rearrangement of adsorbed proteins, which in the initial phase of adsorption are statistically distributed at the surface of the sorbent, but become more densely packed towards the end of the adsorption process. In addition, a reorientation of adsorbed proteins may also take place, directed by specific protein-protein and protein-ligand interactions and leading to the most favoured arrangement of adsorbed proteins at the surface of the sorbent. Such a phenomenon would be less apparent when large particle/pore-size sorbents are employed, since in these cases adsorption of proteins is mainly diffusion-controlled throughout the adsorption process and rearrangement of adsorbed proteins might occur with a similar time scale to diffusional transport. To substantiate this hypothesis, more studies are needed at much lower protein concentrations than utilized in the present study in order to provide data relevant to the linear part of the equilibrium isotherm.

Apart from the asymmetric breakthrough curves discussed above, the adsorption kinetics in the upper part of the curve were consistently slower with small-particle-size than with larger-particle-size sorbents at identical protein concentrations. In order to equate adequately the effect of particle size for various sorbent systems, the experimentally determined breakthrough volumes for sorbents with different particle sizes were corrected by appropriate multiplication factor in order to yield normalized values. Reevaluation of the data then revealed an inverse relationship between adsorption kinetics and particle size for protein loads approaching saturation. This dependency may have its origin in one or more of the possibilities discussed below.

#### *Non-ideal pore connectivity*

The particle-size/pore-size ratio of Nucleosil 4000-5 is very low (12.5) compared to Nucleosil 4000-2540 (> 62.5). Supports having particle-size/pore-size ratios of < 30

are, based on the theoretical considerations of Guiochon and Martin<sup>23</sup>, presumed to experience unimpeded flow through the porous system. However, Nucleosil supports have been reported<sup>24</sup> to show lower performance in size-exclusion chromatography than expected for their particle size. A similar phenomenon might occur during frontal analysis, since the pathway of the protein through the porous system will be impeded by non-ideal pore connectivity. Since residence times of the protein inside the pores of the sorbent will then be shorter, breakthrough might occur earlier and at lower protein concentrations, whilst protein–ligand rearrangements could become more dominant at higher protein concentrations. Further experiments, in which dye affinity sorbents with pore sizes of 30 nm, 100 nm and 400 nm, and a particle size of 5  $\mu\text{m}$  are compared, may confirm this hypothesis. In this connection it is noteworthy that the data for Nucleosil 1000-5 which has a particle-size to pore-size ratio of 50, demonstrated that this dye affinity sorbent performed best in terms of kinetic phenomena (*cf.* Fig. 8).

#### Ligand gradients

Ligand heterogeneities (denser immobilized ligands at the surface than at the centre of the sorbent) have been previously discussed as a major factor in adsorption anomalies. The current evidence<sup>24</sup> on this aspect suggests that for small-particle-size sorbents, chemical modification of the matrix surface results in a more homogeneous layer of immobilized ligands over the accessible surface of the particle than for large-particle-size sorbents. Furthermore, more homogeneous sorbents are believed to perform better than heterogeneous sorbents. In this respect the 5- $\mu\text{m}$  sorbents should perform better, than, *e.g.*, a 25- $\mu\text{m}$  porous sorbent. In our studies, this could only be confirmed at the lower part of the breakthrough curve, but never at the upper part. If rearrangement and, possibly, reorientation of adsorbed proteins<sup>25</sup> are a major contributing factor to the adsorption kinetics at the upper part of the breakthrough curve, no real justification exists *a priori* why sorbents with a more homogeneous ligand densities and distribution over the whole surface of the particle should perform better than those with a ligand gradient in the pores. Sorbents having lower ligand

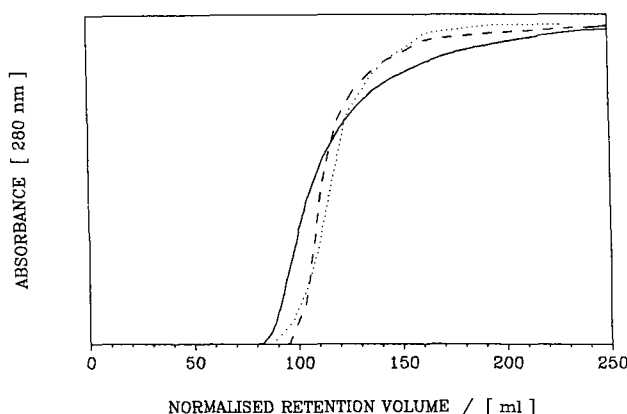


Fig. 8. Profile of breakthrough curves on silica-based affinity sorbents with different pore sizes and constant particle size during the adsorption of lysozyme in 50 mM Tris-HCl (pH 7.8)/0.8 M NaCl at a flow-rate of 0.5 ml/min. .... = Nucleosil 300-5; ---- = Nucleosil 1000-5; — = Nucleosil 4000-5.

densities in the centre of the sorbent than at the outer surfaces may conceivably display better adsorption characteristics and kinetics due to much more specific interaction of the adsorbate with the ligand, in which case reorientation will not be necessary. Invoking this hypothesis would explain the better performance of large particle-size sorbents of both the Nucleosil 300- and Nucleosil 4000-based supports (*cf.* Fig. 7a and b).

#### *Changes in dissociation constants*

Differences in the adsorption capacities and dissociation constants of the various dye affinity sorbents can be considered as an obvious explanation of the observed dependence of kinetics on particle sizes in the overload condition. As shown in Table I, the capacity of the Nucleosil 4000-2540 dye affinity sorbent was higher and the dissociation constant was lower than that of the Nucleosil 4000-5 dye affinity sorbent, whilst for the Nucleosil 300 dye affinity sorbents, the opposite was observed. If the kinetic effect was solely due to differences in the dissociation constants, one would expect the breakthrough curve behaviour of Nucleosil 300 and Nucleosil 4000 to be different. Since this was not the case (*cf.* Fig. 7a and b), other influences, besides dissociation constant differences, must be involved.

#### CONCLUSIONS

With preparative batch chromatographic isolations, feed stock loading of proteins is interrupted when a certain amount of the protein of interest is detected in the effluent. In such situations, slow adsorption kinetics in the upper part of the breakthrough curve will not represent a serious limitation in terms of productivity or performance. If protein rearrangement and/or reorientation plays a central role in the adsorption, for sorbents containing more immobilized ligands than required on a stoichiometric basis to bind the adsorbate (*i.e.* excess ligands are always available) then, the effective capacity of these "high-ligand-density" sorbents may not necessarily be higher than the capacity of a sorbent with a lower amount of immobilized ligands. In such "high-ligand-density" cases a proportion of the immobilized ligands may not be accessible whilst high density patches of ligands may even contribute to slower adsorption kinetics. The use of small-particle-size sorbents will not circumvent this limitation. Beside the technical and economic issues of pressure, cost of manufacture, and packing requirements, the use of small-particle sorbents (*e.g.*,  $d_p < 10 \mu\text{m}$ ) in preparative chromatography does not appear to be justified, especially, if a breakthrough of 10% or 20% of the protein of interest can be tolerated. Such conditions occur commonly in large-scale chromatographic isolations involving recycling capabilities. Collectively, these conclusions argue in favour of larger-particle-diameter sorbents in process applications.

An important outcome of the studies discussed in this publication is the further demonstration of the usefulness of the chromatographic model, based on frontal analysis, in characterizing and providing essential data on the thermodynamic parameters and the dynamic performance of sorbents. Changes in the adsorption behaviour of proteins due, *e.g.*, to steric hindrances is not as obvious in bath experiments and may not be recognized. Furthermore, the influence of changes in the gel structure after packing the columns, as observed for the Fractogel and Blue

Sepharose sorbents, will also not be recognised, if only bath experiments are considered.

The adsorption of proteins on sorbents is still a poorly understood and obviously a very complex process. Interpretation of observed adsorption phenomena often cannot be adequately explained by first order models, which account only for homogeneous protein–ligand interaction. Irreversible adsorption, as observed for example with HSA and some silica-based affinity sorbents, may ultimately become predictable if a full picture of the molecular basis of protein–protein interactions, protein unfolding, or rearrangement of the tertiary structure and reorientation of proteins at the surface of the sorbent were available. To account for—and predict—such effects, much more information about the molecular events occurring between proteins and their environment in adsorption on biomimetic affinity sorbents remains to be acquired. Approaches to such studies on protein adsorption and chromatographic behaviour form part of associated investigations to be described in subsequent publications<sup>25,26</sup>. As eloquently noted by Jacobsen *et al.* in a seminal publication<sup>7</sup> on the measurement of adsorption isotherms “The continued importance of adsorption and chromatographic processes in various areas of science and technology has made them a common focus of study”.

#### ACKNOWLEDGEMENTS

The support of the Australian Research Grants Committee and Monash University Special Research Grants (to M.T.W.H.) is gratefully acknowledged. F.B.A. is a recipient of a Monash University Postdoctoral Fellowship. Furthermore this work was part of a research project supported by the Deutsche Forschungsgemeinschaft, F.R.G. A.J. is a recipient of a Monash University Graduate Scholarship.

#### REFERENCES

- 1 M. Guthridge, J. Bertolini and M. T. W. Hearn, *J. Chromatogr.*, 476 (1989) 445.
- 2 F. B. Anspach, A. Johnston, H.-J. Wirth, K. K. Unger and M. T. W. Hearn, *J. Chromatogr.*, 476 (1989) 205.
- 3 H. A. Chase, *J. Chromatogr.*, 297 (1984) 179.
- 4 F. H. Arnold, S. A. Schofield and H. W. Blanch, *J. Chromatogr.*, 355 (1986) 1.
- 5 B. H. Arve and A. T. Liapis, *AIChE J.*, 33 (1987) 179.
- 6 A. T. Liapis, B. Anspach, M. F. Findley, J. Davies, K. K. Unger and M. T. W. Hearn, *Biotechnol. Bioeng.*, (1989) in press.
- 7 J. Jacobsen, J. Frenz and Cs. Horváth, *J. Chromatogr.*, 316 (1984) 53.
- 8 K.-I. Kasai, Y. Oda, M. Nishikata and S.-I. Ishi, *J. Chromatogr.*, 376 (1986) 33.
- 9 G. Guiochon and A. Katti, *Chromatographia*, 24 (1987) 165.
- 10 D. J. Graves and Y.-T. Wu, *Methods Enzymol.*, 34 (1974) 140.
- 11 B. J. Horstmann, C. N. Kenney and H. A. Chase, *J. Chromatogr.*, 376 (1986) 179.
- 12 I. M. Chaiken, *J. Chromatogr.*, 376 (1986) 11.
- 13 D. J. Winzor and E. J. Yon, *Biochem. J.*, 217 (1984) 867.
- 14 F. H. Arnold, H. W. Blanch and C. R. Wilke, *Chem. Eng. J. (Lausanne)*, 30 (1985) 9.
- 15 L. W. Nichol, A. G. Ogston, D. J. Winzor and W. H. Sawyer, *Biochem. J.*, 143 (1974) 435.
- 16 B. Anspach, H. J. Wirth, K. K. Unger, P. Stanton, J. Davies and M. T. W. Hearn, *Anal. Biochem.*, 179 (1989) 171.
- 17 B. Anspach, K. K. Unger, J. Davies and M. T. W. Hearn, *J. Chromatogr.*, 457 (1988) 195.
- 18 A. Yelayudhan and C. Horváth, *J. Chromatogr.*, 443 (1988) 13.
- 19 W. Kopaciewicz, S. Fulton and S. Y. Lee, *J. Chromatogr.*, 409 (1987) 111.

- 20 L. A. Larew and R. R. Walters, *Anal. Biochem.*, 164 (1987) 537.
- 21 C. DeLisi, H. W. Hethcote and J. W. Brettler, *J. Chromatogr.*, 240 (1982) 283.
- 22 P. G. H. Byfield, S. Copping and R. L. Himsworth, *Mol. Immunol.*, 21 (1984) 647.
- 23 G. Guiochon and M. Martin, *J. Chromatogr.*, 326 (1985) 3.
- 24 K. K. Unger, *Porous Silica*, Elsevier, Amsterdam, 1984.
- 25 M. T. W. Hearn, M. I. Aguilar and A. N. Hodder, *J. Chromatogr.*, in press.
- 26 M. T. W. Hearn, A. N. Hodder and M. I. Aguilar, submitted for publication.



CHROM. 21 787

## FACTORS INFLUENCING THE PERFORMANCE OF PEPTIDE MAPPING BY REVERSED-PHASE HIGH-PERFORMANCE LIQUID CHROMATOGRAPHY

MICHAEL W. DONG\*

*The Perkin-Elmer Corporation, 761 Main Avenue, Norwalk, CT 06859-0250 (U.S.A.)*

and

AN D. TRAN

*Ortho Pharmaceutical Corporation, Raritan, NJ 08869-0602 (U.S.A.)*

---

### SUMMARY

Factors controlling the performance of peptide mapping on reversed-phase columns were systematically evaluated. Performance criteria included resolution (peak capacity and selectivity), system reproducibility, sensitivity and analysis speed. Column configuration, characteristics of packing materials, mobile phase composition, operating variables and instrumental designs were found to influence the performance of peptide mapping. Considerations for peptide identification techniques are discussed.

---

### INTRODUCTION

Peptide mapping is a powerful method for the structural identification of proteins<sup>1,2</sup>. In peptide mapping, a sample protein is selectively cleaved by enzymes (*e.g.*, trypsin, chymotrypsin, endoproteinase Lys-C, V8 proteinase from *Staphylococcus aureus*, pepsin, subtilisin, clostripain, etc.) or by chemical digestions (*e.g.*, cyanogen bromide). Trypsin, the most common agent, cleaves the carboxyl side of the peptide bonds of lysine, arginine and aminoethyl cysteine and forms many fragments averaging 7–12 amino acid residues<sup>3</sup>. In contrast, cyanogen bromide cuts the protein at the methionine site and yields relatively large fragments.

The digest is then analyzed by liquid chromatography to yield a peptide map. Reversed-phase high-performance liquid chromatography (RP-HPLC) is the primary mode used because of its high resolution and selectivity<sup>4</sup>. The resultant peptide map is a unique “fingerprint” profile of the protein and may be compared to a reference chromatogram to establish equivalency.

Fig. 1 shows two comparative tryptic maps of recombinant tissue-type plasminogen activator (rt-PA), a glycosylated protein of approximately 64 000 daltons which was recently approved by the Food and Drug Administration (FDA) for treating heart attack patients<sup>5–7</sup>. The bottom map of a mutant rt-PA is virtually identical to the reference map except the retention time of one peptide is shifted. This is due to the substitution of glutamic acid for arginine in position 275. Such a variance in peak retention is used to identify changes in the amino acid sequence of the protein.

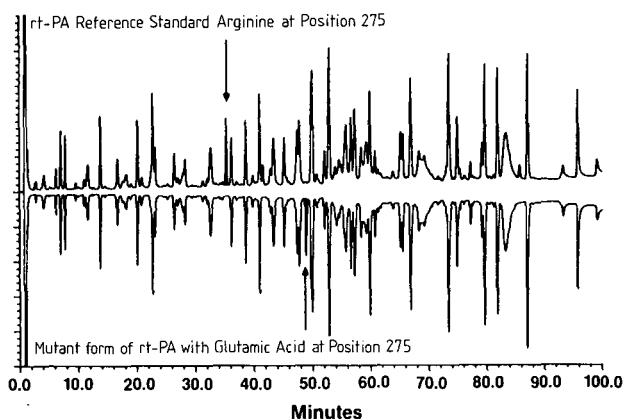


Fig. 1. Tryptic map chromatograms of the rt-PA reference standard and a mutant form of rt-PA with a glutamic acid residue in place of the normal arginine residue at position 275. Arrows illustrate the differences in the two chromatograms caused by the substitution. Courtesy of Garnick *et al.*, from ref. 6.

Peptide mapping is the premier method for the structural elucidation of newly discovered proteins. Since 80–90% of the eukaryotic proteins cannot be sequenced directly due to blocked amino-termini<sup>8</sup>, peptide mapping is used to isolate fragments for sequence analysis. The technique is also used to locate glycosylation sites<sup>9,10</sup> and disulfide linkages<sup>11</sup>. Today, peptide mapping is increasingly used in biotechnology for the quality control of recombinant proteins. Mapping provides vital information on lot-to-lot product consistency, expression errors, and mutation or deamidation sites<sup>5,6</sup>.

Peptide mapping is one of the most demanding applications of HPLC. A typical map contains 20–150 peaks, all of which should be totally resolved (or near totally resolved). A high level of column resolution and system precision is required to accurately reproduce the maps, often in sub-nanomole quantities. This places stringent demands on both the compositional and flow repeatability of the solvent delivery system and also the sensitivity and stability of the detection system.

This paper describes a systematic study of the factors controlling the performance of peptide mapping by RP-HPLC. Performance criteria include resolution, system reproducibility, sensitivity and analysis speed. Factors (column, operating conditions and instrumentation) leading to optimized peptide mapping as well as considerations for sequence analysis and peptide identification are discussed.

## EXPERIMENTAL

### *Apparatus*

The LC system used in this study consisted of a Model 250 binary LC pump, a Rheodyne Model 7125 injector, an LC-135 dual-channel diode array detector, and a GP-100 printer/plotter. In addition, an LC-101 oven for column temperature control and an ISS-100 automatic sampler were used for evaluating system reproducibility. Solvent degassing was accomplished by helium sparging and pressurization in polyethylene solvent bottles (2-l and 4-l capacity). All equipment was from Perkin-Elmer (Norwalk, CT, U.S.A.).

### Columns

Vydac columns packed with polymeric C<sub>18</sub> bonded phase were used. These columns, available from Perkin-Elmer or from the Separations Group (Hesperia, CA, U.S.A.) had the following dimensions: 250 mm × 4.6 mm I.D.; 150 mm × 4.6 mm I.D.; 50 mm × 4.6 mm I.D. and 250 mm × 2.1 mm I.D. The packings had nominal particle diameter and pore size of 5 μm and 300 Å, respectively. An experimental column (83 mm × 4.6 mm I.D.) packed with 3-μm C<sub>8</sub> materials was also evaluated.

A scavenger column (33 mm × 4.6 mm I.D.) packed with 10-μm C<sub>18</sub> particles placed between the pump and the injector protects the analytical column from mobile phase contaminants<sup>12</sup>. This precolumn eliminates the need for solvent filtration through membrane filters, which can introduce gradient artifacts<sup>13</sup>, and also helps to prolong column lifetime. A low-capacity guard column (30 mm × 2.1 mm I.D.) dry-packed with 40-μm C<sub>18</sub> pellicular materials was also found to be satisfactory in offering protection against sample contaminants without adversely affecting performance of the analytical columns<sup>12</sup>.

### Chemicals and reagents

All sample proteins, L-1-tosylamide-2-phenylethyl chloromethyl ketone (TPCK)-treated trypsin, and trifluoroacetic acid (TFA) were obtained from Sigma (St. Louis, MO, U.S.A.). Other chemicals and reagents were obtained from Aldrich (Milwaukee, WI, U.S.A.) and Fisher Scientific (Fairlawn, NJ, U.S.A.). HPLC-grade acetonitrile was obtained from EM Science (Gibbstown, NJ, U.S.A.). Water was filtered and purified by passage through mixed-bed, ion-exchange, and activated charcoal cartridges.

### Mobile phase preparation

Three mobile phase systems were used:

Mobile phase system	Strong solvent (A)	Weak solvent (B)
(I) 0.1% TFA	0.1% TFA acetonitrile	0.1% TFA in water
(II) Balanced absorbance	0.054% TFA in acetonitrile-water (80:20)	0.06% TFA in water
(III) Phosphate	Acetonitrile	50 mM NaH <sub>2</sub> PO <sub>4</sub> (pH 2.6)

Most proteins/peptides yield better peak shapes under acidic pH<sup>14</sup>. The use of 0.1% TFA with acetonitrile has been adopted by most analysts as the "standard" mobile phase for RP-HPLC of proteins. However, use of mobile phase system I (0.1% TFA) is limited to low sensitivity applications because baseline shifts due to unbalanced absorbance preclude its use in mapping below 250 pmol levels.

### Procedure for preparing tryptic digests

Reduction and S-carboxymethylation of proteins were carried out according to the procedure of Crestfield *et al.*<sup>15</sup> with the exception that mercaptoethanol was replaced by dithiothreitol (DTT)<sup>16</sup>. The procedure works well for milligram quantities of protein. However, lower levels are problematic because of the loss of proteins during the dialysis and lyophilization steps. An alternate tryptic digestion procedure suitable

for subnanomole levels of proteins in which these low yield steps were replaced with a dilution step with water, was used for the human transferrin sample<sup>17</sup>.

## RESULTS AND DISCUSSION

Table I lists the performance criteria and the key factors controlling the performance of peptide mapping by liquid chromatography. These factors fall into three distinct categories: column parameters, operating conditions and instrumentation. Each performance criterion and its influencing factors are discussed in detail below.

### *Resolution*

The primary goal in mapping is the resolution of all peptide fragments. Since their size and hydrophobicity vary, gradient elution techniques are used. Resolution is a function of column efficiency ( $N$ ), retention ( $k'$ ), and selectivity ( $\alpha$ ). In complex maps in which all peaks need to be resolved, the overall peak capacity is the most important criterion<sup>18</sup>. In contrast, for resolving co-eluting peaks, increasing the chromatographic selectivity by changing the gradient time ( $t_G$ ), the mobile phase or the bonded phase is often sufficient. Above all, the peptide columns used must yield symmetrical peak shapes with quantitative mass recovery for all fragments.

*Peak capacity.* Peak capacity is an empirical parameter defined as the maximum number of peaks that can theoretically be resolved in the chromatogram. Peak capacity is calculated by dividing the net retention time of the last peak in the chromatogram by the average peak width<sup>18</sup>. It is primarily a function of  $N$ , gradient time ( $t_G$ ), and flow-rate ( $F$ ).

Fig. 2 shows how peak capacity varies with  $t_G$  and column length ( $L$ ). Three Vydac C<sub>18</sub> columns of 5, 15 and 25 cm length were used in the experiments. Peak

TABLE I  
FACTORS INFLUENCING THE PERFORMANCE OF PEPTIDE MAPPING BY LC

<i>Criteria</i>	<i>Key factors</i>
Resolution	Column efficiency
Column peak capacity	Flow-rate and gradient time
Selectivity	Mobile phase, bonded phase, gradient time
Peak shape and mass recovery	Silica type, pore size
System reproducibility	Pump flow and gradient precision Temperature fluctuations LC system reliability Column lot-to-lot reproducibility and lifetime
Detection sensitivity	Detector noise and drift Mobile phase purity and absorbance Monitoring wavelength Column diameter Flow-rate
Analysis speed	Column length, particle size Flow-rate and gradient time

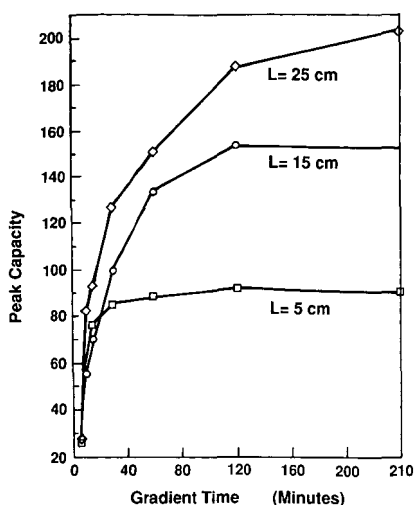


Fig. 2. Graph showing the variation of peak capacity vs. gradient time and column length ( $L$ ). Columns were packed with  $5\text{-}\mu\text{m}$  Vydac  $C_{18}$  materials. Mobile phase: A = 0.1% TFA in acetonitrile, B = 0.1% TFA in water; Gradient conditions: 2% A to 32% A, 1 ml/min and  $40^\circ\text{C}$ ; sample = lysozyme digest. Peak capacities were calculated from peaks 4, 8, 12 and 15 of the digest (see Fig. 6a).

capacity was found to increase with column length and gradient time. The lower curve (5-cm column) shows that peak capacity increases rapidly with  $t_G$  up to about 30 min and flattens out beyond 40 min to a value of 90. Fig. 2 also demonstrates that to achieve high peak capacities ( $>150$ ), longer columns (15 or 25 cm) should be used with gradient times of 80–120 min. For gradient times beyond 2 h, peak capacities appear to reach a constant level for the 15-cm column and a point of diminishing return for the 25-cm column (at 1 ml/min).

Fig. 3 shows a high-resolution tryptic map of human transferrin (unmodified molecular weight 75 000 daltons) using a 25-cm column and a  $t_G$  of 95 min at 1 ml/min. The complexity of the chromatogram is typical for tryptic maps of larger proteins. As Fig. 2 indicates, these operating conditions are near optimum for the  $5\text{-}\mu\text{m}$  Vydac columns used.

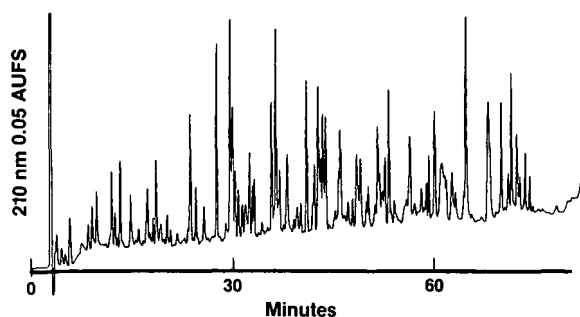


Fig. 3. High-resolution tryptic map of human transferrin (140 pmol). LC conditions: column:  $5\text{-}\mu\text{m}$  Vydac  $C_{18}$  ( $250 \times 4.6$  mm I.D.). Mobile phase: A = 0.056% TFA in acetonitrile–water (80:20); B = 0.06% TFA in water; gradient conditions 2–37% A in 63 min, 37–75% A in 32 min, 75–98% A in 10 min, 1 ml/min, ambient temperature, pressure drop 1200 p.s.i. From ref. 35.

A systematic treatment relating peptide resolution to gradient parameters is found elsewhere<sup>19</sup>. Gradient parameters have a profound effect on peptide resolution because they control average retention ( $\bar{k}$ ) as shown in eqn. 1<sup>19</sup>.

$$\bar{k} = \frac{t_G (F)}{1.15 (\Delta\varphi) V_m S} \quad (1)$$

Where  $\bar{k}$  = Average solute capacity factor under gradient  
 $\varphi$  = Fraction of organic solvent in the mobile phase  
 $\Delta\varphi$  = Change of  $\varphi$  during gradient  
 $V_m$  = Column void volume  
 $S$  = Solute parameter (slope of  $\log k'$  vs.  $\varphi$ )

$\bar{k}$  describes the average solute retention under gradient conditions and is analogous to  $k'$  for isocratic separations. Eqn. 1 indicates that an increase in  $t_G$  (holding  $F$  constant) leads to higher values of  $\bar{k}$ . Higher  $\bar{k}$  is equated to higher resolution (or peak capacity) since greater volumes of a lower strength mobile are passed through the column. This phenomenon was confirmed by data presented in Fig. 2.

Fig. 4 demonstrates the relationship between peak capacity and  $\bar{k}$  at different flow-rates for the 15-cm Vydac column. Peak capacity was found to increase with  $\bar{k}$  (1–40) over a flow-rate range of 0.5 to 3 ml/min. Fig. 4 also shows that for constant retention (e.g.,  $\bar{k} = 10$ ), peak capacity decreases as flow-rate increases. This is caused by a loss of column efficiency at high flow-rates due to the low diffusivities of peptides (see Fig. 9). The highest value of peak capacity in the graph (peak capacity = 168) was

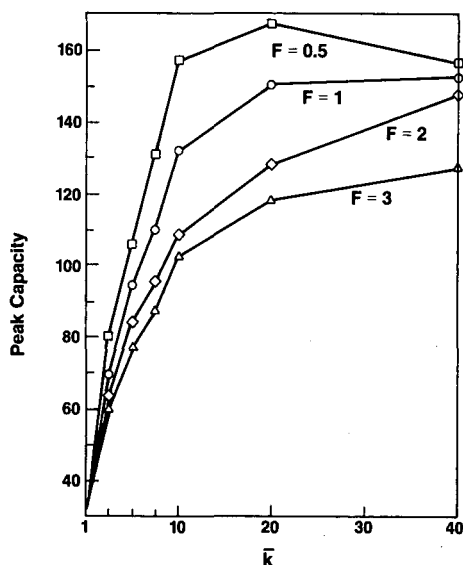


Fig. 4. Graph showing the variation of peak capacity vs.  $\bar{k}$  using different flow-rates. Column: 5- $\mu$ m Vydac C<sub>18</sub> (150 mm  $\times$  4.6 mm I.D.). Mobile phase and sample were identical to that used in Fig. 2.

achieved at  $F = 0.5$  ml/min and  $\bar{k} = 20$  ( $t_G = 208$  min). Thus, for high resolution mapping, these data suggest the use of 15 to 25 cm column lengths, operating at flow-rates of 0.5 to 1 ml/min and gradient times between 60 and 200 min or  $\bar{k}$  between 10 and 20.

**Selectivity.** Chromatographic selectivity ( $\alpha$ ) is primarily a function of the mobile phase composition (e.g., ion-pairing reagent, pH, organic solvent)<sup>14</sup> and the nature of the bonded phase (e.g., C<sub>4</sub>, C<sub>8</sub>, C<sub>18</sub>, phenyl)<sup>20,21</sup>.

Fig. 5 shows two comparative tryptic maps of  $\beta$ -lactoglobulin A (molecular weight 34 000 daltons) using different mobile phases. The figure illustrates how co-eluting fragments can be resolved completely by just changing the mobile phase. Further more, compared to 0.1% TFA (system I), phosphate buffer (system III) yields sharper peaks and less gradient baseline shift due to its higher transparency at 220 nm<sup>22,23</sup>.

The use of bonded phases with shorter alkyl chains (e.g., C<sub>4</sub>–C<sub>8</sub>) often yields sharper peaks and different selectivity than C<sub>18</sub> phases for hydrophobic peptides<sup>21,22</sup>. However, the retention of small or hydrophilic peptides found in many tryptic digests is also lower in these phases.

**Peak symmetry and peptide mass recovery.** Peptide separations are sensitive to silica types<sup>23–25</sup>. The purity, acidity and residual silanophilic activity of the silica material appear to be the critical factors. Residual silanols interact with basic amino acid groups and cause peak tailing or even adsorption. The suitability of bonded phases for peptide mapping can be assessed by basic test probes such as N,N-diethyl-aniline<sup>26</sup> or standard peptides<sup>27</sup>. Alternatively, the peptide map on a new column can be compared to that of a known reference column (e.g., Vydac C<sub>18</sub>) for the total number of peaks and peak symmetries. Pore size of packing materials should be 125–300 Å<sup>6</sup> for peptides to prevent band broadening due to “restricted diffusion”<sup>19,23</sup>. Wide-pore packings (i.e., 300 Å) are preferred for partial digests or if substantial levels of undigested proteins are present in the sample.

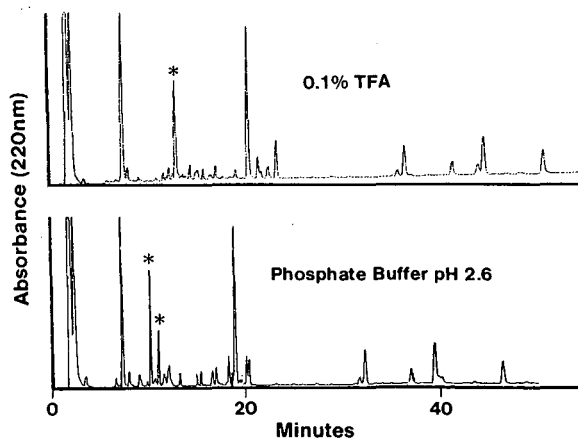


Fig. 5. Comparative tryptic maps of  $\beta$ -lactoglobulin A using mobile phase system I (upper) and III (lower). Gradient conditions: 0–15% A in 15 min, 15–30% A in 40 min, 1 ml/min at 40°C. The peak marked with an asterisk in the upper chromatogram was resolved in the bottom chromatogram by changing chromatographic selectivity.

*Optimizing resolution in peptide mapping.* The utility of predictive modeling in gradient optimization of peptide mapping has been demonstrated<sup>28,29</sup>. Primary structures of individual fragments of known proteins, best separation mode and retention order can also be predicted<sup>30,31</sup>. For very complex maps, the use of sequential digestions<sup>32</sup> and combined ion-exchange/reversed-phase chromatography<sup>3,34</sup> might be required to resolve all peaks.

#### *System reproducibility*

In peptide mapping, shifts in retention time might be interpreted as a variance of primary protein structure<sup>6</sup>. Thus, retention reproducibility of the LC system is a prime prerequisite. Shallow gradients (0–30% acetonitrile in water in 60–120 min) under low flow (0.2–1 ml/min), conditions that are optimal for mapping, are difficult to reproduce for many LC pumps<sup>6,26,35,36</sup>. Inaccurate mixing at low percentages of organic solvent (0–10%) is exacerbated by peptides which have steep elution isotherms or large  $S$  values<sup>23</sup>.

Retention time reproducibility can be evaluated by calculating the standard deviation of retention time of selected fragments from 6–10 repetitive runs or by visual inspection of the plotted chromatograms in an overlay (Fig. 6A) or splitscreen format (Fig. 6B). In our study, relative standard deviations (R.S.D.) of 0.1 to 0.25% in retention times were demonstrated under various operating conditions ( $F = 0.3$ – $2.5$  ml/min and  $t_G = 10$ – $95$  min). These experiments were conducted with thermostatted columns at 40°C to eliminate column temperature fluctuations and with pressurized solvent reservoirs (since even gentle continuous helium sparging tends to reduce TFA levels in the mobile phase).

While short-term reproducibility is attained with precise LC pumps<sup>35,36</sup>, long-term reproducibility is dependent on factors not easily controlled by the analyst (*e.g.*, long-term LC system reliability, column stability and lifetime, and batch-to-batch reproducibility of the packing materials).

Column batch-to-batch reproducibility is dependent on the exactness of the silica manufacturing process and the quality control procedures of the vendor. Column stability and lifetime can be extended by judicious column maintenance and washing procedures<sup>23</sup>, sample cleanup techniques and the use of scavenger and guard columns<sup>12</sup>.

Limited data suggested a column life expectancy of 200–300 injections or 10–30 l of mobile phase<sup>18,37</sup>. The shortened column life (compared to several thousand injections for general RP-HPLC<sup>38</sup>) might be caused by the prolonged use of an acidic mobile phase (0.1% TFA, pH 2) which can cleave the bonded groups or the end caps, exposing the silanols that cause peak tailing<sup>23</sup>. This problem might be addressed via the use of polymerized C<sub>18</sub> phases (*e.g.*, Vydac), novel bonding chemistries<sup>39</sup> and other proprietary treatment techniques (*e.g.*, Phase Separations pH-stable phases).

#### *Sensitivity*

Sensitivity is important in biochemical research because of the limited amount of sample protein available for characterization. Since digestion procedures for sub-nanomoles of proteins have previously been demonstrated<sup>17</sup> and sequencing can be performed routinely at the low picomole levels<sup>40</sup>, enhancing the detection sensitivity in peptide mapping is therefore the next logical step.



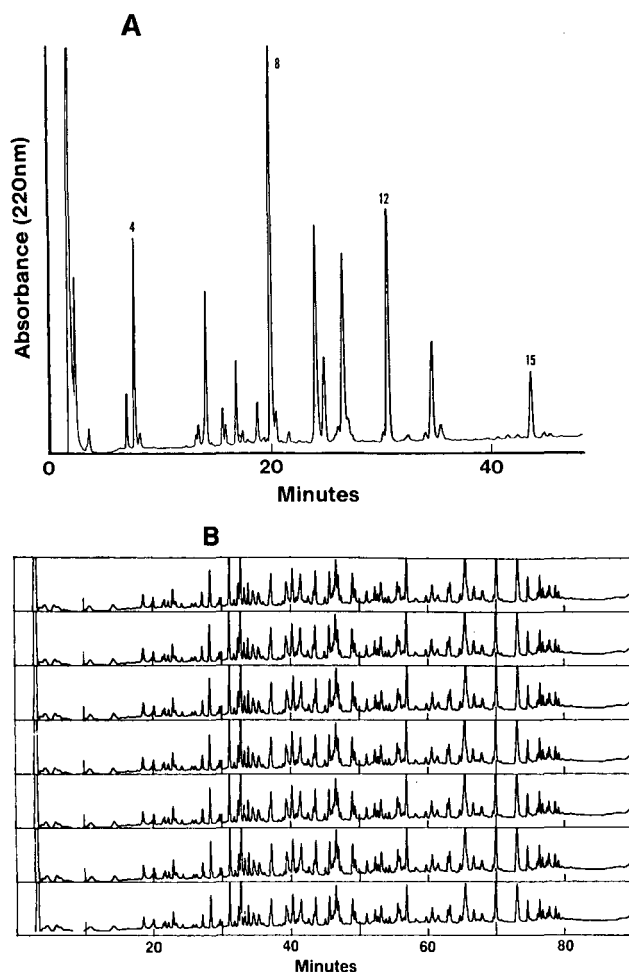


Fig. 6. System reproducibility. (A) an overlay of six tryptic maps of lysozyme. Column and mobile phase conditions identical to those used in Fig. 5 (upper). Retention time R.S.D. < 0.25%; peak area R.S.D. < 0.4%. From ref. 35. (B) Split-screen format of seven tryptic maps of human transferrin using a narrow-bore column at 0.3 ml/min. LC conditions: column: 5- $\mu$ m Vydac C<sub>18</sub> (250  $\times$  2.1 mm I.D.); mobile phase: A = 0.056% TFA in acetonitrile-water (80:20), B = 0.06% TFA in water, gradient conditions: 2–37% A, in 63 min, 37–75% A in 32 min, 75–98% A in 10 min, 0.3 ml/min, 40°C, pressure drop 1800 p.s.i.

Analytical sensitivity in peptide mapping is limited by mobile phase purity and absorbance as well as by detector noise and drift<sup>41</sup>. Fig. 7 shows a high-sensitivity tryptic map of lysozyme at the 15-pmol level using mobile phase system III (phosphate). Note that all peaks are readily identifiable with an acceptable signal to noise ratio at this very low level. A detection limit of about 1 pmol was achieved under these conditions.

Sensitivity is enhanced by using a lower monitoring wavelength (*i.e.*, 210 nm) and by reducing the column diameter. Lowering the monitoring wavelength from 220 nm to 210 nm increases the molar absorptivity of most peptides by a factor of two to

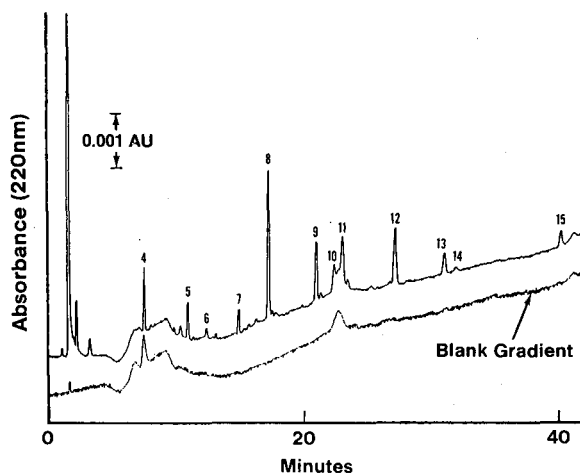


Fig. 7. High-sensitivity tryptic map of  $0.2 \mu\text{g}$  or  $15 \text{ pmol}$  of lysozyme shown with the elution profile of a blank gradient (data sampling rate was higher for the blank gradient run). LC conditions are identical to those used in Fig. 5 (lower). From ref. 35.

four. However, 0.1% TFA mobile phase (system I) cannot be used effectively at 210 nm due to the increased gradient baseline shifts caused by the unbalanced absorbance. Since phosphate buffer (system III) might be less compatible with commercial sequencers ( $> 200 \mu\text{l}$ ), the use of the balanced absorbance TFA mobile phase (system II) is recommended for general high-sensitivity mapping<sup>41</sup>.

Reducing the column diameter from 4.6 mm to 2.1 mm while maintaining the same linear flow velocity further enhances the mass sensitivity by a factor of five. This is due to the reduction of column void volume which leads to a lower sample dilution. This results in higher peak concentrations in the detector flow cell<sup>42</sup>. Fig. 8 is a tryptic map of 60 pmol of human transferrin using a narrow-bore Vydac  $\text{C}_{18}$  column ( $250 \text{ mm} \times 2.1 \text{ mm I.D.}$ ) at 0.3 ml/min. The mobile phase system II was used here at 210 nm. Substantial increases in mass sensitivity are apparent when the peak heights are compared with those found in Fig. 3 (after normalization). Any remaining gradient shift can be eliminated by making fine adjustments with TFA<sup>41</sup>.

Sensitivity can be further enhanced by using 1-mm microbore columns<sup>41</sup>.

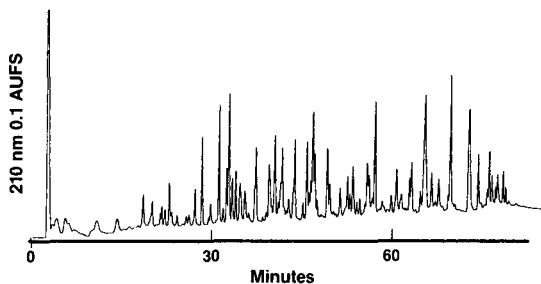


Fig. 8. High-sensitivity tryptic map of human transferrin (60 pmol) using narrow-bore column. Column and mobile phase conditions are identical to those used in Fig. 6B. From ref. 35.

However, their resolution performance might be limited by the column packing technique and also severely hampered by the extracolumn band broadening effects from the instrument<sup>42</sup>.

Lowering the flow-rate while maintaining  $t_G$  can dramatically increase detection sensitivity since retentions ( $\bar{k}$ ) are reduced (see eqn. 1). Although the peak capacity is adversely affected (see Fig. 4), the number of detected peaks which can be collected might not be substantially reduced<sup>41</sup>. This approach is particularly useful for collection runs because the decrease of peak volumes facilitates direct applications to commercial sequencers.

#### Analysis speed

Fast separation is desirable to increase productivity in quality control labs if other performance characteristics are not sacrificed (*e.g.*, resolution, sensitivity, reproducibility, column lifetime)<sup>23,38</sup>. This can be achieved by using shorter columns packed with small particles (2–3  $\mu\text{m}$ ) operated at faster flow-rates. Fig. 9 shows the Van Deemter curves of columns packed with 10-, 5- and 3- $\mu\text{m}$  particles for peptides. 3- $\mu\text{m}$  particles display lower minimum plate heights (*i.e.*, more plates per unit length) and less resistance to mass transfer (or lower  $C$  term, *i.e.*, less efficiency loss at high flows)<sup>32</sup>. The use of elevated column temperatures (40–50°C) enhances performance of fast separations by increasing peptide diffusivities<sup>37,43</sup>.

By using an 8 cm long column packed with 3- $\mu\text{m}$  porous  $\text{C}_8$  materials at high flow-rates (3 ml/min) and short  $t_G$ , tryptic maps of small proteins can be generated in 3–4 min (Fig. 10). These columns generate very high resolution maps at low flow (1 ml/min) and longer  $t_G$  (20–60 min)<sup>38</sup>. Fast peptide analysis is particularly well suited for checking peptide identity and purity from collected fractions.

The elimination of intraparticle diffusion in non-porous particles constitutes a novel approach to fast peptide mapping as demonstrated by Kalghatgi and Horváth

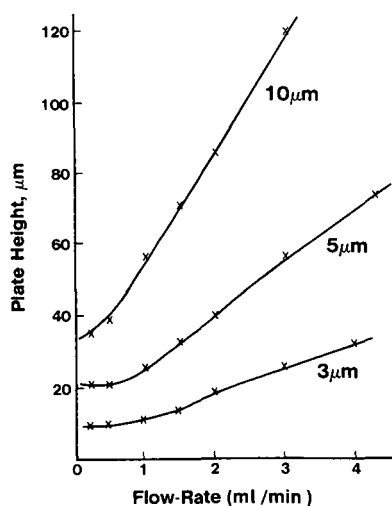


Fig. 9. Van Deemter curves for 10-, 5- and 3- $\mu\text{m}$  particle columns. Mobile phase: acetonitrile–0.1% TFA (25:75), 40°C; sample: met-enkephalin.

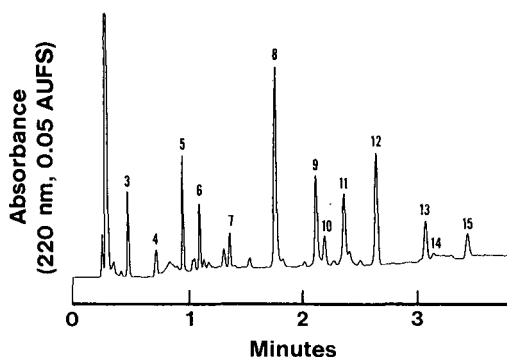


Fig. 10. Fast peptide mapping using an experimental 3- $\mu\text{m}$  porous  $\text{C}_8$  bonded phase column. LC conditions: experimental fast peptide mapping column packed with 3- $\mu\text{m}$  porous  $\text{C}_8$  bonded phase particles (83  $\times$  4.6 mm I.D.); mobile phase: A = acetonitrile, B = 50 mM phosphate buffer (pH = 2.6); Gradient conditions: 0–15% A in 0.8 min, 15–30% A in 3 min, 3.0 ml/min at 40°C, pressure drop = 3200 p.s.i. Sample is a 50-pmol tryptic digest of lysozyme. Peak numbers refer to tryptic fragments of lysozyme in order of elution. Injection was coincidental with the onset of the gradient. From ref. 35.

(Fig. 11)<sup>16</sup>. A very complex tryptic map of rt-PA is achieved in 16 min compared with an analysis time of 100 min (see Fig. 1) on conventional columns.

#### Peptide identification techniques

Traditional methods of peptide identification by amino acid analysis or sequence analysis can be supplemented by on-line detection techniques. Fig. 12 shows a dual-wavelength tryptic map of protein A. The 220-nm map (which monitors all peptide bonds) is very complex but the 280-nm map is more selective because only peptides containing the aromatic amino acids, phenylalanine, tryptophan and tyrosine, are detected. Typical diode array UV spectra of non-aromatic and aromatic peptides are also shown in Fig. 12. The non-aromatic peptide is not present in the 280-nm map due to a lack of absorbance at that wavelength.

Dual-wavelength detection is a powerful means for peptide identification. Research in spectral deconvolution techniques might eventually lead to an improved

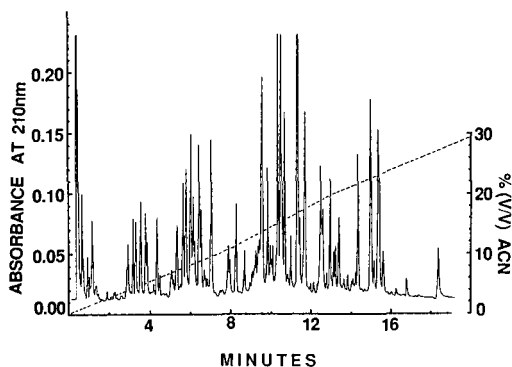


Fig. 11. Tryptic map of rt-PA using an experimental 2- $\mu\text{m}$  micropellicular  $\text{C}_{18}$  column (75  $\times$  4.6 mm I.D.). Flow-rate 1.5 ml/min, temperature 80°C; ACN = acetonitrile. Courtesy of Kaighatgi and Horváth, from ref. 16.

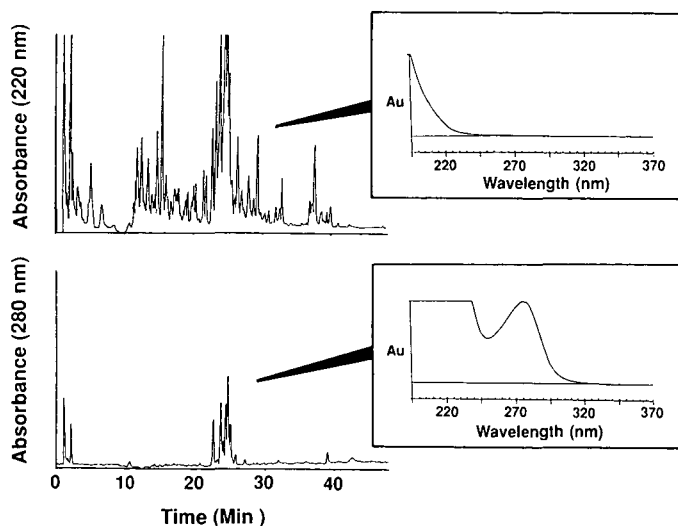


Fig. 12. Tryptic maps of protein A using dual-wavelength detection. Column and mobile phase identical to Fig. 5 (upper).

identification method of aromatic peptides<sup>44</sup>. In addition, coupling the UV detector with a fluorescence<sup>4</sup> or electrochemical detector<sup>11</sup> offers very selective detection for peptides containing tryptophan or cysteine residues.

#### SUMMARY OF PARAMETERS FOR PEPTIDE MAPPING BY RP-HPLC

Table II summarizes some recommended guidelines on column parameters, operating variables and instrumental requirements for peptide mapping.

TABLE II  
GUIDELINES FOR PEPTIDE MAPPING

<i>Column parameters</i>	
Packings	3–5 $\mu\text{m}$ C <sub>8</sub> or C <sub>18</sub> bonded phase 125–300 Å pores
Dimension	100–250 mm long 1–2 mm I.D. for high-sensitivity
<i>Operating variables</i>	
Mobile phase	Strong solvent: 0.052% TFA in acetonitrile–water (80:20) Weak solvent : 0.06% TFA in water
Flow-rates	0.5–2 ml/min for 4.6 mm columns 0.2–0.4 ml/min for narrow-bore columns
Gradient time	30–120 min
Column temperature	Ambient to 50°C
<i>Instrumental requirements</i>	
Pump	Excellent flow and composition precision Low pulsation and gradient delay volume Solvent degassing and pressurization
Detector	Low dispersion and long pathlength Low noise and drift Dual-channel (210 and 280 nm)

High-resolution mapping is achieved by using column 150–250 mm long, packed with 5- $\mu\text{m}$  low-silanophilic materials operating at low flow-rate and long gradient time. Reproducibility is achieved with precise LC pumps and stable analytical columns protected by precolumns. High sensitivity is achieved with sensitive detectors operating at 210 nm and by using the balanced absorbance TFA mobile phase. Narrow-bore columns are used to further maximize sensitivity. Fast peptide mapping is achieved by using short columns packed with 3- $\mu\text{m}$  porous or 2- $\mu\text{m}$  non-porous materials. Dual-wavelength and selective detection techniques are effective for quick peptide identification.

#### ACKNOWLEDGEMENTS

The authors thank F. Vandemark, E. Katz and T. Dion of Perkin-Elmer, C. duMee of Genentech and K. Kalghatgi, K. Stone and K. Williams of Yale University for previewing the manuscript. We also thank R. Garnick of Genentech and K. Kalghatgi of Yale University for allowing us to reproduce Fig. 1 and 11 and K. Stone of Yale University for providing us the human transferrin sample digest.

#### REFERENCES

- 1 S. Borman, *Anal. Chem.*, 59 (1987) 969.
- 2 W. A. Schroeder, in W. S. Hancock (Editor), *CRC Handbook of the Separation of Amino Acids, Peptides and Proteins*, Vol. II, CRC Press, Boca Raton, FL, 1984, pp. 283–300.
- 3 F. Regnier, *LC · GC, Mag. Liq. Gas Chromatogr.*, 5 (1988) 393 and 473.
- 4 P. A. Hartman, J. D. Stodola, G. C. Harbour and J. G. Hoogerheide, *J. Chromatogr.*, 360 (1986) 385.
- 5 W. S. Hancock, *Chromatogr. Forum*, 2 (1986) 57.
- 6 R. L. Garnick, N. J. Solli and P. A. Papa, *Anal. Chem.*, 60 (1988) 2546.
- 7 R. C. Chloupek, R. J. Harris, C. K. Leonard, R. G. Keck, B. A. Keyt, M. W. Spellman, A. J. S. Jones and W. S. Hancock, *J. Chromatogr.*, 463 (1989) 375.
- 8 J. L. Brown and W. K. Robert, *J. Biol. Chem.*, 251 (1976) 1009.
- 9 L. Varady, K. Kalghatgi and Cs. Horváth, *J. Chromatogr.*, 458 (1989) 207.
- 10 J. J. L'Italien, *J. Chromatogr.*, 359 (1986) 712.
- 11 C. Lazure, J. Rochemont, N. G. Seidah and M. Chrétien, *J. Chromatogr.*, 326 (1985) 339.
- 12 M. W. Dong, J. R. Gant and P. Perrone, *LC, Liq. Chromatogr. HPLC Mag.*, 3 (1985) 786.
- 13 K. L. Stone and K. R. Williams, *J. Chromatogr.*, 359 (1986) 203.
- 14 K. D. Nugent, E. G. Burton, T. K. Slaterry, B. F. Johnson and L. R. Snyder, *J. Chromatogr.*, 443 (1988) 381.
- 15 A. M. Crestfield, S. Moore and W. H. Stein, *J. Biol. Chem.*, 238 (1963) 622.
- 16 K. Kalghatgi and Cs. Horváth, *J. Chromatogr.*, 443 (1988) 343.
- 17 K. L. Stone, M. B. LoPresti and K. R. Williams, in C. Fini (Editor), *Focus on Laboratory Methodology in Biochemistry*, CRC Press, Boca Raton, FL, 1989, in press.
- 18 A. J. Banes, G. W. Link and L. R. Snyder, *J. Chromatogr.*, 326 (1985) 419.
- 19 L. R. Snyder and M. A. Stadalius, in Cs. Horváth (Editor), *High Performance Liquid Chromatography — Advances and Perspectives*, Vol. 4, Academic Press, New York, 1986, pp. 195–309.
- 20 N. H. C. Cooke, B. G. Archer, M. J. O'Hare, E. C. Nice and M. Capp, *J. Chromatogr.*, 255 (1983) 115.
- 21 J. D. Pearson and F. E. Regnier, *J. Liq. Chromatogr.*, 6 (1983) 497.
- 22 E. G. Burton, K. D. Nugent, T. K. Slaterry, B. R. Summes and L. R. Snyder, *J. Chromatogr.*, 443 (1988) 363.
- 23 M. W. Dong, J. R. Gant and B. Larsen, *BioChromatography*, 4 (1989) 19.
- 24 J. Köhler and J. J. Kirkland, *J. Chromatogr.*, 385 (1987) 125.
- 25 J. D. Pearson, N. T. Lin and F. E. Regnier, *Anal. Biochem.*, 124 (1982) 217.
- 26 N. D. Danielson and J. J. Kirkland, *Anal. Chem.*, 59 (1987) 2501.
- 27 C. T. Mant and R. S. Hodges, *Chromatographia*, 24 (1987) 805.

- 28 B. F. D. Ghrist and L. R. Snyder, *J. Chromatogr.*, 459 (1989) 25.
- 29 M. A. Stadalius, M. A. Quarry and L. R. Snyder, *J. Chromatogr.*, 327 (1988) 93.
- 30 C. T. Mant, T. W. L. Burke, J. A. Black and R. S. Hodges, *J. Chromatogr.*, 458 (1989) 193.
- 31 R. S. Hodges, J. M. R. Parker, C. T. Mant and R. R. Sharma, *J. Chromatogr.*, 458 (1989) 147.
- 32 G. E. Deibler, L. F. Boyd, R. E. Martenson and M. W. Kies, *J. Chromatogr.*, 326 (1985) 433.
- 33 C. T. Mant and R. S. Hodges, *J. Chromatogr.*, 326 (1985) 349.
- 34 N. Takahashi, N. Isioka, Y. Takahashi and F. W. Putnam, *J. Chromatogr.*, 326 (1985) 407.
- 35 M. W. Dong, J. R. Gant and F. L. Vandemark, *Am. Biotechnol. Lab.*, 716 (1989) 10.
- 36 E. Hoff, *LC · GC*, 7 (1989) 320.
- 37 M. W. Dong, unpublished results.
- 38 M. W. Dong and J. R. Gant, *LC, Mag. Liq. Chromatogr. HPLC*, 2 (1984) 294.
- 39 J. L. Glajch, J. J. Kirkland and K. Kohler, *J. Chromatogr.*, 384 (1987) 81.
- 40 M. W. Hunkapillar, in A. J. Bhowm (Editor), *Proteins/Peptide Sequence Analysis, Current Methodologies*, CRC Press, Boca Raton, FL, 1988, p. 87.
- 41 K. L. Stone, M. B. LoPresti, J. M. Crawford, R. DeAngelis and K. R. Williams, in R. S. Hodges (Editor), *HPLC of Peptides and Proteins: Separation, Analysis and Conformation*, CRC Press, Boca Raton, FL, 1989, in press.
- 42 R. P. W. Scott, *Small Bore Liquid Chromatography Columns*, Wiley, New York, 1984.
- 43 F. D. Antia and Cs. Horváth, *J. Chromatogr.*, 435 (1988) 1.
- 44 L. Servillo, G. Colonna, C. Balestrieri, R. Ragone and I. Gaetano, *Anal. Biochem.*, 126 (1982) 251.





CHROMSYMP. 1652

## BINARY AND TERNARY SALT GRADIENTS IN HYDROPHOBIC-INTERACTION CHROMATOGRAPHY OF PROTEINS

ZIAD EL RASSI\*, LUCILA F. DE OCAMPO and MARIA D. BACOLOD

*Department of Chemistry, Oklahoma State University, Stillwater, OK 74078-0447 (U.S.A.)*

---

### SUMMARY

Hydrophobic-interaction chromatography of mixtures of acidic and basic proteins having a wide range of molecular weights and hydrophobic character was carried out by using binary and ternary salt gradients. Chaotropic and antichaotropic salts as well as organic salts were incorporated in the eluents. The stationary phase consisted of macroporous silica with surface-bound polyether moieties. At constant eluent surface tension, gradient elution with two or three aqueous salt solutions was found to be superior to single-salt gradients in modulating hydrophobic-interaction chromatography retention and selectivity. The effect was attributed to the competitive salt-specific binding to the protein molecule and/or the stationary phase surface. Chaotropic/antichaotropic salt gradient systems exhibited vastly different selectivities upon changing the nature and concentrations of salts in the eluents. In general, the retention of basic proteins increased while that of acidic proteins either decreased or remained unchanged with the use of chaotropic salts. At the same surface tension of the eluent, KSCN and KClO<sub>4</sub> yielded different selectivities. The addition of organic salts, such as tetrabutylammonium bromide was found to be suitable for the separation of proteins having a wide range of isoelectric points.

---

### INTRODUCTION

Hydrophobic-interaction chromatography (HIC) with rigid, microparticulate stationary phases is increasingly used for the analysis and purification of proteins. Due to the weakly hydrophobic character of the stationary phase, proteins are first adsorbed to the column, equilibrated with an eluent of relatively high salt concentration at or near neutral pH, and subsequently eluted by a decreasing salt concentration gradient.

The retention behavior of proteins in HIC can be described by the thermodynamic model of Horváth and co-workers<sup>1,2</sup> based on the solvophobic theory of Sinanoğlu and co-workers<sup>3,4</sup>. According to the model, at relatively high salt concentrations in the eluent the retention increases with the salt molality and at constant salt concentration with the molal surface tension increment of the salt used in the aqueous eluent. The validity of the model requires that there be no specific binding of the salt

to the protein molecule. The retention–surface tension dependency parallels the Hofmeister series, which is based on the ability of the salts to cause precipitation of proteins from aqueous solutions. Proteins are more retained on an HIC column with antichaotropic salts (*e.g.*, phosphates, sulfates, tartrates and citrates) than with chaotropic salts (*e.g.*, perchlorates and thiocyanates). The solvophobic theory was successfully applied to treat the retention behavior of proteins in HIC as a function of the salt concentration in the eluent<sup>2,5</sup>, the hydrophobic character of the proteins<sup>6</sup>, and the hydrophobicity of the stationary phase ligates<sup>7</sup>.

Selectivity in HIC is altered by means of several operating parameters, including the nature and concentration of the salt used in the eluent<sup>8,9</sup>, slope of the salt gradient<sup>10,11</sup>, eluent pH<sup>12–14</sup>, addition of organic solvents<sup>15,16</sup>, denaturing agents<sup>12</sup> and surfactants<sup>17</sup> to the eluent, column temperature<sup>15,18</sup> and the nature of the stationary phase ligates<sup>19–21</sup>.

This study is concerned with investigating the potential of binary and ternary salt gradients in modulating retention and selectivity in HIC of proteins. The terms binary and ternary salt gradients refer to changing the composition of two and three salts in the eluent, respectively. The significance of such an approach resides in its analytical and preparative applicability to a wide range of separation problems of relevance to many areas of the life sciences.

## EXPERIMENTAL

### *Instrumentation*

The liquid chromatograph was assembled from an LDC/Milton Roy (Riviera Beach, FL, U.S.A.), Model CM4000, solvent delivery pump with a dual-beam variable-wavelength detector, Model SpectroMonitor 3100. The column effluent was monitored at 280 nm. Samples were injected by a Model 7125 sampling valve with a 100- $\mu$ l sample loop (Rheodyne, Cotati, CA, U.S.A.). Chromatograms were recorded with a Shimadzu (Columbia, MD, U.S.A.) Model C-R6A integrator, interfaced with a single floppy disk drive.

### *Columns*

Zorbax PSM 300, a spherical silica, having mean particle and pore diameters of 7.5  $\mu$ m and 300 Å, respectively, was obtained from DuPont (Wilmington, DE, U.S.A.). The polyether stationary phase was prepared by covalent attachment of polyethelene glycol (PEG) of average mol. wt. 1000 to the surface of the Zorbax silica gel, using well-established procedures<sup>6,22</sup>. The silica-bound polyether was packed from a methanol slurry at 8000 p.s.i., using a Shandon column packer instrument (Keystone Scientific, Bellefonte, PA, U.S.A.). All columns were made of 100  $\times$  4.6 mm I.D. No. 316 stainless-steel tubes (Alltech, Deerfield, IL, U.S.A.).

### *Materials*

The proteins used in this study are listed in Table I. They were purchased from Sigma (St. Louis, MO, U.S.A.). Reagent-grade hydrochloric acid, glacial acetic acid, phosphoric acid, sodium hydroxide, ammonium sulfate, sodium chloride, disodium hydrogen phosphate, sodium tartrate, sodium citrate, potassium thiocyanate, potassium perchlorate and methanol (HPLC grade) were obtained from Fisher (Pitts-

burgh, PA, U.S.A.) or J. T. Baker (Phillipsburg, NJ, U.S.A.). Tetrabutylammonium bromide was obtained from Aldrich (Milwaukee, WI, U.S.A.).

#### Procedure

Proteins were dissolved in water at concentration of 5 mg/ml for fetuin, ovalbumin,  $\beta$ -lactoglobulin A, and ribonuclease A and at 2 mg/ml for lysozyme, cytochrome *c*, and  $\alpha$ -chymotrypsinogen A. They were chromatographed by using 30-min linear gradient elution of one, two, or three salts at room temperature and a flow-rate of 1.0 ml/min.

The surface tension,  $\gamma$ , of aqueous salt solutions was estimated from the molal salt concentration,  $m$ , the molal surface tension increment,  $\sigma$ , of the salt, and the surface tension of pure water,  $\gamma_0$  (72 dynes/cm at 25°C), using the equation  $\gamma = \gamma_0 + \sigma m$ . An extensive listing of molal surface tension increments of salts can be found in ref. 1.

#### RESULTS AND DISCUSSION

A mixture of seven proteins (Table I), having a wide range of isoelectric points, molecular weights and hydrophobic character was chromatographed on a silica-bound PEG (mol.wt = 1000) column by using single, binary, or ternary salt gradients. In this regard, several salts were used including ammonium sulfate, sodium tartrate, sodium citrate, sodium chloride, potassium perchlorate, potassium thiocyanate and tetrabutylammonium bromide. In all cases, a 30-min linear gradient was used and the background buffer was 50 mM phosphate (pH 6.5).

Linear gradients of decreasing ammonium sulfate, sodium tartrate or sodium citrate concentrations in the eluent (single-salt gradients) were first used in order to evaluate their effectiveness in HIC of the proteins under investigation and to establish a reference to which the retention data obtained by using binary and ternary salt gradients could be compared. Binary salt gradients were carried out (i) by decreasing the concentration of two antichaotropic salts in the eluent, (ii) by decreasing the concentration of an antichaotropic salt while increasing the concentration of a chaotropic salt in the eluent or (iii) by decreasing the concentration of an antichaotropic salt while increasing the concentration of an organic salt in the eluent. Ternary salt gradients were run by decreasing the concentration of two antichaotropic salts while increasing the concentration of a third salt, a chaotropic salt.

TABLE I  
PROTEINS USED IN THIS STUDY

<i>Protein</i>	<i>Symbol</i>	<i>Mol. wt.</i>	<i>pI</i>	<i>Source</i>
Cytochrome <i>c</i>	a	12 200	10.6	Horse heart
Ribonuclease A	b	13 700	9.5	Bovine pancreas
$\beta$ -Lactoglobulin A	c	35 000	5.1	Bovine milk
Lysozyme	d	14 000	11.0	Chicken egg white
Ovalbumin	e	44 000	4.7	Chicken egg
$\alpha$ -Chymotrypsinogen A	f	25 500	9.5	Bovine pancreas
Fetuin	g	48 400	3.2-4.4	Fetal calf serum

The adjusted retention volumes of proteins, measured with single-salt gradients at decreasing ammonium sulfate, sodium tartrate or sodium citrate concentrations in the eluent, are reported in Table II (gradients I, III and V). Sodium citrate and tartrate yielded higher retention than ammonium sulfate at approximately the same eluent surface tension (76.9 dynes/cm). The effectiveness of these salts in protein adsorption on the HIC matrix increased in the order: ammonium sulfate < sodium tartrate < sodium citrate. The adjusted retention volumes of basic proteins, such as cytochrome *c*, ribonuclease A and lysozyme increased to a larger extent than those of other proteins in the sample when changing ammonium sulfate to either sodium citrate or sodium tartrate. A reversal in the elution order for the eluite pair lysozyme and ovalbumin was observed with both sodium citrate and tartrate, when compared with ammonium sulfate. It is believed that both citrate and tartrate (but to a larger extent citrate) form ion pairs with the proteins and especially the basic ones, which make these proteins more hydrophobic than with ammonium sulfate. At the pH of the experiment, *i.e.* pH 6.5, citrates are trivalent anions ( $pK_{a1} = 3.06$ ,  $pK_{a2} = 4.74$  and  $pK_{a3} = 5.40$ ), whereas tartrates are divalent anions ( $pK_{a1} = 2.96$  and  $pK_{a2} = 4.24$ ).

As expected, binary salt gradients of decreasing concentrations of both ammonium sulfate and sodium citrate in the eluent, from 1.0 to 0 *M* and from 0.69 to 0 *M*, respectively, yielded an elution pattern significantly different from that obtained by using either ammonium sulfate or sodium citrate gradients while maintaining the surface tension of the eluents constant (compare gradient IX with gradients I and V in Table II). The adjusted retention volumes of fetuin and  $\alpha$ -chymotrypsinogen A in-

TABLE II  
ADJUSTED RETENTION VOLUMES OF PROTEINS

Polyether column (100 × 4.6 mm I.D.) with linear gradient elution in 30 min. The background buffer was 50 mM phosphate (pH 6.5); flow-rate, 1 ml/min; temperature, 25°C. Gradients: I = ammonium sulfate gradient from 2.0 to 0 *M*; II = ammonium sulfate and potassium thiocyanate gradients from 2.0 to 0 *M* and from 0 to 0.5 *M*, respectively; III = sodium tartrate gradient from 1.70 to 0 *M*; IV = sodium tartrate and potassium thiocyanate gradients from 1.70 to 0 *M* and from 0 to 0.5 *M*, respectively; V = sodium citrate gradient from 1.38 to 0 *M*; VI = sodium citrate and potassium thiocyanate gradients from 1.38 to 0 *M* and from 0 to 0.5 *M*, respectively; VII = ammonium sulfate and sodium tartrate gradients from 1.0 to 0 *M* and 0.85 *M* to 0 *M*, respectively; VIII = ammonium sulfate, sodium tartrate and potassium thiocyanate gradients from 1.0 to 0 *M*, from 0.85 to 0 *M* and from 0 *M* to 0.5 *M*, respectively; IX = ammonium sulfate and sodium citrate gradients from 1.0 *M* to 0 *M* and from 0.69 *M* to 0 *M*, respectively; X = ammonium sulfate, sodium citrate and potassium thiocyanate gradients from 1.0 to 0 *M*, from 0.69 to 0 *M* and from 0 to 0.5 *M*, respectively.

Protein	Gradient									
	I	II	III	IV	V	VI	VII	VIII	IX	X
Cytochrome <i>c</i>	0.30	0.85	0.70	1.40	2.13	5.71	0.40	0.77	0.53	1.93
Ribonuclease A	5.77	5.59	7.50	9.50	12.62	12.64	6.93	7.85	9.02	9.98
$\beta$ -Lactoglobulin A	10.98	13.27	13.80	13.70	15.07	15.48	11.36	13.22	13.98	14.55
Lysozyme	12.66	22.10	17.13	24.27	19.05	26.95	17.13	23.96	18.60	24.96
Ovalbumin	13.28	14.72	14.18	13.70	16.97	16.69	14.39	14.63	17.00	15.98
$\alpha$ -Chymotrypsinogen A	20.14	24.63	21.60	25.40	23.26	26.20	21.10	23.70	23.69	25.37
Fetuin	19.97	22.89	22.12	22.60	23.25	24.97	21.60	22.65	24.43	24.02

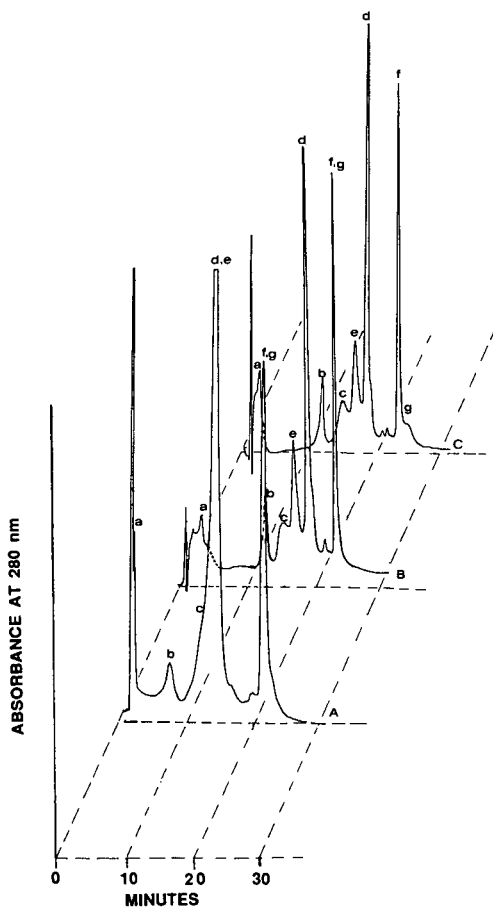


Fig. 1. Hydrophobic-interaction chromatography of proteins. Column, silica-bound polyether,  $100 \times 4.6$  mm I.D.; temperature  $25^{\circ}\text{C}$ ; flow-rate, 1 ml/min. (A) Ammonium sulfate gradient from 2.0  $M$  to 0  $M$ ; (B) sodium citrate gradient from 1.38 to 0  $M$ ; (C) binary salt gradient of ammonium sulfate and sodium citrate from 0.375 to 0  $M$  and from 1.125 to 0  $M$ , respectively. In all cases, a linear gradient of 30 min was used. The background buffer was 50 mM phosphate (pH 6.5). For symbols see Table I.

creased and a reversal in their elution order was observed with the binary salt gradient as compared to ammonium sulfate or sodium citrate gradients. Whereas the adjusted retention volume of ovalbumin, measured with the binary salt gradient, equaled that obtained by using sodium citrate gradient, the retention volumes of other components of the protein mixture ranked between those obtained by using individual salt gradients of ammonium sulfate and sodium citrate, respectively.

Upon changing the composition of ammonium sulfate and sodium citrate in the starting eluent to 0.375  $M$  and 1.125  $M$ , respectively, while keeping the eluent surface tension roughly the same as in the preceding experiment, the elution profile of proteins under investigation became slightly different. As seen in Fig. 1C, with the binary salt gradient, the seven proteins were retained to an extent closer to that obtained by

using a sodium citrate gradient than an ammonium sulfate gradient. However, the eluite pairs ribonuclease A and  $\beta$ -lactoglobulin A, ovalbumin and  $\beta$ -lactoglobulin A, and fetuin and  $\alpha$ -chymotrypsinogen A are better resolved with the binary salt gradient than with single-salt gradients at virtually equal eluent surface tension (compare Fig. 1C with Figs. 1A and 1B).

Also, binary salt gradients of decreasing concentrations of both ammonium sulfate and sodium tartrate in the eluent (gradient VII in Table II) produced an elution pattern different from that obtained by using single-salt gradients of ammonium sulfate (gradient I) or sodium tartrate (gradient III) at practically the same eluent surface tension of *ca.* 76.9 dynes/cm. Whereas an increase in the adjusted retention volume of ovalbumin was observed with the binary salt gradient as compared to ammonium sulfate or sodium tartrate gradients, the retention of lysozyme measured with the binary salt gradient was identical to that obtained by using sodium tartrate

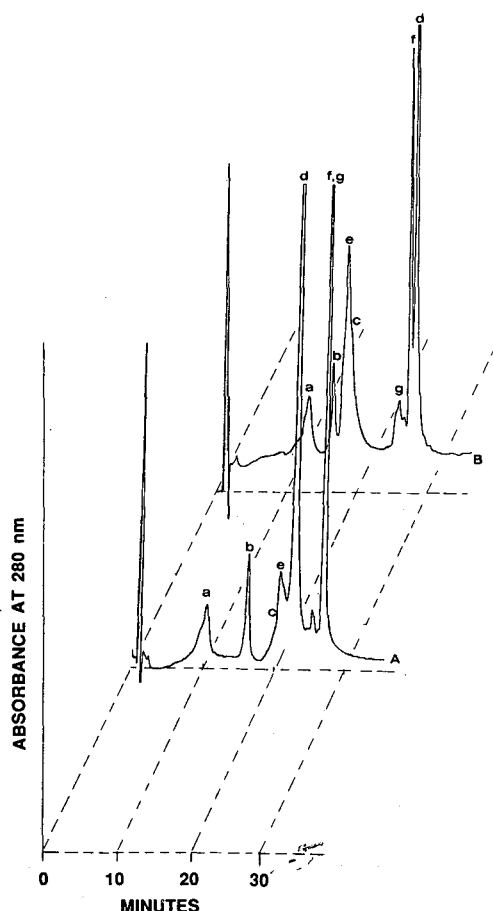


Fig. 2. Hydrophobic-interaction chromatography of proteins. (A) Sodium citrate gradient from 1.5 to 0 *M*; (B) binary salt gradient of sodium citrate and potassium thiocyanate from 1.5 to 0 *M* and from 0 to 0.5 *M*, respectively. Other conditions as in Fig. 1.

gradient. The adjusted retention volumes of other proteins, measured with the binary salt gradient, fell in between those obtained by using single-salt gradients. However, the elution order with the binary salt gradient paralleled that obtained by using a sodium tartrate gradient.

Salt selectivity in HIC arises from quantitative differences in salt-specific binding to proteins<sup>5,23-25</sup> and/or from differential hydration of both stationary phase and protein surfaces. In the light of the above results, by using binary salt gradients of different salt composition and types of salts, different selectivities can be generated. This may be due to competitive, salt-specific binding to protein and/or the stationary phase.

Other types of binary salt gradients were also tested for their effectiveness in modulating retentivity and selectivity in HIC. Fig. 2B depicts the chromatogram obtained by using a binary salt gradient of decreasing sodium citrate and increasing potassium thiocyanate concentrations in the eluent. Comparison of this chromatogram to that in Fig. 2A, which was obtained by using sodium citrate gradient, reveals that the binary salt gradient has resolved most of the proteins in the mixture and yielded a different selectivity, as manifested by the reversal in the elution order of the elute pair  $\beta$ -lactoglobulin A and ovalbumin and the pair lysozyme and  $\alpha$ -chymotrypsinogen A as well as the pair fetuin and  $\alpha$ -chymotrypsinogen A. The addition of 0.5 M KSCN to the gradient former, *i.e.* the strong eluent, increased the surface tension by only 0.22 dynes/cm. However, lysozyme, and to lesser extent cytochrome *c* and  $\alpha$ -chymotrypsinogen A were much more retained in the presence than in the absence of KSCN. In addition, whereas the retention of ribonuclease A was not affected by the presence of KSCN, acidic proteins, such as ovalbumin and  $\beta$ -lactoglobulin A were less retained with than without KSCN in the gradient former.

Keeping the concentration of KSCN in the gradient former identical to that used in the above binary salt gradient, but using 1.38 M instead of 1.5 M sodium citrate in the starting eluent (gradient VI in Table II) produced an elution pattern different from that in Fig. 2B as far as the elution order of the elute pair ovalbumin and  $\beta$ -lactoglobulin A is concerned. The selectivity of the sodium citrate-KSCN gradient system toward the proteins has also changed upon reducing the concentration of KSCN from 0.5 M to 0.2 M in the gradient former. Binary salt gradients of decreasing antichaotropic salt concentration and increasing chaotropic salt concentration in the eluent offer the opportunity for the optimization of selectivity in HIC, because changing the concentration of the salts in the starting eluent and the gradient former leads to widely different selectivities.

When using chaotropic/antichaotropic salt gradient systems, sample selectivity can also be varied by keeping the eluent surface tension constant while exchanging one antichaotropic salt for another in the starting eluent. The adjusted retention volumes of proteins, measured with ammonium sulfate-, sodium tartrate- or sodium citrate-KSCN gradients, are summarized in Table II (gradients II, IV and VI, respectively). The adjusted retention volumes of proteins were the highest with the sodium citrate-KSCN gradient and the lowest with the ammonium sulfate-KSCN gradient. When using a citrate-KSCN gradient the elution order of the following elutes was: fetuin <  $\alpha$ -chymotrypsinogen A < lysozyme. It changed to fetuin < lysozyme <  $\alpha$ -chymotrypsinogen A and to lysozyme < fetuin <  $\alpha$ -chymotrypsinogen A when using tartrate-KSCN and sulfate-KSCN gradients, respectively, instead of the sodium citrate-KSCN gradient.

In order to examine the influence of the nature of the chaotropic salt on HIC selectivity in a binary salt gradient system, gradient elution of decreasing ammonium sulfate concentration and increasing  $\text{KClO}_4$  concentration was carried out. The concentration of  $\text{KClO}_4$  in the gradient former was adjusted to give approximately the same surface tension as with  $\text{KSCN}$  (*ca.* 72.22 dynes/cm). The chromatogram ob-

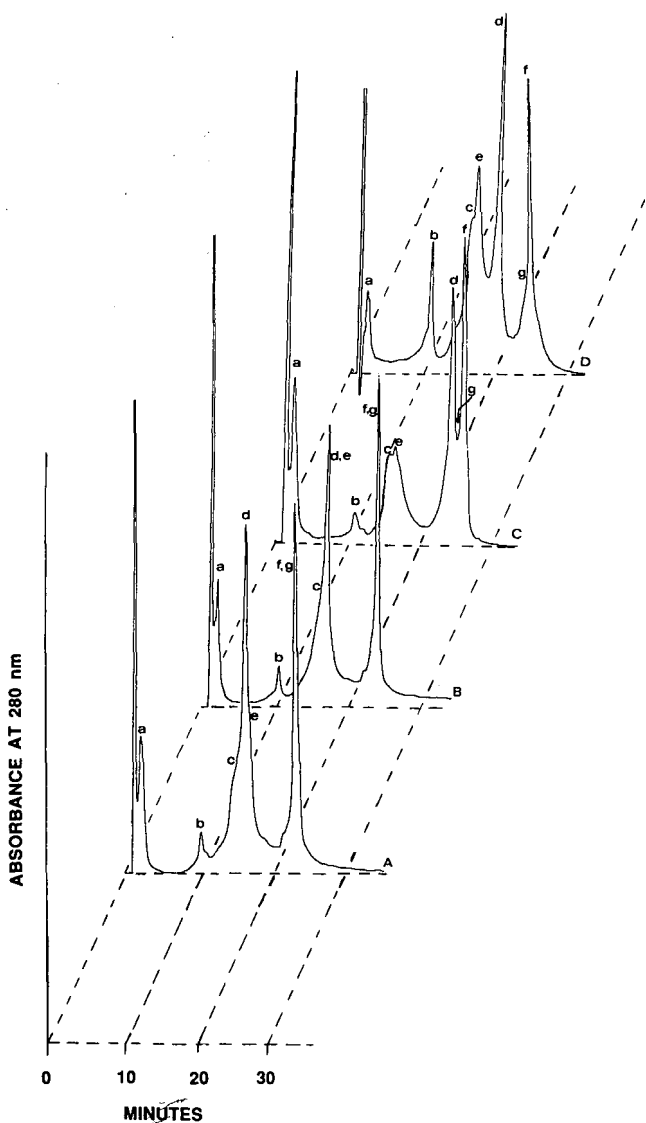


Fig. 3. Hydrophobic-interaction chromatography of proteins. (A) Ammonium sulfate gradient from 2.16 to 0  $M$ ; (B) binary salt gradient of ammonium sulfate and sodium chloride from 2.16 to 0  $M$  and from 0 to 0.15  $M$ , respectively; (C) binary salt gradient of ammonium sulfate and potassium thiocyanate from 2.16 to 0  $M$  and from 0 to 0.5  $M$ , respectively; (D) binary salt gradient of ammonium sulfate and potassium perchlorate from 2.16 to 0  $M$  and from 0 to 0.16  $M$ , respectively. Other conditions as in Fig. 1.



tained with this binary salt gradient is illustrated in Fig. 3D. It can be seen that the potassium perchlorate–ammonium sulfate gradient system exhibited less retentivity toward the proteins and yielded different modulation of selectivity than the potassium thiocyanate–ammonium sulfate gradient at the same eluent surface tension (*cf.* Figs. 3D and 3C).

Based on the above results, thiocyanates and perchlorates are likely to bind electrostatically to the protein molecule<sup>23</sup>, causing different structural alterations. Indeed, replacing KSCN or KClO<sub>4</sub> by sodium chloride in the gradient former and keeping the surface tension constant (72.22 dynes/cm) did not result in improvement of resolution and selectivity; instead, the retention of all proteins in the sample increased slightly in the same way (*cf.* Figs. 3B and 3A). The salt-specific binding to protein would likely be responsible for selectivity changes in HIC of proteins when KSCN or potassium perchlorate are present in the eluent. This is in agreement with

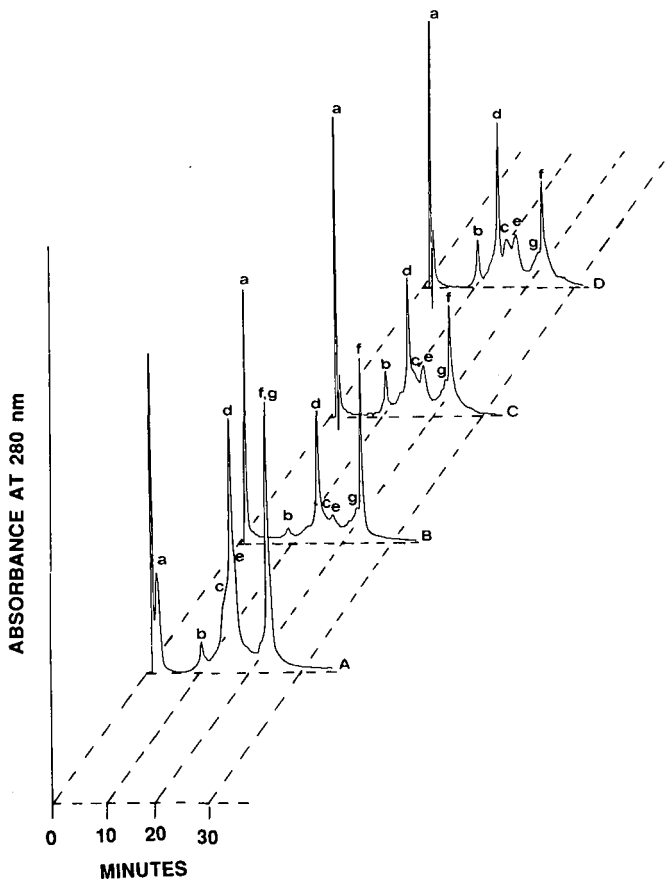


Fig. 4. Hydrophobic-interaction chromatography of proteins. (A) Ammonium sulfate gradient from 2.16 to 0 *M*; (B) ammonium sulfate and tetrabutylammonium bromide gradients from 2.16 to 0 *M* and from 0 to 10 *mM*, respectively; (C) ammonium sulfate and tetrabutylammonium bromide gradients from 2.16 to 0 *M* and from 0 to 20 *mM*, respectively; (D) ammonium sulfate and tetrabutylammonium bromide gradients from 2.16 to 0 *M* and from 0 to 40 *mM*, respectively. Other conditions as in Fig. 1.

the finding that the retention volumes of some proteins decreased while those of others increased with increasing sodium-perchlorate concentration in the eluent<sup>2</sup>.

Binary salt gradients of decreasing ammonium sulfate concentration and increasing tetrabutylammonium ( $\text{Bu}_4\text{N}^+$ ) bromide concentration (organic salt of negative molal surface tension increment) in 50 mM phosphate buffer (pH 6.5) were carried out. The chromatograms obtained by using 0, 10, 20 or 40 mM  $\text{Bu}_4\text{N}^+$  in the gradient former are depicted in Fig. 4. Whereas cytochrome *c* was eluted in the void volume of the column in the presence of  $\text{Bu}_4\text{N}^+$ , ribonuclease A was slightly more retained at 10 and 20 mM than at 0 or 40 mM  $\text{Bu}_4\text{N}^+$  in the eluent. Lysozyme,  $\alpha$ -chymotrypsinogen A, and fetuin retention decreased monotonically but at different rates with increasing  $\text{Bu}_4\text{N}^+$  concentration in the eluent. In contrast, the retention of  $\beta$ -lactoglobulin A first increased when going from 0 to 10 mM  $\text{Bu}_4\text{N}^+$  in the gradient former and then remained unchanged as the concentration of the organic salt increased in the concentration range studied, while the retention of ovalbumin increased almost monotonically with the concentration of the organic salt in the gradient former.

The effect of  $\text{Bu}_4\text{N}^+$  concentration on protein retention can be explained by ion-pair formation in the eluent as well as by the adsorption of such ions on the stationary phase surface. Both mechanisms can explain the general increase and decrease in retention of acidic and basic proteins, respectively, with increasing  $\text{Bu}_4\text{N}^+$  concentration in the eluent. The exception that fetuin (an acidic protein) retention decreased with increasing  $\text{Bu}_4\text{N}^+$  concentration can be explained by the decrease in surface tension of the eluent, since fetuin was eluted at the end of the gradient run. Ion-pair formation between  $\text{Bu}_4\text{N}^+$  and the acidic residues of proteins would increase the hydrophobicity of the proteins and therefore their retention. On the other hand, at relatively high salt concentrations in the eluent,  $\text{Bu}_4\text{N}^+$  ions are likely to be adsorbed on the surface of the stationary phase, thus creating a dynamically coated surface with positively charged sites. It has been shown<sup>24</sup> that a hydration layer deficient in salt exists on a protein surface when in contact with aqueous solutions containing high concentrations of salt. Hydrophobic interactions are of short range, allowing a close association of the protein and the stationary phase. Therefore, in the presence of positively charged sites on the hydrophobic surface, cooperative hydrophobic and coulombic interactions may take place at the contact surface area between the analyte and the stationary phase. This may explain the increase in retention for ovalbumin and  $\beta$ -lactoglobulin A upon adding  $\text{Bu}_4\text{N}^+$  to the mobile phase. In contrast, the presence of adsorbed  $\text{Bu}_4\text{N}^+$  ions on the stationary phase surface would explain the decrease in retention for basic proteins, due to weak electrostatic repulsion between species of same charges. Indeed, El Rassi and Horváth<sup>26,27</sup> and Kennedy *et al.*<sup>28</sup> have shown that ion-exchange stationary phases could be used in the HIC mode with eluents containing a high salt concentration. The elution pattern of proteins with such phases was different from that obtained by using neutral and weakly hydrophobic stationary phases, due to the interplay of hydrophobic and electrostatic interactions. Due to the specific binding of  $\text{Bu}_4\text{N}^+$  to the proteins and/or the stationary phase, the observed retention behavior is different from that predicted by the surface tension argument of the original retention model of Horváth and co-workers<sup>1,2</sup> (see Introduction). Such binding may affect retention to a certain degree, thereby leading to changes in selectivity.

HIC selectivity can be further manipulated by using ternary salt gradients. The adjusted retention volumes of proteins, measured with a linear gradient of increasing both ammonium sulfate and sodium tartrate concentrations and decreasing potassium thiocyanate concentrations in the eluent are reported in Table II; gradient VIII. It is seen that the elution pattern with a ternary salt gradient is quite different from that obtained by using any of the binary salt gradients (compare gradient VIII with gradients III, IV and VII in Table II) at virtually the same eluent surface tension. Comparison of ternary gradient VIII with the binary gradient VII reveals that protein retention has increased and a reversal in the elution order of the elute pair lysozyme and  $\alpha$ -chymotrypsinogen A and the pair fetuin and  $\alpha$ -chymotrypsinogen A has occurred when going from the binary to the ternary salt gradient.

The adjusted retention volumes of proteins, measured with a ternary salt gradient of decreasing ammonium sulfate and sodium citrate concentrations and increasing potassium thiocyanate concentrations in the eluent are shown in Table II; gradient X. The comparison of retention data, obtained by using the ternary gradient (X in Table II) with those measured with the binary gradient (IX in Table II) shows that the adjusted retention volumes of all the components of the mixture increased, except for ovalbumin, which decreased when using the ternary gradient instead of the binary gradient. In addition, the elution order, which was lysozyme <  $\alpha$ -chymotrypsinogen A < fetuin with the binary salt gradient, has changed to fetuin < lysozyme <  $\alpha$ -chymotrypsinogen A with the ternary gradient.

In conclusion, sample selectivity in HIC can be varied conveniently by holding the surface tension of the eluent constant while (i) exchanging one salt for another in single-salt gradients or (ii) varying the composition and nature of salts in binary and ternary salt gradients. Gradient elution with two or three salts is more efficient than single-salt gradients in modulating HIC selectivity. Work is continuing in this laboratory on the use of mixed aqueous salt solutions in HIC of proteins; isocratic elution is being carried out, and the results will be reported in an upcoming article.

#### ACKNOWLEDGEMENTS

The authors wish to thank R. W. Stout for his generous gift of Zorbax silica gel. This work was supported by grant No. HN9-004 from the Oklahoma Center for the Advancement of Science and Technology (Oklahoma Health Research Program) and by the College of Arts and Sciences, Dean Incentive Grant Program at Oklahoma State University.

#### REFERENCES

- 1 W. R. Melander and Cs. Horváth, *Arch. Biochem. Biophys.*, 183 (1977) 200.
- 2 W. R. Melander, D. Corradini and Cs. Horváth, *J. Chromatogr.*, 317 (1984) 67.
- 3 O. Sinanoğlu and S. Abdunur, *Fed. Proc., Fed. Am. Soc. Exp. Biol.*, 24 (1965) s-12.
- 4 T. Halicioğlu and O. Sinanoğlu, *Ann. N.Y. Acad. Sci.*, 158 (1969) 308.
- 5 J. L. Fausnaugh and F. E. Regnier, *J. Chromatogr.*, 359 (1986) 131.
- 6 Z. El Rassi and Cs. Horváth, *J. Liq. Chromatogr.*, 9 (1986) 3245.
- 7 A. Katti, Y.-F. Maa and Cs. Horváth, *Chromatographia*, 24 (1987) 646.
- 8 J. L. Fausnaugh, L. A. Kennedy and F. E. Regnier, *J. Chromatogr.*, 317 (1984) 141.
- 9 M. N. Schmuck, M. P. Nowlan and K. M. Gooding, *J. Chromatogr.*, 371 (1986) 55.
- 10 N. T. Miller and B. L. Karger, *J. Chromatogr.*, 326 (1985) 45.

- 11 Y. Kato, T. Kitamura and T. Hashimoto, *J. Chromatogr.*, 333 (1985) 202.
- 12 Y. Kato, T. Kitamura and T. Hashimoto, *J. Chromatogr.*, 298 (1984) 407.
- 13 H. Engelhardt and U. Schon, *J. Liq. Chromatogr.*, 9 (1986) 3225.
- 14 S. Hjerten, K. Yao, K.-O. Eriksson and B. Johansson, *J. Chromatogr.*, 359 (1986) 99.
- 15 S. C. Goheen and S. C. Engelhorn, *J. Chromatogr.*, 317 (1984) 55.
- 16 M. L. Heinitz, L. Kennedy, W. Kopaciewicz and F. E. Regnier, *J. Chromatogr.*, 443 (1988) 173.
- 17 D. B. Wetlaufer and M. R. Koenigbauer, *J. Chromatogr.*, 359 (1986) 55.
- 18 S.-L. Wu, K. Benedek and B. L. Karger, *J. Chromatogr.*, 359 (1986) 3.
- 19 A. J. Alpert, *J. Chromatogr.*, 359 (1986) 85.
- 20 D. L. Gooding, M. N. Schmuck and K. M. Gooding, *J. Chromatogr.*, 296 (1984) 141.
- 21 Y. Kato, T. Kitamura and T. Hashimoto, *J. Chromatogr.*, 360 (1986) 260.
- 22 J.-P. Chang, Z. El Rassi and Cs. Horváth, *J. Chromatogr.*, 319 (1985) 396.
- 23 T. Arakawa and S. N. Timasheff, *Biochemistry*, 21 (1982) 6545.
- 24 T. Arakawa and S. N. Timasheff, *Biochemistry*, 23 (1984) 5912.
- 25 T. Arakawa and S. N. Timasheff, *Methods Enzymol.*, 114 (1985) 49.
- 26 Z. El Rassi and Cs. Horváth, *J. Chromatogr.*, 326 (1985) 79.
- 27 Cs. Horváth and Z. El Rassi, *Chromatography Forum*, 1 (1986) 49.
- 28 L. A. Kennedy, W. Kopaciewicz and F. E. Regnier, *J. Chromatogr.*, 359 (1986) 73.

CHROMSYMP. 1638

## HIGH-PERFORMANCE ADSORPTION CHROMATOGRAPHY OF TRANSFER RIBONUCLEIC ACIDS AND PROTEINS ON 2- $\mu$ m SPHERICAL BEADS OF HYDROXYAPATITE

### INFLUENCE OF SODIUM CHLORIDE AND MAGNESIUM IONS ON THE RESOLUTION

JOHAN LINDEBERG, TASANEE SRICHAISO and STELLAN HJERTÉN\*

*Institute of Biochemistry, Biomedical Center, University of Uppsala, P.O. Box 576, S-751 23 Uppsala (Sweden)*

---

#### SUMMARY

The influence of sodium chloride and magnesium chloride on the adsorption of tRNA and proteins on a high-performance liquid chromatographic column of 2- $\mu$ m spherical hydroxyapatite beads was investigated. The resolution of  $^{14}$ C-labelled aminoacyl-tRNA isoacceptors was improved in the presence of sodium chloride. Inclusion of magnesium chloride in the buffers led to a separation of two tRNA species that could not be fractionated with or without sodium chloride in the eluting buffers (the original properties of the column were lost, however, and could not be regenerated by simply returning to magnesium chloride-free phosphate buffer). Also, the adsorption of some proteins was affected when salt was included in the buffers. For instance, the elution order of proteins could be changed by choosing an appropriate concentration of sodium chloride. This finding might be utilized to facilitate the purification of certain proteins.

---

#### INTRODUCTION

Spherical beads of hydroxyapatite have been developed recently for use in high-performance liquid chromatographic (HPLC) systems. We have previously described some basic properties of this bed material, and we also briefly discussed the effects of including sodium chloride in the eluting phosphate buffer in connection with the purification of  $\gamma$ -globulin from whole serum<sup>1</sup>. The general influence of sodium chloride on the adsorption of proteins on hydroxyapatite has been studied by Gorbunoff<sup>2,3</sup> and Gorbunoff and Timasheff<sup>4</sup>, but has not in our knowledge been used for the fractionation of ribonucleic acids. In this paper we report some further investigations on the application of this technique to both protein and tRNA. In addition, as magnesium ions are known to change the three-dimensional structure of tRNA<sup>5</sup>, the effect of including magnesium chloride in the eluting buffers was investigated.

## EXPERIMENTAL

The chromatographic equipment included a Model 2152 HPLC controller, a Model 2150 HPLC pump and a Model 2210 recorder (LKB, Brömme, Sweden), a Model 786 variable-wavelength detector (Micromeritics, Norcross, GA, U.S.A.), a Model 7125 injector (Rheodyne, Cotati, CA, U.S.A.), a Microcol TDC 80 fraction collector (Gilson, Villiers le Bel, France) and a Model LS 2800 liquid scintillation system (Beckman, Irvine, CA, U.S.A.).

The high-performance hydroxyapatite columns (100 mm × 7.5 mm I.D.) were a gift from Toa Nenryo Kogyo (Tokyo, Japan). DEAE-Sepharose and Sepharose 6B were obtained from Pharmacia (Uppsala, Sweden), sodium chloride from KEBO Lab. (Stockholm, Sweden), sodium dihydrogenphosphate, disodium hydrogenphosphate, potassium dihydrogenphosphate, dipotassium hydrogenphosphate, potassium chloride, magnesium chloride, sodium acetate and hydrochloric acid (37%) from E. Merck (Darmstadt, F.R.G.), L-[U-<sup>14</sup>C]leucine (340 mCi/mmol), L-[U-<sup>14</sup>C]valine (265 mCi/mmol) and L-[U-<sup>14</sup>C]phenylalanine (536 mCi/mmol) from New England Nuclear (Dreieich, F.R.G.), the xylene-based scintillation liquid (Quickszint 212) from Zinsser Analytic (Maidenhead, U.K.), tris(hydroxymethyl)aminomethane (Tris), chicken egg albumin and lysozyme from Sigma (St. Louis, MO, U.S.A.) and chymotrypsinogen A from Pharmacia (Uppsala, Sweden). Human serum albumin and human transferrin were gifts from KabiVitrum (Stockholm, Sweden).

*Preparation of bulk tRNA*

Bulk tRNA was prepared from *Escherichia coli* MRE 600 as described by Zubay<sup>6</sup>. After deacylation at pH 9.0 in 1 M Tris-HCl for 1 h, high-molecular-weight RNA was removed by chromatography on Sepharose 6B<sup>7</sup>.

*Preparation of aminoacyl-tRNA ligase*

A crude extract of aminoacyl-tRNA ligase was prepared from *Escherichia coli* B according to Muench and Berg<sup>8</sup>. The preparation was stored at -70°C in portions of 0.1 ml.

*Preparation of [<sup>14</sup>C]aminoacyl-tRNA isoacceptors*

Pools of specific tRNA isoacceptors, obtained from chromatography on cross-linked agarose beads<sup>9</sup> (see Fig. 1), were labelled with their cognate <sup>14</sup>C-labelled amino acids. The reaction mixture contained 1 volume (100–200 μl) of the chosen tRNA pool, 1 volume of amino acid mixture (see Table I), 2 volumes of distilled water and 0.01 volume of ligase. After incubation at 37°C for 20 min, the reaction was interrupted by addition of 0.25 volume of 1 M sodium acetate buffer (pH 4.5).

The solution obtained was diluted with an equal volume of 0.02 M sodium acetate (pH 4.5) and applied to a DEAE-Sepharose column (20 mm × 10 mm I.D.), equilibrated with 20 mM sodium acetate (pH 4.5). The column was then washed with the equilibration buffer, containing 0.3 M sodium chloride, until UV-absorbing material (unreacted amino acids, ligase, ATP, etc.) ceased to appear in the effluent. The tRNA isoacceptor was finally eluted with the same buffer, containing 1 M sodium chloride. The eluted tRNA fraction was precipitated with 2 volumes of 95% ethanol, then vacuum dried and stored at -20°C.

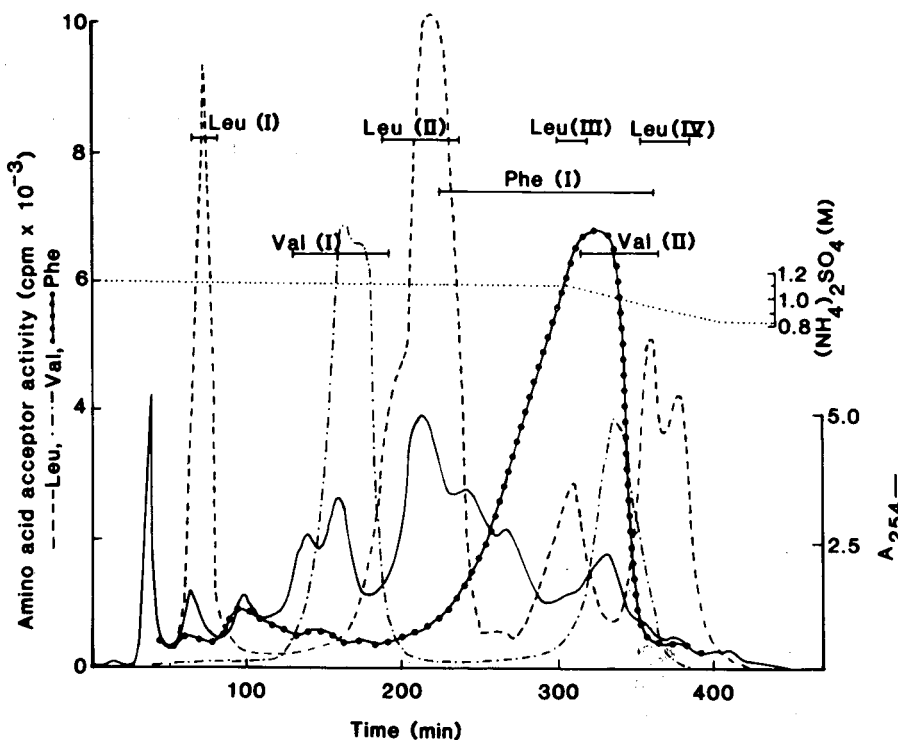


Fig. 1. Fractionation of *E. coli* tRNA by HPLC on cross-linked agarose beads<sup>9</sup>. Aliquots of each fraction were assayed for leucine, valine and phenylalanine acceptance. The fractions corresponding to each activity peak were pooled as indicated: Leu(I), Leu(II), Leu(III), Leu(IV), Val(I), Val(II) and Phe(I). tRNA in each pool was labelled with its cognate <sup>14</sup>C-labelled amino acid prior to hydroxyapatite chromatography (see Figs. 3-6).

*Radioactivity measurements*

Scintillation liquid (3.0 ml) was carefully mixed in a scintillation tube with 0.9 ml of each fraction collected in the agarose and hydroxyapatite chromatography experiments, and counted in a scintillation system for 10 min. The radioactive decay in counts per minute (cpm) was calculated and plotted on the chromatograms.

TABLE I

COMPOSITIONS OF AMINO ACID MIXTURES

HEPES = N-2-Hydroxyethylpiperazine-N'-2-ethanesulphonic acid; ATP = adenosine 5'-triphosphate; DTT = dithiothreitol; 2-ME = 2-mercaptoethanol.

Amino acid	[ <sup>14</sup> C]Amino acid (μM)	0.4 M buffer		Concentration (mM)					
		Type	pH	Mg <sup>2+</sup>	K <sup>+</sup>	NH <sub>4</sub> <sup>+</sup>	ATP	DTT	2-ME
Leucine	3.08	HEPES	8.0	40	—	24	16	—	80
Valine	5.68	Sodium cacodylate	7.1	40	40	—	8	—	—
Phenylalanine	1.50	HEPES	7.1	40	—	20	16	4	—

## RESULTS

*Influence of sodium chloride on the adsorption of bulk tRNA on hydroxyapatite*

A solution of bulk tRNA ( $27 A_{260}$  units) was applied to the column and eluted immediately with a gradient in phosphate concentration from 0.044 to 0.102 M at pH 6.8 over 180 min. Fractions of 1.0 ml were collected and measured for radioactivity. The experiment was then repeated with 0.1 M sodium chloride included in all buffers.

The absorbance pattern at 260 nm (see Fig. 2) was altered when sodium chloride was added to the buffers, and showed that some peaks became narrower and that the resolution seemed to be improved. The recovery was 99% in the presence and 100% in the absence of salt, as determined by absorbance measurements and the "cut-and-weigh" technique.

*HPLC of  $^{14}\text{C}$ -labelled aminoacyl-tRNA isoacceptors on hydroxyapatite in the absence and presence of sodium chloride*

In order to investigate the influence of sodium chloride on the separate aminoacyl-tRNA isoacceptors, a series of [ $^{14}\text{C}$ ]aminoacyl-tRNA isoacceptors were prepared as described above (see Experimental).

The vacuum-dried isoacceptor was dissolved in 30  $\mu\text{l}$  of 5 mM sodium phosphate buffer (pH 6.8). Of this sample, 29  $\mu\text{l}$  were applied to the hydroxyapatite column and eluted immediately with a phosphate gradient from 0.044 to 0.102 M over 180 min. Fractions of 1.0 ml were collected and analysed for radioactivity. A similar experiment was then performed with 0.1 M sodium chloride added to the buffers.

This procedure was repeated for each of the aminoacyl-tRNAs used. Also, when an aminoacyl-tRNA appeared in several peaks on chromatography on cross-linked agarose beads (see Fig. 1), each peak was studied separately on the hydroxyapatite column.

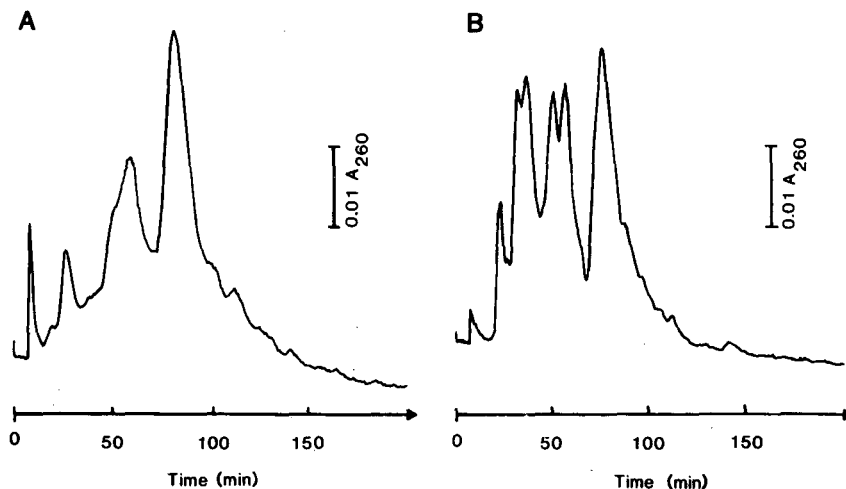


Fig. 2. Influence of sodium chloride on the adsorption of tRNA on hydroxyapatite. Samples, bulk tRNA ( $0.7 A_{260}$  units); volume, 29  $\mu\text{l}$ ; column dimensions, 100 mm  $\times$  7.5 mm I.D.; flow-rate, 0.4 ml/min. Elution: (A) a gradient from 0.044 M sodium phosphate buffer (pH 6.8) to 0.102 M over 180 min; (B) as in A, but the buffers also contained 0.1 M sodium chloride.



Following the course described above, four [ $^{14}\text{C}$ ]leucyl-, one [ $^{14}\text{C}$ ]phenylalanyl- and two [ $^{14}\text{C}$ ]valyl-tRNA isoacceptor pools (see Fig. 1) were used to investigate the influence of sodium chloride on the adsorption to hydroxyapatite (see Figs. 3–5).

The resolution seemed to be improved for all [ $^{14}\text{C}$ ]aminoacyl-tRNAs when 0.1 *M* sodium chloride was included in the buffers, with the possible exception of the second [ $^{14}\text{C}$ ]valyl-tRNA sample [Val(II) in Fig. 1] and the two [ $^{14}\text{C}$ ]leucyl-tRNA samples [Leu(I) and Leu(II) in Fig. 1], which appeared more heterogeneous in the absence of salt (see Figs. 3 and 4). The fourth [ $^{14}\text{C}$ ]leucyl-tRNA [Leu(IV)], which in the sodium chloride-free chromatography experiment seemed to consist of a single component, could be resolved easily into two distinct peaks when sodium chloride was present in the buffers (see Fig. 3).

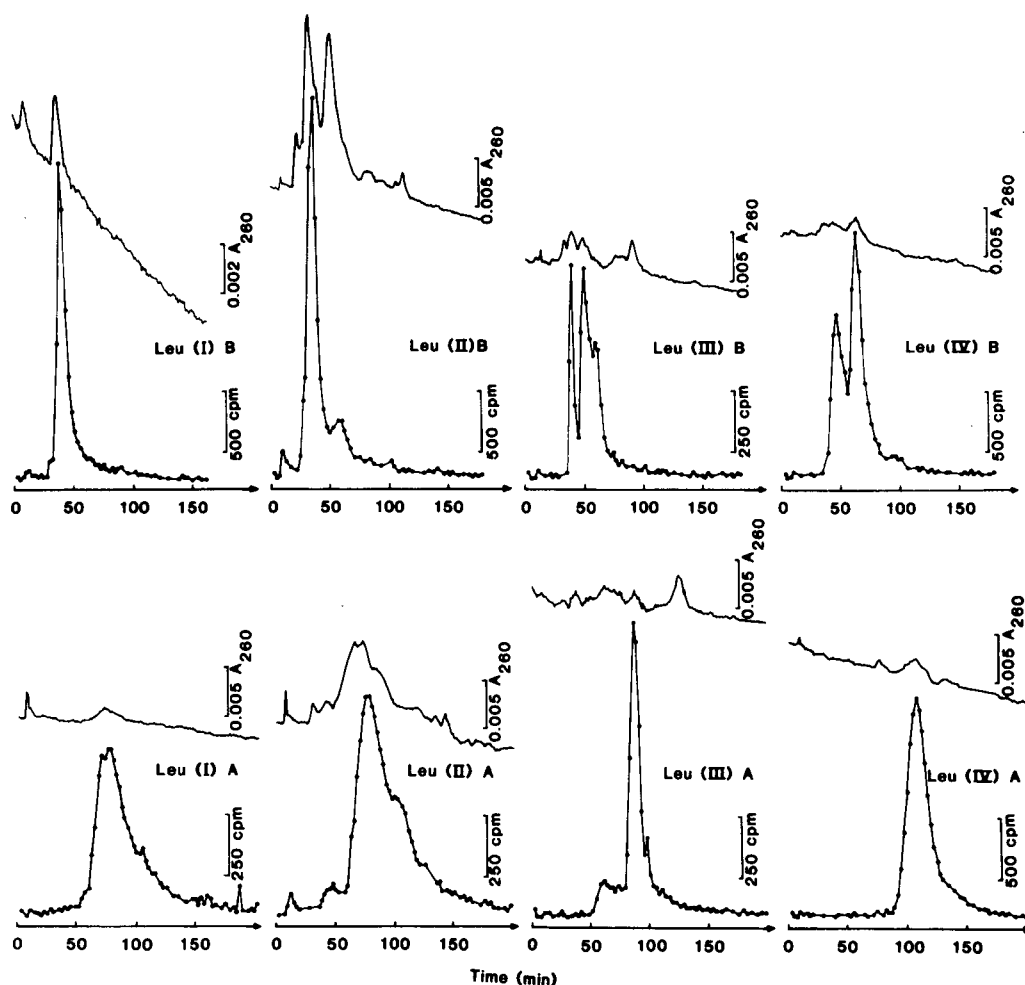


Fig. 3. HPLC of  $^{14}\text{C}$ -labelled leucyl-tRNA isoacceptors on hydroxyapatite in (A) the absence and (B) the presence of 0.1 *M* sodium chloride. Samples, [ $^{14}\text{C}$ ]leucyl-tRNA isoacceptors [Leu(I)–Leu(IV) in Fig. 1]. Conditions and elution (A and B) as in Fig. 2.

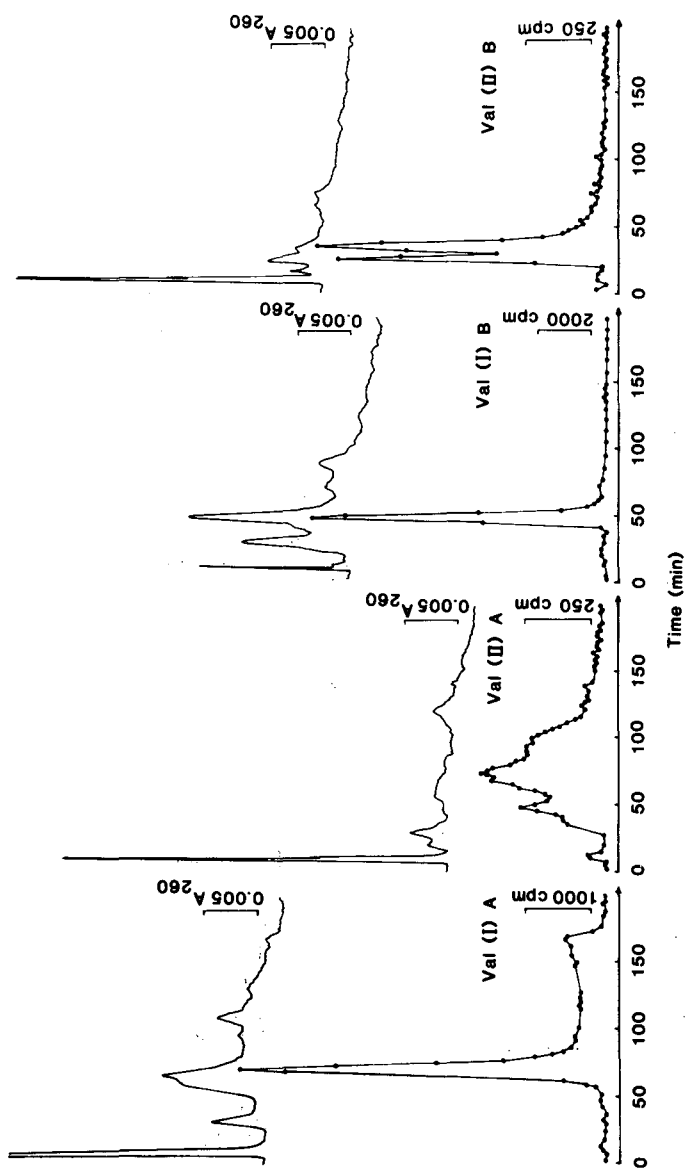


Fig. 4. HPLC of  $^{14}\text{C}$ -labelled valyl-tRNA isoacceptors on hydroxyapatite in (A) the absence and (B) the presence of 0.1 M sodium chloride. Samples, [ $^{14}\text{C}$ ]valyl-tRNA isoacceptors [Val(I) and Val(II) in Fig. 1]. Conditions and elution (A and B) as in Fig. 2.

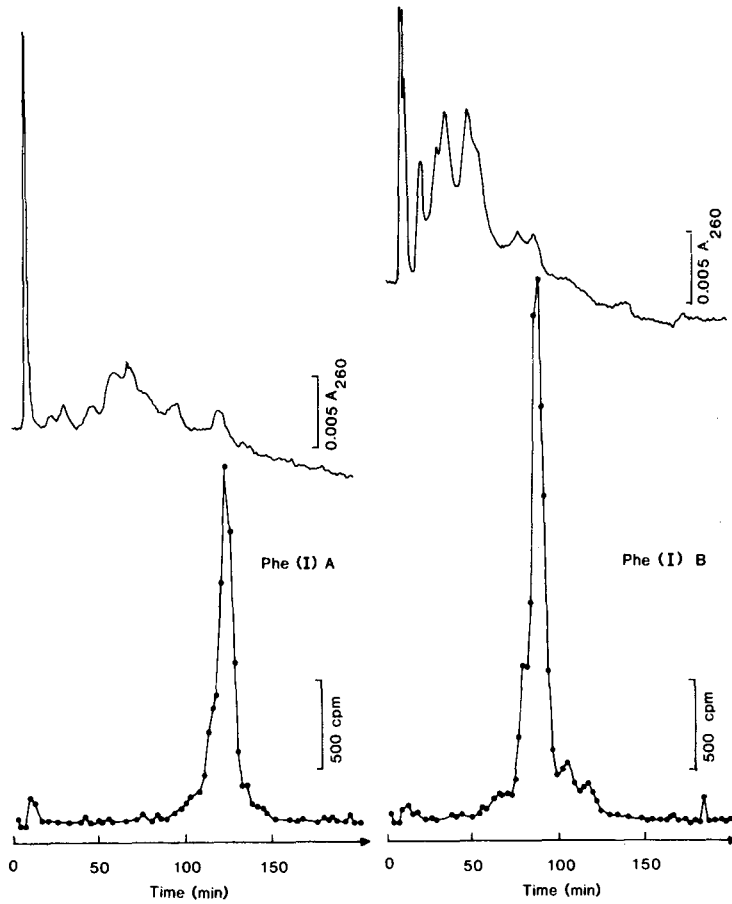


Fig. 5. HPLC of  $^{14}\text{C}$ -labelled phenylalanyl-tRNA isoacceptors on hydroxyapatite in (A) the absence and (B) the presence of 0.1  $M$  sodium chloride. Sample, [ $^{14}\text{C}$ ]phenylalanyl-tRNA isoacceptors [Phe(I) in Fig. 1]. Conditions and elution (A and B) as in Fig. 2.

#### *HPLC of $^{14}\text{C}$ -labelled valyl-tRNA on hydroxyapatite in the presence of magnesium chloride*

As magnesium ions are known to influence the three-dimensional structure of tRNA<sup>5</sup>, the adsorption of tRNA on hydroxyapatite might be expected to change on inclusion of magnesium chloride in the buffers (magnesium might also interact with the phosphate ions in the hydroxyapatite and thereby change its chromatographic properties).

To examine this, the [ $^{14}\text{C}$ ]valyl-tRNA isoacceptor I [Val(I) in Fig. 1] was applied again and eluted from the hydroxyapatite column, but in this experiment the sodium chloride was replaced with 10  $mM$  magnesium chloride.

The apparently homogeneous peak observed in both the absence and presence of sodium chloride (Fig. 4) was split into two distinct peaks when 10  $mM$  magnesium chloride was included in the phosphate buffers (see Fig. 6).

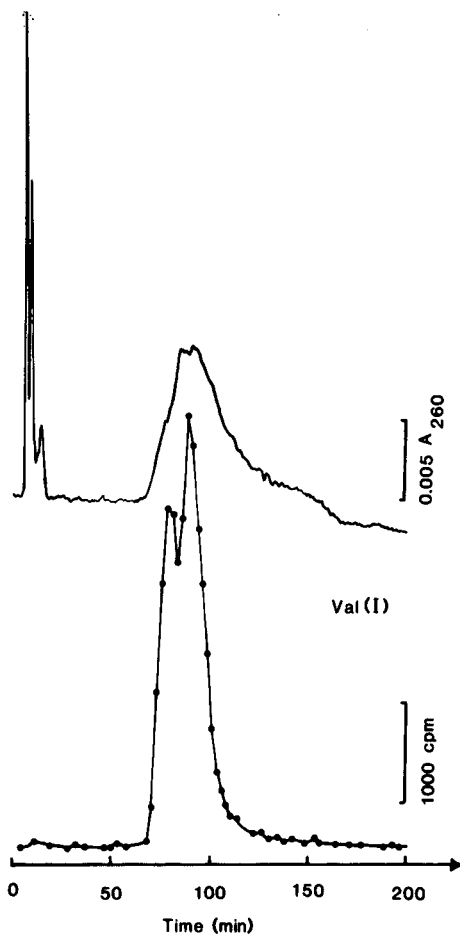


Fig. 6. HPLC of  $^{14}\text{C}$ -labelled valyl-tRNA isoacceptors on hydroxyapatite in the presence of 10 mM magnesium chloride. Sample,  $^{14}\text{C}$ valyl-tRNA isoacceptors [Val(I) in Fig. 1]. Conditions as in Fig. 2. Elution, gradient of sodium phosphate buffer (pH 6.8), including 10 mM magnesium chloride, from 0.044 to 0.102 M over 180 min. The chromatogram in the absence of magnesium chloride is shown in Fig. 4.

*Influence of sodium chloride and potassium chloride on the adsorption of proteins on hydroxyapatite*

Chloride ions at moderate concentrations are known to elute mainly basic proteins from hydroxyapatite columns<sup>2-4</sup>. If chloride ions were included at non-eluting concentrations in the eluting buffer, one could expect the elution order of the proteins to change. To investigate this, the hydroxyapatite column was equilibrated with 0.01 M phosphate buffer (pH 6.8). A sample consisting of 90  $\mu\text{g}$  of ovalbumin, 90  $\mu\text{g}$  of human transferrin, 340  $\mu\text{g}$  of human serum albumin, 16  $\mu\text{g}$  of lysozyme and 21  $\mu\text{g}$  of chymotrypsinogen A dissolved in 120  $\mu\text{l}$  of the equilibration buffer was applied to the column and allowed to be adsorbed for 10 min. The proteins were then eluted with a gradient in phosphate concentration from 0.01 to 0.19 M over 90 min.

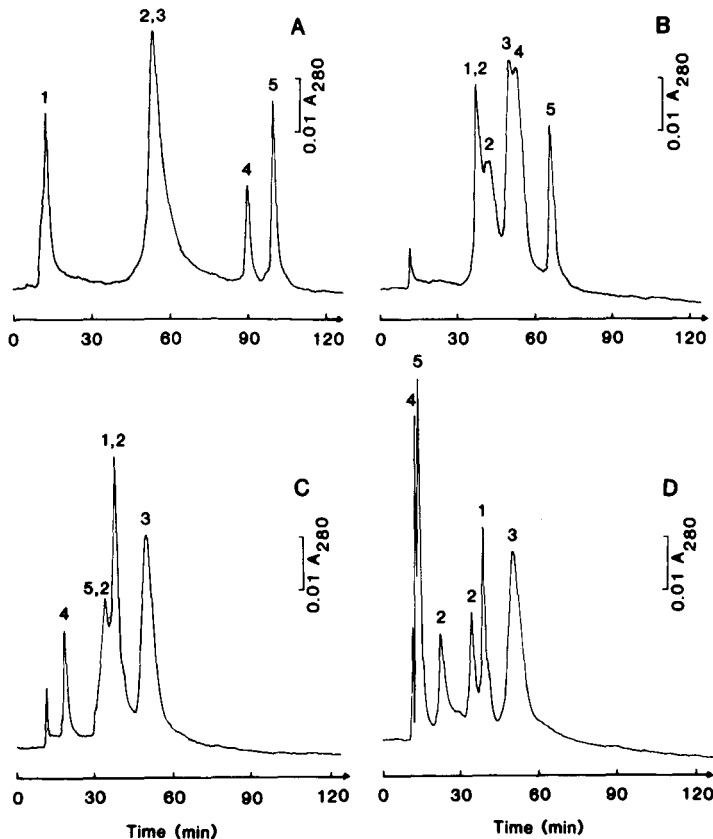


Fig. 7. HPLC of a model protein mixture in the presence of increasing sodium chloride concentrations: 1 = chicken egg albumin (90  $\mu\text{g}$ ); 2 = human transferrin (90  $\mu\text{g}$ ); 3 = human serum albumin (340  $\mu\text{g}$ ); 4 = lysozyme (16  $\mu\text{g}$ ); 5 = chymotrypsinogen A (21  $\mu\text{g}$ ). Sample volume, 120  $\mu\text{l}$ ; column dimensions, 100 mm  $\times$  7.5 mm I.D.; flow-rate, 0.3 ml/min. Elution: (A) 0.01 M sodium phosphate buffer (pH 6.8) for 28 min, then a gradient from 0.01 to 0.19 M over 90 min; (B), (C) and (D) as in A, but the buffers also included 0.1, 0.2 and 0.5 M sodium chloride, respectively.

This procedure was followed four times, using sodium phosphate containing 0.0, 0.1, 0.2 and 0.5 M sodium chloride. In order to investigate the influence of the cation, the experiment was repeated using potassium phosphate and potassium chloride.

As expected, the two basic proteins, lysozyme ( $pI$  10.5–11) and chymotrypsinogen A ( $pI$  8.8–9.6), showed markedly decreased adsorption on inclusion of sodium chloride in the buffers (Fig. 7). Human transferrin, although fairly acidic ( $pI$  5.2–6.2), was also eluted earlier at increasing chloride concentrations. On the other hand, chicken egg albumin ( $pI$  4.6) was adsorbed more strongly when chloride ions were included. Finally, the elution of human serum albumin ( $pI$  5.8) was more or less independent of the chloride concentration in the buffers.

Only minor differences in the elution patterns were seen on using sodium or potassium as cations.

## DISCUSSION

In HPLC of any kind it is generally preferable to keep the elution conditions as simple as possible in order to maximize reproducibility. Sometimes, however, it can be of advantage to utilize an additional parameter to manipulate the appearance of the chromatogram.

We have shown that although sodium chloride alone cannot desorb tRNA from a hydroxyapatite column, it does have the attractive property of improving the separation of tRNA compared with elution by sodium phosphate buffers alone. A general narrowing of the eluting zones was observed (Figs. 2–5), and sometimes an apparently homogeneous peak split into two parts [Leu(IV) in Fig. 3] when sodium chloride was present in the buffers. This zone-narrowing effect may be attributed to a reduction in the number of ways tRNA can be adsorbed on hydroxyapatite. The sodium chloride concentration (0.1 *M*) was found to be suitable in our experiments, but may not be the optimum concentration for all separations.

Magnesium ions are known to alter the three-dimensional structure of tRNA<sup>5</sup> and should also compete with the calcium ions of the hydroxyapatite for the phosphodiester bridges of the ribonucleic acids. In addition, it should interact with phosphate groups on the column, and might therefore be expected to influence the adsorption of tRNA on hydroxyapatite. We have demonstrated here that a valyl-tRNA isoacceptor appearing homogeneous in both the presence and absence of sodium chloride [Val(I) in Fig. 4] could be resolved into two distinct components when magnesium chloride was included in the buffers (Fig. 6). Unfortunately, the column could not be regenerated by washing with phosphate buffers not containing magnesium chloride, and thereby lost its original properties.

Inclusion of sodium chloride in the eluting phosphate buffer has previously been used for the specific purification of  $\gamma$ -globulin from whole serum<sup>1,10</sup>. In this work we further demonstrated this phenomenon by separating a model protein mixture with increasing concentrations of sodium chloride in the eluting buffers. As expected, the adsorption of the basic proteins lysozyme (*pI* 10.5–11) and chymotrypsinogen A (*pI* 8.8–9.6) was lowered considerably in the presence of sodium chloride<sup>2</sup> but, surprisingly, that of human transferrin (*pI* 5.2–6.2) was also reduced. Chicken egg albumin (*pI* 4.6), on the other hand, was bound more strongly to the column when sodium chloride was included in the buffers, whereas human serum albumin (*pI* 5.8) was hardly affected. By an appropriate choice of chloride and phosphate concentrations in the eluting buffers, one might be able to elute selectively one specific protein out of several proteins adsorbed on the column (*e.g.*,  $\gamma$ -globulin from whole serum as in ref. 1) or to elute all but one particular protein from the column. An example of the latter possibility might be human serum albumin in Fig. 7D, provided that the eluting phosphate concentration is chosen properly. This cannot be achieved with only sodium phosphate in the eluting buffer (see Fig. 7A).

The reproducibility was high for both the tRNA and the protein experiments.

## ACKNOWLEDGEMENTS

This work was financially supported by the Swedish Natural Science Research Council and the Knut and Alice Wallenberg, Carl Trygger and Bengt Lundqvist Memorial Foundations.

## REFERENCES

- 1 S. Hjertén, J. Lindeberg and B. Shopova, *J. Chromatogr.*, 440 (1988) 305–313.
- 2 M. J. Gorbunoff, *Anal. Biochem.*, 136 (1984) 425–432.
- 3 M. J. Gorbunoff, *Anal. Biochem.*, 136 (1984) 433–439.
- 4 M. J. Gorbunoff and S. N. Timasheff, *Anal. Biochem.*, 136 (1984) 440–445.
- 5 V. Swaminathan and M. Sundaralingam, *CRC. Crit. Rev. Biochem.*, 6 (1979) 318–323.
- 6 G. Zubay, *J. Mol. Biol.*, 4 (1962) 347–356.
- 7 U. Hellman and I. Svensson, *Prep. Biochem.*, 10 (1980) 375–386.
- 8 K. H. Muench and P. Berg, in G. L. Cantoni and D. R. Davies (Editors), *Procedures in Nucleic Acid Research*, Vol. I, Harper and Row, New York, 1966, p. 375.
- 9 T. Srichaiyo and S. Hjertén, *J. Liq. Chromatogr.*, 12 (1989) 809–826.
- 10 S. Hjertén, *Biochim. Biophys. Acta*, 31 (1959) 216–235.





CHROMSYMP. 1668

## UNEXPECTED ELUTION BEHAVIOUR OF PEPTIDES WITH VARIOUS REVERSED-PHASE COLUMNS

H. ENGELHARDT\*

*Angewandte Physikalische Chemie, Universität des Saarlandes, 6600 Saarbrücken (F.R.G.)*

G. APPELT

*Forschungsabteilung Gastroenterologie, Med.-Poliklinisches Institut, Karl-Marx-Universität, 7010 Leipzig (G.D.R.)*

and

E. SCHWEINHEIM

*Angewandte Physikalische Chemie, Universität des Saarlandes, 6600 Saarbrücken (F.R.G.)*

---

### SUMMARY

Gastrin and cholecystokinin peptides were separated by reversed-phase chromatography on conventional bristle-type and polymer-coated stationary phases. The retention of the sulphated and non-sulphated isomeric forms of both peptides is governed by the structure of the peptide, the net charge and additional polar interactions with the stationary phases. Polymer-coated phases are optimum for separations according to chain length, whereas polar interactions are required for the separation of sulphated and non-sulphated peptides of identical chain length.

---

### INTRODUCTION

Gastrin and cholecystokinin (CCK), peptides of the CCK family, are present in both the gut and brain tissues and the circulation<sup>1,2</sup>. Both peptides are structurally related. They have the same carboxyl-terminal pentapeptide, and a further structural similarity is a sulphated tyrosine at the C-terminus<sup>3,4</sup>. The release of gastrin and cholecystokinin peptides into the peripheral blood occurs in response to a protein- and fat-rich meal. In the gut, the physiological role of CCK is to regulate gall-bladder contraction and pancreatic exocrine secretion, whereas gastrin stimulates the gastric acid secretion<sup>5</sup>. Various multiple molecular forms of gastrin and cholecystokinin peptides, varying in peptide length and charge, have been identified and separated by means of gel-filtration column chromatography and reversed-phase high-performance liquid chromatography (RP-HPLC), followed by radioimmunoassay<sup>1,6</sup>. Further, the octapeptide of CCK (CCK8) and the CCK variant containing 33 amino acids (CCK33), and also the heptadecapeptide (G 17) and the 34 amino acid sequence (G 34) of gastrin, exist naturally in both a sulphated and non-sulphated form<sup>1,7</sup>. Because the concentrations of these peptides in body fluids are below the usual detection sensitivity, optimization of separation must be performed using standards. The

resolution should be high in order to obtain fractions at expected elution windows and to use the fractions for the more sensitive immunological assays.

There have been long and lively discussions about the effects of stationary-phase properties on peptide and protein retention<sup>8,9</sup>. The use of silica-based materials in the RP-HPLC of peptides and proteins has at least two inherent disadvantages. First, the presence of silanols at the surface, which have not been covered or shielded by the "classical" silanization process, is responsible for irreversible adsorption of basic solutes or elution with asymmetric peak shapes<sup>10</sup>. This has been extensively discussed for RP-HPLC of low-molecular-weight solutes<sup>11</sup>. Anomalous behaviour of peptides, *i.e.*, increase in retention at high acetonitrile concentrations<sup>12</sup>, could be attributed to such silanophilic interactions. It has been shown that with "good" stationary phases, where surface silanols have been completely shielded, this behaviour could no longer be observed<sup>13</sup>. The second problem is the stability of the silica matrix or the cleavage of the siloxane bonds to the organosilane, resulting in a loss of carbon and non-reproducible retention times, owing to the harsh elution conditions required for peptide separations<sup>14</sup>. Standard peptide separation conditions are gradient elution at low pH (<3) or addition of ion-pairing reagents, such as trifluoroacetic acid (TFA). Several strategies have been described to overcome these restrictions. The influence of silica gel structure on hydrolysis<sup>15</sup> was studied and the use of new silanization reagents<sup>16</sup> for preparing more stable modified silicas was discussed. The use of cross-linked polymeric stationary phases has been discussed<sup>17,18</sup>. They are stable toward hydrolysis<sup>9</sup> and show different selectivities, but do not generate the efficiency of silica-based stationary phases of identical particle diameter<sup>19</sup>.

Polymer-coated or polymer-encapsulated silicas seem to combine the advantages of microparticulate silica (defined pore structure, mechanical rigidity) and the polymeric phases by totally shielding of surface silanols. Different approaches led to this new type of stationary phase by either coating the silica with a convenient prepolymer, which is then immobilized at the silica surface<sup>20,21</sup>, or by allowing the silica to react with an olefinic silane and polymerizing an olefin coated onto the surface<sup>22</sup>. Both methods give stationary phases with excellent retention properties for basic solutes and show normal elution behaviour of proteins.

For optimization of the separation of gastrin and CCK, commercially available peptides, such as the sulphated and non-sulphated forms of cholecystokinin and gastrin, have been used. The influence of stationary phase properties on absolute and relative retention has been evaluated. In addition to conventional bristle-type RP systems, new polymer-coated reversed-phase materials have been included in the study<sup>21,22</sup>. Because they should exhibit only hydrophobic and very few silanophilic properties.

## EXPERIMENTAL

A modular liquid chromatograph, consisting of two M 510 pumps (Waters Assoc., Milford, MA, U.S.A.), a Waters Chromatography Data Station 840, a multi-wavelength detector (Knauer, Berlin, F.R.G.), detection wavelength 220 nm, and a Rheodyne 7125 sample injector (Rheodyne, Berkeley, CA, U.S.A.) with a 20- $\mu$ l loop, was used.

Different stationary phases with classical modification by organosilanes or with

TABLE I  
COLUMNS USED

<i>Material</i>	<i>Particle size, (<math>\mu\text{m}</math>)</i>	<i>Pore size (nm)</i>	<i>Column length <math>\times</math> I.D. (cm)</i>	<i>Distributor</i>
Macherey, Nagel & Co.:				
Nucleosil C <sub>8</sub>	5	12	12.5 $\times$ 0.4	Bischoff, Leonberg, F.R.G.
Nucleosil C <sub>18</sub>	5	12	12.5 $\times$ 0.4	Bischoff
Nucleosil C <sub>8</sub>	5	30	12.5 $\times$ 0.4	Bischoff
Merck:				
Lichrospher C <sub>18</sub>	10	30	25 $\times$ 0.4	Bischoff
Vydac C <sub>4</sub> 214 TPB	10	30	25 $\times$ 0.4	Macherey, Nagel & Co., Düren, F.R.G.
PolyEncap	10	10	25 $\times$ 0.4	Laboratory prepared <sup>a</sup>
Silica:LiChrosorb				
Vinyl ether C <sub>18</sub>	10	10	12.5 $\times$ 0.4	Laboratory prepared <sup>a</sup>
Silica: LiChrosorb				
MH 1	5	12	25 $\times$ 0.4	Gynkotek, Germering, F.R.G.
Silica: Nucleosil				
PolyEncap	5	30	12.5 $\times$ 0.4	Bischoff
Silica: Nucleosil				

<sup>a</sup> Prepared in our laboratory, as described in ref. 22.

polymer-coating were used. The columns, their dimensions and the distributors are summarized in Table I. The Vydac C<sub>4</sub> phase was purchased as bulk material and packed into columns in our laboratory with a standard slurry-packing technique. The synthesis of the PolyEncap and the octadecyl vinyl ether phases have been described recently<sup>22</sup>.

Mixtures of water (purified with a Milli-Q equipment; Millipore, Eschborn, F.R.G.) and acetonitrile of HPLC grade (ACN) (Baker, Gross-Gerau, F.R.G.); were used isocratically (30% ACN) or in gradients (28% to 40% ACN in 30 min for 12.5-cm columns and 60 min for 25-cm columns). All eluents contained 0.1% TFA. The ionic strength was adjusted with potassium chloride.

Cholecystokinin (Pancreomycin) octapeptide (CCK8), sulphated and non-sulphated, and gastrin-17 (peptide with 17 amino acids), sulphated and non-sulphated, were purchased from Sigma (Munich, F.R.G.). The amino acid sequence of CCK8 is Asp-Tyr-Met-Gly-Trp-Met-Asp-Phe-NH<sub>2</sub>. Sulphatation occurs on tyrosine. The sequence of gastrin-17 is *p*-Glu-Gly-Pro-Trp-Leu-(Glu)<sub>5</sub>-Ala-Tyr-Gly-Trp-Met-Asp-Phe-NH<sub>2</sub>. Sulphatation also occurs on tyrosine.

## RESULTS AND DISCUSSION

### *Peptide separations with gradient elution*

For protein and peptide analysis, several brands of specially designed reversed-phase columns are now available. One of the most widely applied is the Vydac RP column with C<sub>4</sub> bristles and this system was used for the first experiment. As can be seen in Fig. 1, under standard gradient conditions the two CCK8 peptides (1 and 2)

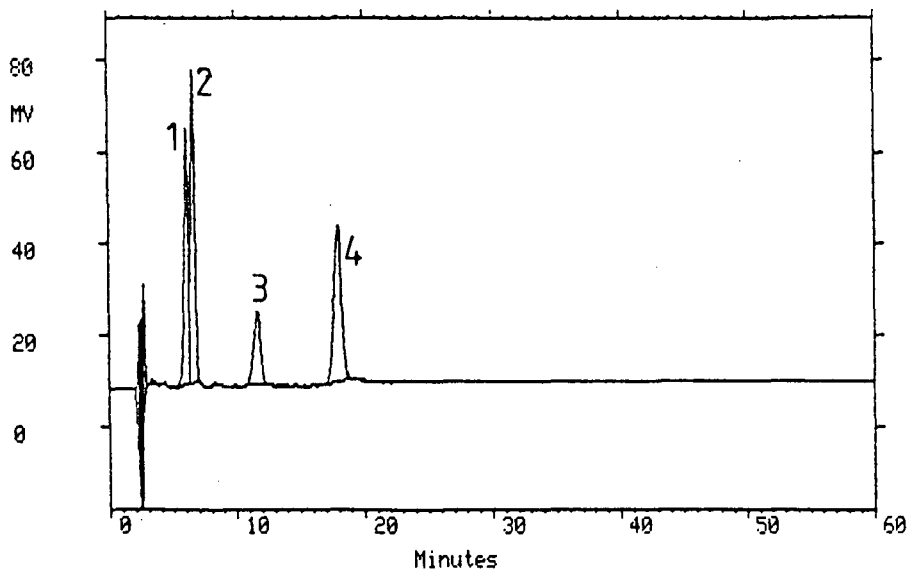


Fig. 1. Separation of gastrin and CCK8 peptides on Vydac C<sub>4</sub> 30 nm. Solutes, 1 = CCK8 sulphated; 2 = CCK8 desulphated; 3 = gastrin-17 sulphated; 4 = gastrin-17 desulphated. Column, Vydac C<sub>4</sub> 30 nm (see Table I); eluent, gradient from 28% aqueous ACN-0.1% TFA to 40% ACN-0.1% TFA in 60 min.

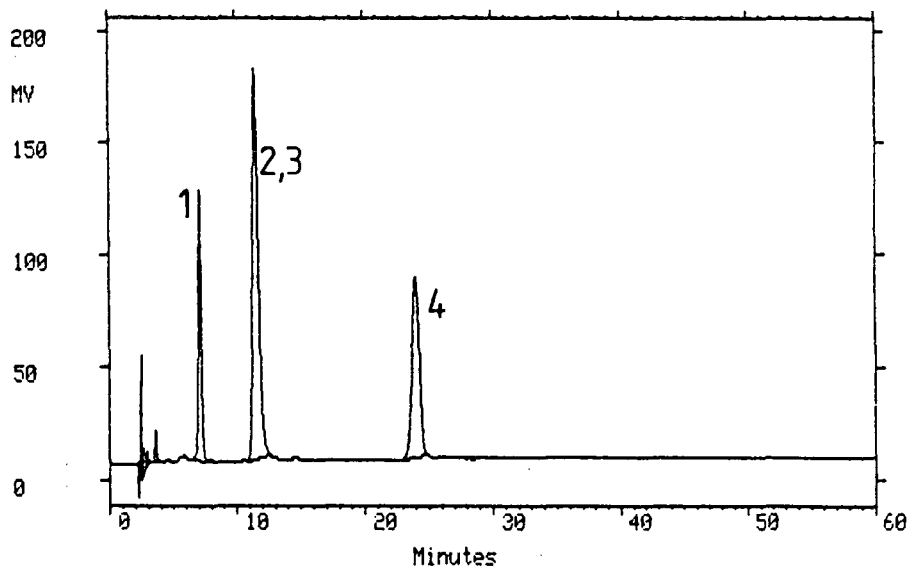


Fig. 2. Separation of standard peptides on LiChrospher C<sub>18</sub> 30 nm. Column, see Table I. Samples and conditions as in Fig. 1.

are not adequately separated for the desired collection of fractions. The elution order is as expected, the octapeptides being eluted before the non-sulphated ones. This finding led us to increase retention by increasing the carbon content of the stationary phase. The separation obtained under the standard gradient conditions with an RP C<sub>18</sub> coating on silica with identical surface area and pore diameter (LiChrospher C<sub>18</sub>, 30 nm) is shown in Fig. 2. The retention of the non-sulphated peptides (2 and 4) increased, as expected, with increasing carbon content of the stationary phase. However, the elution of the sulphated peptides (1 and 3) was hardly affected by the change in carbon content, thus leading to simultaneous elution of non-sulphated CCK8 with gastrin-17, sulphated. These observations can be explained with the superposition of at least two retention mechanisms: hydrophobic and ionic interactions.

Ionic interactions, which always play a role in the separation of nitrogen-containing pharmaceuticals, have been minimized in HPLC by the introduction of polymeric-coated stationary phases. With these columns, even strongly basic solutes, which are extremely sensitive to silanophilic interactions, are eluted with symmetrical peaks<sup>22</sup>. Fig. 3 shows the separation of the peptides from such a polymeric phase where octadecyl vinyl ether had been polymerized on the surface of a silica modified with vinylsilane<sup>22</sup>. Owing to the high carbon content, the retentions are relatively high, the sulphated and non-sulphated solutes cannot be separated and, surprisingly, the elution order for the sulphated and non-sulphated forms of CCK8 (1 and 2, respectively) has changed. Another difference from the separations shown in Figs. 1 and 2 was that here a silica base material with a specific surface area of 300 m<sup>2</sup>/g was used. To differentiate between the influence of the surface area and the type of coating, a conventional reversed phase with the same surface area was also used. In Fig. 4 a standard separation with a Nucleosil C<sub>18</sub> column is shown. With this column, the separation of all four peptides is possible and the elution order was identical with that on the wide-pore materials (30 nm).

In order to evaluate the different retention mechanisms and their influence on elution sequence more closely, additional isocratic studies of absolute and relative retention with stationary phases of different types were performed.

#### *Polymer-coated vs. bristle-type phases*

It is impossible to study the retention behaviour of proteins by isocratic elution. However, with the short-chain peptides used in this work, isocratic measurements of absolute and relative retentions are possible. Hence, it seems feasible to use these peptides for more general observations of protein retention in RP-HPLC. Figs. 1–4 show that sulphated and non-sulphated peptides exhibit different and surprising behaviour on conventional bristle-type and polymer-coated columns. Because of the low molecular weights and the greater variability of phases, silica with standard pore diameters of *ca.* 10 nm were used. Behaviour identical with that described for this material has been observed with wide-pore material (pore diameter 30 nm). Differences in absolute retention between the various stationary phases have been observed and could easily be related to the carbon content of the stationary phase and peptide chain length. However, the selectivities of the stationary phases are different for the separations according to peptide chain length and for sulphated and non-sulphated species. In Fig. 5 the relative retentions of CCK8 and gastrin-17 and their sulphated isomers are shown. In contrast to this selectivity according to chain length, Fig. 6

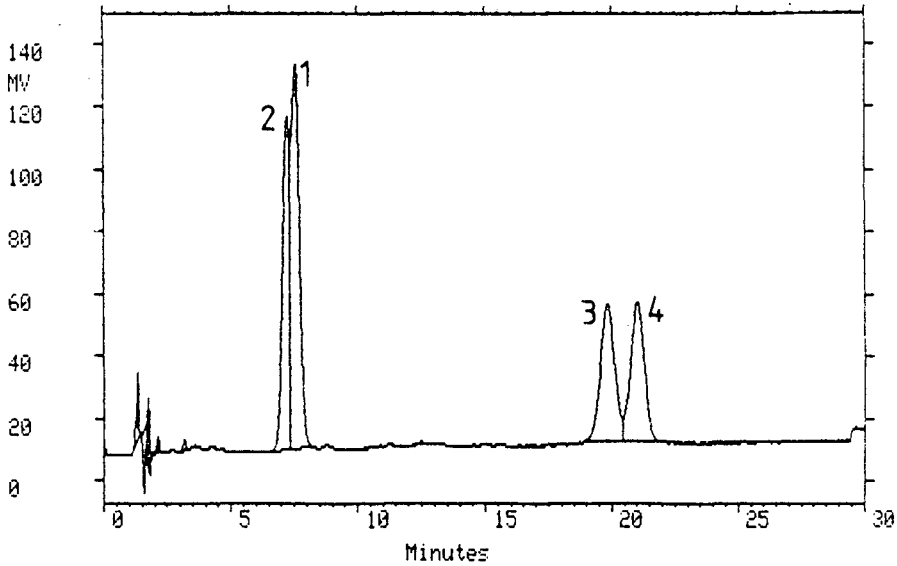


Fig. 3. Separation of standard peptides on  $C_{18}$  vinyl ether. Column, see Table I. Samples and conditions as in Fig. 1; gradient time, 30 min.

shows the polar selectivities of the sulphated and non-sulphated species of identical chain length. The polymer-coated stationary phases (e.g.,  $C_{18}$  vinyl ether) show the highest hydrophobic selectivity. However, this column shows the lowest polar selec-

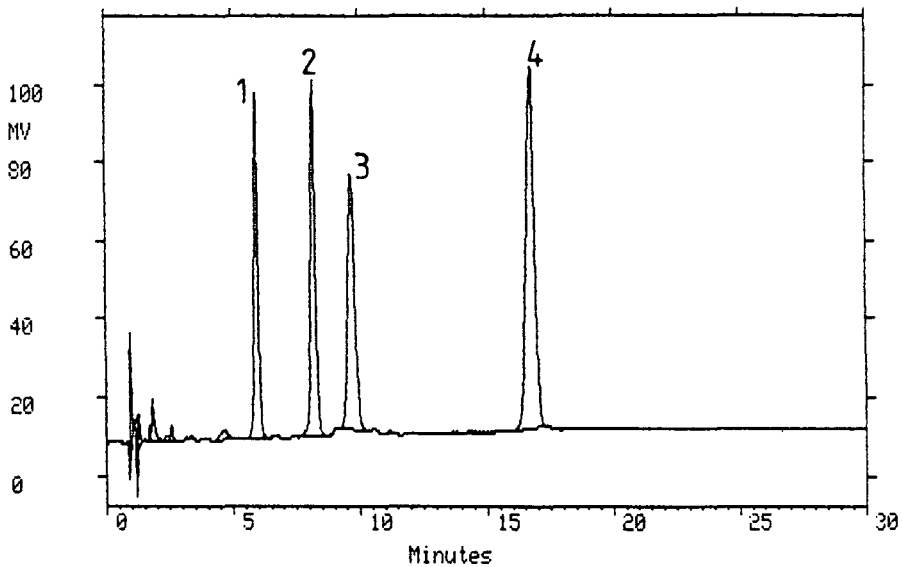


Fig. 4. Separation of standard peptides on MN Nucleosil  $C_{18}$  12 nm. Column, see Table I. Samples and conditions as in Fig. 1; gradient time, 30 min.

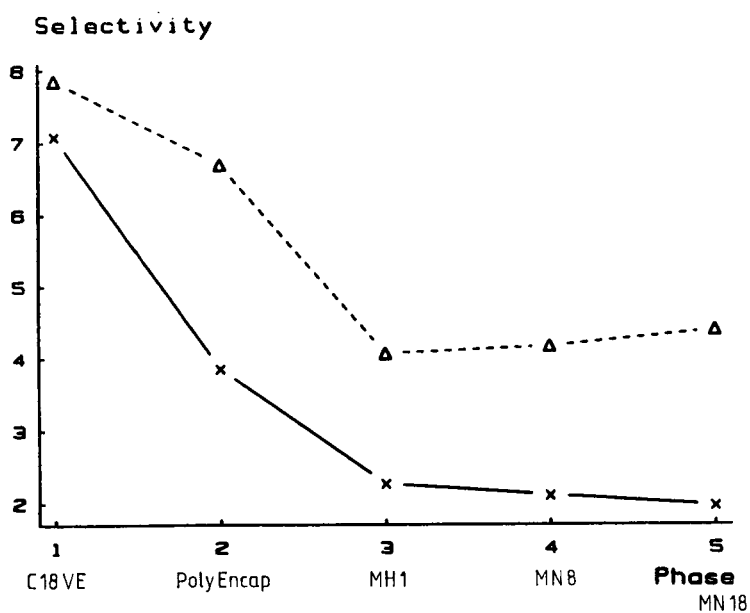


Fig. 5. Hydrophobic selectivity of stationary phases. Columns, see Table I. Isocratic measurements with 30% aqueous ACN-0.1% TFA. ×, Gastrin sulphated-CCK sulphated; Δ, gastrin-CCK.

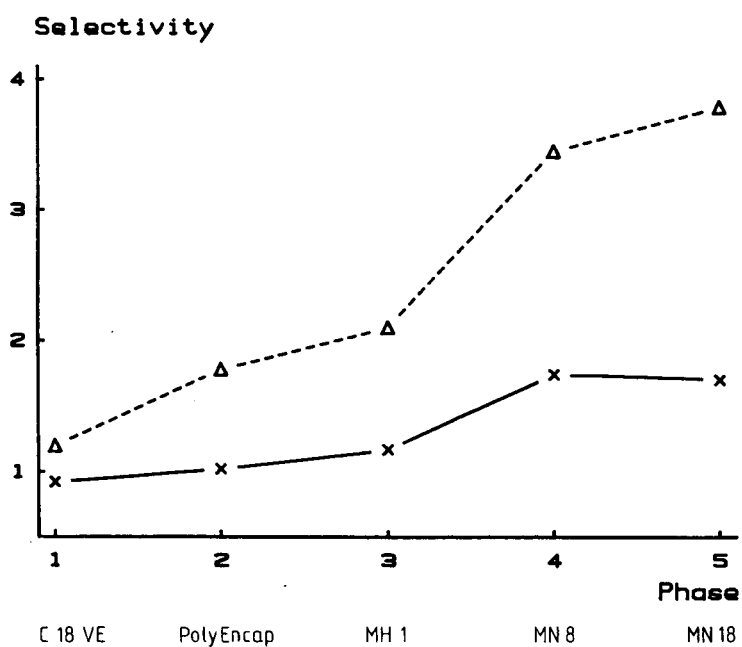


Fig. 6. Polar selectivity of stationary phases. Conditions as in Fig. 5. ×, CCK8-CCK8 sulphated; Δ, gastrin-17-gastrin-17 sulphated.

tivity for the separation of sulphated and non-sulphated peptides, as can be seen in Figs. 3 and 6. In contrast, the opposite is true for the conventional bristle-type stationary phases MN 8 (Nucleosil C<sub>8</sub>), where the hydrophobic selectivity is much lower. The two other polymer-coated stationary phases also included in Figs. 5 and 6 are in between these two extremes. Owing to its more polar surface groups the stationary phase (PolyEncap) where a butyl acrylate had been polymerized on silica modified with vinylsilane<sup>22</sup>, shows, despite the small change in carbon content from C18 vinyl ether (less than 3%), less hydrophobic selectivity and a slightly enhanced polar selectivity. The other polymer-coated stationary phase (MH 1) resembles the conventional bristle-type phases much more. This can be explained by the preparation technique used for this type of stationary phase. In this instance, a trimethylsilylated silica is covered with a polysiloxane containing octadecyl groups<sup>21</sup>.

From these findings, it may be concluded that stationary phases for peptide and protein separations require not only optimum coverage of surface silanols, usually determined by measurement of the peak symmetry of basic solutes, but also additional centres for polar interactions to permit the separation of isomers differing only in a polar functional group.

#### *Influence of ionic strength*

In protein and peptide separations with silica-based stationary phases, silanophilic interaction with unmodified surface silanols is observed in addition to the main retention mechanism, *i.e.*, hydrophobic interaction. It has been demonstrated<sup>23</sup> that these silanophilic interactions, like ion exchange of basic peptides and ion exclusion of acidic peptides, can be minimized by increasing the ionic strength of the buffer solution by the addition of salts, such as potassium chloride. As can be seen in Fig. 7, the retention of the non-sulphated CCK 8 decreases with increasing ionic strength, whereas the retention of the sulphated isomer is only slightly affected by increasing the ionic strength, especially up to 0.15 *M* potassium chloride solutions. At first glance, this is not understandable, because for the sulphated species ion exclusion should be expected. However, if one calculates the net charge for the two isomers at pH 2.5, the sulphated CCK has a net charge of zero (positively charged, terminal amino group and a negatively charged sulphate group), whereas the non-sulphated CCK has a net charge of +1 (positively charged terminal amino group only). Consequently, this species (non-sulphated) can interact with surface silanols by an ion-exchange mechanism. Enhancement of retention by increasing salt concentration, usually applied in hydrophobic-interaction chromatography (HIC), could not be observed for this small peptide up to a concentration of 1 *M*.

In Fig. 8, the influence of ionic strength on retention is shown for a polymer-coated stationary phase. Here, the retention increases for both isomers at low ionic strength. In their preparation surface silanols are totally covered by a polymeric layer. The increase in eluent hydrophilicity due to increasing potassium chloride concentration increases the retention of both solutes. The retention of the non-sulphated isomer with larger hydrophobicity increases continuously, whereas that of the sulphated species remains constant. The polar ester functionalities in the polymeric layer may be the reason for this behaviour.

The differences between the two types of stationary phases can be seen much more clearly from the dependence of relative retentions on ionic strength, as shown in



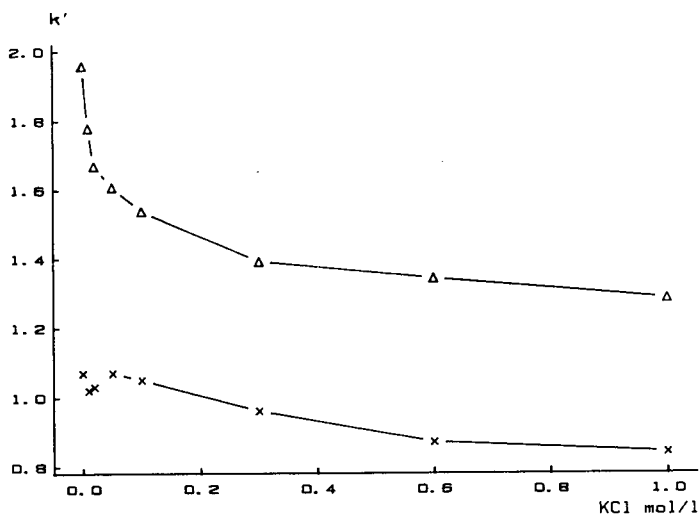


Fig. 7. Influence of ionic strength on peptide retention with a bristle-type stationary phase. Column, Lichrospher  $C_{18}$ , 30 nm (see Table I). Other conditions as in Fig. 5.  $\times$ , CCK8 sulphated;  $\Delta$ , CCK desulphated.

Fig. 9. The selectivity with the conventional bristle-type stationary phase decreases as ionic strength increases, because for the non-sulphated CCK (one positive charge) the additional contribution of ion exchange for the non-sulphated CCK (one positive charge) decreases with increasing ionic strength. At a salt concentration above 0.5 M, additional contributions to the retention mechanism are excluded, and selectivity is

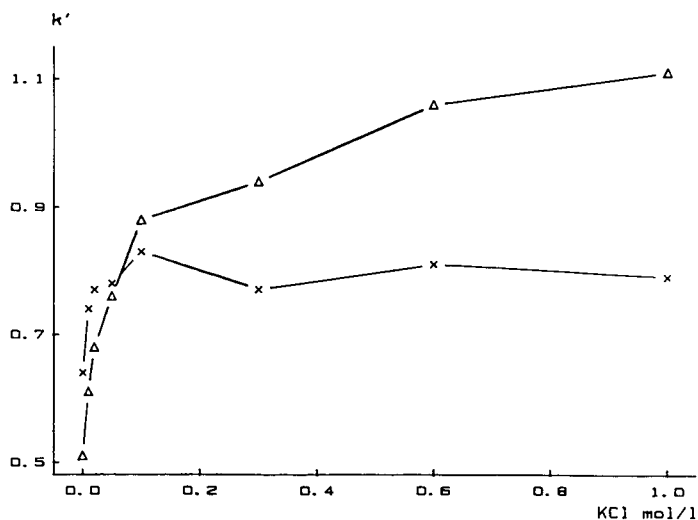


Fig. 8. Influence of ionic strength on peptide retention with a polymer-coated phase. Column, PolyEncap 30 nm (see Table I). Other conditions as in Fig. 5.  $\times$ , CCK8 sulphated;  $\Delta$ , CCK desulphated.

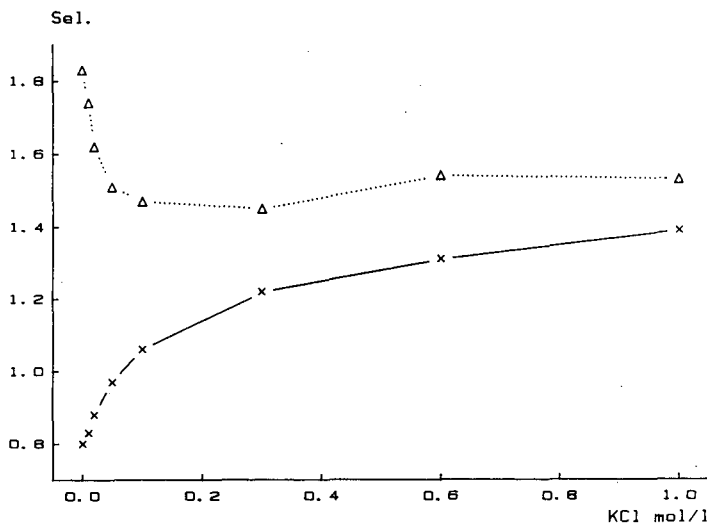


Fig. 9. Influence of ionic strength on selectivity (CCK8 desulphated–CCK8 sulphated) with different types of stationary phases. Columns: ×, PolyEncap 30 nm; Δ, LiChrospher C<sub>18</sub>, 30 nm; see Table I. Other conditions as in Fig. 5.

determined solely by differences in peptide hydrophobicity. It has also been observed in size-exclusion chromatography of proteins<sup>23</sup> that a salt concentration of 0.5 M is necessary for suppression of electrostatic interactions.

With a polymer-coated stationary phase at low ionic strength the sulphated peptide is more strongly retarded than the non-sulphated peptide. At a salt concentration of *ca.* 0.05 M the elution sequence changes, and the selectivity increases with increasing ionic strength. This is due to the stronger dependence of the retention of the non-sulphated peptide on ionic strength (see Fig. 8). At salt concentrations above 0.5 M the dependence of selectivity on ionic strength is identical with that observed for conventional bristle-type stationary phases, indicating an identical separation mechanism. It should be mentioned that all polymer-coated phases investigated behave identically, in spite of differences in functional groups and pore sizes (data not shown). This demonstrates the advantages of polymer-coated stationary phases due to the absence of additional retention mechanisms.

## CONCLUSIONS

The complexity of peptide and protein structures, together with the heterogeneity of stationary phases for HPLC, can cause surprising retention behaviour. The charges of peptides cause, in addition to hydrophobic interactions, electrostatic interactions with polar surface groups on the stationary phases. At present, two different types of stationary phases are used for RP-HPLC of proteins: conventional bristle-type phases and polymeric-coated phases. The latter have been developed for the analysis of basic nitrogen-containing pharmaceuticals to reduce silanophilic interactions, which usually cause peak asymmetry. Both types of stationary phase exhibit

different retention behaviour in protein analysis. With "good" conventional bristle-type stationary phases (symmetrical peaks for peptides with one positive net charge) at low ionic strength (below 0.3), an ion-exchange mechanism contributes to peptide retention. With polymer-coated stationary phases the ion exchange does not contribute noticeably to retention. However, for the separation of isomeric peptides, differing by one sulphonic acid group, polar interactions with either surface silanols (bristle-type phases) or siloxanes (polysiloxane-coated phases) are necessary for separation.

#### ACKNOWLEDGEMENT

The stay of G. A. in Saarbrücken was made possible by the scientific exchange programme of the Karl-Marx-Universität, Leipzig, and the Universität des Saarlandes, Saarbrücken.

#### REFERENCES

- 1 M. M. Wolfe and J. E. McGuigan, *Gastroenterology*, 87 (1984) 323.
- 2 J. F. Rehfeld, *J. Anat. Nerv. Syst.*, 9 (1983) 113.
- 3 J. F. Rehfeld, *Am. J. Physiol.*, 240 (1981) G255.
- 4 G. J. Dockray, A. Varro and R. Dimaline, in J. de Bellerode and Dockray (Editors), *Cholecystokinin in the Nervous System*, Verlag Chemie, Weinheim, Deerfield Beach, Basle, 1984.
- 5 G. Nilsson and V. Mutt, in L. Martin (Editor), *Comprehensive Endocrinology*, G. B. J. Glass (Editor), *Gastrointestinal Hormones*, Raven Press, New York, 1980.
- 6 P. N. Maton, A. C. Selden and V. S. Chadwick, *Regul. Pept.*, 8 (1984) 9.
- 7 E. J. Dravian, G. H. Greeley, R. D. Beauchamp and J. C. Thompson, *J. Liq. Chromatogr.*, 10 (1987) 1431.
- 8 W. S. Hancock and J. T. Sparrow, in Cs. Horváth (Editor), *High Performance Liquid Chromatography, Advances and Perspectives*, Vol. 3, Academic Press, New York, 1983, p. 50.
- 9 W. G. Burton, K. D. Nugent, T. K. Slattery, B. R. Summers and L. R. Snyder, *J. Chromatogr.*, 443 (1988) 363.
- 10 C. T. Mant and R. S. Hodges, *Chromatographia*, 24 (1987) 805.
- 11 W. R. Melander and Cs. Horváth, in Cs. Horváth (Editor), *High Performance Liquid Chromatography, Advances and Perspectives*, Vol. 2, Academic Press, New York, 1980, p. 114.
- 12 M. T. W. Hearn and B. Grego, *J. Chromatogr.*, 218 (1981) 497.
- 13 H. Engelhardt and H. Müller, *Chromatographia*, 19 (1984) 77.
- 14 J. L. Glajch, J. J. Kirkland and J. Köhler, *J. Chromatogr.*, 384 (1987) 81.
- 15 J. Köhler and J. J. Kirkland, *J. Chromatogr.*, 385 (1987) 125.
- 16 J. J. Kirkland, J. L. Glajch and R. D. Farlee, *Anal. Chem.*, 61 (1989) 2.
- 17 J. W. Dautkins, L. L. Lloyd and F. R. Warner, *J. Chromatogr.*, 352 (1986) 157.
- 18 D. Mac Blane, N. Kitagawa and J. R. Benson, *Am. Lab.*, 2 (1987) 134.
- 19 H. W. Stuurman, J. Köhler, S. O. Jansson and A. Litzén, *Chromatographia*, 23 (1987) 341.
- 20 U. Bien-Vogelsang, A. Deege, H. Figge, J. Köhler and G. Schomburg, *Chromatographia*, 19 (1984) 170.
- 21 H. Figge, A. Deege, J. Köhler and G. Schomburg, *J. Chromatogr.*, 35 (1986) 393.
- 22 H. Engelhardt, H. Löw, W. Eberhardt and M. Mauss, *Chromatographia*, 27 (1989) 535.
- 23 H. Engelhardt and D. Mathes, *Chromatographia*, 14 (1981) 325.



CHROMSYM. 1672

## HYDROPHILIC-INTERACTION CHROMATOGRAPHY FOR THE SEPARATION OF PEPTIDES, NUCLEIC ACIDS AND OTHER POLAR COMPOUNDS

ANDREW J. ALPERT

*\*PolyLC, 9052 Bellwart Way, Columbia, MD 21045 and Department of Medicine, The Johns Hopkins School of Medicine, Baltimore, MD 21205 (U.S.A.)*

---

### SUMMARY

When a hydrophilic chromatography column is eluted with a hydrophobic (mostly organic) mobile phase, retention increases with hydrophilicity of solutes. The term hydrophilic-interaction chromatography is proposed for this variant of normal-phase chromatography. This mode of chromatography is of general utility. Mixtures of proteins, peptides, amino acids, oligonucleotides, and carbohydrates are all resolved, with selectivity complementary to those of other modes. Typically, the order of elution is the opposite of that obtained with reversed-phase chromatography. A hydrophilic, neutral packing was developed for use in high-performance hydrophilic-interaction chromatography. Hydrophilic-interaction chromatography is particularly promising for such troublesome solutes as histones, membrane proteins, and phosphorylated amino acids and peptides.

Hydrophilic-interaction chromatography fractionations resemble those obtained through partitioning mechanisms. The chromatography of DNA, in particular, resembles the partitioning observed with aqueous two-phase systems based on polyethylene glycol and dextran solutions.

---

### INTRODUCTION

A hydrophilic, strong-cation-exchange (SCX) material, poly(2-sulfoethyl aspartamide)-silica (PolySulfoethyl A) was introduced recently<sup>1</sup> for high-performance liquid chromatography (HPLC) of peptides. The material is a complement or alternative to reversed-phase chromatography (RPC). Columns of this material are eluted with a salt gradient in a buffer at pH 2.8-3.0, often with some acetonitrile present. At low levels of CH<sub>3</sub>CN, retention and selectivity are governed primarily by the number of basic residues or positive charges in peptides<sup>1-3</sup>. This property permits isolation and analysis of specific entities, such as C-terminal peptides<sup>4</sup>, disulfide-linked peptides<sup>5</sup>, and pyroglutamyl-terminated peptides<sup>6</sup>. The material is also useful, in combination with RPC, for peptide mapping<sup>7</sup> and purification of natural or synthetic peptides<sup>1,5</sup>.

The selectivity changes markedly when the mobile phase contains high levels of organic solvent: (1) Retention increases dramatically above 70% CH<sub>3</sub>CN, while elec-

trostatic effects on the retention of Gly-Tyr diminish in importance<sup>1</sup>; (2) Hydrophilic peptides([Arg<sup>8</sup>]-vasopressin,  $\beta$ -endorphin (1-16)) are retained more strongly relative to more hydrophobic peptides (somatostatin,  $\beta$ -endorphin (1-17))<sup>1</sup>; (3) A mixture of four decapeptide standards, differing only in hydrophobic character, is largely resolved with 50% CH<sub>3</sub>CN<sup>1</sup>, but not with lower concentrations<sup>8</sup>. The order of elution is least to most hydrophilic<sup>8</sup>, opposite from the order in RPC.

These data suggest that increasing the proportion of organic solvent in the mobile phase increases the sensitivity of the sorbent to the hydrophilic residues of peptides. Retention due to such residues, normally a minor "mixed-mode" effect, seems to become a major factor above 70% CH<sub>3</sub>CN. The same effect has been observed with a variety of stationary phases<sup>9-11</sup>. This is "normal-phase" chromatography in that elution is promoted by the use of more polar (here, more aqueous) mobile phases. However, a new term, hydrophilic-interaction chromatography, is proposed to describe the combination of hydrophilic stationary phases and hydrophobic, mostly organic mobile phases. A suitable acronym would be HILIC (HIC having been preempted by Hydrophobic-Interaction Chromatography). This is descriptive, as will be evident from the data to follow, and thus more accurate than the historical term "normal-phase chromatography".

The conditions of HILIC have been used extensively for the analysis of sugars and oligosaccharides<sup>12-19</sup> but only in isolated cases for other classes of compounds. The objectives of this report are: (1) to find out whether these disparate applications involve a single mode of chromatography; (2) to explore the utility of HILIC for the separation of polar solutes; (3) to introduce a packing designed for use in HILIC.

## EXPERIMENTAL

### *HPLC apparatus and columns*

Isocratic HPLC was performed with a Model 300 pump from Scientific Systems (State College, PA, U.S.A.), a spectroMonitor 3100 detector from LDC (Riviera Beach, FL, U.S.A.), and a Lloyd Instruments recorder, Model GRAPHIC 1000 (Vector Group, Newburgh, NY, U.S.A.). Gradient elution HPLC was performed with a 5500 liquid chromatograph, a VISTA 402 data system and a UV200 detector, all from Varian (Walnut Creek, CA, U.S.A.). The HPLC columns are manufactured by PolyLC (Columbia, MD, U.S.A.). PolySulfoethyl A and PolyHydroxyethyl A are available under the tradenames PolySulfoethyl Aspartamide and PolyHydroxyethyl Aspartamide, respectively. The C<sub>18</sub> column was manufactured by Column Engineering (Ontario, CA, U.S.A.). The particle diameter was 5  $\mu$ m unless noted otherwise; the pore diameter was 300 Å.

Titanium frits were obtained from Mott Metallurgical (Farmington, CT, U.S.A.). Ultra High Molecular Weight (UHMW) polyethylene frits were a gift from Upchurch Scientific (Oak Harbor, WA, U.S.A.). Alumina frits were purchased from Alltech (Deerfield, IL, U.S.A.).

### *Reagents*

Cyclo(Ala-Ser), cyclo(Ala-Gly) and cyclo(Ser-Ser) were purchased from Research Plus (Bayonne, NJ, U.S.A.); [Des-Gln]-Substance P from Chemical Dynamics (S. Plainfield, NJ, U.S.A.); oxytocin, [Arg<sup>8</sup>]-vasopressin, somatostatin, Substance

P(4-11) and Substance P(5-11) from Bachem (Torrance, CA, U.S.A.); Substance P(6-11) and Substance P(7-11) from Peninsula Laboratories (Belmont, CA, U.S.A.); and oligothymidylic acid pd(T)<sub>25-30</sub> from Pharmacia LKB (Piscataway, NJ, U.S.A.). Oligothymidylic acid pd(T)<sub>12-18</sub> and pd(T)<sub>19-24</sub> and all other peptides, amino acids, phosphorylated amino acids, organic acids, and oligonucleotides were obtained from Sigma (St. Louis, MO, U.S.A.).

The mixture of homologous 3-hydroxy-2-nitropyridinyl- $\beta$ -D-maltooligoglycosides, as well as purified calibration standards, were a gift from Dr. A. M. Fathy (Diagno-Chemie, Stolberg, F.R.G.).

Organic reagents were purchased from Aldrich (Milwaukee, WI, U.S.A.). All reagents and solvents were of HPLC grade or of the purest grade available.

#### *Preparation of mobile phases*

Stock solutions of triethylamine phosphate (TEAP), 2 M in phosphate, were prepared by addition of triethylamine (TEA) to a concentrated solution of phosphoric acid till the desired pH was obtained, followed by appropriate dilution. This stock solution was stored in the refrigerator when not in use. The same method was used to prepare stock solutions of other salts not readily obtainable. Since the pH of amine salt buffers tends to drift, stock solutions should be prepared fresh monthly.

Mobile phases containing CH<sub>3</sub>CN were prepared by addition of stock solution and the required volume of water to a volumetric flask, followed by addition of CH<sub>3</sub>CN to a level several ml below the mark. After mixing, the flask was placed in a sonicator bath for 5 min, which both degasses and warms the cool solution. CH<sub>3</sub>CN was then added to the mark.

#### *Preparation of PolyHydroxyethyl A*

PolyHydroxyethyl A was prepared by the incorporation of ethanolamine into a coating of polysuccinimide, covalently bonded to silica, using a procedure similar to that detailed in previous papers on polysuccinimide-based coatings<sup>20,21</sup>.

## RESULTS

#### *Retention vs. hydrophilicity*

Fig. 1 shows the separation of amino acids with a column of PolySulfoethyl A and a mostly organic mobile phase. The order of elution is approximately the opposite of that expected for RPC. This is quite evident in Fig. 2, which compares the relative order of elution of the non-basic amino acids (except for cysteine, which tailed badly) on several types of columns. PolySulfoethyl A and PolyHydroxyethyl A (described below) were used in the HILIC mode and displayed elution orders similar to each other and nearly the opposite of that reported for RPC<sup>22</sup>. Minor changes in the order of elution were observed with changes in the pH and salts used in the HILIC mobile phases (*e.g.*, a reversal of the position of Gly and Ser). The elution order is also given for a sulfonated polystyrene-divinylbenzene (PS-DVB) SCX packing, typically used in amino acid analyzers<sup>23</sup>. The elution orders in Fig. 2 suggest that separation on this column is due to relative hydrophobic interaction.

The same effects are observed with non-electrolytes, albeit at higher concentrations of CH<sub>3</sub>CN. The cyclopeptides listed in Fig. 3 lack ionizable groups, the N- and

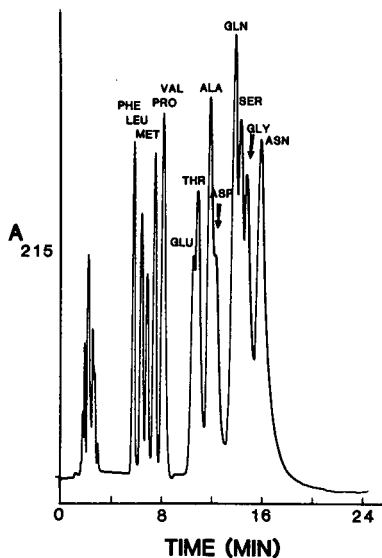


Fig. 1. HILIC of amino acids. Column, PolySulfoethyl A, 200 × 4.6 mm; mobile phase (isocratic), 5 mM TEAP (pH 2.8) with 80% CH<sub>3</sub>CN; flow-rate, 2 ml/min.

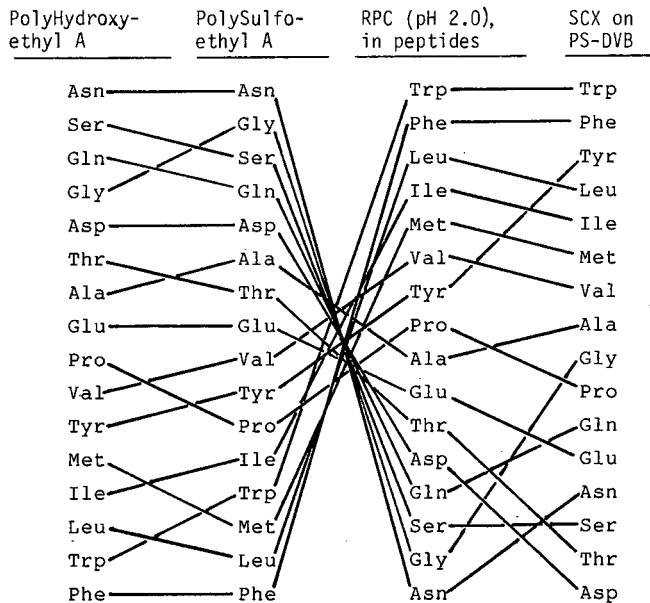


Fig. 2. Relative order of elution of amino acids from various columns. Tie lines connect the same amino acid. PolyHydroxyethyl A and PolySulfoethyl A: columns, 200 × 4.6 mm; mobile phase (isocratic), 10 mM TEAP (pH 2.8) containing 80% (v/v) CH<sub>3</sub>CN. RPC: from ref. 22; Linear AB gradient from water to CH<sub>3</sub>CN (0.1% TFA in each). SCX: from ref. 23; Step gradient of increasing salt and pH.



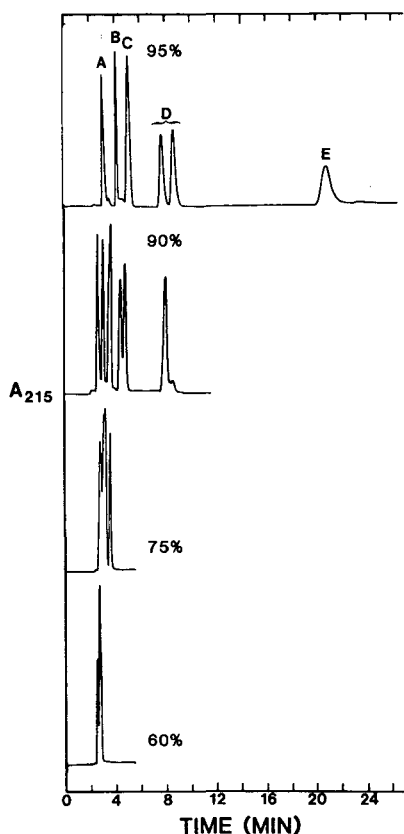


Fig. 3. HILIC of cyclopeptides. Column, as in Fig. 2; mobile phase (isocratic), 15 mM TEAP (pH 2.8) with 95, 90, 75 or 60%  $\text{CH}_3\text{CN}$  as noted; flow-rate, 1 ml/min. Peaks: A = cyclo(Leu-Gly); B = cyclo(Phe-Ser); C = cyclo(Ala-Gly); D = cyclo(Ala-Ser); E = cyclo(Ser-Ser).

C-termini being linked in an amide bond to form a diketopiperazine ring. Nonetheless, retention increases with hydrophilicity of the residues involved and is inversely proportional to the polarity of the mobile phase.

All these cyclopeptides were eluted in doublets depending on the mobile phase used, as is evident here for cyclo(Ala-Ser). Presumably these correspond to geometric isomers, since the corresponding linear peptides, with blocked termini, gave single peaks (data not shown).

#### *Preparation of poly(2-hydroxyethyl aspartamide)-silica*

To facilitate the study of the HILIC mode, a new HPLC packing was synthesized (Fig. 4). This material is poly(2-hydroxyethyl aspartamide)-silica, or Poly-Hydroxyethyl A. The new material, more hydrophilic than PolySulfoethyl A (see below) but lacking its charged character, is well suited for the study of HILIC.

#### *HILIC of amino acids on SCX and neutral supports*

The graphs in Fig. 5 show HILIC effects on retention of ordinary and

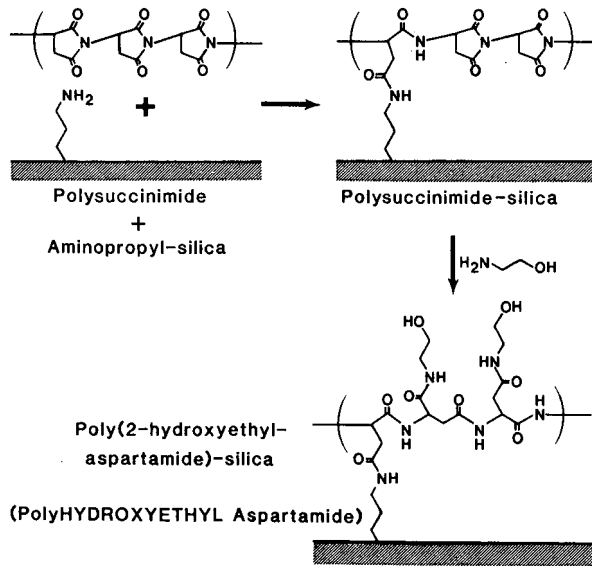


Fig. 4. Preparation of PolyHydroxyethyl A.

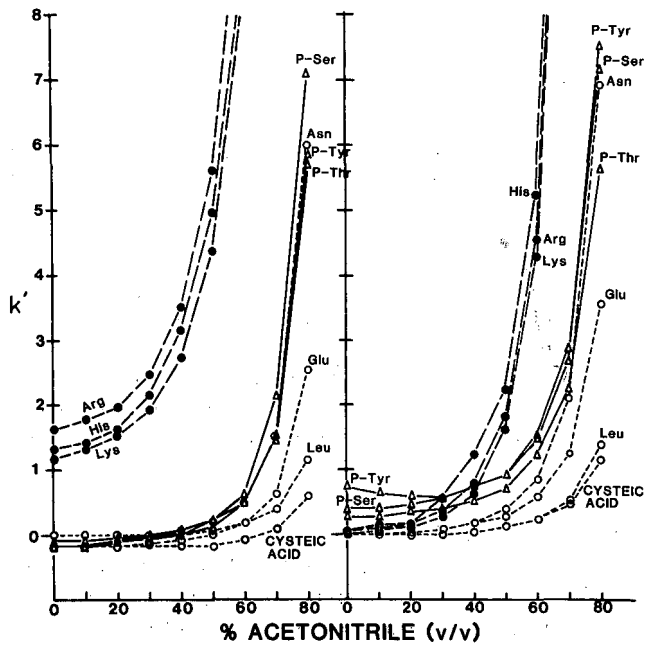


Fig. 5. HILIC (isocratic) of amino acids. The capacity factor was determined from the formula  $k' = (t_R - t_0)/t_0$ , where  $t_0$  is the elution time for toluene, a non-retained solute, at a given flow-rate. Columns,  $200 \times 4.6$  mm, with titanium frits; mobile phase, 25 mM TEAP (pH 5.0) with  $\text{CH}_3\text{CN}$  as noted. Left: Poly-Sulfoethyl A; right: PolyHydroxyethyl A.

phosphorylated amino acids. In the absence of an organic solvent, Arg- and His- are retained on PolyHydroxyethyl A (Fig. 5, right) to an insignificant extent. All other ordinary amino acids are eluted in the void volume. There is a dramatic increase in retention of the basic amino acids as the organic solvent content of the mobile phase is increased. This suggests that positively charged amino acids are quite hydrophilic. The same is true of negatively charged amino acids, as evidenced by the pronounced retention of phosphorylated amino acids in the HILIC mode; for example, phosphorylation increases the capacity factor ( $k'$ ) of Tyr- by one order of magnitude. However, not all charged species are equally hydrophilic;  $k'$  increases markedly for the series cysteic acid < glutamic acid < phosphorylated amino acids. In fact, cysteic acid is less well retained than is Leu-. Neutral amino acids are well retained and resolved, starting at *ca.* 70% CH<sub>3</sub>CN.

HILIC effects on PolySulfoethyl A (Fig. 5, left) are similar, but are superimposed on electrostatic effects. Even in the absence of organic solvents, the basic amino acids are well retained. Values for  $k'$  increase with organic solvent concentration, probably due to hydrophilic interactions, since the shape of the retention curves are the same in both graphs. Above 50% CH<sub>3</sub>CN, hydrophilic interactions are more prominent than electrostatic effects, which contribute to retention as a minor "mixed-mode" component.

The negatively charged Glu-, cysteic acid, and phosphorylated amino acids are eluted from PolySulfoethyl A before the void volume ( $k' = -0.15$ ) in the absence of or at low levels of organic solvent, indicating electrostatic repulsion. However, at CH<sub>3</sub>CN levels above 50%, HILIC effects overcome this repulsion, and thereafter, retention is similar on both columns.

Phosphorylated amino acids are retained and resolved on PolyHydroxyethyl A, even in the absence of organic solvents (Figs. 5 and 6). This makes their analysis in protein hydrolyzates convenient, since other amino acids are not retained under these conditions (Fig. 6), although the separation of P-Thr- and P-Ser- needs to be optimized. The order of elution does not correlate with that of the corresponding non-phosphorylated amino acids (Fig. 2). P-Tyr- is anomalously well retained. This is also

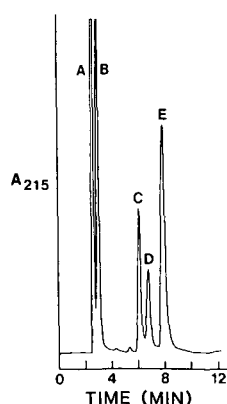


Fig. 6. HILIC of phosphorylated and non-phosphorylated amino acids. Column, PolyHydroxyethyl A (3  $\mu$ m), 100  $\times$  4.6 mm, with titanium frits; mobile phase (isocratic), 10 mM TEAP (pH 2.8); flow-rate, 0.5 ml/min. Peaks: A = His-; B = Ser-, Leu- (void volume); C = P-Thr-; D = P-Ser-; E = P-Tyr-.

the order of elution observed with anion-exchange columns<sup>24,25</sup>. This suggests that the PolyHydroxyethyl A column may be operating as a low-capacity anion-exchange column, a view supported by the elution of basic amino acids in doublets with mobile phases of low ionic concentration. One peak of the doublets coincides with and the other precedes the void volume, suggesting an element of electrostatic repulsion. This would be readily apparent in Fig. 6, for example, except that the presence of Ser- and Leu- in the void volume masks the void volume peak of the His- doublet. However, raising the concentration of the mobile phase from 10 to 25 mM (Fig. 5) not only eliminates the peak splitting, but leads to negligible retention of Arg- and His- ( $k' = 0.1$ ). Thus, the interpretation of Fig. 6 may not be a straightforward matter. In any case, the selective retention of phosphorylated amino acids raises the possibility of the selective isolation of phosphorylated peptides from a protein digest.

In the course of this study, it was observed that phosphorylated amino acids did not pass through HPLC columns with stainless-steel frits from certain manufacturers. The problem was not encountered with frits of titanium, alumina, or UHMW polyethylene. It was subsequently learned<sup>26</sup> that the recovery of phosphorylated peptides

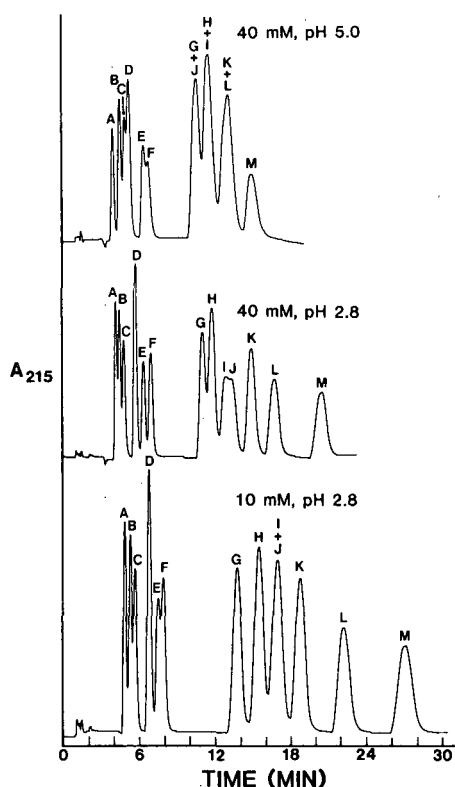


Fig. 7. HILIC of dipeptide standards. Column, PolyHydroxyethyl A, 200 x 4.6 mm; mobile phase (isocratic), TEAP buffer (concentration and pH as noted) with 80% CH<sub>3</sub>CN; flow-rate, 2 ml/min. Peaks: A = Gly-Phe; B = Gly-Leu; C = Gly-Ile; D = Gly-Met; E = Gly-Val; F = Gly-Tyr; G = Gly-Ala; H = Gly-Glu; I = Gly-Asp; J = Gly-Thr; K = Gly-Gly; L = Gly-Ser; M = Gly-Asn.

from HPLC columns improved significantly when stainless-steel frits were replaced by titanium frits. These data imply that non-ferrous frits should be used in HPLC of phosphorylated species.

#### *HILIC of peptides*

Fig. 7 shows the separation, under HILIC conditions, of dipeptides with the composition Gly-X on a column of PolyHydroxyethyl A. As with the amino acids, retention appears to be governed by hydrophilic interactions, increasing with polarity of the solute. Retention is inversely proportional to pH and ionic concentration.

Fig. 8 (I) shows the resolution by HILIC of peptide standards with varied composition. The coincidence of Tyr-Gly and Gly-Tyr is an example of the insensitivity of the HILIC mode to a change of sequence that does not affect charge (and thus hydrophilicity). By contrast, location of the acidic residue of Asp-Val next to the N-terminus probably creates an ion pair in which the charged centers are close enough to neutralize each other. Evidently this decreases their hydrophilicity, in view of the greater retention of Val-Asp, where the charged centers are more isolated. Glu-Ala-Glu provides a good demonstration of the sensitivity of HILIC to the composition of the hydrophilic residues in a peptide, since addition of an Asn- residue nearly doubles the  $k'$  of the peptide. This addition also moves the C-terminal carboxyl group further away from the carboxyl of the side chain of Glu-. However, the Asn-residue probably does not promote retention through electrostatic effects, since a similar increase is observed with the addition of Gln- residues to the N-terminus of small peptides with neutral N-terminal residues (see Fig. 9).

Chromatogram II of Fig. 8 shows the (non-optimized) separation by HILIC of

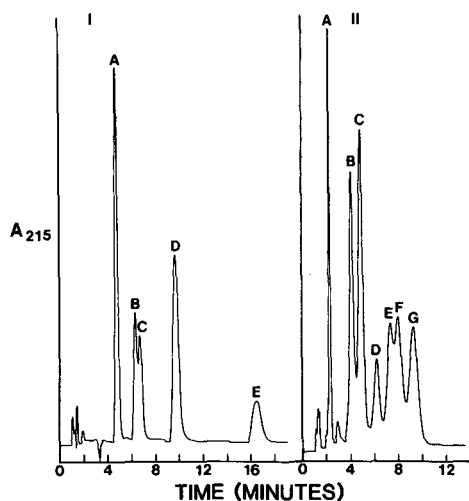


Fig. 8. HILIC of peptide standards (isocratic). Column, as in Fig. 7; mobile phase, 40 mM TEAP (pH 2.8) with 80% (I) or 70% (II)  $\text{CH}_3\text{CN}$ ; flow-rate, 2 ml/min. Peaks: (I) A = Asp-Val; B = Val-Asp; C = Tyr-Gly + Gly-Tyr; D = Glu-Ala-Glu; E = Glu-Ala-Glu-Asn; (II) A = Oxytocin; B = [Tyr<sup>1</sup>]-somatostatin; C = somatostatin; D = [Tyr<sup>11</sup>]-somatostatin; E = [Des-Gln]-Substance P; F = Substance P; G = [Arg<sup>8</sup>]-vasopressin.

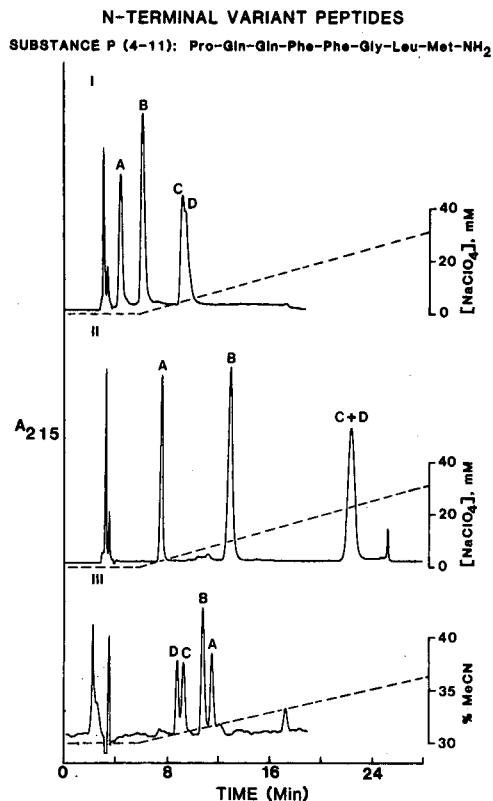


Fig. 9. Gradient elution of Substance P fragments from (I) a PolyHydroxyethyl A column (HILIC mode); (II) a PolySulfoethyl A column (HILIC mode); (III) a C<sub>18</sub> column (RPC mode). Column dimensions, 200 × 4.6 mm; flow-rate, 0.8 ml/min; detection, absorbance at 215 nm, 0.5 a.u.f.s. Elution: (I), (II) 90-min linear gradient, 0–100% eluent B. Eluent A, 10 mM TEA-methylphosphonate (pH 3.0) with 80% CH<sub>3</sub>CN. Eluent B, same + 125 mM sodium perchlorate. (III) 90-min linear gradient, 0–100% eluent B. Eluent A, 0.1% TFA in 30% CH<sub>3</sub>CN; eluent B, 0.1% TFA in 55% CH<sub>3</sub>CN. Peaks: Substance P fragments: A = (7–11); B = (6–11); C = (4–11); D = (5–11). MeCN = Acetonitrile.

some polypeptide hormones. The concentration of CH<sub>3</sub>CN used was lower than for chromatogram I in order to achieve isocratic elution of these peptides in a reasonable time. With the exception of oxytocin, the order of elution is the opposite of that observed for RPC<sup>27</sup> and HIC<sup>28</sup>. As may be surmised from the amino acid data, basicity of a peptide promotes retention, but to a much lesser extent than would be the case with a PolySulfoethyl A column operated in the cation-exchange mode; the time for the isocratic elution of peptides of +1, +2 and +3 charge is considerably shorter. At the same time, the sensitivity of the hydrophilicity of the nonbasic residues results in a selectivity complementary to that of cation exchange. Thus, while [Arg<sup>8</sup>]-vasopressin has a charge of +2, it is eluted after somatostatin, Substance P and their analogues, all with a +3 charge but also with more hydrophobic character.

#### *N-Terminal variant peptides*

Eucaryotic proteins, manufactured by recombinant methods, are sometimes

found to vary in composition, particularly at the N-terminus. There may be an additional N-terminal Met- or N-formyl Met- residue; conversely, exoprotease activity may remove one or two residues from the end. Assessment of the purity of a recombinant protein involves digestion of the product and analysis of the N-terminal peptide fraction for the presence of such variant sequences. RPC often fails to distinguish between such variants.

Fig. 9 shows the separation of a series of Substance P fragments with residues removed in sequence at the N-terminus. HILIC was used to obtain chromatograms I and II, while chromatogram III is RPC. Gradient rates were chosen to give comparable peak widths in both modes. While RPC features the best overall selectivity in this case, the degree of separation of these variant peptides is greatest with HILIC. This is particularly the case when the capacity is increased by the superposition of electrostatic effects and hydrophilic interactions, as with PolySulfoethyl A (chromatogram II). Selectivity differences with PolyHydroxyethyl A may reflect the "contact region" of the peptides (see Discussion).

Peptides may be eluted from HILIC columns with decreasing organic gradients as well as increasing salt gradients. This topic is addressed in the Discussion section, as is the selection of the salts.

#### *Partition mechanisms and HILIC of carbohydrates*

HPLC of carbohydrates has been performed since 1975<sup>12-15,17,19</sup> with columns of silica with an aminopropylsilane coating (NH<sub>2</sub>-silica); mobile phases typically contain about 80% CH<sub>3</sub>CN. These conditions are effectively those of HILIC. This implies that NH<sub>2</sub>-silica retains carbohydrates not directly through its basic charge<sup>15-17</sup> but because the basic groups are hydrophilic. The uncharged, hydrophilic PolyHydroxyethyl A also works well for HILIC of carbohydrates. This is demonstrated in Fig. 10 with a homologous series of oligoglycosides and various concentrations of CH<sub>3</sub>CN. Other hydrophilic stationary phases can also be used, such as diol-<sup>15</sup> and polyol-<sup>16-18</sup> type packings. PolySulfoethyl A can be used, but retention times are 25% less than with PolyHydroxyethyl A. Presumably, this reflects the relative hydrophilicity of these stationary phases.

Reducing sugars are well retained and resolved on PolyHydroxyethyl A, but are eluted in doublets corresponding to the  $\alpha$ - and  $\beta$ -anomers (data not shown). This complicates the elution pattern. The problem is overcome by addition of a small amount of amine to the mobile phase; this speeds up the rate of mutarotation<sup>15-17</sup> and collapses the doublets.

Chromatography of carbohydrates as conducted above has been shown to involve a partitioning mechanism<sup>29-31</sup>. The stationary phase retains a semi-immobilized layer of mobile phase enriched with water. Chromatography of carbohydrates involves partitioning between this stagnant aqueous layer and the bulk of the (mostly organic) mobile phase. It would be reasonable to suppose that the partition mechanism advanced for the chromatography of carbohydrates represents the mechanism of HILIC fractionations of other classes of polar solutes as well.

#### *Aqueous two-phase systems and HILIC of oligonucleotides*

In order to gain additional insight into the mechanism of HILIC, the chromatography of oligonucleotides was studied. Nucleic acids can be fractionated by parti-

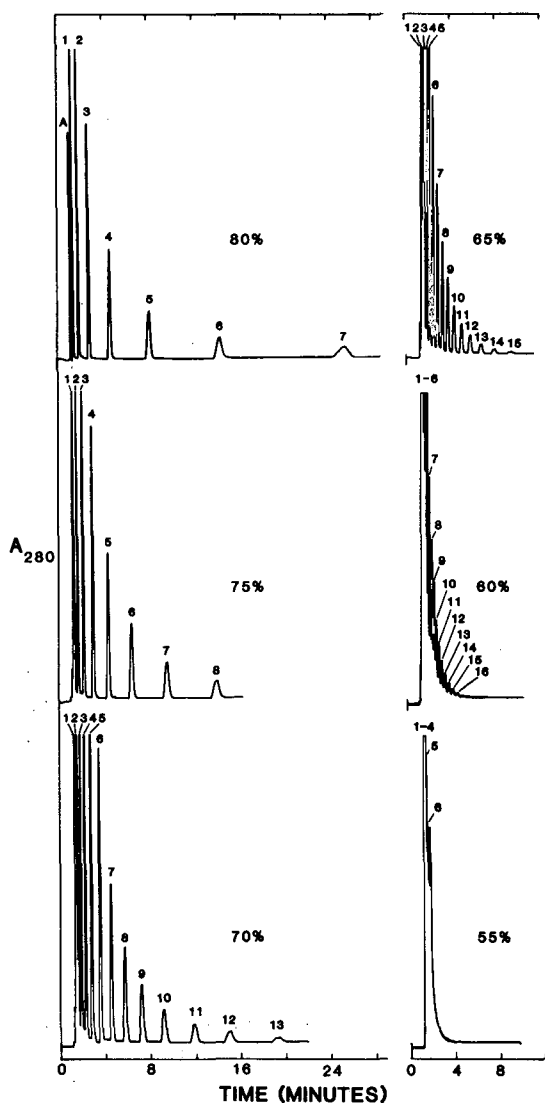


Fig. 10. HILIC (isocratic) of a homologous mixture of 3-hydroxy-2-nitropyridinyl- $\beta$ -D-maltooligoglycosides. Peaks were identified with purified standards. Column, PolyHydroxyethyl A,  $200 \times 4.6$  mm,  $5 \mu\text{m}$ ; mobile phase, acetonitrile-water, 80, 75, 70, 65, 60 or 55% acetonitrile as noted; flow-rate, 2 ml/min. Peaks: 1, 2, 3 ... = degree of polymerization; A = aglycon.

tioning between two aqueous phases, rendered immiscible by small amounts of two polymers that differ sufficiently in hydrophilicity, such as polyethylene glycol (PEG) and dextran. Albertsson<sup>32</sup> has developed the potential of such systems for the bulk fractionation of cells and proteins as well as nucleic acids, and Müller and Kute-meier<sup>33,34</sup> have applied the phenomenon to the chromatographic fractionation of nucleic acids.



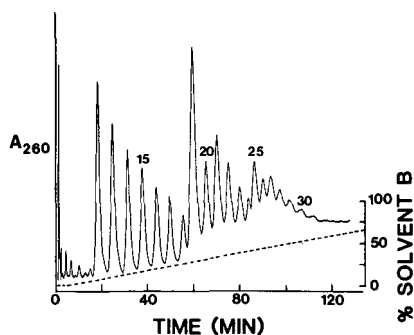


Fig. 11. HILIC (gradient elution) of oligothymidylic acid,  $pd(T)_{12-30}$ . Column, PolyHydroxyethyl A (3  $\mu m$ ),  $100 \times 4.6$  mm; gradient, 200 min linear, 0–100% eluent B. Eluent A, 40 mM TEAP (pH 5.0) with 70% (v/v)  $CH_3CN$ . Eluent B, 75 mM TEAP (pH 5.0) with 80% (v/v)  $CH_3CN$ ; flow-rate, 1 ml/min; detection, absorbance at 260 nm, 0.1 a.u.f.s.

Fig. 11 shows a homologous series of thymidylic acid [ $pd(T)$ ] oligomers. A gradient of increasing salt was used; in addition, a slightly increasing gradient of  $CH_3CN$  concentration was employed to promote retention near the end of the salt gradient and thus increase resolution of closely related species. The results obtained with HILIC resemble those obtained with the above partitioning systems in the following respects: (1) Retention increases with oligomer size; (2) Retention of oligo- $pd(A)_6$  was about three times greater than that of oligo- $pd(T)_6$ , while retention of oligo- $pd(C)_6$  and oligo- $pd(G)_6$  was more than one order of magnitude greater (the opposite of the trend observed with anion-exchange HPLC<sup>35</sup>); (3) Retention was extremely sensitive to the ionic strength of the mobile phase (permitting elution with unusually shallow salt gradients).

#### *HILIC of organic acids and bases*

A column of PolyHydroxyethyl A was eluted with 75 mM TEAP (pH 5.0), containing 70%  $CH_3CN$ . Glyceric acid, tartronic acid and phosphoglyceric acid were completely resolved, with  $k'$  values of 0.46, 1.29 and 1.75, respectively. This demonstrates once again the hydrophilicity of charged groups, especially phosphate groups.

Organic bases contain hydrophilic functional groups, and should lend themselves well to analysis by HILIC. In fact, HILIC conditions are already used for the analysis of basic drugs, both with uncoated silica<sup>36,37</sup> and  $NH_2$ -silica<sup>38,39</sup>.

## DISCUSSION

### *The mechanism of HILIC*

The mechanism by which the HILIC mode operates can be discussed at several levels:

At the empirical level, HILIC is a variant of normal-phase chromatography. Retention is proportional to the polarity of the solute and inversely proportional to the polarity of the mobile phase.

The data in this paper suggest that the mechanism of HILIC involves partitioning between the (hydrophobic) mobile phase and a layer of mobile phase enriched

with water and partially immobilized on the stationary phase. This distinguishes this variant of normal-phase chromatography from other variants involving adsorption directly on the stationary phase. The following observations support a partitioning mechanism: (1) Analogy with the partitioning mechanism already worked out for the fractionation of carbohydrates; (2) The decreasing differences between charged and uncharged stationary phases with increasing levels of organic solvent in the mobile phases (*cf.* Fig. 5); (3) In HILIC of oligonucleotides, the sensitivity to factors known to affect the partitioning of nucleic acids between PEG-containing aqueous phases and (more-hydrophilic) dextran-containing aqueous phases: ionic concentration, base composition, and molecular weight. In fact, 25% CH<sub>3</sub>CN can substitute for the PEG in such two-phase systems<sup>40</sup>.

The phenomena responsible for the partitioning of solutes between the two layers are obscure. Some form of dipole-dipole interactions may be involved, although Nikolov and Reilly<sup>31</sup> found that retention of sugars under HILIC conditions was better correlated with their hydration number than with the potential to form hydrogen bonds. The partitioning of solutes in aqueous two-phase systems is not well understood either<sup>32</sup>. A great deal of study will be required to clarify these questions.

#### *HILIC as a mixed-mode effect in RPC*

One can increase the retention of solutes through hydrophilic interactions by increasing the concentration of organic solvent in the mobile phase. For example, when Nikolov and Reilly<sup>31</sup> eluted a column of uncoated silica with 90% CH<sub>3</sub>CN, they obtained  $k'$  values for sugars comparable to those obtained by elution of NH<sub>2</sub>-silica with 80% CH<sub>3</sub>CN. This raises the question of how hydrophobic a stationary phase can be and still be used in the HILIC mode if one is prepared to use levels of organic solvent approaching 100%. An extreme case of this may be RPC packings that are not end-capped. On such columns, the retention of many proteins and peptides as a function of % CH<sub>3</sub>CN is a U-shaped curve<sup>41-49</sup>. Bij *et al.*<sup>41</sup> have ascribed retention at lower CH<sub>3</sub>CN levels—the conventional RPC region—to “solvophobic” interactions and retention on the other side of the minimum to “silanophilic” interactions.

A reinterpretation of these observations may be warranted by the data in the present study. Retention in the organic solvent-rich region of the U-shaped curves may reflect hydrophilic interactions. In that case, the order of elution of solutes should be the reverse of that in the other branch of the curve. This is in fact the case for peptides<sup>42,43</sup>, proteins<sup>46-49</sup>, and small molecules<sup>9</sup>. Bij *et al.*<sup>41</sup> even obtained U-shaped curves for polar solutes by eluting silica in a reversed-phase mode. Their explanation is succinct: “...it simply demonstrates that the polarity of the eluent relative to that of the stationary phase determines whether the retention behavior is ‘normal’ or ‘reversed’.” This explanation will serve as well, at the empirical level, for the results presented here.

Cyclodextrin-bonded phases offer vivid examples of these effects. With mobile phases low in organic solvent, retention is of the RPC type, through inclusion-complex formation with the hydrophobic cyclodextrin cavity<sup>50</sup>. Retention at high levels of organic solvent is evidently due to HILIC, reflecting the hydrophilic nature of the exterior of the cyclodextrins. Thus, plots of  $k'$  vs. % CH<sub>3</sub>CN are U-shaped curves for dansylated amino acids<sup>51</sup>, showing at least partial inversion of the elution order.

These stationary phases also resolve carbohydrates satisfactorily at high  $\text{CH}_3\text{CN}$  levels<sup>52,53</sup>, again reflecting a possible HILIC mechanism.

RPC is probably a "mixed-mode" process, reflecting the presence of both hydrophobic and hydrophilic interactions. The hydrophobic interactions are negligible at high levels of organic solvent. The data from this study suggest that the hydrophilic interactions are negligible at low levels of organic solvent, except for the most hydrophilic solutes observed here: organic bases. Such compounds are notorious for tailing in RPC. The phenomenon is usually ascribed to electrostatic attraction to silanols. A gradient of increasing organic solvent decreases retention through hydrophobic interactions, but would increase hydrophilic interactions. The presence of the latter as a mixed-mode effect would lead to the opposite of the focussing effect normally expected from gradient elution and cause tailing. It should be noted that any mobile phase component that decreases retention in HILIC also decreases tailing of basic compounds in RPC. Agents used for this purpose include amines<sup>41</sup>, amine salts<sup>41</sup> and inorganic salts<sup>27</sup>. Hydrophilic amines are less effective for this purpose than hydrophobic amines<sup>41</sup>, an observation difficult to explain in terms of electrostatic effects but consistent with HILIC effects. It may also be noted that U-shaped curves are not obtained if no hydrophilic interactions are possible, whether due to a lack of polar sites in the stationary phase<sup>9,54</sup> or to the non-polar nature of a particular solute<sup>41</sup>.

#### *The contact region of peptides*

Some HILIC effects can be understood in terms of the "contact region" concept developed to describe the region of a protein's surface that preferentially makes contact with a chromatographic sorbent<sup>55</sup>. For example, Substance P has basic (and thus hydrophilic) and hydrophobic domains at opposite ends of the molecule. This could permit the selective adsorption of the hydrophilic domain on a HILIC stationary phase surface. No such segregation of domains is obtained with somatostatin; a hydrophobic region is bracketed by two basic residues. This may explain the lesser retention of somatostatin compared to Substance P on both PolySulfoethyl A<sup>1</sup> and PolyHydroxyethyl A.

The same concept can account for the relatively poor ability of RPC to resolve N-terminal variant peptides and the success noted with HILIC (Fig. 9). As with other basic groups, a charged N-terminus is quite hydrophilic. In RPC, this will tend to exclude the N-terminus as a preferred contact region. An example of this was observed<sup>28</sup> in RPC of several nonapeptides with the same composition but different sequences. With a blocked N-terminus, retention was greater with three Leu- residues at this terminus than when they were located in the interior, presumably reflecting steric accessibility. The elution positions were reversed when the N-termini were unmodified.

The best mode for the analysis of N-terminal variant peptides must be determined on a case-by-case basis. The modes of greatest utility may be those in which the N-terminus is a preferred contact region. Cation-exchange certainly qualifies, as does a combination of cation-exchange and hydrophilic interaction (Fig. 9, chromatogram II). However, the electrostatic effects may be so marked as to lead to some insensitivity to the composition of the non-basic residues relative to the basic residues and the N-terminus itself. Thus, PolyHydroxyethyl A, operating purely through hydrophilic interaction, is better able than PolySulfoethyl A to discriminate between some peptides differing in the composition of non-basic residues (Fig. 9).

### *HILIC on miscellaneous stationary phases*

A number of reports in the literature describe the use of hydrophilic stationary phases under HILIC conditions. Mant *et al.*<sup>10</sup> studied the use of SynChropak GPC for size separation of peptides. This neutral, reasonably hydrophilic packing displayed HILIC effects when the mobile phase contained over 60% CH<sub>3</sub>CN (Fig. 6 in ref. 10). A similar packing, LiChrosorb DIOL, has also been used for HILIC (see below).

Carunchio *et al.*<sup>11</sup> coated LiChrosorb with chitosan. The resulting material was a hydrophilic, low-capacity anion exchanger. Nucleotides, amino acids and dipeptides were resolved under HILIC conditions; a mixture of hydrophilic interactions and electrostatic effects was evident. For example, electrostatic repulsion appears to have counteracted the pronounced hydrophilic interaction of the basic amino acids, leading to their elution in the same period of time as the other amino acids.

### *HILIC of proteins*

Perhaps the first purifications of proteins with HILIC conditions were those of Rubenstein *et al.*<sup>56,57</sup>. Interferon<sup>56</sup> and serum proteins<sup>57</sup> were purified on LiChrosorb DIOL, using a decreasing gradient of 1-propanol.

Soluble proteins tend to become denatured in the presence of CH<sub>3</sub>CN concentrations above 20%. Thus, HILIC would not be useful for the purification of most soluble enzymes. However, for many proteins a high organic solvent content in the eluent is of no concern. For example, some enzymes and proteins function in the hydrophobic milieu of membranes, and might be expected to respond well to chromatography with a mostly organic solvent mobile phase. Several reports have described the purification of integral membrane proteins by "ion-exchange" chromatography with such mobile phases; the sorbents used were the hydrophilic packings CM-Trisacryl<sup>58-60</sup> and DEAE-cellulose<sup>61</sup>. Yields and purity were appreciably higher than with the standard aqueous mobile phases containing surfactants.

With some protein mixtures, the objective may be simply to determine the number of components present. In the case of H1 histone from chicken erythrocytes<sup>62</sup>, RPC yields 3 peaks, while HILIC on the cation exchanger PolyCAT A<sup>20</sup> yields 21 (using an increasing gradient of sodium perchlorate).

### *Practical aspects of HILIC mobile phases and gradients*

Gradient elution in HILIC can be accomplished by increasing the polarity of the mobile phase, using either a decreasing organic solvent or an increasing salt gradient. When ion-exchange columns are used in the HILIC mode for a sample of unknown characteristics, then a salt gradient is preferable, since it insures the elution of most solutes in a reasonable time. By contrast, uncharacterized solutes are probably best eluted from PolyHydroxyethyl A columns with gradients of decreasing organic solvent<sup>63</sup>. This guarantees elution of all components in the sample, since they are retained by PolyHydroxyethyl A only through hydrophilic interactions. Salt gradients may then be evaluated for complementary selectivity. CH<sub>3</sub>CN is a convenient solvent to use, since it yields less viscous mobile phases and greater retention of solutes than mobile phases containing equivalent amounts of methanol or 2-propanol. At levels of CH<sub>3</sub>CN above 70%, every 1% increase leads to an increase of about 10% in the (isocratic) *k'* values for small molecules.

One of the problems with HILIC is the poor solubility of many salts in mobile phases containing high concentrations of organic solvents. Sodium perchlorate is one salt that is quite soluble in such media and which also does not absorb light at the low wavelengths (*ca.* 215 nm) frequently used for detection of peptides. Organic salts also offer reasonable solubility. Salts of phosphonic acids, such as sodium methylphosphonate, are promising. The buffering ranges and optical transparency of these salts are similar to those of the corresponding phosphate salts, and the solubility in HILIC mobile phases is superior. The same is true of amine salts such as TEAP. Unfortunately, TEA salts sometimes yield rising baselines and artifactual peaks in gradient elutions; this reflects the accumulation of oxidation products of TEA<sup>64</sup>. Sodium, potassium, and ammonium salts do not possess this liability. However, substitutions involving either counterion of a salt can affect the selectivity, sometimes in a dramatic fashion. This topic will be addressed in a future study.

Peptides can be purified for sequencing purposes using PolyHydroxyethyl A columns with volatile mobile phases, due to the low concentrations of salt required with this column. In such cases, a descending gradient of CH<sub>3</sub>CN is convenient. A suitable salt is the triethylamine salt of trifluoroacetic acid<sup>64</sup>. This salt is both volatile and transparent at 215 nm. The TEA must be scrupulously purified to avoid the baseline artifacts described above. An alternative volatile salt is ammonium formate<sup>65</sup>, although this is less volatile than the triethylamine salt of trifluoroacetic acid, and absorbs below 240 nm.

It is not necessary to include salts in the mobile phase for HILIC of non-electrolytes, such as carbohydrates. However, omission of salt leads to broad peaks and variable retention times for amino acids and peptides.

The selectivity of HILIC complements that of RPC. The two modes, used in sequence, may afford useful fractionations of complex mixtures. It would be convenient to use HILIC as the second step, since a fraction collected from the RPC column would merely need to receive sufficient additional organic solvent to assure good binding to the HILIC column. The capacity of PolyHydroxyethyl A columns for peptides is several times less than that of suitable ion-exchange columns, and is comparable to that of an RPC column.

It may be difficult to elute polyelectrolytes from ion-exchange columns in the HILIC mode, owing to the high levels of salt required. An example would be the elution of very basic peptides from PolySulfoethyl A. In such cases, PolyHydroxyethyl A is a suitable alternative, requiring one-fifth to one-tenth as much salt. For the preparative purification of oligonucleotides, it is a particularly promising alternative to anion-exchange HPLC<sup>35,66-70</sup>, which typically requires 0.5-2.0 *M* salt and often 5 *M* urea (which will interfere with sensitive biological experiments).

## CONCLUSIONS

HILIC is potentially as general a mode as reversed-phase and ion-exchange chromatography. It affords good resolution within every class of polar solutes evaluated to date, and works best with hydrophilic solutes least suitable for fractionation by RPC. Thus, it has the potential to resolve mixtures not heretofore amenable to fractionation by chromatography. A variety of hydrophilic stationary phases can be used in the HILIC mode; the choice depends on the application. For example, an

ion-exchange column may display superior selectivity which reflects the superposition of electrostatic and HILIC effects, while PolyHydroxyethyl A may be preferred if a volatile mobile phase is necessary. Some properties of columns other than HILIC columns can also be ascribed to hydrophilic interaction, present as a mixed-mode effect.

Perhaps the most important single property described in this study is the pronounced hydrophilicity of charged, basic groups, which influences the chromatography of any solute to which they are attached. This hydrophilicity can account for the successful analysis of some mixtures by HILIC that are not successfully analyzed by RPC, as well as the tailing of basic compounds in RPC.

There are some applications for which HILIC seems to be especially well suited. PolyHydroxyethyl A shows a particular affinity for phosphorylated amino acids under some conditions, and may be useful for the selective isolation of phosphorylated peptides. Another is the analysis and purification of polyelectrolytes, such as very basic peptides and oligonucleotides, which are eluted from columns of PolyHydroxyethyl A at levels of salt far lower than those needed for ion-exchange columns. Purification of some membrane proteins and histones seems to be easier to achieve by HILIC than by other modes of chromatography.

PolyHydroxyethyl A is promising as a stationary phase for which HILIC effects are the only ones of significance. It is possible to prepare uncharged stationary phases that are still more hydrophilic. This would permit the operation of HILIC at lower levels of organic solvent. Such stationary phases are currently under development. The polyaspartamide coatings used in this work are stable polymers of derivatives of asparagine, the most hydrophilic neutral amino acid, and the packing materials developed by this laboratory for HILIC will continue to be based on such coatings.

#### ACKNOWLEDGEMENTS

I am indebted to W. V. Willis, M. C. Linder, D. R. McLachlan, C. A. Mizzen, M. Brasseur, J. F. Leykam, and H. E. Meyer for communicating results prior to publication, and to A. M. Fathy for donating the oligoglycosides. The advice and encouragement of Patricia Wirth-Nugent were crucial to the formulation of this study. Support came in part from NIH grant HL 36260 (NHLBI section).

#### REFERENCES

- 1 A. J. Alpert and P. C. Andrews, *J. Chromatogr.*, 443 (1988) 85.
- 2 D. L. Crimmins, J. Gorka, R. S. Thoma and B. D. Schwartz, *J. Chromatogr.*, 443 (1988) 63.
- 3 D. L. Crimmins, R. S. Thoma, D. W. McCourt and B. D. Schwartz, *Anal. Biochem.*, 176 (1989) 255.
- 4 D. H. W. Cheng, P.-J. Lee and K. W. K. Watt, presented at *7th International Symposium on HPLC of Proteins, Peptides and Polynucleotides, Washington, DC, Nov. 1987*, abstract 311.
- 5 P. C. Andrews, *Pept. Res.*, 1 (1988) 93.
- 6 D. L. Crimmins, D. W. McCourt and B. D. Schwartz, *Biochem. Biophys. Res. Commun.*, 156 (1988) 910.
- 7 T. D. Schlabach, J. C. Colburn, R. J. Mattaliano and S. Yuen, in T. E. Hugli (Editor), *Techniques in Protein Chemistry*, Vol. 1, Academic Press, New York, 1989, Ch. 48.
- 8 R. S. Hodges and C. T. Mant, University of Alberta, personal communication.
- 9 Y.-B. Yang and M. Verzele, *J. Chromatogr.*, 387 (1987) 197.
- 10 C. T. Mant, J. M. R. Parker and R. S. Hodges, *J. Chromatogr.*, 397 (1987) 99.

- 11 V. Carunchio, A. M. Girelli and A. Messina, *Chromatographia*, 23 (1987) 731.
- 12 J. C. Linden and C. L. Lawhead, *J. Chromatogr.*, 105 (1975) 125.
- 13 J. K. Palmer, *Anal. Lett.*, 8 (1975) 215.
- 14 F. M. Rabel, A. G. Caputo and E. T. Butts, *J. Chromatogr.*, 126 (1976) 731.
- 15 C. Brons and C. Olieman, *J. Chromatogr.*, 259 (1983) 79.
- 16 M. Verzele and F. Van Damme, *J. Chromatogr.*, 362 (1986) 23.
- 17 M. Verzele, G. Simoens and F. Van Damme, *Chromatographia*, 23 (1987) 292.
- 18 B. Bendiak, J. Orr, I. Brockhausen, G. Vella and C. Phoebe, *Anal. Biochem.*, 175 (1988) 96.
- 19 K. Koizumi, T. Utamura and Y. Okada, *J. Chromatogr.*, 321 (1985) 145.
- 20 A. J. Alpert, *J. Chromatogr.*, 266 (1983) 23.
- 21 A. J. Alpert, *J. Chromatogr.*, 359 (1986) 85.
- 22 D. Guo, C. T. Mant, A. K. Taneja, J. M. R. Parker and R. S. Hodges, *J. Chromatogr.*, 359 (1986) 499.
- 23 Z. Deyl, J. Hyaneek and M. Horakova, *J. Chromatogr.*, 379 (1986) 177.
- 24 J. C. Robert, A. Soumarmon and M. J. M. Lewin, *J. Chromatogr.*, 338 (1985) 315.
- 25 M. C. McCroskey, J. R. Colca and J. D. Pearson, *J. Chromatogr.*, 442 (1988) 307.
- 26 H. E. Meyer, Ruhr-Universität Bochum, personal communication.
- 27 M. J. O'Hare and E. C. Nice, *J. Chromatogr.*, 171 (1979) 209.
- 28 A. J. Alpert, *J. Chromatogr.*, 444 (1988) 269.
- 29 L. A. Th. Verhaar and B. F. M. Kuster, *J. Chromatogr.*, 234 (1982) 57.
- 30 P. Orth and H. Engelhardt, *Chromatographia*, 15 (1982) 91.
- 31 Z. L. Nikolov and P. J. Reilly, *J. Chromatogr.*, 325 (1985) 287.
- 32 P.-Å. Albertsson, *Partition of Cells and Macromolecules*, 3rd ed., Wiley, New York, 1986.
- 33 W. Müller and G. Kutemeier, *Eur. J. Biochem.*, 128 (1982) 231.
- 34 W. Müller, *Eur. J. Biochem.*, 155 (1986) 213.
- 35 W. Müller, *Eur. J. Biochem.*, 155 (1986) 203.
- 36 R. W. Schmid and Ch. Wolf, *Chromatographia*, 24 (1987) 713.
- 37 R. M. Smith and J. O. Rabuor, *J. Chromatogr.*, 464 (1989) 117.
- 38 H. Hosotbuso, S. Takahara and N. Taenaka, *J. Chromatogr.*, 432 (1988) 340.
- 39 H. Hosotbuso, *J. Chromatogr.*, 487 (1989) 421.
- 40 G. Johansson and M. Joelsson, *J. Chromatogr.*, 464 (1989) 49.
- 41 K. E. Bij, Cs. Horváth, W. R. Melander and A. Nahum, *J. Chromatogr.*, 203 (1981) 65.
- 42 B. Grego and M. T. W. Hearn, *Chromatographia*, 14 (1981) 589.
- 43 M. T. W. Hearn and B. Grego, *J. Chromatogr.*, 255 (1983) 125.
- 44 D. W. Armstrong and R. E. Boehm, *J. Chromatogr. Sci.*, 22 (1984) 378.
- 45 H. Engelhardt and H. Müller, *Chromatographia*, 19 (1984) 77.
- 46 R. S. Blanquet, K. H. Bui and D. W. Armstrong, *J. Liq. Chromatogr.*, 9 (1986) 1933.
- 47 R. J. Simpson, R. L. Moritz, E. E. Nice and B. Grego, *Eur. J. Biochem.*, 165 (1987) 21.
- 48 R. J. Simpson and R. L. Moritz, *J. Chromatogr.*, 474 (1989) 418.
- 49 R. J. Simpson, L. D. Ward, G. E. Reid, M. P. Batterham and R. L. Moritz, *J. Chromatogr.*, 476 (1989) 345.
- 50 D. W. Armstrong and W. Li, *Chromatography*, 2 (1987) 43.
- 51 S. M. Han and D. W. Armstrong, *J. Chromatogr.*, 389 (1987) 256.
- 52 H. L. Jin, A. M. Stalcup and D. W. Armstrong, *J. Liq. Chromatogr.*, 11 (1988) 3295.
- 53 D. W. Armstrong and H. L. Jin, *J. Chromatogr.*, 462 (1989) 219.
- 54 H. Engelhardt, H. Löw, W. Eberhardt and M. Mauss, *Chromatographia*, 27 (1989) 535.
- 55 J. Fausnaugh-Pollitt, G. Thevenon, L. Janis and F. E. Regnier, *J. Chromatogr.*, 443 (1988) 221.
- 56 M. Rubenstein, S. Rubenstein, P. C. Familletti, R. S. Miller, A. A. Waldman and S. Pestka, *Proc. Natl. Acad. Sci. USA*, 76 (1979) 640.
- 57 M. Rubenstein, *Anal. Biochem.*, 98 (1979) 1.
- 58 G. Helyneck, B. Luu, J.-L. Nussbaum, D. Picken, G. Skalidis, E. Trifilieff, A. Van Dorsselaer, P. Seta, R. Sandeaux, C. Gavach, F. Heitz, D. Simon and G. Spach, *Eur. J. Biochem.*, 133 (1983) 689.
- 59 P. Boyot, E. Trifilieff, A. Van Dorsselaer and B. Luu, *Anal. Biochem.*, 173 (1988) 75.
- 60 P. Boyot, B. Luu, L. R. Jones and E. Trifilieff, *Arch. Biochem. Biophys.*, 269 (1989) 639.
- 61 M. H. Tadros, H. Zuber and G. Drews, *Eur. J. Biochem.*, 127 (1982) 315.
- 62 D. R. McLachlan and C. A. Mizzen, in preparation.
- 63 P. C. Andrews, in preparation.
- 64 J. F. Leykam, in preparation.

- 65 M. Brasseur, in preparation.
- 66 M. Colpan and D. Riesner, *J. Chromatogr.*, 296 (1984) 339.
- 67 R. R. Drager and F. E. Regnier, *Anal. Biochem.*, 145 (1985) 47.
- 68 L. W. McLaughlin and R. Bischoff, *J. Chromatogr.*, 418 (1987) 51.
- 69 R. Hecker and D. Riesner, *J. Chromatogr.*, 418 (1987) 97.
- 70 M. Sieber, in *Nucleosil 4000-7 PEI*, Macherey-Nagel, Düren, 1989, Fig. 6.



CHROMSYMP. 1650

## INVESTIGATION OF SOME $\alpha$ -AMYLASES BY HIGH-PERFORMANCE HYDROPHOBIC-INTERACTION CHROMATOGRAPHY

LÁSZLÓ SZEPESY\* and LÁSZLÓ VIDA

*Department of Chemical Technology, Technical University of Budapest, Budafoki u.8, 1521 Budapest (Hungary)*

and

MIHÁLY TÓTH and ELEMÉR LÁSZLÓ

*Department of Agricultural Chemical Technology, Technical University of Budapest, Budafoki u.8, 1521 Budapest (Hungary)*

---

### SUMMARY

$\alpha$ -Amylases of different origins were investigated with a Synchronapak propyl column and a linearly descending salt gradient in order to isolate the active fraction from among the inactive proteins present. Fractions collected by several injections were assayed for enzymatic activity by the modified Wohlgemut method. An experimental hydroxypropyl packing was tested for the separation of  $\alpha$ -amylases under isocratic conditions, using a dilute buffer or plain water as eluent. The chromatograms obtained can serve as fingerprints for the quality control of some industrial proteins.

---

### INTRODUCTION

Hydrophobic-interaction chromatography (HIC) was first developed in the early 1970s, using agarose gels with bonded alkylamine ligands<sup>1-3</sup>. High-performance HIC is a relatively new addition to the rapidly advancing methods of protein separation.

The retention mechanism is based essentially on the same forces (London-type dispersion) as in reversed-phase chromatography. In both instances hydrophobic functional groups are bound to the substrate and used as the stationary phase. However, in reversed-phase packings the functional groups are very densely distributed, producing a strong hydrophobic interaction between the proteins and the stationary phase. As a result, organic solvents must be used to elute the proteins, which then lose some of their activity.

By contrast, the functional groups in hydrophobic-interaction packing materials are much more sparsely distributed, short, hydrophobic ligands, so that elution can be accomplished by buffers without appreciably denaturing the proteins. This is generally achieved by using reverse gradients in which the sample is eluted by going from high to low salt concentrations. Because proteins retain their structures under such conditions, it is especially suitable for studies where enzymatic activity is of prime importance.

Melander and Horváth<sup>4,5</sup> have given an explanation for the role of neutral salts in the hydrophobic interaction of proteins, based on the solvophobic theory of Sinanoglu and co-workers<sup>6,7</sup>. According to their treatment, the effect of salt type on protein retention can be related to the molal surface tension increment of the salt<sup>4</sup>. Thus, salts with higher molal surface tension increments produce increased retention at equal molal salt concentrations. The magnitude of the effect depends also on the properties of the protein and the stationary phase. The effect of the stationary phase and the operational variables<sup>8-19</sup> have been extensively investigated. Separation and investigation of  $\alpha$ -amylases by HIC have also been reported<sup>9,20</sup>.

In our laboratory, hydrophobic-interaction HPLC has been used to study a series of industrial enzymes such as  $\alpha$ -amylases, glycoamylases and glycooxidases. In this paper, we report some results obtained in the investigation of  $\alpha$ -amylases. The goal of this investigation was to isolate the active fraction from among the inactive proteins present in enzyme preparations of different origins.

## EXPERIMENTAL

### *Materials*

The investigation was carried out on a Merck-Hitachi HPLC system consisting of a Model 655A-11 pump, a Model L-5000 low-pressure gradient system, a Rheodyne (Berkeley, CA, U.S.A.) 7125 injector valve with a 20- $\mu$ l loop and a Model 655A-22 variable-wavelength UV detector. Chromatograms were recorded and evaluated with a Merck-Hitachi Model D-2000 chromato-integrator.

Separations were performed on a SynChropak propyl (particle size 6.5  $\mu$ m) column (250 x 4.1 mm I.D.), obtained from SynChrom (Linden, IN, U.S.A.) and an experimental hydroxypropyl (particle size 10  $\mu$ m) column (250 x 4.6 mm I.D.) developed by Dr. R. Ohmacht at the University Medical School, Pécs, Hungary.

Protein standards (ribonuclease A, ovalbumin, chymotrypsin, chymotrypsinogen A) and  $\alpha$ -amylase (Type II A, bacterial) were obtained from Sigma (St. Louis, MO, U.S.A.), Brew-n-zyme AT, a thermostable bacterial  $\alpha$ -amylase, from Jan Dekker BV, Naarden International (Wormerveer, The Netherlands) and Termamyl 60 L thermostable  $\alpha$ -amylase from Novo (Denmark).

Analytical-reagent-grade ammonium sulphate and potassium dihydrogenphosphate were obtained from Reanal (Budapest, Hungary). Distilled water was prepared by double distillation in glass.

### *Methods*

On the SynChropak propyl column, a descending linear salt gradient was used from 1.0 to 0.1 *M* ammonium sulphate in 0.02 *M* potassium dihydrogenphosphate buffer at pH 7.0. The flow-rate was 1 ml/min, and detection was accomplished at 280 nm. On the experimental hydroxypropyl column, isocratic elution was carried out by using 0.1 *M* ammonium sulphate in 0.02 *M* potassium dihydrogenphosphate buffer at pH 7.0 or plain distilled water containing 20 ppm of  $\text{Ca}^{2+}$ .

Samples were prepared by dissolving about 10 mg of  $\alpha$ -amylase in 1 ml distilled water. The industrial enzyme samples were diluted with distilled water in a 1:9 ratio. Each sample was chromatographed at least in triplicate.

### Determination of enzymatic activity

The enzymatic activity of  $\alpha$ -amylase was determined by the modified Wohlge-  
mut method<sup>21</sup> (Naarden Assay No. 2-124). This assay is based on determining the  
time required to hydrolyse starch to dextrin of a definite size, as indicated by the  
colour of the dextrin-iodine complex. This colour is compared with a colour standard  
of glass disks (Hellige No. 620 S-5).

### RESULTS AND DISCUSSION

Before injection of the  $\alpha$ -amylase samples, the SynChropak propyl column was  
tested by injection of some protein standards generally used for the evaluation of HIC  
columns. First, a 30-min linear gradient was used in accordance with the test chro-  
matogram published. In order to shorten the analysis time and improve peak sharp-  
ness, a steeper 20-min linear gradient was also applied, as shown in Fig. 1. Since with  
the 20-min gradient the retention times decreased and the peaks became sharper  
without a significant decrease in resolution, the enzyme samples were investigated  
under these conditions.

Fig. 2 shows the chromatogram of the Sigma  $\alpha$ -amylase standard. After the first  
chromatogram, sample injection was repeated five times and the eluent fractions  
corresponding to the individual peaks were pooled. In this instance, only two frac-  
tions were collected. Enzymatic activity in the collected fractions was determined by  
the modified Wohlgemut method. The enzyme activity measured is indicated in Fig. 2  
by the dashed line.

In Fig. 3 the chromatogram of Brew-n-Zyme AT is shown. Again, the separated  
fractions from five chromatograms were pooled. In this instance, three fractions were  
collected and tested for enzyme activity. The dashed line shows the enzyme activity of  
the fractions.

Fig. 4 shows the chromatogram of Termamyl 60 L. Three separate fractions

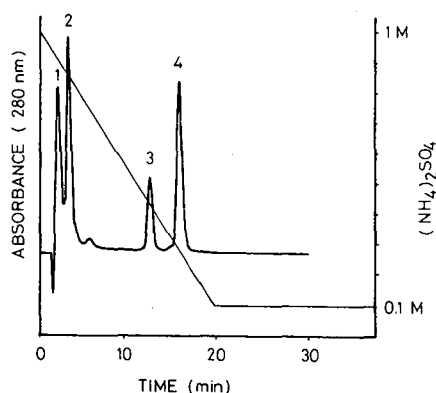


Fig. 1. Separation of a standard protein mixture by HIC. Column, SynChropak propyl; mobile phase A, 1 M  $(\text{NH}_4)_2\text{SO}_4$ -0.02 M  $\text{KH}_2\text{PO}_4$  (pH 7.0); mobile phase B, 0.1 M  $(\text{NH}_4)_2\text{SO}_4$ -0.02 M  $\text{KH}_2\text{PO}_4$  (pH 7.0); 20-min linear gradient from A to B; flow-rate, 1 ml/min. Standards: 1 = ribonuclease A; 2 = ovalbumin; 3 =  $\alpha$ -chymotrypsin; 4 = chymotrypsinogen A.

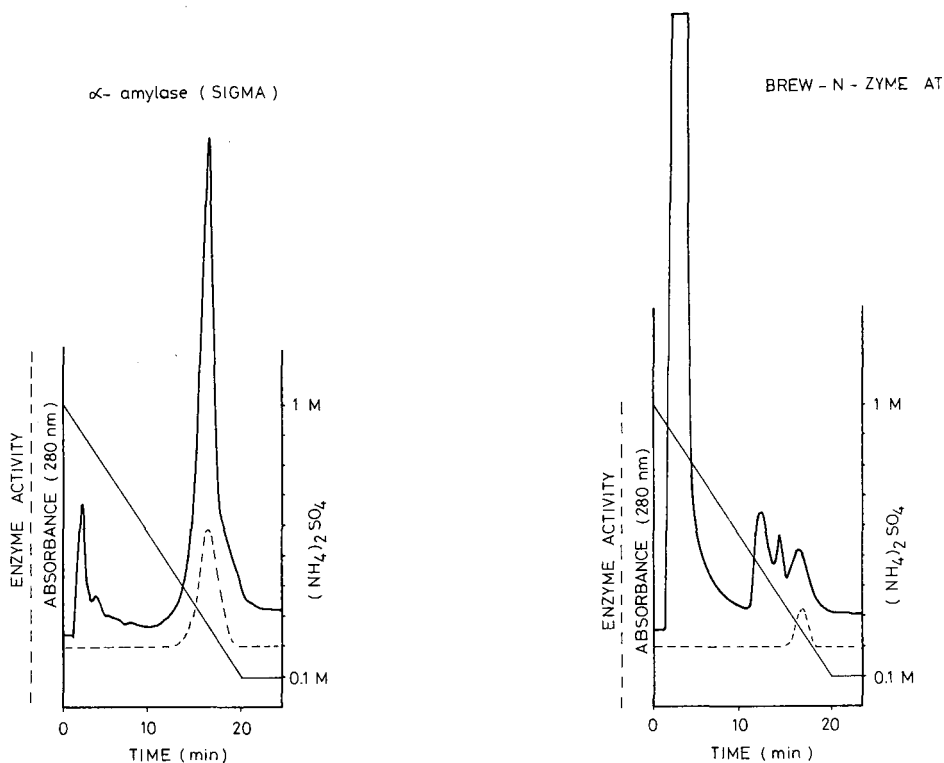


Fig. 2. Chromatogram of  $\alpha$ -amylase (Sigma). Conditions as in Fig. 1.

Fig. 3. Chromatogram of Brew-n-zyme AT industrial enzyme. Conditions as in Fig. 1.

were collected and tested for enzyme activity. Again, the fraction eluted between 16 and 18 min contains the activity, as shown by the dashed line.

Fig. 2 shows that in the purified Sigma product almost all proteins present are responsible for the enzymatic activity. In contrast, in the industrial enzyme preparations a large amount of other proteins can also be found. For instance, in the Brew-n-Zyme chromatogram (Fig. 3), there are other proteins in the vicinity of the active protein, which may represent other types of enzymatic activity. The chromatograms shown demonstrate at the same time that HIC can also be efficiently used for preparative purposes, producing enzyme preparations of high purity and high specific activity.

Next, some preliminary results will be reported on the use of the experimental hydroxypropyl packing. This packing shows an intermediate retention capacity between reversed-phase and HIC columns. A test mixture containing dimethyl, dipropyl and dibutyl phthalate was used to compare the hydrophobicity of the two columns investigated. With methanol-water (1:1) as the mobile phase, the hydroxypropyl column provided a well resolved chromatogram with symmetrical peaks and retention times of 5.6, 10.0 and 16.1 min, respectively. Under the same conditions the Syn-Chropack propyl column furnished two overlapped peaks at 3–3.6 min. On this column a much weaker mobile phase, methanol-water (1:9), provided a similar sep-

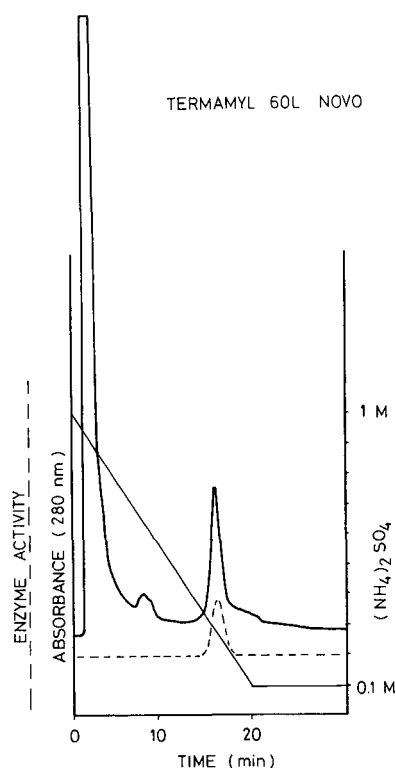


Fig. 4. Chromatogram of Termamyl 60 L industrial enzyme. Conditions as in Fig. 1.

aration of the test mixture to that obtained on the hydroxypropyl column (retention times 4.6, 7.6 and 14.2 min, respectively).

The retention of proteins on the hydroxypropyl column at high salt concentrations was very strong, resulting in long retention times and broad peaks under HIC conditions. For this reason we tried to use this column under isocratic conditions, instead of the reverse gradient used for HIC columns.

First, we compared the performance of the column with buffer B of the previous buffer system (0.1 M ammonium sulphate in 0.02 M potassium dihydrogenphosphate) or distilled water containing 20 ppm of  $\text{Ca}^{2+}$  in the form of calcium acetate. According to the literature<sup>21,22</sup>, metal ions have been used to protect  $\alpha$ -amylase activity against pH, temperature and proteases. Calcium has been found the most effective metal ion in preserving the activity of the enzyme.

With both eluents we obtained chromatograms containing a large number of completely or partially resolved peaks. However, the chromatograms obtained with water as eluent were superior, the peaks being better resolved than in the buffer system. In Fig. 5, the chromatogram of the Sigma  $\alpha$ -amylase shows that, in contrast to the two large peaks obtained by HIC, a large number of peaks (about 10–12) can be distinguished in the chromatogram. In Fig. 6 the chromatogram of Brew-n-zyme and in Fig. 7 the chromatogram of Termamyl 60 L are shown. There are a large number of peaks of different proportions and partly at different retention times.

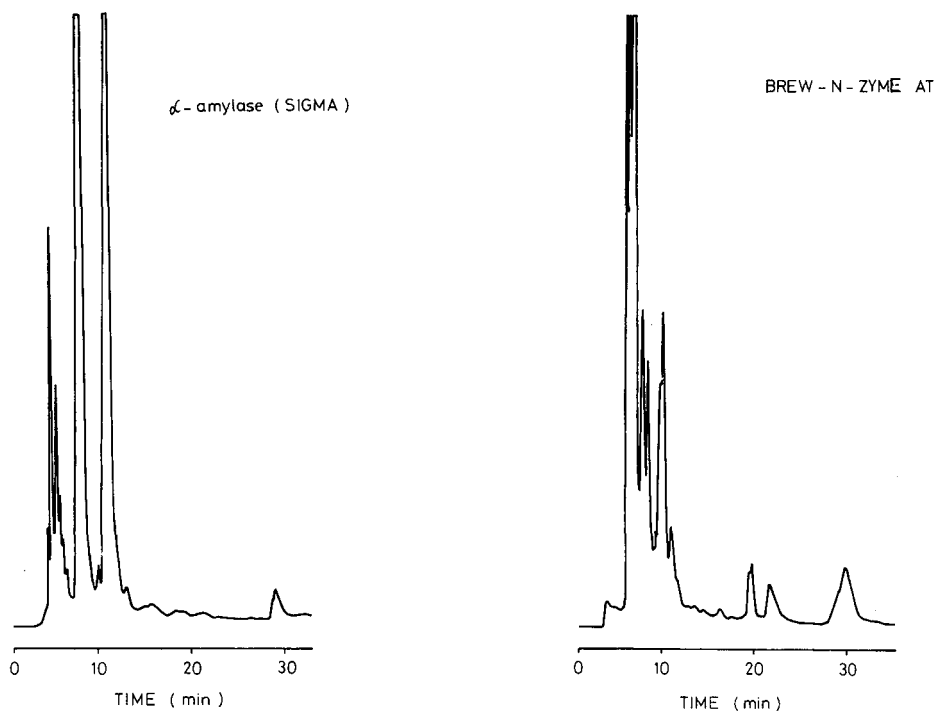


Fig. 5. Chromatogram of  $\alpha$ -amylase (Sigma). Column, hydroxypropyl (experimental); mobile phase, distilled water (20 ppm  $\text{Ca}^{2+}$ ); flow-rate, 1 ml/min (isocratic).

Fig. 6. Chromatogram of Brew-n-zyme AT industrial enzyme. Conditions as in Fig. 5.

Culture filtrates of *Bacillus subtilis* are the richest sources of  $\alpha$ -amylase and different proteases, and the industrial enzyme preparations are more or less purified culture filtrates. For this reason, several other proteins of different molecular weights, even peptides, may be present in the enzyme preparations<sup>21,23</sup>.

The chromatograms obtained under isocratic conditions and using plain water or very dilute buffers as eluent were highly reproducible and can serve as fingerprints for the characterization of some industrial protein products.

#### CONCLUSIONS

High-performance HIC can be used for the comparison and characterization of industrial enzymes of different origin. In addition, HIC can be efficiently used for preparative purposes, producing enzyme preparations of high purity and high specific activity.

Packings with intermediate retention capacity (hydrophobic character) between reversed-phase and HIC columns seem to possess a high resolving power for certain proteins under isocratic elution conditions and can be used for the quality control of some industrial protein products.



Fig. 7. Chromatogram of Termamyl 60 L industrial enzyme. Conditions as in Fig. 5.

#### ACKNOWLEDGEMENTS

The authors gratefully acknowledge the loan of the HPLC equipment by the Analytical Instruments and Chemical Reagents Division of Merck (Darmstadt, F.R.G.), and thank Dr. R. Ohmacht for providing the experimental hydroxypropyl column.

#### REFERENCES

- 1 Z. Er-el, Y. Zaidenzaig and S. Shaltiel, *Biochem. Biophys. Res. Commun.*, 49 (1972) 383.
- 2 S. Shaltiel and Z. Er-el, *Proc. Natl. Acad. Sci. U.S.A.*, 70 (1973) 778.
- 3 S. Hjertén, *J. Chromatogr.*, 87 (1973) 325.
- 4 W. Melander and Cs. Horváth, *Arch. Biochem. Biophys.*, 183 (1977) 200.
- 5 W. Melander and Cs. Horváth, *J. Solid Phase Biochem.*, 2 (1977) 141.
- 6 O. Sinanoglu and S. Abdalnur, *Fed. Proc., Fed. Am. Soc. Exp. Biol.*, 24 (1965) 12.
- 7 T. Halicioğlu and O. Sinanoglu, *Ann. N.Y. Acad. Sci.*, 158 (1969) 308.
- 8 J. L. Fausnaugh, L. A. Kennedy and F. E. Regnier, *J. Chromatogr.*, 317 (1984) 141.
- 9 J. L. Fausnaugh, E. Pfannkoch, S. Gupta and F. E. Regnier, *Anal. Biochem.*, 137 (1984) 464.
- 10 N. T. Miller, B. Feibush and B. L. Karger, *J. Chromatogr.*, 316 (1985) 202.
- 11 J. P. Chang, Z. El Rassi and Cs. Horváth, *J. Chromatogr.*, 396 (1985) 399.
- 12 Z. El Rassi and Cs. Horváth, *J. Liq. Chromatogr.*, 9 (1986) 3245.
- 13 D. L. Gooding, M. N. Schmuck and K. M. Gooding, *J. Chromatogr.*, 296 (1984) 107.
- 14 K. Benedek, S. Dong and B. L. Karger, *J. Chromatogr.*, 317 (1984) 227.
- 15 S. L. Wu, K. Benedek and B. L. Karger, *J. Chromatogr.*, 395 (1986) 3.
- 16 W. R. Melander, D. Corradini and Cs. Horváth, *J. Chromatogr.*, 317 (1984) 67.

- 17 J. L. Fausnaugh and F. E. Regnier, *J. Chromatogr.*, 359 (1986) 131.
- 18 A. Katti, Y. F. Maa and Cs. Horváth, *Chromatographia*, 24 (1987) 646.
- 19 L. Szepesy and Cs. Horváth, *Chromatographia*, 26 (1988) 13.
- 20 Y. Kato, T. Kitamura and T. Hashimoto, *J. Chromatogr.*, 360 (1986) 260.
- 21 B. Hagihara, *Annual Report of Scientific Works*, Vol. 2, Faculty of Science, Osaka University, Osaka, 1954, p. 35.
- 22 T. Isamura and S. Fujita, *J. Biochem. (Tokyo)*, 47 (1964) 548.
- 23 A. J. Wieg, *Ph.D. Thesis*, Technical University of Budapest, Budapest, 1972.



CHROMSYMP. 1647

## ANALYSIS OF GLYCOPROTEIN-DERIVED OLIGOSACCHARIDES BY HIGH-pH ANION-EXCHANGE CHROMATOGRAPHY

LOUISETTE J. BASA and MICHAEL W. SPELLMAN\*

*Department of Medicinal and Analytical Chemistry, Genentech, Inc., South San Francisco, CA 94080 (U.S.A.)*

---

### SUMMARY

The technique of high-pH anion-exchange chromatography with pulsed amperometric detection has recently been shown to be a powerful method for resolving closely related oligosaccharides [M. R. Hardy and R. R. Townsend, *Proc. Natl. Acad. Sci. U.S.A.*, 85 (1988) 3289–3293]. This report describes separations involving a total of nineteen different high-mannose, hybrid and complex-type oligosaccharides isolated after peptide:N-glycosidase F (PNGase F) or *endo*- $\beta$ -N-acetylglucosaminidase H digestion of glycoproteins. Separations were carried out at a constant base concentration (0.1 M NaOH) using linear gradients from 0 to 0.2 M sodium acetate. The applicability of this chromatography for profiling the N-linked oligosaccharides of glycoproteins was demonstrated by generating “oligosaccharide maps” of PNGase F-liberated oligosaccharides from recombinant human tissue plasminogen activator, ribonuclease *b*, human transferrin, and bovine fetuin. Methods for recovering salt-free oligosaccharides after this chromatography were also investigated. On-line ion suppression with an anionic micromembrane suppressor cartridge was found to be capable of effective desalting up to a total sodium ion concentration of 0.15–0.2 M at a flow-rate of 1 ml/min. After high-pH anion-exchange chromatography with ion suppression, collected oligosaccharides were analyzed by fast-atom bombardment mass spectrometry after conversion to permethyl derivatives or after reductive amination with *p*-aminobenzoic acid ethyl ester.

---

### INTRODUCTION

A significant recent development in carbohydrate analysis has been the application of high-pH anion-exchange chromatography (HPAEC) for monosaccharide analysis<sup>1</sup> and for the separation of oligosaccharides<sup>2–4</sup>. These separations take advantage of the fact that the hydroxyl groups of carbohydrates are weakly acidic<sup>5</sup> and, at pH values greater than 12, the resulting oxyanion derivatives can be separated by anion-exchange chromatography. When used in conjunction with pulsed amperometric detection<sup>6</sup> (PAD), HPAEC permits carbohydrate analysis to be carried out at the picomole level.

The use of HPAEC for separations of neutral oligosaccharides was described

first by Hardy and Townsend<sup>2</sup>, who reported on the separation of positional isomers of chemically synthesized, neutral oligosaccharides. They found that the separations were sensitive to molecular size, sugar composition and linkage of the monosaccharide units. In most cases, the elution order within a series of compounds was consistent either with the known hierarchy of acidities (hemiacetal > 2-OH > 6-OH > 3-OH > 4-OH) of the unsubstituted hydroxyl groups<sup>5</sup> or with the accessibility of the ionized groups to the functional groups of the anion exchange column. One limitation of that work was that many of the model oligosaccharides used were structurally related, but not identical, to typical N-linked oligosaccharides that would be obtained after digestion of a glycoprotein with peptide:N-glycosidase F (PNGase F) or *endo*- $\beta$ -N-acetylglucosaminidase H (*endo* H). HPAEC has also been shown to be useful in the separation of sialylated and phosphorylated oligosaccharides<sup>3</sup> and in separating high-mannose and hybrid oligosaccharides<sup>4</sup>.

In this paper we report on separations of a variety of N-linked oligosaccharides including high-mannose and hybrid oligosaccharides released by *endo* H, and di-, tri-, and tetra-antennary complex oligosaccharides released by PNGase F. We also describe methods for on-line desalting of oligosaccharides to permit subsequent identification by chemical or spectroscopic techniques.

## EXPERIMENTAL

### *Materials*

Recombinant human tissue plasminogen activator (rt-PA; Activase<sup>TM</sup>) is the product of Genentech. Recombinant gp120 (rgp120) was produced by expression in Chinese hamster ovary (CHO) cells and immunoaffinity purified<sup>7</sup>. Ribonuclease *b*, human transferrin and bovine fetuin were purchased from Sigma. *Endo* H was obtained from Genzyme. PNGase F and  $\alpha$ -fucosidase were purchased from Boehringer-Mannheim.

### *Model oligosaccharides*

Compounds **1–4**, **15**, **18**, **19** and the sialylated counterparts of compounds **11–13** were isolated from CHO-expressed rt-PA. Their structures were confirmed by methylation analysis, fast-atom bombardment mass spectrometry (FAB-MS) and 500 MHz <sup>1</sup>H nuclear magnetic resonance (NMR) spectroscopy<sup>8</sup>. Compounds **5–7** were isolated from rgp120<sup>9,10</sup>. Compound **10** was purchased from Biocarb AB. Compound **17** was isolated from human transferrin. Compounds **8**, **9** and **11–13** were prepared by treatment of their sialylated counterparts with 0.02 M trifluoroacetic acid for 60 min at 80°C to remove sialic acid. Compounds **14** and **16** were prepared by treatment of compounds **13** and **15**, respectively, with  $\alpha$ -fucosidase (40 mU) in 0.1 M sodium phosphate buffer (pH 4.5) at 37°C overnight.

### *Reduction and S-carboxymethylation of glycoproteins*

Samples of rt-PA, rgp120, ribonuclease B, human transferrin and bovine fetuin were reduced and S-carboxymethylated prior to glycosidase digestion, as follows. Samples were dialyzed into 0.36 M Tris-HCl buffer (pH 8.6) containing 8 M urea and 3 mM EDTA. Dithiothreitol (DTT) was added to a final concentration of 10 mM. After 4 h at room temperature, iodoacetic acid was added to a final concentration of

25 mM and the samples were incubated at 25°C for 30 min in the dark. Samples were then quenched with excess DTT, dialyzed into 100 mM  $\text{NH}_4\text{HCO}_3$  and lyophilized.

#### *Digestion with PNGase F*

Reduced and S-carboxymethylated glycoprotein samples to be digested (typically 0.5 mg) were reconstituted in 0.25 M sodium phosphate buffer (pH 8.6) containing 10 mM EDTA and 0.02% (w/v) sodium azide. PNGase F (3.2 units) was added, and the samples were incubated overnight at 37°C.

#### *Digestion with endo H*

Reduced and S-carboxymethylated glycoprotein samples (typically 0.5 mg) were reconstituted in 0.05 M sodium phosphate buffer (pH 6) containing 0.02% sodium azide. Endo H (0.05 units) was added and the samples were incubated overnight at 37°C.

#### *Chromatography on Sephadex G-15*

Glycosidase digestion mixtures were applied to a column (47 × 1 cm I.D.) of Sephadex G-15 equilibrated in 0.1 M  $\text{NH}_4\text{HCO}_3$ . The flow-rate was 0.6 ml/min. Carbohydrate-containing fractions were detected by the phenol-sulfuric acid assay<sup>11</sup>.

#### *C<sub>18</sub> Sep-Pak*

Glycosidase digestion mixtures were applied to C<sub>18</sub> Sep-Pak cartridges that had been preconditioned with ethanol and acetonitrile<sup>12</sup> and then equilibrated in water. After sample application the cartridge was washed with 0.3 ml of water. Oligosaccharides were eluted with 0.5 ml of water followed by 1 ml of 40% (v/v) aqueous acetonitrile and then dried on a centrifugal evaporator.

#### *Ethanol precipitation*

At the termination of glycosidase digestion, samples were mixed with three volumes of ice-cold ethanol<sup>13</sup> and centrifuged at 11 600 g for 10 min at 4°C. Pellets were washed three times with ice-cold 75% ethanol. The combined supernatants were evaporated under a stream of nitrogen and then reconstituted in water for chromatography.

#### *HPAEC conditions*

HPAEC was carried out on a Dionex BioLC system (Dionex, Sunnyvale, CA, U.S.A.) equipped with a pellicular anion exchange column (AS6) and a pulsed amperometric detector (Dionex PAD-2). The detector potentials used were 0, +0.75 and -0.85 V with a duration of 180 ms at each potential. Detection was facilitated by the addition of 0.5 M NaOH (at a flow-rate of 0.75 ml/min) to the column effluent upstream of the detector cell. Semipreparative runs were made without any post-column addition of base, and the column effluent was passed through an anion micro-membrane suppressor unit (Dionex AMMS) for on-line desalting. The regenerant solution for the AMMS unit was 0.03 M  $\text{H}_2\text{SO}_4$  at a flow-rate of 6.5 ml/min.

The chromatograms shown here were generated using either of two gradient programs. For both gradient programs, solvent A was 0.1 M NaOH, solvent B was 0.1 M NaOH containing 0.5 M sodium acetate and the flow-rate was 1 ml/min.

*Gradient program 1:* the column was pre-equilibrated in 100% solvent A; after a 5-min hold, oligosaccharides were eluted with a linear gradient from 0 to 20% solvent B in 40 min. *Gradient program 2:* the column was pre-equilibrated in 5% solvent B; after a 2-min hold, oligosaccharides were eluted with a two-stage linear gradient from 5% to 15% solvent B in 5 min, and from 15% to 40% solvent B in 25 min.

#### *Methylation analysis*

Collected oligosaccharides were prereduced with sodium borohydride and permethylated using methyl iodide and methylsulfinyl-carbanion in methyl sulfoxide<sup>12</sup>. The permethylated oligosaccharides were recovered by chromatography on C<sub>18</sub> Sep-Pak cartridges (Waters Assoc.).

#### *Derivatization with p-aminobenzoic acid ethyl ester (ABEE)*

Oligosaccharides collected after HPAEC with ion suppression were lyophilized and then reconstituted in 0.01 ml of water. To this was added 0.04 ml of a reagent consisting of 165 mg of ABEE, 35 mg of sodium cyanoborohydride, 0.041 ml of acetic acid and 0.35 ml of methanol<sup>14,15</sup>. Samples were incubated at 80°C for 30 min. After cooling, the samples were partitioned between water (0.3 ml) and chloroform (0.3 ml). The aqueous phase was subjected to reversed-phase high-performance liquid chromatography (HPLC) on a Novapak C<sub>18</sub> column (15 cm × 4.6 mm I.D., Waters Assoc.) using an acetonitrile-water gradient system to recover the ABEE derivatives. The HPLC column effluent was monitored for absorbance at 254 nm.

#### *FAB-MS*

FAB mass spectra were acquired on a JEOL HX110HF/HX110HF tandem mass spectrometer operated in a normal two-sector mode. All other conditions were as previously described<sup>8</sup>.

## RESULTS AND DISCUSSION

#### *Separation of neutral oligosaccharides*

HPAEC provides efficient separation of neutral oligosaccharides of the types found attached to asparagine residues of glycoproteins. Chromatograms obtained by HPAEC analysis of high-mannose oligosaccharides are shown in Fig. 1. Fig. 1A shows the separation of a mixture of Man<sub>5</sub>GlcNAc (1), Man<sub>6</sub>GlcNAc (2) and Man<sub>7</sub>GlcNAc (3 and 4) structures released by endo H digestion of CHO-expressed rt-PA. These oligosaccharides have been characterized by other methods<sup>8</sup> and shown to have the structures indicated in Table I. In particular, <sup>1</sup>H NMR analysis indicated that the Man<sub>7</sub>GlcNAc structures consisted of a mixture of two isomers. These isomers are partially resolved by HPAEC (retention time of 32 min, Fig. 1A). Fig. 1B shows the high-mannose oligosaccharides released by endo H digestion of CHO-expressed rgp120. In this case, the size distribution of the high-mannose oligosaccharides is in good agreement with that determined by gel-permeation chromatography of the high-mannose oligosaccharides released by hydrazine treatment of rgp120<sup>9,10</sup>. The rgp120 sample contains the Man<sub>5</sub>GlcNAc (1), Man<sub>6</sub>GlcNAc (2) and both of the Man<sub>7</sub>GlcNAc (3 and 4) structures found in the rt-PA sample. In addition, the rgp120 sample contains another major Man<sub>7</sub>GlcNAc peak (5), at 31.5 min, which is well

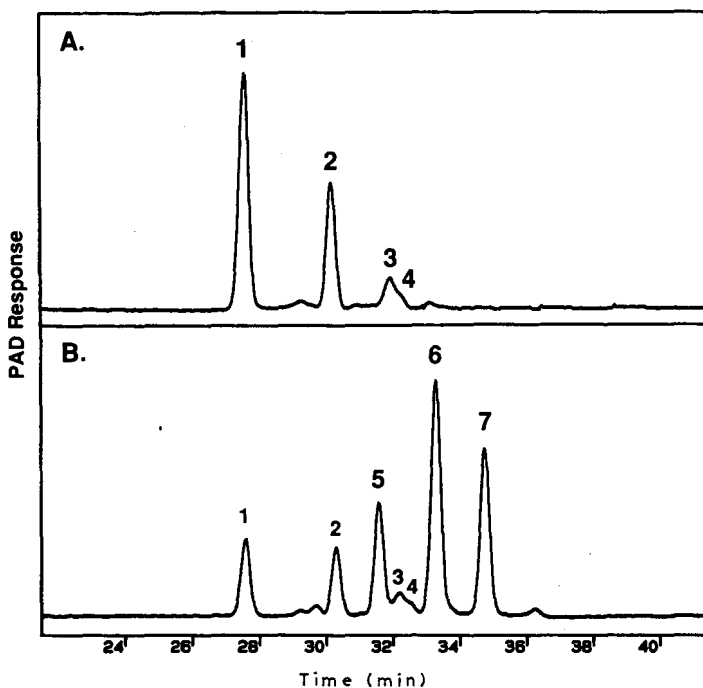


Fig. 1. Separation of high-mannose oligosaccharides. Oligosaccharides from (A) rt-PA and (B) rgp120 were liberated by treatment of the glycoproteins with endo H, recovered by ethanol precipitation, and analyzed by HPAEC using gradient program 1. Peak identifications are given in Table I.

resolved from the other two  $\text{Man}_7\text{GlcNAc}$  isomers. Compounds 6 and 7 are  $\text{Man}_8\text{GlcNAc}$  and  $\text{Man}_9\text{GlcNAc}$ , respectively.

The separation of three, closely related, asialo diantennary complex oligosaccharides is shown in Fig. 2. Compounds 8 and 9 differ in that the former structure has a fucose residue attached  $\alpha(1\rightarrow6)$  to the reducing GlcNAc residue. The addition of fucose to an oligosaccharide has been shown with other model compounds<sup>2</sup> to cause a shift to earlier retention time in HPAEC. Compound 10, which lacks the innermost GlcNAc residue of compound 9, elutes latest of the three diantennary structures. The elution order of the three compounds in Fig. 2 is the opposite of that predicted for a purely size-based separation. Therefore, although the general trend in HPAEC is that oligosaccharides of a homologous series elute in order of increasing size, certain chain extensions can actually result in decreased retention presumably either by substitution of a particularly acidic position or by limiting accessibility of ionized groups to the functional groups of the column.

Separation of a more complex mixture of desialylated di-, tri- and tetraantennary complex oligosaccharides is shown in Fig. 3. Once again, the effect of fucosylation of the reducing GlcNAc residue is a shift to earlier retention time, as is illustrated by the diantennary oligosaccharides plus/minus fucose (peaks 8 and 9) and the tetraantennary oligosaccharides plus/minus fucose (peaks 13 and 14). Two branching isomers of fucosylated triantennary oligosaccharides were also resolved by this technique: the fucosylated 2,4-branched triantennary structure (compound 11) eluted at

TABLE I  
STRUCTURES OF THE MODEL OLIGOSACCHARIDES USED

<i>Compound</i>	<i>Structure</i>
1	$\begin{array}{c} \text{Man}\alpha(1\rightarrow6) \\ \text{Man}\alpha(1\rightarrow3) \end{array} \left. \begin{array}{c} \text{Man}\alpha(1\rightarrow6) \\ \text{Man}\alpha(1\rightarrow3) \end{array} \right\} \text{Man}\beta(1\rightarrow4)\text{GlcNAc}$
2	$\begin{array}{c} \text{Man}\alpha(1\rightarrow6) \\ \text{Man}\alpha(1\rightarrow3) \end{array} \left. \begin{array}{c} \text{Man}\alpha(1\rightarrow6) \\ \text{Man}\alpha(1\rightarrow2)\text{Man}\alpha(1\rightarrow3) \end{array} \right\} \text{Man}\beta(1\rightarrow4)\text{GlcNAc}$
3	$\begin{array}{c} \text{Man}\alpha(1\rightarrow6) \\ \text{Man}\alpha(1\rightarrow3) \end{array} \left. \begin{array}{c} \text{Man}\alpha(1\rightarrow6) \\ \text{Man}\alpha(1\rightarrow2)\text{Man}\alpha(1\rightarrow2)\text{Man}\alpha(1\rightarrow3) \end{array} \right\} \text{Man}\beta(1\rightarrow4)\text{GlcNAc}$
4	$\begin{array}{c} \text{Man}\alpha(1\rightarrow2)\text{Man}\alpha(1\rightarrow6) \\ \text{Man}\alpha(1\rightarrow3) \end{array} \left. \begin{array}{c} \text{Man}\alpha(1\rightarrow6) \\ \text{Man}\alpha(1\rightarrow2)\text{Man}\alpha(1\rightarrow3) \end{array} \right\} \text{Man}\beta(1\rightarrow4)\text{GlcNAc}$
5 <sup>a</sup>	$\text{Man}\alpha(1\rightarrow2) \left\{ \begin{array}{l} \begin{array}{c} \text{Man}\alpha(1\rightarrow6) \\ \text{Man}\alpha(1\rightarrow3) \end{array} \left. \begin{array}{c} \text{Man}\alpha(1\rightarrow6) \\ \text{Man}\alpha(1\rightarrow2)\text{Man}\alpha(1\rightarrow3) \end{array} \right\} \text{Man}\beta(1\rightarrow4)\text{GlcNAc} \end{array} \right.$
6 <sup>a</sup>	$\begin{array}{l} \text{Man}\alpha(1\rightarrow2) \\ \text{Man}\alpha(1\rightarrow2) \end{array} \left\{ \begin{array}{l} \begin{array}{c} \text{Man}\alpha(1\rightarrow6) \\ \text{Man}\alpha(1\rightarrow3) \end{array} \left. \begin{array}{c} \text{Man}\alpha(1\rightarrow6) \\ \text{Man}\alpha(1\rightarrow2)\text{Man}\alpha(1\rightarrow3) \end{array} \right\} \text{Man}\beta(1\rightarrow4)\text{GlcNAc} \end{array} \right.$
7	$\begin{array}{c} \text{Man}\alpha(1\rightarrow2)\text{Man}\alpha(1\rightarrow6) \\ \text{Man}\alpha(1\rightarrow2)\text{Man}\alpha(1\rightarrow3) \end{array} \left. \begin{array}{c} \text{Man}\alpha(1\rightarrow6) \\ \text{Man}\alpha(1\rightarrow2)\text{Man}\alpha(1\rightarrow3) \end{array} \right\} \text{Man}\beta(1\rightarrow4)\text{GlcNAc}$
8	$\begin{array}{c} \text{Gal}\beta(1\rightarrow4)\text{GlcNAc}\beta(1\rightarrow2)\text{Man}\alpha(1\rightarrow6) \\ \text{Gal}\beta(1\rightarrow4)\text{GlcNAc}\beta(1\rightarrow2)\text{Man}\alpha(1\rightarrow3) \end{array} \left. \begin{array}{c} \text{Man}\beta(1\rightarrow4)\text{GlcNAc}\beta(1\rightarrow4)\text{GlcNAc} \\ \text{Fuca}(1\rightarrow6) \end{array} \right\} \text{GlcNAc}$
9	$\begin{array}{c} \text{Gal}\beta(1\rightarrow4)\text{GlcNAc}\beta(1\rightarrow2)\text{Man}\alpha(1\rightarrow6) \\ \text{Gal}\beta(1\rightarrow4)\text{GlcNAc}\beta(1\rightarrow2)\text{Man}\alpha(1\rightarrow3) \end{array} \left. \begin{array}{c} \text{Man}\beta(1\rightarrow4)\text{GlcNAc}\beta(1\rightarrow4)\text{GlcNAc} \\ \text{GlcNAc} \end{array} \right\}$
10	$\begin{array}{c} \text{Gal}\beta(1\rightarrow4)\text{GlcNAc}\beta(1\rightarrow2)\text{Man}\alpha(1\rightarrow6) \\ \text{Gal}\beta(1\rightarrow4)\text{GlcNAc}\beta(1\rightarrow2)\text{Man}\alpha(1\rightarrow3) \end{array} \left. \begin{array}{c} \text{Man}\beta(1\rightarrow4)\text{GlcNAc} \\ \text{GlcNAc} \end{array} \right\}$

TABLE I (continued)

Compound	Structure
11	$\begin{array}{l} \text{Gal}\beta(1\rightarrow4)\text{GlcNAc}\beta(1\rightarrow2)\text{Man}\alpha(1\rightarrow6) \\ \text{Gal}\beta(1\rightarrow4)\text{GlcNAc}\beta(1\rightarrow4) \backslash \\ \text{Gal}\beta(1\rightarrow4)\text{GlcNAc}\beta(1\rightarrow2) \backslash \end{array} \begin{array}{l} \text{Man}\alpha(1\rightarrow3) \\ \text{Man}\beta(1\rightarrow4)\text{GlcNAc}\beta(1\rightarrow4)\text{GlcNAc} \\ \text{Fuca}(1\rightarrow6) \end{array}$
12	$\begin{array}{l} \text{Gal}\beta(1\rightarrow4)\text{GlcNAc}\beta(1\rightarrow6) \backslash \\ \text{Gal}\beta(1\rightarrow4)\text{GlcNAc}\beta(1\rightarrow2) \backslash \\ \text{Gal}\beta(1\rightarrow4)\text{GlcNAc}\beta(1\rightarrow2)\text{Man}\alpha(1\rightarrow3) \end{array} \begin{array}{l} \text{Man}\alpha(1\rightarrow6) \\ \text{Man}\beta(1\rightarrow4)\text{GlcNAc}\beta(1\rightarrow4)\text{GlcNAc} \\ \text{Fuca}(1\rightarrow6) \end{array}$
13	$\begin{array}{l} \text{Gal}\beta(1\rightarrow4)\text{GlcNAc}\beta(1\rightarrow6) \backslash \\ \text{Gal}\beta(1\rightarrow4)\text{GlcNAc}\beta(1\rightarrow2) \backslash \\ \text{Gal}\beta(1\rightarrow4)\text{GlcNAc}\beta(1\rightarrow4) \backslash \\ \text{Gal}\beta(1\rightarrow4)\text{GlcNAc}\beta(1\rightarrow2) \backslash \end{array} \begin{array}{l} \text{Man}\alpha(1\rightarrow6) \\ \text{Man}\beta(1\rightarrow4)\text{GlcNAc}\beta(1\rightarrow4)\text{GlcNAc} \\ \text{Man}\alpha(1\rightarrow3) \\ \text{Fuca}(1\rightarrow6) \end{array}$
14	$\begin{array}{l} \text{Gal}\beta(1\rightarrow4)\text{GlcNAc}\beta(1\rightarrow6) \backslash \\ \text{Gal}\beta(1\rightarrow4)\text{GlcNAc}\beta(1\rightarrow2) \backslash \\ \text{Gal}\beta(1\rightarrow4)\text{GlcNAc}\beta(1\rightarrow4) \backslash \\ \text{Gal}\beta(1\rightarrow4)\text{GlcNAc}\beta(1\rightarrow2) \backslash \end{array} \begin{array}{l} \text{Man}\alpha(1\rightarrow6) \\ \text{Man}\beta(1\rightarrow4)\text{GlcNAc}\beta(1\rightarrow4)\text{GlcNAc} \\ \text{Man}\alpha(1\rightarrow3) \end{array}$
15	$\begin{array}{l} \text{NeuAc}\alpha(2\rightarrow3)\text{Gal}\beta(1\rightarrow4)\text{GlcNAc}\beta(1\rightarrow2)\text{Man}\alpha(1\rightarrow6) \\ \text{NeuAc}\alpha(2\rightarrow3)\text{Gal}\beta(1\rightarrow4)\text{GlcNAc}\beta(1\rightarrow2)\text{Man}\alpha(1\rightarrow3) \end{array} \begin{array}{l} \text{Man}\beta(1\rightarrow4)\text{GlcNAc}\beta(1\rightarrow4)\text{GlcNAc} \\ \text{Fuca}(1\rightarrow6) \end{array}$
16	$\begin{array}{l} \text{NeuAc}\alpha(2\rightarrow3)\text{Gal}\beta(1\rightarrow4)\text{GlcNAc}\beta(1\rightarrow2)\text{Man}\alpha(1\rightarrow6) \\ \text{NeuAc}\alpha(2\rightarrow3)\text{Gal}\beta(1\rightarrow4)\text{GlcNAc}\beta(1\rightarrow2)\text{Man}\alpha(1\rightarrow3) \end{array} \begin{array}{l} \text{Man}\beta(1\rightarrow4)\text{GlcNAc}\beta(1\rightarrow4)\text{GlcNAc} \end{array}$
17	$\begin{array}{l} \text{NeuAc}\alpha(2\rightarrow6)\text{Gal}\beta(1\rightarrow4)\text{GlcNAc}\beta(1\rightarrow2)\text{Man}\alpha(1\rightarrow6) \\ \text{NeuAc}\alpha(2\rightarrow6)\text{Gal}\beta(1\rightarrow4)\text{GlcNAc}\beta(1\rightarrow2)\text{Man}\alpha(1\rightarrow3) \end{array} \begin{array}{l} \text{Man}\beta(1\rightarrow4)\text{GlcNAc}\beta(1\rightarrow4)\text{GlcNAc} \end{array}$
18	$\begin{array}{l} \text{Man}\alpha(1\rightarrow3)\text{Man}\alpha(1\rightarrow6) \\ \text{NeuAc}\alpha(2\rightarrow3)\text{Gal}\beta(1\rightarrow4)\text{GlcNAc}\beta(1\rightarrow2)\text{Man}\alpha(1\rightarrow3) \end{array} \begin{array}{l} \text{Man}\beta(1\rightarrow4)\text{GlcNAc} \end{array}$
19	$\begin{array}{l} \text{Man}\alpha(1\rightarrow6) \\ \text{Man}\alpha(1\rightarrow3) \backslash \\ \text{NeuAc}\alpha(2\rightarrow3)\text{Gal}\beta(1\rightarrow4)\text{GlcNAc}\beta(1\rightarrow2)\text{Man}\alpha(1\rightarrow3) \end{array} \begin{array}{l} \text{Man}\alpha(1\rightarrow6) \\ \text{Man}\beta(1\rightarrow4)\text{GlcNAc} \end{array}$

<sup>a</sup> The attachment positions of the peripheral mannose residues have not been determined for these compounds.

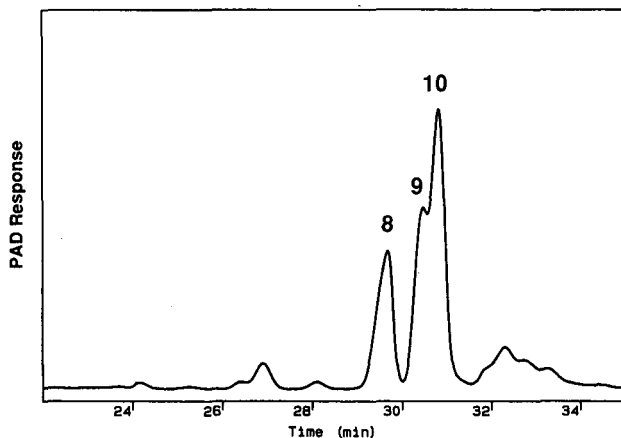


Fig. 2. Separation of three asialo-diantennary complex oligosaccharides. Chromatography was carried out using gradient program 1. Peak identifications are given in Table I.

29.5 min, and the fucosylated 2,6-branched triantennary oligosaccharide (compound **12**) eluted at 31 min. On the basis of the  $pK_a$  values of the unsubstituted hydroxyl groups of these two compounds, one would predict that the 2,4-branched oligosaccharide should elute after the 2,6-branched oligosaccharide (the 2,4-branched structure has an unsubstituted 6-OH, which is more acidic than the unsubstituted 4-OH of the 2,6-branched structure). The observed elution order is the opposite of that predicted solely on the basis of  $pK_a$  values, suggesting that the elution of these two compounds is dominated by the accessibility of the ionized groups to the column matrix. These results are similar to those reported by Hardy and Townsend<sup>2</sup> for a pair of related compounds. Fig. 3 shows only the fucosylated forms of the two trian-

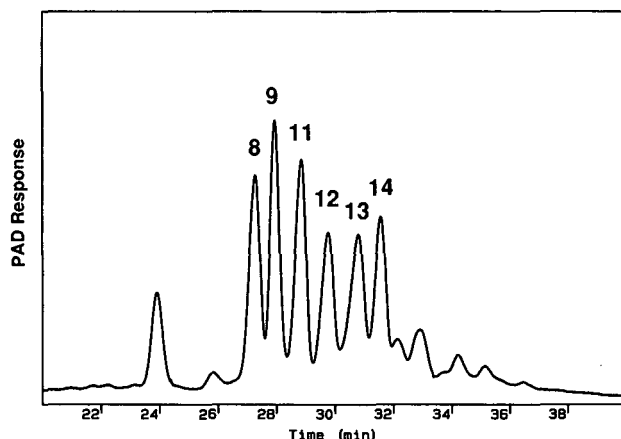


Fig. 3. Separation of asialo-complex oligosaccharides. Chromatography was carried out using gradient program 1. Numbered peaks are identified in Table I. Peaks not numbered are oligosaccharides present as contaminants in the model compounds.



tennary structures. Defucosylation of the triantennary structures caused the expected shift to later retention times. In the elution program used to generate Fig. 3, the defucosylated 2,4-branched triantennary oligosaccharide coelutes with the fucosylated 2,6-branched structure, and the defucosylated 2,6-branched oligosaccharide coelutes with the fucosylated tetraantennary structure (not shown).

#### *Separation of sialylated oligosaccharides*

Several experiments were performed to examine the ability of HPAEC to resolve structurally related sialylated oligosaccharides. As would be expected, the separation is dominated by the number of residues of sialic acid attached to an oligosaccharide. However, significant resolution was still attainable among related structures with the same formal charge. Fig. 4 shows that a fucosylated di- $\alpha(2\rightarrow3)$ -sialylated diantennary oligosaccharide (compound **15**) is well resolved from the equivalent, non-fucosylated, di- $\alpha(2\rightarrow3)$ -sialyl-diantennary oligosaccharide (compound **16**). The separation is also affected by the attachment position of sialic acid to galactose, as shown in Fig. 5. Both of the compounds in Fig. 5 are non-fucosylated diantennary complex oligosaccharides; they differ only in that compound **17** has sialic acid attached to the 6 position of galactose whereas the sialic acid in compound **16** is attached to the 3 position of galactose.

The separation of two (monosialyl) hybrid oligosaccharides is shown in Fig. 6. Compound **19** contains one more mannose residue than compound **18**, which causes a shift to later retention time. The elution characteristics of these hybrid oligosaccharides are similar to those reported previously for oligosaccharides isolated from ovalbumin<sup>4</sup>.

#### *"Mapping" of oligosaccharides released from glycoproteins*

The speed, sensitivity and selectivity of HPAEC make it a promising technique for profiling the oligosaccharides of glycoproteins. This is illustrated in Fig. 7, which

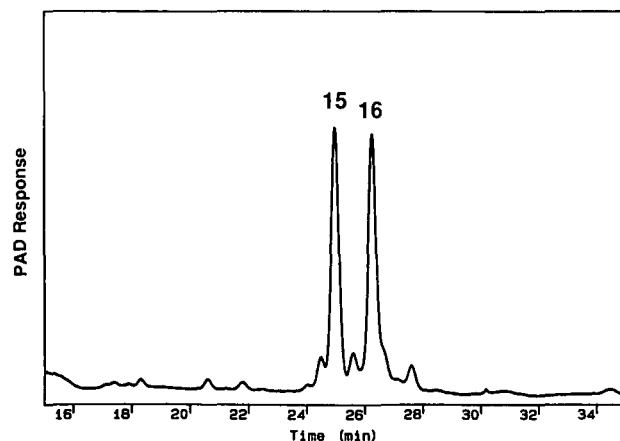


Fig. 4. Influence of fucosylation on the elution of sialylated diantennary oligosaccharides. Both compounds are di- $\alpha(2\rightarrow3)$ -sialyl diantennary oligosaccharides. They differ by the presence (**15**) or absence (**16**) of fucose attached to the reducing GlcNAc residue. Elution was with gradient program 2.

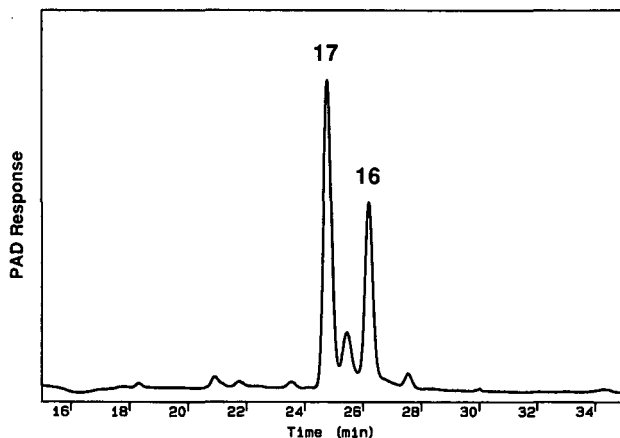


Fig. 5. Influence of sialylation position on the elution of diantennary oligosaccharides. Both compounds are disialyl diantennary oligosaccharides. Sialic acid is linked  $\alpha(2\rightarrow3)$  to galactose in compound **16** and  $\alpha(2\rightarrow6)$  to galactose in compound **17**. Elution was with gradient program 2.

shows the HPAEC profiles obtained after PNGase F treatment of four glycoproteins to release their N-linked oligosaccharides. As described above, the separations are dominated by the number of sialic acid residues on a particular oligosaccharide; as a result, the chromatograms contain regions where neutral, mono-, di-, tri- and tetrasialyl oligosaccharides elute (designated N, 1, 2, 3 and 4, respectively, in Fig. 7). For each glycoprotein, the HPAEC profile agrees well with what has been published previously on the N-linked oligosaccharides of the glycoprotein. rt-PA (Fig. 7A) is known to contain attached high-mannose, hybrid, and mono-, di-, tri- and tetrasialyl complex oligosaccharides<sup>9</sup>. Ribonuclease *b* (Fig. 7B) contains exclusively neutral (high-mannose) oligosaccharides<sup>16</sup>. The predominant oligosaccharide structure of

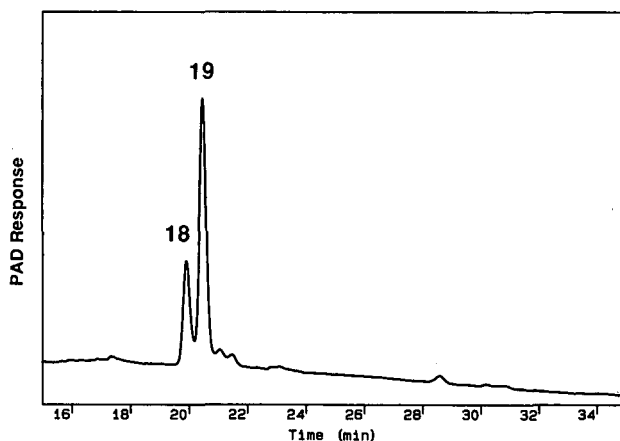


Fig. 6. Separation of hybrid oligosaccharides. Compounds **18** and **19** were released by endo H digestion of rt-PA. Elution was with gradient program 2.

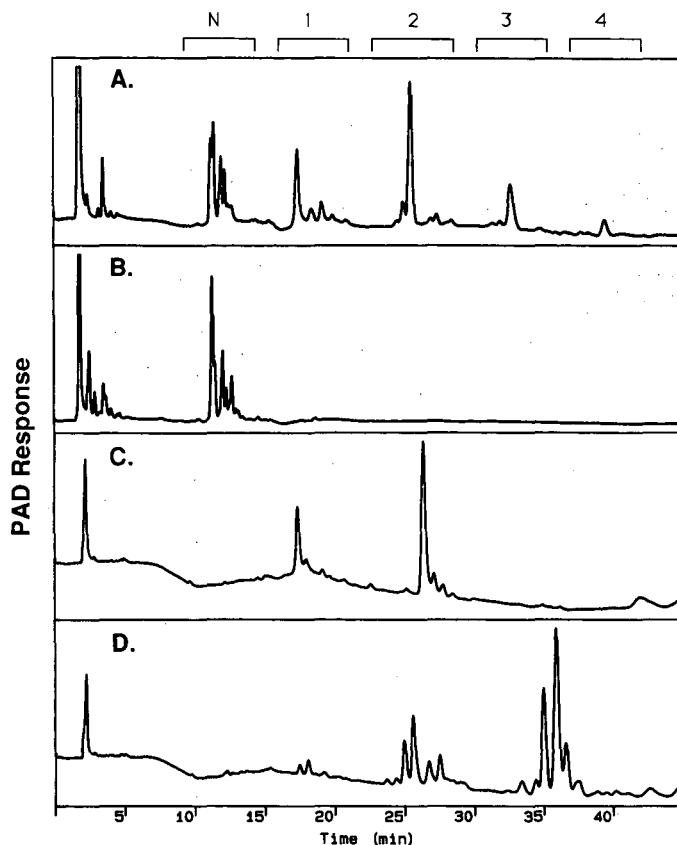


Fig. 7. Oligosaccharide profiles of four glycoproteins. The glycoproteins were reduced and S-carboxymethylated and then treated with PNGase F. The oligosaccharides released were recovered by ethanol fractionation and analyzed by HPAEC using gradient program 2. (A) rt-PA; (B) ribonuclease *b*; (C) human transferrin; (D) bovine fetuin. The labels at the top indicate the elution positions of neutral (N), monosialyl (1), disialyl (2), trisialyl (3) and tetrasialyl (4) oligosaccharides.

human transferrin (Fig. 7C) is a non-fucosylated disialyl diantennary oligosaccharide in which sialic acid is attached to the 6-position of galactose<sup>17</sup>. The carbohydrate structures of bovine fetuin (Fig. 7D) are quite heterogeneous, differing in the extent of sialylation, the number of peripheral branches (*i.e.* diantennary *vs.* triantennary), and the linkage ( $\beta$ 1,4 *vs.*  $\beta$ 1,3) of galactose residues<sup>18</sup>. Hardy and Townsend<sup>2</sup> have demonstrated with fetuin glycopeptides that HPAEC is capable of resolving structures that contain  $\beta$ 1,3-linked galactose from those with  $\beta$ 1,4-linked galactose<sup>2</sup>.

It should be noted that HPAEC is not able to resolve closely related acidic molecules as efficiently as it resolves their desialylated counterparts. For example, rt-PA contains nearly equimolar amounts of (trisialyl) fucosylated 2,4-branched and 2,6-branched triantennary oligosaccharides. These oligosaccharides coelute in Fig. 7A (retention time of 30.5 min), whereas their desialylated equivalents are well resolved by HPAEC (see Fig. 3).

### Methods of preparing oligosaccharides for HPAEC

HPAEC separations depend upon ionizing oligosaccharides at high pH to promote their interaction with the anion exchange resin. As a consequence, the separations are easily perturbed by the presence of buffer salts in the sample matrix. We have investigated several techniques to recover oligosaccharides released by glycosidase digestion, with the goal of conveniently and reproducibly obtaining suitably salt- and protein-free samples for HPAEC analysis. Fig. 8 compares the HPAEC profiles obtained when oligosaccharides were recovered by gel-permeation chromatography (Fig. 8A), by chromatography on a  $C_{18}$  Sep-Pak cartridge (Fig. 8B) or by ethanol precipitation (Fig. 8C). The chromatograms obtained after ethanol precipitation were superimposable with those obtained after gel permeation. The  $C_{18}$  Sep-Pak cartridges did not prove to be efficient for this application, since desalting was incomplete (not shown) and varying recoveries were observed for different oligosaccharides (compare traces A and B in Fig. 8). As a result, we routinely use ethanol precipitation for sample preparation because it is simple, lends itself to the preparation of multiple samples in parallel, and gives results comparable to those obtained after gel-permeation chromatography.

### On-line desalting of oligosaccharides

The high-resolution oligosaccharide separations attainable by HPAEC make

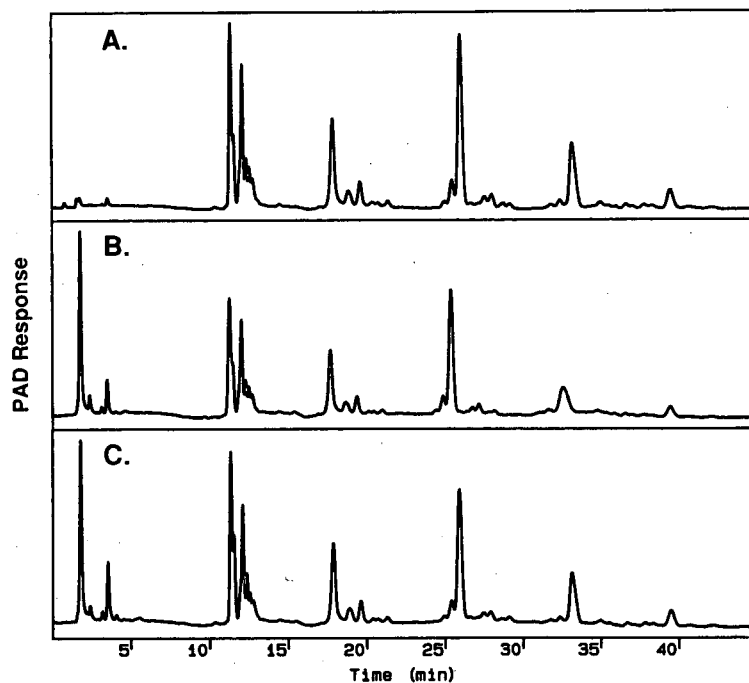


Fig. 8. Comparison between three methods of recovering oligosaccharides after PNGase F digestion. Identical aliquots of reduced and S-carboxymethylated rt-PA were treated with PNGase F, and the released oligosaccharides were recovered by (A) gel permeation chromatography, (B) reversed-phase chromatography on  $C_{18}$  Sep-Pak, and (C) ethanol precipitation. Elution was with gradient program 2.

the technique useful for general carbohydrate characterization. However, in the absence of supporting analytical results (*e.g.* mass spectrometry and/or NMR), chromatographic retention time alone is not sufficient to identify an oligosaccharide. One difficulty with HPAEC is that the eluents contain high concentrations of non-volatile salts (typically sodium acetate and sodium hydroxide); therefore, an unidentified oligosaccharide must be desalted prior to carrying out conventional methods of structure elucidation.

We have evaluated the use of an anionic micromembrane suppressor (AMMS; Dionex) downstream of the detector to achieve on-line desalting. Within the AMMS cartridge, the column effluent passes along one face of a polyanionic membrane, which is permeable to cations but impermeable to anions. Sodium ions in the effluent stream are exchanged for protons from an aqueous sulfuric acid regenerant solution on the other face of the membrane, thus converting the sodium hydroxide and sodium acetate to water and acetic acid, respectively. After "ion suppression", salt-free oligosaccharides can be recovered by lyophilization of column fractions. The main limitation of this approach is the exchange capacity of the AMMS cartridge: the cartridge is able to exchange *ca.* 0.15–0.2 *M* sodium ions at a flow-rate of 1 ml/min. Thus, although the capacity of the cartridge is generally satisfactory for desalting neutral oligosaccharides, it may be overwhelmed by the sodium acetate concentrations necessary to elute multiply charged oligosaccharides.

We have used this approach successfully to desalt high-mannose and hybrid oligosaccharides, separated by HPAEC, and mono-, di-, tri- and tetrasialyl complex oligosaccharides, separated by neutral-pH anion-exchange chromatography on a Mono Q column. The lyophilized oligosaccharides collected in this manner were then analyzed by  $^1\text{H}$  NMR at 500 MHz, which yielded good spectra that contained only minimal acetate signals (not shown; see ref. 8).

Although oligosaccharides can be prepared successfully for NMR analysis after HPAEC, the inherent insensitivity of NMR and the low capacity of the HPAEC columns make it desirable to be able to prepare samples for more sensitive analytical methods, most notably mass spectrometry. Preparation of samples for FAB-MS analysis requires thorough desalting, since even small amounts of contaminating salt adversely affect ionization and result in reduced sensitivity<sup>19</sup>. We have examined two methods for derivatizing oligosaccharides after HPAEC with ion suppression. The goal with both techniques was to make a derivative that could be purified by reversed-phase HPLC and would be suitable for FAB-MS analysis.

The first approach was to reduce and permethylate oligosaccharides that had been separated by HPAEC and desalted by on-line ion suppression (Fig. 9). Permethylated oligosaccharide alditols are suitably non-polar for reversed-phase chromatography and have been shown to exhibit good ionization and useful fragmentation in FAB-MS<sup>19</sup>. Fig. 9A shows the HPAEC separation of a mixture of high-mannose oligosaccharides released by endo H treatment of rt-PA. The peak indicated with the arrow was collected, recovered by lyophilization, reduced and permethylated. The resulting permethylated oligosaccharide alditol was recovered by reversed-phase chromatography on a  $\text{C}_{18}$  Sep-Pak cartridge<sup>12</sup> and analyzed by FAB-MS (Fig. 9B). The mass spectrum of this derivative contained abundant  $[\text{M} + \text{H}]^+$  ( $m/z$  1328.4) and  $[\text{M} + \text{Na}]^+$  ( $m/z$  1350.4) ions.

We were able to use this technique successfully to obtain mass spectra of a

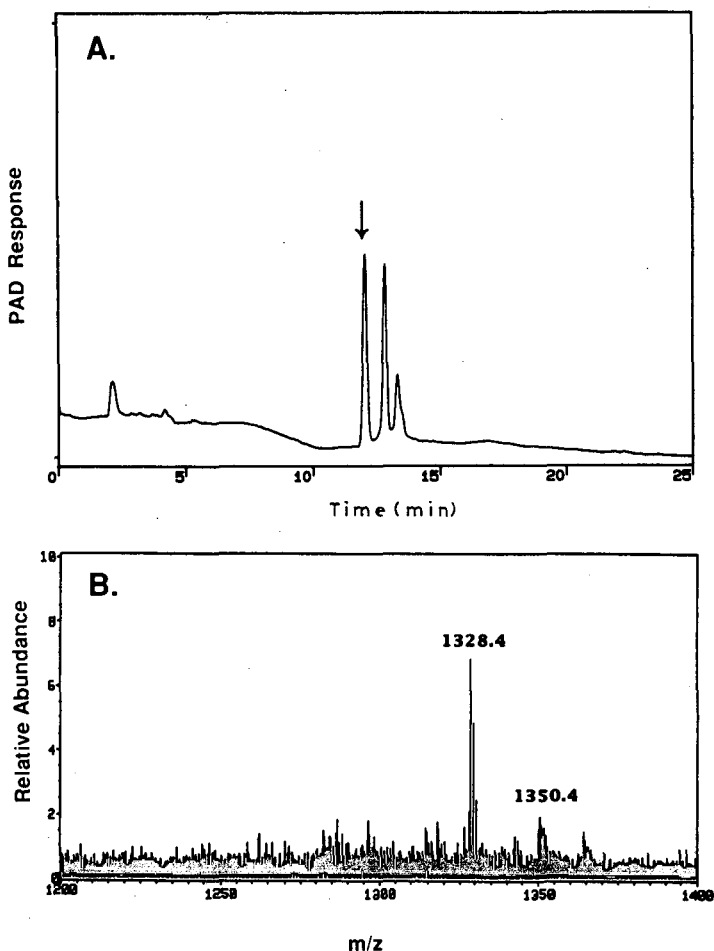


Fig. 9. FAB-MS analysis of the permethylated derivative of a high-mannose oligosaccharide after HPAEC. (A) Separation of a mixture of high-mannose oligosaccharides by HPAEC using gradient program I. The column effluent was passed through an anionic micromembrane suppressor cartridge for on-line desalting. The collected oligosaccharide (arrow) was recovered by lyophilization, permethylated and analyzed by FAB-MS. (B) The FAB-MS spectrum of the derivatized oligosaccharide. The ions at  $m/z$  1328.4 and  $m/z$  1350.4 correspond to  $[M + H]^+$  and  $[M + Na]^+$ , respectively, for reduced and permethylated  $\text{Man}_5\text{GlcNAc}$  (compound 1, Table I).

variety of high-mannose and desialylated complex oligosaccharides<sup>8</sup>. There are, however, several disadvantages to using permethylated derivatives for this application: (1) sample preparation is rather laborious and time-consuming; (2) the presence of even fairly low levels of salt can interfere with the permethylation chemistry, resulting in undermethylation<sup>20</sup>; and (3) the permethylated derivatives lack a good UV chromophore, which would be useful for monitoring the reversed-phase purification.

To overcome the limitations of the permethyl derivatives, we examined a different derivatization method: reductive coupling of *p*-aminobenzoic acid ethyl ester

(ABEE) to reducing oligosaccharides collected after HPAEC and ion suppression. ABEE derivatives<sup>14,15</sup> and derivatives with longer-chain alkyl esters of *p*-aminobenzoic acid<sup>21</sup> have been demonstrated to have desirable properties for FAB-MS. This type of derivatization chemistry offers several advantages over permethylation for use after HPAEC: (1) the derivatization should not be affected by residual sodium acetate resulting from incomplete ion suppression; (2) the derivatization introduces a UV chromophore, which simplifies subsequent reversed-phase HPLC purification; and (3) the longer-chain alkyl esters of *p*-aminobenzoic acid have been demonstrated to yield derivatives that ionize extremely efficiently, making sub-nanomole sensitivity feasible<sup>21</sup>.

To test the suitability of ABEE derivatives for FAB-MS analysis after HPAEC separations, an aliquot of an asialo diantennary oligosaccharide (compound **10**, Table I) was collected after HPAEC using gradient program 1 with ion suppression. The sample was derivatized with ABEE and the derivative isolated by reversed-phase HPLC, as described in Experimental. The FAB mass spectrum of the isolated ABEE derivative is shown in Fig. 10 and contains a prominent  $[M + H]^+$  ion ( $m/z$  1587.5). Thus it appears to be quite feasible to analyze ABEE derivatives of oligosaccharides after HPAEC separations. As has been demonstrated by Poulter *et al.*<sup>21</sup>, the use of longer-chain alkyl esters of *p*-aminobenzoic acid results in significantly improved sensitivity over ABEE derivatives and, therefore, will probably prove to be the reagents of choice for this application.

In conclusion, the results presented here demonstrate that HPAEC is a versatile method for separating both neutral and acidic oligosaccharides of the types commonly found as N-linked substituents of glycoproteins. The resolution and reproducibility of the separations make the technique suitable for oligosaccharide profiling. When used in conjunction with on-line ion suppression, HPAEC can be a "semipreparative"

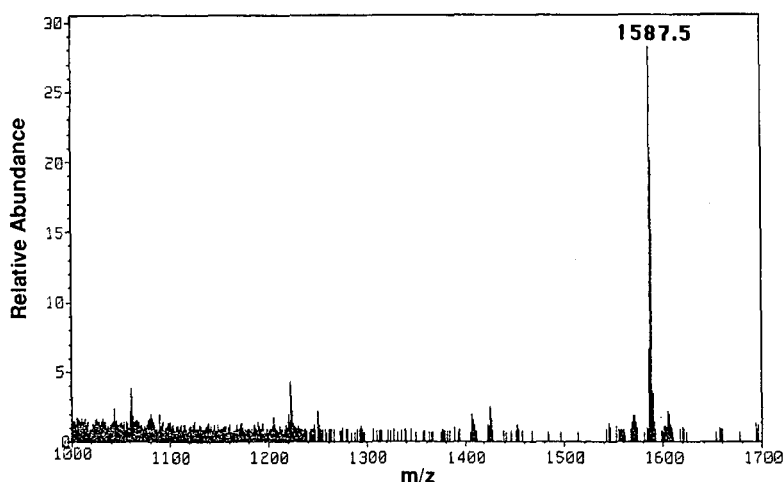


Fig. 10. FAB-MS analysis of the ABEE derivative of compound **10**. Compound **10** was subjected to HPAEC and collected as described in the legend to Fig. 9. The collected oligosaccharide was derivatized with ABEE as described in Experimental, and analyzed by FAB-MS. The ion at  $m/z$  1587.5 corresponds to  $[M + H]^+$  for the ABEE derivative of compound **10**.

technique, permitting identification of collected oligosaccharides by conventional chemical and spectroscopic methods. It should be noted that, although pulsed amperometry is a destructive method of detection, only a small percentage of the column effluent ever comes into contact with the detection electrode. Therefore, in our semi-preparative work it has been possible to collect oligosaccharides downstream of the detector without stream splitting. We have not observed significant degradation products in NMR spectra, in mass spectra, or by rechromatography of collected oligosaccharides.

#### ACKNOWLEDGEMENT

The authors thank Dr. John Stults for carrying out the FAB-MS analyses.

#### REFERENCES

- 1 M. R. Hardy, R. R. Townsend and Y. C. Lee, *Anal. Biochem.*, 170 (1988) 54-62.
- 2 M. R. Hardy and R. R. Townsend, *Proc. Natl. Acad. Sci. U.S.A.*, 85 (1988) 3289-3293.
- 3 R. R. Townsend, M. R. Hardy, O. Hindsgaul and Y. C. Lee, *Anal. Biochem.*, 174 (1988) 459-470.
- 4 L.-M. Chen, M.-G. Yet and M.-C. Shao, *FASEB J.*, 2 (1988) 2819-2824.
- 5 J. A. Rendlemen, in R. F. Gould (Editor), *Carbohydrates in Solution (Advances in Chemistry Series, Vol. 117)*, American Chemical Society, Washington, DC, 1971, pp. 51-69.
- 6 S. Hughes and D. C. Johnson, *Anal. Chim. Acta*, 132 (1981) 11-22.
- 7 L. A. Lasky, J. E. Groopman, C. W. Fennie, P. M. Benz, D. J. Capon, D. J. Dowbenko, G. R. Nakamura, W. M. Nunes, M. E. Renz and P. W. Berman, *Science (Washington, D.C.)*, 233 (1986) 209-212.
- 8 M. W. Spellman, L. J. Basa, C. K. Leonard, J. A. Chakel, J. V. O'Connor, S. Wilson and H. van Halbeek, *J. Biol. Chem.*, 264 (1989) 14100-14111.
- 9 T. Mizuochi, M. W. Spellman, M. Larkin, J. Solomon, L. J. Basa and T. Feizi, *Biochem. J.*, 254 (1988) 599-603.
- 10 T. Mizuochi, M. W. Spellman, M. Larkin, J. Solomon, L. J. Basa and T. Feizi, *Biomed. Chromatogr.*, 2 (1988) 260-270.
- 11 M. DuBois, K. A. Gilles, J. K. Hamilton, P. A. Rebers and F. Smith, *Anal. Chem.*, 28 (1956) 350-356.
- 12 T. J. Waeghe, A. G. Darvill, M. McNeil and P. Albersheim, *Carbohydr. Res.*, 123 (1983) 281-304.
- 13 S. Hirani, R. J. Bernasconi and J. R. Rasmussen, *Anal. Biochem.*, 162 (1987) 485-492.
- 14 W. T. Wang, N. C. LeDonne, Jr., B. Ackerman and C. C. Sweeley, *Anal. Biochem.*, 141 (1984) 366-381.
- 15 J. W. Webb, K. Jiang, B. L. Gillece-Castro, A. L. Tarentino, T. H. Plummer, J. C. Byrd, S. J. Fisher and A. L. Burlingame, *Anal. Biochem.*, 169 (1988) 337-349.
- 16 C.-J. Liang, K. Yamashita and A. Kobata, *J. Biochem.*, 88 (1980) 51-58.
- 17 G. Spik, V. Debruyne, J. Montreuil, H. van Halbeek and J. F. G. Vliegthart, *FEBS Lett.*, 185 (1985) 65-69.
- 18 E. D. Green, G. Adelt, J. U. Baenziger, S. Wilson and H. van Halbeek, *J. Biol. Chem.*, 263 (1988) 18 253-18 268.
- 19 A. Dell, *Adv. Carbohydr. Chem. Biochem.*, 45 (1987) 19-72.
- 20 H. Rauvala, J. Finne, T. Krusius, J. Karkkainen and J. Jarnefelt, *Adv. Carbohydr. Chem. Biochem.*, 38 (1981) 389-416.
- 21 L. Poulter, R. Karrer, K. Jiang, B. L. Gillece-Castro and A. L. Burlingame, *36th ASMS Conference on Mass Spectrometry and Allied Topics, San Francisco, 1988*, Abstracts, pp. 921-922.



CHROM. 21 785

## AUTOMATED EVALUATION OF TRYPTIC DIGEST FROM RECOMBINANT HUMAN GROWTH HORMONE USING ULTRAVIOLET SPECTRA AND NUMERIC PEAK INFORMATION<sup>a</sup>

HANS-JURGEN P. SIEVERT\*

*Hewlett-Packard Company, Route 41 and Starr Road, P.O. Box 900, Avondale, PA 19311 (U.S.A.)*  
and

SHIAW-LIN WU, ROSANNE CHLOUPEK and WILLIAM S. HANCOCK

*Genentech, Incorporated, 460 Point San Bruno Boulevard, South San Francisco, CA 94083 (U.S.A.)*

---

### SUMMARY

UV spectra were successfully employed in identifying peptide fragments from a tryptic digest of recombinant-DNA-derived human growth hormone (r-hGH). It was possible to distinguish very similar peptides utilizing a digital comparison of the UV spectra. An automated procedure was developed to generate a calibration library for the tryptic digest of a reference standard. The calibration library was then evaluated for reproducibility and selectivity and found to provide superior performance in correctly identifying ambiguous peaks as compared to the use of a conventional calibration table.

Spectral match factors together with numerical information, derived from peak retention time, area and height, were used to arrive at a “peak score” descriptive of the similarity between standard and sample peaks. “Peak scores” could be combined to calculate a “sample score” indicative of overall similarity between an unknown and a standard. The scoring procedure was automated to generate a final report without operator intervention and successfully assigned appropriate scores to similar as well as dissimilar samples, *e.g.*, native and oxidized r-hGH.

---

### INTRODUCTION

One method for the characterization of recombinant-DNA-derived proteins or peptides utilizes digestion with trypsin to obtain a number of characteristic peptide fragments which can be separated and quantified using high-performance liquid chromatography (HPLC)<sup>1,2</sup>. This “tryptic map” provides a key analytical technique that can be applied during the development stage as well as in the routine quality control of manufactured lots. However, the unambiguous identification of all peaks in the tryptic map is a laborious exercise which cannot be repeated on a day-to-day basis.

---

<sup>a</sup> Presented as paper No. 892 at the 39th Pittsburgh Conference and Exhibition, held at New Orleans, February 22–26, 1988.

Thus, a typical lot release procedure relies on comparing replicate analyses of the tryptic map for the sample in question with those of well characterized reference material.

The comparison makes use of numerical peak data such as retention time, area and height. A major challenge in this context is that of assigning the correct identity to the chromatographic peaks obtained for each tryptic map. Careful control of the chromatographic equipment and separation conditions are required to reduce the variability of peak data to a minimum.

Peak assignment, however, becomes very difficult if more than one candidate peak is found in a given search window, a situation that is not uncommon with tryptic digests of larger proteins. Traditionally, the peak with the largest response in the window is considered to be the correct match. If additional chromatographic signals are available from parallel detection with the same or a second detector, the response of the standard under the different conditions of detection can also be used. With the advent of the diode array detector it becomes possible to obtain spectral information for each of the peaks in the tryptic map. This information has tremendous potential to facilitate peak identification by comparing the UV spectra of standard and unknown.

For a number of years, algorithms for the point by point numerical comparison of two spectra have been available and have been used successfully to distinguish between very similar compounds<sup>3,4</sup>. Utilizing one such algorithm, this study tried to determine whether UV spectra can be of use in the identification of the tryptic peptide fragments of recombinant human growth hormone (r-hGH). A critical question in this context was whether the spectra contain enough information to allow one to differentiate between compositionally very similar peptides, especially in the absence of aromatic amino acids.

Our study proceeded in four stages: (1) develop a procedure for the generation of a calibration library from reference standards; (2) determine the sensitivity and selectivity of this calibration library; (3) define an algorithm for calculating a peak score which reflects the confidence of correct identification; (4) combine individual peak scores to arrive at an overall similarity score to characterize a tryptic map.

## EXPERIMENTAL

### *Chemicals and solvents*

Acetonitrile (UV-grade, Burdick and Jackson), trifluoroacetic acid (spectrograde, Pierce), water (purified by a Milli-Q system, Millipore) and trypsin (TPCK-treated, Sigma) were used. r-hGH (Protropin®) was produced as described previously<sup>5</sup>.

### *Oxidation of r-hGH*

Samples were oxidized by adding 50  $\mu$ l of chilled performic acid (9 parts 88% formic acid and 1 part 30% hydrogen peroxide) to 1 mg r-hGH and reacting the mixture for 1 h at 0°C.

### *Tryptic digest of r-hGH*

Samples were digested in a buffer solution containing 100 mM sodium acetate, 10 mM Tris base and 1 mM calcium chloride at pH 8.3 at 37°C by addition of 1:100 trypsin (trypsin: r-hGH, by weight) at time zero and at 2 h. Samples were acidified after

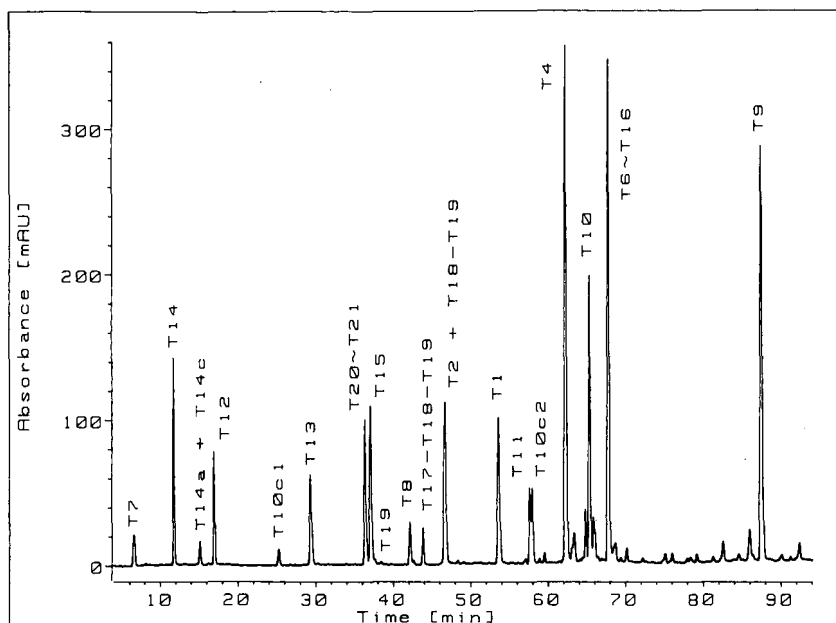


Fig. 1. Tryptic map of r-hGH separated with gradient I (TFA). A 100- $\mu$ g sample was loaded in 0.2 ml of 0.1 M ammonium bicarbonate and separated using gradient system I as outlined in the Experimental section. The tryptic fragments as identified by FAB-MS are indicated in the figure, actual amino acid composition is as follows (c indicates a chymotrypsin-like cleavage; a indicates a pyroglutamic acid (q) containing residue; ~ denotes a disulfide bridge): T7 = EETQQK; T14 = QTYSK; T14a = qTYSK; T14c = QTY; T12 = LEDGSPR; T10c1 = SVFAN; T13 = TGQIFK; T20~T21 = IVQCR~SVEGSCGF; T15 = FDTNSHNDDALLK; T19 = VETFLR; T8 = SNLELLR; T17~T18~T19 = K~DMDK~VETFLR (incomplete digestion); T2 = LFDNAMLRL; T18~T19 = DMDK~VETFLR (incomplete digestion); T1 = MFPTIPLSR; T11 = DLEEGIQTLMGR; T10c2 = SLVYGASDSNVYDLLK; T4 = LHQLAFDITYQEFEEAYIPK; T10 = SVFANSLVYGASDSNVYDLLK; T6~T16 = YSFLQNPQTSLCFSESIPTPSNR~. NYGLLYCFR; T9 = ISLLLIQSWLEPVQFLR.

a total of 4 h with 100  $\mu$ l of phosphoric acid (pH < 3) per ml of sample and analyzed directly or stored for up to three days at 2–8°C. It had been determined elsewhere (unpublished results) that digestion of r-hGH was complete after 4 h.

#### High-performance liquid chromatography

Separations were performed using a Hewlett-Packard 1090M HPLC system equipped with a DR5 ternary pumping system, an automated injection and sampling system, a heated column compartment and a diode array detector and controlled by an HP 79994A ChemStation.

Two gradient systems were employed for the separation of the tryptic fragments. System I used trifluoroacetic acid (TFA) in water at 0.1% as solvent A, solvent B being 0.08% TFA in acetonitrile. The gradient was linear from 0 to 60% B between 0 and 120 min at a flow-rate of 1 ml/min with the oven temperature set at 40°C. System II utilized 50 mM sodium phosphate in water, pH 2.85, as solvent A, solvent B was acetonitrile. The gradient profile was linear from 0 to 40% B over 120 min at a flow-rate of 1 ml/min

with the oven temperature set to 40°C. For both gradient systems we used a 15 cm × 0.46 cm Nucleosil C<sub>18</sub> reversed-phase column, particle size 5 μm, particle size 100 Å, packed by Alltech Assoc. Fig. 1 shows a typical chromatogram of a mixture of tryptic peptides derived from an r-hGH reference standard analyzed with the TFA gradient system.

#### Data processing

For all analyses, spectra were acquired at one-second intervals over the range from 200 to 350 nm. In addition, chromatographic signals were recorded at 220, 230, 254, 274, 280, and 292 nm with a reference wavelength of 350 nm in all cases. Rawdata were stored on magnetic media and were processed on the ChemStation using the built-in spectral library functions as well as additional evaluation software which was written for that purpose using a high-level command language available on the ChemStation.

#### Spectral matching

Numerical point by point comparison of two UV spectra is implemented on the ChemStation with the COMPARE command<sup>6</sup> and is illustrated in Fig. 2 where spectra for peptides T13 and T14 are compared (Fig. 2a). At each wavelength, absorbance

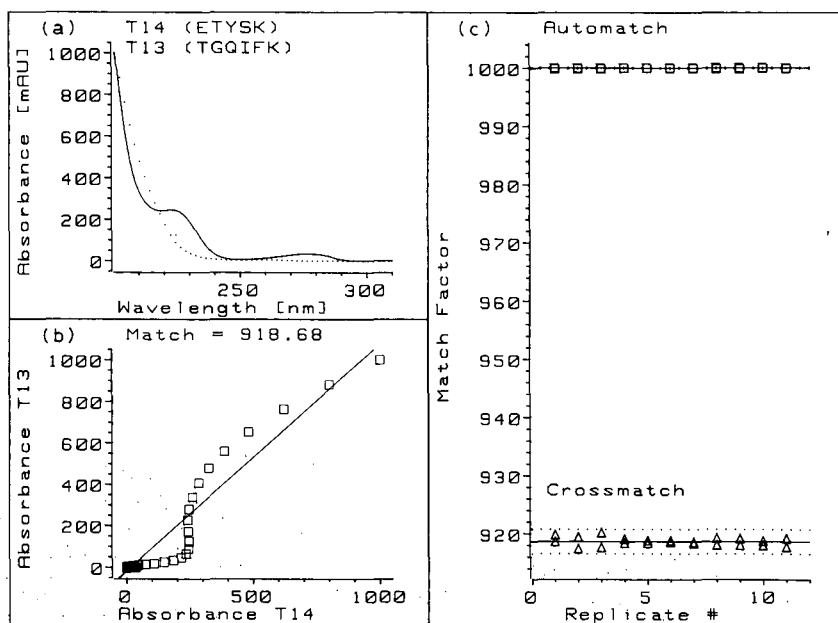


Fig. 2. Spectral match between tryptic peptides T14 and T13 as an example of moderate similarity. Part a shows the UV spectra for the two peptides (T13 shown as dotted line). Part b presents the distribution arising from plotting pairwise absorbance values for both peptides at identical wavelengths; the solid line is the linear least squares fit through the data. The square of the correlation coefficient multiplied by 1000 is defined as the match factor and is shown at the top of part b. Part c shows a comparison of the match factor for all of 11 spectra for the two peptides, either comparing each with its own average spectra (automatch) or with the average for the other peptide (crossmatch). The mean match factor is given as solid line in each case, the dotted lines indicate the upper and lower limits of  $\pm 3$  standard deviations, respectively.

values for the two peptide spectra are plotted as abscissa and ordinate and a linear regression is applied to the resulting scatter plot (Fig. 2b). The square of the correlation coefficient, multiplied by 1000, is defined as the match factor for the two spectra. A value of 0 indicates no match at all, a value of 1000 would characterize a perfect match. The two peptides shown in Fig. 2a differ in the nature of the aromatic amino acid residue which is phenylalanine for T13 and tyrosine for T14. Their spectra are clearly different, even on visual comparison, and the match factor accordingly has a low value of 919. Thus, even though a match factor could be as low as 0, spectral similarities are quite apparent to the naked eye once the match factor drops below 900.

Fig. 3 illustrates how the match factor is affected when we compare T13 with T12, a peptide fragment which does not contain any aromatic amino acid at all (Fig. 3a). The spectra now are very similar and the match factor increases to 997 (Fig. 3b), approaching the value expected for identical spectra. Visual identification of the two compounds could at best be considered ambiguous. We will show later how the significance of a given match factor, even in close proximity of 1000, can be assessed in statistical terms.

RESULTS AND DISCUSSION

*Spectral calibration library*

The first step towards characterizing the tryptic map of r-hGH was to compile a library of standard spectra for the various fragments in the map. For this purpose a reference standard was injected four times and analyzed with gradient systems

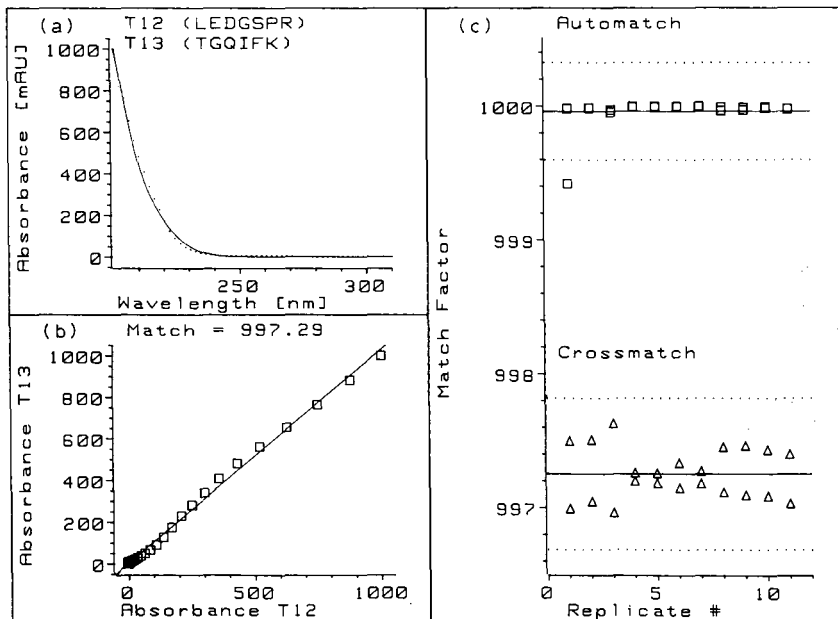


Fig. 3. Spectral match between tryptic peptides T12 and T13 as an example of strong similarity. The presentation of data is as explained in the legend to Fig. 2.

I (TFA based) and II (phosphate based). Each of the resulting data files was processed in the following fashion. After integration of the signal at 220 nm, apex spectra were identified for all integrated peaks. They were corrected for solvent background by subtracting a reference spectrum which was interpolated from two baseline spectra at either side of the peak. The resulting peak spectra were then stored into a library file which we referred to as a sample library since it contained all spectra characteristic of a given sample.

The two-point reference correction employed here is especially important in the case of gradient I, since TFA undergoes a significant change in spectral properties as the acetonitrile concentration is increased during the course of the gradient elution<sup>7</sup>. Fig. 4 illustrates how the uncorrected upslope and downslope spectra for fragment T9 differ significantly from the apex spectrum and each other (Fig. 4a). After baseline correction all three spectra match closely (Fig. 4b).

We next used a retention time window of  $\pm 0.5$  min centered on the apex of each peak from the first standard to find the spectrum with the best match from each of the other three standards. Those spectra that were common to all four standards were then averaged, normalized, smoothed, and transferred into a new spectral library file which we named the calibration library. For each peak of the tryptic map, this library file contains the UV spectrum and values for area, height, retention time, and scaling factor, all based on averages from the four standard runs.

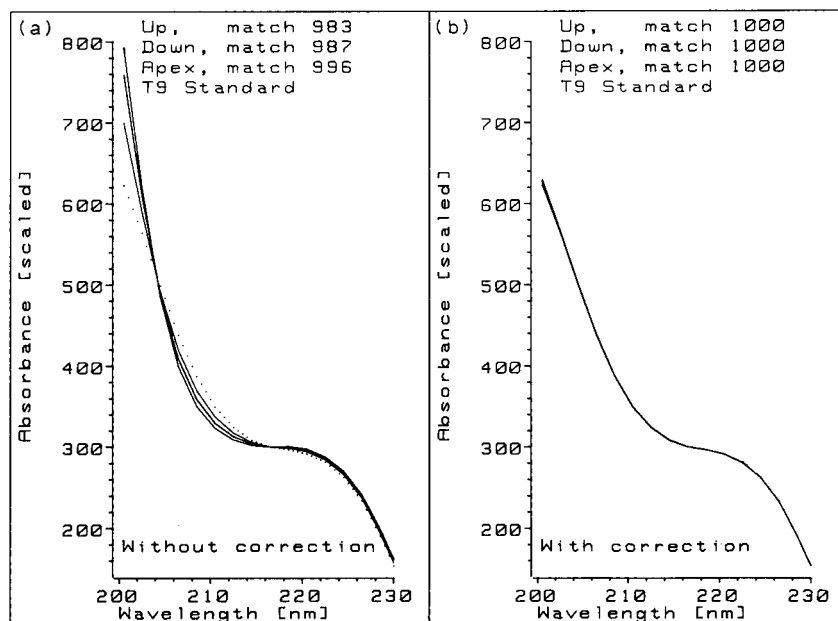


Fig. 4. Background correction for peak spectra as demonstrated for the tryptic peptide T9 separated with gradient I (TFA). Part a shows the comparison of uncorrected upslope, downslope and apex spectra for the T9 peak with a standard T9 spectrum (dotted line); match factors are given to indicate the degree of similarity. Part b presents the same spectra after background correction had been applied, match factors again refer to comparison with T9 standard.

From previous characterization studies the identity of the tryptic fragments had been determined by amino acid analysis and fast atom bombardment (FAB) mass spectrometry (MS)<sup>1</sup>. Library entries for peaks eluting prior to the first and after the last tryptic fragment as well as entries for peaks with area or height below one percent of total area or height were then removed. It had also been shown<sup>1</sup> that most of the minor peaks were not related to r-hGH but were nonspecific background, presumably derived from trypsin or due to other interferences like baseline noise or solvent impurities. The final calibration library for the TFA system contained 40 entries, 19 of which represented tryptic fragments of known identity; the phosphate library in its final form consisted of 31 entries. These two calibration libraries were used in all subsequent experiments.

Correlation of data from different standard runs relies heavily on good chromatographic reproducibility. In Fig. 5, chromatographic traces from four replicates analyzed with gradient II are overlaid to demonstrate that instrument performance is excellent even towards the end of the gradient. Statistical analysis of retention time variations showed the average standard deviation for all peaks incorporated into the calibration library to be 0.027 min (1.6 s) and 0.021 min (1.3 s) for gradient system I and II, respectively.

#### *Reproducibility and selectivity of the calibration library*

Two key properties of the match factor that determine the usefulness of the spectral data incorporated into the calibration library are reproducibility and

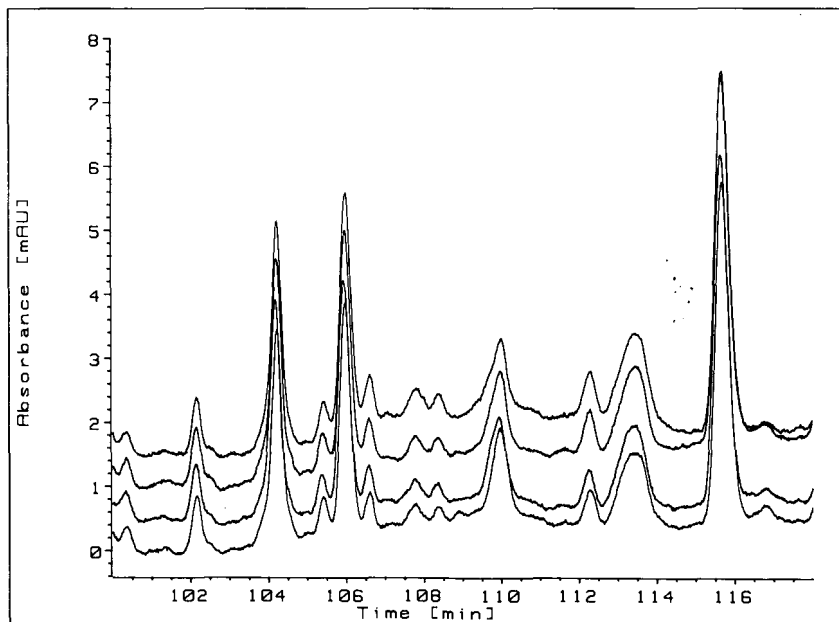


Fig. 5. Reproducibility of the tryptic map analyzed with gradient II (phosphate). A 100- $\mu$ g sample was loaded in 0.2 ml of 0.1 M ammonium bicarbonate and separated using gradient system II as outlined in the Experimental section. The figure shows the superimposition of four replicate elution profiles. Some of the data have been shifted along the absorbance axis to provide greater clarity.

selectivity. We therefore decided to investigate these properties in a systematic fashion in order to obtain some quantitative guidelines. Results in this section were obtained using gradient I, since TFA, when employed as modifier, presents a greater challenge for LC detector and pump than does phosphate.

Reproducibility of the match factor determines the absolute limit for the similarity between any two spectra and thus defines the sensitivity of spectral matching. Two spectra can be considered different only when mean and standard deviation for the match between the two differ significantly from those obtained by repeatedly matching identical spectra. It is not sufficient to use a match factor cutoff as criterion for positive identification, additional statistical information is needed to determine the significance of a given match factor.

Spectra for T13 or T14 derived from eleven different injections were averaged to obtain a representative spectrum for each peptide. All individual spectra were then matched against their respective average (Fig. 2c, automatch; T13  $\leftrightarrow$  T13av, T14  $\leftrightarrow$  T14av) and the resulting distribution of match factors was compared with that obtained from matching individual T13 spectra against the average T14 spectrum and *vice versa* (Fig. 2c, crossmatch; T13  $\leftrightarrow$  T14av, T14  $\leftrightarrow$  T13av). It can be seen that the means for automatch and crossmatch are quite different, the match factor for the crossmatch of 918.6 is certainly a good indication of dissimilarity. More importantly, confidence intervals of three standard deviations above and below each mean as indicated in Fig. 2c do not overlap, but show a significant gap. Thus, we can distinguish T13 from T14 with a great degree of confidence.

Fig. 3c shows the corresponding plot of automatch and crossmatch for T13 and T12. These peptides are very similar in their spectral characteristics as can be seen by the mean crossmatch score of 997.25. Nonetheless, there is still a clear gap between the confidence intervals for automatch and crossmatch, indicating that it is possible to differentiate between compounds of extreme similarity. In statistical terms, if we apply Student's *t*-test for unequal variances to the data in Fig. 3c, we obtain a *t*-value of 57 and a probability of better than 99.99% that the mean values obtained for automatch and crossmatch are indeed different.

The *t*-test for the comparison of T13 and T14 (Fig. 2c) results in a *t*-value of 542 and a probability of 100.00% that the spectra are different. *t*-Values expressing the similarity among the four aliphatic peptides (T7, T8, T11, and T12) ranged from 13 to 133 which is sufficient for a statistically valid distinction. (For a population size of 11 a *t*-value of at least 6.2 is required to provide greater than 99.99% probability that two means are different.)

When we analyzed the reproducibility of match factors for the four standard runs using gradient I, we found that the mean match factor ranged from 998.76 to 1000.00 with standard deviations from less than 0.001 to 1.306. This indicated to us that we could employ very stringent match criteria for spectral identity. Since variability of the match factor increases as peak concentration decreases and since the relative concentrations of the tryptic fragments from r-hGH should be fairly constant, we decided to define individual match criteria for each entry in the calibration library rather than using a fixed match threshold. To be considered a positive match, an unknown spectrum had to have a match score above a threshold of three standard deviations below the mean match for a given standard. This gives us a 99.8% probability that only correct matches are assigned.



Our next concern was the selectivity of the calibration library, that is, its stability against false positive matches. To establish selectivity, each standard in the calibration library had to be matched against every entry from a typical sample library to determine the number of potential mismatches. A mismatch in this context was defined as a standard entry for which more than one match candidate was found with a match factor inside the confidence limits established earlier. Selectivity can be greatly enhanced by defining a retention time window around a given standard to limit the number of search candidates.

When we used a retention time window of  $\pm 1$  min, which is twice the window employed for later experiments, we found incorrect matches only for three standards. These mismatches were all minor peaks with peak heights between 3 and 6 mAU and did not correspond to any known tryptic fragments of r-hGH. With a  $\pm 0.5$  min window no mismatches were found at all. We concluded from this that, with selection of an appropriate retention time window, the calibration library for r-hGH provides accurate identification of all fragments.

Traditional calibration procedures for peak identification based only on retention times resulted in mismatches for 5–8 standards inside a  $\pm 0.5$  min retention time window. When the window was increased to  $\pm 1$  min, nearly all standards exhibited mismatched peaks. Thus, the spectral information contained in our calibration library presents some clear advantages in reducing the potential for incorrect peak matching.

#### *Definition and application of the peak score*

Since chromatographic conditions are not always stable, resolution between adjacent peaks might change or additional peaks might appear in a tryptic map making it difficult to positively identify an unknown peak even when spectral matching is employed. However, in addition to peak spectra, other quantitative information is available for each peak and could be utilized to develop a procedure that would assign a numerical similarity score to each match between a standard and an unknown peak. Table I shows the variability of the different parameters available to construct this score. Based on the relative standard deviations, it is obvious that the greatest confidence can be placed in the match factor. Retention time information on one hand and peak area and height on the other hand exhibit deviations larger than those for the match factor by one and two orders of magnitude, respectively.

These findings are not surprising, if one considers that variability of area and height can be attributed not only to the chromatographic separation but also to the sample preparation, particularly the tryptic digestion. Retention time deviations, in turn, are primarily affected by variations in the chromatography. Assuming proper background correction, UV spectra should be completely invariant even under conditions that lead to noticeable fluctuations in retention times. The major cause for variability of the match factor would be detector noise, especially for fragments present at low concentrations.

Based on the statistical information in Table I, we can empirically define the following peak score (PS) which weights each parameter according to its variability:

$$PS = \{10 \times \Delta(MF) + \Delta(RT) + 1/10 \times [\Delta(AR) + \Delta(HT)]\}/11.2 \quad (1)$$

with

$$\Delta(\text{MF}) = [\text{MF}(\text{Std}) - \text{MF}(\text{Unk})] / [3 \times \text{sdev}(\text{MF})], \text{MF}(\text{Std}) > \text{MF}(\text{Unk}) \quad (2)$$

$$\Delta(\text{MF}) = 0, \quad \text{MF}(\text{Std}) \leq \text{MF}(\text{Unk})$$

$$\Delta(\text{RT}) = |\text{RT}(\text{Std}) - \text{RT}(\text{Unk})| / [3 \times \text{sdev}(\text{RT})] \quad (3)$$

$$\Delta(\text{RA}) = |\text{RA}(\text{Std}) - \text{RA}(\text{Unk})| / [3 \times \text{sdev}(\text{RA})] \quad (4)$$

$$\Delta(\text{RH}) = |\text{RH}(\text{Std}) - \text{RH}(\text{Unk})| / [3 \times \text{sdev}(\text{RH})] \quad (5)$$

Unk refers to the unknown, Std to the standard, and sdev indicates the standard deviation obtained for the four replicate standards. MF, RT, RA and RH are match factor, retention time, relative area and relative height, respectively; area and height values are expressed relative to a reference peak to eliminate concentration effects. To avoid unrealistically high delta values, we established minimum values for sdev of 0.1 (MF), 0.05 min (RT) and a 1% relative standard deviation for RA and RH.

Eqn. 1 accounts for the fact that the spectral match is the most significant parameter for peak recognition and therefore is weighted most heavily. Even if all other parameters indicate a perfect match, a large deviation in the match factor

TABLE I

STANDARD DEVIATIONS FOR RETENTION TIME, AREA, HEIGHT, AND MATCH FACTOR OF TRYPTIC DIGESTS FROM r-hGH ANALYZED WITH TWO DIFFERENT CHROMATOGRAPHY METHODS

	<i>Gradient I (TFA)<sup>a</sup></i>			<i>Gradient II (phosphate)<sup>b</sup></i>		
	<i>Mean<sup>c</sup></i>	<i>Low<sup>d</sup></i>	<i>High<sup>e</sup></i>	<i>Mean<sup>c</sup></i>	<i>Low<sup>d</sup></i>	<i>High<sup>e</sup></i>
Retention time						
Standard deviation (min)	0.027	0.007	0.174	0.021	0.004	0.041
Relative standard deviation (%)	0.136	0.008	1.882	0.075	0.007	0.594
Peak area <sup>f</sup>						
Standard deviation (mAU · s)	0.568	0.006	3.498	0.403	0.006	2.847
Relative standard deviation (%)	6.265	0.006	33.508	4.004	0.006	40.485
Peak height <sup>f</sup>						
Standard deviation (mAU)	0.501	0.006	5.476	0.464	0.000	2.682
Relative standard deviation (%)	3.281	0.006	16.425	3.109	0.000	41.555
Match factor						
Standard deviation	0.156	0.000	1.306	0.080	0.000	0.661
Relative standard deviation (%)	0.016	0.000	0.131	0.008	0.000	0.066

<sup>a</sup> Standard deviations are based on a calibration library of 40 peaks.

<sup>b</sup> Standard deviations are based on a calibration library of 31 peaks.

<sup>c</sup> Overall mean for all peaks in the calibration library of standard deviations calculated for each individual peak from four replicate injections of r-hGH.

<sup>d</sup> Minimum value for the standard or relative standard deviations as defined in *c*.

<sup>e</sup> Maximum value for the standard or relative standard deviations as defined in *c*.

<sup>f</sup> Peak area and peak height counts were normalized to fragment T10 as 100.

indicates that the peak in question has the wrong identity. The scaling factor of 11.2 is the sum of all weighting factors and normalizes the peak score to unit weight. The use of a one-sided delta value for the match factor in eqn. 2 reflects the fact that only match factors below the standard should be penalized.

By definition, a perfect peak score would be zero, a score of 1 will give us a 99.8% probability that we would not miss any positive matches but usually indicates rather marginal similarity between standard and unknown. Peak scores for all entries in the four sample libraries used to construct the calibration library ranged from 0.002 to 0.465 with an average score of 0.051. Because the score is open-ended, we somewhat arbitrarily decided that a score of 2 or larger indicated a totally mismatched peak. The probability that a positive match would result in a score of 2 is less than 0.000002%.

#### *Automated evaluation of digests using a sample score*

At this point we had in our hands a quantitative procedure to describe how well a peak from a calibration library is matched by any given peak in an unknown sample. Our next step was therefore aimed towards developing a scoring procedure that describes the overall similarity between all the peaks in an unknown and a calibration sample. Such a sample score would make it possible to evaluate and score a tryptic digest in completely automated fashion requiring no operator intervention.

Our definition of the sample score (SS) is:

$$SS = \frac{1}{N} \left( \sum_{i=1}^N SS_i + 2 \times MP + EP \right) \quad (6)$$

where MP is the number of missed standard peaks, EP the number of extra peaks in the sample, and N the number of standard entries in the calibration library.

The sample score allows us to account for missed calibration peaks as well as supernumerary peaks found in a sample. Furthermore, the score is normalized so as to be independent of the number of entries in the calibration library which becomes important if the library is modified. A peak score larger than 2 has previously been defined as a mismatch, therefore all peak scores are truncated to 2 so that missed and mismatched peaks have the same peak score. The penalty score of 1 for extra peaks is strictly empirical at this point, another possible approach could be to have the penalty reflect the size of the extra peak.

Even though a perfect sample score is easily defined as being exactly zero, it is more difficult to arrive at a criterion for what constitutes the limit between a passing and a failing score. Meaningful limits will have to be established through statistical analysis of typical sample scores for reference standards to account for variability due to different lots of growth hormone and trypsin as well as overall chromatographic variability.

Table II gives the sample scores for the four sample libraries (1A–D) used to construct the calibration library as well as for additional samples (2A–C and 3A–D) derived from the same reference standard but injected in different amounts. As expected, the calibration samples themselves, (1A–D), injected at 100  $\mu\text{g}$ , show a very good score of 0.076 or less, with an average value of 0.050 indicative of the extreme similarity between all four replicates.

TABLE II  
SIMILARITY BETWEEN REPLICATE SAMPLES OF TRYPTIC DIGESTS OF r-hGH ANALYZED WITH GRADIENT I (TFA)

Sample <sup>a</sup>	Amount ( $\mu\text{g}$ )	Individual sample scores <sup>b</sup>				Average sample score <sup>b</sup>
		A	B	C	D	
1	100	0.076	0.025	0.048	0.052	0.050
2	50	0.882	0.793	0.719	—	0.798
3	200	0.341	0.499	0.553	0.379	0.443

<sup>a</sup> All samples were tryptic digests of r-hGH reference material analyzed as described in the Experimental section.

<sup>b</sup> Sample score as defined in eqn. 6.

The increase in sample score for the 50- $\mu\text{g}$  injections (2A–2C) to an average value of 0.798 is partly due to a drift in chromatographic conditions resulting in resolution changes for several peaks. The coeluting fragments T14a and T14c were separated into two peaks, each with a spectrum different from the composite spectrum contained in the calibration library. The partially resolved peak pair T11 and T10c2 (Fig. 1), on the other hand, was not separated at all and consequently neither fragment was identified. Furthermore, the fragment with the lowest concentration (T19) was not detected at this smaller sample size.

The 200- $\mu\text{g}$  injections (3A–D) show an average score of 0.443 and thus fall between the 100- and the 50- $\mu\text{g}$  samples. The increased sample score results from the same problematic peaks encountered with the 50- $\mu\text{g}$  injection. In both the 50- and the 200- $\mu\text{g}$  injections, the additional standard peaks which were missing were all small peaks of unknown identity. This would indicate that the significance of these unidentified peaks with respect to sample identity needs to be investigated in some more detail.

For the phosphate gradient system (gradient II), similar data are shown in Table III. Again, the four calibration samples (1A–D) exhibit very low scores of 0.064 and

TABLE III  
SIMILARITY BETWEEN REPLICATE SAMPLES OF NATIVE AND OXIDIZED TRYPTIC DIGESTS OF r-hGH ANALYZED WITH GRADIENT II (PHOSPHATE)

Sample	Amount ( $\mu\text{g}$ )	Individual sample scores <sup>a</sup>				Average sample score <sup>a</sup>
		A	B	C	D	
1 <sup>b</sup>	100	0.025	0.016	0.037	0.064	0.036
2 <sup>b</sup>	100	0.671	—	—	—	0.671
3 <sup>c</sup>	100	1.687	1.723	1.677	1.681	1.692

<sup>a</sup> Sample score as defined in eqn. 6.

<sup>b</sup> Sample was tryptic digest of r-hGH reference material analyzed as described in the Experimental section.

<sup>c</sup> Sample was tryptic digest of oxidized r-hGH reference material analyzed as described in the Experimental section.

less, with the average at 0.036. An additional sample (2), which also contained reference material, but was analyzed at a different time, shows a higher score of 0.671. This score is in the range of scores obtained for the 50- and 200- $\mu\text{g}$  injections of reference material with gradient I. Closer inspection revealed that here, too, changes in peak resolution had an adverse effect on the sample score.

To provide some data on the kind of sample score obtained with a sample that is known to differ from the standard, we also analyzed samples of r-hGH which was oxidized prior to digestion with trypsin to simulate potential degradation pathways. As can be seen quite clearly (Table III, 3A-D), the average sample score of 1.692 lies significantly above the scores obtained for reference material and reflects the difference between oxidized and native r-hGH. Furthermore, reproducibility for the four samples is very good, indicative of the similarity among replicate injections of the oxidized samples.

To relate this abstract score to the more traditional visual method of evaluation, Fig. 6 shows a chromatogram for the oxidized r-hGH digest. Peaks that disappeared due to oxidation and those peaks that appear as new fragments and are not encountered in native r-hGH are clearly labeled. Although it is quite obvious, even to the casual observer, that the chromatogram in Fig. 6 differs considerably from the standard fragmentation pattern as indicated by the arrows, there are two clear advantages to the use of the sample score: (1) the whole evaluation procedure can be automated to obtain a final sample score without the need for operator intervention; (2) the scoring procedure is completely digital and therefore not subject to observer bias.

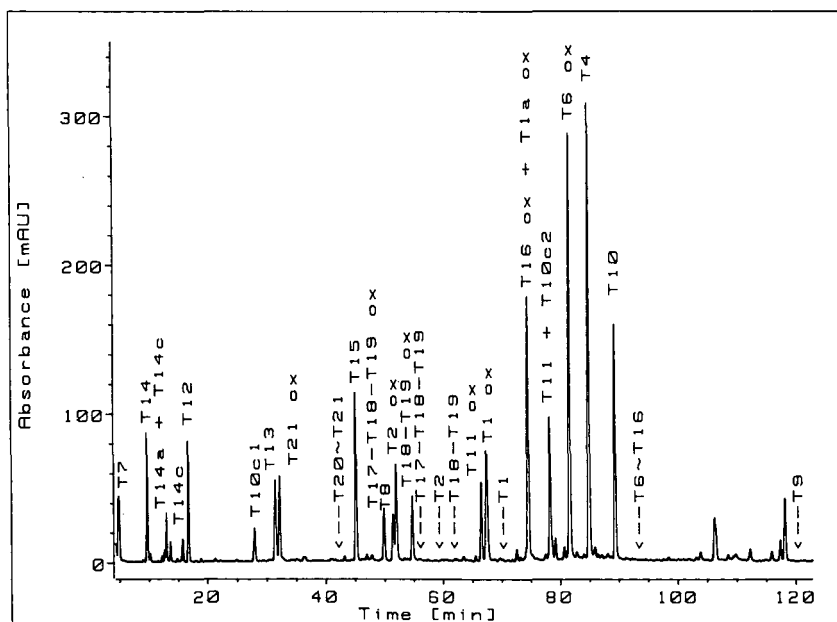


Fig. 6. Tryptic map for oxidized r-hGH analyzed with gradient II (phosphate). A 100- $\mu\text{g}$  sample of oxidized r-hGH was loaded in 0.2 ml of 0.1 M ammonium bicarbonate and separated using gradient system II as outlined in the Experimental section. The elution position for the unoxidized peptides is indicated by arrows, oxidized peptides are denoted by "ox".

## CONCLUSION

We believe that we have been able to show that, in spite of the overall similarity in their UV spectra, the individual peptides of the tryptic digest of r-hGH can be identified with a great deal of confidence. We developed a scoring procedure for tryptic digests that incorporates the cumulative similarity between the peaks in unknown and standard samples to assign a digital score to the match between the two.

At this point there are three major areas where further work is needed. The problem of mixed component spectra has to be addressed, possibly with the use of multi-component analysis. The significance of the small peaks of unknown identity, which might reflect lot to lot variability of either growth hormone or trypsin, requires further investigation. Finally, more data on the overall variability of the scoring procedure are needed to define the criteria that determine the cutoff between a pass or fail score.

Refinements in both the peak and the sample score could incorporate very specific knowledge about the expected behaviour of the r-hGH digest after chemical modification. Disappearance of peaks characteristic of oxidation, for instance, could be coupled to a search for the known oxidation products with a corresponding adjustment to the sample score. System suitability criteria like resolution between critical peak pairs could also be used to modify the sample score. For quality control applications, the peak score could be adjusted to place a greater weight on area and height deviations.

The methodology described here is by no means limited to r-hGH, tryptic digests from other proteins could be analyzed in a similar fashion, although the validation of selectivity for the calibration library has to be undertaken for each tryptic map. Peptide fragments, by nature of their rather non-descript and similar spectra, probably are more difficult to deal with than other chromatographic samples of comparable complexity but with more spectral variety. Tryptic maps might therefore be a good test case in the development of future expert systems for compound identification in complex samples.

## REFERENCES

- 1 W. S. Hancock, E. Canova-Davis, R. Chloupek, S. Wu, I. P. Baldonado, J. E. Battersby, M. W. Spellman, L. J. Basa and J. A. Chakel, *Banbury Report 29: Therapeutic Peptides and Proteins: Assessing the New Technologies*, Cold Spring Harbor Laboratory, Cold Spring Harbor, NY, 1988, p. 95.
- 2 W. S. Hancock, *Chromatogr. Forum*, 1 (1986) 57.
- 3 D. M. Demorest, J. C. Fetzer, I. S. Lurie, S. M. Carr and K. B. Chatson, *LC · GC, Mag. Liq. Gas Chromatogr.*, 5 (1986) 128.
- 4 D. H. Hill, T. R. Kelly and K. J. Langner, *Anal. Chem.*, 59 (1987) 350.
- 5 K. C. Olson, J. Fenno, N. Lin, R. N. Harkins, C. Snider, W. H. Kohr, M. J. Ross, D. Fodge, G. Prender and N. Stebbing, *Nature (London)*, 293 (1981) 408.
- 6 A. Drouen, *The COMPARE Command, Information Note*, Hewlett-Packard, Waldbronn, Publication Number 12-5952-3725, 1987.
- 7 G. Winkler, *LC · GC, Mag. Liq. Gas Chromatogr.*, 5 (1986) 1044.

CHROMSYMP. 1651

## PROTEIN CHROMATOGRAPHY WITH PYRIDINE- AND ALKYLTHIOETHER-BASED AGAROSE ADSORBENTS

SVEN OSCARSSON\* and JERKER PORATH

*Institute of Biochemistry (Box 576) and Biochemical Separation Centre (Box 577), Biomedical Center, University of Uppsala, S-751 23 Uppsala (Sweden)*

---

### SUMMARY

In an attempt to identify the part of the ligand of 3-(2-pyridylthiol)-2-hydroxypropylagarose that is responsible for the specific adsorption of immunoglobulins and  $\alpha_2$ -macroglobulin from serum, nine agarose derivatives were prepared: (I) 3-(N-2-iminopyridyl)-2-hydroxypropyl-, (II) 3-(4-pyridylthio)-2-hydroxypropyl-, (III) 3-(2-pyridylthio-N-oxide)-2-hydroxypropyl-, (IV) 3-(2-pyridylthio)-2-hydroxypropyl-, (V) 3-(ethylthio)-2-hydroxypropyl-, (VI) 3-(*n*-butylthio)-2-hydroxypropyl-, (VII) 3-(2-aminoethylthio)-2-hydroxypropyl-, (VIII) 3-(2-hydroxyethylthiol)-2-hydroxypropyl- and (IX) 3-(N-2-pyridyl-2-one)-2-hydroxypropylagarose. The selective adsorption of the above serum proteins to these derivatives was analysed by chromatography. The electron distributions were calculated for three of the investigated pyridine derivatives in order to establish whether there is any relationship between the electron distribution in the molecule and the absorption properties of the pyridine derivatives. By optimizing the preparation methods for the different derivatives, the possible side-reactions were minimized and checked. The adsorbed serum proteins were determined by the Ouchterlony technique and electrophoresis. The concentration of human serum albumin in the different fractions was determined by conventional radioimmunological methods. These data make it possible to classify the adsorbents according to their selectivity and hydrophobic thiophilic behaviour.

---

### INTRODUCTION

Ligands of different types coupled to matrices have been investigated as potential adsorbents for chromatography, and we have attempted to identify the structural features responsible for the cooperative effects often observed between the ligand, the polymer matrix of the adsorbent and the protein<sup>1-7</sup>. In 1985 Porath *et al.*<sup>8</sup> reported a new type of adsorbent, the thiophilic gels, typified by T-gel, which exhibited a characteristic, group-specific adsorption of immunoglobulins, C3, C4 and  $\alpha_2$ -macroglobulin. This explorative work was based on the use of divinyl sulphone-activated agarose gel. The sulphone group, together with a thioether, seemed to be essential for the characteristic salt-promoted adsorption of proteins. However, on further investigation of the thiophilic adsorption, we discovered that epichlorohydrin-activated gels to which 2-mercaptopyridine had been coupled exhibit similar behaviour<sup>9</sup>.

In an attempt to correlate structure and adsorption properties we have undertaken a chromatographic study of a number of adsorbents with ligands differing with respect to the presence or absence of atoms or groups of atoms.

## EXPERIMENTAL

### *Chemicals*

Sephacrose 6B, 2-aminoethanethiol, 1-ethanethiol and the human serum albumin-radioimmunological assay (HSA-RIA) kit for HSA detection were kindly supplied by Pharmacia (Uppsala, Sweden). Potassium sulphate, 1-butanethiol, 2-mercaptopyridine and 2-mercaptopyridine-1-oxide sodium salt were purchased from Fluka (Buchs, Switzerland), 2-aminopyridine and 4-mercaptopyridine from Aldrich (Steinheim, F.R.G., and Milwaukee, WI, U.S.A., respectively), sodium borohydride, ethylene glycol, 2-propanol,  $\text{NaH}_2\text{PO}_4 \cdot \text{H}_2\text{O}$ , hydrochloric acid and epichlorohydrin from Merck (Darmstadt, F.R.G.), Trisma base from Sigma (St. Louis, MO, U.S.A.), acetone and  $\text{NaHCO}_3$  from May and Baker (Dagenham, U-K-), toluene from Riedel-de Haan (Seelze, F.R.G.), 2-mercaptoethanol from Carl Roth (Karlsruhe, F.R.G.) and ethanol (99.5%) from Svensk Sprit (Stockholm, Sweden). Normal human serum was obtained from the Blood Bank at the University Hospital (Uppsala, Sweden) and gradient polyacrylamide gels (PAA 4/30) for electrophoresis and PD 10 columns for desalting from Pharmacia. Antisera against human serum proteins were kindly supplied by Professor C. B. Laurell (Department of Clinical Chemistry, Malmö Hospital, Malmö, Sweden).

### *Preparation methods*

*Epoxy-activated agarose gel beads.* Thoroughly washed and suction-dried Sepharose 6B (50 g) was added to a stirred mixture of 25 ml of 4 M NaOH, 4.25 ml of 1-chloro-2,3-epoxypropane and 0.17 g of  $\text{NaBH}_4$ . After reaction for 30 min with stirring, 10 ml of 4 M NaOH were added to the suspension, followed by continuous addition of 20 ml of 1-chloro-2,3-epoxypropane over a period of 1 h. After a total reaction time of 15 h, the slurry was washed with deionized water on a sintered-glass filter until the filtrate was neutral.

(I) *3-(N-2-Iminopyridyl)-2-hydroxypropylagarose (PyNH<sub>2</sub>-gel).* Suction-dried epoxy-activated agarose (25 g), prewashed with 0.1 M sodium phosphate buffer (pH 7.0), was added with stirring to a mixture of 50 ml of 0.1 M sodium phosphate buffer and 10 g of aminopyridine at pH 7.0. After 24 h at room temperature with stirring, the gel was transferred to a glass filter and washed with deionized water, ethanol and again with deionized water. The gel was found to contain 1343  $\mu\text{mol}$  N per gram of dried product.

(II) *3-(4-Pyridylthio)-2-hydroxypropylagarose (Py-S-4-gel).* Suction-dried epoxy-activated agarose (25 g), prewashed with 0.1 M sodium phosphate buffer (pH 6.8), was added to the reaction vessel. While nitrogen was allowed to flow through the reaction vessel for 10 min, 1.5 g of  $\text{NaBH}_4$  was successively added to 100 ml of 0.1 M sodium phosphate buffer (pH 7.5) containing 3 g of 4-mercaptopyridine. The pH of this solution was adjusted to 6.8 before addition to the gel in the reaction vessel. After a 3-h reaction time with stirring in a nitrogen atmosphere at room temperature, the gel was washed with deionized water, ethanol and again with deionized water. The



ligand concentration was found to be 759 and 724  $\mu\text{mol}$  per gram of dried product, as calculated from the sulphur and nitrogen content, respectively.

(III) *3-(2-Pyridylthio-N-oxide)-2-hydroxypropylagarose (Py-S-NO-gel)*. The preparation was performed according to the same method as described for 3-(4-pyridylthio)-2-hydroxypropylagarose. The ligand concentration was found to be 768 and 750  $\mu\text{mol}$  per gram of dried product, as calculated from the sulphur and nitrogen content, respectively.

(IV) *3-(2-Pyridylthio)-2-hydroxypropylagarose (Py-S-2-gel)*. The preparation was performed according to the same method as described for 3-(4-pyridylthio)-2-hydroxypropylagarose. The ligand concentration was found to be 825 and 793  $\mu\text{mol}$  per gram of dried product, as calculated from the sulphur and nitrogen content, respectively.

(V) *3-(Ethylthio)-2-hydroxypropylagarose (Et-S-gel)*. Suction-dried epoxy-activated agarose (25 g), prewashed with 0.1 M sodium phosphate buffer (pH 8.5), was added to 40 ml of 0.1 M sodium phosphate buffer (pH 8.5), then 20 ml of ethanethiol were added to the reaction vessel with stirring, followed by 40 ml of ethanol. The pH of the solution was adjusted to 8.5. After a total reaction time of 24 h at room temperature with stirring, the gel was transferred to a glass filter and washed thoroughly with deionized water, ethanol and again with deionized water. The washing procedure was repeated four times in the course of 2 days with 1–2-liter portions of the respective washing solutions. The ligand concentration was found to be 797  $\mu\text{mol}$  per gram of dried product, as calculated from the sulphur content.

(VI) *3-(n-Butylthio)-2-hydroxypropylagarose (Bu-S-gel)*. The preparation was performed according to the method described for 3-(ethylthio)-2-hydroxypropylagarose. The ligand concentration was found to be 771  $\mu\text{mol}$  per gram of dried product, as calculated from the sulphur content.

(VII) *3-(2-Aminoethylthio)-2-hydroxypropylagarose (NH<sub>2</sub>-et-S-gel)*. Suction-dried, epoxy-activated agarose (25 g), prewashed with 0.2 M NaHCO<sub>3</sub>, was added to 75 ml of 0.2 M NaHCO<sub>3</sub> (pH 8.5), then 0.5 g NaBH<sub>4</sub> was added gradually to 25 ml of 0.2 M NaHCO<sub>3</sub> containing 1 g of aminoethanethiol. After adjusting the pH to 8.5, the aminoethanethiol solution was added to the stirred gel suspension. After a total reaction time of 15 h at room temperature, the slurry was washed with deionized water, ethanol and again with deionized water on a sintered-glass filter. The ligand concentration was found to be 832 and 922  $\mu\text{mol}$  per gram of dried product, as calculated from the sulphur and nitrogen content, respectively.

(VIII) *3-(2-Hydroxyethylthio)-2-hydroxypropylagarose (OH-et-S-gel)*. Suction-dried, epoxy-activated agarose (25 g), prewashed with 0.1 M sodium phosphate buffer (pH 7.5), was added to 50 ml of 0.1 M sodium phosphate buffer (pH 7.5), then 20 ml of mercaptoethanol were added to the stirred gel suspension. After a total reaction time of 21 h at room temperature, the slurry was washed with deionized water, ethanol and again with deionized water. The ligand concentration was found to be 881  $\mu\text{mol}$  per gram of dried product, as calculated from the sulphur content.

(IX) *3-(N-Pyridyl-2-one)-2-hydroxypropylagarose (PyO-gel)*. The gel was prepared according to ref. 9, except that the reaction time was 3 h. The ligand concentration was found to be 729  $\mu\text{mol}$  per gram, as calculated from the nitrogen content.

### *Analytical procedures*

Nitrogen and sulphur analyses were performed by Microkemi (Uppsala, Sweden). The effluent from the chromatographic column was monitored at 280 nm on an Ultrospec II Biochrom spectrophotometer (LKB, Bromma, Sweden). Electrophoretic analyses of the pooled and concentrated fractions were performed in slabs of 4–30% polyacrylamide gradient gel according to the manufacturer's manual (Pharmacia). Serum proteins were immunologically identified by the conventional Ouchterlony technique, using monospecific antibodies against  $\alpha_2$ -macroglobulin, orosomucoid, hemopexin, IgG, IgA, IgM, albumin, prealbumin, transferrin,  $\alpha_1$ -antitrypsin, ceruloplasmin, haptoglobin, chymotrypsin, C3 and C4. The concentration of human serum albumin in the pooled fractions was determined by conventional immunological methods, such as radioimmunoassay (RIA) or enzyme-linked immunosorbent assay (ELISA). Chromatography was performed according to standard procedures by use of a fast procedure liquid chromatographic (FPLC) system from Pharmacia, equipped with a programmable LCC-500 control unit.

### *Thiol and disulphide content in the prepared agarose derivatives*

*Disulphide determination.* To a glass test-tube, 0.1 g of freeze-dried product of the respective gel and 5 ml of 50 mM dithioerythritol (DTE) in 0.1 M Tris buffer (pH 7.5) were added. After a total reaction time of 180 min at room temperature, the gel was suction-dried on a glass filter and the absorbance of the eluate was measured at 343 or 324 nm against a blank solution, consisting of 50 mM DTE in 0.1 M Tris buffer (pH 7.5). The concentration and amount of mercaptopyridine released from the gel were calculated by use of molar absorptivity of  $0.71 \cdot 10^4 \text{ l mol}^{-1}$  for 2-mercaptopyridine<sup>10</sup> and  $1.98 \cdot 10^4 \text{ l mol}^{-1} \text{ cm}^{-1}$  for 4-mercaptopyridine<sup>10</sup>.

*Thiol determination.* To a glass test tube, 0.1 g of the respective freeze-dried gel and 5 ml of 5 mM 2,2-dipyridyl disulphide in 0.1 M Tris buffer (pH 8.1) were added. After a total reaction time of 180 min at room temperature, the gel was suction-dried on a glass filter and the absorbance of the eluate was measured at 343 nm against a blank solution consisting of 5 mM 2,2-dipyridyl disulphide in 0.1 M Tris (buffer (pH 8.1).

### *MO calculations*

The electron distribution in the investigated molecules was calculated at the Department of Quantum Chemistry, University of Uppsala, by use of an Alliant FX 80 computer at the Faculty of Sciences (University of Uppsala) and a program, SCF/MO SCF Sirius, developed by Jensen and Ågren<sup>11,12</sup>. *Ab initio* MO wave functions were derived for the three molecules, using standard minimal basis sets of contracted Gaussian orbitals (STO/4G). All computations were carried out using the parameters published for 2-hydroxypyridine in ref. 13, for 2-mercaptopyridine in ref. 14 and for 2-aminopyridine in ref. 15. The coordinates for the last two molecules were transformed to the orthorhombic system. The coordinates for the hydrogens in 2-mercaptopyridine were calculated by use of a bond length of 1.738 Å and the same Z-coordinate as the corresponding carbon.

### *Chromatography*

A  $10 \times 1 \text{ cm}$  I.D. column was packed with the test gel to obtain a bed volume

of 4.6–4.7 ml, while maintaining a flow-rate of  $50 \text{ ml/cm}^2 \cdot \text{h}$  during the sedimentation. The column was equilibrated with  $0.1 \text{ M}$  Tris buffer (pH 7.5), containing  $0.5 \text{ M}$   $\text{K}_2\text{SO}_4$ . Potassium sulphate was added to the sample to a final concentration of  $0.5 \text{ M}$ . A  $500\text{-}\mu\text{l}$  sample (containing  $68 \text{ mg protein/ml}$ ) of centrifuged human serum (a pool of fifteen different serum samples) was applied to the column. A pump (P-500; Pharmacia) maintained a flow-rate of  $25 \text{ ml/cm}^2 \cdot \text{h}$  via an injection valve (V7; Pharmacia), equipped with a  $500\text{-}\mu\text{l}$  sample loop. The chromatographic procedure was programmed by use of a LCC-500 control unit (Pharmacia). The experiments were performed at room temperature. Fractions of  $5 \text{ ml}$  were collected. The adsorbed material was eluted from the column in three successive desorption steps: the first with  $0.1 \text{ M}$  Tris (pH 7.5), the second with 40% (v/v) ethylene glycol in  $0.1 \text{ M}$  (pH 7.5) and the third with 30% (v/v) 2-propanol in  $0.1 \text{ M}$  Tris (pH 7.5).

## RESULTS

Nine different types of ligands have been studied in order to clarify the effect of one essential factor in the adsorption process, the ligand structure. In two earlier studies<sup>9,16</sup> we investigated 2-(N-pyridyl-2-one)-2-hydroxypropyl-, 3-(phenylthio)-2-hydroxypropyl-, 3-(phenyloxy)-2-hydroxypropyl- and 3-(2-pyridyldisulphanyl)-2-hydroxypropylagarose. The effect of the pyridine nucleus in combination with the exocyclic sulphur in gel preparation IV (see Fig. 1) was investigated by replacing the pyridine nucleus with alkylmercaptans of different length (gel preparations V and VI) and alkylmercaptans with hydroxyl or amino groups as functional groups (gel preparations VII and VIII). The role of the exocyclic sulphur in gel preparation IV was investigated by replacing sulphur with nitrogen (gel preparation I) or oxygen (gel preparation IX) (see Fig. 1). The cooperative effect between the exocyclic sulphur and nitrogen in pyridine was investigated by comparing the adsorption on gel preparations III and II with the adsorption on gel preparation IV. We shall now classify all the investigated structures according to their ability to absorb proteins, especially immunoglobulins, in the presence of  $0.5 \text{ M}$   $\text{K}_2\text{SO}_4$  and at a ligand concentration of about  $800 \mu\text{mol S}$  per gram of dried product.

### *Ligand structure vs. protein adsorption*

Of nine ligands investigated, four can adsorb significant amounts of proteins, which can also be desorbed. All of the adsorbing ligands contain sulphur, but sulphur is effective as an adsorption promoter only when combined with either a fully aromatic ring, as in thiophenol, with a less aromatic ring, such as pyridine, or with an unsubstituted alkyl group with a chain length of at least two carbon atoms without hydroxyl or amino groups as functional groups (see Table I).

Simultaneous adsorption of immunoglobulins and a minor amount of albumin is possible only with gel preparations II and IV. When the pyridine nucleus is replaced by an alkyl chain, at least two carbon atoms long, the albumin will be adsorbed preferentially, and the amount of albumin adsorbed will increase from 0.28% of the total applied albumin to 11.5% for ethanethiol- and 18% for butanethiol-derivatized gels (see Table I and Fig. 2).

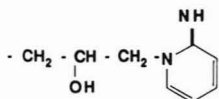
TABLE I  
DISTRIBUTION OF PROTEINS IN THE CHROMATOGRAPHIC FRACTIONS ON GELS I-IX AFTER CHROMATOGRAPHY IN THE PRESENCE OF 0.05 M  $K_2SO_4$ -0.1 M TRIS (pH 7.5)

Fractions	Recovery (%) in $A_{280}$ units								
	I	II	III	IV	V	VI	VII	VIII	IX
Non-adsorbed fractions	99.4	70.0	92.2	53.0	32.8	78.8	102	103.0	95.5 <sup>a</sup>
Desorbed by deleting $K_2SO_4$	0 <sup>b</sup>	16.4	0 <sup>c</sup>	35.9	48.4	12.8	—	0 <sup>c</sup>	1.4 <sup>a</sup>
Desorbed with ethylene glycol	0 <sup>c</sup>	1.0	0 <sup>c</sup>	1.0	11.8	0 <sup>c</sup>	—	0 <sup>c</sup>	0 <sup>c</sup>
Desorbed with 2-propanol	0 <sup>c</sup>	0 <sup>c</sup>	—	—	0 <sup>c</sup>	5.3	—	0 <sup>c</sup>	0 <sup>c</sup>
% of the totally applied proteins still on the gel <sup>c</sup>	1.1	3.7	2.4	3.7	0.4	1.3	0.4	0.4	—
Total	100.5	91.1	94.6	93.6	93.4	98.5	102.5	103.4	96.9

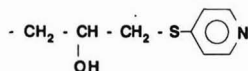
<sup>a</sup> Results obtained by amino acid analyses.

<sup>b</sup> The registered value has an absorbance  $<0.5$ .

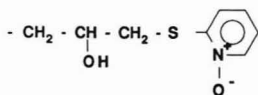
<sup>c</sup> The registered values have absorbance  $<0.1$ .



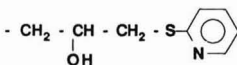
I: 3 - ( N - 2 - iminopyridyl ) - 2 - hydroxypropyl



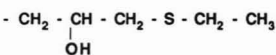
II: 3 - ( 4 - pyridylthio ) - 2 - hydroxypropyl



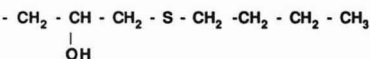
III: 3 - ( 2 - pyridylthio - N - oxide ) - 2 - hydroxypropyl



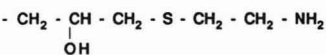
IV: 3 - ( 2 - pyridylthio ) - 2 - hydroxypropyl



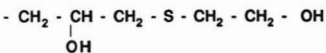
V: 3 - ( ethylthio ) - 2 - hydroxypropyl



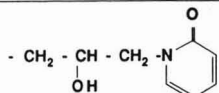
VI: 3 - ( n - butylthio ) - 2 - hydroxypropyl



VII: 3 - ( 2 - aminoethylthio ) - 2 - hydroxypropyl



VIII: 3 - ( 2 - hydroxyethylthio ) - 2 - hydroxypropyl



IX: 3 - ( N - 2 - pyridyl - 2 - one ) - 2 - hydroxypropyl

Fig. 1. Structures of the ligands in the prepared agarose gels.

*Synthesis of mercaptopyridine gel derivatives*

In the synthesis of mercaptopyridine gel derivatives, several problems must be defined and solved. The mercaptopyridines tend to become oxidized, and the resulting product, 2,2'-dipyridyl disulphide or 4,4'-dipyridyl disulphide, can also react with

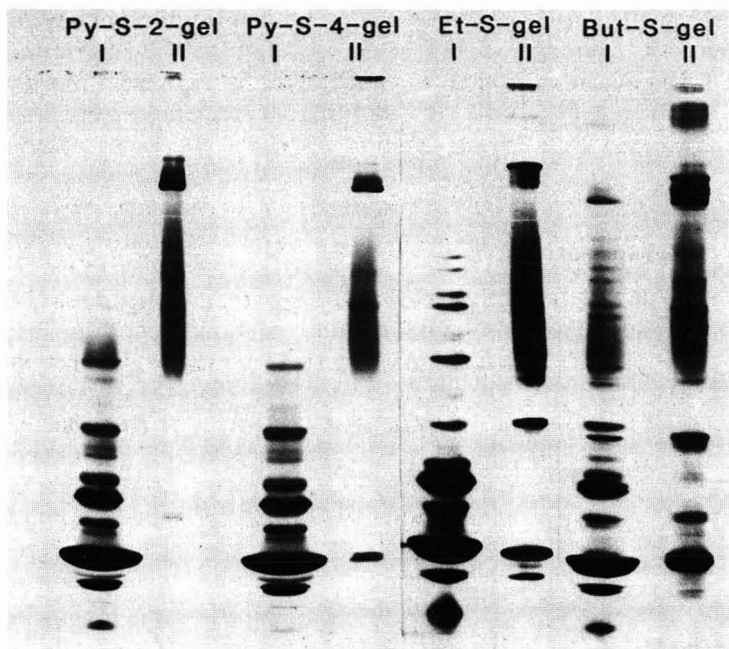


Fig. 2. Gel electropherogram of human serum that had passed the chromatographic bed of the adsorbent (I) and the material that was eluted deleting  $K_2SO_4$  from the buffer (II).

oxirane to yield a ligand having an undesired structure (Fig. 3). Therefore, a thiol-disulphide exchange reaction should, if possible, be avoided, as should also the formation of a mixture of ligands, caused by simultaneous coupling to both nitrogen and sulphur. The first problem was minimized by using  $NaBH_4$  and a nitrogen atmo-

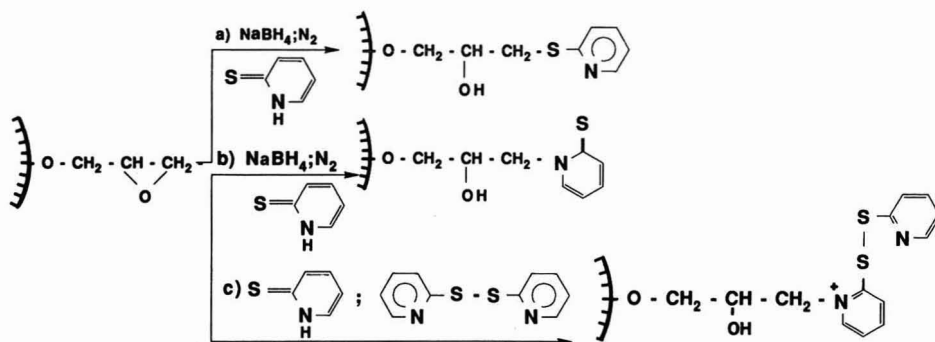


Fig. 3. Three possible pathways for the reaction of oxirane structures on the agarose with mercaptopyridine. (a) In the presence of  $NaBH_4$  and in a nitrogen atmosphere the undesired disulphide structures are minimized. (b) The presence of two nucleophilic centres in the mercaptopyridine molecule can result in a coupling of the mercaptopyridine via the nitrogen atom instead of the exocyclic sulphur, as in reaction pathway (a). (c) In the absence of  $NaBH_4$  and in air in the presence of 2,2-dipyridyl disulphide in the reaction mixture, a mixture of reaction products can result from either pathway (a) or (b) together with the undesired disulphide product.

sphere during the synthesis. With gel preparation II (Fig. 1), the protein remaining on the gel after desorption was reduced from 13.6 to 1.6%, and for gel preparation IV (Fig. 1) from 6.8 to 1.5%, after a final reduction of proteins on the gel with DTE, followed by amino acid analyses of these gels. The second problem has been investigated, and coupling will occur only via sulphur<sup>17</sup>.

*Determination of the amount of thiol and disulphide groups on the agarose derivatives*

To complement the above-mentioned analyses, the thiol concentration in the prepared gels was also determined according to a modified version of the method of Grassetti and Murray<sup>10</sup>. The thiol content was found to be low for gel preparation IV (see Table II) but was about five times higher for gel preparation II. The possible presence of disulphides in gel preparations II and IV was investigated by reduction with DTE, followed by spectrophotometric detection of released 2-mercaptopyridine and 4-mercaptopyridine at 343 and 324 nm, respectively. Two gel preparations of 3-(2-pyridylthio)-2-hydroxypropyl- (gel preparation IV) and two of 3-(4-pyridylthio)-2-hydroxypropylagarose (gel preparation II) were compared. Preparations 2 and 4 were performed under nitrogen in the presence of NaBH<sub>4</sub> and show the lowest disulphide content. In order to minimize the disulphide content, it is therefore necessary both to include NaBH<sub>4</sub> and to exclude oxygen.

*Molecular orbital calculation of the electron distribution in the ligands calculated by an MO method*

The results (Fig. 4) obtained on calculation of the electron distribution show that the electron excess is of nearly the same magnitude in the three molecules and is concentrated on the exocyclic atom and the pyridine nitrogen. 2-Mercaptopyridine has a lower electron density in the ring ( $-0.40$  electrons) compared with 2-hydroxypyridine ( $-0.03$  electrons) and 2-aminopyridine ( $-0.05$  electrons). These figures were obtained by summing the calculated electron density values contributed by the different atoms in the ring. These figures were subtracted from the sum of electron in the ring, where each carbon contributes six electrons, nitrogen seven electrons and hydrogen one electron.

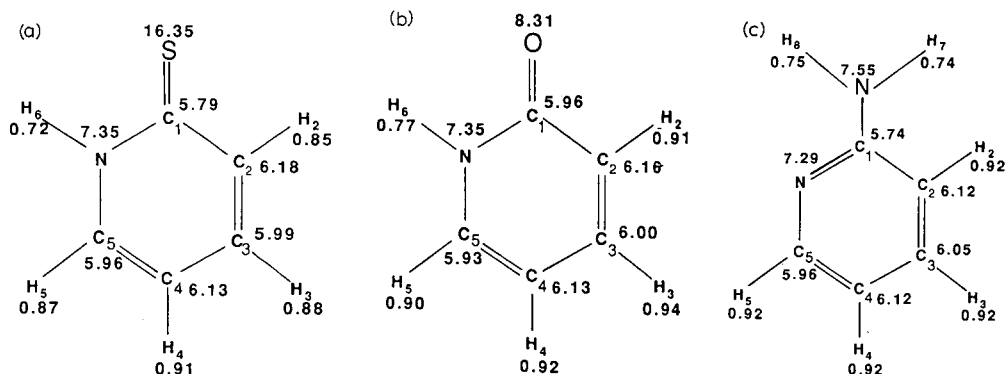
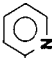



Fig. 4. Calculated electron densities (SCF/MO SCF Sirius) for (a) 2-mercaptopyridine, (b) 2-hydroxypyridine and (c) 2-aminopyridine. The value for each respective atom represents the total number of electrons.

TABLE II  
CONTAMINATION OF THIOL<sup>a</sup>- AND DISULPHIDE<sup>b</sup>-CONTAINING LIGANDS IN GEL PREPARATIONS II AND IV

Main ligand and preparation		Total ligand concentration ( $\mu\text{mol S/g}$ dried product)	Preparation method	$\mu\text{mol thiol/g}$ dried product	Thiol groups in total ligand (%)	$\mu\text{mol disulphide groups/g}$ dried product	Disulphide groups in total ligand (%)
Ligand:	$-\text{CH}_2-\underset{\text{OH}}{\text{CH}}-\text{CH}_2-\text{S}-$ 						
1	Prep. No.:	909	$\text{NaBH}_4$	1.9; 2.1 <sup>c</sup>	0.21; 0.23	4.78; 1.71 <sup>c</sup>	0.53; 0.19 <sup>c</sup>
2		653	$\text{NaBH}_4$ , $\text{N}_2$ atmosphere	0.5	0.08	1.24	0.19
Ligand:	$-\text{CH}_2-\underset{\text{OH}}{\text{CH}}-\text{CH}_2-\text{S}-$ 						
3	Prep. No.:	896	$\text{NaBH}_4$	3.0	0.33	3.2; 3.7 <sup>c</sup>	0.36; 0.41 <sup>c</sup>
4		718	$\text{NaBH}_4$ , $\text{N}_2$ atmosphere	3.3	0.45	0.58	0.08

<sup>a</sup> The number of thiol groups determined by reaction between the agarose derivatives and 2,2'-dipyridyl disulphide.

<sup>b</sup> The number of disulphide groups determined as released 2-mercaptopyridine and 4-mercaptopyridine when reduced with 5 mM DTE.

<sup>c</sup> Mean of two determinations.



TABLE III

## PROTEINS ADSORBED ON Py-S-2-, Py-S-4-, Et-S- AND Bu-S-GELS

The serum sample was applied to the column in the presence of 0.5 M K<sub>2</sub>SO<sub>4</sub>-0.1 M Tris. After elution of the proteins not adsorbed on the gel, the column was desorbed by deleting K<sub>2</sub>SO<sub>4</sub> from the buffer. These fractions were collected, and the amounts of IgG and HSA were determined. For Ouchterlony analysis, the pooled fractions were concentrated to an  $A_{280}$  value of 1.0.

<i>Gel type</i>	<i>Preparation No.</i>	<i>Amount of HSA (μg)</i>	<i>Identified components (major components in italics)</i>
Py-S-2-	IV	65	albumin, <i>IgG</i> , $\alpha_2$ -macroglobulin, <i>IgA</i> , C3, C4, <i>IgM</i>
Py-S-4-	II	42	albumin, C3, C4, $\alpha_2$ -macroglobulin, <i>IgG</i> , <i>IgA</i>
Et-S-	V	2880	<i>albumin</i> , C4, <i>IgA</i> , $\alpha_1$ -antitrypsin, C4, $\alpha_2$ -macroglobulin, <i>IgG</i> , chymotrypsin
Bu-S-	VI	4550	$\alpha_2$ -macroglobulin, <i>IgG</i> , <i>IgA</i> , <i>albumin</i> , $\alpha_1$ -antitrypsin, C3, C4

## DISCUSSION

In our first publication on the pyridine agarose gels<sup>9</sup>, we pointed out that the ligands studied could be arranged in order of increasing hydrophobicity. The mercaptopyridine-derivatized gel was found to be weakly hydrophobic. A relationship seems to exist between the water solubility of the ligand-forming substances (their degree of hydrophilicity or hydrophobicity) and adsorption capacity of the type of protein being adsorbed. This is confirmed by the results obtained for the ligands studied here. The ligand affinity for proteins can be arranged in order of decreasing water solubility. 2-Mercaptopyridine and 4-mercaptopyridine are more hydrophilic than thiophenol. The thiophenol gel therefore adsorbs comparatively more albumin per ligand equivalent, and the electrophoretic pattern of the adsorbed proteins is different and more complex. Albumin adsorption on the thiophenol gel reflects the fact that the hydrophobicity of the thiophenol ligand is higher than that of the pyridylsulphido group.

When the pyridine nucleus in gel preparation IV is replaced by alkylthioethers, such as ethanethiol or butanethiol, the hydrophobicity of gel preparations V and VI increases, and consequently also the albumin adsorption (Table III). The introduction of functional groups, such as hydroxyl or amino, into the alkylthioethers (gel preparations VII and VIII) lowers the hydrophobicity of the ligands and consequently the capacity to adsorb proteins.

If mercaptopyridine in 3-(2-pyridylthio)-2-hydroxypropyl agarose (preparation IV) is replaced with aminopyridine (gel preparation I) or hydroxypyridine (gel preparation IX) or oxygen, the adsorption capacity is drastically reduced (see Table I).

In an attempt to investigate the factors responsible for the different adsorption capacities for the pyridine derivatives, the following parameters were investigated: (1) the sites of attachment of the pyridine nucleus to the matrix; (2) the hydrophobicity, and (3) the difference in electron distribution between the mercaptopyridine derivative and the distribution in 2-amino- and 2-hydroxypyridine derivatives.

The exact position of attachment of the pyridine derivatives (amino-, thio- and hydroxypyridines) to the epoxide groups on agarose has been determined. These results<sup>17</sup> show that amino- and hydroxypyridine (gel preparations I and IX, respectively) are attached only via the pyridine nitrogen, whereas mercaptopyridine is attached only via the sulphur (see Fig. 1). During the isolation of synthesized model substances of pyridine derivatives by flash chromatography, the relative hydrophobicities of the different pyridine derivatives could be compared, as the solvent used for elution of the different pyridine derivatives from the silica in flash chromatography reflects the hydrophobicity of the substances. The aminopyridine derivative could be eluted with methanol, whereas the mercapto- and hydroxypyridine derivatives could be eluted with diethyl ether. These results clearly show that there is no difference in hydrophobicity between the hydroxypyridine and mercaptopyridine derivatives.

The arylthioether gels treated here are only weakly hydrophobic in nature, as shown by their extremely low affinity for serum albumin. However, it is evident that the pyridine adsorbents possess affinity properties of a different kind (Table III). It is possible that they are electron donor to acceptor adsorbents<sup>18</sup>. Clearly, therefore, it is of interest to know the electron distribution over the ligands. The results of *ab initio* calculations have revealed a deficit of electrons on the pyridine-S-gels. It is highly unlikely that the water medium would convert the ligand properties to those of an electron donor. Admittedly, neglecting the influence of water in the calculation is a weakness in our attempt to formulate the basis for a theory, but that weakness is shared with application of quantum mechanics in other areas. As a parallel to our attempts to apply calculations of electron distributions in the gas phase to experimental results obtained in solution at room temperature, we can refer to results where the chemical shift value obtained from NMR studies in solution at room temperature shows a good correlation with the electron density calculated for the corresponding atom in the gas phase<sup>19,20</sup>.

Unsubstituted pyridine nitrogen is a prerequisite for the characteristic protein affinity, as is also demonstrated by the properties of gel preparations I and IX.

#### ACKNOWLEDGEMENTS

We thank Dr. Hans Ågren, Department of Quantum Chemistry, for all his support, advice and valuable discussions, Mr. David Nordfors at the same department for his technical support with the computer, Mrs. Marie Sundqvist at our Institute for excellent technical assistance and Dr. David Eaker for critical and linguistic revision of this work.

We are grateful to the Swedish Board for Technical Development and Pharmacia-LKB for financial support.

#### REFERENCES

- 1 S. Hjertén, J. Rosengren and S. Pählman, *J. Chromatogr.*, 101 (1974) 281–288.
- 2 J. Rosengren, S. Pählman, M. Glad and S. Hjertén, *Biochim. Biophys. Acta*, 412 (1975) 51–61.
- 3 J. Porath and K. Dahlgren Caldwell, *J. Chromatogr.*, 133 (1977) 180–183.
- 4 J. Porath and B. Larsson, *J. Chromatogr.*, 155 (1978) 47–68.
- 5 J. M. Egly and J. Porath, *J. Chromatogr.*, 168 (1978) 35–47.
- 6 M. A. Vijayalakshmi and J. Porath, *J. Chromatogr.*, 177 (1979) 201–208.

- 7 G. Halperin, M. Breitenbach, M. Tauber-Finkelstein and S. Shaltiel, *J. Chromatogr.*, 215 (1981) 211–228.
- 8 J. Porath, F. Maisano and M. Belew, *FEBS Lett.*, 185 (1985) 306–310.
- 9 J. Porath and S. Oscarsson, *Makromol. Chem., Macromol. Symp.*, 17 (1988) 359–371.
- 10 D. R. Grasseti and J. F. Murray, *Arch. Biochem. Biophys.*, 119 (1967) 41–49.
- 11 H. J. Aa. Jensen and H. Ågren, *Chem. Phys. Lett.*, 110 (1984) 170.
- 12 H. J. Aa. Jensen and H. Ågren, *Chem. Phys.*, 104 (1986) 229.
- 13 B. R. Penfold, *Acta Crystallogr.*, 6 (1953) 591–600.
- 14 B. R. Penfold, *Acta Crystallogr.*, 6 (1953) 707–713.
- 15 M. Chao, E. Schempp and R. D. Rosenstein, *Acta Crystallogr. Sect. B.*, 31 (1975) 2922–2924.
- 16 S. Oscarsson and J. Porath, *Anal. Biochem.*, 176 (1989) 330–337.
- 17 A. Gogoll and S. Oscarsson, *Heterocycles*, submitted for publication.
- 18 J. Porath, in T. W. Hutchens (Editor), *Protein Recognition of Immobilized Ligands, UCLA Symp.*, Vol. 80, Alan R. Liss, New York, 1989, pp. 101–122.
- 19 K. Konishi and K. Takahashi, *Bull. Chem. Soc. Jpn.*, 50 (1977) 2512–2516.
- 20 M. Witanowski, T. Saluvere, L. Stefaniak and G. A. Webb, *Mol. Phys.*, 23 (1972) 1071–1081.



CHROM. 21 986

## NEW LATEX-BONDED PELLICULAR ANION EXCHANGERS WITH MULTI-PHASE SELECTIVITY FOR HIGH-PERFORMANCE CHROMATOGRAPHIC SEPARATIONS

JOHN R. STILLIAN\* and CHRISTOPHER A. POHL

*Dionex Corporation, 1228 Titan Way, P.O. Box 3603, Sunnyvale, CA 94088-3603 (U.S.A.)*

---

### SUMMARY

A new polymeric “multi-phase” chromatographic packing material that combines ion exchange in a pellicular format with adsorption and ion-pair retention on a neutral macroporous core bead is described. The material is stable from pH 0 to 14 and from 1 to 100% (v/v) of common reversed-phase solvents in aqueous mixtures. The ability to independently control ion exchange and adsorption or ion-pair retention is demonstrated on a variety of inorganic and organic analytes.

---

### INTRODUCTION

In 1973 Horváth wrote “Ion-exchange resins are particularly suitable stationary phases because of their versatility and stability. Although their application has been mostly aqueous systems, it is not so restricted, and it is safe to say that ion-exchange resins represent the most universal class of stationary phases in liquid chromatography. The favorable chromatographic properties of ion-exchange resins are enhanced by the pellicular structure, although at the cost of reduced column loading capacity”<sup>1</sup>. Some of the most successful ion chromatography columns today are pellicular. To realize their full potential for liquid chromatography, they lack only solvent compatibility. This limitation of current pellicular ion-exchange materials is related to the low cross-link of the core bead polymer. Traditionally ion chromatography applications were entirely aqueous and low cross-linked materials were adequate. As ion chromatography progressed to organic ion problem solving, the need for a solvent amenable ion-exchange packing material became obvious. In the process of developing solvent-stable pellicular ion-exchange materials a new type of “multi-phase” material, that combines the features of a pellicular ion-exchange phase with the features of high-adsorption surface area of reversed phase on the same packing material, was developed. A multi-phase material provides multiple modes of retention during the separation process, including ion exchange, ion pair when a “pairing agent” is added, and adsorption retention. This paper will describe the new multi-phase material, will describe some of the effects of different solvents on ion-exchange selectivity and will postulate on mechanisms of retention during multi-mode separations.

## BACKGROUND

Pellicular ion-exchange materials have come to be recognized as materials that have a relatively inert core with a thin layer or "skin" of active ion-exchange material applied to the outer surface. This ion-exchange layer is fully functionalized and is applied either as an encapsulating layer, where there is no physical attachment of the active layer to the core, or as a layer that is electrostatically bonded to the core and usually takes the form of latex beads. Pellicular materials are desirable over fully functionalized gel ion-exchange materials because capacity is controlled allowing reasonable eluent ionic concentrations. They are also chromatographically more desirable because the pellicular layer guarantees a much shorter analyte diffusion path allowing column efficiencies approaching that of reversed-phase columns.

Until Small and Stevens<sup>2</sup> made the first electrostatically agglomerated pellicular ion-exchange materials in the 1970s<sup>2</sup>, encapsulation techniques developed in the 1960s<sup>3</sup> were the only method known for making pellicular ion-exchange materials. Encapsulation techniques, however, suffer from non-reproducible thickness of the pellicular layer and delamination of the pellicular layer as a result of shrinking and swelling of the pellicular layer with use. Encapsulation is nonetheless a viable pellicular ion-exchange packing. Recently a pellicular cation-exchange column, based on encapsulation, for the analytical determination of alkali metals and alkaline earths, was introduced<sup>4</sup>. Fig. 1a is a schematic of an encapsulated pellicular ion exchanger. Methods for making surface functionalized anion and cation polystyrene-divinylbenzene (PS-DVB) "pseudo" pellicular ion exchangers have also been known for some time, but these had poor analytical performance, because swelling, due to hydration of the sulfonated or aminated sites in the surface functionalized layer, was non-uniform. This non-uniform swelling was a result of a high to low gradient of functional sites with respect to depth.

### *Electrostatic agglomeration*

Most of the ion chromatography columns in use today are electrostatically latex-coated pellicular ion exchangers. These materials consist of three regions: (1) an inert PS-DVB core, (2) a shallow sulfonated layer on the surface of the inert core, (3) a mono-layer coating of colloidal ion-exchange particles which are permanently attached to the oppositely charged, functionalized surface of the inert core. The latex coating consists of fully functionalized anion-exchange latex particles made from vinylbenzylchloride (VBC) polymer cross-linked with DVB and fully functionalized with an appropriate tertiary amine for desired anion-exchange selectivity<sup>5,6</sup>. Fig. 1b is a schematic representation of an electrostatically agglomerated ion-exchange packing.

Ion-exchange materials prepared by electrostatic agglomeration have several distinct advantages over the encapsulated materials. First, agglomerates are easily prevented during the attachment process using electrostatic agglomeration since the core beads and the latex beads are polymerized independently and any agglomerates can be removed by filtration before the attachment step. Phase thickness is also easily controlled because only a mono-layer of essentially mono-disperse latex beads can be attached. Therefore phase thickness and uniformity is controlled by the latex bead diameter. Because the latex is fully functionalized, column capacity increases as latex

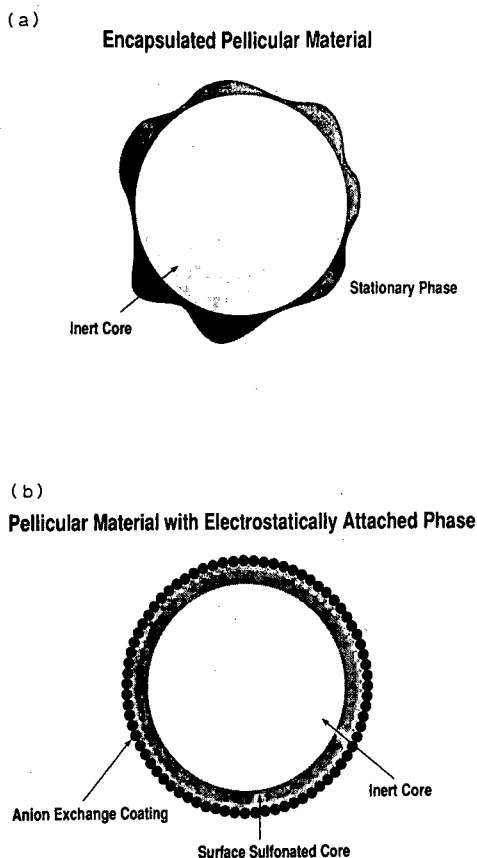


Fig. 1. (a) Schematic of an encapsulated pellicular ion-exchange packing. (b) Schematic of an electrostatically agglomerated latex-coated pellicular ion exchanger.

diameter increases, so latex diameter is also used to control column capacity. The diameters of the different latexes that are commonly used range from 50 to 500 nm and column capacity ranges from 5 to 150  $\mu\text{equiv./column}$ . Because the core beads and latex beads are independently manufactured and brought together only at the last steps of making a column, each can be subjected to independent quality control in their manufacture. This provides very reproducible pellicular ion-exchange materials, with respect to capacity and selectivity, and greatly improves manufacturing efficiency. The electrostatic forces of adhesion are so strong that it is virtually impossible to separate the two phases. Theoretically there can be as many as several hundred electrostatic bonds holding a single aminated latex bead to the surface sulfonated core bead. Finally, the surface of the functionalized core has the same charge as that of the analyte. This means the analyte is effectively excluded from the core, thus concentrating analytes in the active pellicular layer, maintaining chromatographically favorable short diffusion paths into and out of the stationary phase. This is analogous to the very hydrophilic core of  $\text{C}_{18}$  derivatized silica which excludes hydrophobic analytes from the core in reversed-phase high-performance liquid chromatography (HPLC).

Electrostatic agglomeration has two major disadvantages. The latex functionalization chemistry must be aqueous compatible to maintain the aqueous latex suspension prior to agglomeration. This effectively limits available chemistries to rather hydrophilic reagents. Also the functional groups on the surface of the inert core can also interact with sample components causing chromatographic anomalies. For example, transition metals in the sample matrix can concentrate on the residual cation-exchange sites and result in the complexation or precipitation of analyte ions such as phosphate and sulfate on subsequent injections.

## EXPERIMENTAL

### *Instrumentation*

The chromatographic system used for all chromatograms shown was a Dionex 4500i gradient ion chromatograph (Dionex, Sunnyvale, CA, U.S.A.) equipped with 0.010 in. I.D., 0.063 in. O.D. polyetherether ketone (PEEK) tubing on the high-pressure side of the analytical pump. The instrument was equipped with a conductivity detector (Dionex CDM-II) and a multi-wavelength UV-VIS detector (Dionex CDM-II). A helium headspace was maintained on the eluents with a Dionex eluent degas module (EDM-II). The ion chromatograph was interfaced to a Dionex AutoIon 450 data system. The AutoIon 450 is an IBM-compatible computer system with software for complete system control, data collection and data reprocess that is written within the Microsoft Windows operating environment.

### *Columns*

The ion-exchange columns used are the Dionex OmniPac™ PAX-100, OmniPac PAX-500 and the Hamilton PRP™-X100 (Hamilton, Reno, NV, U.S.A.). Both Dionex columns are 250 mm × 4 mm I.D. These columns are latex-coated pellicular anion-exchange columns. The substrate is 8- $\mu$ m diameter particles made from ethylvinylbenzene (EVB) cross-linked with > 50% DVB. The PAX-100 is made with a microporous substrate with no significant adsorption surface area and is strictly a solvent compatible anion-exchange column. The substrate for the PAX-500 is macroporous with approximately 300 m<sup>2</sup>/g of adsorption surface area and 60-Å pores. The latex for both columns is approximately 60 nm in diameter, fully quaternized, polyVBC, cross-linked with 4% DVB. Both column types have the same ion-exchange selectivity and average 40  $\mu$ equiv./column ion-exchange capacity. Because it is macroporous the PAX-500 packing is a less dense material and measures approximately 25  $\mu$ equiv./g whereas the microporous PAX-100 packing has approximately 16  $\mu$ equiv./g ion-exchange capacity.

The Hamilton PRP-X100 is a surfaced quaternized (trimethylamine) macroporous PS-DVB 10  $\mu$ m packing in 250 mm × 4.6 mm I.D. column and has approximately 200  $\mu$ equiv./g ion-exchange capacity<sup>7</sup>. The column used measured 580  $\mu$ equiv./column ion-exchange capacity.

Ion-pair chromatography was performed on a 250 × 4 mm I.D. Dionex Ionpac™ NS1 column packed with 10  $\mu$ m neutral, macroporous EVB-DVB with an average of 300 m<sup>2</sup>/g surface area and an average pore size of 60 Å.

For conductivity detection the system was equipped with a Dionex micromembrane suppressor (AMMS)<sup>8</sup>. A Dionex micromembrane suppressor for Mobile Phase



Ion Chromatography (MPIC<sup>TM</sup>) (AMMS-MPIC) was used if an ion-pair reagent is used in the eluent since the membranes in this suppressor are optimized for transport of the large hydrophobic alkyl quaternary ammonium ion-pair reagents used in ion-pair chromatography. Both the AMMS and the AMMS-MPIC suppressors are compatible with any concentration of acetonitrile, methanol, ethanol, isopropanol and other common reversed-phase HPLC solvents. In all cases the suppressor regenerant solution was 0.02 *N* sulfuric acid, flowing at 10 ml/min using a Dionex AutoRegen system.

### *Reagents*

Sodium hydroxide eluents were made from 50% analytical grade (J. T. Baker, Phillipsburg, NJ, U.S.A.). Sulfuric acid was of J. T. Baker Instra-analyzed grade. Sodium chloride and sodium carbonate were Mallinckrodt (Mallinckrodt, Paris, KY, U.S.A.) analytical-reagent grade. Tetrabutylammonium hydroxide (TBAOH) was MPIC grade 0.1 *M* concentrate from Dionex. Acetonitrile, isopropanol and methanol were Fisher brand "Optima" grade solvents for HPLC (Fisher Scientific, Fair Lawn, NJ, U.S.A.07410).

Substrate resin and latex were polymerized from EVB-DVB and VBC-DVB respectively (Dow, Midland, MI, U.S.A.).

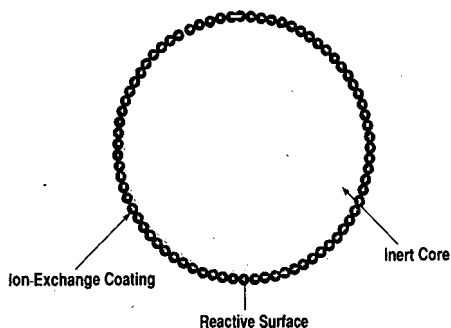
## RESULTS AND DISCUSSION

### *Synthesis*

In this paper we are presenting a new method for latex attachment in order to generate a pellicular ion-exchange material and a new multi-phase column packing made possible by the new latex attachment method. The new pellicular material consists of three regions: (1) a highly cross-linked (> 50%) EVB-DVB polymer, microporous substrate bead which is compatible with all common reversed-phase HPLC solvents, (2) a highly reactive surface on the substrate bead created at the time of polymerization, and (3) an ion-exchange pellicular phase comprised of a polymeric VBC latex cross-linked with DVB that is electrostatically or covalently attached to the inert substrate bead. During manufacture, neutral latex can either be covalently attached to the substrate bead via the reactive surface and subsequently functionalized, or functionalized prior to electrostatic attachment to the substrate bead. As in traditional electrostatic attachment the inert core and the latex are independently polymerized regardless of the attachment mechanism.

The reactive surface on the substrate bead is generated by a proprietary method. During polymerization another polymer is added to the polymerizing solution, and is ultimately incorporated only onto the exterior surface of the substrate bead polymer. The concentration of polymer added controls the density of reactive sites on the surface of the core bead and a very low density of "reactive sites" can be achieved. For example, the added polymer can be chosen that has sulfonate, carboxylate or amine functional groups. These functional groups then allow electrostatic agglomeration of previously functionalized latex beads of opposite charge to the substrate. However, contrary to traditional electrostatic agglomeration, after agglomeration there is no measurable residual ion-exchange capacity on the surface of the substrate bead. This was verified by measuring breakthrough capacity for cation exchange on a

(a)

**Pellicular Material with Covalently Attached Phase**

(b)

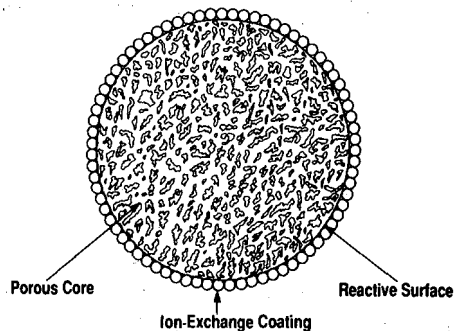
**Multi-Phase Pellicular Material**

Fig. 2. (a) Schematic of a covalently attached, latex-coated pellicular ion exchanger. (b) Schematic of a multi-phase pellicular material with a macroporous substrate and latex ion-exchange coating.

column agglomerated as described. The column was treated with 0.001 *M* LiCl (pH 8 with LiOH) at 1 ml/min for 30 min. Then the column was connected to a pump primed with 0.001 *M* KCl (pH 8 with KOH) and KCl was pumped at 1 ml/min. The effluent was monitored, using direct conductance, until breakthrough of the KCl was indicated by the increase in the effluent conductance. The milliliters of column void volume (previously determined) is subtracted from the total milliliters of KCl to breakthrough. The net milliliters of KCl times the normality of KCl in  $\mu\text{equiv./ml}$  gives  $\mu\text{equiv./column}$  cation-exchange capacity. Using this method the residual cation-exchange capacity was measured for three columns and all three measured less than 1  $\mu\text{equiv./column}$  capacity, below the detection limits of the technique. A column of the same dimensions, made by traditional electrostatic agglomeration, measured 11  $\mu\text{equiv./column}$  residual cation-exchange capacity by the same method. The method as described was used so that there was no interference from anion-exchange selectivity and so that weak and strong acid cation-exchange capacity both were measured.

In a second possibility, the added polymer can be chosen with reactive functional groups allowing covalent attachment of neutral latex beads for agglomeration. The neutral, covalently agglomerated latex beads can then be functionalized after agglomeration allowing non-aqueous functionalization chemistries. Latex can be selectively functionalized in the presence of the core bead polymer by judiciously choosing the latex polymer and functionalization chemistry. For example, if an EVB–DVB substrate is covalently agglomerated with DVB cross-linked polyVBC latex, then the latex can be selectively aminated via traditional amination chemistry. Alternatively the latex can be selectively sulfonated, for example, by first reacting VBC with thiourea in alcohol to generate a thiuronium quaternary amine site, followed by hydrogen peroxide oxidation to a benzyl sulfonate cation-exchange functional group. Neither of these routes generates anion-exchange or cation-exchange groups on the core bead surface because the chemistries are not reactive with EVB–DVB.

This new attachment method has the advantages that no measurable residual ion-exchange sites exist on the substrate bead after agglomeration in either of the new attachment schemes, and latex is attached prior to functionalization in the covalent scheme of latex attachment and therefore functionalization is not limited to aqueous chemistries to maintain a latex suspension as in the traditional electrostatic attachment method. This allows for the possibility of amination with amines with low water solubility and for functionalization with chelating groups where functionalization chemistry is non-aqueous<sup>9</sup>. A schematic of a latex coated, highly cross-linked, microporous resin bead made by the new attachment process is shown in Fig. 2a.

#### *Effect of solvent on ion-exchange selectivity*

The ability to add significant concentrations of solvents, e.g. 1–100% acetonitrile or methanol, to ion-exchange eluents gives the added selectivity control of the influence of solvent on ion exchange. The degree of hydration of the ions in the bulk eluent, and the enthalpy of hydration of a hydrated ion in solution, which determines how easily an ion sheds waters of hydration to become associated with an ion-exchange site and *vice versa*, is a major determining factor in ion-exchange selectivity<sup>10</sup>. Ions that are highly hydrated tend to have shorter retention times than ions of lower hydration. This is generally the argument given for the order of elution of halides by anion exchange<sup>5,6</sup>. Divalent and polyvalent selectivity is generated by the three-dimensional orientation of adjacent ion-exchange sites combined with the degree of hydration of the gel polymer phase<sup>11</sup>. For example, for a particular divalent ion to be retained as a divalent it must find two adjacent fixed ion-exchange sites that are appropriately spaced. Also, these sites must have the right degree of hydration to make it thermodynamically favorable for the divalent ion to shed waters of hydration and become associated with both sites, displacing the co-ions (other analyte ions or eluent ions) which then become fully hydrated in the bulk eluent. Latex cross-linking is one of the three major parameters about the stationary phase that controls ion-exchange selectivity<sup>6</sup>, the other two being the nature of the amine used to generate the quaternary anion-exchange site<sup>6</sup> and the nature of the base polymer of the active ion-exchange layer. Higher latex cross-linking results in higher density of ion-exchange sites (because of the higher polymer density) and therefore, statistically a higher number of sites that will thermodynamically “fit” a particular divalent ion over another divalent ion. Just about everything that affects ion-exchange selectivity is related to the enthalpy of hydration of ions and ion-exchange sites.

Adding a solvent to an ionic eluent disrupts the water structure in the bulk solution and changes the degree of hydration of the ions in solution and the ion-exchange sites in the polymer. The degree to which hydration changes is probably dependent on the degree of hydration in the 100% aqueous solution. Ions that are highly hydrated, *e.g.* have high enthalpies of hydration, tend to hold on to waters of hydration more strongly and will lose fewer waters of hydration than ions that are less hydrated and tend to give up waters of hydration more readily. Protic solvents like alcohols can also affect ionic eluents containing hydroxide by the formation of alkoxide ions.

Fig. 3a, b and c indicate an unexpected affect on the selectivity of ion exchange on a latex-coated pellicular ion exchanger with the addition of solvent. Fig. 3a shows the selectivity of a pellicular ion-exchange material with 4% cross-linked latex with no solvent in the eluent. Fig. 3b shows that by adding 20% (v/v) acetonitrile without changing the ionic concentration of the eluent, the selectivity has greatly changed. This chromatogram is approximately the same as would be seen on a 1% cross-linked latex anion exchanger with a 100% aqueous eluent. The chromatogram in Fig. 3c, generated with 40% acetonitrile in the eluent is equivalent to approximately a 0.25% cross-linked latex with a 100% aqueous eluent. In general, the addition of acetonitrile to the eluent tends to decrease the retention of analytes, apparently by changing (lowering) the "effective" cross-linking of the latex.

Table I is a summary of experiments where the concentration of the ionic component of the eluent (25 mM sodium hydroxide) is kept constant while the nature and concentration of the solvent is varied. The trend for eluent systems in Table I containing increasing amounts of methanol is for steadily increasing the capacity factor,  $k'$ . It might be predicted that adding solvent to a hydroxide eluent would tend to cause increasing retention since hydroxide is a highly hydrated ion and would tend to shed fewer waters of hydration on the addition of a solvent, as compared to other ions in solution or the ion-exchange sites in the polymer. This should tend to decrease the selectivity of the stationary phase ion-exchange sites for the hydroxide eluent ion

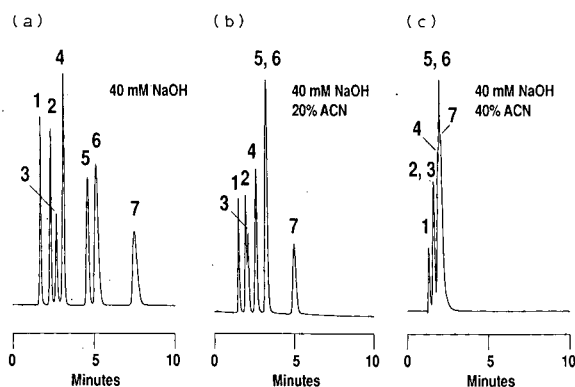


Fig. 3. Effect of acetonitrile on retention with OmniPac PAX-100 multi-phase column. Analytes are: 1 = 1 ppm fluoride; 2 = 2 ppm chloride; 3 = 3 ppm nitrite; 4 = 5 ppm sulfate; 5 = 5 ppm bromide; 6 = 8 ppm nitrate; 7 = 8 ppm phosphate. Flow-rate 1 ml/min; 10- $\mu$ l injection loop; suppressed conductivity 10  $\mu$ S/cm full scale. Eluents as indicated on figures. ACN = Acetonitrile.

TABLE I  
ANALYTE  $k'$  VS. SOLVENT TYPE AND CONCENTRATION ON OMNIPAC PAX-100

Analyte	Solvent	Solvent concentration in 0.025 M sodium hydroxide				
		0%	5%	30%	50%	80%
Fluoride	Acetonitrile	0.05	0.05	0.01	0.01	0.0
	Methanol	0.05	0.03	0.07	0.09	0.15
	Isopropanol	0.05	0.13	0.18	nd	nd
Chloride	Acetonitrile	0.55	0.71	0.38	0.24	0.0
	Methanol	0.55	0.37	0.62	0.79	0.15
	Isopropanol	0.55	1.4	1.1	nd	nd
Nitrate	Acetonitrile	1.1	1.4	1.2	0.56	1.9
	Methanol	1.1	1.2	2.4	5.9	8.4
	Isopropanol	1.1	7.0	3.4	nd	nd
Sulfate	Acetonitrile	2.6	2.4	1.7	1.0	1.9
	Methanol	2.6	2.5	2.4	2.8	2.5
	Isopropanol	2.6	8.8	8.0	nd	nd
Phosphate	Acetonitrile	4.0	3.7	6.0	1.9	1.9
	Methanol	4.0	1.9	5.2	5.9	8.4
	Isopropanol	4.0	>15	>15	nd	nd

causing a general increasing of retention for other ions. Methanol is also a protic solvent and capable of reacting with hydroxide to form a methoxide ion which is generally a weaker eluting ion than hydroxide. Although significant numbers of methoxide ions are usually only formed at high methanol concentrations, the hydrophobic polymer backbone of the ion-exchange latex will tend to concentrate methanol causing higher methanol concentrations in the stationary phase compared to the bulk eluent. The affect of a solvent on the hydration of ions, combined with methoxide formation, probably accounts for methanol containing eluents causing an increase in the  $k'$  of analytes with increasing methanol concentration. Methanol does not appear to change the effective cross-linking of the latex like acetonitrile.

The data in Table I indicate that, of the solvents tested, acetonitrile has the greatest influence on decreasing the  $k'$  values of the test analytes. With 30% acetonitrile added to the eluent there is a significant decrease in  $k'$  values of all the analytes except phosphate, which has increased. The  $k'$  of phosphate ion has probably increased due to the pH change as a result of the addition of acetonitrile to the eluent. The pH of 0.025 M NaOH is 12.4, the "apparent" pH of 0.025 M NaOH in 30% acetonitrile in water measures approximately 12.8, and the last pH of phosphate is 12.36 (at 25°C). By the addition 50% acetonitrile to the eluent, the influence of pH on phosphate is overcome by the selectivity influence of the solvent on the ion-exchange phase and phosphate has a much shorter  $k'$  along with the rest of the test ions. It's interesting that at 80% acetonitrile the  $k'$  actually begins to increase again for nitrate and sulfate.

We hypothesize that the pellicular ion-exchange phase formed by a latex with low cross-linking is probably swollen to a greater extent in an acetonitrile-water

mixture than in water alone. The result of this swelling is lower effective cross-linking since there is just less polymer, and therefore fewer ion-exchange sites, per unit volume of latex. Acetonitrile probably does cause a change in hydration of ions like other solvents but this effect is over-ridden by the swelling effect until high acetonitrile concentrations where the polymer is swollen to its maximum. This may explain the increase in retention for nitrate and sulfate at 80% acetonitrile in Table I.

Isopropanol seems to have the similar effect of reducing retention times for some ions but not for all ions tested. It certainly seems reasonable that the more hydrophobic alcohol isopropanol is capable of swelling the ion-exchange gel polymer to some extent while the more hydrophilic alcohol methanol can not. 5% Isopropanol causes an increase in  $k'$  for all ions tested probably due to the effect of the low dielectric constant of isopropanol on ion exchange<sup>10</sup>. It is also possible that even at only 5% isopropanol there is sufficient isopropanol concentrated in the stationary phase polymer to cause a significant concentration of alkoxide ion formation. With the addition of 30% isopropanol, chloride, nitrate and sulfate all have a lower  $k'$  value than with 5% isopropanol, nitrate showing the greatest change. Fluoride and phosphate, however have increased in  $k'$  at 30% isopropanol. The fact that some ions have increased  $k'$  and some decreased  $k'$  suggests that the effect of isopropanol is not simply swelling but also the competing effect of a solvent on ion hydration and therefore ion-exchange selectivity.

Before the advent of these solvent amenable pellicular ion-exchange packings the only way to change the effective cross-link of a material was to change the synthesis parameters. The ability to control active phase cross-link with the addition of acetonitrile, and ion-exchange selectivity with the addition of other solvents means that separations that previously required several different ion-exchange columns can be performed on one ion-exchange column. Although other types of non-latex-coated ion-exchange columns may be solvent compatible, the only solvent selectivity effect that can be achieved is the influence on the degree of hydration of the ion-exchange site and the analyte, which tends to increase retention.

Table II is a tabulation of  $k'$  values from the Hamilton PRP-X100 anion-exchange column with 0, 5 and 50% acetonitrile, and 0, 5, 50 and 80% methanol in a sodium carbonate eluent using chemically suppressed conductance detection. Note that the retention of ions on the PRP-X100 is generally increasing with increasing acetonitrile concentration. This is different from the effect of acetonitrile on the pellicular latex-coated ion-exchange column where  $k'$  first decreases as the solvent concentration is increased, due to solvent swelling effects on cross-linking, and then  $k'$  tends to increase due to solvent effects on the ion-exchange process directly. Because methanol is a poorer latex swelling solvent, the trend for methanol on the PAX-100 column is the same as the PRP-X100 where the retention of the ions tends to increase due to direct effects of solvent on ion exchange as described earlier.

Carbonate was used as the eluent for the PRP-X100 because this column does not have the hydroxide selectivity the PAX-100 does. The PRP-X100 is designed for use with ionic aromatic eluents commonly used in single column ion chromatography such as potassium phthalate and is therefore too hydrophobic for hydroxide to be an efficient eluent. For this reason  $k'$  changes for analytes on each column cannot be directly compared but trends in  $k'$  values due to solvents used on each column can. 80% acetonitrile selectivity could not be determined on the PRP-X100 because 0.010

TABLE II

ANALYTE  $k'$  VS. SOLVENT TYPE AND CONCENTRATION ON HAMILTON PRP-X100ND = Not determined due to insolubility of 0.010 M Na<sub>2</sub>CO<sub>3</sub> in acetonitrile.

Analyte	Solvent	Solvent concentration in 0.010 M Na <sub>2</sub> CO <sub>3</sub>			
		0%	5%	50%	80%
Fluoride	Acetonitrile	0.65	0.63	0.68	ND
	Methanol	0.65	0.66	0.90	1.5
Chloride	Acetonitrile	2.4	2.6	3.2	ND
	Methanol	2.4	2.4	2.7	4.3
Nitrate	Acetonitrile	15	16	19	ND
	Methanol	15	9.6	13	8.0
Sulfate	Acetonitrile	6.0	7.2	9.3	ND
	Methanol	6.0	6.2	6.5	8.0
Phosphate	Acetonitrile	4.6	5.9	7.8	ND
	Methanol	4.6	4.6	7.3	17

*M* carbonate is not soluble in 80% acetonitrile. To allow the comparison of at least two analytes on both columns under similar eluent conditions fluoride and chloride were chromatographed on the PRP-X100 using 0.040 *M* sodium hydroxide with 30% (v/v) methanol and 0.040 *M* sodium hydroxide with 30% (v/v) acetonitrile. Retention times for fluoride were 5.5 and 6.0 min and for chloride 24.5 and 32.0 min, respectively. Acetonitrile actually seemed to cause slightly longer retention times than methanol on the PRP-X100. Although the PRP-X100 is not a true pellicular ion exchanger as defined earlier, the surface of the resin is fully functionalized and should have a gel-like nature similar to a latex coating. Because the bead is made up of a polymer with very high cross-linking, however, the fully functionalized ion-exchange gel-like surface is resistant to swelling in acetonitrile, unlike the latex coating.

Fig. 4 demonstrates another example of the advantage of using solvent in conjunction with pellicular latex-coated ion-exchange packing. By adding 20% acetonitrile to the eluent, enough to prevent any significant interfering adsorption retention, a mixture of mono- and polyvalent aromatic carboxylates and sulfonates are separated with a simple salt gradient. Sodium hydroxide is added (0.0002 *M* initially) to ensure all the acids are ionized. Sodium hydroxide is increased linearly, along with sodium chloride, to 0.0016 *M* to maintain a constant chloride-hydroxide ratio in the eluent which facilitates a more rapid equilibration of the ion-exchange phase back to initial conditions for the next gradient. When the ratios of different ions of the same valency in the gradient eluent are kept constant throughout the gradient, typical reequilibration times are 5 to 10 min. This is a difficult separation for reversed-phase HPLC and is usually done in the ion-suppression or ion-pair mode, as shown on a NovaPak C<sub>18</sub> column in Fig. 5. The peaks have poorer symmetry in the ion-suppression mode and peak resolution in either chromatogram is not as good as the ion-exchange separation for the same analysis time. Also notice there is a logical order to the elution by ion exchange; monovalents elute first followed by divalents followed by trivalents.

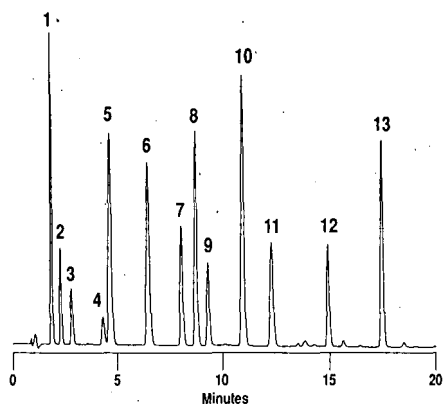


Fig. 4. Separation of aromatic acids on OmniPac PAX-100. Eluent: 20% (v/v) acetonitrile isocratic, 0.050 to 0.40 *M* NaCl gradient in 20 min, 0.0002 to 0.0016 *M* NaOH gradient in 20 min simultaneous with NaCl gradient. Detection: absorbance 254 nm 0.1 AUFS. Peaks: 1 = benzoate; 2 = benzenesulfonate; 3 = toluenesulfonate; 4 = *p*-chlorobenzenesulfonate; 5 = *p*-bromobenzoate; 6 = 3,4-dinitrobenzoate; 7 = phthalate; 8 = terephthalate; 9 = *p*-hydroxybenzoate; 10 = *p*-hydroxy-benzenesulfonate; 11 = gentisate; 12 = trimesate; 13 = pyromellitate.

### Multi-phase packing

In addition to forming conventional pellicular ion-exchange materials, the new covalent attachment method allows the production of an entirely new class of multi-phase materials combining ion-exchange, ion-pair and reversed-phase retention mechanisms. The multi-phase material is comprised of the same three regions as described earlier. In the case of the multi-phase materials, the core bead is macroporous with an average surface area of about 300 m<sup>2</sup>/g and an average pore size of approximately 60 Å. Latex is attached only to the exterior surface of the macro-

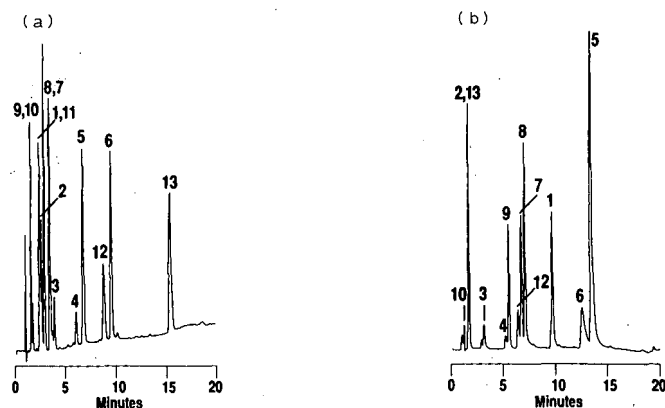


Fig. 5. HPLC separation of aromatic organic acids, Column: NovaPak C<sub>18</sub>, 5 μm. Flow-rate: 1.0 ml/min. UV absorbance detection 0.1 AUFS. (a) Ion-pair separation. Peaks as in Fig. 4. Eluent: 0.010 *M* tetrabutyl ammonium phosphate, pH 6.5; 25–50% (v/v) acetonitrile gradient in 20 min. (b) Ion-suppression separation. Peaks as in Fig. 4. Eluent: 0.020 *M* phosphoric acid, 0.020 *M* ammonium sulfate buffer; 10–80% (v/v) acetonitrile gradient in 20 min.



porous bead, using less than 1% of the total surface area. The latex beads are too large to enter the pores, defining two distinctly different areas for retention, ion exchange in the latex coating and adsorption on the surface area of the interior of the pores. Fig. 2b is a schematic representation of a multi-phase bead. The new latex attachment route (covalent or electrostatic) allows the production of the multi-phase packing since the method generates no significant residual ion-exchange sites on the high surface area that would otherwise interfere with reversed-phase or ion-pair retention processes.

Pinkerton and Hagestam<sup>27</sup> describe a material that has two distinct and separate phases in one packing material. The external of the macroporous bead defines one phase that is neutral and very hydrophilic, designed to prevent retention of proteins. The internal phase in the interstices of the macroporous bead is functionalized with peptides containing hydrophobic moieties. This packing material is designed to allow sample preparation or direct injection of physiological, high protein containing samples for drug analysis with minimal protein interference or fouling since proteins or other macromolecules are too large to enter the pores and the external surface is too hydrophilic for their retention. Although this material has two distinct phases, only one of the phases is designed for analyte retention, the other is intended to prevent retention.

This multi-phase material is also distinctly different from the mixed-mode supports described by Hartwick and co-workers<sup>12-14</sup>. Specifically, the mixed-mode supports, besides being silica based, are a heterogeneous mixture of ion-exchange and hydrophobic ligands in a single active layer. Because they are mixed together it is not possible to take full advantage of the properties of ion-exchange selectivity which rely on a three dimensional relationship of ion-exchange sites. To understand the properties of the new multi-phase material it is important to understand the difference between ion-exchange and ion-pair selectivity.

#### *Mixed ion-exchange/ion-pair selectivity*

The literature suggests that for the most part, ion-exchange selectivity is an enthalpy driven process<sup>6,11,15</sup>. A net free energy decrease for an ion from the bulk solution associating with an ion-exchange site in the active phase and displacing a previously associated co-ion, is due to a favorable enthalpy change in the hydration energy difference of the eluent ion, the analyte ion and the ion-exchange site. Ion-exchange selectivity is due to differences in the net change in free energy of the ion-exchange process for different analyte ions resulting from differences in the free energy of analytes and the free energy of fixed ion-exchange sites. The free energies of analytes are relatively constant in the bulk solution but are usually different for each analyte due to differences in hydration energies. Ion-exchange site free energies vary as a result of the degree of hydration of the ion-exchange site, which is determined by its environment in the polymer. Polymers do not have uniform density throughout the latex bead. Areas of higher density (higher cross-linking) are less hydrated and have less hydrated ion-exchange sites. Areas of lower density (lower cross-linking) are more hydrated and have somewhat more hydrated ion-exchange sites. This heterogeneity in the degree of hydration of the fixed ion-exchange sites creates good selectivity for either ions of high hydration energy, or ions of low hydration energy but not both on the same ion-exchange phase. It is not possible to affect the heterogeneity of a

single ion-exchange phase dramatically enough to provide optimum selectivity for very high and very low hydration energy ionic analytes.

Ion exchange has good selectivity for polyvalent ions particularly polyvalent ions of the same charge because ion-exchange site density is high in the gel structure of a fully functionalized ion exchanger such as the latex coating. Polyvalent ions can more often be retained with some or all charges satisfied by the charges of the fixed ion-exchange sites as discussed earlier.

Ion exchange is rather narrow in the scope of ions that can be separated on one ion-exchange phase of a given selectivity. This limitation results in the requirement for several ion-exchange columns with different selectivities to separate a broad spectrum of analytes.

Ion-pair chromatography, originally described by Haney and Wittmer<sup>16</sup>, is for the most part an entropy driven system and, whether one subscribes to the ion-pair formation theory<sup>17,18</sup>, the dynamic ion-exchange theory<sup>19-21</sup> or the ion-interaction theory<sup>22-24</sup> of retention, is a surface phenomenon. As with adsorption retention the entropy of the system has to be thermodynamically favorable for "ion-pair" retention to take place<sup>19,25</sup>. That is the hydrated analyte ion is driven from the bulk solution onto the stationary phase to form an ion pair because the analyte ion pair imparts less order to the water already ordered in the vicinity of the stationary phase as compared to the much less ordered water in the bulk solution. Contrast this to ion exchange which is a three dimensional phenomenon where ions penetrate into the gel network of the active ion-exchange phase, as described earlier. The resulting ion pair is not very useful for divalent ions because retention is essentially only in two dimensions and divalent ions are not likely to be retained in a unique environment where they "fit" better thermodynamically than other divalent ions because the fit for any analyte ion only has two degrees of freedom.

Ion-pair chromatography has quite different strengths and weakness compared to ion exchange. Selectivity strengths include (1) good resolution of monovalent ions particularly when monovalent ions have low and very similar hydration energies (*e.g.* nitrate and chlorate) because "absorption" based ion-pair retention is mostly entropy driven and is not dependent on enthalpies of hydration as is ion exchange. This is why fluoride, a highly hydrated ion, is unretained by ion exchange but is retained by ion pair; (2) good resolution and selectivity for surface active, or large hydrophobic ions because the technique allows the hydrophobic tail to enhance the retention mechanism; (3) good selectivity for large polarizable ions like iodide since they readily form ion pairs in the solvent rich environment near the hydrophobic surface of the substrate; (4) a broad scope of ions can be eluted and resolved due to the generally lower overall selectivity of the method as compared to ion exchange. The weaknesses of ion-pair chromatography are mainly polyvalent ions. In particular, polyvalent ions of the same valency (*e.g.* sulfate and many divalent organic acids) are difficult or impossible to resolve by ion pair.

Obviously the advantages of the two techniques are complimentary. The new multi-phase material takes advantage of this by providing the selectivity of both retention mechanisms on the same column at the same time. Ion exchange takes place in the pellicular layer, ion pair on the high surface area of the rest of the macroporous core bead, when an ion-pair reagent is added to the eluent. Since the latex is agglomerated only to the exterior surface of the macroporous bead, it takes up less than

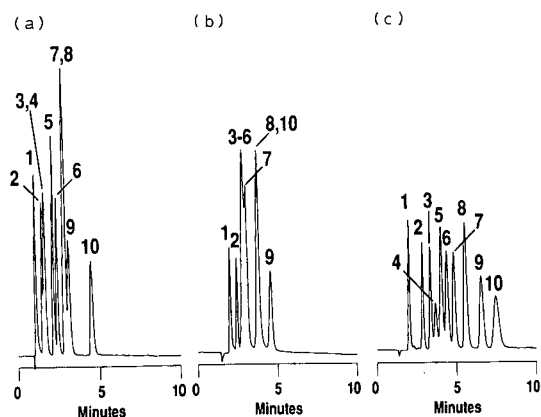


Fig. 6. Comparison of ion-exchange (a), ion-pair (b) and multi-phase (ion-exchange and reversed-phase, (c) selectivity. Peaks: 1 = fluoride 1 ppm; 2 = chloride 2 ppm; 3 = nitrite 3 ppm; 4 = succinate 10 ppm; 5 = sulfate 10 ppm; 6 = oxalate 10 ppm; 7 = bromide 5 ppm; 8 = nitrate 8 ppm; 9 = chlorate 10 ppm; 10 = phosphate 8 ppm. Flow-rate: 1 ml/min; suppressed conductivity 10  $\mu$ S/cm full scale; 10- $\mu$ l injection loop. Eluent: 17% acetonitrile, 42 mM NaOH, 1 mM TBAOH. Column: (a) OmniPac PAX-100; (b) IonPac NS1; (c) OmniPac PAX-500.

0.1% of the total available surface area in the bead. Fig. 6 illustrates that multi-mode ion pair/ion exchange is a combination of the selectivities of the two retention mechanisms. Fig. 6a shows only ion-exchange selectivity on a pellicular latex agglomerated phase that is agglomerated on a highly cross-linked but microporous core bead so there is no neutral surface area available for adsorption retention. This shows the strengths of ion exchange, with the divalent components sulfate, oxalate and succinate are separated from each other, but bromide, nitrate and chlorate, however, are poorly resolved and fluoride is in the void. Note that there is no evidence of ion-pair selectivity with 1 mM TBAOH in the eluent. Fig. 6b is strictly an ion-pair separation of the same set of analytes with the same eluent on a neutral macroporous stationary phase. The ion-pair separation displays good resolution of bromide, nitrate and chlorate and fluoride is retained, but the divalent ions are co-eluting. Actually, with ion-pair there are about two dozen divalent inorganic anions and divalent organic acids that all have the same selectivity and all co-elute under any eluent conditions. Fig. 6c shows the same analytes with the same eluent on the multi-phase material. The multi-phase material is actually the sum of the two selectivities. Notice that to a first approximation the  $k'$  values for the multi-phase separation are the sum of the  $k'$  values of ion exchange and ion pair. The divalent ions are resolved, and bromide, nitrate and chlorate are resolved. Fluoride is retained from the void.

#### *Ion exchange/adsorption*

If ion-pair reagent is added to the eluent the high, neutral hydrophobic surface area of the substrate in the multi-phase column is available for adsorption retention. The separation shown in Fig. 7 demonstrates the differences between ion-exchange selectivity with the added advantage of solvent selectivity control and multi-phase selectivity this time combining ion-exchange and adsorption retention.

Fig. 7a shows a chromatogram generated on the Omnipac PAX-100 with sul-

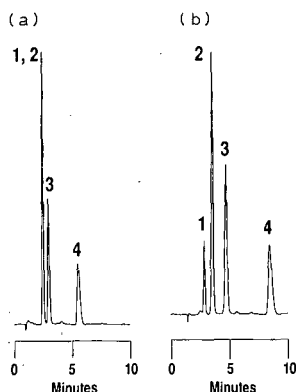


Fig. 7. Control of selectivity with the OmniPac PAX-100 (a) and PAX-500 (b) columns. Eluent: 40 mM NaOH, 20% acetonitrile. Suppressed conductivity, 10  $\mu$ S/cm full scale; flow-rate = 1 ml/min; 10  $\mu$ l injection loop. Peaks: 1 =  $\text{SO}_4^{2-}$ ; 2 = benzenesulfonate; 3 = *p*-toluenesulfonate; 4 = *p*-chlorobenzenesulfonate.

fate and benzene sulfonate co-eluting. Using the PAX-500 (Fig. 7b) with the same eluent conditions sulfate and benzene sulfonate are resolved. Benzene sulfonate is retained longer on this column due to the combination of ion-exchange and adsorption retention. The concept of combining ion-exchange and adsorption retentions on multi-phase materials can be extended to combinations of neutral and ionic analytes as shown in Table III.

Table III shows retention times of 2-aminopyrimidine, a neutral compound in the pH of the eluent throughout the gradient, and 2-thiouracil and 5-carboxy-2-thiouracil which are anionic over the full pH range of the gradient. Note that the anionic analytes, 2-thiouracil and 5-carboxy-2-thiouracil decrease in retention as the ionic portion of the gradient is made steeper, whereas 2-aminopyrimidine retention stays constant. The retention of 2-aminopyrimidine changes only as a result of a change in the solvent gradient from 1–23% acetonitrile to 1–27% acetonitrile in 10 min. This is because 2-aminopyrimidine is the only one of the three to be retained only by adsorption retention.

TABLE III

EFFECT OF IONIC AND SOLVENT GRADIENT CHANGE ON THE RETENTION TIME OF NEUTRAL AND IONIC ANALYTES ON A MULTI-PHASE COLUMN

Retention time R.S.D. < 1%.

Analyte	Gradient conditions		
	1 to 30 mM Sodium carbonate, 1 to 27% acetonitrile	1 to 50 mM Sodium carbonate, 1 to 23% acetonitrile	1 to 75 mM Sodium carbonate, 1 to 23% acetonitrile
2-Thiouracil	8.15 min	7.85 min	7.57 min
2-Aminopyrimidine	8.65 min	8.90 min	8.90 min
5-Carboxy-2-thiouracil	17.4 min	15.4 min	13.9 min

2-Thiouracil, a monovalent anion, was affected to a lesser extent than 5-carboxy-2-thiouracil, a divalent anion, as a result of the change in ionic strength because the change in retention of a monovalent analyte due to a change in the concentration of a divalent eluent ion ( $\text{CO}_2^-$ ) is one-half that of a divalent analyte<sup>26</sup>. Table III indicates that during methods development on a multi-phase column adsorption retention selectivity for neutral compounds and ion-exchange selectivity can be manipulated independently providing relatively easy control over the selectivity power of the column. Carrying this to a logical extreme, Fig. 8 shows it is possible to elute analytes by class. Neutral analytes are eluted first with an eluent containing solvent and water only, with no buffer added. After all neutral compounds are eluted the eluent is changed to lower solvent and a gradient of ionic strength to elute the anionic analytes. This capability has implications for "on-column" sample clean-up as well as two dimensional selectivity control on one column. We have already begun demonstrating in our lab the feasibility of selectively eluting otherwise interfering neutral compounds prior to elution of ionic compounds of interest, or *vice versa*, within one injection.

## CONCLUSIONS

A new type of multi-phase material that combines strong base anion-exchange retention and adsorption retention has been developed. The construction of this multi-phase column allows simultaneous ion-exchange and ion-pair or adsorption retention combining the positive attributes of both retention mechanisms. The ability to use solvents in conjunction with ion-exchange was discussed and the significant improvement of gradient focusing power (efficiency) of an ion-exchange salt gradient for some organic ions, over reversed-phase ion pair or ion suppression was demonstrated. Pellicular ion-exchangers built on a highly cross-linked, neutral, hydrophobic

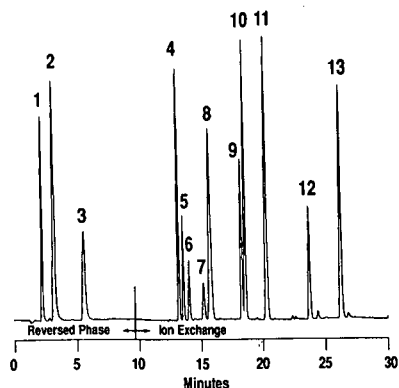


Fig. 8. Two-dimensional chromatography with a single column. OmniPac PAX-500 column, 1 ml/min. Absorbance detection 254 nm, 0.1 AUFS. 10- $\mu$ l injection loop. Gradient: 80% (v/v) acetonitrile isocratic for 10 min; at 10.1 min: 20% (v/v) acetonitrile, 0.050 M NaCl, 0.0002 M NaOH, which is ramped to 20% (v/v) acetonitrile, 0.4 M NaCl, 0.0016 M NaOH in 10 min and held isocratic for 10 min. Peaks: 1 = benzylalcohol; 2 = diethyltoluamide; 3 = benzene; 4 = benzoic acid; 5 = benzenesulfonic acid; 6 = toluenesulfonic acid; 7 = *p*-chlorobenzenesulfonic acid; 8 = *p*-bromobenzoic acid; 9 = phthalic acid; 10 = terephthalic acid; 11 = *p*-hydroxybenzenesulfonic acid; 12 = 1,3,5-benzenetricarboxylic acid; 13 = 1,2,4,5-benzenetetracarboxylic acid.

substrate allow a new dimension in selectivity control for ion exchange, by allowing control of the ion-exchange gel phase cross-link with solvent concentration as well as changing ion-exchange selectivity by the nature of the solvent. Because ion exchange and adsorption are independent retention mechanisms they can be independently controlled on the multi-phase column providing two-dimensional selectivity control that has on-column sample preparation implication as well as analyte selectivity control. Ion-pair and ion-suppression techniques practiced on reversed-phase systems are a means for dealing with ionic organic analytes with a technique that doesn't handle ionic analytes well. The new multi-phase columns could well eventually replace reversed-phase ion-pair and ion-suppression techniques for many applications, and realize the potential of ion exchange alluded to by Horváth.

#### ACKNOWLEDGEMENTS

We thank S. Heberling, V. Barretto and V. Summerfelt for their many hours of laboratory work in the process of development of multi-phase materials and for their undaunted enthusiasm and diligence on the project.

#### REFERENCES

- 1 Cs. Horváth, in J. Marinsky (Editor), *Ion Exchange, A Series of Advances*, Vol. 5, Marcel Dekker, New York, 1966, Ch. 7.
- 2 H. Small and T. Stevens, *U.S. Pat.*, 4 252 644 (1981).
- 3 H. Giddings, *U.S. Pat.*, 3 488 922 (1970).
- 4 G. Schomberg, P. Kolla and M. W. Laubi, *Am. Lab. (Fairfield, Conn.)*, May (1989) 92.
- 5 F. Helfferich, *Ion Exchange*, McGraw-Hill, New York, 1962.
- 6 R. W. Slingsby and C. A. Pohl, *J. Chromatogr.*, 458 (1988) 41.
- 7 *Doc. No. L-80013*, Hamilton, Reno, NV, January 1989.
- 8 J. Stillian, *LC Mag.*, 3 (1985) 802.
- 9 S. D. Alexandratos, M. A. Strand, D. R. Quillen and A. J. Walder, *Macromolecules*, 18 (1985) 829.
- 10 B. Karger, J. N. LePage and N. Tanaka, in Cs. Horváth (Editor), *High Performance Liquid Chromatography*, Vol. 1, Academic Press, New York, 1980, Ch. 3.
- 11 R. M. Diamond and D. C. Whitney, in J. Marinsky (Editor), *Ion Exchange, A Series of Advances*, Vol. 1, Marcel Dekker, New York, 1966, Ch. 8.
- 12 J. Crowther, S. Fasio and R. Hartwick, *J. Chromatogr.*, 282 (1983) 619.
- 13 T. Floyd, L. Yu and R. Hartwick, *Chromatographia*, 21 (1986) 402.
- 14 T. Floyd, J. Crother and R. Hartwick, *LC Mag.*, 3 (1985) 508.
- 15 D. Reichenberg, in J. Marinsky (Editor), *Ion Exchange, A Series of Advances*, Vol. 1, Marcel Dekker, New York, NY, 1966, Ch. 7.
- 16 W. G. Haney and D. Wittmer, *U.S. Pat.*, 4 042 327 (1977).
- 17 D. P. Wittmer, N. O. Nuessle and W. G. Haney, Jr., *Anal. Chem.*, 47 (1975) 1422.
- 18 Cs. Horváth, W. Melander, I. Molnar and P. Molnar, *Anal. Chem.*, 49 (1977) 2295.
- 19 N. H. C. Cooke and K. Olsen, *J. Chromatogr. Sci.*, 12 (1980) 512.
- 20 R. A. Hux and F. F. Cantwell, *Anal. Chem.*, 56 (1984) 1258.
- 21 J. C. Kraak, K. M. Jonker and J. F. K. Huber, *J. Chromatogr.*, 142 (1977) 671.
- 22 P. T. Kissinger, *Anal. Chem.*, 49 (1977) 883.
- 23 B. A. Bidlingmeyer, S. N. Deming, W. P. Price Jr., B. Sachok and M. Petrusek, *J. Chromatogr.*, 186 (1979) 419.
- 24 Z. Iskandarani and D. J. Pietrzyk, *Anal. Chem.*, 54 (1982) 1065.
- 25 C. Horváth, W. Melander and I. Molnar, *J. Chromatogr.*, 125 (1976) 129.
- 26 O. Samuelson, *Ion Exchange Separations in Analytical Chemistry*, Wiley, New York, 1963, Ch. 5.
- 27 T. C. Pinkerton and H. Hagestam, *Anal. Chem.*, 57 (1985) 508.

CHROMSYMP. 1665

## MICROPELLICULAR STATIONARY PHASES FOR RAPID PROTEIN ANALYSIS BY HIGH-PERFORMANCE LIQUID CHROMATOGRAPHY

KRISHNA KALGHATGI

*Department of Chemical Engineering, Yale University, New Haven, CT 06520-2159 (U.S.A.)*

---

### SUMMARY

The high separating speed, efficiency and operational stability of various micropellicular stationary phases are demonstrated in the high-performance liquid chromatography (HPLC) of biopolymers. The micropellicular sorbents were prepared from 2- $\mu\text{m}$  fluid-impervious silica microspheres as the support, with a thin layer of different retentive materials at the surface. These include a molecular fur of octyl or stearyl chains for reversed-phase chromatography as well as a hydrophilic layer with amino groups and polyethyleneglycol chains for anion-exchange and hydrophobic interaction chromatography, respectively. The use of appropriate micropellicular stationary phases for protein separation by metal-interaction and affinity chromatography is also illustrated. In most cases, operation at elevated column temperature was found to be preferable for rapid separations. Preliminary results show that the stability of micropellicular columns compares very favorably with that of columns conventionally used in HPLC and that they are easy to maintain.

---

### INTRODUCTION

Reversed-phase chromatography (RPC) continues to be a leading analytical technique for separation of proteins and peptides. The success of this method is due to its general applicability, availability of highly efficient columns and of highly sophisticated (HPLC) instrumentation. By virtue of its versatility, RPC has successfully met the new challenges of modern biotechnology in both analytical and preparative chromatography of biological macromolecules<sup>1-3</sup>. Recently, there has been considerable interest in further improvement of speed and column efficiency by employment of micropellicular stationary phases for the separation of biopolymers<sup>4-11</sup>. In comparison to the usual porous sorbents, pellicular sorbents allow faster mass transfer due to the absence of intraparticle diffusional resistances. This leads to higher column efficiency, particularly at relatively high flow velocities and for large molecules with low diffusivity. Due to the solid, fluid-impervious core and low surface area, the micropellicular stationary phases are generally more stable at elevated temperature than conventional, porous column materials. An increase in temperature results in the improvement of sorption kinetics as well as an increase in solute diffusivity, with a concomitant decrease in the viscosity of the mobile phase. Therefore, use of small-

particle, pellicular stationary phases and elevated temperatures, together, are expected to facilitate rapid analysis of proteins, peptides and other biopolymers.

#### *Historical background*

The role and importance of mass transfer in chromatographic processes is well described in the literature<sup>12-15</sup> and therefore, appropriate choice of conditions that provide favorable mass-transfer properties is essential for high-efficiency separations. Particle size is an important parameter contributing to the efficiency of the column and reduction in particle size leads to greater column efficiency. However, this approach is generally restricted by the concomitant decrease in column permeability due to excessive pressure. Another important factor is the support material itself. In column liquid chromatography of proteins the packing material has consisted of porous particles, which are characteristically weak and have a low efficiency, due to diffusional resistances in the stagnant mobile phase in the retentive material. Attempts to improve mass-transfer properties of the stationary phase have been met, with limited success, in the 1950s by the use of surface-coated packings, such as Celite, coated with a layer of ion-exchange resins for the separation of proteins<sup>16,17</sup> or by the use of polyethylenimine (PEI)-coated cellulose for the separation of nucleic acid constituents by thin-layer chromatography<sup>18</sup>. With the advent of HPLC, another approach was used to reduce diffusional resistance to mass transfer by reducing the diffusional path length in the stationary-phase support. Horváth and co-workers<sup>19-24</sup> were first to demonstrate the merits of pellicular stationary phases in HPLC, and this approach was further pursued by Kirkland<sup>25,26</sup>. The separation of nucleic acid constituents on the pellicular ion exchangers, prepared from relatively large glass beads [particle size ( $d_p$ )  $\approx$  40  $\mu$ m] as supports, marked an advance in stability at elevated temperature and pressure, in separation efficiency, and in high-speed analysis by HPLC. The concept of pellicular sorbents was successfully extended also to the use of immobilized enzymes<sup>27,28</sup>. In the early years of HPLC, a wide variety of these sorbents found commercial applications<sup>15</sup>. They were made from relatively large glass beads and used for the separation of small molecules.

Advances in particle classification technology in the late sixties led to the commercial availability of 5- or 10- $\mu$ m particles with narrow particle size distribution. This was the beginning of an era of bonded phases on totally porous microparticulate supports. This brought about the decline in the use of pellicular sorbents of much greater particle size. The microparticulate porous bonded phases had greater efficiency and higher sample load capacity. In addition, availability in the last decade of a wide variety of totally porous supports in a wide range of particle sizes and porosities has established such porous microparticulate stationary phases as a standard in HPLC of small molecules.

In recent years HPLC has made very significant advances in the separation of large molecules of biological origin. Such compounds are generally analyzed by gradient elution by the use of columns packed with small particles (3-10  $\mu$ m in size) with relatively large pores (300-500 Å). However, low diffusivity of biopolymers and restricted mass transfer in the porous interior of the column packings often results in long analysis times for high-molecular-weight substances. Even the macroporous (pore size > 50 nm) stationary phases have been described as showing poor performance, as well as low recovery of mass and biological activity<sup>5</sup>. Although an increasing



pore diameter is expected to alleviate some of these problems, particles with very large pores ( $> 1000 \text{ \AA}$ ) do not possess sufficient mechanical strength for use in HPLC. In the mid-1980s, Unger and co-workers<sup>5,29,30</sup> revived the concept of pellicular sorbents, and introduced 1.5- $\mu\text{m}$ , monodisperse, non-porous, reversed-phase silica packings into biopolymer chromatography. This was followed by other micropellicular sorbents, based on siliceous<sup>8-10,31</sup>, or polymeric<sup>4,7,11,32,33</sup> supports for the HPLC of large molecules. Recent work<sup>8-10,33</sup> from our laboratory has demonstrated the merits of micropellicular sorbents in allowing high speed of analysis and high column efficiency. Furthermore, their superior stability at elevated temperature for protein separation and peptide mapping, has also been established<sup>8</sup>. This study illustrates the versatility of micropellicular stationary phases in HPLC for rapid separation of proteins by different types of chromatography.

## EXPERIMENTAL

### *Materials*

Insulin, ribonuclease A,  $\alpha$ -chymotrypsinogen A (all from bovine pancreas), cytochrome *c* (horse heart), lysozyme (chicken egg white), myoglobin (sperm whale),  $\beta$ -lactoglobulin A (bovine milk), ovalbumin (chicken egg), concanavalin A (Con A) (jack bean),  $\alpha$ -methylmannoside and trifluoroacetic acid (TFA) were purchased from Sigma (St. Louis, MO, U.S.A.). r-Human growth hormone (r-hGH) and tissue plasminogen activator (r-tPA) were from Genentech (South San Francisco, CA, U.S.A.). N-Tosyl-L-phenylalanine chloromethylketone (TPCK)-treated trypsin was obtained from Worthington (Freehold, NJ, U.S.A.). Iminodiacetic acid (IDA) disodium salt, ethylene diamine tetraacetic acid (EDTA) tetrasodium salt, polyethylene glycol (PEG) 600, polyethylenimine (PEI) 600,  $\gamma$ -glycidoxypropyltrimethoxysilane, boron trifluoride etherate,  $\text{NiSO}_4 \cdot 7\text{H}_2\text{O}$  were obtained from Aldrich (Milwaukee, WI, U.S.A.). HPLC-grade acetonitrile, methanol, reagent-grade orthophosphoric acid and buffer salts were from J. T. Baker (Phillipsburg, NJ, U.S.A.). Tetraethylammonium hydroxide (TEAH) and octylsodium sulfate were products of Eastman Kodak (Rochester, NY, U.S.A.). Eluents were prepared with deionized water, prepared with a NanoPure system (Barnstead, Boston, MA, U.S.A.); filtered through a 0.45- $\mu\text{m}$  filter, and degassed by sparging with helium before use.

### *Instruments*

A Hewlett Packard Model 1090 Series M liquid chromatograph (Avondale, PA, U.S.A.), equipped with a ternary DR5 solvent delivery system, diode-array detector, ColorPro graphic plotter and autosampler, were used. The chromatographic system and data evaluation were controlled by Series 79994A Chem Station computer. The column effluent passed through heat exchangers in the diode-array detector before entering the flow cell.

Other experiments were carried out with a Series 400 pump and a Model LC 95 detector, both from Perkin Elmer (Norwalk, CT, U.S.A.), which were assembled with a heat exchanger coil and a Model 7125 injector (Rheodyne, Cotati, CA, U.S.A.). temperature circulating bath (Haake Buchler, Saddlebrook, NJ, U.S.A.). The flow cell of the detector was pressurized, and the chromatograms were processed by C-R3A Chromatopak integrator (Shimadzu, Columbia, MD, U.S.A.).

Column stability measurements were performed by using a chromatograph assembled together with a Series 10 pump, Model LC 65T detector/oven (both from Perkin Elmer), and a Model 728 autosampler from (Micromeritics, Norcross, GA, U.S.A.). Silica microspheres were sized by Model CAPA-700 particle size analyzer (courtesy of M. Perlstein, Horibo Instruments, Irvine, CA, U.S.A.).

### Columns

Non-porous silica microspheres ( $d_p = 2 \mu\text{m}$ ) and Hy-Tach  $C_{18}$  micropellicular reversed-phase columns were obtained from Glycotech (Hamden, CT, U.S.A.). Concanavalin A (Con A) was bound to non-porous silica microspheres according to the procedure described previously<sup>10</sup>. The micropellicular anion exchanger was prepared by reaction with  $\gamma$ -glycidoxypropyltrimethoxysilane to form epoxy silica, followed by treatment with PEI, according to the procedure of Regnier and Noel<sup>34</sup>. Similarly, the micropellicular stationary phase for hydrophobic interaction chromatography (HIC) was prepared by reaction of epoxy silica with PEG in the presence of boron trifluoride. In most cases, the stationary phases were packed into  $30 \times 4.6 \text{ mm}$  I.D. columns. The  $0.5\text{-}\mu\text{m}$  dual-density frits (Mott Metallurgical, Farmington, CT, U.S.A.) and connecting lines were made of No. 316 stainless-steel.

Experiments with a totally porous stationary phase were carried out by using a Vydac  $C_{18}$  column (Type 218TP54,  $250 \times 4.6 \text{ mm}$  I.D., Separations Group, Hesperia, CA, U.S.A.).

### Procedures

Reduction, S-carboxymethylation of r-tPA, and subsequent digestion with trypsin were carried out according to the procedure described previously<sup>9</sup>. Sample injections were made to coincide with the commencement of the gradient, and actual gradient profiles were determined by tracer technique<sup>9</sup>.

## RESULTS AND DISCUSSION

### Stability of micropellicular sorbents

A scanning electron micrograph of non-porous silica microspheres is shown in Fig. 1. These particles have a nominal diameter of  $2 \mu\text{m}$  and exhibit a narrow particle size distribution, as shown in Fig. 2. The specific surface area was found to be  $1.20 \text{ m}^2/\text{g}$  by the BET method. This is in agreement with the calculated value ( $1.35 \text{ m}^2/\text{g}$ ) for the geometric surface area, of solid spheres  $2 \mu\text{m}$  in diameter and, thus, suggests the absence of internal pore structure in the silica microspheres. Due to very small size and lack of porosity, the columns packed with such silica particles are expected to be much more stable at high inlet pressures and elevated temperature than traditional HPLC packings made from porous silica or polymeric supports. The stability of micropellicular  $C_{18}$  stationary phase was investigated at elevated temperature in acidic and moderately alkaline medium. The column performance was tested for the separation of standard proteins at various stages of elution with the mobile phases given in Table I. The chromatograms in Fig. 3 showed no sign of deterioration of the column after pumping 35 000 and 30 500 column void volumes of acidic and alkaline eluents, respectively, at  $80^\circ\text{C}$ . Stability was also tested under conditions analogous to those employed in protein chromatography for cleaning of the column by injecting an

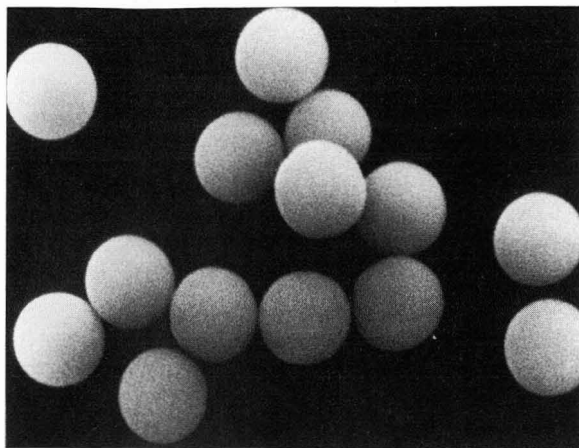


Fig. 1. Electron micrograph of micropellicular silica.

appropriate cleansing agent. Micropellicular  $C_{18}$  sorbents were stable after 128 injections ( $70 \mu\text{l}$  each) of 0.25% TEAH (pH 12), and perfusion with 6000 column void volumes of the mobile phase at pH 9.0. However, the column performance was severely affected by injection of TEAH at a higher concentration (1%, pH 13) or 0.1 M sodium hydroxide.

#### *Reversed-phase chromatography*

*Rapid analysis.* RPC is an increasingly used method of analysis for proteins and peptides. It is employed successfully for the determination of sample composition, assay of purity for the detection of trace impurities in protein samples, and for monitoring of biological processes<sup>1,2</sup>. Previous work from this laboratory has shown that silica-based micropellicular stationary phases can be successfully used for rapid protein analysis<sup>8</sup>, peptide mapping<sup>9</sup> and trace analysis<sup>3,5</sup>. The absence of pore structure in micropellicular sorbents, which provide significant advantages, such as complete

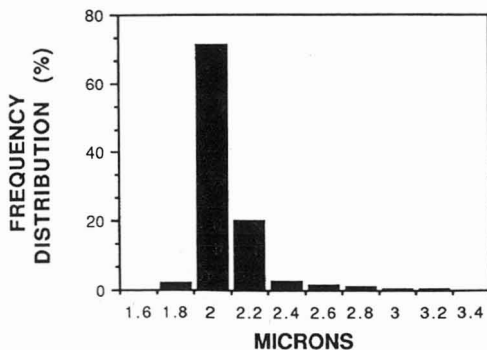


Fig. 2. Particle size distribution of micropellicular silica. A suspension of silica beads (100 mg) in 25 ml of water was sonicated for 30 min and the particle size was analyzed with a Model CAPA-700 particle size analyzer.

TABLE I

## STABILITY OF MICROPELLICULAR STATIONARY PHASES

Micropellicular C<sub>18</sub> columns, 30 × 4.6 mm I.D., were maintained at 80°C in an oven and perfused with the eluents listed below. The performance of the column at each step was tested for separation of proteins, as described in Fig. 3.

Column perfusate	pH	Volume <sup>a</sup>	Injection <sup>b</sup>	Test of efficiency <sup>c</sup>
Methanol-water (1:1, v/v) + 0.1% TFA	2.0	3500	—	NC
Methanol-water (45:55, v/v) + 0.1% TFA	2.0	8000	—	NC
Methanol-water (15:85, v/v) + 0.1% TFA	2.0	5500	—	NC
Methanol-water (15:85, v/v) + 0.1% TFA	2.0	9000	—	NC
50 mM Ammonium bicarbonate	8.5	9000	—	NC
50 mM Tris-orthophosphoric acid	8.5	9000	—	NC
Methanol-50 mM Tris (15:85, v/v)	9.0	12500	—	NC
50 mM Trisodium phosphate	11.0	5500	—	LE
50 mM Tris-phosphoric acid	8.5	6000	0.25% TEAH	NC
50 mM Tris-phosphoric acid	8.5	3000	1.0% TEAH	LE
50 mM Tris-phosphoric acid	8.5	3000	0.1 M NaOH	LE

<sup>a</sup> Expressed as column void volumes.

<sup>b</sup> Sample (70 μl) injected 64 times at 5-min intervals during perfusion of the column.

<sup>c</sup> NC = no change in column performance; LE = loss of column efficiency.

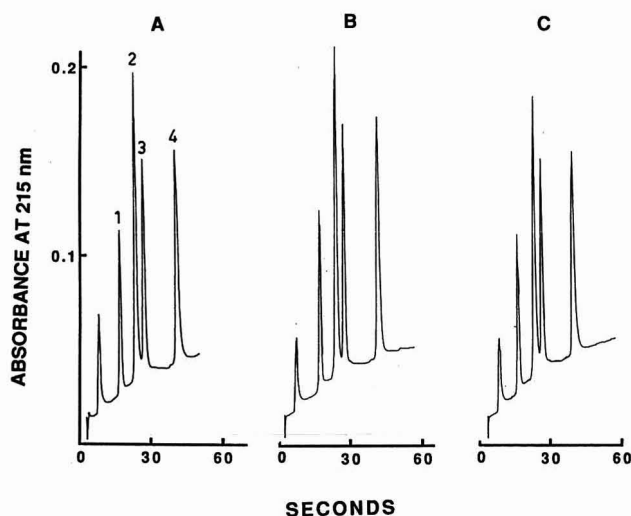


Fig. 3. Stability of micropellicular C<sub>18</sub> stationary phase. Columns (30 × 4.6 mm I.D.) were eluted with various mobile phases under conditions described in Table I. Sample, 20 μl, containing 0.5 μg each of ribonuclease A (1), cytochrome *c* (2), lysozyme (3) and β-lactoglobulin A (4); flow-rate, 3 ml/min; temperature, 80°C; eluent A, 0.1 (v/v) aqueous TFA; eluent B, 95% aqueous acetonitrile containing 0.1% (v/v) TFA. The sample components were eluted by a linear increase of eluent B from 20 to 90% in 1.5 min. Chromatogram A was obtained at initial stage of a newly packed column, whereas B and C were obtained with the same column after elution with 26 000 column void volumes of aqueous methanol containing 0.1% (v/v) TFA, 9000 column void volumes each of 50 mM NH<sub>4</sub>HCO<sub>3</sub>, Tris-orthophosphoric acid (both pH 8.5) and 50 mM Tris (pH 9.0).

exposure to large molecules and rapid solute equilibration with the stationary phase, is demonstrated in Fig. 4 by high-speed analysis of five proteins in less than 8 s. Current practice of protein chromatography does not require analyses to be carried out in seconds, and analysis on a time scale of seconds imposes additional constraints on the instrumentation<sup>35-37</sup>. The results presented here demonstrate the potential of micropellicular sorbents for fast analysis of biological macromolecules.

*Comparison with totally porous stationary phases.* Columns packed with micropellicular (2  $\mu\text{m}$ ) and totally porous (5  $\mu\text{m}$ ; 300  $\text{\AA}$ ) reversed-phase sorbents were used for the separation of proteins. The analyses were carried out at constant temperature. Column inlet pressure and gradient conditions were optimized for each column to achieve base-line resolution of all components. Although both columns provided excellent resolution of five proteins at room temperature, the analysis time was three times shorter with the micropellicular column (Fig. 5A and B). Since the speed of analysis is proportional to the velocity of the mobile phase, it is necessary to operate the column at flow-rate as high as possible without significant loss in separation efficiency. This approach is limited by (i) pressure constraints due to low permeability of the columns packed with micropellicular sorbents and (ii) significant departure from the minimum of the Van Deemter curve, resulting in loss of efficiency for porous particles<sup>15</sup>. At elevated temperature, the solute diffusivity and sorption rates increase,

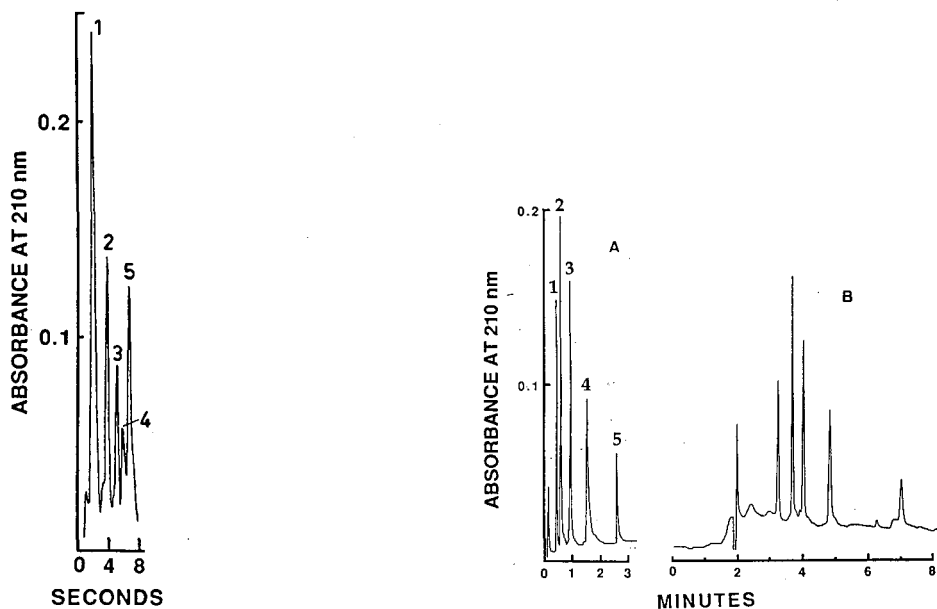


Fig. 4. High-speed analysis of proteins. Column, 5.0  $\times$  4.6 mm I.D. micropellicular C<sub>18</sub>; flow-rate, 5 ml/min; temperature, 80°C; sample, ca. 100 ng each of ribonuclease A (1), cytochrome *c* (2), lysozyme (3), L-asparaginase (4) and  $\beta$ -lactoglobulin A (5). Elution was carried out by a linear gradient of acetonitrile from 18 to 90% in 30 s.

Fig. 5. Reversed-phase chromatography of proteins on micropellicular (A) and totally porous (B) stationary phases. Sample components were ribonuclease A (1), insulin (2), lysozyme (3), myoglobin (4) and r-hGH (5); temperature, 22°C. For details see Table II.

TABLE II  
COMPARISON OF OPERATING CONDITIONS IN THE REVERSED-PHASE CHROMATOGRAPHY OF PROTEINS BY MICROPELLICULAR AND TOTALLY POROUS STATIONARY PHASES

Column	Temperature (°C)	Flow-rate (ml/min)	Pressure (p.s.i.)	Gradient	Analysis time (min)	Regeneration time <sup>a</sup> (min)	Cycle time (min)	Solvent consumption per run (ml)
Micropellicular (30 × 4.6 mm I.D.)	22	1.3	2530	15-90% B in 4 min	2.5	1.5	4.0	5.2
	40	1.7	2600	15-90% B in 1.5 min	1.1	0.9	2.0	3.4
Total porous (250 × 4.6 mm I.D.)	22	1.3	1800	15-90% B in 9 min	7.8	7.0	14.8	19.2
	40	2.0	1800	15-90% B in 9 min	7.3	6.0	13.3	26.6

<sup>a</sup> Determined by the time required for the detector signal to return to initial value.

leading to reduction of plate height and abatement of pressure restrictions<sup>38</sup>. In contrast with porous supports, the micropellicular packings can be used at elevated temperatures without adverse effect on column performance. Due to the absence of pores in micropellicular sorbents, columns packed with such stationary phases can be regenerated faster than those with porous stationary phases after gradient elution. A comparison of operating conditions and productivity of protein chromatography with micropellicular and totally porous stationary phases is given in Table II. Whereas both types of columns yielded satisfactory results for the resolution of sample components, the micropellicular column had a shorter cycle time and consumed less solvent than the column with porous stationary phase. On the other hand, the columns with conventional porous stationary phases have certain advantages, such as greater column permeability and higher load capacity, which can be important in certain applications.

*Other methods of protein chromatography.* The surface of non-porous silica microspheres was modified with appropriate functions and the stationary phases thus obtained were used in the separation of proteins by ion-exchange HIC and metal-interaction chromatography (MIC). A commercial sample of ovalbumin was analyzed in 2 min with a salt gradient on a micropellicular PEI column. Various peaks in Fig. 6 represent the microheterogeneity of ovalbumin due to glycosylation and phosphorylation of the protein<sup>39,40</sup>. Figs. 7 and 8 illustrate the rapid separation of proteins by HIC and MIC, respectively.

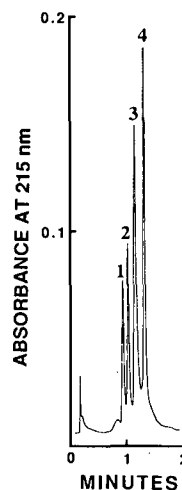
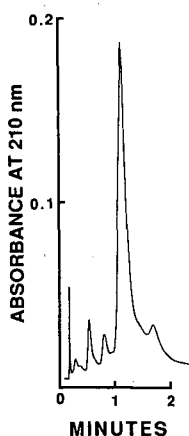


Fig. 6. Ion-exchange chromatography of commercial ovalbumin. Column, micropellicular PEI ( $30 \times 4.6$  mm I.D.). The sample components were eluted by a linear increase of NaCl from 0 to 0.5 *M* in 5 min with 25 *mM* phosphate buffer (pH 7.5). The main peak represents ovalbumin and its glycosylated/phosphorylated conformers are shown by the minor peaks. Flow-rate, 2 ml/min; temperature, 70°C.

Fig. 7. Hydrophobic interaction chromatography. Column: micropellicular polyether ( $30 \times 4.6$  mm I.D.); flow-rate, 3 ml/min; temperature, 50°C. Sample components, cytochrome *c* (1), ribonuclease A (2), lysozyme (3) and  $\alpha$ -chymotrypsinogen (4). Eluent, decreasing gradient of ammonium sulfate from 3 to 0 *M* in 3 min.

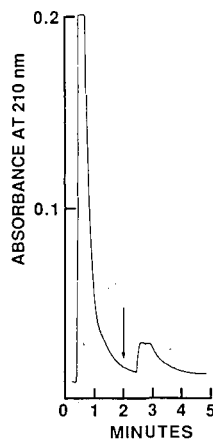
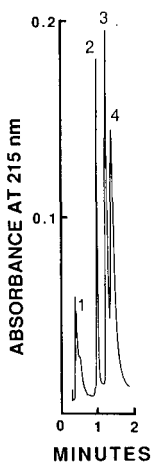


Fig. 8. Metal-interaction chromatography. Column, micropellicular IDA complexed with nickel ( $30 \times 4.6$  mm I.D.). Sample components:  $\beta$ -lactoglobulin A (1), chymotrypsinogen A (2), cytochrome *c* (3) and lysozyme (4). Eluent, linear gradient of NaCl from 0 to 0.5 *M* in 3 min; flow-rate, 2 ml/min; temperature, 50°C.

Fig. 9. Separation of glycopeptides and non-glycopeptides in a tryptic digest of r-tPA. Column, micropellicular Con A ( $30 \times 4.6$  mm I.D.). The protein digest (25  $\mu$ g) was injected and the bound fraction, containing the glycopeptides, was eluted with 50 mM  $\alpha$ -methylmannoside (2 min) in the starting eluent, consisting of 25 mM Tris-0.15 mM NaCl (pH 7.5); flow-rate, 1 ml/min; temperature, 25°C.

*Combination of chromatographic techniques (LC-LC).* Since micropellicular stationary phases are suitable for rapid analysis of proteins and peptides on a time scale of a few minutes or less, it seemed appropriate to explore a combination of more than one chromatographic technique (LC-LC) for the separation of complex mixtures of biological substances. An example shown is the separation of glycopeptides and non-glycopeptides in the tryptic digest of r-tPA by rapid affinity and RPC. A micropellicular Con A column was used for fractionation of glycopeptides and non-glycopeptides (Fig. 9). In this experiment, various peptides in the original digest as well as the glyco- and non-glycopeptides fractions were separated off-line by RPC. As shown in Fig. 10, excellent separation of peptides was obtained in less than 15 min. The glycopeptide fraction contained a predominant peptide, eluted shortly after 8 min and a few components in trace amounts with retention times of 0.6 and 7.5–8.0 min. Although no effort was made to characterize the sugar moiety in the peptide (a retention time of 8.2 min), its absence in the non-glycopeptide map is taken as sufficient evidence for a glycopeptide. These results are in agreement with the chromatographic profiles described by Spellman<sup>41</sup>.

## CONCLUSION

Micropellicular stationary phases have particle diameters about 20 times smaller than those of conventional pellicular sorbents which played an important role in the early days of HPLC. Columns packed with micropellicular sorbents are emi-



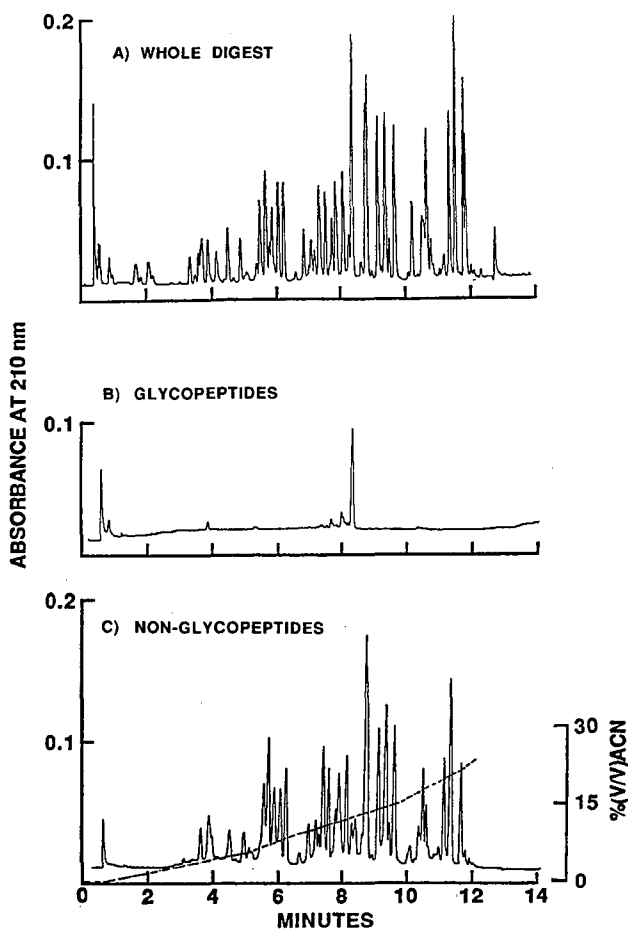


Fig. 10. Separation of tryptic fragments of r-tPA. Column, micropellicular  $C_{18}$  ( $75 \times 4.6$  mm I.D.). The flow-through fraction (non-glycopeptides) and glycopeptide fraction (Fig. 9) were freeze-dried prior to injection into the column. Eluent A, 50 mM phosphate buffer, containing 1 mM octyl sodium sulfate (pH 2.8); eluent B, 60% (v/v) acetonitrile (ACN) in 50 mM phosphate buffer (pH 2.8); flow-rate, 1.5 ml/min; temperature, 80°C.

nently suitable for the chromatography of proteins and offer a gain in separating speed, efficiency, stability and reproducibility comparable to that brought about by the introduction of microparticulate stationary phases in HPLC. The advantages of micropellicular sorbents demonstrated here are expected to secure for them an important place in the growing list of novel stationary phases for HPLC.

#### ACKNOWLEDGEMENTS

The author is indebted to Prof. Csaba Horváth for encouragement. Generous gift of r-hGH and r-tPA from Drs. W. Hancock and M. Spellman of Genentech is greatly appreciated. Contributions of Drs. G. Bonn (University of Innsbruck, Aus-

tria) and I. Fellegvári in some of the experiments are gratefully acknowledged. This work was supported by Grants GM 20993 and CA 21948 from the National Institute of Health, U.S. Department of Health and Human Services.

## REFERENCES

- 1 W. S. Hancock, *Chromatogr. Forum*, 2 (1986) 57.
- 2 S. Borman, *Anal. Chem.* 59 (1987) 969A.
- 3 R. L. Garnick, N. J. Solli and P. A. Papa, *Anal. Chem.*, 60 (1988) 2546.
- 4 D. J. Burke, J. K. Duncan, L. C. Dunn, L. Cummings, C. J. Siebert and G. S. Ott, *J. Chromatogr.*, 353 (1986) 425.
- 5 K. K. Unger, G. Jilge, J. N. Kinkel and M. T. W. Hearn, *J. Chromatogr.*, 359 (1986) 61.
- 6 R. Janzen, K. K. Unger, H. Giesche, J. N. Kinkel and M. T. W. Hearn, *J. Chromatogr.*, 397 (1987) 91.
- 7 Y. Kato, T. Kitamura, A. Mitsui and T. Hashimoto, *J. Chromatogr.*, 398 (1987) 327.
- 8 K. Kalghatgi and Cs. Horváth, *J. Chromatogr.*, 398 (1987) 335.
- 9 K. Kalghatgi and Cs. Horváth, *J. Chromatogr.*, 443 (1988) 343.
- 10 L. Varady, K. Kalghatgi and Cs. Horváth, *J. Chromatogr.*, 459 (1988) 207.
- 11 I. Mazsaroff, M. Rounds and F. E. Regnier, *J. Chromatogr.*, 411 (1987) 452.
- 12 J. J. van Deemter, F. J. Zuiderweg and A. Klengenber, *Chem. Eng. Sci.*, 5 (1956) 271.
- 13 Cs. Horváth and H.-J. Lin, *J. Chromatogr.*, 126 (1976) 401.
- 14 Cs. Horváth and H.-J. Lin, *J. Chromatogr.*, 149 (1987) 43.
- 15 L. R. Snyder and J. J. Kirkland, *Introduction to Modern Liquid Chromatography*, Wiley, New York, 1979, pp. 168–268.
- 16 J. Feitelson and S. M. Partridge, *Biochem. J.*, 64 (1956) 607.
- 17 N. K. Boardman, *J. Chromatogr.*, 2 (1959) 388.
- 18 K. Randerath, *Thin Layer Chromatography*, Academic Press, New York, 2nd ed., 1956, pp. 229–243.
- 19 Cs. Horváth, B. Preiss and S. R. Lipsky, *Anal. Chem.*, 39 (1967) 1422.
- 20 Cs. Horváth and S. R. Lipsky, *Anal. Chem.*, 41 (1967) 1227.
- 21 Cs. Horváth and S. R. Lipsky, *J. Chromatogr.*, 7 (1969) 109.
- 22 Cs. Horváth, in J. A. Marinsky and Y. Marcus (Editors), *Ion Exchange and Solvent Extraction*, Vol. 5, Marcel Dekker, New York, 1973, pp. 207–260.
- 23 Cs. Horváth, in D. Glick (Editor), *Methods of Biochemical Analysis*, Vol. 21, Wiley, New York, 1973, pp. 79–154.
- 24 Cs. Horváth, in E. Grushka (Editor), *Bonded Stationary Phases in Chromatography*, Ann Arbor Science Publishers, Ann Arbor, MI, 1974, p. 59.
- 25 J. J. Kirkland, *J. Chromatogr. Sci.*, 7 (1969) 361.
- 26 J. J. Kirkland, *J. Chromatogr. Sci.*, 8 (1970) 72.
- 27 Cs. Horváth and J. M. Engasser, *Ind. Eng. Chem. Fundam.*, 12 (1973) 229.
- 28 Cs. Horváth, *Biochim. Biophys. Acta*, 358 (1974) 164.
- 29 B. Anspach, K. K. Unger, H. Giesche and M. T. W. Hearn, *Proceedings of the 4th International Symposium on HPLC of Proteins, Peptides and Polynucleotides, Baltimore, MD, December 1984*, paper 103.
- 30 K. K. Unger, G. Jilge, R. Janzen, J. Giesche and J. N. Kinkel, *Chromatographia*, 22 (1986) 379.
- 31 L. F. Colwell and R. A. Hartwick, *J. Liq. Chromatogr.*, 10 (1987) 2721.
- 32 D. P. Lee, *J. Chromatogr.*, 443 (1987) 71.
- 33 Y.-F. Maa and Cs. Horváth, *J. Chromatogr.*, 445 (1987) 71.
- 34 F. E. Regnier and R. Noel, *J. Chromatogr. Sci.*, 14 (1976) 316.
- 35 K. Kalghatgi and Cs. Horváth, in B. Wittman-Liebold (Editor), *Methods in Protein Sequence Analysis*, Springer Verlag, Berlin, 1989, p. 248.
- 36 M. W. Dong, J. R. Gant and B. R. Larsen, *Biochromatography*, 4 (1989) 19.
- 37 G. Rozing and H. Goetz, *J. Chromatogr.*, 476 (1989) 3.
- 38 F. D. Antia and Cs. Horváth, *J. Chromatogr.*, 435 (1988) 1.
- 39 G. D. Longmore and H. Schatcher, *Carbohydr. Res.*, 100 (1982), 365.
- 40 C. Ceccarini, P. Lorernzoni and P. H. Atkinson, *Biochim. Biophys. Acta*, 759 (1983) 214.
- 41 M. Spellman, in B. Karger and F. Regnier (Editors), *Proceedings of the Intensive Seminars in Analytical Biotechnology*, Bioseparations, Baltimore, MD, 1987, paper 4.

CHROMSYMP. 1658

## COMPARISON OF RETENTION BEHAVIOR ON POLYMERIC RESINS AND AN ALKYL-BONDED SILICA PHASE IN REVERSED-PHASE HIGH-PERFORMANCE LIQUID CHROMATOGRAPHY

SUSAN PEDIGO and LARRY D. BOWERS\*

*Department of Chemistry and Department of Laboratory Medicine and Pathology, University of Minnesota, 420 Delaware St. S.E., Minneapolis, MN 55455 (U.S.A.)*

---

### SUMMARY

The two most obvious differences between alkyl-bonded silica phases and polystyrene–divinylbenzene resins as reversed-phase chromatographic supports are the aromaticity and the lack of hydrogen bonding ability in the polymeric resin. The effect of these differences on the selectivity for a set of small solutes was studied through the use of a solvatochromic comparison method. For retention on a polymeric phase for mobile phases with the modifiers methanol and acetonitrile, the linear solvation energy relationship indicated an increased dependence on the polarizability/dipolarity of solutes. For the modifier tetrahydrofuran, retention on the polystyrene–divinylbenzene resin was indistinguishable from that on the alkyl-bonded silica phase. The hydrogen bonding ability of a solute was found to play a greater role in retention on alkyl-bonded silica than on the polymeric resin for all three modifiers. Since the mobile phase compositions were chosen such that the Hildebrand solubility parameters were equal, the dependence of retention on molar volume was found to be the same for all mobile phase–stationary phase combinations examined.

---

### INTRODUCTION

Silica-based bonded phases currently dominate the high-performance chromatographic field as stationary phase materials. In order to be chromatographically useful, stationary phases must meet many requirements, such as mechanical stability at high pressure and chemical inertness toward chromatographic solvents. Although these characteristics are met by siliceous stationary phase materials, problems inherent in the silica support material present limitations. Instability at high pH and the presence of residual silanol groups, which have been implicated as a source of poor protein recovery<sup>1</sup> and poor peak symmetry in amine chromatography<sup>2</sup>, are most frequently mentioned. These problems have generated interest in exploring non-siliceous alternatives as reversed-phase sorbents.

Polystyrene–divinylbenzene (PS–DVB) polymeric materials meet the requirements of mechanical stability and chemical inertness. Since they are stable in alkaline solution, they present an alternative to alkyl-bonded silica as a reversed-phase

material. There are two obvious structural differences between alkyl-bonded silica phases and PS-DVB resins as reversed-phase materials. These are the aromaticity of the polymeric phase and its lack of silanol groups. These differences are significant because they may influence selectivity. Because of the potential impact of polymeric stationary phases, it is important to characterize their chromatographic behavior, particularly in comparison with alkyl-bonded silica phases.

The behavior of PS-DVB as a reversed-phase sorbent has been studied under a variety of mobile phase conditions including pH<sup>3-7</sup>, electrolyte concentration<sup>3,4</sup> and mobile phase modifier<sup>4,8</sup>. Of these factors the role of the mobile phase modifier has been studied most extensively. Mori<sup>8</sup> and Robinson *et al.*<sup>4</sup> discussed the influence of solvent polarity on the chromatographic separation mode. They found that as the solvent became more polar, the separation mode changed from adsorption to gel permeation and then to reversed-phase partition. Several authors have used a retention index scale to compare solvent-dependent selectivity differences for the elution of solutes from PS-DVB resins<sup>9-11</sup>.

In a previous paper<sup>12</sup>, we reported the solvent-dependent differences between the performance of a hydrophobic polymeric resin and an alkyl-bonded silica phase. A distinct correlation exists between peak symmetry and the swelling of the polymeric stationary phase. The observed changes in the polymer beads appear to be intraparticulate. Some solvents, such as tetrahydrofuran (THF), swell the polymer with a concomitant improvement in the peak symmetry. Conversely, a more hydrophilic solvent, such as methanol, shrinks the polymer and asymmetric peaks are observed. This suggests a significant difference in the nature of the stationary phase or the retention mechanism depending upon the mobile phase modifier. Although interesting, none of the work done so far elucidates the role of aromaticity and hydrogen bonding in the retention process.

Several recent reports in the literature on the comparison of solvatochromic polarity measurements with chromatographic retention<sup>13,14</sup> will allow us to address these issues directly. These research workers have utilized a solvatochromic comparison technique to isolate several properties of a solvent previously dealt with under a collective "polarity" value. The solvent properties include the hydrogen bond accepting (HBA) basicity<sup>15</sup>, hydrogen bond donating (HBD) acidity<sup>16</sup> and the polarizability/dipolarity<sup>17</sup> of a solvent. In a linear solvation energy relationship (LSER), these solvatochromic parameters are useful for discussing solute-solvent interactions<sup>18</sup>. Taft *et al.*<sup>19</sup> used LSER to predict octanol-water partition coefficients. Sadek *et al.*<sup>13</sup> used the same approach for examining retention in reversed-phase high-performance liquid chromatography (RP-HPLC). The combination of the solvatochromic parameters of the solute with the molar volume of the solute in a LSER were shown to correlate with log *k'* (capacity factor) values, determined experimentally. We chose this method for the present study because of the information it can yield about the stationary phases involved.

According to the solvatochromic comparison method, a solubility property (SP) of a solute is given by the following equation.

$$SP = SP_0 + M(\delta_1^2 - \delta_2^2)\bar{V}_3/100 + S(\pi_2^* - \pi_1^*)\pi_3^* + B(\alpha_2 - \alpha_1)\beta_3 + A(\beta_2 - \beta_1)\alpha_3 \quad (1)$$

Previously established<sup>19</sup> rules for the symbols will be followed: *i.e.* 1, 2, and 3 denote

the mobile phase, stationary phase and the solute, respectively; the molar volume, dipolarity/ polarizability, hydrogen bond donating acidity and accepting basicity are denoted by  $V$ ,  $\pi^*$ ,  $\alpha$ , and  $\beta$ , respectively. The last term in eqn. 1 will be omitted for reasons discussed elsewhere<sup>18</sup>. Eqn. 1 may be represented as follows

$$SP = SP_0 + mV/100 + s\pi^* + b\beta \quad (2)$$

The magnitudes of the coefficients  $m$ ,  $s$ , and  $b$  are due to a *difference* between mobile phase and stationary phase properties. The sign of the coefficient is determined by whether the term represents an exoergic or endoergic factor in the retention process. In the case of reversed-phase chromatography,  $SP$  is the logarithm of the capacity factor.

In the present study, two types of stationary phase were examined, an octadecyl-bonded silica (ODS) and two PS-DVB polymeric resins. The retention of twelve test solutes was compared for the two stationary phase materials under the same mobile phase conditions. We correlated retention data for the solutes with their solvatochromic parameters. In identical mobile phases, differences in the coefficients in eqn. 2 indicate differences in the stationary phases. In addition, we looked at overall selectivity differences between the phases under the same conditions.

#### EXPERIMENTAL

Table I lists the test solutes and their solvatochromic parameter values. All of the solutes are small aromatic compounds, which were chosen to span a wide range of  $V$ ,  $\pi^*$  and  $\beta$  values. This is important in order to have a statistically meaningful correlation in eqn. 2 with a limited number of solutes. All of the solutes were obtained from Aldrich (Milwaukee, WI, U.S.A.), and diluted in the mobile phase prior to injection. Samples contained 1 to 2  $\mu\text{g}$ , depending upon the solute. Because of apparent problems with isotherm non-linearity at relatively low solute concentrations (5  $\mu\text{g}$ /injection), a study was performed for each test solute to ensure that data were taken in a linear portion of the isotherm. The non-linearity was observed on all polymeric columns tested.

Mobile phases were prepared with water purified by the Milli Q system (Millipore, Milford, MA, U.S.A.). Unless otherwise noted, the mobile phase modifiers methanol, acetonitrile and THF (Fisher Scientific, Fairlawn, NJ, U.S.A.) are in the concentrations 70%, 50% and 40%, respectively. At these volume fractions, the Hildebrand solubility parameters<sup>20</sup> are nearly equal for the mixtures. The system dead-volume was determined with either uracil or  $^2\text{H}_2\text{O}$  (Aldrich).

Three columns were used in this study. They included a PLRP-S column (40  $\times$  4.6 mm I.D., 300 Å pores, 8- $\mu\text{m}$  particle diameter) from Polymer Labs. (Amherst, MA, U.S.A.), a PRP-1 column (150  $\times$  4.6 mm I.D., 10- $\mu\text{m}$  particle diameter) from Hamilton (Reno, NV, U.S.A.), and a Hypersil ODS column (20  $\times$  4.6 mm I.D., 5- $\mu\text{m}$  particle diameter) from Shandon (Sewickley, PA, U.S.A.). The last column was upward-slurry-packed in methanol in our laboratory.

The chromatographic system consisted of a Beckman 110A pump (Fullerton, CA, U.S.A.), Rheodyne Model 7125 valve (Cotati, CA, U.S.A.) with a 20- $\mu\text{l}$  loop, and a Perkin Elmer LC-15 detector (Norwalk, CT, U.S.A.) at 254 nm. The detector was equipped with a Max-N flow-cell and associated electronics (LDC/Milton Roy,

TABLE I  
SOLVATOCHROMIC PARAMETERS<sup>a</sup> FOR SELECTED SOLUTES AND SOLVENTS

	$\pi^*$	$\beta$	$V/100$	$\alpha$
<i>Solutes</i>				
Benzene	0.59	0.10	0.989	
Toluene	0.55	0.11	1.139	
<i>tert.</i> -Butylbenzene	0.49	0.12	1.649	
Chlorobenzene	0.71	0.07	1.118	
Iodobenzene	0.81	0.05	1.215	
Benzyl alcohol	0.80	0.55	1.169	
Anisole	0.73	0.22	1.186	
2-Phenyl-2-propanol	0.75	0.61	1.305	
Acetophenone	0.90	0.49	1.269	
Nitrobenzene	1.01	0.30	1.129	
3-Nitrotoluene	0.97	0.31	1.285	
Benzonitrile	0.90	0.37	1.130	
<i>Solvents</i>				
Methanol	0.60			0.93
Acetonitrile	0.75			0.19
Tetrahydrofuran	0.58			0.00
Water	1.09			1.17
Aliphatics	0.00			0.00

<sup>a</sup> Taken from ref. 25. Solvatochromic parameters defined in text.

Riviera Beach, FL, U.S.A.). All experiments were performed at room temperature. Quadruplicate experiments were performed for all solutes. The data were taken on a strip-chart recorder. When the peaks were asymmetrical ( $B/A > 1.6$ )<sup>21</sup>, the data were acquired with an Apple IIe computer equipped with an Adalab board (Interactive Microware, State College, PA, U.S.A.) and stored with the Vidichart program. The data were subsequently analysed for the peak centroid via a moments program. The experimental  $k'$  values were regressed against the solvatochromic parameters via a standard multivariable least-squares linear regression program.

## RESULTS AND DISCUSSION

As an initial test of our solute set, we compared values obtained on a ODS-bonded phase with values in the literature for similar conditions. Table II contains the regression results for eqn. 2 for alkyl-bonded silica data sets. These include the present data, the data of Smith<sup>22</sup> and the data of Haky and Young<sup>23</sup>. The regression results of the data of Smith and of Haky and Young were previously reported by Sadek *et al.*<sup>13</sup>. The present data and Smith's data were obtained with identical mobile phase systems and columns (Hypersil ODS). Even though only three of the test solutes were common to the two data sets, the correlations were statistically equivalent. Likewise, the regression results were the same for our data and the data of Haky and Young, even though the mobile phase compositions and the size of the solute data sets were different. We take this agreement as evidence that our selection of solutes is valid for evaluating the solvatochromic parameters. Table III contains the regression results for

TABLE II  
SOLVATOCROMIC PARAMETERS FOR OCTADECYL-BONDED PHASE COLUMNS

SP<sub>0</sub>, *m*, *b*, and *s* are defined by eqn. 2. The correlation coefficient is given by *r*; *n* represents the number of solutes studied.

Solvent	Methanol		Acetonitrile		Tetrahydrofuran		
	Present <sup>a</sup>	Smith <sup>b</sup>	Haky <sup>c</sup>	Present <sup>a</sup>	Smith <sup>b</sup>	Present <sup>a</sup>	Smith <sup>b</sup>
SP <sub>0</sub> <sup>d</sup>	-1.10 ± 0.39	-0.48 ± 0.014	-0.27 ± 0.09	-0.71 ± 0.32	-0.38 ± 0.17	-0.28 ± 0.26	-0.13 ± 0.17
<i>m</i>	1.57 ± 0.36	0.90 ± 0.09	1.53 ± 0.07	1.15 ± 0.19	1.11 ± 0.15	1.03 ± 0.16	0.97 ± 0.11
- <i>b</i>	1.49 ± 0.18	1.28 ± 0.14	1.97 ± 0.12	1.83 ± 0.18	1.77 ± 0.17	1.63 ± 0.15	1.80 ± 0.17
<i>s</i>	-0.55 ± 0.19	-0.13 ± 0.13	-0.54 ± 0.10	0.12 ± 0.22	0.28 ± 0.16	-0.09 ± 0.18	0.17 ± 0.16
<i>r</i>	0.972	0.981	0.992	0.976	0.984	0.981	0.983
<i>n</i>	10	9	28	12	9	12	9
Av. res. <sup>d</sup>	0.08	0.08	0.07	0.10	0.06	0.08	0.04

<sup>a</sup> The chromatographic system consisted of a Hypersil ODS column and 70:30 MeOH-H<sub>2</sub>O, 50:50 MeCN-H<sub>2</sub>O, and 40:60 THF-H<sub>2</sub>O.

<sup>b</sup> Recalculated from data presented in ref. 29. Chromatographic system same as above.

<sup>c</sup> Recalculated from data presented in ref. 30 as in ref. 28. The chromatographic system consisted of an Alltech RP-18 column and methanol-0.05 M (NH<sub>4</sub>)<sub>2</sub>HPO<sub>4</sub> buffer (55:45).

<sup>d</sup> Av. res. = Average residual observed in the fit of eqn. 2 to log *k'* of the solute retention data.

TABLE III

LOG  $k'$  DATA AND SOLVATOCHROMIC PARAMETERS FOR A PLRP-S STATIONARY PHASE

Chromatographic conditions and terms defined in Table II.

<i>Solute</i>	<i>Methanol</i>	<i>Acetonitrile</i>	<i>Tetrahydrofuran</i>
Benzene	1.139	0.769	0.611
Toluene	1.559	0.999	0.820
<i>tert.</i> -Butylbenzene	—	1.458	1.163
Chlorobenzene	1.547	1.056	0.801
Iodobenzene	—	1.387	0.963
Benzyl alcohol	0.093	-0.197	-0.247
Anisole	1.381	0.755	0.576
2-Phenyl-2-propanol	0.400	0.071	0.075
Acetophenone	0.959	0.382	0.134
Nitrobenzene	1.218	0.649	0.482
3-Nitrotoluene	1.405	0.886	0.709
Benzonitrile	0.850	0.446	0.247
$SP_0$	$-1.75 \pm 0.63$	$-0.65 \pm 0.29$	$-0.41 \pm 0.39$
$m$	$2.80 \pm 0.59$	$1.31 \pm 0.18$	$1.04 \pm 0.20$
$-b$	$3.39 \pm 0.30$	$2.60 \pm 0.16$	$2.06 \pm 0.19$
$s$	$0.73 \pm 0.31$	$0.64 \pm 0.20$	$0.31 \pm 0.23$
$r$	0.979	0.988	0.976
Average residual	0.12	0.09	0.10

the data obtained with the two polymeric stationary phases. The differences between the two phases will be discussed as they are reflected in the individual coefficients.

Generally, the molar volume coefficient ( $m$ ) is always large and positive. The cavity-forming process is energetically unfavorable in the aqueous mobile phase. As a result, an increase in the molar volume of a solute results in an increase in retention. For the sake of simplicity, the specific forces determining the magnitude of  $m$  are neglected, except for its dependence upon the Hildebrand solubility parameter (see eqn. 1). Since the  $\delta^2$  values for the solvent systems are nearly equal and  $\delta^2$  for the non-polar stationary phases is small, the value of  $m$  (molar volume coefficient) should be nearly equal for the data correlations involving all solvent-stationary phase combinations tested in this experiment (see Tables II and III). The single obvious exception is methanol-water (70:30). In this case the organic modifier is also a hydrogen-bond donor, as will be discussed below.

The dependence of retention upon the hydrogen bond forming abilities of the stationary and mobile phases is a complex issue. One would expect that if a solute can form a hydrogen bond, it will do so with the mobile phase, thereby decreasing its retention relative to a non-hydrogen bond-forming solute. For this reason, the coefficient  $b$  is negative and always significant in the correlation of  $\log k'$  with the solvatochromic parameters in eqn. 2. Hydrogen bonding in the mobile phase can occur with water and, in some situations, with the modifier, depending upon the nature of the modifier. Generally, the water in the mobile phase would be expected to dominate the hydrogen bond donating character of that phase. A mobile phase mixture with less water will show less of a dependence upon the hydrogen bond accepting ability of a solute. Our data yield two examples of this. For acetonitrile-water mobile phases on



PLRP-S, the magnitude of  $b$  (coefficient of hydrogen bond-donating acidity) decreases as the water content changes from 50% to 30%. The same decrease is seen for methanol–water mixtures. The  $-b$  for 70% methanol is  $3.39 (\pm 0.30)$  (see Table III), and for 85% methanol it is  $2.56 (\pm 0.37)$ . This decrease in the magnitude of the coefficient of hydrogen bond-donating acidity ( $b$ ) does not indicate that an increased modifier concentration increases retention; rather it indicates a decrease in the importance of the hydrogen bond-accepting basicity of a solute as a factor in the retention process as the concentration of water in the mobile phase is decreased.

As mentioned earlier, the ability of the modifier to form a hydrogen bond will influence the hydrogen bond donating acidity of the mobile phase. Of the three modifiers used in this study, methanol is the strongest hydrogen bond donor (see Table I). For equal modifier concentrations in the mobile phase—and assuming the stationary phase does not have significant hydrogen bond-donating character—the  $b$  coefficient for the methanol should have the greatest magnitude. This is seen for the polymeric resin in Table III [ $|b(70\% \text{ methanol})| > |b(70\% \text{ acetonitrile})|$ ].

The assumption that the polymeric phase is a poor hydrogen bond donating acid is probably valid. There are no hydrogen bond donating functionalities in the polymeric phase itself, but some researchers have reported oxidation of the PS–DVB or traces of initiator or catalyst. The absence of hydrogen bond donating ability in our studies suggests that this was not a problem, although we did not specifically test for their presence. In addition, PS–DVB shows poor solvent uptake of water or methanol<sup>24</sup>, either of which could lend hydrogen bond donating character to the phase. ODS, on the other hand, is likely to have significant hydrogen bond donating character. Yonker *et al.*<sup>25</sup> have shown that methanol and a significant amount of water are adsorbed on alkyl-bonded silica phases which, in addition to the residual silanol groups, further increases their hydrogen bond donating (HBD) character. As mentioned earlier, the coefficient,  $b$ , for PLRP-S (poor HBD acidity) in methanol–water mobile phases (good HBD acidity) is greater than  $b$  for the other two modifiers. Because of the enhanced HBD character of ODS in methanol (*e.g.*, modification of the stationary phase), this is not seen for the ODS phase, where  $(b(\text{methanol}) = b(\text{acetonitrile}) = b(\text{THF}))_{\text{ODS}}$ .

The greatest difference in the behavior of the polymeric and alkyl-bonded phases is seen in  $s$ , the coefficient for the dipolarity/polarizability term in eqn. 2. Because of the aromaticity of the polymeric phase, the coefficient  $s$  for the correlations is always positive. This indicates that a solute with a large  $\pi^*$  is relatively more retained on a polymeric phase than a solute with a low  $\pi^*$ . In contrast to PLRP-S, alkyl-bonded silica phases show  $s$  values close to zero (THF and acetonitrile) or negative (methanol), indicating that the polarizability and dipolarity of a solute are less important in retention on ODS phases.

The values of  $s$  on PLRP-S are all positive. However, they are not equal. There appears to be a relationship between the mobile phase modifier and the dependence of retention on the solute  $\pi^*$ . In a study performed by Pietrzyk<sup>24</sup>, THF was found to be adsorbed on a polystyrene resin to a greater extent than acetonitrile. Methanol and water are also adsorbed on the aromatic resin, but to a lesser extent than either THF or acetonitrile. There is an inverse correlation between the amount of adsorbed solvent and the dependence of retention upon the solute  $\pi^*$  ( $s(\text{THF}) < s(\text{acetonitrile}) < s(\text{methanol})$ ). The relatively small  $s$  value for PLRP-S in a THF environment indicates

that there is less of a difference in the  $\pi^*$  parameters between the PS-DVB stationary phase and THF-water mobile phase. We postulate that the adsorbed THF creates an environment on the adsorbent which is more similar to the environment in the mobile phase, and therefore the influence of the polarizability of the polymeric phase is reduced. In contrast, the relatively small amount of methanol adsorbed on the polymeric phase from methanol-water mobile phases will not significantly alter the polarizability of the polymeric phase. As a result, the  $s$  value for PLRP-S in methanol-water is large and positive.

Alkyl-bonded silica phases also exhibit a solvent dependent  $s$  value. Our ODS data show that methanol yields an  $s$  value that is significantly different from that with the other two modifiers. One possible explanation for this involves the amount of modifier adsorbed on ODS and the polarizability of that modifier. Since all of the modifiers are more polarizable than the aliphatic phase, the adsorption of modifier will increase the polarizability of ODS, thereby decreasing the value of  $s$ . Yonker *et al.*<sup>26</sup> found methanol to be adsorbed to a lesser extent than either THF or acetonitrile. The relatively low amount of adsorbed methanol and the low  $\pi^*$  of methanol indicate that it will not enhance the polarizability of the ODS phase to the same extent as either THF or acetonitrile. This results in a large negative  $s$  value for methanol-water mixtures.

In order to determine whether the behavior observed for PLRP-S was characteristic of PS-DVB phases in general, a similar set of experiments was performed on PRP-1 at 70% acetonitrile (Table IV). The correlation for the test solutes was identical on the two polymeric phases.

TABLE IV  
COMPARISON OF TWO POLYSTYRENE-DIVINYLBENZENE HPLC SORBENTS

Columns as described in Experimental; mobile phase, 70:30 MeCN-H<sub>2</sub>O. Solvatochromic terms defined in Table II.

Solute	PLRP-S	PRP-1
<i>log k'</i>		
Benzene	0.195	0.467
Toluene	0.485	0.617
<i>tert.</i> -Butylbenzene	0.786	0.885
Chlorobenzene	0.550	0.664
Iodobenzene	0.884	0.917
Benzyl alcohol	-0.445	-0.264
Anisole	0.308	0.439
2-Phenyl-2-propanol	-0.325	0.172
Acetophenone	-0.017	-0.078
Nitrobenzene	0.154	0.348
3-Nitrotoluene	0.348	0.512
Benzonitrile	0.018	0.211
<i>Solvatochromic parameters</i>		
SP <sub>0</sub>	-0.87 ± 0.26	-0.45 ± 0.23
<i>m</i>	1.03 ± 0.16	0.83 ± 0.14
- <i>b</i>	2.13 ± 0.15	1.91 ± 0.13
<i>s</i>	0.58 ± 0.18	0.47 ± 0.16
<i>r</i>	0.985	0.985
Ave. residual	0.08	0.07

The modulus concept, as introduced by Melander *et al.*<sup>27</sup>, compares differences in retention between two stationary phases. The modulus, or the selectivity for a solute between two columns in identical mobile phase systems, is given by:

$$\mu = \frac{k'_{A-1}}{k'_{A-2}} = \frac{\varphi_1}{\varphi_2} \exp[(\Delta G_{A-2}^0 - \Delta G_{A-1}^0)/RT] \quad (3)$$

The solute is denoted by A and the two columns by 1 and 2. In identical mobile phases, assuming that only solvophobic interactions<sup>6</sup> are responsible for retention, the modulus cancels out the mobile phase effects. Retention differences would then be due to preferential interactions with either phase 1 or phase 2. If  $\mu$  is not constant, there is a difference in the selectivity between the two columns.

Using the modulus technique for examining the selectivity differences between stationary phase materials, Melander *et al.*<sup>27</sup> compared several aromatic bonded phases with alkyl-bonded silica phases. Even though the selectivity differences were much smaller than those reported for the present data on a PS-DVB phase, they found differences which were due to more than just a difference in the phase ratio ( $\varphi$ ). There was greater selectivity for alkyl benzenes on the alkyl-bonded phases and greater selectivity for polyaromatic compounds on the aromatic bonded phases. This would clearly be the situation if we considered the differences in the relative  $\pi^*$  values of polyaromatic molecules (more polarizable) and alkylbenzenes (less polarizable). Other authors have discussed the unique selectivity afforded by the polarizable phenyl groups in phenyl-bonded silica phases<sup>27-30</sup>. However, the role of the aromatic groups in retention on phenyl-bonded phases is not clear, owing to the variation of phase ratio and the effect of the residual silanol groups<sup>31</sup>.

As Fig. 1 shows, methanol produces very drastic differences in relative retention for the test solutes on PS-DVB in comparison with alkyl-bonded phases. The large average modulus ( $\mu = 16.8$ ) indicates how much more strongly the solutes are retained on the polymer. The large variation in the modulus values shows the wide range of relative retention between the solutes. It is interesting to note that in MeOH solutions,

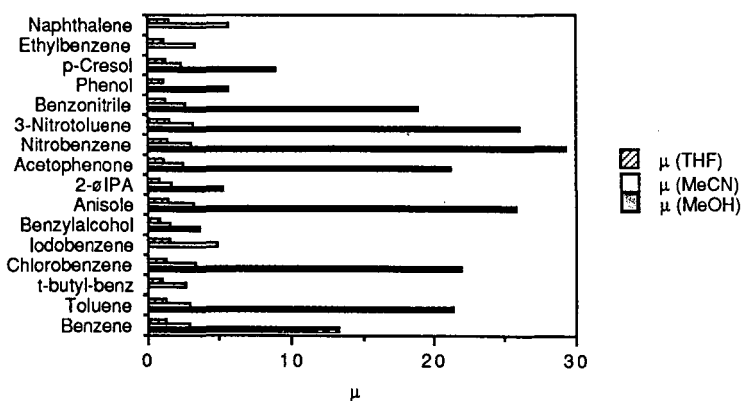


Fig. 1. The modulus for the retention of fourteen test solutes on PLRP-S in comparison with their retention on ODS. The mobile phases were 40% THF, 70% methanol and 50% acetonitrile, 2-φIPA = 2-phenyl-2-propanol; t-butyl-benz = *tert.*-butylbenzene.

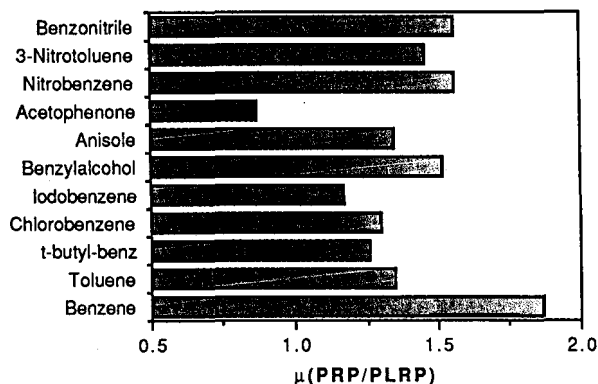


Fig. 2. The modulus for the retention of twelve test solutes on PRP-1 in comparison with their retention on ODS. The mobile phase was acetonitrile–water (70:30, v/v).

alcohols (HBD acids) are more retained on ODS relative to the mean modulus (Fig. 1, solutes 1–4). This is additional confirmation that the ODS phase has enhanced HBA basicity in methanol–water mobile phases. Fig. 1 also shows that solutes with high  $\pi^*$  values are more retained on PLRP-S relative to the mean modulus for a methanolic mobile phase. This agrees with the results from the solvatochromic comparison technique study discussed previously ( $s(\text{methanol})_{\text{PLRP-S}}$  is large and positive). With methanol–water mixtures, PLRP-S offers an advantage in selectivity over ODS, the potential limitations are lengthy analysis times and asymmetrical peaks ( $B/A = 3$ ) (ref. 12).

The mean modulus for acetonitrile is 3.1. Acetonitrile–water mobile phases afford significant selectivity when a polymeric column is used. THF has a mean modulus very close to unity ( $\mu = 1.2$ ), which indicates a similarity between the ODS and polymeric phases when in the THF environment. Little selectivity enhancement is obtained by using an aromatic phase with this organic modifier in comparison with alkyl-bonded silica sorbents:

For comparison purposes, data taken for a different polymeric column (PRP-1) are shown (Fig. 2). The retention of test solutes on the two columns is very similar. The fact that the mean modulus is greater than unity may reflect a difference in the phase ratio. Because of a smaller pore size (60–100 Å pore diameter), the PRP-1 has a larger surface area than the PLRP-S column.

## CONCLUSIONS

Significant differences exist between polymeric phases, such as PS–DVB, and alkyl-bonded silica phases. In addition to the extended usable pH range of polymeric supports, unique selectivity is observed. For organic solvents, such as methanol, which are not adsorbed on the support, the aromatic nature of the backbone is clearly expressed, as shown by the increase in the  $s$  term of the solvatochromism studies. For solvents such as THF, which are adsorbed on the polymer, a similarity exists between the polymeric and bonded silica phases. This finding confirms the importance of solvent modification of the stationary phase as a major factor in reversed-phase

chromatography. It also presents the chromatographer with two additional advantages. If a separation at high pH is desired, but the aromatic nature of the solutes is not significantly different, the use of THF will be the best organic co-solvent, since the overall hydrophobicity of the solutes will be the major factor in the separation. The unique selectivity of the polymeric phase for halogen-substituted compounds and other compounds with polarizable groups presents additional means of separation.

In contrast to the differences observed with alkyl-bonded phases, polymeric phases from different manufacturers seem to show more similarities than differences. It remains to be seen whether the polymeric phases are more reproducible from lot-to-lot than the silica-based chromatographic materials.

#### ACKNOWLEDGEMENTS

The authors thank Frank Warner of Polymer Laboratories, Ltd., for the donation of the polymeric supports used in this work. The project was supported in part by the Industry/University Cooperative Research Center for Biocatalytic Process Technology of the University of Minnesota.

#### REFERENCES

- 1 E. C. Nice, M. W. Capp, N. Cooke and M. J. O'Hare, *J. Chromatogr.*, 218 (1981) 569.
- 2 P. C. Sadek and P. W. Carr, *J. Chromatogr. Sci.*, 21 (1981) 314.
- 3 D. J. Pietrzyk and C. H. Chu, *Anal. Chem.*, 49 (1981) 757.
- 4 J. L. Robinson, W. J. Robinson, M. J. Marshall, A. D. Barnes, K. J. Johnson and D. S. Salas, *J. Chromatogr.*, 189 (1980) 145.
- 5 D. P. Lee, *J. Chromatogr. Sci.*, 20 (1982) 203.
- 6 J. Bontemps, L. Bettendorff, J. Lombet, C. Grandfils, G. Dandrifosse, E. Schoffeniels, F. Nevejans and J. Crommen, *J. Chromatogr.*, 295 (1982) 486.
- 7 H. Takahagi and S. Seno, *J. Chromatogr.*, 108 (1975) 354.
- 8 S. Mori, *Anal. Chem.*, 50 (1977) 745.
- 9 R. M. Smith, *J. Chromatogr.*, 291 (1984) 372.
- 10 F. Smejkal, M. Popl, A. Cihova and M. Zazvorkova, *J. Chromatogr.*, 148 (1980) 147.
- 11 M. Popl, V. Dolansky and J. Fahnrich, *J. Chromatogr.*, 148 (1978) 195.
- 12 L. D. Bowers and S. Pedigo, *J. Chromatogr.*, 371 (1986) 243.
- 13 P. C. Sadek, P. W. Carr, R. M. Doherty, M. J. Kamlet, R. W. Taft and M. H. Abraham, *Anal. Chem.*, 57 (1986) 2971.
- 14 P. W. Carr, R. M. Doherty, M. J. Kamlet, R. W. Taft, W. Melander and Cs. Horvath, *Anal. Chem.*, 58 (1986) 2674.
- 15 M. J. Kamlet and R. W. Taft, *J. Am. Chem. Soc.*, 98 (1976) 377.
- 16 R. W. Taft and M. J. Kamlet, *J. Am. Chem. Soc.*, 98 (1976) 2886.
- 17 M. J. Kamlet, J. L. Abboud and R. W. Taft, *J. Am. Chem. Soc.*, 99 (1977) 6027.
- 18 M. J. Kamlet, J. L. M. Abboud, M. H. Abraham and R. W. Taft, *J. Org. Chem.*, 48 (1983) 2877.
- 19 R. W. Taft, M. H. Abraham, G. R. Famini, R. M. Doherty, J. L. M. Abboud and M. J. Kamlet, *J. Pharm. Sci.*, 74 (1985) 807.
- 20 B. L. Karger, L. R. Snyder and Cs. Horvath, *An Introduction to Separation Science*, Wiley, New York, 1973, p. 55.
- 21 L. R. Snyder and J. J. Kirkland, *Introduction to Modern Liquid Chromatography*, Wiley, New York, 1979, p. 222.
- 22 R. M. Smith, *Anal. Chem.*, 56 (1984) 256.
- 23 J. E. Haky and M. A. Young, *J. Liq. Chromatogr.*, 7 (1984) 675.
- 24 D. J. Pietrzyk, *Talanta*, 16 (1969) 169.
- 25 C. R. Yonker, T. A. Zweier and M. F. Burke, *J. Chromatogr.*, 241 (1982) 257.

- 26 C. R. Yonker, T. A. Zweier and M. F. Burke, *J. Chromatogr.*, 241 (1982) 269.
- 27 W. R. Melander, J. X. Huang, Cs. Horvath, W. R. Stout and J. J. DeStefano, *Chromatographia*, 20 (1985) 641.
- 28 W. T. Cooper and Y. T. Lin, *Chromatographia*, 21 (1986) 335.
- 29 T. Hanai and J. Hubert, *J. Chromatogr.*, 291 (1984) 81.
- 30 R. M. Smith, *J. Chromatogr.*, 237 (1982) 144.
- 31 P. E. Antle, A. P. Goldberg and L. R. Snyder, *J. Chromatogr.*, 321 (1985) 1.

CHROM. 21 788

## PHYSICAL AND CHEMICAL CHARACTERIZATION OF MICROPOROUS ZIRCONIA

M. P. RIGNEY<sup>a,\*</sup>, E. F. FUNKENBUSCH<sup>b</sup> and P. W. CARR

*Department of Chemistry, University of Minnesota, 207 Pleasant St. S.E., Minneapolis, MN 55455 (U.S.A.)*

---

### SUMMARY

Small ( $< 10 \mu\text{m}$ ) microporous zirconia has been prepared and evaluated as an alkaline stable high-performance liquid chromatographic support. Zirconia is an amphoteric metal oxide which exhibits both anion- and cation-exchange properties depending on the solution pH and the nature of the buffer. The affinity of zirconia for polyoxy anions, particularly the effect of phosphate on the properties of the zirconia, is examined. Most significantly, the exceptional stability of zirconia, even under extreme conditions, is demonstrated and compared to the stability of alumina.

---

### INTRODUCTION

At present, 3- and 5- $\mu\text{m}$  microparticulate silica gels, and related bonded phase supports are the most versatile and advanced chromatographic supports available. The popularity of silica as a chromatographic support results from the cumulative impact of its excellent mechanical strength, availability in a wide range of pore sizes, nearly ideal pore structure (and hence mass transfer properties), the great versatility of the silanization chemistry and the availability of reagents for altering the chemical properties of its surface. However, silica gel also has a number of significant limitations, particularly its solubility in aqueous alkaline media.

The dissolution of silica in aqueous mobile phases is widely recognized and has been extensively documented<sup>1–6</sup>. The stability of silica-based bonded phase supports is also limited in acidic solution due to the acid-catalyzed hydrolysis of the siloxane bonds (Si–O–Si) anchoring the bonded phase to the surface<sup>7–9</sup>. Silica and bonded phase supports can be stabilized to alkali by acid and base pretreatment of the silica<sup>10</sup>, the use of a sacrificial presaturation column<sup>11</sup>, and by cladding the silica surface with alkaline-stable metal oxides such as zirconia and titania<sup>12–20</sup>. Although all such measures improve the stability, and in some cases the support can be used at a pH as high as 10, the stability is not as great as one could desire for a number of applications, particularly for biological separations.

---

<sup>a</sup> Present address: Ecolab, Inc., Ecolab Center, St. Paul, MN 55102, U.S.A.

<sup>b</sup> Present address: 3M Company, 3M Center, St. Paul, MN 55144, U.S.A.

A variety of substrates have been evaluated in an effort to develop chemically stable chromatographic supports. For example, rigid and semi-rigid organic polymers, particularly polystyrene-divinylbenzene (PS-DVB) supports, have been widely studied as alternatives to silica-based reversed-phase supports<sup>21-24</sup>. The two major advantages of PS-DVB supports in comparison to silica-based supports are their excellent stability over a broad pH range, and the absence of silanol groups on their surface. However, reversed-phase chromatography on these support materials is often characterized by asymmetric peaks and undesirably long retention times, particularly for aromatic solutes. Although improvements have been made with these supports, the chromatographic efficiency attainable on PS-DVB supports is generally not comparable to the efficiencies attainable on silica-based bonded phase microparticulate supports<sup>21,24</sup>.

Carbon (in the form of charcoal) was widely used as an adsorbent in the early days of chromatography, particularly in the displacement and frontal modes<sup>25-29</sup>. Since that time various carbonaceous adsorbents have continued to attract interest as reversed-phase chromatographic supports, primarily because of their excellent stability over a broad pH range. However, it was clear even in the early work of Tiselius cited above<sup>27-29</sup> that the surface of charcoal is very heterogeneous as reflected in peak asymmetry and irreversible adsorption of many solutes. The most homogeneous form of carbon is graphite, but most forms of graphite have a very low surface area or are too fragile for use as a high-performance liquid chromatographic (HPLC) support. Knox and Gilbert<sup>30</sup> developed a method of preparing porous graphitic carbon (PGC) by pyrolysis of a phenol-formaldehyde polymer coated on silica followed by dissolution of the silica "template" and thermal treatment to improve surface homogeneity. PGC has adequate mechanical stability for use as an HPLC support, but the surface remains somewhat heterogeneous and is likely to be subject to the type of long term oxidation common to all carbon surfaces.

The search for a material which possesses the desirable mechanical and physical properties of silica but with improved aqueous stability has also led to the preparation and evaluation of alumina-based stationary phases. Alumina has historically been widely used as a support for normal phase adsorption chromatography, although its use has not been as widespread as that of silica due at least in part to the greater complexity of the adsorption mechanism on alumina. Recently, high-performance ion-exchange and reversed-phase supports have been prepared by coating polymers onto the surface of alumina<sup>31,32</sup>, and these supports have shown considerable improvement relative to silica with respect to alkaline stability.

We believe there are potential advantages to the use of an inorganic support, particularly for applications at the preparative and process scale, and our objective is to develop and characterize a microparticulate, zirconia-based support with the desirable physical and mechanical properties of silica, but with chemical stability superior to any other inorganic support. We are also interested in chemically modifying this support for use in a variety of chromatographic modes, including reversed-phase (RP) HPLC<sup>33</sup>.

Zirconia and zirconium phosphate have been widely used as ion-exchange chromatographic supports, particularly in the nuclear industry for applications such as the treatment of reprocessing solutions<sup>34</sup>, high-level waste treatment, recovery of fission products and high-temperature ion-exchange separations. The attributes of



zirconia and zirconium phosphate that have made them particularly appealing in these applications are their extreme chemical and thermal stability. For example, hydrous zirconia is stable to water treatment at temperatures as high as 300°C<sup>35</sup>, and zirconium phosphate has also been used at temperatures as high as 300°C for extended periods of time<sup>36,37</sup>.

The porous zirconia spherules used in this work were comprised of monoclinic zirconia crystals. Crystalline zirconia has an extremely high melting point (2700°C), exceptional resistance to attack by both acids and alkalis, and excellent mechanical properties. The surface of zirconia, like most metal oxides, is highly hydroxylated. The existence of hydroxyl groups on the surface of zirconia has been confirmed spectroscopically<sup>38-41</sup>. Two distinct hydroxyl infrared bands have been reported<sup>38,39,41</sup> and have been assigned to surface bridging and terminal hydroxyl groups. We expect that the bridging hydroxyl, being strongly polarized by two zirconium(IV) ions will be more acidic while terminal hydroxyls more basic.

As with other metal oxides, the surface hydroxyl groups on zirconia control the surface chemistry, particularly with respect to the acid-base properties. Zirconia is an amphoteric metal oxide. The isoelectric point (IEP) and/or point-of-zero charge (PZC), range from less than 3 to higher than 10<sup>42-48</sup>. It is obvious from the wide range of these values that the source, type, chemical and thermal pretreatment and method of measurement can have a profound effect on the apparent acidity and basicity.

The presence of acidic and basic groups on the surface of zirconia is reflected in its cation- and anion-exchange properties. Zirconia has anion-exchange properties in neutral and acid solution and cation-exchange properties in alkali solutions<sup>49-51</sup>. Zirconia has a unique selectivity for polyoxy anions such as borate, carbonate, phosphate, sulfate, chromate, arsenate, arsenite, molybdate and tungstate<sup>52</sup>. A particularly interesting property, first observed by Amphlett *et al.*<sup>48</sup> is that treatment of zirconium oxide with phosphoric acid converts it to zirconium phosphate and that the treated support displays cation-exchange properties at 2 < pH < 14.

There has only been one previous report on the use of zirconia as a HPLC support<sup>53</sup>, and this work involved the use of a low-surface-area zirconia (9 m<sup>2</sup>/g even after hydrothermal treatment) that was dynamically modified with a hydrophobic quaternary ammonium salt. No attempt was made to characterize the chromatographic properties of the zirconia nor to develop a permanent means of surface modification.

On the basis of this brief review it is obvious that, despite more desirable chemical stability, the potential of zirconia as an HPLC support has not been evaluated. The objective of the present paper was to study the properties of unmodified zirconia as a prelude to other studies in which its surface is chemically modified<sup>33</sup>.

## EXPERIMENTAL

### *Chemicals*

All reagents were obtained from commercial sources and were reagent grade or better unless noted below. Triphenyl phosphine oxide, diphenyl phosphoric acid and diphenyl phosphinic acid were obtained from Aldrich (Milwaukee, WI, U.S.A.). Phenyl phosphonic acid was obtained from Alfa Chemicals (Danvers, MA, U.S.A.). The disodium salt of nicotineamide adenine dinucleotide, reduced form (grade III) was

obtained from Sigma (St. Louis, MO, U.S.A.). Methanol and 2-propanol were CHROMAR grade obtained from Mallinckrodt (St. Louis, MO, U.S.A.). The water used in all experiments was from a Barnstead Nano-Pure system with an "Organic-Free" final cartridge. All chromatographic mobile phases were filtered through 0.45- or 0.22- $\mu\text{m}$  filters prior to use. Water for use in the preparation of solutions for the alkaline stability tests can be boiled to remove carbon dioxide prior to use.

#### *Chromatographic supports*

The porous zirconia spherules were provided by the Ceramic Technical Center of 3M Co. (St. Paul, MN, U.S.A.). The spherules were prepared by a proprietary process, fired at high temperature (typically 600°C), and sized by air classification. During the course of this work several different lots of zirconia with widely different physical properties were used. Some of the relevant physical properties, as determined by the BET nitrogen adsorption isotherm technique, are summarized in Table I.

The alumina used was from two sources: Woehlm acidic alumina, activity grade 1 obtained from Alupharm Chemicals (New Orleans, LA, U.S.A.), and 5- $\mu\text{m}$  Spherisorb 5AY alumina (Phase Separations, Norwalk, CT, U.S.A.). The physical properties of these supports are also given in Table I.

#### *Apparatus*

HPLC studies were carried out on one of two chromatographic systems. System 1 consisted of a Hewlett-Packard (Palo Alto, CA, U.S.A.) Model 1090L liquid chromatograph with a DR5 binary solvent delivery system and a filter photometric detector with a 254-nm filter installed. For stability testing with alkaline mobile phases an expanded pH range kit was installed. Absorbance data were digitized, integrated and plotted using a Hewlett-Packard Model 3393A integrator interfaced to the chromatograph via a HP-IL interface loop.

System 2 consisted of an IBM Instruments (Danbury, CT, U.S.A.) Model 9533 liquid chromatograph, a Rheodyne Model 7125 injection valve and an IBM Model 9522 fixed-wavelength UV detector with a 254-nm filter installed. Absorbance data were typically digitized and stored on an IBM 9000 computer using the chromato-

TABLE I  
PROPERTIES OF POROUS ZIRCONIA SPHERULES

NA = Data not available.

<i>Sample</i>	<i>Particle size (<math>\mu\text{m}</math>)</i>	<i>Surface area (<math>\text{m}^2/\text{g}</math>)</i>	<i>Pore diameter (<math>\text{Å}</math>)</i>	<i>Porosity (%)</i>
ZrO <sub>2</sub> 1	50	50	100	NA
2	30-40	30	106	30
3	1-40	41	150	48
4	20-40	50	24	47
5	5-10	55	146	53
6	<8	61	96	45
7A	5-10	62	95	35
7B	10-15	62	95	35
Al <sub>2</sub> O <sub>3</sub>	5	92	132	NA

graphic applications package (CAP), version 1.4 provided by IBM. Chromatograms from System 2 were printed either on the IBM 9000 printer or on a Hewlett-Packard Model 7470 plotter using a BASIC program to read the data files and drive the plotter.

System 2 was used with a Tracor Model 965 photoconductivity detector for the chromatography of inorganic anions on zirconia. In order to make a differential conductivity measurement, the photoreactor coil was disconnected and a "T" placed in the eluent stream between the pump and the injector to divert mobile phase into the reference cell of the conductivity detector.

For experiments in which chromatographic supports were exposed to hot (100°C) 1 M sodium hydroxide, an Altex (Berkeley, CA, U.S.A.) Model 110A pump and a Fisher (Pittsburgh, PA, U.S.A.) Isotemp oven were used.

The columns used in the experiments were packed in 5 cm × 0.46 cm I.D. or 5 cm × 0.21 cm I.D. column blanks of 316 stainless-steel (316 SS). Two different end fitting configurations based on ¼-in., 316 SS Parker-Hanifin end fittings were used. Type 1 used an unmodified end fitting with a ¼ in. × ⅜ in. 2-μm titanium frit. Type 2 used a 2-μm 316 SS screen in a specially modified Parker-Hanifin end fitting as described by Sadek<sup>54</sup>. Particles greater than 15 μm diameter were packed by preparing a dilute slurry of the support material in methanol or isopropyl alcohol, and then drawing this slurry through a column with a type 2 end fitting by house vacuum (or aspirator). Particles smaller than 15 μm were packed at 6000–9000 p.s.i. from a methanol or isopropyl alcohol slurry using a stirred upward slurry packing technique.

#### *Acid-base titrations*

The titrations of zirconia and silica with 0.1 M hydrochloric acid and 0.1 M sodium hydroxide were performed by preparing a 10-mg/ml slurry of the support in 20% (w/v) sodium chloride in a beaker thermostatted at 30°C and blanketed with a flow of nitrogen. The titrant was dispensed in increments of 0.025 ml with a 2.5-ml capacity Radiometer pH Stat autoburette, and after each addition the pH of the slurry was measured with an Orion Model 801 pH meter equipped with an Orion Ross combination pH electrode.

#### *Stability testing*

The stability of zirconia and alumina at pH 1, 3, 10, 12 and 14 was examined under static conditions by adding 100 mg of support to 900 ml of the appropriate solution and monitoring the appearance of zirconium or aluminum in the supernatant solution. Solutions at pH 10, 12 and 14 were 0.0001, 0.01 and 1.0 M carbon dioxide-free sodium hydroxide, respectively. Solutions at pH 1 and pH 3 were 0.1 M hydrochloric acid and 0.001 M hydrochloric acid, respectively. The solutions were stored at ambient temperature and were agitated twice per day. Testing was performed at various time intervals by withdrawing 10 ml from the supernatant solution, filtering through a 0.45-μm filter and determining the concentration of zirconium or aluminum by inductively coupled plasma emission spectrometry (ICP-ES). The amount of zirconia and alumina dissolved was determined as follows:

$$\% \text{ zirconia dissolved} = \frac{\text{zirconium}_f \cdot V_s \cdot 123.22 \cdot 100\%}{91.22 \cdot M_z}$$

where zirconium<sub>f</sub> =  $\mu\text{g/ml}$  of zirconium found by ICP-ES;  $V_s$  = ml of solution before sample aliquot is removed;  $M_z$  = mass of zirconia in sample solution.

$$\% \text{ alumina dissolved} = \frac{\text{aluminum}_f \cdot V_s \cdot 101.96 \cdot 100\%}{26.9815 \cdot 2 \cdot M_A}$$

where aluminum<sub>f</sub> =  $\mu\text{g/ml}$  found by ICP-ES;  $V_s$  = ml of solution before sample aliquot is removed;  $M_A$  = mass of alumina in sample solution.

The stability of zirconia under "sterilizing conditions" was determined by exposing a 5 cm  $\times$  0.46 cm I.D. zirconia column (type 1 end fitting) to a mobile phase of 1 *M* sodium hydroxide for 3.25 h at 100°C and determining the amount of zirconium in the column effluent by ICP-ES.

## RESULTS AND DISCUSSION

The proprietary procedure for preparing porous microparticulate zirconia produces very regular spherical particles. Initially, zirconia with a mean particle diameter as large as 50  $\mu\text{m}$  was produced, however, considerable progress has been made through the course of the work in the production of small zirconia particles. Mean particle diameters in the 5–10- $\mu\text{m}$  range can now be prepared routinely. The mechanical stability of the zirconia particles appears to be comparable to that of silica. Columns have been slurry packed at pressures as high as 9000 p.s.i. and operated under extreme conditions for long periods of time without any evidence of mechanical instability.

The surface areas given in Table I are low when compared to the surface areas of the silica supports typically used in HPLC, however, it is important to recognize when considering the surface area data that the true density of monoclinic zirconia is approximately 5.8 g/ml<sup>55</sup>, whereas the true density of a common commercial silica packing is approximately 2.3 g/ml (ref. 2). Due to its higher density, the surface area of zirconia is comparable to that of silica when considered in terms of surface area per unit volume. It has been estimated that a high-performance silica column usually has a surface area to volume ratio of 125 m<sup>2</sup>/ml<sup>56</sup>. By comparison, a typical zirconia column has a ratio of 122 m<sup>2</sup>/ml<sup>57</sup>.

The particle size distribution for a 5–10- $\mu\text{m}$  fraction of zirconia is shown in Fig. 1. A typical pore size distribution, determined by mercury intrusion porosimetry, is shown in Fig. 2. Note that the size distribution is fairly uniform although there is some skewing of the distribution towards small particle diameters. Because of the high density of zirconia the size classification of the particles has been somewhat problematic, however, considerable improvement continues to be made in the classification of zirconia particles and hence narrower size distributions can be obtained.

As noted above, the reported acid–base properties of zirconia vary over a wide range. Many previous reports<sup>58–61</sup> examined the acid–base properties of zirconia by adsorption of acidic and basic compounds from the gas phase, however, in most chromatographic applications zirconia will be used in a partially aqueous environment, therefore the determination of its acid–base properties in aqueous media seemed most relevant to its end use. Consequently the acid–base properties of zirconia were briefly studied by titration in aqueous media. Titration of zirconia with hydrochloric

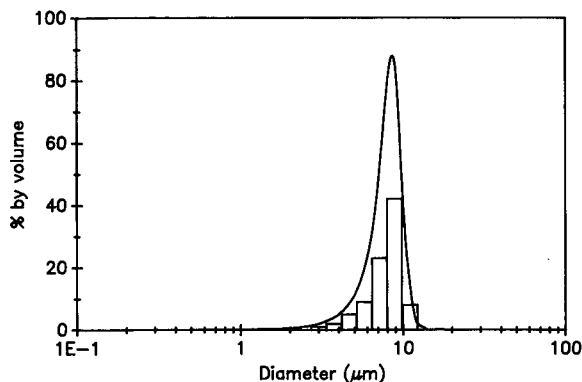


Fig. 1. Particle size distribution of zirconia sample 7A from Table I.

acid gave no indication of any strongly basic sites. As shown in Fig. 3, a titration with sodium hydroxide gave very similar results to those obtained for silica, when the data are presented per unit area. The pH of the 1% aqueous suspension of zirconia was 5.5, compared to a pH of 4.2 for the 1% suspension of silica. These titration results are consistent with other reports in the literature<sup>47</sup>.

In addition to its acid-base properties, another consideration relevant to the derivatization and chromatographic use of zirconia is the concentration of adsorptive sites on its surface. The concentration of these sites was roughly estimated from the thermogravimetric analysis curve (TGA) shown in Fig. 4. Based on the water loss determined by TGA, a value of  $9.8 \mu\text{mol}/\text{m}^2$  of active sites is obtained if we arbitrarily assume that the mass decrease from 205–455°C is due primarily to the loss of strongly hydrogen-bonded water and that the mass decrease from 455–810°C results from the condensation of neighboring zirconium hydroxides. This is not a truly quantitative

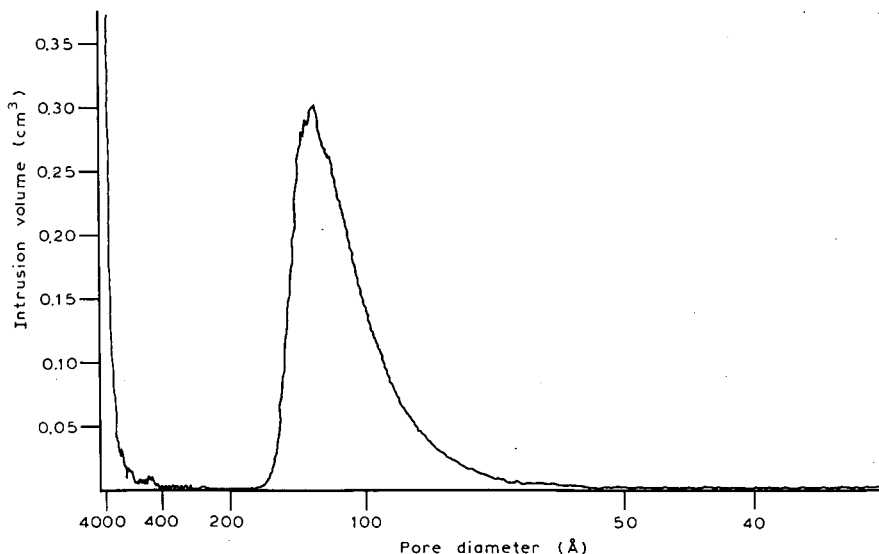


Fig. 2. Pore size distribution of zirconia sample 5 from Table I.

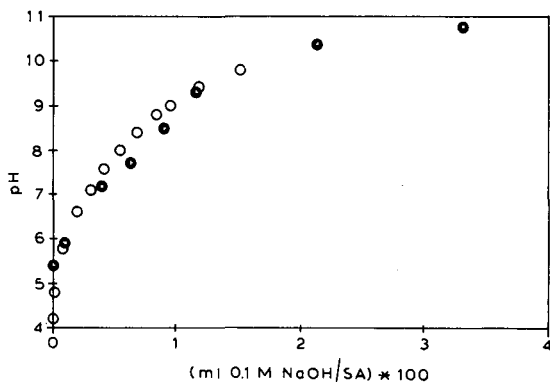


Fig. 3. Titration of zirconia ( $ZrO_2$ , ●) and silica (Nucleosil 100-30, ○) with 0.1 M NaOH. SA = Surface area.

measure of the surface population of ZrOH groups but it does provide a rough estimate of the hydroxyl content of the zirconia surface. Estimates of the surface hydroxyl population based on adsorption of organic and inorganic phosphates are of the same order of magnitude and indicate that  $9.8 \mu\text{mol}/\text{m}^2$  is an upper limit.

As already noted, the primary motivation for evaluating zirconia as a support material is its stability at extreme pH values, particularly under alkaline conditions. Therefore, its stability from pH 1–14 was determined under static conditions and compared to that of alumina. Alumina was chosen as a “reference” because it has been studied and is being used as an alkaline-stable alternative to silica as a chromatographic support material. No comparison was made to silica since it is known to dissolve in aqueous alkaline media<sup>1–6</sup>. The results of the static stability test for zirconia, as well as for alumina are shown in Fig. 5. Note that there was no zirconium detected in the supernatant solutions at any pH (detection limit =  $0.03 \mu\text{g}/\text{ml}$ ). By contrast, detectable levels of aluminum were found at pH 1, 3, 12 and 14. The superior stability of zirconia relative to alumina at  $\text{pH} \geq 12$  and  $\text{pH} \leq 3$  is obvious. Although it is very likely that different forms and sources of alumina will have different relative

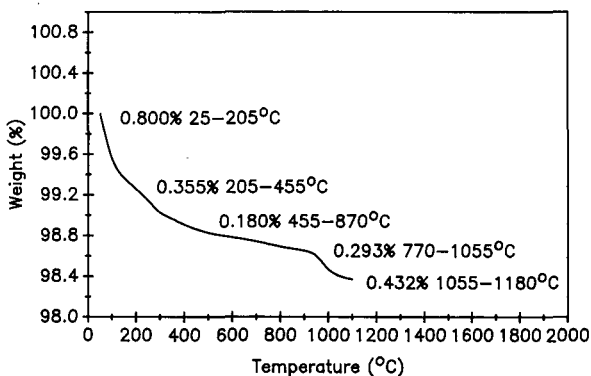


Fig. 4. Thermogravimetric analysis of zirconia.

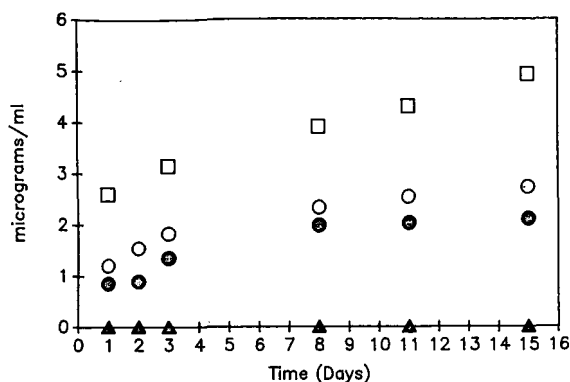


Fig. 5. Alkaline stability of zirconia and alumina. ▲ = ZrO<sub>2</sub>, pH 1-14; □ = Al<sub>2</sub>O<sub>3</sub>, pH 14; ○ = Al<sub>2</sub>O<sub>3</sub>, pH 12; ● = Al<sub>2</sub>O<sub>3</sub>, pH 3.

stabilities, it is still clear that in terms of stability in aqueous mobile phases at extreme pH (either acidic or basic), zirconia is the material of choice, not silica or alumina. It should be noted that the static conditions used in this experiment constitute a much less stringent test of stability than the dynamic conditions inherent in typical chromatographic usage.

The stability of zirconia under alkaline conditions was further tested by exposing a column of zirconia particles to a mobile phase of 1 *M* sodium hydroxide at 100°C for 3.25 h at a flow-rate of 1 ml/min. There was no zirconium detected in the column effluent after this treatment. Even if zirconium were present at just below the detection limit (0.03 μg/ml) this corresponds to the dissolution of less than 0.001% of the mass of zirconia originally present in the column under these very extreme conditions.

Given that the extreme stability of the zirconia makes it a viable alternative inorganic support, it is important to understand its surface chemistry. The ion-exchange retention of a variety of organic ionic solutes on zirconia was studied in order to develop a better understanding of its surface properties. The capacity factors ( $k'$ ) for these test solutes under a variety of conditions are given in Table II. Several qualitative conclusions can be made based on this data. Zirconia acts as an anion exchanger at pH 5 in an acetate buffer and at pH 8 in a Tris buffer. Note that as the pH is increased from 5 to 8 the retention of anionic solutes decreased as expected. However, even at pH 8 there was still no retention of cationic solutes. At pH 9.2 in a borate buffer, only cations are retained on the zirconia. Although zirconia has been reported to have a very strong interaction with borate (and other oxygen containing polyanions), the addition of borate did not cause any irreversible changes in the properties of the zirconia. This is indicated by the agreement between the capacity factors obtained in acetate buffer before and after exposure of the column to borate, as shown in Table II. The data in Table II also show that at pH 8 in Tris buffer, treatment of the column with 5 *mM* phosphate resulted in retention of only cations. This conversion of zirconia from an anion exchanger to a cation exchanger at pH 8 by treatment with phosphate was not readily reversible as evidenced by the fact that overnight flushing with a Tris buffer containing no phosphate followed by a redetermination of the retention of the test solutes in Tris buffer at pH 8 (again with no phosphate present in the mobile phase)

TABLE II  
ION-EXCHANGE PROPERTIES OF ZIRCONIA

Column: 5 cm × 0.21 cm I.D. packed with 30–40 μm zirconia. Mobile phase: 100 mM aqueous buffer as specified in table heading. Flow-rate: 1 ml/min. Column temperature: 25°C.

Solute	$pK_a$	Acetate (pH 5) <sup>a</sup>		Tris (pH 8) <sup>b</sup>			Borate (pH 9.2)
		A	B	A	B	C	
Benzylamine	9.3	0	0	0	1.9	1.9	0.3
Diphenyl cyclam	12 ( $pK_1$ )	0	0	0	6.0	6.0	1.0
<i>p</i> -Nitrobenzoic acid	3.4	2.2	2.3	0	0	0	0
Benzoic acid	4.2	5.8	6.2	1.7	0	0	0
<i>cis</i> -Cinnamic acid	3.9	7.0	6.7	2.3	0	0	0
<i>trans</i> -Cinnamic acid	4.4						
Hydroxybenzoic acid	4.5 ( $pK_1$ )	14.8	14.6	8.6	0	0	0
	9.3 ( $pK_2$ )						
Acetophenone		0	0	0	0	0	0

<sup>a</sup> A = Before exposure to borate buffer; B = after exposure to borate buffer.

<sup>b</sup> A = Before exposure to phosphate buffer; B = 50 mM phosphate in mobile phase; C = no phosphate in mobile phase after extensive flush with Tris buffer.

gave essentially the same results as those obtained in Tris buffer with 5 mM phosphate present in the mobile phase. Thus, although the acid–base titration data gave no indication of amphoteric acid–base properties, the ion-exchange results do show both anion- and cation-exchange properties, depending on the solution pH and the nature of the buffer. The transition from an anion exchanger to a cation exchanger occurs between pH 8 and pH 9.2.

An example of a separation of four weak organic acids at pH 5 in an acetate buffer is shown in Fig. 6. The efficiency of the zirconia column was determined as a function of flow-rate in the same mobile phase. The results are given in Fig. 7. Note that there is a strong dependence of efficiency on flow-rate, with the efficiency decreasing as the flow-rate increases. The efficiencies achieved are comparable to those observed for ion exchange on unmodified alumina<sup>62</sup> and silica<sup>63</sup>.

The retention of a variety of inorganic anions on zirconia in a 10 mM acetate buffer at pH 5.0 is summarized in Table III. Note that the oxyanions  $\text{NO}_3^-$ ,  $\text{SO}_4^{2-}$ ,  $\text{BrO}_3^-$ ,  $\text{B}_4\text{O}_7^{2-}$  and  $\text{S}_2\text{O}_3^{2-}$  are strongly retained on zirconia, as expected given the strong interaction between zirconia and oxygen-containing anions which was noted

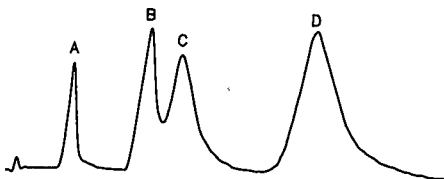


Fig. 6. Anion-exchange separation on zirconia. 5 cm × 0.46 cm I.D. column packed with 10–15 μm zirconia. Mobile phase: 10 mM acetate buffer at pH 5.0. Flow-rate: 1 ml/min. Column temperature: 40°C. A = *p*-Nitrobenzoic acid; B = benzoic acid; C = cinnamic acid; D = hydroxybenzoic acid.



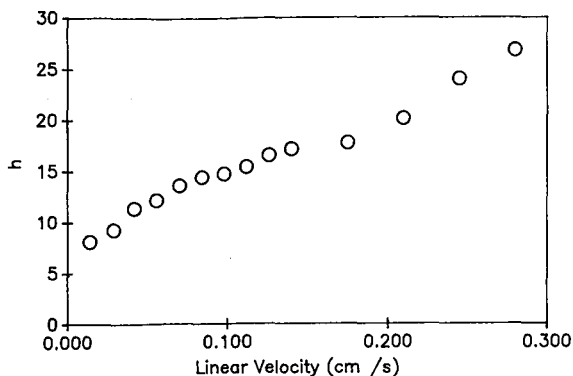


Fig. 7. Efficiency of zirconia column as determined from width at half height of hydroxybenzoic acid peak ( $k' \approx 25$ ). Chromatographic conditions are given in Fig. 5.

above. The halides elute in the order  $\text{Cl}^-$ ,  $\text{Br}^-$ ,  $\text{I}^-$  which is consistent with their elution order on polystyrene-divinylbenzene  $\text{R}_4\text{N}^+$  type ion exchangers<sup>64,65</sup>. The elution sequence for these anions on alumina is reversed<sup>66</sup>. The chromatographic efficiencies determined for these anions were comparable to those reported for the organic acids.

As already noted when describing the ion-exchange behavior of zirconia, phosphate has an essentially irreversible effect on the properties of zirconia. This strong interaction with phosphate has many implications for the use of zirconia as a chromatographic support and we have therefore examined the adsorption of several different phosphate species on zirconia. The adsorption of NADH onto the zirconia surface was studied a static adsorption experiment in the summarized in Table IV. Clearly NADH does adsorb onto zirconia.  $3.5 \mu\text{mol/g}$  adsorbed under the experimental conditions, although this is not necessarily an upper limit. Zirconia pretreated with inorganic phosphate did not adsorb NADH to a measurable extent. Washing the zirconia with  $0.1 M$  sodium hydroxide after phosphate treatment gave a product which adsorbed some NADH, although not as much as the untreated zirconia. This is not surprising since it is known that phosphate is stripped from zirconium phosphate at high pH. Washing the phosphate-treated zirconia with  $0.1 M$  nitric acid had no apparent effect, that is, it did not adsorb NADH after washing

TABLE III

RETENTION OF INORGANIC ANIONS ON ZIRCONIA

Column:  $5 \text{ cm} \times 0.46 \text{ cm}$  I.D. packed with  $10\text{--}15 \mu\text{m}$  zirconia. Mobile phase:  $10 \text{ mM}$  acetate buffer, pH 5. Flow-rate:  $1 \text{ ml/min}$ . Injection volume:  $20 \mu\text{l}$ . Solute concentration: *ca.*  $15 \text{ mM}$ . Detector: Tracor 965 photoconductivity detector.

Solute	$k'$	Solute	$k'$
Chloride	2.2	Sulfate	6.2
Bromide	3.0	Bromate	6.5
Iodide	3.5	Tetraborate	10.6
Nitrate	4.9	Thiosulfate	15.0

TABLE IV  
NADH ADSORPTION ON ZIRCONIA

$\mu\text{mol}$  of NADH adsorbed onto 100 mg of zirconia from 5 ml of 100 mM pH 8 Tris buffer.

Sample treatment <sup>a</sup>	$\mu\text{mol}$ NADH added	$\mu\text{mol}$ NADH adsorbed	NADH Adsorbed $\mu\text{mol/g ZrO}_2$
None	0.5	0.15	3.5
100 mM phosphate, pH 8, NaOH wash <sup>b</sup>	0.5	0.28	2.8
100 mM phosphate, pH 8	0.5	0	0
100 mM phosphate, pH 8, HNO <sub>3</sub> wash <sup>c</sup>	0.5	0	0
100 mM phosphate, pH 8, NaOH wash <sup>d</sup>	0.5	0.082	0.82
100 mM borate, pH 8	0.5	0.25	2.5

<sup>a</sup> 100 mg of support were washed with 2 × 2 ml of the designated buffer *before* addition of NADH.

<sup>b</sup> Sample of zirconia with 3.5  $\mu\text{mol/m}^2$  adsorbed NADH washed with 1 × 0.2 ml of 1 M phosphate, pH 8.

<sup>c</sup> 100 mg of phosphate-treated zirconia were washed with 2 × 2 ml of 0.1 M HNO<sub>3</sub> *before* addition of NADH.

<sup>d</sup> 100 mg of phosphate-treated zirconia were washed with 2 × 2 ml of 0.1 M NaOH *before* addition of NADH.

with 0.1 M nitric acid. This finding is consistent with the known stability of zirconium phosphate in acidic solutions. Inorganic phosphate was able to displace some fraction of previously adsorbed NADH. The presence of borate reduced the extent of NADH adsorption, but not as dramatically as phosphate.

Additional experiments were done to more clearly define the variables effecting the adsorption of oxyphosphorus compounds onto zirconia. In these experiments, the static adsorption of phenylphosphonic acid, diphenyl phosphate, diphenyl phosphinic acid and triphenyl phosphine oxide on zirconia was studied under a variety of solvent conditions. As shown by the data in Table V, all three compounds with an hydroxyl group adsorb to nearly the same extent in methanol. In carbon dioxide-free water diphenyl phosphate and diphenyl phosphinic acid adsorb to a greater extent than in methanol, presumably due to their lower solubility in water. In the absence of a strong adsorption competitor it is not surprising that the solubility

TABLE V  
STATIC ADSORPTION OF ORGANOPHOSPHORUS COMPOUNDS ON ZIRCONIA

$\mu\text{mol}$  of compound adsorbed from 100  $\mu\text{M}$  solution onto 100 mg of zirconia. Determined by decrease in absorbance of solution at 214 nm after 1 h of exposure to zirconia.

Compound	$\mu\text{mol adsorbed per g zirconia}$		
	50 mM Tris	CO <sub>2</sub> -free water	Methanol
Phenyl phosphonic acid	3.2	3.3	2.0
Diphenyl phosphate	0	0.9	1.7
Diphenyl phosphinic acid	0	2.6	2.0
Triphenyl phosphine oxide	0	0	0

would determine the extent of adsorption. The adsorption of diphenyl phosphate was significantly reduced in water relative to methanol. In 50 mM Tris buffer only phenyl phosphonic acid adsorbed to a measurable extent. The Tris, present at a much higher concentration than the adsorbates, is preferentially adsorbed except in the case of the phenyl phosphonic acid which has two hydroxyl groups. We have interpreted this as evidence for the formation of a "bidentate" surface complex. In fact, the formation of bidentate surface complexes between phosphonic acids and metal oxides has previously been demonstrated spectroscopically<sup>67,68</sup>. In general, these adsorption results seem to indicate that hydroxyl groups on the organophosphorus compounds are essential for adsorption and that adsorption of phosphonates, with two hydroxyl groups per molecule is stronger than that of other phosphate species.

#### CONCLUSIONS

The evaluation of porous microparticulate zirconia spherules is reported. The physical and mechanical properties of these spherules make them appropriate for use as HPLC supports. Zirconia has both anion- and cation-exchange properties, depending on solution pH and buffer composition. Inorganic phosphate adsorbs onto zirconia and alters its anion-exchange properties, transforming it from an anion exchanger below pH 9 to a cation exchanger. Organophosphates and organophosphonates, particularly the latter, are strongly adsorbed on zirconia. Most importantly, it has been demonstrated that these porous zirconia spherules are stable at pH 1–14 under static conditions and that their alkaline stability is superior to that of chromatographic alumina.

#### ACKNOWLEDGEMENTS

This work was supported in part by grants from the University of Minnesota Center for Biological Process Technology and 3M Company.

#### REFERENCES

- 1 R. E. Iler, *The Chemistry of Silica*, Wiley-Interscience, New York, 1979.
- 2 K. K. Unger, *Porous Silica (Journal of Chromatography Library, Vol. 16)*, Elsevier, Amsterdam, 1979.
- 3 R. P. W. Scott, *Adv. Chromatogr.*, 20 (1982) 167.
- 4 C. T. Wehr and R. E. Majors, *LC·GC, Mag. Liq. Gas Chromatogr.*, 5 (1987) 942.
- 5 A. Wehrli, J. C. Hildenbrand, H. P. Keller, R. Stampeli and R. W. Frei, *J. Chromatogr.*, 149 (1978) 199.
- 6 K. Krummen and R. W. Frei, *J. Chromatogr.*, 132 (1977) 27.
- 7 J. J. Glajch, J. J. Kirkland and J. Köhler, *J. Chromatogr.*, 384 (1987) 81.
- 8 K. K. Unger, N. Becker and P. Roumeliotis, *J. Chromatogr.*, 125 (1976) 115.
- 9 C. Horvath, W. Melander and I. Molnar, *Anal. Chem.*, 49 (1977) 142.
- 10 J. Köhler and J. J. Kirkland, *J. Chromatogr.*, 385 (1987) 125.
- 11 J. G. Atwood, G. J. Schmidt and W. Slavin, *J. Chromatogr.*, 171 (1979) 109.
- 12 P. P. Wickramanayake, A. Chatt and W. A. Aue, *Can. J. Chem.*, 59 (1981) 1045.
- 13 R. Aigner-Held, W. A. Aue and E. E. Pickett, *J. Chromatogr.*, 189 (1980) 139.
- 14 W. H. Tomb and H. H. Weetall, *U.S. Pat.*, 3 783 101 (1974).
- 15 R. W. Stout and J. J. DeStefano, *J. Chromatogr.*, 326 (1985) 63.
- 16 R. W. Stout, *U.S. Pat.*, 4 600 646 (1986).
- 17 D. R. Marsh and G. T. Tsao, *Biotechnol. Bioeng.*, 18 (1976) 349.
- 18 H. H. Weetall and N. B. Havewala, *Biotechnol. Bioeng.*, 3 (1972) 241.
- 19 R. W. Stout, S. I. Sivakoff, R. D. Ricker, H. C. Palmer, M. A. Jackson and T. J. Odiorne, *J. Chromatogr.*, 352 (1986) 381.

- 20 A. Barkatt and P. B. Macedo, *U.S. Pat.*, 4 648 975 (1987).
- 21 J. R. Benson and D. J. Woo, *J. Chromatogr. Sci.*, 22 (1984) 386.
- 22 F. Nevejans and M. Verzele, *Chromatographia*, 20 (1985) 173.
- 23 L. D. Bowers and S. Pedigo, *J. Chromatogr.*, 371 (1986) 243.
- 24 T. Hanai, in S. Hara, S. Mori and T. Hanai (Editors), *Chromatography —The Separation System*, Maruzen, Tokyo, 1981, p. 121.
- 25 H. G. Cassidy, *J. Am. Chem. Soc.*, 62 (1940) 3073.
- 26 H. G. Cassidy and S. E. Wood, *J. Am. Chem. Soc.*, 63 (1941) 2628.
- 27 A. Tiselius and L. Hagdahl, *Acta Chem. Scand.*, 4 (1950) 394.
- 28 L. Hagdahl, R. J. P. Williams and A. Tiselius, *Ark. Kem.*, 7 (1952) 1.
- 29 A. Tiselius, *Kolloid-Z.*, 105 (1943) 101.
- 30 J. H. Knox and M. T. Gilbert, *U.K. Pat.*, 7 939 449 (1979); *U.S. Pat.*, 4 263 268 (1979); *G.R.F. Pat.*, P2 946 688-4 (1979).
- 31 U. Bien-Vogelsang, A. Deege, H. Figge, J. Köhler and G. Schomburg, *Chromatographia*, 19 (1984) 170.
- 32 R. M. Chicz, Z. Shi and F. E. Regnier, *J. Chromatogr.*, 359 (1986) 121.
- 33 M. P. Rigney, T. P. Weber and P. W. Carr, *J. Chromatogr.*, 484 (1989) 273.
- 34 E. R. Russel, A. W. Adamson, J. Schubert and G. E. Boyd, *United States Atomic Energy Commission Report CN-508* (1943).
- 35 C. B. Amphlett, L. A. McDonald and M. J. Redman, *J. Inorg. Nucl. Chem.*, 6 (1958) 236.
- 36 N. Michael, W. D. Fletcher, D. E. Croucher and M. J. Bell, *Westinghouse Report CVNA-135* (for the United States Atomic Energy Commission) (1961).
- 37 C. B. Amphlett, L. A. McDonald and M. J. Redman, *J. Inorg. Nucl. Chem.*, 6 (1958) 220.
- 38 P. A. Agron, E. L. Fuller, Jr. and H. F. Holmes, *J. Colloid Interface Sci.*, 52 (1975) 553.
- 39 T. Yamaguchi, Y. Nakano and K. Tanabe, *Bull. Chem. Soc. Jpn.*, 51 (1978) 2482.
- 40 N. E. Tretyakov, D. V. Dozdyakov, O. M. Ornskaya and V. N. Filiminov, *Zh. Fiz. Khim.*, 44 (1970) 1077.
- 41 A. J. Tench and R. L. Nelson, *Trans. Faraday Soc.*, 63 (1967) 2254.
- 42 E. J. W. Verwey, *Rec. Trav. Chim.*, 60 (1941) 625.
- 43 S. Mattson and A. J. Pugh, *Soil Sci.*, 38 (1934) 229.
- 44 G. W. Smith and T. Salman, *Can. Met. Q.*, 5 (1966) 93.
- 45 G. A. Parks, *Adv. Chem. Ser.*, 67 (1967) 121.
- 46 G. A. Parks, *Chem. Rev.*, 65 (1964) 177.
- 47 H. Kita, N. Henmi, K. Shimazu, H. Hattori and K. Tanabe, *J. Chem. Soc., Faraday Trans. I*, 77 (1981) 2451.
- 48 C. B. Amphlett, L. A. McDonald and M. J. Redman, *J. Inorg. Nucl. Chem.*, 6 (1958) 236.
- 49 C. B. Amphlett, *Inorganic Ion Exchangers*, Elsevier, Amsterdam, New York, 1964.
- 50 K. A. Kraus and H. O. Phillips, *J. Am. Chem. Soc.*, 78 (1956) 249.
- 51 C. B. Amphlett, in *Proceedings of the Second International Conference on the Peaceful Uses of Atomic Energy, Geneva, 1958, P/271*, United Nations, Geneva, 1958, p. 17.
- 52 K. A. Kraus, H. O. Phillips, T. A. Carlson and J. S. Johnson, in *Proceedings of the Second International Conference on the Peaceful Uses of Atomic Energy, Geneva, 1958, P/1832*, United Nations, Geneva, 1958, p. 3.
- 53 Y. Ghaemi and R. A. Wall, *J. Chromatogr.*, 174 (1979) 51.
- 54 P. C. Sadek, *Ph.D. Thesis*, University of Minnesota, Minneapolis, MN, 1985.
- 55 R. Stevens, *Zirconia and Zirconia Ceramics*, Publication No. 113, Magnesium Elektron, Twickenham, 1986.
- 56 K. K. Unger and U. Trudinger, in P. R. Brown and R. A. Hartwick (Editors), *High Performance Liquid Chromatography*, Wiley, New York, 1989, Ch. 3, p. 159.
- 57 T. P. Weber, personal communication.
- 58 E. Paukstis, R. I. Soltanov and E. N. Yurchenko, *React. Kinet. Catal. Lett.*, 19 (1982) 105.
- 59 K. Esumi and K. Meguro, *Bull. Chem. Soc. Jpn.*, 55 (1982) 315.
- 60 T. Yamaguchi, Y. Nakano and K. Tanabe, *Bull. Chem. Soc. Jpn.*, 51 (1978) 2482.
- 61 N. E. Tretyakov, D. V. Dozdyakov, O. M. Ornskaya and V. N. Filiminov, *Zh. Fiz. Khim.*, 44 (1970) 1077.
- 62 C. Laurent, H. A. H. Billiet and L. de Galan, *Chromatographia*, 17 (1983) 253.
- 63 R. L. Smith and D. J. Pietrzyk, *Anal. Chem.*, 56 (1984) 610.
- 64 J. S. Fritz, D. T. Gjerde and C. Pohlandt, *Ion Chromatography*, Hüthig, Heidelberg, 1982.
- 65 F. C. Smith, Jr. and R. C. Chang, *The Practice of Ion Chromatography*, Wiley, New York, 1983.
- 66 G. L. Schmitt and D. J. Pietrzyk, *Anal. Chem.*, 57 (1985) 2247.

## EFFECT OF COVERAGE DENSITY ON THE RETENTION MECHANISM IN REVERSED-PHASE HIGH-PERFORMANCE LIQUID CHROMATOGRAPHY

BOGUSŁAW BUSZEWSKI<sup>a</sup>, ZDZISŁAW SUPRYNOWICZ and PIOTR STASZCZUK

*Faculty of Chemistry, Maria Curie Skłodowska University, PL-20 031 Lublin (Poland)*

and

KLAUS ALBERT, BETTINA PFLEIDERER and ERNST BAYER\*

*Institut für Organische Chemie, Auf der Morgenstelle 18, D-7400 Tübingen (F.R.G.)*

---

### SUMMARY

The chromatographic properties of reversed-phase high-performance liquid chromatographic (RP-HPLC) packings with chemically bonded C<sub>18</sub> groups of controlled coverage were characterized by correlation of the capacity factor and the composition of the mobile phase, taking physico-chemical properties of the packings into account. On the basis of a cylindrical model of pores and the dependence of retention on density and homogeneity of the surface coverage with alkylsilyl ligands, an attempt was made to describe the retention mechanism in the RP-HPLC system. It was found that packings with a coverage density higher than 3.8 μmol/m<sup>2</sup> were dense, homogeneous and shielded the unblocked surface silanol groups sufficiently.

---

### INTRODUCTION

The separation mechanism in reversed-phase high-performance liquid chromatography (RP-HPLC) is based on the hydrophobic interactions between the solute and alkylsilyl groups chemically bonded to the support surface<sup>1–6</sup>. In previous papers<sup>7–11</sup> the controlled preparation of packings with chemically bonded C<sub>18</sub> groups resulting in materials with various surface coverages of alkylsilyl ligands was discussed. A maximum density of the stationary phase of α<sub>RP</sub> > 4 μmol/m<sup>2</sup> can be obtained. In most of the previous papers<sup>7–14</sup>, however, the correlation between the physico-chemical properties of the phases and the separation of various substances was only partially discussed.

The determination of the free surface energy of packings has been demonstrated to be very useful<sup>13</sup>. Depending on the coverage with octadecyl ligands<sup>15–18</sup>, the surface of the packing showed significantly different properties and interactions, especially<sup>13</sup> for C<sub>18</sub> ligands with a coverage density α<sub>RP</sub> ≥ 3.8 μmol/m<sup>2</sup>. It follows from the literature<sup>1–3,7,10–12,17–20</sup> that during elution in the RP-HPLC system, C<sub>18</sub> ligands

---

\* Present address: Institut für Organische Chemie, Auf der Morgenstelle 18, D-7400 Tübingen, F.R.G.

change their conformation<sup>13,15,21</sup> which significantly influences the retention, resolution and peak shape. This can result from (i) the presence of free, unblocked silanol groups, which causes an increase in the interactions at the mobile phase–solute–stationary phase interface, (ii) specific interactions between individual alkylsilyl ligands (especially when the surfaces are blocked homogeneously) and (iii) the composition of the mobile phase and the nature of the sample.

Investigation of the separation mechanism in columns of packings with different surface coverages of C<sub>18</sub> alkylsilyl ligands therefore appears to be very interesting. Correlations between the retention data of the solutes and the coverage density ( $\alpha_{RP}$ ) and the mobile phase composition were therefore studied. In addition, an evaluation of the density and the homogeneity of the coverage density of the packings was attempted on the basis of the experimental data.

## EXPERIMENTAL

### Materials

Monochlorooctadecylsilane (Petrarch Systems, Bristol, PA, U.S.A.) mixed with dried morpholine (Reakhim, Moscow, U.S.S.R.) and specially dried toluene<sup>22</sup> (POCh, Gliwice, Poland) was used as the modifying reagent.

TABLE I  
PHYSICO-CHEMICAL CHARACTERISTICS OF THE PREPARED PACKING MATERIALS

A = activator; ODMCS = monochlorooctadecylsilane;  $\alpha_{RP}$  = concentration of chemically bonded C<sub>18</sub> groups ( $\mu\text{mol}/\text{m}^2$ );  $\alpha_{\text{SiOH}}$  = concentration of accessible silanol groups ( $^{\circ}\text{mol}/\text{m}^2$ );  $D$  = mean pore diameter (nm);  $V_p$  = pore volume ( $\text{cm}^3/\text{g}$ );  $S_{\text{BET}}$  = specific surface area ( $\text{m}^2/\text{g}$ ).

No. of packing	Type of packing	A:ODMCS ratio (mol/mol)	Surface coverage			Porosity		
			C (%)	$\alpha_{RP}$	$\alpha_{\text{SiOH}}$	$D$	$V_p$	$S_{\text{BET}}$
	Bare silica gel (SG)	—	—	—	5.21	20.00	2.10	361
1	Silica gel C <sub>18</sub>	2.60:1	5.08	0.72	4.53	18.28	1.92	338
2	monomeric structure	2.35:1	11.69	1.61	3.45	17.37	1.81	323
3		2.10:1	17.20	2.60	2.52	15.71	1.65	314
4		1.85:1	21.20	3.46	1.58	15.24	1.60	203
5		1.60:1	24.50	4.24	0.42	14.28	1.55	175

Spherical silica gel (SG-7/G) (Polymer Institute, Bratislava, Czechoslovakia)<sup>23</sup> was used as the support for the chemically bonded phase. Its characteristic data are given in Table I. The solvents used (analytical-reagent grade) were toluene, benzene, methanol and dimethyl ether (POCh). Binary eluents for RP-HPLC systems (methanol–water) were prepared as described previously<sup>22</sup> using water with a conductivity of  $10^{-5}$  S/m. In measurements carried out by gel permeation chromatography (GPC), tetrahydrofuran (THF) (VEB Laborchemie, Apolda, G.D.R.) was used as the mobile phase. Stainless-steel tubes (100 × 4 mm I.D.) were purchased from the Chemical Reagent Factory–ZOCh (Lublin, Poland).

### *Apparatus*

Chromatographic measurements were made using a liquid chromatograph consisting of an LC-20 piston pump (Pye Unicam, Cambridge, U.K.), a Model 7120 injection valve (Rheodyne, Berkeley, CA, U.S.A.) equipped with a 10- $\mu$ l injection loop, a Model 254 M ultraviolet detector (Techma Robot, Warsaw, Poland) equipped with an 8- $\mu$ l flowcell and a TZ-4100 linear recorder (Laboratorní Přístroje, Prague, Czechoslovakia). The dead volume was determined on the basis of the solvent peaks.

The porosity parameters characterizing the starting material and chemically modified packings (the specific surface area,  $S_{\text{BET}}$ , the pore volume,  $V_p$ , and the mean pore diameter,  $D$ ) were determined by low-temperature adsorption and desorption of nitrogen using a Model 1800 automatic apparatus (Carlo Erba, Milan, Italy).

The concentration of surface silanol groups ( $\alpha_{\text{SiOH}}$ ) before and after modification was determined using the method proposed by Nondek and Vyskočil<sup>24</sup>. The degree of coverage of the surface with alkyl ligands ( $\alpha_{\text{RP}}$ ) was calculated as described elsewhere<sup>25</sup>. The percentage of carbon was determined using a Model 185 CHN analyser (Hewlett-Packard, Palo Alto, CA, U.S.A.).

Solid-state NMR measurements were performed on a Bruker MSL 200 spectrometer with samples of 200–300 mg in double-bearing rotors of  $\text{ZrO}_2$ . Magic-angle spinning (MAS) was carried out at a spinning rate of 4 kHz.  $^{29}\text{Si}$  cross-polarization (CP)-MAS-NMR spectra were recorded with a pulse length of 5  $\mu$ s together with a contact time of 5 ms and a pulse repetition time of 2 s. For  $^{13}\text{C}$  CP-MAS-NMR spectra a contact time of 12 ms was used. All NMR spectra were externally referenced to liquid tetramethylsilane (TMS) and the chemical shifts are given in parts per million (ppm).

### *Chemical bonding procedure*

Chemical modification of the surface of silica supports was carried out as described elsewhere using only monofunctional silanes<sup>8,9</sup>. Changes in the molar ratio of the modifier monochlorooctadecylsilane (ODMCS) and activator (morpholine) permit the preparation of supports with strictly defined amounts of carbon on the support surface<sup>10,11</sup>. Numerical volumes of the molar ratio are given in Table I, which also contains the physico-chemical characteristics of the surface of the prepared packings after their chemical modification.

### *Column packing procedure*

The columns were packed under a pressure of 450 Pa using a laboratory-built apparatus described previously<sup>26</sup>. An 8% (v/v) solution of carbon tetrachloride in methanol was used as the dispersing medium. The prepared columns were evaluated by determining characteristic basic parameters such as the number of theoretical plates ( $N_T$ ), reduced parameters:  $h$  (plate height) and  $v$  (velocity), column resistance ( $\phi$ ) and asymmetry coefficient ( $f_{\text{As}}$ )<sup>27,28</sup>. The columns prepared can be described according to Bristow and Knox<sup>28</sup> as "good" or even "very good", as confirmed by the data presented in Table II.

## RESULTS AND DISCUSSION

Table I lists the physico-chemical data of the monofunctionally modified silica gels ( $C_{18}$ ) with different carbon contents. The data indicate that a change in the activator—modifier (ODMCS) molar ratio permits the preparation of packings with different carbon contents. The data show that with increasing  $\alpha_{RP}$  a decrease in  $\alpha_{SiOH}$  is obtained. The sum of  $\alpha_{RP}$  and  $\alpha_{SiOH}$  is approximately constant and equal to the initial  $\alpha_{SiOH}$  value. The densest packing (No. 5) is an exception, because the sum of  $\alpha_{RP}$  and  $\alpha_{SiOH}$  is significantly smaller. This can be explained by steric masking of unreacted silanol groups<sup>10–12,15–18,29,30</sup> on the whole surface by the dense population of alkylsilyl ligands. An analysis of the porosimetric data indicates similar conclusions (Table I).

In all instances the decrease in  $D$ ,  $V_p$  and  $S_{BET}$  values can be correlated with an increase in the percentage of carbon. From the typical GPC curves presented in Fig. 1 it can be concluded that in spite of the increase in carbon content, even packing 5, with the highest degree of modification, is capable of typical GPC separations, which means that the pores are not blocked by long  $C_{18}$  chains. A correlation between porosimetric (Table I) and chromatographic data is possible. The increase in  $\alpha_{RP}$  values leads to an decrease in the elution volume ( $V_e$ )<sup>10,14</sup>.

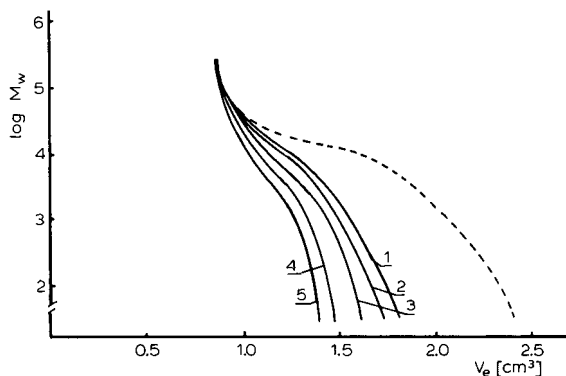


Fig. 1. Plot of log mol.wt. ( $M_w$ ) of polystyrene standards vs. elution volume ( $V_e$ ) for unmodified support (dashed line) and for packings with chemically bonded  $C_{18}$  groups (continuous line).  $\alpha_{RP}$ : (1) 0.72; (2) 1.61; (3) 2.60; (4) 3.46; (5) 4.25  $\mu\text{mol}/\text{m}^2$ . Chromatographic conditions: mobile phase, THF; flow-rate, 0.5 ml/min; detection, UV (254 nm).

We showed recently that in material of dense coverage ( $\alpha_{RP} \geq 4.0 \mu\text{mol}/\text{m}^2$ ), about 85% of the silanol groups are blocked and the surface area decreases by about 60%<sup>10,11</sup>. These findings are supported by  $^{29}\text{Si}$  CP-MAS-NMR data. In Fig. 2A the  $^{29}\text{Si}$  CP-MAS-NMR spectrum of native silica gel is depicted. The existence of geminal silanol groups  $Q_2$ , silanol groups  $Q_3$  and siloxane units  $Q_4$  can easily be recognized by the corresponding signals at  $-90$ ,  $-100$  and  $-110$  ppm, respectively<sup>15,16</sup>. With modified silica gel with an 11.69% carbon loading (packing 2), a new signal arises at 14.0 ppm due to the introduced Si–O–Si moiety (Fig. 2B). Correspondingly, the signal intensity of the  $Q_2$  and  $Q_3$  units decreases.



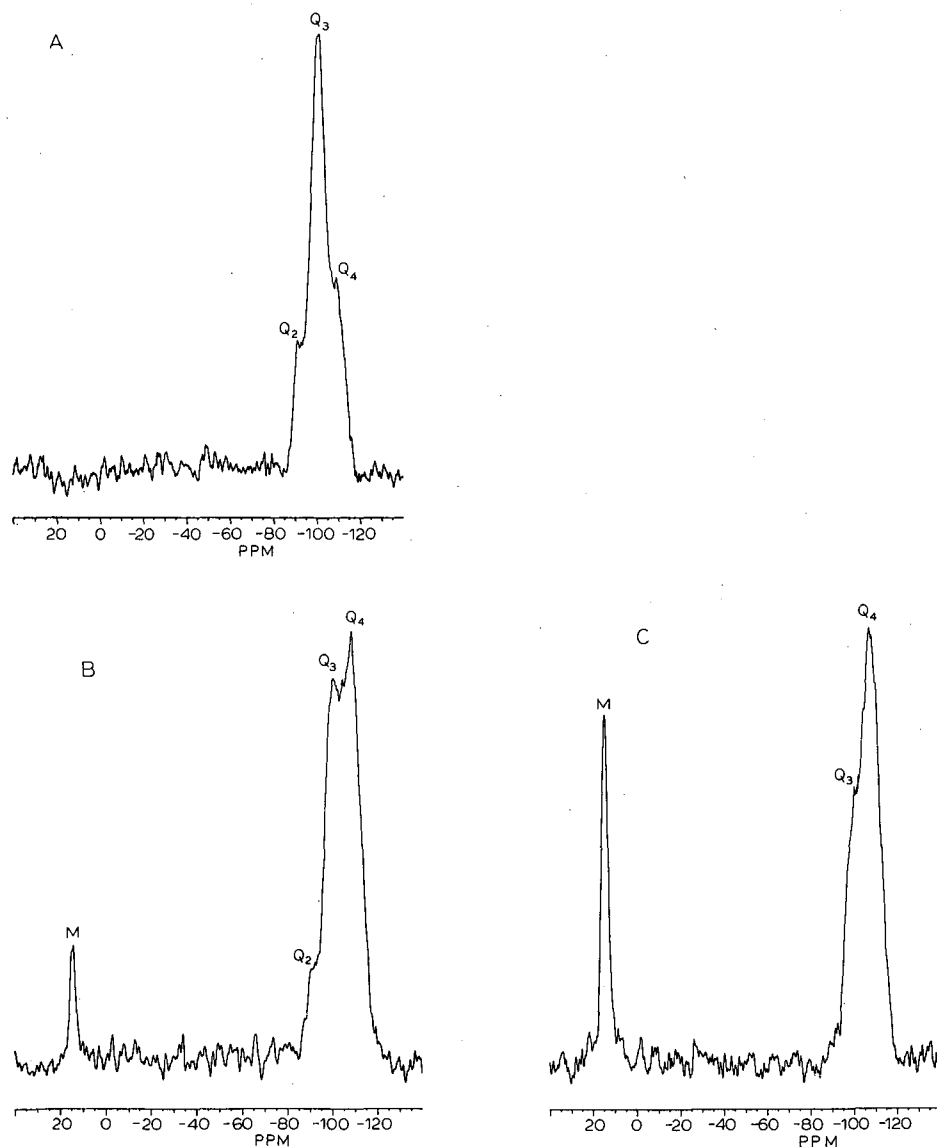


Fig. 2.  $^{29}\text{Si}$  CP-MAS-NMR spectra (39.75 MHz) of silica gel samples: (A) unmodified silica gel; (B) monofunctionally modified silica gel with a carbon loading of 11.67% (packing 2); (C) monofunctionally modified silica gel with a carbon loading of 24.5% (packing 5).

In the spectrum of the modified silica gel with the highest carbon loading (packing 5, Fig. 2C), the  $\text{Q}_2$  units can no longer be detected and the signal intensity of  $\text{Q}_3$  units is also dramatically reduced. In contrast to Fig. 2A, the signal of  $\text{Q}_4$  units dominates the spectral pattern between  $-90$  and  $-110$  ppm.

The CP excitation technique used for recording of the  $^{29}\text{Si}$  NMR spectra is dependent on the number of protons associated with the investigated species.

Therefore, at a distinct contact time, only the  $M/(Q_2 + Q_3)$  ratio can be quantitatively determined<sup>16</sup>. The decreasing signal intensity of  $Q_2$  and  $Q_3$  units in Fig. 2B and C is consistent with an increasing signal intensity of the M unit. This clearly confirms the formation of a covalent Si-O-Si linkage even at a high surface loading.

In the  $^{13}\text{C}$  CP-MAS-NMR spectrum of the modified material with the highest carbon loading (packing 5), no signal of adsorbed material can be found, in contrast to earlier observations<sup>15</sup> (Fig. 3).

Experiments permitting the determination of the free surface energy of packings prepared were also carried out<sup>13</sup>. From these investigations it follows that the materials with a coverage above  $3.8 \mu\text{mol}/\text{m}^2$  are so dense and homogeneous that the free surface energy decreases by a factor of 5 in comparison with unmodified silica gel and is very similar to that of a hydrocarbon surface. These data are consistent with the results obtained from elemental and porosimetric analysis<sup>14</sup>.

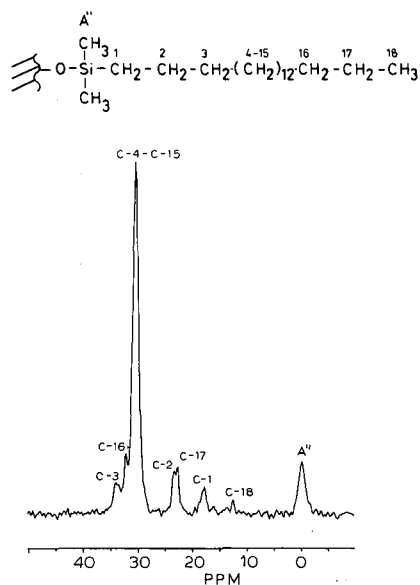


Fig. 3.  $^{13}\text{C}$  CP-MAS-NMR spectrum (50.33 MHz) of monofunctionally modified silica gel with a carbon loading of 24.5% (packing 5).

The prepared phases were investigated in the RP-HPLC system and compounds of different chemical natures were used as test substances. Fig. 4 presents the results for the five columns packed with the materials described in Table I. The column data are given in Table II. Correlation of the capacity factors ( $k'$ ) of benzene derivatives and the composition of the binary mobile phase ( $\Phi$ ) showed a dependence of the selectivity on the surface loading. An increase in the coverage density results in an increase in the separation selectivity for different substances. In all instances the  $k'$  values of individual substances increase with increase in the water content in the mobile phase (when the water content exceeds 50%, v/v). This effect, however, is most significant for materials with  $\alpha_{\text{RP}}$  values of 3.46 and  $4.24 \mu\text{mol}/\text{m}^2$  (Fig. 4D and E, respectively). The selectivity improves when the mobile phase contains 60–80% of methanol.

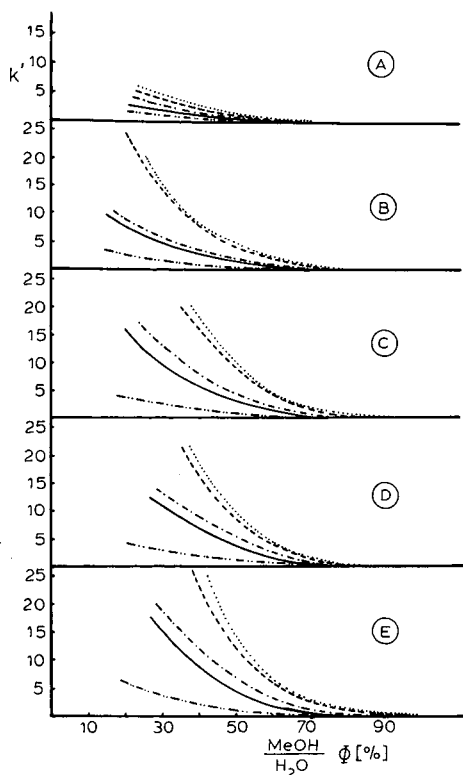


Fig. 4. Relationship between the capacity factor ( $k'$ ) and the composition of the mobile phase ( $\Phi$ ) for benzene derivatives obtained on columns packed with materials with a controlled content of  $C_{18}$  groups on the surface.  $\alpha_{RP}$ : (A) 0.72; (B) 1.60; (C) 2.60; (D) 3.46; (E) 4.25  $\mu\text{mol}/\text{m}^2$ . (····) chlorobenzene; (-----) toluene; (-·-·-) benzene; (—) nitrobenzene; (- - - -) phenol. MeOH = Methanol.

It can be concluded that hydrophobic interactions between the mobile phase and chemically bonded hydrophobic  $C_{18}$  ligands should be especially observed for materials with high surface loading ( $\alpha_{RP} = 4.24 \mu\text{mol}/\text{m}^2$ ). In such materials, polar molecules of benzene derivatives cannot interact because of great cohesive (chain-

TABLE II

COLUMN PROPERTIES

Mobile phase: methanol-water (70:30, v/v).  $k'$  = capacity factor;  $N_T$  = number of theoretical plates per 100 mm column length;  $h$  = reduced plate height;  $v$  = reduced velocity;  $\varphi$  = column resistance parameter;  $f_{As}$  = asymmetry factor.

No. of packing	Solute naphthalene					
	$k'$	$N_T$	$h$	$v$	$\varphi$	$f_{As}$
1	0.29	2620	5.45	6.2	782	1.42
2	1.09	2835	5.05	5.95	778	1.39
3	2.79	2978	4.80	5.80	742	1.20
4	3.26	3215	4.45	5.09	717	1.19
5	4.40	3605	3.96	4.90	695	1.11

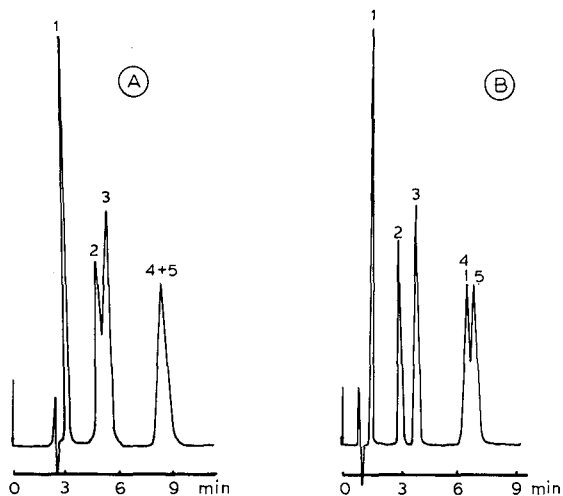


Fig. 5. Examples of the separation of benzene derivatives on columns packed with materials with different coverage densities of  $C_{18}$  groups.  $\alpha_{RP}$ : (A) 3.46; (B) 4.25  $\mu\text{mol}/\text{m}^2$ . Chromatographic conditions: mobile phase, methanol-water (60:40, v/v); flow-rate, 1 ml/min; detection, UV (254 nm). Peaks: 1 = phenol; 2 = nitrobenzene; 3 = benzene; 4 = toluene; 5 = chlorobenzene.

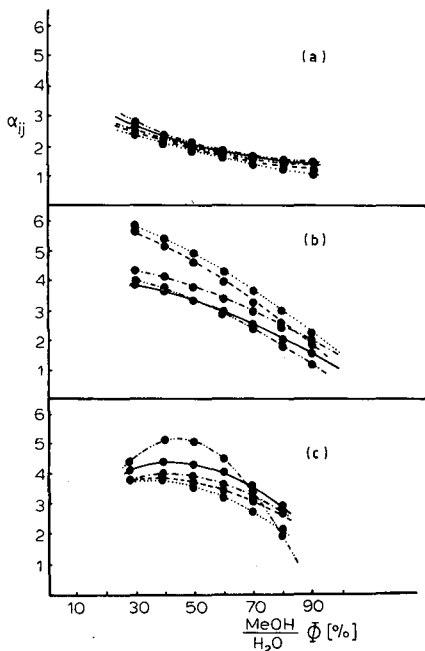


Fig. 6. Selectivity coefficients ( $\alpha_{ij}$ ) for three pairs of substances as a function of the mobile phase composition ( $\Phi$ ). (a)  $\alpha_{ij} = k'_{\text{toluene}}/k'_{\text{benzene}}$ ; (b)  $\alpha_{ij} = k'_{\text{nitrobenzene}}/k'_{\text{phenol}}$ ; (c)  $\alpha_{ij} = k'_{\text{benzene}}/k'_{\text{phenol}}$ ; (····) packing 1; (---) packing 2; (- - -) packing 3; (—) packing 4; (- · - · -) packing 5. For column packing characteristics, see Tables I and II.

chain) interactions. It seems that for the materials with a high coverage density, the mechanism of separation can be described as a partition process<sup>1-6</sup>, because the resolution of peaks 2 and 3 and 4 and 5 is improved with increasing coverage density. This suggestion is confirmed by the chromatograms in Fig. 5, which shows the separation of the test mixture obtained on columns containing packings 4 and 5 (Table D).

In order to explain more precisely the processes that occur in the packings during the HPLC test, three other test mixtures were used: benzene-toluene, phenol-nitrobenzene and phenol-benzene. The relationship between the selectivity of separation ( $\alpha_{ij} = k_j/k_i$ ) and composition of the mobile phase is plotted in Fig. 6, from which it can be concluded that their slopes change depending on the chemical nature of the test substances and on the properties of the surface<sup>14</sup>. In two cases (Fig. 6A and C) the elution order correlates with the changes in percentage of carbon (Table I) and with increasing  $\alpha_{ij}$ . In Fig. 6B, the sequence of the curves is the opposite of that in Fig. 6A and C. In this connection, it can be assumed that the mechanism of the elution is slightly different.

Fig. 6A presents the plots determined for the non-polar mixture, benzene-toluene. The form of these plots is consistent with hydrophobic theory<sup>1-7,12,29,31-33</sup>, where interactions between the mobile phase and the support surface dominate. Thus  $\alpha_{ij}$  values will change with increase in the hydrophobic nature of the prepared packing and a small concave in the course of the curves can be observed. Fig. 6B presents the curves plotted for the phase containing polar components, which can interact with the unblocked surface silanol groups. The lack of any interactions results in a smaller selectivity for the separation of polar substances chromatographed on the material of high coverage (packing 5). The resolution improves, however, owing to prolongation of the retention time on the materials characterized by less dense coverage (packings 1 and 2). This behaviour is indicated by different slopes of the curves corresponding to the materials characterized by a low percentage of carbon (the  $\alpha_{RP}$  values for these materials are 0.72 and 1.61  $\mu\text{mol}/\text{m}^2$ , respectively, see Table I). Hence the previous conclusion about a different mechanism (adsorption type) for these materials is supported. Free silanol groups also seem to play a role. With a low surface loading the surface is not masked sufficiently by the "mobile" bonded  $\text{C}_{18}$  chains, in contrast to materials with a high surface loading<sup>9,12,29,30</sup>.

The curves corresponding to packings 3, 4 and 5 are similar in general, but the significantly hydrophobic nature of the packing with a coverage density  $\alpha_{RP} = 4.24 \mu\text{mol}/\text{m}^2$  increases with increase in methanol content in the mobile phase (stronger interactions of the chain-chain type). This phenomenon is probably responsible for the penetration of polar solute molecules to silanol groups. For this reason, the  $\alpha_{ij}$  values are significantly lower. Considering Fig. 6C, where the plots of the mixture of non-polar (benzene) and polar (phenol) solutes are shown, typical slopes for the materials of a hydrophobic nature are observed<sup>10,14</sup>. The high-coverage material (packing 5) shows the smallest retention of phenol, because the  $\alpha_{ij} = k_{\text{benzene}}/k_{\text{phenol}}$  values are the highest. This is due to the shielding of residual silanol groups by  $\text{C}_{18}$  ligands. From the point of view of separation selectivity, the slope of the curve corresponding to packing 5 ( $\alpha_{RP} = 4.24 \mu\text{mol}/\text{m}^2$ ) seems to be optimal.

The significant maximum of the selectivity ( $\alpha_{ij}$ ) in relation to the changes in composition of mobile phase ( $\Phi$ ) indicates different interactions of the substances

separated between the mobile phase and the packing surface<sup>31-33</sup>. The 6-fold increase in coverage density for packing 5 compared with packing 1 (Table I) leads to an increase in separation selectivity of about 30%.

The slopes of the curves for packings 1, 2 and 3 are similar, but differ significantly from those of packings 4 and 5. The slight differences in selectivity probably result from the increase in interactions between the test substances and the stationary phases and the increase in the hydrophobic nature of the packings investigated. This may also indicate a different accessibility of these surfaces for polar phenol molecules.

Convergence of the results is observed as in the calculations of surface free energy<sup>13</sup> on the basis of adsorption of two different substances, *n*-octane and water. Similar conclusions can also be drawn from the linear relationship between  $\log(k'/S_{\text{BET}})$  and the number of carbon atoms ( $n_c$ ) for the benzene homologues, which are presented in Fig. 7.

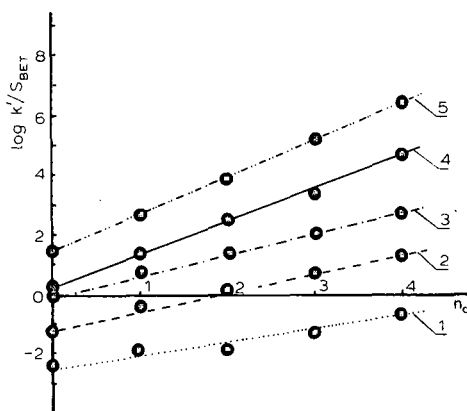


Fig. 7. Dependence of  $\log(k'/S_{\text{BET}})$  on the number of methylene groups ( $n_c$ ) in the homologous series of alkylbenzenes (benzene, toluene, ethylbenzene, propylbenzene and butylbenzene). For packings 1-5, see Tables I and II.

Correlations with the slopes in Fig. 4A-E can be found. A different slope corresponding to the materials with higher  $\alpha_{\text{RP}}$  values shows a homogeneous coverage of the support surface, and the unblocked silanols are shielded by the  $\text{C}_{18}$  ligands in materials with a high surface loading.

The slopes of the straight lines corresponding to packings 1, 2 and 3 (Fig. 7) characterized by smaller degrees of coverage (specific solvent-surface interactions are preferred to cohesive and hydrophobic interactions), in contrast, show a different elution mechanism and it seems that these materials show an adsorption mechanism. This can only be explained by a larger number of free silanol groups. These unblocked silanol groups are especially susceptible to interactions with polar substances having free electron pairs or  $\pi$  electrons. For this reason, the most sensitive test to define the nature of the surface and its density and homogeneity is undoubtedly the elution of organic bases, *e.g.*, amines<sup>12,29</sup>. In these instances not only the retention data but also

the tailing effect due to the specific interactions with unblocked silanols can reveal the separation mechanism. For these investigations, pyridine and 2,6-dimethylpyridine (lutidine) were used as the test substances in the RP-HPLC system [methanol–water (70:30, v/v)] (Fig. 8).

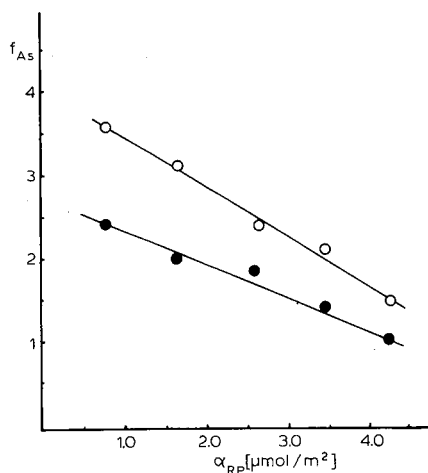


Fig. 8. Effect of coverage density of  $C_{18}$  groups ( $\alpha_{RP}$ ) on the peak asymmetry ( $f_{As}$ ) for ( $\circ$ ) lutidine and ( $\bullet$ ) pyridine. Chromatographic conditions: mobile phase, methanol–water (70:30, v/v); flow-rate, 1 ml/min; detection, UV (254 nm).

The relationship between the asymmetry coefficient ( $f_{As}$ ) and concentration of  $C_{18}$  ligands ( $\alpha_{RP}$ ) indicates that the more hydrophobic packing No. 5 ( $\alpha_{RP} = 4.24 \mu\text{mol}/\text{m}^2$ ) shows for both amines the smallest  $f_{As}$  value calculated according to Buszewski *et al.*<sup>27</sup> and Bristow and Knox<sup>28</sup>. The increase in the amount of free silanol groups leads to an increase in tailing (*i.e.*,  $f_{As}$  value)<sup>10</sup>. It can be concluded that the presence of polar basic substances changes not only the mechanism of the process, but also the “mobility” and the conformation of  $C_{18}$  ligands<sup>12,16,17,19</sup>. In this connection, the assumption that for the materials with a coverage density  $\alpha_{RP} \geq 3.46 \mu\text{mol}/\text{m}^2$  (packing 4) the  $f_{As}$  values are less than 2 seems to be reasonable. The behaviour of the packings with a coverage density of  $\alpha_{RP} \geq 3.46 \mu\text{mol}/\text{m}^2$  is similar to that with  $\alpha_{RP} \geq 4 \mu\text{mol}/\text{m}^2$  (No. 5), although the coverage is not dense.

## CONCLUSIONS

The CP-MAS-NMR data confirm the high surface coverage of the investigated materials. In materials with a high surface loading ( $4.24 \mu\text{mol}/\text{m}^2$ ), the *n*-alkyl ligands are exclusively covalently bonded to the silica surface. For dense coverages ( $\alpha_{RP} = 4.24 \mu\text{mol}/\text{m}^2$ ), 85% of the accessible silanol groups are blocked by alkylsilyl ligands.

The retention mechanism based on hydrophobic interactions is dependent on the surface coverage. In materials having a dense coverage ( $\alpha_{RP} \geq 3.8 \mu\text{mol}/\text{m}^2$ ), the partition process predominates, whereas in materials with less dense coverages ( $\alpha_{RP} < 3.8 \mu\text{mol}/\text{m}^2$ ), the adsorption process is of increasing importance.

## ACKNOWLEDGEMENT

One of us (B.B.) is grateful to the Alexander von Humboldt-Foundation for financial support.

## REFERENCES

- 1 A. Nahum and Cs. Horváth, *J. Chromatogr.*, 203 (1981) 53.
- 2 R. K. Gilpin and A. Squires, *J. Chromatogr. Sci.*, 19 (1981) 195.
- 3 K. G. Wahlund and A. Sokolowski, *J. Chromatogr.*, 151 (1978) 299.
- 4 D. E. Martire and R. E. Bohem, *J. Phys. Chem.*, 87 (1983) 1045 A.
- 5 B. L. Karger, J. R. Gant, A. Hartkopf and P. H. Weiner, *J. Chromatogr.*, 128 (1976) 65.
- 6 Cs. Horváth, *LC, Mag. Liq. Chromatogr. HPLC*, 1 (1983) 552.
- 7 B. Buszewski, L. Nondek, A. Jurášek and D. Berek, *Chromatographia*, 23 (1987) 442.
- 8 B. Buszewski, A. Jurášek, J. Garaj, L. Nondek, I. Novák and D. Berek, *J. Liq. Chromatogr.*, 10 (1987) 2325.
- 9 B. Buszewski, *Chemia Stosow.*, 32 (1988) 203.
- 10 B. Buszewski and Z. Suprynowicz, *Chromatographia*, 24 (1987) 573.
- 11 B. Buszewski and Z. Suprynowicz, *Anal. Chim. Acta*, 208 (1988) 263.
- 12 J. Nawrocki and B. Buszewski, *J. Chromatogr.*, 448 (1988) 1.
- 13 P. Staszczuk and B. Buszewski, *Chromatographia*, 25 (1988) 881.
- 14 B. Buszewski, D. Berek, J. Garaj, I. Novák and Z. Suprynowicz, *J. Chromatogr.*, 446 (1988) 191.
- 15 K. Albert, B. Pfeleiderer and E. Bayer, in D. E. Leyden and W. T. Collins (Editors), *Chemically Modified Surfaces*, Vol. 2, Gordon & Breach, New York, 1988, p. 287.
- 16 E. Bayer, A. Paulus, B. Peters, G. Laupp, J. Reiners and K. Albert, *J. Chromatogr.*, 364 (1986) 25.
- 17 K. Albert, B. Evers and E. Bayer, *J. Magn. Reson.*, 62 (1985) 428.
- 18 R. K. Gilpin, *J. Chromatogr. Sci.*, 22 (1984) 371.
- 19 C. H. Lochmüller, A. S. Colborn, M. L. Hunnicutt and J. M. Harris, *Anal. Chem.*, 55 (1983) 1344.
- 20 E. Bayer, K. Albert, J. Reiners, M. Nieder and D. Müller, *J. Chromatogr.*, 264 (1983) 197.
- 21 L. Nondek, B. Buszewski and D. Berek, *J. Chromatogr.*, 360 (1986) 241.
- 22 B. Buszewski, R. Lodkowski and J. Trocewicz, *J. High Resolut. Chromatogr. Chromatogr. Commun.*, 10 (1987) 527.
- 23 D. Berek and I. Novák, *U.S. Pat.*, 4 255 286 (1981) and 4 382 070 (1983).
- 24 L. Nondek and V. Vyskočil, *J. Chromatogr.*, 206 (1981) 581.
- 25 E. Berendsen and L. de Galan, *J. Liq. Chromatogr.*, 1 (1978) 403.
- 26 B. Buszewski, Z. Suprynowicz and T. Pastuszak, *Chem. Anal. (Warsaw)*, 28 (1983) 513.
- 27 B. Buszewski, D. Berek and J. Garaj, *Wiad. Chem.*, 40 (1986) 369.
- 28 P. A. Bristow and J. H. Knox, *Chromatographia*, 10 (1977) 279.
- 29 E. Bayer and A. Paulus, *J. Chromatogr.*, 400 (1987) 1.
- 30 A. Paulus, K. Albert, B. Peters and E. Bayer, in press.
- 31 H. Colin and G. Guiochon, *J. Chromatogr.*, 119 (1976) 41.
- 32 H. Colin and G. Guiochon, *J. Chromatogr.*, 158 (1978) 183.
- 33 H. Colin, N. Ward and G. Guiochon, *J. Chromatogr.*, 149 (1978) 169.



CHROM. 21 845

## STUDIES ON THE STABILITY OF *n*-ALKYL-BONDED SILICA GELS UNDER BASIC pH CONDITIONS

N. T. MILLER\* and J. M. DiBUSSOLO

*The PQ Corporation, Research and Development Center, Conshohocken, PA 19428 (U.S.A.)*

---

### SUMMARY

Mobile phase and stationary phase parameters that influence stability of silica-based reversed phases are examined under high pH conditions. Mobile phases containing 0.1 M NaOH and variable methanol content were cycled through columns packed with various alkyl-bonded phases. Chromatography of small molecules and %C analysis were used to probe changing chromatographic performance as phase hydrolysis proceeded. It was evident that the rate of bonded phase hydrolysis was increased when the 0.1 M NaOH solution contained a high amount of organic solvent, especially when followed by a high organic-containing acidic wash. C<sub>4</sub> bonded phases were less stable than C<sub>18</sub> bonded phases. In the latter case, low bonded ligand coverage or the lack of endcapping also reduced stability against base hydrolysis. Reversed phases bonded to acid-washed silica showed greater base stability than those bonded to non-treated silica. The use of a silica precolumn did not serve to increase system usefulness. However, the use of soluble sodium silicate in the NaOH solution increased column lifetime for both short (*i.e.* C<sub>4</sub>) and long (*i.e.* C<sub>18</sub>) *n*-alkyl chain reversed phases.

---

### INTRODUCTION

Recent advances in synthesis and characterization of *n*-alkyl-bonded silicas for reversed-phase liquid chromatography (RPLC) have resulted in improved reproducibility and stability of these packings. While a number of reports are concerned with the use of silica-based column packings in mobile phases of pH *ca.* 2-7<sup>1-4</sup>, several groups have been concerned with packing stability in the region of eluent pH > 7. Various approaches to this problem have included the use of metal oxide doped silica<sup>5,6</sup>, polymer coatings on silica<sup>7-9</sup>, alumina or polymers as alternative stationary phase supports<sup>10-12</sup>, as well as mobile phase additives including organic amines or aluminum salts<sup>13,14</sup>. A frequently employed approach is the use of a short precolumn loosely packed with silica gel or the bonded phase placed between the pump and injector to allow equilibration of the mobile phase with silica<sup>15</sup>.

A distinction should be made between the use of basic pH eluent conditions in order to achieve the separation as opposed to a column cleaning step. The former case may employ relatively dilute basic conditions (*e.g.* 10-100 mM triethylamine or am-

monium acetate) for longer periods of time, while column washing may require a more concentrated base (e.g. 0.1 M NaOH) for a relatively short time (ca. five column volumes). Apparently, the use of 0.1 M NaOH as a column regeneration solution stems from the conventional biochemical practices on agarose and dextran-type gels<sup>16</sup>. Several advantages of this 0.1 M NaOH solution include cost-effective disinfectant action for pyrogen removal, safe presence in the final product, and easy disposal. Interestingly, although so-called base-stabilized reversed phases are commercially available, the problem of packing stability under basic conditions can be of greater concern for more hydrophilic bonded phases, *i.e.* ion-exchange and size-exclusion packings<sup>17-19</sup>. Moreover, acidic solutions of high organic content are frequently promoted as cleaning recipes for silica-based reversed phases<sup>17,20</sup>. Thus, column stability across a wide pH range is often given as a general reason for the use of polymer-based stationary phases<sup>21</sup>.

It is well known that silica-based packings can be unstable in basic pH systems. The solubility of silica in water at room temperature is roughly 100–150 ppm over the pH range 2–9<sup>22</sup>. From pH 9–10.7, there is an increase in silica solubility to ca. 1000 ppm, owing to the formation of silicate ion and monomeric Si(OH)<sub>4</sub>. At high pH conditions, the solubility of silica decreases from ca. 75 ppm in 25% aqueous methanol to ca. 15 ppm in 75% aqueous methanol. The reduction in silica solubility with increase in organic modifier content may explain in part the successful use of silica columns for polar solute separation using alkaline (e.g. ammonium acetate or ammonium nitrate) mobile phases rich in organic modifier (e.g. methanol)<sup>23,24</sup>. Impurities in the silica or organic coatings on the silica can provide altered solubility depending on the type of impurity or coating and its distribution on the surface<sup>22</sup>.

In this paper, we describe several results of our studies on the stability of *n*-alkyl-bonded silicas at high pH. We will show that base stability of C<sub>18</sub> reversed phases in 0.1 M NaOH is a function of organic modifier content in the mobile phase as well as stationary phase variables, including bonded alkyl chain length, coverage, endcapping and acid-washing of the base silica gel. Lastly, we will show that column lifetime can be extended by the use of soluble sodium silicate in the mobile phase. Taken together, these data can serve to improve the knowledge base concerning the reliability of silica-based reversed-phase systems under basic pH solution conditions.

## EXPERIMENTAL

### *Equipment and materials*

The liquid chromatograph was composed of a Series 410 four-solvent delivery liquid chromatography (LC) pump, a Model ISS-100 autosampler with injector, and a Model LC-95 variable-wavelength UV detector (Perkin-Elmer, Norwalk, CT, U.S.A.). Data were collected on a C-R6A Chromatopac integrator (Shimadzu, Columbia, MD, U.S.A.) and processed using a Nelson Analytical (Cupertino, CA, U.S.A.) Model 2600 chromatography software package on an IBM-PC AT (Boca Raton, FL, U.S.A.).

Alkylsilanes were obtained from Petrarch Systems (Bristol, PA, U.S.A.). IM-PAQ<sup>®</sup> RG2010Si, RG2010-C18, RG2020-C18 and RG2010-C4 silicas and bonded phases (nominal 200 Å pore diameter, 10 μm or 20 μm diameter packings) were obtained from The PQ Corporation (Conshohocken, PA, U.S.A.). The physical and

TABLE I  
CHARACTERISTICS OF SILICA GELS USED

	RG2010 Si	RG2020 Si
Pore volume (ml/g) <sup>a</sup>	1.34	1.37
Surface area (m <sup>2</sup> /g) <sup>a</sup>	246	257
Median pore diameter (Å) <sup>a</sup>	198	196
Particle size properties		
$D_v, 50$ (μm) <sup>b</sup>	8.92	17.15
$D_v, 50/D_p, 50$ <sup>b</sup>	1.22	1.14
$D_v, 10/D_v, 90$ <sup>b</sup>	1.72	1.66
Metals, anions (ppm) <sup>c</sup>		
Al	77	85
Ca	<25	<25
Fe	54	51
Na	30	36
SO <sub>4</sub> <sup>2-</sup>	<25	<25
Cl <sup>-</sup>	<25	<25
pH <sup>d</sup>	5.1	5.2
Loss on drying <sup>e</sup>	5.6	4.6

<sup>a</sup> Porosimetry determined by nitrogen sorption (BET method).

<sup>b</sup> Particle-size analysis by Coulter counter.  $D_{v,50}$  = 50% point on the cumulative volume (mass) distribution of particle size;  $D_{p,50}$  = 50% point on the cumulative population (frequency) distribution of particle size.

<sup>c</sup> Cation analysis by HF digestion of silica followed by flame atomic absorption spectroscopy for Na and inductively coupled plasma spectroscopy for Al, Ca, Fe and Mg determination. Anion analysis was by ion chromatography of water extracts of the silica.

<sup>d</sup> pH measured of a 10% slurry of silica in water.

<sup>e</sup> Loss on drying determined by the weight change of the silica after heating at 105°C for 2 h.

chemical characteristics of these silica gels are shown in Table I. The bonded packings utilize monomeric *n*-alkylsilane chemistry with endcapping on acid-washed silica. In certain experiments to study stationary phase variables, *n*-alkyl-bonded silicas were synthesized using a modified procedure of Kinkel and Unger<sup>25</sup>. Elemental analyses were determined on a Perkin-Elmer Model 2400 CHN analyzer with a precision of *ca.* 1% R.S.D.

Column hardware was obtained from Extrudhone (Irwin, PA, U.S.A.) and Valco Instruments (Houston, TX, U.S.A.). Small molecule solutes were obtained from Sigma (St. Louis, MO, U.S.A.) and Aldrich (Milwaukee, WI, U.S.A.) and used as received. Orthophosphoric acid was a "Baker Analyzed" grade reagent (J. T. Baker, Phillipsburg, NJ, U.S.A.), while monobasic and dibasic sodium phosphate were obtained from Sigma. Urea was from Bio-Rad (Richmond, CA, U.S.A.). Sodium hydroxide, HPLC-grade methanol and isopropanol (IPA) were from E. M. Science (Cherry Hill, NJ, U.S.A.). Sodium silicate "N" Clear was obtained from PQ Corporation. HPLC-grade water was prepared in-house.

#### Chromatographic procedures

The stationary phases were packed into 15 × 0.46 cm I.D. columns using standard slurry procedures with methanol as the driving solvent. Methanol-water

and IPA-water mobile phases were prepared by adding the correct volumes of organic solvent and water following by dissolution of the appropriate acid or buffer salt. pH was adjusted as desired by use of the appropriate acid or base.

The multi-solvent LC pump and autosampler were programmed to automate column testing with repeated exposure of the column to alkaline mobile phases. In the typical experiment, an initial evaluation was performed on the freshly packed reversed-phase column using a standard test mixture of uracil, N-acetylprocainamide (NAP), caffeine and phenol<sup>2</sup> in a standard mobile phase (*i.e.* solvent A) of methanol-water (20:80) containing 0.1% (*ca.* 15 mM) orthophosphoric acid. This analysis lasted 20 min. Keeping the flow-rate constant at 1 ml/min, the pump then delivered a 5-min linear gradient to reach 100% solvent B consisting of 0.1 M NaOH in methanol-water (80:20 or 20:80, see Table III). Solvent B was then pumped isocratically for 15 min and was followed by a 5-min linear gradient to 100% solvent C consisting of 0.1 M or 25 mM HNO<sub>3</sub> in aqueous IPA. After isocratic operation of solvent C for 15 min to wash away any hydrolyzed hydrocarbon chains from the packing, the LC pump then delivered a 5-min linear gradient back to 100% solvent A. After equilibration of the column in solvent A for 15 min, the autosampler made an injection of the standard test mixture for reevaluation of solute retention. This solvent program

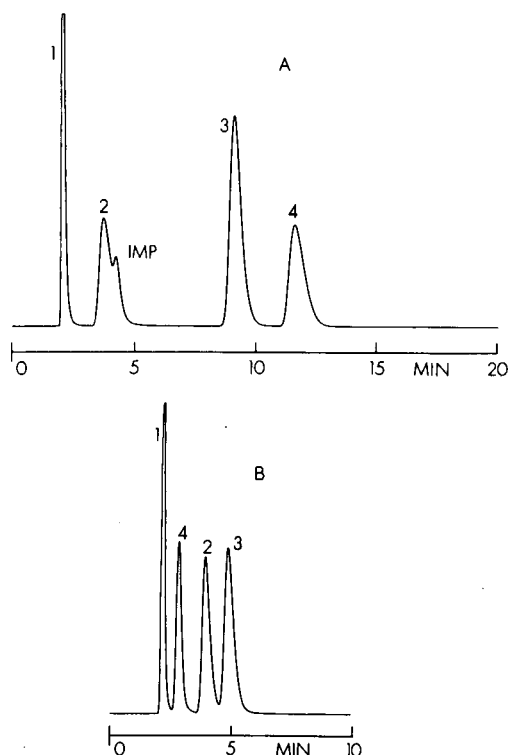


Fig. 1. Chromatography of uracil (1), NAP (2), caffeine (3) and phenol (4) on C<sub>18</sub> columns. The solutes were chromatographed in a mobile phase of 20% (v/v) aqueous methanol containing 15 mM H<sub>3</sub>PO<sub>4</sub> at 1.0 ml/min and 25°C. (A) Bonded silica containing 3.41 μmol/m<sup>2</sup> C<sub>18</sub> groups. (B) Bonded silica containing 1.97 μmol/m<sup>2</sup> C<sub>18</sub> groups. IMP = Impurity.

could be recycled as many times as needed. At the end of the study, the columns were washed with IPA and sacrificed to obtain elemental analysis data.

## RESULTS AND DISCUSSION

The aim of this paper was to evaluate the effects of basic pH eluents on *n*-alkyl phases bonded to silica gel. Our first experiments involved the development of a small molecule test mixture to characterize the reversed-phase columns prior to treatment with a NaOH solution. Fig. 1 compares chromatograms of the solute mixture uracil, NAP, caffeine and phenol from a fully bonded (*i.e.* 3.41  $\mu\text{mol}/\text{m}^2$ )  $\text{C}_{18}$  packing and from a partially bonded (*i.e.* 1.97  $\mu\text{mol}/\text{m}^2$ )  $\text{C}_{18}$  packing, both based on high purity 10- $\mu\text{m}$  granular silica gel having 200- $\text{\AA}$  pores (Table I). Note that altered selectivity for NAP, caffeine and phenol is obtained on the two  $\text{C}_{18}$  bonded phases. Table II shows the results of alterations in the methanol-water (20:80) mobile phase to investigate the retention behavior of these solutes on the fully bonded  $\text{C}_{18}$  reversed phase. Decreases in mobile phase pH or increases in ionic strength caused a decrease in  $k'$  or band sharpening of NAP, suggesting a largely ionic interaction of this solute with the surface (*i.e.* with acidic silanols). The NAP solute is also retained relatively longer on the partially bonded  $\text{C}_{18}$  packing, which is known to have accessible silanols. Caffeine retention is largely independent of pH, but is reduced upon addition of urea (or acetonitrile) to the mobile phase. This result suggests that caffeine is mainly sensitive to hydrogen bonding with the surface silanols<sup>26</sup>. Lastly, the solute phenol can be used to gauge the hydrophobicity of the bonded phase except at high pH ( $\text{p}K_a$  of phenol is *ca.* 10<sup>27</sup>). The results obtained for caffeine and phenol for the partially bonded  $\text{C}_{18}$  reversed phase in Fig. 1B support the above explanation.

In the next sections of this paper, we will examine the role of mobile phase components and stationary phase variables on column stability under high pH conditions. Lastly, we will briefly examine the use of soluble sodium silicate as an aid to extended column lifetime. Taken together, the results provide a perspective on parameters that control the stability of silica-based *n*-alkyl reversed phases at high pH.

### *Effect of mobile phase variables*

In this study, we examined mobile phase parameters of the basic pH solution that influence the stability of *n*-alkyl-bonded silicas. Several 15  $\times$  0.46 cm I.D. columns of a fully bonded  $\text{C}_{18}$  reversed phase based on 10- $\mu\text{m}$  granular silica of 200  $\text{\AA}$  pore diameter were packed and evaluated using the standard 20 min separation of uracil, NAP, caffeine and phenol. Subsequent to this result, the mobile phase was changed to 0.1 *M* NaOH in aqueous methanol as outlined in Experimental. A final wash of the column with acidic aqueous IPA was programmed before return to the standard conditions for reevaluation of the column.

Table III summarizes the variables studied in this set of experiments including NaOH concentration, and the effects of methanol and IPA content in the wash solutions and reports initial and final %C and  $k'$  results. Interestingly, losses in %C do not correlate well with observed changes in  $k'$ . For example, the  $\text{C}_{18}$  packing of experiment 3 shows a loss of 1.76% C with reduction in  $k'$  for NAP, caffeine and phenol, while in experiment 5, a loss in selectivity for caffeine and phenol is observed with roughly the same *ca.* 10% loss in bonded carbon. Note that experiment 7 in-

TABLE II  
RETENTION BEHAVIOR ( $k'$  VALUES) OF N-ACETYLPROCAINAMIDE (NAP), CAFFEINE AND PHENOL ON A HIGH-COVERAGE  $C_{18}$  BONDED SILICA

Mobile phase, methanol-water (20:80) with additives as indicated; flow-rate, 1.0 ml/min; detection at 254 nm, 0.2 a.u.f.s.; temperature, 25°C; column: 3.41  $\mu$ mol/m<sup>2</sup>  $C_{18}$  groups on 10  $\mu$ m silica of 200 Å pores; column dimensions, 15 × 0.46 cm. I.D. pH values measured in hydro-organic mixture.

Solute	Mobile phase additives									
	None	15 mM $H_3PO_4$ pH 2.3	15 mM $NaH_2PO_4$ pH 5.0	15 mM $NaH_2PO_4$ pH 7.0	15 mM $NaH_2PO_4$ pH 9.2	15 mM $Na_2HPO_4$ pH 13	0.1 M NaOH, pH 13	15 mM $H_3PO_4$ , 1 M urea	1 mM NaCl	10 mM NaCl
NAP	— <sup>a</sup>	0.60	0.94	1.91	— <sup>a</sup>	— <sup>a</sup>	— <sup>a</sup>	0.58	1.26 <sup>b</sup>	1.40
Caffeine	3.45	3.51	3.51	3.54	3.68	3.90	2.79	3.61	3.61	3.61
Phenol	4.35	4.23	4.23	4.25	4.13	0.42	3.96	4.38	4.38	4.40

<sup>a</sup> No elution observed.

<sup>b</sup> Eluted with tailing.

dicates bonded phase hydrolysis is not due to the acidic aqueous IPA as observed previously<sup>2</sup>. It is likely that chromatographic performance is more sensitive to phase hydrolysis than %C measurements. Moreover, the entire column was sacrificed to provide a sample for %C, which may represent an "averaging" of the result. More study is required.

Fig. 2 presents a plot of caffeine-phenol selectivity change as a function of base-catalyzed hydrolysis of the C<sub>18</sub> bonded silica surface, while Fig. 3 shows chromatograms from the C<sub>18</sub> column through 12 cycles of the 0.1 M NaOH wash conditions causing the greatest degradation, experiment 5 (see Table III). Typically, the change in chromatography occurs as a loss of *k'* for phenol and a *k'* increase for caffeine, *i.e.* a loss in caffeine/phenol selectivity. We also frequently noticed an increase in operating pressure of the LC system, often enough (*i.e.* > 6000 p.s.i.) to shut down the HPLC solvent pump. Interestingly, NAP retention was not often affected in these experiments. Fig. 2 indicates that the most deleterious condition results from washing the C<sub>18</sub> bonded silica with a basic solution high in organic modifier content. One may speculate that the organic modifier solvates the hydrophobic surface and permits access of OH<sup>-</sup>; however, it is not possible at this time to identify the point of hydrolytic cleavage on the packing. The increased IPA content (80%) of the acidic solution decreased the C<sub>18</sub> column stability only when this solution was used in conjunction with the 80% aqueous methanol containing 0.1 M NaOH. This result suggests that the high IPA content is needed for elution of the cleaved stationary phase ligands. In fact, washing the columns at the end of experiments 1 and 2 with IPA-water (80:20) containing 25 mM HNO<sub>3</sub> did not change retention of caffeine or phenol.

In separate experiments, we found that 20% aqueous methanol did not wet the C<sub>18</sub> bonded silica upon suspension of the bonded phase with this mobile phase in a test tube. Chromatography of the small molecules using this mobile phase on an originally "dry" column resulted in one peak eluting at the V<sub>0</sub> position. After passage of methanol (either during the column packing operation or as a separate step) and return to the 20% aqueous methanol, retention and separation of the small molecule probes occurs. This phenomenon probably relates to the presence of a solvent layer enriched in methanol sorbed to the C<sub>18</sub> bonded surface<sup>28</sup>. Thus, if NaOH is chosen to sanitize a column, one caveat is to minimize the organic content of the basic solution where possible, such that the desired cleaning action is still obtained and column lifetime is maximized.

#### *Effect of stationary phase variables*

We next examined in greater detail the role of stationary phase parameters on the stability of the column to basic pH conditions. Table IV lists the characteristics of several packings synthesized for this study, while Fig. 4 plots caffeine-phenol selectivity as a function of passage of 0.1 M NaOH in 80% aqueous methanol. With the exception of the partially bonded C<sub>18</sub> packing (experiment 4) and the C<sub>4</sub> reversed phase (experiment 5) based on 10- $\mu$ m silica of 200 Å pore diameter, the remaining bonded phases were synthesized on 20- $\mu$ m silica with 200 Å pores with similar surface chemistry to the 10- $\mu$ m material (see Table I). In each of the experiments in Table IV, we varied some aspect of the bonding chemistry ranging from a fully bonded material with endcapping on a acid-washed silica (experiment 1) to a partial bonding with no

TABLE III  
INFLUENCE OF MOBILE PHASE PARAMETERS ON BASE STABILITY OF C<sub>18</sub> BONDED SILICA

Experiment No.	Hydrolytic solvent	Wash solvent	Vol. of each solution passed (ml)	Final %C <sup>a</sup>	Final <i>k'</i> values <sup>b</sup>		
					NAP	Caffeine	Phenol
1	Methanol-water (20:80), 0.1 M NaOH	IPA-water (40:60) 0.1 M HNO <sub>3</sub>	90	16.17	0.48	3.26	4.27
2	Methanol-water (20:80), 0.2 M NaOH	IPA-water (40:60) 0.2 M HNO <sub>3</sub>	60	15.45	0.44	3.24	4.19
3	Methanol-water (20:80), 0.1 M NaOH	IPA-water (80:20), 25 mM HNO <sub>3</sub>	165	15.09	0.44	3.16	4.06
4	Methanol-water (80:20), 0.1 M NaOH	IPA-water (40:60), 0.1 M HNO <sub>3</sub>	165	15.57	0.41	3.73	4.0
5	Methanol-water (80:20), 0.1 M NaOH	IPA-water (80:20), 25 mM HNO <sub>3</sub>	165	15.32	0.44	4.36	4.36
6	Methanol-water (80:20), 0.1 M NaOH	None	165	15.46	0.40	3.56	3.98
7	None	IPA-water (80:20), 0.1 M HNO <sub>3</sub>	165	16.51	0.51	3.14	4.65

<sup>a</sup> The freshly synthesized C<sub>18</sub> bonded phase on 10 μm silica of 200 Å pore diameter showed 16.85% C by elemental analysis.

<sup>b</sup> Initial *k'* values were 0.71, 3.23 and 4.53 for NAP, caffeine and phenol, respectively.



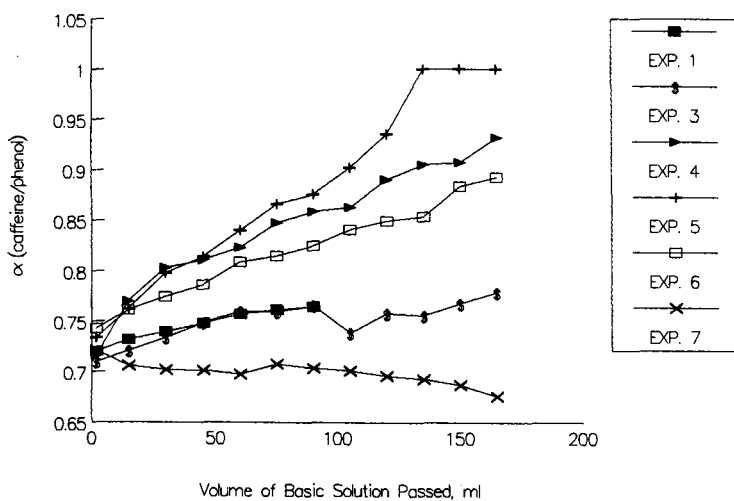


Fig. 2. Caffeine-phenol selectivity on several  $C_{18}$  columns as a function of 0.1  $M$  NaOH solution passed through the column. Caffeine and phenol  $k'$  values were measured on each column using the conditions of Fig. 1. See Table III and text for the conditions of experiments 1-7.

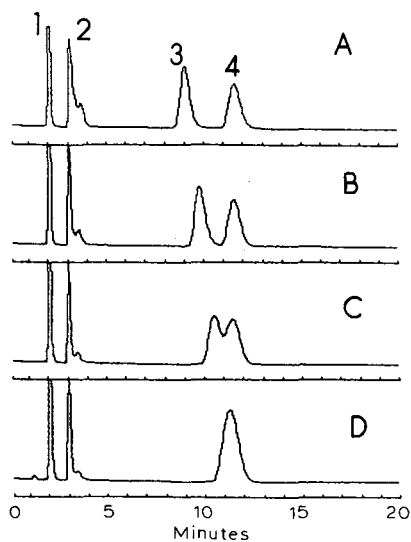


Fig. 3. Chromatography of uracil (1), NAP (2), caffeine (3) and phenol (4) on a  $C_{18}$  column through twelve cycles of 0.1  $M$  NaOH aqueous methanol solution passed. The solutes were chromatographed on the  $C_{18}$  column using the conditions of Fig. 1. See Experimental, Table III, and experiment 5 in Fig. 2 for description of the 0.1  $M$  NaOH treatment. (A) Initial evaluation; operating pressure was 150 p.s.i. (B) Column evaluation after cycle 4 of treatment, equivalent to passage of 60 ml each of 0.1  $M$  NaOH in 80% aqueous methanol and 25  $mM$   $HNO_3$  in 80% aqueous IPA through the column. (C) Column evaluation after cycle 7, equivalent to 105 ml of each of the wash solvents in (B) passed through the column. (D) Column evaluation after cycle 11, equivalent to 165 ml of each of the wash solutions in (B) passed through the column. Operating pressure was 180 p.s.i.

TABLE IV  
 INFLUENCE OF STATIONARY PHASE PROPERTIES ON BASE STABILITY OF *n*-ALKYL-BONDED SILICAS<sup>a</sup>

Experiment No.	Bonded phase	Basic solution passed (ml) <sup>b</sup>	Initial %C		Final %C		NAP		Caffeine		Phenol	
			Initial %C	Final %C	Final k'	Initial k'	Final k'	Initial k'	Final k'	Initial k'		
1	C <sub>18</sub> , endcapped (acid-washed)	75	16.33	14.29	0.74	0.83	3.83	3.21	4.46	4.47		
2	C <sub>18</sub> , endcapped (non-acid-washed)	75	17.16	14.70	0.88	1.08	4.07	3.22	4.07	4.46		
3	C <sub>18</sub> , non-endcap (non-acid-washed)	75	16.87	12.71	0.84	1.10	4.96	3.37	4.24	4.38		
4	C <sub>18</sub> , non-endcap <sup>c</sup> (non-acid-washed)	15	10.11	7.39	0.84 <sup>d</sup>	0.78	1.31 <sup>d</sup>	1.21	0.32 <sup>d</sup>	0.29		
5	C <sub>4</sub> , endcapped <sup>c</sup> (acid-washed)	45	5.97	4.88	0.27	0.43	2.09	1.94	2.09	2.63		

<sup>a</sup> Except as noted, all bonded phases were monomeric *n*-alkylsilyl groups bonded to 20  $\mu$ m granular silica gel having 200 Å diameter pores.

<sup>b</sup> The basic solution employed in this study was methanol-water (80:20) containing 0.1 *M* NaOH followed by a rinse with 25 *mM* HNO<sub>3</sub> in IPA-water (80:20).

<sup>c</sup> These bonded phases (C<sub>18</sub> or C<sub>4</sub>) were monomeric *n*-alkylsilyl groups bonded to 10  $\mu$ m silica of 200 Å pore diameter. The C<sub>18</sub> packing was a partially bonded phase.

<sup>d</sup> High operating pressure terminated this experiment after only one cycle.

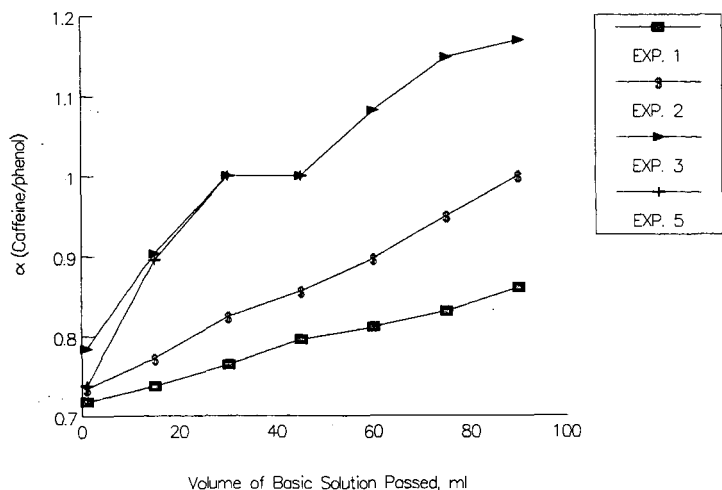


Fig. 4. Caffeine-phenol selectivity as a function of passage of 0.1 *M* NaOH solutions through columns of various stationary phase chemistries. The solutes were chromatographed under the conditions of Fig. 1. See Table IV and text for the conditions of experiments 1-5.

endcap or acid-washing (experiment 4). Finally, a  $C_4$  bonded phase was synthesized with endcapping on the acid-washed silica as indicated in experiment 5. Each of the packings was exposed to the most deleterious conditions of Table III, *i.e.* the 0.1 *M* NaOH in 80% aqueous methanol followed by the 25 *mM*  $HNO_3$  in 80% aqueous IPA wash. In these experiments, a rough correlation was observed between %C loss in the packing and loss of caffeine-phenol selectivity. Thus, the  $C_{18}$  column of experiment 1 showed the greatest resistance to hydrolysis corresponding to a *ca.* 13% loss of %C, while the partially bonded  $C_{18}$  column of experiment 4 deteriorated (*i.e.* excessive operating pressure) within one cycle with a *ca.* 27% loss of bonded carbon. Fig. 4 indicates that full  $C_{18}$  coverage with endcapping on an acid-washed silica provides the greatest resistance to base hydrolysis. Interestingly, inverted elution order of caffeine and phenol was obtained on the non-endcapped (non-acid-washed)  $C_{18}$  column (experiment 3) by the fourth cycle (Fig. 4). This column also showed a *ca.* 25% loss in bonded carbon by the end of the experiment. Lastly, the short chain  $C_4$  column (experiment 5) deteriorated within two cycles and high column back-pressure had shut off the LC system by the fourth cycle. Thus, for the same bonded phase chemistry and the same basic pH eluent conditions, the  $C_4$  column appears less stable relative to the  $C_{18}$  column. This result agrees with column stability under acidic conditions, in that a more hydrophobic surface shows greater stability to hydrolysis<sup>2</sup>. In the next section, we briefly examine stability of the columns against base hydrolysis using soluble sodium silicate.

#### Use of sodium silicate

In the past, workers have used precolumns containing silica or bonded phase to presaturate the mobile phase with stationary phase such that the analytical column is not degraded<sup>15</sup>. In a single experiment, we dry-packed a  $5 \times 0.46$  cm I.D. precolumn with 10- $\mu$ m silica of 200 Å pore diameter and used it in the system in conjunction with

TABLE V  
INFLUENCE OF SOLUBLE SODIUM SILICATE ON THE BASE STABILITY OF *n*-ALKYL-BONDED SILICAS<sup>a</sup>

Experiment No.	Bonded phase	Basic solution passed (ml)	Initial %C	Final %C	NAP		Caffeine		Phenol	
					Final k'	Initial k'	Final k'	Initial k'	Final k'	Initial k'
1	C <sub>18</sub>	165 <sup>b</sup>	16.85	15.32	0.44	0.92	4.36	3.28	4.36	4.59
2	C <sub>18</sub>	165 <sup>c</sup>	16.85	15.88	0.44	0.74	3.59	3.28	4.39	4.60
3	C <sub>4</sub>	45 <sup>b,d</sup>	5.97	4.88	0.27	0.43	2.09	1.94	2.09	2.63
4	C <sub>4</sub>	120 <sup>c,e</sup>	5.97	5.45	0.25	0.42	2.26	2.13	2.26	2.90

<sup>a</sup> All reversed phases were monomeric *n*-alkyl groups on 200 Å, 10- $\mu$ m silica.

<sup>b</sup> The basic solution passed was methanol-water (80:20) containing 0.1 M NaOH followed by a rinse with IPA-water (80:20) containing 25 mM HNO<sub>3</sub>.

<sup>c</sup> The basic solution passed was a silicate-saturated 0.1 M NaOH in methanol-water (80:20) followed by a rinse with 25 mM HNO<sub>3</sub> in IPA-water (80:20), see

text.

<sup>d</sup> Excessive operating pressure shut this experiment down in the fourth cycle.

<sup>e</sup> Excessive operating pressure shut this experiment down in the ninth cycle.

a freshly packed 15 × 0.46 cm I.D. column of the fully bonded C<sub>18</sub> (endcapped, acid-washed) bonded phase based on the same silica. The wash solutions employed were the 0.1 M NaOH in 80% aqueous methanol followed by the 25 mM HNO<sub>3</sub> in 80% aqueous IPA.

Initially, the operating pressure of the chromatograph was *ca.* 150 p.s.i. By the fourth cycle, the instrument had shut down owing to the 5000 p.s.i. back-pressure of the precolumn. The analytical column showed only *ca.* 180 p.s.i. Note that in the absence of the precolumn we could achieve all eleven of the cycles on this C<sub>18</sub> packing (see experiment 5 in Fig. 2 and Fig. 3) with initial and final operating pressures of 150 and 180 p.s.i. respectively.

We next examined the use of a commercially available sodium silicate solution in the 0.1 M NaOH in 80% aqueous methanol for the purpose of pre-saturating this solution with silica. This solution has a weight ratio of 3.22 SiO<sub>2</sub>/Na<sub>2</sub>O with 8.9% Na<sub>2</sub>O and a pH of 11.3<sup>29</sup>. We diluted this solution by *ca.* 400 times with water to obtain concentrations of *ca.* 12 mM SiO<sub>2</sub> (*ca.* 1000 ppm silicate) and *ca.* 7.2 mM NaOH. We then dissolved additional NaOH (*ca.* 20 g/l of solution) into this solution to raise the NaOH concentration to 0.5 M such that the mixture of 200 ml of this solution with the 800 ml of methanol would bring the final NaOH concentration to 0.1 M. Upon addition of the methanol, silica was observed to precipitate from solution, which was not unexpected as the literature indicates a *ca.* 15 ppm solubility of silica in this system<sup>22</sup>. After stirring, the solution was filtered and placed in the chromatograph. All of the solutions and dilutions were done in polyethylene containers to avoid dissolution of silica from the walls of glass solvent bottles. As with use of any mobile phase containing salt, compatibility with other solvents used in gradients is mandatory. We did not notice any precipitation of silica when aliquots of the 25 mM HNO<sub>3</sub> in 80% aqueous IPA were contacted with the silica-saturated 0.1 M NaOH in 80% aqueous methanol. Table V and Fig. 5 present the results of substitution of this

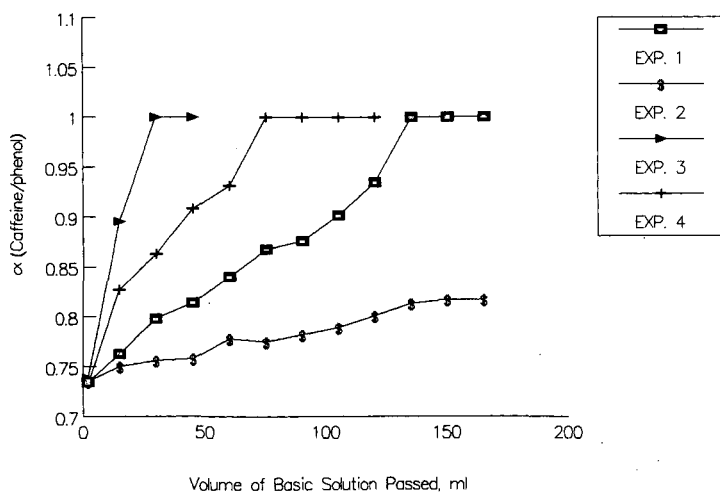


Fig. 5. Caffeine-phenol selectivity on C<sub>18</sub> and C<sub>4</sub> columns as a function of 0.1 M NaOH solution passed through the column with and without silicate-saturation of the basic solution. The solutes were chromatographed under the conditions of Fig. 1. See Table V and text for the conditions of experiments 1-4.

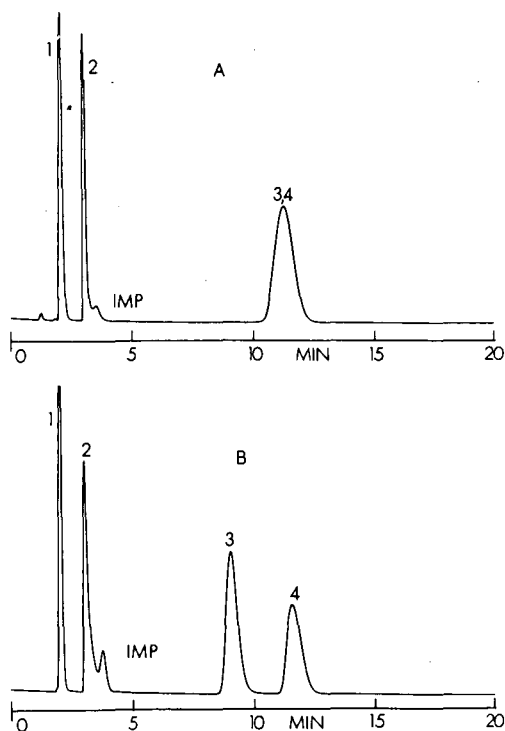


Fig. 6. Chromatography of uracil (1), NAP (2), caffeine (3) and phenol (4) on  $C_{18}$  columns after passage of 0.1  $M$  NaOH in 80% aqueous methanol with and without dissolved silicate. The solutes were chromatographed using the conditions of Fig. 1. (A) 165 ml each of 0.1  $M$  NaOH in 80% aqueous methanol and 25  $mM$   $HNO_3$  in 80% aqueous IPA were passed through the column. Operating pressure was 180 p.s.i. (B) The same volumes of the same solutions as in (A) were cycled through the column except the 0.1  $M$  NaOH in 80% aqueous methanol was saturated with silicate, see text. Operating pressure was 260 p.s.i. IMP = Impurity.

silica-saturated basic solution for that containing no silicate. Loss of bonded carbon was reduced by *ca.* 40% in the  $C_{18}$  system and by *ca.* 50% in the  $C_4$  system by virtue of silica-saturation of the 0.1  $M$  NaOH solution. Increased column lifetime in terms of caffeine-phenol selectivity was observed for both the  $C_4$  and  $C_{18}$  columns using this approach. Undoubtedly, with adjustment of the organic modifier content of the wash solutions in the  $C_4$  system as appropriate for cleaning, the column lifetime could be improved further. Fig. 6 presents the chromatograms on the  $C_{18}$  columns after passage of *ca.* 165 ml of the unsaturated (Fig. 6A) and saturated (Fig. 6B) silicate solutions of basic pH. It is obvious that the addition of silicate to the mobile phase improved the column stability. Note that some increase in operating pressure is observed in Fig. 6B, but that the result achieved is acceptable. Thus, silicate-saturated basic pH solutions can be used to wash silica-based reversed phases with extended lifetimes of the columns.

## CONCLUSION

This paper examined several variables in the stability of silica-based reversed phases to basic pH. Chromatography of small molecule test probes and %C measurements proved to be valuable in qualitatively evaluating bonded phase stability as a function of passage of hydro-organic solutions of 0.1 M NaOH. Increased organic modifier content of the 0.1 M NaOH wash solution decreases the operating lifetime of the reversed-phase column as measured by resolution and operating pressure. High organic modifier content of an acidic wash following the 0.1 M NaOH solution also high in organic modifier further decreases column lifetime, probably because cleaved ligand chains are more effectively washed away. High coverage and endcapped bonded phases containing long chains (*i.e.* C<sub>18</sub>) based on a acid-washed silica showed an increased lifetime under basic pH conditions relative to those cases where any one of these conditions was not met. The use of a silica precolumn does not serve to enhance system usefulness. Finally, the use of silica-saturated (via soluble sodium silicates) mobile phases of high pH can increase column lifetime for long or short (*i.e.* C<sub>4</sub>) chain columns over the case where silica-presaturation is not used.

## ACKNOWLEDGEMENTS

The authors acknowledge several valuable discussions concerning silicate science with M. Robert Derolf. Joseph Kowalewski is thanked for elemental analyses of bonded silicas and the packing of several columns.

## REFERENCES

- 1 J. J. Kirkland, J. L. Glajch and R. D. Farlee, *Anal. Chem.*, 61 (1989) 2.
- 2 N. Sagliano, T. R. Floyd, R. A. Hartwick, J. M. DiBussolo and N. T. Miller, *J. Chromatogr.*, 443 (1988) 155.
- 3 J. Kohler, D. B. Chase, R. D. Farlee, A. J. Vega and J. J. Kirkland, *J. Chromatogr.*, 352 (1986) 275.
- 4 H. A. Claessens, J. W. de Haan, L. J. M. van de Ven, P. C. de Bruyn and C. A. Cramers, *J. Chromatogr.*, 436 (1988) 345.
- 5 R. W. Stout and J. J. DeStefano, *J. Chromatogr.*, 326 (1985) 63.
- 6 L. S. Lysjuk and A. A. Chuiko, *J. Chromatogr.*, 407 (1987) 189.
- 7 H. Figge, A. Deege, J. Kohler and G. Schomburg, *J. Chromatogr.*, 351 (1986) 393.
- 8 W. Kopaciewicz and F. E. Regnier, *J. Chromatogr.*, 358 (1986) 119.
- 9 Y. Ohtsu, H. Fukui, T. Kanda, K. Nakamura, M. Nakano, O. Nakata and Y. Fujiyama, *Chromatographia*, 24 (1987) 380.
- 10 R. M. Chiciz, Z. Shi and F. E. Regnier, *J. Chromatogr.*, 359 (1986) 121.
- 11 U. Bien-Vogelsang, A. Deege, H. Figge, J. Kohler and G. Schomburg, *Chromatographia*, 19 (1984) 170.
- 12 J. W. Novak and M. L. Moskovitz, presented at the *Third Washington Symposium on Preparative Scale Liquid Chromatography*, Washington, DC, May 4-5, 1987.
- 13 A. Wehrli, J. C. Hildenbrand, H. P. Keller, R. Stampfli and R. W. Frei, *J. Chromatogr.*, 149 (1978) 199.
- 14 E. A. Pfannkoch and W. Kopaciewicz, presented at the *Twelfth International Symposium on Column Liquid Chromatography*, Washington, DC, June 19-24, 1988, paper M-L-11.
- 15 J. G. Atwood, G. J. Schmidt and W. Slavin, *J. Chromatogr.*, 171 (1979) 109.
- 16 G. Sofer, *BioTechnology*, 2 (1984) 1035.
- 17 W. Kopaciewicz, personal communication, April 10, 1989.
- 18 S. A. Berkowitz, M. P. Henry, D. R. Nau and L. J. Crane, *Am. Lab.*, 19 (1987) 33.
- 19 R. W. Stout, S. I. Sivakoff, R. D. Ricker, H. C. Palmer, M. A. Jackson and T. J. Odiorne, *J. Chromatogr.*, 352 (1986) 381.

- 20 C. T. Wehr, *Methods Enzymol.*, 104C (1984) 133.
- 21 H. W. Stuurmand, J. Kohler, S.-O. Jansson and A. Litzen, *Chromatographia*, 23 (1987) 341.
- 22 R. K. Iler, *The Chemistry of Silica*, Wiley-Interscience, New York, 1979, pp. 40–62.
- 23 B. B. Wheals, *J. Chromatogr.*, 187 (1980) 65.
- 24 B. Law and P. F. Chan, *J. Chromatogr.*, 467 (1989) 267.
- 25 J. N. Kinkel and K. K. Unger, *J. Chromatogr.*, 316 (1984) 193.
- 26 L. R. Snyder and J. J. Kirkland, *Introduction to Modern Liquid Chromatography*, Wiley-Interscience, New York, 2nd ed., 1979, p. 799.
- 27 *Merck Index*, Merck & Co., Rahway, NJ, 10th ed., 1983, p. 7117.
- 28 R. M. McCormick and B. L. Karger, *Anal. Chem.*, 52 (1980) 2249.
- 29 *Bulletin 17-Z*, The PQ Corporation, Valley Forge, PA, 1980.



CHROM. 21 706

## MECHANISM OF RETENTION IN HIGH-PERFORMANCE LIQUID CHROMATOGRAPHY ON POROUS GRAPHITIC CARBON AS REVEALED BY PRINCIPAL COMPONENT ANALYSIS OF STRUCTURAL DESCRIPTORS OF SOLUTES

ROMAN KALISZAN\*

*Department of Biopharmaceutics and Pharmacodynamics, Medical Academy, K. Marksa 107, 80-416 Gdansk (Poland)*

KRZYSZTOF OŚMIAŁOWSKI

*Department of Inorganic Chemistry, Medical Academy, K. Marksa 107, 80-416 Gdansk (Poland)*

and

BARBARA J. BASSLER and RICHARD A. HARTWICK

*Department of Chemistry, Rutgers University, Piscataway, NJ 08854 (U.S.A.)*

---

### SUMMARY

High-performance liquid chromatographic retention data derived for a set of non-congeneric aromatic solutes on a graphitic carbon stationary phase with hexane as the eluent were analysed. The capacity factors were quantitatively related to structural information extracted from nineteen molecular descriptors of solutes by multivariate analysis. The descriptors considered included molecular weight, molecular refractivity, topological indices, information content indices, quantum chemical indices and structural indices based on electron charge distribution within a molecule. The first three principal components obtained by factor analysis of nineteen structural descriptors appeared meaningful for the description of retention. Most important for retention were structural features reflecting abilities of solutes to participate in intermolecular interactions of the electron pair donor-acceptor and dipole-induced dipole type. The structural factor related to molecular size appeared less important for retention but decisive for the prediction of boiling points. Multivariate analysis of structural descriptors was demonstrated to provide systematic information useful for the explanation of the mechanism of a chromatographic process.

---

### INTRODUCTION

Quantitative structure-retention relationships (QSRR) have been extensively studied in the last decade for three main purposes: explanation of the mechanism of retention, retention prediction and parameterization of the structures of solutes<sup>1</sup>. Most published QSRR were derived by means of a multiple regression analysis of a set of retention data (dependent variable) and various empirical, semiempirical and theoretical structural parameters assumed to be independent variables. Unfortunately, the independent (*i.e.*, explanatory) variables considered have often been interrelat-

ed by simple or multiple correlations. Sets of intercorrelated chemical data are unsuitable for multiple regression but can be the subject of multivariate analysis with factorial methods.

Factor analysis was first applied to chromatographic data in the early 1970s<sup>2-4</sup>. More recent examples of the application of multivariate analysis in chromatography may be found in refs. 5-15. The analyses reported were mostly aimed at the prediction of the retention of a particular set of solutes with various mobile-stationary phase systems. However, Wold and co-workers<sup>14,15</sup> used chromatographic data to extract some structural properties of amino acids. Little attention has been paid to the multivariate analysis of structural descriptors of solutes. In fact, Massart and co-workers<sup>6,7</sup> performed factor analysis of a set of topological and quantum chemical indices of a series of compounds but did not relate the factors extracted quantitatively to the gas chromatographic retention indices studied.

It appeared soon after Knox *et al.*<sup>16</sup> introduced porous graphitic carbon as a high-performance liquid chromatographic (HPLC) stationary phase that the retention behaviour observed was different to that expected for a reversed-phase material. Our QSRR studies<sup>17</sup> demonstrated that specific, polar, size-independent solute-stationary phase interactions are decisive for retention. In this work we attempted to apply multivariate analysis in order to obtain some insight into the mechanism of HPLC retention on graphitic carbon.

## EXPERIMENTAL

### *Materials*

The test solutes selected for study are simple aromatic derivatives. The whole set of 20 solutes is diverse enough to avoid congenericity and includes various functionalities. On the other hand, a subgroup of phenol derivatives can be separated to allow specific comparisons.

For the sake of comparison, boiling point data were collected<sup>18</sup> for the solutes analysed and these data are given in Table I together with chromatographic and structural indices.

### *Chromatographic determinations*

Solutes dissolved in heptane were chromatographed with neat heptane as the mobile phase on 30 cm × 1 mm I.D. columns slurry-packed with porous graphitic carbon material. A standard HPLC system was applied. Details of the analytical procedure have been given previously<sup>17</sup>.

The column void volume was determined by the change in the refractive index of an injection of pentane in hexane. Logarithms of capacity factors ( $\log k'$ ) are given in Table I.

### *Structural descriptors*

Non-empirical structural descriptors were considered, *i.e.*, molecular parameters that can be calculated based exclusively on the structural formula of a solute. The total of nineteen descriptors determined included molecular weight (molwt), molecular refractivity (bondrefr), four topological indices, three information content indices, six quantum chemical indices and four modifications of quantum chemical data.

Molecular refractivity (bondrefr) was calculated as the sum of the bond refractivities for all pairs of connected atoms according to Iophphe<sup>19</sup>. A list of individual increments can be found in ref. 1, p. 96.

The following indices based on molecular topology were considered: (i) indices of molecular shape (kappa values) of second and third order,  $\kappa^2$  and  $\kappa^3$  (kappa2 and kappa3), according to Kier<sup>20</sup>; (ii) the Kier and Hall<sup>21</sup> generalized molecular connectivity index of second order,  $\chi^{2v}$  (chi2v); and (iii) the average distance sum connectivity index of Balaban<sup>22</sup> calculated according to Barysz *et al.*<sup>23</sup> (balaban). It should be mentioned that being in full agreement with mathematical topology, one can compare topological indices derived for closely congeneric compounds only, such as aliphatic hydrocarbons. The indices considered here are empirical modifications of graph theoretical indices and were introduced to provide the diversity of structures observed in real chemical systems.

The next group of structural indices considered were information indices of neighbourhood symmetry of zeroth order, ic0, first order, ic1, and second order, ic2 (ref. 24). These information content indices were calculated by means of the general information theory equation (Shannon's equation) from probabilities of finding equivalent atoms (ic0) or patterns of atoms in a given structural formula.

The separate group of non-empirical structural descriptors studied were quantum chemical indices. The indices were calculated for each solute by using the MNDO3 method<sup>25</sup> on molecular coordinate files obtained from the Cambridge Crystallographic Database<sup>26</sup>. Calculations were done on a VAX 780 computer with an array processor. The following quantum chemical indices were considered: total energy (etotal), heat of formation (heatf), energy of core-core repulsion (corer), energy of highest occupied molecular orbital (ehomo), energy of lowest unoccupied molecular orbital (elumo), dipole moment (dipolem) and electron excess charges on individual atoms.

The last group of molecular descriptors considered here were parameters derived from excess charge distribution within a molecule. These were submolecular polarity parameters,  $\Delta$  (delta), electronic-geometric index,  $T^E$  (geoli), and the local dipole index,  $D_L$  (diploc). The submolecular polarity parameter delta1 was calculated as the largest difference of excess charges for a pair of atoms in a molecule<sup>27</sup>. The second-order submolecular polarity parameter, delta2, was determined analogously as the second largest difference of excess charges. Determination of the local dipole index according to Kikuchi<sup>28</sup> is based on the equation

$$D_L = \sum |Q_A - Q_B| / N_{AB}$$

where  $Q_A$  and  $Q_B$  are net charges of atoms A and B which are bonded together. The summation is made over all pairs of bonded atoms and  $N_{AB}$  is the number of such pairs. The electronic-geometric index,  $T^E$  (geoli), is based on excess charge distribution and on molecular geometry, as proposed previously<sup>29</sup>.

#### Statistical analysis

Principal component analysis (PCA)<sup>30,31</sup> was performed on a set of nineteen structural descriptors of twenty solutes. The resulting principal component object scores were related to chromatographic data and boiling points by means of a step-wise multiple regression.

By PCA, a multi-dimensional parameter space may be reduced to a few significant components which concentrate the information distributed over many variables. In other words, all those original parameters which are interrelated by simple or multiple correlations are combined (linear combination) to a few orthogonal principal components.

Principal component loadings (vectors) and principal component object scores are usually displayed graphically on the plane spanned by two principal component axes. A vector representation of the original parameters in the principal component space is obtained by plotting the loading values of the principal components on the variable against each other.

In PCA, high loadings of almost all variables on the first principal component are usually observed, whereas the other PCs contain much less information. In such a situation it may be difficult to interpret the meaning of individual principal components and rotation of the principal coordinate system is often applied. The VARI-MAX procedure was applied here using standard statistical software.

## RESULTS AND DISCUSSION

For the set of twenty solutes studied, logarithms of HPLC capacity factors,

TABLE I

RETENTION DATA ( $\log k'$ ), BOILING POINTS AND NINETEEN NON-EMPIRICAL STRUCTURAL DESCRIPTORS FOR THE SET OF SOLUTES ANALYSED

No.	Solutes	$\log k'$	<i>b.p.</i> (K)	<i>molwt</i> <sup>a</sup>	<i>bondrefr</i> <sup>b</sup>	<i>kappa2</i> <sup>c</sup>	<i>kappa3</i> <sup>d</sup>	<i>chi2v</i> <sup>e</sup>	<i>balaban</i> <sup>f</sup>	<i>ic0</i> <sup>g</sup>	<i>ic1</i> <sup>h</sup>
1	Phenol	0.431	454.7	94.11	27.768	1.755	1.016	1.336	8.640	1.314	1.914
2	<i>p</i> -Cresol	0.456	474.9	108.14	32.416	1.968	1.331	1.836	9.717	1.272	2.272
3	4-Ethylphenol	0.277	492	122.17	37.064	2.646	1.541	2.020	10.600	1.236	2.325
4	4- <i>n</i> -Propylphenol	0.312	505.6	136.19	41.712	2.194	1.229	2.416	11.365	1.207	2.275
5	2-Isopropylphenol	-0.171	486	136.19	41.712	2.843	1.834	2.517	11.992	1.207	2.275
6	2- <i>tert.</i> -Butylphenol	-0.419	494	150.22	46.360	2.666	1.808	3.767	13.351	1.183	2.209
7	4- <i>tert.</i> -Butylphenol	-0.022	512.5	150.22	46.360	2.666	2.054	3.797	13.064	1.183	2.209
8	Carvacrol	-0.194	510.7	150.22	46.360	3.055	1.808	3.001	13.192	1.183	2.259
9	Thymol	-0.148	506	150.22	46.360	3.055	1.808	3.217	13.262	1.183	2.259
10	Benzene	-1.060	353.2	78.11	26.184	1.606	0.845	1.155	7.330	1.000	1.194
11	Toluene	-0.791	383.6	92.14	30.832	1.783	1.038	1.411	8.435	0.997	1.533
12	<i>o</i> -Xylene	-0.433	417.4	106.17	35.480	1.994	1.101	2.084	9.661	0.991	1.658
13	<i>m</i> -Xylene	-0.666	412.1	106.17	35.480	1.994	1.353	2.158	9.596	0.991	1.658
14	<i>p</i> -Xylene	-0.658	411.3	106.17	35.480	1.994	1.353	2.155	9.542	0.991	1.658
15	Anisole	-0.317	428	108.14	32.616	2.468	1.331	1.517	9.711	1.272	1.774
16	Benzyl alcohol	-0.211	478.3	108.14	32.416	2.478	1.331	1.644	9.420	1.272	2.046
17	Chlorobenzene	-0.606	405	112.56	31.018	1.987	1.204	1.296	8.928	1.325	1.650
18	Acetophenone	0.283	475.6	120.15	35.618	2.444	1.389	1.922	10.770	1.264	1.993
19	Nitrobenzene	0.799	483.8	123.11	31.858	2.259	1.253	1.654	11.376	1.727	2.006
20	Methyl benzoate	0.236	472.6	136.15	37.232	3.129	1.662	1.858	12.034	1.392	2.192

<sup>a</sup> Molecular weight. <sup>b</sup> Sum of bond refractivities<sup>20</sup>. <sup>c</sup> Index of molecular shape of second order<sup>19</sup>. <sup>d</sup> Index of molecular shape of third order<sup>19</sup>. <sup>e</sup> Valence connectivity index of second order<sup>21</sup>. <sup>f</sup> Modified Balaban index<sup>23</sup>. <sup>g,h,i</sup> Information content indices of zeroth, first and second order, respectively<sup>24</sup>. <sup>j</sup> Total energy (eV). <sup>k</sup> Heat of formation (kcal). <sup>l</sup> Energy of core-core repulsion (eV). <sup>m</sup> Energy of the highest occupied molecular orbital (eV). <sup>n</sup> Energy of the lowest empty molecular orbital (eV). <sup>o</sup> Dipole moment calculated quantum chemically (D). <sup>p</sup> Submolecular polarity parameter of first order (electrons). <sup>q</sup> Submolecular polarity parameter of second order (electrons). <sup>r</sup> Local dipole index<sup>28</sup> (electrons). <sup>s</sup> Geometric electronic index<sup>29</sup> (electrons/Å<sup>2</sup>).

boiling points and nineteen non-empirical structural descriptors are collected in Table I. The correlation matrix (not included) for all 21 data sets reflects high intercorrelations among most of the structural descriptors under study.

Stepwise multiple regression analysis of  $\log k'$  data against the nineteen non-empirical structural descriptors of the solutes did not yield any statistically significant multi-parameter equation.

Intercorrelations among structural parameters limit the applicability of multiple regression analysis in QSRR studies. On the other hand, according to current chemometric theory, as many relevant data as possible should be used because this increases the probability of good characterization of the solutes<sup>15</sup>. The large data tables resulting from such an assumption can be subjected to multivariate analysis to extract the systematic information contained in the data. The set of structural data considered here consisted of the last nineteen columns in Table I.

Basing on the eigenvalues of the correlation matrix, we decided to extract five main factors from the data. The first factor accounted for 57% of the variance in structural data, the second for 21%, the third for 7%, the fourth for 6% and the fifth for 3% of the variance. Altogether, the principal components extracted accounted for about 95% of the variance in the structural data considered.

Subsequently, we calculated loadings (eigenvectors) of the five principal components extracted. The loadings were next subjected to VARIMAX rotation. The VARIMAX-rotated PC loadings, PCvr1 to PCvr5, are given in Table II. In Fig. 1 the loadings of two first principal components by individual structural descriptors are graphically depicted.

<i>ic</i> <sup>2j</sup>	<i>etotal</i> <sup>j</sup>	<i>heat</i> <sup>k</sup>	<i>corer</i> <sup>l</sup>	<i>ehomo</i> <sup>m</sup>	<i>elum</i> <sup>n</sup>	<i>dipolem</i> <sup>o</sup>	<i>delta1</i> <sup>p</sup>	<i>delta2</i> <sup>q</sup>	<i>diploc</i> <sup>r</sup>	<i>geol</i> <sup>s</sup>
2.661	1172.37	12.443	3336.19	-9.3347	-0.0245	1.55	0.444	0.347	0.1411	2.436
3.203	1328.68	10.938	4272.77	-9.2302	0.1309	1.52	0.441	0.361	0.1578	3.001
3.471	1484.60	18.407	5320.72	-9.0901	0.1767	1.36	0.435	0.342	0.1251	3.102
3.698	1639.92	39.683	6360.13	-9.1356	-0.0370	1.68	0.450	0.338	0.1045	3.080
3.482	1639.88	40.626	6723.87	-9.4610	0.0874	1.66	0.453	0.346	0.1056	3.472
3.152	1794.76	71.972	8189.62	-9.5373	0.0712	1.56	0.462	0.350	0.1028	4.217
2.992	1795.46	55.862	7919.10	-9.1947	0.1701	1.50	0.440	0.347	0.1236	4.219
3.593	1795.88	53.090	7828.34	-9.2813	0.0302	1.46	0.454	0.372	0.1133	4.091
3.593	1795.77	48.596	7920.80	-9.3971	0.0472	1.66	0.453	0.368	0.1038	4.000
2.661	848.65	249.257	2255.72	-7.4078	-0.4751	0.13	0.168	0.164	0.7960	1.506
2.386	1006.14	59.026	3319.61	-9.2088	0.1824	0.03	0.204	0.169	0.0851	1.727
2.419	1157.34	175.358	4451.23	-9.3617	0.2491	0.14	0.201	0.200	0.0796	2.318
2.530	1157.88	160.664	4343.00	-9.0636	0.0498	0.16	0.231	0.223	0.9170	2.440
2.197	1158.56	147.252	4298.57	-9.3161	0.2503	0.02	0.218	0.217	0.9440	2.309
2.858	1327.77	31.882	4321.22	-8.8705	0.2100	1.35	0.501	0.388	0.1901	3.540
3.031	1328.13	23.574	4293.52	-9.3306	0.2758	1.46	0.531	0.494	0.1655	3.488
2.459	1190.88	41.735	3192.70	-9.6014	-0.1082	1.43	0.126	0.124	0.5100	1.008
3.013	1455.63	33.040	5002.93	-9.8255	-0.3894	2.66	0.550	0.416	0.1327	2.936
2.700	1683.97	71.757	5139.94	-10.2590	-1.0730	4.88	0.842	0.819	0.2428	3.666
3.155	1777.78	-6.123	6161.55	-9.7408	-0.3392	1.76	0.764	0.716	0.2399	5.150

TABLE II

VARIMAX-ROTATED LOADINGS OF THE EXTRACTED PRINCIPAL COMPONENTS BY INDIVIDUAL STRUCTURAL DESCRIPTORS DENOTED AS IN TABLE I

<i>Structural descriptor</i>	<i>PCvr 1</i>	<i>PCvr 2</i>	<i>PCvr 3</i>	<i>PCvr 4</i>	<i>PCvr 5</i>
molwt	0.9411	0.1939	0.2309	0.0404	0.0422
bondrefr	0.9812	-0.1106	0.1058	0.0650	-0.0114
kappa2	0.7672	0.1657	0.2620	0.1219	0.4263
kappa3	0.9148	-0.0014	0.1633	0.0234	0.2406
chi2v	0.9570	-0.1417	-0.0115	0.0224	-0.0605
balaban	0.9476	0.2351	0.1739	0.0377	0.0993
ic0	-0.0039	0.8805	0.3678	-0.0455	0.1296
ic1	0.5796	0.2746	0.3280	0.6257	0.1320
etotal	0.8451	0.3942	0.2930	0.0901	0.1687
heatf	-0.1619	-0.2388	-0.8694	0.0240	-0.2526
corer	0.9688	0.0949	0.1654	0.0971	0.0826
ehomo	-0.3170	-0.4787	-0.4550	0.6322	-0.0343
elumo	0.1390	-0.8985	0.3036	-0.0758	0.1436
dipolem	0.1863	0.9190	0.2916	-0.0120	-0.0287
delta1	0.2626	0.7589	0.3085	0.0940	0.4708
delta2	0.1773	0.8080	0.1819	0.0074	0.5053
diploc	-0.2855	-0.1426	-0.8155	-0.1542	0.0290
geoeli	0.6868	0.3201	0.2065	0.1365	0.5749

The principal component scores for the set of twenty solutes studied, scaled to a variance of 1, obtained after VARIMAX rotation, are collected in Table III. For illustration the first two PC scores for the solutes considered are presented in Fig. 2.

As can be observed in Table II (see also Fig. 1), the first principal component, PCvr1, is loaded mostly by such structural descriptors as molecular refractivity (bondrefr), energy of core-core repulsion (corer), valence connectivity index of second order (chi2v), Balaban index (balaban), molecular weight (molwt), kappa parameter of third order (kappa3) and total energy (etotal). To a lesser extent PCvr1 is loaded by kappa2, electronic-geometric index (geoeli) and information content indices of first and second order (ic1 and ic2). It is evident that all these structural descriptors strongly loading PCvr1 reflect basically the size (bulkiness) of the solutes. In such a situation PCvr1 condenses information on molecular size.

The second principal component, PCvr2, is loaded predominantly by the following structural descriptors: dipole moment (dipolem), energy of LUMO (elumo), information content index of zeroth order (ic0) and the submolecular polarity parameters of the first and second order (delta1 and delta2). Hence it may be concluded that PCvr2 concentrates structural information related to the so-called molecular polarity. Specific, polar properties of chemical compounds are the result of electron distribution within a molecule. From the chromatographic point of view, such properties determine the ability of a solute to participate in intermolecular interactions with the stationary and/or mobile phase of the dipole-dipole, dipole-induced dipole and electron pair donor-acceptor type.

A separate discussion requires high loading of PCvr2 by ic0. The index ic0 reflects the diversity in the atom composition of a molecule. For the set of solutes

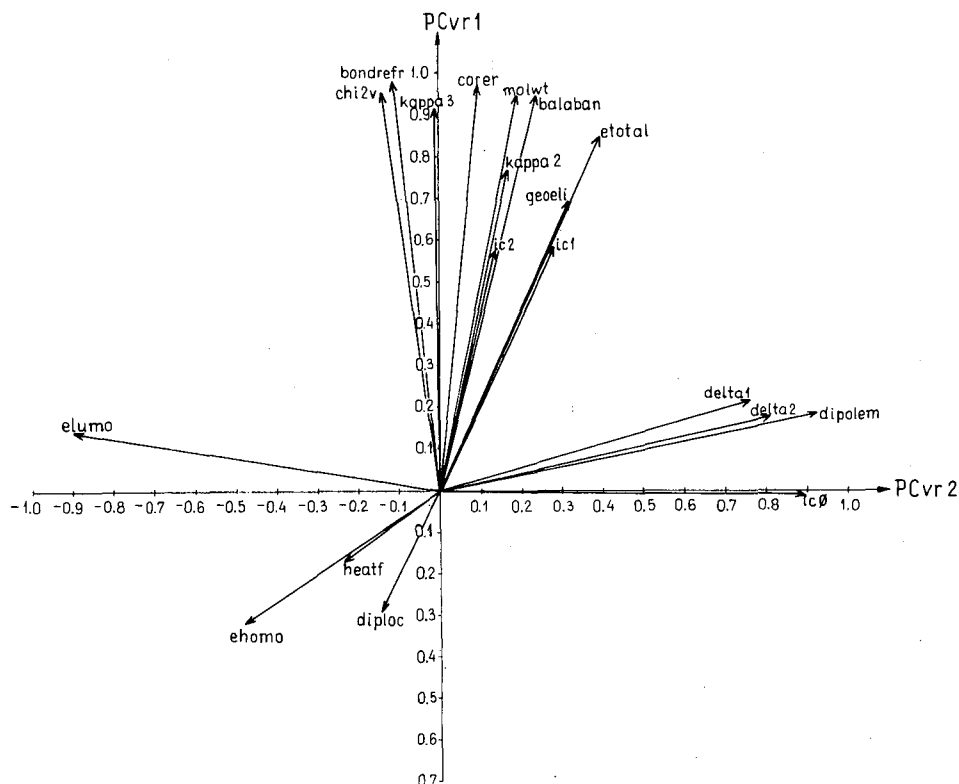


Fig. 1. VARIMAX-rotated loadings of two first principal components by individual structural descriptors denoted as in Table I.

studied it also reflects their molecular polarity as demonstrated by correlation of  $ic0$  with dipole moment ( $r = 0.93$ ) and with the submolecular polarities  $\delta 1$  and  $\delta 2$  ( $r = 0.81$  and  $0.82$ , respectively).

The third VARIMAX-rotated principal component, PCvr3, is highly loaded by the heat of formation ( $heatf$ ) and the local dipole index ( $diploc$ ). The next loading structural descriptor would be the energy of HOMO ( $ehomo$ ), with a contribution of  $-0.4550$ . The parameter  $ehomo$  is one of the three structural descriptors most significantly loading PCvr4, the other two being  $ic1$  and  $ic2$ . The loading values for these descriptors are  $0.6322$ ,  $0.6257$  and  $0.6377$ , respectively. Loadings of PCvr4 by the remaining parameters are insignificant ( $< 0.15$ ). There is no parameter strongly loading PCvr5 but several descriptors provide contributions of about  $0.5$ ;  $geeli$ ,  $\delta 1$ ,  $\delta 2$  and  $kappa2$ . It may be speculated that PCvr5 contains some information on the molecular shape of the solutes.

The principal component scores after VARIMAX rotation for the solutes studied (Table III and Fig. 2) differentiate a subgroup of phenolic solutes from the remaining benzene derivatives. As illustrated in Fig. 2, phenols are distributed along the PCvr1 axis and are characterized by low values of PCvr2. The reverse situation is observed for non-phenolic compounds.

It seemed interesting to apply the structural information condensed in five prin-

TABLE III  
 VARIMAX-ROTATED PRINCIPAL COMPONENT SCORES FOR THE SOLUTES ANALYSED  
 The solutes are numbered as in Table I.

Solute No.	PCvr 1	PCvr 2	PCvr 3	PCvr 4	PCvr 5
1	1.4096	-0.1692	1.0508	-0.1146	-0.1675
2	0.7181	0.0879	1.0513	0.8746	-0.0358
3	0.0823	0.3454	0.9058	1.1894	0.2208
4	-0.3910	-0.1595	0.6249	1.3567	-1.2177
5	-0.8082	0.1659	0.5300	0.4910	-0.0839
6	-1.7161	0.1006	-0.1624	-0.2756	-0.4645
7	-1.7017	0.3733	-0.2055	-0.2137	-0.0352
8	-1.4317	0.1615	0.0534	0.6297	0.0020
9	-1.5090	0.1269	0.1492	0.4699	-0.2106
10	1.4856	0.0749	-2.6331	2.5015	-0.5728
11	1.1533	1.1636	0.7842	-0.9680	-0.5168
12	0.2404	0.9928	-0.1926	-0.9950	-0.7277
13	0.0362	0.6940	-1.8420	-0.8304	0.3305
14	0.0419	0.9590	-1.6122	-1.5784	0.5789
15	0.7642	0.3651	0.4583	-0.0071	1.5090
16	0.7810	0.2429	0.8289	0.1247	1.5695
17	0.7581	-0.0330	0.4278	-1.3157	-1.8248
18	0.1020	-0.9377	0.4288	-0.3581	-0.6119
19	0.2569	-3.5829	-0.6015	-0.8545	-0.3883
20	-0.2719	-0.9712	-0.0440	-0.1264	2.6470

principal components to correlation studies with HPLC data derived on graphitic carbon as stationary phase with hexane as the eluent. The stepwise regression analysis of  $\log k'$  against PCvr1 to PCvr5 for the whole set of 20 solutes yielded the following equation:

$$\log k' = -0.145 - 0.323 \text{ PCvr2} + 0.259 \text{ PCvr3} \quad (1)$$

characterized by a correlation coefficient  $R = 0.85$ , standard error of estimate  $s = 0.271$  and  $F$ -test value 22.2. The equation is significant at the  $1.8 \cdot 10^{-5}$  level and the significance levels for the coefficients at the variables PCvr2 and PCvr3 are 0.0001 and 0.0005, respectively.

On analysing eqn. 1, one notes the absence of the molecular size-related PCvr1. As is well known, the bulkiness of chemical compounds determines their ability to participate in non-specific dispersive intermolecular interactions. The lack of significance of PCvr1 for a description of the retention of the whole set of diverse solutes means that the net London-type attraction of solutes and stationary phase is comparable to that between solutes and mobile phase molecules. The PCvr2 term in eqn. 1 can be interpreted as compromising the charge-transfer attractive interactions of the solutes and the graphitic carbon stationary phase on the one hand and the solute-hexane inductive interactions on the other. The contribution of PCvr3 to eqn. 1 is difficult to interpret in terms of the retention mechanism. Bearing in mind the input by the local dipole index to the third PC, one could consider PCvr3 as reflecting



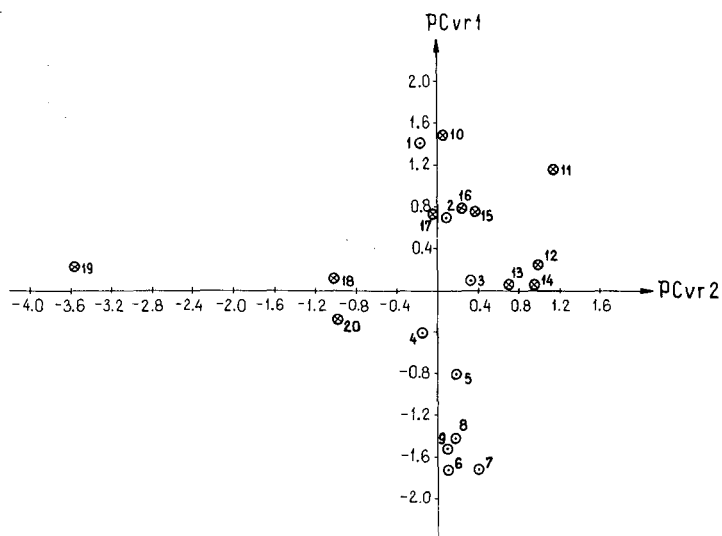


Fig. 2. Principal component scores after VARIMAX rotation for the solutes numbered as in Table I.

dipole-induced dipole interactions involving solute molecules and the molecules of both chromatographic phases.

Eqn. 1 may give some insight into the mechanism of separations in the graphitic carbon-hexane HPLC system. Its statistical value, however, is too low for the reliable prediction of retention. When phenolic derivatives are excluded from regression then the equation derived for the remaining eleven benzene derivatives has much increased predictive properties:

$$\log k' = -0.100 - 0.373 \text{ PCvr1} - 0.299 \text{ PCvr2} + 0.159 \text{ PCvr3} \quad (2)$$

Eqn. 2 is characterized by the statistical parameters  $R = 0.977$ ,  $s = 0.140$  and  $F$ -value = 49.5. The significance level for eqn 2 is  $4.4 \cdot 10^{-5}$  and for the variables PCvr1, PCvr2 and PCvr3 the respective values are 0.001, 0.00001 and 0.002. The relationship between the measured  $\log k'$  data and values calculated by eqn. 2 is illustrated in Fig. 3.

On comparing eqn. 1 and 2, one notes that in the latter the term PCvr1, related to molecular size, becomes significant. It may also be noted that PCvr1 scores for the solutes studied (Table III) attain higher values for smaller compounds. Thus, a negative coefficient for PCvr1 suggests that more bulky non-phenolic solutes will be more strongly retained in the HPLC system under study. This in turn can be interpreted as a result of weaker dispersive interactions between a solute and the solvent than the respective solute-stationary phase interactions. The terms PCvr2 and PCvr3 in eqn. 2 may be interpreted analogously as in eqn. 1 for a whole set of solutes. Again, the term PCvr2 predominates over others.

The following regression equation was derived for a subset of nine phenolic derivatives:

$$\log k' = 0.204 + 0.247 \text{ PCvr1} \quad (3)$$

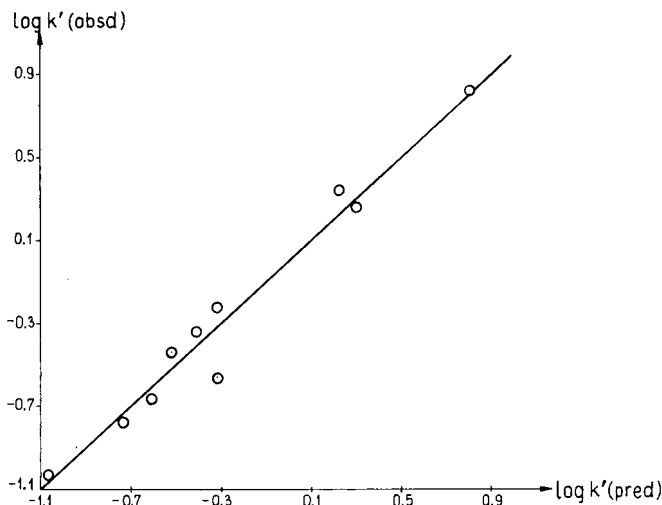


Fig. 3. Plot of observed values against values calculated from eqn. 2 of  $\log k'$  for non-phenolic solutes.

For eqn. 3 the statistical characteristics are  $R = 0.884$ ,  $s = 0.158$  and  $F$ -value = 25.0. The significance levels for eqn. 3 and the variable PCvr1 are 0.002 and 0.001, respectively. As could be expected, similarity of the electronic properties of a closely congeneric group of phenols made the terms PCvr2 and PCvr3 insignificant for the retention differentiation. In such a situation, retention within a series depends on the ability of an individual member to participate in non-specific dispersive interactions. This does not mean that there are no polar intermolecular interactions present in the system. These interactions, as revealed by the general eqn. 1, may still be decisive for the retention of the whole homogeneous group of phenols studied. The contributions of polar interactions to the retention of individual phenols must be similar, however. The principal components extracted from the nineteen structural descriptors considered are not precise enough to account for changes in polar properties within a closely congeneric set of phenolic compounds. Hence the structural information contained in the non-empirical descriptors considered here does not suffice for the precise prediction of retention.

The same fundamental intermolecular interactions that determine chromatographic separations are also responsible for various physico-chemical properties of chemical compounds. These interactions, for instance, take place among molecules of a substance in a liquid state. It therefore seemed interesting to establish whether and to what extent the structural information extracted by PCA would be of value for the calculation of the boiling points of the solutes studied.

A stepwise regression analysis of boiling point data of the solutes, b.p., against the VARIMAX-rotated principal component scores yielded the following four-parameter regression equation:

$$\text{b.p.} = 457.9 - 33.2 \text{ PCvr1} - 15.2 \text{ PCvr2} + 23.0 \text{ PCvr3} + 9.2 \text{ PCvr4} \quad (4)$$

Eqn. 4 includes all twenty solutes studied and is characterized by  $R = 0.944$ ,  $s = 17.3$

and  $F$ -value = 30.9. The significance levels for eqn. 4 and the variables PCvr1, PCvr2, PCvr3 and PCvr4 are 0.0001, 0.00001, 0.001, 0.00001 and 0.03, respectively. The variable PCvr4 is hardly significant and thus the relationship described by eqn. 4 resembles eqn. 2. In both eqns. 2 and 4 the coefficients at PCvr1 and PCvr2 are negative whereas that at PCvr3 is positive. In eqn. 4, however, the variable PCvr1 predominates, reflecting strong dispersive attractions among molecules in liquid state. Also, the significance of PCvr3 is higher than that of PCvr2 in eqn. 4, in contrast to eqn. 2. Therefore, it may be concluded that in order to hold the solutes considered in the liquid state, dispersive intermolecular interactions are decisive, supplemented by specific polar interactions, whereas the reverse is true for HPLC retention in the graphitic carbon-hexane system.

The QSRR studies using principal components extracted from nineteen non-empirical structural descriptors provide evidence for the decisive role of specific, polar, electronic intermolecular interactions for the separation of solutes in a graphitic carbon-hexane HPLC system. This is in agreement with the general conclusions of our earlier work, in which we analysed retention on graphitic carbon from the point of view of the metallic character of the stationary phase and electron pair donor-acceptor interactions of solutes<sup>17</sup>.

The principal component analysis of nineteen well established topological, information content and quantum chemical structural indices confirmed that these indices provide information mainly about the molecular size of chemical compounds. The information on electronic properties of the compounds which was condensed in PCvr2 and PCvr3 was also meaningful. Information contained in PCvr4 and PCvr5 is difficult to identify and has little relevance for the physico-chemical properties of the solutes considered here. The non-empirical molecular descriptors most often applied in QSRR studies still lack the full structural information required for the reliable prediction of molecular properties, including chromatographic retention. A further search for more specific structural parameters is required.

## REFERENCES

- 1 R. Kaliszan, *Quantitative Structure-Chromatographic Retention Relationships*, Wiley, New York, 1987.
- 2 P. H. Weiner, C. J. Dack and D. G. Howery, *J. Chromatogr.*, 69 (1972) 249.
- 3 J. F. K. Huber, C. A. M. Meijers and J. A. R. J. Hulsman, *Anal. Chem.*, 44 (1972) 111.
- 4 J. F. K. Huber, E. T. Alderlieste, H. Harren and H. Poppe, *Anal. Chem.*, 45 (1973) 1337.
- 5 R. F. Hirsch, R. J. Gaydosch and J. R. Chrétien, *Anal. Chem.*, 52 (1980) 723.
- 6 L. Buydens, D. L. Massart and P. Geerlings, *Anal. Chem.*, 55 (1983) 738.
- 7 L. Buydens, D. Coomans, M. Vanbelle, D. L. Massart and R. Vanden Driessche, *J. Pharm. Sci.*, 72 (1983) 1327.
- 8 M. N. Hasan and P. C. Jurs, *Anal. Chem.*, 55 (1983) 263.
- 9 T. Cserháti, B. Bordás, L. Ekiert and J. Bojarski, *J. Chromatogr.*, 287 (1984) 385.
- 10 J. R. Chrétien, K. Szymoniak, C. Lion and J. K. Haken, *J. Chromatogr.*, 324 (1985) 355.
- 11 B. Walczak, M. Dreux, J. R. Chrétien, K. Szymoniak, M. Lafosse, L. Morrin-Allory and J. P. Doucet, *J. Chromatogr.*, 353 (1986) 109.
- 12 B. Walczak, J. R. Chrétien, M. Dreux, L. Morrin-Allory, M. Lafosse, K. Szymoniak and F. Membrey, *J. Chromatogr.*, 353 (1986) 123.
- 13 K. Szymoniak and J. R. Chrétien, *J. Chromatogr.*, 404 (1987) 11.
- 14 S. Wold, L. Eriksson, S. Hellberg, J. Jonsson, M. Sjöström, B. Skageberg and C. Wikström, *Can. J. Chem.*, 65 (1987) 1814.
- 15 L. Eriksson, J. Jonsson, M. Sjöström and S. Wold, *Quant. Struct.-Act. Relat.*, 7 (1988) 144.

- 16 J. H. Knox, B. Kaur and G. R. Millward, *J. Chromatogr.*, 352 (1986) 3.
- 17 B. J. Bassler, R. Kaliszán and R. A. Hartwick, *J. Chromatogr.*, 461 (1989) 139.
- 18 R. C. West, M. J. Astle and W. H. Beyer (Editors), *CRC Handbook of Chemistry and Physics*, CRC Press, Boca Raton, FL, 1986–87.
- 19 B. V. Iophphe, *Refraktometricheskie Metody Khimii*, GNTIKhL, Leningrad, 1960.
- 20 L. B. Kier, *Acta Pharm. Jugosl.*, 36 (1986) 171.
- 21 L. B. Kier and L. H. Hall, *J. Pharm. Sci.*, 65 (1976) 1806.
- 22 A. T. Balaban, *Chem. Phys. Lett.*, 89 (1982) 399.
- 23 M. Barysz, G. Jashari, R. S. Lall, V. K. Srivastava and N. Trinajstić, in R. B. King (Editor), *Chemical Applications of Topology and Graph Theory*, Elsevier, Amsterdam, 1983, pp. 222–230.
- 24 R. Sarkar, A. B. Roy and P. K. Sarkar, *Math. Biosci.*, 39 (1978) 299.
- 25 M. J. S. Dewar, *QCPE*, 11 (1975) 279.
- 26 *Cambridge Crystallographic Database*, Cambridge Crystallographic Data Centre, Cambridge, 1979.
- 27 K. Ośmiałowski, J. Halkiewicz, A. Radecki and R. Kaliszán, *J. Chromatogr.*, 346 (1985) 53.
- 28 O. Kikuchi, *Quant. Struct.-Act. Relat.*, 6 (1987) 179.
- 29 K. Ośmiałowski, J. Halkiewicz and R. Kaliszán, *J. Chromatogr.*, 361 (1986) 63.
- 30 K.-J. Schaper and R. Kaliszán, in E. Mutschler and E. Winterfeldt (Editors), *Trends in Medicinal Chemistry*, VCH, Weinheim, Berlin, 1987, pp. 125–139.
- 31 J. R. Llinas and J. M. Ruiz, in G. Vernin and M. Chanon (Editors), *Computer Aids to Chemistry*, Ellis Horwood, Chichester, 1986, pp. 200–256.

CHROMSYMP. 1635

## PREPARATION OF SILICONE-COATED 5-25- $\mu\text{m}$ I.D. FUSED-SILICA CAPILLARY COLUMNS FOR OPEN-TUBULAR LIQUID CHROMATOGRAPHY

O. VAN BERKEL-GELDOF, J. C. KRAAK and H. POPPE\*

*Laboratory for Analytical Chemistry, University of Amsterdam, Nieuwe Achtergracht 166, 1018 WV Amsterdam (The Netherlands)*

---

### SUMMARY

Fused-silica capillaries of I.D. of 5, 10 and 25  $\mu\text{m}$  were coated with PS-255 or PS-264 in order to achieve highly efficient columns for reversed-phase open-tubular liquid chromatography. Various coating solvents were tested, of which Freon-114 showed the most promising features with respect to speed of coating and ease of handling. The highest efficiency was obtained with a 1 m  $\times$  5.0  $\mu\text{m}$  I.D. column, showing 250 000 and 58 800 plates for solutes with capacity factors 0.2 and 2.6, respectively, at approximately six times the optimum linear velocity.

---

### INTRODUCTION

Open-tubular liquid chromatography (OTLC) will only be competitive with packed-column LC with respect to speed of separation and efficiency provided that capillaries with inner diameters of 5-10  $\mu\text{m}$  can be coated with a uniform, non-extractable layer 0.1-1  $\mu\text{m}$  thick<sup>1-4</sup>. The requirements put on the magnitude of the external peak broadening, which should be kept at about 1 nl (ref. 2), can be met by applying the techniques of on-column laser-induced fluorescence detection<sup>5-9</sup> and split injection<sup>10</sup>.

For on-column optical detection and for practical reasons, fused-silica capillaries are to be preferred to glass capillaries. However, deposition of a retentive layer by chemical bonding on the fused-silica surface is difficult because of the inertness of this material. Recently, the techniques used for coating and immobilization of silicone phases on fused-silica capillaries to prepare columns for gas chromatography (GC) and supercritical fluid chromatography (SFC) have been applied successfully to the preparation of 5-50- $\mu\text{m}$  I.D. columns for LC<sup>11-14</sup>.

An important factor in the coating of thick films is the viscosity of the coating solution. On the one hand too high a viscosity of the stationary phase may prevent the coating of thick films because of poor solubility in the coating solvent, and on the other too low a viscosity of the stationary phase appeared to cause droplet formation during evaporation and cross-linking<sup>14</sup>. In addition, the physical properties of the coating solvent may play a crucial role in the successful preparation of fused-silica open-tubular columns. The application of different coating solvents is discussed below.

It is known that the methylvinylsilicone gum PS-255 is to be preferred in the preparation of thick, immobilized layers<sup>15</sup>. In this study, PS-255 and PS-264, a methylphenylvinylsilicone gum, were selected for coating small-diameter capillaries.

## EXPERIMENTAL

### Materials

Fused-silica capillaries of I.D. 10 and 25  $\mu\text{m}$  were obtained from SGE (Ringwood, Australia) and 5- $\mu\text{m}$  I.D. fused-silica capillary from Polymicro Technologies (Phoenix, AZ, U.S.A.).

The stationary phases were polymethylsilicone fluid OV-101 purchased from Chrompack (Middelburg, The Netherlands), PS-255 (dimethyl- + 1–3% methylvinyl-silicone gum) and PS-264 (dimethyl- + 3–7% diphenyl- + 0.5–1% methylvinyl-silicone gum) from Fluka (Buchs, Switzerland) and polymethylhydrosilane and dicumyl peroxide from Merck (Darmstadt, F.R.G.).

The coating solvents were *n*-pentane (J. T. Baker, Deventer, the Netherlands), *n*-butane (Matheson, Oevel, Belgium) and 1,2-dichlorotetrafluoroethane (Freon-114) (Ucar, Nieuw Vennep, The Netherlands).

Polyaromatic hydrocarbons and anthracene derivatives, used as test compounds, were obtained from Janssen (Beerse, Belgium). Stock solutions of these compounds were prepared in acetonitrile–water (40:60, v/v).

All solvents were of spectroscopic quality and were filtered through a 0.2- $\mu\text{m}$  Optex filter (Millipore, Molsheim, France) prior to use.

### Apparatus

The chromatographic system is shown schematically in Fig. 1. For 25- $\mu\text{m}$  I.D. columns and low flow-rates, the system was equipped with a helium-pressurized vessel, acting as a constant-pressure pump, which was replaced with an LC pump (Orlita,

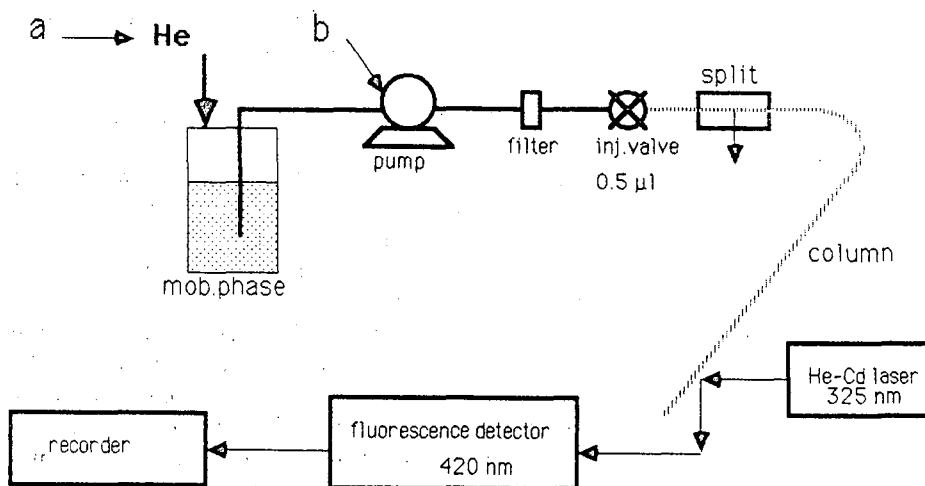


Fig. 1. Schematic representation of the chromatographic OTLC set-up. Supply of the mobile phase by (a) helium pressurized vessel and (b) LC pump.

Giessen, F.R.G.) for 5- and 10- $\mu\text{m}$  I.D. columns. Injections were made by means of a 0.5- $\mu\text{l}$  injection valve (Model 7520, Rheodyne, Berkely, CA, U.S.A.) combined with a laboratory-made splitting device, allowing injection volumes of a few picolitres.

On-column laser induced fluorescence detection was performed with a He-Cd laser as excitation source, excitation wavelength,  $\lambda_{\text{ex}} = 325 \text{ nm}$  (Model 4207 NB, Liconix, Sunnyvale, CA, U.S.A., or Model 56X, Omnicrome, Chino, U.S.A.) and a modified fluorimeter (M4Q III, Zeiss, Jena, G.D.R.) as photodetector, with emission wavelength,  $\lambda_{\text{em}} = 420 \text{ nm}$ .

#### Column preparation

The capillaries were pretreated and coated as described previously<sup>14</sup>. Briefly, after hydrothermal treatment with a 10% (v/v) solution of hydrochloric acid and deactivation of the fused-silica surface by polymethylhydrosilane, the capillaries were coated by the static method. Stationary phase solutions were prepared in *n*-pentane, *n*-butane or Freon-114.

Fig. 2 shows the reservoir for filling the capillaries at ambient temperature with a coating solution, prepared in *n*-pentane at least one day before use. Dicumyl peroxide was added in the ratio stationary phase: dicumyl peroxide = 20:1 (w/w) just before filling.

The filling vessel for coating solutions in either *n*-butane or Freon-114 is shown in Fig. 3. The cooled vessel containing the stationary phase and dicumyl peroxide in the ratio 20:1 (w/w) was filled with the solvent, closed and allowed to stand overnight at room temperature to dissolve the silicone. The capillaries were filled at a temperature of 5°C below the boiling point of the applied solvent (*n*-butane, b.p. =  $-0.5^\circ\text{C}$ ; Freon-114, b.p. =  $3.8^\circ\text{C}$ )

After filling, the capillaries were connected to a vacuum pump with both ends when *n*-pentane was used and with one end in the case of *n*-butane or Freon-114. In the latter instances one end of the capillaries was closed by means of a septum. Evacuation was carried out at 10–15°C above the boiling point of the applied solvent.

Next, the columns were purged with helium to remove traces of solvent and oxygen and, after flame-sealing, the silicone phase was immobilized by cross-linking at 260°C. Finally, the column was rinsed with acetonitrile–water (40:60, v/v) and dried at 140°C under a stream of helium.

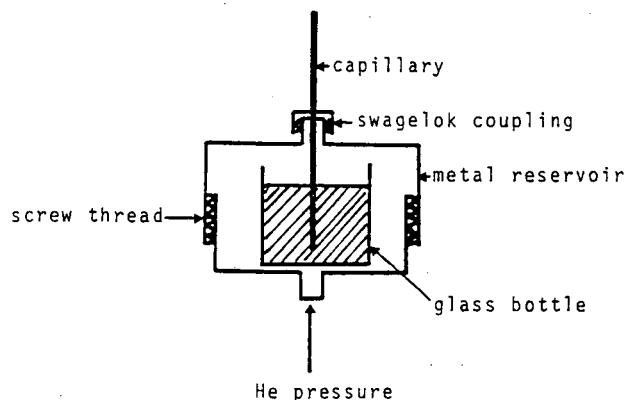


Fig. 2. Schematic representation of the reservoir to rinse and fill the fused-silica capillaries.

TABLE I  
DIMENSIONS AND COATING CONDITIONS OF FUSED-SILICA CAPILLARY COLUMNS

Column No.	Length (cm)	I.D. <sup>a</sup> ( $\mu$ m)	Stationary phase	Concentration (mg/ml)	Coating solvent	I.D. <sup>b</sup> ( $\mu$ m)	$d_f$ ( $\mu$ m)	Phase ratio	Coating yield (%)
1	94	25.10	PS-255(OV-101)	120	<i>n</i> -Pentane	23.77	0.67	0.126	84
2	98	26.09	PS-255	50	<i>n</i> -Butane	25.51	0.29	0.047	86
3	67	26.09	PS-255	100	<i>n</i> -Butane	24.95	0.57	0.100	84
4	100	28.46	PS-255		Freon-114	27.82	0.32	0.048	
5	124	10.24	PS-255	60	<i>n</i> -Pentane	10.08	0.08	0.032	50 <sup>c</sup>
6	67	10.18	PS-255	40	<i>n</i> -Butane	10.11	0.04	0.016	34 <sup>c</sup>
7	100	5	PS-255	20	<i>n</i> -Pentane	5.00	0.02 <sup>d</sup>	0.017 <sup>d</sup>	79
8a <sup>e</sup>	83	5	PS-255	35	<i>n</i> -Pentane	5.38	0.045 <sup>d</sup>	0.035 <sup>d</sup>	93
8b <sup>e</sup>	69	5	PS-255				0.02 <sup>d</sup>	0.016 <sup>d</sup>	
9	67	25.13	PS-264		Freon-114	24.44	0.34	0.059	

<sup>a</sup> Before coating.

<sup>b</sup> After coating and rinsing.

<sup>c</sup> Untreated fused-silica capillary.

<sup>d</sup> Calculated from capacity factor *versus* phase ratio plot.

<sup>e</sup> 8a and 8b before and after removal of a blocked part, respectively.



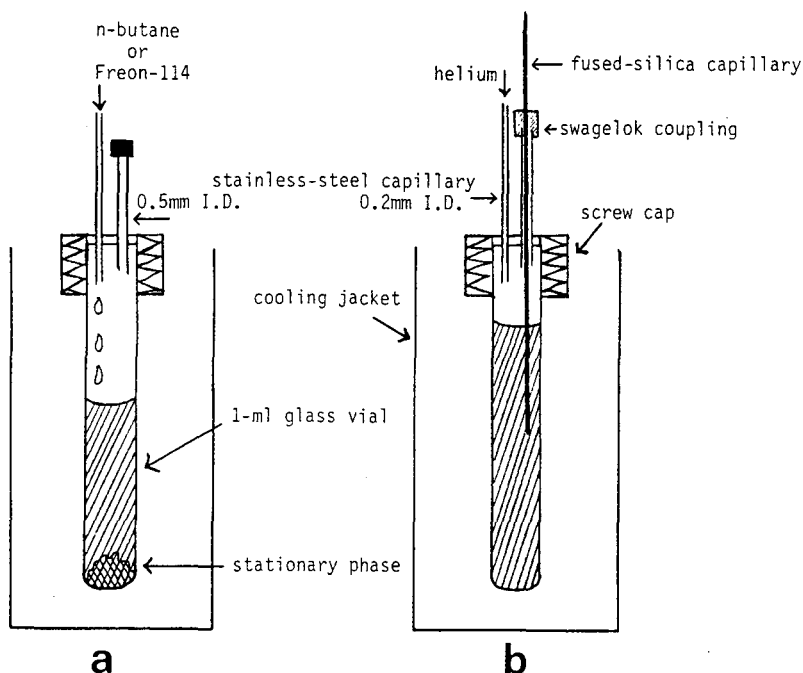


Fig. 3. Schematic representation of the device for (a) dissolving the stationary phase and (b) filling the fused-silica capillaries with the coating solution in *n*-butane or Freon-114.

#### Film thickness

Before and after coating, the inner diameter of the capillaries was determined by an aerodynamic method, based on the Hagen-Poiseuille relationship, as described previously<sup>16</sup>. The dimensions of the fused-silica capillary columns and coating conditions are given in Table I. The expected film thickness,  $d_f$ , was calculated from the column diameters before coating and the amount of silicone material applied, according to the equation

$$d_f = \frac{d}{2} \left( 1 - \sqrt{1 - \frac{C}{\rho}} \right) \quad (1)$$

where  $C$  = concentration of the coating solution in  $\text{g ml}^{-1}$ ,  $d$  = capillary diameter before coating and  $\rho$  = density of the silicone phase ( $0.98 \text{ g ml}^{-1}$ ). For the calculation of the immobilization yield, the film thickness obtained from measurement of the column diameter before and after the treatment was compared with the expected film thickness. The stationary to mobile phase ratio was found from the equation

$$V_s/V_m = d_c d_f / (0.5 d_c - d_f)^2 \quad (2)$$

where  $V_s$  = volume of stationary phase,  $V_m$  = volume of mobile phase, and  $d_c$  = column diameter after coating and rinsing.

It should be noted that for the 5- $\mu\text{m}$  I.D. columns the film thickness and phase ratio were calculated from the capacity factor *versus* phase ratio plots (see Fig. 4).

#### Retention and efficiency

Capacity factors ( $k'$ ) were calculated from  $k' = (t_r/t_0) - 1$ , where  $t_r$  and  $t_0$  are the retention times of a retained and an unretained solute (anthranilic acid), respectively.

The experimental data for plate heights ( $H$ ) and linear velocities ( $v$ ) were fitted to the theoretical values as calculated with the Golay equation:

$$H = \frac{2D_m}{v} + \frac{(1 + 6k' + 11k'^2)d_c^2v}{96D_m(1 + k')^2} + \frac{2k'd_f^2v}{3D_s(1 + k')^2}$$

The diffusion coefficients of the test solutes in the mobile phase,  $D_m$ , calculated according to the Wilke–Chang equation<sup>17</sup>, are given in Table II.

TABLE II

DIFFUSION COEFFICIENTS OF THE TEST SOLUTES IN ACETONITRILE–WATER (40:60, v/v) CALCULATED ACCORDING TO THE WILKE–CHANG EQUATION

Solute	Diffusion coefficient, $D_m$ ( $\text{m}^2 \text{s}^{-1}$ )	Solute	Diffusion coefficient, $D_m$ ( $\text{m}^2 \text{s}^{-1}$ )
Anthranilic acid	$0.70 \cdot 10^{-9}$	9-Methylanthracene	$0.54 \cdot 10^{-9}$
Anthracene	$0.57 \cdot 10^{-9}$	9-Vinylanthracene	$0.51 \cdot 10^{-9}$
9-Cyanoanthracene	$0.54 \cdot 10^{-9}$	9-Phenylanthracene	$0.46 \cdot 10^{-9}$

Diffusion coefficients in the stationary phase,  $D_s$ , of anthracene and pyrene in immobilized polymethylsilicones have been found to be  $5 \cdot 10^{-12}$ – $27 \cdot 10^{-12} \text{m}^2 \text{s}^{-1}$  (ref. 14). It was assumed that the diffusion coefficients using a different stationary phase in the present systems are of the same order of magnitude and a value for  $D_s$  of  $10^{-11} \text{m}^2 \text{s}^{-1}$  was assumed in calculations of the theoretical plate height.

## RESULTS AND DISCUSSION

### Column preparation

*Effect of pretreatment.* Although it has been reported that fused-silica capillaries possess sufficient wettability for polymethylsilicones<sup>18,19</sup>, others have found that it is necessary to pretreat this inert material before coating in order to achieve highly efficient columns<sup>20–22</sup>. Then the coating procedure should involve four steps: hydrothermal treatment, deactivation, static coating and cross-linking.

The effect of the pretreatment was examined by coating untreated fused-silica capillaries and comparing the coating yield with that for pretreated capillaries. From Table I it can be seen that in the two instances of coating untreated fused-silica capillaries only half of the expected film thickness was obtained. This phenomenon is probably due to a loss of stationary phase by solvent rinsing, which leads to the conclusion that the immobilization of the stationary phase is insufficient. In contrast, hydrothermally treated and deactivated fused-silica columns show a coating and immobilization yield of 84–90%.

*Coating solvent.* Apart from the structure of the stationary phase and the nature of the capillary surface, the successful coating of capillaries also depends on the choice of the coating solvent and coating temperature<sup>23</sup>. The use of dicumyl peroxide as cross-linking agent prevented the application of high coating temperatures. Coating with *n*-pentane as coating solvent at 45°C took several days, leading to an increasing risk of blockage during evaporation, possibly also due to premature decomposition of dicumyl peroxide and cross-linking. A high coating speed at low temperature has been reported by application of liquefied gases as coating solvents<sup>24,25</sup>. Because of their favourable boiling points and solubility of the stationary phase, *n*-butane (b.p. -0.5°C) and Freon-114 (b.p. 3.8°C) were tested for their applicability as coating solvents. It appeared to be impossible to dissolve over 6% (w/v) of the gum phases in Freon-114 and therefore with this solvent the phase ratio is limited to about 0.05.

In *n*-butane, up to 15% (w/v) of the silicone gums could be dissolved easily. The main drawback of these concentrated coating solutions was the high viscosity, resulting in longer times for filling and evaporation at an increasing risk of blocking and "bubble bursting", especially when coating small-diameter capillaries. Nevertheless, the use of *n*-butane rather than *n*-pentane is to be preferred, because coating is less time consuming (a few hours *versus* a few days).

Probably the long coating times with *n*-pentane at 45°C had an adverse effect on the column stability. During chromatographic testing of the columns, columns 1 and 8a became blocked at high flow-rates and, after removal of the blocked part of the column, a significantly smaller phase ratio was indicated by lower capacity factors. It is assumed that the insufficient immobilization of the stationary phase is due to degradation of the cross-linking agent DCuP under these coating conditions. The coating times with Freon-114 appeared to be similar to those with *n*-butane.

The choice of the coating solvent should be based on the speed of coating at low temperatures, the film thickness required and ease of handling. Considering these aspects, Freon-114 appears to be the preferred choice as a solvent for coating a layer on the inner wall of fused-silica capillaries, unless very thick layers are required, in which case *n*-butane could be used.

#### *Performance of prepared columns*

*Retention.* A linear relationship between the phase ratios of different columns coated with PS-255 and the capacity factor of various test solutes was found, as shown in Fig. 4. The good reproducibility of the coating method is demonstrated by the fact that no significant differences in the retention behaviour of columns with various inner diameters were observed.

As shown in Table III, the capacity factors of the test solutes obtained with the PS-264 column are approximately double those with comparable PS-255 columns. A further increase in capacity factors can be achieved by coating a thicker film of PS-264 with *n*-butane as coating solvent.

*Efficiency.* A number of columns prepared with the described procedure were tested with respect to efficiency by measuring chromatograms of mixtures of anthracene derivatives at various mobile phase velocities and by the construction of  $H/v$  plots from the data obtained. Figs. 5-10 show some results acquired during this study, which will now be discussed briefly in the order 25- $\mu$ m I.D. columns (Figs. 5 and 6), 10- $\mu$ m I.D. columns (Figs. 7 and 8) and 5- $\mu$ m I.D. columns (Figs. 9 and 10).

TABLE III  
 COMPARISON OF CAPACITY FACTORS OF ANTHRACENE DERIVATIVES ON COLUMNS COATED WITH PS-255 AND PS-264 WITH  
 ACETONITRILE-WATER (40:60, v/v) AS THE MOBILE PHASE

Stationary phase	Phase ratio	Solute				
		9-Cyanoanthracene	Anthracene	9-Methylanthracene	9-Vinyanthracene	9-Phenylanthracene
PS-255	0.048	0.3	1.3	1.7	2.8	5.1
PS-264	0.059	0.9	3.0	4.0	6.6	13.5

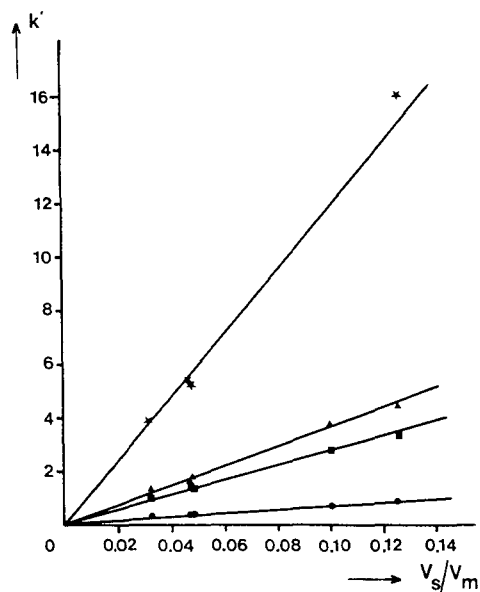


Fig. 4. Capacity factors of test solutes *versus* the phase ratio on different fused-silica columns coated with PS-255. Mobile phase: acetonitrile-water (40:60, v/v). ● = 9-Cyanoanthracene; ■ = anthracene; ▲ = 9-methylanthracene; ★ = 9-phenylanthracene.

The chromatogram in Fig. 5 illustrates the mediocre efficiency that can be obtained with these large-diameter columns. In fact, a packed HPLC column leads to higher resolution in the same or a shorter analysis time. The study of such columns was included, however, in order to obtain a clear idea of the performance as a function of

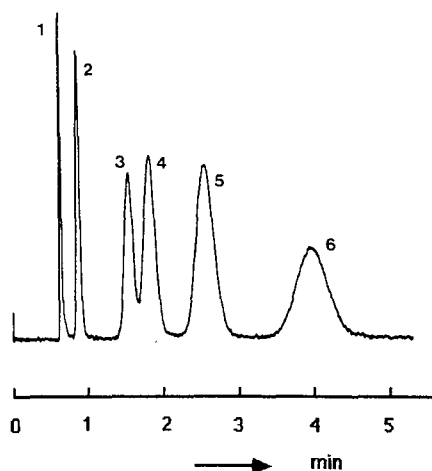


Fig. 5. Chromatogram of a test mixture of anthracene derivatives on column 2, 66.5 cm  $\times$  26.1  $\mu$ m I.D. fused silica coated with PS-255. Film thickness, 0.3  $\mu$ m; mobile phase, acetonitrile-water (40:60, v/v); pressure, 6 bar; linear velocity, 15.6 mm s<sup>-1</sup>. Peaks: 1 = anthranilic acid; 2 = 9-cyanoanthracene; 3 = anthracene; 4 = 9-methylanthracene; 5 = 9-vinyanthracene; 6 = 9-phenylanthracene.

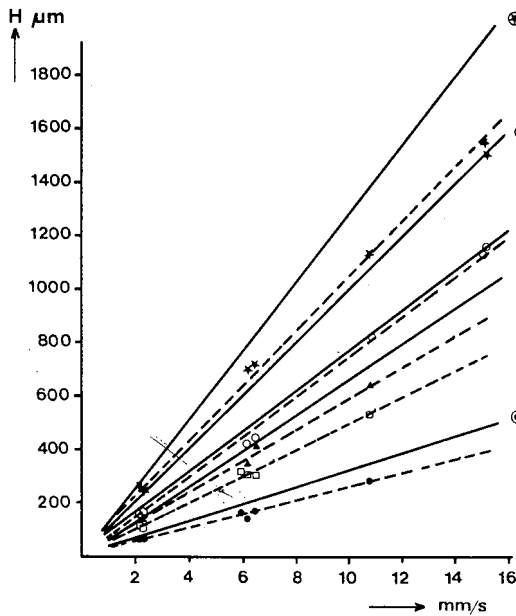


Fig. 6. Theoretical and experimental  $H$  versus  $v$  plots for anthracene derivatives on column 2. Mobile phase, acetonitrile-water (40:60, v/v). Theoretical curves calculated with  $D_m$  values from Table II and  $D_s$  values equal to  $10^{-11} \text{ m}^2 \text{ s}^{-1}$ . Solid lines, theoretical calculated  $H$  values; broken lines, experimental  $H$  values. ● = 9-Cyanoanthracene,  $k' = 0.35$ ; □ = anthracene,  $k' = 1.34$ ; ▲ = 9-methylanthracene,  $k' = 1.75$ ; ○ = 9-vinylanthracene,  $k' = 2.9$ ; ★ = 9-phenylanthracene,  $k' = 5.0$ .

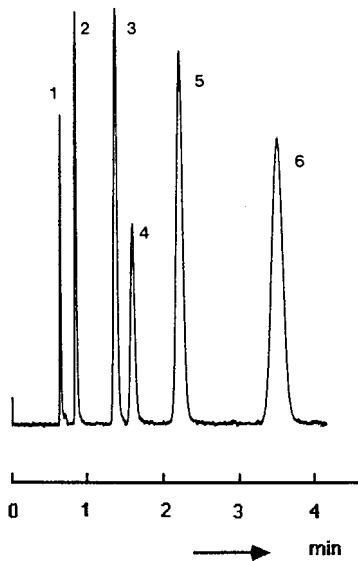


Fig. 7. Chromatogram of a test mixture of anthracene derivatives on column 5, 112 cm  $\times$  10.2  $\mu\text{m}$  I.D. fused silica, coated with PS-255. Film thickness, 0.08  $\mu\text{m}$ ; pressure, 80 bar; linear velocity, 29  $\text{mm s}^{-1}$ . Other experimental conditions and peaks as in Fig. 5.

diameter. The experimental  $H/v$  plots obtained with these columns, illustrated in Fig. 6, are straight lines that pass through the origin. This is in accordance with theory, as the axial diffusion can be neglected at these large diameters. For comparison, the theoretical lines, calculated with the extended Golay equation, are shown.

The diffusion coefficient in the mobile phase,  $D_m$ , was calculated by means of the original form of the Wilke–Chang equation, while the value for the stationary phase was set at  $10^{-11} \text{ m}^2 \text{ s}^{-1}$ . It should be noted that for all columns the contribution of the stationary phase term,  $H_{Es}$ , is less than 10%.

Although the discrepancy between the calculated and experimental curves in Fig. 6 is not dramatic, a systematic deviation occurs, the experimental values for the retained components being 20–40% smaller than the predicted values. This indicates first that uniform stationary layers were probably obtained and second that some inaccuracies were present in the calculation of theoretical  $H$  values. Possible causes include inaccurate capacity factors, inaccurate  $D_m$  and/or  $D_s$  values or secondary flow effects. The first is not likely as the unretained marker (anthranilic acid) elutes together with, or earlier than, compounds such as uranyl acetate, 2-naphthol and salicylic acid.

Inaccuracies in  $D_m$  values may occur; *e.g.*, Snyder<sup>26</sup> published another calculation scheme for which a higher accuracy is claimed and that generally leads to

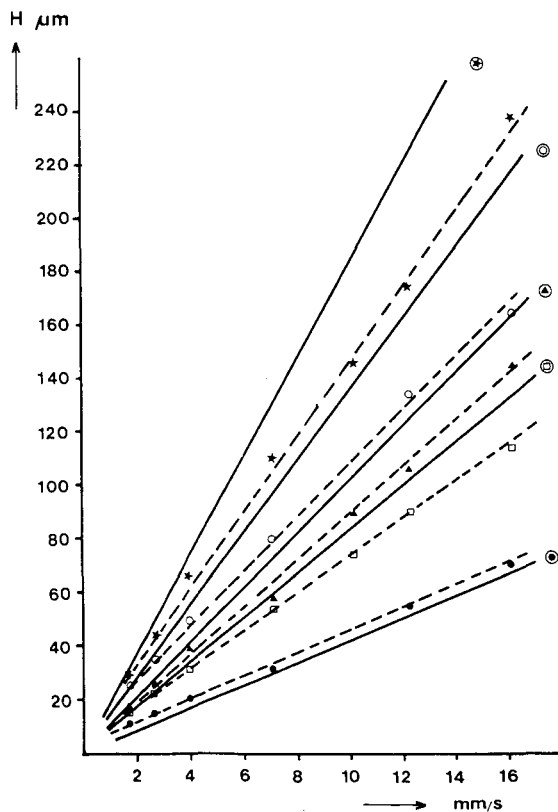


Fig. 8. Theoretical and experimental  $H$  versus  $v$  plots for anthracene derivatives on column 5. Details as in Fig. 6. ●:  $k' = 0.27$ ; □:  $k' = 0.97$ ; ▲:  $k' = 1.28$ ; ○:  $k' = 2.11$ ; ★:  $k' = 3.77$ .

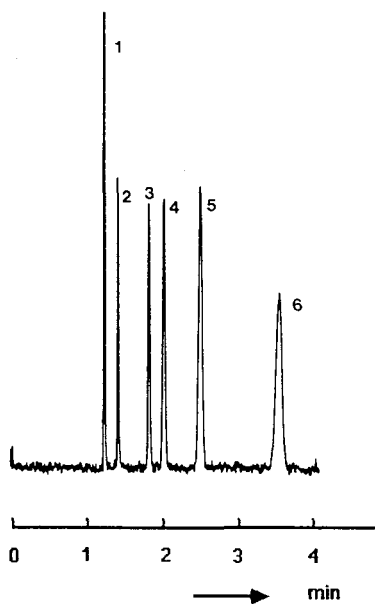


Fig. 9. Chromatogram of a test mixture of anthracene derivatives on column 8b, 67 cm  $\times$  5.4  $\mu$ m I.D. fused silica, coated with PS-255. Film thickness, 0.02  $\mu$ m; pressure, 50 bar; linear velocity, 9.2 mm  $s^{-1}$ . Other experimental conditions and peaks as in Fig. 5.

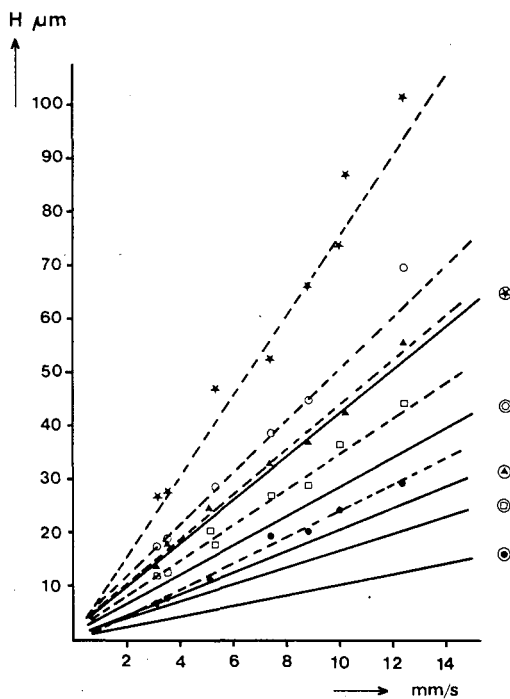


Fig. 10. Theoretical and experimental  $H$  versus  $v$  plots for anthracene derivatives on column 8b. Details as in Fig. 6.  $\bullet$ :  $k' = 0.18$ ;  $\square$ :  $k' = 0.51$ ;  $\blacktriangle$ :  $k' = 0.68$ ;  $\circ$ :  $k' = 1.08$ ;  $\star$ :  $k' = 1.96$ .



about 30% higher values. The method of choice, of course, would be the experimental evaluation of  $D_m$  values, *e.g.*, based on the Aris–Taylor equation as described by Huber and van Vught<sup>27</sup>. In fact, the  $H$  measurements of the unretained solute constitute such a determination in rudimentary form. Unfortunately, the virtual coincidence of the calculated and experimental values for anthranilic acid does not support the assumption of higher values of  $D_m$ . As a rough estimate of  $D_s$  is inserted for all solutes, inaccuracies in these values are very large. The observed deviation, however, cannot be explained by these inaccuracies as the term containing  $D_s$  in the expression for the plate height constitutes less than 10% of the total  $H$  value.

As for the secondary flow effect, calculation according to the work of Tijssen<sup>28</sup> shows that this effect will not exert any significant influence with the narrow tubes used here. At present, therefore, one has to conclude that the 30% deviation between the theoretical and experimental  $H$  values remains unexplained.

The data for the analytically more interesting experiments with 10- $\mu\text{m}$  I.D. columns show a similar deviation, although of smaller magnitude. The experimental curves for the unretained solute are slightly lifted upward, which may indicate the onset of the influence of external volume broadening effects. However, this would hardly affect the  $H$  values for more retained solutes.

According to the analysis by Knox and Gilbert<sup>1</sup>, 10- $\mu\text{m}$  I.D. columns would be preferable to packed columns when plate numbers,  $N$ , in excess of 30 000 are required. Fig. 7 illustrates this. Although the  $N$  value is only 4000 for component 5 ( $k' = 2.1$ ), the retention time and pressure are very favourable. Therefore, the operation of a similar column with, *e.g.*, five times this length at the same linear velocity would indeed constitute a very good performance.

Columns of 5- $\mu\text{m}$  I.D. are even more attractive from the point of view of application. In the chromatogram in Fig. 9, peak 5 has 16 800 plates, generated with  $t_0 = 73$  s. A few of these short columns in series or one 2-m long, would generate over 50 000 plates in a few minutes. The comparison of the experimental and calculated values for  $H$  gives completely different results, the experimental values being 1.5–2.5 times higher than expected. The deviation is more severe for the less retained solutes. It is noteworthy that the peaks are slightly fronting on this column (8b), resulting in peak asymmetries with  $A$  values from 0.95 to 0.77 for all solutes. With column 7 (1 m  $\times$  5.0  $\mu\text{m}$  I.D.), the peaks were symmetrical, which leads to a higher efficiency. Plate numbers of 250 000 ( $k' = 0.2$ ) and 58 800 ( $k' = 2.6$ ) were obtained at a linear velocity of 3 mm/s, which is about six times the optimal linear velocity. However, with this column the experimental  $H$  values are about 30% higher than expected on the basis of theory.

Although at present we are not in the position to account fully for these deviations, we believe that the following effects play a role:

(i) External peak broadening, especially important for the less retained compounds. This would explain the decrease in the relative deviation at increased retention.

(ii) Stationary phase overload. This, to our knowledge, is the only mechanism that explains the fronting of peaks. For better analytical utility, the layer thickness should be increased by a factor of 4–10, allowing for higher mass loadability.

(iii) Possibly non-uniformity of the stationary layer also contributes to the high  $H$  values.

Although these results still leave numerous questions open, we believe that the

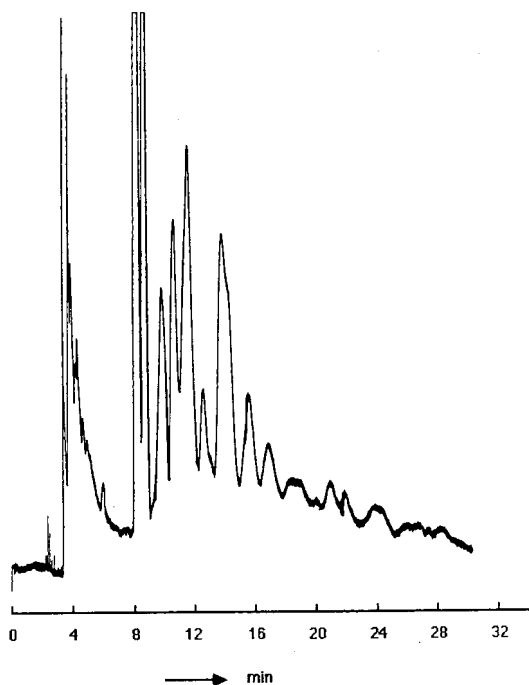


Fig. 11. Chromatogram of a coal tar extract on column 5, 101 cm  $\times$  10.1  $\mu$ m I.D. fused silica, coated with 0.08  $\mu$ m PS-255. Mobile phase, acetonitrile-water (40:60, v/v); pressure, 15 bar; linear velocity, 5.6 mm s<sup>-1</sup>;  $\lambda_{\text{ex}}$  = 325 nm;  $\lambda_{\text{em}}$   $\geq$  385 nm.

successful demonstration of OTLC performance, close to theoretical predictions (*i.e.*, generally within a factor of 1.5–2), is an important step towards the development of analytically useful OTLC systems. The immobilization of silicones appears to be a viable route towards such systems.

An example of the high separation power of a 10- $\mu$ m I.D. column is given in Fig. 11, showing the separation of polyaromatic hydrocarbons in a tar extract.

#### ACKNOWLEDGEMENT

This work was supported by Pye Unicam Ltd., Cambridge, U.K.

#### REFERENCES

- 1 J. H. Knox and M. T. Gilbert, *J. Chromatogr.*, 186 (1979) 405.
- 2 J. H. Knox, *J. Chromatogr. Sci.*, 18 (1980) 453.
- 3 H. Poppe, presented at the 9th International Symposium on Column Liquid Chromatography, Edinburgh, July 1–5, 1985.
- 4 J. W. Jorgenson and E. J. Guthrie, *J. Chromatogr.*, 255 (1983) 335.
- 5 H. P. M. van Vliet and H. Poppe, *J. Chromatogr.*, 346 (1985) 149.
- 6 S. Folestad, L. Johnson, B. Josefsson and B. Galle, *Anal. Chem.*, 54 (1982) 925.
- 7 S. Folestad, B. Josefsson and B. Galle, *J. Chromatogr. Sci.*, 23 (1985) 273.
- 8 E. J. Guthrie and J. W. Jorgenson, *Anal. Chem.*, 56 (1984) 483.
- 9 F. J. Yang, *J. High Resolut. Chromatogr. Chromatogr. Commun.*, 4 (1981) 83.

- 10 V. L. McGuffin and M. Novotny, *Anal. Chem.*, 55 (1983) 580.
- 11 A. Farbrot, S. Folestad and M. Larsson, *J. High Resolut. Chromatogr. Chromatogr. Commun.*, 9 (1986) 117.
- 12 S. Folestad, B. Josefsson and M. Larsson, *J. Chromatogr.*, 391 (1987) 347.
- 13 S. Folestad and M. Larsson, *J. Chromatogr.*, 394 (1987) 455.
- 14 O. van Berkel, H. Poppe and J. C. Kraak, *Chromatographia*, 24 (1987) 739.
- 15 K. Grob and G. Grob, *J. High Resolut. Chromatogr. Chromatogr. Commun.*, 6 (1983) 133.
- 16 P. P. H. Tock, G. Stegeman, R. Peerboom, H. Poppe, J. C. Kraak and K. K. Unger, *Chromatographia*, 24 (1987) 617.
- 17 S. Bretsznajder, *Prediction of Transport and Other Physical Properties of Fluids*, Pergamon Press, Oxford, 1971, pp. 33–39 and 358–383.
- 18 K. D. Bartle, B. W. Wright and M. L. Lee, *Chromatographia*, 14 (1981) 387.
- 19 B. W. Wright, P. A. Peadar, M. L. Lee and T. J. Stark, *J. Chromatogr.*, 248 (1982) 17.
- 20 K. Markides, B. J. Tarbet, C. L. Woolley, C. M. Schregenberger, J. S. Bradshaw and M. L. Lee, *J. High Resolut. Chromatogr. Chromatogr. Commun.*, 8 (1985) 378.
- 21 C. L. Woolley, R. C. Kong, B. E. Richter and M. L. Lee, *J. High Resolut. Chromatogr. Chromatogr. Commun.*, 9 (1985) 329.
- 22 C. P. M. Schutjes, E. A. Vermeer and C. A. Cramers, *J. Chromatogr.*, 279 (1983) 49.
- 23 R. C. Kong, S. M. Fields, W. P. Jackson and M. L. Lee, *J. Chromatogr.*, 289 (1984) 105.
- 24 T. Wännman, L. Blomberg and S. Schmidt, *J. High Resolut. Chromatogr. Chromatogr. Commun.*, 8 (1985) 32.
- 25 K. Janák, V. Kahle, K. Tesarik and M. Morká, *J. High Resolut. Chromatogr. Chromatogr. Commun.*, 8 (1985) 843.
- 26 L. R. Snyder and P. E. Antle, *LC Mag.*, 3 (1985) 98.
- 27 J. F. K. Huber and G. van Vught, *Ber. Bunsenges. Phys. Chem.*, 69 (1965) 821.
- 28 R. Tijssen, *Ph.D. Thesis*, Technical University Delft, Delft, 1979.



CHROMSYMP. 1666

## PREDICTION OF THE HIGH-PERFORMANCE LIQUID CHROMATOGRAPHIC RETENTION BEHAVIOUR OF SOME BENZODIAZEPINE DERIVATIVES BY THIN-LAYER CHROMATOGRAPHY

KLÁRA VALKÓ\*

*Central Research Institute for Chemistry, Hungarian Academy of Sciences, P.O. Box 17, H-1525 Budapest (Hungary)*

SAROLTA OLAJOS

*National Institute for Nervous and Mental Diseases, Laboratory of Pharmacokinetics, Budapest (Hungary)*  
and

TIBOR CSERHÁTI

*Central Research Institute for Chemistry, Hungarian Academy of Sciences, P.O. Box 17, H-1525 Budapest (Hungary)*

---

### SUMMARY

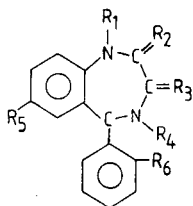
The reversed-phase retention behaviour of eighteen benzodiazepine derivatives was studied using high-performance liquid chromatography (HPLC) and thin-layer chromatography (TLC). In each instance the retention decreased with increasing concentration of the organic mobile phase in the eluent, that is, no anomalous effect was observed. In reversed-phase TLC the  $R_M$  value of benzodiazepine derivatives depended linearly on the organic phase concentration and logarithmically on the buffer concentration in the eluent. A highly significant correlation was found between the HPLC  $\log k_0$  value and the reversed-phase TLC parameters, suggesting that TLC can be used for predicting the HPLC retention behaviour of benzodiazepine derivatives. As the TLC parameters explained about 75% of the total variance, the predictive power of TLC is limited.

---

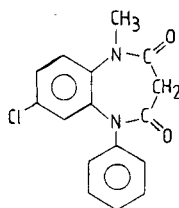
### INTRODUCTION

Benzodiazepine derivatives (BZDs) have found growing acceptance and application in the modern therapeutic practice<sup>1</sup>. BZDs are of considerable importance, having hypnotic, tranquillizing and anticonvulsant properties. As the range of BZDs available has expanded rapidly over the last 10 years, many chromatographic methods have been developed for their separation and identification. The early separations were based on adsorption thin-layer chromatography<sup>2,3</sup> (TLC) or pH-gradient TLC<sup>4</sup>. Earlier high-performance liquid chromatographic (HPLC) methods have been reviewed<sup>5</sup>. Both adsorption<sup>6</sup> and reversed-phase methods<sup>7</sup> have been used in the HPLC separation of BZDs, and gas chromatography (GC) has also been frequently applied<sup>8,9</sup>. The performances of the various chromatographic methods (TLC, GC and HPLC) have been compared<sup>10</sup>.

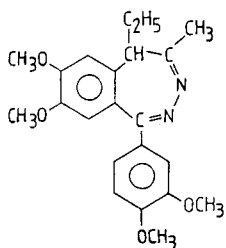
TABLE I  
STRUCTURES OF BENZODIAZEPINE DERIVATIVES



Compound	Common name	$R_1$	$R_2$	$R_3$	$R_4$	$R_5$	$R_6$
1	7-Aminonitrazepam	H	=O	H	H	NH <sub>2</sub>	H
2	Bromazepam	H	=O	H	H	Br	<sup>a</sup>
3	Uxepam	CH <sub>3</sub>	=O	H	CONH <sub>2</sub>	Cl	H
4	Oxazepam	H	=O	OH	H	H	H
5	Lorazepam	H	=O	H	H	Cl	Cl
6	Nitrazepam	H	=O	H	H	NO <sub>2</sub>	H
7	Clonazepam	H	=O	H	H	NO <sub>2</sub>	Cl
8	Chlordiazepoxide	H	NHCH <sub>3</sub>	H	O	Cl	H
9	Alprazolam	R <sub>1</sub> C(CH <sub>3</sub> )=NN=R <sub>2</sub>		H	H	Cl	H
10	Desmethyldiazepam	H	=O	H	H	Cl	H
11	Flunitrazepam	CH <sub>3</sub>	=O	H	H	NO <sub>2</sub>	F
12	Clorazepat	H	(OH) <sub>2</sub>	COOH	H	Cl	H
13	Diazepam	CH <sub>3</sub>	=O	H	H	Cl	H
14	Midazolam	R <sub>1</sub> C(CH <sub>3</sub> )=NCH <sub>2</sub> R <sub>2</sub>		H	H	Cl	F
15	Medazepam	CH <sub>3</sub>	H	H	H	Cl	H
16	Prazepam	CH <sub>2</sub> -cP <sup>b</sup>	=O	H	H	Cl	H



17 Clobazam



18 Tofisopam

<sup>a</sup> 2-Pyridinyl instead of phenyl group.

<sup>b</sup> cP = cyclopropyl.

The biological activity of a molecule is controlled by many factors, one of the most important being its lipophilicity, because penetration of the membranes of target organisms is governed by molecular lipophilicity<sup>11,12</sup>. Lipophilicity can be determined by the traditional method of partition between water and *n*-octanol<sup>13</sup>, by HPLC<sup>14,15</sup> and by reversed-phase TLC (RP-TLC)<sup>16</sup>. The use of GC methods for determining lipophilicity has its limitations<sup>17,18</sup> and the results have sometimes been contradictory<sup>19</sup>. Chromatographic methods have some advantages: they are rapid and relatively simple, require only small amount of the compounds and the compounds need not to be very pure. When a compound contains one or more dissociable polar substituents, the pH of the eluent<sup>20,21</sup> and the ionic strength<sup>22–24</sup> modify the lipophilicity. As chromatographic retention data are used extensively in quantitative structure–activity relationship (QSAR) studies<sup>25</sup>, comparison of the performances of various chromatographic techniques to determine lipophilicity is of great practical and theoretical importance.

The objectives of this work were to determine the lipophilicity of some benzodiazepine derivatives, to compare the lipophilicity values determined by HPLC and RP-TLC and to test the predictive power of RP-TLC for the HPLC retention behaviour of BZDs<sup>26</sup>.

#### EXPERIMENTAL

The structures of the BZDs are given in Table I. The compounds were purchased from Hoffman-La Roche (Basle, Switzerland) (compounds 1, 2, 11 and 14), Gedeon Richter (Budapest, Hungary) (compounds 3, 4, 6, 10, 13 and 15), Wyeth Laboratories (Princeton, NJ, U.S.A.) (compound 5), VEB Arzneimittelwerk (Jena, G.D.R.) (compound 7), POLFA Pharmaceutical Works (Yelenia Gora, Poland) (compound 8), Upjohn Pharmaceutical Works (Kalamazoo, MI, U.S.A.) (compound 9), Mack Chemische Pharmazeutische Fabrik (Illertissen, F.R.G.) (compound 12), Gödecke (Augsburg, F.R.G.) (compound 16), Hoechst (Frankfurt, F.R.G.) (compound 17) and Egis Pharmaceutical Works, (Budapest, Hungary) (compound 18).

The HPLC system consisted of a Model 750 pump (Micromeritics, Norcross, GA, U.S.A.), Model OE-308 20- $\mu$ l injector (Labor-MIM, Budapest, Hungary), a LiChrosorb RP-C18 column (250  $\times$  4.6 mm I.D.) (Merck, Darmstadt, F.R.G.), a Model OE-308 variable-wavelength UV detector (Labor-MIM and a Type OH-850 recorder (Radelkis, Budapest, Hungary). The separations were carried out at room temperature, with detection at 230 nm. The compounds were dissolved in methanol to give a 1 mg/ml stock solution, which was then diluted with the eluent in a 1:19 (v/v) ratio. The dead volume was determined with 0.5 mM sodium nitrate solution. The retention times were determined with acetonitrile–0.06 M KH<sub>2</sub>PO<sub>4</sub> (pH 4.8) eluent mixtures. The acetonitrile concentration was varied from 30 to 70 vol.-% in steps of 5%. The retention parameters of the BZDs were also determined in 0.15 M Sørensen buffer<sup>27</sup> (pH 7.4) at 40 and 50 vol.-% acetonitrile concentrations. Five independent determinations were performed with each eluent system.

The log  $k'$  values, measured with KH<sub>2</sub>PO<sub>4</sub> buffer, were extrapolated to zero acetonitrile concentration separately for each BZD:

$$\log k' = \log k_0 + b \cdot C \quad (1)$$

where  $\log k'$  is the actual  $\log k'$  value of a BZD determined at  $C$  vol.-% acetonitrile concentration,  $\log k_0$  is the  $\log k'$  value of a compound extrapolated to zero acetonitrile concentration,  $b$  is the decrease in the  $\log k'$  value caused by a 1% increase in the acetonitrile concentration and  $C$  (vol.-%) is the acetonitrile concentration.

For reversed-phase TLC at pH 4.8, Silcoflat F<sub>254</sub> plates (Labor-MIM) were impregnated with paraffin oil, as previously described<sup>28</sup>. The stock solution for the HPLC experiments was applied; 3  $\mu$ l of each solution were spotted on the plates. The eluent contained from 0 to 32.5 vol.-% of acetonitrile in steps of 2.5% and 6, 12, 30, 60 and 90 mM KH<sub>2</sub>PO<sub>4</sub> solution. After development, the plates were dried at 105°C and the BZDs were detected by their UV absorption spectra. As it was previously established that the mobility of various buffers in RP-TLC may deviate from that of the eluent<sup>29</sup>, the phosphate front was detected by use of the ammonium molybdate-tin(II)chloride reagent<sup>30</sup>. All experiments were performed in quadruplicate. The  $R_M$  values were calculated separately for each individual spot and each eluent. It was assumed that the buffer and acetonitrile concentrations of the eluent may simultaneously influence the  $R_M$  value. Moreover, the exact type of correlation (linear or logarithmic) between independent (acetonitrile and buffer concentrations) and dependent ( $R_M$  value) variables was not previously established. We used stepwise regression analysis to select the independent variables influencing significantly the  $R_M$  value<sup>31</sup>. The  $R_M$  values were taken as dependent variables and the linear and logarithmic forms of acetonitrile and buffer concentrations (a total of four variables) as independent variables.

The significance level of accepted variables was set at 95%. This calculation allows the separation and determination of the relative effects of the acetonitrile and buffer concentrations on the retention behaviour of the BZDs, which in our case cannot be determined experimentally.

To study the effect of various organic modifiers on the RP-TLC retention of BZDs, their  $R_M$  values were determined at 40 and 50 vol.-% acetonitrile and methanol concentrations, the aqueous phase being Sørensen buffer (pH 7.4).

To assess the predictive power of RP-TLC for HPLC, two different methods were applied. The HPLC retention parameters of eqn. 1. were correlated with the results of the stepwise regression analysis described above. The  $\log k_0$  and slope ( $b$ ) values were separately taken as dependent variables. The  $R_{M0}$  value and the regression coefficients of the independent variables significantly influencing the RP-TLC retention of BZDs were taken as independent variables. Referring to the previous considerations, their linear, quadratic and logarithmic (if mathematically possible) forms were included in the calculations. The stepwise regression analysis was applied in this case under the same conditions as before.

The retention data obtained in Sørensen buffer (two HPLC and four RP-TLC retention parameters) were compared by principal component analysis (PCA)<sup>32</sup>. The data matrix consisted of the chromatographic parameters of the BZDs. The sum of variance explained was set at 99%. The non-linear map of PCA loadings and variables was also calculated<sup>33</sup>.

## RESULTS AND DISCUSSION

The dependence of the retention of some BZDs on the acetonitrile concentration in the eluent is shown in Fig. 1. In each instance the correlation follows the



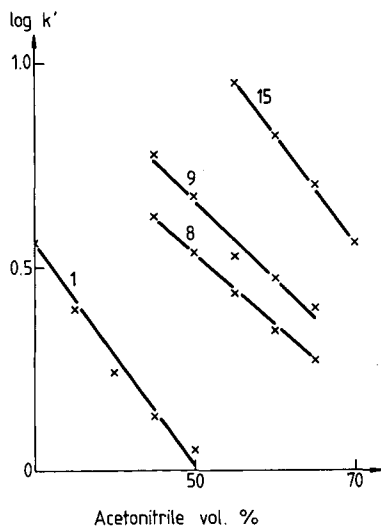


Fig. 1. Dependence of the HPLC retention of BZDs on the acetonitrile concentration in the eluent. Numbers refer BZDs in Table I.

general rule that the retention decreases logarithmically with increasing concentration of organic modifier. The parameters of eqn. 1 are given in Table II. The equation agrees well with the experimental data, the significance level in each instance being

TABLE II

HIGH-PERFORMANCE LIQUID CHROMATOGRAPHIC RETENTION CHARACTERISTICS OF BENZODIAZEPINE DERIVATIVES: PARAMETERS OF EQN. 1

Numbers refer to BZDs in Table I.

Compound	$\text{Log } k_o$		Slope $\cdot 10^3$	
	Mean	Standard deviation	Mean	Standard deviation
1	1.186	0.103	-23.07	2.41
2	1.231	0.038	-16.79	0.83
3	1.807	0.022	-29.10	0.47
4	1.802	0.090	-28.84	1.97
5	1.746	0.038	-27.00	0.76
6	1.479	0.020	-20.76	0.37
7	1.754	0.103	-25.47	1.95
8	1.448	0.042	-18.31	0.75
9	1.628	0.106	-19.26	1.91
10	1.699	0.032	-22.43	0.58
11	1.806	0.026	-23.97	0.43
12	1.618	0.054	-20.95	0.90
13	1.849	0.042	-22.01	0.70
14	1.514	0.056	-20.41	2.79
15	2.376	0.085	-25.86	1.30
16	2.328	0.094	-26.59	1.45
17	1.736	0.035	-22.64	0.59
18	1.799	0.059	-22.11	0.94

higher than 99.9% (the lowest regression coefficient was 0.9860). This result indicates that the linear approximation describes well the dependence of the  $\log k'$  values of the BZDs on the acetonitrile concentration in the concentration range applied.

The coefficient of variation between the parallel determinations in RP-TLC never exceeded 6%. The mobility of the phosphate front in the RP-TLC experiments was near that of the eluent; the mean  $R_F$  value was 0.95. As the  $R_F$  value did not change systematically with either the acetonitrile or buffer concentration, we did not correct our retention data for the different mobilities of the phosphate front<sup>34</sup>.

The dependence of the  $R_M$  value of some BZDs on the buffer concentration in the eluent is shown in Fig. 2. The data show that the dependence is markedly non-linear. The change is high at lower buffer concentration range and levels out at higher concentrations. This phenomenon can be explained by the assumption that the paraffin oil does not cover the active adsorption centers of the silica surface entirely. The free silanol groups also influence the retention; in our case they increase it. As the buffer is in a more or less dissociated form, its ions may be adsorbed on the silanol groups not covered by the impregnating agent. This adsorption results in a lower retention capacity.

The concentration dependence is of saturation character, because the number of active silanol groups is limited and decreases non-linearly with increasing concentration of free ions<sup>35</sup>. We are well aware that our data can also be explained by the salting-in effect<sup>36</sup>. However, taking into consideration the highly lipophilic character of BZDs this is not probable.

The parameters of the equations describing the dependence of the  $R_M$  values of BZDs on the acetonitrile and buffer concentrations are given in Table III. The blank entries in Table III are due to the fact that with compounds 1, 6, 7, 9, 11, 13 and 18

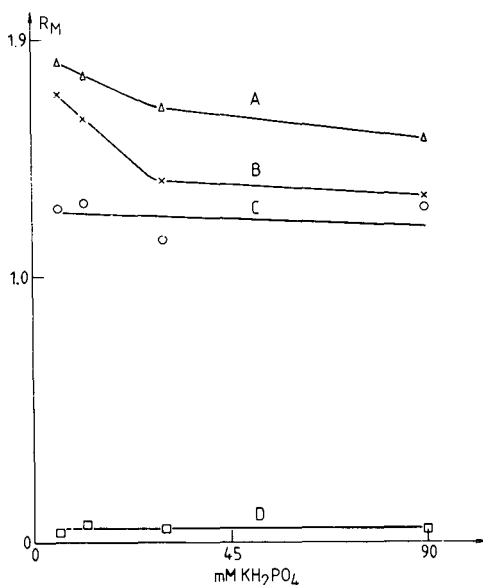


Fig. 2. Dependence of  $R_M$  values of some BZDs on the  $\text{KH}_2\text{PO}_4$  concentration in the eluent at 25 vol.-% acetonitrile concentration. A = medazepam (compound 15); B = midazolam (compound 14); C = diazepam (compound 13); D = 7-aminonitrazepam (compound 1).

only the acetonitrile concentration influenced significantly the retention of BZDs. Therefore, the beta weights,  $b_2$ , and the standard deviation of the  $b_2$  value are zero. In these instances, the beta weights of  $b_1$  are equal to  $r^2$ . The equations fit the experimental data well; the significance level of the correlation in each instance was over 99.9% (see  $F$  values). The change in the independent variables accounts for about 91.75 and 98.40% of the change in the  $R_M$  value (see  $r^2$  values). Except for compound 1, which is a metabolite, each compound has considerable lipophilicity (see  $R_{M0}$

TABLE III

DEPENDENCE OF  $R_M$  VALUES OF BENZODIAZEPINE DERIVATIVES ON THE ACETONITRILE ( $C_1$ ) AND BUFFER ( $C_2$ ) CONCENTRATIONS IN THE ELUENT

Results of stepwise regression analysis.  $R_M = R_{M0} + b_1C_1 + b_2\log C_2$ . Numbers refer to BZDs in Table I.

Parameter	Compound					
	1	2	3	4	5	6
Sample number	23	20	18	20	18	19
$R_{M0}$	1.41	2.68	2.85	2.68	3.16	2.30
$s$	0.13	0.08	0.08	0.09	0.08	0.07
$b_1$	-5.30	-7.32	-7.37	-6.70	-7.92	-6.18
$s$	0.28	0.34	0.46	0.42	0.51	0.24
Beta weight		-1.08	-1.08	-1.09	-1.15	
$b_2$		-15.38	-12.94	-16.25	-23.38	
$s$		5.67	5.92	6.99	6.55	
Beta weight		-0.14	-0.15	-0.16	-0.26	
$r^2$	0.9451	0.9708	0.9666	0.9596	0.9599	0.9741
$F$		378.5	217.1	202.0	179.7	
Sample number	7	8	9	10	11	12
$R_{M0}$	2.51	3.28	3.46	3.45	2.83	3.26
$s$	0.08	0.07	0.09	0.08	0.09	0.06
$b_1$	-6.67	-8.19	-8.89	-8.74	-7.53	-8.19
$s$	0.30	0.44	0.45	0.51	0.40	0.39
Beta weight		-1.11		-1.08		-1.08
$b_2$		-18.01		-15.10		-13.33
$s$		5.64		6.55		5.01
Beta weight		-0.19		-0.15		-0.14
$r^2$	0.9675	0.9740	0.9625	0.9709	0.9559	0.9806
$F$		281.0		250.2		379.1
Sample number	13	14	15	16	17	18
$R_{M0}$	3.36	4.82	4.27	4.10	3.25	3.62
$s$	0.09	0.08	0.10	0.11	0.07	0.10
$b_1$	-8.44	-11.21	-8.67	-9.80	-8.19	-9.69
$s$	0.45	0.68	0.73	0.85	0.34	0.50
Beta weight		-1.26	-1.24		-1.08	
$b_2$		-38.94	-35.08		-13.82	
$s$		6.48	8.00		5.01	
Beta weight		-0.46	-0.46		-0.12	
$r^2$	0.9587	0.9656	0.9319	0.9175	0.9840	0.9613
$F$		168.6	88.9		490.9	

values), which makes it probable that they bind preferably to the lipophilic membrane substructures and/or to the hydrophobic core of proteins. The logarithmic form of the acetonitrile and the linear form of the buffer concentration do not influence the retention of BZDs significantly, *i.e.*, the lipophilicity depends linearly on the concentration of the organic modifier and, with some derivatives, logarithmically on the buffer concentration. The increase in both the acetonitrile and buffer concentration decreases the retention (see  $b_1$  and  $b_2$  values). The fact that the retention of some derivatives did not depend significantly on the buffer concentration in the eluent does not prove that the retention of these compounds is not influenced by the buffer concentration. This finding only indicates that in these instances the impact of the buffer concentration on the retention is probably low. Therefore, it is below the detection limit of our method. The relative importance of the two independent variables differs considerably (see beta weights). The impact of the acetonitrile concentration is 3–9 times higher than that of the buffer concentration. This result indicates that in the determination of the retention of BZDs the buffer concentration is of secondary importance.

The parameters of the equation describing the dependence of the log  $k_0$  values on the RP-TLC characteristics of BZDs are given in Table IV. The changes in the independent variables selected by the stepwise regression analysis account for *ca.* 75% of the variance of the log  $k_0$  value (see  $r^2$  value). The calculated  $F$  value (see Table IV) is higher than the tabulated  $F$  value corresponding to the 99.9% significance level ( $F = 9.34$ ), that is, the equation is highly significant.

Each RP-TLC parameter showed a significant correlation with the HPLC log  $k_0$  value. However, their relative impacts were different. The beta weights show that the  $R_{M0}$  value has the highest and the buffer sensitivity the lowest impact on the log  $k_0$  value. This is understandable because the  $R_{M0}$  and log  $k_0$  values are theoretically similar parameters in RP-TLC and HPLC. As the correlation between the RP-TLC and HPLC retention data is highly significant, it can be assumed that the HPLC retention can be predicted on the basis of RP-TLC measurements. However, from a practical point of view, the fit of the equation (the RP-TLC parameters explain *ca.* 75% of the variance) is not sufficient to predict exactly the HPLC retention. We conclude that with BZDs the RP-TLC retention data are of limited value for predicting HPLC retention behaviour. This observation is supported by the finding that there was no significant correlation between the slope value of eqn. 1 and the RP-TLC parameters. This phenomenon can be explained by the assumption that the coverages

TABLE IV

DEPENDENCE OF THE LOG  $k_0$  VALUES OF BENZODIAZEPINE DERIVATIVES ON THEIR RP-TLC PARAMETERS

Results of stepwise regression analysis. Log  $k_0 = a + b_3 R_{M0} + b_4 b_1 + b_5 b_2$ , where  $R_{M0}$ ,  $b_1$  and  $b_2$  are the parameters of the equation in Table III.  $n = 18$ ;  $F = 13.94$ ;  $a = 2.00$ ;  $r^2 = 0.7492$ .

Parameter	$R_{M0}$	$b_1 \cdot 10$	$b_2 \cdot 10^2$
$b$	1.22	4.93	1.74
$s$	0.21	1.07	0.45
Beta weight	3.11	2.28	0.71

of the silica surface are different in RP-TLC and HPLC, resulting in different responses of the chromatographic system to changes in the organic modifier concentration.

The data matrix for the PCA is shown in Table V. The first PCA component contains most of the variance (eigenvalue 5.11; variance explained 85.24%). This finding indicates a strong relationship between the reversed-phase chromatographic systems studied. This result is in accordance with that of stepwise regression analysis, *i.e.*, the RP-TLC and HPLC retention mechanisms are similar but not identical. The second PCA component (eigenvalue 0.60; variance explained 9.92%) is of negligible importance.

The  $F_1$  and  $F_2$  axes of the two-dimensional non-linear maps do not have any concrete physical or chemical meanings. They only show the relative (projected in two dimensions) distances between the BZDs chromatographic systems in multi-dimensional space. The BZDs did not form separate groups on the two-dimensional non-linear map of PCA variables (Fig. 3). This finding indicates that the various substituents influence the retention to similar extents, *i.e.*, that there is no single substituent that governs retention. The six chromatographic systems on the two-dimensional non-linear map of PCA loadings form two distinct groups, one for the HPLC and the other for the RP-TLC systems (Fig. 4). This result supports our previous conclusions that the two methods may produce slightly different but correlated retention parameters.

TABLE V

## RETENTION PARAMETERS OF BENZODIAZEPINE DERIVATIVES AT pH 7.4

Numbers refer to BZDs in Table I. I =  $\log k'$  at 40 vol.-% acetonitrile concentration; II =  $\log k'$  at 50 vol.-% acetonitrile concentration; III =  $R_M$  value at 40 vol.-% acetonitrile concentration; IV =  $R_M$  value at 50 vol.-% acetonitrile concentration; V =  $R_M$  value at 40 vol.-% methanol concentration; VI =  $R_M$  value at 50 vol.-% methanol concentration.

Compound	No. of parameter					
	I	II	III	IV	V	VI
1	0.222	0.035	-0.50	-0.58	-0.28	-0.40
2	0.581	0.301	-0.35	-0.47	-0.11	-0.19
3	0.653	0.216	-0.46	-0.56	-0.21	-0.41
4	0.669	0.390	-0.37	-0.53	-0.09	-0.31
5	0.734	0.368	-0.29	-0.41	-0.02	-0.23
6	0.734	0.368	-0.20	-0.41	0.15	-0.15
7	0.761	0.426	-0.11	-0.35	0.21	-0.11
8	0.778	0.442	-0.33	-0.45	-0.10	-0.27
9	0.928	0.558	-0.24	-0.37	-0.04	-0.24
10	0.932	0.561	-0.15	-0.37	0.18	-0.14
11	0.942	0.592	-0.12	-0.34	0.19	-0.10
12	0.885	0.515	-0.14	-0.35	0.16	-0.16
13	1.151	0.772	-0.09	-0.32	0.22	-0.08
14	1.431	1.014	-0.17	-0.37	0.05	-0.13
15	1.645	1.149	-0.10	-0.27	0.00	0.23
16	1.446	0.970	0.16	-0.16	0.59	0.09
17	0.934	0.584	-0.19	-0.40	-0.02	-0.25
18	1.073	0.661	-0.22	-0.40	-0.10	-0.29

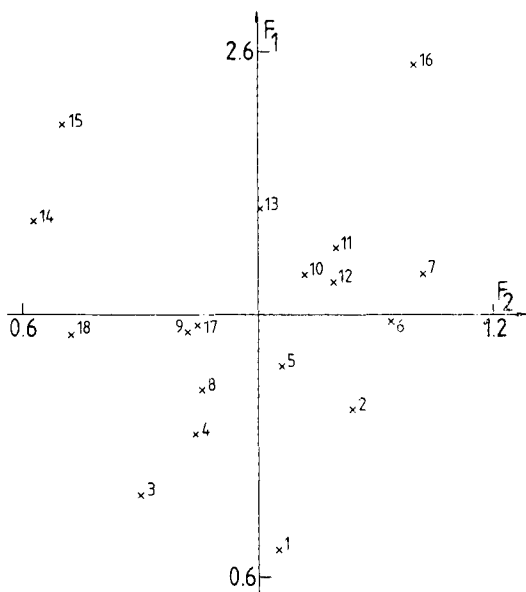


Fig. 3. Two-dimensional non-linear map of principal component variables. Number of iterations, 49; maximum error,  $9.46 \cdot 10^{-6}$ . Numbers refer to BZDs in Table I.

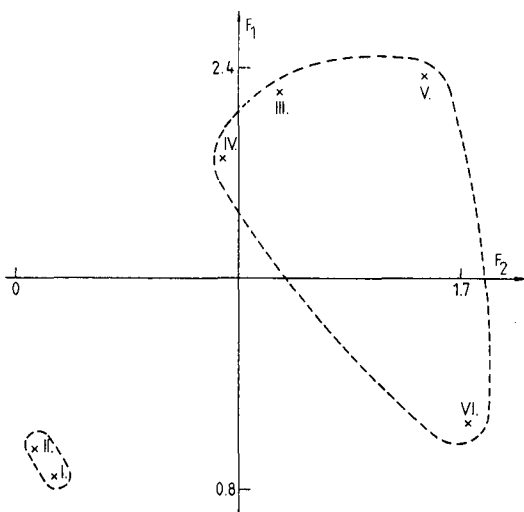


Fig. 4. Two-dimensional non-linear map of PCA loadings. Number of iterations, 142; maximum error,  $3.73 \cdot 10^{-5}$ . Numbers refer to chromatographic systems in Table IV.

## REFERENCES

- 1 W. E. Müller, *Drugs Today*, 24 (1988) 649.
- 2 H. Schütz, *J. Anal. Toxicol.*, 2 (1978) 147.
- 3 I. Wouters, E. Roets and J. Hoogmartens, *J. Chromatogr.*, 179 (1979) 381.
- 4 E. Stahl and J. Müller, *J. Chromatogr.*, 209 (1981) 484.
- 5 A. C. Mehta, *Talanta*, 31 (1984) 1.
- 6 I. Fellegvári, K. Valkó, M. Simonyi, P. Sándor and T. Láng, in H. Kalász and L. S. Ettre (Editors), *Chromatography '87*, Akadémiai Kiadó, Budapest, 1988, p. 193.
- 7 R. Gill, B. Law and J. P. Gibbs, *J. Chromatogr.*, 356 (1986) 37.
- 8 K. Verebey, D. Jukofsky and J. Mule, *J. Anal. Toxicol.*, 6 (1982) 305.
- 9 C. Drouet-Coassolo, C. Aubert, P. Coassolo and J. P. Cano, *J. Chromatogr.*, 487 (1989) 295.
- 10 M. Chiarotti, N. De Giovanni and A. Fiori, *J. Chromatogr.*, 358 (1986) 169.
- 11 C. Hansch and W. J. Dunn, *J. Pharmacol. Sci.*, 61 (1972) 1.
- 12 C. Hansch and I. M. Clayton, *J. Pharmacol. Sci.*, 62 (1973) 1.
- 13 C. Hansch and S. M. Anderson, *J. Org. Chem.*, 32 (1967) 2583.
- 14 J. M. McCall, *J. Med. Chem.*, 18 (1975) 549.
- 15 K. Valkó, *J. Liq. Chromatogr.*, 7 (1984) 1405.
- 16 C. B. C. Boyle and B. V. Milborrow, *Nature (London)*, 208 (1965) 537.
- 17 K. Bocek, *J. Chromatogr.*, 162 (1979) 209.
- 18 K. Valkó and A. Lopata, *J. Chromatogr.*, 252 (1982) 77.
- 19 É. János, *J. Chromatogr.*, 365 (1986) 117.
- 20 B. Rittich, M. Polster and O. Králik, *J. Chromatogr.*, 197 (1980) 43.
- 21 Gy. Vigh, J. Varga-Puchony, J. Hlavay and E. Papp-Hites, *J. Chromatogr.*, 236 (1982) 51.
- 22 T. Cserhádi, Y. M. Darwish and Gy. Matolcsy, *J. Chromatogr.*, 241 (1982) 223.
- 23 E. Pap and Gy. Vigh, *J. Chromatogr.*, 258 (1983) 49.
- 24 T. Cserhádi, M. Szögyi and L. Györfi, *Chromatographia*, 20 (1985) 253.
- 25 R. Kaliszan, *Quantitative Structure-Chromatographic Retention Relationships*, Wiley, New York, 1987.
- 26 T. Cserhádi and T. Bellay, *Acta Phytopathol. Entomol. Hung.*, 23 (1988) 257.
- 27 S. P. L. Sörensen, *Biochem. Z.*, 21 (1909) 131.
- 28 T. Cserhádi, B. Bordás, E. Fenyvesi and J. Szejtli, *J. Chromatogr.*, 259 (1983) 107.
- 29 T. Cserhádi and J. Gasparic, *J. Chromatogr.*, 394 (1987) 368.
- 30 E. Stahl, *Dünnschichtchromatographie.*, Springer, Berlin, 1962, p. 495.
- 31 H. Mager, *Moderne Regressionsanalyse*, Salle, Sauerlander, Frankfurt am Main, 1982, p. 135.
- 32 K. V. Mardia, J. T. Kent and J. M. Bibby, *Multivariate Analysis*, Academic Press, London, 1979.
- 33 J. Sammon, Jr., *IEEE Trans. Comput.*, C18 (1969) 401.
- 34 T. Cserhádi and M. Szögyi, *J. Liq. Chromatogr.*, 11 (1988) 3067.
- 35 H. Engelhardt and H. Müller, *J. Chromatogr.*, 218 (1981) 395.
- 36 K. E. Bij, Cs. Horváth, W. R. Melander and A. Nahum, *J. Chromatogr.*, 203 (1981) 65.





CHROM. 21 886

## STUDY OF PARTITION MODELS IN REVERSED-PHASE LIQUID CHROMATOGRAPHY BASED ON MEASURED MOBILE PHASE SOLUTE ACTIVITY COEFFICIENTS

WON JO CHEONG and PETER W. CARR\*

*Department of Chemistry, Smith Hall, 207 Pleasant Street, University of Minnesota, Minneapolis, MN 55455 (U.S.A.)*

---

### SUMMARY

Lack of accurate values for solute activity coefficients in aqueous organic solvent mixtures has been an impediment to the development of a detailed model of reversed-phase liquid chromatography (RPLC). In this study we have employed a recently measured set of infinite dilution activity coefficients for the alkylbenzenes (benzene to *n*-butylbenzene) in mixtures of water with four of the more common organic cosolvents in order to explore the mechanism of the retention process in RPLC. The work indicates that the solvophobic theory of reversed-phase chromatography is essentially correct, that is, most of the free energy of transfer arises from processes taking place in the mobile phase. Analysis of relative solute activity coefficients of two solutes in the bonded phase shows that the stationary phase environment is considerably more polar than that of a bulk long chain alkane. This supports the idea that sorbed organic modifier plays a substantial role in establishing the chemistry in the bonded phase domain. The fact that measurements of the activity coefficients of non-polar solutes in methanol-saturated hexadecane are insignificantly different from those in pure hexadecane strongly suggests that the vastly different surface area to volume ratio of bonded and bulk phases is vitally important in bonded-phase RPLC.

---

### INTRODUCTION

The primary purpose of this study was to examine the effect of mobile phase composition on the retention of a series of non-polar solutes and to apply the results to the study of the retention mechanism of reversed-phase liquid chromatography (RPLC).

In this work we choose to study the retention of the alkylbenzenes for many reasons. First we felt that the solute-condensed phase interaction would be simplest with a non-polar solute thereby making data interpretation easier. Secondly the alkylbenzenes can be readily measured with common liquid chromatographic detectors. Finally and most importantly the use of non-polar solutes would circumvent the complexities introduced when solutes interact with underivatized silanol groups which are inevitably present in bonded phases<sup>1,2</sup>.

*The partition model*

The retention of a series of homologous alkylbenzenes was studied and the results were analyzed in terms of three partition-like models of bonded-phase chromatography. The retention mechanism in RPLC has been the subject of a great deal of attention and controversy. Many mechanisms<sup>3-10</sup> have been proposed, but none has been conclusively demonstrated. This is due to the complexity of RPLC with bonded phases and difficulties in obtaining the appropriate experimental data needed to test the proposed mechanisms. It should be noted that most, but certainly not all, studies of RPLC have been rather qualitative. In many studies  $\ln k'$  was correlated with some property of the mobile phase (e.g. its surface tension<sup>8</sup>, or empirical solvent strength parameters (e.g. a solvatochromic property of the solvent<sup>11,12</sup>). In contrast, there have been few attempts to relate observed capacity factors to capacity factors computed from the amount of stationary and mobile phases and fundamental theories involving specific properties of the phases and the probe solutes. The work of Schantz *et al.*<sup>13</sup> is a notable exception to this generalization.

Fundamentally a detailed mechanism of the retention process requires the development of an equation which predicts the free energy of transfer of the solute from the mobile to stationary phase in terms of independently measurable properties. This can be done at many levels of sophistication. In this work we choose to rely upon measurements of as many properties as possible and to minimize the need for estimating unknown parameters.

In the simplest terms retention can be viewed as a distribution of a solute between a mobile and stationary phase. The free energy change for the transfer process can be related to the activity coefficients of the solute in both phases under a given set of conditions (mobile phase, stationary phase, temperature). Technical and fundamental difficulties arise from the fact that the stationary phase in bonded-phase RPLC is not a uniform bulk liquid. Several different definitions of what constitutes the effective stationary phase in RPLC have been proposed<sup>3-6,14-18</sup>.

Some workers have paid particular attention to the interaction of the solute and mobile phase with the hydrophobic surface<sup>6,19-21</sup>. Such models are most appropriately termed adsorption mechanisms. The above cited papers employed Everett's specific definition of the surface activity coefficient<sup>22,23</sup>. In these approaches one deals with an effective surface phase activity coefficient that is represented as the product of two terms. The first of these terms takes into account the contribution of the interfacial tension of the system to the solute chemical potential in the bonded phase. The second term is a more conventional activity coefficient, that is, it is related to the transfer free energy as if the interfacial contribution to the free energy of transfer were zero.

This emphasis on surface-solute and surface-eluent interaction terms can be contrasted with Snyder's view of normal phase liquid chromatography<sup>24</sup>. Snyder assumed that the difference between the surface-eluent and surface-solute interaction is the major driving force for solute retention in normal-phase chromatography and that the mobile phase effects are small compared to stationary phase effects.

In RPLC most models minimize the importance of the solute-surface interaction<sup>3-5,7-9</sup>. In contrast, work which emphasizes the adsorption model considers the surface effect to be a major term<sup>19-21</sup>. Everett's definition of a surface activity coefficient was used and consequently the surface interaction effect was separated

from the other energy terms. Of the many studies of the retention mechanism of RPLC the work of Locke<sup>6</sup> and Lochmuller and Wilder<sup>4</sup> are closely related. Locke<sup>6</sup> based his estimate of a solute's activity coefficient on its solubility in water and was able to demonstrate a linear relationship between the logarithm of this activity coefficient in the mobile phase and the logarithm of the capacity factor.

The study of Schantz *et al.*<sup>13</sup>, who examined the partition model in detail, is very relevant to the present study. These authors compared measured partition coefficients ( $K$ ) for a series of alkylbenzenes between various methanol-water mixtures and bulk phase hexadecane to the net retention volume ( $V_N$ ) of the same solutes on a bonded-phase RPLC column operated at the same mobile phase composition. The ratio of  $K$  to  $V_N$  is completely independent of the solute activity coefficient in the mobile phase. They found that this ratio was not independent of the solute. The difference in the ratio varied by 0.4 ln units from benzene to *n*-butylbenzene. This is unambiguous evidence that the effective activity coefficient of the solute in the bonded phase is not the same as the activity coefficient in bulk hexadecane. If they were identical there could be no variation upon change in solute.

More importantly they observed that the ratio of retention in bulk phase hexadecane to bonded phase octadecane decreased, roughly linearly, by 0.9 ln units as the mobile phase composition varied from pure methanol to about 50% (v/v) methanol. This implies that there is a very substantial differential effect of the mobile phase on the solute activity coefficient in the bonded and bulk phases. This ratio depends upon the amount of both phases. It is evident from their data that the volume of stationary phase will decrease with an increase in the fraction of water in the mobile phase thereby decreasing the bonded phase activity coefficients as water is added to the mobile phase. Martire and his co-workers also showed by direct measurement that the amount of methanol in hexadecane when equilibrated against pure methanol is very small (approximately 0.003 mole of methanol per mole of hexadecane). This seems to be a trivial quantity and ought not alter the activity coefficient of a solute in bulk hexadecane.

## THEORY

The thermodynamic equilibrium constant for a partition model can be written as follows:

$$K_{th} = \frac{X_1^s \gamma_1^s}{X_1^m \gamma_1^m} = 1 \quad (1)$$

where

$$X_1^s = n_1^s/n_2^s \quad (2)$$

$$X_1^m = n_1^m/n_2^m \quad (3)$$

The terms  $X$  and  $\gamma$  denote the mole fraction and the activity coefficient of the solute (subscript 1) in the mobile (m) and stationary (s) phases, respectively. In addition the

terms  $n_1$  designate the number of moles of solute in each phase whereas  $n_2^s$  and  $n_2^m$  represent the total number of moles of stationary phase and mobile phase in the column.

Certainly in the case of liquid-liquid chromatography with two perfectly immiscible fluids the meaning of the number of moles of stationary and mobile phase is quite clear. It is far more ambiguous in bonded-phase chromatography. For example we can certainly disregard the number of moles of silica in the column for all solutes that do not interact with silica. However, it is not clear whether sorbed organic modifier<sup>18</sup> should be counted as part of the stationary phase. If it can be shown that the sorbed organic modifier alters the properties of a solute when it is in the stationary phase then it is reasonable to include it as being part of the total number of moles in the stationary phase. The number of moles of ligand chemically bonded to the support should constitute a minimum estimate of the amount of stationary phase in any simple partition model of bonded-phase RPLC. Thus at this point we feel that it is best to defer a precise definition of what we mean by  $n_2^s$ .

The capacity factor can be defined as follows:

$$k' = n_1^s/n_1^m \quad (4)$$

Combining eqn. 1-4 we obtain

$$k' = (\gamma_1^m/\gamma_1^s) (n_2^s/n_2^m) \quad (5)$$

$$\ln k' = \ln \gamma_1^m - \ln \gamma_1^s + \ln n_2^s - \ln n_2^m \quad (6)$$

We now examine the above equations in terms of those quantities that are measurable. The capacity factor and the solute activity coefficient<sup>25</sup> in the mobile phase can be measured. Assuming that the column void volume is a good measure of the volume of mobile phase in the column the number of moles of the mobile phase in the column can be computed without further approximation as follows:

$$n_2^m = V_m d_m [w_o/M_o + (1 - w_o)/M_w] \quad (7)$$

where  $V_m$  is the void volume of the column,  $d_m$  the density of the mobile phase,  $M_o$  the molecular weight of the organic modifier,  $M_w$  the molecular weight of water,  $w_o$  the weight fraction of organic modifier in the mobile phase, and  $w_w$  the weight fraction of water in the mobile phase. Eqn. 6 can be rewritten as follows:

$$A = \ln k' + \ln (n_2^m/\gamma_1^m) = \ln (n_2^s/\gamma_1^s) \quad (8)$$

In eqn. 8, all of the measurable mobile phase terms are placed on the left and the stationary phase terms on the right. A very important idea is that the parameter  $A$  can be measured and studied as a function of the volume fraction of organic modifier in the mobile phase ( $\varphi$ ). When  $A$  is independent of  $\varphi$  then it must follow, based only on thermodynamics, that  $n_2^s/\gamma_1^s$  will be independent of  $\varphi$ .

In an effort to define what actually constitutes the number of moles of material comprising the stationary phase we will consider three distinct "partition" type models

of the stationary phase. In model I we assume that the stationary phase only consists of the bonded phase ligand. It follows in this case that the number of moles of stationary phase must be independent of  $\varphi$ . The number of moles of stationary phase would also appear to be independent of  $\varphi$  if, beyond some minimum value of  $\varphi$ , the stationary phase were saturated with organic modifier. Thus in model II the stationary phase is assumed to consist, over the range in  $\varphi$  studied, of the bonded ligands and a fixed amount of sorbed modifier. In both of the above models it follows that the solute activity coefficient will not depend on  $\varphi$  since the solute's environment is fixed. A final possibility (model III), which will provide a solute environment that is independent of  $\varphi$ , is based on the idea that active stationary phase, that is the region into which the solute partitions, is comprised of a sorbed multilayer of pure organic modifier. In this model the bonded phase ligands serve only as a substrate onto which the multilayer of modifier sorbs. In model III the amount of stationary phase might vary with  $\varphi$  due to an increase in the number of multilayers but since the solute's environment is fixed one expects, as a first approximation, that the activity coefficient in the multilayer will be independent of  $\varphi$ .

In all of the above models a solute molecule in the stationary phase experiences an environment that is independent of  $\varphi$ . Consequently the stationary phase solute activity coefficient will be independent of  $\varphi$ . For cases I and II we must conclude on purely thermodynamic grounds that when the stationary phase composition is independent of  $\varphi$  the term  $A$  will be independent of  $\varphi$ . This is not true in case III.

Obvious cases II and III cannot hold over the entire range of  $\varphi$  (0–1.0). There must come a point where  $\varphi$  becomes so small that the amount of modifier in the stationary phase (case II) or the number of multilayers (case III) decreases. We will show below that for a variety of mobile phase modifiers and for a series of alkylbenzenes the term  $A$  and therefore  $n_2^s/\gamma_1^s$  does depend on  $\varphi$  but the dependence is weak.

A purely arithmetic examination of eqn. 8 indicates that  $A$  can appear to be independent of  $\varphi$  in two different ways. This will be so when both the solute activity coefficient in the stationary phase and the number of moles of stationary phase are both independent of  $\varphi$ . A second is that both the solute activity coefficient in the stationary phase and the number of moles of stationary phase vary with  $\varphi$  in such a fashion that the measured ratio appears to be independent of  $\varphi$  (see the right-hand side of eqn. 8).

In attempting to differentiate between these two possibilities we will consider the ratio of capacity factors for two similar solutes. Eqn. 5 can be rewritten for solutes 1 and 2 as follows:

$$k'(1) n_2^m/\gamma_1^m(1) = n_2^s/\gamma_1^s(1) \quad (9)$$

$$k'(2) n_2^m/\gamma_1^m(2) = n_1^s/\gamma_1^s(2) \quad (10)$$

Dividing eqn. 10 by 9 we get

$$[k'(2)/k'(1)] [\gamma_1^m(1)/\gamma_1^m(2)] = \gamma_1^s(1)/\gamma_1^s(2) = B_{2/1} \quad (11)$$

In this approach the number of moles of stationary phase drops out. If the left-hand

side of eqn. 11 is independent of  $\phi$  then the ratio ( $B_{2/1}$ ) of the stationary phase activity coefficients of the two solutes must be independent of  $\phi$ . We hypothesize that when the ratio of activity coefficients is independent of  $\phi$  then the individual activity coefficients will also be independent of  $\phi$  or else the two activity coefficients must vary so similarly with  $\phi$  that the ratio appears to be constant. This point will be discussed in more detail later.

## EXPERIMENTAL

### Activity coefficients

The activity coefficients of the alkylbenzenes in aqueous solvents were measured by head space gas chromatography (HSGC)<sup>25</sup>. The background and experimental details can be found in a previous report<sup>26</sup> and other references<sup>27,28</sup>.

### HPLC

Retention data for the methanol–water system<sup>29,30</sup> and the acetonitrile–water system<sup>31</sup> were taken from the literature. The data for the isopropanol–water and tetrahydrofuran–water systems were measured in this laboratory. A Hypersil ODS column (100 × 4.6 mm I.D., 5  $\mu$ m, Hewlett-Packard, Avondale, PA, U.S.A.) was used throughout this study. The column was placed in a water jacket and the temperature was controlled at 25 ± 0.2°C. An Altex pump with a pulse dampener (Model 110AQ, Altex Scientific, Berkeley, CA, U.S.A.) was used to deliver the mobile phase. Samples were injected via a home-made auto-injector by using a Valco air-actuated injector (Model AC6W, Valco Instruments, Houston, TX, U.S.A.) equipped with a 10- $\mu$ l loop. A Hitachi variable-wavelength UV–VIS detector (Model 100-10, NSI/Hitachi Scientific Instruments, Mountain View, CA, U.S.A.) was used to generate the solute elution profiles. All retention times were based on the peak maximum position. The eluent flow-rate was varied from 0.2 to 1.0 ml/min depending on the mobile phase composition. Water was used as the void volume marker<sup>32</sup>.

The capacity factor data for the isopropanol–water and tetrahydrofuran–water systems measured in this study are given in Tables I and II. Some important column characteristics were obtained from the literature<sup>33,34</sup> and are summarized in Table III.

TABLE I

### CAPACITY FACTORS OF ALKYL BENZENES IN ISOPROPANOL–WATER MIXTURES

Measured in a Hypersil ODS column (46 × 100 mm, 5  $\mu$ m) at 25°C with a 10- $\mu$ l sample loop.

Solute	Volume fraction of isopropanol							
	1.0	0.9	0.8	0.7	0.6	0.5	0.4	0.3
Benzene	0.220	0.258	0.374	0.579	0.948	1.666	3.052	7.50
Toluene	0.224	0.306	0.455	0.722	1.253	2.425	5.031	14.78
Ethylbenzene	0.227	0.347	0.513	0.878	1.579	3.250	7.633	27.37
Propylbenzene	0.233	0.372	0.612	1.051	2.015	4.512	12.0	55.06
Butylbenzene	0.242	0.401	0.739	1.269	2.596	6.213	18.34	107.9
Cumene	0.238	0.346	0.589	0.972	1.852	4.097	10.64	–
tert.-Butylbenzene	0.256	0.382	0.648	1.099	2.174	5.008	14.04	–

TABLE II  
CAPACITY FACTORS OF ALKYL BENZENES IN TETRAHYDROFURAN-WATER MIXTURES  
Measured in a Hypersil ODS column (46 × 100 mm, 5 μm) at 25°C with a 10-μl sample loop.

Solute	Volume fraction of tetrahydrofuran						
	0.9	0.8	0.7	0.6	0.5	0.4	0.3
Benzene	0.210	0.312	0.572	0.955	1.674	3.292	7.486
Toluene	0.217	0.354	0.673	1.181	2.302	4.980	13.87
Ethylbenzene	0.253	0.378	0.754	1.401	2.972	7.350	25.07
Propylbenzene	0.261	0.423	0.849	1.720	3.965	11.18	47.27
Butylbenzene	0.274	0.452	0.965	2.048	5.130	17.10	—
Cumene	0.261	0.406	0.834	1.637	3.804	10.32	—
<i>tert.</i> -Butylbenzene	0.273	0.426	0.897	1.852	4.580	13.47	—

## RESULTS AND DISCUSSION

Plots of  $\ln k'$  and  $\ln \gamma_1^m$  versus  $\phi$  are shown in Fig. 1. We believe that these results provide unequivocal thermodynamic evidence that the principal driving force for the change in retention in RPLC upon variation in  $\phi$  are due to changes in the solute-solvent interactions in the mobile phase and are only secondarily due to solute-solvent interactions in the stationary phase. The variation in the stationary phase contributions to  $k'$  are represented by the parameter  $A$ . Comparison of Fig. 2 to Fig. 1 shows that the variations due to the mobile phase interactions are much greater than those due to the stationary phase interactions. Note that the scale of the ordinate in Fig. 1 is five-fold larger than the ordinate in Fig. 2.

TABLE III  
COLUMN CHARACTERISTICS

$V$  = Column volume (ml), calculated by using the column dimensions;  $d_s$  = packing density of stationary phase (g/ml);  $V_m$  = column void volume (ml);  $W_s$  = weight of stationary phase (g);  $A_{sp}$  = specific surface area of silica substrate.

Column characteristic	LiChrosorb RP-C <sub>18</sub> <sup>a</sup>	Zorbax ODS <sup>b</sup>	Develosil ODS-5 <sup>c</sup>	Hypersil ODS <sup>d</sup>
$V$	3.77	2.492	2.492	1.661
$d_s$	0.5	0.783	0.8	0.8
$V_m$	2.26 <sup>e</sup>	1.414	1.495 <sup>e</sup>	1.150
$W_s$	1.885	1.95	1.99	1.329
$A_{sp}$	343	150 <sup>f</sup>	150 <sup>f</sup>	150 <sup>f</sup>

<sup>a</sup> Used in work of Schoenmakers *et al.*<sup>29</sup>.

<sup>b</sup> Used in Barmam's work<sup>30</sup>.

<sup>c</sup> Used in Hanai and Hubert's work<sup>31</sup>.

<sup>d</sup> Used in this study.

<sup>e</sup> Calculated assuming the total porosity is 0.6.

<sup>f</sup> Best available estimate.

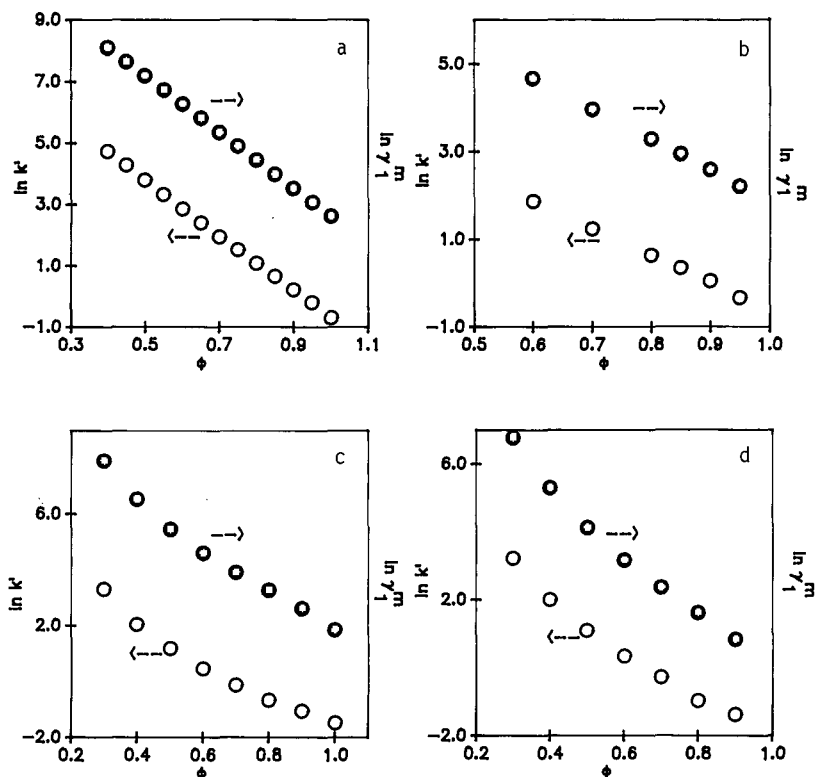


Fig. 1. The variation in capacity factor ( $\circ$ ) and solute activity coefficients ( $\bullet$ ) in the mobile phase. The solute in all cases is ethylbenzene. Solvent system: (a) methanol-water; (b) acetonitrile-water; (c) isopropanol-water; (d) tetrahydrofuran-water.

It is evident from the data summarized in Fig. 1 that the variations in  $k'$  and  $\gamma_1^m$  with  $\phi$  are both very large and strikingly similar. The data for ethylbenzene shown in Fig. 1 are quite typical. For all solutes examined plots of  $\ln k'$  and  $\ln \gamma_1^m$  versus  $\phi$  were almost parallel. In contrast the variation in factors related to the stationary phase (see Fig. 2), summarized in term  $A$  (see eqn. 8), are much smaller compared to the variation in  $\ln k'$  and  $\ln \gamma_1^m$ . We note that for ethylbenzene in methanol a 270-fold greater change occurs in the mobile phase than in the stationary phase. For the other mobile phase modifiers the changes in the term  $A$  with  $\phi$  are smaller (see Fig. 2) and in the case of isopropanol and tetrahydrofuran they are not monotonic. Because the variations in  $\ln \gamma_1^m$  and  $\ln k'$  with  $\phi$  are quite large a 1% change in  $\phi$  will cause a 10% change in  $k'$  or  $\gamma_1^m$ . Clearly small experimental errors in establishing the  $\phi$  value for both  $k'$  and  $\gamma_1^m$  could easily account for some of the non-monotonic trends. It is unrealistic to believe that the  $A$  values are accurate to better than 0.1–0.2 ln units. On the whole it is clear that  $A$  does vary with  $\phi$  in the methanol-water and tetrahydrofuran-water systems, possibly in the acetonitrile-water system and at most very slightly in the isopropanol-water system.

The data presented above do not prove that the major overall driving forces for retention in RPLC are the processes going on in the mobile phase. It is possible, but



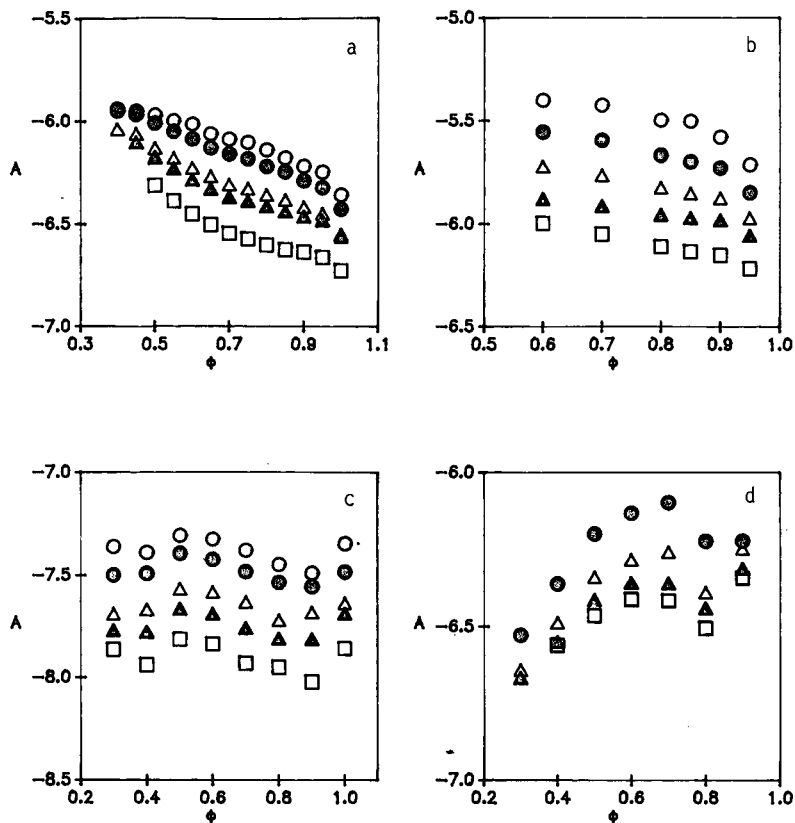


Fig. 2. The variation in  $A$  with mobile phase volume fraction. Solvent system: (a) methanol-water; (b) acetonitrile-water; (c) isopropanol-water; (d) tetrahydrofuran-water. Solutes:  $\circ$  = benzene;  $\bullet$  = toluene;  $\triangle$  = ethylbenzene;  $\blacktriangle$  = *n*-propylbenzene;  $\square$  = *n*-butylbenzene.

very unlikely, that the large  $k'$  values are due to very low stationary phase activity coefficients. We addressed this issue by estimating the activity coefficients in the bonded phase by the use of bulk phase analogs. Two extreme points of view can be adopted in estimating the solute activity coefficients in the bonded phase. First one can assume, as in model I above, that a non-polar environment is established by the bonded alkyl chains. In this case solute stationary phase activity coefficients should be modeled by their values in, for example, *n*-hexadecane. In another study<sup>35</sup> we found that the activity coefficient of toluene in hexadecane was equal to 0.96. The values for the activity coefficients of a series of alkylbenzenes in hexadecane, as measured by Schantz and Martire<sup>36</sup>, along with those computed by the UNIFAC method<sup>37</sup> for estimating limiting activity coefficients are given in Table IV. We see that all of the values are, in accord with intuition, similar and close to unity.

Values measured in this work by HSGC for benzene, toluene, ethyl benzene and propyl benzene are in good agreement with the literature. The value for *n*-butylbenzene disagrees with that of Schantz and Martire. The error in activity coefficients measured by HSGC for very low volatility solutes such as *n*-butylbenzene (b.p. 180°C) could be

TABLE IV  
MEASURED AND COMPUTED SOLUTE ACTIVITY COEFFICIENTS IN HEXADECANE

Solute	Activity coefficients			
	Measured <sup>a</sup>	Measured <sup>b</sup>	Measured <sup>c</sup>	Computed by UNIFAC
Benzene	1.09	1.07	1.08	0.91
Toluene	1.03	1.05	1.07	1.03
Ethylbenzene	1.15	1.16	1.18	1.05
<i>n</i> -Propylbenzene	1.14	1.21	1.22	1.09
<i>n</i> -Butylbenzene	1.14	1.30	1.31	1.13

<sup>a</sup> From Schantz and Martire<sup>36</sup>.

<sup>b</sup> In this work.

<sup>c</sup> In hexadecane saturated with methanol.

greater than 10% due to adsorption/condensation of the solute in the transfer lines especially when the solvent is also non-volatile.

In any instance it is evident that if bulk hexadecane were a good model for the stationary phase activity coefficients then the  $B_{2/1}$  values would be close to unity and would not vary from solute to solute nearly as much as do the mobile phase values. Consequently based on model I we conclude that the principal driving force for retention in RPLC lies in the mobile phase.

A second perspective is that the stationary phase solute activity coefficient is completely controlled by the sorbed organic modifier as would be the case if model III were to prevail. Here the activity coefficients in the stationary phase should be modeled by their values in the pure bulk organic modifier. We measured these quantities as part of this study (see Table V). Relative to the huge activity coefficients in the

TABLE V  
ACTIVITY COEFFICIENTS IN PURE ORGANIC LIQUIDS

Measured by head space gas chromatography in the indicated solvent at infinite dilution at 25°C. Based on the mole fraction concentration scale and Raoult's law reference state.

Solute	Methanol	Acetonitrile	Isopropanol	Tetrahydrofuran
Benzene	6.82	2.83	4.24	—
Toluene	9.67	4.03	5.08	0.84
Ethylbenzene	13.2	5.59	6.07	0.90
<i>n</i> -Propylbenzene	17.5	7.79	6.95	0.91
<i>n</i> -Butylbenzene	24.5	11.1	8.51	0.90
<i>Reciprocal relative activity coefficients<sup>a</sup></i>				
Benzene	1.42	1.43	1.20	—
Ethylbenzene	0.73	0.72	0.83	0.93
<i>n</i> -Propylbenzene	0.55	0.52	0.74	0.93
<i>n</i> -Butylbenzene	0.39	0.37	0.60	0.94

<sup>a</sup> The activity coefficient of toluene divided by the activity coefficient of the solute of interest.

hydro-organic mobile phase these values are on the order of unity. Therefore regardless of the two extreme points of view outlined above it is unreasonable to expect that the non-polar solutes studied here will be "pulled" into the stationary phase by virtue of a very small stationary phase activity coefficient. In addition the differences in the solute activity coefficients in the pure organic modifiers are not nearly large enough to account for the solute to solute variations in  $k'$ .

Based on the above we believe that the basic concept that retention in RPLC is due to the solvophobic effect is validated. This is not to say that any specific solvophobic model, such as that of Horváth and co-workers<sup>8,9</sup>, is correct in detail. Given that the mobile phase provides the major driving force for retention this does not mean that changes in the type of non-polar bonded ligand will be chromatographically unimportant. The results of Schantz *et al.*<sup>13</sup>, as do our  $A$  values, indicate that solute activity coefficients in a bonded stationary phase are significantly altered by the mobile phase. One must expect that the type of the bonded phase will modify its propensity for sorption of the mobile phase. Based on the very large difference in the solubility of methanol in hexane and in hexadecane it would be surprising if there were no differences in the amount of organic modifier sorbed by bonded octyl and octadecyl groups. Further in view of the fact that a reasonably efficient column can easily sense differences in transfer free energies of two solutes of less than 100 cal/mol, subtle changes in the stationary phase can significantly alter chromatographic selectivity factors.

We next examine the relative retention of two solutes on the same column as a function of  $\varphi$ . The term  $B_{2/1}$  is the relative stationary phase activity coefficient of two solutes. The data given in Table VI summarize our results using toluene as the reference solute. In view of the fact that the mobile phase activity coefficients are only precise to a few percent the relative stationary phase activity coefficients are, within experimental error, almost independent of  $\varphi$  over the range 0.3–1.0 for all four mobile phase modifiers (see Table V, and Figs. 3 and 4). The variation in  $B_{2/1}$  with  $\varphi$  is much smaller, particularly for the methanol–water system, than the variation in  $A$  with  $\varphi$ . The sole possible exception being the tetrahydrofuran–water system where there does appear to be a significant increase in  $B_{2/1}$  as the volume fraction of tetrahydrofuran approaches unity. These results may, however, be due to the experimental difficulties encountered in measuring the very low  $k'$  values in this system. This data should not be taken to mean that the stationary phase is not modified by the organic constituent of the mobile phase. We believe that it is (see below).

It is extremely interesting to note that despite the considerable variations of the solute activity coefficients in the pure polar organic solvents (see Table V) the differences in the relative stationary phase solute activity coefficients among the four types of organic modifiers are surprisingly small. In addition variations in the relative stationary phase activity coefficient from solute to solute are much greater than are those based on the use of bulk hexadecane as a model for the stationary phase. That is the variation in  $B_{2/1}$  (see Table V) from benzene to *n*-butylbenzene is much greater than one would predict based on the activity coefficients in hexadecane given in Table IV.

Given the two-fold change in  $B_{2/1}$  between benzene and *n*-butylbenzene we must conclude that the stationary phase environment is more polar than hexadecane. Thus case I, described above, is ruled out. This conclusion is in agreement with many fundamental studies of chromatography that indicate that a substantial amount of

TABLE VI  
RELATIVE STATIONARY PHASE SOLUTE ACTIVITY COEFFICIENTS

Relative activity coefficients computed from eqn. 11.  $\phi_{org}$  = Volume fraction of organic component in the mobile phase.  $\gamma_1^{PA}(1)\gamma_1^{PA}(2)$  = The ratio of the activity coefficient of toluene in bulk isopropanol to the activity coefficient of the indicated solute in isopropanol.

Solvent system	$\phi_{org}$	Benzene	Ethylbenzene	Propylbenzene	Butylbenzene	Cumene	tert.-Butylbenzene
Methanol-water	1.00	1.07	0.872	0.881	0.742	—	—
	0.95	1.08	0.879	0.852	0.714	—	—
	0.90	1.07	0.878	0.839	0.709	—	—
	0.85	1.07	0.870	0.823	0.686	—	—
	0.80	1.08	0.870	0.822	0.684	—	—
	0.75	1.08	0.863	0.813	0.679	—	—
	0.70	1.07	0.860	0.809	0.681	—	—
	0.65	1.07	0.868	0.816	0.689	—	—
	0.60	1.08	0.867	0.819	0.696	—	—
	0.55	1.05	0.878	0.834	0.715	—	—
	0.50	1.04	0.884	0.846	0.741	—	—
	0.45	1.02	0.908	0.871	—	—	—
	0.40	0.99	0.905	—	—	—	—
Average		1.06	0.87	0.84	0.71	—	—
S.D.		0.03	0.01	0.02	0.03	—	—
Acetonitrile-water	0.95	1.15	0.882	0.811	0.693	—	—
	0.90	1.16	0.863	0.776	0.657	—	—
	0.85	1.21	0.857	0.761	0.649	—	—
	0.80	1.18	0.853	0.749	0.644	—	—
	0.70	1.19	0.841	0.726	0.636	—	—
	0.60	1.17	0.845	0.722	0.645	—	—
Average		1.18	0.85	0.76	0.66	—	—
S.D.		0.03	0.01	0.03	0.02	—	—

Isopropanol- water	1.0	1.15	0.857	0.814	0.689	0.828	0.841
	0.9	1.07	0.879	0.771	0.628	0.754	0.723
	0.8	1.09	0.828	0.758	0.661	0.789	0.721
	0.7	1.11	0.861	0.758	0.640	0.769	0.703
	0.6	1.10	0.852	0.766	0.662	0.776	0.719
	0.5	1.09	0.838	0.762	0.658	0.770	0.712
	0.4	1.11	0.836	0.749	0.640	0.759	0.697
	0.3	1.15	0.825	0.761	0.695	—	—
	Average	1.11	0.84	0.77	0.66	0.78	0.73
	S.D.	0.03	0.02	0.02	0.03	0.02	0.05
Tetrahydrofuran- water	0.9	— <sup>a</sup>	0.974	0.913	0.888	0.968	0.949
	0.8	—	0.845	0.802	0.754	0.825	0.780
	0.7	—	0.850	0.769	0.728	0.815	0.768
	0.6	—	0.859	0.797	0.757	0.824	0.790
	0.5	—	0.868	0.806	0.768	0.850	0.824
	0.4	—	0.879	0.825	0.818	0.854	0.828
	0.3	—	0.891	0.868	—	—	—
	Average	—	0.88	0.83	0.79	0.86	0.82
S.D.	—	0.04	0.04	0.06	0.05	0.06	
$\gamma_1^{\text{IPA}}(1)/\gamma_1^{\text{IPA}}(2)^d$	1.20	0.83	0.74	0.60	0.77	0.69	

<sup>a</sup> The mobile phase activity coefficient of benzene in tetrahydrofuran was not measurable by HSGC due to overlap with the solvent peak.

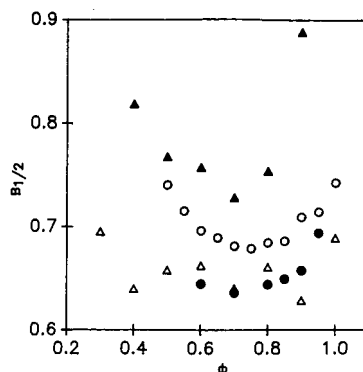
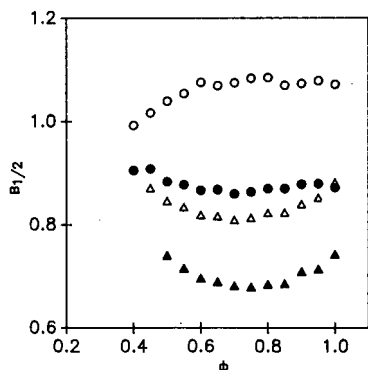


Fig. 3. Dependence of the relative stationary phase activity coefficient ( $B_{2/1}$ ) on the solute and volume fraction of organic modifier in the mobile phase. All results are for the indicated solute relative to toluene in methanol-water mobile phases. Solutes:  $\circ$  = benzene;  $\bullet$  = ethylbenzene;  $\triangle$  = *n*-propylbenzene;  $\blacktriangle$  = *n*-butylbenzene.

Fig. 4. Dependence of the relative stationary phase activity coefficient ( $B_{2/1}$ ) on the type of mobile phase modifier and volume fraction of organic modifier in the mobile phase. All results are for the *n*-butylbenzene relative to toluene in the indicated mobile phases: methanol-water ( $\circ$ ), acetonitrile-water ( $\bullet$ ), isopropanol-water ( $\triangle$ ), tetrahydrofuran-water ( $\blacktriangle$ ).

mobile phase is sorbed by the stationary phase<sup>14,18</sup>. More importantly it agrees with the solvatochromic studies of Stahlberg and Almgren<sup>38</sup>, and Carr and Harris<sup>39</sup> in which the stationary phase polarity was directly probed with pyrene.

The  $B_{2/1}$  values in all four organic modifiers are strikingly similar to those measured in bulk isopropanol (see the last line in Table V). This suggests the very simple idea that perhaps the absolute values of the stationary phase activity coefficients of all of the solutes in all of the mobile phases can be modeled by setting them equal to or proportional to their activity coefficient in pure bulk isopropanol (hereafter denoted as  $\gamma_1^{\text{IPA}}$ ).

We will now investigate the consequences of making the following universal approximation:

$$\gamma_1^s = \alpha \gamma_1^{\text{IPA}} \quad (12)$$

Based on the approximate constancy of  $A$  and  $B_{2/1}$  as  $\phi$  is changed over the range 0.3–1.0 we believe that it is reasonable to make the rough approximation that the number of moles of stationary phase is constant. This is consistent with case II described above. We now combine eqn. 12 with eqns. 2 and 7 to give

$$k' = [\gamma_1^m / (\alpha \gamma_1^{\text{IPA}})] (n_2^s / \{V_m d_m [w_0/M_0 + (1 - w_0)/M_w]\}) \quad (13)$$

Since we have assumed that the number of moles of stationary phase is a constant the capacity factor can be computed as a function of  $\phi$  to within an unspecified constant of proportionality. Taking the logarithm of both sides of eqn. 13 after combining the constants yields the following equation:

$$\begin{aligned} \ln k' &= C + \ln \gamma_1^m - \ln \gamma_1^{\text{PA}} - \ln \{V_m d_m [w_0/M_0 + (1 - w_0)/M_w]\} \\ &= C + \ln k'_{\text{calc}} \end{aligned} \quad (14)$$

We will refer to the sum of all the known terms on the right-hand side of eqn. 14 as  $\ln k'_{\text{calc}}$ . In view of the above arguments the difference between  $\ln k'$  and  $\ln k'_{\text{calc}}$  is an unknown offset that should not affect the slope of a plot of  $\ln k'$  versus  $\ln k'_{\text{calc}}$ . The resulting plots for all four mobile phases for all solutes are shown in Fig. 5. Linear least squares analysis of this data was carried out and the results are summarized in Table VII. These are in all cases very good correlations, as are those based on the data shown in Figs. 6 and 7 (see below). The average least squares slopes for methanol, acetonitrile, isopropanol and tetrahydrofuran are: 1.089, 1.078, 1.007, and 0.941, respectively. For all but the isopropanol system there is a slight downward trend in the slope and a more distinct trend in the intercept as the solute size increases.

The slope for the isopropanol system is closest to unity and shows only random variations among the seven solutes investigated. The same is true of the intercepts, that

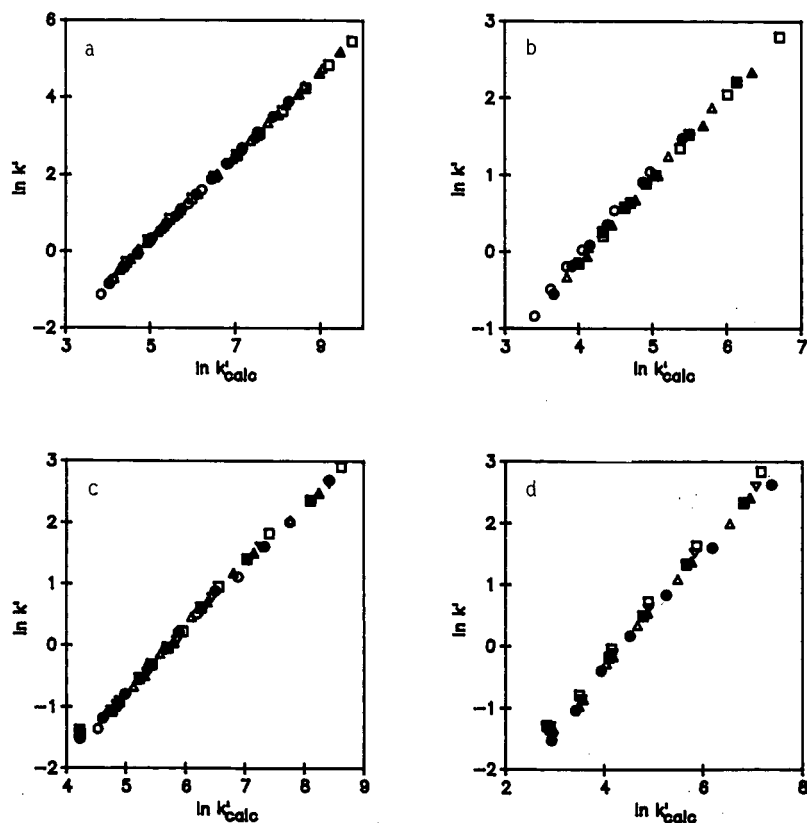


Fig. 5. Plot of measured  $\ln k'$  vs  $\ln k'_{\text{calc}}$  based on the isopropanol model for the stationary phase activity coefficient. The values of  $\ln k'_{\text{calc}}$  were obtained from eqn. 14. Solvent system: (a) methanol-water; (b) acetonitrile-water; (c) isopropanol-water; (d) tetrahydrofuran-water. Solutes:  $\circ$  = benzene;  $\bullet$  = toluene;  $\triangle$  = ethylbenzene;  $\blacktriangle$  = *n*-propylbenzene;  $\square$  = *n*-butylbenzene.

TABLE VII

REGRESSION ANALYSIS OF EFFECT OF  $\phi$  ON SOLUTE RETENTION

The data below are the results of regressing the  $\ln k'$  vs. the  $\ln k'_{\text{calc}}$  as defined in eqn. 14. In all cases the solute activity coefficient in the stationary phase was assumed to be equal to that in bulk isopropanol. The results were obtained by regression of the individual solutes one at a time. The average result was obtained by regression of all of data for all of the solutes in the indicated solvent simultaneously.

<i>Solute</i>	<i>Intercept (S.D.)</i>	<i>Slope (S.D.)</i>	<i>r</i>	<i>n</i>
<i>Methanol-water</i>				
Benzene	-5.27(0.042)	1.103(0.007)	0.9999	13
Toluene	-5.23(0.026)	1.104(0.004)	0.9999	13
Ethylbenzene	-5.18(0.029)	1.095(0.004)	0.9999	13
Propylbenzene	-5.06(0.032)	1.076(0.005)	0.9999	12
Butylbenzene	-5.01(0.036)	1.068(0.005)	0.9999	11
Average	-5.15(0.02)	1.089(.003)	0.99976	62
<i>Acetonitrile-water</i>				
Benzene	-4.77(0.174)	1.177(0.043)	0.9974	6
Toluene	-4.73(0.111)	1.153(0.025)	0.9990	6
Ethylbenzene	-4.59(0.077)	1.116(0.016)	0.9995	6
Propylbenzene	-4.45(0.055)	1.070(0.011)	0.9997	6
Butylbenzene	-4.50(0.034)	1.087(0.006)	0.9999	6
Cumene	-4.54(0.063)	1.102(0.013)	0.9997	6
Average	-4.42(0.06)	1.078(0.011)	0.99797	36
<i>Isopropanol-water</i>				
Benzene	-5.870(0.110)	1.018(0.019)	0.9989	8
Toluene	-5.769(0.088)	1.010(0.015)	0.9993	8
Ethylbenzene	-5.709(0.084)	1.000(0.013)	0.9994	8
Propylbenzene	-5.724(0.086)	0.999(0.013)	0.9995	8
Butylbenzene	-5.750(0.092)	1.010(0.013)	0.9994	8
Cumene	-5.751(0.131)	1.007(0.022)	0.9988	7
<i>tert.</i> -Butylbenzene	-5.650(0.155)	0.989(0.025)	0.9983	7
Average	-5.76(0.04)	1.007(0.005)	0.99915	54
<i>Tetrahydrofuran-water</i>				
Toluene	-4.126(0.129)	0.927(0.026)	0.9980	7
Ethylbenzene	-4.088(0.096)	0.930(0.018)	0.9990	7
Propylbenzene	-4.124(0.071)	0.943(0.013)	0.9995	7
Butylbenzene	-4.063(0.085)	0.966(0.017)	0.9993	6
Cumene	-4.121(0.110)	0.953(0.021)	0.9990	6
<i>tert.</i> -Butylbenzene	-4.122(0.111)	0.958(0.020)	0.9989	6
Average	-4.090(0.056)	0.941(0.012)	0.99749	39

is, for the isopropanol system the intercepts for the various solutes do not differ beyond their individual standard deviations. In contrast the slope for the tetrahydrofuran system is the smallest, although it does not differ from unity as much as does the slope for methanol. We note that activity coefficients in bulk tetrahydrofuran are quite close to unity whereas the other bulk solvents induce much larger activity coefficients (see Table IV).

In three of the solvent systems the intercepts for the various solutes are so similar that the above approximation for  $\gamma_1^s$  leads to a universal curve for the retention of



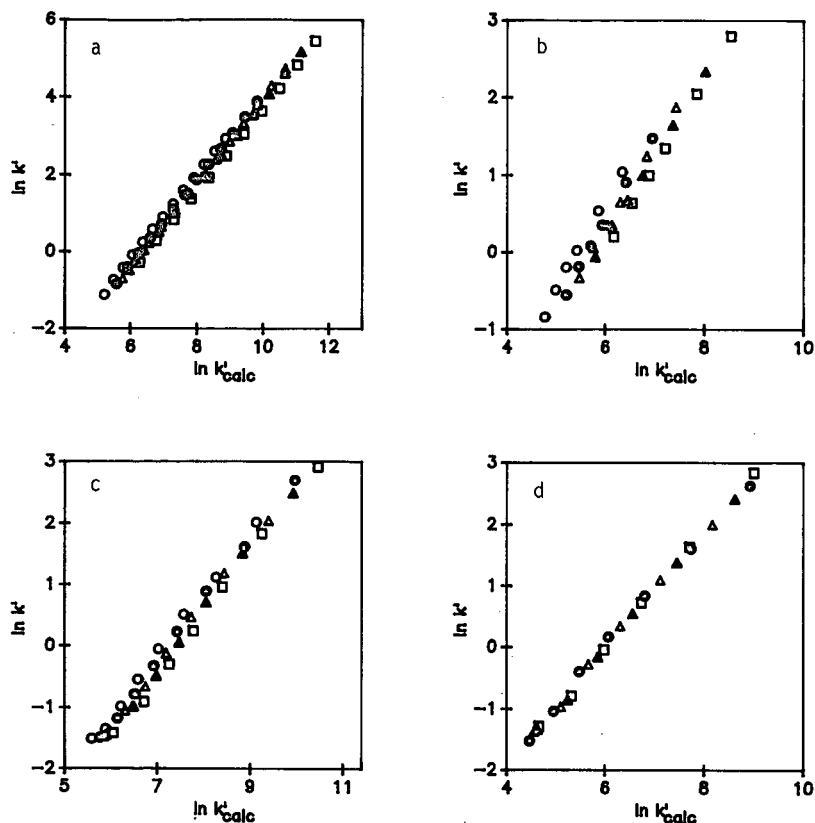


Fig. 6. Plot of measured  $\ln k'$  vs.  $\ln k'_{\text{calc}}$  based on the hexadecane model for the stationary phase activity coefficient. Solvent system: (a) methanol-water; (b) acetonitrile-water; (c) isopropanol-water; (d) tetrahydrofuran-water. Solutes:  $\circ$  = benzene;  $\bullet$  = toluene;  $\triangle$  = ethylbenzene;  $\blacktriangle$  = *n*-propylbenzene;  $\square$  = *n*-butylbenzene.

non-polar solutes. In other words three of the data sets are very similar except for the presence of an offset in the plot; this amounts to a proportional difference in  $k'$  which corresponds to the term  $\alpha$  in eqns. 12 and 13.

Other approaches to estimating the solute activity coefficient in the stationary phase were tested including the assumption that the activity coefficients are equal (or proportional) to those in bulk hexadecane (see Fig. 6), and assuming that they are equal (or proportional) to that in the pure bulk organic solvent used in the mobile phase (see Fig. 7). Systematic, that is solute dependent deviations, are evident in Figs. 6 and 7. It is clear that except for the tetrahydrofuran-water system the best single unifying factor is the isopropanol approximation (see eqn. 12).

We believe that this supports the idea that the effect of a change in stationary phase composition and the concomitant change in environment sensed by a solute immersed in the stationary phase are quite small relative to the enormous change in the solute environment in the mobile phase over the range in mobile phase compositions explored in this work. At this time we do not have an explanation for the different

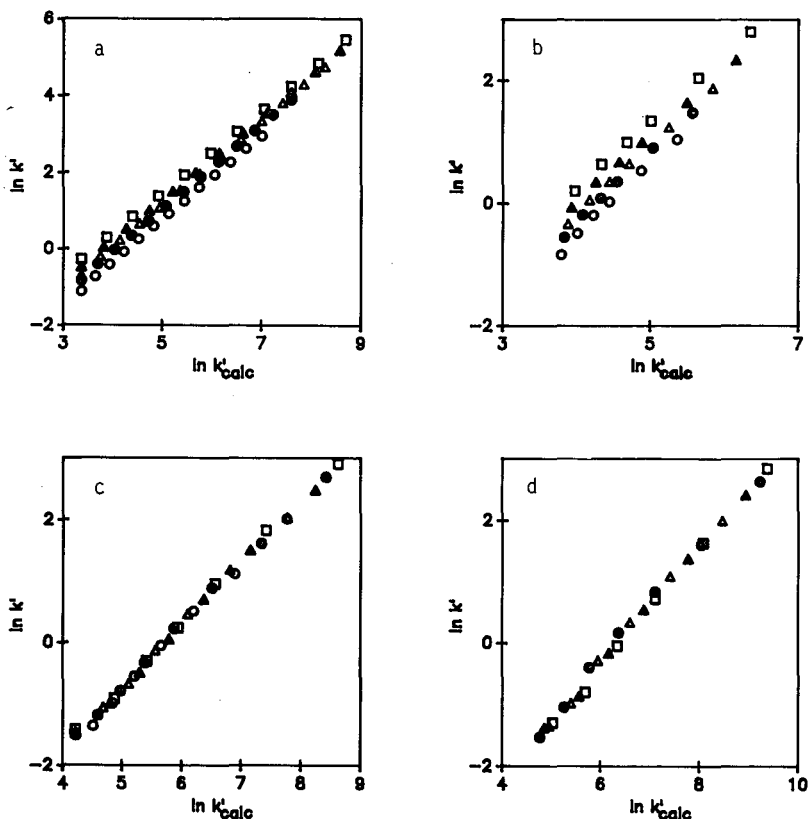


Fig. 7. Plot of measured  $\ln k'$  vs.  $\ln k'_{\text{calc}}$  based on the use of the solute activity coefficient in the bulk pure organic modifier used in the mobile phase as the stationary phase activity coefficient. Solvent system: (a) methanol-water; (b) acetonitrile-water; (c) isopropanol-water; (d) tetrahydrofuran-water. Solutes:  $\circ$  = benzene;  $\bullet$  = toluene;  $\triangle$  = ethylbenzene;  $\blacktriangle$  = *n*-propylbenzene;  $\square$  = *n*-butylbenzene.

behavior of tetrahydrofuran other than the fact that it is the least polar of all of the modifiers based on factors such as its dielectric constant, Kamlet-Taft  $\pi^*$  dipolarity/polarizability<sup>40</sup> and the fact that the activity coefficients of non-polar solutes in tetrahydrofuran are close to unity. When the solute's activity coefficient in the stationary phase is set equal to its activity coefficient in bulk tetrahydrofuran the slope of the regression line of  $\ln k'$  versus  $\ln k'_{\text{calc}}$  is equal to 0.943 which is not different from that based on the isopropanol assumption.

An important point that should be addressed is why do the three modifiers act as if the stationary phase environment has a polarity similar to isopropanol. We have no solid answer to this question but believe that isopropanol may simply be the best model for the combined effect of the bonded phase ligands, sorbed mobile phase components, including water, and the polarity of the accessible silanol groups on the stationary phase chemical potential of the solute.

The intercepts of all of the plots shown in Fig. 5 are significantly different. Physically the intercepts correspond to the offset term in eqn. 14. If we assume that  $\alpha$  in

TABLE VIII

COMPARISON OF MOLES OF BONDED PHASE FROM COLUMN CHARACTERISTICS AND VALUES CALCULATED FROM THE PARTITION MODEL

<i>Data set</i>	<i>Amount of stationary phase (mmoles)</i>	
	<i>A<sup>a</sup></i>	<i>B<sup>b</sup></i>
Methanol <sup>c</sup>	1.3	5.8
Acetonitrile <sup>d</sup>	0.6	12
Isopropanol <sup>e</sup>	0.4	3.2
Tetrahydrofuran <sup>e</sup>	0.4	17

<sup>a</sup> Computed from the column characteristics given in Table III and ligand surface coverage = 2  $\mu\text{mol}/\text{m}^2$ .

<sup>b</sup> Computed from the intercept given in Table VII.

<sup>c</sup> This is the Zorbax column used by Barman<sup>30</sup>.

<sup>d</sup> This is the Develosil column used by Hanai and Hubert<sup>31</sup>.

<sup>e</sup> This is the Hypersil column used in this work.

eqn. 12 is unity, that is, the activity coefficient of the solute in the stationary phase is equal to the value in pure bulk isopropanol, then we can compute the number of moles of stationary phase. The results are summarized in Table VIII. It is evident that the number of moles of stationary phase is, in all cases, much larger than that computed based on estimates of the amount of bonded phase by using the column characteristics given in Table III. For the Hypersil column used in this work we find that the amount of stationary phase is much larger for the tetrahydrofuran mobile phase than for the isopropanol mobile phase despite the fact that the same column was used. In addition the number of moles of stationary phase is impossibly large. For example the data for the tetrahydrofuran system corresponds to a volume of 1.4  $\text{cm}^3$ . This is larger than the void volume of the column (1.15  $\text{cm}^3$ ). The above computations are contingent upon the assumed value of the constant of proportionality ( $\alpha$ ) between the bulk phase activity coefficient and the activity coefficient in the stationary phase being unity. It is much more likely that the actual stationary phase activity coefficient is intermediate between the value in hexadecane and that in the pure organic liquid. A decrease in  $\alpha$  will decrease our estimate of the number of moles of stationary phase to more reasonable values. However, activity coefficients in tetrahydrofuran are very close to those in hexadecane and the extraordinarily large amount of sorbed modifier computed based on a partition model cannot be rationalized. This suggests that the data analysis is not consistent with a "pure" partition model<sup>41</sup>.

It seemed to us that, no matter how small, within reason, one chooses to make the activity coefficients in the stationary phase, one cannot deny that a considerable amount of the organic modifier is sorbed into the bonded phase thereby altering its properties. However, given the very small amount of methanol needed to saturate bulk hexadecane (0.3 mole %) we felt that it would be impossible for this minute amount of methanol to exert a substantial effect on the activity coefficient of a non-polar solute. This was verified by measuring the activity coefficient of a series of alkylbenzenes in bulk methanol-saturated hexadecane (see Table IV). Our assumption is clearly validated; saturation of bulk hexadecane with methanol does not change the environment experienced by a non-polar solute.

Based on this we are convinced that the very high surface to volume ratio of a bonded phase column, relative to that of a bulk liquid, must allow for the sorption of a much larger amount of organic modifier into the bonded phase than occurs in experiments with bulk liquid phases such as our HSGC experiment or the "sit flask" experiment of Schantz and Martire<sup>36</sup>. Using literature data on sorption of organic modifiers<sup>7,14,18,34</sup>, we infer that at least 1–2 moles of the organic modifier per mole of bonded ligand can be adsorbed into the bonded phase. In essence then we feel that bonded-phase RPLC cannot be accurately described as a pure partition process even for non-polar solutes.

We turn now to reconciling our observations to those of Schantz *et al.*<sup>13</sup>. If one assumes that the activity coefficient of the solute in bulk hexadecane is independent of the amount of methanol that can partition into the phase then the change in our  $A$  term with  $\varphi$  should be directly comparable to the change in the natural logarithm of the ratio of the hexadecane partition coefficient to net retention volume studied by Schantz *et al.*<sup>13</sup>. For the methanol–water system  $A$  varied by about 0.5 ln units in the same direction and over the same range in  $\varphi$  that the parameter of Schantz *et al.*<sup>13</sup> varied by 0.9 ln units. Given the vastly different methodologies and the different experimental difficulties we believe that these results are only marginally inconsistent. Nonetheless if the difference is real it can be reconciled. Based on our preceding results that the bonded phase acts as if it is more polar than an alkane we hypothesize that one must include some number of moles of organic modifier in the number of moles of stationary phase (see eqn. 8). Consequently the term  $A$  must vary less than the ratio of the sit flask partition coefficient to the net retention volume because of a cancellation of effects. That is the amount of stationary phase increases by sorbing the organic modifier and very possibly some water into the bonded phase domain. This has the effect of simultaneously increasing the stationary phase solute activity coefficient and the number of moles of stationary phase. Since the term  $A$  is a ratio of these two factors it appears to vary less than either factor alone.

## CONCLUSION

It is clear from the above results that the solute–mobile phase activity coefficient is tremendously important in RPLC. Consequently all models of RPLC, such as that of Geng and Regnier<sup>42,43</sup>, which do not incorporate this term should be re-examined. Because mobile phase interactions are the dominant factor in establishing the dependence of  $k'$  on  $\varphi$  and the  $\gamma^m$  values are so large it is evident that the solvophobic mechanism of RPLC is correct in spirit if not in detail. This does not mean that the stationary phase is a non-participating spectator. The results clearly show the importance of the very high surface area in bonded-phase RPLC. Solute activity coefficients in the stationary phase cannot be modeled by treating the solute as being dissolved in a non-polar bulk phase such as hexadecane.

## ACKNOWLEDGEMENT

This work was supported by the National Science Foundation and the Petroleum Research Foundation.

## REFERENCES

- 1 A. Nahum and Cs. Horváth, *J. Chromatogr.*, 203 (1981) 53.
- 2 K. E. Bij, Cs. Horváth, W. R. Melander and A. Nahum, *J. Chromatogr.*, 203 (1981) 65.
- 3 Cs. Horváth (Editor), *High Performance Liquid Chromatography—Advances and Perspectives*, Vol. 2, Academic Press, New York, 1980, p. 113.
- 4 C. H. Lochmuller and D. R. Wilder, *J. Chromatogr. Sci.*, 17 (1979) 574.
- 5 M. Jaroniec and J. A. Jaroniec, *J. High Resolut. Chromatogr. Chromatogr. Commun.*, 9 (1986) 236.
- 6 D. C. Locke, *J. Chromatogr. Sci.*, 15 (1977) 393.
- 7 R. P. W. Scott and P. Kucera, *J. Chromatogr.*, 149 (1978) 93.
- 8 Cs. Horváth, W. Melander and I. Molnar, *J. Chromatogr.*, 125 (1976) 129.
- 9 Cs. Horváth and W. Melander, *J. Chromatogr. Sci.*, 15 (1977) 393.
- 10 D. E. Martire and R. E. Bohem, *J. Phys. Chem.*, 87 (1983) 1045.
- 11 B. P. Johnson, M. G. Khaledi and J. G. Dorsey, *J. Chromatogr.*, 384 (1987) 221.
- 12 B. P. Johnson, M. G. Khaledi and J. G. Dorsey, *Anal. Chem.*, 58 (1986) 2354.
- 13 M. Schantz, B. N. Barman and D. E. Martire, *J. Res. Natl. Bur. Stand. U.S.*, 93 (1988) 161.
- 14 R. M. McCormick and B. L. Karger, *Anal. Chem.*, 52 (1980) 2249.
- 15 J. H. Knox and A. J. Pryde, *J. Chromatogr.*, 112 (1975) 171.
- 16 P. J. Schoenmakers, H. A. H. Billiet and L. de Galan, *J. Chromatogr.*, 185 (1979) 179.
- 17 D. Westerlund and A. J. Theodorsen, *J. Chromatogr.*, 144 (1977) 27.
- 18 C. R. Yonker, T. A. Zwier and M. F. Burke, *J. Chromatogr.*, 241 (1982) 257.
- 19 C. H. Eon, *Anal. Chem.*, 47 (1975) 1871.
- 20 H. Colin and G. Guiochon, *J. Chromatogr.*, 158 (1978) 183.
- 21 W. E. Hammers, G. J. Meurs and C. L. de Ligny, *J. Chromatogr.*, 24 (1982) 169.
- 22 D. H. Everett, *Trans. Faraday Soc.*, 60 (1964) 1803.
- 23 D. H. Everett, *Trans. Faraday Soc.*, 61 (1965) 2478.
- 24 L. R. Snyder, *Principles of Adsorption Chromatography*, Marcel Dekker, New York, 1968.
- 25 W. J. Cheong and P. W. Carr, *J. Chromatogr.*, 500 (1990) 215.
- 26 A. Hussam and P. W. Carr, *Anal. Chem.*, 57 (1985) 793.
- 27 J. R. Conder and C. L. Young, *Physicochemical Measurements by Gas Chromatography*, Wiley, New York, 1979.
- 28 B. V. Ioffe and A. G. Vitenberg, *Head Space Analysis and Related Methods in Gas Chromatography*, Wiley, New York, 1984.
- 29 P. J. Schoenmakers, H. A. H. Billiet and L. de Galan, *J. Chromatogr.*, 282 (1983) 107.
- 30 B. N. Barman, *Ph.D. Thesis*, Georgetown University, Washington, DC, 1985.
- 31 T. Hanai and J. Hubert, *J. Chromatogr.*, 290 (1984) 197.
- 32 R. A. Djerki and R. J. Laub, *J. Liq. Chromatogr.*, 10 (1987) 1749.
- 33 E. Engelhardt and G. Ahr, *Chromatographia*, 14 (1981) 227.
- 34 E. H. Slaats, W. Markovski, J. Fekete and H. Poppe, *J. Chromatogr.*, 207 (1981) 299.
- 35 J. H. Park, A. Hussam, P. Couasnon, D. Fritz and P. W. Carr, *Anal. Chem.*, 59 (1987) 1970.
- 36 M. Schantz and D. E. Martire, *J. Chromatogr.*, 391 (1987) 35.
- 37 J. Gmehling, P. Rasmussen and A. Fredenslund, *Ind. Eng. Chem. Process Des. Dev.*, 21 (1982) 118.
- 38 J. Stahlberg and M. Almgren, *Anal. Chem.*, 57 (1985) 817.
- 39 J. W. Carr and J. M. Harris, *Anal. Chem.*, 58 (1986) 626.
- 40 M. J. Kamlet, M. H. Abraham and R. J. Taft, *J. Org. Chem.*, 48 (1983) 2877.
- 41 M. Jaroniec, D. E. Martire and J. Oscik, *J. Liq. Chromatogr.*, 9 (1986) 2555.
- 42 X. Geng and F. E. Regnier, *J. Chromatogr.*, 332 (1985) 147.
- 43 X. Geng and F. E. Regnier, *J. Chromatogr.*, 402 (1987) 41.



CHROMSYMP. 1648

## RETENTION CHARACTERISTICS OF SEVERAL COMPOUND CLASSES IN REVERSED-PHASE LIQUID CHROMATOGRAPHY WITH $\beta$ -CYCLODEXTRIN AS A MOBILE PHASE MODIFIER

REZA M. MOHSENI and ROBERT J. HURTUBISE\*

*Chemistry Department, University of Wyoming, Laramie, WY 82071 (U.S.A.)*

---

### SUMMARY

$\beta$ -Cyclodextrin was investigated as a mobile phase modifier in the reversed-phase liquid chromatography of polycyclic aromatic hydrocarbons, nitrogen heterocycles and hydroxyl aromatics. A wide range of  $\beta$ -cyclodextrin concentrations was employed, and the retention properties of the compound classes were compared in methanol–water and ethanol–water mobile phases at 25°C.  $\beta$ -Cyclodextrin–solute dissociation constants were obtained for the compounds in several methanol–water and ethanol–water mobile phase compositions, using the chromatographic data. The trends in the retention data and dissociation constants for the compound classes were discussed. Several conclusions were drawn concerning the mechanism of retention when  $\beta$ -cyclodextrin is present in the mobile phases. Also, comparisons were made between the structural features of the compounds and their capacity factors and dissociation constants.

---

### INTRODUCTION

Cyclodextrins (CDs) are cyclic oligosaccharides, constructed from  $\alpha$ -(1,4)-linked glucose units arranged in a torus<sup>1</sup>. The most common cyclodextrins are  $\alpha$ -,  $\beta$ - and  $\gamma$ -cyclodextrin, containing six, seven and eight glucose units, respectively. Because the cavity of a CD molecule contains C–H groups and glucosidic oxygens, the interior part of the molecule is relatively hydrophobic<sup>2</sup>. Generally, the external part of the CD molecule is hydrophilic compared to its cavity. The hydrophilic nature of the external portion of the molecule is due to primary and secondary hydroxyl groups being located on the smaller and larger sides of the CD molecule, respectively. Cyclodextrins have the ability to form inclusion complexes with a variety of molecules. The formation of an inclusion complex depends upon shape, size and spatial geometry of the solute, the diameter of the CD cavity and other factors<sup>1,2</sup>.

There are essentially two approaches for applying CDs in liquid chromatography (LC). The first involves the use of CDs bonded to silica gel, and the second involves the use of CDs as a mobile phase additive. Armstrong and DeMond<sup>3</sup> have reviewed cyclodextrin-bonded phases for LC separations. Tarr *et al.*<sup>4</sup> studied the influence of mobile phase alcohol modifiers on the separation of polynuclear aromatics

with a  $\beta$ -CD bonded phase column. However, relatively little work has been reported on the chromatographic aspects of CDs added to mobile phases when a  $C_{18}$  column is used. Armstrong<sup>5</sup> and Hinze and Armstrong<sup>6</sup> used CD mobile phase modifiers in thin-layer chromatography (TLC) for separating structural isomers. Debowski *et al.*<sup>7,8</sup> resolved enantiomers of mandelic acid and mandelic acid derivatives by using reversed-phase liquid chromatography (RPLC) for  $\alpha$ - and  $\beta$ -CD inclusion complexes. Gazdag *et al.*<sup>9</sup> employed  $\alpha$ -,  $\beta$ - and  $\gamma$ -CDs as mobile phase additives in RPLC for enantiomer separation of D,L-norgestrels. Gazdag *et al.*<sup>10</sup> added a mixture of CDs to the mobile phase to develop a simple optimization technique for the separation of isomeric compounds. They studied the effects of CD concentration, pH and ionic strength on the capacity factors of model compounds. Armstrong *et al.*<sup>11</sup> resolved a variety of racemic compounds, including drugs, nicotinoids, amino derivatives, sulfonates, metallocenes and crown ethers with  $\beta$ -CD in the mobile phase by RP-TLC.

The separation of structural isomers<sup>12-14</sup> and aromatic amino acids<sup>15</sup> has been achieved by the addition of CDs to the mobile phase. Bazant *et al.*<sup>16</sup> used either  $\beta$ -CD as the mobile phase additive or  $\beta$ -CD, chemically bonded to the stationary phase, for the separation of structural isomers of some biologically important hydroxy-, methoxy- and amino-substituted aromatic carboxylic acids by LC. They emphasized that CDs can be applied to the separation of compounds that are difficult to separate in other systems.

The formation of inclusion complexes between host/guest molecules is mainly responsible for altering solute retention in RPLC. There have been some reports relating the concentration of CD and stability constants of inclusion complexes to retention characteristics<sup>17-21</sup>. For example, Fujimura *et al.*<sup>20</sup> derived an equation relating capacity factor to CD concentration in the mobile phase and the stability constant of the CD complex. Zukowski *et al.*<sup>19</sup> derived a similar equation that relates the observed capacity factors to the total CD concentration.

Because very little retention data and mechanistic information have been published on the effects of  $\beta$ -CD added to the mobile phase in RPLC, the retention characteristics of several polycyclic aromatic hydrocarbons (PAHs), nitrogen heterocycles and aromatic hydroxyl compounds as a function of both  $\beta$ -CD concentration and organic modifier concentration were investigated. Furthermore, the dissociation constants of the inclusion complexes for the model compounds were obtained by using equilibrium concentrations of  $\beta$ -CD, and various mechanistic aspects of the chromatographic interactions with  $\beta$ -CD were investigated.

## EXPERIMENTAL

### Materials

The liquid chromatograph used was a Waters unit with a Model 6000A pump (Waters Assoc., Milford, MA, U.S.A.), a U6K injector, a dual-channel ultraviolet detector, set at 254 nm, and a dual-channel 10-mV strip-chart recorder. A Model FE Haake (Saddle Brook, NJ, U.S.A.) constant temperature bath was used to keep the temperature of the column at 25°C. The column employed was a  $\mu$ Bondapack  $C_{18}$  (300 mm  $\times$  4 mm I.D.) purchased from Phenomenex (Torrance, CA, U.S.A.). PAHs and nitrogen heterocycles were obtained from commercial sources. The model compounds and  $\beta$ -CD were purchased from Aldrich (Milwaukee, WI, U.S.A.). Table I



lists the structures of the model compounds studied in this work. Methanol was of HPLC-grade and purchased from Baker (Phillipsburg, NJ, U.S.A.).

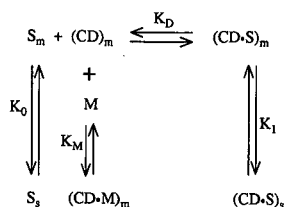
### Methods

Methanol and water were prefiltered through a Millipore type FH 0.5- $\mu\text{m}$  filter.  $\beta$ -CD was vacuum dried at 0.78 atm pressure at 75°C for 8 h prior to use. Then,  $\beta$ -CD was dissolved in purified water, and methanol was added to the  $\beta$ -CD solution. The maximum amount of  $\beta$ -CD that dissolved in all the mobile phases investigated was 6.81 g in 1 l of methanol–water (30:70). The largest analytical concentrations of  $\beta$ -CD in methanol–water mixtures of 30:70, 40:60, 50:50 and 60:40 were 6.0, 5.0, 4.0, 3.0 mM, respectively. The largest analytical concentration of  $\beta$ -CD in ethanol–water solvents was 5.0 mM. Eqn. 11 was used to calculate the equilibrium concentrations of  $\beta$ -CD. The formation constants for methanol and ethanol used in eqn. 11 were 0.32 and 0.93  $M^{-1}$ , respectively<sup>22</sup>. The methanol–water mixtures used for the PAHs were 55:45, 60:40, 65:35, 70:30 and 75:25, and those for the nitrogen heterocycles were 50:50, 55:45, 60:40 and 65:35. The methanol–water compositions that were used for the hydroxyl aromatics were 30:70, 40:60, 50:50 and 60:40. The ethanol–water compositions used for the hydroxyl compounds were 35:65, 40:60, 45:55 and 50:50. The concentrations of all the samples injected were 1 mg/ml in methanol, except for the concentration of anthracene, which was 0.5 mg/ml. The temperature was kept constant at 25°C, and the column void volume was obtained by injecting a methanol solution of potassium nitrite.

## RESULTS AND DISCUSSION

### Theoretical considerations

The following equilibria occur when a solute (S) is involved in a reversed-phase chromatographic system with  $\beta$ -CD in the mobile phase:



where subscripts m and s refer to the mobile and stationary phase, respectively, and M is the organic modifier. The distribution constants of the solute and the inclusion complex are given in eqns. 1 and 2, respectively.

$$K_0 = [S_s]/[S_m] \quad (1)$$

$$K_1 = [(CD \cdot S)_s]/[(CD \cdot S)_m] \quad (2)$$

The dissociation constant of the inclusion complex is given in eqn. 3, and

$$K_D = [S_m][(CD)_m]/[(CD \cdot S)_m] \quad (3)$$

TABLE I  
NAMES AND STRUCTURES OF MODEL COMPOUNDS

<i>Compound</i>	<i>Structure</i>	<i>Compound</i>	<i>Structure</i>
(1) Naphthalene		(12) 1-Indanol	
(2) Biphenyl		(13) 5-Indanol	
(3) Acenaphthene		(14) 1,7-Dihydroxynaphthalene	
(4) Phenanthrene		(15) 2,3-Dihydroxynaphthalene	
(5) Anthracene		(16) <i>o,o'</i> -Biphenol	
(6) Quinoline		(17) <i>p,p'</i> -Biphenol	
(7) Isoquinoline		(18) 1-Naphthol	
(8) Benzo( <i>f</i> )quinoline		(19) 2-Naphthol	
(9) Benzo( <i>h</i> )quinoline		(20) 2-Phenylphenol	
(10) 1,3-Dihydroxybenzene		(21) 3-Phenylphenol	
(11) 1,4-Dihydroxybenzene		(22) 4-Phenylphenol	

the formation constant for the formation of  $(CD \cdot M)_m$  is given in eqn. 4:

$$K_M = \frac{[(CD \cdot M)_m]}{[(CD)_m][M]} \quad (4)$$

The capacity factor ( $k'$ ) of the solute is defined as

$$k' = \frac{\varphi([S_s] + [(CD \cdot S)_s])}{([S_m] + [(CD \cdot S)_m])} \quad (5)$$

where  $\varphi$  is the phase ratio of the column. Since the external part of the CD is hydrophilic, the interaction between CD and the stationary phase is considered negligible<sup>20</sup>. Thus, eqn. 5 can be written as

$$k' = \varphi[S_s]/([S_m] + [(CD \cdot S)_m]) \quad (6)$$

Substituting into eqn. 6 for  $[S_s]$  and  $[(CD \cdot S)_m]$  by using eqns. 1 and 3, respectively, results in

$$k' = \varphi K_0 K_D / (K_D + [(CD)_m]) \quad (7)$$

Since  $k'_0 = \varphi K_0$ , where  $k'_0$  is the capacity factor with no  $\beta$ -CD present, eqn. 7 is written as

$$1/k' = 1/k'_0 + [(CD)_m]/k'_0 K_D \quad (8)$$

Eqn. 8 is similar to the equation derived by Fujimura *et al.*<sup>20</sup>. However, the equilibrium concentration of  $\beta$ -CD appears in the equation instead of total  $\beta$ -CD concentration. The main reason for using the equilibrium concentration of  $\beta$ -CD is that methanol weakly competes with the solute for the formation of an inclusion complex with  $\beta$ -CD<sup>22</sup>.

To obtain the equilibrium concentration of  $\beta$ -CD, the mass balance for CDs is used:

$$[(CD)_T] = [(CD)_m] + [(CD \cdot M)_m] + [(CD \cdot S)_m] + [(CD \cdot S)_s] \quad (9)$$

If it is assumed that the last two terms on the right side of eqn. 9 are negligible compared to the first two terms, because the solute concentration is very small, then the following equation results:

$$[(CD)_T] = [(CD)_m] + [(CD \cdot M)_m] \quad (10)$$

By substituting  $[(CD \cdot M)_m]$  from eqn. 4 into eqn. 10 the following equation is obtained:

$$[(CD)_m] = [(CD)_T]/(1 + K_M[M]) \quad (11)$$

Zukowski *et al.*<sup>19</sup> used eqn. 11 to obtain the equilibrium concentrations of  $\beta$ -CD in reversed-phase chromatographic systems.

#### *Dependence of capacity factors on organic modifier at a given $\beta$ -CD concentration*

Methanol (used as the main organic modifier in this work) competed somewhat with the solute in occupying the  $\beta$ -CD cavity. This aspect has not been considered in detail in chromatographic systems. Matsui and Mochida<sup>22</sup> determined the stability constants of  $\alpha$ - and  $\beta$ -CD complexes for several alcohols, using a spectrophotometric method. According to their data, the association constant of methanol with  $\beta$ -CD was  $0.32 M^{-1}$ . The small value for the association constant shows that methanol interacts weakly with  $\beta$ -CD, and the interaction with  $\beta$ -CD can normally be considered a constant effect at a given methanol composition. However, because of the relatively large concentration of methanol used in the mobile phase, a substantial amount of methanol can interact with  $\beta$ -CD. This aspect will be discussed in more detail later. Fig. 1 illustrates the effect of methanol concentration on  $\log k'$  for the PAHs in the

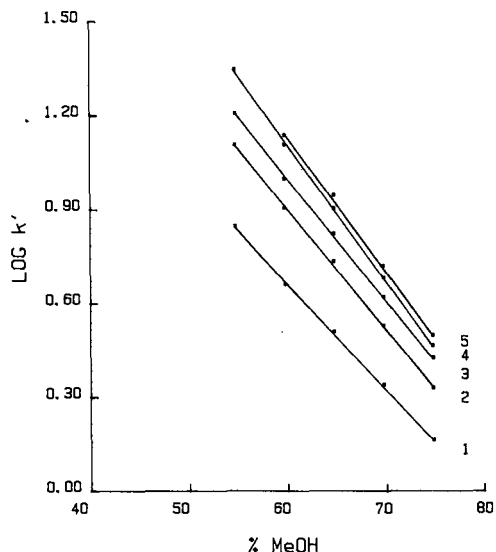


Fig. 1. Plot of  $\log k'$  vs. percentage of methanol (MeOH) for PAHs on a  $C_{18}$  column with 1.5 mM  $\beta$ -CD.

presence of 1.5 mM  $\beta$ -CD. This figure shows that with increasing amounts of methanol the capacity factors decrease for a given compound in the presence of the same amount of  $\beta$ -CD, as would be expected. The other mobile phases containing different amounts of  $\beta$ -CD gave similar graphs. The dependence of  $\log k'$  on the organic modifier concentration and  $\beta$ -CD concentration for quinoline, isoquinoline, benzo(*f*)quinoline [B(*f*)Q], and benzo(*h*)quinoline [B(*h*)Q] was also investigated. The same general retention characteristics were found for these compounds as were found for PAHs as the methanol concentration increased at a given  $\beta$ -CD concentration. The other set of compounds investigated was hydroxyl aromatics. Linear relationships were also obtained between  $\log k'$  and methanol concentration in the presence and absence of  $\beta$ -CD for the hydroxyl aromatics.

#### *Dependence of capacity factors on $\beta$ -CD concentration*

The capacity factors of the PAHs and nitrogen heterocycles for different analytical concentrations of  $\beta$ -CD (0.0, 0.5, 1.0, 1.5, 2.0 and 2.5 mM) in methanol–water were obtained. The methanol–water ratios employed were 75:25, 70:30, 65:35, 60:40 and 55:45. The  $k'$  values showed relatively small decreases for the PAHs on the  $C_{18}$  column with increasing concentration of  $\beta$ -CD. For example, the  $k'$  value of naphthalene changed from 3.51 with no  $\beta$ -CD in the mobile phase to 3.15 with 2.5 mM  $\beta$ -CD in the methanol–water (65:35) mobile phase. These results indicated that weak inclusion complexes were formed and that the uncomplexed PAHs interacted readily with the hydrocarbonaceous ligand of the stationary phase. The small change in the  $k'$  values was essentially the same for all the PAHs investigated. Pyrene had a long retention time with a methanol–water (65:35) mobile phase, and its chromatographic band was much broader compared to the other PAHs investigated. Pyrene only partially fits into the cavity of  $\beta$ -CD<sup>23</sup>, and thus  $\beta$ -CD would have little influence on its retention under the experimental conditions used in this work.

Quinoline and isoquinoline showed little change in  $k'$  values with the addition of  $\beta$ -CD to the mobile phase. Also, addition of  $\beta$ -CD caused the bands to broaden to some extent. The broadening of the bands with the addition of  $\beta$ -CD could possibly be explained by an increased interaction between the nitrogen atom of the solute with residual silanol groups of the stationary phase<sup>24</sup>. However, additional work is needed to substantiate this. The broad bands and small  $k'$  values for quinoline and isoquinoline indicated that they did not form strong complexes with  $\beta$ -CD. The  $k'$  value for quinoline in the absence of  $\beta$ -CD was 1.36, whereas with 2.5 mM  $\beta$ -CD present it was 1.24. B(f)Q and B(h)Q gave well-defined chromatographic bands, although  $\beta$ -CD had little effect on the  $k'$  values for B(f)Q and B(h)Q. This indicates that these nitrogen heterocycles interacted with C<sub>18</sub> more readily than with  $\beta$ -CD. For example, B(f)Q had a  $k'$  value of 3.13 with no  $\beta$ -CD, but a  $k'$  value of 3.01 with 2.5 mM  $\beta$ -CD.

The retention characteristics of thirteen hydroxyl aromatics over a wide range of methanol–water compositions with different concentrations of  $\beta$ -CD were also studied (Table I). This class of compounds showed much greater changes in  $k'$  values than the PAHs and nitrogen heterocycles. In fact, several of the hydroxyl aromatics showed rather dramatic changes in  $k'$  values as a function of  $\beta$ -CD concentration. Table II lists the capacity factors of the solutes in methanol–water (40:60) on a C<sub>18</sub> column at 25°C with different amounts of  $\beta$ -CD. Fig. 2 shows the effect of  $\beta$ -CD on the retention of 2-, 3- and 4-phenylphenol and indicates that addition of  $\beta$ -CD to the mobile phase causes a substantial decrease in the retention of all three solutes. The relatively large changes in  $k'$  values occur because of the formation of strong inclusion complexes between the  $\beta$ -CD and the hydroxyl aromatics, and thus the solutes interact less with the hydrocarbonaceous ligand of the stationary phase.

TABLE II

$k'$  VALUES OF HYDROXYL AROMATIC COMPOUNDS FOR METHANOL–WATER (40:60) WITH DIFFERENT CONCENTRATIONS (mM) OF  $\beta$ -CD

The names and structures of the compounds are given in Table I.

Solute	$\beta$ -CD (mM)					
	0.0	1.0	2.0	3.0	4.0	5.0
10	0.732	0.682	0.651	0.624	0.544	0.530
11	0.496	0.450	0.422	0.395	0.337	0.330
12	4.33	4.06	3.96	3.73	3.46	3.40
13	9.98	8.64	7.70	6.74	5.94	5.47
14	4.37	4.06	3.91	3.63	3.32	3.22
15	5.35	4.86	4.56	4.11	3.70	3.50
16	9.62	9.06	8.86	8.42	7.92	7.69
17	5.90	3.61	2.74	2.14	1.71	1.45
18	11.64	10.04	8.99	7.98	7.06	6.50
19	10.18	9.05	8.34	7.55	6.82	6.35
20	22.95	20.14	18.28	16.39	14.72	13.65
21	25.89	19.23	15.30	12.47	10.36	9.02
22	25.40	17.49	13.34	10.57	8.56	7.40

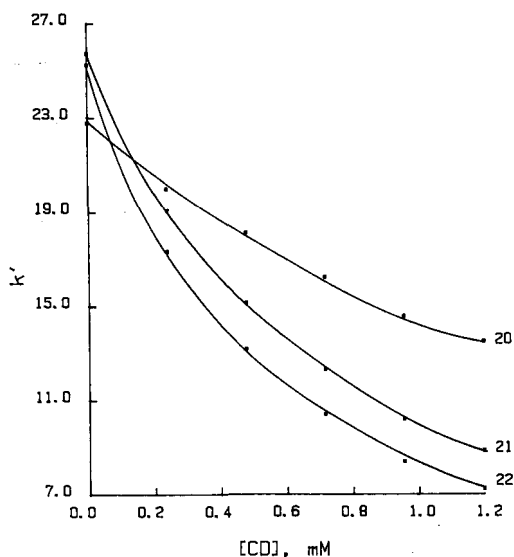


Fig. 2. Plot of  $k'$  values vs. equilibrium of  $\beta$ -CD concentration for 2-phenylphenol (20), 3-phenylphenol (21) and 4-phenylphenol (22) with methanol-water (40:60).

#### *Dependence of $K_D$ values on the methanol content*

Eqn. 8 relates the capacity factor to the dissociation constant of the inclusion complex and the equilibrium concentration of  $\beta$ -CD and shows that a graph of  $1/k'$  vs.  $[(\text{CD})_m]$  would give a straight line with an intercept of  $1/k'_0$  and a slope of  $1/k'_0 K_D$ . Therefore,  $K_D$  values can be obtained by using eqn. 8. The linear relationship between  $1/k'$  and  $\beta$ -CD concentration also indicates a 1:1 ratio between the solute and  $\beta$ -CD<sup>20</sup>.

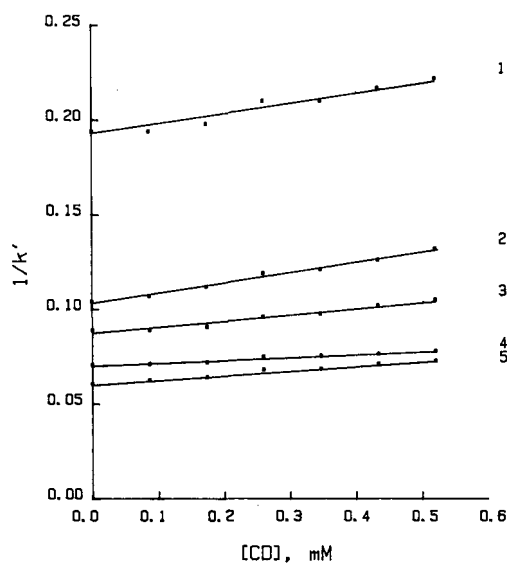


Fig. 3. Plot of  $1/k'$  vs. equilibrium of  $\beta$ -CD concentration for PAHs with methanol-water (60:40).

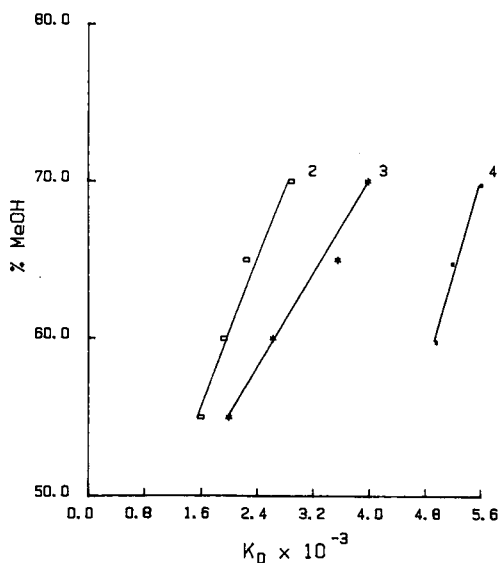
TABLE III

 $K_D$  ( $M$ ) VALUES OF PAHs FOR METHANOL-WATER MOBILE PHASES IN THE PRESENCE OF  $\beta$ -CD

Solute	Methanol-water				
	55:45	60:40	65:35	70:30	75:25
Naphthalene	$3.14 \cdot 10^{-3}$	$3.30 \cdot 10^{-3}$	$3.25 \cdot 10^{-3}$	$3.87 \cdot 10^{-3}$	$2.53 \cdot 10^{-3}$
Biphenyl	$1.62 \cdot 10^{-3}$	$1.95 \cdot 10^{-3}$	$2.27 \cdot 10^{-3}$	$2.91 \cdot 10^{-3}$	$2.12 \cdot 10^{-3}$
Acenaphthene	$2.02 \cdot 10^{-3}$	$2.65 \cdot 10^{-3}$	$3.57 \cdot 10^{-3}$	$4.00 \cdot 10^{-3}$	$2.99 \cdot 10^{-3}$
Phenanthrene	—	$4.88 \cdot 10^{-3}$	$5.11 \cdot 10^{-3}$	$5.52 \cdot 10^{-3}$	$3.33 \cdot 10^{-3}$
Anthracene	—	$2.58 \cdot 10^{-3}$	$3.38 \cdot 10^{-3}$	$4.20 \cdot 10^{-3}$	$2.50 \cdot 10^{-3}$

In addition, it is important to mention that the equilibrium concentration of  $\beta$ -CD should be used in obtaining  $K_D$  values rather than the analytical concentration of  $\beta$ -CD. This is because the effect of methanol interaction with  $\beta$ -CD can be substantial due to the large amount of methanol present in the mobile phase. For example, a methanol-water (75:25) mobile phase is 18.4  $M$  in methanol.

Fig. 3 shows the linear relationships between  $1/k'$  values and the equilibrium concentration of  $\beta$ -CD for the PAHs, investigated with methanol-water (60:40). The equilibrium concentrations of  $\beta$ -CD were calculated from eqn. 11. The slopes of these lines were small, indicating that  $\beta$ -CD concentration had little effect on the retention of the solutes. The nitrogen heterocycles showed fairly good linear relationships between  $1/k'$  and  $\beta$ -CD concentration. However, as stated above, the change in  $k'$  values was even smaller than for PAHs. Table III lists dissociation constants of the inclusion complexes of the PAH model compounds obtained from eqn. 8 for several different methanol-water compositions. Table III shows that by increasing the methanol

Fig. 4. Plot of percentage of methanol vs.  $K_D$  values for PAHs with methanol-water.

concentration in the mobile phase from 55 to 70%, the dissociation constants of PAHs increase. Thus, the higher the methanol content, the weaker the association of the solute with  $\beta$ -CD. The methanol concentration in the mobile phase as a function of the dissociation constant in the range of 55–70% methanol is shown in Fig. 4 for biphenyl, acenaphthene and phenanthrene. Naphthalene and anthracene also showed the same general trend. As Fig. 4 shows, there is an approximate linear relationship between methanol concentration and  $K_D$  values of 55–70% methanol. However, the 75% methanol data points did not fall near the lines (Table III). It is possible that another mechanism is operative at 75% methanol. Additional information is needed to explain the results at 75% methanol.

Linear relationships were also found for  $1/k'$  vs. the equilibrium concentration of  $\beta$ -CD for the hydroxyl aromatics. The largest slope in this series of compounds was obtained for the hydroxyl aromatics in methanol–water (30:70) and the smallest slope was obtained in methanol–water (60:40). Fig. 5 illustrates the linear relationships between  $1/k'$  and equilibrium concentration of  $\beta$ -CD for some of the hydroxyl compounds in methanol–water (40:60). Table IV lists the dissociation constants for the hydroxyl compounds in different methanol–water mobile phases at 25°C. Table IV shows that with the addition of the methanol to the mobile phase the  $K_D$  values generally become larger, except for the two dihydroxybenzene compounds. The increasing methanol content causes more competition between the solute and the methanol for binding to the  $\beta$ -CD, even though methanol binds relatively weakly to  $\beta$ -CD<sup>22</sup>. As a result, the inclusion complex of the solute is dissociated to a greater extent in stronger mobile phases. Fig. 6 shows typical relationships between  $K_D$  and methanol concentration for two hydroxyl aromatics. These graphs contrast with the graphs for PAHs in Fig. 4. This is probably related to the much smaller changes in  $k'$  values for PAH compared to hydroxyl aromatics. Table V lists typical intercepts,

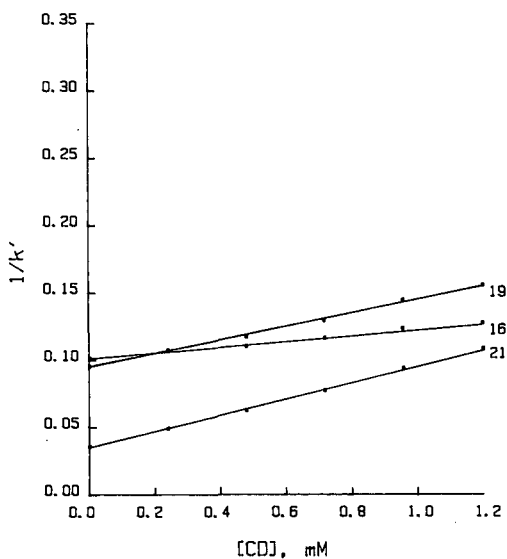


Fig. 5. Plot of  $1/k'$  vs. equilibrium values of  $\beta$ -CD concentration for 2-naphthol (19), *o,o'*-biphenol (16) and 3-phenylphenol (21) with methanol–water (40:60).



TABLE IV

 $K_D$  ( $M$ ) VALUES OF HYDROXYL AROMATICS FOR METHANOL-WATER MOBILE PHASES IN THE PRESENCE OF  $\beta$ -CD

See Table I for the names and structures of the compounds.

Solute	Methanol-water			
	30:70	40:60	50:50	60:40
10	$3.76 \cdot 10^{-3}$	$3.01 \cdot 10^{-3}$	$1.75 \cdot 10^{-3}$	$8.65 \cdot 10^{-3}$
11	$2.42 \cdot 10^{-3}$	$2.24 \cdot 10^{-3}$	$1.08 \cdot 10^{-3}$	$3.27 \cdot 10^{-3}$
12	$4.10 \cdot 10^{-3}$	$4.20 \cdot 10^{-3}$	$3.74 \cdot 10^{-3}$	$7.06 \cdot 10^{-3}$
13	$1.07 \cdot 10^{-3}$	$1.41 \cdot 10^{-3}$	$1.95 \cdot 10^{-3}$	$3.27 \cdot 10^{-3}$
14	$2.18 \cdot 10^{-3}$	$3.24 \cdot 10^{-3}$	$3.21 \cdot 10^{-3}$	$4.43 \cdot 10^{-3}$
15	$1.52 \cdot 10^{-3}$	$2.17 \cdot 10^{-3}$	$2.57 \cdot 10^{-3}$	$3.62 \cdot 10^{-3}$
16	$3.98 \cdot 10^{-3}$	$4.75 \cdot 10^{-3}$	$4.57 \cdot 10^{-3}$	$7.70 \cdot 10^{-3}$
17	$1.66 \cdot 10^{-4}$	$4.10 \cdot 10^{-4}$	$7.94 \cdot 10^{-4}$	$1.90 \cdot 10^{-3}$
18	$8.89 \cdot 10^{-4}$	$1.49 \cdot 10^{-3}$	$2.24 \cdot 10^{-3}$	$3.88 \cdot 10^{-3}$
19	$1.25 \cdot 10^{-3}$	$1.93 \cdot 10^{-3}$	$2.58 \cdot 10^{-3}$	$4.27 \cdot 10^{-3}$
20	$1.05 \cdot 10^{-3}$	$1.74 \cdot 10^{-3}$	$2.52 \cdot 10^{-3}$	$4.72 \cdot 10^{-3}$
21	$2.18 \cdot 10^{-4}$	$6.18 \cdot 10^{-4}$	$1.17 \cdot 10^{-3}$	$2.38 \cdot 10^{-3}$
22	$2.95 \cdot 10^{-4}$	$4.72 \cdot 10^{-4}$	$9.27 \cdot 10^{-4}$	$1.95 \cdot 10^{-3}$

slopes and correlation coefficients of the hydroxyl compounds with methanol-water (40:60). The correlation coefficients indicate good linearity between  $1/k'$  and  $\beta$ -CD concentration, showing that 1:1 complexes were formed.

As discussed in the derivation of eqn. 8, it was assumed that the interaction of the CD · S complex with the stationary phase was negligible. The linear relationship obtained from the  $1/k$  vs.  $[(CD)_m]$  graphs support this view for the compounds

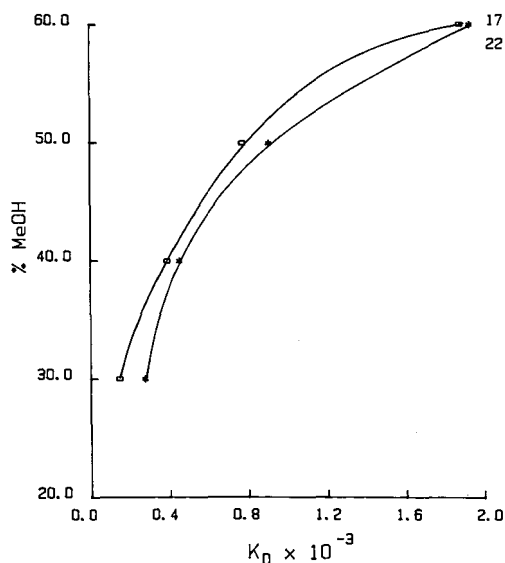
Fig. 6. Plot of percentage of methanol vs.  $K_D$  values for  $p,p'$ -biphenol (17) and 4-phenylphenol (22).

TABLE V  
SLOPE, INTERCEPT AND CORRELATION COEFFICIENT VALUES OF HYDROXYL AROMATICS FOR METHANOL-WATER (40:60) WITH  $\beta$ -CD

See Table I for the names and structures of the compounds.

Solute	Intercept	Slope	Correlation coefficient
10	1.35	0.449	0.976
11	1.99	0.889	0.981
12	0.230	0.548	0.988
13	0.0988	0.0702	0.999
14	0.228	0.0703	0.992
15	0.184	0.0847	0.995
16	0.104	0.0219	0.996
17	0.174	0.424	0.999
18	0.0853	0.0574	0.998
19	0.0973	0.0504	0.999
20	0.0434	0.0250	0.999
21	0.0376	0.0608	0.999
22	0.0381	0.0807	0.999

investigated. However, there is the possibility that the CD · S complex could interact with the stationary phase, and the mechanism is more complex. By using an equation proposed by Zukowski *et al.*<sup>19</sup>, in which the distribution of the CD · S complex between the stationary and mobile phase was taken into consideration, very little of our experimental data could be fitted to this equation. The data from the phenylphenols though did correlate reasonably well with the equation considered by Zukowski *et al.*<sup>19</sup>. These results suggest that the CD · S complexes of the phenylphenols interacted with the stationary phase. More work would be needed to establish the extent to which the CD · S complexes interacted with the stationary phase.

#### *Effect of ethanol content on the retention of hydroxyl compounds*

The model compounds investigated with ethanol-water mobile phases were 1- and 2-naphthol, 2-, 3- and 4-phenylphenol. Ethanol-water mobile phases were investigated because ethanol forms a stronger complex with  $\beta$ -CD than does methanol. The formation constant for ethanol with  $\beta$ -CD has been reported as  $0.93 M^{-1}$  and for methanol  $0.32 M^{-1}$  (ref. 22). The retention characteristics of the solutes were obtained in different ethanol-water mixtures in the presence of increasing amounts of  $\beta$ -CD. The ethanol-water mixtures used were 35:65, 40:60, 45:55 and 50:50. Table VI gives the capacity factors of the compounds in ethanol-water (40:60). The overall change in  $k'$  values with the addition of  $\beta$ -CD was less than that for methanol-water (40:60) for any given solute. Graphs of  $1/k'$  vs.  $\beta$ -CD concentration gave fairly good linear relationships. However, the correlation coefficients indicated that better linearity was obtained with methanol-water than that with ethanol-water.

The dissociation constants of the inclusion complexes of the compounds for ethanol-water compositions are listed in Table VII. It shows that the  $K_D$  values depend upon the ethanol content in the mobile phase. By comparing the  $K_D$  values of the inclusion complexes for methanol-water (40:60) with the corresponding  $K_D$  values for

TABLE VI

$k'$  VALUES OF SEVERAL HYDROXYL AROMATICS FOR ETHANOL-WATER (40:60) IN THE PRESENCE OF DIFFERENT CONCENTRATIONS (mM) OF  $\beta$ -CD

See Table I for the names and structures of the compounds.

Solute	$\beta$ -CD (mM)					
	0.0	1.0	2.0	3.0	4.0	5.0
18	5.20	4.73	4.58	4.22	4.20	3.97
19	4.37	3.91	3.86	3.54	3.51	3.36
20	8.43	7.70	7.55	7.05	7.09	6.61
21	8.48	7.55	7.22	6.54	6.40	5.86
22	8.47	7.35	7.01	6.18	5.92	5.36

TABLE VII

$K_D$  VALUES (M) OF THE HYDROXYL COMPOUNDS FOR ETHANOL-WATER IN THE PRESENCE OF  $\beta$ -CD

See Table I for the names and structures of the compounds.

Solute	Ethanol-water			
	35:65	40:60	45:55	50:50
18	$1.86 \cdot 10^{-3}$	$2.32 \cdot 10^{-3}$	$2.18 \cdot 10^{-3}$	$1.53 \cdot 10^{-3}$
19	$2.17 \cdot 10^{-3}$	$2.46 \cdot 10^{-3}$	$2.48 \cdot 10^{-3}$	$1.63 \cdot 10^{-3}$
20	$2.31 \cdot 10^{-3}$	$2.83 \cdot 10^{-3}$	$2.82 \cdot 10^{-3}$	$1.84 \cdot 10^{-3}$
21	$1.12 \cdot 10^{-3}$	$1.61 \cdot 10^{-3}$	$1.98 \cdot 10^{-3}$	$1.71 \cdot 10^{-3}$
22	$8.28 \cdot 10^{-4}$	$1.22 \cdot 10^{-3}$	$1.56 \cdot 10^{-3}$	$1.38 \cdot 10^{-3}$

ethanol-water (40:60) (Tables IV and VII), it can be concluded that the solutes associate with the  $\beta$ -CD cavity more readily in methanol-water than that in the corresponding ethanol-water mixtures. A similar comparison of methanol-water with ethanol-water at 50:50 shows that the  $K_D$  values are greater in methanol-water for compounds 18, 19 and 20, but the  $K_D$  values for compounds 21 and 22 are smaller than the  $K_D$  in ethanol-water (Tables IV and VII). Generally more stable inclusion complexes were obtained in methanol-water mixture than that in ethanol-water. However, as discussed above, there are exceptions to this.

#### Structural features

The dissociation constants can be considered as a measure of how tightly a solute fits inside the  $\beta$ -CD cavity. They also indicate the importance of the molecular structure in determining whether the solute fits into the  $\beta$ -CD cavity. Table IV shows that the  $K_D$  value of *o,o'*-biphenol is greater than that of *p,p'*-biphenol in methanol-water (30:70), namely,  $3.98 \cdot 10^{-3}$  and  $1.66 \cdot 10^{-4}$ , respectively. This was the case for all of the methanol-water mixtures investigated for these two compounds. The  $K_D$  values of *o,o'*- and *p,p'*-biphenol showed that *p,p'*-biphenol fits more readily into the  $\beta$ -CD cavity than *o,o'*-biphenol. The comparison between  $K_D$  values of 1- and 2-naphthol

shows that the  $K_D$  value of 2-naphthol is larger than that of 1-naphthol. If the two compounds were to approach the  $\beta$ -CD cavity from their wide sides, there would be more steric hindrance for 2-naphthol in forming an inclusion complex with  $\beta$ -CD than for 1-naphthol. Table IV shows that the  $K_D$  values for 2-naphthol are greater than those for 1-naphthol. Thus, steric considerations are more important for 2-naphthol. 4-Phenylphenol gave smaller  $K_D$  values than 2-phenylphenol (Table IV). This result indicates the importance of the spatial geometry of solutes in forming an inclusion complex. 4-Phenylphenol fits more readily into the  $\beta$ -CD cavity than 2-phenylphenol because the hydroxyl functionality is in the *para* position, causing less hindrance than in the case where the hydroxyl group is in the *ortho* position. For 3-phenylphenol the  $K_D$  values are greater than the  $K_D$  values for 4-phenylphenol, except in the methanol–water (30:70) mobile phase. These data again indicate the importance of steric factors.

Fig. 2 and Table II illustrate that among the phenylphenols, 4-phenylphenol shows very large changes in  $k'$  values. From 0.0 to 5.0 mM  $\beta$ -CD, the  $\Delta k'$  was 18.0 units. On the other hand, 3-phenylphenol gave a  $\Delta k'$  of 16.9, and 2-phenylphenol showed a relatively smaller change in  $k'$  values with a  $\Delta k'$  of 9.3. The  $\Delta k'$  values show that 4-phenylphenol fits in the cavity of  $\beta$ -CD more completely than 3- and 2-phenylphenol. As another example, *o,o'*-biphenol had a  $\Delta k'$  of 1.93, whereas *p,p'*-biphenol gave a  $\Delta k'$  of 4.45 (Table II). Thus, *p,p'*-biphenol fits more effectively into the  $\beta$ -CD cavity than *o,o'*-biphenol. The relatively smaller changes in  $k'$  values for 2-phenylphenol and *o,o'*-biphenol are most likely due to the positions of the hydroxyl groups in the molecules. The position of the hydroxyl groups would not permit these compounds to fit as readily into the  $\beta$ -CD cavity as the compounds with hydroxyl groups in the *para* positions. The  $\Delta k'$  for 1-naphthol was 5.14, and for 2-naphthol it was 3.83 (Table II). This showed that 1-naphthol fits into  $\beta$ -CD more completely than 2-naphthol. 1,3-Dihydroxybenzene showed a  $\Delta k'$  of 0.20 in methanol–water (40:60), and for 1,4-dihydroxybenzene the  $\Delta k'$  was 0.17 (Table II). Because of the small changes in  $k'$  values for these two compounds, they did not interact readily with the  $\beta$ -CD. These two compounds are small relative to the size of the  $\beta$ -CD cavity and would not fit tightly into the  $\beta$ -CD cavity. The number of polar groups in the solute also affects the capacity factors. For instance, 2,3-dihydroxynaphthalene showed a  $\Delta k'$  value of 1.85, while 1-naphthol had a  $\Delta k'$  of 5.14. This implies that 1-naphthol fits in the cavity more tightly than 2,3-dihydroxynaphthalene.

The nature of the binding forces for the formation of an inclusion complex is not completely understood. Some researchers believe that London dispersion forces between guest and host molecules are a major driving force in the formation of an inclusion complex<sup>25</sup>. However, others believe that hydrogen bonding between the guest and the hydroxyl groups of CDs is important<sup>1,2</sup>. The release of high-energy water molecules or release of strain in the macromolecular ring of CDs are also considered to be important<sup>1,2</sup>. Some insights into the interactions in inclusion complex formation can be obtained by comparing  $K_D$  values. For convenience, the  $K_D$  values of several hydroxyl aromatics, naphthalene and biphenyl are compared in Table VIII. Biphenyl, 4-phenylphenol and *p,p'*-biphenol have essentially the same dissociation constants in methanol–water (60:40). This implies that hydrogen bonding is not very important in the formation of an inclusion complex for these compounds. If hydrogen bonding were a major driving force, the dissociation constants would most likely

TABLE VIII

$K_D$  VALUES ( $M$ ) OF SEVERAL COMPOUNDS FOR METHANOL-WATER (60:40) IN THE PRESENCE OF  $\beta$ -CD

Solute	$K_D$	Solute	$K_D$
Biphenyl	$1.95 \cdot 10^{-3}$	<i>p,p'</i> -Biphenol	$1.90 \cdot 10^{-3}$
4-Phenylphenol	$1.95 \cdot 10^{-3}$	Naphthalene	$3.30 \cdot 10^{-3}$
3-Phenylphenol	$2.38 \cdot 10^{-3}$	1-Naphthol	$3.88 \cdot 10^{-3}$
2-Phenylphenol	$4.72 \cdot 10^{-3}$	2-Naphthol	$4.27 \cdot 10^{-3}$
<i>o,o'</i> -Biphenol	$7.70 \cdot 10^{-3}$		

decrease in going from biphenyl to 4-phenylphenol to *p,p'*-biphenol. As another example, naphthalene has a  $K_D$  value similar to the  $K_D$  values of 1- and 2-naphthol. However, if hydrogen bonding were important, a larger difference would be seen in the  $K_D$  values of 1- and 2-naphthol compared to naphthalene.

The same questions can be raised about compounds with the same, or essentially the same  $K_D$  values, but different  $k'$  values under the same chromatographic conditions. For example, 4-phenylphenol and biphenyl have the same  $K_D$  value in methanol-water (60:40), but different  $k'$  values in this mobile phase as the  $\beta$ -CD concentration increases. For example, in 1.5 mM  $\beta$ -CD with methanol-water (60:40), biphenyl has a  $k'$  of 8.3, whereas 4-phenylphenol has a  $k'$  of 2.5.  $K_D$  can be considered as a function of the ratio  $[(CD)_m]/[(CD \cdot S)_m]$  and  $[S_m]$ , showing that three concentration terms are involved. However, by rearranging eqn. 8, it can be solved for  $k'$ , and by multiplying the numerator and denominator by  $1/k'_0 K_D$ , one obtains

$$k' = \frac{1}{1/k'_0 + [(CD)_m]/k'_0 K_D} \quad (12)$$

Eqn. 12 shows that for two compounds at a fixed value of  $[(CD)_m]$  and with the same  $K_D$  value, the magnitude of  $k'_0$  will be a major factor in determining the value of  $k'$ . For example, the  $k'_0$  for 4-phenylphenol is 3.18 for a methanol-water (60:40) composition, whereas it is 9.40 for biphenyl. Thus, one would not expect the same change in  $k'$  for 4-phenylphenol as for biphenyl as the  $\beta$ -CD concentration changes. Obviously,  $k'$  is not just a function of  $K_D$ , as shown in eqn. 12.

## CONCLUSIONS

The retention properties of PAHs and nitrogen heterocycles were affected little by the presence of  $\beta$ -CD in the mobile phase, because the solutes interacted more readily with the stationary phase than with  $\beta$ -CD. However, the retention characteristics of most of the hydroxyl aromatics were affected significantly with  $\beta$ -CD as a mobile phase modifier, showing that  $\beta$ -CD could compete with the  $C_{18}$  column for the solute. The linear relationship obtained for  $1/k'$  vs.  $[\beta\text{-CD}]$  showed that 1:1 complexes were obtained between the solutes and  $\beta$ -CD.

Methanol-water was a better mobile phase than ethanol-water, because the chromatographic data were more reproducible and methanol-water permitted greater

selectivity to be achieved for the solutes. Ethanol competed somewhat more effectively for  $\beta$ -CD than did methanol, and this partly explains the better selectivity for methanol-water.

The structural features of the hydroxyl aromatics played an important part in determining whether the hydroxyl aromatics would interact strongly with  $\beta$ -CD. The  $K_D$  values for the hydroxyl aromatics and changes of  $k'$  values as a function of  $\beta$ -CD concentration were shown to be good indicators of which structural isomer would interact the strongest with  $\beta$ -CD. However, it was shown that  $K_D$  values alone could not be used to predict the change in  $k'$  values because  $k'$  is also a function of  $k'_0$  and  $[(CD)_m]$  at any given mobile phase composition.

#### ACKNOWLEDGEMENT

This research was supported partially by the U.S. Department of Energy under contract No. DE-AC22-83PC 60015.

#### REFERENCES

- 1 J. Szejtli, *Cyclodextrins and Their Inclusion Complexes*, Akademiai Kiado, Budapest, 1982.
- 2 M. L. Bender and M. Komiyama, *Cyclodextrin Chemistry*, Springer Verlag, New York, 1978.
- 3 D. W. Armstrong and W. DeMond, *J. Chromatogr. Sci.*, 22 (1984) 411.
- 4 M. A. Tarr, G. Nelson, G. Patonay and I. M. Warner, *Anal. Lett.*, 21 (1988) 843.
- 5 D. W. Armstrong, *J. Liq. Chromatogr.*, 3 (1980) 895.
- 6 W. L. Hinze and D. W. Armstrong, *Anal. Lett.*, 13 (1980) 1093.
- 7 J. Debowski, D. Sybilska and J. Jurczak, *J. Chromatogr.*, 237 (1982) 303.
- 8 J. Debowski, J. Jurczak and D. Sybilska, *J. Chromatogr.*, 282 (1983) 83.
- 9 M. Gazdag, G. Szepesi and L. Huszar, *J. Chromatogr.*, 351 (1986) 128.
- 10 M. Gazdag, G. Szepesi and L. Huszar, *J. Chromatogr.*, 436 (1988) 31.
- 11 D. W. Armstrong, F.-Y. He and S. M. Han, *J. Chromatogr.*, 448 (1988) 345.
- 12 D. Sybilska, J. Lipkowski and J. Woycikowski, *J. Chromatogr.*, 253 (1982) 95.
- 13 D. Sybilska, J. Debowski, J. Jurczak and J. Zukowski, *J. Chromatogr.*, 286 (1984) 163.
- 14 J. Debowski, G. Grassini-Strazza and D. Sybilska, *J. Chromatogr.*, 349 (1985) 131.
- 15 J. Debowski, J. Jurczak, D. Sybilska and J. Zukowski, *J. Chromatogr.*, 329 (1985) 206.
- 16 L. Bazant, M. Wurst and E. Smolkova-Keulemansova, *J. Chromatogr.*, 445 (1988) 337.
- 17 K. Uekama, F. Hirayama and T. Irie, *Chem. Lett.*, (1978) 661.
- 18 K. Uekama, F. Hirayama, S. Nasu, N. Matsuo and T. Irie, *Chem. Pharm. Bull.*, 26 (1978) 3477.
- 19 J. Zukowski, D. Sybilska and J. Jurczak, *Anal. Chem.*, 57 (1985) 2215.
- 20 K. Fujimura, T. Ueda, M. Kitagawa, H. Takayanagi and T. Ando, *Anal. Chem.*, 58 (1986) 2668.
- 21 B. Sebillé, N. Thaud, J. Piquion and N. Behar, *J. Chromatogr.*, 409 (1987) 61.
- 22 Y. Matsui and K. Mochida, *Bull. Chem. Soc. Jpn.*, 52 (1979) 2808.
- 23 K. Kano, I. Takenoshita and T. Ogawa, *J. Phys. Chem.*, 86 (1982) 1833.
- 24 M. A. Stadalius, J. S. Berus and L. R. Snyder, *LC · GC, Mag. Liq. Gas Chromatogr.*, 6 (1988) 494.
- 25 R. J. Bergeron, M. A. Channing, G. J. Gibely and D. M. Pillor, *J. Am. Chem. Soc.*, 99 (1977) 5146.

CHROM. 21 786

## REVERSED-PHASE ION-PAIR LIQUID CHROMATOGRAPHY OF GLUCURONIDES

### RETENTION AND SELECTIVITY

MORGAN STEFANSSON and DOUGLAS WESTERLUND\*

*Department of Analytical and Pharmaceutical Chemistry, Uppsala University Biomedical Center, P.O. Box 574, S-751 23 Uppsala (Sweden)*

---

#### SUMMARY

The parameters that influence the retention and selectivity of glucuronides in reversed-phase ion-pair liquid chromatography were investigated. The extent of ion-pair retention was dependent on the degree of substitution of the ammonium counter ion used and increased in the order 4- < 2- < 3- < 1-substituted, comparing counter ions with the same number of carbon atoms. The retentions and selectivities were influenced by the type of buffer system, solid phase and organic modifier used. The selectivities obtained were so high that a urine sample spiked with four glucuronides could be analysed by a direct injection technique and UV detection (254 nm).

---

#### INTRODUCTION

Glucuronides are metabolic conjugation reaction products<sup>1</sup>, *i.e.* phase II metabolites, and for a long time have been considered to be inactive end products. However, later work suggested<sup>1</sup> that some compounds do form pharmacologically active conjugates or may be hydrolysed to reform the active parent compound.

The glucuronic acid that is covalently coupled to the parent compound by UDP-glucuronyltransferases transforms the parent compound to a considerably more polar and also ionizable compound,  $pK_a$  3–4<sup>1</sup>, making bioanalysis more difficult.

By using a hydrophobic ammonium compound as counter ion<sup>2</sup>, the glucuronides can be retained as ion pairs in reversed-phase (RP) high-performance liquid chromatographic (HPLC) systems. This technique made the simultaneous and selective analysis of glucuronides and parent compounds possible when direct injections of incubated homogenates (liver microsomes) and UDP-glucuronyltransferase preparations were performed<sup>3</sup>.

In this study, the retention and selectivity of glucuronides and parent compounds were investigated using different organic modifiers and solid phases. The character of the buffer system and the amine used as counter ion were shown to be efficient parameters in the regulation of retention and selectivity. By choosing appropriate conditions, direct injection of a spiked urine sample for UV detection of four glucuronides was possible.

## EXPERIMENTAL

*Instrumentation*

An Altex Model 100 A HPLC pump, Rheodyne 7125 injector with a 20- $\mu$ l loop, Waters Assoc. Model 440 UV detector, Kipp & Zonen BD 40 recorder and HETO Type 02 PT 923 water-bath (Birkerød, Denmark) for thermostating the chromatographic system were used. The pH measurements were made with a Metrohm (Herisau, Switzerland) 632 pH meter.

*Chemicals and solid phases*

2-Aminophenyl- $\beta$ -D-glucuronide, 4-nitrophenyl- $\beta$ -D-glucuronide, phenyl- $\beta$ -D-glucuronide, 2-aminophenol, 4-nitrophenol and 2-(N-morpholino)ethanesulphonic acid were obtained from Sigma (St. Louis, MO, U.S.A.). All other chemicals were of HPLC or analytical-reagent grade and were used without further purification.

The column packings were Partisil-10 ODS (10  $\mu$ m), 5% carbon loading (Whatman, Maidstone, U.K.), TSK-gel LS 410 (5  $\mu$ m), 24% carbon loading (Toyo Soda, Tokyo, Japan), Nucleosil C<sub>18</sub> (5  $\mu$ m), 14.5% carbon loading, Nucleosil CN (10  $\mu$ m) (Machery-Nagel, Düren, F.R.G.), and PRP-1 (10  $\mu$ m) (Hamilton, Bonaduz, Switzerland).

*Column preparation and chromatographic conditions*

The TSK-gel, Partisil-10 ODS, Nucleosil C<sub>18</sub> and CN were packed into stainless-steel columns (50  $\times$  4.6 mm I.D.) with a slurry medium containing methanol-propanol (6:4, v/v), followed by 200 ml of methanol. The PRP-1 column was packed with a slurry medium containing 2.5% sodium chloride, 10% glycerol and a small amount of acetone in water, followed by 200 ml of slurry medium and 100 ml of water. The column dimensions were 100  $\times$  4.6 mm I.D.

Prior to analysis, the systems were equilibrated with at least 100 ml of mobile phase. The mobile phases were prepared by dissolving the counter ion, as base or salt, in the organic modifier. The buffer phase and organic modifier were then mixed together and degassed in an ultrasonic bath. The mobile phase flow-rate was 1.0 ml/min at 25.0°C (thermostated water-bath). The volume of the mobile phase in the column,  $V_m$ , was obtained from the front disturbance in the chromatogram by injection of water and monitoring the UV signal at 254 nm. The capacity ratio,  $k'$ , was calculated from  $k' = (V_r - V_m)/V_m$ , where  $V_r$  is the retention volume. The solutes were dissolved in deionized water (Millipore) and stored at -20°C before analysis.

*Retention models*

In this study it is assumed that the general retention models evaluated according to the ion-pair adsorption mechanism<sup>2</sup> are valid. No efforts have been made to calculate the equilibrium constants involved, the reason being that in most experiments the data points are too few in relation to the large number of constants present in the equations. The qualitative discussions are based on the following equations:

Uncharged solute (S):

$$k'_S = \frac{qK^0K_D}{1 + K_{BO}[B^-][Q^+]} \quad (1)$$



Anion ( $G^-$ ):

$$k_{G^-} = \frac{qK^0[K_D a_H + K_{GQ}[Q^+][K'_a]}{(K'_a + a_H)(1 + K_{BQ}[B^-][Q^+])} \quad (2)$$

Cation ( $HA^+$ ):

$$k'_{HA^+} = \frac{qK^0 [K_D K'_a + K_{HAB}[B^-]a_H]}{(K'_a + a_H)(1 + K_{BQ}[B^-][Q^+])} \quad (3)$$

Zwitterion ( $^+Z^-$ ):

$$k'_{+z^-} = \frac{qK^0 K_{BZQ}[B^-][Q^+]}{1 + K_{BQ}[B^-][Q^+]} \quad (4)$$

The retention of a zwitterion will change with pH. At low pH it will distribute as cationic solute (eqn. 3), whereas at high pH it becomes anionic (eqn. 2).

In these equations:

$K^0$  = capacity of the solid phase;

$q$  = phase ratio (the ratio of the solid phase in grams to the volume of the mobile phase in millilitres);

$K_D$  = distribution constant for an uncharged solute;

$K_{GQ}$  = stoichiometric distribution constant for the ion pair;

$K_{BQ}$  = stoichiometric distribution constant for the ion pair of an anionic buffer component and an ammonium counter ion;

$K_{HAB}$  = stoichiometric distribution constant for the ion pair of a cationic solute and an anionic buffer component;

$K_{BZQ}$  = stoichiometric distribution constant for the ion-pair complex of zwitterionic solute, ammonium cation and anionic buffer component;

$K'_a$  = acid dissociation constant;

$a_H$  = hydrogen activity

The equations are valid on the assumptions that (i) a linear distribution isotherm, *i.e.*, a constant capacity factor independent of concentration, prevails, (ii) a zwitterionic solute distributes as an ion pair, not as uncharged species, and (iii) the solid phase has one active site of adsorption.

## RESULTS AND DISCUSSION

### *Influence of pH*

In Fig. 1 the logarithm of the retention is plotted *versus* pH for three glucuronides differing in character by the substituents on the phenyl ring. At low pH two of the glucuronides are retained as uncharged acids (eqn. 1), but as the pH is increased the retention increases as the glucuronides become charged and they are retained as ion pairs (eqn. 2) with dodecylethyldimethylammonium (DDEDA). The additional decrease in retention at low pH for 2-aminophenyl- $\beta$ -D-glucuronide is caused by the protonation of the aromatic amino function ( $pK'_a \approx 5$ ) (*cf.*, eqn. 3). The

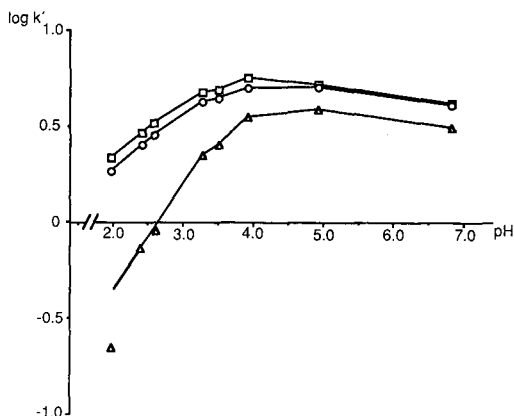


Fig. 1. Log  $k'$  versus pH. Column, TSK-Gel  $C_{18}$  ( $5 \mu\text{m}$ ),  $50 \times 4.6$  mm I.D.; mobile phase, phosphate buffer ( $\mu = 0.1$ ), 50% (v/v) methanol and 20.0 mM DDEDA-Br.  $\circ$  = Phenyl- $\beta$ -D-glucuronide;  $\triangle$  = 2-aminophenyl- $\beta$ -D-glucuronide;  $\square$  = 4-nitrophenyl- $\beta$ -D-glucuronide.

slight decrease in retention with increasing pH ( $> 5$ ) is probably caused by the change in buffer composition with pH. At higher pH a higher concentration of divalent phosphate anion will be present. This anion may compete more efficiently for the hydrophobic counter ion than the monovalent ion (see *Influence of buffer components in the mobile phase*, below).

#### *Influence of organic modifier*

The retention and the selectivity (defined as the ratio  $k'_{\text{parent compound}} : k'_{\text{glucuronide}}$ ) of glucuronides and their parent compounds were investigated using methanol, acetonitrile and tetrahydrofuran as organic modifiers (Table I). The percentage of organic modifier were chosen in order to give about the same magnitude of the capacity ratios. The influence on the selectivity differs depending on the structure of the parent compound. For the simple monoprotolytic compounds, phenol and

TABLE I

#### INFLUENCE OF ORGANIC MODIFIER

Column, Nucleosil  $C_{18}$  ( $5 \mu\text{m}$ ),  $50 \times 4.6$  mm I.D.; mobile phase: phosphate buffer (pH 4.95,  $\mu = 0.1$ ), 20.0 mM DDEDA and modifier [methanol, acetonitrile (ACN) or tetrahydrofuran (THF)].

Substrate	50% Methanol		25% ACN		22% THF	
	$k'$	$\alpha^a$	$k'$	$\alpha^a$	$k'$	$\alpha^a$
Phenyl- $\beta$ -D-glucuronide	5.21	0.58	4.79	1.23	3.73	2.64
Phenol	3.01		5.90		9.83	
2-Aminophenyl- $\beta$ -D-glucuronide	3.93	0.32	3.37	0.56	2.96	0.93
2-Aminophenol	1.25		1.88		2.75	
4-Nitrophenyl- $\beta$ -D-glucuronide	5.28	1.14	7.50	1.84	9.44	2.64
4-Nitrophenol	6.04		13.8		24.9	

<sup>a</sup>  $\alpha = k'_{\text{parent compound}}/k'_{\text{glucuronide}}$

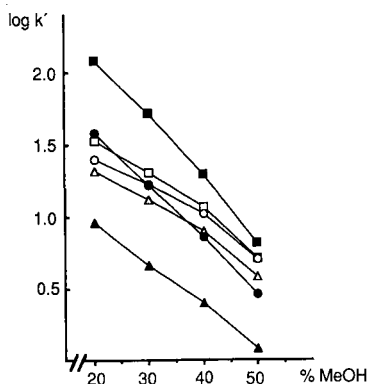


Fig. 2. Log  $k'$  versus methanol concentration. Column, TSK-Gel  $C_{18}$  ( $5 \mu\text{m}$ ),  $50 \times 4.6$  mm I.D.; mobile phase, phosphate buffer (pH 4.95,  $\mu = 0.1$ ), 20.0 mM DDEDA-Br and methanol (MeOH).  $\circ$  = Phenyl- $\beta$ -D-glucuronide;  $\triangle$  = 2-aminophenyl- $\beta$ -D-glucuronide;  $\square$  = 4-nitrophenyl- $\beta$ -D-glucuronide;  $\bullet$  = phenol;  $\blacktriangle$  = 2-aminophenol;  $\blacksquare$  = 4-nitrophenol.

4-nitrophenol, the selectivity increases on changing from methanol to acetonitrile to tetrahydrofuran.

This indicates that a hydrogen-accepting solvent is to be preferred when a high selectivity is needed for such compounds. On the other hand, for 2-aminophenol the selectivity decreases with a change in solvents in the same direction. However, using pH as a parameter, the selectivity can easily be modified. The retentions for the parent compounds and the 4-nitrophenyl- $\beta$ -D-glucuronide increase on changing the solvent from methanol to acetonitrile to tetrahydrofuran, whereas they decrease for the remaining two compounds.

No general guidelines can be drawn from these limited studies, but they indicate that each pair of compounds has to be studied separately regarding retention and selectivity effects.

As expected, the retentions of all the compounds decrease with increasing concentration of methanol in the mobile phase (Fig. 2), but there are no linear relationships. For the phenol pair there is even a retention reversal at methanol concentrations higher than 30% when the glucuronide has the highest retention. This is another illustration of the complex retention mechanism, which is to be expected considering the many equilibria prevailing in systems of this kind. A change in the concentration of the organic modifier in the mobile phase leads to several changes. When the concentration of methanol is increased, there is a non-linear decrease in the adsorption of a quaternary ammonium counter ion<sup>4</sup>, and there is also a non-linear increase in the solvating ability of the mobile phase. Recent studies<sup>5</sup> on solute retention in methanol–water mixtures showed that the “free” (*i.e.*, not associated with water) methanol concentration increases non-linearly with increasing methanol content. The relative adsorption of buffer components and solutes may change on increasing the content of organic modifier. Finally, the possibility of solutes being retained by more than one site of adsorption on the solid phase must be taken into account<sup>6</sup>. With this background, it is obvious that a linear relationship between  $k'$  and the concentration of organic modifier in the mobile phase is not to be expected in this kind of system.

TABLE II  
INFLUENCE OF SOLID PHASE

Mobile phase, phosphate buffer (pH 4.95,  $\mu = 0.1$ ), 20.0 mM DDEDA and 50% (v/v) methanol.

Substrate	Nucleosil-CN <sup>a</sup>		PRP-1		Partisil ODS <sup>b</sup>		Nucleosil C <sub>18</sub> <sup>c</sup>		TSK-GEL <sup>d</sup>	
	k'	$\alpha$	k'	$\alpha$	k'	$\alpha$	k'	$\alpha$	k'	$\alpha$
Phenyl- $\beta$ -D-glucuronide	5.50	0.90	5.84	1.85	3.29	0.51	5.21	0.58	4.95	0.58
Phenol	4.94		10.8		1.68		3.01		2.90	
2-Aminophenyl- $\beta$ -D-glucuronide	4.58	0.56	4.32	0.73	2.73	0.32	3.93	0.32	3.80	0.32
2-Aminophenol	2.56		3.16		0.86		1.25		1.20	
4-Nitrophenyl- $\beta$ -D-glucuronide	9.41	1.34	9.42	3.60	3.41	1.40	5.28	1.14	5.10	1.31
4-Nitrophenol	12.6		33.9		4.77		6.04		6.68	

<sup>a</sup> 30% methanol.

<sup>b</sup> Carbon load 5%.

<sup>c</sup> Carbon load 14.5%.

<sup>d</sup> Carbon load 24%.

*Influence of the solid phase*

The retention and selectivity were investigated using different solid phases (Table II). The character of the solid phase may have an influence on many parameters involved in the retention eqns. 1–4: the capacity ( $K^0$ ), the equilibrium constants ( $K_{GQ}$ ,  $K_D$ , etc.) and the phase ratio ( $q$ ). The selectivities obtained for different carbon loadings (5, 14.5 and 24%) are fairly constant whereas the retentions increase up to the level of 14.5% (Nucleosil). A further increase in carbon content does not increase the retention except for 4-nitrophenol. The different solid phases were obtained from different suppliers and the methods used to produce the solid phases may differ, including the character of the basic silica used as raw material. However, non-derivatized silanol groups and steric hindrance may also play a part in the total retention<sup>7</sup>.

For the PRP-1 phase, which is highly hydrophobic and has  $\pi$ - $\pi$  interaction possibilities, the glucuronides are relatively less retained compared with their parent compounds. The cyano phase gave lower retentions in general, and the methanol concentration in the mobile phase had to be decreased. This might prove useful with a coupled column system, assuming that the glucuronide is retained on a precolumn of the nitrile type during the clean-up step and later transferred on-line to the analytical column by changing the mobile phase.

*Influence of buffer components in the mobile phase*

According to the retention models many parameters may influence the retention of solutes. For charged solutes a hydrophobic counter ion often dominates the retention. However, if its concentration is kept constant, other parameters such as the concentration of buffer components may have an influence on the retention. This is demonstrated in Fig. 3, where two commonly used buffer systems, citrate and phosphate, plus a zwitterionic buffer system, 2-(N-morpholino)ethanesulphonic acid (MES), were compared at pH 4.95. Phosphate and citrate had an ionic strength of 0.1, equivalent to 98.0 and 35.0 mM, respectively. MES was 50.0 mM and the pH was adjusted by addition of sodium hydroxide. There is a dramatic effect on glucuronide retention and the selectivity depending on the buffer used. The parent compounds are

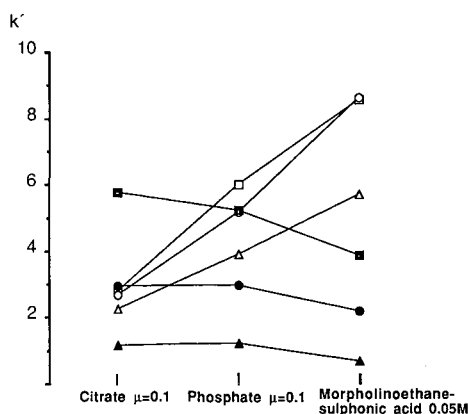


Fig. 3. Variation of  $k'$  with buffer system. Column, Nucleosil C<sub>18</sub> (5  $\mu$ m), 50  $\times$  4.6 mm I.D.; mobile phase, buffer (pH 4.95) in 50% (v/v) methanol and 20.0 mM DDEDA-Br. Solutes as in Fig. 2.

only slightly affected; MES buffer gives the lowest retentions. At this pH there are differences in the concentrations of the monovalent anions of citrate and phosphate and also MES, being 21.3, 97.5 and 3.0 mM, respectively.

The character and concentration of the buffer components determine their influence on the retention of the solutes. The citrate buffer, which gives the lowest retentions of the glucuronides, contains in addition to the monovalent anion about the same concentration of divalent anion. Divalent buffer ions may have a higher competing ability than a monovalent ion for the hydrophobic counter ion. Hence, the MES buffer exhibits the lowest competing ability and gives the highest retentions for the glucuronides. Undoubtedly, large selectivity differences can be obtained by choosing an appropriate buffer system, as will be demonstrated below.

#### *Influence of counter ion in the mobile phase*

In RP ion-pair LC the distribution of an ion pair is governed by its hydrophobicity and interaction with the solid phase. Ammonium compounds of similar size, but differing in carbon chains and substitution at the nitrogen, were compared as counter ions (Fig. 4). Clearly, the existence of one long chain favours retention rather than several short chains (compare decylamine, dipentylamine and tetrapropylammonium). Also, nonyltrimethylammonium gives a higher retention than tetrapropylammonium. Dimethyloctylamine and octylamine both have the same main chain but differ in nitrogen substitution. At 50 mM they give approximately the same retention for 2-aminophenyl- $\beta$ -D-glucuronide, although octylamine contains two carbons less and hence is less hydrophobic. Apparently, the increased polarity (low degree of substitution at the nitrogen) counteracts the decreased hydrophobicity by an increased interaction in ion-pair formation with the glucuronic moiety and/or the solid phase, probably by hydrogen bonding.

In order to obtain a high retention, the counter ion should be a primary amine with a long carbon chain. Unfortunately, the solubility in water-based mobile phases is

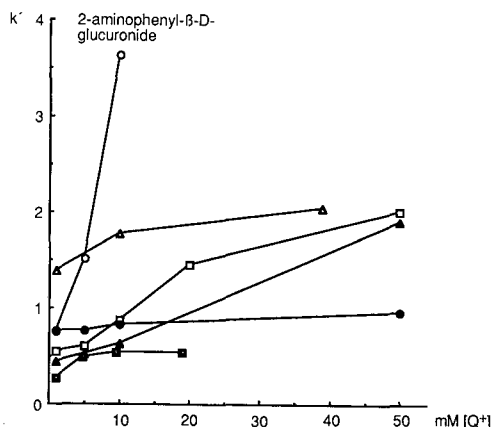


Fig. 4. Variation of  $k'$  for 2-aminophenyl- $\beta$ -D-glucuronide with  $Q^+$  concentration. Column, Nucleosil  $C_{18}$  (5  $\mu$ m), 50  $\times$  4.6 mm I.D.; mobile phase, phosphate buffer (pH 4.95,  $\mu = 0.1$ ), 25% (v/v) acetonitrile and  $Q$ .  $\circ$  = Decylamine  $\cdot$  HCl;  $\Delta$  = nonyltrimethylammonium  $\cdot$  Br;  $\square$  = dimethyloctylamine;  $\blacktriangle$  = octylamine  $\cdot$  HCl;  $\bullet$  = dipentylamine;  $\blacksquare$  = tetrapropylammonium  $\cdot$  OH.

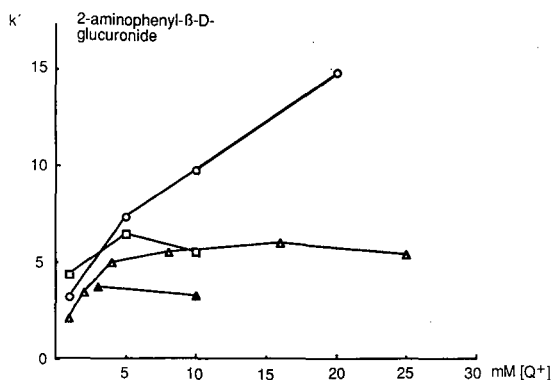


Fig. 5. As Fig. 4. ○ = Dodecylamine · HCl; □ = hexadecyltrimethylammonium · Br; △ = dimethyldodecylamine; ▲ = tetrahexylammonium · Br.

low for this kind of compound and further one long carbon chain favours micelle formation. Differently substituted ammonium compounds with as many methylene groups as possible preventing micelle formation were tested as counter ions (Fig. 5). Again, the primary amine, dodecylamine, gives the highest retention. Fig. 6 shows the retention for three glucuronides and their parent compounds when using dodecylamine in combination with the zwitterionic MES buffer, 40% methanol and 5% tetrahydrofuran as organic modifiers. The retention can be varied over a wide range and suitable selectivities can be selected by varying the counter-ion concentration. The parent compounds have all capacity factors below 4 at all dodecylamine concentrations.

#### Direct injection of spiked urine sample

A chromatogram from a direct injection of a urine sample, spiked with four

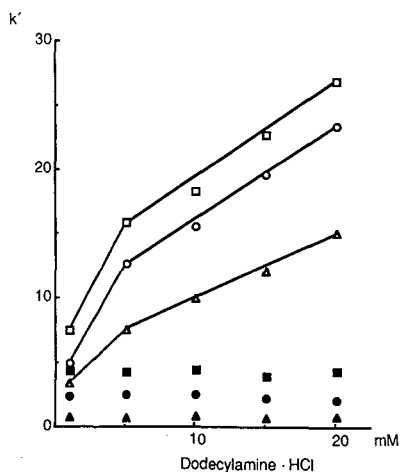


Fig. 6. Variation of  $k'$  with dodecylamine concentration. Column, Nucleosil  $C_{18}$  ( $5\ \mu\text{m}$ ),  $50 \times 4.6\ \text{mm}$  I.D.; mobile phase, MES buffer ( $0.05\ \text{M}$ , pH 4.95), 40% (v/v) methanol, 5% (v/v) tetrahydrofuran and dodecylamine · HCl. Solutes as in Fig. 2.

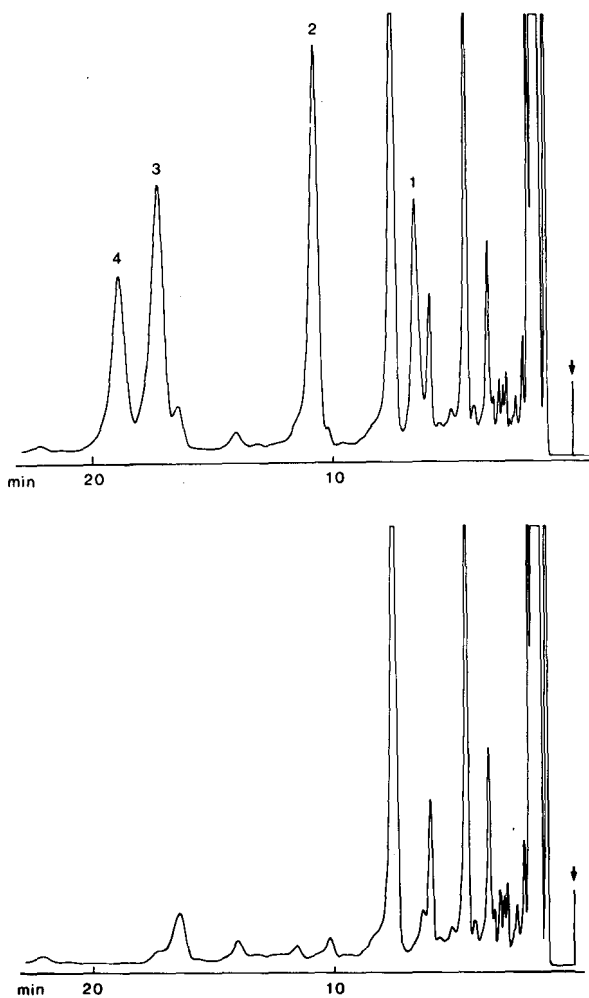


Fig. 7. Top chromatogram: 20- $\mu$ l injection of a spiked urine sample containing 12–40 nmol of each glucuronide. Bottom chromatogram: Blank urine sample. The urine was filtered and diluted 5-fold before analysis. Column, Nucleosil C<sub>18</sub> (5  $\mu$ m), 150  $\times$  4.6 mm I.D.; mobile phase, glycine buffer (0.05 M, pH 3.00), 50% (v/v) methanol and 20.0 mM dodecylamine  $\cdot$  HCl. UV detection at 254 nm. Peaks: 1 = 2-aminophenyl- $\beta$ -D-glucuronide; 2 = 8-hydroxyquinoline- $\beta$ -D-glucuronide; 3 = 4-nitrophenyl- $\beta$ -D-glucuronide; 4 = Phenyl- $\beta$ -D-glucuronide.

glucuronides, together with the blank urine sample is shown in Fig. 7. In this instance a pH of 3.0 was used to suppress the ionization of acids, present in the urine, with  $pK_a$  values of 4–5. The zwitterion glycine was used as the buffer system. The small glycine probably acts as a strong dipole<sup>8</sup> which, in combination with its polarity, should minimize competition on the solid phase. Even the highly polar and charged 2-aminophenyl- $\beta$ -D-glucuronide is well retained, showing the suitable selectivity obtained with this system.



## CONCLUSIONS

RP ion-pair LC of glucuronides has been shown to be considerably influenced by many parameters. Suitable retention and selectivity can be obtained by appropriate choices of the buffer system, organic modifier, pH, solid phase and concentration and character of the counter ion. Of the counter ions tested, dodecylamine exhibited the greatest influence on retention, but also the concentration of organic modifier in the mobile phase had a large effect. On direct injection of a urine sample spiked with four glucuronides, the pH could successfully be utilized to suppress the ionization of endogenous acids present, hence improving the glucuronide selectivity. Character, concentration and charge are distinctive features for the choice of the buffer system. The introduction of zwitterionic buffer components decreased the competition for the counter ions, thereby promoting the ion-pair formation and retention of an anionic solute. When using coupled columns, a less hydrophobic precolumn should be used for the preconcentration of the glucuronide during the clean-up step. The glucuronide could then be desorbed by changing the mobile phase and transferred on-line to a more hydrophobic analytical column where it will be enriched on the top of the column. Several conjugation reaction products are possible, often present in low concentrations, which is why the enhanced selectivity and sensitivity possible with coupled column systems would make this a suitable technique for metabolic studies of polar and ionizable compounds.

## REFERENCES

- 1 G. J. Dutton (Editor), *Glucuronic Acid. Free and combined*, Academic Press, New York, 1966.
- 2 A. Tilly Melin, Y. Askemark, K.-G. Wahlund and G. Schill, *Anal. Chem.*, 51 (1979) 976.
- 3 M. Stefansson and D. Westerlund, in preparation.
- 4 A. Bartha and Gy. Vigh, *J. Chromatogr.*, 260 (1983) 337.
- 5 E. D. Katz, C. H. Lochmüller and R. P. W. Scott, *Anal. Chem.*, 61 (1989) 349.
- 6 A. Tilly Melin, M. Ljungcrantz and G. Schill, *J. Chromatogr.*, 185 (1979) 225.
- 7 R. E. Majors, in Cs. Horváth (Editor), *High-Performance Liquid Chromatography — Advances and Perspectives*, Vol. 1, Academic Press, New York, 1980, p. 77.
- 8 G. Scatchard and J. G. Kirkwood, *Phys. Z.*, 33 (1932) 297.



CHROM. 21 790

## BASIS OF THE RATIONAL SELECTION OF THE HYDROPHOBICITY AND CONCENTRATION OF THE ION-PAIRING REAGENT IN REVERSED-PHASE ION-PAIR HIGH-PERFORMANCE LIQUID CHROMATOGRAPHY

AKOS BARTHA<sup>a</sup> and GYULA VIGH\*

*Chemistry Department, Texas A&M University, College Station, TX 77843-3255 (U.S.A.)*

and

ZITA VARGA-PUCHONY

*Institute for Analytical Chemistry, University of Chemical Engineering, Veszprem (Hungary)*

---

### SUMMARY

The retention of ionic solutes in ion-pair chromatographic separations can be controlled efficiently only when the surface concentration of the pairing ion, and the resulting surface potential, vary over a reasonably broad range. To achieve a broad operating range, the hydrophobicity and the mobile phase concentration of the pairing ion must be matched to the organic modifier concentration of the eluent. Preferred combinations of the eluent methanol concentrations and the commonly used alkylsulphonate and tetraalkylammonium pairing ions are reported, allowing for the rational selection of these parameters.

---

### INTRODUCTION

The effects of the chain length and the concentration of ion-pairing reagents on the retention of ionic solutes have been studied since the early applications of ion-pair chromatography. Horváth *et al.*<sup>1</sup>, Deelder and co-workers<sup>2,3</sup> and Knox and Hartwick<sup>4</sup>, among many others<sup>5–11</sup>, pioneered this subject. In addition to pH, organic modifier and pairing ion concentrations of the eluent, the hydrophobicity (length of the alkyl chain) of the pairing ion is one of the main parameters in the optimization of retention<sup>12</sup>. Generally, the retention of oppositely charged ionic solutes increases with increasing hydrophobicity of the pairing ions when used at identical mobile phase concentrations.

An important step in the progress of ion-pair chromatography was the recognition that solute retention depends primarily on the surface concentration of the adsorbed ion-pairing reagent<sup>2–5</sup>. Alkylsulphonate pairing ions of different chain length at similar surface concentrations were shown to result in identical solute retention<sup>4,10</sup>. This implies that the hydrophobicity of ion-pairing reagents affects solute retention only through their hydrophobicity-controlled adsorption<sup>4,10,11</sup>.

---

<sup>a</sup> On leave from the University of Chemical Engineering, Veszprem, Hungary.

Goldberg *et al.*<sup>13</sup> also suggested that, in principle, a single pairing ion can be used for the optimization of separation selectivity, provided that its adsorption covers a sufficiently wide range. On the other hand, studies by Bartha and co-workers<sup>10,14</sup> have shown that the organic modifier concentration of the eluent greatly influences the adsorption of both positively and negatively charged ion-pairing reagents. No single, commercially available pairing ion could ensure sufficiently high surface concentrations in eluents with widely differing organic modifier concentrations.

Pairing ion selection is still largely a trial-and-error procedure in most optimization schemes and previous chromatographic experience plays a large role. A rule of thumb calls for the replacement of the pairing ion with a more hydrophobic ion when sufficient retention shifts are not obtained.

Unfortunately, most optimization strategies<sup>13-16</sup>, and even some expert systems<sup>17</sup>, continue to adopt this very simple approach. They rely on the (convenient) use of a single (positively or negatively charged) pairing ion, irrespective of the organic modifier concentration in the eluent. Arguments used to support pairing ion selection (such as solubility and column equilibration time<sup>13</sup> or "reasonable effect on solute retention"<sup>17</sup>) apply only over a limited range of organic modifier concentrations. Popular choices tend to favour the less hydrophobic reagents.

Low *et al.*<sup>18</sup> suggested a rational approach for the selection of the types and ranges of the mobile phase variables to be used in the optimization of ion-pair chromatographic separations. The primary parameters include the charge type of the pairing ion, the pH and/or the methanol (or other organic modifier) concentration of the eluent. Essentially, these parameters are determined by the nature (charge type and relative hydrophobicity) of the sample solutes<sup>18</sup>.

This approach can be extended to the selection of the hydrophobicity (chain length) and mobile phase concentration of the pairing ion. Until now, however, the complexity of this problem (*i.e.*, the interrelationship of the mutually dependent parameters ionic strength, chain length and concentration of the pairing ion and organic modifier concentration) prevented the rational selection of these parameters. Recently, two important developments in the electrostatic theory of ion-pair chromatography<sup>19-21</sup> contributed to an improved understanding of the simultaneous effects of these parameters. The basic assumption of this theory is that the adsorbed amphiphilic ions and the counter ions form an electrical double layer at the surface and create a surface potential. This surface potential will influence both the adsorption isotherm of the pairing ion and the retention of ionic solutes. The magnitude of the surface potential depends primarily on three parameters: the surface concentration of the pairing ion, the dielectric constant and the ionic strength of the mobile phase<sup>19</sup>.

Stahlberg and Hagglund<sup>22</sup> have shown that the type and concentration of the electrolyte influences both solute retention and pairing ion adsorption through the surface potential, confirming the notion that eluent pH and ionic strength can be considered independent parameters.

Stahlberg and Bartha<sup>23</sup> demonstrated that the hydrophobicity of the pairing ion and the concentration of the organic modifier affect the surface potential by influencing the adsorption of the pairing ions.

In this paper, we discuss the interrelationship of the organic modifier and the hydrophobicity and concentration of the pairing ion, and provide a rational basis for their selection. We show that the use of a single pairing ion irrespective of the concen-

tration of the organic modifier may be convenient, but it is not efficient. Based on an extensive compilation of adsorption isotherms and retention data, recommendations are made for matching the hydrophobicity and mobile phase concentration of typical positively charged (tetraalkylammonium) and negatively charged (alkylsulphonate) ion-pairing reagents to the organic modifier concentration in the eluent. Pairing ions used in special applications, such as indirect UV detection and enantiomer or peptide separations, will not be discussed.

## EXPERIMENTAL

All chemicals were of analytical-reagent grade. Drugs and ion-pairing reagents were obtained from Janssen (Beerse, Belgium), Fluka (Buchs, Switzerland) and Merck (Darmstadt, F.R.G.). Distilled, ion-exchanged water was used for the preparation of buffer solutions and eluents. An LC 5000 liquid chromatograph, equipped with UV (254 nm) and RI detectors (all from Varian Aerograph, Walnut Creek, CA, U.S.A.) and two Model 7010 six-port injection valves (Rheodyne, Cotati, CA, U.S.A.) were used. Columns were thermostated at 25°C. The chromatographic system allowed the determination of both the breakthrough curves of the pairing ions (surface concentrations) and the retention data (capacity factors) of the solutes, as described previously<sup>24</sup>. The analytical columns (120 × 4.6 mm I.D.) were slurry packed with 5- $\mu$ m ODS-Hypersil (Shandon, London, U.K.), Nucleosil C<sub>18</sub> (Macherey-Nagel, Bad Dürkheim, F.R.G.), Supelco S C<sub>18</sub> (Supelco, Bellefonte, PA, U.S.A.) and 5- $\mu$ m LiChrosorb RP-8 and RP-18 (Merck). Three non-commercial stationary phases, received as gifts, were also used: DiMeODS (10- $\mu$ m dimethyloctadecylsilica) (Prof. E. Sz. Kovats, Ecole Polytechnique, Lausanne, Switzerland), BST C<sub>18</sub> (5- $\mu$ m octylsilica) (Bio-Separation Technologies, Budapest, Hungary) and HTS RP6 (10- $\mu$ m dimethylhexylsilica) (Prof. Th. Welsch, Karl-Marx University, Leipzig, G.D.R.). Details of the stationary phase studies will be published elsewhere<sup>25</sup>.

The eluents were prepared by weighing as described previously<sup>24</sup>. They contained 25 mM phosphoric acid, 25 mM sodium dihydrogenphosphate and different concentrations of ion-pairing reagents and sodium bromide (to maintain the ionic strength constant). Methanol was used as an organic modifier.

## RESULTS AND DISCUSSION

### *Role of the surface concentration of the pairing ion in the optimization of separations*

A nine-component mixture of strong bases and weak acids (catecholamines and some of their acidic metabolites) was taken as an example to demonstrate the importance of pairing-ion selection in the retention control of ionic solutes. All solutes are considered to be of interest and must be separated from each other.

In Fig. 1 the solute capacity factors are shown as a function of pH using a methanol-aqueous buffer (10:90, v/v) eluent. The curves represent the idealized behaviour of weak acids (solutes 1-4) and strong bases (solutes 5-9) between pH 2.5 and 7.5. This separation problem can be solved fairly simply: the retention of the early eluting solutes must be increased. One alternative is to decrease the methanol concentration at high pH in order to increase the retention of all ionized solutes. However, their retention remains very low even in pure aqueous buffer. The same strategy at

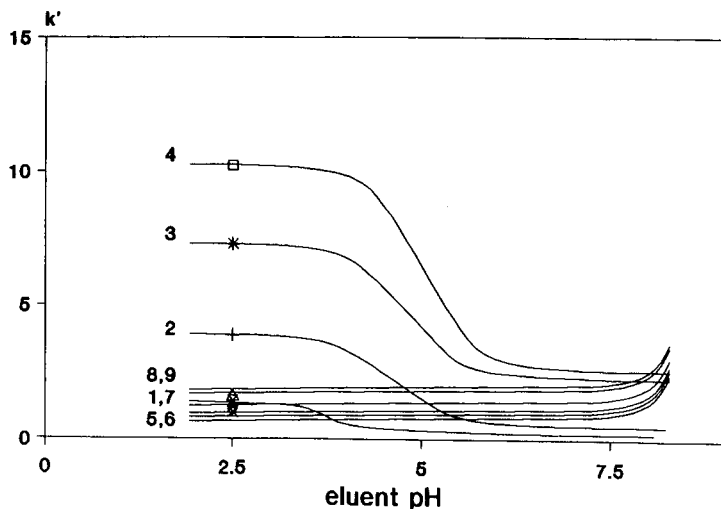


Fig. 1. Variation of the capacity factors ( $k'$ ) of a mixture of weak acids and strong bases as a function of the eluent pH. Column,  $5\text{-}\mu\text{m}$  ODS-Hypersil; eluent, 10% (v/v) methanol in  $50\text{ mM}$  aqueous phosphate buffer, constant ( $175\text{ mM}$ ) ionic strength adjusted with sodium bromide. Solutes: 1 = homovanilmandelic acid; 2 = 3,4-dihydroxyphenylacetic acid; 3 = 3,4-dihydroxymandelic acid; 4 = 5-hydroxyindole-3-acetic acid; 5 = noradrenaline; 6 = adrenaline; 7 = octopamine; 8 = dopamine; 9 = 3,4-dihydroxyphenylalanine.

low pH results in excessively retained weak acids. The only good alternative is to increase the retention of the strong bases by adding a negatively charged pairing ion to the eluent. However, this must be done at low pH, because at high pH, owing to the ionic repulsion of the ion-pairing reagent, all acids elute close to the solvent front. These considerations result in a simple optimization vector space: a single line [pH 2.5, 10% (v/v) methanol and varying concentration of a negatively charged pairing ion], shown in a three-dimensional representation in Fig. 2. Next, the concentration limits and the hydrophobicity of the pairing ion to be used along this single line must

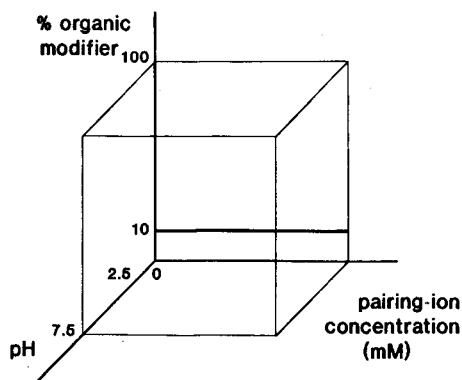


Fig. 2. Three-dimensional representation of the combination of eluent optimization parameters: eluent pH, methanol concentration and ion-pairing reagent concentration. The bold horizontal line at 10% (v/v) methanol represents the selected optimization parameter space.

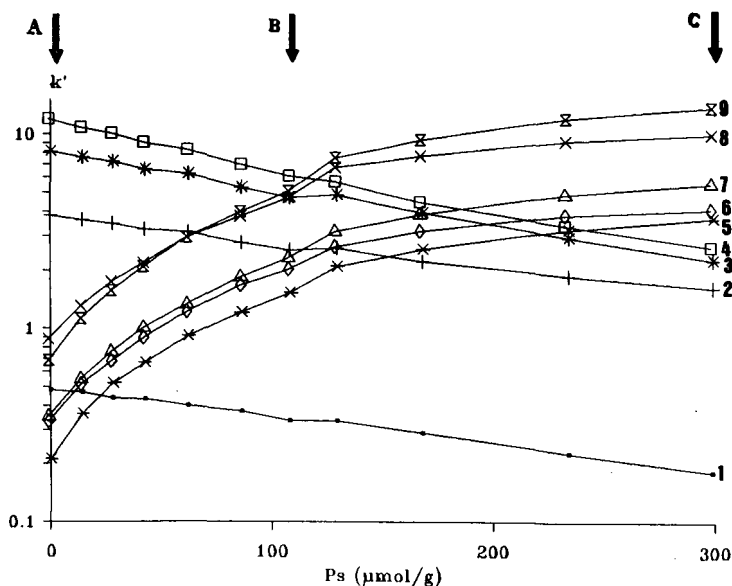


Fig. 3. Capacity factors ( $k'$ ) of solutes 1–9 in Fig. 1 as a function of the surface concentration ( $P_s$ ) of hexyl- and octylsulphonate pairing ions. Mobile phases between arrows A and B contained 0 to 70 mM hexylsulphonate and those between B and C contained 0.5 to 10 mM decylsulphonate pairing ion. Other conditions as in Fig. 1.

be selected. First, we shall analyse the possible consequences of an improper choice, and in the last part of the paper we show a practical solution to this problem.

The use of two alkylsulphonate pairing ions of different hydrophobicity was evaluated experimentally. The mobile phase concentration was varied from 0 to 70 mM for sodium hexylsulphonate and from 0 to 10 mM for sodium decylsulphonate. In Fig. 3 the solute capacity factors are plotted against the surface concentration ( $P_s$ ) of the alkylsulphonates. All strong bases become more retained as the pairing ion is added, while the retention of the four weak acids (1–4) gradually decreases. Although there is a small break in the retention curves as hexylsulphonate is replaced with decylsulphonate, the difference is negligible, in accordance with earlier findings<sup>10,11</sup>.

The chromatograms shown in Fig. 4 were obtained as follows: (A) without any ion pairing reagent, (B) with 70 mM sodium hexylsulphonate and (C) with 10 mM decylsulphonate. Although sodium hexylsulphonate enhanced the retention of the positively charged solutes, certain solute pairs (*e.g.*, 2–7 and 3–8) could not be separated. The highest surface concentration of this pairing ion is 110  $\mu\text{mol/g}$ . When sodium decylsulphonate is used, higher surface concentrations (and potentials) are obtained; the positively charged basic solutes become more retained than the weak acids. High surface concentrations of decylsulphonate result not only in increased retention, but also in improved separation selectivity as indicated by the complete separation of the components in chromatogram C in Fig. 4. (Incidentally, a number of local optima can be found in this high surface concentration range.)

Thus, the main question is how one can find the eluent composition limits that probably contain the global selectivity optimum. According to our experience, the

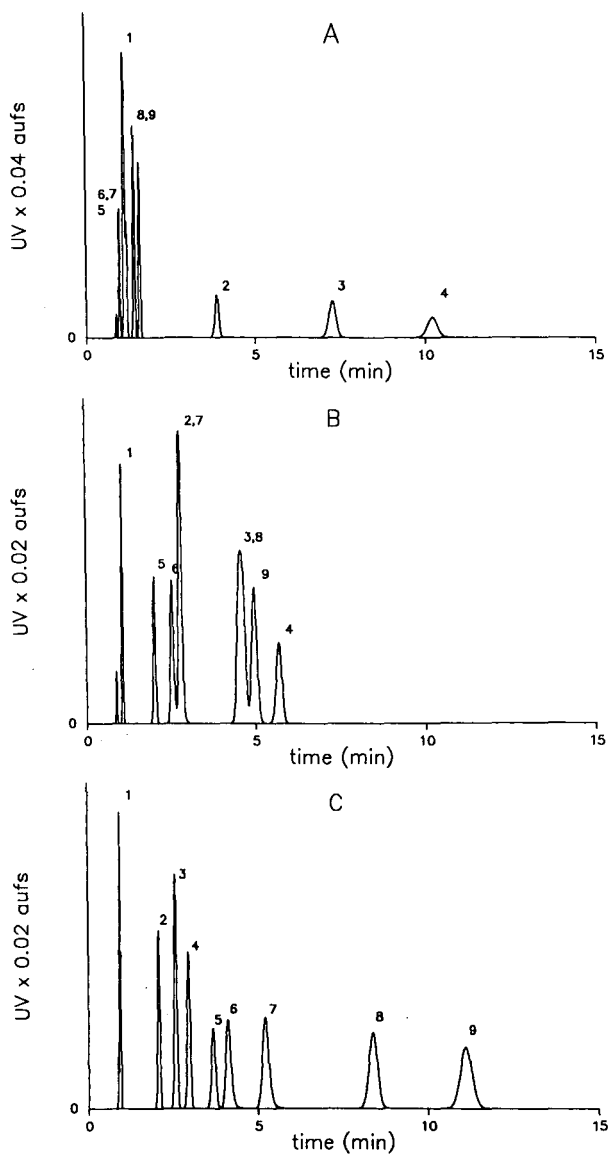


Fig. 4. Chromatograms of the catecholamine mixture shown in Fig. 1. (A) No pairing ion added; (B) eluent containing 70 mM sodium hexylsulphonate; (C) eluent containing 10 mM sodium decylsulphonate. Other conditions as in Fig. 1.

surface concentration of the ion-pairing reagents should reach at least 100–200  $\mu\text{mol/g}$  if the solute retention is to be affected significantly (see, *e.g.*, Fig. 3). One possibility is to increase the concentration of hexylsulphonate even further and another is to use a more hydrophobic pairing ion.



This example highlights some important points that any optimization strategy must confront. If the hydrophobicity and/or the concentration range of the pairing ion are not selected appropriately, then the surface concentration of the pairing ion (and the retention controlling surface potential) will vary only over a limited range. Higher surface potentials can only be reached by decreasing the ionic strength of the eluent (if possible at all)<sup>19</sup> and/or by increasing the mobile phase concentration and the hydrophobicity of the ion-pairing reagent. Although a given pairing ion can perform well at a certain organic modifier concentration, its effects may not be large enough in a less polar eluent.

The separation selectivity does not necessarily improve as surface concentrations are increased even higher. At very high surface concentrations, the retention of oppositely charged solutes will reach a maximum (see Fig. 3) and a number of secondary effects (which are difficult to handle both theoretically<sup>23</sup> and empirically) might influence the separation selectivity.

*Limitations following from the use of a single pairing ion irrespective of the concentration of the organic modifier in the eluent*

Ionic solute retention is best controlled through ionic interactions established by sufficiently high surface potentials, *i.e.*, pairing-ion surface concentrations. In this respect, all optimization strategies that rely on the use of a single pairing ion are limited. This limitation becomes obvious when one compares the adsorption isotherms of ion-pairing reagents measured at different organic modifier concentrations.

In Fig. 5 the adsorption isotherms of sodium octylsulphonate are shown for 0, 10, 25 and 40% (v/v) methanol–aqueous phosphate buffer (pH 2.1) eluents. With increasing methanol concentration, the surface concentration of the pairing ion decreases rapidly. This effect is shown in Fig. 6 in a different representation: the corresponding methanol concentrations and pairing-ion adsorption data (for hexyl-, octyl- and decylsulphonates) are plotted at constant mobile phase pairing-ion concentrations. The adsorption decreases almost three-fold when the methanol concentration is increased to 40% (v/v).

Mixture designs used for mobile phase optimization often require the addition of pure methanol to a base eluent with a given pairing-ion concentration<sup>13,15</sup>. This results in even lower surface concentrations, because dilution and weakened adsorption strength act in concert [*i.e.*, the eluent at 40% (v/v) methanol will contain only 3 mM octylsulphonate<sup>15</sup>]. Alternatively, one could increase the mobile phase concentration of the selected pairing ion to compensate for the decreased adsorption strength. The limitations of this method are demonstrated by Fig. 6. Compared with octylsulphonate (5 mM curve), four-fold higher mobile phase concentrations of sodium hexylsulphonate (20 mM curve) still result in much lower (30–50%) surface concentrations.

A more efficient approach adapts the hydrophobicity and concentration of the pairing ion to the organic modifier concentration that is required for the separation. A lower concentration of a more hydrophobic pairing ion can extend the range in which the surface concentration (and potential) can be varied (see data for decylsulphonate in Fig. 6).

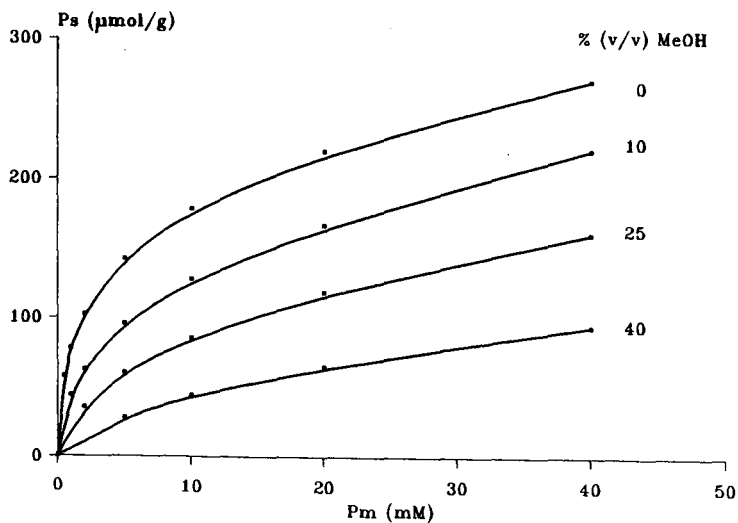


Fig. 5. Adsorption isotherms of sodium octylsulphonate from 0, 10, 25 and 40% (v/v) methanol (MeOH). pH, 2.1; aqueous phosphate buffer eluents on ODS-Hypersil at constant temperature (25°C) and ionic strength (175 mM).  $P_s$  = surface concentration;  $P_m$  = mobile phase concentration.

#### *Practical recommendations for pairing-ion selection*

Often one must face the problem of pairing-ion selection without a knowledge of the adsorption isotherms of the pairing ions and their dependence on the organic modifier concentrations. Instead of attempting to describe mathematically the effects on the surface potential of the chain length and eluent concentration of the pairing

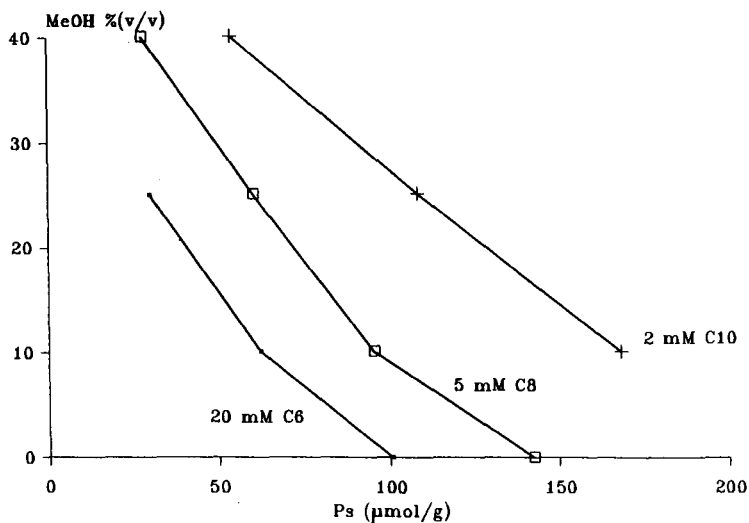


Fig. 6. Variation of the surface concentration ( $P_s$ ) of hexyl- (C6), octyl- (C8) and decylsulphonate (C10) pairing ions at constant (20, 5 and 2 mM) mobile phase concentrations with increasing methanol (MeOH) concentration of the eluent. Other conditions as in Fig. 5.

ion and the organic modifier concentration (which would require a very large and complete dataset for all these variables), we used our extensive solute retention and adsorption isotherm<sup>10,14,23-25</sup> datasets and derived recommended pairing ion-organic modifier combinations which can help the chromatographer to select the appropriate pairing ions. These operating ranges were defined such that the selected pairing ions must (i) be sufficiently soluble to yield at least 100  $\mu\text{mol/g}$  surface concentrations in the organic modifier range assigned, (ii) permit fast column equilibration and regeneration and (iii) not form micelles.

Figs. 7 and 8 summarize our recommendations (which represent a compromise between the above requirements) for the different chain length, ion-pairing reagent and methanol concentration combinations for both alkylsulphonate and tetraalkylammonium ions. These pairing ions are thought to cover most of the common ion-pair chromatographic applications. The bars represent the methanol and highest practical pairing-ion mobile phase concentration combinations that lead to surface concentrations of 100  $\mu\text{mol/g}$  or higher for each reagent, and which can be safely dissolved without micelle formation. The initial electrolyte concentration in these eluents must not exceed 100 mM. Once the methanol concentration of the eluent has been selected, the appropriate pairing ion and its concentration limits (typically between 0 and Pm mM) can be selected from the diagrams. When the bars of several pairing ions overlap, those most centered around the selected methanol concentrations are to be preferred.

Certain other popular pairing ions, such as pentyl- and heptylsulphonates, were not included because sufficient adsorption and retention data were not available. However, their respective limits can be estimated by extrapolation between the neighbouring members of the homologous series. Owing to the possibility of irreversible adsorption on reversed-phase columns, very hydrophobic asymmetric quaternary ammonium salts also were not considered in Fig. 7. However, published adsorption

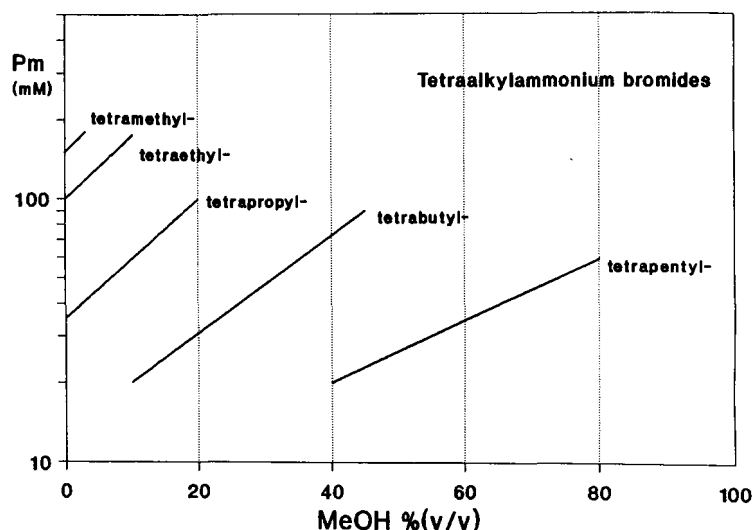


Fig. 7. Recommended maximum mobile phase concentrations (Pm) of tetraalkylammonium pairing ions and their application ranges as a function of the methanol (MeOH) concentration of the mobile phase.

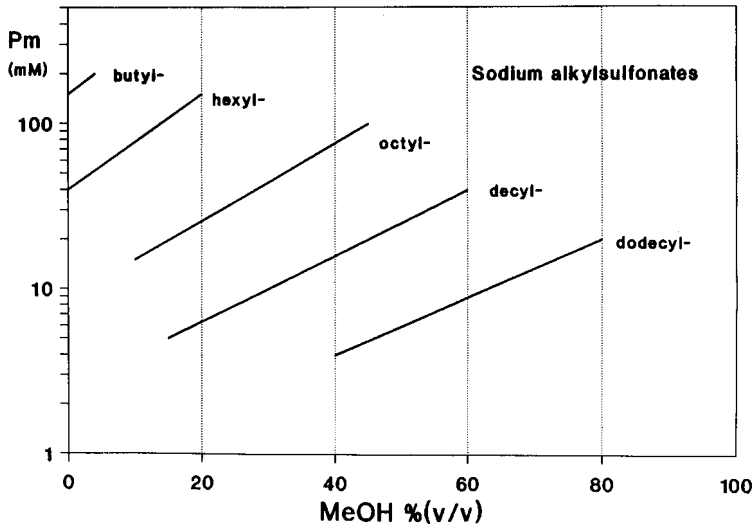


Fig. 8. Recommended maximum mobile phase concentrations ( $P_m$ ) of alkylsulphonate pairing ions and their application ranges as a function of the methanol (MeOH) concentration of the mobile phase.

data for cetrimide<sup>6,7</sup> indicate that it can be used over a wide range of organic modifier concentrations with characteristics close to the tetrapentylammonium ion.

In Fig. 9 the capacity factors of the positively charged octopamine are plotted against the mobile phase concentration of sodium octylsulphonate for eight different

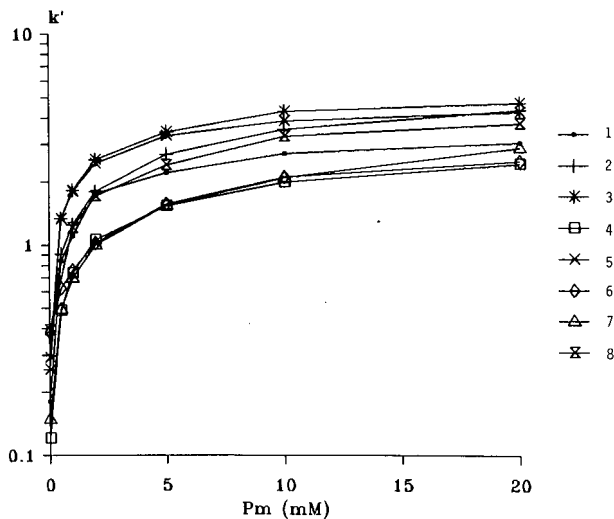


Fig. 9. Capacity factor ( $k'$ ) of positively charged octopamine as a function of the mobile phase concentration ( $P_m$ ) of sodium octylsulphonate on eight reversed-phase columns. All measurements were made in methanol-aqueous phosphate buffer (pH 2.1) (10:90, v/v) eluents of constant ionic strength (175 mM, adjusted with sodium bromide) at 25°C. 1 = LiChrosorb RP-18; 2 = Nucleosil C<sub>18</sub>; 3 = DiMeODS; 4 = LiChrosorb RP-8; 5 = Supelco S C<sub>18</sub>; 6 = BST C<sub>18</sub>; 7 = HTS RP6; 8 = ODS-Hypersil.

reversed-phase columns. The eluent pH (2.1), organic modifier concentration [10% (v/v) methanol] and ionic strength (175 mM, adjusted with sodium bromide) were kept constant throughout these experiments. The most notable feature is that a comparable increase in retention is observed on these diverse packings, indicating that the recommendations in Figs. 7 and 8 are fairly generally applicable. The effects of the stationary phase will be discussed in detail in another paper<sup>25</sup>.

A further generalization is possible by extension of the electrostatic theory of ion-pair chromatography to include the effects of the type and concentration of the organic modifier<sup>26</sup>. Using "isopotential" binary methanol-, acetonitrile- and tetrahydrofuran-water eluents, diagrams similar to Figs. 7 and 8 can be obtained.

The recommendations described here are part of a knowledge base used in the development of an ion-pair chromatographic expert system. This expert system is intended to aid users in the selection of the mobile phase optimization parameters by considering the nature (charge type and relative retention) of the solutes in the sample. Once the primary parameters (pH, organic modifier concentration and charge type of the pairing ion) have been selected, the hydrophobicity and concentration of the pairing ion are matched with the organic modifier concentration of the eluent.

## CONCLUSIONS

We have shown that one must be able to vary the surface concentration of the pairing ion, *i.e.*, the surface potential, over a reasonably broad range in order to optimize the separation of a complex mixture of differently charged solutes. When the organic modifier concentration is increased, the mobile phase concentration and/or the hydrophobicity of the pairing ion must also be increased to counter the weakened adsorption strength. Based on a comprehensive dataset which contains pairing-ion adsorption isotherms and solute retention data, preferred combinations of typical (both positively and negatively charged) pairing ions (hydrophobicity and concentration) and organic modifier concentrations have been selected. The need for facile column regeneration, solubility and/or the prevention of micelle formation have also been used as constraints.

## REFERENCES

- 1 Cs. Horváth, R. W. Melander and I. Molnár, *Anal. Chem.*, 49 (1977) 142.
- 2 R. S. Deelder, H. A. J. Linssen, A. P. Konijnendijk and J. L. M. van de Venne, *J. Chromatogr.*, 185 (1979) 241.
- 3 R. S. Deelder and J. H. M. van den Berg, *J. Chromatogr.*, 218 (1981) 327.
- 4 J. H. Knox and R. C. Hartwick, *J. Chromatogr.*, 204 (1981) 3.
- 5 E. Tomlinson, C. M. Riley and T. M. Jefferies, *J. Chromatogr.*, 173 (1979) 89.
- 6 C. T. Hung and R. B. Taylor, *J. Chromatogr.*, 202 (1980) 333.
- 7 C. T. Hung and R. B. Taylor, *J. Chromatogr.*, 209 (1981) 175.
- 8 I. S. Lurie and S. M. Demchuk, *J. Liq. Chromatogr.*, 4 (1981) 337.
- 9 W. R. Melander and Cs. Horváth, in M. T. W. Hearn (Editor), *Ion-Pair Chromatography*, Marcel Dekker, New York, 1985, Ch. 2.
- 10 A. Bartha, Gy. Vigh, H. A. H. Billiet and L. de Galan, *J. Chromatogr.*, 303 (1984) 29.
- 11 A. Bartha and Gy. Vigh, *J. Chromatogr.*, 395 (1987) 503.
- 12 P. J. Schoenmakers, *Optimization of Chromatographic Selectivity, A Guide for Method Development*, Elsevier, Amsterdam, 1986, Ch. 3.
- 13 A. P. Goldberg, E. Nowakowska, P. E. Antle and L. R. Snyder, *J. Chromatogr.*, 316 (1984) 241.

14. A. Bartha and Gy. Vigh, *J. Chromatogr.*, 260 (1983) 337.
15. P. M. J. Coenegracht, N. V. Tuyen, H. J. Metting and P. M. J. Coenegracht-Lamers, *J. Chromatogr.*, 389 (1987) 351.
16. H. A. H. Billiet, J. Vuik, J. K. Strasters and L. de Galan, *J. Chromatogr.*, 384 (1987) 153.
17. Y. Hu, A. Peeters, G. Musch and D. L. Massart, *Anal. Chim. Acta*, 223 (1989) 1.
18. G. K.-C. Low, A. Bartha, H. A. H. Billiet and L. de Galan, *J. Chromatogr.*, 478 (1989) 21.
19. J. Stahlberg, *J. Chromatogr.*, 356 (1986) 231.
20. J. Stahlberg and A. Furangen, *Chromatographia*, 24 (1987) 783.
21. J. Stahlberg, *Chromatographia*, 24 (1987) 820.
22. J. Stahlberg and I. Hagglund, *Anal. Chem.*, 60 (1988) 1958.
23. J. Stahlberg and A. Bartha, *J. Chromatogr.*, 456 (1988) 253.
24. A. Bartha and Gy. Vigh, *J. Chromatogr.*, 265 (1983) 171.
25. Z. Varga-Puchony, A. Bartha and Gy. Vigh, in preparation.
26. A. Bartha, Gy. Vigh and J. Stahlberg, *J. Chromatogr.*, 485 (1989) 403.

CHROM. 21 710

## ESTIMATION OF THE REVERSED-PHASE LIQUID CHROMATOGRAPHIC LIPOPHILICITY PARAMETER $\log k'_w$ USING ET-30 SOLVATOCHROMISM

JAMES J. MICHELS<sup>a</sup> and JOHN G. DORSEY<sup>\*b</sup>

*Department of Chemistry, University of Florida, Gainesville, FL 32611 (U.S.A.)*

---

### SUMMARY

The estimation of the reversed-phase liquid chromatographic lipophilicity parameter  $\log k'_w$  has been studied using the solvatochromic  $E_T(30)$  polarity scale. Over 200 sets of chromatographic retention data were used to compare the  $\log k'_w$  estimates made from the volume percent of organic modifier (%) and  $E_T(30)$  models of mobile phase strength. It was found that linear extrapolations of  $\log k'$  versus  $E_T(30)$  plots to the polarity of unmodified aqueous mobile phase gave a more reliable value of  $\log k'_w$  than linear regressions of  $\log k'$  versus volume percent. This evaluation was based upon the relative value of the 95% confidence interval about  $\log k'_w$ , the point of intersection of  $\log k'$  versus solvent strength plots for different modifiers, the scatter of estimations with different modifiers and the goodness-of-fit of the data to the linear model. Estimations of  $\log k'_w$  using the solvatochromic approach are found to give a more sensitive lipophilicity description than the volume percent approach. Recommended procedures for carrying out lipophilicity estimations with reversed-phase liquid chromatography are also discussed.

---

### INTRODUCTION

A growing application of reversed-phase liquid chromatography (RPLC) is the estimation of the physico-chemical properties of chemical compounds, also known as quantitative structure-retention relationships (QSRR). QSRR constitutes a large subset of quantitative structure-activity relationships (QSAR). One such physico-chemical property, lipophilicity, is a descriptor of the hydrophobic partitioning character of a compound and has many uses in the environmental and biological sciences<sup>1,2</sup>. A recent *Chemical Abstracts* database search performed by this laboratory revealed that since 1975 the number of papers published each year regarding chromatography and QSAR has increased steadily. In 1975, the percentage of those papers concerning high-performance liquid chromatography (HPLC) was approximately 12% and as of 1988 that portion has expanded to about 25%.

---

<sup>a</sup>Present address: The NutraSweet Company, 601 E. Kensington Road, Mt. Prospect, IL 60056, U.S.A.

<sup>b</sup>Present address: Department of Chemistry, University of Cincinnati, Cincinnati, OH 45221, U.S.A.

Recent reviews have covered research studying the use of RPLC retention data as an estimator of lipophilicity<sup>3-7</sup>. The major advantages of using RPLC over shake-flask methods are that it is faster, shows a larger dynamic range of  $\log P$ , is more convenient to perform experimentally, is extremely reproducible and can be automated. RPLC also works well because precise peak-height or -area quantitation is not necessary and the sample need not be 100% pure. An experiment is usually carried out by obtaining the logarithm of the capacity factor for a solute,  $\log k'$ . Since the capacity factor is directly proportional to the chromatographic partition coefficient<sup>8</sup>, capacity factors have been used to estimate  $P$ .

Various approaches have been devised to obtain capacity factors for lipophilicity information, but one that has received much attention is the parameter  $\log k'_w$ , the logarithm of the capacity factor using only an aqueous phase as the eluent. The advantage of using  $\log k'_w$  is that it is independent of any organic modifier effects, reflects polar-non-polar partitioning in a manner similar to shake-flask methods<sup>9,10</sup> and is dependent on the solute's structure and polar functionalities<sup>11</sup>.

The  $\log k'_w$  parameter, however, is difficult to measure directly in an RPLC experiment because of poor partitioning kinetics across the stationary phase-mobile phase interface and prohibitively long retention times. It is arduous both to detect and locate a peak centroid because of the skewing of the peaks.

$\log k'_w$  can be estimated by the intercept of the regression equation<sup>12</sup>:

$$\log k' = S\% + \log k'_w \quad (1)$$

where  $S$  is Snyder's strength value and  $\%$  is the volume percent of organic modifier in the mobile phase. The retentivity of the chromatographic system with respect to changes in mobile phase "strength", denoted here by  $\%$ , is inferred by  $S$ . It has been suggested that  $\log k'_w$  itself be a direct measure of lipophilicity for neutral solutes because it minimizes hydrogen bonding effects<sup>13</sup> and has been found to be reproducible between  $C_{18}$  columns used<sup>14</sup>. These columns must be from the same manufacturer, however, since  $\log k'_w$  should vary from column to column because of bonding density and phase ratio differences.

Despite the utility of  $\log k'_w$  as a lipophilicity descriptor, a problem exists in the fundamental detail of its estimation. While eqn. 1 holds on a qualitative basis, curvature exists in these plots<sup>15-17</sup> and could lead to erroneous extrapolation results. A solution to this problem of mobile phase strength characterization for QSRR has been to describe retention data with the equation<sup>18,19</sup>

$$\log k' = A\%^2 + B\% + \log k'_w \quad (2)$$

where  $A$  and  $B$  are the mobile phase- and solute-dependent first and second coefficients of the second-order polynomial regression. While a second-order or higher polynomial will almost always give a better fit to the data, additional uncertainty in an extrapolation occurs due to the  $A\%^2$  term and that uncertainty can only be reduced by measuring extra data points closer to the point of extrapolation.

One possible solution to the problem of describing mobile phase strength for lipophilicity studies lies in empirical solvatochromic solvent polarity scales. These methods are useful for this purpose because they quantify some of the significant



intermolecular interactions experienced by a solute in the chromatographic system. One such scale,  $E_T(30)^{20}$ , is attractive for use in RPLC because the ET-30 molecule is readily soluble in RPLC solvents, is spectrally influenced by interactions characteristic to those solvents such as hydrogen bonding, dipolar and charge-transfer interactions, and is extremely sensitive to small changes in organic modifier. It has been shown previously<sup>21</sup> with 332 sets of RPLC retention data that when solute retention is modeled by the equation

$$\log k' = m[E_T(30)] + b \quad (3)$$

a more linear relationship is found than when using eqn. 1.

If eqn. 3 provides a more linear description of the retention process than eqn. 1, a more accurate estimation of  $\log k'_w$  should result upon extrapolation to the polarity of mobile phase containing no organic modifier. It has been reported<sup>9</sup> that values of  $\log k'_w$  estimated by eqn. 1 are dependent on the modifier used. Also, since the  $E_T(30)$  polarity scale shows a linear relationship with  $\log k'$ , eqn. 3 should produce results rivaling or surpassing results from using eqn. 2. A prior study using homologous alcohols and acetonitrile as RPLC organic modifiers<sup>22</sup> has shown two important conclusions. When the retention data for solutes were plotted with both eqns. 1 and 3 using methanol, ethanol and acetonitrile as single organic modifiers, (i) the average difference between estimated  $\log k'_w$  values between two different modifiers was improved by 40% with the  $E_T(30)$  model compared to volume % modifier and (ii)  $E_T(30)$  plots for all three modifiers converged toward the polarity of water while volume percent plots diverged at 0% modifier. These conclusions imply that a solvatochromic model of eluent strength, like  $E_T(30)$ , may yield reliable values of  $\log k'_w$  in more than just one modifier.

These types of convenient linearizations are likely the best application of solvatochromic measurements in liquid chromatography as it is not clear that any type of true fundamental information can be obtained from them. This paper compares the estimation of  $\log k'_w$  by the  $E_T(30)$  and % models of solute retention through the calculation of comparative figures of merit. A brief discussion of recommended execution of lipophilicity experiments using estimated  $\log k'_w$  values is also presented.

## EXPERIMENTAL

### *Solvatochromic measurements*

Solvatochromic solvent polarity measurements were made on binary solutions of pure organic solvent and aqueous buffer using ET-30 (Reichardt's dye) (Aldrich, Milwaukee, WI, U.S.A.). The organic solvents were Fisher (Austin, TX, U.S.A.) HPLC-grade methanol and acetonitrile and all water used was purified using a Barnstead (Newton, MA, U.S.A.) purification system. One buffer was composed of 0.02 M 3-morpholinopropanesulfonic acid (MOPS) (Kodak, Rochester, NY, U.S.A.) and 0.2% (v/v) *n*-decylamine (Aldrich) and another made up of 66.6 mM ACS certified sodium phosphate monobasic (Fisher). Both buffers were adjusted to a pH of 7.4 with aqueous sodium hydroxide. Binary organic-buffer solutions were prepared by mixing additive volumes of pure organic solvent and buffer solution in increments ranging from 0 to 100% organic modifier for MOPS buffer and from 0 to 70% for phosphate

buffer. ET-30 was added to the simulated mobile phases to a final concentration of approximately 100 mg/l. Samples were placed into a Fisher 5-cm path length glass cell and spectra obtained with an IBM Instruments (Danbury, CT, U.S.A.) Model 9420/9430 UV-visible spectrophotometer. Six spectra were acquired for each sample and the  $E_T(30)$  values averaged. Maximum absorbance wavelengths were determined using a first-derivative algorithm on the instrument. The  $E_T(30)$  data were taken every 10% organic and fit to an appropriate degree polynomial using the Crickett Software (Philadelphia, PA, U.S.A.) program STATWORKS run on an Apple (Cupertino, CA, U.S.A.) Macintosh SE microcomputer. Any unmeasured  $E_T(30)$  values (*i.e.*, 45% methanol in MOPS buffer) were determined by interpolation.  $E_T(30)$  polarity values for methanol-water, acetonitrile-water and ethanol-water mobile phases were the same as those used in previous studies<sup>21-23</sup>.

#### Retention measurements

All retention measurements were taken from the literature<sup>18,19,21,22,24,25</sup>. Each reference employed a C<sub>18</sub> column and Table I summarizes the pertinent experimental details.

#### Calculations

All computations were done on the Apple Macintosh SE computer with the exception of the polynomial confidence intervals, which were done on an Apple II 48K microcomputer using the program POLYCONFINT written in this laboratory. Linear and polynomial regression were performed with STATWORKS and all other calculations accomplished with the Microsoft (Redmond, WA, U.S.A.) spreadsheet EXCEL.

TABLE I

EXPERIMENTAL CONDITIONS FOR REVERSED-PHASE RETENTION DATA TAKEN FROM THE LITERATURE FOR LOG  $k'_w$  STUDY

Ref.	Column	Modifiers	$t_0$ method	Solutes
22	Ultrasphere ODS	Methanol Ethanol Acetonitrile	Solvent elution	Nitro-, amino-, alkyl-, keto- and polycyclic aromatics
18	LiChrosorb RP-18	Methanol Acetonitrile MOPS <sup>a</sup> <i>n</i> -Decylamine	Solvent elution	Nicotinate esters
21	Ultrasphere ODS	Methanol Acetonitrile	Solvent elution	Alkylbenzenes
24	Spherisorb S5 ODS-2	Methanol Ethanol	NaNO <sub>3</sub> elution	5-Dimethylamino- 1-sulfonyl derivatives
25	Nucleosil 10-RP-18	Methanol Acetonitrile Tetrahydrofuran	Set $t_0 = 125$ s	Nitro-, amino-, alkyl-, keto-, halo- and polycyclic-aromatics, alcohols, heterocyclics

<sup>a</sup> Morpholinopropanesulfonic acid.

## RESULTS AND DISCUSSION

*Solvatochromic solvent polarity measurements for neutral electrolyte solutions*

Studies have been previously performed on the solvatochromic polarity of surfactant and electrolyte solutions. One study of ionic surfactant solutions<sup>26</sup> showed that the  $E_T(30)$  polarity of a surfactant solution was dependent on the presence of added buffer salts. Using NMR data, it was shown<sup>26,27</sup> that the charged groups of ET-30 are coulombically influenced and align with the other oppositely charged groups of the surfactants. Another study using Kosower's Z scale<sup>28</sup>, which uses a probe similar to ET-30, has also shown solvatochromic polarity increasing with the addition of electrolyte. Table II presents our results showing the effects of increasing the amount of electrolyte on  $E_T(30)$  polarity.  $E_T(30)$  values were measured for mixtures of organic modifier with neutral buffers and sodium chloride solutions. Within an experimental error of about 0.10 kcal/mole, an increase in polarity is observed with increase in electrolyte concentration.  $E_T(30)$  values of electrolyte solutions, however, should be viewed with caution when directly compared to values taken in non-electrolyte solutions because of the added coulombic interactions between the charged functional groups of the dye and the electrolytes. This is evident when comparing the water-organic to electrolyte-organic mixtures.

The  $E_T(30)$  polarity of a solution is also influenced by acidity. Langhals<sup>29</sup> has shown that  $E_T(30)$  values cannot be measured in acidic electrolyte solutions because the phenoxide group of ET-30 becomes protonated and the character of the charge-

TABLE II

DEPENDENCE OF  $E_T(30)$  POLARITY ON THE CONCENTRATION OF ELECTROLYTE IN NEUTRAL AQUEOUS-ORGANIC MIXTURES

<i>Solution<sup>a</sup></i>	$E_T(30)$ (kcal/mole)	<i>Solution<sup>a</sup></i>	$E_T(30)$ (kcal/mole)
Water- 50% (v/v) methanol	58.30	99 mM phosphate- 40% (v/v) acetonitrile	57.76
1 mM NaCl- 50% (v/v) methanol	58.03	Water- 60% (v/v) methanol	57.46
10 mM NaCl- 50% (v/v) methanol	58.03	10 mM MOPS- 0.2% (v/v) DA- 60% (v/v) methanol	58.08
100 mM NaCl- 50% (v/v) methanol	58.25	20 mM MOPS- 0.2% (v/v) DA- 60% (v/v) methanol	58.73
Water- 40% (v/v) acetonitrile	57.46	31 mM MOPS 0.2% (v/v) DA- 60% (v/v) methanol	59.29
31 mM phosphate- 40% (v/v) acetonitrile	57.40		
66 mM phosphate- 40% (v/v) acetonitrile	57.48		

<sup>a</sup> NaCl = sodium chloride; phosphate = sodium phosphate monobasic; MOPS = morpholinopropanesulfonic acid; DA = *n*-decylamine.

transfer functionality is destroyed. There are no problems of complete protonation of the dye with the work presented here on account of ET-30 spectra being obtained in mobile phases buffered at pH 7.4. The  $pK_a$  of the dye has been reported to be 8.4 in 50% methanol–water<sup>26</sup>. Based on its  $pK_a$  and the pH of the solutions used, ET-30 can sense acidic interactions. Reichardt<sup>30</sup> has defined polarity as the total solvating power of the solvent and thus these forces can be included in the  $E_T(30)$  “polarity” of basic solutions.

The relationships between the  $E_T(30)$  polarity and the volume percent of methanol and acetonitrile added to the buffer solutions are shown in Figs. 1 and 2. The methanol–MOPS buffer curve in Fig. 1 expressed non-linear behavior from 0 to 100%. One explanation of the shape of this plot could be that the probe is more specifically solvated by the MOPS and *n*-decylamine molecules at the high and low percentage methanol regions. Furthermore, the random mixing approximation is likely to fail at these composition extremes. Mobile phases of compositions between 30 and 70% methanol give almost a linear polarity response with respect to %. The acetonitrile–MOPS buffer curve in Fig. 1 shows the polarity decreasing non-linearly from 0 to 80% acetonitrile and rapidly decreasing from 80 to 100%. This behavior is similar to what has been seen with acetonitrile–water mixtures<sup>21</sup>.

Mixtures of phosphate buffer with both methanol and acetonitrile were studied and their polarity profiles are presented in Fig. 2. The  $E_T(30)$  polarity for these solutions also exhibited non-linear behavior in the range of % organic compositions studied for both solvent systems. Due to problems with solubility of the phosphate buffer salt with the organic modifiers, the maximum mobile phase compositions allowed were 70% methanol and 60% acetonitrile, so no polarity measurements could be made at organic compositions greater than these.

#### *Estimation of $\log k'_w$ by extrapolation methods*

Values of  $\log k'_w$  were estimated by extrapolating linear regression plots of  $\log k'$  versus % organic for each solute to 0% organic modifier and plots of  $\log k'$  versus  $E_T(30)$  to the polarity of pure water. If a buffer solution was used as the aqueous component of the mobile phase, the  $E_T(30)$  plots were extrapolated to the measured  $E_T(30)$  polarity of the pure buffer (63.36 kcal/mole for the MOPS–decylamine buffer).

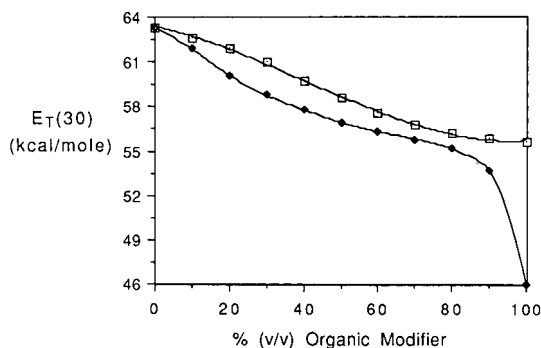


Fig. 1.  $E_T(30)$  polarity change as a function of the volume % of organic modifier in a mixture with 0.02 *M* MOPS (pH 7.4)–0.2% (v/v) *n*-decylamine buffer. □, methanol; ◆, acetonitrile.

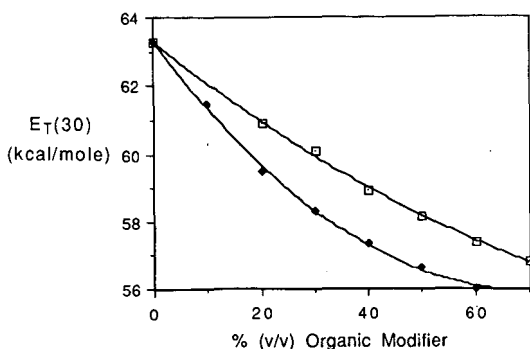


Fig. 2.  $E_T(30)$  polarity change as a function of the volume % of organic modifier in a mixture with 66.6 mM phosphate buffer (pH 7.4). □, methanol; ◆, acetonitrile.

Literature data sets were used that had reported  $\log k'$  versus % organic on a  $C_{18}$  column for both methanol and a second solvent modifier, such as acetonitrile or ethanol<sup>18,21,22,24,25</sup>. A data set refers to a collection of  $\log k'$  values for one solute taken at different mobile phase conditions using one modifier. A summary of the experimental conditions from all of the references can be found in Table I.

Three restrictions were placed on each set of  $\log k'$  data used. The first restriction was to not use  $\log k'$  values above 90% methanol or 80% of the second modifier. It has previously been discussed<sup>21,22</sup> that a limitation of the  $E_T(30)$  polarity scale used as a measure of mobile phase "strength" for RPLC is the occurrence of specific solvation effects between the probe molecule and the solvent components at high percentages of organic modifier. Changes in the solvent polarity above these % values were found not to relate linearly to  $\log k'$ ; this is no problem, however, because  $\log k'$  values measured with more aqueous-rich mobile phases should be used to extrapolate to  $\log k'_w$ . This reasoning will be explained later in the discussion dealing with confidence intervals. A second restriction was not to use  $\log k'$  values much less than  $-0.30$  to try to minimize measurement errors associated with small values of  $\log k'$ . The last restriction is directly related to the first two such that if a data set contained less than four  $\log k'$  values, it was not used. This will also be explained by the confidence interval discussion.

In order to compare the reliability of the  $\log k'_w$  values estimated by both the % and  $E_T(30)$  models, four figures of merit (FOM) were calculated using a total of 204 data sets. Final results for each reference based entirely on linear extrapolations are summarized in Table III. The first FOM was the correlation coefficient,  $r$ , which is a descriptor of the "goodness-of-fit" of a linear model to a set of data. It would be desirable to use a model that gives the most linear description to the data to minimize errors associated with forcing a line through data points that do not express linear behavior. In the previous study of linearity of  $\log k'$  versus  $E_T(30)$ <sup>21</sup>, only ten data sets on a  $C_{18}$  column were obtained, so  $r$  was monitored in this study as well to check if similar linearity improvements over the % model are obtained. From Table III, it can be seen that the average correlation coefficient was greater using the  $E_T(30)$  model with the only exception being where the average  $r$  for both models was the same. The overall apparent correlation improvement using  $E_T(30)$  over % may only be consid-

TABLE III  
COMPARATIVE FIGURES-OF-MERIT FOR LOG  $k'_w$  STUDY BASED ON LINEAR REGRESSION FOR BOTH THE  $E_T(30)$  AND % ORGANIC MODELS

Ref.	$r^a$		$\Delta \log k'_w$		$E_T(30)$		Intersection <sup>c</sup>		RCI <sup>d</sup>	
	%	$E_T(30)$	%	$E_T(30)$	$E_T(30)$	% (v/v)	$E_T(30)$ (kcal)	%	$E_T(30)$	
22	0.9966	0.9972	0.3939	0.2435	216.95	65.65	12.41	10.39		
	$\pm 0.0036$	$\pm 0.0021$	$\pm 0.3170$	$\pm 0.2123$	$\pm 584.37$	$\pm 11.60$	$\pm 7.50$	$\pm 4.01$		
	(N = 30)	(N = 30)	(N = 30)	(N = 30)	(N = 29)	(N = 30)	(N = 27)	(N = 30)		
18	0.9936	0.9986	0.5551	0.2864	- 93.22	68.75	22.28	9.82		
	$\pm 0.0045$	$\pm 0.0014$	$\pm 0.4395$	$\pm 0.4048$	$\pm 938.95$	$\pm 16.86$	$\pm 10.76$	$\pm 4.78$		
	(N = 36)	(N = 36)	(N = 18)	(N = 18)	(N = 18)	(N = 18)	(N = 35)	(N = 35)		
21	0.9972	0.9991	0.5530	0.4740	- 81.94	59.70	9.58	7.06		
	$\pm 0.0021$	$\pm 0.0006$	$\pm 0.2405$	$\pm 0.2562$	$\pm 630.13$	$\pm 0.78$	$\pm 5.72$	$\pm 3.17$		
	(N = 10)	(N = 10)	(N = 5)	(N = 5)	(N = 5)	(N = 5)	(N = 9)	(N = 10)		
24	0.9908	0.9983	0.9741	0.7749	182.72	60.21	11.08	4.72		
	$\pm 0.0064$	$\pm 0.0011$	$\pm 0.2293$	$\pm 0.2311$	$\pm 107.77$	$\pm 0.28$	$\pm 3.79$	$\pm 1.47$		
	(N = 36)	(N = 36)	(N = 18)	(N = 18)	(N = 18)	(N = 18)	(N = 36)	(N = 35)		
25	0.9952	0.9952	0.3931	0.4144	80.90	67.84	15.60	14.56		
	$\pm 0.0034$	$\pm 0.0036$	$\pm 0.2744$	$\pm 0.3552$	$\pm 620.55$	$\pm 62.28$	$\pm 8.02$	$\pm 7.74$		
	(N = 92)	(N = 92)	(N = 46)	(N = 46)	(N = 46)	(N = 46)	(N = 86)	(N = 92)		
Total	0.9945	0.9968	0.5144	0.4089	96.68	65.13	15.24	11.04		
	$\pm 0.0047$	$\pm 0.0030$	$\pm 0.3675$	$\pm 0.3552$	$\pm 625.80$	$\pm 39.90$	$\pm 8.69$	$\pm 6.91$		
	(N = 204)	(N = 204)	(N = 117)	(N = 117)	(N = 116)	(N = 117)	(N = 193)	(N = 202)		

<sup>a</sup>  $r$  = correlation coefficient.

<sup>b</sup>  $\Delta \log k'_w$  = difference between  $\log k'_w$  values estimated using two different modifiers.

<sup>c</sup> Intersection = % or  $E_T(30)$  intersection point between regressions using two different modifiers.

<sup>d</sup> RCI = relative confidence interval about  $\log k'_w$ .

ered marginal, however, since all of the average  $r$  values are greater than 0.99. It was found that retention plots using methanol as the modifier were comparable between the two models but acetonitrile and ethanol showed much better linearity with the  $E_T(30)$  model as compared to volume %. An  $F$ -test<sup>31</sup> of 95% confidence performed on the variances of the averaged correlation coefficients for both models, however, determined the two average  $r$  values ( $n = 204$ ) to be significantly different. These results solidify previous findings on linearity improvements and support the observation that a solvatochromic polarity scale such as  $E_T(30)$  provides a more linear description of the strength of the mobile phase than the bulk organic modifier composition.

A second FOM was  $\Delta \log k'_w$ , the difference between the  $\log k'_w$  values estimated by two different modifiers. Since it would often be useful to employ another modifier, the difference between estimations by the two modifiers should be minimized. Furthermore, agreement of  $\log k'_w$  values from two (or more) modifiers lends confidence to the accuracy of the extrapolated value. Previous work has shown that for 27 data sets a 40% decrease in the  $\Delta \log k'_w$  occurred when using the  $E_T(30)$  model over %<sup>22</sup>. Table III shows a  $\Delta \log k'_w$  improvement of roughly 21% when using the  $E_T(30)$  model for all reference data sets ( $N = 117$ ) [ $\Delta \log k'_w = 0.4089$  for  $E_T(30)$  and 0.5144 for %].

The third FOM is the extrapolated intersection point of linear regressions for a solute using two different modifiers. This intersection determines if two different retention plots converge toward a point indicating an unmodified aqueous mobile phase. If a given retention model describes the strength of the mobile phase in a useful manner, then % plots should converge to 0% organic or the  $E_T(30)$  plots to 63.11 kcal/mole (the polarity of pure water). It will be defined here that % intersections less than 50% organic and  $E_T(30)$  intersections greater than a polarity of 58 kcal/mole (the approximate polarity of 50% organic mobile phase) will be considered converging toward  $\log k'_w$ . From Table III it can be seen that all of the average intersections of the  $E_T(30)$  data sets converged toward the polarity of water while it is difficult to infer the same about the % data. Some of the average % intersections were negative, some were positive and the standard deviations of those averages were large.

In order to extract more meaning out of the intersection results, frequency histograms were constructed to demonstrate the distribution of these values. Fig. 3 shows the spread of the % intersections covering a range from -200 to 500% organic for 97 of the 114 total data sets. Some intersections could not be calculated because the two retention plots of interest were parallel. It was found that 70% of those intersections occurred at values greater than 50% organic, with 41% of the total sets being in the range between 100 and 200% organic. Fig. 4 illustrates the spread of the  $E_T(30)$  intersections in the range from 55 to 70 kcal/mole for 94 of the 117 total data sets. It was found that 78% of these intersections were greater than 58 kcal/mole, with 42% of the total sets occurring between 60 and 63 kcal/mole. The mentioned intersection results indeed show that linear regressions of  $\log k'$  versus  $E_T(30)$  do converge toward the polarity of a pure aqueous mobile phase while  $\log k'$  versus % plots diverge at 0% organic modifier. Based on these intersection results, a more useful estimation of the partitioning processes occurring in a chromatographic system at 100% aqueous mobile phase may be obtained with the  $E_T(30)$  solvent strength model.

A last FOM is the relative confidence interval, RCI. The RCI for a solute using a particular organic modifier indicates the relative uncertainty in a  $\log k'_w$  value and

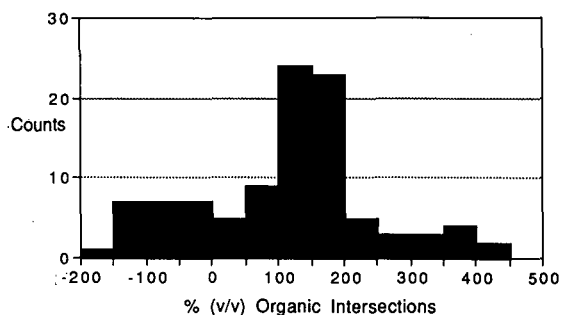


Fig. 3. Frequency histogram of the distribution of linear-linear intersections between plots of  $\log k'$  versus % methanol and  $\log k'$  versus % acetonitrile or ethanol.

can be compared with other solutes in the same and another retention model. For a given solute this figure is calculated by the equation

$$RCI = [(95\% \text{ CI})/\log k'_w] \cdot 100 \quad (4)$$

where 95% CI is the 95% confidence interval at  $\log k'_w$  and is the product of Student's  $t$ -value and the standard deviation of the regression at  $\log k'_w$ <sup>31,32</sup>. The 95% confidence interval is a function of the residual error of the regression, the number and spread of the data points on the ordinate (or  $x$ ) axis and the difference between the centroid of the  $x$  values and the predicting  $x$  value [0% organic or the aqueous  $E_T(30)$ ]. A minimum in an RCI would occur for a predicted  $y$  value that was positioned near the mean of the  $x$  values of a regression model having a correlation coefficient near 1 and consisting of a large number of data points ( $N > 10$ ) spanning a wide range of  $x$  values. Based on these statistical criteria, the data points taken to perform the extrapolation to  $\log k'_w$  should be done with water-rich mobile phases as close to 0% modifier added as possible. This is why the limitation of the  $E_T(30)$  polarity scale at very high organic compositions does not become a limiting factor, because at high % organic the extrapolated value is much less reliable. Also, at least four  $\log k'$  values are needed for a linear extrapolation (where the degrees of freedom for the regression equal the number of data points minus the number of parameters in the regression

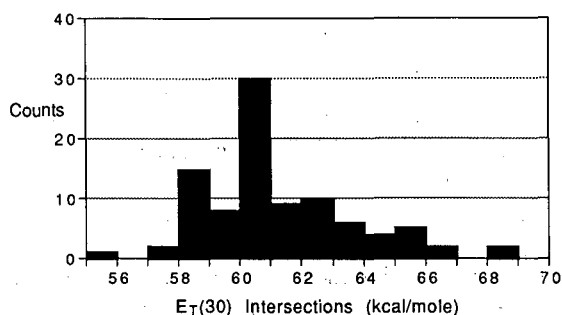


Fig. 4. Frequency histogram of the distribution of linear-linear intersections between plots of  $\log k'$  versus  $E_T(30)$  for methanol-water mixtures and  $\log k'$  versus  $E_T(30)$  for acetonitrile-water or ethanol-water mixtures.



model,  $N - P$ ) because the Student's  $t$ -value for less than four data points increases significantly<sup>32</sup>.

The RCI results are shown in Table III. For all data sets ( $N = 193$  for % and 202 for  $E_T$ ), the overall relative uncertainty in the estimated  $\log k'_w$  values is lower when using the  $E_T(30)$  model. An  $F$ -test statistically verified this observation. The greatest difference in RCI between the two retention models is with the data sets of Reymond *et al.*<sup>18</sup> and Lehtonen<sup>24</sup> because data points were taken as low as 10% organic in many cases and the  $E_T(30)$  plots were very linear. The average of the RCI data of Johnson *et al.*<sup>21</sup>, Michels and Dorsey<sup>22</sup> and Schoenmakers *et al.*<sup>25</sup> did not favor the  $E_T(30)$  model to as large an extent, but the standard deviation of those RCIs was also lower. As was seen with  $\Delta \log k'_w$ , the magnitude of improvement in RCI varied with the data reference because some experiments were done with more  $\log k'$  data points than others but in all cases the  $E_T(30)$  data was more favorable than the % data.

The four figures of merit in this study were also recalculated for the data sets using the second modifiers acetonitrile and ethanol in which a polynomial regression was fit to the data. Table IV presents a comparison of the polynomial % and the  $E_T(30)$  results from Table III. The  $r$  and RCI results are only for the polynomial regressions of acetonitrile and ethanol and the  $\Delta \log k'_w$  and intersection results are for linear methanol data used with polynomial acetonitrile or ethanol data. As statistically expected, the polynomial regression yielded correlation coefficients of almost 1. Another positive aspect of using the polynomial over the linear regression is seen in the  $\Delta \log k'_w$  and intersections data, where the scatter in the  $\log k'_w$  values was reduced and the regression models intersected near 0% organic. Fig. 5 exhibits the frequency histogram for the intersections between the linear methanol plots and the polynomial acetonitrile or ethanol plots. All of these data were found to converge to 0% organic with 82% of them occurring between -10 and 20% organic.

Relative confidence intervals were also calculated for the polynomial-extrapolated  $\log k'_w$  values. It was found that the RCIs for the % polynomial fits were still larger than those for  $E_T(30)$  and determined to be statistically different by an  $F$ -test. An added level of uncertainty is contributed to the % organic retention model by the squared-term of the second-order polynomial equation. The number of degrees of freedom when calculating a second-order polynomial will be a value of one larger than that for a linear regression because the value of  $P$  increases by 1. A solution with which to improve the RCI for polynomial estimated  $\log k'_w$  is to measure at least five or six points on the  $\log k'$  versus % plot toward 0% organic and thus increase the number of degrees of freedom of the regression. While this a worthy solution, the time of analysis would be greatly increased over using a linear solvatochromic model which only requires four or five points.

#### *Procedures for the estimation of $\log k'_w$*

Certain procedures should be followed to ensure reliable results from the estimation of  $\log k'_w$  by extrapolation methods. Both the solvatochromic and linear-polynomial % models give reasonable statistical results. It is recommended that only polynomial fits should be used for acetonitrile or ethanol % plots. The  $\log k'_w$  values estimated by both models, however, are different and deciding which model gives the most accurate estimation of the lipophilic properties of solutes could only be done by

TABLE IV  
 COMPARATIVE FIGURES OF MERIT FOR LOG  $k'_w$  STUDY BASED ON LINEAR REGRESSION FOR  $E_T(30)$  AND % MODELS USING METHANOL AS MODIFIER AND SECOND-ORDER POLYNOMIAL REGRESSION FOR % MODEL USING ETHANOL AND ACETONITRILE AS MODIFIERS (ONLY % MODEL POLYNOMIAL DATA SHOWN FOR  $r$  AND RCI)

Ref.	$\Delta \log k'_w$ <sup>b</sup>		Intersection <sup>c</sup>		RCI <sup>d</sup>	
	$E_T(30)$	%	$E_T(30)$	% ( $v/v$ )	$E_T(30)$ (kcal)	%
22	0.9996 ±0.0005 ( $N = 20$ )	0.3207 ±0.2029 ( $N = 30$ )	0.2435 ±0.2123 ( $N = 30$ )	9.54 ±16.55 ( $N = 24$ )	65.65 ±11.60 ( $N = 30$ )	19.74 ±14.77 ( $N = 20$ )
18	0.9999 ±0.0000 ( $N = 18$ )	0.1241 ±0.1011 ( $N = 18$ )	0.2864 ±0.4048 ( $N = 18$ )	-1.24 ±5.73 ( $N = 18$ )	68.75 ±16.86 ( $N = 18$ )	11.71 ±4.78 ( $N = 35$ )
21	0.9998 ±0.0001 ( $N = 5$ )	0.1599 ±0.0420 ( $N = 5$ )	0.4740 ±0.2562 ( $N = 5$ )	6.00 ±1.60 ( $N = 5$ )	59.70 ±0.78 ( $N = 5$ )	8.03 ±3.17 ( $N = 10$ )
24	0.9993 ±0.0009 ( $N = 18$ )	0.4198 ±0.1597 ( $N = 18$ )	0.7749 ±0.2311 ( $N = 18$ )	9.33 ±3.24 ( $N = 18$ )	60.21 ±0.28 ( $N = 18$ )	7.73 ±2.82 ( $N = 35$ )
25	0.9991 ±0.0018 ( $N = 47$ )	0.1739 ±0.1381 ( $N = 46$ )	0.4144 ±0.3552 ( $N = 46$ )	4.13 ±12.78 ( $N = 45$ )	67.84 ±62.28 ( $N = 46$ )	13.53 ±6.33 ( $N = 46$ )
Total	0.9995 ±0.0008 ( $N = 107$ )	0.2411 ±0.1838 ( $N = 117$ )	0.4089 ±0.3532 ( $N = 117$ )	5.37 ±12.03 ( $N = 110$ )	65.13 ±39.90 ( $N = 117$ )	13.15 ±9.68 ( $N = 107$ )

<sup>a</sup>  $r$  = correlation coefficient.

<sup>b</sup>  $\Delta \log k'_w$  = difference between  $\log k'_w$  values estimated using two different modifiers.

<sup>c</sup> Intersection = % or  $E_T(30)$  intersection point between regressions using two different modifiers.

<sup>d</sup> RCI = relative confidence interval about  $\log k'_w$ .

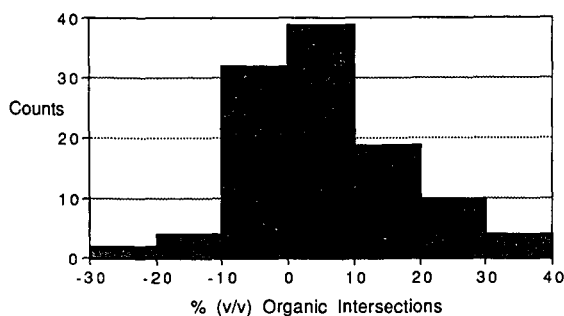


Fig. 5. Frequency histogram of the distribution of intersections between linear plots of  $\log k'_w$  versus % methanol and polynomial plots of  $\log k'_w$  versus % acetonitrile or ethanol.

comparative QSSR or QSAR studies with real biological and environmental partitioning data. This work is currently underway in our laboratory. Table V shows the results of correlation analysis between  $\log k'_w$  and  $\log P_{ow}$  for the data of Reymond *et al.*<sup>18</sup>, Michels and Dorsey<sup>22</sup> and Schoenmakers *et al.*<sup>25</sup>. The values of  $\log P_{ow}$  were taken from shake-flask measurements<sup>33</sup> and calculation<sup>18</sup>. A separate correlation was done for each mobile phase system and the slopes, intercepts and correlation coefficients are reported. Fig. 6 shows an example correlation between  $E_T(30)$ -estimated  $\log k'_w$  from the data of Schoenmakers *et al.*<sup>25</sup> and  $\log P_{ow}$ . It can be seen from Table V that for all solvent systems the  $E_T(30)$ -estimated  $\log k'_w$  values give larger slopes and comparable correlation coefficients. This implies that the solvatochromic method gives a more sensitive scale with which to measure solute lipophilicity, but not a direct measure of  $\log P_{ow}$  values.  $\log k'_w$  has been proposed to be a useful lipophilicity descriptor by itself<sup>14</sup> and these results support this belief.

A recent paper by Minick *et al.*<sup>34</sup> reported attempting the use of the  $E_T(30)$  polarity scale for  $\log k'_w$  extrapolations. The authors, however, did not carry out any

TABLE V

RESULTS OF THE CORRELATION ANALYSIS OF  $\log k'_w$  VERSUS  $\log P_{ow}$  USING DIFFERENT BINARY HYDROORGANIC MOBILE PHASES FOR THE  $E_T(30)$  AND % MODELS

Parameter	Methanol-water		Ethanol-water		Acetonitrile-water	
	%(v/v)	$E_T(30)$	%(v/v)	$E_T(30)$	%(v/v)	$E_T(30)$
Slope <sup>a</sup>	0.936	1.41	0.979	1.25	0.871	1.11
Intercept <sup>a</sup>	0.203	-0.166	0.366	0.187	0.338	0.700
$r^a$	0.971	0.970	0.924	0.937	0.976	0.983
Slope <sup>b</sup>	0.880	1.28			0.832	0.958
Intercept <sup>b</sup>	0.148	-0.622			0.243	-0.040
$r^b$	0.982	0.976			0.970	0.982
Slope <sup>c</sup>	0.814	1.53			0.769	1.10
Intercept <sup>c</sup>	0.536	-0.287			0.662	0.510
$r^c$	0.960	0.959			0.907	0.881

<sup>a</sup>  $N = 10$  from ref. 22.

<sup>b</sup>  $N = 18$  from ref. 18 (ethanol-water not used).

<sup>c</sup>  $N = 34$  from ref. 25 (ethanol-water not used).

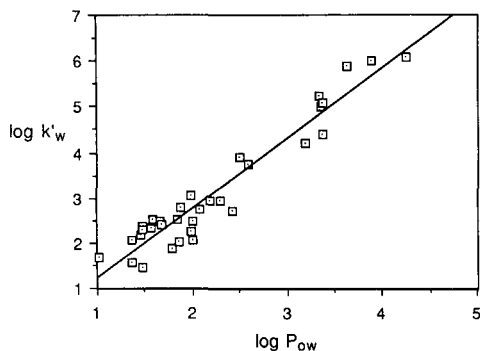


Fig. 6. Correlation between  $E_T(30)$ -estimated  $\log k'_w$  from the data of Schoenmakers *et al.*<sup>25</sup> and octanol-water partition coefficients<sup>33</sup>.

extrapolations of  $\log k'$  versus  $E_T(30)$  plots because of observed non-linearity. A normalization procedure producing " $\Delta E_T(30)$ " values was used as the solvent strength descriptor instead of directly measured  $E_T(30)$ . Using any type of normalized  $E_T(30)$  values, such as Reichardt's  $E_T^N$  values<sup>30</sup>, distorts the behavior of the retention model and is not recommended. They did show graphically, however, that the extrapolated  $\log k'_w$  values give a more accurate measure of lipophilicity than using isocratic values. The elution order of solutes can invert at lower % organic ranges to yield incorrect lipophilicity assignments.

Following sound statistical practice is important for estimating  $\log k'_w$  values of minimal uncertainty. Data points on a plot of  $\log k'$  versus mobile phase strength should be taken in water-rich eluents as close as possible to the value of unmodified aqueous mobile phase. The variance in the regression model is dependent on the centroid as well as the spread and number of the data points along the ordinate axis. Ideally,  $\log k'$  values should be taken down to 10% modifier, but the chromatographic partition coefficient limits this process so that the lowest modifier composition for the elution of some compounds is roughly 50% methanol. Since the solvatochromic  $E_T(30)$  model yields linear retention behavior for modifiers that are slightly stronger than methanol, like acetonitrile and ethanol, and  $E_T(30)$  plots for all three of these modifiers converge toward the polarity of unmodified mobile phase, a solvatochromic model would be useful for this type of experiment. Using organic modifiers stronger than acetonitrile or ethanol, such as propanol or tetrahydrofuran, is not desirable, however, because of specific solute<sup>35</sup> and stationary phase<sup>22,36</sup> solvation effects that produce a different mechanism of retention. It is also crucial to measure accurately the void time of the chromatographic system since  $t_0$  is dependent on the bulk composition of the mobile phase, but there is much debate over the best way to measure this parameter<sup>37-41</sup>.

To study statistically how the reliability of a  $\log k'$  versus solvent strength extrapolation changes with the range and centroid of the data points, a data set with twelve points covering a wide range of solvent compositions was used. In Table VI the data point closest to pure water was removed in succession until five data points remained in the high organic portion of the plot. As the range and number of data points became smaller and more removed from water, the value of the RCI became larger. Also note that for both solvent strength models the value of  $\log k'_w$  became

TABLE VI

CHANGE IN THE RELATIVE CONFIDENCE INTERVAL (RCI) ABOUT  $\log k'_w$  ESTIMATED WITH METHANOL-WATER MOBILE PHASES FOR METHYLAMINO-5-DIMETHYLAMINO-1-SULFONATE<sup>24</sup> AS A FUNCTION OF THE SPANNING OF  $\log k'_w$  VALUES TOWARD PURE WATER

Lowest % (v/v)	N	$E_T(30) \log k'_w$	$E_T(30) RCI$	% $\log k'_w$	% RCI
35	12	3.5781	4.48	2.7730	12.92
40	11	3.4789	3.57	2.6267	12.53
45	10	3.4775	4.53	2.4895	12.08
50	9	3.4390	5.53	2.3742	13.50
55	8	3.4415	8.04	2.2246	14.60
60	7	3.3964	14.15	2.0761	— <sup>a</sup>
65	6	3.2276	16.78	1.8999	25.24
70	5	3.0366	29.74	1.6880	32.39

<sup>a</sup> Calculation yielded an empty set result.

smaller when the data points were in the organic-rich region. Table VII shows the effects of shifting the centroid of the ordinate axis further from water when the range of the data points is kept constant. As the centroid reaches a value of 75% organic, the uncertainty in the extrapolation with both models becomes very large. These results illustrate that  $\log k'$  values must be measured in water-rich mobile phases to keep the uncertainty about the extrapolated  $\log k'_w$  value at as low a level as possible.

Of the 117 intersections calculated in this paper using the  $E_T(30)$  model, fourteen were found not to converge to the polarity of unmodified mobile phase. Of those fourteen divergent sets, ten included a nitrogen-containing functional group that could be highly interactive with a surface silanol (eighteen nitrogen-containing sets altogether). We have also investigated the use of  $E_T(30)$ -estimated  $\log k'_w$  values for the calculation of solute-solvent contact free energy in RPLC<sup>36</sup> and have found the same problem of nitrogen-containing compounds interacting with surface silanols.

Employing a stationary phase that provides the most possible non-polar surface would be desirable since the influence of residual silanols would be minimized. Silanol interactions can be negated by using masking agents in the mobile phase or by

TABLE VII

CHANGE IN THE RELATIVE CONFIDENCE INTERVAL (RCI) ABOUT  $\log k'_w$  ESTIMATED WITH METHANOL-WATER MOBILE PHASES FOR METHYLAMINO-5-DIMETHYLAMINO-1-SULFONATE<sup>24</sup> AS A FUNCTION OF THE MOVEMENT OF THE ORDINATE CENTROID FROM PURE WATER

Four values of  $\log k'$  are taken in each % range, with each  $\log k'$  taken every 10% organic.

% (v/v) range	$E_T(30) RCI$	Average $E_T(30)$	% RCI	Average %
35-65	10.18	58.28	22.91	50
40-70	6.29	57.94	16.27	55
45-75	— <sup>a</sup>	57.56	15.84	60
50-80	11.13	57.24	25.20	65
55-85	8.67	56.93	29.83	70
60-90	33.08	56.64	49.70	75

<sup>a</sup> Calculation yielded an empty set result.

using monomeric stationary phases of very high alkyl ligand bonding density. Studies using masking agents like tetraethylamine or *n*-decylamine in the mobile phase<sup>42,43</sup> have observed that for hydrogen-bond accepting solutes, the masking agent binds to the silanol and allows the polar solute to interact primarily with hydrophobic ligands. A disadvantage with using these agents, however, is that they can form ion pairs with specific solutes and alter the measured hydrophobicity. Another method of minimizing silanol interactions is by exhaustively end-capping and/or producing a high bonding density C<sub>18</sub> phase. It has been shown that exhaustive end-capping with a C<sub>1</sub> functional group deactivates surface silanols<sup>44</sup> and for small, polar solutes, directly measured log  $k'_w$  values are more reproducible<sup>45</sup>.

## CONCLUSION

The RPLC estimation of solute lipophilicity, in the form of the parameter log  $k'_w$ , has been discussed using the solvatochromic  $E_T(30)$  solvent polarity scale. Comparative figures of merit were calculated for 204 data sets to contrast the % and  $E_T(30)$  models of mobile phase strength. Results show that the  $E_T(30)$  model is more useful than the linear % model because of increased statistical confidence in log  $k'_w$  values. Calculations done with a polynomial % model on retention data generated with acetonitrile and ethanol modifiers found log  $k'_w$  values statistically comparable to those estimated by linear % extrapolations of methanol-generated data. The  $E_T(30)$ -estimated log  $k'_w$  values, however, were still statistically more certain than polynomial % estimated values. Correlations relating log  $k'_w$  and log  $P_{ow}$  have shown  $E_T(30)$ -estimated log  $k'_w$  values producing a more sensitive scale of hydrophobicity than %-estimated values.

Suggested guidelines for the execution of RPLC lipophilicity estimations have been presented. The most desirable chromatographic system would be an end-capped high bonding density C<sub>18</sub> stationary phase and an aqueous mobile phase modified with methanol, ethanol or acetonitrile. A high bonding density stationary phase would minimize interactions between the solute and surface residual silanols and maximize the partitioning capabilities of the chromatographic system. Using organic modifiers stronger than acetonitrile or ethanol such as propanol or tetrahydrofuran would be undesirable because the mechanism of retention changes with the stronger solvents. Retention measurements for a solute of interest should be taken over a minimal range of 40% organic modifier with the most water-rich mobile phase used being as close to unmodified eluent as possible. Qualitative structure-activity relationships for solutes of biological and environmental interest also need to be performed using log  $k'_w$  values estimated by  $E_T(30)$ , and this work is ongoing in this laboratory.

## ACKNOWLEDGEMENTS

The authors are grateful to Dr. John Cornell of the University of Florida Statistics Department for his helpful advice and to Drs. John Baty and Sheila Sharp of the Department of Biochemical Medicine of Ninewells Hospital (Dundee, U.K.) for generously contributing retention data. They also acknowledge NIH GM33382 and Merck Sharp & Dohme for support of this work.

## REFERENCES

- 1 N. Nirmalakhandan and R. E. Speece, *Environ. Sci. Technol.*, 22 (1988) 606–615.
- 2 C. Hansch, in N. B. Chapman and J. Shorter (Editors), *Correlation Analysis in Chemistry and Biology*, Plenum Press, New York, 1978, pp. 397–438.
- 3 R. Kalizan, *J. Chromatogr.*, 220 (1981) 71–83.
- 4 C. F. Carney, *J. Liq. Chromatogr.*, 8 (1985) 2781–2804.
- 5 T. Braumann, *J. Chromatogr.*, 373 (1986) 191–225.
- 6 R. Kalisz, *CRC Crit. Rev. Anal. Chem.*, 16 (1986) 323–382.
- 7 R. Kalisz, *Chromatography*, 2, No. 5 (1987) 19–29.
- 8 R. P. W. Scott and P. Kucera, *J. Chromatogr.*, 142 (1977) 213–232.
- 9 T. Braumann, G. Weber and L. H. Grimme, *J. Chromatogr.*, 261 (1983) 329–343.
- 10 M. M. Schantz and D. E. Martire, *J. Chromatogr.*, 391 (1987) 35–51.
- 11 L. R. Snyder, M. A. Quarry and J. L. Glajch, *Chromatographia*, 24 (1987) 33–44.
- 12 L. R. Snyder, J. W. Dolan and J. R. Gant, *J. Chromatogr.*, 165 (1979) 3–30.
- 13 K. Miyake, N. Mizuno and H. Terada, *J. Chromatogr.*, 439 (1988) 227–235.
- 14 T. Braumann, H. Genieser, C. Lüllman and B. Jastorff, *Chromatographia*, 24 (1987) 777–782.
- 15 P. J. Schoenmakers, H. A. H. Billiet, R. Tijssen and L. de Galan, *J. Chromatogr.*, 149 (1978) 519–537.
- 16 M. Borówko, M. Jaroniec and J. Piotrowska, *J. Liq. Chromatogr.*, 10 (1987) 2033–2045.
- 17 P. Jandera, *J. Chromatogr.*, 314 (1984) 13–36.
- 18 D. Reymond, G. N. Chung, J. M. Mayer and B. Testa, *J. Chromatogr.*, 391 (1987) 97–109.
- 19 J. D. Baty and S. Sharp, *J. Chromatogr.*, 437 (1988) 13–31.
- 20 C. Reichardt, *Angew. Chem., Int. Ed. Engl.*, 4 (1965) 29–40.
- 21 B. P. Johnson, M. G. Khaledi and J. G. Dorsey, *Anal. Chem.*, 58 (1986) 2354–2365.
- 22 J. J. Michels and J. G. Dorsey, *J. Chromatogr.*, 457 (1988) 85–98.
- 23 J. G. Dorsey and B. P. Johnson, *J. Liq. Chromatogr.*, 10 (1987) 2695–2706.
- 24 P. Lehtonen, *J. Chromatogr.*, 314 (1984) 141–153.
- 25 P. J. Schoenmakers, H. A. H. Billiet and L. de Galan, *J. Chromatogr.*, 218 (1981) 261–284.
- 26 K. A. Zachariasse, V. P. Nguyen and B. Kozankiewicz, *J. Phys. Chem.*, 85 (1981) 2676–2683.
- 27 P. Plieninger and H. Baumgärtel, *Justus Liebigs Ann. Chem.* (1983) 860–875.
- 28 M. Mohamad and E. Kosower, *J. Phys. Chem.*, 74 (1970) 1153–1154.
- 29 H. Langhals, *Tetrahedron*, 43 (1987) 1771–1774.
- 30 C. Reichardt, *Solvent Effects in Organic Chemistry*, VCH, Weinheim, 2nd ed., 1988.
- 31 R. L. Anderson, *Practical Statistics For Analytical Chemists*, Van Nostrand Reinhold, New York, 1987.
- 32 D. Draper and M. Smith, *Applied Regression Analysis*, Wiley, New York, 2nd ed., 1981.
- 33 C. Hansch and A. Leo, *Substituent Constants for Correlation Analysis in Chemistry and Biology*, Wiley, New York, 1979.
- 34 D. J. Minick, J. H. Frenz, M. A. Patrick and D. A. Brent, *J. Med. Chem.*, 31 (1988) 1923–1933.
- 35 A. Nahum and Cs. Horváth, *J. Chromatogr.*, 192 (1980) 315–322.
- 36 P. T. Ying, K. A. Dill and J. G. Dorsey, *Anal. Chem.*, in press.
- 37 G. E. Berendsen, P. J. Schoenmakers, L. de Galan, G. Vigh, Z. Varga-Puchony and J. Inczedy, *J. Liq. Chromatogr.*, 3 (1980) 1669–1686.
- 38 H. Engelhardt, H. Müller and B. Dreyer, *Chromatographia*, 19 (1985) 240–245.
- 39 L. Margarit-Roig, A. Diaz-Marot and M. Gassiot-Matas, *Afinidad*, 43 (1986) 525–529.
- 40 M. C. Hennion and R. Rosset, *Chromatographia*, 25 (1988) 43–50.
- 41 W. R. Melander, J. F. Erard and Cs. Horváth, *J. Chromatogr.*, 282 (1983) 211–228.
- 42 N. El Tayar, A. Tsantili-Kakoulidou, T. Roethlisberger, B. Testa and J. Gal, *J. Chromatogr.*, 439 (1988) 237–244.
- 43 E. Bayer and A. Paulus, *J. Chromatogr.*, 400 (1987) 1–4.
- 44 J. H. Knox, J. Kriz and E. Adamcová, *J. Chromatogr.*, 447 (1988) 13–27.
- 45 L. A. Cole and J. G. Dorsey, unpublished results.





CHROMSYMP. 1673

## STRATEGIES OF MOBILE PHASE TRANSFER FROM THIN-LAYER TO MEDIUM-PRESSURE LIQUID CHROMATOGRAPHY WITH SILICA AS THE STATIONARY PHASE

SZABOLCS NYIREDY, KARIN DALLENBACH-TOELKE, GEORG C. ZOGG and OTTO STICHER\*

*Department of Pharmacy, Swiss Federal Institute of Technology (ETH) Zurich, CH-8092 Zürich (Switzerland)*

---

### SUMMARY

The location of the fronts in thin-layer chromatography (TLC) with multi-component mobile phases is discussed with reference to the possibilities of mobile phase transfer via analytical overpressured-layer chromatography (OPLC) to preparative medium-pressure liquid chromatography (MPLC). The advantage of this procedure is that the mobile phase of the TLC separation where the substance zones are distributed over the whole  $R_F$  range can be transferred to preparative column chromatography without limitations. Because OPLC may be used as equilibrated or non-equilibrated planar column systems and all mobile-phase fronts may be seen, it can be applied as a pilot method for preparative MPLC. Depending on the results of the analytical OPLC separation, four possibilities exist for mobile phase transfer to MPLC; these are discussed.

The generally useful method is to equilibrate the dry-filled column (silica of TLC quality with an average particle size of 15  $\mu\text{m}$ ) with a solvent in which the substances to be separated do not migrate and which was used for the prerun in analytical OPLC. The separation is then started with the optimized TLC mobile phase where the substances are distributed over the whole  $R_F$  range. Transfer of the optimized TLC mobile phase via OPLC to MPLC is demonstrated by the separation of furocoumarin isomers from the roots of *Heracleum sphondylium* and the ginsenosides from *Panax ginseng* C. A. Meyer. The separation of anthraquinone aglycones from *Rhamnus frangula* is an example of the direct transfer of the mobile phase from TLC to MPLC.

---

### INTRODUCTION

High-performance liquid chromatography (HPLC) is the best established method<sup>1,2</sup> for scale-up to different preparative column liquid chromatographic (CLC) methods. Thin-layer chromatography (TLC) is accepted in many laboratories as a rapid pilot method for preparative normal-phase (NP) CLC<sup>3–7</sup>. However, the disadvantage is that, for a successful preparative separation, the TLC separation

should be obtained below  $R_F = 0.3^8$ . It is almost impossible to achieve a separation in this small range for complex separation problems, and the result cannot always be predicted by using multi-component mobile phases.

In this paper we report different strategies for transfer of the optimized TLC mobile phase via analytical overpressured-layer chromatography (OPLC) to preparative NP medium-pressure liquid chromatography (MPLC)<sup>9</sup>, using the whole  $R_F$  range (0.1–0.9) of the TLC plate for the analytical separation.

## EXPERIMENTAL

The analytical separations were carried out on silica 60 F<sub>254</sub> TLC Alufoils from Merck (Darmstadt, F.R.G.) in unsaturated chromatographic chambers. MPLC glass columns obtained from Labomatic (Schönenbuch, Switzerland) (735 × 26 mm I.D. and 584 × 37 mm I.D.) and from Büchi (Flawil, Switzerland) (460 × 36 mm I.D.) were dry-filled with TLC silica gel GF<sub>254</sub> having an average particle size of 15 μm (Merck).

Analytical reagent grade solvents were used for all separations. The mobile phase was delivered with either a Labomatic MD-80/100 MPLC pump, a Lewa (Leoberg, F.R.G.) Lab M5 pump or a Büchi 681 chromatography pump.

The prepurified extract of furocoumarins was obtained from *Heracleum sphondylium*<sup>10</sup>, the ginsenosides from *Panax ginseng* C. A. Meyer<sup>11</sup> and anthraquinone aglycones from a hydrolysed extract from *Rhamnus frangula*<sup>12</sup>. Samples were applied with a Linomat IV TLC spotter from Camag (Muttens, Switzerland) for the analytical separations. For MPLC separations, sample injection was performed with a Rheodyne (Cotati, CA, U.S.A.) four-way valve.

For OPLC separations a Chrompres 10 apparatus (Labor-MIM, Budapest, Hungary) was used at 10 bar overpressure. For the one-directional linear OPLC separations all four sides of the plates were impregnated with Impres II polymer suspension (Labor-MIM). Two channels were scratched out at a distance of 18 cm for the solvent inlet and outlet.

The densitograms in the absorption mode were recorded at 313 nm for furocoumarins (mercury source lamp) and at 254 nm for the anthraquinone aglycones with a Camag TLC scanner II, coupled with an HP 9000-216 computer (Camag) and an SC-920 high-speed TLC scanner (Shimadzu, Kyoto, Japan). For visual detection of ginsenosides, 1% vanillin in sulphuric acid was used and the densitograms were recorded at 540 nm.

For the on-line preparative MPLC separations, an LKB (Bromma, Sweden) detector with a 313-nm filter for furocoumarins and a 254-nm filter for anthraquinone aglycones, coupled with an LKB 2210 recorder and an LKB 7000 Ultracrac fraction collector, was used.

## RESULTS AND DISCUSSION

### *Theoretical aspects*

The main difference between TLC and CLC is that TLC is a non-equilibrated system, whereas CLC is generally a system equilibrated with the mobile phase. The rule that the substances have to be separated below  $R_F = 0.3$  in TLC for a successful

transfer to preparative CLC<sup>8</sup> is based on the fact that below  $R_F = 0.3$  the TLC system is generally also equilibrated, meaning that all compounds migrate within the last front of a multi-component mobile phase (see Fig. 1a). In all theoretical cases shown in Fig. 1 the mobile phase consists of four solvents. The fronts ( $\alpha$ ,  $\beta$ ,  $\gamma$ ,  $\delta$ ) are rarely visible in TLC, except for the  $\alpha$ -front. On transferring the mobile phase of the TLC separation shown in Fig. 1b to CLC, the compounds migrating between the  $\gamma$  and  $\delta$  front will be eluted together, because the TLC solvent composition between these two fronts is not identical with the eluent of the equilibrated column. All other compounds could be separated under these conditions by CLC.

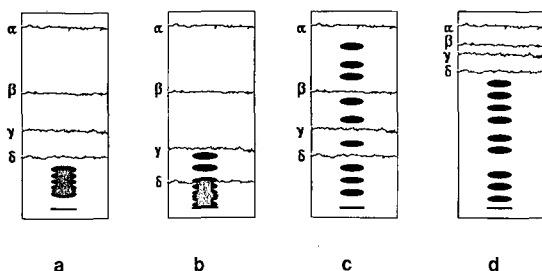


Fig. 1. Location of the fronts of a multi-component mobile-phase system and the compound zones in TLC (for explanation, see text).

On using the whole  $R_F$  range for the separation of the compounds in TLC, an ideal distribution, as depicted in Fig. 1c, is obtained, with all compounds separated. However, owing to the several fronts occurring between these compounds, a preparative CLC separation would not be possible with this mobile phase. A special case is shown in Fig. 1d, where all compounds migrate within the last front and are well separated. This mobile phase could be used for CLC separation and a good result would be obtained.

Because OPLC can be used as an equilibrated or non-equilibrated "planar column", this method may be employed as a pilot technique for the transfer of the optimized TLC mobile phase to the various CLC methods, *e.g.*, MPLC with silica as stationary phase. The plates must be prepared as described under Experimental. The optimized TLC mobile phase obtained from an unsaturated chromatographic tank cannot generally be transferred to analytical OPLC because gas and/or air are adsorbed on the surface of the stationary phase. This causes a disturbing zone<sup>13</sup> in the completely closed OPLC chamber, which distorts the substance zones within its range. The location of the disturbing zone depends on the mobile phase composition and pressure relationships, which are influenced primarily by the flow-rate.

As shown in an earlier study on the disturbing zone, three possibilities exist for transfer of the TLC mobile phase to analytical OPLC<sup>14,15</sup>:

- (1) Variation of the flow-rate to either extremely high or low values to place the disturbing zone in an  $R_F$  range where it does not distort the separation.
- (2) Reduction of the solvent strength of the mobile phase and further development. This method can be used only for the separation of closely related structures, where the reduction of the solvent strength does not result in a change in order of elution of consecutive compounds.

(3) A prerun with a suitable solvent, in which the applied samples do not migrate and which is miscible with the mobile phase. For non-polar compounds this solvent is usually *n*-hexane; for polar compounds such a solvent must be considered during the TLC mobile phase optimization<sup>16</sup>. The plate is developed with this solvent until no more air bubbles are eluted from the plate. The separation may then be started with the mobile phase.

Among these possibilities, the third is generally applicable to the transfer of the optimized TLC mobile phase to analytical OPLC. Because OPLC is used in this way as a specially equilibrated planar column, the OPLC mobile phase (including prerun) can also be transferred to preparative MPLC.

#### *Mobile phase transfer to preparative MPLC*

The mobile phase transfer strategy for preparative MPLC separation can be deduced from the results of the analytical OPLC experiments used as a pilot method. As the TLC/OPLC experiments are carried out on plates with an average particle size of 11  $\mu\text{m}$ , silica with an average particle size of 15  $\mu\text{m}$  is used for preparative MPLC. The column is dry-filled with the aid of a vacuum and nitrogen overpressure<sup>9</sup>. Theoretically, all transfer possibilities described above for OPLC can also be applied to preparative MPLC.

(1) A good preparative separation is problematic when starting with a dry column with an adequate mobile phase velocity, because the location of the disturbing zone is difficult to predict. This method can only be used when the substances to be separated are in the lower  $R_F$  ( $R_F < 0.3$ ) range in the OPLC separation.

(2) The same effect can be achieved by reduction of the solvent strength ( $S_T$ ) of the TLC mobile phase. The influence of the solvent strength reduction on the separation must always be checked in analytical OPLC. This method is applicable to the separation of compounds with different structures only in certain instances.

(3) The dry-filled column must be equilibrated with the solvent used in the OPLC prerun, and then the separation may be started with the TLC/OPLC mobile phase. This method can be used independently of the structures of the substances to be separated and the location of the fronts (see Fig. 1c). With this method a certain dilution of the mobile phase has to be considered for the first-eluted compounds ( $R_F < 0.8$  in TLC). With on-line detection, a shift of the baseline may be observed owing to the different mobile-phase compositions between the various fronts. Substances migrating on or near these fronts give very sharp peaks, but this can also be predicted from analytical OPLC. However, these effects have almost no influence on the quality of the preparative separation.

(4) In the special case where all substances are spread over the whole  $R_F$  range, and migrate within the last front of the multi-component mobile phase (in both TLC experiments and analytical OPLC as well), the column can be equilibrated with the TLC mobile phase (see Fig. 1d). As a result, the preparative separation will be similar to that in analytical OPLC.

In all transfer possibilities mentioned above for the determination of the amount of sample for MPLC, the TLC plate will be overloaded in analytical fully off-line OPLC until the densitometric resolution is no longer satisfactory. Calculation is performed approximately according to the amount of extract per unit volume of the stationary phase (*e.g.*, 6.5 ml for the TLC plate and 468 ml for the glass columns investigated for the separation of furocoumarins).

*Separation of furocoumarin isomers from Heracleum sphondylium roots*

Separation of the five main furocoumarin isomers from *Heracleum sphondylium* is shown as a typical example of the separation of apolar compounds. Optimization was started with TLC preassays, where diethyl ether, ethyl acetate and chloroform were selected. Optimization with the regular part of the PRISMA model<sup>16,17</sup> gave the best separation at a solvent strength of  $S_T = 1.6$  [ethyl acetate–chloroform–diethyl ether–*n*-hexane (8.8:17.6:17.6:56)]. The densitogram of the TLC separation with this mobile phase is shown in Fig. 2a.

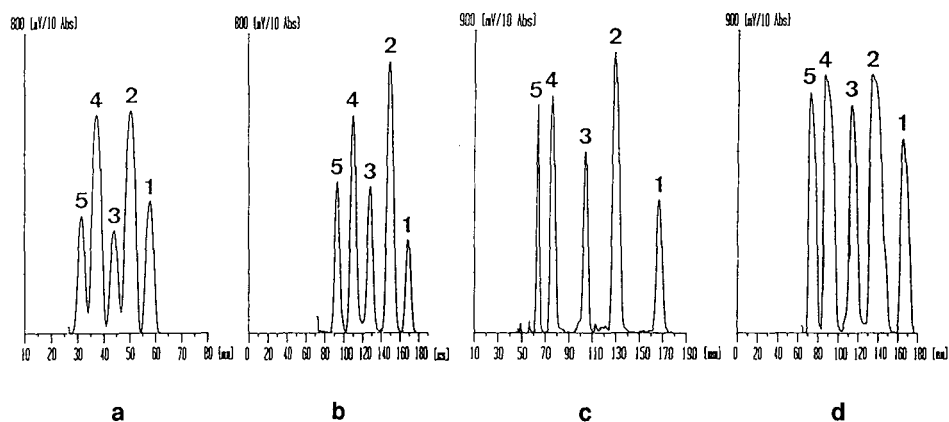


Fig. 2. Analytical TLC and OPLC separations of *Heracleum sphondylium* extract on TLC plates. 1 = Isobergapten; 2 = pimpinellin; 3 = bergapten; 4 = isopimpinellin; 5 = sphondin. (a) TLC separation in unsaturated chamber (separation distance, 8.5 cm); (b) OPLC separation after an *n*-hexane prerun; conditions, flow-rate 0.5 ml/min, development distance 18 cm, overrunning; (c) OPLC separation with reduced solvent strength ( $S_T = 1.0$ ); (d) overloaded OPLC separation on TLC plate (volume, 6.5 ml) with a 4-mg sample and an *n*-hexane prerun.

The TLC mobile phase was transferred directly to analytical OPLC over an 18-cm separation distance. The adsorbed air or gas was eliminated either by a prerun with *n*-hexane (Fig. 2b) or by decreasing the solvent strength of the mobile phase to  $S_T = 1.0$  (Fig. 2c). All five main compounds could be baseline separated by these methods. In the next step, under the same chromatographic conditions, the plate was overloaded to find the maximum amount of sample that could just be separated on a TLC plate by the OPLC technique (Fig. 2d).

In the next step, the mobile phase was transferred to MPLC. The results of the various mobile phase transfer procedures are shown in Figs. 3 and 4.

First, the separation was carried out with a dry-filled column to which the sample was applied. Separation was started with a mobile phase that was diluted with *n*-hexane, as an alternative method for eliminating adsorbed air and gas. Of course, the effectiveness of this procedure was tested first by analytical OPLC. The chromatogram of this MPLC separation is shown in Fig. 3.

Using the generally applicable method similar to analytical OPLC, the column was first equilibrated with *n*-hexane, then the sample was applied and the separation was started with the optimized TLC mobile phase. The resulting separation is depicted in Fig. 4a. Because in the analytical OPLC separation all compounds to be separated were migrating within the last front of the four-component eluent, the

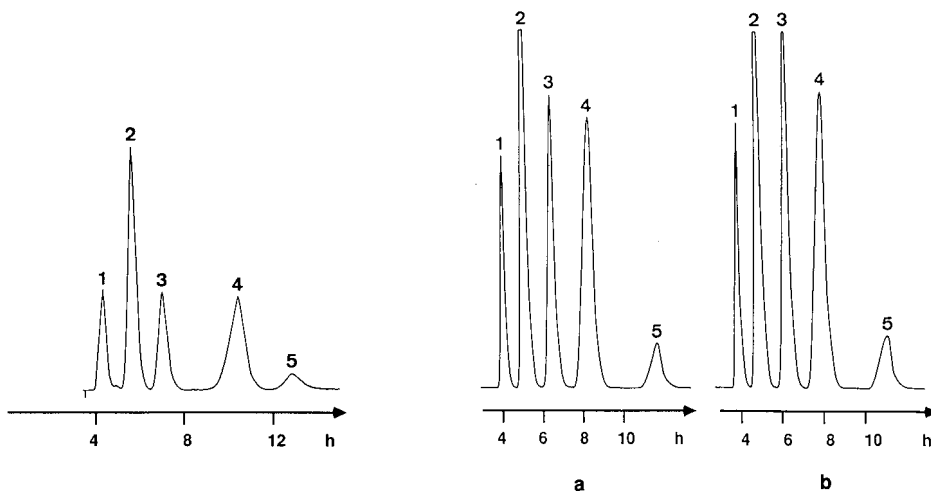


Fig. 3. MPLC separation of *Heracleum sphondylium* extract on non-equilibrated column. 1 = Isobergapten; 2 = pimpinellin; 3 = bergapten; 4 = isopimpinellin; 5 = sphondin. Column dimensions, 460 × 36 mm I.D. (468 ml); dry-filled with TLC silica gel GF<sub>254</sub>; mobile phase, ethyl acetate–chloroform–diethyl ether–*n*-hexane (5.5:11:11:72.5); flow-rate, 5 ml/min; sample amount, 300 mg.

Fig. 4. MPLC separations of *Heracleum sphondylium* extract on an equilibrated column. 1 = Isobergapten; 2 = pimpinellin; 3 = bergapten; 4 = isopimpinellin; 5 = sphondin. Column dimensions: 460 × 36 mm I. D. (468 ml); dry-filled with TLC silica gel GF<sub>254</sub>; TLC mobile phase, ethyl acetate–chloroform–diethyl ether–*n*-hexane (8.8:17.6:17.6:56); flow-rate, 5 ml/min; sample amount, 300 mg. (a) Equilibration with *n*-hexane; (b) equilibration with the TLC mobile phase.

separation of the furocoumarin-containing extract was also carried out on a column that had been equilibrated with the TLC mobile phase. The resulting chromatogram is shown in Fig. 4b.

On comparing the chromatograms obtained using the three mobile phase transfer possibilities, all methods are seen to give high-resolution separations. As expected, the longest separation time was observed with the lowest solvent strength, although the flow-rate was increased by 70%.

Equilibration of the column with *n*-hexane exerts a very small effect on the retention times, especially on those of the first-eluted compounds. Because all compounds migrated within the last front in OPLC, the chromatograms of the separation started with an *n*-hexane-equilibrated column or with a column equilibrated with the mobile phase are almost identical. As may be concluded from Figs. 3 and 4, the separation time could be reduced dramatically<sup>18</sup> by increasing the flow-rate, but this was not the aim of these experiments.

#### *Separation of ginsenosides from Panax ginseng roots*

Separation of the main ginsenosides (Rg2, Rg1, Rf, Re, Rd, Rc, Rb2, Rb1) from *Panax ginseng* is given as a typical example of the transfer of the optimized TLC mobile phase for polar compounds. From the TLC preassays in unsaturated chambers, methyl ethyl ketone, methanol and water were finally selected for further optimization of the mobile phase with the irregular top part of the PRISMA model<sup>19,20</sup>.

In the next step, the optimized TLC mobile phase [methyl ethyl ketone–metha-

nol–water (70:22:8)] was transferred to analytical OPLC. The prerun was carried out with methyl ethyl ketone, in which the substance do not migrate. Then the separation was started with the mobile phase from the TLC separation. The densitogram of the analytical OPLC separation on a TLC plate is shown in Fig. 5a; the separation distance was 17 cm.

For the MPLC separation of the ginsenosides, the column, dry-filled with 15- $\mu\text{m}$  silica of TLC quality, was equilibrated with methyl ethyl ketone. Thus, starting conditions were obtained that were similar to those in the OPLC separations. After the application of 150 mg of sample to a 73.5  $\times$  2.6 cm I.D. column, the separation was started with the optimized mobile phase from the TLC separation. The eight main ginsenosides could be isolated almost without mixed fractions, as demonstrated in Fig. 5b.

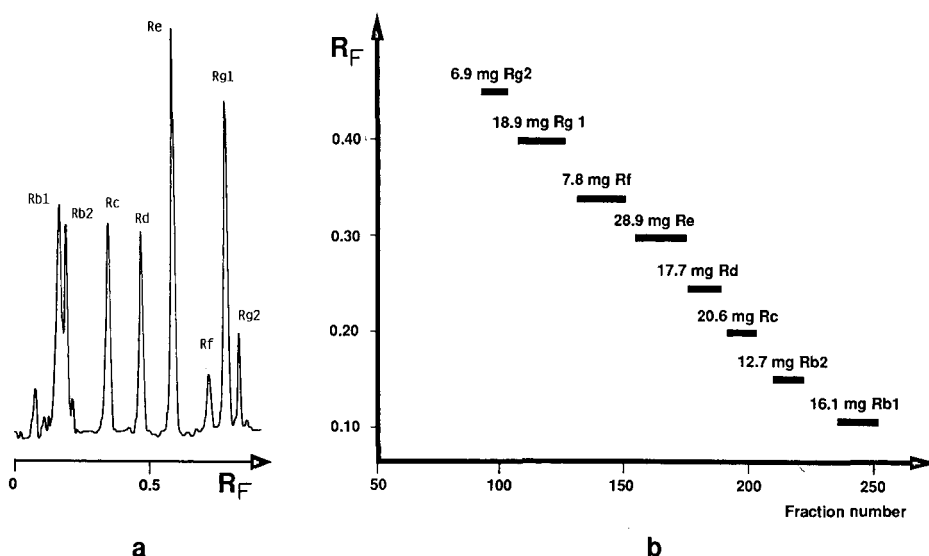


Fig. 5. Analytical OPLC and preparative MPLC separation of *Panax ginseng* extract. Mobile phase, methyl ethyl ketone–methanol–water (70:22:8) (a) OPLC separation on TLC plate after a methyl ethyl ketone prerun; conditions, flow-rate 0.5 ml/min; development distance 18 cm; (b) MPLC separation; column dimensions, 735  $\times$  26 mm I.D. (410 ml), dry-filled with TLC silica gel HF<sub>254</sub>; flow-rate 2 ml/min; sample amount 150 mg.

#### *Separation of anthraquinone aglycones from Rhamnus frangulae cortex*

The TLC separation of a prepurified, hydrolysed extract, containing three anthraquinone aglycones (chrysophanic acid, physcion and frangula emodin) was achieved in two steps: chrysophanic acid and physcion were separated with a mobile phase of tetrahydrofuran–*n*-hexane (1:7) (mobile phase A), as shown in Fig. 6a; then, to facilitate rapid migration of frangula emodin, tetrahydrofuran–*n*-hexane (3:7) (mobile phase B) was employed (see Fig. 6b).

This latter mobile phase was not suitable for the complete separation, as chrysophanic acid and physcion were not adequately resolved in this system. Therefore, the MPLC separation of the three compounds was carried out with a solvent strength

step gradient. The dry-filled (15- $\mu\text{m}$  silica) column (584  $\times$  37 mm I.D.) was first equilibrated with *n*-hexane. After the sample application, the separation was started with mobile phase A at a flow-rate of 9 ml/min. After elution of chrysophanic acid and physcion, the mobile phase was changed to B. The on-line MPLC trace is depicted in Fig. 6c. From a 1200-mg extract, 37.2 mg of chrysophanic acid, 48.4 mg of physcion and 819 mg of frangula emodin could be obtained.

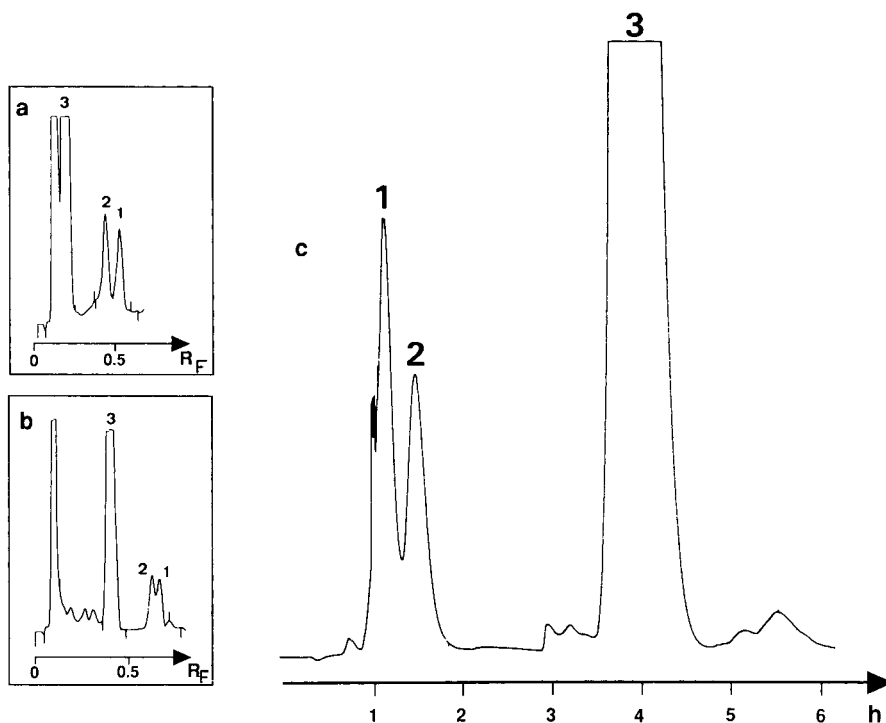


Fig. 6. Analytical TLC and preparative MPLC separation of anthraquinone aglycones. 1 = Chrysophanic acid; 2 = physcion; 3 = frangula emodin. (a) TLC separation in an unsaturated chromatographic tank with tetrahydrofuran-*n*-hexane (1:7); development distance, 9 cm. (b) TLC separation in an unsaturated chromatographic tank with tetrahydrofuran-*n*-hexane (3:7); development distance, 8.5 cm. (c) MPLC separation with a step gradient (for explanation see text); column dimensions, 584  $\times$  37 mm I.D. (615 ml), dry-filled with TLC silica HF<sub>254</sub>; flow-rate, 9 ml/min; sample amount, 1200 mg.

## CONCLUSION

Four basic possibilities exist for mobile phase transfer from TLC to MPLC with silica as stationary phase. It is advantageous to use OPLC as a pilot method, because it is a forced-flow "planar-column" chromatographic system. OPLC separations may be carried out in both the fully off-line mode and the fully on-line mode<sup>21,22</sup>, and both techniques can be applied to these transfer strategies. Transfer possibilities via analytical OPLC and directly from TLC to MPLC are summarized in Fig. 7.

If MPLC separation is carried out starting with a dry column, solvent strength reduction at a higher flow-rate is a good approach, provided that the influence of the



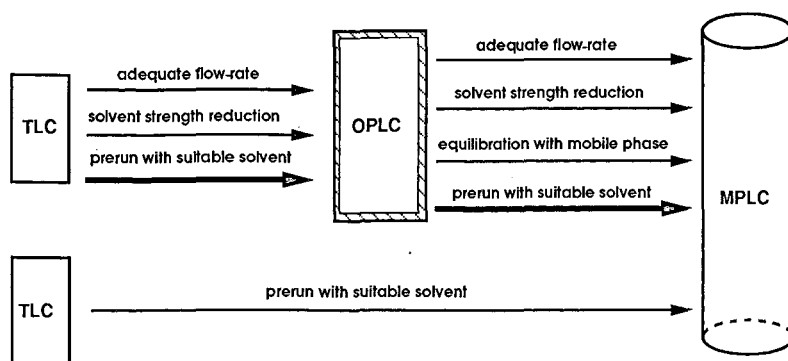


Fig. 7. Mobile phase transfer possibilities from TLC to MPLC with silica as stationary phase.

change of these parameters has been checked in analytical OPLC. This mobile phase transfer is possible if the correlation between solvent strength and  $R_F$  values is similar for all compounds to be separated. An extremely high mobile phase velocity can be employed only for the separation of non-polar compounds.

Equilibration of dry-filled MPLC columns with the optimized TLC/OPLC mobile phase is possible only if all compounds migrate within the last front of the multi-component eluent. This behaviour may be tested by analytical OPLC. Generally, the MPLC columns can be equilibrated with the solvent used for the prerun in analytical OPLC. This method is feasible regardless of the structures and properties of the substances to be separated. The solvent for the prerun is always *n*-hexane for non-polar compounds; for polar compounds, it must be decided during the mobile phase optimization process<sup>6</sup>. The compounds to be separated should not migrate in this solvent, and it should be either part of the mobile phase or at least miscible with the eluent.

The major advantage of the strategies presented is that mobile phase transfer starts from a TLC separation where the whole  $R_F$  range is used, in contrast to the general rule applied until now that all zones should be below  $R_F = 0.3$  in TLC. However, prediction of the final MPLC result can be improved, especially when using the OPLC technique as a pilot method. Needless to say, these strategies can also be applied for the mobile phase transfer from TLC to all preparative column liquid chromatographic methods in which silica is used as the stationary phase.

#### ACKNOWLEDGEMENTS

Financial support from the Swiss KWF Commission is gratefully acknowledged. The authors express their thanks to Labomatic (Schönenbuch, Switzerland) for the loan of an MPLC system.

#### REFERENCES

- 1 P. D. McDonald and B. A. Bidlingmeyer, in B. A. Bidlingmeyer (Editor), *Preparative Liquid Chromatography*, Elsevier, Amsterdam, Oxford, New York, Tokyo, 1987, p. 1.
- 2 D. Schaufelberger and K. Hostettmann, *J. Chromatogr.*, 346 (1985) 396.
- 3 E. Soczewinski and T. Wawrzynowicz, *J. Chromatogr.*, 218 (1981) 729.

- 4 P. Rahn and M. Woodman, *Am. Lab.*, 13 (1981) 96.
- 5 W. Jost, H. E. Hauck and F. Eisenbeiss, *Fresenius Z. Anal. Chem.*, 318 (1984) 300.
- 6 J. K. Rozylo, I. Malinowska and M. Poniewaz, *Fresenius Z. Anal. Chem.*, 318 (1984) 307.
- 7 A. Talamona, *GIT Fachz. Lab.*, No. 3 (1987) 205.
- 8 K. Hostettmann, M. Hostettmann and A. Marston, in K. Hostettmann, M. Hostettmann and A. Marston (Editors), *Preparative Chromatography Techniques*, Springer, Berlin, 1986, p. 27.
- 9 Sz. Nyiredy, K. Dallenbach-Tölke and O. Sticher, 17th International Symposium on Chromatography, Vienna, 1988, Abstr. No. I.P.64.
- 10 C. A. J. Erdelmeier, *Ph. D. Thesis*, No. 7924, ETH, Zürich, 1983.
- 11 K. Dallenbach-Tölke, *Ph. D. Thesis*, No. 8178, ETH, Zürich, 1986.
- 12 Sz. Nyiredy, C. A. J. Erdelmeier and O. Sticher, in R. E. Kaiser (Editor), *Planar Chromatography*, Vol. 1, Hüthig, Heidelberg, Basle, New York, 1986, pp. 119–164.
- 13 Sz. Nyiredy, S. Y. Mészáros, K. Dallenbach-Toelke, K. Nyiredy-Mikita and O. Sticher, *J. High Resolut. Chromatogr. Chromatogr. Commun.*, 10 (1987) 352.
- 14 Sz. Nyiredy, C. A. J. Erdelmeier and O. Sticher, in E. Tyihák (Editor), *Proceedings of the International Symposium on TLC with Special Emphasis on Overpressured Layer Chromatography (OPLC)*, Labor-MIM, Budapest, 1986, pp. 222–231.
- 15 Sz. Nyiredy, *Application of the "PRISMA" Model for the Selection of Eluent-systems in Overpressured Layer Chromatography (OPLC)*, Labor-MIM, Budapest, 1987.
- 16 Sz. Nyiredy, K. Dallenbach-Tölke and O. Sticher, *J. Planar Chromatogr.*, 1 (1988) 336.
- 17 Sz. Nyiredy, C. A. J. Erdelmeier, B. Meier and O. Sticher, *Planta Med.*, 51 (1985) 241.
- 18 G. C. Zogg, Sz. Nyiredy and O. Sticher, *Chromatographia*, 27 (1989) 591.
- 19 K. Dallenbach-Toelke, Sz. Nyiredy, B. Meier and O. Sticher, *J. Chromatogr.*, 365 (1986) 63.
- 20 K. Dallenbach-Toelke, Sz. Nyiredy, S. Y. Mészáros and O. Sticher, *J. High Resolut. Chromatogr. Chromatogr. Commun.*, 10 (1987) 362.
- 21 E. Mincsovcics, E. Tyihák and A. M. Siouffi, *J. Planar Chromatogr.*, 1 (1988) 141.
- 22 G. C. Zogg, Sz. Nyiredy and O. Sticher, *J. Planar Chromatogr.*, 1 (1988) 351.

CHROMSYMP. 1674

## INVESTIGATION AND IMPROVEMENT OF THE HORVÁTH-LIN EQUATION OF STATE

PÁL BENEDEK\* and TAMÁS JANKÓ

*Department of Chemistry, L. Eötvös University, P.O. Box 32, H-1518 Budapest 112 (Hungary)*

---

### SUMMARY

In connection with a thermodynamic analysis of high-performance liquid chromatography, Horváth and Lin developed a three-parameter equation of state. The dimensionless multipliers of this equation were correlated with the critical compressibility factor,  $z_c$ . A different temperature-correction relationship is now suggested. It is shown that the coefficient  $m$  in the modified temperature correction is component-specific and, with polar substances, it is also temperature dependent. Equations that correlate it with the acentric factor and with the polarity factor are given.

---

### INTRODUCTION

Horváth and Lin<sup>1</sup> proposed the following three-parameter equation of state with a critical compressibility factor correlation:

$$P = RT/(v - b) - a/v(v + c) \quad (1)$$

where

$$a = \alpha a[T_r] (R^2 T_c^2 / P_c) \quad (2)$$

with  $a[T_r]$  given by eqn. 15;

$$b = \beta (RT_c / P_c) \quad (3)$$

$$c = \gamma b \quad (4)$$

The root of eqn. 1 at the critical temperature,  $T_c$ , and critical pressure,  $P_c$ , is the reference volume of the fluid,  $v_0$ ;  $\alpha$ ,  $\beta$  and  $\gamma$  are dimensionless multipliers which are interrelated and dependent on the reference compressibility factor,  $z_0$ :

$$z_0 = (P_c v_0) / (RT_c) \quad (5)$$

The dimensionless multipliers are involved in the following system of equations derived from the canonical form of the critical isotherm:

$$z_0^3 = \alpha\beta \quad (6)$$

$$3z_0^2 = -\gamma\beta^2 - \gamma\beta + \alpha \quad (7)$$

$$3z_0 = -\gamma\beta + \beta + 1 \quad (8)$$

The numerical solution of this non-linear system of equations is given as the following cubic polynomials of the reference compressibility factor,  $z_0$ :

$$\alpha = 0.12233 + 5.22425z_0 - 22.4011z_0^2 + 28.43065z_0^3 \quad (9)$$

$$\beta = 1.494495 - 14.62351z_0 + 47.4259z_0^2 - 48.69008z_0^3 \quad (10)$$

$$\gamma = 1657.483 - 16001.19z_0 + 51711.96z_0^2 - 55874.32z_0^3 \quad (11)$$

$$b_r - b_r^0 = 3.287697 - 35.07038z_0 + 116.9788z_0^2 - 124.1009z_0^3 \quad (12)$$

where  $b_r$  is the reduced limiting volume ( $b_r = b/v_0$ ).

The Horváth–Lin equation of state is one of the possible realizations of the three-parameter corresponding states principle:

$$f[P, v, T; P_c, T_c, z_c] = 0 \quad (13)$$

with the critical compressibility factor,  $z_c$ , selected as the third parameter. The correlation between the critical compressibility factor,  $z_c$ , and the reference compressibility factor,  $z_0$ , is calculated from the data in the original Horváth–Lin paper and is

$$z_0 = -0.4734192 + 7.320713z_c - 23.58415z_c^2 + 27.45711z_c^3 \quad (14)$$

It is obvious that eqn. 14 and the relationships expressed in eqns. 9–12 generate a family of Horváth–Lin equations of state (eqn. 1) with critical compressibility factor correlation. For example, if we take the premultiplier  $\gamma$  as equal to unity, then  $b = b_r^0$  and eqn. 1 simplifies to the Redlich–Kwong equation of state<sup>2</sup>. It can be seen that the presence of the third parameter,  $c$ , in the Horváth–Lin equation of state is responsible for the value of the component-specific reduced limiting volume,  $b_r = b/v_0$ , and consequently for the profile of the isotherm. Because of this, the calculated isotherm fits the experimental  $P$ – $v$  curve.

In the original Horváth–Lin paper, the dimensionless coefficient  $a[T_r]$  is suggested to be given by

$$a[T_r] = 1/T_r \quad (15)$$

Our investigations proved that this relationship limits the performance of eqn. 1.

## IMPROVEMENT OF THE HORVÁTH-LIN EQUATION OF STATE FOR APOLAR SUBSTANCES

The coefficient  $a[T_r]$  is certainly component-specific and its temperature dependence is slightly more complicated than suggested by eqn. 15. We selected another relationship, which was first proposed by Soave<sup>3</sup>:

$$a[T_r] = [1 + m(1 - T_r^{0.5})]^2 \quad (16)$$

Here the component-specific parameter  $m = m_s$  is correlated with Pitzer's acentric factor<sup>4</sup>,  $\omega$ :

$$m_s = 0.48036 + 1.5701\omega - 0.16814\omega^2 \quad (17)$$

Pitzer's acentric factor is very component-specific:

$$\omega = -\log P_r^0 - 1 \quad (T_r = 0.7) \quad (18)$$

However, in the case of the Horváth-Lin equation of state, not only  $\alpha$ ,  $\beta$ ,  $\gamma$  and  $b_r$  are functions of  $z_0$ , but also the parameter from eqn. 16. We have found that the following two-variable polynomial shows this phenomenon:

$$\begin{aligned} m_{0.7} = & (0.48036 + 1.5701\omega - 0.16814\omega^2) + \\ & + (0.57200 + 0.48044\omega - 0.08144\omega^2)(b_r - b_r^0) + \\ & + (-5.0607 - 4.2736\omega + 0.80413\omega^2)(b_r - b_r^0)^2 \end{aligned} \quad (19)$$

Applying eqn. 1 together with eqn. 16 and with the correction expressed in eqn. 19 represents the first improvement of the Horváth-Lin equation of state. In the class of apolar substances there is a correlation between  $\omega$  and  $z_c$ :

$$z_c = 0.291 - 0.08\omega \quad (20)$$

Taking into account this relationship, we can consider that the acentric factor,  $\omega$ , and the critical compressibility factor,  $z_c$ , carry the same information about the shape and size of a molecule. Thus, with this first improvement of the Horváth-Lin equation of state suggested here for apolar substances we do not leave the domain of the three-parameter corresponding states principle.

*Improvement of the Horváth-Lin equation of state for polar substances*

The correlation expressed in eqn. 20 loses its validity with polar substances. It is true that the critical compressibility factor,  $z_c$ , and the acentric factor,  $\omega$ , carry different information about the size and shape of a molecule on the one hand, and about its polarity on the other. There is a departure from the relationship expressed in eqn. 20, however, and its interpretation would be very difficult. Consequently, we have to apply the four-parameter corresponding states principle for polar substances.

We selected the polarity factor as the fourth parameter, by a definition similar to eqn. 16:

$$\omega_p = -\log P_r^0 - 1 \quad (T_r = 0.6) \quad (21)$$

This definition corresponds to the fact that the lower the temperature, the better will the polarity of the molecule manifest itself. Hence the difference in the acentric factor,  $\omega$ , and the polarity factor is very significant. We have found a two-variable polynomial for the component-specific parameter  $m_{0.6}$ :

$$\begin{aligned} m_{0.6} = & (-0.07725 + 1.0699\omega_p - 0.1252\omega_p^2 + 0.013377\omega_p^3) + \\ & + (-0.36434 + 0.3236\omega_p - 0.6249\omega_p^2 + 0.009049\omega_p^3)(b_r - b_r^0) + \\ & + (-3.2220 - 2.8792\omega_p - 0.5501\omega_p^2 + 0.0791225\omega_p^3)(b_r - b_r^0)^2 \quad (22) \end{aligned}$$

The value of  $m$  in eqn. 16 at the reduced temperature of  $T_r = 0.7$  has to be  $m = m_{0.7}$ , and at the reduced temperature of  $T_r = 0.6$  it has to be  $m = m_{0.6}$ . This means that  $m$  is a temperature-dependent coefficient in eqn. 16. One can calculate  $m$  for temperatures  $T_r > 0.34$  by the following linear relationship:

$$m = (10T_r - 6)(m_{0.7} - m_{0.6}) + m_{0.6} \quad (23)$$

Applying eqn. 1 with eqn. 16 and together with the correlations expressed in eqns. 10 and 22 involved in the relationship expressed in eqn. 23 represents, for polar substances, the second improvement of the Horváth-Lin equation of state.

#### HOW TO USE THE IMPROVED HORVÁTH-LIN EQUATION OF STATE

Let us consider eqn. 1 in a detailed form:

$$\frac{[RT/(v - \beta[z_0](RT_c/P_c)) - \{\alpha[z_0](R^2T_c^2/P_c)\{1 + m[\omega, \omega_p, (b_r - b_r^0)[z_0]]\}(1 - T_r^{0.5})^2\}]/v}{v\{v - \gamma[z_0]\beta[z_0](RT_c/P_c)\}} - P[v, T] = 0 \quad (24)$$

This is a non-linear equation with only one unknown variable,  $z_0$ . Fitting eqn. 24 to a single experimental point  $[P, v, T]$ , one can calculate the value of the unknown variable,  $z_0$ . Knowing  $z_0$ ,  $\omega$  and  $\omega_p$  for the given substance, one can use the improved Horváth-Lin equation of state for direct calculation.

The correlations between  $z_c$  and  $z_0$  for polar and apolar substances would eliminate the determination of  $z_0$  by the mentioned fitting procedure. Elaboration of such correlations will be the subject of another paper.

## ACKNOWLEDGEMENTS

The authors are grateful to Professor Csaba Horváth (Yale University, New Haven, CT, U.S.A.) for consultations and suggestions related to this paper. This work was supported by Grant No. 1288-86 of the Hungarian National Scientific Research Fund OTKA.

## REFERENCES

- 1 Cs. Horváth and H.-J. Lin, *Can. J. Chem. Eng.*, 55 (1977) 450.
- 2 O. Redlich and J. N. S. Kwong, *Chem. Rev.*, 44 (1955) 233.
- 3 G. Soave, *Chem. Eng. Sci.*, 27 (1972) 1197.
- 4 K. S. Pitzer, *J. Am. Chem. Soc.*, 77 (1955) 3427.





CHROMSYMP. 1645

## REVERSED-PHASE LIQUID CHROMATOGRAPHIC STUDIES OF NON-IONIC SURFACTANTS AND RELATED SOLUTES

P. VARUGHESE<sup>a</sup>, M. E. GANGODA and R. K. GILPIN\*

*Department of Chemistry, Kent State University, Kent, OH 44242 (U.S.A.)*

---

### SUMMARY

Homologous series of alkyl ester, ether and amide polyoxyethylene non-ionic surfactants have been synthesized and their retention properties have been studied under reversed-phase conditions. In addition, methylene group selectivities have been determined for the three types of surfactants as well as for a homologous series of ethyl esters of alkanolic acids. In the composition range studied for a given mobile phase, methylene selectivity was nearly independent of the head group of the surfactants. This supports the idea that the retention mechanism is governed by hydrophobic interactions between the alkyl tail of the surfactant and the bonded stationary phase.

---

### INTRODUCTION

The analytical chemistry of non-ionic surfactants has been summarized in a recently published monograph<sup>1</sup>. Only relatively few studies have systematically dealt with the retention properties of this class of compounds. Examples of these studies may be found in refs. 2–5.

In the current investigation, homologous series of three types of alkyl oxyethylene monodispersed non-ionic surfactants with differing head groups and identical hydrocarbon tails were synthesized. The compounds which were prepared fit the general formulas:  $\text{CH}_3(\text{CH}_2)_{n-1}\text{CO}_2(\text{C}_2\text{H}_4\text{O})_4\text{H}$ ,  $\text{CH}_3(\text{CH}_2)_{n-1}(\text{OC}_2\text{H}_4)_4\text{OH}$ , and  $\text{CH}_3(\text{CH}_2)_{n-1}\text{CONH}(\text{C}_2\text{H}_4\text{O})_2\text{H}$ . The retention behavior of these three classes of surfactants were studied under reversed-phase liquid chromatographic conditions, using aqueous methanol as the mobile phase and an octyl surface as the stationary phase. The incremental changes in retention per addition of a methylene carbon in the tail of the surfactant (*i.e.*, methylene selectivity<sup>6</sup>) have been determined for alkyl chain lengths varying from C<sub>3</sub> to C<sub>8</sub> for each of the three different head groups. Additionally, the changes in solute retention have been correlated with the hydrophil/lipophil balance (HLB) determined by the Griffin equation<sup>7,8</sup>.

---

<sup>a</sup> Permanent address: Department of Chemistry, Indiana University of Pennsylvania, Indiana, PA 15705, U.S.A.

## EXPERIMENTAL

*Surfactant synthesis*

All chemicals were purchased from Aldrich (Milwaukee, WI, U.S.A.).

The ether surfactants (*i.e.*,  $\text{CH}_3(\text{CH}_2)_{n-1}(\text{OC}_2\text{H}_5)_m\text{OH}$ , where  $n = 3-8$  and  $m = 2-4$ ) were prepared by addition of a 1:5:1 molar ratio of sodium hydroxide pellets, appropriate polyethylene glycol, and a given alkyl bromide. The resulting mixture was refluxed for several hours, cooled, and digested with water. The product was extracted with multiple portions of chloroform, and the extract was dried over anhydrous sodium sulfate. The extract was filtered, the chloroform removed in a rotary evaporator, and the remaining oily residue was fractionally distilled under reduced pressure to obtain the purified surfactant.

The amide surfactants, (*i.e.*,  $\text{CH}_3(\text{CH}_2)_{n-1}\text{CONH}(\text{C}_2\text{H}_4\text{O})_2\text{H}$  where  $n = 5-8$ ) were prepared by the method of Afzal *et al.*<sup>9</sup> with a slight modification in the work-up procedure.

The ester surfactants (*i.e.*,  $\text{CH}_3(\text{CH}_2)_{n-1}\text{CO}_2(\text{C}_2\text{H}_4\text{O})_4\text{H}$ , where  $n = 5-8$ ) were prepared by refluxing a given alkanolic acid with tetraethylene glycol (1:5 mol ratio) in the presence of a cation-exchange resin, which was used as a catalyst ( $\text{H}^+$  form). A Dean-Stark trap was attached, and 50 ml of toluene were added to the flask. After *ca.* 6 h of refluxing, the toluene was distilled off; the mixture was cooled and then filtered to remove the resin. Subsequently, the mixture was digested with a saturated solution of NaCl and extracted with chloroform. The product was isolated from the chloroform in a similar fashion to that described for the ether surfactants.

In all of the above cases the purity and identity of the surfactants were established by thin-layer chromatography, infrared and nuclear magnetic resonance spectrometry.

*Chromatographic experiments*

All chromatographic analyses were performed on an IBM Instruments (Danbury, CT, U.S.A.) Model LC/9533 liquid chromatograph, using a 250 mm  $\times$  4.6 mm I.D. IBM column packed with an octyl stationary phase (Part No. 8635316). The refractive index detector used was an IBM Model LC/9525 instrument. The HPLC-grade methanol was obtained from Fisher Scientific (Pittsburgh, PA, U.S.A.) and the deionized water was prepared using a Milli-Q (Millipore, Milford, MA, U.S.A.) purification system. Mobile phases were prepared on a v/v basis and degassed before using.

After switching mobile phases, the column was conditioned with at least 20–30 column volumes of the new mobile phase. Retention data were collected at a flow-rate of 1.0 ml/min. The surfactant test solutes were prepared in either methanol or in binary mixtures of methanol and water at an approximate concentration of 1.0 mg/ml. Reported capacity factors,  $k'$ , are mean values from 2–5 replicate injections, calculated using  $^2\text{H}_2\text{O}$  to determine the void volume.

## RESULTS AND DISCUSSION

Free energies of transfer of straight-chain solutes from water to a non-polar phase are linear with respect to the number of carbons in the chain<sup>10,11</sup>. Thus, for

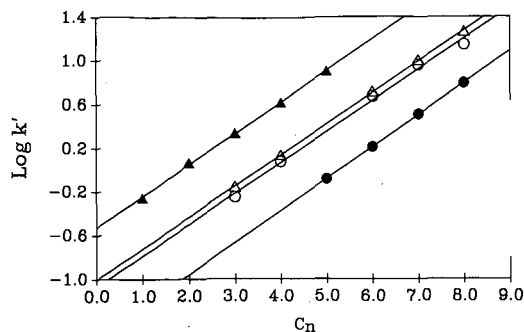


Fig. 1.  $\log k'$  vs.  $C_n$  for homologous series of solutes. Mobile phase: methanol-water (55:45). Solutes:  $\circ$  = ester surfactants;  $\triangle$  = ether surfactants;  $\bullet$  = amide surfactants;  $\blacktriangle$  = ethyl alkanooates. Correlation coefficients for all plots are 0.998 or better.

homologous series of solutes  $\log k'$  also is linearly related to the number of carbon atoms<sup>12-20</sup>. This latter relationship can be expressed as

$$\log k' = aC_n + b \quad (1)$$

where the slope,  $a$ , is the incremental change in retention as a function of increasing carbon number,  $C_n$ . The intercept,  $b$ , is related to the functional groups in the solute and their influence on retention<sup>15,21</sup>.

The plots of  $\log k'$  vs.  $C_n$  for homologous series of surfactants (ester, ether and amide) and for comparison purposes of ethyl esters of alkanooic acids using methanol-water (55:45) as the mobile phase are shown in Fig. 1. Similar plots were observed in methanol-water (65:35) and (75:25) mobile phases. Values for  $a$  and  $b$  for the three classes of non-ionic surfactants and simple esters are given in Table I. These values are consistent with those reported by others<sup>22</sup>.

The above results reflect several trends. Firstly, the methylene selectivity,  $a$ , increased directly with the water content of the mobile phase. Tanaka and Thornton<sup>21</sup> have reported similar observations for homologous series of alkanes, alcohols and carboxylic acids. Secondly, the slopes were nearly constant for a given mobile phase composition, irrespective of the homologous series (*i.e.*, the ester, ether or

TABLE I  
SLOPE ( $a$ ) AND INTERCEPT ( $b$ ) VALUES OF  $\log k'$  VS.  $C_n$

Solute	Methanol-water					
	55:45		65:35		75:25	
	$a$	$b$	$a$	$b$	$a$	$b$
Ether surfactants	0.285	-1.005	0.235	-1.149	0.191	-1.29
Ester surfactants	0.284	-1.140	0.229	-1.136	0.196	-1.33
Amide surfactants	0.293	-1.544	0.241	-1.572	0.191	-1.68
Ethyl esters	0.282	-0.505	0.233	-0.669	0.188	-0.85

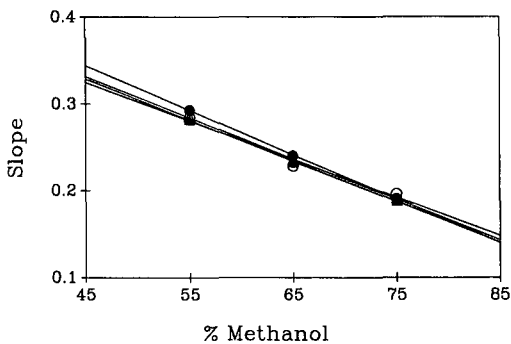


Fig. 2. Methylene selectivity vs. percent methanol. Solutes:  $\circ$  = ester surfactants;  $\triangle$  = ether surfactants;  $\bullet$  = amide surfactants;  $\blacktriangle$  = ethyl alkanooates. The correlation coefficient is 0.992.

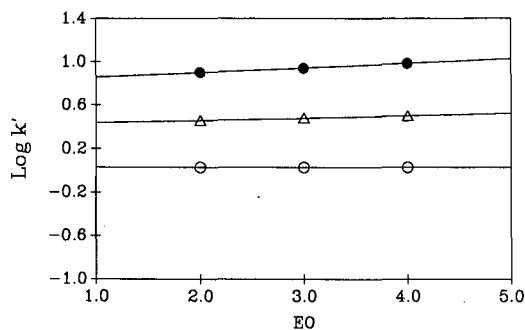


Fig. 3.  $\log k'$  vs. number of ethylene oxide (EO) units in the heptyl polyoxyethylene ethers,  $\text{CH}_3(\text{CH}_2)_6(\text{EO})_n\text{OH}$ . Mobile phase: methanol-water:  $\bullet$  = 55:45;  $\triangle$  = 65:35;  $\circ$  = 75:25. The correlation coefficient is 0.999.

TABLE II  
CALCULATED VALUES OF HLB

Surfactant	HLB	Surfactant	HLB
$\text{C}_3\text{H}_7\text{CO}_2(\text{C}_2\text{H}_4\text{O})_4\text{H}$	16.74	$\text{C}_7\text{H}_{15}\text{O}(\text{C}_2\text{H}_4\text{O})_4\text{H}$	13.22
$\text{C}_4\text{H}_9\text{CO}_2(\text{C}_2\text{H}_4\text{O})_4\text{H}$	15.90	$\text{C}_8\text{H}_{17}\text{O}(\text{C}_2\text{H}_4\text{O})_4\text{H}$	12.61
$\text{C}_6\text{H}_{13}\text{CO}_2(\text{C}_2\text{H}_4\text{O})_4\text{H}$	14.44	$\text{C}_7\text{H}_{15}\text{O}(\text{C}_2\text{H}_4\text{O})_2\text{H}$	10.29
$\text{C}_7\text{H}_{15}\text{CO}_2(\text{C}_2\text{H}_4\text{O})_4\text{H}$	13.81	$\text{C}_7\text{H}_{15}\text{O}(\text{C}_2\text{H}_4\text{O})_3\text{H}$	12.02
$\text{C}_8\text{H}_{17}\text{CO}_2(\text{C}_2\text{H}_4\text{O})_4\text{H}$	13.23	$\text{C}_5\text{H}_{11}\text{CONH}(\text{C}_2\text{H}_4\text{O})_2\text{H}$	13.00
$\text{C}_3\text{H}_7\text{O}(\text{C}_2\text{H}_4\text{O})_4\text{H}$	16.36	$\text{C}_6\text{H}_{13}\text{CONH}(\text{C}_2\text{H}_4\text{O})_2\text{H}$	12.17
$\text{C}_4\text{H}_9\text{O}(\text{C}_2\text{H}_4\text{O})_4\text{H}$	15.44	$\text{C}_7\text{H}_{15}\text{CONH}(\text{C}_2\text{H}_4\text{O})_2\text{H}$	11.43
$\text{C}_6\text{H}_{13}\text{O}(\text{C}_2\text{H}_4\text{O})_4\text{H}$	13.88	$\text{C}_8\text{H}_{17}\text{CONH}(\text{C}_2\text{H}_4\text{O})_2\text{H}$	10.78

amide head groups). Thirdly, as shown in Fig. 2, there was a linear and nearly superimposable correlation between the methylene selectivity and volume percent of methanol in the mobile phase for all four homologous series. These latter results also demonstrate that the hydrophilic head groups do not influence the methylene selectivity.

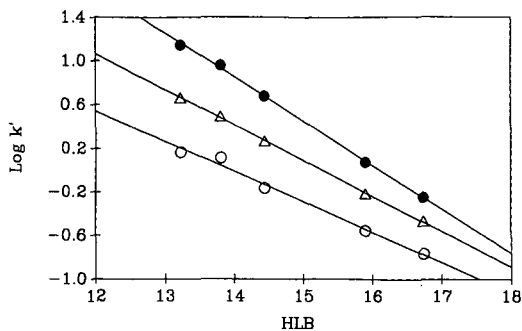


Fig. 4.  $\text{Log } k'$  vs. HLB for the ester surfactants. Mobile phase: methanol-water: ● = 55:45;  $\Delta$  = 65:35; ○ = 75:25. The correlation coefficient is 0.995.

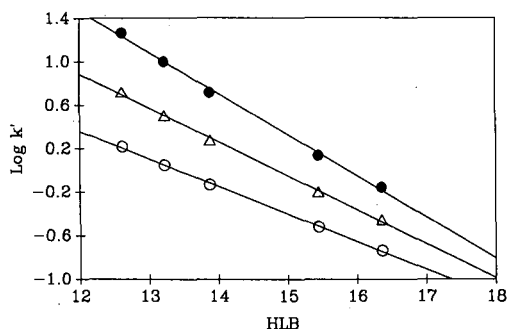


Fig. 5.  $\text{Log } k'$  vs. HLB for the ether surfactants. Mobile phase: methanol-water: ● = 55:45;  $\blacktriangle$  = 65:35; ○ = 75:25. The correlation coefficient is 0.998.

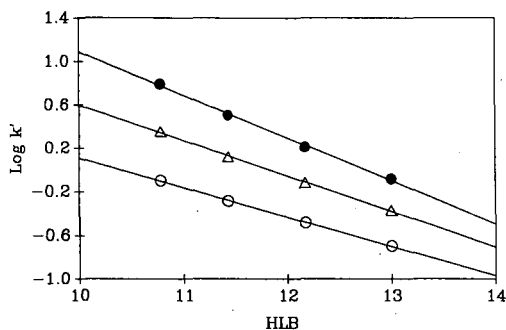


Fig. 6.  $\text{Log } k'$  vs. HLB for amide surfactants. Mobile phase: methanol-water: ● = 55:45;  $\Delta$  = 65:35; ○ = 75:25. The correlation coefficient is 0.999.

The retention behavior was also studied for a series of heptyl ethers containing 2, 3 and 4 ethylene oxide units by using three different aqueous methanol mobile phase compositions. Plots of  $\log k'$  vs. the number of ethylene oxide groups for methanol-water (55:45), (65:35) and (75:25) mobile phases are given in Fig. 3. The plots are nearly parallel and the slopes very small. These data further support the idea that the interactions between the hydrophobic tail of the surfactant and the stationary phase are primarily responsible for the observed changes in retention for the ethylene oxides studied.

Approximately forty years ago Griffin<sup>7,8</sup> proposed an empirical relationship, which he termed the hydrophil/lipophil balance (HLB), to quantify the relationship between the two parts of a surfactant molecule, the hydrophilic and the lipophilic groups. This relationship is given in eqn. 2.

$$\text{HLB} = \frac{\text{Mol. wt. of hydrophilic part} \times 20}{\text{Mol. wt. of the surfactant}} \quad (2)$$

The HLB, which increases with increasing polarity of the molecule, has been employed in a general sense for characterizing surfactants<sup>1</sup>.

Calculated HLB values are given in Table II for the various surfactants examined in the current study. When these values were plotted against  $\log k'$ , linear correlations were observed, as shown in Figs. 4–6 for the ester, ether, and amide surfactants, respectively. The overall negative slopes indicate that retention decreases with decreasing hydrophobicity of the surfactant. The nearly identical slopes between surfactant type for the compounds are consistent with the above hydrophobic retention mechanism. Further studies are needed to determine the generality of this relationship for other classes of surfactants.

#### ACKNOWLEDGEMENTS

Support from DARPA-ONR Contract NOO14-86-K-0772 is acknowledged.

#### REFERENCES

- 1 J. Cross (Editor), *Non-ionic Surfactants, Chemical Analysis*, Marcel Dekker, New York, 1987.
- 2 A. Nakae and K. Kunihiro, *J. Chromatogr.*, 156 (1978) 167.
- 3 A. Otsuki and H. Shiraishi, *Anal. Chem.*, 51 (1979) 2329.
- 4 K. Nakamura, Y. Morikawa and I. Matsumoto, *J. Am. Oil Chem. Soc.*, 58 (1981) 72.
- 5 M. Kudoh, *J. Chromatogr.*, 291 (1984) 327.
- 6 P. Sadek, P. Carr and M. Ruggio, *Anal. Chem.*, 59 (1987) 1032.
- 7 W. C. Griffin, *J. Soc. Cosmet. Chem.*, 1 (1949) 311.
- 8 W. C. Griffin, *J. Soc. Cosmet. Chem.*, 5 (1954) 249.
- 9 J. Afzal, B. Fung and E. O'Rear, *J. Fluor. Chem.*, 34 (1987) 385.
- 10 C. Tanford, *The Hydrophobic Effect: Formation of Micelles and Biological Membranes*, Wiley, New York, 1973, p. 50.
- 11 R. Smith and C. Tanford, *Proc. Natl. Acad. Sci. U.S.A.*, 70 (1973) 289.
- 12 R. B. Sleight, *J. Chromatogr.*, 83 (1973) 31.
- 13 K. K. Unger, N. Becker and P. Roumeliotis, *J. Chromatogr.*, 125 (1976) 115.
- 14 E. Tomlinson, H. Poppe and J. C. Kraak, *J. Pharm. Pharmacol., Suppl.*, 28 (1976) 43.
- 15 H. Colin and G. Guiochon, *J. Chromatogr. Sci.*, 18 (1980) 54.
- 16 A. Tchaplá, H. Colin and G. Guiochon, *Anal. Chem.*, 56 (1984) 621.

- 17 H. Colin, G. Guiochon, Z. Yun, J. C. Diez-Masa and J. Jandera, *J. Chromatogr. Sci.*, 21 (1983) 179.
- 18 P. Jandera, *J. Chromatogr.*, 314 (1984) 13.
- 19 R. M. Smith, *J. Chromatogr.*, 236 (1982) 313.
- 20 M G. Khaledi, *Anal. Chem.*, 60 (1988) 876.
- 21 N. Tanaka and E. R. Thornton, *J. Am. Chem. Soc.*, 99 (1977) 7300.
- 22 C. R. Yonker, T. A. Zwier and M. F. Burke, *J. Chromatogr.*, 241 (1982) 269.





CHROM. 21 789

## EFFECT OF ALCOHOL CHAIN LENGTH, CONCENTRATION AND POLARITY ON SEPARATIONS IN HIGH-PERFORMANCE LIQUID CHROMATOGRAPHY USING BONDED CYCLODEXTRIN COLUMNS

IBRAHIM Z. ATAMNA, GARY M. MUSCHIK and HALEEM J. ISSAQ\*

Program Resources, Inc., NCI-Frederick Cancer Research Facility, P.O. Box B, Frederick, MD 21701 (U.S.A.)

---

### SUMMARY

The effect of alcohol chain length, concentration and polarity on separation in high-performance liquid chromatography using  $\beta$ -cyclodextrin-bonded silica is discussed. The results show that retention times cannot be predicted merely from the polarity of the binary mobile phase. Although organic modifiers with the same physico-chemical properties and from the same solvent group were used, the retention times obtained using binary mobile phases having the same polarity, were different. It was also observed that normal-chain carbon alcohols gave retention times shorter than those obtained with a branched-chain alcohol (*n*-propanol vs. isopropanol), and the longer the alcohol chain the shorter the retention times. A plot of  $\ln k'$  vs. alcohol volume fraction for benzene, toluene, ethylbenzene, propylbenzene, butylbenzene, 1-phenylhexane and 1-phenyloctane gave a linear relationship in methanol, ethanol and propanol (except for 1-phenylhexane). A non-linear relationship was obtained for all the solutes in isopropanol, *tert.*-butanol and 1-butanol, in the alcohol volume fraction studied.

---

### INTRODUCTION

Since the introduction of bonded cyclodextrins (CDs) as stable high-performance liquid chromatography (HPLC) stationary phases in 1984 by Armstrong<sup>1</sup>, many applications have been generated which show the potential of these materials<sup>2-6</sup>. These phases have been used for reversed-phase type separations, including polycyclic aromatic hydrocarbons<sup>2</sup>, mycotoxins<sup>2</sup>, quinones<sup>2</sup> cyclic and acyclic nitrosoamines<sup>7</sup>, and for normal phase type separations for mixtures of substituted anilines<sup>8</sup> (positional isomers), and for the separation of chiral, geometrical, optical and positional isomers<sup>5,6</sup> in addition to enantiomers; epimers and conformers<sup>9,10</sup>. Most separations achieved using CD-bonded phases are caused by differential migration of the solutes based on the formation of inclusion complexes by the different solutes entering the CD cavity.

The retention time of a given solute using CD-bonded phases is a function of many factors (eluotropic strength of mobile phase, temperature, mobile phase flow-

rate, type and shape of solute, pH and chirality), which determines the formation constant.

Manipulation of the mobile phase composition is undoubtedly the most powerful and the easiest means of adjusting both retention and selectivity in LC. In reversed-phase type separations (inclusion complexes) not only the volume of water can be changed but also the volume and nature of the organic modifier. Tarr *et al.*<sup>11</sup> recently showed the effect of *tert.*-butanol on retention of selected polynuclear aromatic compounds using a  $\beta$ -CD-bonded column. They found a significant effect on retention by adding 1% of *tert.*-butanol to the mobile phase. For example, the retention of 1-methylnaphthalene increased from 7.7 min in 100% water to 13.4 min in *tert.*-butanol-water (1:99), while the retention of 2-methylnaphthalene decreased to 11.0 min in 1% *tert.*-butanol, from 23.0 min in 100% water. A literature survey showed that there is no systematic study on the effect of different alcohols in the range 0–100% in water (where possible) on the retention time and selectivity of solutes using  $\beta$ -CD-bonded columns.

In this study the effect of different alcohols, methanol, ethanol, propanol, isopropanol, butanol and *tert.*-butanol and their content in the mobile phase on retention of several alkylbenzenes was evaluated. Also, the effect of using different alcohol-water mobile phases having the same polarity index on retention, selectivity and resolution were studied.

## EXPERIMENTAL

### Materials

The  $\beta$ -CD column (50.0  $\times$  4.6 mm I.D.) was a gift from Advanced Separation Technologies (Whippany, NJ, U.S.A.). Methanol, isopropanol, propanol, benzene and toluene were purchased from Burdick & Jackson Labs. (Muskegon, MI, U.S.A.). Ethanol (spectroscopic grade) was obtained from NSI Chemicals (Newark, NJ, U.S.A.). 1-Butanol and *tert.*-butanol (99.7%), ethylbenzene (99%), propylbenzene (98%), 1-phenylhexane (97%) and 1-phenyloctane (99%), biphenyl, 2-phenylphenol, diphenylamine and fluorene were purchased from Aldrich (Milwaukee, WI, U.S.A.). Water was deionized glass distilled. All chemicals were used as received without further purification.

### Methods and apparatus

A Hewlett-Packard Model 1090 liquid chromatograph equipped with built-in oven for temperature control, a photodiode array detector, an automatic injector, a strip-chart recorder, a Hewlett-Packard Model 3392A integrator and a Hewlett-Packard Model 85 computer/controller was used. All the alkylbenzenes were dissolved in methanol at concentrations of approximately  $4 \cdot 10^{-4}$  M. Test samples were run in all the different alcohol modifiers at different concentrations with water. Note that of the alcohols selected for this study methanol, ethanol, propanol, isopropanol and *tert.*-butanol are freely miscible in water, while butanol is not. Also, the test solutes may not be retained and will elute with the dead volume in mobile phases with a high content of alcohols. The experiments and the results will, therefore, reflect these two restrictions, where applicable.

During all the experiments, the flow-rate was kept constant at 1 ml/min, and the

temperature at 40°C, unless stated otherwise. Approximately 150–300 column volumes were allowed for column equilibration with each new mobile phase composition. All the retention times of the different solutes in all the different concentrations and types of the alcohol modifiers are an average of three injections of 5  $\mu\text{l}$  each. The value of  $t_0$  was determined by injecting 5  $\mu\text{l}$  of  $10^{-3}$  M sodium nitrite at each mobile phase used.

## RESULTS AND DISCUSSION

Interactions of the solutes in HPLC with bonded-phase CDs and other constituents of the stationary phase sorbents are governed to a large extent by the composition of the mobile phase. The elution volume of a given solute is a function of the formation constant which depends on many factors such as mobile phase composition, temperature, barriers to the formation of inclusion complexes, stabilization energies, etc. Tarr *et al.*<sup>11</sup> proposed that the apparent equilibrium constant may be used to estimate the chromatographic interactions of the solute with both the stationary and the mobile phase, because it expresses the ratio between the solute fraction included (inclusion complex) to the free solute in the mobile phase. Increased mobile phase hydrophobicity is expected to increase the free fraction of the solute resulting in decrease of retention time. Therefore, measuring the retention times of different alkylbenzenes at different concentrations of organic modifiers (alcohols) would be a valuable information which would aid chromatographers in the prediction of solute retention.

### *Effect of methanol content on retention*

There are quite a few articles dealing with the dependence of the capacity ratio on the modifier when reversed-phase columns were used<sup>12–17</sup>. The exact dependence is still a contested issue. The two most frequently used relationships are a linear function:

$$\ln k' = Ax + B$$

and a quadratic function

$$\ln k' = A'x^2 + B'x + C$$

where  $A$ ,  $A'$ ,  $B$ ,  $B'$  and  $C$  are coefficients, the values of which depend on the solute. Recently Geng and Regnier<sup>18,19</sup> detailed a study for the dependence of the coefficients  $A$ ,  $A'$  and  $B'$  on the structure of the solute molecule in reversed-phase systems. They concluded that an increase in the non-polar surface area of a solute would lead to an increase in retention which would require a larger number of solvent molecules for solute displacement. In contrast, increasing the surface area of the solvent will cause a decrease in the number of solvent molecules required for displacement of a particular solute. Figs. 1 and 2 show the variation of the  $\ln k'$  values for seven solutes as a function of the methanol concentration in the range between 0.2 and 0.8 of the fraction of methanol in water. The figures represent the best possible linear fit of the data. The correlation coefficients, slopes and intercepts for the different solutes are

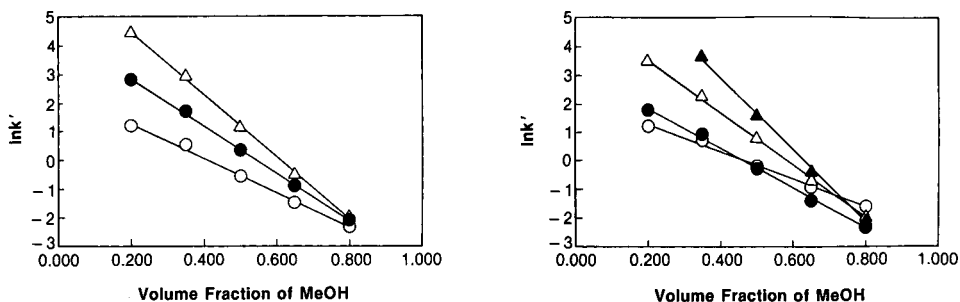


Fig. 1. Variation of retention with the binary mobile phase composition for methanol-water mixtures on a  $\beta$ -CD column. Solutes:  $\circ$  = toluene;  $\bullet$  = propylbenzene;  $\triangle$  = 1-phenylhexane. The flow-rate was 1.0 ml/min, the temperature was  $40 \pm 0.1^\circ\text{C}$  using a  $\beta$ -CD (cyclobond II) bonded silica gel column,  $5 \mu\text{m}$  spherical ( $50.0 \times 4.6 \text{ mm I.D.}$ ). Detection was carried out at 254 nm. MeOH = Methanol.

Fig. 2. Variation of retention with the binary mobile phase composition for methanol-water mixtures on a  $\beta$ -CD column. Solutes:  $\circ$  = benzene;  $\bullet$  = ethylbenzene;  $\triangle$  = butylbenzene;  $\blacktriangle$  = 1-phenyloctane. Experimental conditions as in Fig. 1. MeOH = Methanol.

shown in Table I. It is observed that the longer the side chain of the benzene ring the greater the decrease in retention as methanol content increases. These results (slope values are increased with solute size) agree with the displacement model postulation of Geng and Regnier<sup>18,19</sup>. However, this sharp decrease in retention is not seen for benzene. According to standard reversed-phase LC theory one should get an orderly change in retention behavior with change in the alkyl chain length as mentioned above. However, benzene behaves as if it was not a member of the homologous series. Since all the solutes examined in this study are small enough to be included in the  $\beta$ -CD cavity, it seems that factors other than size are affecting retention. In fact, benzene seems to be too strongly retained. If it behaves as a normal member of the homologous series it should be less retained than toluene. This means that the binding constant of benzene is greater to  $\beta$ -CD than one might expect. Another interesting observation is that as the percentage of the organic modifier increases, the benzene molecules compete even more effectively for the  $\beta$ -CD relative to other compounds. It is difficult to find the exact answer to this behavior but it may be entropic in nature.

TABLE I

SUMMARY OF RETENTION PARAMETERS FOR BONDED  $\beta$ -CYCLODEXTRIN OF ALKYL-BENZENES, WHEN METHANOL WAS USED AS MODIFIER

Compound	Intercept	Slope	Correlation coefficient ( <i>r</i> )
Benzene	2.25	-4.84	0.9973
Toluene	2.50	-6.03	0.9983
Ethylbenzene	3.23	-6.99	0.9989
Propylbenzene	4.47	-8.18	0.9994
Butylbenzene	5.38	-9.18	0.9995
1-Phenylhexane	6.64	-10.83	0.9996
1-Phenyloctane	7.97	-12.65	0.9989

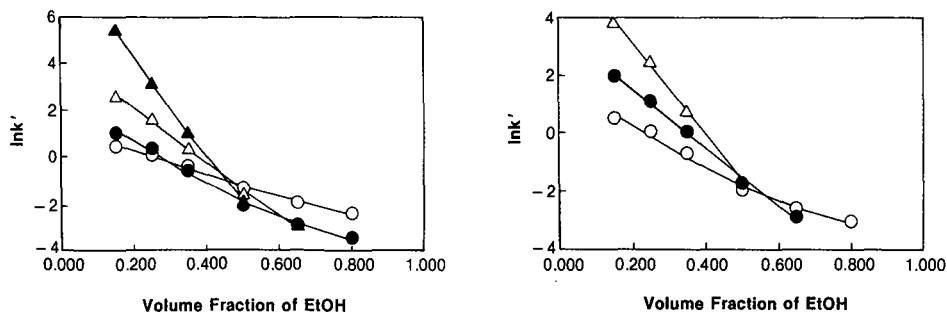


Fig. 3. Variation of retention with the binary mobile phase composition for ethanol-water mixtures on a  $\beta$ -CD column. Solutes:  $\circ$  = benzene;  $\bullet$  = ethylbenzene  $\triangle$  = butylbenzene  $\blacktriangle$  = 1-phenyloctane. Experimental conditions as in Fig. 1. EtOH = Ethanol.

Fig. 4. Variation of retention with the binary mobile phase composition for ethanol-water mixtures on a  $\beta$ -CD column. Solutes:  $\circ$  = toluene;  $\bullet$  = propylbenzene;  $\triangle$  = 1-phenylhexane. Experimental conditions as in Fig. 1. EtOH = Ethanol.

The other solutes all have aliphatic groups which would carry them into the CD. This hydrophobic binding to CD may restrict their motion and geometry in the CD cavity (less entropy) which is not helpful for binding<sup>20</sup>. Benzene on the other hand, is free to assume many orientations and positions in the CD cavity (*i.e.*, high entropy).

#### *Effect of ethanol content on retention*

As mentioned in the introduction several alcohols with different side chain length are used to examine the effect of their content in the mobile phase on retention. The second alcohol is ethanol, which is rarely used in practice for chromatographic separations. Figs. 3 and 4 show the effect of increasing ethanol content in the mobile phase on retention. It was found that the correlation coefficient ( $R$ ) for the linear and quadratic fits between  $\ln k'$  and ethanol volume fraction are very close, as seen from Table II. Most of the values for both linear and quadratic fits are close to or higher than 0.99. For practical considerations it is assumed here to be linear. Several points are worth mentioning here: the slope values (Table II) for the different solutes, show that as the non-polar surface area of the solute increases the retention decreases with

TABLE II

SUMMARY OF RETENTION PARAMETERS FOR BONDED  $\beta$ -CYCLODEXTRIN OF ALKYL-BENZENES, WHEN ETHANOL WAS USED AS MODIFIER

Compound	Intercept	Slope	$r$ (linear fit)	$r$ (quadratic fit)
Benzene	1.11	-4.50	0.9932	0.9956
Toluene	1.33	-5.87	0.9863	0.9941
Ethylbenzene	2.02	-7.28	0.9882	0.9959
Propylbenzene	3.52	-10.00	0.9981	0.9984
Butylbenzene	4.38	-11.46	0.9977	0.9982
1-Phenylhexane	6.31	-15.87	0.9994	0.9996
1-Phenyloctane	8.44	-20.78	0.9989	1.0000

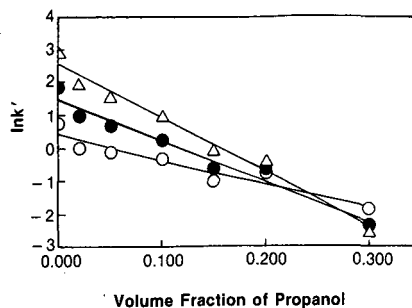
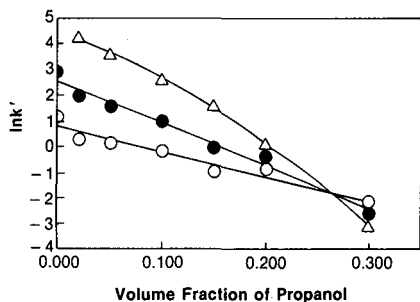


Fig. 5. Variation of retention with the binary mobile phase composition for propanol–water mixtures on a  $\beta$ -CD column. Solutes:  $\circ$  = benzene;  $\bullet$  = ethylbenzene;  $\triangle$  = butylbenzene. Experimental conditions as in Fig. 1.

Fig. 6. Variation of retention with the binary mobile phase composition for propanol–water mixtures on a  $\beta$ -CD column. Solutes:  $\circ$  = toluene;  $\bullet$  = propylbenzene;  $\triangle$  = 1-phenylhexane. Experimental conditions as in Fig. 1.

increase in ethanol content. However, for the solutes 1-phenylhexane and 1-phenyloctane there is a noticeable drop in retention as ethanol content increases. For example, the retention time of 1-phenyloctane was close to the dead volume at 35% (v/v) ethanol, while it was 15 min at 25% ethanol. This change in retention for small changes in ethanol content can be explained by the competition of the formation of inclusion complexes between the ethanol molecules and the solutes. It seems that at higher concentrations of ethanol the stabilization energy and the barriers for the formation of inclusion complexes favors the ethanol. The second competing factor is the increase in hydrophobicity of the mobile phase, which causes an increase in the free fraction of solute, a decrease in formation constant and thus decrease in retention.

#### *Effect of 1-propanol content on retention*

Figs. 5 and 6 show the plots of  $\ln k'$  of the test solutes against the volume content of 1-propanol in the mobile phase. At 30% 1-propanol all the test solutes eluted with the dead volume. The same effect was observed with 80% methanol and 65% ethanol. This is due to the fact that the solubility of the different solutes is much better in the long-chain alcohol, because of the increase in hydrophobicity. Table III

TABLE III

SUMMARY OF RETENTION PARAMETERS FOR BONDED  $\beta$ -CYCLODEXTRIN OF ALKYL-BENZENES, WHEN PROPANOL WAS USED AS MODIFIER

Compound	Intercept	Slope	$r$ (linear fit)	$r$ (quadratic fit)
Benzene	0.378	-7.32	0.9480	0.9499
Toluene	0.757	-9.59	0.9675	0.9683
Ethylbenzene	1.46	-12.50	0.9818	0.9819
Propylbenzene	2.56	-16.62	0.9899	0.9899
Butylbenzene	3.38	-19.57	0.9949	0.9963
1-Phenylhexane	5.03	-25.93	0.9930	0.9996

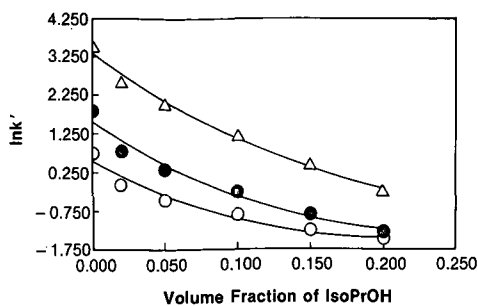


Fig. 7. Variation of retention with the binary mobile phase composition for isopropanol-water mixtures on a  $\beta$ -CD column. Solutes:  $\circ$  = benzene;  $\bullet$  = ethylbenzene;  $\triangle$  = butylbenzene. Experimental conditions as in Fig. 1. IsoPrOH = Isopropanol.

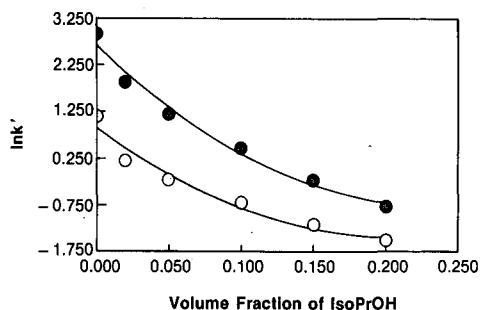


Fig. 8. Variation of retention with the binary mobile phase composition for isopropanol-water mixtures on a  $\beta$ -CD column. Solutes:  $\circ$  = toluene;  $\bullet$  = propylbenzene. Experimental conditions as in Fig. 1. IsoPrOH = Isopropanol.

shows that the correlation coefficient values of the linear and quadratic fits are very close. Here also, as in the case of ethanol, a linear fit is assumed. The decrease in retention of the solutes benzene and toluene, over the whole range of propanol content, is moderate relative to the decrease in retention of other solutes as can be seen from the slope values. This is attributed to the relatively free movement of these solutes, in and out of the cavity, because of their small molecular volume, as compared to the size of the CD cavity. The solute 1-phenylhexane, exhibits a more gradual decrease in retention, high slope values than the other solutes.

At this point it is clear that the longer the side chain of the alcohol used the less volume fractions are needed in the mobile phase to obtain the same decrease in retention time using a shorter chain alcohol, *i.e.*, methanol, as discussed earlier. Such behavior was observed using micellar chromatography where water forms the bulk of the mobile phase<sup>21</sup> and reversed-phase chromatography<sup>15,17</sup>.

#### *Effect of isopropyl alcohol content on retention*

It was of interest to examine the effect of the same number of carbon alcohols but with different geometry on the retention of the same solutes. Figs. 7 and 8 give the plots of the behaviour of the  $\ln k'$  against the isopropanol content in the mobile phase. A small change in mobile phase alcohol content caused a sharp decrease in retention times for all the solutes. At 20% isopropanol all the test solutes eluted close to the dead volume. The best fit was found to be a quadratic one, this means that the mechanism of separation (or retention) is a complex function of both the mobile and stationary phases, in 1-propanol it was mostly linear. Overall the retention time of the solutes was shorter in isopropanol than in 1-propanol.

#### *Effect of tert.-butanol content on retention*

Tarr *et al.*<sup>11</sup> found that the retention of some of the polycyclic aromatic hydrocarbons decreased with the addition of 1% butanol to the mobile phase butanol-water (1:99) and increased for others. This small change in the content of alcohol in the mobile phase is not enough to give the chromatographer a clear idea of the

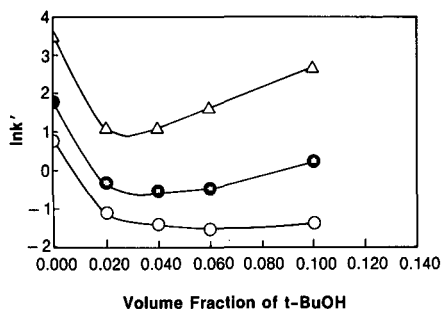


Fig. 9. Variation of retention with the binary mobile phase composition for *tert*-butanol–water mixtures on a  $\beta$ -CD column. Solutes: ○ = benzene; ● = ethylbenzene; △ = butylbenzene. Experimental conditions as in Fig. 1. *t*-BuOH = *tert*-Butanol.

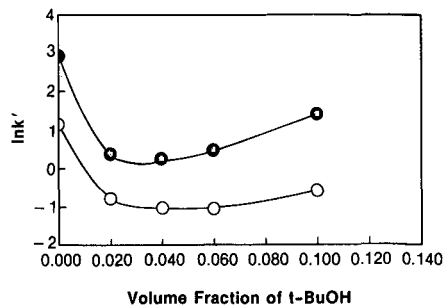
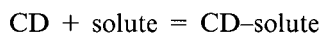


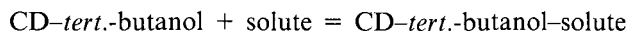
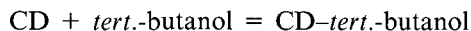
Fig. 10. Variation of retention with the binary mobile phase composition for *tert*-butanol–water mixtures on a  $\beta$ -CD column. Solutes: ○ = toluene; ● = propylbenzene. Experimental conditions as in Fig. 1. *t*-BuOH = *tert*-Butanol.

behavior of several classes of compounds when higher quantities of *tert*-butanol is used. Therefore, it was important to examine the effect of higher concentrations of *tert*-butanol on the retention of the alkylbenzenes and to compare the results to those obtained using *n*-butanol. Figs. 9 and 10, which are the plots of  $\ln k'$  against volume fraction of *tert*-butanol, show that the retention time is a complex function of the alcohol content. At 2–4% alcohol a decrease in retention time for all the solutes except butylbenzene at 4% is observed. However, the addition of higher percentages of alcohol results in higher retention times, except for benzene and toluene where the change in retention is minimal.

This decrease in retention at the low concentrations of *tert*-butanol and retention increase at the higher quantities of the alcohol supports the explanation given by Tarr *et al.*<sup>11</sup> and Nelson *et al.*<sup>22</sup>. The presence and type of alcohol have a substantial effect on the fluorescence lifetime of the pyrene–CD inclusion complex systems<sup>22</sup>. This observation indicates that the changes in the  $\alpha$ -CD interactions are not merely a solvent effect due to the bulk presence of alcohol outside the  $\alpha$ -CD cavity. If no local participation of the alcohol molecules with the pyrene–CD complex occurs then a change in the fluorescence lifetime of the complex would not be expected. It was proposed that the increased solvent hydrophobicity and enhancement by coinclusion of alcohols are the two competing factors that influence the retention behavior. So at the low *tert*-butanol concentrations the equilibrium reaction for the inclusion complex formation is:



and for the higher *tert*-butanol concentrations is:





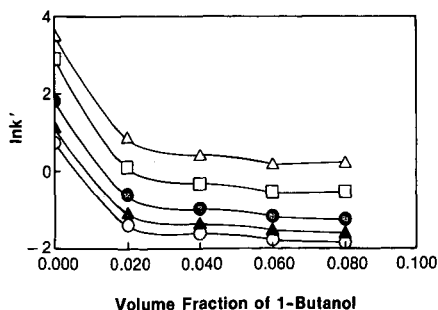


Fig. 11. Variation of retention with the binary mobile phase composition for 1-butanol–water mixtures on a  $\beta$ -CD column. Solutes:  $\circ$  = benzene;  $\blacktriangle$  = toluene;  $\bullet$  = ethylbenzene;  $\square$  = propylbenzene;  $\triangle$  = butylbenzene. Experimental conditions as in Fig. 1.

Deactivation of the amphiphilic hydroxyls of the CD outer surface, causes an increase in the core hydrophobicity.

Fig. 11 gives the behavior of  $\ln k'$  against the volume percentage of 1-butanol. The maximum solubility of 1-butanol in water was 8%. An addition of 2% 1-butanol resulted in a large decrease in retention for all the solutes. Increasing 1-butanol volume fraction from 6 to 8% in the mobile phase caused a minor decrease in retention of the small molecules benzene, toluene and ethylbenzene but a slight increase in retention of the solutes propylbenzene and butylbenzene. The decrease in retention at the low percentages of the alcohol is the same for the two alcohols (1-butanol and *tert.*-butanol). The effect is caused by an increase in the hydrophobicity of the mobile phase.

*Effect of different binary alcohol–water mobile phases having the same polarity on separation and selectivity*

In a previous work<sup>23</sup> the effect of mobile phase composition on separation and selectivity using reversed-phase thin-layer chromatography plates and a water–alcohol mobile phase was studied. As an extension to the present study it was of interest to see what effect the different alcohols in the mobile phase would have, if all the mobile phases had the same polarity index. The polarity of each mobile phase was calculated according to Snyder<sup>24</sup> based on the following equation:

$$P' = \Phi_1 P_1 + \Phi_2 P_2$$

where  $P'$  is the polarity of the mixture,  $P_1$  and  $P_2$  are the polarity of the pure solvents and  $\Phi_1$  and  $\Phi_2$  are the volume fractions of the two solvents.

The experiment was run at room temperature, using a 5- $\mu$ m spherical  $\beta$ -CD colume (125  $\times$  4.6 mm I.D.), at a flow-rate of 1 ml/min. The solutes used were 2-phenylphenol diphenylamine, fluorene and biphenyl. The alcohols used in the binary mobile phase mixture were methanol, ethanol, *n*-propanol, isopropanol and *tert.*-butanol. Butanol and isobutanol were not miscible in water at the required volume.

Table IV shows the results obtained with the above mentioned five alcohols. All the mobile phases had a polarity index of approximately 8.94. Several interesting features are clear from examining the results.

TABLE IV  
EFFECT OF ALCOHOL TYPE ON RETENTION IN HPLC USING BINARY ALCOHOL-WATER MOBILE PHASES HAVING THE SAME POLARITY

Compound	Methanol-water <sup>a</sup> (25:75)		Ethanol-water (21:79)		Propanol-water (20:80)		Isopropanol-water (20:80)		tert.-Butanol-water (20:79)	
	$t_R$	$\alpha$	$t_R$	$\alpha$	$t_R$	$\alpha$	$t_R$	$\alpha$	$t_R$	$\alpha$
2-Phenylphenol	10.9	—	6.7	—	2.4	—	3.2	—	2.2	—
Diphenylamine	12.0	1.10	7.8	1.16	2.8	1.17	3.8	1.19	2.5	1.14
Fluorene	20.2	1.68	16.1	2.06	5.6 <sup>b</sup>	1.24	12.8 <sup>b</sup>	1.68	6.1 <sup>b</sup>	1.91
Biphenyl	36.2	1.79	21.9	1.36	4.5	1.61	7.6	2.0	3.2	1.28

<sup>a</sup> All binary mobile phase mixtures have a polarity index of 8.9

<sup>b</sup> Peak reversal in this alcohol.

The selectivity, solute elution order, of the four test compounds is divided into two groups: one in methanol and ethanol, the other in propanol, isopropanol and tertiary butanol, but different than in the first two alcohols. The difference between the two groups is the peak reversal of biphenyl which eluted last in methanol and ethanol, but eluted before fluorene in the second group. A second observation is that although the percent of alcohol decreased in the mobile phase from methanol, ethanol to propanol, the retention times decreased considerably almost 8-fold for biphenyl. Increasing the chain length of the alcohol increases the hydrophobic properties of the alcohol, *i.e.* increasing the chain length increases the solubility of the solutes in the mobile phase and also weakens the formation of the inclusion complex in the CD cavity which results in a decrease in retention time.

A third observation is that when the retention times in *n*-propanol are compared to those in isopropanol better separation and longer retention times are obtained using the isopropanol mobile phase. The explanation for this was given earlier.

A fourth observation is that when the retention times obtained using isopropanol and *tert.*-butanol are compared (isopropanol is not soluble in water at the required level), the retention times decreased with increasing the total number of carbons as was observed with the straight-chain alcohols. A fifth and final observation is that although all the mobile phases (with the five alcohols) had the same polarity, the retention times obtained were different in each case. On the other hand this behavior can be used to an advantage in that when the components of a mixture are not resolved in one alcohol, using a different alcohol may resolve them.

#### ACKNOWLEDGEMENTS

The authors would like to thank Professor Armstrong for helpful discussions. This project has been funded at least in part with Federal funds from the Department of Health and Human Services under contract number NO1-CO-74102. The content of this publication does not necessarily reflect the views or policies of the Department of Health and Human Services, nor does mention of trade names, commercial products, or organizations imply endorsement by the U.S. Government.

#### REFERENCES

- 1 D. W. Armstrong, *U.S. Pat.*, 4 539 399 (1985).
- 2 D. W. Armstrong, A. Alak, W. DeMond, W. L. Hinze and T. E. Riehl, *J. Liq. Chromatogr.*, 8 (1985) 261.
- 3 E. Smolkova-Keulemansova, *J. Chromatogr.*, 17 (1985) 251.
- 4 D. W. Armstrong and T. J. Ward, *J. Liq. Chromatogr.*, 9 (1986) 407.
- 5 D. W. Armstrong, X. Yang, S. M. Han and R. A. Menges, *Anal. Chem.*, 59 (1987) 2594-2596.
- 6 T. E. Beesley, *Am. Lab. (Fairfield, Conn.)*, May (1985) 78-87.
- 7 H. J. Issaq, M. Glennon, D. E. Weiss, G. N. Chmurny and J. E. Saavedra, *J. Liq. Chromatogr.*, 9 (1986) 2763.
- 8 C. A. Chang and Q. Wu, *J. Liq. Chromatogr.*, 10 (1987) 1359.
- 9 W. L. Hinze, T. E. Riehl, D. W. Armstrong, W. DeMond, A. Alak and T. Ward, *Anal. Chem.*, 57 (1985) 237.
- 10 T. Takenchi, H. Asai and D. Ishii, *J. Chromatogr.*, 357 (1986) 409.
- 11 M. A. Tarr, G. Nelson, G. Patonay and I. M. Warner, *Anal. Lett.*, 21 (1988) 843-856.
- 12 M. J. M. Wells and C. R. Clark, *J. Chromatogr.*, 235 (1982) 31.
- 13 W. Melander, B. K. Chen and Cs. Horváth, *J. Chromatogr.*, 185 (1979) 99.

- 14 L. R. Snyder, J. W. Dolan and J. R. Gant, *J. Chromatogr.*, 165 (1979) 3.
- 15 P. J. Schoenmakers, H. A. H. Billiet, R. Tijssen and L. de Galan, *J. Chromatogr.*, 149 (1978) 519.
- 16 B. L. Karger, J. R. Gant, A. Hartkopf and P. H. Wiener, *J. Chromatogr.*, 128 (1976) 65.
- 17 L. R. Snyder, in Cs. Horváth (Editor), *High Performance Liquid Chromatography*, Vol. 1, Academic Press, New York, 1980, p. 207.
- 18 X. Geng and F. E. Regnier, *J. Chromatogr.*, 296 (1984) 15.
- 19 X. Geng and F. E. Regnier, *J. Chromatogr.*, 332 (1985) 332.
- 20 H. J. Issaq, M. L. Glennon, D. E. Weiss and S. D. Fox, in W. L. Hinze and D. W. Armstrong (Editors), *Ordered Media in Chemical Separations (ACS Symposium Series, 342)*, American Chemical Society, Washington, DC, 1987, pp. 260–271.
- 21 J. G. Dorsey, M. T DeEchegaray and T. S. Landy, *Anal. Chem.*, 55 (1983) 924.
- 22 G. Nelson, G. Patonay and I. M. Warner, *Anal. Chem.*, 60 (1988) 274.
- 23 H. J. Issaq, J. R. Klose and W. Cutchin, *J. Liq. Chromatogr.*, 5 (1982) 625.
- 24 L. R. Snyder, *J. Chromatogr. Sci.*, 16 (1978) 223.

CHROM. 21 791

## OPTIMIZATION OF SELECTIVITY, DETECTABILITY AND ANALYSIS TIME IN HIGH-PERFORMANCE LIQUID CHROMATOGRAPHY

S. AHUJA

*Development Department, Pharmaceuticals Division, Ciba-Geigy Corporation, Old Mill Rd., Suffern, NY 10901 (U.S.A.)*

---

### SUMMARY

The resolution requirements in pharmaceutical analysis by high-performance liquid chromatography are frequently higher than those for other multicomponent separations where the components are present in similar proportion. Furthermore, it is often necessary to separate a large number of components most of which are present at very low levels and have unknown structures. This places extraordinary requirements in terms of selectivity of separation and resolution of minor components as they may not be detected because of variability of stationary phase, improper selectivity evaluations, or poor resolution at the tail end of the major peak. Discussion with respect to resolution, detectability/quantitation, and analysis time is included.

---

### INTRODUCTION

It is possible to separate a variety of compounds even at ultratrace levels by high-performance liquid chromatography (HPLC)<sup>1</sup>. Unfortunately, it is not easy to determine *ab initio*, from the published literature, the specific condition for a given separation<sup>2–5</sup>. The difficulty stems from a narrow focus provided by most researchers, *i.e.* the publications tend to deal primarily with the separations of components of interest to them. The theory in many cases has been oversimplified to provide simple equations. When a significant number of compounds are present with different aromaticity, functional groups, and acidic, basic, or neutral character in a given sample, the development of a separation method becomes very difficult. These points will be addressed with regard to reversed-phase separations of pharmaceutical compounds by HPLC. The discussion should be useful for separation of pharmaceutical compounds as well as other multifunctional compounds.

### EXPERIMENTAL

A variety of C<sub>8</sub> and C<sub>18</sub> HPLC columns were investigated with different mobile phases. To evaluate various C<sub>18</sub> columns, the mobile phase was composed of methanol–water–acetic acid (70:23:2) and the flow-rate ranged from 0.8 to 1.6 ml/min. Detailed molecular probe investigations were conducted on the selected C<sub>8</sub> Whatman column that proved to be most useful for a complex separation of acidic, basic, and

neutral compounds after investigation of various manufacturer's columns (see case I under *Separation of peak pairs*). Details on mobile phases and columns used are provided in the text.

#### THEORY

The following resolution equation is familiar to most chromatographers<sup>3</sup>:

$$R_s = \frac{1}{4}(\alpha - 1) \sqrt{N} \frac{k'}{1 + k'} \quad (1)$$

Where  $R_s$  = resolution;  $N$  = number of theoretical plates;  $\alpha$  = separation factor;  $k'$  = capacity factor. It should be noted that this equation has been oversimplified since the following assumptions are made for the two components whose resolution is to be determined: (a)  $k_1'$  is approximately equal to  $k_2'$  therefore their average value ( $k'$ ) is used; (b) peak width is equal; (c)  $N$  is same. This equation is useful when  $\alpha$  value is  $\approx 1$ ; the resolution value is inflated by 1% at  $\alpha = 1.01$  and  $> 50\%$  at  $\alpha = 1.5$  as compared to eqn. 2. In general, the average of the  $R_s$  values predicted by these two equations is often better than with either equation.

If we assume  $N$  to be the same for both components but use the peak width of the second peak in calculations, the equation takes the following form:

$$R_s = \frac{1}{4} \frac{\alpha - 1}{\alpha} \sqrt{N} \frac{k'}{1 + k'} \quad (2)$$

In those cases where the assumptions stated above do not hold, appropriate equations should be derived and used<sup>6</sup>. In most practical work, however, the resolution is calculated by eqn. 3:

$$R_s = \frac{t_2 - t_1}{\frac{1}{2}(w_1 + w_2)} \quad (3)$$

Where  $t_2$  and  $t_1$  = retention times of the two components;  $w_2$  and  $w_1$  = peak widths of the same components.

For reliable quantitation, the goal should be to obtain a value of  $R_s \geq 1.5$  for every peak pair<sup>3</sup>. However, this resolution is not always possible when a significant number of multifunctional compounds are present. For two bands of equal size one can use  $R_s = 1.0$  (2% of one band overlaps the other), since most electronic integrators can easily calculate peak areas. However, for a given value of  $R_s$ , band overlap becomes more serious when one of the two bands is much smaller than the other. For example, this resolution is insufficient when the concentration of the minor component is 1 in 16. Furthermore, as the relative concentration of the minor band decreases, there is decreasing accuracy in the measured area of the minor band. This suggests that resolution requirements increase as the concentration of the minor component

decreases to trace or ultratrace levels. Discussed below are a few examples of separations with respect to resolution, detectability/quantitation, and analysis time.

## RESULTS AND DISCUSSION

Impurities in pharmaceutical compounds originate mainly during the synthetic process from raw materials, solvents, intermediates, and by-products<sup>7</sup>. Degradation products and contaminants of various types make up some of the other sources of impurities. As a result, it is necessary to incorporate stringent tests to control impurities in pharmaceutical compounds. This fact is evident from the requirements of the United States Food, Drug & Cosmetic Act and various pharmacopeias which provide tests for control of specific impurities. It is interesting to note that specifications for impurities can vary between pharmacopeias. Because a pharmaceutical compound can be prepared by a variety of methods, the need for methodologies suitable for controlling low levels of impurities and rational limits becomes apparent. This is essential to assure that the observed toxicologic or pharmacologic effects are due to the compound of interest and not due to impurities.

Analytical methods that can control impurities to ultratrace levels are available<sup>1,8-10</sup>; however, the level to which any impurity should be controlled is primarily determined by its pharmacologic and toxicologic effects. This should include all impurities: those originating from synthesis and those originating from other sources such as degradation<sup>11</sup>. For example, penicillins and cephalosporins have been known to undergo facile cleavage of the  $\beta$ -lactam bond in aqueous solution. This is of special interest since some studies on penicillins have shown that their instability may effect possible reactions involved in penicillin allergy<sup>12</sup>. The control of low levels of impurities is extremely important when a drug is taken in large quantities for

TABLE I  
STATIONARY PHASE EVALUATIONS

Mobile phase, methanol-water-acetic acid (70:23:2); 0.8 ml/min, except flow-rate, with column E and F = 1 ml/min and with column G = 1.6 ml/min.

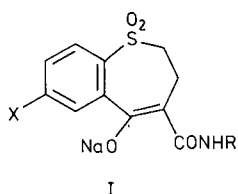
Column	Manufacturer	$d_p$ ( $\mu\text{m}$ )	$N$ claimed (minimum)	$L$ (cm)	$N$ (found <sup>a</sup> )	Impurities
A	Nucleosil C <sub>18</sub> (Chromapak)	5	10 000	25	5384	5
B	Partisil ODS (Whatman)	5	10 000	25	2800	6
C	Ultrasphere ODS (Altex)	5	25 000	25	3900	9
D	Zorbax ODS	5	10 000	25	1410	7
E	$\mu$ Bondapak C <sub>18</sub> (Waters)	10	5000	30	864	7
F	$\mu$ Bondapak C <sub>18</sub> (Waters)	10	5000	30	1369	7
G	Radial compression C <sub>18</sub>	10	5000	10	2340 (calc.)	6

<sup>a</sup> For compound I.

therapeutic purposes or as a fad, such as the use of methotrexate (10–20 g) to treat neoplasia or faddist use of vitamins, especially vitamin C.

#### *Variabilities in stationary phase*

Resolution of impurities or by-products in pharmaceutical compounds depends on appropriate selection of a mode of chromatography, column, mobile phase, and detector. Even when all other conditions are optimum, variability in columns from manufacturer to manufacturer or from the same manufacturer can affect separations. Table I lists evaluations of impurities in a potential anti-inflammatory compound (I) with the following structure<sup>1,3</sup>:



A review of the table reveal that almost a two-fold number of impurities (9 vs. 5) can be seen when column C is used as opposed to column A. The differences can be attributed to variability in selectivity offered by these columns rather than the theoretical plates, because *N* (found) for compound I was higher in column A than in column C. A comparison of columns from the same manufacturer, *i.e.*, columns E and F, shows that *N* (found) is significantly different; however, the number of impurities found is the same and lies between those of columns A and C. Again, there is no correlation with the number of theoretical plates. The radial compression column G from the same manufacturer actually shows one impurity less even though the calculated number of theoretical plates is higher than columns E and F. Smaller particle size (5  $\mu\text{m}$ ) alone is not responsible for higher resolution as is obvious from differences in results for columns A–D. Also columns E–G with twice the particle size show almost the same number of impurities as columns B and D. The result of this study shows that resolution of components is clearly a function of the selected stationary phase (which is variable from manufacturer to manufacturer and even from the same manufacturer) and the mobile phase. This investigation suggests the need of select probes to assure that the selected stationary phase is providing the desired resolution and detectability.

#### *Studies with select probes*

Columns from various manufacturers were evaluated for a separation that entailed mixture of acidic, basic, and neutral compounds<sup>14</sup>. The columns that were not end-capped were found unsuitable for further investigations. From the remaining, one manufacturer's column (Whatman) was selected for in-depth investigation. The type of data provided by this manufacturer is given in Table II. It is readily apparent that the probes given in Table II (benzene, naphthalene, and biphenyl) are similar in structure, *i.e.*, they are all aromatic hydrocarbons, and the effect of polar groups cannot be determined with this approach.

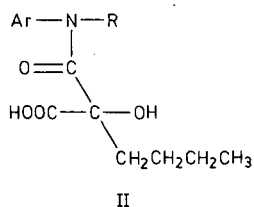


TABLE II  
TYPICAL MANUFACTURER'S DATA FOR A C<sub>8</sub> COLUMN (10 μm)  
Whatman column, 25 cm × 4.6 mm I.D.; methanol-water (80:20).

	<i>Benzene</i>	<i>Naphthalene</i>	<i>Biphenyl</i>
Retention time ( $t_R$ , min)	4.53	5.90	7.31
Peak width at 60% height ( $W_{60\%}$ , min)	0.102	0.139	0.173
Efficiency ( $N$ )	7890	7207	7142
Capacity factor ( $k'$ )	0.69	1.20	1.73
Asymmetry ratio	1.41	1.33	1.29

Many workers<sup>15-30</sup> have discussed the types of silanols that can exist and the problems of separations of basic samples in the presence of free silanols. Frequently, mobile phase additives are used to circumvent problems resulting from silanols. A large number of solutes have been used for characterizing selectivity of the reversed-phase columns<sup>17</sup>, however, no single test solute is useful for this purpose. Of the various solutes used for evaluating silanols, nitrobenzene is the most well-known and, perhaps, as useful as any. Therefore, it was selected to evaluate three columns from different batches with a mobile phase of *n*-heptane to determine the differences in terms of residual silanol sites in these columns. The results are given in Table III. The data do not permit clear differentiation, *e.g.*, column 1585 has the highest number of theoretical plates, a desirable characteristic for a column, but it gives the same peak width for nitrobenzene as column 1887 (the column with the lowest  $N$ ).

The same three columns could be differentiated more clearly with a new molecular probe (II). It has the following characteristics: (1) aromatic character; (2) carbonyl group and substituted nitrogen in its structure; (3) hydroxyl and carboxyl groups on the same asymmetric C atom; (4) a short carbon chain (C<sub>4</sub>).



The data with the new molecular probe are given in Table IV. With a mobile phase containing acetonitrile-0.02 *M* acetate buffer (41:59, v/v) (pH 4.1), significant differences can be observed among the three columns from the same manufacturer. At the 0.1 μg level, the new molecular probe was not detected with column 1887, whereas the other two columns gave a peak for it. With column 1646, the peak tails and has a width two times that of column 1585. It should be noted that the number of theoretical plates is also significantly higher ( $\approx 3.5 \times$ ) with column 1585 (the number of theoretical plates was calculated for the tailing peak with column 1646 to provide a relative value).

As can be seen from the data in Table IV, column 1887 behaves very differently

TABLE III  
EVALUATION C<sub>8</sub> COLUMNS WITH NITROBENZENE<sup>14</sup>

Whatman column, 10  $\mu\text{m}$ , 25 cm; mobile phase, *n*-heptane; flow-rate, 1 ml/min; amount injected, 0.04  $\mu\text{g}$  (15  $\mu\text{l}$ ).

	Column number		
	IR 1585	IR 1646	IR 1887
Retention time ( $t_R$ , min)	13.7	14.5	11.4
Peak width ( $W$ , min)	1.2	1.4	1.2
Retention ( $t_R$ ) benzene	8.5	8.4	8.0
Capacity factor ( $k'$ )	0.6	0.7	0.4
Theoretical plates ( $N$ )	2027	1789	1447

from the other two in that 0.1  $\mu\text{g}$  of the new probe is not detected (0.2  $\mu\text{g}$  and upward were detected). A plot of this data, when extrapolated down to the 0.1  $\mu\text{g}$  level, indicates a much broader peak width (2.3 min) for this column as compared to the other columns ( $\leq 1$  min). This shows that detectability of a component at low levels (0.1  $\mu\text{g}$  or  $\approx 0.1\%$ ) can vary from one batch of columns to the next. Detectability decreases because there is a concomitant loss of peak height due to peak broadening. As the peak broadens, the resolution for closely resolved peaks is also affected negatively; this can eventually result in the complete loss of resolution and detectability as observed at the 0.1  $\mu\text{g}$  level for column 1887. Hence it is important to select a probe that is useful for monitoring selectivity and detectability of a given separation while recognizing no single probe is likely to be universal for this purpose.

#### Separation of peak pairs

Selectivity optimizations generally entail improving the separation of a pair of peaks where the observed resolution is minimum or more simply, the  $\alpha$  value is low. However, this rule does not work well in pharmaceutical analysis for a very large number of cases because a significant number of compounds have to be simultaneously resolved that may vary in aromaticity, functional groups and their acidic, basic or neutral character. Two such cases are discussed below.

TABLE IV  
EVALUATION OF THE COLUMNS WITH THE NEW PROBE (COMPOUND II)<sup>14</sup>

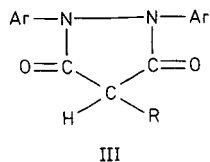
Whatman C<sub>8</sub> 10  $\mu\text{m}$ , 25 cm; 0.1  $\mu\text{g}$  molecular probe injected; mobile phase, acetonitrile-0.02 *M* acetate buffer (pH 4.1) (41:59, v/v); flow-rate, 2.4 ml/min.

	1585	1646	1887
Retention time (min)	3.4	3.8	Not detected <sup>b</sup>
Peak width	0.5	1.0 <sup>a</sup>	Not detected <sup>b</sup>
Capacity factor ( $k'$ )	1.9	2.2	—
Theoretical plates ( $N$ )	740	214	—

<sup>a</sup> Tails.

<sup>b</sup> Sample of 1  $\mu\text{g}$  gives  $t_R = 4.4$  min;  $W = 6.0$  (large tail);  $k' = 2.7$ .

*Case I.* An optimum separation, both in time and resolution, was developed for a substituted diphenylhydrazino compound (III) on a 25 cm  $\times$  4.6 mm I.D. C<sub>8</sub> column with a mobile phase containing acetonitrile-acetate buffer pH 4.1 (44:56).



The HPLC method (Fig. 1) resolves various potential transformation products from compound III<sup>31</sup>. Of interest in this separation are the peak pairs 7, 8 and 8, 9. Peak 7 is well resolved from peak 8. The calculated resolution of this peak pair is  $\leq 1.0$  and is more than adequate for quantitation of peak 7. However, this resolution is not enough for the component at the tail end of peak 8, *i.e.*, see peak 9. This is due to the fact that in pharmaceutical analysis it is necessary to inject sufficient amounts of the active ingredient to allow quantitation of low levels of impurities. In this case it is 7  $\mu\text{g}$  per injection, an amount which allows quantitation of impurities down to a few hundredths of percent. This produces a very broad peak for the main component which can have a width  $\approx 10 \times$  that of a minor component. The calculated required

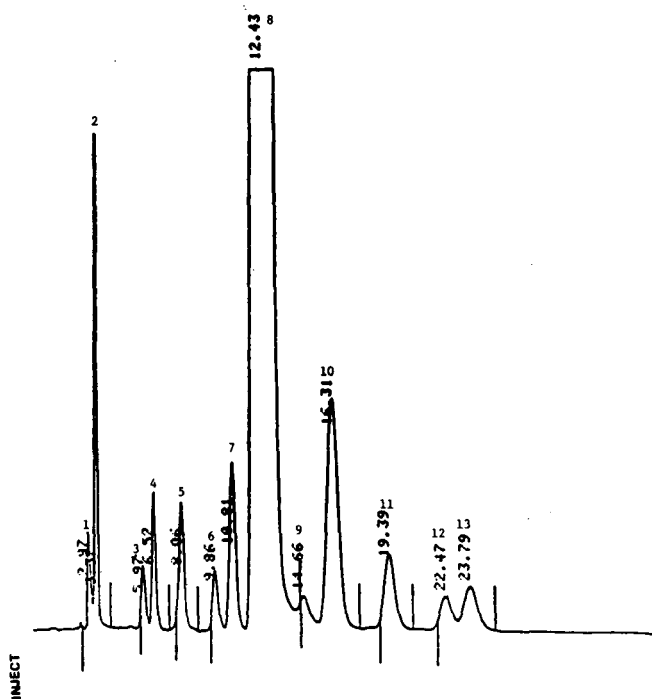


Fig. 1. Resolution of transformation products of a diphenylhydrazino compound<sup>31</sup>.

resolution is  $\geq 1.25$  for peaks 8 and 9. This puts an extra premium on mobile phase optimization and selectivity. Furthermore, it becomes necessary to assure that no component is eluting under the substantial area of the main peak. These requirements were met in the mobile phase optimization for this compound.

*Case 2.* Frequently separations are encountered where one of the components has unusually long retention time. For example, with separation of compound IV, the elution of the thioether impurity takes an unduly long time on a 25 cm  $\times$  4.6 mm I.D. C<sub>8</sub> column packed with 5- or 10- $\mu$ m particles.

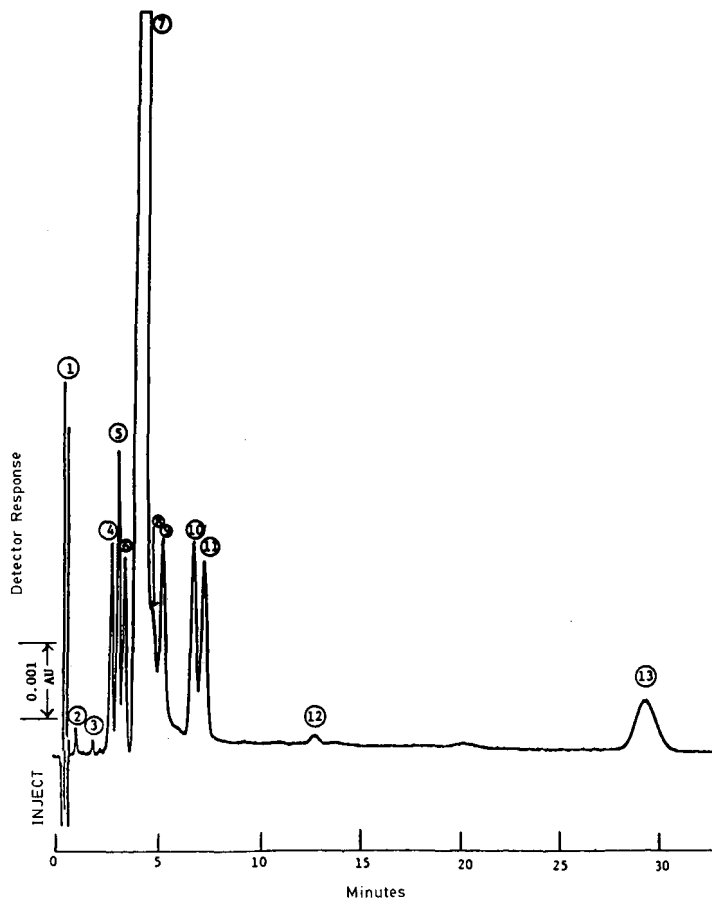
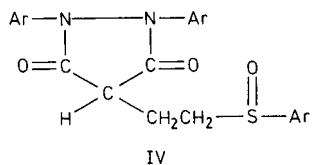


Fig. 2. Resolution of transformation products of Compound IV<sup>32</sup>.

The problem primarily required a reduction in analysis time with a minimal loss of resolution. This was attained by selection of a smaller column length, *i.e.*, 10 cm with the mobile phase containing 0.3% phosphoric acid–(acetonitrile–tetrahydrofuran, 4:1) (65:35). Fig. 2 shows such a chromatogram<sup>32</sup>. It can be seen that most of the components, except component 8, are fairly well resolved and the retention time of the thioether impurity (peak 13) is  $\approx 30$  min, a reasonable analysis time for most practical purposes. A component, peak 8, eluting at the tail of the main peak is poorly resolved and requires much higher resolution. Poor resolution can affect quantitation significantly. For example, alteration of the aqueous content of the mobile phase to 70% can provide excellent separation with  $R_s = 1.3$  and much better quantitation<sup>33</sup>. However, this improvement in resolution is possible at the expense of a significant increase in analysis time. Hence, it is important to assess various priorities in the optimization of mobile phase.

#### CONCLUSIONS

(1) Variabilities in the stationary phase, *i.e.*, differences in columns from different manufacturers or the same manufacturer can significantly influence the number of impurities resolved with a given mobile phase.

(2) Studies with the selectal probes can help select reliable columns and assure the same detectability for the observed components.

(3) It is important to work with  $R_s$  values greater than 1.25 for close peak pairs especially when the component of interest elutes at the tail end of the main peak. It is best to let the concentration of the minor component and the analysis time dictate the acceptable  $R_s$  value.

#### REFERENCES

- 1 S. Ahuja, *Ultratrace Analysis of Pharmaceuticals and Other Compounds of Interest*, Wiley, New York, 1986.
- 2 S. Ahuja, *Selectivity and Detectability Optimizations in HPLC*, Wiley, New York, 1989.
- 3 L. R. Snyder, J. L. Glajch and J. J. Kirkland, *Practical HPLC Method Development*, Wiley, New York, 1988.
- 4 P. J. Schoenmakers, *Optimization of Chromatographic Selectivity*, Elsevier, Amsterdam, 1986.
- 5 J. C. Berridge, *Techniques for Automated Optimization of HPLC Separation*, Wiley, New York, 1985.
- 6 K. Suematsu and T. Okamoto, *J. Chromatogr. Sci.*, 27 (1989) 13.
- 7 S. Ahuja, *Drug Quality Lecture*, Indian Pharmaceutical Congress, Madras, December, 1974.
- 8 S. Ahuja, *CHEMTECH*, November (1980) 702.
- 9 S. Ahuja, *J. Chromatogr. Sci.*, 17 (1979) 168.
- 10 S. Ahuja, *J. Pharm. Sci.*, 65 (1976) 163.
- 11 J. A. Mollica, S. Ahuja and J. Cohen, *J. Pharm. Sci.*, 67 (1978) 443.
- 12 T. Yamana and A. Tsuji, *J. Pharm. Sci.*, 65 (1976) 1563.
- 13 S. Ahuja, S. Shiromani and J. Smith, unpublished results.
- 14 S. Ahuja, *Proceedings Ninth Australian Symposium on Analytical Chemistry, Sydney, April 27, 1987*, p. 530.
- 15 M. A. Stadalius, J. S. Berus and L. R. Snyder, *LC · GC Mag. Liq. Gas Chromatogr.*, 6 (1988) 494.
- 16 K. K. Unger, *Porous Silica*, Elsevier, Amsterdam, 1979.
- 17 P. E. Antle and L. R. Snyder, *LC*, 2 (1984) 840.
- 18 J. B. Peri and A. L. Hensley, *J. Phys. Chem.*, 72 (1968) 2926.
- 19 R. K. Iler, *The Chemistry of Silica*, Wiley-Interscience, New York, 1979.
- 20 J. Köhler, D. B. Chase, R. D. Farlee, A. J. Vega and J. J. Kirkland, *J. Chromatogr.*, 352 (1986) 275.

- 21 P. C. Sadek, C. J. Koester and L. D. Bowers, *J. Chromatogr. Sci.*, 25 (1987) 489.
- 22 P. J. van den Driest, H. J. Ritchie and S. Rose, *LC · GC, Mag. Liq. Gas Chromatogr.*, 6 (1988) 124.
- 23 W. G. Tramposch and S. G. Weber, *Anal. Chem.*, 56 (1984) 2567.
- 24 J. Nawrocki, *J. Chromatogr.*, 407 (1987) 171.
- 25 P. C. Sadek and P. W. Carr, *J. Chromatogr. Sci.*, 21 (1983) 314.
- 26 A. Sokolowski and K.-G. Wahlund, *J. Chromatogr.*, 189 (198) 299.
- 27 P.-O. Lagerstrom, I. Marle and B.-A. Persson, *J. Chromatogr.*, 273 (1983) 151.
- 28 B.-A. Persson, S.-O. Jansson, M.-L. Johansson and P.-O. Lagerström, *J. Chromatogr.*, 316 (1984) 291.
- 29 J. W. Dolan, *LC · GC*, 4 (1986) 222.
- 30 E. Bayer and A. Paulus, *J. Chromatogr.*, 400 (1987) 1.
- 31 S. Ahuja, S. Shiromani, G. Thompson and J. Smith, unpublished results, 1984.
- 32 K. Parashkevov, R. Piskorik and J. Smith, unpublished results, 1983.
- 33 S. Ahuja, J. Ashman and J. Smith, unpublished results, 1986.

CHROM. 21 634

## STRATEGY FOR PEAK TRACKING IN LIQUID CHROMATOGRAPHY ON THE BASIS OF A MULTIVARIATE ANALYSIS OF SPECTRAL DATA

JOOST K. STRASTERS, HUGO A. H. BILLIET\* and LEO DE GALAN

*Delft University of Technology, Department of Analytical Chemistry, De Vries van Heystplantsoen 2, 2628 RZ Delft (The Netherlands)*

and

BERNARD G. M. VANDEGINSTE

*Catholic University of Nijmegen, Department of Analytical Chemistry, Toernooiveld, 6525 ED Nijmegen (The Netherlands)*

---

### SUMMARY

Peak tracking, required for the interpretive optimization of the mobile phase in reversed-phase high-performance liquid chromatography, is performed by means of multiwavelength detection followed by a multivariate analysis of the resulting data. A combination of techniques (target factor analysis and iterative target transformation factor analysis) is necessary to circumvent problems caused by a limited resolution or lack of knowledge regarding spectral characteristics and to determine the number of relevant components. A procedure to perform the actual peak tracking, which combines data related to the spectral characteristics and relative peak areas of separated and coeluting components, is presented.

---

### INTRODUCTION

A number of strategies developed to optimize the mobile phase composition in high-performance liquid chromatography (HPLC)<sup>1–5</sup> requires knowledge of the individual retention behaviour of all components in the sample, irrespective of whether the separation of all or only a part of the solutes is desired<sup>6</sup>. One of these so-called interpretive optimization strategies is the iterative regression design<sup>7</sup>, which estimates the retention at various mobile phase compositions on the basis of a limited number of chromatograms of a given sample under various experimental conditions and a linear retention model. In order to derive this model, the location of the components in successive chromatograms must be known. The determination of the elution order in a set of chromatograms is referred to as peak tracking.

A simple method of peak tracking uses the relative areas of the peaks to derive the individual retention characteristics. Because of the expected peak overlap (one of the reasons to optimize the separation), some of the individual peak areas will be difficult to determine without assumptions on peak shape. Although an algorithm using combinations of areas to analyse coeluting peaks has been described<sup>8</sup>, the result

will depend heavily on the number of components assumed in the mixture, usually defined as the maximum number of peaks observed in any chromatogram. Otto *et al.*<sup>9</sup> circumvented problems related to the variation in area of peaks of the same component by applying fuzzy set theory and assuming a limited variation in the retention behaviour.

Drouen *et al.*<sup>10</sup> described the use of wavelength ratios, which should result in a characteristic level for every component. However, due to the variability of the spectra in different mobile phase systems and disturbances in the ratios caused by drifting or shifted baselines, a direct matching of levels is not always possible. Furthermore, in cases of severe overlap (resolution lower than 0.5) the individual levels of the components are no longer observed. The logical extension to multiwavelength detection by means of linear photodiode array detection (LPDA) and a subsequent comparison by eye of the resulting spectral data was described by the same authors<sup>11</sup>. Although individual spectra of the components are not always observed in peak clusters containing more than two components with severe chromatographic overlap, a simultaneous visual evaluation of a number of spectra recorded in a peak group can be used to estimate the number of components and select specific adsorption characteristics to aid in the peak tracking.

For a further automation of the method and an extension to more complex mixtures, we recently described the application of various multivariate analysis techniques to spectral data resulting from multiwavelength detection of peak clusters<sup>12</sup>: depending on the amount of information available, one or more of these techniques can be applied to assist in the determination of separate elution profiles and/or spectra of components in peak clusters. The multicomponent analysis applied to separate mixture spectra requires no resolution, but all components should be available in a library containing reference spectra measured in the same mobile phase. A selection of the relevant library spectra by means of a target factor analysis lowers the demands on the spectral quality of these spectra, but requires some chromatographic resolution. Various techniques related to self-modelling curve resolution such as the iterative target transformation factor analysis determine both spectral characteristics and elution profiles, but produce reliable results only when the chromatographic resolution is sufficiently large<sup>13,14</sup>.

In this study we have used a combination of these techniques in a systematic approach to track peaks in various chromatograms of the same sample. The procedure is described by referring to two practical examples with special emphasis on a practical method to determine the number of relevant components.

## THEORETICAL

### *The principal component analysis (PCA)*<sup>15</sup>

The two multivariate methods applied in the peak-tracking procedure are the target factor analysis<sup>15</sup> and the iterative target transformation factor analysis<sup>16</sup>. Both methods use the results of an abstract analysis of the spectral data: since the spectra observed are a linear combination of contributions of individual components present in the cluster, the original data matrix, **D**, of  $n_s$  spectra over  $n_w$  wavelengths can be written as a product of the spectral characteristics of the components and the corresponding concentration profiles (Beer's law):



$$\mathbf{D} = \mathbf{S}\mathbf{C}^T \quad (1)$$

$\mathbf{S}$  contains the  $n_c$  pure component spectra over  $n_w$  wavelengths and  $\mathbf{C}$  contains the  $n_c$  individual elution profiles over  $n_s$  points. An analysis of the variance observed in the data by means of a principal component analysis<sup>15</sup> produces an alternative decomposition:

$$\mathbf{D} = \mathbf{R}\mathbf{V}^T \quad (2)$$

When this description is derived from the covariance matrix  $\mathbf{D}^T\mathbf{D}$ , the matrix  $\mathbf{V}$  contains the  $n_s$  principal components (dimensions  $n_s \times n_s$ ) which correspond to the eigenvectors of the covariance matrix. The matrix  $\mathbf{R}$  (dimensions  $n_w \times n_s$ ) is derived by a projection of  $\mathbf{D}$  on  $\mathbf{V}$ . When only the significant eigenvectors are considered (described in the next section) an equation with reduced matrices,  $\mathbf{R}'$  (dimensions  $n_w \times n_c$ ) and  $\mathbf{V}'$  (dimensions  $n_s \times n_c$ ), is derived which results in a reconstructed data matrix,  $\mathbf{D}'$ . Apart from the experimental noise,  $\mathbf{D}'$  is equal to  $\mathbf{D}$ . The reduced matrices,  $\mathbf{R}'$  and  $\mathbf{V}'$ , can be transformed to their physically meaningful counterparts,  $\mathbf{S}$  and  $\mathbf{C}$ :

$$\mathbf{D}' = \mathbf{R}'\mathbf{V}'^T \quad (3a)$$

$$= \mathbf{R}'\mathbf{T}\mathbf{T}^{-1}\mathbf{V}'^T \quad (3b)$$

$$= \mathbf{S}\mathbf{C}^T \quad (3c)$$

The matrix  $\mathbf{T}$  is the transformation matrix (dimensions  $n_c \times n_c$ ). Different methods indicated by the general descriptor "factor analysis" try to derive either  $\mathbf{T}$  or  $\mathbf{T}^{-1}$  depending on the available information on the system and/or by imposing a number of boundary conditions.

*The target factor analysis*<sup>15,17</sup>

The target factor analysis (TFA) selects the appropriate components from a library by an individual examination of the spectral characteristics: every reference spectrum is approximated in a least squares sense by means of the columns of  $\mathbf{R}$  (the reference spectrum,  $\mathbf{s}$ , is projected onto the hyperspace defined by  $\mathbf{R}$  and is compared with its projection,  $\mathbf{s}'$ ):

$$\mathbf{s}' = \mathbf{R}(\mathbf{R}^T\mathbf{R})^{-1}\mathbf{R}^T\mathbf{s} \quad (4a)$$

$$= \mathbf{R}\mathbf{t} \quad (4b)$$

If the projection is valid, *i.e.*, if the spectrum resembles its projection closely and consequently is a component present in the examined cluster the required projection produces one of the columns of  $\mathbf{T}$ ,  $\mathbf{t}$ . Once all components present in the cluster have been identified,  $\mathbf{T}$ , and hence  $\mathbf{T}^{-1}$ , is known and the corresponding elution profiles are calculated.

The requirements for this analysis to work are the following: the spectral characteristics for all components should be (slightly) different and some resolution

(approximately  $R = 0.1$ ) should be present in order to derive an hyperplane with the correct dimensionality. A slight change in spectral characteristics, for instance caused by a change in the mobile phase composition, is acceptable as long as the correct components are selected from the library<sup>12</sup>.

*The iterative target transformation factor analysis (ITT-FA)*<sup>13,14,16</sup>

Like other forms of self-modelling curve resolution<sup>18,19</sup>, the ITT-FA derives both elution profiles and spectra by imposing a number of boundary conditions on the derived solution, *i.e.*, non-negativity of concentrations and a restriction to unimodal profiles. However, as the name indicates, no specific peak model is assumed.

The ITT-FA starts with a first estimate of the elution profile, which is a spike at the location derived by means of an orthogonal abstract rotation (the varimax rotation). This estimate,  $e_1$ , is projected onto the hyperplane described by  $V$ , and the resulting projection,  $e'_1$ , is corrected for negative concentrations and secondary maxima. The resulting profile,  $e_2$ , is again projected and corrected until no significant improvement in subsequent projections is observed:

$$e'_i = V(V^T V)^{-1} V^T e_i \quad (5a)$$

$$= V t_i \quad (5b)$$

$$e_{i+1} = (e'_i)_{\text{corrected}} \quad (6)$$

The final transformation found to derive the profile,  $t_i$ , is one of the rows of  $T^{-1}$  in eqn. (3b). Once all profiles in a peak cluster have been determined in this way, the transformation matrix,  $T$ , is constructed and the corresponding spectra are calculated (eqn. 3c).

Similar to TFA, the spectra should show some dissimilarity in order to derive the correct hyperplane used for the derivation of the elution profiles. However, the amount of resolution required for a correct analysis is significantly greater in comparison with TFA (approximately  $R = 0.4$  for components present in equal concentrations). The quality of the resulting spectra, used in a subsequent comparison between various chromatograms of the same sample, will also depend on the spectral similarity of the components and the relative quantities. In a previous publication<sup>13</sup> we described a selection criterion to decide on the reliability of the derived spectra based on the observed values of these parameters (as opposed to the real, unknown values).

*The number of relevant components*

A specific problem confronting the analyst in practical optimization problems is how to determine the number of components in an unknown mixture that can be detected by UV spectroscopy. Often, one assumes this number to be equal to the maximum number of peaks in any chromatogram of the sample. However, this number is a good guess at best. A similar problem must be dealt with in the case of separate peak clusters: the individual elution profiles (TFA) or spectra (ITT-FA) can be calculated only once all spectra or profiles have been determined. Consequently, a knowledge of the number of (relevant) components is essential to obtain the desired information.

A much better estimate as compared to the observed number of peak maxima can be derived by a multivariate treatment of the spectral data. As indicated before, the number of principal components (PCs) derived is originally equal to the number of columns,  $n_s$ , in the data matrix, *i.e.*, the number of spectra recorded. However, because each PC describes the maximum amount of variation in the data which is not described by the previous ones, only the first  $n_c$  PCs are related to the relevant information with regard to spectra and elution profiles. The remaining PCs are required only to describe the experimental noise and can be removed without changing the information content of the resulting data matrix,  $\mathbf{D}'$  (eqn. 3a). A number of methods to determine the number of significant PCs has been described in the literature<sup>15,20-22</sup> and can be roughly divided into two depending on the knowledge of the experimental error.

When the experimental error is known, one can reconstruct the data matrix  $\mathbf{D}'_{n_c}$  using the reduced matrices  $\mathbf{R}'_{n_c}$  and  $\mathbf{V}'_{n_c}$ ;  $n_c$  indicates the number of columns and hence the assumed dimensionality of the data, *i.e.*, the number of components.  $\mathbf{D}'_{n_c}$  is compared with  $\mathbf{D}$  and when the difference falls just within the experimental error the correct number of components is used. Adding more components to the description corresponds to overfitting of the data and will not result in a significant improvement of the quality. When using the reduced matrices,  $\mathbf{R}'$  and  $\mathbf{V}'$ , part of the experimental error is removed from the data. Malinowski and Howery<sup>15</sup> defined this removed error by the term "extracted error" (XE):

$$\text{XE}_{n_c}^2 = \sum_{i=1}^{n_s} \sum_{j=1}^{n_w} [d_{ij} - (d'_{ij})_{n_c}]^2 / n_s n_w \quad (7)$$

This error can be used to estimate the real error, RE, in the data:

$$\text{RE}_{n_c}^2 = \text{XE}_{n_c}^2 n_s / (n_s - n_c) \quad (8)$$

Several short-cuts to determine the value of RE exist, using the eigenvalues  $\lambda$  related to the eigenvectors of the covariance matrix,  $\mathbf{Z}$  (the PCs). Since the last  $n_s - n_c$  eigenvalues are related only to the experimental error, this error can be estimated from:

$$\text{RE}_{n_c}^2 = \sum_{i=n_c+1}^{n_s} \lambda_i / [n_w(n_s - n_c)] \quad (9)$$

The real error is estimated for different values of  $n_c$  and the value of  $n_c$  where the error drops below the known experimental error is taken as the number of components. A similar measure of uncertainty, the chi-squared criterion of Bartlett, is also based on the difference between the original and the reconstructed data matrix (see ref. 15, p. 76)

$$\chi_{n_c, \text{exptl.}}^2 = \sum_{i=1}^{n_s} \sum_{j=1}^{n_w} [d_{ij} - (d'_{ij})_{n_c}]^2 / \sigma^2 \quad (10)$$

where the known experimental error,  $\sigma$ , is assumed to be constant over the full wavelength range, which is acceptable to a first approximation. This value is compared with the theoretical value:

$$\chi_{n_c, \text{th.}}^2 = (n_w - n_c)(n_s - n_c) \quad (11)$$

The value of  $n_c$  where the difference between  $\chi_{n_c, \text{exptl.}}$  and  $\chi_{n_c, \text{th.}}$  is minimal is taken as the correct dimensionality of the data.

When the experimental error is not known, one has to evaluate the amount of variance added to the data by the inclusion of an additional PC as compared to the remaining variance in the non-significant PCs. One of the functions used for this evaluation is the indicator function, IND, described by Malinowski<sup>20</sup>:

$$\text{IND}_{n_c} = \text{RE}_{n_c}/(n_s - n_c)^2 \quad (12)$$

This value should reach a minimum when the correct number of factors is used in the reproduction. However, this minimum is observed clearly only when the real (true) factors underlying the data are significantly different, *i.e.*, the angles between axes representing these factors in the data space are sufficiently large to distinguish differences between spectra or elution profiles from deviations caused by the experimental error. A computationally more complicated but also more fundamental approach is the so-called cross-validation<sup>21</sup>: the principal component analysis is repeated a number of times with part of the data omitted from the data matrix. This data section is predicted on the basis of models derived from the PCs by applying varying dimensionalities. This is repeated for all sections of the data matrix (preferably all individual elements). The resulting estimates are compared to the true values and the decrease in the remaining error observed with an increase in the number of factors used for the prediction is evaluated to derive the correct number of components.

All methods described in this section have one important characteristic in common: they are all devised to determine the number of statistically significant factors or components. Unfortunately, this also includes deviations in the normally distributed experimental error caused by drifting baselines, non-linearities in the absorbance characteristics of the diode array, insignificantly small contributions of impurities, etc. What we are really interested in is the number of relevant components, *i.e.*, those components exhibiting significant UV absorption and physical meaningful chromatographic behaviour. When the ITT-FA is used to analyse the above disturbances, a unimodal is possibly forced upon non-unimodal profiles, resulting in large errors in the subsequent inverse transformation (eqn. 3b) and consequently in erroneous spectral characteristics. Incorrect profiles can influence other spectra derived for the cluster under examination, including those related to physical significant solutes, or give rise to apparent components without any physical significance.

In order to avoid these kinds of deviations, we propose an alternative procedure. The ITT-FA is repeated a number of times using different dimensionalities,  $n_c$ . Each analysis, the resulting profiles and spectra are corrected for negative absorbances and concentrations in case the procedure was stopped before physically meaningful elements were derived. The calculated and corrected profiles and spectra are used to recalculate the data matrix:

$$\mathbf{D}'_{n_c} = \mathbf{S}'_{n_c} \mathbf{C}'_{n_c}^T \quad (13)$$

By a comparison of this reproduced data matrix with the original one, the extracted error is calculated (eqn. 7). When XE reaches a minimum, the cluster is described by the  $n_c$  most reliable profiles and spectra which can be derived given the aforementioned boundary conditions. Although the neglect of small impurities, drifting baseline, etc., will result in a larger extracted error than would be expected on the basis of the experimental error, this deviation is less serious than the one resulting from the use of forced unimodal profiles and is a better indication of the number of relevant components in a cluster.

## EXPERIMENTAL

### *Chromatographic conditions*

The full peak-tracking procedure will be described on the basis of two examples. The first example consists of two chromatograms of a mixture of thirteen components listed in Table I. The mixture was eluted on a Novapak C<sub>18</sub> column (Millipore Waters, Milford, MA, U.S.A.), 10 cm × 8 mm I.D. and particle size 5 μm, using 1.5 ml/min of tetrahydrofuran (THF)-water (40:60) and methanol-water (60:40) as mobile phases, respectively (Fig. 1).

The second example was part of a study on full and limited optimization<sup>6</sup> and consists of three chromatograms of a mixture of nine components (Table I). The mixture was eluted on a 20 cm × 4.6 mm I.D. column packed with 5-μm ODS-Hypersil using 1.0 ml/min of THF-water (31:69), methanol-water (50:50) and acetonitrile-water (38:62) as mobile phases, respectively (Fig. 2).

Retention times of the nine-component mixture observed during the subsequent steps of the optimization procedure can be found in ref. 6. The solutes were obtained from Fluka (Buchs, Switzerland) and E. Merck (Darmstadt, F.R.G.) and used in suitable concentrations (0.1–0.2 mg/ml).

TABLE I

THE COMPOSITION OF THE TWO MIXTURES USED IN THE EXAMPLES

<i>Mixture A</i>	<i>Mixture B</i>
1 Acetanilide	1 Benzyl alcohol
2 Methylparaben	2 Dimethyl phthalate
3 Benzaldehyde	3 Phenol
4 Acetophenone	4 Benzonitrile
5 Cinnamyl alcohol	5 <i>p</i> -Cresol
6 Nitrobenzene	6 Diethyl phthalate
7 Methyl benzoate	7 3,4-Dimethylphenol
8 Anisole	8 Benzene
9 Diethyl phthalate	9 2,4-Dimethylphenol
10 Methyl salicylate	
11 Ethyl benzoate	
12 1-Nitronaphthalene	
13 Benzophenone	

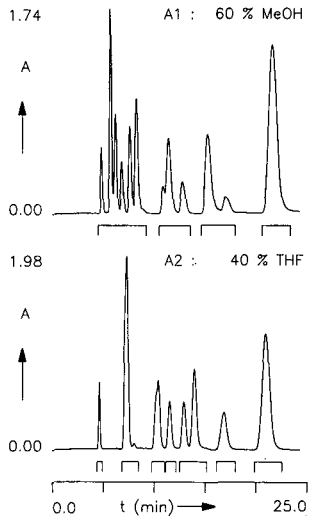


Fig. 1. Two chromatograms of a thirteen-component mixture (composition in Table I). Experimental conditions in the text. The peak clusters selected for the multivariate analysis are indicated by the brackets below the chromatograms. MeOH = methanol.

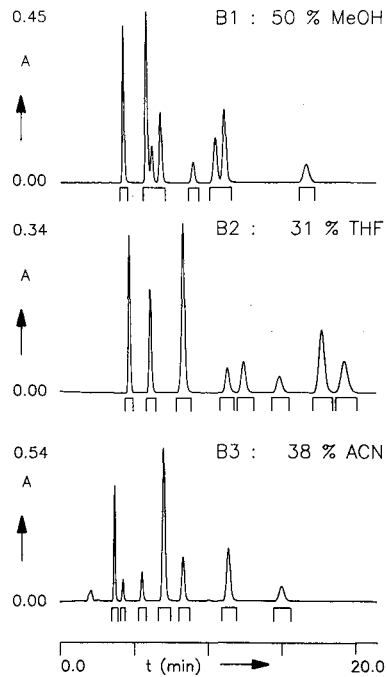


Fig. 2. Three chromatograms of a nine-component mixture (composition in Table I). ACN = Acetonitrile. Other details as in Fig. 1.

### *Instrumentation*

The chromatographic system consisted of an HP 1090 chromatograph, equipped with an HP 1040A linear photodiode array detector (Hewlett-Packard, Waldbronn, F.R.G.). The detector was connected to an HP-85 desktop computer, equipped with an HP-IB IEEE-488 interface and RS-232C serial interface. The data were temporarily stored on 5¼-in. flexible disks using an HP82910M disk-drive.

The data files collected by means of the detector were transferred to an Olivetti M24 personal computer (Olivetti, Ivrea, Italy) by means of serial interfaces on both computers. Further analysis of the data was performed on an IBM-PC (IBM, U.S.A.), equipped with two 5¼-in. disk-drives, an expansion unit with two 10-Mbyte hard disks, the Intel 8087 mathematical coprocessor and an HP-7470A graphics plotter with serial interface.

The spectra were recorded between 210 and 400 nm. The first 10 min of the chromatograms were sampled with approximately 30 spectra per minute. The remainder was analysed using 20 spectra per minute, since broadening of the peaks reduced the requirements on the sampling frequency.

### *Software*

All software used in the procedure was developed using the Turbo Pascal compiler version 4.0 (Borland International, CA, U.S.A.). The algorithm for the TFA was adapted from the description by Malinowski and Howery<sup>15</sup>; the ITT-FA was adapted from the description by Vandeginste *et al.*<sup>16</sup>. Correlation coefficients were calculated according to Reid and Wong<sup>23</sup>. The eigenvectors and eigenvalues of the covariance matrix of the data matrix were determined by the HQR II algorithm<sup>24</sup>.

Curve fitting, to estimate resolutions and concentrations, was performed on the basis of bigaussian profiles and a non-linear procedure described by Bevington<sup>25</sup>. This procedure was preferred to a direct calculation of peak width and areas based on the calculated profiles, because of the limited sampling frequency over the chromatographic peaks, and the inherent uncertainty in the derived results.

## RESULTS AND DISCUSSION

In order to illustrate the procedure currently under investigation, two mixtures were eluted under varying chromatographic conditions (Table I and Figs. 1 and 2). In the following discussion the thirteen-component mixture will be referred to as mixture A, and the corresponding chromatograms as A1 (60% methanol) and A2 (40% THF). The nine-component mixture is referred to as mixture B, and the chromatograms will be identified by B1 (50% methanol), B2 (32% THF) and B3 (38% acetonitrile). Although the composition of both mixtures was accurately known, the strategy as such assumes no prior knowledge of the number of components or their identities, hence chromatograms of "unknown" mixtures can be analysed in the same way.

An overview of the full procedure is given in Fig. 3. In the following sections the separate steps of the strategy will be discussed in more detail.

### *Processing of separate clusters*

The first step is the partition of every chromatogram in peak clusters. These clusters are for instance selected on the basis of a critical absorbance threshold. This

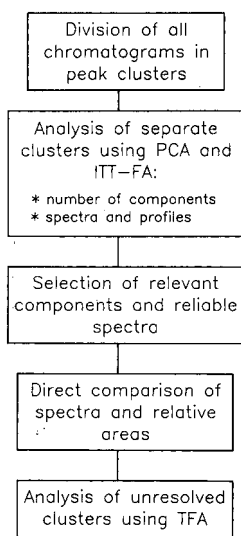


Fig. 3. Overview of the peak tracking procedure.

level is tested for at all wavelengths, thus ensuring detection of all components in the mixture exhibiting significant absorption at any wavelength. Once all regions with significant UV activity have been selected, the corresponding mixture spectra are subjected to the principal component analysis, resulting in the abstract matrices  $\mathbf{R}$  and  $\mathbf{V}$ .

Fig. 4 illustrates the procedure applied to the separate peak clusters (step 2 in Fig. 3). After the principal component analysis, the maximum number of components,

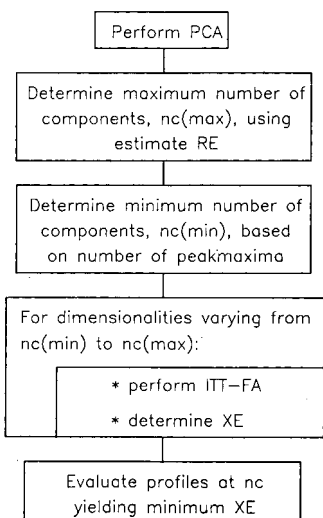


Fig. 4. The analysis of an individual peak cluster.



$n_{c_{\max}}$ , present in the cluster is determined on the basis of the real error (RE, eqn. 9) determined for different dimensionalities,  $n_c$ , and compared with the known experimental error of 0.15 ma.u. The minimum number of components,  $n_{c_{\min}}$ , is defined by the number of observed peak maxima in the cluster. Of course,  $n_{c_{\max}}$  should be larger than or equal to  $n_{c_{\min}}$ , otherwise one is confronted with split peaks or components with high spectral similarity and a correct analysis of the cluster by means of the ITT-FA will not be possible. The next step consists of a repeated execution of the ITT-FA varying the number of components from  $n_{c_{\min}}$  to  $n_{c_{\max}}$ . The extracted error, XE, is calculated for every dimensionality as the difference between the elements of the original and of the reconstructed data matrix (eqn. 7). The dimensionality yielding the smallest XE is taken to be the true number of components,  $n_c$ .

The last step in Fig. 4 consists of an evaluation of the calculated profiles: by a non-linear fitting procedure a bigaussian profile is used to estimate the area and peak width for every profile determined by means of ITT-FA. The area is based on profiles corresponding with normalized spectra (normalization to the norm, *i.e.*, the sum of squared absorbances equals 1), and is used to distinguish between minor components (less than 1% of the mixture) and major components. The minor components are ignored in the remainder of the analysis and the relative peak areas of the other components are calculated. The peak width is used to determine the resolution from neighbouring components, for the subsequent selection of reliable spectra.

The above procedure is illustrated in Fig. 5 for the third cluster in chromatogram A1. The number of components based on the value of RE was four. Since the number of peak maxima observed was two, the ITT-FA was performed with two, three and four components, resulting in XE values of 0.9, 2.6 and 6.9. As a comparison, the ITT-FA was also performed with an assumed dimensionality of 1, resulting in XE = 310.3. The latter value is extremely high, as expected, since two peaks are clearly observed in the original chromatogram. The spectrum which corresponds with this profile will be equal to the first column of **R**, hence it will be a mixture spectrum containing elements of the spectra of both components. When three components are assumed to be present, a small profile is observed fronting the first real component, which is characterized by a rather "noisy" spectrum. This deviation is probably caused by a shift in the baseline or a small impurity in the front of the peak. Although the profile derived for this disturbance is not correct, as expressed by the increased value of XE, the confusion caused by a profile like this will be minimal since the peak area derived is negligible. However, if four components are assumed to be present, a large additional peak is observed, probably corresponding with non-linearities in the observed absorptions as indicated by the similarity of spectra 1 and 4. Since this fourth profile is in fact bimodal, the error introduced by the ITT-FA will be more noticeable, as indicated by the value of XE. Obviously, these kind of disturbances will cause confusion with regard to the correct number of components in the mixture and must be avoided. By selecting the dimensionality corresponding with the minimum value of XE, the best profiles and spectra are derived to define the cluster. Consequently the number of components in the cluster was taken to be two.

The full results for all chromatograms in the two examples are summarized in Tables II (mixture A) and III (mixture B). In most cases the number of components based on the value of RE,  $\chi^2$  and/or IND is too high because of the disturbances mentioned in the Theoretical section. Especially the IND function is much too

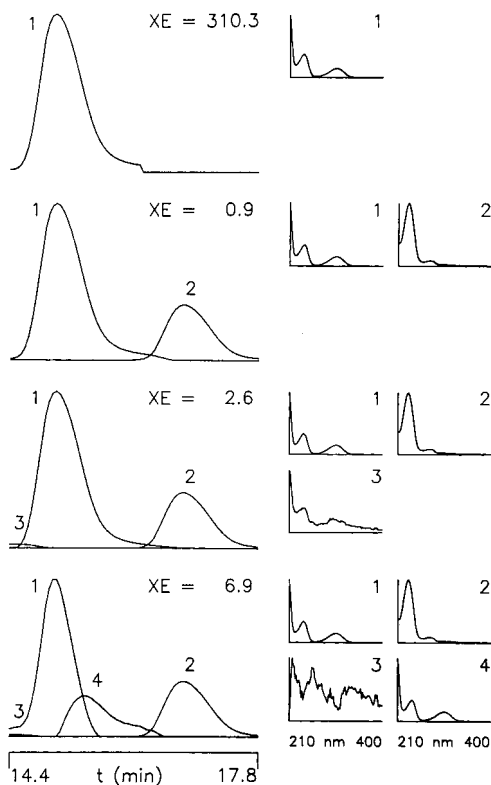


Fig. 5. The results of the ITT-FA for the third peak cluster in chromatogram A1. The analysis is performed for different dimensionalities of the cluster, resulting in the individual elution profiles and the corresponding spectra. The value of the extracted error, XE, is indicated for each analysis.

sensitive to disturbances in the chromatographic process, even in the case of pure peaks. By comparison, the repeated execution of ITT-FA is much better, although it still overestimates the total number of solutes in the sample. If we impose a threshold of 1% for the relative peak area of a component to be considered as significant, the numbers reduce to  $N_{\text{est}}$  which are equal to the true numbers,  $N_{\text{act}}$ , in the three chromatograms. Indeed, only two discrepancies remain: in cluster 2 of chromatogram A1 and cluster 3 of chromatogram B2 an additional component is detected. The relative areas of the peaks are equal to 1.5 and 2.0% respectively of those of the total mixtures and are probably due to minor impurities or disturbances in the chromatographic process. When these solutes are also detected in chromatograms A2, B1 and B3, they will be regarded as impurities in the mixtures. However, if they are not detected in the other chromatogram(s), either because we are dealing with an artefact, or because of close coelution with a component present in excess, they are ignored because of the low concentrations. Since only thirteen components are detected in chromatogram A2 and nine components in both chromatograms B1 and B3, these two solutes will not be detected in the other chromatograms. The point is stressed here because in practical experiments it is almost impossible to avoid these kinds of disturbances, and automated procedures should be equipped to handle them.

TABLE II

ESTIMATED DIMENSIONALITIES OF THE CLUSTERS IN THE TWO CHROMATOGRAMS OF THE THIRTEEN-COMPONENT MIXTURE, BASED ON THE KNOWN EXPERIMENTAL ERROR (RE), THE  $\chi^2$  TEST, THE INDICATOR FUNCTION OF MALINOWSKI (IND) AND THE RESULTS OF THE ITT-FA (ITT)

In addition the number of significant components selected after examination of the concentrations,  $N_{est}$ , and the actual number of components, based on knowledge of the mixture,  $N_{act}$ , are listed. The two chromatograms are identified as A1, recorded in 60% methanol, and A2, recorded in 42% THF (Fig. 1).

Cluster	RE	$\chi^2$	IND	ITT	$N_{est}$	$N_{act}$
A1-1	10	10	21	8	6	6
A1-2	5	5	10	4	4	3
A1-3	4	4	9	2	2	2
A1-4	4	4	12	3	2	2
A1 total	23	23	52	17	14	13
A2-1	3	2	7	2	1	1
A2-2	6	5	11	5	4	4
A2-3	3	3	7	2	2	2
A2-4	2	2	5	1	1	1
A2-5	4	4	13	3	3	3
A2-6	2	2	8	1	1	1
A2-7	3	3	13	1	1	1
A2 total	23	21	64	15	13	13

#### *The selection of reliable spectra*

Step 3 in Fig. 3 refers to an evaluation of the calculated spectra and profiles. The results of the ITT-FA are dependent on the extent of chromatographic resolution, the spectral similarity between the components and the relative concentrations of the components<sup>13</sup>. Since the peak tracking is based primarily on a comparison of spectra, the quality of the calculated spectra, *i.e.*, the similarity between the true and calculated spectrum expressed by the correlation coefficient,  $\rho$ , is essential. Based on simulations of two-component clusters, described by bigaussian profiles, relationships to derive this quality by evaluating the observed chromatographic resolution, observed spectral similarity of both components and observed relative concentrations were developed. Especially in the case of low resolution, these observed values will deviate from the true ones due to reconstruction errors in the ITT-FA. In general, when two components are reasonably resolved (resolution > 0.4), not too dissimilar ( $\rho_{12}$  > 0.5) and present in approximately equal concentrations, the calculated spectra will have a high quality ( $\rho$  > 0.999), sufficient for reliable results in comparison with spectra observed in other chromatograms. However, at lower resolution or in the case of large differences in relative concentrations, this quality will not be obtained for one or both calculated spectra, in which case they will not qualify for use in a direct comparison. Although the relationships applied were derived for two-component clusters, an extension to larger clusters by means of a pairwise evaluation of subsequent peaks seems justified to a first approximation<sup>26</sup>.

However, application of the above procedure in practical situations sometimes

TABLE III

## ESTIMATED DIMENSIONALITIES OF THE CLUSTERS IN THE THREE CHROMATOGRAMS OF THE NINE-COMPONENT MIXTURE

The three chromatograms are identified as B1, recorded in 50% methanol, B2, recorded in 32% THF and B3, recorded in 38% acetonitrile (Fig. 2). Other details as in Table II.

<i>Cluster</i>	<i>RE</i>	$\chi^2$	<i>IND</i>	<i>ITT</i>	$N_{est}$	$N_{act}$
B1-1	3	2	6	3	2	2
B1-2	3	3	9	3	3	3
B1-3	1	1	3	1	1	1
B1-4	3	3	7	2	2	2
B1-5	2	1	3	1	1	1
B1 total	12	10	28	10	9	9
B2-1	2	2	5	1	1	1
B2-2	1	1	4	1	1	1
B2-3	3	3	6	3	3	2
B2-4	2	1	3	2	1	1
B2-5	2	1	5	1	1	1
B2-6	1	1	2	1	1	1
B2-7	2	2	4	1	1	1
B2-8	2	2	3	1	1	1
B2 total	15	13	32	11	10	9
B3-1	1	1	4	1	1	1
B3-2	2	1	3	1	1	1
B3-3	1	1	3	1	1	1
B3-4	3	3	7	3	3	3
B3-5	2	1	3	1	1	1
B3-6	2	2	4	1	1	1
B3-7	1	1	3	1	1	1
B3 total	12	10	27	9	9	9

leads to acceptance of components not quite fulfilling the demands imposed on the spectral quality, *i.e.*, in the case of closely coeluting components (resolution  $R < 0.4$ ) with high spectral similarity ( $\rho_{12} > 0.9$ ) and increased tailing not very well described by the bigaussian model used in the derivation of the relationships used in the evaluation. In order to make the selection procedure more flexible, spectra derived from closely coeluting solutes will remain suspect and candidates for improvement. Furthermore, the selection procedure is directed only at the quality of the spectra and consequently may result in incorrect relative areas in the case of components with similar spectra but different concentrations at low resolutions. If the relative areas are required in order to derive an unambiguous identification, the conclusions with regard to these clusters based on the results of the ITT-FA must be regarded with caution.

In view of the previous discussion, we make the following distinctions.

A cluster is considered fully resolved when only one component is present or when all components are sufficiently resolved with respect to the concentrations (minimum resolution 0.4) to rely on both spectral data and related concentrations.

A cluster is unresolved when one or more of the components involved are uncertain with respect to the spectra and/or relative areas. These clusters are analysed in more detail in the next steps of the procedure.

A component is fully defined when both its spectral characteristics and its relative area are known.

A component is tentative when some assumptions are available with respect to its spectrum, but due to the close proximity of other undefined or tentative components the exact characteristics are not yet defined.

A component is undefined when, due to its low concentration or close proximity to other components, its spectral characteristics are unknown.

The spectra selected on the basis of the above evaluation, are stored in a library identified by the code of the chromatogram. For instance, chromatogram A1 will produce library A1, which will be compared with library A2 derived from chromatogram A2.

The result of the selection procedure for the first example is illustrated in Fig. 6a. The required spectral quality was set at 0.995, a practical compromise between an high correlation, ensuring acceptance of only correct spectra, and a larger deviation from the ideal value of 1 in order to include most components in the library. Since some changes in the spectra are often observed due to differences in the mobile phase, extreme high demands on the quality of the spectra will be impractical. Obviously, the resolution in the second cluster of chromatogram A2 is too low to rely on the derived

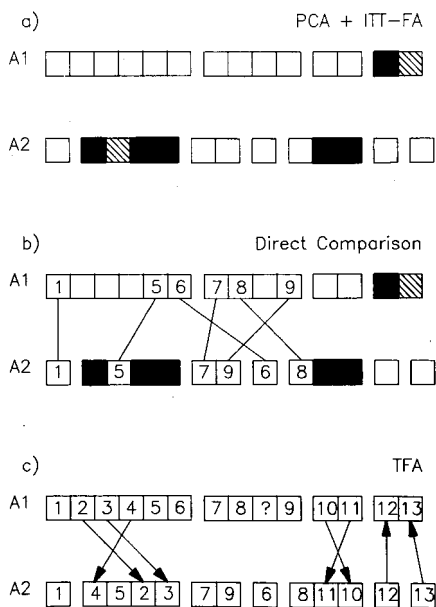


Fig. 6. The results of the three steps in the peak tracking procedure for the two chromatograms of the thirteen-component mixture, A1 and A2. Numbers refer to Table I. The unknown component is indicated by "?". (a) The conclusions of the evaluation of the spectra. Spectra are defined as: reliable ( $\square$ ), tentative ( $\equiv$ ) or unreliable ( $\blacksquare$ ). (b) Components recognized by a direct comparison, indicated by a line connecting matched solutes. (c) Components recognized by means of TFA. Arrows point from the targets to the clusters.

pure component spectra (the observed resolutions were 0.33, 0.40 and 0.26 and consequently the real resolutions are approximately 0.25, 0.34 and 0.10; ref. 13). Only the spectrum of the second component is included in the library as tentative, because of an higher concentration and consequently a more reliable spectrum. The same holds for the last two components in the fifth cluster (observed resolution 0.28, real resolution 0.15). The last cluster of chromatogram A1 contains two components with resolution 0.29 (real resolution approximately 0.17). Since the concentration (UV activity) of the second component is much higher than that of the first one, its spectrum is tentatively used in the subsequent comparison. As a result, the first example contains thirteen (perhaps fourteen) components (Table II), and produces two spectral libraries: A1, containing twelve reliable and one tentative spectrum, and A2 containing seven reliable and one tentative spectrum. In chromatogram A1 one unresolved cluster remains to be analysed in the next steps of the procedure since it contained one unreliable spectrum. In chromatogram A2 two unresolved clusters remain: cluster 2 (three unreliable spectra) and cluster 5 (two unreliable spectra).

The same procedure is followed for the second example (Fig. 7a): the chromatographic resolution in the first cluster of chromatogram B1 is very low (observed 0.32, estimated 0.23), however, due to the large difference in concentration, the spectrum of the first component is tentatively used in the spectral comparison. The resolution between the first and second components in the third cluster of chromatogram B2 is 0.48 (estimated real resolution 0.44) but, due to the fact that the concentration of the first component seems very low (observed fraction in the cluster 0.13, estimated true fraction 0.09), its spectral characteristics are not included in the library. The same holds true for the last component (impurity) in the cluster. The spectral characteristics of the central component are probably sufficiently accurate, but the component is regarded as tentative because of the overall uncertainty in the cluster. Although a fraction of 0.13 cannot be considered negligible, the ITT-FA does not perform well when used to analyse a cluster with widely varying concentrations<sup>13</sup>. The identity of the component(s) present in low concentration must be determined by other methods (step 5 in Fig. 3). Finally, the resolutions between the three components in the fourth cluster of chromatogram B3 are estimated to be 0.25 and 0.32. Despite an high spectral similarity, the spectral characteristics and relative areas cannot be relied upon, and are not included in the library. Apparently we are dealing with a nine- (perhaps ten) component mixture (Table III) which produces three spectral libraries: B1 and B2, both with seven reliable and one tentative spectrum and B3, with six reliable spectra. In chromatogram B1 the first cluster is unresolved (one spectrum was unreliable), in chromatogram B2 the third cluster is unresolved (two unreliable spectra) and in chromatogram B3 the fourth cluster must be examined in the next steps of the procedure (three unreliable spectra).

#### *The direct comparison of spectra*

The fourth step in the peak tracking procedure consists of a direct comparison of the spectra (both the reliable and tentative ones) derived from the chromatograms. When all components differ sufficiently in their spectral characteristics a close match between the spectra, expressed by a correlation coefficient, is adequate for identification purposes. However, when two or more components have very similar spectral characteristics, for instance in the case of homologues, an additional source of

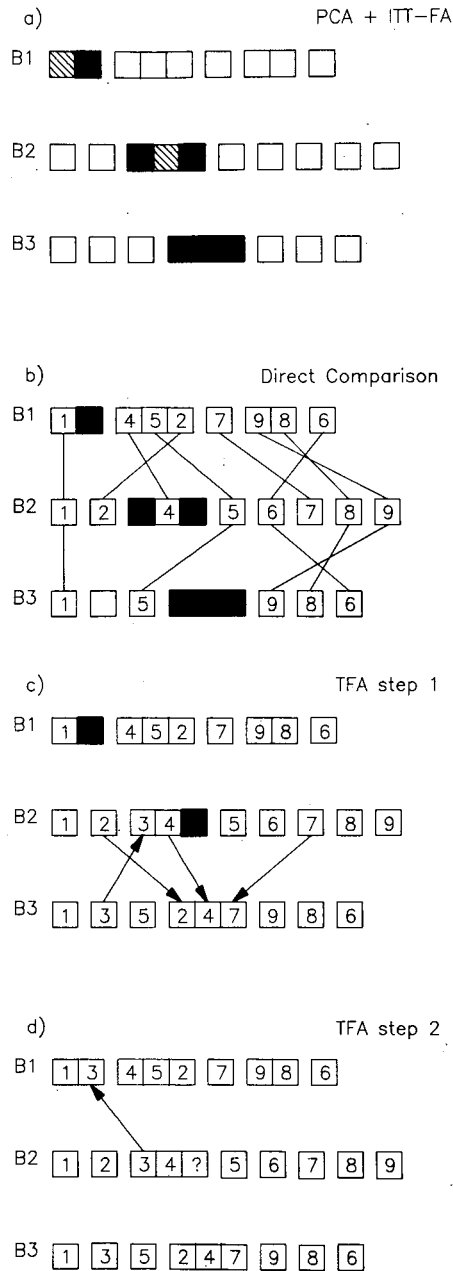


Fig. 7. The results of the four steps in the peak tracking procedure for the three chromatograms of the nine-component mixture, B1, B2 and B3. Numbers refer to Table I. The unknown component is indicated by "?". (a) The conclusions of the evaluation of the spectra. Spectra are defined as: reliable ( $\square$ ), tentative ( $\text{▨}$ ) or unreliable ( $\blacksquare$ ). (b) Components recognized by a direct comparison, indicated by a line connecting matched solutes. (c) Components recognized by means of TFA using spectral data from chromatograms B2 and B3. Arrows point from targets to clusters. (d) Component recognized by means of TFA using the updated spectral library of chromatogram B2.

information is required. This is supplied by the relative areas of the peaks. In the rare situation that two different components in the sample have identical spectra as well as equal areas, it will be impossible to distinguish between them and one has to work with two or more hypotheses to describe the retention behaviour of the mixture. As a first assumption, the hypothesis without cross-over of peaks seems the most reasonable one, since homologues will usually react in a similar fashion to changes in the specificity of the solvent. This assumption is equivalent to the assumption of limited variation in retention<sup>12</sup>.

During the comparison of the spectra (and areas) of two chromatograms, two additional libraries are produced containing those spectra which are not observed in the other chromatogram. Again this is decided on the basis of a critical value of the correlation coefficient, for instance  $\rho > 0.995$ , and an assumed variance in the relative area, for instance 10%. Due to the variable nature of the chromatographic process, the spectral comparison is used as a first selection criterion, and the relative area is used to check the validity of the identification. When a solute from a series of spectrally similar components is not yet included in a library, this will be detected by the comparison of relative areas as well (provided the solutes do not have both similar spectra and equal area). This is illustrated in Table IV: when comparing the spectrum of the second component of chromatogram B2 with the spectra in library B1, two spectra with high correlation are observed. By examining the relative areas of the two components and comparison with the relative area of component B2-2, component B1-5 is clearly matched with the component in question. Since this component is missing in library B3 due to close overlap with other components, only a considerable similarity with one of the other solutes is observed. This is detected by a large difference in the relative areas (13.8 vs. 7.9%), and consequently component B2-2 is not yet found in chromatogram B3, so that its spectral characteristics are retained for use in the next step of the procedure.

When processing more than two chromatograms, one starts by selecting the chromatogram with the maximum number of reliable spectra. Next, the contents of the

TABLE IV

ILLUSTRATION OF THE COMPARISON OF THE SPECTRA AND RELATIVE AREAS RESULTING FROM THE ANALYSIS OF CHROMATOGRAMS B1, B2 AND B3

$\rho$  is the correlation coefficient of spectrum B2-2 (library B2) with the spectra in libraries B1 and B3. When the correlation exceeds a value of 0.995, the relative areas are compared with the relative area of component B2-2 (13.8%). An unambiguous identification is indicated by an asterisk.

<i>Component library B1</i>	$\rho$	<i>Area (%)</i>	<i>Component library B3</i>	$\rho$	<i>Area (%)</i>
B1-1	0.83245		B3-1	0.82032	
B1-3	0.90942		B3-2	0.87021	
B1-4	0.90383		B3-3	0.90818	
B1-5	0.99976	13.9*	B3-7	0.92077	
B1-6	0.91285		B3-8	0.76801	
B1-7	0.91648		B3-9	0.99942	7.9
B1-8	0.76731				
B1-9	0.99983	7.9			



library related to this chromatogram are compared to all other libraries collected during the previous step in the procedure.

The results for both examples are presented in Figs. 6b and 7b. Example A is based on a comparison of spectral characteristics only, resulting in a recognition of five components. The tentative spectrum (corresponding with component 13) is not matched with any of the spectra in library A2. Consequently a library A1a containing the spectra of solutes 2–4, 10, 11 and 13 (tentative) of chromatogram A1 is created. At the same time a library A2a with solutes 12 and 13 of chromatogram A2 is constructed.

Example B is analysed in two steps. First the library derived from chromatogram B2 is compared with library B1. The tentative components are recognized since both spectra and areas are matched with solutes in B1 and consequently are now considered as “defined”. Since all components in library B2 are matched with the spectra in library B1, no spectra remain to be used in the next step of the analysis. The next comparison involves libraries B2 and B3. Five components are identified unambiguously, indicated by the lines and numbers in Fig. 7b. Despite high correlation between the spectra of components 2, 4 and 7 with the spectra in library B3, no direct match is observed because of large differences in the relative areas. As a consequence a new library, B2a, is developed containing the spectra of these compounds. Simultaneously, a library B3a is created containing the spectrum of the second component of library B3, since no direct match was observed between this spectrum and the spectra in library B2.

#### *Analysis of unresolved clusters*

The unresolved clusters remaining after the PCA and ITT-FA are analysed using the libraries created in the previous step in a TFA. Since the requirements with respect to the resolution are considerably reduced, clusters which cannot be analysed by means of the ITT-FA can be resolved, provided the spectra of the components are known.

The procedure continues as follows: for every unresolved cluster one determines which pure component spectra (“defined components”) are available from the cluster itself because of a reliable performance of the ITT-FA for the corresponding section of the cluster, for instance component 8 when analysing the fifth cluster in chromatogram A2. These components are required to determine the complete transformation matrix **T** and have often been identified in the previous step of the procedure. The spectra are added to the library containing the unidentified spectra from the other chromatogram and the TFA is performed. On the basis of the results of the projection (eqn. 4), the relevant spectra are selected from the library. The inverse transformation is applied to derive the corresponding elution profiles. However, before the profiles, and hence retention times (required for the optimization procedure!), can be determined, spectra of all components in the cluster should be available. When only minor components in a cluster are not yet identified, the retention times can be estimated by performing the TFA assuming a reduced dimensionality. In the case of severe spectral similarity within the mixture, the relative areas of the profiles can now be determined and used as an additional indication of the identity.

An example of this approach is given in Table V: the library A1a is used in a target test on the unresolved clusters of chromatogram A2, starting with the second cluster. First the library is extended by including the spectrum of component 5 as determined by means of ITT-FA in step 2 of the procedure. After projecting the spectra, the components 2–4 (and obviously component 5) are selected as solutes

TABLE V

RESULTS OF THE TFA WITH FIVE SPECTRA SELECTED FROM LIBRARY A1, STORED IN LIBRARY A1a, ON THE SECOND AND FOURTH CLUSTERS OF CHROMATOGRAM A2

The success of the test is expressed by means of the correlation coefficients,  $\rho_2$  and  $\rho_4$ , between the target spectra and their projections on the hyperplanes related to the clusters. The conclusion expresses the number of the cluster in which the components are situated in chromatogram A2.

<i>Target spectrum</i>	<i>Cluster A2-2</i> $\rho_2$	<i>Cluster A2-4</i> $\rho_4$	<i>Tested spectrum present in cluster</i>
A1-2	0.99623	0.42776	2
A1-3	0.99722	0.55250	2
A1-4	0.99962	0.70628	2
A1-10	0.83222	0.99818	4
A1-11	0.92815	0.99974	4

present in cluster 2 on the basis of the high correlation between the target spectra and their projections. Since all major components have been identified in this cluster, the inverse transformation is performed and the cluster is fully resolved. Similarly, the components 10 and 11 (in combination with component 8) are identified in cluster 5 and used to determine the individual profiles. In this way, all unresolved clusters are analysed and the locations of the missing components are determined.

When more than two chromatograms are involved, the procedure is repeated a number of times: when a new component has been identified on the basis of TFA, its spectrum is removed from the library used in the TFA and added to the library corresponding with the chromatogram in which the compound has been identified. This adjusted library is then used in a direct comparison with the other chromatograms involving only those components not yet recognized in a previous step. New components not identified in a chromatogram by a direct comparison are added to the library used in the TFA of unresolved clusters in that chromatogram, etc. These steps are repeated until all components are identified or the contents of the libraries remain constant. This is summarized in Fig. 8.

The results for example A are illustrated in Fig. 6c. By a combination of the spectral data in both chromatograms all components in chromatogram A2 are identified, and only one impurity in chromatogram A1 remains unrecognized. Example B requires two steps, illustrated in Fig. 7c and d: first the unresolved cluster in chromatogram B3 is analysed with the reliable, but as yet unidentified spectra from chromatogram B2. The three components (2,4,7) contained in library B2a are all located in the fourth cluster of chromatogram B2. Since it was the only remaining cluster, this result was expected, but the principle can be applied when more unresolved clusters are present in the chromatogram (example A); *visé versa*, the only remaining unidentified spectrum from B3 is found in the unresolved cluster of chromatogram B2 (correlation 0.99924). We are left with chromatogram B1. In the preceding step all of the known reliable spectra from B2 were matched. From B3 we have found a new, ninth component (3). Not surprisingly, in a TFA this component is found to be located in the unresolved cluster of chromatogram B1 (Fig. 7d). Since an high correlation is observed, nine components are now recognized in all three chromatograms, and only

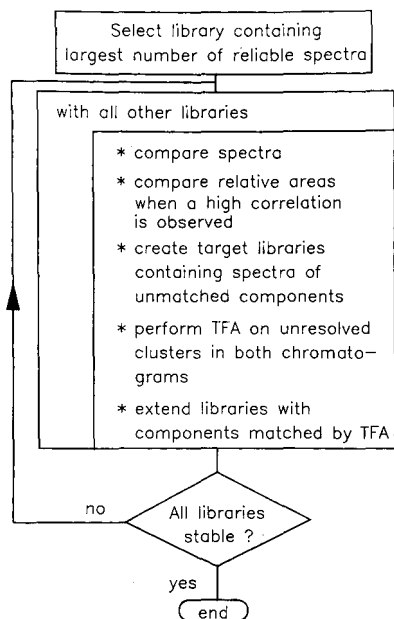


Fig. 8. The comparison and combination of spectral data derived from the separate chromatograms.

the impurity observed in the third cluster of the second chromatogram remains unidentified.

The conclusions with respect to the peak tracking in the two examples are summarized in Figs. 9 and 10. Tables with retention times corresponding to the individual solutes are now available for use in an interpretive optimization strategy<sup>6</sup>.

### Limitations

The procedure described in this section has a number of limitations. First and foremost it is assumed that the spectral characteristics of the components do not change too much with varying experimental circumstances. It is clear that none of the methods described in the introduction can be applied if the absorption characteristics of the components change, for instance because of dissociation or association with varying pH. If reversed-phase chromatography is restricted to a change in organic modifier such as methanol, tetrahydrofuran and acetonitrile, such strong conformational changes do not occur. Although shifts and other changes in the spectra have been reported<sup>10,12</sup>, the shape of the spectra remains fairly constant throughout, and an unambiguous identification is usually possible, although slight distortions are observed in the profiles derived by means of TFA. However, when other modes of liquid chromatography are involved (for instance ion-pairing chromatography) these assumptions no longer hold and peak tracking is limited to those components which have stable spectral characteristics. Increased uncertainty will result in the case of coelution of components with unstable spectra.

Also in the case where the spectra of the components do not change too much, a number of limitations exists. When a particular component is coeluted closely with

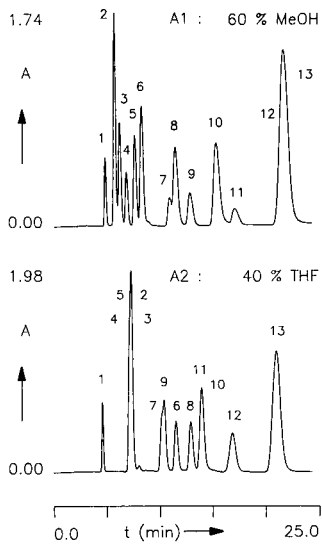


Fig. 9. The results of the peak tracking procedure for the two chromatograms of the thirteen-component mixture. Numbers refer to Table I. MeOH = methanol.

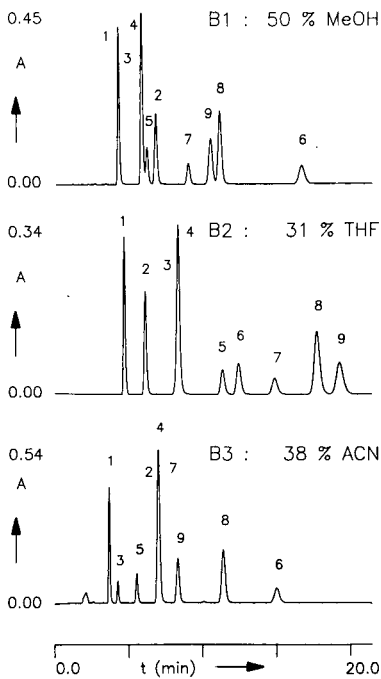


Fig. 10. The results of the peak tracking procedure for the three chromatograms of the nine-component mixture. Numbers refer to Table I. MeOH is methanol.

other components in all available chromatograms, no reliable spectrum is obtained for tracking that component. Here two situations may be observed: if the same components are coeluted together in all chromatograms, the changes of finding a suitable optimum are limited. On the other hand, a given component may be closely coeluted with different components in subsequent chromatograms. For example, between chromatograms B1 and B2 only, it would have been impossible to find the spectral characteristics, and hence the exact retention times, of component 3. Now, as long as only one component remains unknown, its uniqueness automatically allows approximate tracking. When two or more components are involved, only a limited peak tracking might be possible, resulting in several alternatives with respect to the retention behaviour of a number of components. Often it will be possible to choose one of the alternatives on the basis of subsequent chromatograms. Otherwise an increase in peak capacity (decrease in elution strength) will often result in the additional resolution required for reliable spectral data.

#### CONCLUSIONS

The procedure described is capable of unambiguous peak tracking in chromatograms of unknown mixtures based on a multivariate handling of spectral data resulting from multiwavelength detection. The number of analytically significant components is best estimated on the basis of the results of the ITT-FA, combined with an examination of the responses involved (UV activity).

The combination of TFA and ITT-FA eliminates the limitations of each method separately: unknown spectra of moderately coeluting components are determined by means of the ITT-FA. Clusters with too little resolution for the ITT-FA are resolved by means of TFA, using spectra derived from other chromatograms.

When components with very similar spectra are present in a mixture, additional information such as the relative areas of the peaks must be used in order to perform an unambiguous identification. Clearly, by limiting the comparison to the areas of spectrally similar components, the number of possible matches is greatly reduced, and hence the accuracy of the analysis is increased.

The major assumption is that the spectral characteristics of the components do not change much with varying experimental conditions. However, the probability of erroneous identifications is limited and the procedure issues a warning when not all components have been tracked in all chromatograms. The influence of the remaining components on the quality of the separation can be determined on the basis of a measure of concentration. Especially if procedures are to be implemented in automated systems, this last point is of great importance: a procedure should be able to indicate success or failure, rather than issue an answer at any cost.

#### REFERENCES

- 1 P. J. Schoenmakers, *Optimization of Chromatographic Selectivity (Journal of Chromatography Library, Vol. 35)*, Elsevier, Amsterdam, 1986.
- 2 J. C. Berridge, *Techniques for the Automated Optimization of HPLC Separations*, Wiley, Chichester, 1986.
- 3 J. L. Glajch, J. J. Kirkland and J. M. Minor, *J. Liq. Chromatogr.*, 10 (1987) 1727.
- 4 L. R. Snyder and M. A. Quarry, *J. Liq. Chromatogr.*, 10 (1987) 1789.

- 5 S. N. Deming, J. G. Bower and K. D. Bower, *Adv. Chromatogr. (N.Y.)*, 24 (1984) 35.
- 6 A. Bartha, H. A. H. Billiet and L. de Galan, *J. Chromatogr.*, 458 (1988) 371.
- 7 A. C. J. H. Drouen, H. A. H. Billiet, P. J. Schoenmakers and L. de Galan, *Chromatographia*, 16 (1982) 48.
- 8 H. J. Issaq and K. McNitt, *J. Liq. Chromatogr.*, 5 (1982) 1771.
- 9 M. Otto, W. Wegscheider and E. P. Lankmayr, *Anal. Chem.*, 60 (1988) 517.
- 10 A. C. J. H. Drouen, H. A. H. Billiet and L. de Galan, *Anal. Chem.*, 56 (1984) 971.
- 11 A. C. J. H. Drouen, H. A. H. Billiet and L. de Galan, *Anal. Chem.*, 57 (1985) 962.
- 12 J. K. Strasters, H. A. H. Billiet, L. de Galan, B. G. M. Vandeginste and G. Kateman, *J. Chromatogr.*, 385 (1987) 530.
- 13 J. K. Strasters, H. A. H. Billiet, L. de Galan, B. G. M. Vandeginste and G. Kateman, *Anal. Chem.*, 60 (1988) 2745.
- 14 G. G. R. Seaton and A. F. Fell, *Chromatographia*, 24 (1987) 208.
- 15 E. R. Malinowski and D. G. Howery, *Factor Analysis in Chemistry*, Wiley, New York, 1980.
- 16 B. G. M. Vandeginste, W. Derks and G. Kateman, *Anal. Chim. Acta*, 173 (1985) 253.
- 17 M. McCue and E. R. Malinowski, *Appl. Spectrosc.*, 37 (1983) 463.
- 18 W. H. Lawton and E. A. Sylvestre, *Technometrics*, 13 (1971) 617.
- 19 M. Maeder and A. Zilian, *Chemometr. Intell. Lab. Syst.*, 3 (1988) 205.
- 20 E. R. Malinowski, *Anal. Chem.*, 49 (1977) 612.
- 21 H. T. Eastment and W. J. Krzanowsky, *Technometrics*, 24 (1982) 73.
- 22 E. R. Malinowski, *J. Chemometrics*, 3 (1988) 49.
- 23 J. C. Reid and E. C. Wong, *Appl. Spectrosc.* 20 (1966) 220.
- 24 Y. Beppu and I. Ninomiya, *Computers Chem.*, 6 (1982) 87.
- 25 P. R. Bevington, *Data Reduction and Error Analysis for the Physical Sciences*, McGraw-Hill, New York, 1989, Ch. 11.
- 26 J. K. Strasters, H. A. H. Billiet, L. de Galan, B. G. M. Vandeginste and G. Kateman, *Abstracts 12th International Symposium on Column Liquid Chromatography, Washington, 1988*, Tu-L-13.

CHROM. 21 635

## PEAK TRACKING AND SUBSEQUENT CHOICE OF OPTIMIZATION PARAMETERS FOR THE SEPARATION OF A MIXTURE OF LOCAL ANAESTHETICS BY HIGH-PERFORMANCE LIQUID CHROMATOGRAPHY

JOOST K. STRASTERS, FRANK COOLSAET, AKOS BARTHA, HUGO A. H. BILLIET\* and LEO DE GALAN

*Delft University of Technology, Department of Analytical Chemistry, De Vries van Heystplantsoen 2, 2628 RZ Delft (The Netherlands)*

---

### SUMMARY

A peak tracking strategy based on multivariate analysis of multiwavelength spectral data was applied to four chromatograms of a mixture of eight local anaesthetics and extended to cope with coelution of components having identical spectral characteristics. The resulting characterization of the retention behaviour of the individual components was used to select a suitable parameter space for the subsequent improvement of the observed separation.

---

### INTRODUCTION

During recent years a number of strategies for a systematic optimization of the mobile phase composition for high-performance liquid chromatographic (HPLC) separations has been developed<sup>1,2</sup>. Especially reversed-phase HPLC has been extensively studied, resulting in a number of so-called interpretive optimization methods, which base the prediction of the location of the optimum on a model of the retention behaviour of the individual components in a mixture<sup>3,4</sup>. By a suitable concentration of organic modifier, determined by means of a gradient scan, the retention range is fixed. By using isoelutropic mixtures of different types of organic modifiers [methanol, acetonitrile or tetrahydrofuran (THF)] the specificity of the mobile phase is varied, hopefully resulting in the desired separation of all components. Depending on the number of modifiers in the mixture, a one- or two-parameter optimization is performed: with a mixture of two isoelutropic solvents, the mixing ratio is the only parameter. When three solvents are involved two mixing ratios are varied and accordingly a two-parameter optimization is performed.

The above procedure is mainly restricted to mixtures containing uncharged solutes. When one is dealing with more complex samples, with both charged and uncharged species, different mobile phase additives, such as ion-pairing reagents, are required to ensure sufficient retention<sup>5,6</sup>. Consequently the number of parameters involved increases dramatically: apart from the type and concentration of organic modifier, the type and concentration of ion-pairing reagent and the pH will influence

both the overall retention and the specificity of the separation. However, current strategies become extremely time consuming when a large number of parameters is involved. Furthermore, a large number of initial experiments will be required to gauge the influence of the parameters on the retention of the individual solutes in sufficient detail and to construct a response surface describing the quality of the separation for different values of the parameters. Consequently, the optimization is usually restricted to a smaller number of parameters, one of which is the ion-pair concentration<sup>5</sup>. This selection of parameters is done on the basis of experience.

Apart from practical considerations in the restriction of the parameter space with respect to the number of experiments and the limitations of the software, this restriction is often fundamentally correct, since large areas in the extended parameter space will never produce a suitable separation and will play no rôle of importance in the actual optimization. Recent studies by Low *et al.*<sup>6,7</sup> were directed at an efficient selection of parameters and determination of a suitable range of values based on a limited number of preliminary experiments. An important aspect is the characterization of the mixture: the type of components determine which parameters will influence the retention behaviour. For instance, when a (strong) acid is fully dissociated at low pH, inclusion of the pH as a parameter will be useless to influence the retention of this component and will only increase the number of experiments.

With this in mind, the following distinctions can be made between different types of solutes<sup>6</sup>: neutral solutes (N), not ionized within the specified pH range; strong acids and bases (SA/SB), fully ionized within the specified pH range; weak acids and bases (WA/WB) which change their ionic state in the specified pH range. Once all components in a mixture have been characterized according to this specification, a suitable selection of parameters for the optimization will be possible: the retention of neutral solutes is influenced solely by the type and concentration of the organic modifier(s). Weak acids and bases are sensitive to changes in the pH of the mobile phase. All charged solutes are influenced by the concentration of ion-pairing reagent. Acids are retained by a positively charged reagent such as quaternary ammonium salts, and bases by negatively charged ones, for instance sodium octanesulphonate. It is often possible to perform this characterization on the basis of a limited number of experiments, as will be demonstrated in the following discussion.

A separate problem, both in the interpretive optimization strategies and in the characterization of unknown mixtures, is peak recognition: in order to describe the influence of a change in the values of the parameters on the retention of the individual solutes, one must be able to identify the peaks between the chromatograms. Since one is not immediately interested in an identification of the solutes, but in which peaks in two chromatograms of the same mixture correspond to the same solute, this process is referred to as peak tracking. A number of methods are available to perform peak tracking based on relative areas<sup>8,9</sup> or wavelength ratios<sup>10</sup>. Introduction of linear photodiode array detection (LPDA) increased the potential of tracking considerably, since full spectra can now be compared<sup>11</sup>.

Recently, we described a strategy for further automation of the tracking procedure based on a multivariate analysis of spectral data, collected by means of LPDA<sup>12</sup>. In order to compare the spectral characteristics of overlapping components in peak clusters, these characteristics must be extracted from a set of mixture spectra. In peak clusters with more than two more or less closely coeluting solutes, pure



component spectra are not observed directly and must be determined in some other way. By means of a multicomponent analysis or target factor analysis (TFA) deconvolution of peak groups is possible, but these techniques require library spectra<sup>13</sup>. Other techniques referred to as "self-modelling curve resolution", such as the iterative target transformation factor analysis (ITT-FA)<sup>14</sup>, require no spectral information from other sources, but are more sensitive to the amount of chromatographic resolution<sup>15</sup>. We have demonstrated<sup>12</sup> for two examples of typical complexity that the combination of ITT-FA and TFA assisted by peak areas allowed unambiguous identification of nine and thirteen components, respectively. In both examples all solutes were uncharged.

Of course, additional problems arise when two or more components have similar spectra. When these components are fully separated, additional information on peak areas can be used to track the peaks. However, if these components are present in the same cluster a correct analysis is no longer possible, as will be discussed in the following sections. More seriously, all methods indicated above assume that the spectral characteristics of the components do not change too much with varying experimental conditions. This is generally true for uncharged solutes, but is not necessarily the case for solutes with different states of dissociation in various mobile phases. However, peak tracking in chromatograms of mixtures containing ionized solutes is not *a priori* a waste of time, since some conclusions with respect to the uncharged or fully ionized solutes can always be drawn.

In order further to test the potential of the tracking procedure in other applications, this paper focusses on a mixture of eight local anaesthetics. With a minimum of knowledge regarding this mixture, *i.e.*, a reasonable retention in 50% methanol and the presence of basic solutes, we will try fully to characterize the mixture by means of peak tracking in order to select a suitable parameter space where improvement of the separation can be expected.

#### THEORETICAL

In order to describe some of the phenomena observed during the analysis of the mixture, a short description is provided here of the mathematical background. For further details the reader is referred to refs. 12–16.

Every mixture spectrum observed during the elution of a peak cluster can be described as a sum of the contributions of the individual pure component spectra, weighted by means of a concentration factor. When a component does not contribute to a spectrum, its concentration is equal to zero. When this decomposition is performed for every mixture spectrum of the cluster, the set of spectral data can be expressed by means of a matrix

$$\mathbf{D} = \mathbf{S} \mathbf{E}^T \quad (1)$$

where the mixture spectra are the columns of the data matrix  $\mathbf{D}$  (dimensions  $n_w$  wavelengths  $\times$   $n_s$  spectra). When  $n_c$  components are present, this decomposition results in a matrix  $\mathbf{S}$  (dimensions  $n_w \times n_c$ ) containing the pure component spectra and a matrix  $\mathbf{E}$  (dimensions  $n_s \times n_c$ ) with the contributions, *i.e.*, the elution profiles.

Without knowledge of the pure component spectra, an alternative decomposition is possible, based on a principal component analysis (PCA)<sup>16</sup>:

$$\mathbf{D} = \mathbf{R} \mathbf{V}^T \quad (2)$$

The matrix  $\mathbf{V}$  (dimensions  $n_s \times n_s$ ) contains the eigenvectors of the covariance matrix of  $\mathbf{D}$  and can be thought of as an abstract description of the elution profiles: every elution profile in the mixture can be described as a linear combination of the columns of  $\mathbf{V}$ . The same holds for matrix  $\mathbf{R}$  (dimensions  $n_w \times n_s$ ) which can be used to reconstruct the pure component spectra. Since the columns of  $\mathbf{V}$  and  $\mathbf{R}$  are ordered according to the amount of variance they describe in the original data, only the first  $n_c$  columns are required to reconstruct the original data within the experimental error. The other columns describe the experimental noise. The reduced matrices,  $\mathbf{R}'$  (dimensions  $n_w \times n_c$ ) and  $\mathbf{V}'$  (dimensions  $n_s \times n_c$ ), can be transformed into their physical counterparts,  $\mathbf{S}$  and  $\mathbf{E}$ , by means of a suitable transformation,  $\mathbf{T}$  (dimensions  $n_c \times n_c$ ), resp.  $\mathbf{T}^{-1}$ :

$$\mathbf{D}' = \mathbf{R}' \mathbf{V}'^T \quad (3a)$$

$$= \mathbf{R}' \mathbf{T} \mathbf{T}^{-1} \mathbf{V}'^T \quad (3b)$$

$$= \mathbf{S} \mathbf{E}^T \quad (3c)$$

Different techniques to determine  $\mathbf{T}$  are available and described by the general term factor analysis. The target factor analysis (TFA) first determines the separate factors which are thought to contribute to the overall variance in the data by projecting an assumed factor, for instance a spectrum, on the relevant hyperspace, in this case  $\mathbf{R}'$ . When the target and projection coincide, the factor is accepted and the transformation required for the projection is used as an element of  $\mathbf{T}$ . Once all factors (components) have been identified, the inverse transformation is calculated and the elution profiles are derived.

The ITT-FA<sup>14</sup> does not require pure component spectra or profiles to test as factors, but searches for solutions which conform to two boundary conditions, *i.e.*, non-negativity of the concentrations and unimodality of the derived profiles. Once all profiles have been determined, the inverse transformation is used to calculate the spectra.

One way to check whether the correct dimensionality, *i.e.*, the correct value of  $n_c$ , has been applied in the analysis, is to compare the reconstructed data matrix,  $\mathbf{D}'$ , with the original data matrix,  $\mathbf{D}$ . The difference, expressed in the form of a sum of squares, was defined by Malinowski and Howery<sup>16</sup> as the extracted error,  $\mathbf{XE}$ :

$$\mathbf{XE}^2 = \sum_{i=1}^{n_w} \sum_{j=1}^{n_s} (d_{ij} - d'_{ij})^2 / n_w n_s \quad (4)$$

When the analysis is performed with different values of  $n_c$ , that value is accepted as correct which yields the smallest extracted error.

## EXPERIMENTAL

*Mixture and chromatographic conditions*

The composition of the mixture was selected on the basis of separation problems described in the literature<sup>17,18</sup>. The molecular formulas of the eight components are given in Fig. 1. Reference to the components is made by the numbers in this figure. The concentration of all components was 1 mg/ml, except for bupivacaine (0.5 mg/ml). An examination of the spectral similarities in a solvent of methanol–15 mM triethylamine (TEA) (50:50), pH 7 (Fig. 2), expressed by means of a correlation coefficient<sup>19</sup>, indicated an extreme similarity between components 2 and 5 and between components 3, 4 and 7 (Table I). Comparison of the structures of the components (Fig. 2) endorses these conclusions, since the chromophoric groups (aromatic structures) are identical for the components specified.

The mixture was eluted on a Novapak C<sub>18</sub> column, particle size 5 μm, 7.5 cm × 3.9 mm I.D. (Millipore Waters, Milford, MA, U.S.A.) using a mobile phase of methanol–15 mM TEA (50:50). The flow-rate was set at 1 ml/min. The pH of the buffer was fixed at 3 and 7. At each pH value two experiments were performed, one without the ion-pairing reagent, the other with 5 mM sodium octanesulphonate added to the mobile phase. The four chromatograms resulting from these preliminary experiments are shown in Fig. 3; only the one at pH 7 with the ion-pairing reagent reveals eight significantly, but widely differently, resolved peaks.

*Instrumentation*

The chromatographic system consisted of an HP 1090 chromatograph, equipped with an HP 1040A linear photodiode array detector (Hewlett-Packard, Waldbronn, F.R.G.). The detector was connected to an HP-85 desktop computer, equipped with an HP-IB IEEE-488 interface and RS-232C serial interface. The data were temporarily stored on 5 $\frac{1}{2}$ -in. flexible disks using an HP82910M disk-drive.

The data files collected by means of the detector were transferred to an Olivetti M24 personal computer (Olivetti, Ivrea, Italy) by means of serial interfaces on both

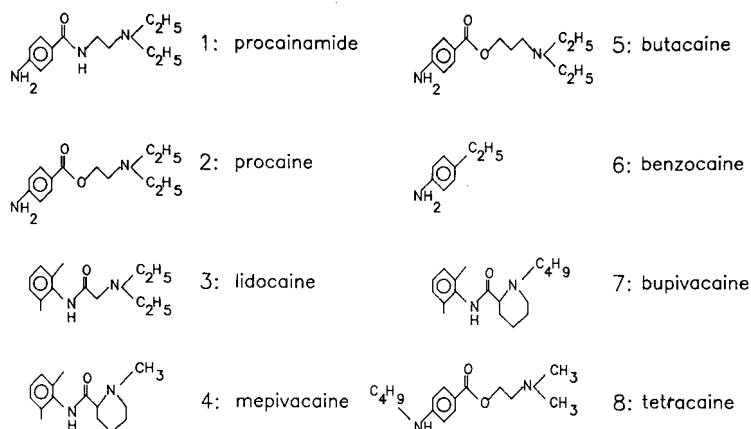


Fig. 1. The molecular structures of the eight local anaesthetics in the mixture.



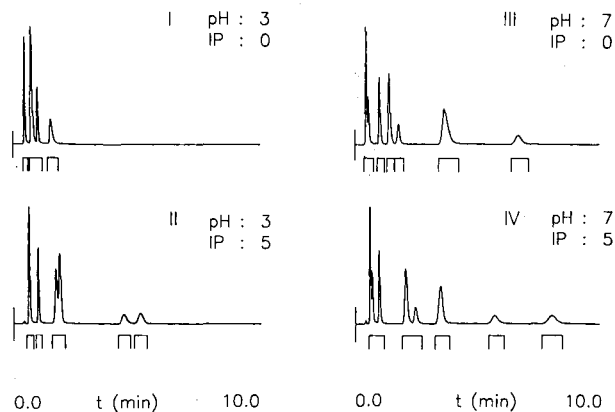


Fig. 3. The four preliminary chromatograms of the mixture at 210 nm, recorded in 50% methanol at pH 3 and 7, without and with 5.0 mM sodium octanesulphonate (IP). Further experimental details in the text. The clusters selected for further analysis according to the peak tracking procedure are indicated by brackets.

to Reid and Wong<sup>19</sup>. The eigenvectors and eigenvalues of the covariance matrix of the data matrix were determined by the HQR II algorithm<sup>20</sup>.

Curve fitting, performed to estimate resolutions and concentrations, was performed on the basis of bigaussian profiles and a non-linear procedure described by Bevington<sup>21</sup>. This procedure was preferred to a direct calculation of the peak width and areas based on the calculated profiles, because of the limited sampling frequency over the chromatographic peaks, and the inherent uncertainty in the derived results.

## RESULTS AND DISCUSSION

The following discussion is split into two parts. The first section will concentrate on the peak tracking in the four chromatograms of Fig. 3, referred to as I–IV. Consequently, we will assume that no further prior knowledge of the mixture is available apart from the assumptions mentioned in the Introduction. In the second part, the results of the peak tracking will be used to select the appropriate parameters to improve the separation.

### Peak tracking

The results of the peak tracking strategy are summarized in Fig. 4. The strategy consists of a number of steps, performed sequentially and aimed at a combination of the results derived for the individual chromatograms. The first step is the selection of clusters on the basis of an absorbance threshold. The clusters selected are indicated in Fig. 3. The next step consists of a separate analysis of all peak clusters by means of a PCA, followed by the ITT-FA. The results of the ITT-FA, estimates of the individual elution profiles and pure component spectra, are corrected for negative concentrations and absorbances and used to calculate a reconstructed data matrix,  $\mathbf{D}'$  (eqn. 3c). The difference between the reconstructed data matrix and the original one is a measure of the success of the analysis. By repeating the ITT-FA a number of times with different dimensionalities, *i.e.*, assuming a different number of components, and selecting the

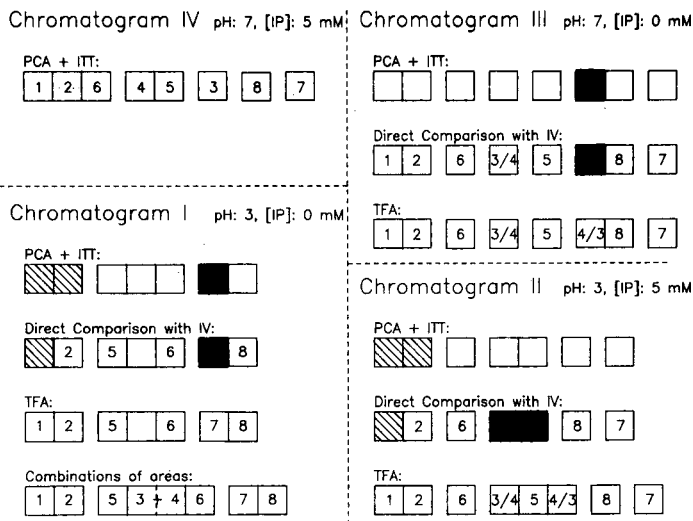


Fig. 4. A schematic representation of the results of the peak tracking procedure. Components in clusters are categorized with respect to the quality of the corresponding spectral and quantitative data as reliable ( $\square$ ), tentative ( $\square$  with diagonal lines) or unreliable ( $\blacksquare$ ). The component numbers refer to the components in Fig. 1. Chromatograms are indicated by Roman numbers corresponding to Fig. 3. Chromatogram IV is the reference to which the other three are correlated as discussed in the text.

best result indicated by the extracted error (eqn. 4), the number of components in the cluster best described by unimodal profiles and physically realistic spectra is selected. On the basis of a 1% concentration threshold, possible impurities, described by an additional unimodal profile in negligible quantity, are rejected. The conclusions of this step, the number of components,  $N_C$ , in each cluster, are summarized in the third column of Table II.

The first observation is that more components are found in chromatograms III and IV than in chromatograms I and II, *e.g.*, eight and seven respectively. However, all concentrations exceeded the threshold value of 1%, so that none can be considered as an impurity. There are two possible explanations to account for this observation: two components are eluted at exactly the same time, *i.e.*, the observed mixture spectra all contain the same ratio of pure component spectra and consequently one of the degrees of variation is removed from the observed data. Only one profile and one corresponding mixture spectrum is formed which will not be found in any of the other chromatograms (if this coelution occurs in every chromatogram the problem passes undetected since the analysis will simply be performed with one component less than those thought to be present in the mixture). However, the chances of a coelution as extreme as this (resolution below approximately 0.01) are remote and will probably only be observed early in the chromatogram close to the dead-volume.

A second explanation, which will occur more frequently, is the coelution of two components with an high spectral similarity ( $p > 0.999$ ). Even when two separate peak maxima may be observed, the variation in the spectral data will still be reduced, and the number of components derived for the cluster will be one less than the true number of components. Two examples will be discussed later.

TABLE II

## THE CONCLUSIONS OF THE FIRST AND SECOND STEPS OF THE PEAK TRACKING PROCEDURE

For every cluster in each chromatogram (identification according to Fig. 3), the number of relevant components,  $N_C$ , as determined after PCA, ITT-FA and evaluation of concentrations is listed. In addition the minimum observed extracted error,  $XE_{min}$ , is displayed. The final column presents the number of reliable or tentative spectra in every cluster,  $N_S$ , based on an evaluation of resolution and spectral similarity (*cf.*, Fig. 4).

Chromatogram	Cluster	$N_C$	$XE_{min}$	$N_S$
I	1	2	1.41	2
	2	3	1.64	3
	3	2	0.12	1
	Total	7		6
II	1	2	0.24	2
	2	1	0.05	1
	3	2	3.73	2
	4	1	0.02	1
	5	1	0.01	1
Total	7		7	
III	1	2	0.54	2
	2	1	0.02	1
	3	1	0.02	1
	4	1	0.02	1
	5	2	0.02	1
Total	8		7	
IV	1	3	1.05	3
	2	2	0.01	2
	3	1	0.01	1
	4	1	0.01	1
	5	1	0.01	1
Total	8		8	

In order to perform the actual peak tracking by a comparison of pure component spectra, the next step consists of a judgement of the reliability of the spectra resulting from the ITT-FA. Due to the fact that errors are introduced in the reconstruction of the profiles when the resolution becomes too low (below approximately  $R = 0.4$  for components present in equal concentration, *i.e.*, equal UV activity), not all calculated spectra are sufficiently free from errors to be used directly. Since the extent of the observed distortion also depends on the spectral similarity of the components and on their concentrations, a further analysis of these quantities is required to select the appropriate spectra. Such an analysis has been presented previously using two-component clusters<sup>15</sup> where the observed resolution, the observed spectral similarity and the apparent concentrations were used to judge the reliability of the derived spectra. The expected similarity between the derived spectra and the true spectra is estimated and expressed by means of a correlation coefficient. However, the demand

that this quality index exceeds for instance 0.995 does not guarantee that the calculated concentrations are accurate. Consequently, three types of components are distinguished after the ITT-FA: reliable components, accurately described with respect to both the spectral characteristics and concentration; tentative components, of which the spectra are sufficiently accurate, but the derived concentration is suspect; and unreliable components, which are present in too low a concentration or coelute too closely with other components to rely on the corresponding calculated spectra. Unreliable spectra can be determined only in a second step involving the TFA where the demands on the resolution for a successful analysis are greatly reduced (the amount of information provided during the analysis is increased since spectra derived from the other chromatograms are used as targets). Tentative components are accepted as such but are candidates for further improvement by means of TFA.

The results of the classification are indicated in Fig. 4 by means of open (reliable), shaded (tentative) or dark (unreliable) blocks. The resolution of the first cluster in chromatograms I and II is fairly low (estimated 0.36) but the spectra are tentatively accepted because of the high spectral similarity of the components, and hence the reduced influence of the error introduced by the distortions in the calculated profiles. The resolutions, in the third cluster of chromatogram I and in the fifth cluster of chromatogram III are definitely too low to rely on the spectrum of the fronting component due to the low relative concentration in comparison with the tailing component.

The resolution in chromatogram IV is sufficient to derive reliable spectra of all components, and thus enables us to decide that we are indeed dealing with an eight-component mixture (Fig. 4). Indeed, a comparison of the spectra, as illustrated in Table I and Fig. 2, gives an indication of the spectral complexity of the mixture. Since three components do have extremely similar spectra, the reduced dimensionality of chromatograms I and II is probably caused by coelution of two of these components in one cluster.

Since chromatogram IV produces the largest number of components and the largest number of reliable spectra (Table II), the resulting library of eight spectra is used as a basis for a direct comparison of pure component spectra and in the TFA performed on unresolved clusters in the other chromatograms. The components can therefore be numbered as indicated in Fig. 4. Although we proceed on the assumption that we are dealing with an unknown mixture, for the convenience of the reader and to facilitate the discussion we use the same numbering as in Fig. 1.

The comparison between the chromatograms III and IV is straightforward. A direct comparison of spectra and concentrations identifies all components, except 3 and 4. Due to the fact that both components have equal spectral characteristics and similar concentrations, an unambiguous identification is not possible. Component 7, though also spectrally identical to 3 and 4, is identified since its concentration is different. Consequently, cluster 3 of chromatogram III contains either component 3 or 4. Since the other is not detected by a direct comparison of spectra, it must be situated in cluster 5 (dark block). This is verified by means of the TFA. A definite choice of the location of components 3 and 4 is discussed in the next section.

The comparison between chromatograms I and IV is more difficult, because of the lower resolution in chromatogram I. A direct comparison of spectra and concentrations tracks the components 2, 5, 6 and 8. Although there is a high



correlation between component 1 and the first component in the first cluster of chromatogram I, no positive identification is possible because the concentrations are too dissimilar. The same is true for components 3, 4 and 7 that correlate highly with the central solute in the second cluster of chromatogram I. The decision on the location of component 1 can be made on the basis of its spectral uniqueness (Table I), although the procedure implies a verification by means of TFA. In the case of components 3, 4 and 7 there is the additional problem of extreme spectral similarity that makes it impossible to determine which of the three components matches. This spectral similarity also complicates the application of TFA: when virtually identical spectra are used as targets they cannot be distinguished. To put it differently: components with identical spectra will not produce meaningful elution profiles. In technical terms, such targets produce closely similar transformations of the columns of  $\mathbf{R}'$  (eqn. 3b). Consequently, in the inverse transformation resulting after a selection of all matching components, the determinant of  $\mathbf{T}$  is very small (an ill conditioned matrix), resulting in large errors in the calculated profiles.

Hence, a library is constructed containing only the spectral characteristics of components 1 and 3, with the latter being representative of solutes 4 and 7 as well. This library is extended with component 2 (already identified but required for the determination of the correct inverse transformation) and used in the TFA performed in cluster 1. Component 1 is now identified unambiguously and is situated in this cluster. The same procedure is followed for cluster 2, after extension of the library with components 5 and 6, and on cluster 3 after extension of the library with the spectrum of component 8. In both cases an high correlation between the spectrum of component 3 and the projections on the spectral description of the clusters (matrix  $\mathbf{R}'$ ) is observed, indicating that all three components, 3, 4 and 7, are located in clusters 2 and 3. The concentration of the peak in cluster 3 corresponds with the concentration of component 7, which leaves components 3 and 4 to be situated in cluster 2. When the concentrations of 3 and 4 are summed, the result equals the concentration of the combined profile derived by means of both the ITT-FA and TFA. Since the two components are poorly resolved, the combined profile can be described by a unimodal profile, as illustrated in Fig. 5, and both the profile and the derived spectra correspond

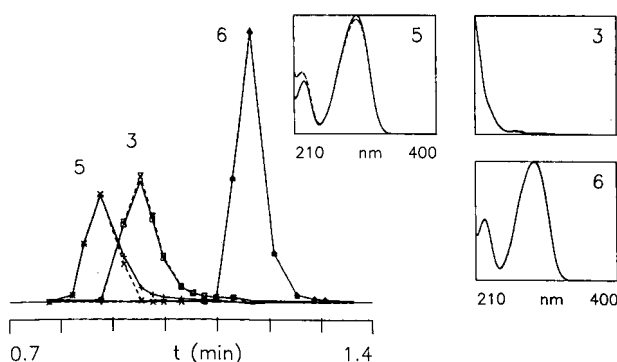


Fig. 5. The results of the ITT-FA performed on cluster 2 of chromatogram I (Fig. 3), indicated by the dashed line, as compared to the results of the TFA (solid line) performed with the pure component spectra of components 3, 5 and 6. The left side of the figure displays the elution profiles, the right side shows the spectra derived by means of ITT-FA (dashed line) compared with the true pure component spectra (solid line).

with the ones derived by means of the TFA. The minor distortion in the spectrum of component 5 derived by means of the ITT-FA is caused by the incorrect reconstruction of the tail of the profile and is not sufficient to hinder a correct identification. In this case the result of the ITT-FA together with a combination of areas can be applied to track all components in the second cluster. The exact identification of components 3 and 4 is not relevant since they have approximately the same retention time.

Similar problems are encountered with the comparison of the spectral data of chromatograms II and IV. The tracking of components 2, 6, 7 and 8 is unambiguous. Component 1 is identified in the same way as above using a library consisting of spectra from components 1, 2 (already identified), 3 and 5. We are left with components 3–5 which must all reside in the third cluster of chromatogram II. It might be surprising that component 5 is not found in this cluster from ITT-FA, despite its reasonable resolution from the fronting component (estimated resolution 0.86). An explanation is found after cluster 3 has been analysed by means of a TFA using the spectra of components 3 and 5, illustrated in Fig. 6. The TFA correctly reconstructs a combined profile of components 3 and 4, containing two distinctive maxima. It should be remembered, however, that ITT-FA assumes an unimodal profile, and thus results in the incorrect profile indicated by the dashed line coinciding with the first peak maximum of the bimodal profile. Through the inverse transformation, this error is introduced in the spectrum derived from the second component, which thus deviates strongly from the spectrum of component 5 (see Fig. 6, dashed *versus* solid line in the spectrum of solute 5). Consequently this distorted spectrum is not observed in the other chromatograms and should not be included in libraries used for peak tracking. By contrast, the results of the TFA can be used to estimate the concentration of the individual profiles, for instance by means of a perpendicular division of the profile, yielding the identification displayed in Fig. 4, with again the exact location of components 3 and 4 uncertain.

The detection of the occurrence of a bimodal profile must be based on one of the following points: when it is observed that one or more spectrally identical solutes are missing in a chromatogram, clusters producing spectra similar to the spectra of these components are suspect and must be checked by means of TFA. If the resulting profiles

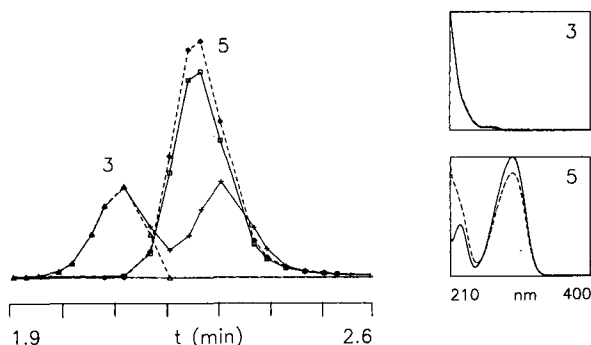


Fig. 6. The results of the ITT-FA performed on cluster 3 of chromatogram II (Fig. 3), indicated by the dashed line, as compared to the results of the TFA (solid line) performed with the pure component spectra of components 3 and 5. Other details as in Fig. 5.

are identical to the ones derived by means of ITT-FA, a direct match or a combination of areas will produce one or more possible solutions. However, when the TFA results in bimodal profiles, other spectra reconstructed previously by ITT-FA for this cluster will become unreliable and must be removed from libraries derived for the chromatogram in question. The tracking of the corresponding solutes can be performed only by means of TFA. It is for this reason that the third cluster of chromatogram II is darkened after the direct comparison of the spectra. Usually, the occurrence of bimodal profiles can also be detected by an increase in the minimum extracted error (Table II) since the removal of part of a profile can be compensated for only partly by other components in the cluster.

After the above procedure, the chromatograms I and IV have been identified as far as the retention times of the components are concerned. In chromatograms II and III, the exact location of the components 3 and 4 remain interchangeable. If one or both of these components are available, a separate injection will solve the dilemma, as has been done to produce Fig. 7. If not, then consecutive experiments must be based on both alternatives. However, often the identity will remain uncertain, even when the separation is complete.

#### Parameter selection

Now that the components have been localized in the four chromatograms, their response to the elution conditions can be analysed. An idealized representation of the observed behaviour is given in Fig. 8. The behaviour of the solutes in Fig. 8 is not measured as such but serves to help the reader better understand the following discussion.

Components 1 and 2 both display very low retention at both low and high pH and only display a (small) increase in retention with the addition of a negatively charged ion-pairing reagent. Apparently they are positively charged solutes, protonated over the full pH range examined with a weak dependence on the ion-pair concentration. Consequently, we are dealing with components which behave like strong bases in the parameter space examined.

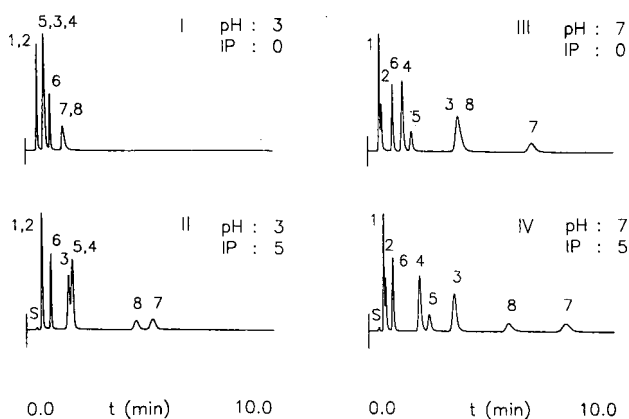


Fig. 7. The results of the peak tracking procedure. The component numbers refer to Fig. 1; the chromatograms are identical to those in Fig. 3. S = Solvent.

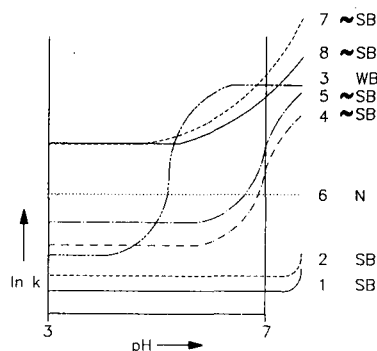


Fig. 8. The characterization of the components in the mixture. On the basis of the retention behaviours at low and high pH, taking the response of the ion-pair reagent concentration into account, the components are identified as behaving like strong bases (SBs), moderately strong bases ( $\sim$ SBs), weak bases (WBs) or neutrals (Ns).

Components 4, 5, 7 and 8 are substantially retained when the pH is increased from 3 to 7, hence the degree of protonation is changed. Since the components react to the addition of an ion-pairing reagent at both low and high pH, they are still charged at high pH. Because of this behaviour, the solutes are categorized as moderately strong bases.

The retention of component 6 is not influenced by either a change in pH or the addition of an ion-pairing reagent and consequently it is considered to be neutral.

The retention of component 3 increases at low pH with the addition of a negatively charged ion-pairing reagent, thus it is protonated at this pH. However, at high pH the (much larger) retention is no longer influenced by the addition of ion-pairing reagent and the component behaves like a neutral solute. Apparently we are dealing with a component with a retention behaviour like a weak base, which is protonated only at low pH. Here we have an additional indication of the identity of components 3 and 4 in chromatogram III, as compared to chromatogram IV. Due to an increase in retention with increasing pH, the components are identified as bases, but a protonated base will not suffer a decrease in retention with the addition of a negatively charged ion-pairing reagent. Consequently the elution order of the components does not change in chromatograms III and IV. This information is essential when interpretive optimization techniques are applied.

When we compare these conclusions with the molecular structures in Fig. 1, a few observations regarding the retention behaviour are immediately confirmed. Component 6, benzocaine, clearly contains no strong basic groups and can be considered as neutral. The tertiary amino groups in the other components are responsible for their basic behaviour, while the long hydrophobic aliphatic chains in the components 7, bupivacaine, and 8, tetracaine, cause the long retention times of these compounds. The reason why component 3 appears less basic than components 4 and 7 is the fact that the piperidine group is a stronger base than a tertiary amine group with alkyl chains<sup>22,23</sup>.

One of the requirements of the applied peak tracking procedure is the invariability of the pure component spectra under varying experimental conditions.

Although this cannot always be expected for charged solutes, in this case the requirement is fulfilled since a direct comparison of the pure component spectra of well resolved components produces correlation coefficients ranging from 0.9996 to 1.0000. Apparently, despite the change in protonation (different behaviours at pH 3 and pH 7), the spectra of the components are fairly constant, probably because the chromophoric groups are not affected by the protonation of the basic tertiary amino groups.

Although most components are reasonably separated in chromatogram IV, the retention of components 1 and 2 is still limited and it is desirable that their separation is improved. An inspection of the four chromatograms recorded so far indicates that the changes of finding a better separation within the parameter space examined (pH from 3 to 7 and ion-pairing reagent concentration from 0 to 5 mM) are minimal, since the critical pair is coeluted in every chromatogram. However, from the characterization of the components we can also draw the following conclusions regarding the retention behaviour of the components outside the above parameter range: due to the limitations of the stationary phase, a further increase in pH will not be possible, and an increase in the retention of components 1 and 2 can be obtained only by an increase in the ion-pairing reagent concentration. However, this will result in a strong increase in the retention of components 8 and 7, leading to impractically long chromatograms. In order to decrease the retention of these latter components one could increase the methanol content, but this would result in a decrease in the retention of component 6, which would then be coeluted with either component 1 or 2. Therefore the best chromatogram is observed at pH 7 and an ion-pairing reagent concentration of 5 mM and further changes in the pH, methanol content or the ion-pairing reagent concentration are not expected to improve the overall separation or quality of the chromatogram. However, there is a possibility that a change in the nature of the organic modifier will provide additional specificity.

The use of isoeluotropic mobile phases, changing the specificity of the mobile phase, but keeping the overall retention constant, has been described extensively<sup>1,2</sup>. When we determine the isoeluotropic mobile phase composition of 50% methanol by means of transfer rules, 38% acetonitrile or 32% THF is advised<sup>24</sup>. However, the retention times observed in chromatograms recorded with these compositions were too short, and corrections were required. The desired retention range was reached at 30% acetonitrile and 18% THF (Fig. 9). A number of changes in specificity are clearly observed. Especially the neutral component 6 shows a considerable change in retention behaviour, eluting in the proximity of component 4 in the chromatogram recorded in acetonitrile and coeluting with component 3 in the chromatogram recorded in THF. Although the retention of the charged solutes is influenced less dramatically by the change of organic modifier, some changes of the elution order are observed, for instance components 7 and 8 change their order in the chromatogram recorded in THF. In addition, the retention of components 1 and 2 is influenced such that the hoped for increase in resolution is obtained. Additional experiments showed that a simple increase in the water content of the mobile phase did not achieve a similar result but actually decreased the resolution of components 1 and 2. Unfortunately the overall separation in the chromatogram recorded in THF is insufficient, due to the coelution of components 3 and 6, but in the chromatogram in 30% acetonitrile sufficient separation of all components is observed. If desired a further optimization

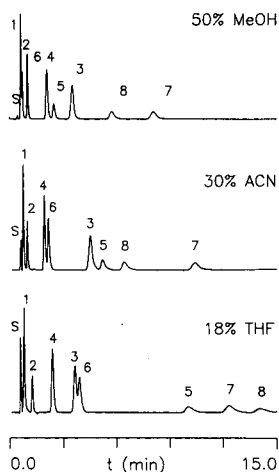


Fig. 9. Three chromatograms of the mixture recorded at 210 nm in isoeluotropic mobile phase compositions consisting of 50% methanol (MeOH), 30% acetonitrile (ACN) and 18% THF respectively. The aqueous phase contained 15 mM TEA and 5 mM octane sulphonate, pH 7. The numbers refer to Fig. 1. S = Solvent.

can be performed according to one of the established methods, for instance the iterative regression design<sup>3</sup>.

An acceptable separation was reached on the basis of a limited number of experiments: four preliminary chromatograms, two chromatograms to determine isoeluotropic compositions and the two actual isoeluotropic binary compositions.

Table III summarizes the retention times of the solutes in the chromatograms of Fig. 9. The exact chromatographic conditions are given in the caption.

TABLE III  
RETENTION TIMES OF THE EIGHT LOCAL ANAESTHETICS (SEE FIG. 1 FOR THE IDENTIFICATION) IN THE CHROMATOGRAMS OF FIG. 9 UNDER THE CHROMATOGRAPHIC CONDITIONS GIVEN IN THE CAPTION

Elution order	Acetonitrile		18% THF	
	Solute no.	$t_R$ (min)	Solute no.	$t_R$ (min)
1	1	0.63	1	0.70
2	2	0.88	2	1.18
3	4	1.84	4	2.33
4	6	2.09	3	3.63
5	3	4.52	6	3.90
6	5	5.23	5	10.20
7	8	6.48	7	12.60
8	7	10.60	8	14.30

## CONCLUSIONS

Peak tracking is not only required in the final stage of interpretive optimization strategies, but can also play a useful role in preliminary scouting procedures, required for an intelligent selection of the optimization parameters. Based on the change in retention, detected by means of the peak tracking procedure in a limited number of chromatograms, the components can be categorized. When the characteristics of the components in the sample examined are known, the response to a change in one of the parameters can be predicted, and the desirability of this change will play a rôle in the decision to include the corresponding parameter in the actual optimization. In this way irrelevant parameters are removed from consideration, reducing the number of experiments required to find an acceptable separation.

Peak tracking procedures which can be applied to chromatograms of unknown mixtures are limited in the sense that the spectral characteristics of the components must not be influenced too much by the experimental circumstances. However, if this requirement is fulfilled the application of advanced detection techniques such as LPDA, in combination with extensive mathematical treatment, will be able to solve most problems related to peak tracking, even in the case of severe peak overlap in one or more chromatograms.

If coelution of components with identical spectra is observed, additional analysis of this cluster by means of TFA is required, since bimodal profiles cannot be derived by means of the ITT-FA and will introduce errors in the spectra derived for other components present in these clusters. Furthermore, a better estimate of the related areas will be possible using the TFA. When coelution of components with identical spectra results in unimodal profiles a systematic combination of areas will be required to affirm the exact location.

By a rigorous analysis of the retention behaviour of the components in a mixture of local anaesthetics, useless experiments involving pH or ion-pairing reagents can be avoided, and an acceptable separation was derived by a variation of the selectivity of the mobile phase.

## REFERENCES

- 1 P. J. Schoenmakers, *Optimization of Chromatographic Selectivity (Journal of Chromatography Library, Vol. 35)*, Elsevier, Amsterdam, 1986.
- 2 J. C. Berridge, *Techniques for the Automated Optimization of HPLC Separations*, Wiley, Chichester, 1986.
- 3 A. C. J. H. Drouen, H. A. H. Billiet, P. J. Schoenmakers and L. de Galan, *Chromatographia*, 16 (1982) 48.
- 4 J. W. Weyland, C. H. P. Bruins and D. A. Doornbos, *J. Chromatogr. Sci.*, 22 (1984) 31.
- 5 H. A. H. Billiet, J. Vuik, J. K. Strasters and L. de Galan, *J. Chromatogr.*, 384 (1987) 153.
- 6 H. A. H. Billiet, G. K.-C. Low, A. Bartha and L. de Galan, *Abstracts 12th International Symposium on Column Liquid Chromatography, Washington, 1988*, W-P-356.
- 7 G. K.-C. Low, A. Bartha, H. A. H. Billiet and L. de Galan, *J. Chromatogr.*, submitted for publication.
- 8 H. J. Issaq and K. McNitt, *J. Liq. Chromatogr.*, 5 (1982) 1771.
- 9 M. Otto, W. Wegscheider and E. P. Lankmayr, *Anal. Chem.*, 60 (1988) 517.
- 10 A. C. J. H. Drouen, H. A. H. Billiet and L. de Galan, *Anal. Chem.*, 56 (1984) 971.
- 11 A. C. J. H. Drouen, H. A. H. Billiet and L. de Galan, *Anal. Chem.*, 57 (1985) 962.
- 12 J. K. Strasters, H. A. H. Billiet, L. de Galan and B. G. M. Vandeginste, *J. Chromatogr.*, in press.
- 13 J. K. Strasters, H. A. H. Billiet, L. de Galan, B. G. M. Vandeginste and G. Kateman, *J. Chromatogr.*, 385 (1987) 530.

- 14 B. G. M. Vandeginste, W. Derks and G. Kateman, *Anal. Chim. Acta*, 173 (1985) 253.
- 15 J. K. Strasters, H. A. H. Billiet, L. de Galan, B. G. M. Vandeginste and G. Kateman, *Anal. Chem.*, 60 (1988) 2745.
- 16 E. R. Malinowski and D. G. Howery, *Factor Analysis in Chemistry*, Wiley, New York, 1980.
- 17 A. N. Masoud and D. M. Krupski, *J. Anal. Toxicol.*, 4 (1980) 305.
- 18 T. A. Cough and P. B. Baker, *J. Chromatogr. Sci.*, 20 (1982) 289.
- 19 J. C. Reid and E. C. Wong, *Appl. Spectrosc.*, 20 (1966) 220.
- 20 Y. Beppu and I. Ninomiya, *Computers Chem.*, 6 (1982) 87.
- 21 P. R. Bevington, *Data Reduction and Error Analysis for the Physical Sciences*, McGraw-Hill, New York, 1969, Ch. 11.
- 22 S. Coffey (Editor), *Rodd's Chemistry of Carbon Compounds*, Vol. IB, Elsevier, Amsterdam, 2nd ed., 1965, p. 121.
- 23 S. Coffey (Editor), *Rodd's Chemistry of Carbon Compounds*, Vol. IVF, Elsevier, Amsterdam, 2nd ed., 1976, p. 213.
- 24 P. J. Schoenmakers, H. A. H. Billiet and L. de Galan, *J. Chromatogr.*, 205 (1981) 13.



CHROM. 21 712

## PERFORMANCE OF MICRO-LIQUID CHROMATOGRAPHIC COLUMNS IN AN INDUSTRIAL ENVIRONMENT: A CASE HISTORY

N. G. F. M. LAMMERS and J. H. M. VAN DEN BERG

*Analytical Development Department, Duphar BV, P.O. Box 2, 1380 AA Weesp (The Netherlands)*

and

M. VERZELE\* and C. DEWAELE

*Laboratory of Organic Chemistry, State University of Ghent, Krijgslaan 281 (S.4 · B-9000 Ghent (Belgium))*

---

### SUMMARY

Packed fused-silica capillary liquid chromatography (micro-LC) columns, with an inner wall polymer coating stabilizing the packed column bed, were evaluated in an industrial laboratory environment. Data on their performance and long-term stability in “real-world practice” are reported. The results indicate that micro-LC is a viable proposition for routine application.

---

### INTRODUCTION

Micro-liquid chromatography (micro-LC) is that form of liquid chromatography (LC) carried out on packed fused-silica (or other capillary) columns of I.D. 50–500  $\mu\text{m}$ . Initially, the most interesting aspect of micro-LC was thought to be the reduced amounts of solvent and packing material needed. Hirose *et al.*<sup>1</sup> showed, however, that micro-LC is a relatively easy route to LC with high plate numbers. Another important feature of packed fused-silica capillary LC is that the columns are more permeable than conventional columns<sup>2</sup>. This high column permeability is the result of the “direct wall effect”, which leads to a less densely packed column bed in columns of capillary dimensions<sup>3</sup>. Possible column instability can be avoided by using an elastic polymeric inner-wall coating which “holds” the packing. This higher permeability with good stability of micro-LC columns made from polymeric inner-wall-coated tubing, leads to a number of important advantages of micro-LC<sup>4–10</sup>.

This contribution to the miniaturization of LC emphasizes the excellent column stability of micro-LC. It is shown that this is available in routine application in an industrial environment. Packed fused-silica capillary LC combined with low-dispersion chemiluminescence detection<sup>11</sup> proved to be a sensitive and suitable method for analyses where only a small sample volume is available. Currently a method is being developed to permit neurotransmitter release studies *in vitro* (brain slices) and *in vivo* (brain dialysis) in which fmol/ $\mu\text{l}$  sensitivity is required. Chemiluminescence and micro-LC are used for this purpose. During the development of this method, the characteristics of the packed fused-silica capillary columns were measured for a period of

nearly 3 years. The reduced plate height,  $h$ , was monitored at several linear velocities,  $u$ , and the column resistance parameter,  $\phi$ , peak asymmetry,  $A_s$ , and retention ratio, (RR)<sup>a</sup>, were determined for the dansyl derivatives of  $\beta$ -histine {2-[2-(methylamino)-ethyl]pyridine dihydrochloride} relative to a by-product of the dansylation. The linear velocity was calculated assuming a total porosity of 0.50.

#### EXPERIMENTAL

The columns were a 500 × 0.5 mm I.D. column packed with 5- $\mu$ m RoSiL-C<sub>18</sub> (a spherical octadecylated silica gel from RSL, Eke, Belgium) and a 270 × 0.32 mm fused-silica capillary packed with 10- $\mu$ m RSiL-C<sub>18</sub> (a highly loaded irregularly shaped octadecylated silica gel phase from RSL). The instrument consisted of an MCP 36 pump (Haskel, Burbank, CA, U.S.A.), a Type 7520 or 7010 six-port injection valve (Rheodyne, Berkeley, CA, U.S.A.), a Perfusor ED2 syringe pump (Braun, Melsungen, F.R.G.), a 25- $\mu$ l glass-coil flow cell of 0.4 mm I.D., a mixing cross (Valco Instruments, Houston, TX, U.S.A.), a Model PR-305 photomultiplier (Products for Research, St. Danvers, MA, U.S.A.), a Type PM 28B power supply (Thorn EMI, Middlesex, U.K.), a Type C-10 photon counter (Thorn EMI) and an HP 3392A integrator (Hewlett-Packard, Waldbronn, F.R.G.).

Further chromatographic conditions are given in the legends to the figures. A detailed description of the instrumental set-up for chemiluminescence LC has been published elsewhere<sup>11</sup>. Eltoprazine [1-(2,3-dihydro-1,4-benzodioxin-5yl)piperazine hydrochloride], a drug under development for the indication of pathological destructive behaviour, was used.

#### RESULTS AND DISCUSSION

Immediately after production, the columns were tested with polycyclic aromatic hydrocarbons as samples and with acetonitrile–water (75:25) as the mobile phase at the optimum linear velocity. The smaller column had a reduced plate height of 2–2.5 whereas for the larger I.D. column it was *ca.* 3–4 (compound and  $k'$  dependent). Under these chromatographic conditions the optimum linear velocity, or the minimum in the Van Deemter plot, is observed at  $u$  values between 1 and 2 mm/s. With the probes and eluting solvents studied here a minimum in the  $h/u$  curve is not observed (even down to 0.3 mm/s) and the efficiencies were generally not as good, although the smaller I.D. column shows astonishingly low  $h$  values at very low flow-rate (Tables I and II). That the  $h/u$  relationship and the  $h$  values are strongly solvent and compound dependent is well recognized and is illustrated again here.

The first column was used to analyse dansylated amino acids and dansylated drugs; the other column was used to analyse catecholamines. Because the concentra-

<sup>a</sup> The retention ratio (RR) is measured instead of the  $\alpha$  value or selectivity factor. This is unusual and needs some clarification. Measuring "dead time" is awkward for two reasons: it was too difficult to find a chemiluminescence active compound that really showed no interaction with the column packing, and in some instances large volumes were injected with deliberately different composition to the eluent. This creates gradient effects which render "dead time" measurement nearly impossible. For these reasons RR values are used to express the degree of separation in the analysis being studied. The aim was to control the RR reproducibility.

TABLE I

## SEPARATIONS OF DANSYLATED DRUGS AND AMINO ACIDS ON THE 0.5 mm I.D. COLUMN

Column, 500 × 0.5 mm I.D., 5- $\mu$ m RoSiL-C<sub>18</sub>. Eluent acetonitrile-water (65:35) with 10 mM imidazole. Samples, dansylated drugs and amino acids (see legend to Fig. 1). RR values for the dansyl derivatives of  $\beta$ -histine relative to a byproduct of the dansylation. Detection, chemiluminescence.

No. of injections	$u$ (mm/s) <sup>a</sup>	$h$	RR	$A_s$	$\phi$
50	0.39	5.6	2.20	1.05	520
	0.70	9.4			
	1.49	17			
	2.40	24			
	3.27	28			
125	0.27	6.4	2.20	1.30	540
	0.51	9.4			
	1.38	18			
	2.19	23			
	3.20	28			
200	1.04	13	2.20	1.27	580
	1.40	18			
	2.14	19			
	2.95	27			
300 <sup>b</sup>	0.47	6.0	2.19	0.96	590
	0.83	13			
	1.10	14			
	1.66	19			
	2.40	22			
	3.08	26			
400	0.49	7.9	2.19	1.02	772
	0.93	10			
	1.53	14			
	2.31	18			
500	0.40	6.9	2.20	1.04	1050
	0.95	9.8			
	1.70	18			

<sup>a</sup>  $u$  measured with  $\epsilon_1$  (total porosity) = 0.50.

<sup>b</sup> Column shortened to 480 mm.

tion of the buffer influences the rate of the chemiluminescence reaction, the concentration was kept constant at 10 mmol/dm<sup>3</sup> (ref. 11). This resulted in a relaxation time of the reaction of less than 1 s, which has only a small influence on the peak width and peak shape. The peak width of the first eluting compound was about 6 s at the indicated flow-rate.

Some column chromatographic characteristics for the 0.5 mm I.D. column as a function of the number of injections are presented in Table I. It can be concluded that the column is stable with respect to asymmetry and selectivity of the peaks. However, it suffers from clogging owing to dirty sample injection, which results in a gradually increasing back-pressure and a higher resistance parameter. A doubled  $\phi$  value was observed after 4 months of regular use.

Similar experience over a period of nearly 3 years is tabulated for the 0.32 mm I.D. column in Table II. Whenever the back-pressure became excessive, a 1-cm piece

TABLE II

## SEPARATION OF DRUGS AND AMINO ACIDS ON THE 0.32 mm I.D. COLUMN

Column, 270 × 0.32 mm I.D., 10- $\mu$ m RSiL-C<sub>18</sub>. Eluent, acetonitrile–water (65:35) with 10 mM imidazole.

<i>No. of injections</i>	<i>u (mm/s)</i>	<i>h</i>	<i>A<sub>s</sub></i>	$\phi$	<i>Date<sup>a</sup></i>
10	0.30	1.3	1.47	870	March 86 (1)
	0.42	1.6			
	0.60	1.9			
	1.52	2.4			
	1.82	4.0			
	3.8	8.0			
	6.4	10.7			
	10.2	14.8			
50	1.4	1.4	1.51	860	March 86 (1)
	2.9	2.7			
	4.3	2.8			
	4.9	3.1			
	11.8	10.7			
250 <sup>d</sup>	1.6	2.1	1.52	1060	Aug. 86 (2)
	10.3	5.8	1.05 <sup>b</sup>		
500 <sup>e</sup>	1.1	2.2		2600 <sup>c</sup>	Oct. 86
1000 <sup>f</sup>	4.6	6.2	1.98	1550	(2)
1250 <sup>g</sup>	2.2	2.9	1.23	2960	Apr. 87 (3)
					May 87 (3)
1600 <sup>h</sup>	8.2	6.2	1.33	1000	Apr. 88 (2)
1900 <sup>i</sup>	4.0	4.0	1.29	1230	Aug. 88 (2)
2000 <sup>j</sup>	2.5	3.5	1.40	1550	Jan. 89 (2)

<sup>a</sup> Measurements with (1) dansylated drugs and amino acids; (2) dansylated catecholamines [acetonitrile–water (85:15) with 10 mM imidazole]; (3) dansylated Eltoprazine in plasma.

<sup>b</sup> Measured under optimum chemiluminescent conditions.

<sup>c</sup> High  $\phi$  reached, leading to shortening of column.

<sup>d–j</sup> Column shortened to 250, 240, 230; 210, 170, 145 and 130 mm, respectively.

of the column top was removed, which restored the performance to acceptable levels. Breaking off a piece of the column has to be carried out carefully so that an even, clean break is produced. We do this with a capillary scoring tool (Supelco, Bellefonte, PA, U.S.A.).

Restoring the column in this way was necessary, with our sample, after about every 250 injections and was kept up for 2000 injections. The peak asymmetry appears high for this column, but the chemiluminescence was not performed under ideal conditions. As soon as these conditions were further optimized<sup>11</sup> a more favourable value for  $A_s$  was observed. As Tables I and II show, the columns were shortened by 1–2 cm every time the back-pressure or the reduced plate height increased excessively. Even after 2000 analyses the reduced plate height had hardly changed. The back-

pressure of the column was higher than at the start, however, probably because clogging occurs not only at the injector site but also at the end frit site. Clogging of the top end is removed by cutting off a piece of the column, but clogging of the bottom frit cannot be repaired so easily. However, the results are acceptable.

The catecholamines were derivatized (in some instances "on-line") with dansyl chloride. For the plasma analysis of Eltoprazine, derivatization was carried out off-line. Examples of this chemiluminescence analysis on both columns are shown in Figs. 1 and 2. In Fig. 1 for the 0.5 mm I.D. column, the separations after 50 and after 300 runs are shown at eluent flow-rates far above the optimum. In Fig. 2 similar chromatograms are shown for the 0.32 mm I.D. column of length 250, 230 and 210 mm. The detection limits for the compounds analysed are in the femtomole range.

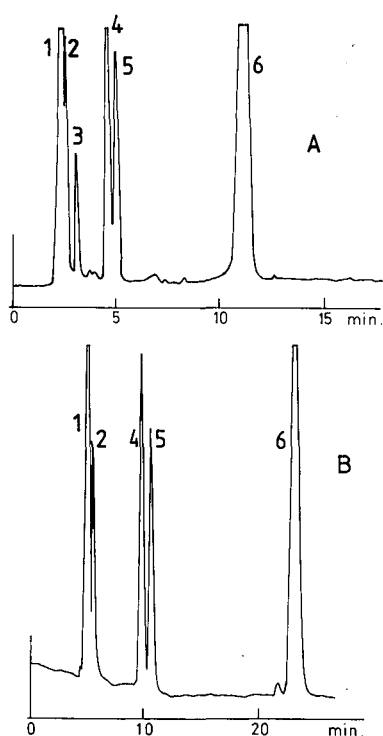


Fig. 1. Separation of dansylated amino acids. Column,  $500 \times 0.5$  mm I.D., packed with  $5\text{-}\mu\text{m}$  RoSiL- $\text{C}_{18}$ . Eluent, acetonitrile-water (65:35) with  $10\text{ mM}$  imidazole. Sample,  $0.2\ \mu\text{l}$  of dansyl derivatives of the compounds mentioned. Dansyl derivative of  $\beta$ -histine at  $1.6\ \text{ng}/\mu\text{l}$ . Peaks in order of appearance: 1, DNS-OH; 2, methionine; 3, tryptophan; 4, mebeverinic acid; 5, byproduct of the dansylation of  $\beta$ -histine; 6,  $\beta$ -histine. Detection, chemiluminescence. Trace A after 50 analyses and at  $15\ \mu\text{l}/\text{min}$  ( $2.4\ \text{mm}/\text{s}$  or far above the optimum). Back-pressure,  $19\ \text{MPa}$ . Trace B after 300 analyses on a  $480\text{-mm}$  column and at  $7\ \mu\text{l}/\text{min}$  ( $1.1\ \text{mm}/\text{s}$ ). Back-pressure,  $10\ \text{MPa}$ .

In Tables I and II, entries which are derived from the chromatograms in Figs. 1 and 2 are given in italics. The chromatograms in Fig. 2B, C and D do not appear in Tables I and II. Table II shows that the  $0.32\ \text{mm}$  I.D. column, finally shortened to nearly half its original length ( $130\ \text{cm}$ ), was still performing well.

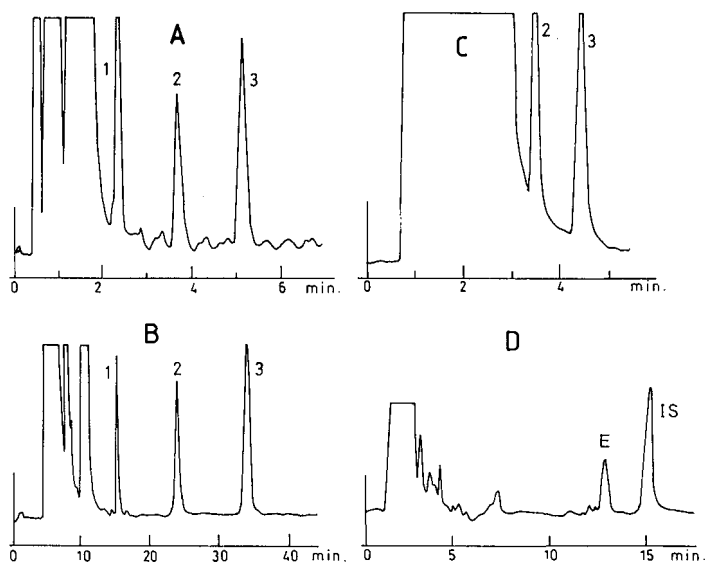


Fig. 2. Separation of dansylated drugs and amino acids. Column,  $250 \times 0.32$  mm I.D. packed with  $10\text{-}\mu\text{m}$  RSiL- $\text{C}_{18}$ . Eluent, acetonitrile-water (85:15) with  $10\text{ mM}$  imidazole. Chemiluminescence detection. Peaks in order of appearance: 1, serotonin (5-HT); 2, noradrenaline (NA); 3, dopamine (DA). (A) Sample,  $5\ \mu\text{l}$  of catecholamines each at  $1\ \text{pg}/\mu\text{l}$ ; flow-rate,  $15\ \mu\text{l}/\text{min}$  ( $u = 6.4\ \text{mm/s}$ ); back-pressure,  $15\ \text{MPa}$ . (B) Same as under A but with  $0.5\ \mu\text{l}$  of a catecholamine solution at  $20\ \text{pg}/\mu\text{l}$  and with a flow-rate of  $2.5\ \mu\text{l}/\text{min}$  ( $u = 1.0\ \text{mm/s}$ ); back-pressure,  $2.5\ \text{MPa}$ . (C) After 1000 analyses with a column shortened to  $230\ \text{mm}$  with a flow-rate of  $20\ \mu\text{l}/\text{min}$  ( $u = 8.3\ \text{mm/s}$ ),  $20\ \mu\text{l}$  of catecholamine solution and on-line derivatization. (D) After 1500 analyses with a column shortened to  $210\ \text{mm}$ . Eluent, acetonitrile-water (65:35) with  $10\text{ mM}$  imidazole;  $0.5\ \mu\text{l}$  of plasma extract. Sample, Eltoprazine at  $25\ \text{pg}/\mu\text{l}$ ; internal standard (an analogue of Elkoprazine) at  $75\ \text{pg}/\mu\text{l}$ . Flow-rate,  $10\ \mu\text{l}/\text{min}$  ( $u = 4.1\ \text{mm/s}$ ); back pressure,  $13\ \text{MPa}$ .

## CONCLUSION

This case study shows that in a practical environment, micro-LC columns behave remarkably well. An increasingly interesting aspect of micro-LC is the low volume of spent solvent.

## ACKNOWLEDGEMENTS

We thank the Duphar management for authorization to publish these results. C. D. thanks the Instituut voor Wetenschappelijk Onderzoek in Nijverheid en Landbouw (IWONL) for a grant.

## REFERENCES

- 1 A. Hirose, D. Wiesler and M. Novotny, *Chromatographia*, 18 (1984) 239.
- 2 M. Verzele and C. Dewaele, *J. High Resolut. Chromatogr. Chromatogr. Commun.*, 10 (1987) 280.
- 3 M. Verzele, C. Dewaele, M. De Weerd and S. Abbott, *J. High Resolut. Chromatogr. Chromatogr. Commun.*, 12 (1989) 164.
- 4 M. Verzele and C. Dewaele, *J. Chromatogr.*, 395 (1987) 85.

- 5 C. Dewaele and M. Verzele, *11th International Symposium on Column Liquid Chromatography, Amsterdam, June 28–July 3, 1987*, Th-P-25, p. 44.
- 6 G. Schuddinck and M. Verzele, *J. Chromatogr.*, 407 (1987) 159.
- 7 M. De Weerd, M. Verzele and C. Dewaele, *J. High Resolut. Chromatogr. Chromatogr. Commun.*, 10 (1987) 553.
- 8 D. Duquet, C. Dewaele and M. Verzele, *J. High Resolut. Chromatogr. Chromatogr. Commun.*, 11 (1988) 252.
- 9 J. Vindevogel, G. Schuddinck, C. Dewaele and M. Verzele, *J. High Resolut. Chromatogr. Chromatogr. Commun.*, 11 (1988) 317.
- 10 M. Verzele, C. Dewaele and M. De Weerd, *LC-GC Mag.*, 6 (1988) 966.
- 11 G. de Jong, N. Lammers, F. Spruit, C. Dewaele and M. Verzele, *Anal. Chem.*, 59 (1987) 1458.





CHROMSYMP. 1664

## DIRECT COUPLING OF CAPILLARY LIQUID CHROMATOGRAPHY WITH CONVENTIONAL HIGH-PERFORMANCE LIQUID CHROMATOGRAPHY

TOYOHIDE TAKEUCHI\*

*Research Centre for Resource and Energy Conservation, Nagoya University, Chikusa-ku, Nagoya 464 (Japan)*

and

MASASHI ASAI, HIROKI HARAGUCHI and DAIDO ISHII

*Department of Applied Chemistry, School of Engineering, Nagoya University, Chikusa-ku, Nagoya 464 (Japan)*

---

### SUMMARY

A capillary column liquid chromatograph was combined with a conventional liquid chromatograph and the system was evaluated by using aromatic hydrocarbons as test analytes. A capillary fused-silica column of 0.35 mm I.D. was employed in the former chromatograph. The combination of normal-phase and reversed-phase separations was possible because the first dimension involved separation with the capillary column, which resulted in very small peak volumes. A whole sample band from the former chromatograph could be transferred to the sample loop of the latter. The system was applied to the normal- and reversed-phase separation of aromatic hydrocarbons in a fuel for body warmers (benzine).

---

### INTRODUCTION

There are inherent limits to improvements of the selectivity in liquid chromatography (LC). Successive column chromatography is one of the best means of increasing the separation efficiency. Giddings<sup>1</sup> defined the peak capacity,  $\varphi$ , as a measure of the separation efficiency:

$$\varphi = 1 + \frac{\sqrt{N}}{m} \ln(1 + k') \quad (1)$$

where  $N$  is the theoretical plate number,  $k'$  is the capacity factor of the last-eluted peak of interest and  $m$  is the number of standard deviations,  $\sigma$ , that are taken as equalling the peak width.

Freeman<sup>2</sup> has shown that if two or more different chromatographic modes are coupled, the total peak capacity of a multi-dimensional separation,  $\varphi_T$ , approaches

$$\varphi_T = \prod_{i=1}^n \varphi_i \quad (2)$$

where  $\phi_i$  are the peak capacities of each mode and  $n$  is the number of modes. Coupled chromatographic systems offer much greater peak capacities than single-column systems, but the addition of band broadening is a critical factor in the design of an interface. In order to combine two conventional LC systems, the heart-cutting method has been proposed, in which a portion of a primary band is transferred into the secondary system<sup>3,4</sup>.

Capillary LC systems facilitate direct combination with conventional LC systems, because the peak volumes of the former systems are so small that a whole primary band can be quantitatively transferred to the secondary systems. Floyd<sup>5</sup> has recently published a paper on "two-dimensional" LC-LC, in which microbore LC systems with 1 mm I.D. columns and conventional LC systems are employed as the primary and secondary systems, respectively.

The attractive features and requirements for coupled LC-LC and LC-gas chromatographic separations have been described<sup>6</sup>. A coupled chromatographic system, capillary LC-conventional LC, was used in this work, and the system assembly was evaluated by using aromatic hydrocarbons at test analytes.

## EXPERIMENTAL

### Apparatus

The coupled system was composed of a capillary liquid chromatograph and a conventional high-performance liquid chromatograph. The former chromatograph was assembled from a Microfeeder (Azumadenki Kogyo, Tokyo, Japan), equipped with an MS-GAN 050 gas-tight syringe (0.5 ml) (Ito, Fuji, Japan) as a pump, an ML-525 micro valve injector (0.02  $\mu$ l) (JASCO, Tokyo, Japan), a laboratory-packed fused-silica column and a UVIDEC-100 UV spectrophotometer (JASCO) with a modified flow cell. A schematic diagram of the modified flow cell is shown in Fig. 1. Stainless-steel tubing of 0.05 mm I.D.  $\times$  0.30 mm O.D. (Nomura Chemical, Seto, Japan) was glued in fused-silica tubing of 0.32 mm I.D. with an epoxy-resin adhesive. The detection volume was *ca.* 0.1  $\mu$ l. The capillary fused-silica columns were prepared according to previous work<sup>7</sup>.

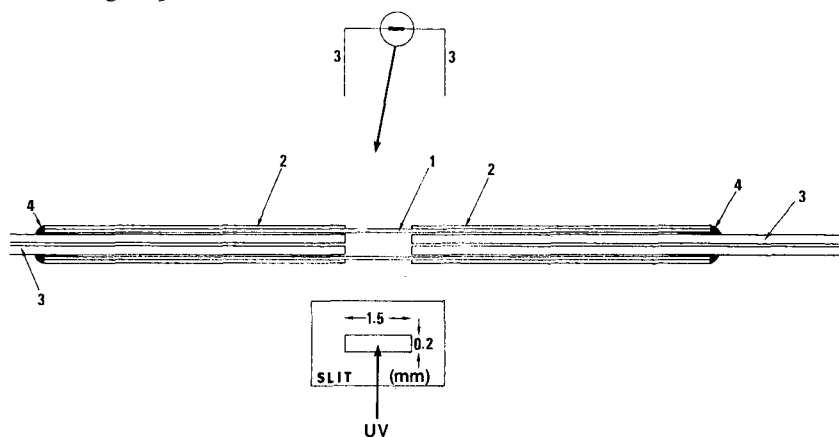


Fig. 1. Schematic diagram of the modified flow cell. 1 = Fused-silica tubing of 0.32 mm I.D.; 2 = polyimide resin; 3 = stainless-steel tubing of 0.05 mm I.D.  $\times$  0.30 mm O.D.; 4 = epoxy-resin adhesive.

The conventional chromatograph was composed of an 880-PU pump (JASCO), a laboratory-modified loop injector, a 100 or 250 × 4.6 mm I.D. column and a UVIDEK-100V UV spectrophotometer (JASCO). The micro LC and the conventional LC instruments were interfaced by small-bore (50–70 μm I.D.) fused-silica or stainless-steel tubing having a dead volume of < 1 μl. The effluent from the capillary LC system was introduced into the loop tubing of the valve injector of the conventional LC system. The valve was manually operated, taking account of the time lag due to the dead volume of the interface. The loop injector of the secondary system was prepared from a Model 7000 switching valve (Rheodyne, Cotati, CA, U.S.A.) and a stainless-steel loop with various volumes.

Aminopropylsilica, TSKgel NH<sub>2</sub>-60 (5 μm) (TOSOH, Tokyo, Japan), Develosil ODS-3K (3 μm) (Nomura Chemical) and Develosil ODS-5 (5 μm) (Nomura Chemical) were employed as packing materials. The capillary LC columns were prepared from fused-silica tubing of 0.35 mm I.D. (Gaskuro Kogyo, Tokyo, Japan) in the laboratory. The conventional columns were supplied by Nomura Chemical.

### Reagents

All the reagents were of analytical-reagent grade, except for HPLC-grade distilled water. The reagents were supplied by Wako (Osaka, Japan) or Tokyo Chemical Industry (Tokyo, Japan) and employed without any treatment.

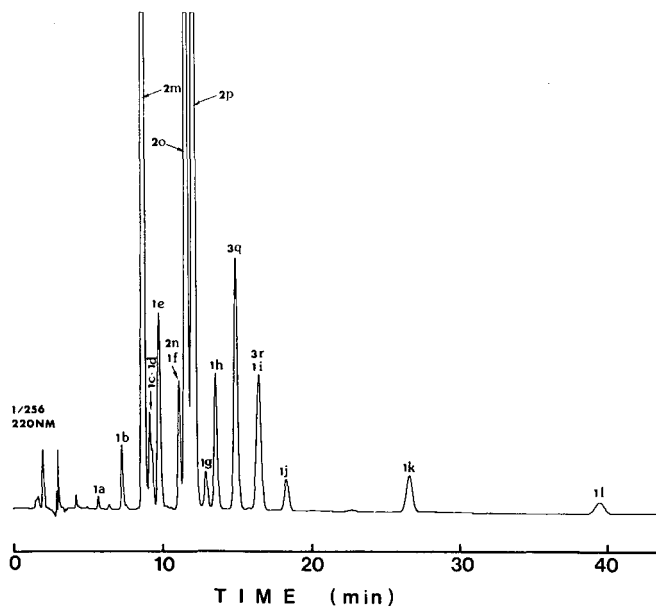


Fig. 2. Reversed-phase separation of an artificial mixture of aromatic hydrocarbons. Column, Develosil ODS (250 × 4.6 mm I.D.); mobile phase, acetonitrile–water (70:30); flow-rate, 1.0 ml/min; sample, *ca.* 0.01% each. 1a = Benzene; 1b = toluene; 1c = *o*-xylene; 1d = *m*- and *p*-xylene; 1e = ethylbenzene; 1f = cumene; 1g = mesitylene; 1h = *n*-propylbenzene; 1i = *sec.*-butylbenzene; 1j = *n*-butylbenzene; 1k = *n*-amylbenzene; 1l = *n*-hexylbenzene; 2m = naphthalene; 2n = biphenyl; 2o = 1-methylnaphthalene; 2p = 2-methylnaphthalene; 3q = phenanthrene; 3r = anthracene. Sample volume, 12 μl; detection, 220 nm.

## RESULTS AND DISCUSSION

The peak volume depends on the column dimensions and efficiency and also on the capacity factors of the analytes when isocratic elution is applied. The peak volumes observed in capillary LC with 100 or 250  $\times$  0.25 or 0.35 mm I.D. columns are *ca.* 10  $\mu$ l or less. This volume is smaller than the acceptable injection volumes for ordinary columns in conventional LC (*ca.* 100  $\mu$ l). This situation facilitates direct combination of the capillary and conventional LC systems<sup>6</sup>. The sample-loop volume of the secondary system must at least be larger than the peak volumes observed in the primary system, because the sample band increases in volume when passing through the interface capillary and the sample loop itself. The loop employed 25 cm  $\times$  *ca.* 0.25 mm I.D. allowed quantitative injection into the secondary system of up to 10  $\mu$ l at a flow-rate of 4.2  $\mu$ l/min.

The two-dimensional separation system was evaluated by using aromatic hydrocarbons as test analytes. The reversed-phase separation of an artificial mixture of aromatic hydrocarbons is demonstrated in Fig. 2. Several peaks overlapped and could not be separated under the operating conditions used. Real samples will give

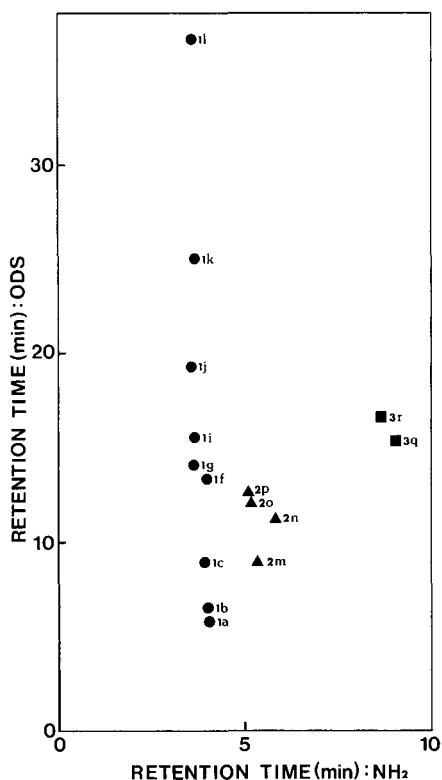


Fig. 3. Retention times on the ODS column *versus* those on the NH<sub>2</sub> column. Columns, Develosil ODS-3K (100  $\times$  0.35 mm I.D.); TSKgel NH<sub>2</sub>-60 (150  $\times$  0.35 mm I.D.); mobile phases, acetonitrile-water (70:30) for the ODS column, hexane for the NH<sub>2</sub> column; flow-rate, 4.2  $\mu$ l/min; sample as in Fig. 2.

much more complicated chromatograms. In such a case, the coupled-column system will improve the separation efficiency and simplify the chromatogram. For example, aromatic hydrocarbons can be separated on the basis of differences in aromatic moieties in the normal-phase mode and then separated on the basis of differences in aliphatic moieties in the reversed-phase mode.

Fig. 3 illustrates relationships between retention times of the analytes on the ODS column in the reversed-phase mode and those on the  $\text{NH}_2$  column in the normal-phase mode. In the normal-phase separation mode the analytes are separated on the basis of differences in the number and size of their aromatic ring moieties, while both aromatic and aliphatic moieties significantly affect the retention times in the reversed-phase mode.

Fig. 4 demonstrates the normal-phase separation of nineteen aromatic hydrocarbons on the  $\text{NH}_2$  column. The first peak contains thirteen monocyclic aromatic hydrocarbons, the second contains three bicyclic aromatic hydrocarbons, the third contains biphenyl and the fourth contains two tricyclic aromatic hydrocarbons. The volume of the last peak is  $5.3 \mu\text{l}$ .

The fraction containing the first peak in Fig. 4 was transferred to the secondary separation system and subjected to reversed-phase separation, as shown in Fig. 5. The detection wavelength was 210 nm. All monocyclic aromatic hydrocarbons examined, except xylenes, were well separated.

Fig. 6 demonstrates the reversed-phase separation of the components in the fraction containing the second and third peaks. Fig. 7 demonstrates the reversed-phase separation of the components in the fraction containing the fourth peak. Fig. 6 was obtained with detection at 220 nm and Fig. 7 at 250 nm. In order to carry out the reversed-phase separation of the components present in each fraction, a normal-phase separation was carried out prior to each reversed-phase separation.

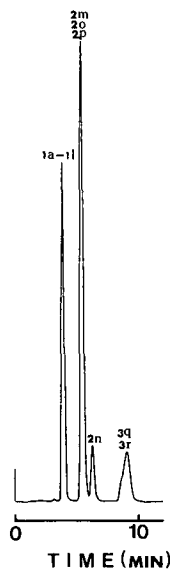


Fig. 4. Normal-phase separation of an artificial mixture of aromatic hydrocarbons. Column, TSKgel  $\text{NH}_2$ -60 ( $150 \times 0.35$  mm I.D.); mobile phase, hexane; flow-rate,  $4.2 \mu\text{l}/\text{min}$ ; sample as in Fig. 2, except concentration (ca. 0.1% each); detection, 220 nm.

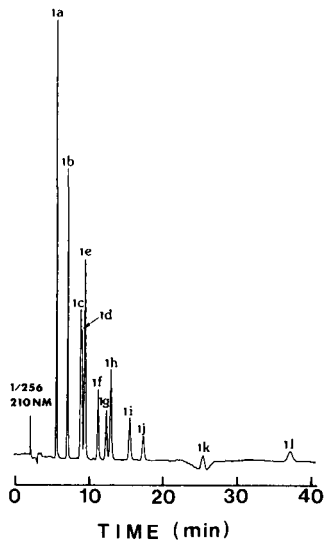


Fig. 5. Reversed-phase separation of a fraction of monocyclic aromatic hydrocarbons. Column, Develosil ODS (250 × 4.6 mm I.D.); mobile phase, acetonitrile–water (70:30); flow-rate, 1.0 ml/min; detection, 210 nm.

The coupled system was applied to the analysis of aromatic hydrocarbons in a fuel for body warmers (benzine). The results are shown in Fig. 8. A few peaks were observed in the normal-phase separation. Fig. 8 also shows the reversed-phase

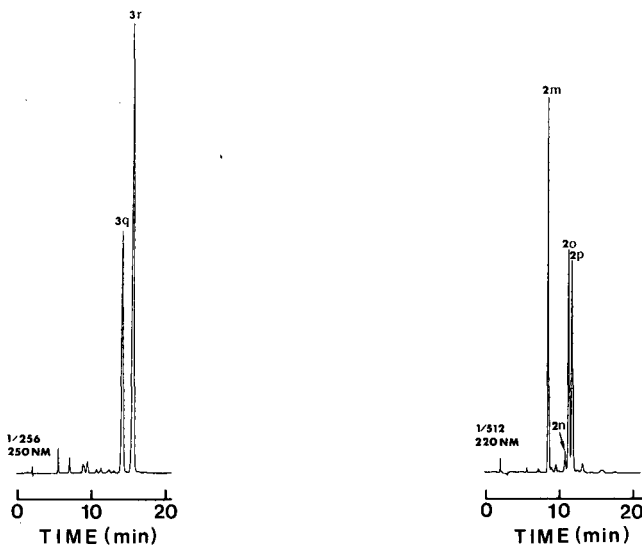


Fig. 6. Reversed-phase separation of a fraction of bicyclic aromatic hydrocarbons and biphenyl. Detection, 220 nm; other operating conditions as in Fig. 5.

Fig. 7. Reversed-phase separation of a fraction of tricyclic aromatic hydrocarbons. Detection, 250 nm; other operating conditions as in Fig. 5.

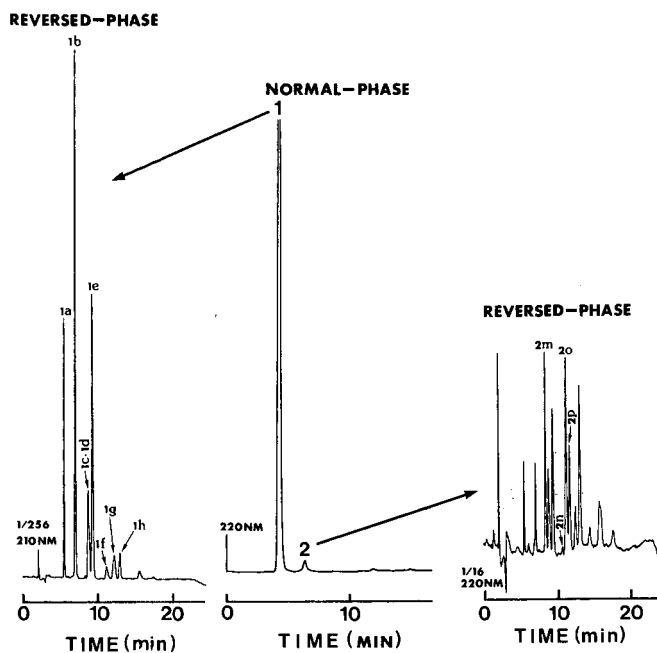


Fig. 8. Coupled-column chromatography of aromatic hydrocarbons in a fuel for body warmers (benzene). Operating conditions of capillary system: column, TSKgel NH<sub>2</sub>-60 (150 × 0.35 mm I.D.); mobile phase, hexane; flow-rate, 4.2 μl/min; sample, 0.02 μl of 10% benzene; detection, 220 nm. Operating conditions of conventional system: column, Develosil ODS (250 × 4.6 mm I.D.); mobile phase, acetonitrile-water (70:30); flow-rate, 1.0 ml/min; detection, 210 nm for monocyclic aromatic hydrocarbons fraction and 220 nm for bicyclic aromatic hydrocarbons fraction.

separation of the components in the fraction containing the first or second peak in the normal-phase separation. Several components were identified on the basis of their retention times. The use of a multi-channel UV detector will give more reliable qualitative information.

In addition to the above separation modes, various other modes are available in LC, *e.g.*, ion exchange, ion pair, size exclusion and chirality recognition. There are many possibilities for selecting two different separation modes for coupled-column chromatography. This technique is generally capable of increasing the peak capacities and will be of practical importance for the separation of complex mixtures.

#### ACKNOWLEDGEMENT

This research was supported by a Grant-in-Aid for Encouragement of Young Scientists (Grant No. 01750719), Science and Culture, The Ministry of Education.

## REFERENCES

- 1 J. C. Giddings, *Anal. Chem.*, 56 (1984) 1258A.
- 2 D. H. Freeman, *Anal. Chem.*, 53 (1981) 2.
- 3 E. L. Johnson, R. Gloor and R. E. Majors, *J. Chromatogr.*, 149 (1978) 571.
- 4 R. E. Majors, *J. Chromatogr. Sci.*, 18 (1980) 571.
- 5 Th. R. Floyd, *Chromatographia*, 25 (1988) 791.
- 6 T. V. Raglione, N. Sagliano, Jr., Th. R. Floyd and R. A. Hartwick. *LC · GC*, 4 (1986) 328.
- 7 T. Takeuchi and D. Ishii, *J. Chromatogr.*, 213 (1981) 25.



CHROMSYMP. 1669

## APPRAISAL OF FOUR PRE-COLUMN DERIVATIZATION METHODS FOR THE HIGH-PERFORMANCE LIQUID CHROMATOGRAPHIC DETERMINATION OF FREE AMINO ACIDS IN BIOLOGICAL MATERIALS

P. FÜRST\*, L. POLLACK, T. A. GRASER<sup>a</sup>, H. GODEL<sup>b</sup> and P. STEHLE

*Institute for Biological Chemistry and Nutrition, University of Hohenheim, Garbenstrasse 30, D-7000 Stuttgart 70 (F.R.G.)*

---

### SUMMARY

Reversed-phase high-performance liquid chromatography (RP-HPLC) is a powerful method for assaying physiological amino acid concentrations in biological fluids. Four pre-column derivatization methods, with *o*-phthaldialdehyde (OPA), 9-fluorenylmethyl chloroformate (FMOC-Cl), phenyl isothiocyanate (PITC) and 1-dimethylaminonaphthalene-5-sulphonyl chloride (dansyl-Cl), were assessed with respect to their applicability in biological research.

The methods permit the measurement of 21–26 major amino acids in 13–40 min. The superior sensitivity favours the use of OPA, FMOC-Cl and dansyl-Cl techniques. Because of instability of the OPA adducts, automated on-line derivatization is required when using this method in general practice. Application of the PITC method, although less sensitive, is useful in clinical chemistry, where sample availability is rarely a problem. Cystine determination is not feasible when using OPA or FMOC-Cl and with PITC the reproducibility and linearity are poor, whereas the dansyl-Cl method allows reliable quantitation.

The four methods are currently used to perform *ca.* 8000 OPA and 5000–6000 FMOC-Cl, PITC and dansyl-Cl analyses of biological samples per year. The results obtained with the RP-HPLC methods compare favourably with those derived from conventional ion-exchange amino acid analyses. When the guard column is regularly changed after 120 analyses, the separation remains satisfactory for at least 700 OPA, 800 FMOC-Cl, 150 PITC and 500 dansyl-Cl analyses. Careful control of factors and limitations inherent in the various methodologies is a prerequisite for proper identification and appropriate quantitation.

---

### INTRODUCTION

For nearly 30 years, amino acid determinations have been carried out mainly by means of various automated ion-exchange post-column derivatization (mostly nin-

<sup>a</sup> Present address: F. Hoffmann-La Roche, CH-4002 Basle, Switzerland.

<sup>b</sup> Present address: Hewlett Packard, D-7517 Waldbronn 2, F.R.G.

hydrin) methods<sup>1-4</sup>. Reversed-phase high-performance liquid chromatography (RP-HPLC) is now recognized as a powerful method in biological research, and the usefulness of this technique for determining amino acids has been amply demonstrated in numerous publications<sup>5-19</sup>. In these reports, adequate separation and subsequent determination of free amino acids in tissues<sup>9,11-14</sup> and reduced analysis times and enhanced sensitivity are claimed in comparison with alternative methods<sup>9,11,15-19</sup>. Although this advanced technology may allow the proper application of HPLC in routine biological practice<sup>20,21</sup>, the validity and value of this approach have not yet been adequately examined and/or verified.

In this paper we compare the applicability of four pre-column derivatization RP-HPLC methods, with *o*-phthalaldehyde (OPA), 9-fluorenylmethyl chloroformate (FMOC-Cl), phenyl isothiocyanate (PITC) and 1-dimethylaminonaphthalene-5-sulphonyl chloride (dansyl-Cl) to the analysis of physiological fluids (plasma, muscle, liver, kidney and leucocytes). Special attention was devoted to the control of factors and limitations inherent in these techniques and in the interpretations of their findings.

## EXPERIMENTAL AND RESULTS

### *o*-Phthalaldehyde method

This derivatization method, introduced as early as 1971<sup>22</sup>, is probably the most commonly used in RP-HPLC for the determination of free amino acids.

*Manual procedure.* In a previous paper<sup>23</sup> we reported analytical conditions allowing the precise measurement of 26 free amino acids in biological samples (plasma, muscle and liver) in the low picomole range. Derivatization was performed manually, and the adducts were detected by fluorescence. Previously reported problems of poor resolution between asparagine and serine and between valine and methionine<sup>24</sup> with 2-mercaptoethanol as a thiol component could be overcome by the use of 3-mercaptopropionic acid (3-MPA) and by substituting acetonitrile for methanol. Applying these optimized conditions, 23 major physiological amino acids can be separated in less than 13 min in the lower picomole range<sup>21</sup>.

These favourable results with 3-MPA are presumably due to the introduction of an  $\alpha$ -carboxyl group into the amino acid adduct, thereby reducing the hydrophobicity of these adducts in comparison with those formed with other mercaptans<sup>24,25</sup>.

We use the manual OPA method commonly at the sensitivity level of 10 pmol amino acid per injection. The limit of sensitivity (0.8 pmol) was determined<sup>21,26</sup> at a signal-to-noise ratio of 2.5:1. Exceptions are histidine and lysine, detected at a minimum of 2.5 and 3.5 pmol, respectively.

The reproducibility was determined on the basis of 25 standard analyses and yielded values between 4.2 and 6.8% [coefficient of variation (C.V.)], respectively. The reliability of the method was assessed by twenty repeated injections of the same derivatized plasma sample, ranging between 1.8% and 6.0% (C.V.), except for tyrosine and histidine (9.8% and 8.6%, respectively)<sup>21</sup>. The error of the method was determined on the basis of twenty duplicate analyses of human plasma samples. The estimate of errors includes the sample preparation and all analytical procedures used. The error in a single determination, based on duplicates, ranged between 4.5 and 8.2% (C.V.) for the individual amino acids. The error in duplicate determinations ranged between 3.2 and 6.1% (C.V.)<sup>21,26,27</sup>.

TABLE I

FREE AMINO ACID CONCENTRATIONS IN HUMAN PLASMA (nmol/ml), DETERMINED BY HPLC (PRE-COLUMN DERIVATIZATION WITH OPA, FMOC AND PITC) AND ION-EXCHANGE CHROMATOGRAPHY (NINHYDRIN POST-COLUMN DERIVATIZATION)

Results are means  $\pm$  S.D. ( $n = 10$ ).

Amino acid	Ion exchange (ninhydrin)	HPLC		
		OPA (automated)	FMOC-Cl	PITC
Glu	23.0 $\pm$ 8.4	16.4 $\pm$ 4.7	19.1 $\pm$ 4.0	11.6 $\pm$ 3.9
Asn	38.4 $\pm$ 7.1	38.4 $\pm$ 10.9	41.2 $\pm$ 7.0	43.8 $\pm$ 9.5
Ser	119.9 $\pm$ 10.6	99.4 $\pm$ 26.6	103.3 $\pm$ 18.3	102.0 $\pm$ 13.5
Gln	574.5 $\pm$ 31.8	556.7 $\pm$ 31.5	547.3 $\pm$ 51.1	493.1 $\pm$ 56.9
Gly	262.2 $\pm$ 46.6	213.5 $\pm$ 34.7	207.1 $\pm$ 29.5	191.8 $\pm$ 23.4
Thr	114.7 $\pm$ 30.3	96.5 $\pm$ 30.1	102.1 $\pm$ 20.3	116.6 $\pm$ 20.8
His	85.7 $\pm$ 23.2	85.5 $\pm$ 16.4	69.7 $\pm$ 20.5	79.8 $\pm$ 20.3
Ala	353.5 $\pm$ 105.1	319.0 $\pm$ 99.4	303.7 $\pm$ 70.7	339.9 $\pm$ 51.5
Tau	60.7 $\pm$ 8.8	38.9 $\pm$ 9.8	38.7 $\pm$ 4.4	59.4 $\pm$ 16.8
Arg	84.8 $\pm$ 7.2	74.3 $\pm$ 29.9	74.9 $\pm$ 19.6	77.5 $\pm$ 11.6
Tyr	66.8 $\pm$ 17.2	48.1 $\pm$ 17.0	51.4 $\pm$ 11.1	54.7 $\pm$ 5.0
Val	198.7 $\pm$ 36.9	209.1 $\pm$ 40.6	185.3 $\pm$ 43.2	222.2 $\pm$ 28.3
Met	28.7 $\pm$ 12.4	35.0 $\pm$ 7.5	25.3 $\pm$ 7.0	25.9 $\pm$ 2.8
Ile	54.2 $\pm$ 12.1	51.1 $\pm$ 6.6	50.4 $\pm$ 13.8	68.7 $\pm$ 10.3
Phe	53.7 $\pm$ 12.9	52.2 $\pm$ 12.3	47.5 $\pm$ 8.2	60.3 $\pm$ 4.8
Trp	45.8 $\pm$ 17.4	34.5 $\pm$ 7.6	—	—
Leu	114.9 $\pm$ 24.7	112.7 $\pm$ 24.2	104.2 $\pm$ 29.2	141.6 $\pm$ 16.8
Orn	80.0 $\pm$ 23.2	81.4 $\pm$ 15.1	78.5 $\pm$ 10.8	—
Lys	195.9 $\pm$ 44.7	182.7 $\pm$ 39.4	178.1 $\pm$ 40.7	202.7 $\pm$ 43.6
Pro	205.3 $\pm$ 40.8	—	193.3 $\pm$ 50.6	240.8 $\pm$ 48.1

Free amino acid concentration in muscle, liver and kidney, as determined by OPA-HPLC, were in the expected physiological range and agree with those obtained by a conventional amino acid analyzer<sup>28,29</sup>. In plasma (Table I), the correlation between the two methods were highly significant ( $r = 0.97$ ,  $p < 0.001$ ) in 120 comparative analyses.

*Automated method.* The instability of the OPA-amino acid adducts seriously limits reproducibility and proper quantification. Hence it is necessary to develop an automated derivatization procedure allowing a given optimum derivatization time for the reaction to be maintained<sup>26,27,30,31</sup>. Another advantage of an automated on-line derivatization system is the considerably higher capacity.

As suitable refrigerated sample injectors were not commercially available at that time, we modified an LKB 2153 autoinjector to permit automated pre-column derivatization and subsequent injection<sup>26,27,30,31</sup>. In this system, the normal digitally pre-set functions of the autoinjector for flush cycles and the injection-fill cycles were changed into digitally pre-set functions for pump time (0–90 s) and derivatization time (0–990 s), respectively. On-line derivatization was facilitated by attaching a peristaltic pump to the autoloader. This permitted mixing of the sample with the OPA-3-MPA reagent in an external mixing T-piece (reaction vessel) in the pumping mode. The prepared samples and the reagent bottle were placed in a thermostated box on

the top of the autoinjector, which was held at ambient temperature (25°C) or cooled to 4°C. As the external reaction vessel was not thermostated, the temperature of the reactants rose to *ca.* 7°C after a 1.5-min reaction time. In the complete, automated HPLC system, the autoinjector was connected to the controller by an interface cable. Full control of the analysis time and gradient profile for each sample injection and of the number of repetitive injections from each vial was then achieved<sup>26,27,30,31</sup>.

Compared with the manual method at similar sensitivity, considerable improvement in reproducibility could be achieved in the range 0.4–2.2%. The reliability of the method, as calculated from twenty consecutive analyses of the same plasma samples, was improved to 0.5–3.8% (C.V.). Exceptions were aspartic acid and  $\alpha$ -aminobutyric acid (5.8% and 6.9%, respectively)<sup>26</sup>. The error of the method was assessed from 180 duplicate analyses of human plasma samples. The resulting variations were in the range 1.0–4.7% (C.V.) (except for aspartic acid, 10.4%), which are considerably less than observed with the manual technique<sup>26</sup>. As expected, the limit of sensitivity (0.8 pmol) is identical with that measured with the manual procedure.

This automated method has been used in our laboratory for analysing biological samples, such as plasma and extracts of leucocytes, muscle, liver, kidney and gut, and has now been introduced in numerous other laboratories. Typical analysis of (A) standard and (B) human plasma are shown in Fig. 1. When the guard column is regularly changed after 100–150 analysis, the separation remains satisfactory for at least 700 analyses, as indicated by unaltered relative retention time and peak width<sup>21,26</sup>. Indeed, the major disadvantage of the OPA method lies in the fact that only primary amines form OPA adducts<sup>22</sup>.

*Ultrasensitive HPLC applications.* In certain very particular and demanding applications, it is necessary to determine trace levels of amino acids in minute amounts of samples. By using microbore HPLC columns, we achieved the resolution of all amino acids present in protein hydrolysates at a sensitivity of 25 fmol of amino acid per injection in less than 30 min (Fig. 2). The limit of sensitivity was 5 fmol at signal-to-noise ratio of 2.5. However, it must be emphasized that elution must be carried out at a flow-rate of 50–80  $\mu$ l/min, and that reliable and reproducible mixing of the gradient solvents is difficult to accomplish at this flow-rate. In addition, fluorescence detection must be performed with a microcuvette of volume less than 3  $\mu$ l. These crucial limitations may render microbore chromatography impractical in most applications.

Another ultrasensitive application is the narrow-bore method, employing RP-HPLC columns of I.D. 1.8 mm<sup>19</sup>. Representative separations from (A) a standard and (B) a plasma sample are shown in Fig. 3. The sensitivity of the analysis is about 1 pmol of amino acid per injection and the reproducibility and reliability range between 4 and 8% (C.V.). The separation of 23 major free amino acids can be accomplished in 22 min. The limit of sensitivity is about 150 fmol at a signal-to-noise ratio of 2.5.

The great advantage of narrow-bore chromatography compared with conventional column technology is the considerably reduced consumption of expensive and polluting organic solvents, the actual use of such reagents with the narrow-bore method being only 15–20% of that with conventional RP-HPLC.

#### *FMOC-Cl-method*

Pre-column derivatization with FMOC-Cl permits the fluorimetric detection of primary and secondary amino acids as stable FMOC adducts<sup>32–34</sup>.

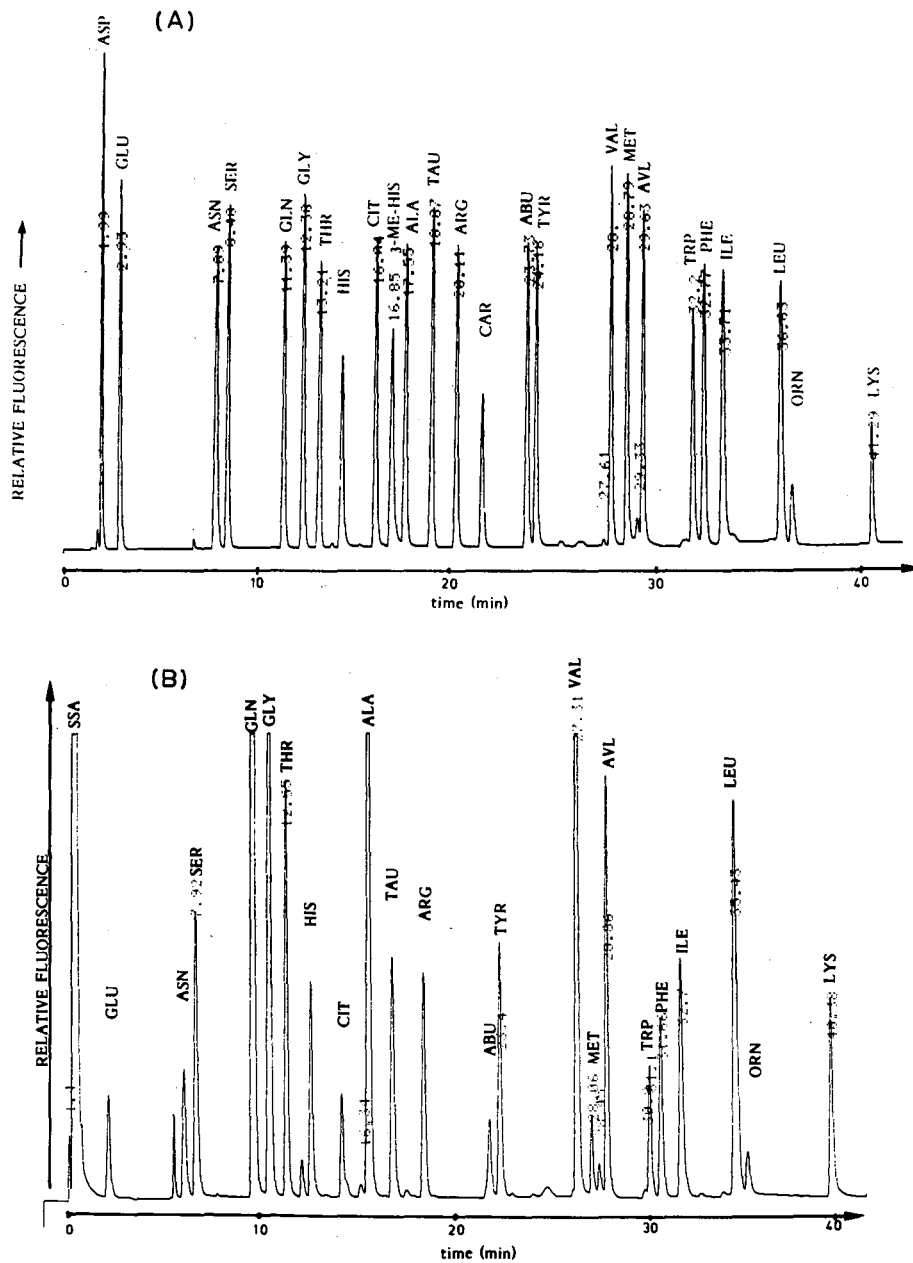


Fig. 1. Typical chromatograms of an (automated) OPA-3-MPA derivatized (A) amino acid standard and (B) human plasma. SSA = sulphosalicylic acid (deproteinization agent); CYA = cysteic acid; CIT = citrullin; TAU = taurine; CAR = carnosine; SAR = sarcosine; ABU =  $\alpha$ -aminobutyric acid; AAD =  $\alpha$ -aminoadipic acid; AVL = norvaline (internal standard); ORN = ornithine. Chromatographic conditions: column, Spherisorb ODS II ( $3 \mu\text{m}$ ) ( $150 \times 4.6 \text{ mm I.D.}$ ); guard column,  $10 \times 4.0 \text{ mm I.D.}$ ; eluent A, 0.5% tetrahydrofuran in  $12.5 \text{ mM}$  sodium phosphate buffer (pH 7.2); eluent B, 35% methanol and 15% acetonitrile in  $12.5 \text{ mM}$  sodium phosphate buffer (pH 7.2); flow-rate,  $1.0 \text{ ml/min}$ ; gradient, 0 min 0% B, 3 min 0% B, 20 min 35% B, 36 min 60% B, 40 min 70% B, 43 min 100% B, 45 min, 100% B, 47 min, 0% B; temperature,  $25^\circ\text{C}$ ; fluorescence detection,  $\lambda_{\text{ex}}$  330 nm,  $\lambda_{\text{em}}$  450 nm; injection volume,  $20 \mu\text{l}$ ; standard, 10 pmol per amino acid.

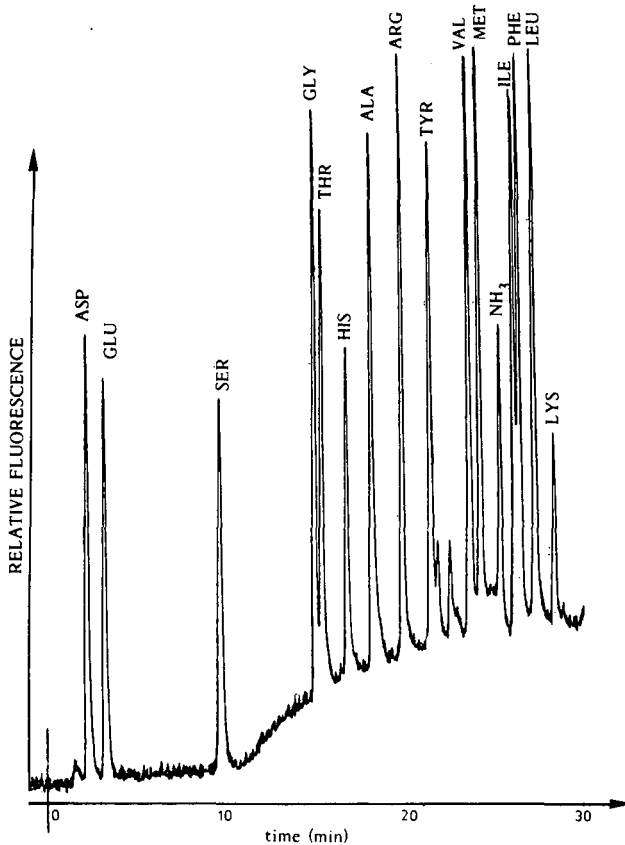


Fig. 2. Typical microbore HPLC of a hydrolysate standard mixture (OPA-3-MPA derivatization). Chromatographic conditions: column, Spherisorb ODS II (3  $\mu$ m) (250  $\times$  1.0 mm I.D.); eluent A, 0.5% acetonitrile + 2.5% methanol in 12.5 mM sodium phosphate buffer (pH 7.2), eluent B, 25% acetonitrile + 5% methanol in 12.5 mM sodium phosphate buffer (pH 7.2); flow-rate, 80  $\mu$ l/min; gradient, 0 min 0% B, 20 min 100% B; room temperature; fluorescence detection,  $\lambda_{ex}$  330 nm,  $\lambda_{em}$  450 nm; injection volume, 1  $\mu$ l; 25 fmol per amino acid.

A typical chromatogram of a physiological standard mixture (Fig. 4A) demonstrates the separation of 22 amino acids in 23 min. An application of this method to biological material (human plasma) is shown in Fig. 4B. Elongation of the column and extension of the running time permit the satisfactory separation of additional amino acids, such as citrulline and hydroxyproline<sup>34</sup>.

The mean free amino acid concentrations in human plasma determined by employing HPLC with FMOC-Cl, as compared with conventional ion-exchange analysis of the same plasma samples from ten healthy subjects, are included in Table I. As shown, the results of these two methods are in good agreement. Exceptions are histidine and taurine, yielding considerably lower concentrations (20 and 30%, respectively) with FMOC-Cl than those found by ion-exchange chromatography. Measurements of free amino acids in muscle, liver or kidney tissues are troublesome with the FMOC-Cl method owing to the low buffering capacity of the reaction mixture.

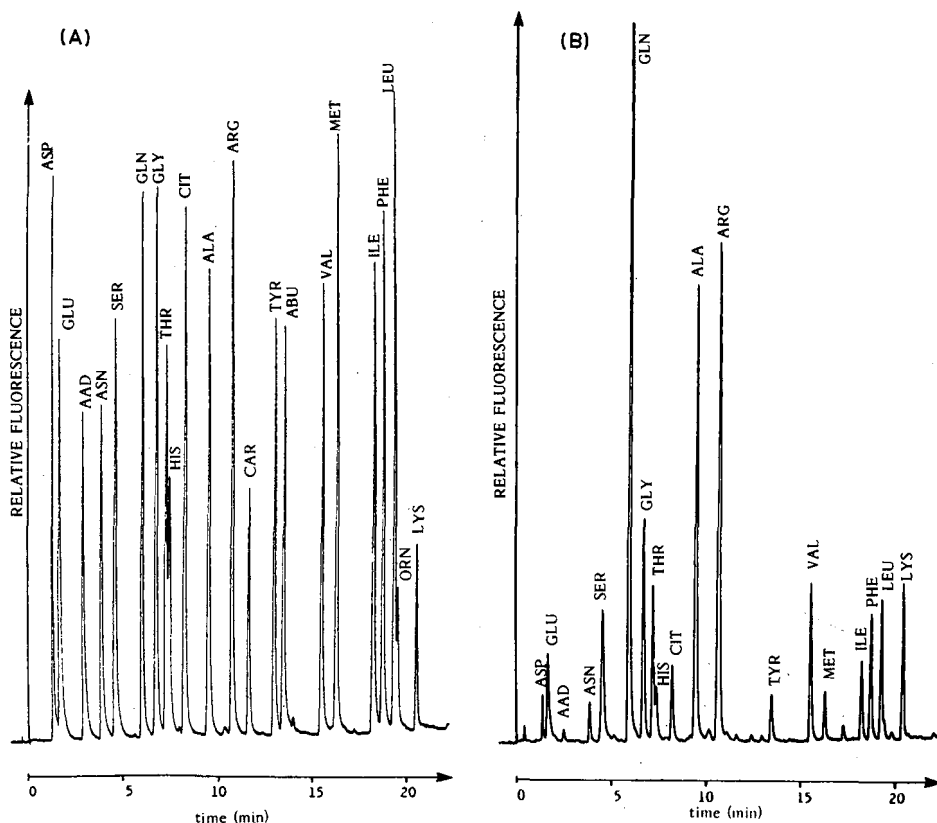


Fig. 3. Narrow-bore HPLC of (A) a standard mixture consisting of 22 amino acids and (B) TCA-precipitated rat plasma after derivatization with OPA-3-MPA. Abbreviations as in Fig. 1. Chromatographic conditions: column, Spherisorb ODS II (3  $\mu$ m) (200  $\times$  1.8 mm I.D.); eluent A, 0.5% tetrahydrofuran in 12.5 mM sodium phosphate buffer (pH 7.2); eluent B, 25% acetonitrile in 12.5 mM sodium phosphate buffer (pH 7.2); flow-rate, 200  $\mu$ l/min; gradient, 0 min 0% B, 20 min 100% B; room temperature; fluorescence detection,  $\lambda_{ex}$  330 nm,  $\lambda_{em}$  450 nm (Merck F-1000); injection volume, 1  $\mu$ l; standard, 1 pmol per amino acid.

The reproducibility of the FMOC-Cl derivatization procedure was calculated from twenty standard analyses. The C.V. ranged between 1.9 and 3.6%, except for histidine (4.6%). This can be explained by the low relative fluorescence response of FMOC-histidine which is only about 20% of that of the other FMOC-amino acids. This difference is probably caused by intramolecular quenching<sup>35</sup>. It is worth noting that determination of free tryptophan and cystine is not feasible with the FMOC-Cl method because the fluorescence of the adducts is also quenched<sup>35,36</sup>. The error of the method, based on 30 duplicate analyses of human plasma samples, ranged between 1.1 and 5.9% (C.V.), with the exception of histidine (9.2%). The detection limit at a signal-to-noise ratio of 2.5 was 1.0 pmol for all amino acids, except histidine (4.5 pmol).

The FMOC-Cl method suffers from the disadvantage that excess of strong fluorescent reagent has to be extracted manually with pentane in order to stop the

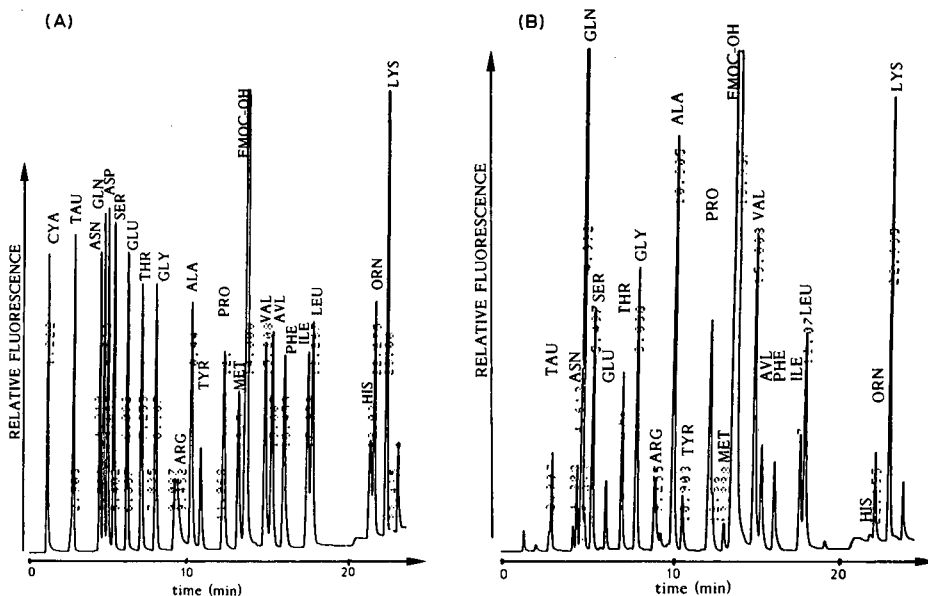


Fig. 4. Elution profiles of (A) an amino acid standard and (B) human plasma after derivatization with FMOCl. Abbreviations as in Fig. 1. Chromatographic conditions: column, Superspher CH-8 (125 × 4.0 mm I.D.); eluent A, 20% acetonitrile in 50 mM sodium acetate buffer (pH 4.2); eluent B, 70% acetonitrile in 50 mM sodium acetate buffer (pH 4.2); flow-rate, 1.5 ml/min; gradient, 0 min 10% B, 3 min 10% B, 9 min 30% B, 17 min 60% B, 18 min 100% B; temperature, 35°C; fluorescence detection,  $\lambda_{\text{ex}}$  265 nm,  $\lambda_{\text{em}}$  310 nm (Merck F-1000); injection volume, 20  $\mu$ l; standard, 5.2 pmol per amino acid, except His (10.4 pmol) and Orn (2.6 pmol).

derivatization reaction and to avoid spontaneous hydrolysis of the FMOCl adducts<sup>34</sup>. This laborious manual extraction procedure prevents the wide acceptance of this method. This shortcoming, however, might be overcome by using specially designed autosamplers and/or a combination of the FMOCl and OPA methods<sup>37</sup>.

#### PITC method

Derivatization with Edman's reagent (PITC) results in the formation of phenylthiocarbonyl (PTC) adducts of primary and secondary amino acids, which can be separated by RP-HPLC<sup>38,39</sup>. After phenylthiocarbonylation (within 5 min at room temperature), excess of coupling reagent must be thoroughly evaporated by vacuum centrifugation (Speed Vac; Savant, Farmingdale, NY, U.S.A.) to furnish acceptable separation conditions and to protect the column. The PTC-amino derivatives are stable for several days and can be automatically injected with an autosampler<sup>27</sup>.

The elution profile of a PITC-derivatized standard mixture containing 21 physiological amino acids, including proline and cystine, is depicted in Fig. 5A and that of a human plasma in Fig. 5B. It is important to note that under the conditions used, tryptophan coelutes with ornithine. The mean free amino acid concentrations of plasma acquired from ten healthy subjects agreed well with values derived from conventional amino acid analyses, with the exception of glutamic acid (Table I).

The reproducibility of the method ranged between 2.6% and 5.5% (C.V.) for all



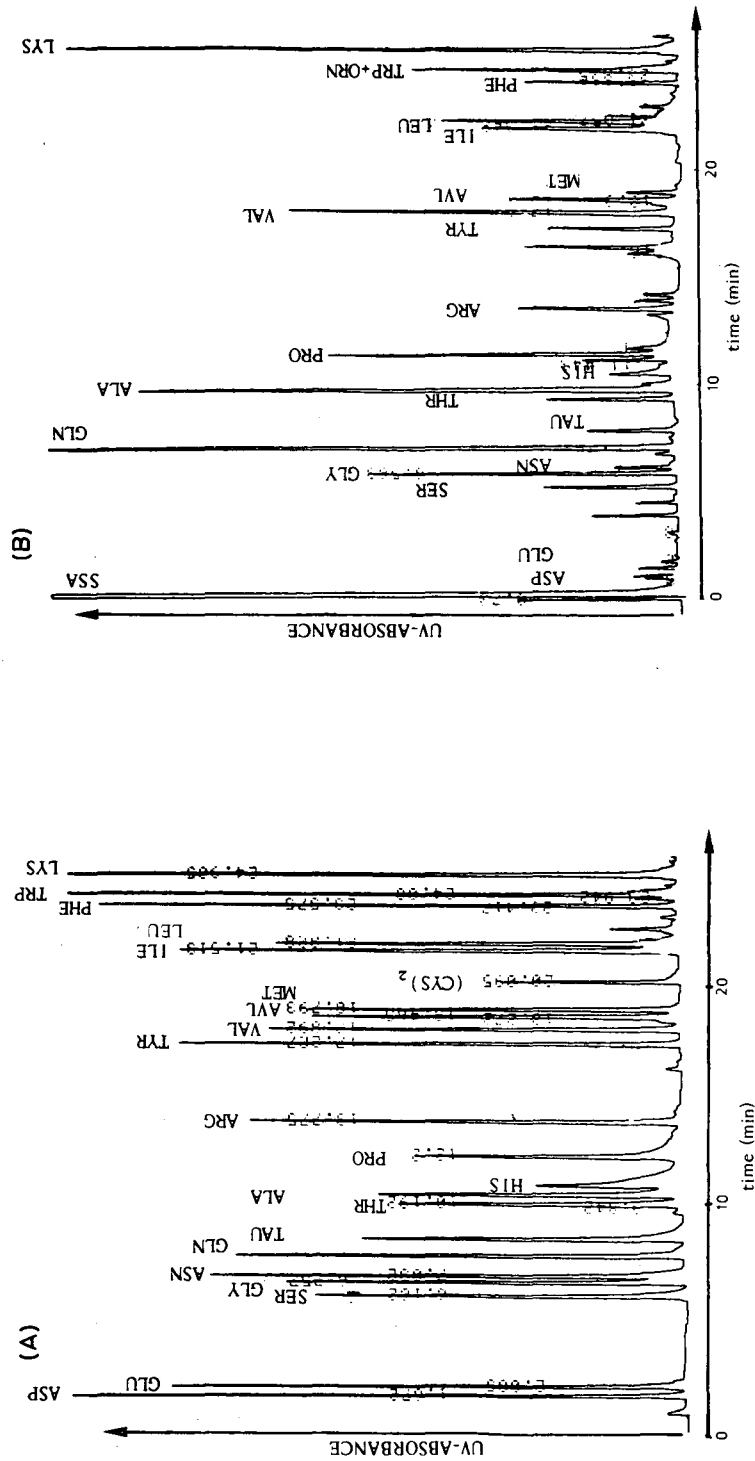


Fig. 5. Elution profiles of (A) an amino acid standard and (B) human plasma after derivatization with PITC. Abbreviations as in Fig. 1. Chromatographic conditions: column, Spherisorb ODS II (3  $\mu$ m) 125  $\times$  4.6 mm I.D.; guard column, 10  $\times$  4.0 mm I.D.; eluent A, 12.5 mM sodium phosphate buffer (pH 6.8); eluent B, 60% acetonitrile in 12.5 mM sodium phosphate buffer (pH 6.8); gradient, 0 min 0% B, 5 min 6% B, 19 min 48% B, 25 min 100% B; temperature, 37°C; UV detection, 254 nm (LKB 2151 variable-wavelength monitor); injection volume, 20  $\mu$ l; standard, 500 pmol per amino acid.

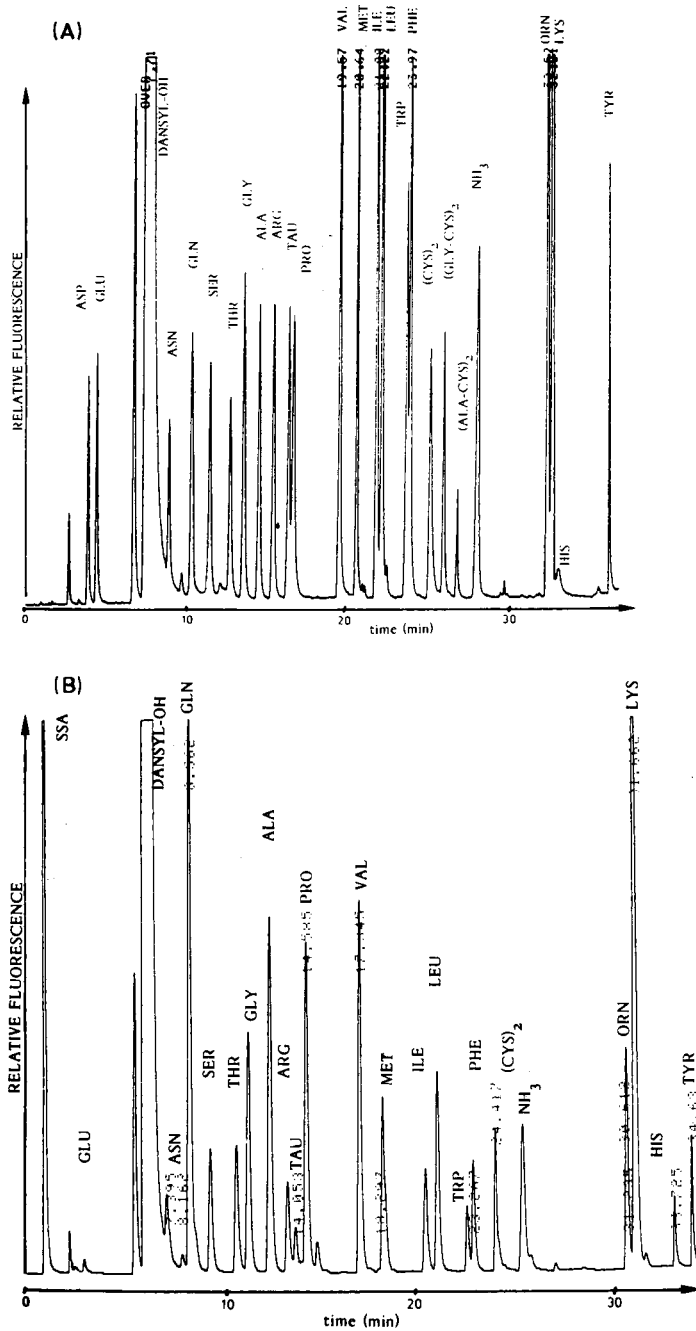


Fig. 6. Elution profile of (A) a standard mixture containing 22 amino acids and the synthetic peptides (Gly-Cys)<sub>2</sub> and (Ala-Cys)<sub>2</sub> and (B) a human plasma after derivatization with dansyl-Cl. Abbreviations as in Fig. 1. Chromatographic conditions: column, Spherisorb ODS II (3  $\mu$ m) (125  $\times$  4.6 mm I.D.); guard column, 10  $\times$  4.0 mm I.D.; eluent A, 3% tetrahydrofuran in 15 mM sodium phosphate buffer (pH 6.3); eluent B, 60% acetonitrile in 15 mM sodium phosphate buffer (pH 6.3); flow-rate, 1.2 ml/min; gradient, 0 min 15% B, 15 min 30% B, 18 min 40% B, 25 min 45% B, 30 min 60% B, 35 min 60% B, 40 min 100% B; temperature, 25°C; fluorescence detection,  $\lambda_{\text{ex}}$  330 nm,  $\lambda_{\text{em}}$  550 nm (Merck F-1000); injection volume, 20  $\mu$ l; standard, 40 pmol per amino acid and peptide except cystine (20 pmol).

amino acids except histidine (6.3%) and cystine (10.0%). Apart from the poor reproducibility, PTC-cystine also revealed an inferior linearity, and therefore the determination of free cystine is not practicable with this method.

As UV detection has to be employed, the sensitivity of the PITC method is low compared with that of the other methods. The limit of sensitivity is 50 pmol at a signal-to-noise ratio of 2.5, which is *ca.* 50 times less sensitive than detection of OPA or FMOc adducts. This is in excellent agreement with most previous studies<sup>38,40</sup>, but is in contrast to Bidlingmeyer *et al.*<sup>39</sup>, who reported a 10-fold lower detection limit (4 pmol at a signal-to-noise ratio of 5) when analysing a standard amino acid mixture. However, such a level is of little practicable value for routine analysis of biological materials.

In addition to poor sensitivity, inferior linearity with cystine and the lengthy sample preparation, we observed rapid deterioration of the columns when analysing biological fluids. This is a serious shortcoming of the PITC method. According to our experience, a maximum of 150 physiological analyses could be performed in spite of the use of rigorous sample preparation and suitable guard columns. The reduced column lifetime is probably caused by traces of the PITC reagent obviously present in the samples, despite careful vacuum evaporation.

#### *Dansyl-Cl method*

Dansyl-Cl is a well known fluorogenic reagent for the determination of primary and secondary amines<sup>41,42</sup>. According to Tapuhi *et al.*<sup>43</sup>, dansyl-amino acid adducts are formed under optimal conditions within 35–50 min at room temperature in the

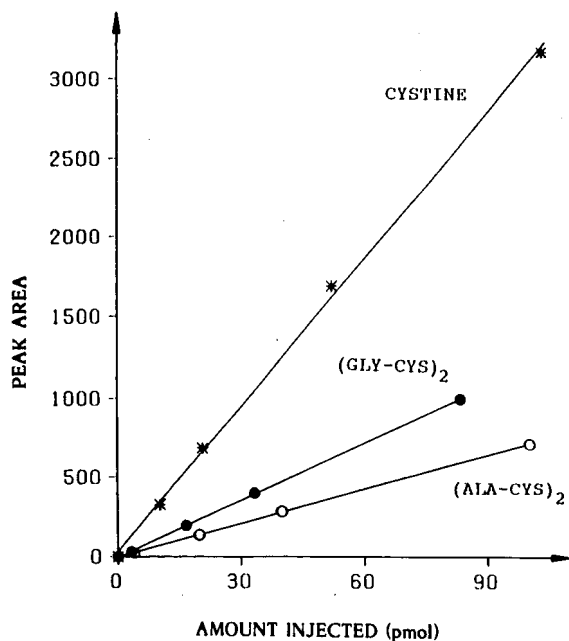


Fig. 7. Linearity obtained with dansyl derivatives of cystine [(Cys)<sub>2</sub>], bis glycyl-L-cystine [(Gly-Cys)<sub>2</sub>] and bis-L-alanyl-L-cystine [(Ala-Cys)<sub>2</sub>] in the range 5–150 pmol.

dark<sup>42</sup>. After separation by RP-HPLC, the dansylated derivatives are detected fluorimetrically. Under these conditions, histidine formed multiple peaks whereas for cystine, ornithine, lysine and tyrosine only the didansyl derivatives were detectable. The minor histidine peak (corresponding to the monoderivatized adduct) eluted between asparagine and glutamine and therefore did not interfere with the determination of the other amino acids.

Fig. 6A shows a typical chromatogram of a dansylated standard mixture containing 22 primary and secondary amino acids, including cystine, and two cystine-containing short-chain peptides. The elution profile of a dansylated human plasma is depicted in Fig. 6B. All the major physiological amino acids can be separated in 35 min.

The reproducibility of the method was calculated from ten standard analyses; the C.V. ranged between 1.5% and 4.1% for amino acids and peptides, except histidine (6.4%). The poor reproducibility for histidine can be explained by the low relative fluorescence response of the didansylated adduct (only about 10% of the other amino acids), which is caused by intramolecular quenching<sup>35</sup> and by the formation of two dansyl derivatives. The error of the method was calculated from 30 duplicate analyses of rat plasma and ranged between 1.7% and 4.5% (C.V.).

In contrast to the PITC method, the dansyl-Cl technique shows excellent linearity for cystine and also for cystine-containing short-chain peptides (Fig. 7). Hence, the dansyl-Cl method appears to offer the only quantitative approach for measuring free cystine in biological material by HPLC techniques<sup>44</sup>.

## CONCLUSION

Each of the four methods investigated permits the measurement of the concentrations of the 21–26 major free amino acids in 13–40 min<sup>21,23,26,27,34,44</sup>. The sensitivity, errors of the methods, advantages and disadvantages and problems with certain “difficult” amino acids are summarized in Table II.

Automated derivatization and the wide range of applicability clearly favour the

TABLE II  
HPLC ANALYSES OF FREE AMINO ACIDS: COMPARISON OF FOUR DERIVATIZATION METHODS

<i>Parameter</i>	<i>OPA</i> ( <i>automated method</i> )	<i>FMOC-Cl</i>	<i>PITC</i>	<i>Dansyl-Cl</i>
Limit of sensitivity, pmol (Signal-to-noise ratio = 2.5)	0.8	1.0	5.0	1.5
Error of the method (C.V.,%) (based on duplicate determinations)	1.0–4.7	1.1–5.9	3.6–7.0	1.7–4.5
Reproducibility (C.V.,%)	0.4–2.2	1.9–4.6	2.6–5.5	1.5–4.1
Stable adducts <sup>a</sup>	N	Y	Y	Y
Detection of secondary amines/cystine <sup>a</sup>	N/N	Y/N	Y/Y	Y/Y
Laborious	–	+++	++	+
Problematic amino acids	Asp, Trp	His, Trp	Orn, Trp, His, (Cys) <sub>2</sub>	His, Asn

<sup>a</sup> Y = yes; N = no.

OPA method for routine analyses of primary free amino acids (except cystine) in biological fluids. If determination of secondary amino acids is desirable, the use of the FMOC-Cl method or a combination of the OPA and FMOC-Cl techniques<sup>37</sup> is recommended. The use of the dansyl-Cl technique is suggested when the determination of free cystine or cystine-containing short-chain peptides is required. Application of the PITC method might be beneficial in frame of clinical and/or protein chemistry, if sufficient sample material is available.

## REFERENCES

- 1 D. H. Spackman, W. H. Stein and S. Moore, *Anal. Chem.*, 30 (1958) 1190.
- 2 K. A. Piez and L. Morris, *Anal. Biochem.*, 1 (1960) 187.
- 3 P. B. Hamilton, *Anal. Chem.*, 35 (1963) 2055.
- 4 G. Ogden, *Nature (London)*, 320 (1986) 771.
- 5 I. Molnar and C. Horvath, *J. Chromatogr.*, 142 (1977) 623.
- 6 P. Lindroth and K. Mopper, *Anal. Chem.*, 51 (1979) 1667.
- 7 D. W. Hill, F. H. Walters, T. E. Wilson and J. D. Stuart, *Anal. Chem.*, 51 (1979) 1338.
- 8 W. S. Gardner and W. H. Miller, III, *Anal. Biochem.*, 101 (1980) 61.
- 9 M. H. Fernstrom and J. D. Fernstrom, *Life Sci.*, 29 (1981) 2119.
- 10 A. Henschen and F. Lottspeich, in A. Henschen (Editor), *High Performance Liquid Chromatography in Biochemistry*, VCH, Weinheim, 1985, p. 141.
- 11 D. C. Turnell and J. D. H. Cooper, *Clin. Chem.*, 28 (1982) 527.
- 12 D. L. Hogan, K. L. Kraemer and J. I. Isenburg, *Anal. Biochem.*, 127 (1982) 17.
- 13 P. Kabus and G. Koch, *Biochem. Biophys. Res. Commun.*, 108 (1982) 783.
- 14 B. H. Jones and J. P. Gilligan, *J. Chromatogr.*, 266 (1983) 471.
- 15 M. Griffin, S. J. Price and T. Palmer, *Clin. Chim. Acta*, 125 (1982) 89.
- 16 M. O. Fleury and D. V. Ashley, *Anal. Biochem.*, 133 (1983) 330.
- 17 K. Venema, W. Leevers, J. O. Bakker, G. Haayer and J. Korf, *J. Chromatogr.*, 260 (1983) 371.
- 18 R. J. Smith and K. A. Panico, *J. Liq. Chromatogr.*, 8 (1985) 1783.
- 19 H. P. Fiedler and A. Plaga, *J. Chromatogr.*, 386 (1987) 229.
- 20 P. Fürst, H. Godel and T. A. Graser, in H. Kalász (Editor), *Chromatography '85*, Akadémiai Kiadó, Budapest, 1985.
- 21 T. A. Graser, H. Godel, S. Albers, P. Földi and P. Fürst, *Anal. Biochem.*, 151 (1985).
- 22 M. Roth, *Anal. Chem.*, 43 (1971) 880.
- 23 H. Godel, T. A. Graser, P. Földi, P. Pfaender and P. Fürst, *J. Chromatogr.*, 297 (1984).
- 24 T. Hayashi, H. Tsuchiya and H. Naruse, *J. Chromatogr.*, 274 (1982) 318.
- 25 P. Kucera and H. Umagat, *J. Chromatogr.*, 255 (1983) 563.
- 26 T. A. Graser, *Thesis*, University of Hohenheim, Stuttgart, 1987.
- 27 P. Fürst, P. Stehle and T. A. Graser, *Infusionstherapie*, 14 (1987) 137.
- 28 J. Christophe, J. Winand, R. Kutzner and M. Hebbelinck, *Am. J. Physiol.*, 221 (1971) 453.
- 29 P. G. Lunn, R. G. Whitehead and B. A. Baker, *Br. J. Nutr.*, 36 (1976) 219.
- 30 H. Brückner, I. Bosch, T. A. Graser and P. Fürst, *J. Chromatogr.*, 386 (1987) 251.
- 31 H. Brückner, I. Bosch, T. A. Graser and P. Fürst, *J. Chromatogr.*, 395 (1987) 569.
- 32 S. Einarsson, B. Josefsson and S. Lagerkvist, *J. Chromatogr.*, 282 (1983) 609.
- 33 S. Einarsson, *J. Chromatogr.*, 348 (1985) 213.
- 34 H. Godel, *Thesis*, University of Hohenheim, Stuttgart, 1986.
- 35 G. G. Guilbault, *Practical Fluorescence. Theory, Methods, and Techniques*, Marcel Dekker, New York, 1973, p. 307.
- 36 A. F. Fell, in J. M. Rattenbury (Editor), *Amino Acid Analysis*, Ellis Horwood, Chichester, 1981, p. 86.
- 37 R. Schuster, *J. Chromatogr.*, 431 (1988) 271.
- 38 R. L. Henrikson and S. C. Meredith, *Anal. Biochem.*, 136 (1984) 65.
- 39 B. A. Bidlingmeyer, S. A. Cohen and T. L. Tarvin, *J. Chromatogr.*, 336 (1984) 93.
- 40 H. Scholze, *J. Chromatogr.*, 350 (1985) 453.
- 41 N. Seiler, *Methods Biochem. Anal.*, 18 (1970) 259.
- 42 V. Neuhoff, in V. Neuhoff (Editor), *Molecular Biology, Biochemistry and Biophysics*, Springer, New York, 1973, p. 85.
- 43 Y. Tapuhi, D. E. Schmidt, W. Lindner and B. L. Karger, *Anal. Biochem.*, 115 (1981) 123.
- 44 P. Stehle, S. Albers, L. Pollack and P. Fürst, *J. Nutr.*, 118 (1988) 1470.



CHROM. 21 988

## PREPARATION OF ELECTROPHORIC DERIVATIVES OF N7-(2-HYDROXYETHYL)GUANINE, AN ETHYLENE OXIDE DNA ADDUCT

KARIMAN ALLAM, MANASI SAHA and ROGER W. GIESE\*

*Department of Medicinal Chemistry in the College of Pharmacy and Allied Health Professions, and Barnett Institute of Chemical Analysis and Materials Science, Northeastern University, Boston, MA 02115 (U.S.A.)*

---

### SUMMARY

Ethylene oxide, a potential human carcinogen, mainly damages DNA by reacting at guanine sites to form N7-(2-hydroxyethyl)guanine. In order to determine this DNA adduct with high sensitivity by gas chromatography, we have prepared, for comparison purposes, four electrophoric derivatives. The two that are most promising to date are bis- and tris-pentafluorobenzyl products prepared by first chemically transforming the N7-(2-hydroxyethyl)guanine to a corresponding xanthine, and then reacting the latter with pentafluorobenzyl bromide. These two derivatives are obtained in good yields and give molar responses of 0.6 and 0.5, respectively, relative to that of lindane by gas chromatography with electron-capture detection.

---

### INTRODUCTION

Ethylene oxide is considered to be a potential human carcinogen<sup>1</sup> and is weakly mutagenic<sup>2</sup>. Its genotoxic effects and their reference to human cancer have been reviewed<sup>3,4</sup>. It causes cancer in exposed animals (see, *e.g.*, ref. 5). This chemical is widely used: approximately  $2.5 \cdot 10^6$  tons per year are consumed in Western Europe, and about  $8 \cdot 10^5$  tons are produced annually in the U.S.A. where roughly 150 000 workers deal with it daily in various industrial processes<sup>4</sup> (1986 data). For example it is commonly used in hospitals to sterilize medical equipment<sup>6</sup>.

As an alkylating agent, ethylene oxide reacts with both proteins and DNA. Hemoglobin adducts of ethylene oxide have been measured to monitor animal or human exposure to this chemical<sup>7-10</sup>. The reaction of ethylene oxide with DNA is probably the reason for its carcinogenic and mutagenic effects. N7-(2-Hydroxyethyl)guanine (**1**) is the main product when it reacts with DNA<sup>7</sup>. Other, less abundant adducts are O<sup>6</sup>-(2-hydroxyethyl)guanine, and N1, N3 and N7 adenine products<sup>11</sup>.

Our approach to quantifying a DNA adduct such as that from ethylene oxide is to isolate the adduct as a modified nucleobase, derivatize it with an electrophore, and quantify the product by gas (GC) or liquid (LC) chromatography with detection by electron-capture negative-ion mass spectrometry (ECNI-MS). Such methodology is attractive because of its potential for high sensitivity and specificity, which is required for measurement of DNA adducts in human samples. Towards this general goal, we

have been optimizing appropriate electrophoric derivatives, sample preparation steps and instrumental conditions (see, *e.g.*, ref. 12). It is useful to form a pentafluorobenzyl derivative of an alkyl and related DNA adduct that can be isolated as a modified nucleobase, because of the excellent GC–ECNI–MS properties of such a derivative. Prior work has included the development of a sensitive electrophoric derivative of O<sup>6</sup>-(2-hydroxyethyl)guanine<sup>1,3</sup>. Here we report the preparation of such a derivative of N7-(2-hydroxyethyl)guanine.

## EXPERIMENTAL

### Materials

N7-(2-Hydroxyethyl)guanine was purchased from Chemical Science Labs. (Lexena, KS, U.S.A.). N7-Methylxanthine was purchased from Sigma (St. Louis, MO, U.S.A.). Pentafluorobenzyl bromide (PFBzBr), potassium carbonate, chloroacetaldehyde, diethyl ether, methyl iodide and tetrabutylammonium hydrogen sulphate were from Aldrich (Milwaukee, WI, U.S.A.). Organic solvents were from American Scientific (Boston, MA, U.S.A.). They were distilled and dried over molecular sieves prior to use. Preparative and analytical thin-layer chromatography (TLC) separations were performed with GHLF silica gel Uniplates with fluorescence indicator (Analtech, Newark, DE, U.S.A.). Flash column chromatography was performed with silica gel 60 (200–300 mesh) from (EM Science, NJ, U.S.A.).

All compositions were v/v unless indicated otherwise.

### Synthesis

*N*<sup>2</sup>,3-*Etheno-N*7-(2-hydroxyethyl)guanine (**2**). A mixture of N7-(2-hydroxyethyl)guanine (30 mg, 0.15 mmol) and chloroacetaldehyde diethyl ether (7 ml, 46 mmol) in 30 ml of water was heated at 80°C for 15 h. The reaction turned clear and homogenous after 6 h. Formation of product was monitored by TLC (fluorescence spot). The residue after rotary evaporation was further evaporated with 10 ml of benzene. The crude product was purified by flash column chromatography using methanol–dichloromethane (15:85), yielding 25 mg (80%) of product. <sup>1</sup>H NMR (300 MHz, C<sup>2</sup>H<sub>3</sub>O<sup>2</sup>H) δ 8.32 (s, 1H), 8.0 (d, 1H), 7.65 (d, 1H), 4.59 (t, 2H), 3.56 (t, 2H).

*N*1-Pentafluorobenzyl-*N*<sup>2</sup>,3-*etheno-N*7-(2-hydroxyethyl)guanine (**3**). To a stirred suspension of **2** (10 mg, 0.046 mmol) in 5 ml of acetonitrile–acetone (4:1) were added 12 mg (0.085 mmol) of potassium carbonate. The reaction mixture was stirred for 3 min and pentafluorobenzyl bromide (0.1 ml, 0.65 mmol) was added. The reaction mixture was stirred at room temperature for 20 h and filtered. The filtrate was vacuum evaporated and the crude product was purified by preparative TLC using methanol–chloroform (1:10), to yield 7.3 mg (45%) of product. <sup>1</sup>H NMR (C<sup>2</sup>H<sub>3</sub>O<sup>2</sup>H) δ 8.01 (s, 1H), 7.65 (d, 1H), 7.35 (d, 1H), 5.49 (s, 2H), 4.59 (t, 2H), 3.95 (t, 2H).

*N*7-(2-Hydroxyethyl)xanthine (**4**). N7-(2-Hydroxyethyl)guanine (20 mg, 0.102 mmol) was dissolved in 1 M hydrochloric acid (1.5 ml) and the solution was cooled to 0°C. A cold solution of sodium nitrite (105 mg, 1.52 mmol) in 0.8 ml 1 M hydrochloric acid was added dropwise and the resulting solution was stirred at room temperature for 30 min and continued at 80°C overnight. TLC indicated the disappearance of starting material and appearance of a new product with higher *R*<sub>F</sub> value using *n*-butanol–acetic acid–water (10:0.5:2). The reaction mixture was neutralized with sodi-



um hydroxide and cooled to 0°C. The precipitated product was isolated by centrifugation, washed three times with cold water and once with hexane. It was vacuum dried yielding product as a white powder (14 mg, 70%). MS (electron impact, EI): 196 ( $M^+$ ), UV:  $\lambda_{\max}$  260, 228 nm (1 M HCl).  $^1\text{H NMR}$  (300 MHz,  $^2\text{H}_2\text{O}/^2\text{HCl}$ )  $\delta$  8.75 (s, 1H), 4.65 (t, 2H), 4.01 (t, 2H).

*1,3-Bis-(pentafluorobenzyl)-N7-(2-hydroxyethyl)xanthine (5)*. To a stirred suspension of potassium carbonate (46 mg, 0.33 mmol) in dry acetone–acetonitrile (1:1, 1 ml) at room temperature was added 6.5 mg (0.033 mmol) of N7-(2-hydroxyethyl)xanthine. Pentafluorobenzyl bromide (0.49 ml, 3.3 mmol) was added followed by continued stirring for 24 h. TLC using ethyl acetate–hexane (85:15), showed the product at  $R_F = 0.54$ . The potassium carbonate was removed by filtration and washed with acetone–acetonitrile (1:1). Evaporation of the solvent yielded a yellow solid which was purified by flash column chromatography using ethyl acetate–hexane (80:20), followed by evaporation. Hexane addition and overnight storage in the refrigerator gave, after filtration and drying, 9.5 mg (52%) of white solid.  $^1\text{H NMR}$  ( $\text{C}^2\text{HCl}_3$ , 300 MHz)  $\delta$  7.67 (s, 1H), 5.29 (s, 2H), 5.40 (s, 2H), 4.45 (t, 2H), 3.95 (t, 2H).

*1,3-Bis-(pentafluorobenzyl)-N7-(2-methoxyethyl)xanthine (7)*. To a stirred solution of **5** (4 mg, 0.007 mmol) in dichloromethane (1.4 ml) was added 0.7 ml of 1 M potassium hydroxide followed by  $(\text{C}_4\text{H}_9)_4\text{NHSO}_4$  (12.2 mg, 0.035 mmol). After the resulting solution was stirred at room temperature for 5 min, methyl iodide (0.028 ml, 0.45 mmol) was added and stirring was continued for 18 h. TLC using ethyl acetate–hexane (1:1), indicated the disappearance of starting material and formation of a new product ( $R_F = 0.4$ ). The organic layer was separated, the aqueous layer extracted three times with dichloromethane and the combined dichloromethane fractions were washed with 5% hydrochloric acid, brine, and dried over anhydrous sodium sulfate. The filtered solution was evaporated *in vacuo* to yield a crude product which was purified by flash column chromatography using ethyl acetate–hexane (1:1), yielding a white solid (3.7 mg, 90%).  $^1\text{H NMR}$  (300 MHz,  $\text{C}^2\text{HCl}_3$ ):  $\delta$  7.68 (s, 1H), 5.04 (s, 2H), 5.25 (s, 2H), 4.25 (t, 2H), 3.79 (t, 2H), 3.25 (s, 3H).

*1,3-Bis-(pentafluorobenzyl)-N7-(2-[pentafluorobenzyloxy]ethyl)xanthine (6)*. To a stirred solution of **5** (2 mg, 0.0035 mmol) in dichloromethane (0.6 ml) was added 0.3 ml of 1 M potassium hydroxide,  $(\text{C}_4\text{H}_9)_4\text{NHSO}_4$  (6.1 mg, 0.018 mmol) and pentafluorobenzyl bromide (0.01 ml, 0.07 mmol). After stirring at room temperature for 20 h, the reaction mixture was worked up the same as for **5**. Flash column chromatography using ethyl acetate–hexane (3:7), yielded a yellow oil (1.2 mg, 47%).  $^1\text{H NMR}$  (300 MHz,  $\text{C}^2\text{HCl}_3$ )  $\delta$  7.58 (s, 1H), 5.45 (s, 2H), 5.25 (s, 2H), 4.64 (s, 2H), 4.45 (t, 2H), 3.80 (t, 2H). MS (EI)  $m/z$  735 ( $M^+$ ), 554 ( $M - \text{PFBz}$ ), 181 ( $\text{PFBz}$ ).

Compound **6** was also synthesized as follows: to a stirred solution of **4** (2.4 mg, 0.012 mmol) in dichloromethane (0.4 ml), 1 M potassium hydroxide (0.2 ml),  $(\text{C}_4\text{H}_9)_4\text{NHSO}_4$  (22 mg, 0.073 mmol) and pentafluorobenzyl bromide was added. The work-up procedure was the same for **6**, giving 8 mg (80%) of product after flash column chromatography.

*1,3-Bis-(pentafluorobenzyl)-N7-methylxanthine (10)*. To a stirred solution of N7-methylxanthine (6.5, 0.039 mmol) in 5 ml of acetonitrile–acetone (1:1), was added 46 mg (0.33 mmol) of potassium carbonate. The reaction mixture was stirred for 1 min and pentafluorobenzyl bromide (0.25 ml, 1.4 mmol) was added. The reaction was stirred for 24 h at room temperature and filtered. The filtrate was rotary-evaporated

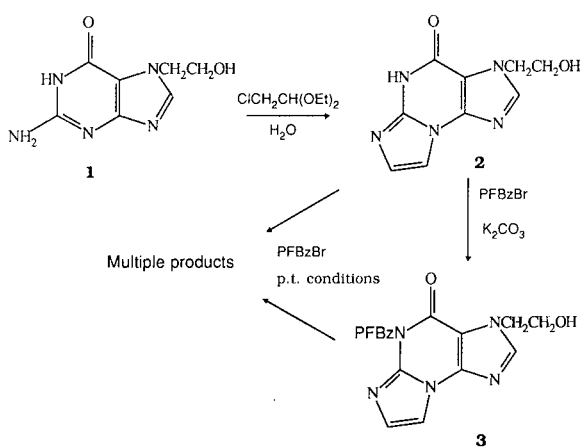
and the crude product was purified by flash column chromatography using ethyl acetate–hexane (5:3), to yield 11.5 mg (55%) of product.  $^1\text{H}$  NMR (300 MHz,  $^2\text{HCl}_3$ ):  $\delta$  7.5 (s, 1H), 5.39 (s, 2H), 5.28 (s, 2H), 3.95, (s, 3H).

## RESULTS AND DISCUSSION

It is attractive to determine alkyl and related DNA adducts by GC–ECNI–MS as their pentafluorobenzyl derivatives, because such derivatives generally are formed easily in high yield, chemically and physically stable, and detected readily with high sensitivity by this technique<sup>13</sup>. Thus we sought such a derivative for N7-(2-hydroxyethyl)guanine, an ethylene oxide DNA adduct.

Unfortunately, the derivatization procedures that we used previously to form pentafluorobenzyl derivatives of a series of pyrimidines and purines<sup>13–15</sup> including O<sup>6</sup>-(2-hydroxyethyl)guanine<sup>13</sup>, were not successful when applied to N7-(2-hydroxyethyl)guanine (**1**). Basically we either recovered unreacted starting material or obtained a complex mixture of products, based on analysis by TLC or HPLC. It appeared that starting material was recovered because it failed to dissolve in the reaction mixture. Efforts to overcome this latter problem by conducting the reactions on smaller amounts of **1**, or starting with **1** predissolved in aqueous acid or base, gave similarly poor results.

Faced with this difficulty, we adopted a strategy of chemically transforming the N7-(2-hydroxyethyl)guanine prior to derivatizing it with pentafluorobenzyl bromide (PFBzBr). One of two approaches that we investigated in parallel is shown in Scheme 1. Following a known procedure<sup>16</sup>, which is a modification of the procedure of Oesch and Doerjer<sup>17</sup>, we subjected **1** to a cyclocondensation reaction with chloroacetaldehyde diethyl ether in water at 80°C. This gave a high yield (see Table I) of N<sup>2</sup>,3-etheno-N7-(2-hydroxyethyl)guanine (**2**), a fluorescent compound. This product in turn could be pentafluorobenzylated under mild conditions (potassium carbonate) to form **3**. However, further derivatization of **3** with PFBzBr under phase transfer con-



Scheme 1.

TABLE I  
PREPARATION AND GC-ECD PROPERTIES OF DERIVATIZED PURINES

Reaction	Product		
	% Yield (preparative)	Retention time (min) <sup>a</sup>	Response <sup>b</sup>
1 → 2	80%	—	—
2 → 3	45%	7.9	0.06
1 → 4	70%	—	—
4 → 5	52%	8.0	0.6
4 → 6	80%	10.7	0.5
5 → 6	47%	10.7	0.5
5 → 7	90%	7.3	0.05
9 → 10	49%	7.2	0.1

<sup>a</sup> For GC conditions, see Fig. 1.

<sup>b</sup> Molar response by GC-ECD based on a comparison of the peak area relative to the peak area relative to that of lindane.

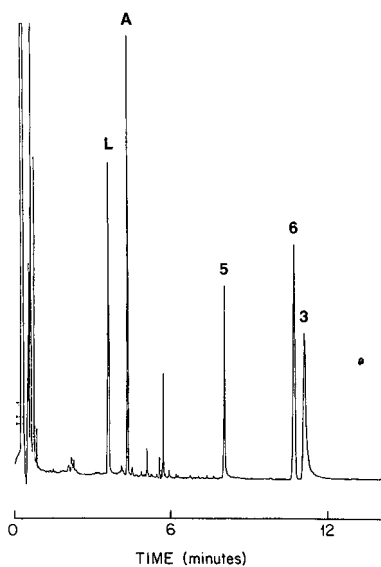


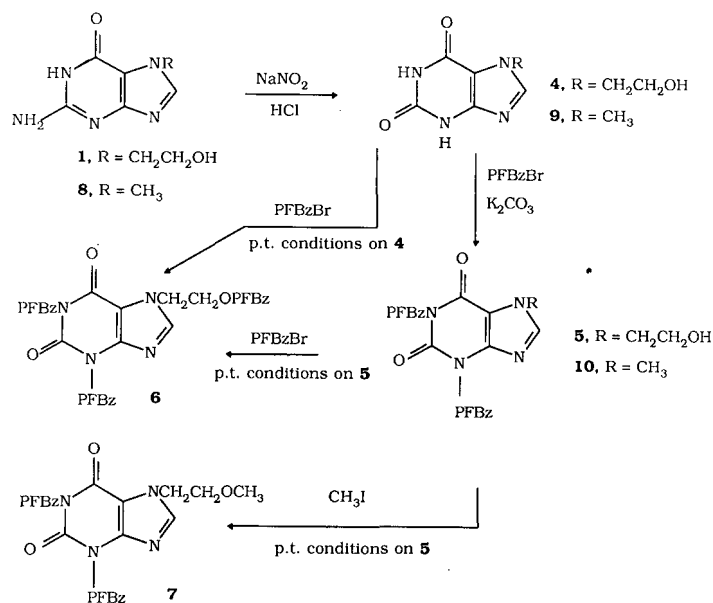
Fig. 1. GC-ECD chromatogram of lindane (L, 6.6 pg), aldrin (A, 6.6); **3** (73.6); **5** (2.5); and **6** (2.7). A 1- $\mu$ l solution of these compounds in toluene was on-column injected onto a 15 m  $\times$  0.321 mm Ultra cross-linked 5% phenyl methyl silicone fused-silica capillary column, 0.17  $\mu$ m film thickness (Hewlett-Packard, Palo Alto, CA, U.S.A.); injector 50°C; column 120°C. The injector was programmed immediately at a setting of 180°C/min up to 260°C, and the column was programmed, after a 2 min hold, at 80°C/min up to 260°C. The carrier gas was helium at 6 ml/min and the make-up gas was nitrogen at 24 ml/min.

ditions, or of **2** directly, gave a complex mixture of products. Although **3** itself could be determined by GC–electron-capture detection (ECD) (Fig. 1, Table I), it gave a tailed GC peak. Further, its inherent fluorescence was considered a drawback as well, since it therefore would tend to decompose upon exposure to light.

The second type of chemical transformation that we investigated is shown in Scheme 2. Using reaction conditions similar to those employed by others to convert guanine to xanthine<sup>18</sup>, we treated **1** with nitrous acid to form N7-(2-hydroxyethyl)-xanthine (**4**), in a 70% yield. Further reaction of **4** with PFBzBr under mild conditions gave **5**. The fully pentafluorobenzylated product **6** could be obtained by reacting either **4** or **5** with PFBzBr under phase transfer conditions. The better of the two pathways is the direct conversion of **4** to **6**, since this saves a step and also gives a slightly higher yield than the two step pathway. We also methylated the hydroxy group of **5** with methyl iodide under phase transfer conditions, forming **7**.

To help establish the generality of the nitrous acid-pentafluorobenzylation reaction sequence (shown in Scheme 2) for similar N7-substituted guanines, and also to provide a related product for comparison purposes, we subjected N7-methylguanine (**8**), to two of the same reactions. This work is summarized as well in Scheme 2, showing the successive formation of N7-methylxanthine (**9**) and then N1,N3-bis-(pentafluorobenzyl)-N7-methylxanthine (**10**).

Table I summarizes the yields for above reactions, along with the retention times and molar responses of the appropriate products of GC–ECD. Basically the behavior of the compounds by GC–ECD is good, as revealed by the moderate retention times and, as shown in Fig. 1, relatively sharp peaks. Noteworthy is the good behavior of the pentafluorobenzyl derivative **5**, in spite of its free, primary hydroxyl group. This makes it puzzling why **7**, the corresponding methyl ether, gives a much



Scheme 2.

lower response. For **10** as well, the related N7-methyl derivative, the response is also low. Whether these differences in response reflect variations in the losses of the compounds in the GC-ECD, or inherent differences in their electrophoricity, is not clear. In studies of other structurally complex, strong electrophores by GC-ECD, we have encountered similar, complex results of this type<sup>19</sup>.

Although it is difficult to prove, we believe that, in the present study, the variations in response reflect differences in the recoveries of these compounds in the GC-ECD. There are two considerations that encourage this hypothesis. First is that the compounds probably all undergo electron capture by the same mechanism: dissociative electron capture forming a parent anion and pentafluorobenzyl radical, based on our studies of related derivatives by ECNI-MS<sup>13</sup>. Secondly, we have observed that surface effects producing losses of structurally complex, strong electrophores in a GC-ECD can be highly specific<sup>19-21</sup>.

Taking into account both the reaction yields and the GC-ECD behavior of the compounds, two emerge as the best ones for the trace determination of N7-(2-hydroxyethyl)guanine by GC-ECD or GC-ECNI-MS: **5** and **6**. They are comparable in terms of ease of formation as well as GC-ECD properties. Whether they will both continue to perform similarly at lower trace levels will be defined in our future studies, including an extension of the method to the determination of N7-(2-hydroxyethyl)guanine in biological samples.

The results presented here are relevant to N7-guanine adducts derived from exposure of DNA to other chemicals of industrial importance besides ethylene oxide. Ethene is metabolized to ethylene oxide, and, not surprising then, also gives rise to hydroxyethylations of nucleophilic sites on protein and DNA<sup>7</sup>. One of the DNA adducts arising from *in vivo* exposure to vinyl chloride, a known human carcinogen, is N7-(2-oxoethyl)guanine<sup>2</sup>. Potentially this adduct could be reduced to the corresponding alcohol for subsequent derivatization by our technique. The carcinogen styrene, via metabolism to styrene-7,8-epoxide, predominantly reacts like ethylene oxide at the N7 position of guanine producing a mixture of positional and diastereomeric hydroxyphenethyl adducts<sup>22</sup>. These products should also be amenable to our procedures.

#### ACKNOWLEDGEMENT

This work was sponsored by Grant 35843 from the National Cancer Institute. Contribution No. 401 from the Barnett Institute.

#### REFERENCES

- 1 P. J. Landrigan, T. J. Munhardt, J. Gordon, J. A. Lipscomb, J. R. Burg, L. F. Mazzuckelli, T. R. Lewis and R. A. Lemen, *Am. J. Ind. Med.*, 6 (1984) 103.
- 2 B. Singer and D. Grunberger, *Molecular Biology of Mutagens and Carcinogens*, Plenum Press, New York, 1983.
- 3 L. Ehrenberg and S. Hussain, *Mutat. Res.*, 86 (1981) 1.
- 4 A. Kolman, M. Naslund and C. J. Calleman, *Carcinogen.*, 1 (1986) 1245.
- 5 W. M. Snellings, C. S. Weil and R. R. Maronpot, *Toxicol. Appl. Pharmacol.*, 75 (1984) 105.
- 6 M. Sun, *Science (Washington, D.C.)*, 231 (1986) 448.
- 7 D. Sergerback, *Chem. Biol. Interact.*, 45 (1983) 139.

- 8 S. Osterman-Golkar, P. B. Farmer, D. Segerback, E. Bailey, C. J. Calleman, K. Svensson and L. Ehrenberg, *Teratogen., Carcinogen, Mutagen.*, 3 (1983) 395.
- 9 P. B. Farmer, E. Bailey, S. M. Gorf, M. Tornquist, S. Osterman-Golkar, A. Kautiainen and D. P. Lewis-Enright, *Carcinogen.*, 7 (1986) 637.
- 10 M. Tornquist, J. Mowrer, S. Jensen and L. Ehrenberg, *Anal. Biochem.*, 154 (1986) 255.
- 11 D. Segerback, *Thesis*, University of Stockholm, Stockholm, 1985.
- 12 R. S. Annan, G. Kresbach, R. Giese and P. Vouros, *J. Chromatogr.*, 465 (1989) 285.
- 13 M. Saha, R. S. Annan, G. M. Kresbach, F. Vouros and R. W. Giese, *Biomed. Environ. Mass Spectrom.*, in press.
- 14 O. Minnetian, S. Saha and R. W. Giese, *J. Chromatogr.*, 410 (1987) 453.
- 15 J. Adams, M. David and R. W. Giese, *Anal. Chem.*, 58 (1986) 345.
- 16 N. Fedtke and J. Swenberg, personal communication.
- 17 F. Oesch and G. Doerjer, *Carcinogen.*, 3 (1982) 663.
- 18 E. Shaw, *J. Org. Chem.*, 27 (1962) 883.
- 19 A. Sentissi, M. Joppich, K. O'Connell, A. Nazareth and R. W. Giese, *Anal. Chem.*, 56 (1984) 2512.
- 20 A. Nazareth, K. O'Connell, A. Sentissi and R. W. Giese, *J. Chromatogr.*, 314 (1984) 219.
- 21 A. Sentissi, K. O'Connell and R. W. Giese, *J. Chromatogr.*, 331 (1985) 396.
- 22 S.-F. Liu, S. M. Rappaport, J. Rasmussen and W. J. Bodell, *Carcinogen.*, 9 (1988) 1401; and references cited therein.

CHROMSYMP. 1637

## APPLICATION OF 3-(2-FUROYL)QUINOLINE-2-CARBALDEHYDE AS A FLUOROGENIC REAGENT FOR THE ANALYSIS OF PRIMARY AMINES BY LIQUID CHROMATOGRAPHY WITH LASER-INDUCED FLUORESCENCE DETECTION

STEPHEN C. BEALE, YOU-ZUNG HSIEH, DONALD WIESLER and MILOS NOVOTNY\*  
*Department of Chemistry, Indiana University, Bloomington, IN 47405 (U.S.A.)*

---

### SUMMARY

3-(2-Furoyl)quinoline-2-carbaldehyde (FQCA) has been synthesized and characterized as a fluorogenic derivatizing reagent for liquid chromatography. The reagent forms highly fluorescent isoindoles upon reaction with primary amines. The spectral properties and optimum reaction conditions for the formation of isoindoles have been investigated. The utility of FQCA for the high-sensitivity analysis of amino acids by laser-induced fluorescence with an argon-ion laser is demonstrated.

---

### INTRODUCTION

Increasing the sensitivity of the determination of primary amines (*e.g.*, amino acids and peptides) resulting from the controlled degradation of biologically important macromolecules is currently a focus of intense research in modern biochemistry. Over the years, a number of chromatographic procedures have been developed for use in this capacity. A suitable derivatizing reagent which adds a chromophore or fluorophore to the molecule, thereby converting the target compounds into a form amenable to high-performance liquid chromatography (HPLC), is often the key to such determinations. Suitable reagents have included ninhydrin<sup>1</sup>, fluorescamine<sup>2,3</sup>, 7-chloro-4-nitrobenzene-2-oxa-1,3-diazole (NBD chloride)<sup>4</sup>, and *ortho*-phthalaldehyde (OPA)<sup>5–8</sup>. Recently, naphthalene-2,3-dicarboxaldehyde (NDA)<sup>9</sup> has been added to the list of effective fluorogenic reagents.

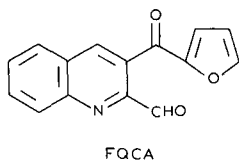
OPA has been perhaps the most popular reagent for use in both pre- and post-column derivatization schemes. This is due to the fact that its reaction with a primary amine results in very rapid formation of an intensely fluorescent isoindole from non-fluorescent starting materials. However, sensitivity of the OPA analysis has typically been limited to the picomole range. Moreover, OPA derivatives have been plagued by their sensitivity to light, air oxidation, and attack by acids<sup>10</sup>. Thus, the isoindoles formed by this reaction tend to be unstable.

A newly developed reagent, NDA<sup>9</sup> is structurally very similar to OPA in that it features the *ortho*-dialdehyde moiety and forms an isoindole in the presence of a primary amine and suitable nucleophile. Considerable work has been done to opti-

mize the nucleophile for the derivatization reaction<sup>9,11</sup>. The cyanide ion was found to be superior to the more conventional thiol, yielding more stable derivatives with a higher quantum yield<sup>11</sup>.

Most fluorogenic reagents have been developed from the perspective of conventional HPLC and commercially available detection systems. As a consequence, the sensitivity exhibited by such methods is adequate for most applications, but not for state-of-the-art protein "nanoscale" isolations<sup>12,13</sup>. Isolation of low picogram quantities of protein has recently been demonstrated with short, packed capillary LC columns<sup>12</sup>. The degradation of a protein on this scale will yield femtogram or lesser amounts of each amino acid. Determinations at such levels require ultra-sensitive detection combined with a separation technique suited to low-volume trace analysis. The combination of capillary LC with laser-induced fluorescence detection provides a unique means for meeting such a challenge.

Since virtually all fluorogenic reagents for primary amines do not yield derivatives with excitation maxima near the lines of convenient high-intensity light sources, such as the helium-cadmium or argon-ion lasers, we have undertaken the task to synthesize and test novel reagents<sup>14</sup>. As the result of our systematic studies in this area, 3-benzoyl-2-quinolinecarboxaldehyde (BQCA)<sup>15</sup> and 3-benzoyl-2-naphthaldehyde (BNA)<sup>16</sup> were prepared and characterized as superior reagents for chromatographic analysis and detection with a helium-cadmium laser at the 442 nm blue line. In this communication we wish to report on yet another promising reagent, 3-(2-furoyl)-quinoline-2-carbaldehyde (FQCA), the structure of which is shown below. FQCA yields fluorescent isoindoles with an excitation maximum near the 488 nm (main line) of the argon-ion laser.



## EXPERIMENTAL

### Chemicals

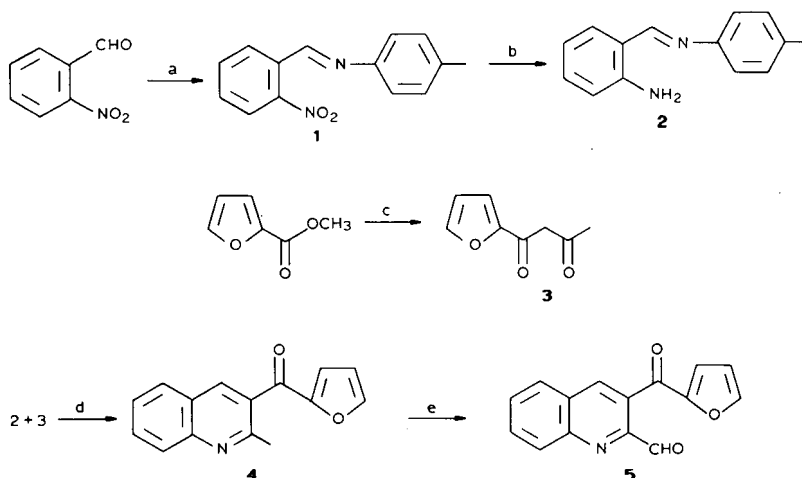
The starting materials for the FQCA synthesis were obtained from Aldrich (Milwaukee, WI, U.S.A.). A set of L-amino acids (Kit No. LAA-21; Sigma, St. Louis, MO, U.S.A.) was used as the amino acid standard. The solvents for the synthesis, chromatography, and fluorescence measurements were from Mallinckrodt (St. Louis, MO, U.S.A.). Water was doubly distilled and deionized in-house.

### Synthesis

The synthetic pathway leading to FQCA is shown below. The identity of all intermediates was established by NMR and/or mass spectral data.

*N*-(*p*-Tolyl)-*o*-nitrobenzalimine (**1**). A mixture of 9.68 g (90.5 mmol) *p*-toluidine and 10.89 g (72.1 mmol) *o*-nitrobenzaldehyde in 25 ml ethanol was kept at 25°C. The precipitate, which began to form after 5 min, was collected on a filter, washed





a: *p*-toluidine; b:  $\text{Na}_2\text{S} \cdot 9\text{H}_2\text{O}$ ; c:  $\text{NaH}$ ,  $(\text{CH}_3)_2\text{CO}$ ; d: piperidine; e:  $\text{SeO}_2$

with cold ethanol, and air-dried. Additional precipitate was obtained by dilution of the filtrate with water and refrigeration. A yield of 16.0 g, 66.7 mmol (93%) was obtained.

*N*-(*p*-Tolyl)-*o*-aminobenzaldehyde (**2**). The procedure for the preparation of **2** was carried out as described by Borsche *et al.*<sup>17</sup>. To a solution of 16.0 g (66.7 mmol) nitroamine **1** in 33 ml 95% ethanol at reflux temperature was added a solution of 31 g (129 mmol)  $\text{Na}_2\text{S} \cdot 9\text{H}_2\text{O}$  in 30 ml 50% aq. ethanol over 15 min, so as to maintain reflux. The mixture was heated under reflux an additional 15 min and cooled to effect crystallization. Solid was collected on a filter, washed with water, and air-dried, yielding 4.09 g (19.5 mmol, 29%) **2**. No attempt was made to secure additional product from the filtrate.

(2-Furoyl)acetone (**3**). Intermediate **3** was prepared according to a modification of the procedure of Swamer and Hauser<sup>18</sup>; 4.27 ml (5.04 g, 40 mmol) methyl 2-furoate was added to a suspension of  $\text{NaH}$  (made from 3.83 g commercial  $\text{NaH}$  slurry by removal of the mineral oil with pentane) in 30 ml anhydrous diethyl ether. To this was added, so as to maintain the temperature below 30°C, 5.87 ml (4.64 g, 80 mmol) acetone (dried over  $\text{CaCl}_2$ ). This mixture was heated under reflux for 2 h, cooled, and divided between diethyl ether and 3 *M*  $\text{HCl}$ . The ether layer was washed with brine, dried ( $\text{MgSO}_4$ ), and concentrated to yield 6.06 g of a red oil (raw yield 99%) which was purified by vacuum distillation (b.p. 85–90°C/1 torr).

3-(2-Furoyl)-2-methylquinoline (**4**). A solution of 410 mg (1.95 mmol) aminoimine **2**, 326 mg (2.15 mmol) diketone **3**, and 50 mg piperidine in 4 ml 95% ethanol was heated overnight under reflux. Removal of the volatile materials left a black, gummy oil which was taken up in dichloromethane and, after being washed with 3 *M*  $\text{NaOH}$ , brine, and dried ( $\text{MgSO}_4$ ), purified by flash chromatography [eluent, 3:2 pentane–diethyl ether (3:2)] yielding 355 mg (1.50 mmol, 77%) product.

3-(2-Furoyl)quinoline-2-carbaldehyde (**5**). A mixture of 355 mg (1.50 mmol) **4** and 183 mg (1.65 mmol)  $\text{SeO}_2$  in 6 ml acetic acid was heated for 17 h in an 80°C bath. The solvent was removed by rotary evaporation. The dichloromethane extract of the

residue was washed with 1 M NaOH and brine and dried ( $\text{MgSO}_4$ ). Concentration yielded 284 mg oil, 1.13 mmol, 75% raw. The ultimate purification was done by LC as discussed below.

#### *Liquid chromatography*

A Perkin-Elmer (Norwalk, CT, U.S.A.) Series 3B liquid chromatograph with detection (Perkin-Elmer LC-55 absorbance detector) at 330 nm was employed for purification of the FQCA reagent. The separation was performed on a Phenomenex (Rancho Palos Verdes, CA, U.S.A.) 5- $\mu\text{m}$ ,  $\text{C}_{18}$  column. A linear gradient from 60% aq. methanol to 100% methanol, in 30 min, was sufficient to isolate FQCA from contaminants introduced during the synthetic procedure.

The micro-LC system consisted of an ISCO (Lincoln, NE, U.S.A.) Model 314 syringe pump equipped with an ISCO HPLC pressure controller and a Model 314 metering pump. Separations were accomplished on a 0.5 m  $\times$  0.25 mm fused-silica (Polymicro Technologies, Phoenix, AZ, U.S.A.) capillary, packed in-house with 5- $\mu\text{m}$   $\text{C}_{18}$  particles (Shiseido Corp., Kyoto, Japan). Detection was accomplished with an argon-ion laser-based detection system similar in design to that described in previous studies<sup>15,16</sup>. Injections were made in the stopped-flow mode. The derivatized amino acids were eluted with a stepwise gradient, beginning with 20% acetonitrile in water containing 0.2% triethylamine and 0.2% acetic acid, in steps of 5% to 50% acetonitrile in water containing 0.2% triethylamine and 0.2% acetic acid.

#### *Fluorescence measurements*

Static fluorescence measurements were made with a Perkin-Elmer 650 spectrofluorometer. For quantum yield studies, the emission spectrum was corrected according to the method of Parker<sup>19</sup>, and compared to that of quinine bisulfate.

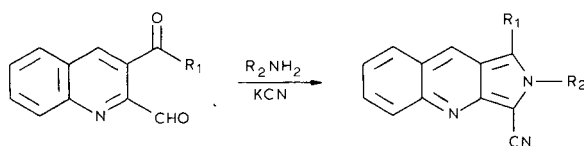
## RESULTS AND DISCUSSION

The development, synthesis, and characterization of fluorogenic derivatizing reagents for primary amines has been of continuing interest to our laboratory<sup>14-16</sup>. We are mainly concerned with the design of reagents that combine the advantages of OPA and NDA with the added feature of an absorbance maximum closely matching the principal output radiation wavelength of an inexpensive and easily maintained laser system. Use of a laser-based detection scheme for HPLC has been shown to enhance the detection limits in a variety of experiments<sup>20-24</sup>. Our efforts have centered on the development of reagents having absorption bands in the visible range. Exploitation of a band in the visible range eliminates many interferences present in biological samples, which typically feature absorption maxima in the UV region. Moreover, two lasers (He-Cd and Ar ion), which are both relatively inexpensive and easy to operate, feature output radiation in the visible range. We have previously described reagents compatible with the 442 nm He-Cd line<sup>14-16</sup>, and in this paper we present a similar reagent for use with the 488 nm line of the Ar-ion laser.

Our design considerations for a fluorogenic reagent include the formation of an isoindole upon reaction with a primary amine and the capability of building a variety of functional moieties into the reagent. The ability to modify the reagent facilitates adaptation to almost any type of detection scheme. In addition, the absorbance of the

derivative should be sufficiently different from that of the reagent itself, thus eliminating interferences from unreacted starting materials. The final criterion of our developmental strategy is the stabilization of the resulting isoindoles so that they may be reliably used in the pre-column derivatization mode, since post-column derivatization is often impractical for capillary LC.

We postulated that the stability of isoindoles can be enhanced through substitution of the proton adjacent to the nitrogen atom of the indole ring. This led us to the *ortho*-aroylaldehyde backbone instead of the more conventional *ortho*-dialdehydes<sup>14</sup>. In the scheme shown below, both positions adjacent to the indolic nitrogen are substituted. Also, the use of a keto-aldehyde:



facilitates the incorporation of various moieties into the parent molecule, resulting in the ability to “fine-tune” the absorption maximum of the derivatized molecule.

In a previous communication<sup>14</sup>, we outlined a number of criteria for comparison of the various fluorogenic reagents developed. These are: (1) high quantum yield; (2) good reaction rate; (3) stability of the derivative with time; and (4) proximity of the absorption maximum to the target laser line. Here, we examine FQCA with respect to these criteria and optimization of the derivatization conditions.

FQCA was originally synthesized as an analogue of BQCA<sup>15</sup>, which has an absorption maximum at 460 nm. In order to effect a hypsochromic wavelength shift,

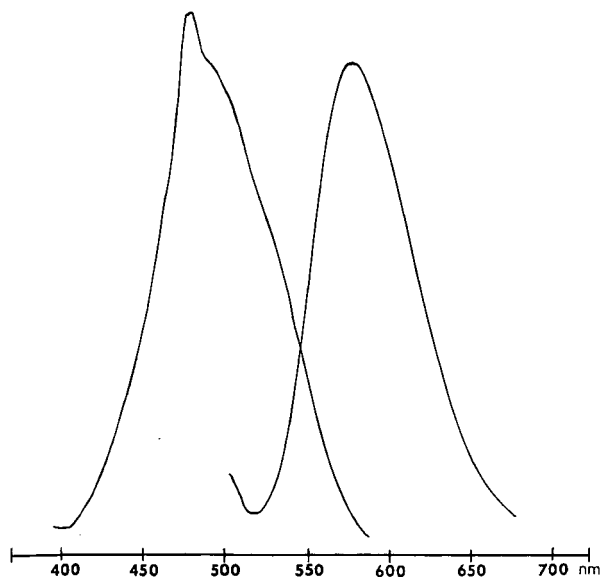


Fig. 1. Absorption and emission spectra of the methionine product.

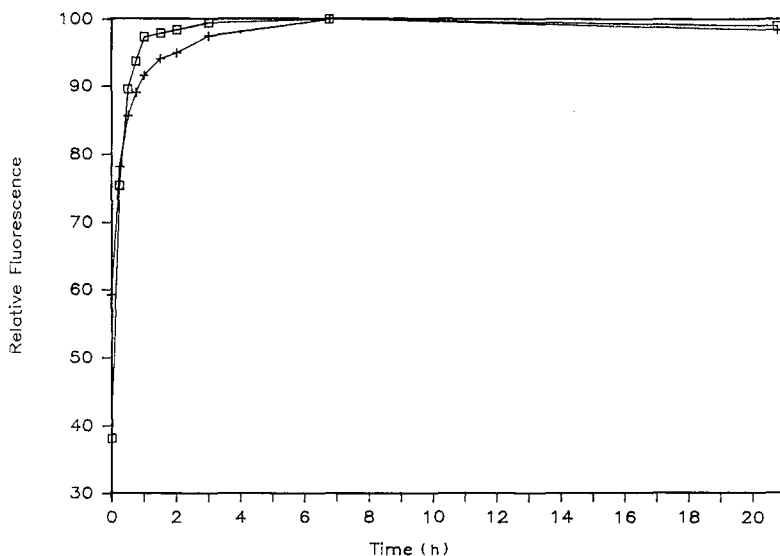


Fig. 2. Stability-time curves for (□) alanine and (+) valine.

we replaced the  $R_1$  (scheme above) phenyl group with a furan moiety. In actuality, the absorption was bathochromically shifted to 480 nm (emission maximum 590 nm), which happens to coincide with the main line (488 nm) of the argon-ion laser. Fig. 1 depicts the absorption and emission spectra for a typical FQCA derivative. Further investigation indicated that the quantum yield of FQCA, derivatized with glycine, is 0.3.

When OPA reacts with primary amines, the fluorescent product forms within 5 min. While FQCA does not react that quickly, the isoindole product reaches its fluorescence maximum in about 45 min. Reaction time on this scale does not present major problems. Primarily, we are concerned with the formation of a stable derivative within a reasonable time and under mild conditions (37°C without stirring or agitation). Fig. 2 depicts the time-stability curve for FQCA-derivatized glycine and lysine. Once the fluorescence maximum has been reached, the derivatives are stable in solution for more than 2 h. In fact, when the dry derivatives are stored in the freezer, they maintain their fluorescence intensity for about 2 weeks.

The optimum concentrations of cyanide ion and reagent for maximum reaction yield have been investigated. The dependence of the reaction yield upon the concentration of cyanide ion and reagent is depicted in Figs. 3 and 4, respectively. These experiments were carried out by allowing FQCA to react with glycine or lysine under the appropriate conditions for 45 min. The reaction mixture was then diluted with methanol to 1.5 ml, and triplicate peak height readings were acquired from the spectrofluorometer, with excitation at 490 nm and emission at 590 nm. Each point on the curve represents an average of three readings. Examination of these data reveals that the fluorescence maximum is reached with *ca.* four-fold molar excess of FQCA and a two-fold excess of cyanide ion. In a previous study<sup>15</sup>, we found that the optimum pH for the derivatization of amino acids is between 7 and 9. This finding also applies to

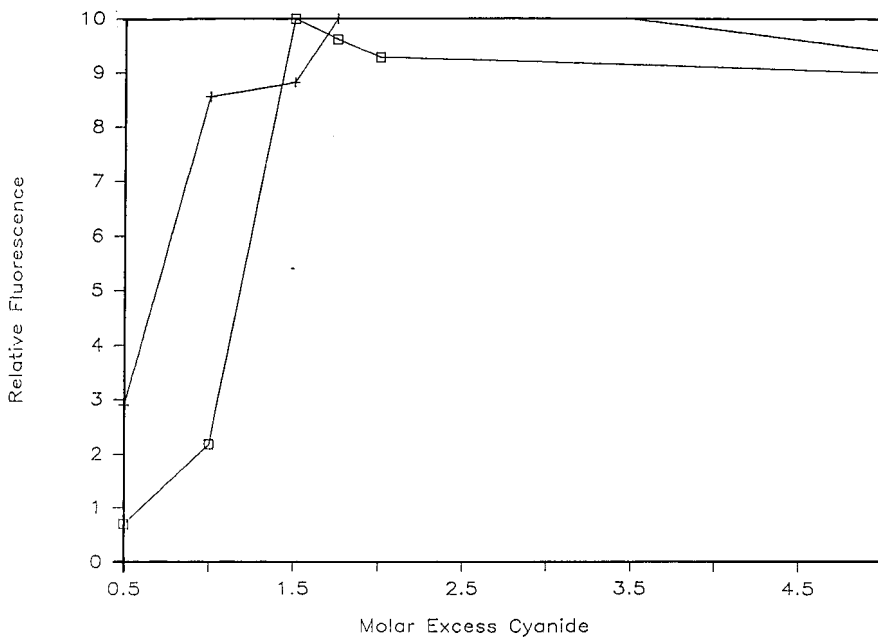


Fig. 3. Dependence of reaction yield on cyanide concentration. □ = Glycine; + = lysine.

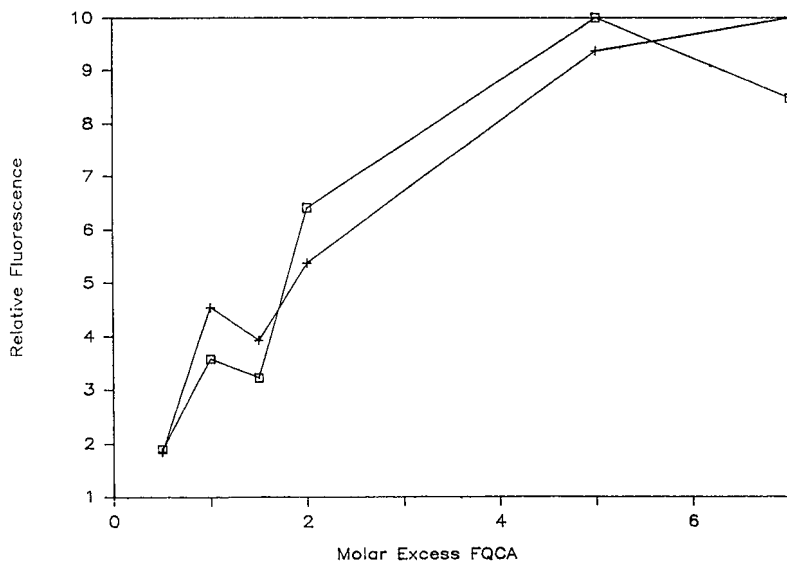


Fig. 4. Reaction yield as a function of reagent concentration. □ = glycine; + = lysine.

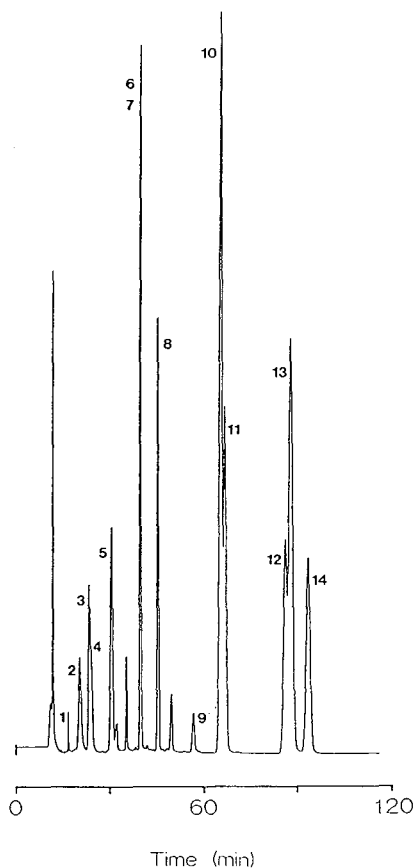


Fig. 5. Standard amino acid chromatogram (conditions given in the text). Peaks 1 = Glu; 2 = Asp; 3 = His; 4 = Ser; 5 = Arg; 6 = Gly; 7 = Tyr; 8 = Ala; 9 = Thr; 10 = Met; 11 = Val; 12 = Phe; 13 = Ile; 14 = Leu.

FQCA, so that the reaction may be carried out in methanol, as opposed to the traditional borate buffer.

Fig. 5 represents a microcolumn LC chromatogram of amino acid standards with high-sensitivity laser-induced fluorescence detection. The chromatographic conditions are as described in the Experimental section. Peak identities are given in the figure legend. The practical detection limits obtained with FQCA-derivatized amino acids were found to be in the femtomole range.

In summary, we have presented the design considerations and synthesis of a fluorogenic reagent for primary amines, rendering them amenable to high-sensitivity detection following microcolumn LC separation. FQCA is shown to be compatible with argon-ion laser-induced fluorescence detection. In addition, flexibility in the design of our reagents through a generalized synthesis scheme<sup>14</sup> is demonstrated.

FQCA in the presence of an amino acid and a suitable nucleophile (cyanide ion, chosen here) forms an intensely fluorescent isoindole the absorption maximum of which closely matches the 488 nm output radiation of the main line of the argon-ion

laser. The reaction proceeds reproducibly under mild conditions (pH 7–9, 37°C) to yield stable products which can be satisfactorily separated chromatographically. Future studies will aim at the optimization of retention.

#### ACKNOWLEDGEMENT

This research was supported by Grant No. PHS R01 GM 24349 from the National Institute of General Medical Sciences.

#### REFERENCES

- 1 M. Rubenstein, S. Chen-Kiang, S. Stein and S. Udenfriend, *Anal. Biochem.*, 95 (1979) 117–121.
- 2 S. Stein, P. Boehlen and S. Udenfriend, *Arch. Biochem. Biophys.*, 163 (1974) 400–403.
- 3 S. DeBernado, M. Weigle, V. Toome, K. Manhart, W. Leimgruber, P. Bohlen, S. Stein and S. Udenfriend, *Arch. Biochem. Biophys.*, 163 (1974) 390–399.
- 4 P. B. Ghosh and M. W. Whitehouse, *Biochem. J.*, 108 (1968) 155–160.
- 5 M. Roth, *Anal. Chem.*, 43 (1971) 880–882.
- 6 P. Lindroth and K. Mopper, *Anal. Chem.*, 51 (1979) 1667–1674.
- 7 J. C. Hodgins, *J. Liq. Chromatogr.*, 2 (1979) 1047–1059.
- 8 Z. Deyl, J. Hyánek and M. Horáková, *J. Chromatogr.*, 379 (1986) 177–250.
- 9 P. De Montigny, J. F. Stobaugh, R. S. Givens, R. G. Carlson, K. Srinivasachar, L. A. Sternson and T. Higuchi, *Anal. Chem.*, 59 (1987) 1096–1101.
- 10 J. D. White and M. E. Mann, *Adv. Heterocycl. Chem.*, 10 (1969) 113–147.
- 11 B. K. Matuszewski, R. S. Givens, K. Srinivasachar, R. G. Carlson and T. Higuchi, *Anal. Chem.*, 59 (1987) 1102–1105.
- 12 C. L. Flurer, C. Borra, S. C. Beale and M. Novotny, *Anal. Chem.*, 60 (1988) 1826–1829.
- 13 C. L. Flurer, C. Borra, F. Andreolini and M. Novotny, *J. Chromatogr.*, 448 (1988) 73–86.
- 14 S. C. Beale, J. C. Savage, D. Wiesler, S. Wietstock and M. Novotny, *Anal. Chem.*, 60 (1988) 1765–1769.
- 15 S. C. Beale, Y.-Z. Hsieh, J. C. Savage, D. Wiesler and M. Novotny, *Talanta*, 36 (1989) 322–325.
- 16 Y.-Z. Hsieh, S. C. Beale, D. Wiesler and M. Novotny, *J. Microcolumn Sep.*, 2 (1989) 96–100.
- 17 W. Borsche, W. Doeller and M. Wagner-Roemmich, *Ber. Dtsch. Chem. Soc.*, 76B (1943) 1099–1104.
- 18 F. W. Swamer and C. R. Hauser, *J. Am. Chem. Soc.*, 72 (1950) 1352–1356.
- 19 C. A. Parker, *Photoluminescence of Solutions*, Elsevier, Amsterdam, 1968, 261–265.
- 20 L. W. Hershberger, J. B. Callis and G. D. Christian, *Anal. Chem.*, 51 (1979) 1444–1446.
- 21 E. S. Yeung and M. J. Sepaniak, *Anal. Chem.*, 52 (1980) 1465A–1481A.
- 22 R. B. Green, *Anal. Chem.*, 55 (1983) 20A–32A.
- 23 R. N. Zare, *Science (Washington, D.C.)*, 226 (1984) 298–303.
- 24 J. Gluckman, D. Shelly and M. Novotny, *J. Chromatogr.*, 317 (1984) 443–453.





CHROMSYMP. 1660

## CHROMATOGRAPHIC STUDIES ON THE BINDING, ACTION AND METABOLISM OF (–)-DEPRENYL

HUBA KALÁSZ\*<sup>a</sup>, LÁSZLÓ KERECSEN and JÓZSEF KNOLL

*Department of Pharmacology, Semmelweis University of Medicine, Nagyvarad ter 4, 1089 Budapest (Hungary)*

and

JÓZSEF PUCSOK

*National Health Institute of Physical Education and Sports, Budapest (Hungary)*

---

### SUMMARY

Serum binding, the effect on striatal dopamine release and the metabolism of (–)-deprenyl [N-methyl-N-propargyl(2-phenyl-1-methyl)ethylammonium chloride], TZ-650 [N-methyl-N-propargyl(2-phenyl)ethylammonium chloride] and J-508 [N-methyl-N-propargyl(indanyl)ammonium chloride] were investigated using various chromatographic methods. A strong interaction between (–)-deprenyl and macroglobulins was found. Deprenyl enhanced the dopamine release from striatal slices of the rat brain and also inhibited the dopamine–DOPAC conversion. Deprenyl analogues showed either smaller or no effect. Hydroxylation of (–)-deprenyl takes place in the *para* position, in addition to the usual oxidative N-dealkylations, which are known from various metabolic studies on N-substituted phenylalkylamines.

---

### INTRODUCTION

(–)-Deprenyl, also called Eldepryl<sup>®</sup>, Jumex<sup>®</sup>, Movergan<sup>®</sup> and Selegiline<sup>®</sup>, is a potent, irreversible and specific inhibitor of the monoamine oxidase B enzyme<sup>1–4</sup>. Its peculiar pharmacological properties and beneficial clinical effects in Parkinson's disease prompted investigations of its binding, action and metabolism and studies of structural analogues.

Johnston<sup>5</sup> reported that clorgyline preferentially inhibits the oxidative deamination of serotonin, while Knoll and Magyar<sup>2</sup> found that (–)-deprenyl is a selective inhibitor of the deamination of benzylamine. These facts furnished indirect evidence that there are two different types of monoamine oxidase enzyme, monoamine oxidase A (MAO-A) and monoamine oxidase B (MAO-B). MAO-A is clorgyline-sensitive, whereas MAO-B is clorgyline-insensitive and deprenyl-sensitive. These inhibitors belong to the so-called suicide inhibitor group, meaning that while the enzyme splits this

---

<sup>a</sup> Present address: Department of Pharmacology and Cell Biophysics, University of Cincinnati, 231 Bethesda Avenue, Cincinnati, OH 45267-0575, U.S.A.

substrate, it suffers covalent binding, which results in an irreversible inhibition. Salach *et al.*<sup>6</sup> provided direct evidence that these enzyme inhibitors covalently interact with the flavin-active site of the enzyme. Ekstedt *et al.*<sup>7</sup> and Birkmayer and Yahr<sup>8</sup> showed that, in spite of repeated administration of (–)-deprenyl, a fairly selective inhibition pattern was maintained in the brain of rats and liver of human subjects.

(–)-Deprenyl is a monoamine oxidase inhibitor lacking the so-called cheese effect. It is not only free of this side-effect of MAO inhibitors but also, as Knoll *et al.*<sup>9</sup> have shown, it inhibits the uptake of tyramine. Similar observations in normal and Parkinsonian volunteers showed no adverse pressor reaction after a challenge with an oral dose of tyramine in amounts considerably larger than those likely to be encountered in a normal diet. These properties of (–)-deprenyl allow its safe administration to Parkinsonian patients on levodopa treatment<sup>3</sup>.

## EXPERIMENTAL

### Materials

(–)-Deprenyl [N-methyl-N-propargyl(2-phenyl-1-methyl)ethylammonium chloride], *o*-methyldeprenyl, *m*-methyldeprenyl, *p*-methyldeprenyl, TZ-650 [N-methyl-N-propargyl(2-phenyl)ethylammonium chloride] and J-508 [N-methyl-N-propargyl(indanyl)ammonium chloride] were kindly supplied by Chinoin (Budapest, Hungary). In some experiments, (–)-deprenyl was labelled in position 2 of the (2-phenyl-1-methyl)ethyl moiety (Fig. 1).

3,4-Dihydroxybenzylamine (DHBA) (Calbiochem, San Diego, CA, U.S.A), dopamine hydrochloride (Serva, Heidelberg, F.R.G.), 3,4-dihydroxyphenylacetic acid (DOPAC) (Fluka, Buchs, Switzerland), alumina, Brockmann Grade II, neutral, and LiChrosorb C<sub>18</sub>, 5 μm (Merck, Darmstadt, F.R.G.) and sodium octanesulphonate (Aldrich, Milwaukee, WI, U.S.A.) were used. All the other chemicals and solvents were of the highest commercially available quality.

Sephadex G-15 and Sephadex G-200 Fine (Pharmacia, Uppsala, Sweden) were used for size exclusion chromatography. They were packed into glass columns 90 or 60 cm × 2.5 or 5.0 cm I.D. For elution 0.05 M ammonium acetate solution was used, and 10-ml fractions of the eluate were collected with an automatic fraction collector (Labor-MIM, Budapest, Hungary). Experiments were carried out with parts of a ReCyChrom system (LKB, Bromma, Sweden) including a cold box adjusted to 4°C, a peristaltic pump, a Uvicord UV detector set at 254 nm and a recorder.

For thin-layer chromatography (TLC), all-glass developing chambers (Desaga, Heidelberg, F.R.G.) were used. The spots were revealed with ninhydrin reagent and by autoradiography by previously published methods<sup>10</sup>.

For high-performance liquid chromatographic (HPLC) experiments a Liqueopump 312 solvent-delivery system with injection valve fitted to a 20-μl loop was used (Labor-MIM). The 250 × 4.6 mm I.D. column (Labor-MIM) was packed with Li-

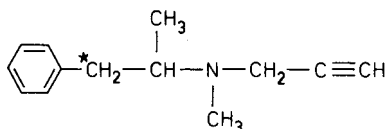


Fig. 1. Structure of deprenyl. The asterisk indicates the position of <sup>14</sup>C labelling.

Chrosorb C<sub>18</sub>. A TL-3 thin-layer electrochemical detector cell with a paraffin oil-based carbon paste working electrode was purchased from Bioanalytical Systems (West Lafayette, IN, U.S.A.). It was used at 0.7 V and connected to an electronic controller, developed by the Biomedical Engineering Workshop of the Department of Pharmacology, Semmelweis University of Medicine (Budapest, Hungary). The signal from the amplifier was observed on an OH 814/1 potentiometric recorder (Radelkis, Budapest, Hungary). The mobile phase was a triethylamine phosphate buffer (pH 3). This buffer also contained 75 mg/l sodium octanesulphonate as an ion-pairing agent and 18 mg/l of Na<sub>2</sub>EDTA to reduce the spike activity of the detector. Finally, 6% (v/v) acetonitrile was added to the mobile phase, which was degassed under vacuum and sonication. The internal standard was 3,4-dihydroxybenzylamine. Results were calculated from the peak-height ratios of dopamine to internal standard and DOPAC to internal standard; the dopamine release from rat brain striata was expressed in pmol/g · min. For statistical evaluations Student's *t*-test for two means was applied. The significance level was set at  $P < 0.05$ .

An HP-5985B gas chromatograph-mass spectrometer (Hewlett-Packard, Palo Alto, CA, U.S.A.) was connected to an HP-2648A data analyser. Separation was achieved by temperature programming from 100 to 320°C at 5°C/min<sup>11</sup>. Glass capillary columns (25 × 0.25 mm I.D.) were used. The stationary phase was 20% diphenyl- and 80% dimethylpolysiloxane (SPB 20) (Supelco, Bellefonte, PA, U.S.A.) and the flow-rate of the helium carrier gas was 1 ml/min. The gas chromatograms and the mass spectra were recorded with a thermal printer.

### Methods

To investigate protein-deprenyl adducts, human serum (obtained from the National Institute for Blood Transfusion, Budapest, Hungary) was incubated with radiolabelled deprenyl for 2 h. The sample was immediately separated by gel chromatography on Sephadex G-15. Protein-deprenyl adducts, eluted at the void volume of the column, were further separated on Sephadex G-200.

The study on dopamine release following chronic pretreatment was performed after three weeks of subcutaneous administration of (-)-deprenyl, TZ-650 or J-508 in one daily dose to rats. Twenty-four hours after the last injection, the rats were decapitated. Striata were immediately removed and halved according to the method of Glowinski and Iversen<sup>12,13</sup>, then soaked in Krebs solution. Four striata were pooled in one organ bath, incubated for 1 h, and then the Krebs solution was replaced. Subsequently, the Krebs solution was changed twice at 10-min intervals. Finally, the Krebs solution was changed to one which contained 20 mM potassium chloride. The striata were exposed to the latter medium for 10 min in order to stimulate the transmitter release. Samples were collected after each 10-min incubation period. The samples were spiked with 40 ng of 3,4-dihydroxybenzylamine (internal standard) and prepurified on a 90-mg alumina microcolumn according to the method of Anton and Sayre<sup>14</sup>. The effluent from the microcolumn was injected into the HPLC column<sup>13</sup>.

For the metabolic study, albino Wistar rats of both sexes, weighing 120–150 g, were used<sup>14</sup>. Solutions of (-)-deprenyl, TZ-650 and J-508 were injected subcutaneously in doses of 50 mg/kg. Urine was collected for 24 h, and either immediately extracted or kept at -40°C until analysed as follows. Urine was adjusted to pH 11

with 0.5 M sodium hydroxide solution and the basic metabolites were extracted with chloroform–ethyl acetate (3:1). The organic layer was re-extracted into the buffer at pH 1.5, and the extraction with chloroform–ethyl acetate (3:1) was repeated after the pH had been adjusted to 11.

## RESULTS

In the study of the binding of (–)-deprenyl to serum proteins the radiolabelled drug was incubated with human serum for 2 h. The gel chromatograms are presented in Fig. 2. The radioactive peak at the void volume of the gel column indicates that there is definite binding between serum proteins and deprenyl (Fig. 2a). A substantial portion of deprenyl was bound to macroglobulins, while the albumins contained the smallest fraction of the radioactivity (Fig. 2b).

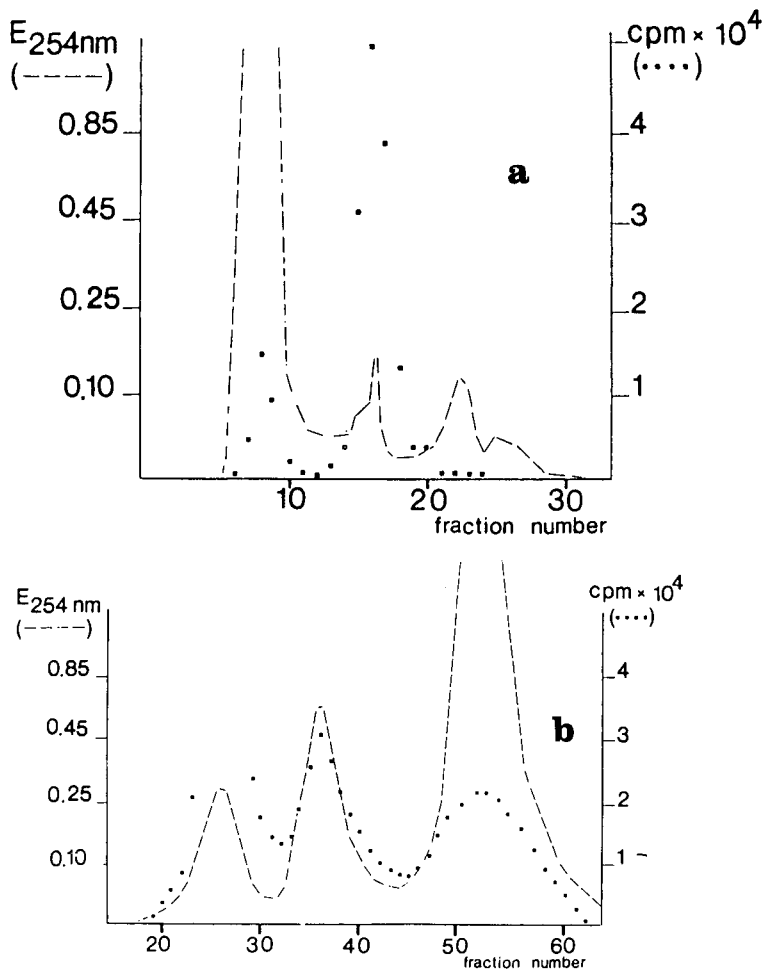


Fig. 2. (a) Gel chromatography of free and protein-bound deprenyl on Sephadex G-15. (b) Gel chromatographic separation of proteins containing deprenyl on Sephadex G-200.  $E_{254\text{nm}}$  = absorbance at 254 nm.

These experiments give direct evidence that the link between deprenyl and serum proteins is strong or irreversible, because deprenyl-protein adducts remained intact even after several hours of gel chromatography. Parallel experiments with reversibly binding substances did not show such a stability of drug-protein adducts in gel chromatography. Similar studies were performed using equilibrium dialysis cells.

Because the specific inhibitory effect of deprenyl on monoamine oxidase B does not explain its effectiveness as medication in Parkinsonism, its action was investigated on the release of dopamine from the striatum. The *in vitro* addition of (-)-deprenyl to the organ bath did not result in a noticeable change in dopamine release, except at very high concentrations, which were well above any therapeutic range. Three weeks of pretreatment with one daily dose of (-)-deprenyl increased the dopamine release and decreased its transformation to DOPAC in rats. Both the so-called resting release and the release induced by 20 mM of potassium were measured. It was found that 3 weeks of pretreatment with a 0.25 mg/kg daily dose of deprenyl increased the dopamine release to *ca.* five times the control level and inhibited the transformation of dopamine to DOPAC. A similar phenomenon was observed in the potassium-stimulated release where the increase was even more expressed (Table I). In experiments with the two structural analogues of (-)-deprenyl, TZ-605 was almost ineffective but J-508 was a stronger MAO inhibitor (less DOPAC was observed) (Table I).

In preliminary investigations of the metabolism of (-)-deprenyl, two-dimensional TLC was used. Development in the first dimension was performed by elution chromatography and displacement chromatography was applied in the second dimension (Fig. 3).

The metabolites of (-)-deprenyl, TX-650 and J-508 were identified by gas chromatography-mass spectrometry (GC-MS). The chromatograms obtained by total ion monitoring are presented in Figs. 4, 5 and 6, respectively. Neither deprenyl nor its

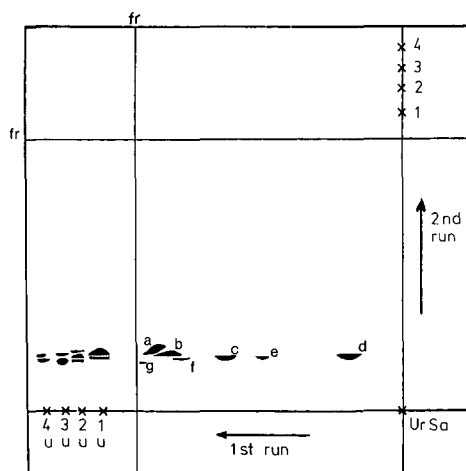


Fig. 3. Displacement TLC of deprenyl metabolites on silica plates with chloroform-methanol-water (29:20:4, v/v/v) and chloroform-triethanolamine (96:4, v/v) in the first and second dimensions, respectively. a = Deprenyl; b = propargylanara; c = methamphetamine; d = amphetamine; e, f and g are unidentified metabolites; u = urine sample; UrSa = urine sample for two-dimensional separation; fr = solvent front.

TABLE I

## RELEASE OF DOPAMINE (DA) AND DOPAC UNDER VARIOUS CONDITIONS

	<i>Release ± S.D. (pmol g<sup>-1</sup> min<sup>-1</sup>)</i>			
	<i>Resting</i>		<i>20 mM KCl stimulated</i>	
	<i>DA</i>	<i>DOPAC</i>	<i>DA</i>	<i>DOPAC</i>
Control	91 ± 7	258 ± 18	200 ± 15	291 ± 19
Deprenyl, 0.25 mg/kg	503 ± 20	72 ± 10	1451 ± 183	120 ± 36
J-508, 0.1 mg/kg	360 ± 27	18 ± 3	650 ± 26	19 ± 3
TZ-650, 0.1 mg/kg	151 ± 18	291 ± 23	272 ± 35	340 ± 36

metabolites gave a molecular ion, but only two main fragments. One of them originates from the benzyl part (the phenolic ring and the neighbouring methyl), which forms a cycloheptatrienium cation in the mass spectrometer, while the other fragment is the tri-, di- or monoalkyl-substituted nitrogen, *i.e.*, the remaining part of the compounds. Thus deprenyl gave fragments with mass numbers 91 + 96, while its de-

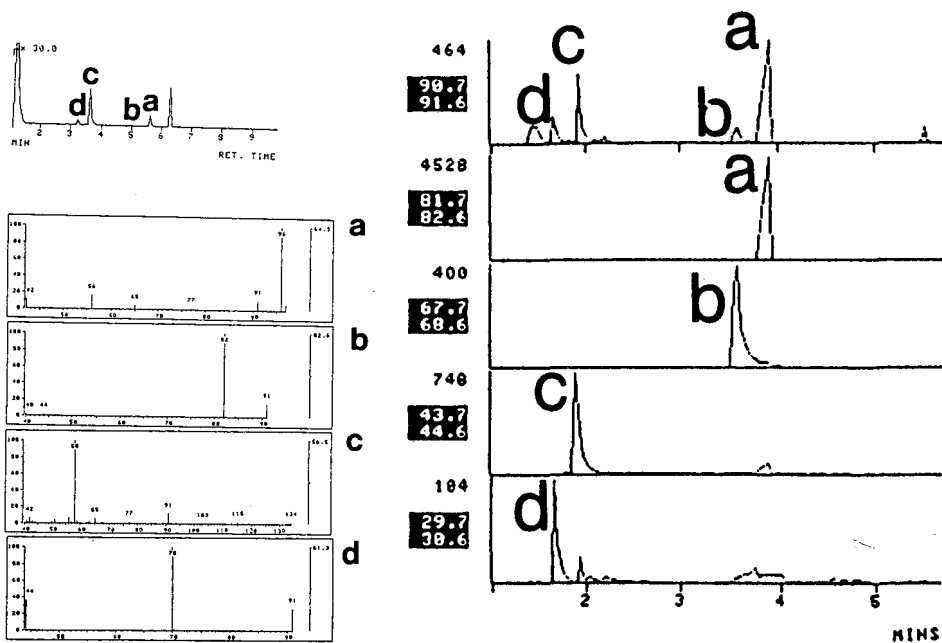


Fig. 4. GC-MS identification of deprenyl metabolites by selected ion monitoring. Peaks a, b, c and d are deprenyl, propargylanara, methamphetamine and amphetamine, respectively.

Fig. 5. GC-MS identification of TZ-650 metabolites by selected ion monitoring. Peaks a, b, c and d are the unaltered drug and its demethylated, depropargylated and didealkylated metabolites, respectively. The white numbers in the black boxes are the scanning ranges of the ion fragments (*e.g.*, 90.7 to 91.6 for *m/z* 91).

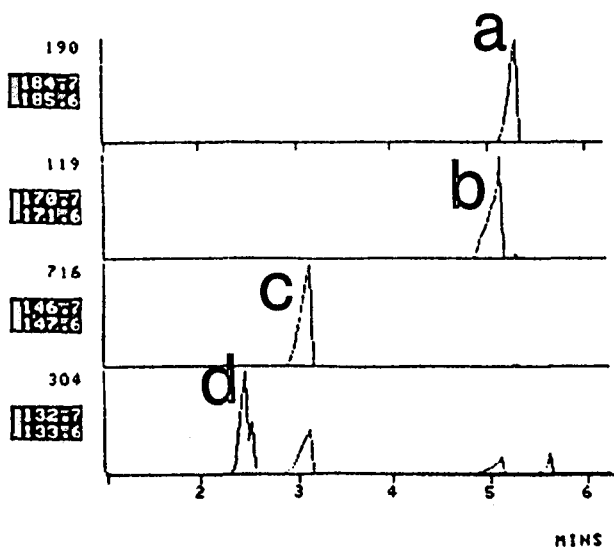


Fig. 6. GC-MS identification of J-508 metabolites using selected ion monitoring. Peaks a, b, c and d are the unaltered drug and its demethylated, depropargylated, and didealkylated metabolites, respectively. For the white numbers in the black boxes, see legend to Fig. 5.

methylated, depropargylated and demethylated/depropargylated products, propargylanara (its other name is propargylamphetamine), methamphetamine and amphetamine gave mass numbers  $91 + 82$ ,  $91 + 58$  and  $91 + 44$ , respectively, indicating the respective losses of the nitrogen substituents. The results are shown in Fig. 4.

Figs. 5 and 6 show the results of the GC-MS investigations of the metabolism of TZ-650 and J-508. Mass fragment 91 characterizes the intact phenolic ring, whereas the ions with mass numbers 82, 68, 44 and 30 represent the intact side-chain of TZ-650 and its demethylated, depropargylated and demethylated/depropargylated derivatives, respectively.

With J-508, molecular ions with mass numbers 185, 171, 147 and 133 indicate the presence of J-508 and its demethylated, depropargylated and demethylated/depropargylated derivatives, respectively.

To find the hydroxylated metabolites of deprenyl, trimethylsilylated derivatives were prepared. This changed the mass fragment belonging to the phenolic ring which contained not only the cycloheptatrienium ion but also its trimethylsilylhydroxy derivative, having a molecular ion of  $m/z$  179. These studies proved that a considerable amount of hydroxymethamphetamine and trace amounts of hydroxypropargylanara were produced during the metabolism of deprenyl, in addition to the earlier known metabolites such as propargylanara, methamphetamine and amphetamine (Fig. 7).

To find the position of (phenolic) hydroxylation during metabolism, some *ortho*-, *meta*- and *para*-methylated deprenyl analogues were investigated. After the administration of the drugs, collection of urine and prepurification by extraction, acetyl derivatives were prepared. With hydroxylated metabolites of the *ortho*- and *meta*-

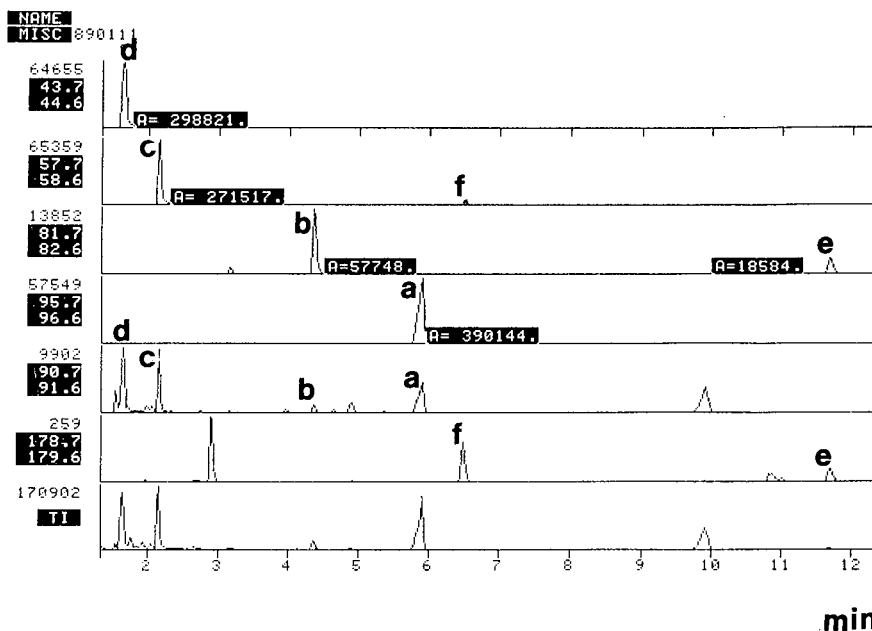


Fig. 7. GC-MS identification of deprenyl metabolites after trimethylsilylation. Peaks a, b, c, d, e and f are deprenyl, propargylanara, methamphetamine, amphetamine, *p*-hydroxypropargylanara and *p*-hydroxymethamphetamine, respectively. For the white numbers in the black boxes, see legend to Fig. 5. Numbers equal to A are the relative amounts of ion fragments.

substituted deprenyl derivatives, the presence of hydroxylated metabolites was detected, whereas they were absent when the metabolites of the *para*-substituted drug were analysed (Fig. 8).

## DISCUSSION

Serum binding of (–)-deprenyl is probably a strong interaction, as the binding remained unaffected by several hours of gel chromatography. The blood level of (–)-deprenyl shows a remarkably fast onset and decline. The maximum deprenyl level in the brain of mice was observable 30 after intravenous injection, whereas the brain and blood levels of (–)-deprenyl decreased to several percent of the peak level after 2 h of intravenous administration to mice.

After 3 weeks of pretreatment with deprenyl, rats showed a highly enhanced dopamine release in the brain striatal slices. This may be important in the explanation of the mechanism of action of (–)-deprenyl.

Ehringer and Hornykiewicz<sup>15</sup> observed that in the brain of Parkinsonian patients the striatal dopamine concentration is lower than that in normal brain. This is probably due to the loss of dopaminergic neurons, and this loss is compensated by glial cells yielding the monoamine oxidase enzyme. Dopaminergic modulation in the brain and especially in the striatum and hypothalamic area declines in senescence. Moreover, an increased monoamine oxidase B activity can be found. This age-related biochemical lesion can be corrected by (–)-deprenyl<sup>3,4,13</sup>



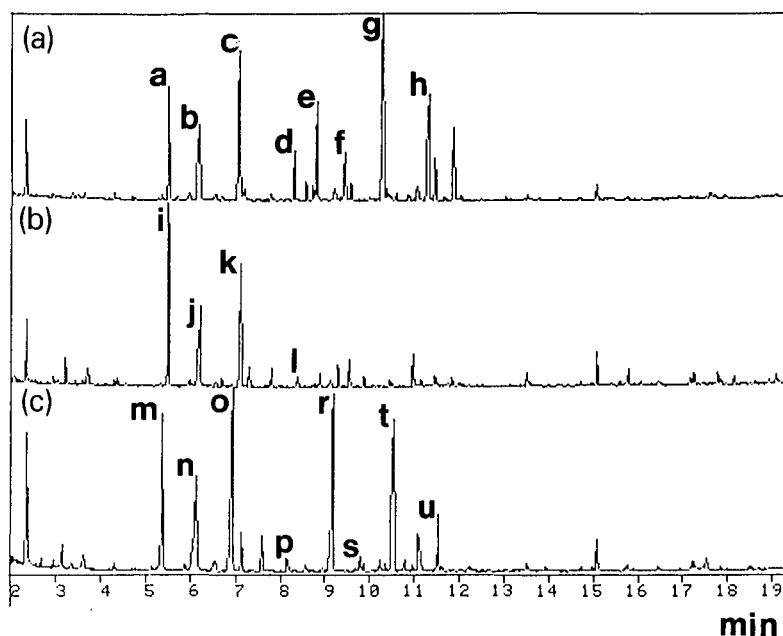


Fig. 8. GC-MS of (A) *o*-methyldeprenyl, (B) *p*-methyldeprenyl and (C) *m*-methyldeprenyl metabolites. Peaks: a = 2-methyldeprenyl; b = 2-methylamphetamine; c = 2-methylmethamphetamine; d = 2-methylpropargylanara; e = 4-hydroxy-2-methyldeprenyl; f = 4-hydroxy-2-methylamphetamine; g = 4-hydroxy-2-methylmethamphetamine; h = 4-hydroxy-2-methylpropargylanara; i = 4-methyldeprenyl; j = 4-methylamphetamine; k = 4-methylmethamphetamine; l = 4-methylpropargylanara; m = 3-methyldeprenyl; n = 3-methylamphetamine; o = 3-methylmethamphetamine; p = 3-methylpropargylanara; r = 4-hydroxy-3-methyldeprenyl; s = 4-hydroxy-3-methylamphetamine; t = 4-hydroxy-3-methylmethamphetamine; u = 4-hydroxy-3-methylpropargylanara.

Reynolds *et al.*<sup>16</sup> also investigated the deprenyl metabolism by GC. They identified amphetamine and methamphetamine in the urine of patients but neither demethylated deprenyl (propargylanara) nor hydroxylated derivatives of deprenyl were found.

The metabolism of deprenyl was explored by displacement TLC. The results indicate the presence of some fragments that are the products of oxidative demethylation, depropargylation and demethylation/depropargylation. However, some additional spots were also present that can be considered to be products of *para*-hydroxylation of either deprenyl or its identified metabolites.

Verification of the presence of dealkylated deprenyl metabolites was obtained by GC-MS. Amphetamine, methamphetamine and propargylanara were found to be metabolites of deprenyl (Fig. 3). Similar experiments were carried out to identify the metabolites of J-508 and TZ-650 (Figs. 4 and 5). The GC-MS identification of further metabolites required derivatization. Acetylation of the urine extract produced adequately volatile derivatives. Their GC-MS spectra showed the presence of *p*-hydroxypropargylanara and a trace amount of *p*-hydroxymethamphetamine among the metabolites (Fig. 7). Similar findings have been published by Yoshida *et al.*<sup>17</sup>

Experiments with *para*-substituted deprenyl derivatives definitely proved that

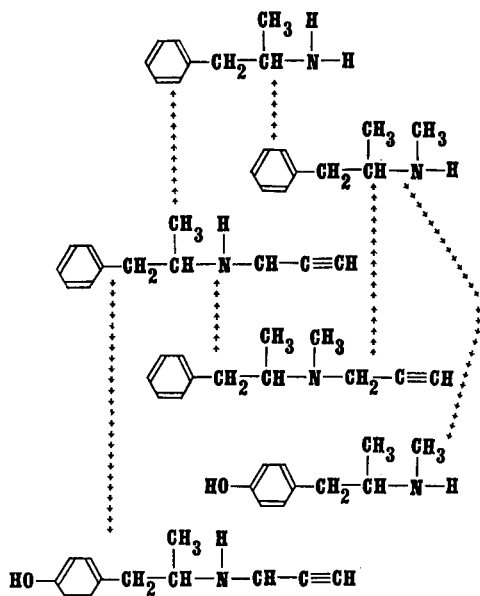


Fig. 9. Metabolic pathway of deprenyl. a, b, c, d, e and f are deprenyl, propargylamara methamphetamine, amphetamine, *p*-hydroxypropargylamara and *p*-hydroxymethamphetamine, respectively.

hydroxylation takes place at the *para* position of the deprenyl, if this process is not hindered by the presence of a *para* substituent in the parent drug (Fig. 8). The metabolic pathway of (–)-deprenyl is shown in Fig. 9.

It is worth mentioning that the very fast onset and decline of the deprenyl level in the brain strongly suggest that the parent drug, (–)-deprenyl, is responsible for the therapeutic effect and that the metabolites do not play any role.

#### ACKNOWLEDGEMENT

This work was financially supported by Grant No. 1892 of the Hungarian Academy of Sciences.

#### REFERENCES

- 1 J. Knoll, Z. Ecsery, J. G. Nivel and B. Knoll, *MTA.V. Osztály Közleményei*, 15 (1964) 231.
- 2 J. Knoll and K. Magyar, *Adv. Biochem. Pharmacol.*, 5 (1972) 393.
- 3 J. Knoll, *Acta Neurol. Scand.*, 95 (1983) 57.
- 4 J. Knoll, *J. Neural Transm.*, 25 (1987) 45.
- 5 J. P. Johnston, *Biochem. Pharmacol.*, 17 (1968) 1285.
- 6 J. I. Salach, K. Detmer and M. B. H. Youdim, *Mol. Pharmacol.*, 16 (1979) 234.
- 7 B. Ekstedt, K. Magyar and J. Knoll, *Biochem. Pharmacol.*, 28 (1979) 919.
- 8 W. Birkmayer and M. Yahr, *J. Neural Transm.*, 43 (1978) 177.
- 9 J. Knoll, E. S. Vizi and G. Somogyi, *Arzneim.-Forsch.*, 18 (1968) 109.
- 10 H. Kalász, *J. High Resolut. Chromatogr. Chromatogr. Commun.*, 6 (1983) 49.
- 11 H. Kalász, L. Kerecsen, J. Knoll, J. Pucso, R. Dobó and I. Hollósi, in H. Kalász and L. S. Ettre (Editors), *Chromatography '87*, Akadémiai Kiadó, Budapest, 1988, p. 275.

- 12 J. Glowinski and L. L. Iversen, *J. Neurochem.*, 13 (1966) 655.
- 13 L. Kerecsen, H. Kalász, J. Tarczali, J. Fekete and J. Knoll, in H. Kalász and L. S. Ettre (Editors), *Chromatography, the State of the Art*, Akadémiai Kiadó, Budapest, 1985, p. 195.
- 14 H. A. Anton and D. F. Sayre, *J. Pharmacol. Exp. Ther.*, 138 (1962) 360.
- 15 H. Ehringer and O. Hornykiewicz, *Wien. Klin. Wochenschr.*, 38 (1960) 1236.
- 16 G. P. Reynolds, J. D. Elswort, K. Blau, M. Sandler, A. J. Dees and G. M. Stern, *Br. J. Clin. Pharmacol.*, 6 (1978) 542.
- 17 T. Yoshida, Y. Yamada, T. Yamamoto and Y. Kuroiwa, *Xenobiotica*, 16 (1986) 129.



CHROMSYMP. 1659

## DETERMINATION OF FLUOXETINE AND NORFLUOXETINE BY HIGH-PERFORMANCE LIQUID CHROMATOGRAPHY

STEVEN H. Y. WONG\*, SANDY S. DELLAFERA and ROSINDA FERNANDES

*Drug Analysis Division, Department of Laboratory Medicine, University of Connecticut School of Medicine, Farmington, CT 06032 (U.S.A.)*

and

HENRY KRANZLER

*Department of Psychiatry, University of Connecticut School of Medicine, Farmington, CT 06032 (U.S.A.)*

---

### SUMMARY

A high-performance liquid chromatographic assay was developed for a recently introduced atypical antidepressant, fluoxetine and its demethylated metabolite, norfluoxetine. Prior to analysis, aliquots of alkalized plasma were extracted with *n*-hexane and isoamyl alcohol, followed by back-extraction with diluted phosphoric acid. These extracts were injected into a 10  $\mu\text{m}$ , reversed-phase  $\text{C}_{18}$  column with phosphate and acetonitrile as the mobile phase and detection at 214 nm. Peak height ratios were linearly correlated up to 800  $\mu\text{g/l}$ . Acceptable coefficients of variation were demonstrated for both within-run and day-to-day studies. Selected drugs were checked for interference. The assay was used to monitor nine patients receiving 20 to 80 mg of fluoxetine per day. Plasma concentrations of fluoxetine and norfluoxetine ranged from 37 to 301  $\mu\text{g/l}$  and 29 to 326  $\mu\text{g/l}$  respectively.

---

### INTRODUCTION

Antidepressant measurement by high-performance liquid chromatography (HPLC) has been advocated for the monitoring of first generation, as well as the recently introduced atypical antidepressants such as trazodone and its metabolite, 1-metachlorophenyl piperazine<sup>1–8</sup>. Currently, the enzyme multiplied immunoassay technique (EMIT) with monoclonal antibodies may be used for quantitative measurement of selected first generation antidepressants such as imipramine, desipramine, amitriptyline and nortriptyline<sup>9</sup>. Rapid screening for these antidepressants may be achieved by using polyclonal antibody-based EMIT and fluorescence polarization immunoassay (FPIA)<sup>4</sup>. However, for newly introduced antidepressants, reversed-phase HPLC is still the method of choice for analysis due to its reproducibility. The current study demonstrated that a newly introduced antidepressant, fluoxetine (FLU) and its demethylated metabolite, norfluoxetine (N-FLU), may be quantitated in plasma by modifying a previously published, simple procedure<sup>5</sup>.

Fluoxetine, N-methyl-8-[4-(trifluoromethyl)phenoxy] benzenepropanamine, is

a non-tricyclic antidepressant<sup>9-13</sup>. It exhibits selective inhibition of serotonin uptake in presynaptic neurons, and is indicated for unipolar depression. After oral administration, peak plasma concentration is reached within 6 to 8 h and absorption is not affected by the presence of food. Mean elimination half-life of FLU is 2 days following a single dose, and 4 days following long-term administration, while that of N-FLU is 7 days, independent of dosage regimen<sup>14</sup>. Fluoxetine is metabolized to norfluoxetine, also an inhibitor of serotonin reuptake, via demethylation, as shown in Fig. 1 (ref. 10). Other unidentified metabolites and glucuronides are also detected in the urine.

FLU and N-FLU were quantified by gas chromatography with electron-capture detection according to Nash *et al.*<sup>15</sup>. Orsulak *et al.*<sup>16</sup> described a procedure using a multi-step extraction and a reversed-phase HPLC analysis with a phenyl column and detection at 226 nm. For 24 patients administered daily doses of 20–60 mg of fluoxetine during the preceding three weeks, the plasma concentrations of FLU and N-FLU were 47–469 and 52–446  $\mu\text{g/l}$ , respectively. More recently, Kelly *et al.*<sup>14</sup> developed an HPLC assay in order to correlate plasma concentrations with clinical response. The assay involved an organic extraction, followed by reversed-phase analysis with a CN column and detection at 226 nm. From data on thirteen patients receiving daily doses of 20 to 60 mg of fluoxetine, the FLU and N-FLU serum concentrations were 73–453, and 54–362  $\mu\text{g/l}$  respectively. Antidepressant response, however, was not correlated with serum concentrations.

For ready adaptation in the clinical laboratory, a previously published HPLC procedure for quantification of antidepressants<sup>5</sup> was modified by using a readily available internal standard, clomipramine, a  $\text{C}_{18}$  column, a binary mobile phase and a readily available UV detection at 214 nm. This assay was used to quantitate plasma concentration of nine patients medicated with fluoxetine.

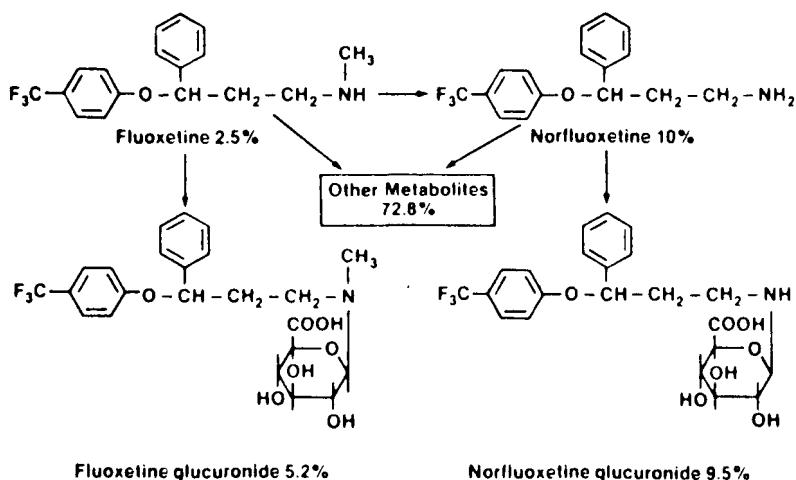


Fig. 1. Metabolites of fluoxetine identified in urine collected for 35 days from normal subjects given [<sup>14</sup>C]fluoxetine. (From ref. 10.)

## EXPERIMENTAL

*Chemicals*

Fluoxetine hydrochloride and norfluoxetine maleate were kindly provided by Eli Lilly (Indianapolis, IN, U.S.A.). Clomipramine, the internal standard, was obtained from Ciba-Geigy (Summit, NJ, U.S.A.). Primary stock solutions of fluoxetine and norfluoxetine, 10 mg/10 ml, were prepared by dissolving the appropriate amounts in 10 ml of distilled water inside volumetric flasks, while methanolic solution of clomipramine was similarly prepared. From these primary stock solutions, working aqueous stock solutions of FLU and N-FLU and working methanolic stock solution of clomipramine were prepared by diluting 100  $\mu$ l of the above solutions in 10 ml of water or methanol. Acetonitrile, *n*-hexane and methanol were "UV" grade, distilled in glass (Burdick and Jackson, Muskegon, MI, U.S.A.). Isoamyl alcohol, potassium dihydrogen phosphate and orthophosphoric acid were "Baker Analyzed" reagent grade (J. T. Baker, Phillipsburg, NJ, U.S.A.). The extraction solvent, *n*-hexane isoamyl alcohol (99:1), was prepared by mixing 990 ml of *n*-hexane with 10 ml of isoamyl alcohol, while 0.05% diluted phosphoric acid was prepared by diluting 59  $\mu$ l of the orthophosphoric acid into 100 ml with distilled water. The mobile phase consisted of 0.05 M, pH 4.7,  $\text{KH}_2\text{PO}_4$ -acetonitrile (6:4). The phosphate solution was prepared by dissolving 13.61 g of monobasic phosphate in 2 l of distilled water, followed by adjusting the pH with diluted potassium hydroxide.

For checking the precision of the assay, quality control samples containing about 200  $\mu$ g/l each of FLU and N-FLU were prepared by mixing 2 ml each of the working stock solutions of FLU and N-FLU with 96 ml of drug-free plasma in a silanized volumetric flask.

*Chromatographic system*

The chromatograph was a Model 5000 liquid chromatography (Varian, Walnut Creek, CA, U.S.A.). The detector was a Spectro-Monitor III variable wavelength UV detector (Laboratory Data Control, Riviera Beach, FL, U.S.A.). Chromatograms were recorded by an Omniscrite recorder (Houston Instruments, Austin, TX, U.S.A.). The analytical column was a  $\mu$ Bondapak  $\text{C}_{18}$  (30 cm  $\times$  4.6 mm I.D.) column, connected to a guard column packed with Bondapak/Corasil  $\text{C}_{18}$  (both from Waters/Millipore, Milford, MA, U.S.A.).

*Sample collection*

A total of ten blood samples were collected from nine patients (one patient had repeat samples drawn), 2 days to 5 months after the initiation of fluoxetine therapy with daily doses of 20 to 80 mg. Sampling was performed at 8 h following a bedtime dose or just before the ingestion of a morning dose. Blood collection was performed with evacuated tubes containing EDTA. Afterward, the sample tubes were centrifuged, followed by transferring the plasma to a polypropylene tube, and kept frozen until subsequent analysis.

*Procedures*

The extraction was a simple three step procedure: alkalinization, organic extraction and back-extraction. To a series of polypropylene tubes, 2-ml aliquots of

drug-free plasma were transferred, followed by addition of 0, 20, 40, 80 and 160  $\mu\text{l}$  of each of the working stock solutions of FLU and N-FLU. The resultant plasma concentrations were 0, 100, 200, 400 and 800  $\mu\text{g/l}$ . To these standards, quality control and patient samples, 160  $\mu\text{l}$  of the working internal standard solution of clomipramine were added. These tubes were vortexed, followed by addition of 2 ml aliquots of 1 M sodium hydroxide and further vortexing. Then, these mixtures were extracted with 5 ml aliquots of n-hexane-isoamyl alcohol (99:1) by rotation for 5 min, and centrifugation for 10 min. The organic layers were transferred to another series of marked polypropylene test tubes, followed by addition of 200  $\mu\text{l}$  of 0.05% dil. phosphoric acid for back-extraction. These tubes were rotated for 5 min and centrifuged for 10 min. The lower aqueous, acidic layer, containing FLU and N-FLU, was carefully pipetted into a small test tube for reversed-phase HPLC analysis.

#### *Chromatographic parameters*

Flow-rate was maintained at 2 ml/min. Column temperature was 50°C. Detection wavelength was 214 nm, 0.01 a.u.f.s. Injection volume ranged from 25 to 50  $\mu\text{l}$ .

#### RESULTS AND DISCUSSION

Fig. 2 shows the chromatograms for the extracts of drug-free plasma, a 200  $\mu\text{g/l}$  standard, and a patient sample. Retention times of N-FLU, FLU and the internal standard were 5.8, 6.8 and 9.5 min respectively, with the corresponding capacity factors ( $k'$ ) of 2.9, 3.5 and 5.3. Fig. 3 shows the linear calibration up to 800  $\mu\text{g/l}$  for both FLU and N-FLU, with excellent correlation coefficients. Precision studies showed acceptable coefficients of variation for both within-run and day-to-day studies, as shown by Table I. Recoveries ranged from 55 to 60% for N-FLU, and 79 to 86% for FLU, comparable to those of other antidepressant assays<sup>3-7</sup>. Sensitivity, defined as signal-to-noise ratio = 3, is estimated to be 6  $\mu\text{g/l}$  for both FLU and N-FLU. Selected drugs, checked for potential interference, their capacity factors are listed in Table II, showing the co-elution of imipramine with N-FLU and amitriptyline with FLU.

In modifying a previously published assay, our goal was to develop a simple and fast procedure that is adaptable by clinical laboratory personnel. Since clinical laboratory personnel would most likely be performing HPLC assays of the first generation tricyclics as well as the newer, atypical antidepressants, the simplicity of the described procedure would allow direct adaptation without lengthy daily change-over of extraction chemicals, solvents and columns. Since different personnel of a given laboratory would be using this procedure, the simplicity of the assay would ensure precision. This approach has been successfully applied in our clinical laboratory where the monitoring of first generation antidepressants, as well as new antidepressants and metabolites is routinely offered.

Simplicity of the procedure is evident in the use of a readily available C<sub>18</sub> column and detection wavelength of 214 nm. This was chosen instead of 226 nm, as in the assays of Orsulak *et al.*<sup>16</sup> and Kelly *et al.*<sup>14</sup>, because 214 nm detectors are readily available in most clinical laboratories as a filter or variable-wavelength detector. In the procedure of Kelly *et al.*<sup>14</sup>, protriptyline was used as an internal standard. In our procedure, clomipramine was used as the internal standard for this as well as other



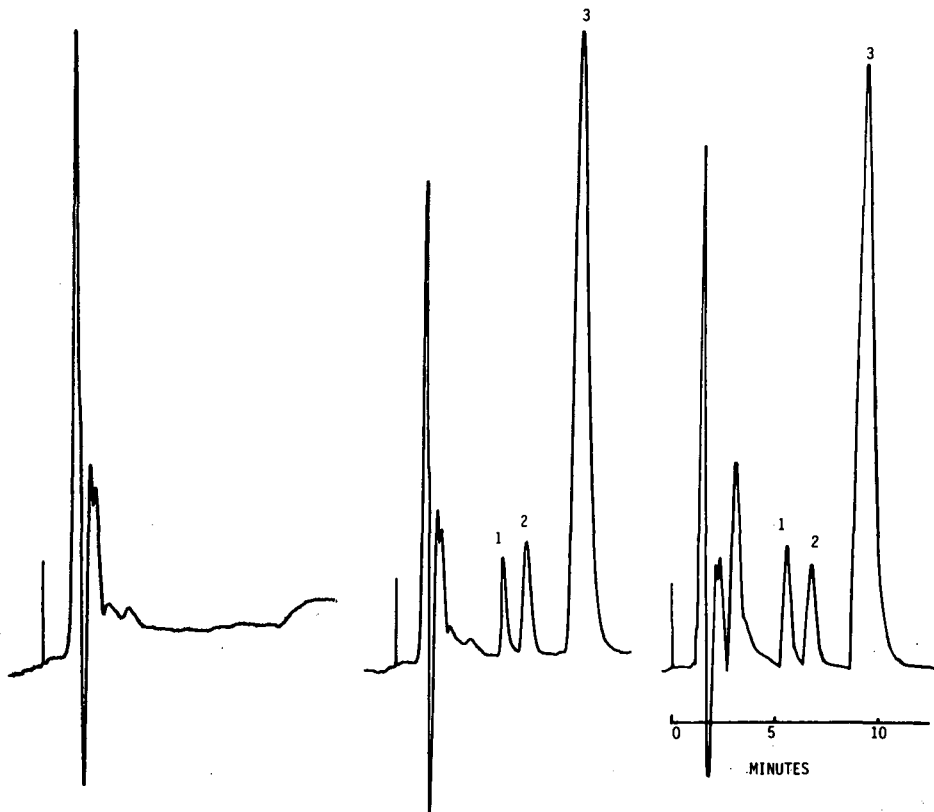


Fig. 2. Chromatograms of extracts of: (left) drug-free plasma (center) plasma with 200 µg/l each of FLU and N-FLU, and (right) a patient's plasma with 163 µg/l of FLU, and 208 µg/l of N-FLU. Peaks: 1 = N-FLU; 2 = FLU; 3 = internal standard, clomipramine.

clinical procedures for the first generation tricyclics. The choice of protriptyline and clomipramine as the internal standards enhances ready clinical adaptation of these procedures, even though the chemical structure of the tricyclic rings of both internal standards are different from those of FLU and N-FLU, as shown by Fig. 1.

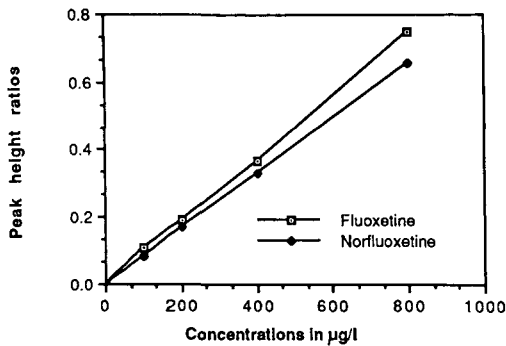


Fig. 3. Calibration curves for FLU and N-FLU. (FLU:  $y = 9.24 \cdot 10^{-4}x - 0.0049$ ,  $r = 0.9999$ ; N-FLU:  $y = 8.19 \cdot 10^{-4}x - 0.0024$ ,  $r = 0.9999$ ).

TABLE I

WITHIN-RUN AND DAY-TO-DAY COEFFICIENTS OF VARIATION (C.V.) IN THE DETERMINATION OF FLU AND N-FLU

	Mean ( $\mu\text{g/l}$ )	C.V. (%)	n
<i>Within-run</i>			
FLU	197.8	1.6	6
N-FLU	201.8	0.7	6
<i>Day-to-day</i>			
FLU	191.4	4.1	18
N-FLU	193.1	5.5	18

Since the precision and recovery of the assay are comparable to those of other antidepressant assays, it was used to check the plasma FLU and N-FLU concentrations of a patient medicated with 80 mg of fluoxetine. Plasma concentration of FLU and N-FLU were 163 and 208  $\mu\text{g/l}$  respectively. Table III lists the data for a group of nine patients medicated with 20–80 mg of fluoxetine and other medications, their FLU and N-FLU plasma concentrations, and relevant clinical information. Since FLU is a newly introduced antidepressant, its use in combination with other drugs may be enhanced by monitoring FLU and N-FLU. It is in this respect that our study differs from those of Orsulak *et al.*<sup>16</sup> and Kelly *et al.*<sup>14</sup> in terms of the observed concentrations. However, the range of FLU and N-FLU are comparable in all three studies.

In general, there was a direct relationship between dosage and the combined fluoxetine and norfluoxetine plasma concentrations measured by us. A similar relationship appears to exist between duration of treatment and plasma concentrations. Notable exceptions to these trends are evidenced by patients 3 and 4, who as out-patients were less likely to have been compliant with the prescribed dosage, and by patients 7 and 9, who were on a variety of medications concomitant with fluoxetine.

TABLE II

CAPACITY FACTORS ( $k'$ ) OF SOME COMMON DRUGS TESTED FOR INTERFERENCE

Drug	$k'$	Drug	$k'$
Acetaminophen	0.00	Desipramine	2.44
Codeine	0.00	Nortriptyline	2.74
Meperidine	0.12	Norfluoxetine	2.90
Phenobarbital	0.84	Imipramine	2.90
Amoxapine	1.67	Propoxyphene	3.48
Phenytoin	1.40	Amitriptyline	3.49
Pentobarbital	1.56	Fluoxetine	3.50
Oxazepam	1.79	Diazepam	3.99
Lorazepam	1.88	Chlorpromazine	4.15
Secobarbital	1.88	Perphenazine	4.92
Flurazepam	2.04	Clomipramine	5.30
Chlordiazepoxide	2.18	Prochlorperazine	6.04
Doxepin	2.20	Thioridazine	8.44
Cimetidine	2.36	Trifluoperazine	8.44

TABLE III  
 PATIENT PLASMA CONCENTRATIONS

Patient	Age	Sex	Inpatient/ outpatient	Daily dosage (mg)	Duration of therapy	Indication	Other medications	FLU( $\mu\text{g/l}$ )	N-FLU( $\mu\text{g/l}$ )
1	28	M	I	20	3 days	Alc. dep. <sup>a</sup>	Atenolol 50 mg	37	29
2	27	M	I	20	13 days	MDD <sup>b</sup>	Perphenazine 4 mg	63	33
3	52	M	O	60	5 months	Somatization disorder	Alprazolam 1.5 mg	98	49
4	37	M	O	40	9 months	MDD <sup>b</sup>	Alprazolam 3 mg Chloral hydrate 2 g	156	156
5	53	F	I	20	9 days	MDD <sup>b</sup>	Perphenazine 4 mg	141	198
6	32	F	O	20	3 months	Adjustment disorder with depressed mood	None	143	220
7	65	M	I	20	13 days	MDD <sup>b</sup>	Glyburide 2.5 mg Chlorpromazine 25 mg Triazolam 0.25 mg	301	65
8	36	M	I	80	5 weeks	Bipolar disorder depressed	Lorazepam 4 mg LiCO <sub>3</sub> 1500 mg	283	60
9	34	F	I	40	2 days	Alc. dep. <sup>a</sup> Agoraphobia with panic disorder	Chlorzoxazone 600 mg Chlordiazepoxide 25 mg	163	208
					2 months	MDD <sup>b</sup>		152	326

<sup>a</sup> Alcohol dependence.

<sup>b</sup> Major depressive disorder.

Repeated sampling from one patient (No. 7) resulted in very similar plasma values for both fluoxetine and norfluoxetine, following a 20 mg oral dose. While the limitations imposed by variability in compliance, concomitant medication, and individual pharmacokinetic factors cannot be disentangled in the present sample of patients, the present study demonstrated the suitability of the assay for typical clinical monitoring of FLU and N-FLU.

As shown by Kelly *et al.*<sup>14</sup>, serum concentrations are not well correlated to clinical response. However, Orsulak<sup>17</sup> has suggested monitoring of fluoxetine may be helpful in the future for patients medicated with fluoxetine and other drugs. Recently, he observed that patients switching medications such as fluoxetine for tricyclics may benefit from monitoring due to possible drug-to-drug interactions. This may be explained by inhibition of the metabolism of first generation tricyclics by fluoxetine, resulting in possibly elevated levels of the first generation tricyclics. However, the described assay is not able to resolve the first generation tricyclics from fluoxetine and norfluoxetine due to co-elution with imipramine and amitriptyline as shown by Table II. Thus, there may be a need for future development of an alternative assay that can resolve combinations of tricyclics and serotonin-inhibiting antidepressants.

#### ACKNOWLEDGEMENT

The authors gratefully thank Dr. Paul J. Orsulak for his many helpful discussions, and his encouragement in the planning of this project.

#### REFERENCES

- 1 S. H. Y. Wong, *Clin. Chem. (Winston-Salem, N.C.)*, 34 (1988) 848–855.
- 2 A. Fazio, E. Spina and F. Pisani, *J. Liq. Chromatogr.*, 10 (1987) 223–240.
- 3 S. H. Y. Wong, in S. H. Y. Wong (Editor), *Therapeutic Drug Monitoring and Toxicology by Liquid Chromatography*, Marcel Dekker, New York, 1985, pp. 39–78.
- 4 S. H. Y. Wong, in B. Gerson (Editor), *Clinics in Laboratory Medicine*, Saunders, Philadelphia, PA, 1987, pp. 415–433.
- 5 S. H. Y. Wong and S. W. Waugh, *Clin. Chem. (Winston-Salem, N.C.)*, 29 (1983) 314–318.
- 6 S. H. Y. Wong, S. W. Waugh, M. Draz and N. Jain, *Clin. Chem. (Winston-Salem, N.C.)*, 30 (1984) 230–233.
- 7 S. H. Y. Wong and N. Marzouk, *J. Liq. Chromatogr.*, 8 (1985) 1379–1395.
- 8 R. F. Suckow, *J. Liq. Chromatogr.*, 6 (1983) 2195–2208.
- 9 S. Pankey, C. Collins, A. Jaklitsch, A. Izutsu, M. Hu, M. Pirio and P. Singh, *Clin. Chem. (Winston-Salem, N.C.)*, 32 (1986) 768–772.
- 10 L. Lemberger, R. G. Bergstrom, R. L. Wolen, N. A. Farid, G. G. Enas and G. R. Aronoff, *J. Clin. Psychiatry*, 46, No. 3 (sec. 2) (1985) 14–19.
- 11 K. Rickels, W. T. Smith, V. Glaudin, J. B. Amsterdam, C. Weise and G. P. Settle, *J. Clin. Psychiatry*, 46, No. 3 (sec. 2) (1985) 38–41.
- 12 P. Stark, R. W. Fuller and D. T. Wong, *J. Clin. Psychiatry*, 46, No. 3 (sec. 2) (1985) 7–13.
- 13 P. Benfield, R. C. Heel and S. P. Lewis, *Drugs*, 32 (1986) 481–508.
- 14 M. W. Kelly, P. J. Perry, S. G. Holstad and M. J. Garvey, *Ther. Drug Monit.*, 11 (1989) 165–170.
- 15 J. F. Nash, R. J. Bopp, R. H. Carmichael and L. Lemberger, *Clin. Chem. (Winston-Salem, N.C.)*, 28 (1982) 2100–2102.
- 16 P. J. Orsulak, J. T. Kenney, J. R. Debus, G. Crowley and P. D. Wittman, *Clin. Chem. (Winston-Salem, N.C.)*, 34 (1988) 1875–1878.
- 17 P. J. Orsulak, personal communication.

CHROMSYMP. 1644

## ON-LINE HIGH-PERFORMANCE LIQUID CHROMATOGRAPHY FOR THE DETERMINATION OF CEPHALOSPORIN C AND BY-PRODUCTS IN COMPLEX FERMENTATION BROTHS

K. HOLZHAUER-RIEGER, W. ZHOU and K. SCHÜGERL\*

*Institut für Technische Chemie, Universität Hannover, Callinstr. 3, D-3000 Hannover 1 (F.R.G.)*

---

### SUMMARY

A fully automated high-performance liquid chromatographic system was developed for optimization of cephalosporin C production. Using a simple, isocratic, reversed-phase method, cephalosporin C, deacetylcephalosporin C, deacetoxycephalosporin C, penicillin N, methionine and its decomposition product 2-hydroxy-4-methylmercaptobutyric acid were determined. The method worked reliably for 250 h and supplied information on the influence of many parameters of the process.

---

### INTRODUCTION

Cephalosporin C (CPC) is a  $\beta$ -lactam antibiotic and its biosynthesis (Fig. 1) is similar to that of penicillin. CPC is produced by the mold *Cephalosporium acremonium* by a fed-batch fermentation technique<sup>1</sup>. Optimization of this process requires accurate and reliable measurements of substrates and products over a long period. Process analysis allows the detection of contamination at an early stage and the monitoring of the ratio of product to by-products to estimate the end-point of cultivation. Further, the influence of dissolved oxygen tension and the feed of substrate solutions [such as methionine (MET) and phosphate] on the production of CPC is particularly interesting. The determination of MET is important because it is a source of sulphur for antibiotic production.

An on-line method for cephalosporin determination using an automatic analyser system has been described<sup>1</sup>. The cephalosporins show an absorbance at 260 nm that disappears when they are treated with cephalosporinase, a  $\beta$ -lactamase. The reaction is specific for all cephalosporin derivatives, so that it only indicates the overall concentration of CPC, deacetylcephalosporin C (DAC) and deacetoxycephalosporin C (DAOC). This disadvantage prompted us to employ high-performance liquid chromatography (HPLC), which offers the possibility of determining several substances simultaneously. Möller *et al.*<sup>2</sup> used an on-line HPLC system for the determination of penicillin V. For several years, HPLC has been used for cephalosporin analysis<sup>3–8</sup> but not for process control. The aim of our investigations was the optimization and automation of a chromatographic method for on-line cephalosporin determination that would work reliably for 250 h. For on-line analysis, a continuous,

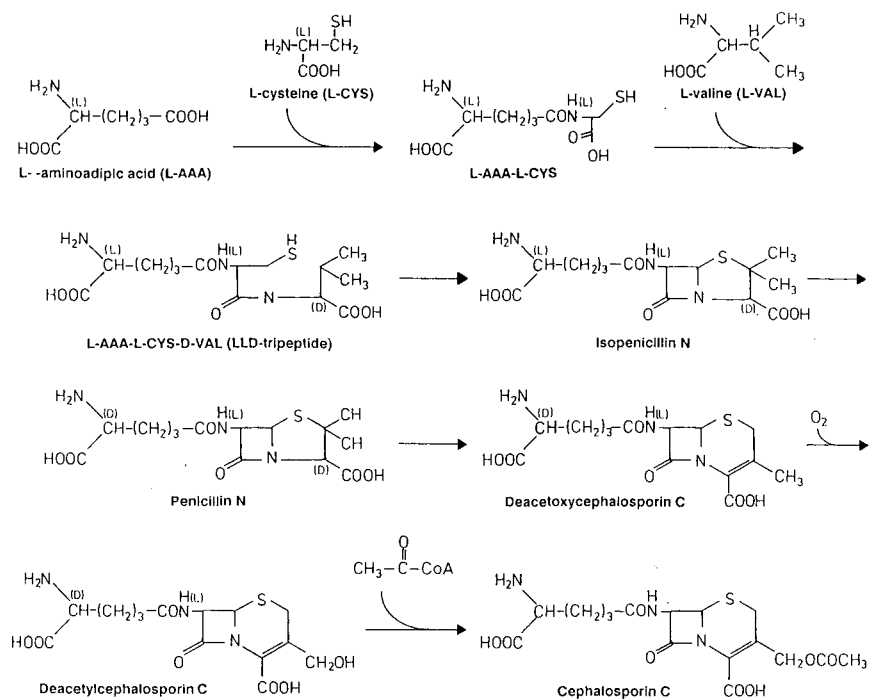


Fig. 1. Biosynthetic cephalosporin pathway.

sterile and cell-free sampling stream is required. The sampling module must work dependably over a period of days. The results are presented in this paper.

## EXPERIMENTAL

### *Fermentation conditions*

CPC production was carried out in a 20 l stirred-tank reactor by fed-batch operation. The complex fermentation medium contained 50–100 g/l of solid peanut flour and other substrates such as glucose, salts and antifoam. A glucose–methionine solution containing 500 g/l of glucose and 20 g/l of MET was used as the feed. In order to avoid catabolic repression, continuous feeding was started after the initial glucose in the medium had been used up. By varying the feeding rates (0.25–1.5 ml/min), a low glucose level could be maintained during the production phase.

### *Materials*

CPC, DAC, DAOC, penicillin N (PEN N) and 2-hydroxy-4-methylcaptopbutyric acid (MMBS) were supplied by Ciba-Geigy (Basle, Switzerland), tetrabutylammonium hydrogensulphate (TBAHS), phosphate salts and MET by Fluka (Neu-Ulm, F.R.G.) and HPLC-grade methanol by Merck (Darmstadt, F.R.G.). Doubly distilled water was obtained using a deionization system from Millipore (Eschborn, F.R.G.). Mobile phases and standard solutions were prepared with Milli-Q water (Millipore). The eluents were degassed with a stream of helium before and during the analysis.

### Sampling system

For continuous sampling, different laboratory-built systems<sup>2,7,8</sup> are in use in our Institute. Two modules were employed for CPC fermentation. One is a flat, porous-plate filter<sup>2,8</sup> with polysulphone membranes (molecular weight cut-off 100 000; Sartorius, Göttingen, F.R.G.). The active filtration area is 47.5 cm<sup>2</sup> and the dead volume is 2.5 ml. For a low solid content in the medium (50 g/l of peanut flour) this sampling system showed very good results, but when using 100 g/l of peanut flour, the filtration rate decreased. This prompted us to employ another type of module (Fig. 2), which had been developed for *E.coli* fermentation. It turned out that it could also be used for CPC production. The module (ABC, Puchheim, F.R.G.) is made of stainless steel and contains a tubular membrane (polypropylene, 200 × 5.5 mm I.D.; pore size, 0.2 μm; Enka, Düsseldorf, F.R.G.). Both modules are positioned in the lower section of the reactor in a well aerated region. They can be steam-sterilized at 121°C. A permeation rate of 0.5–1.0 ml/min could be maintained during fermentation. The filtrate was pumped continuously through capillary Teflon tubes into the injection valve of the HPLC system. For sampling, two tubes were used and alternated daily; one was connected with the sample loop and the other was flushed with formaldehyde and then with water in order to avoid microbial growth. The sampling dead time in the tubes, including the sampling module, was 10 min.

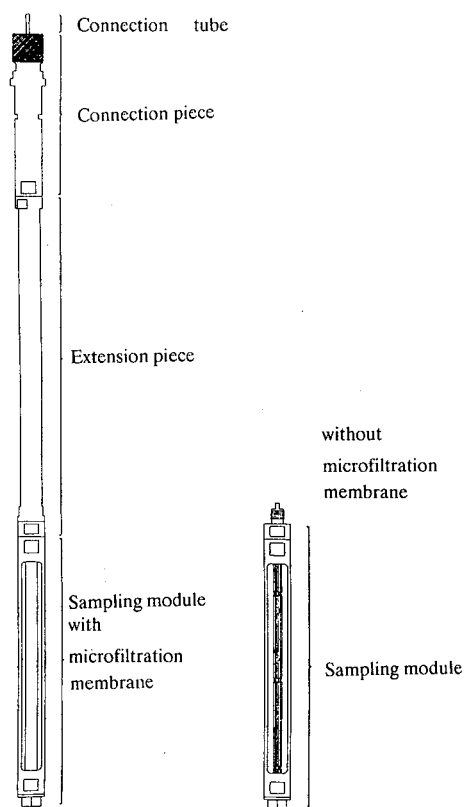


Fig. 2. Sampling module with tubular micromembrane.

### *HPLC equipment*

The HPLC equipment used for cephalosporin analysis consisted of a peristaltic pump (Verder Deutschland, Düsseldorf, F.R.G.), a Spectroflow 400 HPLC pump (Applied Biosystems, Weiterstadt, F.R.G.), an electrical injection valve (VICI Valco Europe, Schenkon, Switzerland) with a 10- $\mu$ l sample loop, a separation column, a Spectroflow 757 variable-wavelength UV detector (Applied Biosystems) and an SP4270 integrator. The analytical column (250  $\times$  4.6 mm) was packed with Nucleosil 100-5C<sub>18</sub> or Nucleosil 100-10C<sub>18</sub> (Macherey-Nagel & Co., Düren, F.R.G.) and was protected by a guard column (50  $\times$  4.6 mm I.D.) containing Vydac-201 SC reversed-phase material (Macherey-Nagel & Co.; 30–40  $\mu$ m, dry packed). The columns were thermostated in a water-bath at 25–30°C.

The HPLC system was controlled by the integrator, which operated the injection valve, started automatically after a previously designated time (0.5–2 runs/h), set the auto-zero-point at the detector, started the pump before the injection (flow-rate 1.0 ml/min) and reduced the flow-rate after the end of the run (0.1 ml/min). Further, the integrator recorded the chromatograms, calculated the concentrations and transmitted them to a process computer (PDP-11/23, Digital Equipment, Munich, F.R.G.) or a PC (Epson, WINner software, Spectra-Physics) for on-line storage.

### RESULTS AND DISCUSSION

During CPC fermentation, the following components are of special interest: CPC and its precursors DAC, DAOC, PEN N in the biosynthesis, MET and its degradation product MMBS. The cephalosporins show a UV maximum at 260 nm due to the cepham chromophore. This O=CNC=C group is not present in PEN N. MET and MMBS also did not show any absorbance at 260 nm. Consequently, the analytical wavelength must be lowered; the most suitable one for monitoring all compounds turned out to be 225 nm.

Different eluents were tested. A mobile phase consisting of 5–10% methanol–90–95% 14 mM phosphate buffer solution, containing 10.3 mM TBAHS (pH adjusted to 6.5), proved to be optimal for the separation of the six compounds. A 2-l volume of the mobile phase was prepared at a time and used during one fermentation by recycling the solvent. A constant flow-rate (1 ml/min) was maintained during the analysis. The methanol content depended on the age of the analytical column. For new separation columns, we started with 10% methanol in the eluent and, if the separation becomes unsatisfactory, the content was reduced to 5%. Further, it was possible to adjust the analysis time by controlling the temperature of the column; during one fermentation, however, the composition of the eluent and the temperature were kept constant. Over a period of 200 h, a 2-min reduction in the retention time for CPC and an increase in the back-pressure was observed. This was due to the complex medium containing proteins which were accumulated on the stationary phase. As the filling material is a highly efficient filter, it was advisable to change the guard column material before each fermentation. The lifetime of the separation column was about three fermentations, after which the selectivity of the column was insufficient so that the separation of the major components from other substances was not satisfactory for quantification.

At the beginning of a fermentation, the HPLC system was calibrated by mea-



asuring the peak areas of a standard solution containing MET, DAC, DAOC, PEN N, CPC and MMBS. During the fermentation, there was no need for any additional calibration. The substances in the chromatograms of the fermentation samples were identified by the retention times of the peaks and by mixing a sample with a standard solution. The recovery for DAC and CPC in fermentation samples was nearly 100%. Fig. 3 shows selected chromatograms of a standard solution and a sample after 75 h of a *C. acremonium* fermentation. It can be seen that the separation of the standard compounds is excellent, but the chromatogram of the fermentation sample shows many unknown substances, particularly at the beginning. Thus, for CPC, DAC and PEN N, the most important components, the resolution was good, but the quantification of MET became difficult at lower concentrations. The linearity of the assay system was established by examining the response of CPC as a function of concentration, and a linear behaviour was obtained from 0.5 to 8.0 g/l. The relative standard deviations (R.S.D.) for the calibration solution (ten runs) are shown in Table I.

The results of typical on-line measurements for the main components involved in the biosynthesis are shown in Fig. 4. DAOC is not included because of its low concentration in the fermentation samples (below 0.5 g/l). After 200 h, a steady state

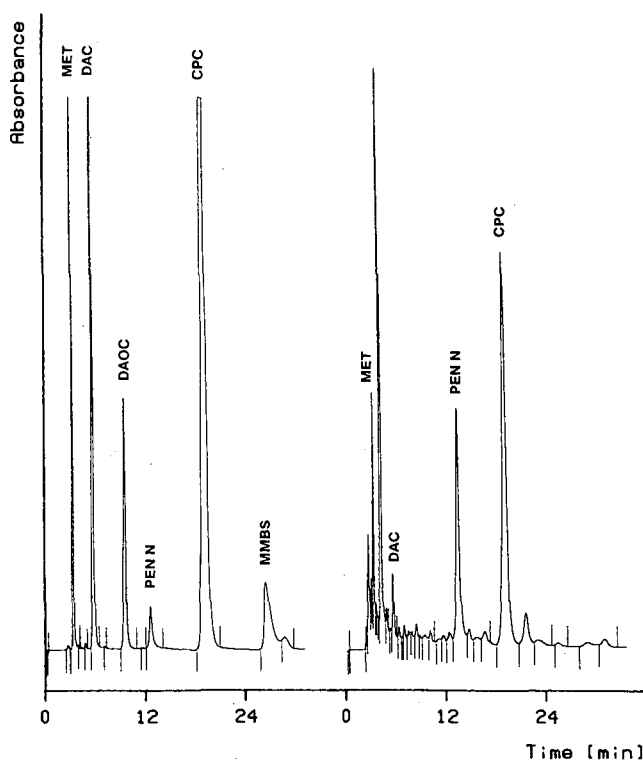


Fig. 3. Chromatograms of a calibration and a fermentation sample. Column, Nucleosil 100-5C<sub>18</sub> (250 × 4.6 mm I.D.); temperature, 30°C; eluent, methanol-14 mM phosphate buffer containing 3.5 g/l TBAHS (pH 6.5) (5:95); flow-rate, 1.0 ml/min; range, 0.1 a.u.f.s. (A) Chromatogram of a standard solution: MET, 2.38 g/l; DAC, 0.4 g/l; DAOC, 0.2 g/l; PEN N, 0.26 g/l; CPC, 1.297 g/l; MMBS, 1.32 g/l. (B) Chromatogram of a CPC fermentation sample.

TABLE I

## MEAN VALUES AND STANDARD DEVIATIONS FOR A CALIBRATION SOLUTION

Results calculated from the integrator for ten chromatograms. Concentrations in the standard solution: MET, 2.09 g/l; DAC, 0.50 g/l; DAOC, 0.20 g/l; PEN N, 0.25 g/l; CPC, 1.29 g/l; MMBS, 1.01 g/l.

Component	Mean concentration (g/l)	S.D. (g/l)	R.S.D. (%)
MET	2.17	0.039	1.8
DAC	0.51	0.005	1.1
DAOC	0.21	0.004	1.8
PEN N	0.26	0.006	2.4
CPC	1.29	0.015	1.1
MMBS	1.09	0.033	3.0

between CPC formation and decomposition was reached, and it was impossible to increase the CPC concentration by longer fermentation times. The main reason is probably the enzymatic degradation of the CPC to DAC by an acetylhydrolase, produced by the fungi, or repression of the last step of the biosynthesis. Therefore, the DAC and PEN N concentrations increased only slightly while the CPC production decreased.

Fig. 4 also shows a comparison of on-line and off-line measurements during fermentation. There is good agreement for the CPC and DAC analytical data. At the end of the production phase, the off-line values for PEN N differ from the on-line measurements, probably owing to inaccurate integration of the small peaks. This demonstrates the advantage of on-line determinations compared with a few off-line data.

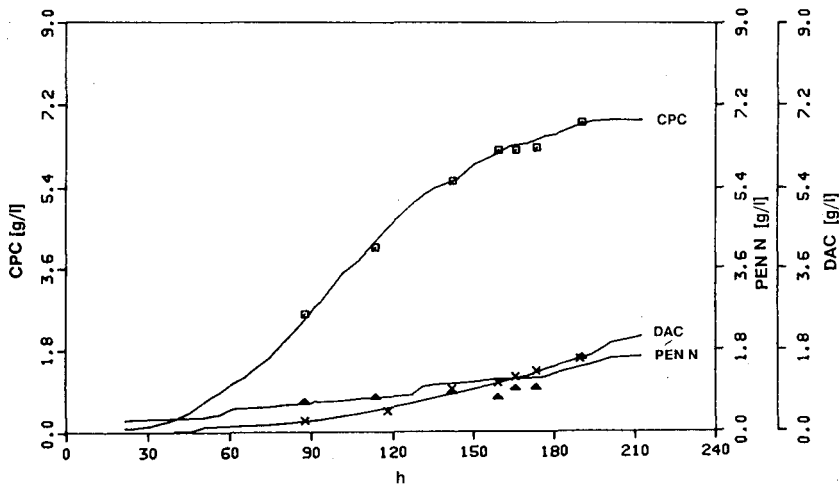


Fig. 4. Cephalosporin C production: comparison of on-line (solid lines) and off-line (points) determinations. Fresh samples:  $\square$  = CPC;  $\triangle$  = PEN N;  $\times$  = DAC.

## REFERENCES

- 1 Th. Bayer, Th. Herold, R. Hiddessen and K. Schügerl, *Anal. Chim. Acta*, 190 (1986) 213–219.
- 2 J. Möller, R. Hiddessen, J. Niehoff and K. Schügerl, *Anal. Chim. Acta*, 190 (1986) 195–203.
- 3 Th. Herold, Th. Bayer and K. Schügerl, *Appl. Microbiol. Biotechnol.*, 29 (1988) 168–173.
- 4 R. D. Miller and N. Neuss, *J. Antibiot.*, 29 (1976) 902.
- 5 E. R. White and J. E. Zarembo, *J. Antibiot.*, 34 (1981) 836.
- 6 E. Crombez, W. Van den Bossche and P. De Moerloose, *J. Chromatogr.*, 169 (1979) 343–350.
- 7 J. Niehoff, J. Möller, R. Hiddessen and K. Schügerl, *Anal. Chim. Acta*, 190 (1986) 205–212.
- 8 K. Schügerl, *Anal. Chim. Acta*, 213 (1988) 1–9.



CHROMSYMP. 1640

## DETERMINATION OF *D*-*myo*-1,2,6-INOSITOL TRISPHOSPHATE BY ION-PAIR REVERSED-PHASE LIQUID CHROMATOGRAPHY WITH POST-COLUMN LIGAND EXCHANGE AND FLUORESCENCE DETECTION

H. IRTH\*, M. LAMOREE, G. J. DE JONG, U. A. Th. BRINKMAN and R. W. FREI<sup>a</sup>

*Department of Analytical Chemistry, Free University, De Boelelaan 1083, 1081 HV Amsterdam (The Netherlands)*

and

R. A. KORNFELDT and L. PERSSON

*Perstorp Pharma, 28480 Perstorp (Sweden)*

---

### SUMMARY

A detection system for *D*-*myo*-1,2,6-inositol trisphosphate (1,2,6-IP<sub>3</sub>) has been developed which is based on the strong complexing properties of the phosphate groups and which includes a post-column ligand-exchange reaction. The weakly fluorescent complex of Fe<sup>III</sup> with methylcalcein blue (MCB) is used as a reagent. Analytes that form a stronger complex with Fe<sup>III</sup> than MCB cause a ligand-exchange reaction; the amount of strongly fluorescent MCB released during this reaction is proportional to the analyte concentration and can be measured sensitively by direct fluorescence detection. The influence of the pH, the reagent concentration, the Fe<sup>III</sup> to MCB ratio, the content of organic modifier and the dimensions of the post-column reaction system on the sensitivity of the detection system are discussed. In combination with ion-pair reversed-phase liquid chromatography, a detection limit of 3–10 ng has been obtained for 1,2,6-IP<sub>3</sub>. The present system has been combined with a preconcentration technique, based on ion-pair formation, which allows the determination of low-ppb concentrations of 1,2,6-IP<sub>3</sub>.

---

### INTRODUCTION

Interest in the biochemistry of inositol phosphates is increasing because of their important role in signal transmission in the living cell<sup>1</sup>. *D*-*myo*-1,4,5-Inositol trisphosphate (1,4,5-IP<sub>3</sub>) was found to act as “second messenger”, being released by hydrolysis of a cell membrane constituent, phosphatidylinositol-4,5-bisphosphate<sup>1,2</sup> after agonist stimulation. Another inositol trisphosphate isomer, *D*-*myo*-1,2,6-inositol trisphosphate<sup>3</sup> (1,2,6-IP<sub>3</sub>), which has interesting pharmacological properties, is currently in a preclinical development phase at Perstorp Pharma (Perstorp, Sweden). The pharmacological properties of 1,2,6-IP<sub>3</sub> include inhibition of platelet thrombus formation,

---

<sup>a</sup> Author deceased.

as shown by Sirén *et al.*<sup>4</sup>, and prevention of complications of diabetes, as described by Renaud *et al.*<sup>5</sup>. The compound also shows antiinflammatory effects<sup>6</sup>. Unlike 1,4,5-IP<sub>3</sub>, 1,2,6-IP<sub>3</sub> does not release calcium from intracellular stores<sup>7</sup>.

Most data published on the determination of inositol phosphates are based on radioisotope techniques. They are applicable to cells and tissue samples, which are incubated with, *e.g.*, *myo*-[<sup>3</sup>H]inositol, in order to obtain labelled inositol phosphates. These techniques have limitations as they do not provide absolute concentrations and are not suitable for the analysis of a large number of samples. In order to obtain and interpret the pharmacokinetics of, *e.g.*, 1,2,6-IP<sub>3</sub>, the need for a direct method is apparent.

Several liquid chromatographic (LC) techniques have been developed for inositol phosphates in order to overcome the problems connected with radioactive labelling. The separation of the inositol phosphates is based on ion-exchange or ion-pairing principles<sup>8-18</sup>. However, the detection of inositol phosphates still remains the main problem for LC, as this type of compound is difficult to detect by conventional methods, such as with UV or electrochemical detectors. The low reactivity of the sugar-type OH groups limits the applicability of derivatization reactions for fluorescence detection. Post-column reaction detection systems developed so far are based on either enzymatic reactions with subsequent determination of the released inorganic phosphate<sup>10,16</sup> or inositol<sup>19</sup>. An alternative is the application of ligand-exchange reactions that make use of the strong complexing properties of the phosphate groups.

The latter principle was used in 1953 by Wade and Morgan<sup>20</sup> as a method to detect phosphate esters in paper chromatography. The reaction is based on the decrease of the colour intensity of the red Fe<sup>III</sup>-sulphosalicylic acid complex at low pH when organic or inorganic phosphate-containing compounds are added. Cilliers and Van Niekerk<sup>12</sup> applied this principle to the LC detection of phytic acid (inositol hexakisphosphate), and Mayr<sup>9</sup> used the same ligand-exchange principle in a system based on coloured complexes of 4-(2-pyridylazo)resorcinol (PAR) with transition metal ions, such as holmium and ytterbium. Meek and Pietrzyk<sup>11</sup> developed a post-column indirect fluorescence detection system based on the quenching of the Al<sup>III</sup>-morin fluorescence by phosphorus oxo acids. Detection limits as low as 15 ng were obtained for, *e.g.*, difluoro(methylene) phosphonic acid.

The colorimetric or fluorescence methods described have the disadvantage that detection is based on the decrease in a steady signal, that is, the analyte signal is measured against a high background signal caused by the reagent. We have previously developed a direct fluorescence detection system based on a post-column ligand-exchange reaction which causes an increase in the signal against a low background<sup>21</sup>. In this paper, we report the application of this principle to the determination of 1,2,6-IP<sub>3</sub>. In order to decrease the detection limit of 1,2,6-IP<sub>3</sub> further, we have also developed an ion-pairing preconcentration system that allows the introduction of larger sample volumes than direct with loop injections.

## EXPERIMENTAL

### *Chemicals*

All reagents were of analytical-reagent grade. The organic solvents and iron-

(III) nitrate were Baker (Deventer, The Netherlands) Analyzed Reagents. 1,2,6-IP<sub>3</sub> and inositol bisphosphate (a mixture of 1,2-IP<sub>2</sub> and 1,6-IP<sub>2</sub>) was purchased from Perstorp Pharma, tetrapentyl- (TPABr) and tetrabutylammonium bromide (TBABr) from Kodak (Rochester, NY, U.S.A.), methylcalcein blue (MCB) from Janssen (Beerse, Belgium) and Tris buffer from Sigma (St. Louis, MO, U.S.A.). Stock solutions (1 mM) of iron(III) nitrate and MCB were prepared in 0.1 M nitric acid and methanol, respectively. The reagent solution (Fe:MCB = 1:3, [Fe<sup>III</sup>] = 6.6 · 10<sup>-6</sup> M) was prepared by adding iron(III) nitrate to a solution of MCB in methanol–20 mM Tris buffer (pH 7.0) (95:5, v/v).

#### *Instrumentation*

Experiments were carried out in an LC system consisting of a Waters Assoc. (Milford, MA, U.S.A.) Model 510 LC pump, a Valco six-port injection valve, a 200 × 4.6 mm I.D. stainless-steel separation column packed with 5- $\mu$ m Hypersil ODS (Shandon Southern, Runcorn, U.K.) and a Kontron (Zürich, Switzerland) SFM 23 fluorescence detector (excitation wavelength 328 nm, emission wavelength 440 nm). The precolumn (10 × 4.6 mm I.D.), used for the preconcentration of 1,2,6-IP<sub>3</sub>, was purchased from Chrompack (Middelburg, The Netherlands) and packed manually with a slurry of 10- $\mu$ m LiChrosorb RP-18 (Merck, Darmstadt, F.R.G.) in methanol. For preconcentration a Kontron 414 LC pump was used at a flow-rate of 2 ml/min. Samples were dissolved in the carrier solution [5 mM Tris buffer (pH 7.0)–2 mM TPABr] and injected onto the preconcentration column via a 1-ml loop. The washing solution was acetonitrile–10 mM Tris buffer (15:85, v/v) containing 1 mM TPABr. The LC mobile phase was acetonitrile–5 mM aqueous Tris buffer (pH 7.0) (37.5:62.5, v/v) containing 1 mM TPABr. The reagent pump was a laboratory-built syringe pump used at a flow-rate of 0.3 ml/min. Mixing of the eluent with the reagent solution was performed by using a T-type mixing union. The reaction coils (volume, 300  $\mu$ l for heating and 180  $\mu$ l for cooling) consisted of 0.3-mm I.D. PTFE tubing; the reaction temperature was 55°C.

## RESULTS AND DISCUSSION

#### *Optimization of the ligand-exchange reaction*

The direct fluorescence detection method developed in our laboratory<sup>21</sup> is based on a post-column ligand-exchange reaction of organosulphur compounds, such as ethylenethiourea, cysteine or glutathione with the non-fluorescent Pd<sup>II</sup>-calcein complex. The sulphur-containing ligands usually possess a higher affinity for Pd<sup>II</sup> than oxygen- and nitrogen-containing ligands, such as calcein (Fig. 1). Therefore, this strongly fluorescing compound is released during the ligand-exchange reaction in an amount proportional to that of the analyte. The fluorescence detection of calcein is favoured by the low background of the reagent because palladium efficiently quenches the calcein fluorescence. However, this system cannot be applied to the detection of inositol phosphates, as the Pd<sup>II</sup>-inositol trisphosphate complex is weaker than the Pd<sup>II</sup>-calcein complex.

We found that the complex stability of 1,2,6-IP<sub>3</sub> with different metal ions at pH 7, obtained by potentiometric titration, increases in the order Hg<sup>II</sup> < Ca<sup>II</sup> < Pb<sup>II</sup> < Ni<sup>II</sup> < Cr<sup>III</sup>  $\approx$  Zn<sup>II</sup>  $\approx$  Cd<sup>II</sup> < Al<sup>III</sup> < Fe<sup>III</sup>. This suggests Al<sup>III</sup> or Fe<sup>III</sup> as the metal ions

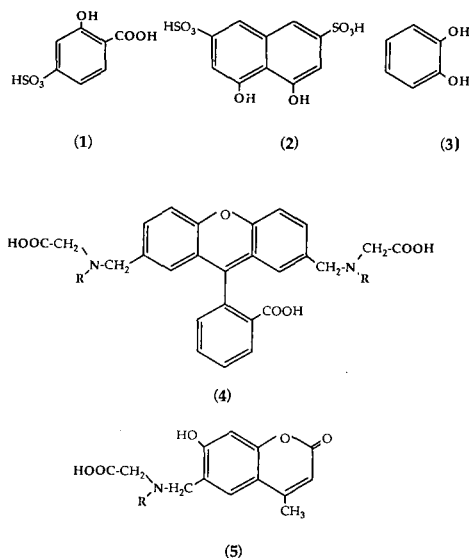


Fig. 1. Ligands investigated with regard to their use in a post-column ligand-exchange detection system. 1 = Sulphosalicylic acid; 2 = chromotropic acid; 3 = catechol; 4 = calcein (R = CH<sub>2</sub>COOH) or methylcalcein (R = CH<sub>3</sub>); 5 = calcein blue (R = CH<sub>2</sub>COOH) or methylcalcein blue (R = CH<sub>3</sub>).

of choice. Preliminary experiments showed that Al<sup>III</sup> does not efficiently quench the fluorescence of the ligands investigated (see Fig. 1). In further work, we therefore investigated only the corresponding Fe<sup>III</sup> complexes. The fluorescence of suitable ligands should efficiently be quenched by Fe<sup>III</sup>, and 1,2,6-IP<sub>3</sub> should form a stronger complex with Fe<sup>III</sup> than the ligand of choice. We found that sulphosalicylic acid, chromotropic acid and MCB meet these requirements. Ligands with an iminodiacetic acid (*e.g.*, calcein and calcein blue) or an *o*-dihydroxy (catechol) group form complexes with Fe<sup>III</sup> that are too strong, while the fluorescence of methylcalcein is hardly quenched by Fe<sup>III</sup>. Table I shows the optimum pH values for the ligand fluorescence and the ligand-exchange reaction with 1,2,6-IP<sub>3</sub> and the detection limits obtained in flow-injection analysis (FIA). MCB ( $\lambda_{\text{exc}} = 370 \text{ nm}$ ,  $\lambda_{\text{em}} = 440 \text{ nm}$ ) is clearly the most

TABLE I

pH RANGE FOR FLUORESCENCE AND LIGAND-EXCHANGE REACTION AND DETECTION LIMIT FOR THE 1,2,6-IP<sub>3</sub>-Fe<sup>III</sup> LIGAND REACTION FOR DIFFERENT LIGANDS

Ligand <sup>a</sup>	pH range for			Detection limit (FIA) (ng)
	Fluorescence	Maximum fluorescence	Ligand exchange	
SSA	> 4.0	> 4.0	1.0–4.5	138
CTA	3.5–5.5	3.5–4.0	1.0–5.0	18
MCB	4.0–10.0	6.0–7.0	1.0–8.0	3

<sup>a</sup> SSA = Sulphosalicylic acid; CTA = chromotropic acid; MCB = methylcalcein blue.



favourable ligand regarding the compatibility of the optimum pH values of ligand exchange and fluorescence and the sensitivity of the detection system. All further experiments were therefore carried out with the system Fe<sup>III</sup>-MCB.

#### *Post-column parameters*

Several parameters that influence the post-column ligand-exchange reaction were investigated by FIA. The mobile phase pumped with the LC pump was the same as the ion-pair LC eluent.

*pH.* pH has a strong influence on (i) the complexing strength of 1,2,6-IP<sub>3</sub>, as it determines the degree of its ionization; (ii) the formation of hydroxo complexes of Fe<sup>III</sup>, which interferes with the formation of Fe-MCB above pH 8 and results in a large increase in the background fluorescence; (iii) the fluorescence of MCB, which has its maximum at pH 6–8, and (iv) the stability of 1,2,6-IP<sub>3</sub> (see below). Batch experiments showed that the ligand-exchange reaction between 1,2,6-IP<sub>3</sub> and Fe-MCB proceeds at a pH as low as 1, but the pH range suitable for the ligand-exchange reaction and fluorescence detection lies between 4 and 8. Owing to the instability of 1,2,6-IP<sub>3</sub> at pH 4–5 (see below), a pH of 7.0, obtained with Tris buffer, was chosen for the post-column reaction system.

*Organic modifier.* The type and content of organic modifier have a strong influence on the fluorescence of MCB, whereas the ligand-exchange reaction between Fe-MCB and 1,2,6-IP<sub>3</sub> is not affected. In aqueous solutions MCB fluoresces only weakly, and a considerable increase in fluorescence is observed if the content of organic modifier, *e.g.*, methanol, is increased above 50%. At a content of 70% methanol the fluorescence of MCB reaches its maximum. As optimum LC conditions were obtained with a mobile phase containing 37.5% acetonitrile, the total, *i.e.*, the post-column, content of organic modifier was increased to about 50% by preparing Fe-MCB in 95% (v/v) methanol and mixing the eluent and reagent solution at a flow-rate ratio of 1.0:0.3.

*Molar ratio of Fe<sup>III</sup> and MCB.* The molar ratio of Fe<sup>III</sup> and MCB has a strong influence on both the 1,2,6-IP<sub>3</sub> response and the fluorescence background and, therefore, on the signal-to-noise ratio. It is obvious that the 1,2,6-IP<sub>3</sub> response will decrease if an excess of Fe<sup>III</sup> is present in the reagent solution, as the analyte will then complex the free Fe<sup>3+</sup> ions before reacting with Fe-MCB. An excess of MCB, on the other hand, will increase the noise level caused by background fluorescence and therefore increase the detection limit of 1,2,6-IP<sub>3</sub>.

Fig. 2 shows the dependence of both the 1,2,6-IP<sub>3</sub> response and the background fluorescence on the MCB:Fe ratio measured by means of FIA experiments. The response factor for 1,2,6-IP<sub>3</sub> increases steadily with increasing MCB:Fe ratio and reaches a more or less constant level at a ratio of 3.5:1. The fluorescence background starts to increase significantly at an MCB:Fe ratio higher than 3:1. The presence of free MCB then leads, as expected, to a higher fluorescence background. An MCB:Fe ratio of 3:1 was chosen for further experiments.

*Reaction time and temperature and concentration of Fe-MCB.* Fig. 3 shows the dependence of the response factor of 1,2,6-IP<sub>3</sub> on the reaction temperature for three different reaction coil volumes at a reagent (*i.e.*, Fe<sup>3+</sup>) concentration of  $6.6 \cdot 10^{-6}$  M. The reaction times (total flow-rate 1.3 ml/min) are 8.3, 13.8, and 23.0 s for the 180-, 300- and 500- $\mu$ l coils, respectively. Fig. 3 shows that the optimum temperature is *ca.*

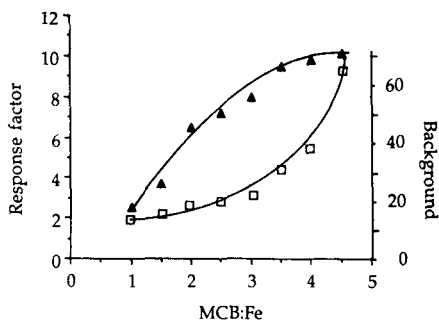


Fig. 2. Dependence of (▲) the response factor for 1,2,6-IP<sub>3</sub> and (□) the fluorescence background on the Fe:MCB molar ratio.

55°C for all the reaction coils tested. The response factors for the 300- and 500- $\mu\text{l}$  reaction coils at 55°C are only slightly different, and a further increase in the reaction time by choosing lower flow-rates or higher reaction-coil volumes did not result in higher response factors; this indicates that the ligand-exchange reaction is virtually complete under these conditions. Decreasing the reagent concentration in order to reduce the background fluorescence caused a decrease in the reaction rate. At a reagent concentration of  $1.6 \cdot 10^{-6} \text{ M}$  the reaction-coil volume had to be increased to 700  $\mu\text{l}$  and the temperature to 60°C in order to obtain similar response factors to those obtained with  $6.6 \cdot 10^{-6} \text{ M}$  at 300  $\mu\text{l}$  and 55°C, but the detector noise was three times lower. A further decrease in the reagent concentration required longer reaction times, *i.e.*, a higher reaction-coil volume, which led to increased peak broadening and did not result in a lower detection limit for 1,2,6-IP<sub>3</sub>.

#### Analytical data

Using a reagent concentration of  $6.6 \cdot 10^{-6} \text{ M}$ , the detection limit for 1,2,6-IP<sub>3</sub> in ion-pair LC amounted to 10 ng (signal-to-noise ratio = 3:1). The detector response was linear ( $r > 0.999$ ,  $n = 4$ ) up to 1000 ng 1,2,6-IP<sub>3</sub>. The relative standard deviation for 10- $\mu\text{l}$  injections of 50 ng of 1,2,6-IP<sub>3</sub> was less than 2% ( $n = 6$ ). If the reagent concentration was decreased to  $1.6 \cdot 10^{-6} \text{ M}$ , the detector response was linear only up to 100 ng, whereas the detection limit could be decreased to 3 ng.

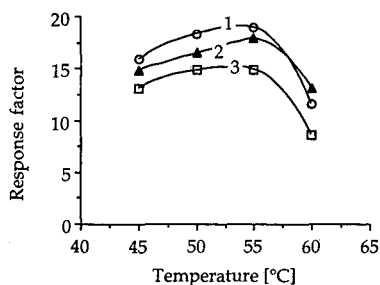


Fig. 3. Dependence of the response factor of 1,2,6-IP<sub>3</sub> on the reaction temperature for reaction-coil volumes of (1) 500, (2) 300 and (3) 180  $\mu\text{l}$ . Reaction-coil volume used for cooling, 180  $\mu\text{l}$ .

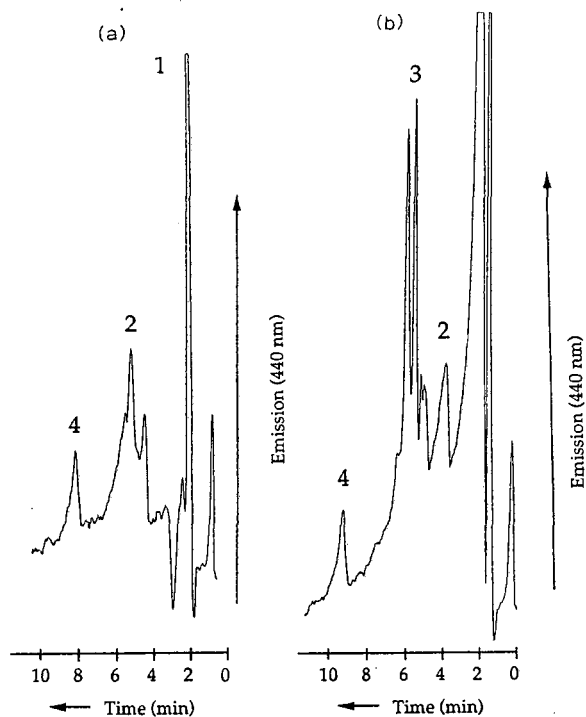


Fig. 4. (a) Chromatogram of a standard solution containing 10 ppb of 1,2,6-IP<sub>3</sub> and 1 mM sodium phosphate. Peaks: 1 = phosphate; 2 = TPABr impurities; 4 = 1,2,6-IP<sub>3</sub>. Conditions: preconcentration to 1 ml; washing of the precolumn with 5 ml of acetonitrile–10 mM Tris buffer (15:85, v/v) containing 1 mM TPABr. For other conditions, see Experimental. (b) Chromatogram of a standard solution containing 10 ppb of 1,2,6-IP<sub>3</sub> and 100 ppb of IP<sub>2</sub>. Peaks: 2 = TPABr impurities; 3 = IP<sub>2</sub>; 4 = 1,2,6-IP<sub>3</sub>. Conditions: preconcentration to 1 ml; no washing step. For other conditions, see Experimental.

#### *Trace enrichment of 1,2,6-IP<sub>3</sub> via ion-pair formation*

Precolumns are frequently applied in LC in order to increase the injection volume and also to achieve an on-line clean-up<sup>22</sup>. For highly ionized compounds, such as 1,2,6-IP<sub>3</sub>, ion-exchange or ion-pairing techniques can be used for trace enrichment. The high capacity ratio of 1,2,6-IP<sub>3</sub> in ion-pair LC with TBABr or TPABr suggested the addition of alkylammonium-type counter ions to the sample in order to preconcentrate 1,2,6-IP<sub>3</sub> from aqueous solutions on C<sub>18</sub>-bonded silica. The desorption of 1,2,6-IP<sub>3</sub> can occur by simply switching the preconcentration column to the analytical column.

By using a 10 × 4.0 mm I.D. precolumn packed with C<sub>18</sub>-bonded silica, breakthrough volumes above 25 ml were obtained with both TBABr and TPABr at a 2 mM concentration. Counter-ion concentrations higher than 5 mM led to a significant decrease in recovery. At pH 7 and 2 mM TPABr the recovery for a 3-ml preconcentration of a solution containing 28 ppb (or  $5.1 \cdot 10^{-8}$  M) 1,2,6-IP<sub>3</sub> was 95% with a relative standard deviation of 1% ( $n = 6$ ). The detection limit for 1-ml preconcentrations was 5 ppb. For both direct injections and preconcentrations the pH of the sample solution had a large influence on the stability of 1,2,6-IP<sub>3</sub>. At pH 4 the recov-

eries for 1,2,6-IP<sub>3</sub> were below 20%, probably owing to hydrolysis of the ester linkages. The recoveries increased steadily with increasing pH and reached a maximum at pH 7.

Owing to the strong retention of 1,2,6-IP<sub>3</sub> as a TPA ion pair on C<sub>18</sub>-bonded silica, the precolumn can be washed with solutions having a low acetonitrile content (5–15%) in order to remove interfering components, such as inorganic phosphates, which are present in a large excess, *e.g.*, in plasma samples. We found that flushing the precolumn with 5 ml of acetonitrile–10 mM Tris buffer (15:85, v/v) containing 1 mM TPABr removed the inorganic phosphate present in the sample without losses of 1,2,6-IP<sub>3</sub>.

A chromatogram for the trace enrichment of a standard solution of 10 ppb of 1,2,6-IP<sub>3</sub> in the presence of 1 mM sodium phosphate [preconcentration of 1 ml, washing with 5 ml of acetonitrile–10 mM Tris buffer (15:85, v/v) containing 1 mM TPABr] is shown in Fig. 4a. Fig. 4b demonstrates the ability of the present method to detect 1,2,6-IP<sub>3</sub> (10 ppb) in the presence of inositol bisphosphates (IP<sub>2</sub>; 100 ppb) which are formed during the metabolic degradation of 1,2,6-IP<sub>3</sub> in blood. IP<sub>2</sub> is probably present as a mixture of isomers, which may explain the occurrence of two peaks. The slightly different retention times in Fig. 4a and b may be caused by slight changes in the LC eluent composition as a result of prolonged re-use. In both chromatograms, peak 2 has the same shape and size for injected blanks and standard solutions and therefore cannot be attributed to hydrolysis products of 1,2,6-IP<sub>3</sub>.

## CONCLUSIONS

The use of a post-column reaction detection system based on ligand exchange between phosphate ions and an Fe<sup>III</sup>–MCB reagent with subsequent fluorescence monitoring allows the successful determination of low-nanogram amounts of 1,2,6-IP<sub>3</sub> with good reproducibility and low standard deviation. If the ion-pair LC–reaction detection system is combined with an on-line trace enrichment step based on ion-pair formation, preconcentration of 1-ml sample volumes permits a detection limit of *ca.* 5 ppb to be achieved.

Preliminary investigations have shown that the present detection technique is, as expected from results with other metal ions and ligands<sup>9,11</sup>, generally applicable to the determination of organic phosphates, such as metabolites of 1,2,6-IP<sub>3</sub> (inositol mono- and bisphosphates). Currently the application of the method to the determination of 1,2,6-IP<sub>3</sub> in plasma is being investigated. Owing to the presence of a large number of phosphate-containing compounds in plasma (including inorganic phosphates), the optimization of the trace-enrichment system is of major concern in this work. Primarily, different washing steps for the removal of interfering anions are being investigated. The preconcentration of inositol phosphates on metal-loaded phases<sup>22</sup> will also be studied.

## REFERENCES

- 1 M. J. Berridge, *Sci. Am.*, 253 (1985) 124.
- 2 J. W. Putney, *Cell Calcium*, 7 (1986) 1.
- 3 M. J. Sirén, *U.S. Pat.*, 4 735 936 (1984).

- 4 M. J. Sirén, A. K. Sim, A. P. McCraw, M. E. Cleland and T. O. Gustafsson, *Thromb Haemostasis*, 62 (1989) 428.
- 5 S. Renaud, J. C. Ruf and M. Ciavatti, *Diabetologia*, 32 (1989) 532A.
- 6 D. Blake, London, U.K., personal communication.
- 7 K. Authi, T. O. Gustafsson and N. Crawford, *Tromb. Haemostasis*, 62 (1989) 250.
- 8 J. A. Shayman and D. M. BeMent, *Biochem. Biophys. Res. Commun.*, 151 (1988) 114.
- 9 G. W. Mayr, *Biochem. J.*, 254 (1988) 585.
- 10 J. L. Meek, *Proc. Natl. Acad. Sci. U.S.A.*, 83 (1986) 4162.
- 11 S. E. Meek and D. J. Pietrzyk, *Anal. Chem.*, 60 (1988) 1397.
- 12 J. J. L. Cilliers and P. J. van Niekerk, *J. Agric. Food Chem.*, 34 (1986) 680.
- 13 V. G. Mahadevappa and B. J. Holub, in A. Kuksis (Editor), *Chromatography of Lipids in Biomedical Research and Clinical Diagnosis (Journal of Chromatography Library, Vol. 37)*, Elsevier, Amsterdam, 1987, p. 225.
- 14 R. A. Minear, J. E. Segars, J. W. Elwood and P. J. Mulholland, *Analyst (London)*, 113 (1988) 645.
- 15 H. Binder, P. C. Weber and W. Siess, *Anal. Biochem.*, 148 (1985) 220.
- 16 J. L. Meek and F. Nicoletti, *J. Chromatogr.*, 351 (1986) 303.
- 17 W. R. Mathews, D. M. Guido and R. M. Huff, *Anal. Biochem.*, 168 (1988) 63.
- 18 A.-S. Sandberg and R. Ahderinne, *J. Food Sci.*, 51 (1986) 547.
- 19 G. Marko-Varga, Lund, Sweden, personal communication.
- 20 H. E. Wade and D. M. Morgan, *Nature (London)*, 171 (1953) 529.
- 21 C. E. Werkhoven-Goewie, W. M. A. Niessen, U. A. Th. Brinkman and R. W. Frei, *J. Chromatogr.*, 203 (1981) 165.
- 22 M. W. F. Nielen, R. W. Frei and U. A. Th. Brinkman, in R. W. Frei and K. Zech (Editors), *Selective Sample Handling and Detection in High Performance Liquid Chromatography, Part A*, Elsevier, Amsterdam, 1988, p. 5.



CHROMSYMP. 1636

## SEPARATION OF CAROTENES ON CYCLODEXTRIN-BONDED PHASES

APRYLL M. STALCUP, HENG L. JIN and DANIEL W. ARMSTRONG\*

*Department of Chemistry, University of Missouri-Rolla, Rolla, MO 65401 (U.S.A.)*

and

PAUL MAZUR, FADILA DERGUINI and KOJI NAKANISHI

*Department of Chemistry, Columbia University, New York, NY 10027 (U.S.A.)*

---

### SUMMARY

The separation of carotenoids and retinoids on a  $\beta$ -cyclodextrin-bonded stationary phase with conventional mobile phases is reported. Compounds studied include  $\beta$ -carotene (*all-trans*), 15,15'-*cis*- $\beta$ -carotene, 7,8,7',8'-dihydro- $\beta$ -carotene,  $\alpha$ -carotene, lycopene, lutein, zeaxanthin, retinal, retinol, retinol palmitate and retinol acetate. The best resolution of carotenes was obtained with low concentrations ( $\leq 1\%$ ) of polar solvents (*e.g.*, 2-propanol or ethyl acetate) in hexane or cyclohexane. Xanthophylls required much higher concentrations of polar solvents. The best solvent for the resolution of lutein and zeaxanthin was found to be dichloromethane. The resolution of *cis/trans*-isomers and the tentative identification of other isomers present in newly synthesized carotenoid standards is also reported. *All-trans*-isomers were found to be eluted before *cis*-isomers.

---

### INTRODUCTION

Retinoids, carotenes and their more polar analogues, the xanthophylls, are ubiquitous in plant and animal tissues. Although the extensive conjugation makes visualization and detection of these compounds fairly straightforward, it also contributes to the instability of these compounds to acid, heat and light<sup>1</sup>. Much of the early work involving carotenes was concerned with the isolation of carotenes from biological matrices and with determining the total carotenoid concentration<sup>2</sup>. In many of these studies thin-layer or paper chromatography was employed as a means of isolating the carotenoids from other materials present in the matrix<sup>3</sup>. One of the difficulties encountered in the application of these methods to the analysis of carotenes was their decomposition or isomerization. Therefore it has been desirable to find an analytical technique that is rapid, highly selective, and requiring minimal sample manipulation to limit the exposure of the sample to factors that contribute to decomposition or isomerization.

High-performance liquid chromatography (HPLC) is rapidly becoming the method of choice for the analysis of carotenoids<sup>4-6</sup>. Although silica gel has proven effective for the separation of some *cis/trans*-isomers, resolution of structural isomers

such as  $\alpha$ - and  $\beta$ -carotene was not accomplished<sup>7</sup>. Adsorption chromatography has been used successfully to separate *cis/trans*-retinal isomers<sup>8</sup>, but silica gel has been suspected of initiating carotenoid decomposition and/or isomerization<sup>9</sup>. Reversed-phase partition chromatography with hydro-organic mobile phases has limited applicability due to the relatively low solubility of carotenoids in aqueous mobile phases and low retention of hydroxycarotenoids, which often are present in carotenoid samples, on non-polar stationary phases. Non-aqueous reversed-phase chromatography was found useful for the isocratic resolution of individual carotenoids but *cis/trans*-isomeric pairs were not included in that study<sup>4</sup>. Separation of *cis/trans*-isomers of  $\beta$ -carotene<sup>10</sup> and canthaxanthin<sup>11</sup> has been achieved on calcium hydroxide columns. Cyclodextrins (CD) have been used extensively to separate a wide variety of optical and geometric isomers<sup>12-16</sup>. Although the most common applications of CD stationary phases involve hydro-organic mobile phases, CD can also be used in the normal-phase mode<sup>17</sup>.

The recent interest in the role of carotenoids in cancer prevention<sup>18,19</sup> necessitates the synthesis and characterization of standards. Several carotenes were synthesized and analyzed chromatographically to determine isomeric purity. The purpose of the work presented here was to evaluate the unique selectivity characteristics of cyclodextrin-bonded phases in the normal-phase mode, as applied to natural and synthetic carotenoid samples.

## EXPERIMENTAL

The chromatographic measurements were made on a LC-6A liquid chromatograph, interfaced with a C-R2AX Chromatopac data system and a SCL-6A system controller (Shimadzu Scientific Instruments, Columbia, MD, U.S.A.). Detection was accomplished using a Shimadzu Model SPD-6A variable-wavelength UV detector (Columbia, MD, U.S.A.).

The chromatographic column was made of 250  $\times$  4.6 mm I.D. stainless steel and packed with 5- $\mu$ m Cyclobond I ( $\beta$ -CD) (Advanced Separations Technology, Whippany, NJ, U.S.A.).

$\alpha$ -Carotene,  $\beta$ -carotene (all-*trans*), lycopene, retinal, retinol, retinol palmitate and retinol acetate were obtained from Sigma (St. Louis, MO, U.S.A.); the xanthophylls (lutein and zeaxanthin) from Atomergic Chemetals Corp. (Farmingdale, NY, U.S.A.); and the solvents (all HPLC grade) from Fisher Scientific (St. Louis, MO, U.S.A.).

15,15'-Didehydro- $\beta$ -carotene was synthesized according to the method of Surmatis and Ofner<sup>20</sup>. The mixture of isomers obtained by this procedure was then thermally isomerized to all-*trans*-15,15'-didehydro- $\beta$ -carotene. 15,15'-*cis*- $\beta$ -Carotene was prepared by catalytic hydrogenation of all-*trans*-15,15'-didehydro- $\beta$ -carotene. 11-*cis* and all-*trans*-15,15'-dihydro- $\beta$ -carotene were synthesized by alkylation of  $\beta$ -ionylideneethylphenylsulfone<sup>21,22</sup> with 1,8-dichloro-2,7-dimethyl-2,6-octadiene<sup>23</sup>, followed by elimination of benzenesulfonic acid with potassium isopropoxide<sup>24</sup>. 15-*cis* and all-*trans*-7,8,7',8'-tetrahydro- $\beta$ -carotene were obtained by  $\text{TiCl}_3/\text{LiAlH}_4$  coupling<sup>25</sup> of all-*trans*-7,8-dihydroretinal<sup>26</sup>.



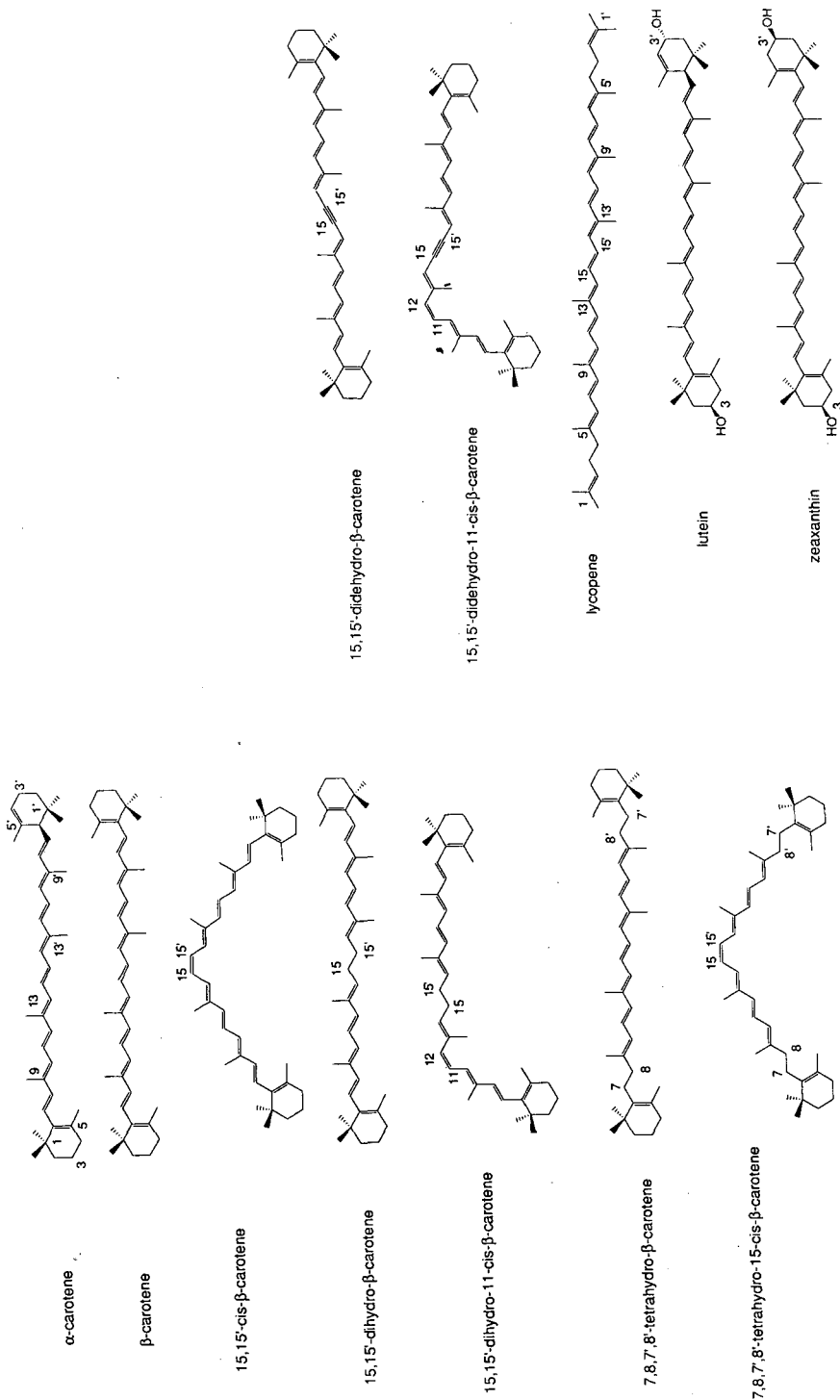


Fig. 1. Structures of compounds used in this study.

TABLE I  
RETENTION TIMES ( $t_R$ ), CAPACITY FACTORS ( $k'$ ), AND CHROMATOGRAPHIC CONDITIONS FOR THE ELUTION OF CAROTENOIDS AND  
RETINOIDS FROM  $\beta$ -CYCLODEXTRIN-BONDED PHASES

Details given in Experimental.

Compounds	$t_R$	$k'$	Mobile phase	Detector (UV, nm)
$\alpha$ -Carotene	5.31	1.62	Dichloromethane-hexane (1:99)	350
	11.60	4.87	Acetone-hexane (1:99)	350
$\beta$ -Carotene	5.41	1.67	Dichloromethane-hexane (1:99)	325
	5.88	1.31	2-Propanol-cyclohexane (0.5:99.5)	350
	2.87	0.49	Ethyl acetate-cyclohexane (1:99)	350
	11.47	4.81	Acetone-hexane (1:99)	350
	4.04	0.98	Chloroform-hexane (1:99)	325
15,15'- <i>cis</i> - $\beta$ -Carotene	6.28	2.10	Dichloromethane-hexane (1:99)	325
	8.08	2.18	2-Propanol-cyclohexane (0.5:99.5)	350
	3.31	0.72	Ethyl acetate-cyclohexane (1:99)	350
	12.29	5.22	Acetone-hexane (1:99)	350
	4.63	1.27	Chloroform-hexane (1:99)	350
15,15'-Dihydro- $\beta$ -carotene	12.49	5.11	Dichloromethane-hexane (1:99)	325
11- <i>cis</i> -15,15'-Dihydro- $\beta$ -carotene	13.43	5.58	Dichloromethane-hexane (1:99)	325
	22.75	10.11	Ethyl acetate-hexane (1:99)	325
7,8,7',8'-Tetrahydro- $\beta$ -carotene	4.39	1.16	Dichloromethane-hexane (1:99)	400
	6.49	2.10	Ethyl acetate-hexane (1:99)	325
	3.61	0.77	Chloroform-hexane (1:99)	400
	4.53	1.23	Dichloromethane-hexane (1:99)	400
15- <i>cis</i> -7,8,7',8'-Tetrahydro- $\beta$ -carotene	6.80	2.25	Ethyl acetate-hexane (1:99)	325
	3.72	0.82	Chloroform-hexane (1:99)	400

15,15'-Didehydro- $\beta$ -carotene	3.30	0.64	Ethyl acetate-hexane (1:99)	450
Retinol palmitate	5.44	1.71	Dichloromethane-hexane (1:99)	330
	4.71	1.46	Ethyl acetate-hexane (1:99)	350
	6.71	2.55	Dichloromethane-cyclohexane (5:95)	350
	4.82	1.47	Acetone-hexane (1:99)	350
Retinyl acetate	17.53	8.26	Dichloromethane-cyclohexane (5:95)	350
	13.62	5.98	Acetone-hexane (1:99)	350
Lycopene	5.07	1.64	Ethyl acetate-cyclohexane (1:99)	350
	4.57	1.42	Dichloromethane-cyclohexane (5:95)	350
	7.11	2.64	Acetone-hexane (1:99)	350
Retinal	2.25	0.21	Ethanol-hexane (5:95)	280
	3.21	0.75	Ethyl acetate-cyclohexane (12:88)	350
	17.41	8.66	Dichloromethane-cyclohexane (15:85)	350
	5.52	1.88	Acetone-hexane (4:96)	350
Retinol	8.16	3.43	Ethyl acetate-cyclohexane 12:88)	350
	3.41	0.83	Ethanol-hexane (5:95)	280
	40.39	21.4	Dichloromethane-cyclohexane (15:85)	350
	22.22	10.6	Acetone-hexane (4:96)	350
Lutein	6.54	2.79	Ethyl acetate-hexane (42:58)	280
	5.74	1.67	Chloroform-hexane (80:20)	280
	11.03	5.21	Dichloromethane	280
	3.83	1.17	Ethanol-hexane (10:90)	280
	5.28	2.02	Ethanol-CH <sub>2</sub> Cl <sub>2</sub> (1:99)	280
	6.50	2.77	Ethyl acetate-hexane (42:58)	280
	7.27	2.38	Chloroform-hexane (80:20)	280
	20.28	10.42	Dichloromethane	280
	5.12	1.89	Ethanol-hexane (10:90)	280
	6.50	2.72	Ethanol-CH <sub>2</sub> Cl <sub>2</sub> (1:99)	280
Zeaxanthin				

## RESULTS AND DISCUSSION

The structures of the carotenoids used in this study are presented in Fig. 1. Various mobile phases were tested to optimize carotenoid separations. In general, the best separations of carotenes and retinoids were observed with fairly low concentrations ( $\leq 1\%$ ) of a polar solvent in hexane or cyclohexane. In order to elute the more polar xanthophylls, it was necessary to employ higher concentrations of more polar solvents (*e.g.*, chloroform or ethanol). The retention times and capacity factors for several carotenoids and retinoids with various mobile phases are presented in Table I and sample chromatograms are shown in Figs. 2 and 3. As expected, the non-polar solutes are eluted first and the more polar solutes are retained the longest. For instance, retinyl palmitate and retinyl acetate are eluted earlier than retinol because they are less polar. The selectivity of the cyclodextrin column resembles that of the silica gel columns in that the cyclodextrin column is unable to resolve  $\alpha$ - and  $\beta$ -carotene but does resolve their xanthophyll analogues, lutein and zeaxanthin.

Separations of compounds on CD-bonded phases when using hydro-organic mobile phases are thought to be the result of preferential formation of inclusion complexes of the more retained solute within the CD cavity<sup>27</sup>. When using non-aqueous mobile phases, the CD cavities are most likely occupied by non-polar solvent molecules. The solutes in this study are probably too large to reside entirely within such a cyclodextrin cavity. Retention and selectivity are, therefore, most probably the result of solute interaction with the hydroxyl groups that line the CD cavity. This would account for the similarity in elution order of the solutes between the CD-bonded phase and silica gel. A similar conclusion regarding the role of the CD hydroxyls on retention and selectivity was drawn in a recent report of the separation of mono- and polysaccharides on CD phases<sup>28</sup>. In addition, the bulky CD groups limit the accessibility of solute molecules to silica surface silanols, which are more acidic than the CD hydroxyls and may contribute to isomerization<sup>9</sup>. Additional studies on this potentially useful aspect of CD-bonded phase are in progress.

The retention times and capacity factors for the carotenoid standards under various chromatographic conditions on the  $\beta$ -CD column are listed in Table I. These include 15,15'-dehydro-, 7,8,7',8'-tetrahydro- and 15,15'-didehydro- $\beta$ -carotene. Proton NMR of the synthetic carotenoid samples revealed the presence of *cis*-isomers along with the predominant *all-trans*-isomers. Based on the NMR, UV, and chromatographic data, the principal contaminants in the standards are tentatively identified and also listed in Table I. The chromatographic factors which aided in the determination of peak identity were elution order (*all-trans*-isomers eluted before *cis*-isomers) and the change in relative peak height with changing wavelength. The retention of 15,15'-dihydro- $\beta$ -carotene seems anomalously long when compared to the retention of the other  $\beta$ -carotenes. It may be that the flexibility about the molecular center of symmetry afford enhanced solute bonded ligand interactions than are possible with the other, more rigid  $\beta$ -carotenes. Resolution and selectivity for geometric and structural isomeric pairs are presented in Table II. Note that *trans*-isomers are linear, while the presence of a *cis*-double bond within the polyene backbone confers a more bent configuration to the molecule. This spatial orientation of the *cis*-isomers may allow a more efficient interaction with the bulky CD moiety than is possible for the linear *all-trans*-isomers<sup>29</sup>.

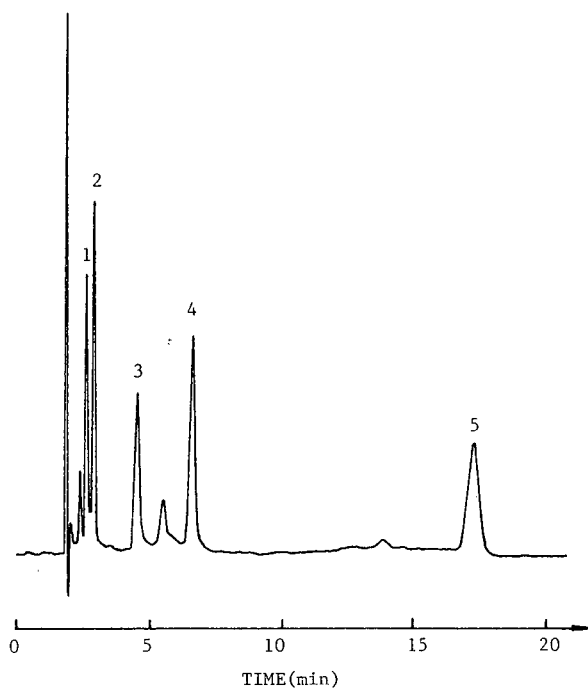


Fig. 2. Chromatographic separation of  $\beta$ -carotene (1), 15,15'-*cis*- $\beta$ -carotene (2), lycopene (3), retinyl palmitate (4) and retinyl acetate (5) on a  $\beta$ -CD column with dichloromethane-cyclohexane (5:95) as mobile phase at 1.5 ml/mn. (Details given in Experimental and tables.)

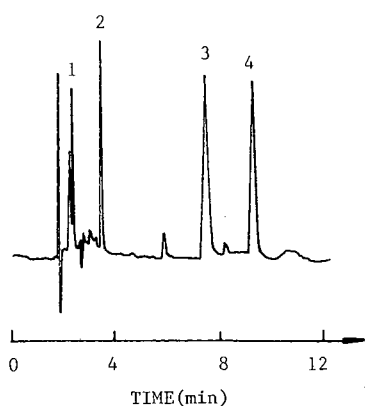


Fig. 3. Chromatographic separation of retinal (1), retinol (2), lutein (3), and zeaxanthin (4) on a  $\beta$ -CD column with ethanol-hexane (5:95) at 1.5 ml/min as mobile phase. (Details given in Experimental and tables.)

TABLE II  
SEPARATION OF *CIS*- AND *TRANS*-ISOMERS AND OF  $\alpha$ - AND  $\beta$ -ISOMERS  
Details given in Experimental.

Compounds	$\alpha^a$	$R_s^b$	Mobile phase
$\beta$ -Carotene (all- <i>trans</i> -)/15,15'- <i>cis</i> - $\beta$ -carotene	1.26	1.74	Dichloromethane-hexane (1:99)
	1.66	2.36	2-Propanol-cyclohexane (95:99.5)
	1.47	1.93	Ethyl acetate-cyclohexane (1:99)
	1.09	0.9	Acetone-hexane (1:99)
	1.30	1.66	Chloroform-hexane (1:99)
Lutein ( $\alpha$ -)/Zeaxanthin ( $\beta$ -)	1.43	4.5	Chloroform-hexane (80:20)
	2.00	10.8	Dichloromethane
	1.62	4.5	Ethanol-hexane (10:90)
	1.35	2.3	Ethanol-dichloromethane (1:99)
15,15'-Dihydro- $\beta$ -carotene (All <i>trans</i> - and 11- <i>cis</i> )	1.09	1.24	Dichloromethane-hexane (1:99)
	1.07	0.8	Ethyl acetate-hexane (1:99)
7,8,7',8'-Tetrahydro- $\beta$ -carotene (All <i>trans</i> and 15- <i>cis</i> )	1.07	0.7	Ethyl acetate-hexane (1:99)
	1.07	0.7	Chloroform-hexane (1:99)
	1.06	0.7	Dichloromethane-hexane (1:99)
15,15'-Didehydro- and 11- <i>cis</i> -15,15'-didehydro- $\beta$ -carotene	1.11	1.25	Dichloromethane-hexane (1:99)

<sup>a</sup>  $k_1/k_2'$

<sup>b</sup> Resolution.

## ACKNOWLEDGEMENTS

Support of this work by the Department of Energy, Office of Basic Sciences (DE FG02 88ER13819) is gratefully acknowledged. Also, we are thankful to Dr. A. Forcault for helpful discussion of this work [Grant (K.N.) NIH GM36564].

## REFERENCES

- 1 G. Britton, *Methods Enzymol.*, 111 (1985) 113.
- 2 M. J. Deutsch, in S. Williams (Editor), *Official Methods of Analysis of the Association of Official Analytical Chemists*, William Byrd Press, Richmond, VA, 14th ed., 1984, p. 830.
- 3 P. Eloranta, *Ann. Bot. Fenn.*, 23 (1986) 153.
- 4 S. K. Hajibrahim, P. J. C. Tibbets, C. D. Watts, J. R. Maxwell, G. Eglinton, H. Colin and G. Guiochon, *Anal. Chem.*, 50 (1978) 549.
- 5 M. Ruddat and O. H. Will III, *Methods Enzymol.*, 111 (1985) 189.
- 6 P. Ruedi, *Pure Appl. Chem.*, 57 (1985) 793.
- 7 A. Fiksdahl, J. T. Mortensen and S. Liaaen-Jensen, *J. Chromatogr.*, 157 (1978) 111.
- 8 R. Bruening, F. Derguini and K. Nakanishi, *J. Chromatogr.*, 361 (1986) 437.
- 9 Y. Tanaka, T. Katayama, K. L. Simpson and C. Chichester, *Bull. Hap. Soc. Sci. Fisheries*, 47(6) (1981) 799.
- 10 K. Tsudika, K. Saiki, T. Takii and Y. Koyama, *J. Chromatogr.*, 245 (1982) 359.
- 11 H. Hashimoto, Y. Koyama and T. Shimamura, *J. Chromatogr.*, 448 (1988) 182.
- 12 D. W. Armstrong, A. Alak, K. Bui, W. DeMond, T. Ward, T. E. Riehl and W. L. Hinze, *J. Incl. Phon.*, 2 (1984) 533.
- 13 D. W. Armstrong, T. J. Ward, A. Czech, B. P. Czech and R. A. Bartsch, *J. Org. Chem.*, 50 (1985) 5556.
- 14 T. J. Ward and D. W. Armstrong, *J. Liq. Chromatogr.*, 9 (1986) 43.
- 15 D. W. Armstrong and W. Li, *Chromatography*, 2 (1987) 407.
- 16 D. W. Armstrong, S. F. Yang, S. M. Han and R. Menges, *Anal. Chem.*, 59 (1987) 2594.
- 17 D. W. Armstrong, A. Alak, W. DeMond, W. L. Hinze and T. E. Riehl, *J. Liq. Chromatogr.*, 8 (1985) 261.
- 18 H. J. C. Nells and A. P. De Leenheer, *Anal. Chem.*, 55 (1983) 270.
- 19 F. Khackik and G. R. Beecher, *J. Chromatogr.*, 449 (1988) 119.
- 20 J. D. Surmatis and A. Ofner, *J. Org. Chem.*, 26 (1961) 1171.
- 21 M. Julia and D. Arnold, *Bull. Soc. Chim. France*, (1973) 746.
- 22 P. S. Manchand, M. Rosenberger, G. Saucy, P. A. Wehrli, H. Wong, L. Chambers, M. P. Ferro and W. Jackson, *Helv. Chim. Acta*, 59 (1976) 387.
- 23 U. T. Bhalerao and H. Rapoport, *J. Am. Chem. Soc.*, 93 (1971) 5311.
- 24 P. Chabardes, J. P. Decor and J. Varagnat, *Tetrahedron*, 33 (1977) 2799.
- 25 J. E. McMurry and M. P. Flemming, *J. Am. Chem. Soc.*, 96 (1974) 4708.
- 26 M. Arnaboldi, M. G. Motto, K. Tsujimoto, V. Balogh-Nair and K. Nakanishi, *J. Am. Chem. Soc.*, 101 (1979) 7082.
- 27 D. W. Armstrong, T. J. Ward, R. D. Armstrong and T. E. Beesley, *Science (Washington, D.C.)*, 232 (1986) 1132.
- 28 D. W. Armstrong and H. L. Jin, *J. Chromatogr.*, 462 (1989) 219.
- 29 A. M. Stalcup, D. E. Martire, S. A. Wise and L. C. Sander, *Chromatographia*, 27 (1989) 405.





CHROM. 21 711

## COMPARATIVE SUPERCRITICAL-FLUID CHROMATOGRAPHIC PROPERTIES OF CARBON DIOXIDE AND SULPHUR HEXAFLUORIDE–AMMONIA MIXTURES WITH PACKED COLUMNS

J. L. VEUTHEY\*

*Département de Chimie Minérale, Analytique et Appliquée, Université de Genève, 30 Quai E. Ansermet, 1211 Genève 4 (Switzerland)*

and

J. L. JANICOT, M. CAUDE and R. ROSSET

*Laboratoire de Chimie Analytique de l'Ecole Supérieure de Physique et de Chimie de Paris, 10 Rue Vauquelin, 75231 Paris Cedex 05 (France)*

---

### SUMMARY

The separation of polar compounds by supercritical-fluid chromatography is difficult with carbon dioxide as mobile phase. In this work, we tested mixtures of ammonia with sulphur hexafluoride as mobile phase and we have compared the solvating power of these mixtures with carbon dioxide for five solutes. The results show that the solvating power of sulphur hexafluoride–ammonia is weak in comparison with carbon dioxide, except for aniline. Ammonia plays only a role as silanol masking agent. Furthermore, ammonia is harmful for the pumping system.

---

### INTRODUCTION

The development of supercritical-fluid chromatography (SFC) was mainly accomplished with carbon dioxide (CO<sub>2</sub>) as the mobile phase<sup>1</sup>. This fluid has numerous advantages: low cost, mild critical parameters and non-toxic nature. However, CO<sub>2</sub> behaves as a non-polar mobile phase (solubility parameters varying between hexane and dichloromethane depending on the pressure and the temperature). Therefore, very few results for polar compounds and particularly basic compounds<sup>2</sup> have been reported with pure CO<sub>2</sub>. For these compounds and with packed columns, polar modifiers are commonly added to CO<sub>2</sub><sup>3–6</sup>. However, the advantages of SFC over liquid chromatography (higher diffusion coefficients, lower viscosities and higher efficiencies per unit time) can be partly lost in this way when the concentration of the polar modifier becomes significant. Further, when modified phases are used it results in a poor or no sensitivity with a flame ionization detector.

It is now recognized that a more polar mobile phase (compatible with a flame ionization detector) is necessary. Sulphur hexafluoride (SF<sub>6</sub>) has not been used extensively as a mobile phase for SFC<sup>7,8</sup> owing to its weak solvating power<sup>9</sup>. On the contrary, ammonia (NH<sub>3</sub>) is known as a polar supercritical fluid, but very few results

are available in SFC<sup>10,11</sup> owing to its critical parameters ( $T_c = 132.4^\circ\text{C}$ ;  $P_c = 111.3$  bar) and because it requires a stationary phase and a device specially designed to work with such a harmful medium<sup>12</sup>. Therefore, a mixture of  $\text{NH}_3$  with an inert fluid, such as  $\text{SF}_6$ , might be a more convenient way to obtain a polar supercritical fluid. This mixture would be less corrosive, have more easily obtainable critical parameters ( $\text{SF}_6$ ,  $T_c = 45.5^\circ\text{C}$ ;  $P_c = 37.1$  bar) and would be compatible with a flame ionization detector. In this work, we tested three mixtures of  $\text{NH}_3$  with  $\text{SF}_6$  for the elution of some model compounds and have compared the results with those obtained with  $\text{CO}_2$ .

## EXPERIMENTAL

### *Apparatus*

The design has been described elsewhere<sup>13</sup>.  $\text{CO}_2$  and the  $\text{SF}_6$ - $\text{NH}_3$  mixture are contained in a cylinder with an eductor tube and supply the pump of a Varian 5500 chromatograph (Varian, Palo Alto, CA, U.S.A.). Cooling of the pump head with cold ethanol ( $5^\circ\text{C}$ ) is necessary to improve the pump efficiency. Temperature control of the fluid and the chromatographic column was achieved by using a constant-temperature water-bath (Polystat 22; Bioblock Science, Illkirch, France). The injector was a Rheodyne 7125 six-way switching valve with a loop of  $10\ \mu\text{l}$ , its rotor being made of Tefzel to be compatible with basic media. A Varian UV 2550 spectrophotometer was used with a detection cell modified in order to withstand pressures up to 350 bar. The pressure in the system was monitored by a back-pressure regulator (Model 26-3220-24004; Tescom, Minneapolis, MN, U.S.A.).

The stainless-steel columns ( $15\ \text{cm} \times 0.46\ \text{cm}$  I.D.) were packed with Nucleosil-100 bare silica ( $5\ \mu\text{m}$ ) (Macherey, Nagel & Co., Düren, F.R.G.) and with MCH-5 reversed-phase RP-18 silica ( $5\ \mu\text{m}$ ) (Varian).

### *Chemicals and reagents*

$\text{CO}_2$  (N45 grade) and three  $\text{SF}_6$ - $\text{NH}_3$  mixtures, containing 1, 2 and 5% (w/w) of ammonia, were obtained from Air Liquide (Paris, France). The ammonia content of the three mixtures was determined by bubbling the  $\text{SF}_6$ - $\text{NH}_3$  through citrated hydrochloric acid solutions and titrating the excess of acid with sodium hydroxide solution. The ammonia contents of the three mixtures were found to be  $1.1 \pm 0.1$ ,  $2.3 \pm 0.3$  and  $5.2 \pm 0.5\%$  (w/w) ( $n = 3$ ), respectively.

Benzonitrile, nitrobenzene, methyl benzoate, phenol and aniline were obtained from Merck (Darmstadt, F.R.G.) and were used without purification. Solutions of solutes in hexane were injected directly into the loop.

## RESULTS AND DISCUSSION

In order to compare the properties of the two supercritical fluids, solutes were chosen on the basis of their adsorption energies on bare silica<sup>14</sup> and of the presence of typical basic or acidic functions such as  $\text{NH}_2$  or  $\text{OH}$ , which can interact strongly with the silica surface or with  $\text{NH}_3$  itself.

Separations were first done on bare silica with  $\text{CO}_2$  as the supercritical mobile phase. Then, with  $\text{SF}_6$ - $\text{NH}_3$  mixtures, bare silica and octadecyl-bonded silica were

used. With both fluids, the influence of pressure and temperature on the retention times of solutes was studied.

### Results with CO<sub>2</sub>

On bare silica, all compounds were eluted with CO<sub>2</sub> as the supercritical mobile phase, as shown in Fig. 1. The order of elution follows the adsorption energies<sup>14</sup>, as in normal-phase liquid chromatography.

Aniline is the most retained solute, because of its strong adsorption energy and the presence of an amino function, which can strongly interact with silanol groups of the silica surface in an apolar medium<sup>15,16</sup>.

For all compounds the capacity factors decrease with increasing pressure at constant temperature. Likewise, at constant pressure, the capacity factors of the solutes increase with increasing temperature, except for aniline, as shown in Table I. Indeed, the density of the mobile phase plays the major role in the retention mechanism, as mentioned previously<sup>1,17</sup>. However, for aniline, the slight decrease in capacity factor with increasing temperature can be explained mainly by its high volatility<sup>17</sup>.

### Results with SF<sub>6</sub>-NH<sub>3</sub> [1, 2 and 5% (w/w) NH<sub>3</sub>]

*On bare silica.* On this stationary phase the order of elution is modified in comparison with the results obtained with CO<sub>2</sub>, methyl benzoate being eluted first (Fig. 1). Phenol is not eluted even with a 5% NH<sub>3</sub> content. The strong retention of phenol can be attributed to the substitution of silanol groups by NH<sub>3</sub> which modifies the acidic character of the support surface. This modification of the stationary phase is clearly confirmed by the results obtained with aniline, where the peak tailing is

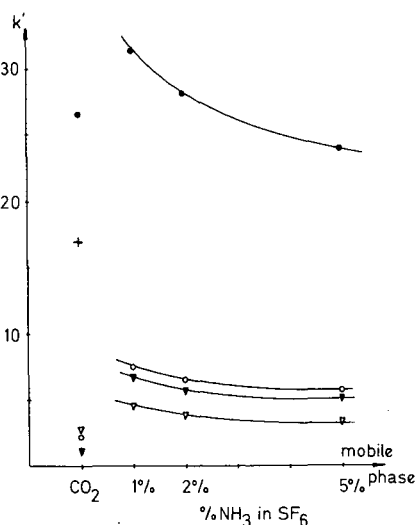


Fig. 1. Capacity factors of test solutes as a function of the supercritical mobile phase. Stationary phase, bare silica, 5- $\mu$ m Nucleosil-100; temperature, 50°C; pressure, 190 bar. Mobile phases: CO<sub>2</sub> ( $P_r = 2.61$ ,  $T_r = 1.06$ ); SF<sub>6</sub>-NH<sub>3</sub> containing 1, 2 and 5% (w/w) of NH<sub>3</sub> ( $P_r = 4.20$ ,  $T_r = 0.99$ ;  $P_r = 3.69$ ,  $T_r = 0.97$ ;  $P_r = 3.01$ ,  $T_r = 0.93$ , respectively); flow-rate, 4 ml min<sup>-1</sup>. Detection: UV at 254 nm. Solutes: ●, aniline; ○, benzonitrile; ▼, nitrobenzene; ▽, methyl benzoate; +, phenol.

TABLE I

CAPACITY FACTORS ( $k'$ ) OF TEST SOLUTES ON BARE SILICA WITH CO<sub>2</sub> AS MOBILE PHASE AS A FUNCTION OF PRESSURE AT CONSTANT TEMPERATURE (313 K) AND AS A FUNCTION OF TEMPERATURE AT CONSTANT PRESSURE (190 bar)

Pressure (bar)	Temperature (K)	Aniline	Methyl benzoate	Benzonitrile	Nitrobenzene
165	313	35.1	2.7	2.4	1.3
215		29.8	2.3	1.9	1.1
265		28.6	2.3	1.9	1.1
288		25.2	1.9	1.6	1.0
190	323	26.5	2.6	2.2	1.1
	333	26.2	2.7	2.7	1.5
	343	26.3	3.1	3.0	1.7
	353	22.6	3.5	3.4	2.1

minimized in comparison with the results obtained with CO<sub>2</sub><sup>16</sup>, the interaction of amino functions with silanols being masked. Moreover, the influence of NH<sub>3</sub> concentration is more important for aniline (Fig. 1) than for other solutes without basic or acidic functions.

The solvating power of SF<sub>6</sub>-NH<sub>3</sub> mixtures is governed by two factors, the composition and the density. The calculated critical parameters of the mixtures are reported in Table II<sup>17</sup>. From these values, it is observed that when the percentage of NH<sub>3</sub> increases, the critical density of the mobile phase decreases. In addition, as NH<sub>3</sub> is far less dense than SF<sub>6</sub> at any given pressure and temperature, the higher the percentage of NH<sub>3</sub> in the mixture, the lower is the final density. As shown in Fig. 1, as the NH<sub>3</sub> concentration increases, the capacity factors decrease. Hence, the change in mobile phase composition has a more important effect on solute retention than density, and finally the mobile phase polarity is enhanced by addition of NH<sub>3</sub>. Nevertheless, as shown in Fig. 1, it is not necessary to increase the NH<sub>3</sub> concentration in SF<sub>6</sub> above 5% as the capacity factor plotted against percentage of NH<sub>3</sub> becomes constant. Indeed, at this percentage the density fall balances the effect of NH<sub>3</sub>.

Hence, under our thermodynamic test conditions, the solvating power of SF<sub>6</sub>-NH<sub>3</sub>, at any percentage of NH<sub>3</sub>, appears to be lower than that of CO<sub>2</sub> for the tested solutes. Only aniline has similar capacity factors in both fluids (Fig. 1). SF<sub>6</sub>, having a weak solvating power in comparison with CO<sub>2</sub><sup>8</sup> [solubility parameters: SF<sub>6</sub> = 5.5

TABLE II

CRITICAL PARAMETERS OF SF<sub>6</sub>-NH<sub>3</sub> MIXTURES AND OF CO<sub>2</sub>

Parameter	CO <sub>2</sub>	SF <sub>6</sub> -NH <sub>3</sub>		
		1.1% NH <sub>3</sub>	2.3% NH <sub>3</sub>	5.2% NH <sub>3</sub>
$\rho_c$ (g cm <sup>-3</sup> )	0.464	0.694	0.653	0.577
$P_c$ (bar)	72.9	43.6	49.6	60.8
$T_c$ (K)	304.3	326.2	333.2	346.4

(cal cm<sup>-3</sup>)<sup>1/3</sup>; CO<sub>2</sub> = 7.5 (cal cm<sup>-3</sup>)<sup>1/3</sup>], a small addition of NH<sub>3</sub> to SF<sub>6</sub> appears to be insufficient to give a more polar mobile phase than CO<sub>2</sub>.

Further, the weak solvating power of SF<sub>6</sub>-NH<sub>3</sub> results in the volatility of the solutes having a more pronounced influence on capacity factors in SF<sub>6</sub>-NH<sub>3</sub> than in CO<sub>2</sub>, as shown in Fig. 2 for aniline. Therefore, if the temperature increases, the capacity factors decrease dramatically, as already mentioned elsewhere<sup>8</sup>.

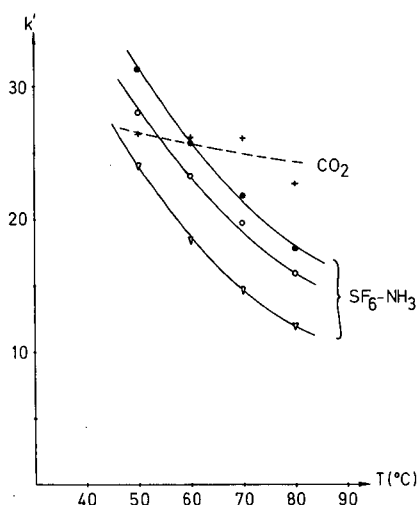


Fig. 2. Influence of temperature at constant pressure ( $P = 190$  bar) on aniline capacity factors as a function of the mobile phase. Other conditions as in Fig. 1. NH<sub>3</sub> concentration: ●, 1%; ○, 2%; ▽, 5% (w/w); +, CO<sub>2</sub>.

*On reversed-phase silica.* On octadecyl-bonded silica and under the same operating conditions with SF<sub>6</sub>-NH<sub>3</sub> as the mobile phase, all solutes are less retained than on bare silica. These results can be explained by the small number of silanol groups available on this stationary phase. Moreover, the elution order for nitrobenzene, benzonitrile and methyl benzoate follows the inverse polarity order as in reversed-phase liquid chromatography; it is exactly the reverse of that obtained on bare silica with supercritical CO<sub>2</sub> as the mobile phase (Fig. 3).

Consequently, two mechanisms can exist on this surface, the most important being a silanophilic interaction which can be decreased by ammonia impregnation as on bare silica (Fig. 3), and the other based on non-polar-non-polar partition.

#### *Practical considerations of the use of SF<sub>6</sub>-NH<sub>3</sub>*

No degradation of the silicas has been observed and the SF<sub>6</sub>-NH<sub>3</sub> mixtures were homogeneous as the capacity factors for test solutes remained constant.

The low solvent power of SF<sub>6</sub>-NH<sub>3</sub> causes problems during the injection process, some solutes diluted in hexane being precipitated in the injection valve. This phenomenon has been observed with some morphinic alkaloids, benzaldehyde and some other moderately polar compounds. These observations indicate that ammonia plays the role of a silanol masking agent rather than of a polar modifier.

The most important drawback to SF<sub>6</sub>-NH<sub>3</sub> mixtures is their corrosive nature

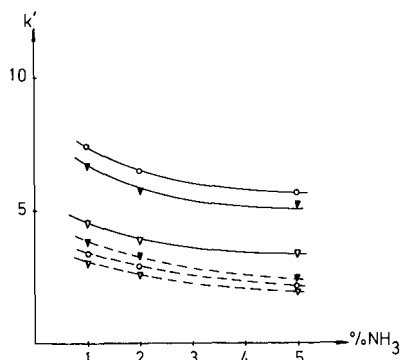


Fig. 3. Influence of percentage of  $\text{NH}_3$  on solute capacity factors on two stationary phases: solid lines, bare silica; and broken lines, reversed-phase silica. Conditions as in Fig. 1. Solutes: O, benzointrile; ▼, nitrobenzene; ▽, methyl benzoate.

toward the pumping system material, even when using a low percentage of  $\text{NH}_3$ . In 1 month, we had to change the inlet-valve seal and the spring-loaded seal twice and the piston itself once.

#### CONCLUSION

The solvating power of  $\text{SF}_6\text{-NH}_3$  (even containing 5% of  $\text{NH}_3$ ) is weak in comparison with  $\text{CO}_2$ , the capacity factors for all the tested solutes being higher in  $\text{SF}_6\text{-NH}_3$  than in  $\text{CO}_2$ . Further, this weak solvating power induces the precipitation of some solutes in the injection valve. The role of ammonia under these conditions is mainly limited to that of a silanol masking agent and therefore it is unnecessary to increase its concentration in  $\text{SF}_6$  above 5% (w/w).

Finally, only basic molecules, such as aniline, show a better behaviour with  $\text{SF}_6\text{-NH}_3$  than with  $\text{CO}_2$ , the silanophilic interactions with the amino groups being minimized by ammonia impregnation.

#### REFERENCES

- 1 R. M. Smith (Editor), *Supercritical Fluid Chromatography*, Royal Society of Chemistry, London, 1988.
- 2 S. M. Fields and K. Grolimund, *J. High Resolut. Chromatogr. Chromatogr. Commun.*, 11 (1988) 727.
- 3 J. R. Wheeler and M. E. McNally, *J. Chromatogr.*, 410 (1987) 343.
- 4 P. Carraud, D. Thiebaut, M. Caude, R. Rosset, M. Lafosse and M. Dreux, *J. Chromatogr. Sci.*, 25 (1987) 395.
- 5 J. L. Janicot, M. Caude and R. Rosset, *J. Chromatogr.*, 437 (1988) 351.
- 6 J. B. Crowther and J. D. Henion, *Anal. Chem.*, 57 (1985) 2711.
- 7 J. C. Giddings, M. N. Myers, L. McLaren and R. A. Keller, *Science (Washington, D.C.)*, 162 (1968) 67.
- 8 J. W. Hellgeth, M. G. Fessehaie and L. T. Taylor, *Chromatographia*, 25 (1988) 172.
- 9 R. D. Smith, B. W. Wright and C. R. Yonker, *Anal. Chem.*, 60 (1988) 1323 A.
- 10 K. Grolimund, W. P. Jackson, M. Joppich, W. Nussbaum, K. Anton and H. M. Widmer, in D. Ishii, K. Jinno and P. Sandra (Editors), *Proceedings of the Seventh International Symposium on Capillary Chromatography, Gifu, Nagoya, May 11-14, 1986*, The University of Nagoya Press, Nagoya, 1986, p. 625.
- 11 J. C. Kuei, K. E. Markides and M. L. Lee, *J. High Resolut. Chromatogr. Chromatogr. Commun.*, 10 (1987) 257.
- 12 P. J. Schoenmakers and F. C. C. J. G. Verhoeven, *Trends Anal. Chem.*, 6 (1987) 10.

- 13 P. Mourier, P. Sassi, M. Caude and R. Rosset, *Analisis*, 12 (1984) 229.
- 14 L. R. Snyder, *Principles of Adsorption Chromatography*, Marcel Dekker, New York, 1968.
- 15 K. E. Bij, Cs. Horváth, W. R. Melander and A. Nahum, *J. Chromatogr.*, 203 (1981) 65.
- 16 J. H. Phillips and R. J. Robey, *J. Chromatogr.*, 465 (1989) 177.
- 17 P. A. Peaden, *J. Liq. Chromatogr.*, 5 (1982) 179.





CHROMSYMP. 1641

## USE OF HIGH-PERFORMANCE LIQUID CHROMATOGRAPHY FOR THE CHARACTERIZATION OF SYNTHETIC COPOLYMERS

GOTTFRIED GLÖCKNER\*

*Department of Chemistry, Dresden University of Technology, Mommsenstrasse 13, DDR 8027 Dresden (G.D.R.)*

and

HOWARD G. BARTH

*Central Research and Development Department, E. I. du Pont de Nemours & Co., Experimental Station, P.O. Box 80228, Wilmington, DE 19880-0228 (U.S.A.)*

---

### SUMMARY

The evaluation of copolymer distribution as a function of molecular weight and chemical composition requires two separations, known as cross-fractionation. This procedure can be substantially improved by using high-performance liquid chromatographic (HPLC) techniques, including size-exclusion chromatography for the separation by molecular size. The separation by chemical composition can be achieved by gradient HPLC. Examples are given for copolymers of styrene and ethyl methacrylate (S-EMA). Gradient HPLC of these and similar copolymers can be performed in both normal-phase and reversed-phase modes with inversion of elution order. In isooctane-tetrahydrofuran (THF) mixtures on polar columns, the elution of S-EMA samples occurs at a higher THF concentration than required by solubility, *i.e.*, with a distinct contribution of adsorption to retention. In contrast, reversed-phase elution with methanol-THF mixtures takes place almost exactly at the solubility borderline of the system.

---

### INTRODUCTION

Synthetic polymers are not the most attractive type of samples for analysis by high-performance liquid chromatography (HPLC). They are composed of such an enormous number of components that, at present, even under favorable conditions scarcely more than the *distribution* of the constituents can be evaluated experimentally. However, no matter how accurate and precise statistical average molecular weights are, polymers cannot be sufficiently characterized by average values alone, because any mean value can be connected to an unlimited number of different distributions. Samples that have identical average data may behave very differently in certain applications because of differences in the distribution of constituents. As a result, efficient separation methods for mixtures as complex as polymers are urgently required.

The basic property of a polymer molecule is the chain length (or degree of polymerization (DP), *i.e.*, the number of repeat units per macromolecule). A typical polymer contains molecules with hundreds or thousands of different DP values. Only with oligomers is there a chance of separating individual species. One of the finest studies in this field is the separation of ethylene oxide oligomers published by Melander *et al.*<sup>1</sup> a decade ago. With oligomer samples of higher molecular weight (MW), baseline separations of individual homologues deteriorate at the high-MW end of the distribution.

The most versatile technique for evaluating the chain-length distribution is size-exclusion chromatography (SEC). Modern equipment consists of columns with inert packings of 3–5  $\mu\text{m}$  particle diameter, pumps which deliver solvents at precise flow-rates and, more recently, molecular-weight-sensitive detectors, based on light scattering or viscosity. Although SEC can be applied satisfactorily to homopolymers, difficulties arise during the SEC analysis of copolymers because copolymer macromolecules are made of more than one kind of repeat unit. The chemically differing units can be composed of blocks or branches, they can alternate or be distributed statistically along the polymer chain. Because SEC separates on the basis of hydrodynamic volume rather than molecular weight, the contents of the detector cell at each elution volume increment consist of a mixture of structurally and chemically different components of the same hydrodynamic volume.

Statistical copolymers, produced by copolymerizing monomer mixtures, have a molecular weight distribution (MWD) similar to that of homopolymers and, in addition, a chemical composition distribution (CCD). Further, there is a sequence distribution which is a distribution along a polymer chain, related to the average composition of the respective chain by the rules of statistics.

Copolymers can be separated by chain length and by composition. Separation by average sequence length is, through the rules of statistical copolymerization, related to a separation by composition. However, any separation by individual sequence lengths, *e.g.*, diads, triads, tetrads, maybe possible only after destructive degradation of the polymer, as is done in pyrolysis–gas chromatography<sup>2</sup>.

The properties of copolymers are determined by the complex distribution in chain length and composition. Chemical compositional heterogeneity can arise from fluctuations of batch composition in the vicinity of a growing chain end. This instantaneous heterogeneity will diminish with increasing MW because, during the sufficiently long lifetime of a growing chain, random fluctuations become more effective.

If, for kinetic reasons, the average composition of a copolymer differs from the batch composition, the latter is depleted in the preferentially consumed monomer. Hence, subsequent portions polymerize from a different batch composition. This gives rise to the chemical heterogeneity due to conversion, which increases with the difference in composition of the starting monomer mixture and of the copolymer formed at the very beginning of the reaction. Mixing problems and changes in reaction conditions by drifting temperature or decreasing initiator concentration may further affect the chemical composition distribution.

The complex MWD/CCD of a binary copolymer can be evaluated by cross-fractionation in bulk solution which requires at least two solvent–non-solvent combinations<sup>3</sup>. (It is not necessary that one combination fractionates, on addition of the

non-solvent, strictly according to MW and the other strictly according to composition.)

Other workers<sup>4,5</sup> have treated the method theoretically in terms of the Flory–Huggins theory of polymer solutions. Unfortunately, effective solvent–non-solvent combinations are not readily available, which may be one reason why only a small number of publications have reported experimental results of cross-fractionation. Another reason may be the time-consuming procedure of fractionation in one direction, subsequent separation of each fraction in another direction and, finally, the characterization of some dozens of subfractions with regard to amount of polymer, molecular weight and chemical composition. In this way, several months of labor-intensive studies are required for the evaluation of the MWD/CCD of a copolymer sample.

Chromatographic cross-fractionation employs the potential of HPLC for separating the copolymer in two different directions<sup>6</sup>. In this way, the limits set by solvent–non-solvent properties can be overcome through specific interactions of the individual solutes with the stationary phase. As an added attraction, the sample size is reduced from  $\geq 10$  g to about 1 mg per copolymer and the time for characterization is decreased from about 10 weeks per sample to about four samples per day<sup>7–9</sup>. Among the possible combinations of methods for chromatographic cross-fractionation are those which employ SEC for separation by molecular size, followed by separation by composition by gradient HPLC<sup>10</sup>.

An interesting version of chromatographic cross-fractionation, called orthogonal chromatography, was introduced by Balke and Patel<sup>11,12</sup>. In this technique, the sample is first fractionated by SEC. The fractionated components are then eluted through a second series of SEC columns, utilizing a different mobile phase that will either change the conformation of the polymer or encourage partitioning.

Investigators who have reported on the chemical composition distribution of styrene–acrylate copolymers by HPLC include Danielewicz and Kubin<sup>13</sup>, Teramachi and co-workers<sup>10,14</sup>, Sato and co-workers<sup>15,16</sup>, Mourey<sup>17</sup> and Mori and co-workers<sup>18–25</sup>.

The applicability of gradient elution HPLC to synthetic polymers is not as commonly used as expected. In view of this, the purpose of this paper is to report studies involving gradient elution HPLC of styrene–ethyl methacrylate (S–EMA) random copolymers with the hope that chromatographers can use this approach to characterize these and other types of copolymers.

## EXPERIMENTAL

### *Samples*

Statistical copolymers of styrene (S) and ethyl methacrylate (EMA) were prepared by radical copolymerization in bulk, as described elsewhere<sup>26</sup>. Sample (codes as used in Figs. 1 and 4) A: 4.7% (w/w) EMA (MW  $51.6 \cdot 10^3$ ), C: 32.2% ( $63.1 \cdot 10^3$ ), E: 54.6% ( $65.2 \cdot 10^3$ ), G: 68.0% ( $83.6 \cdot 10^3$ ), I: 92.5% ( $61.6 \cdot 10^3$ ).

### *Solvents*

Tetrahydrofuran (THF) without stabilizer (BASF, Ludwigshafen, F.R.G.) was distilled over potassium in a silver-coated column. The middle fraction was sub-

sequently refluxed over potassium continuously in a closed apparatus and used as needed in the HPLC and SEC systems. Sample solutions were prepared using analytical-reagent grade THF with 0.025% stabilizer (butylated hydroxytoluene; E. Merck, Darmstadt, F.R.G.). Isooctane (iOct) and methanol were of LiChrosolv grade (Merck). In the HPLC solvent reservoir, the eluents were continuously sparged with helium.

#### *Gradient HPLC*

The liquid chromatograph was a Model 1090 A (Hewlett-Packard, Waldbronn, F.R.G.) with a ternary solvent delivery system (Model DR5), equipped with an auto-sampler and autoinjector, diode-array detector and data-processing unit. The system was controlled by an HP85 personal computer.

The following columns were used: cartridge columns, 60 x 4 mm I.D. (Knauer, Bad Homburg, F.R.G.), packed with either Nucleosil CN (pore diameter,  $d_0 \geq 5$  nm, particle diameter  $d_p = 5 \mu\text{m}$ , column 1), Nucleosil 50 ( $d_0 = 5$  nm,  $d_p = 5 \mu\text{m}$ , column 2) or Nucleosil C<sub>18</sub> ( $d_0 \geq 5$  nm,  $d_p = 5 \mu\text{m}$ , column 3). Column 4 (150 x 4.6 mm I.D.) was packed with Polygosil 60-5 ( $d_0 = 6$  nm,  $d_p = 5 \mu\text{m}$ ).

The gradient conditions were as follows: gradient 1, iOct-THF with 1% methanol throughout, THF concentration = 0% at time zero, 30% (1 min), 70% (9 min), flow-rate 0.5 ml/min; gradient 2, iOct-(THF + 10% methanol), THF + 10% methanol concentration = 10% at time zero, 50% (8 min), 80% (10 min), 100% (11 min), flow-rate 1 ml/min, reduced to 0.3 ml/min between 9.9 and 10 min; gradient 3, iOct-methanol, injection of iOct-methanol (98:2) solution, followed by a sudden transition in THF content to the indicated level (see Fig. 4), after which a 5%/min linear increase in methanol concentration was used at a flow-rate of 0.5 ml/min.

#### *Size-exclusion chromatography*

A Model BT 3020 HPLC pump (Biotronik, Maintal, F.R.G.) was connected to a Model 7010 injection valve (Rheodyne, Lathrop, Heidelberg, F.R.G.), a bank of two GMH6 mixed-gel columns (Toyo Soda, Japan), each 600 x 7.8 mm I.D.,  $d_p = 8-10 \mu\text{m}$  and a Model 51.78 refractive index detector (Knauer). The following conditions were used: THF flow-rate, 1 ml/min; injection volume, 0.2 ml; and sample concentration, 0.5% for preparative fractionations.

## RESULTS

#### *Normal-phase gradient HPLC of statistical S-EMA copolymers [stat-copoly(S-EMA)]*

A model mixture of five S-EMA samples was prefractionated by SEC and the fractions were analysed by gradient HPLC (see Fig. 1). The elution curve gives no indication of a mixed sample. This can be understood from the similarity of the MWs, which are within the limits 51 600 (sample A) and 83 600 (sample G). The presence of different copolymers is clearly visible in the HPLC traces. In the normal-phase (NP) system employed, retention increases with increasing EMA content. The comparatively high MW of sample G is reflected in the appearance of this component in the HPLC trace of SEC fraction 1, which contains the high-MW portions of the mixture and by its predominance in SEC fraction 2. The predominance of Sample A with MW

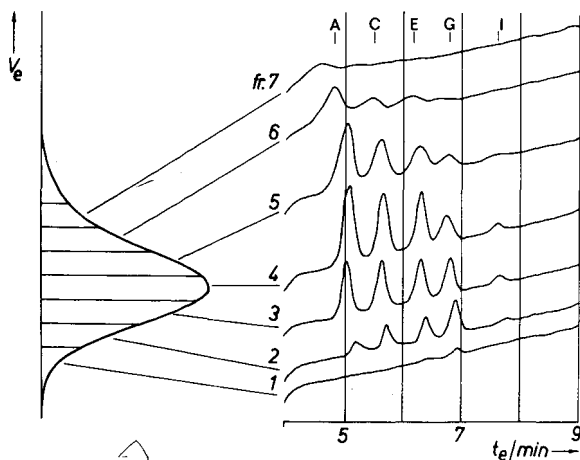


Fig. 1. Separation of a mixture of five *stat*-copoly(styrene-ethyl methacrylate) samples by SEC and normal-phase gradient HPLC on CH-bonded phase (column 1) by gradient elution with *i*Oct-THF (No. 1). Temperature, 50°C; flow-rate, 0.5 ml/min; injection volume for gradient HPLC, 100  $\mu$ l; detection at 259 nm.  $V_e$  = Elution volume;  $t_e$  = elution time; fr = fraction.

51 600 in the low-MW SEC fractions 5–7 is also straightforward. (In comparing the HPLC peaks in Fig. 1, it must be acknowledged that only styrene units are monitored at 259 nm. This accounts for, *e.g.*, the small peak area of sample I.)

Without SEC prefractionation, the copolymers were not baseline separated under the conditions used for Fig. 1. This can be understood as the superimposition of a molecular-weight effect. Separate injections of the individual copolymers yielded well shaped peaks. Their first moment was used for calculating the eluent composi-

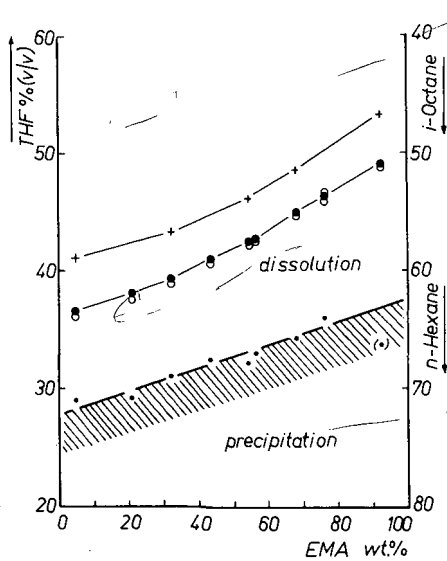


Fig. 2. Elution characteristics in *i*Oct-THF gradients and solubility of *stat*-copoly(styrene-ethyl methacrylate) samples. + = Silica column 2, gradient 1; O, ● = gradient elution from two CN-bonded phase columns of the same size (see column 1) with *i*Oct-THF (0–100% in 10 min). Solubility borderline determined by turbidmetric titration (dots) with *n*-hexane at 20°C. (From ref. 27, with permission from Wiley).

tion at the elution of a given sample. These data (obtained in two laboratories) are shown as open and filled circles in Fig. 2. The curve marked by crosses is from a similar investigation but on a silica column. The higher activity of the latter accounts for the fact that *ca.* 5% more THF is needed for elution from silica than from a nitrile-bonded phase.

The elution characteristics of both columns are well above the solubility borderline. Although the latter had been determined with *n*-hexane non-solvent and at 20°C, both solvent systems are comparable because of the similar solubility parameters of *n*-hexane (14.9 MPa<sup>0.5</sup>) and *i*Oct (15.3 MPa<sup>0.5</sup>)<sup>27</sup>.

The separation of S-EMA copolymers according to composition is more difficult than the separation of *stat*-copoly(styrene-methyl methacrylate) (S-MMA) samples. This can be appreciated from a synoptic presentation of the elution characteristics (see Fig. 3) of S-MMA (curva a), S-EMA (curve b) and *stat*-copoly(styrene-*tert.*-butyl methacrylate) samples (S-TBMA, curve c). The shielding effect of the alkyl groups increases with the bulkiness of the latter and diminishes the adsorption interactions between the ester linkages and polar groups on the surface of the stationary phase.

#### Normal-phase HPLC with separate adjustment of solubility and polarity

The differences between elution characteristics and solubility line in Fig. 2 indicate that retention is due to adsorption. However, the parallelism between the two different types of curves suggests that solubility behavior may also play a role in

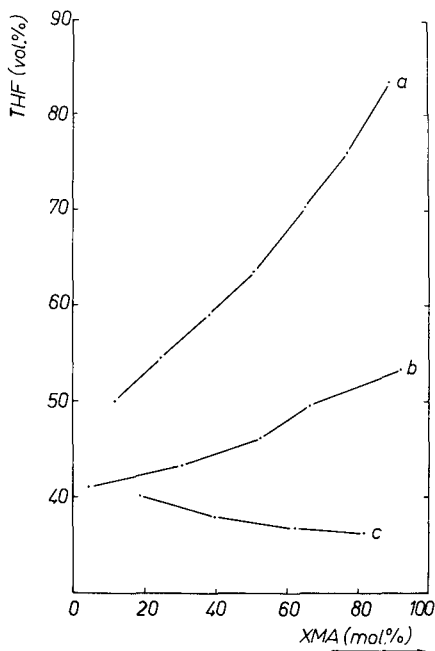


Fig. 3. Shielding effect of alkyl groups in poly(methacrylate esters) on the adsorption of styrene copolymers. Elution characteristics as in Fig. 2 on silica columns. (a) S-MMA, column 4, gradient 2; (b) S-EMA; (c) S-TBMA; (b) and (c) on column 2 with *i*Oct-THF gradient (0-100% in 10 min).

retention. (From past studies<sup>27</sup>, we believe that polymer HPLC is generally governed by solubility and adsorption effects. A pure adsorption mechanism or a pure precipitation–redissolution mechanism are limiting cases.)

Usually, we performed normal-phase gradient elution with THF as gradient eluent B. THF is more polar than iOct, which was used as eluent A, but THF is at the same time a better solvent for all of the copolymers investigated. Thus, in the usual gradient technique we increased simultaneously the dissolution power and elution strength of the eluent. The chromatograms shown in Fig. 4 were obtained under modified conditions, where solubility and displacement effects could be adjusted separately. A linear gradient of increasing methanol concentration was used after a sudden increase in THF content from zero to a selected level. The starting eluent was iOct, which contained 2% methanol in order to suppress adsorption of any impurities during the pre-run period.

The starting eluent contained no THF. As a strong precipitant and poor eluent, it should enable the injected polymer to be retained at the beginning of the column. Of course, the sudden transition in THF concentration caused disturbances of the baseline but, fortunately, the latter became stable again before the sample components were eluted (the trace at 20% THF concentration shows this by the flat section between 3 and 3.5 min). At 20% THF content, all five components were properly eluted when methanol was used, but the resolution was poor. Optimum resolution was found at 25–30% THF. At 35% THF content, the first component of the model mixture disappeared in the 'noise' which had been caused by the transition in THF concentration. The elution in iOct–methanol–THF (63:2:35) is in accordance with the elution characteristics of this copolymer sample in iOct–THF (see Fig. 2).

The independent adjustment of polarity at a selected level of solubility has several advantages in optimizing a separation. In the present instance, *i.e.*, with THF as the solvent and UV detection, elution at a constant THF level has the additional

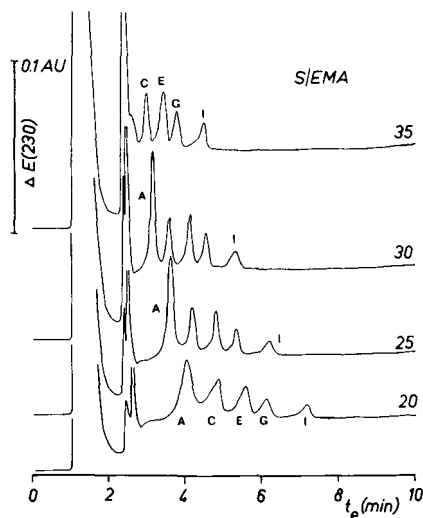


Fig. 4. Separation of a mixture of five *stat*-copoly (styrene–ethyl methacrylate) samples by linear gradients of iOct–methanol after a sudden increase in THF content from 0% to the indicated level (CN column 1, gradient 3). Detection at 230 nm; flow-rate 0.5 ml/min.

benefit that detection is possible at shorter wavelengths. The chromatograms in Fig. 4 were monitored at 230 nm, where THF usually shows adsorption. In the gradients used for Fig. 4, the THF absorption causes a difference in baseline level only before and after the addition of THF, but no baseline rise. The change in baseline can be suppressed within certain limits, whereas a rising baseline renders quantitative evaluation more difficult. Further, for the present system, the effect of copolymer composition on signal size is less severe at 230 than at 259 nm (compare the peaks of sample I in Figs. 4 and 1).

*Reversed-phase chromatography with inversion of elution order*

Low-MW and polymer HPLC may have the same physico-chemical basis<sup>28,29</sup>. Some peculiarities of the latter can be understood as a consequence of the narrow solubility window of polymers, the possibility of multiple attachment of flexible chains on a rigid surface and the fact that synthetic polymers are not chemically uniform substances but mixtures of a huge number of similar homologs. It should be noted, however, that Boehm and Martire<sup>30</sup> have recently developed a theory that suggests that homopolymer HPLC cannot be predicted from small-molecule results.

Gradient HPLC of low-MW substances can be performed in normal-phase (NP) or reversed-phase (RP) modes. Retention in NP chromatography increases with increasing polarity of the samples. The NP retention of S-EMA copolymers is in accordance with the general rule. In RP gradient HPLC, samples of equal molecular

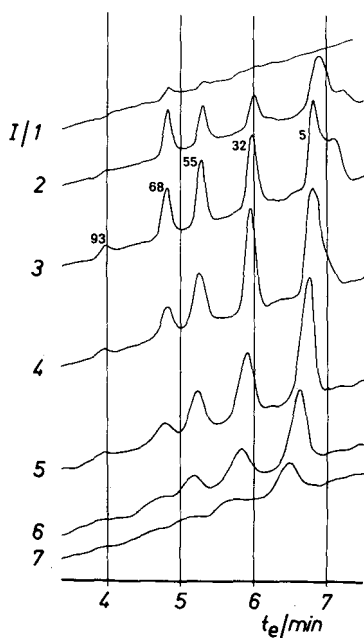


Fig. 5. Reversed-phase separation of the mixture of five *stat*-copoly(styrene-ethyl methacrylate) samples after prefractionation by SEC. Same sample as in Fig. 1;  $C_{18}$ -bonded phase (column 3), methanol-THF gradient (0-100% in 10 min); flow-rate 0.5 ml/min; temperature 50°C; detection at 259 nm. Numbers refer to the % (w/w) of ethyl methacrylate.



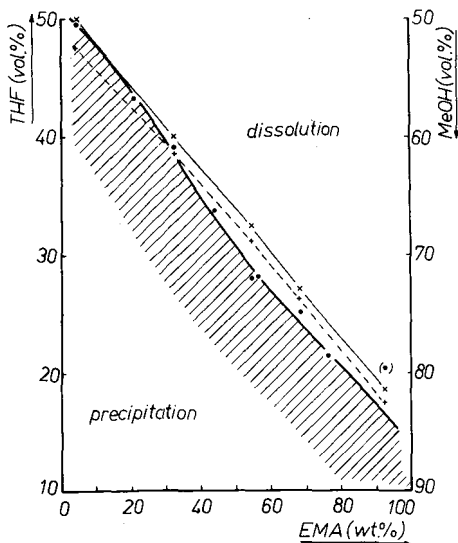


Fig. 6. Elution characteristics in methanol-THF gradients and solubility of *stat*-copoly(styrene-ethyl methacrylate) samples.  $\times$  = elution characteristic of fraction I/2 in Fig. 5;  $+$  = same for fraction I/5. Solubility borderline determined by turbidimetric titration with methanol (MeOH) at 20°C (dots). (From ref. 27, with permission from Wiley).

size have greater retention the less polar they are, *i.e.*, with S-EMA copolymers, the less EMA units they contain.

S-EMA samples have been chromatographed on RP  $C_{18}$  columns with methanol-THF gradients<sup>31,32</sup>. Fig. 5 shows that retention indeed increased with decreasing EMA content. An analogous inversion of elution order in NP- from that in RP-HPLC has been independently observed with *stat*-copoly(S-MMA) samples<sup>14,15</sup>.

Fig. 6 shows the elution characteristic of SEC fractions I/2 and I/5 from Fig. 5, together with the solubility line. In contrast with the behavior on polar columns, S-EMA copolymers are eluted almost precisely at the solubility borderline.

## CONCLUSIONS

Interactive HPLC of SEC-fractionated samples is a useful approach for the characterization of copolymers. By analyzing components of similar hydrodynamic volumes, the uncertainty due to the superimposition of molecular weight and composition is removed. By a judicious choice of mobile phases and gradient conditions, as outlined in this paper, separations of copolymers can be effected. Also, the applicability of this approach for protein characterization has recently been reported<sup>33</sup>. In addition to NP and RP separations, it should also be possible to use ion-exchange chromatography, combined with aqueous SEC, to cross-fractionate polyelectrolytes.

## ACKNOWLEDGEMENTS

Thanks are due to Drs. K. Albrecht, M. Stickler and W. Wunderlich, Darmstadt, for the preparation of S-EMA copolymers and their prefractionation by SEC,

to Dr. A. Müller, Mainz, for supplying THF of the required quality, and to Mrs. Ch. Meissner, Dresden, for light-scattering and turbidimetric measurements. Gottfried Glöckner is indebted to the Sonderforschungsbereich 41 der Johannes-Gutenberg-Universität Mainz for the opportunity to perform the HPLC investigations.

## REFERENCES

- 1 W. Melander, A. Nahum and Cs. Horváth, *J. Chromatogr.*, 185 (1979) 129.
- 2 S. Tsuge, Y. Sugimura, T. Kobayashi, T. Nagaya and H. Ohtani, *Adv. Chem. Ser.*, No. 203 (1983) 625.
- 3 A.J. Rosenthal and B. B. White, *Ind. Eng. Chem.*, 44 (1952) 2693.
- 4 A. V. Topčiev, A. D. Litmanovič, V. Ya. Štern, *Dokl. Akad. Nauk SSSR*, 147 (1962) 1389.
- 5 S. Teramachi and M. Nagasawa, *J. Macromol. Sci. Chem.*, A2 (1968) 1169.
- 6 G. Glöckner and R. Koningsveld, *Makromol. Chem., Rapid. Commun.*, 4 (1983) 529.
- 7 G. Glöckner, J. H. M. van den Berg, N. L. J. Meijerink and Th. G. Scholte, in L. A. Kleintjens and P. J. Lemstra (Editors), *Integration of Fundamental Polymer Science and Technology*, Elsevier Applied Science, Barking, 1986, p. 95.
- 8 G. Glöckner, J. Stejskal and P. Kratochvil, *Makromol. Chem.*, 190 (1989) 425.
- 9 G. Glöckner, in G. Allen and J. C. Bevington (Editors), *Comprehensive Polymer Science*, Vol. 1, C. Booth and C. Price (Editors), Pergamon Press, Oxford, 1989, p. 313.
- 10 S. Teramachi, A. Hasegawa, Y. Shima, M. Akatsuka and M. Nakajima, *Macromolecules*, 12 (1979) 992.
- 11 S. T. Balke and R. D. Patel, *Adv. Chem. Ser.*, No. 203 (1983) 281.
- 12 S. T. Balke, *Sep. Purif. Methods*, 11 (1982) 1.
- 13 M. Danielewicz and M. Kubin, *J. Appl. Polym. Sci.*, 26 (1951) 1981.
- 14 S. Teramachi, A. Hasegawa and K. Motoyama, *Polym. Prep. Jpn.*, 36 (1987) 3169, E441.
- 15 H. Sato, K. Mitsutani, I. Shimizu and Y. Tanaka, *J. Chromatogr.*, 447 (1988) 387.
- 16 H. Sato, H. Takeuchi and Y. Tanaka, *Macromolecules*, 19 (1986) 2613.
- 17 T. H. Mourey, *J. Chromatogr.*, 357 (1986) 101.
- 18 S. Mori, Y. Uno and M. Suzuki, *Anal. Chem.*, 58 (1986) 303.
- 19 S. Mori and Y. Uno, *Anal. Chem.*, 59 (1987) 90.
- 20 S. Mori, *J. Chromatogr.*, 411 (1987) 355.
- 21 S. Mori and Y. Uno, *J. Appl. Polym. Sci.*, 34 (1987) 2689.
- 22 S. Mori, *Anal. Chem.*, 60 (1988) 1125.
- 23 S. Mori, *Anal. Sci.*, 4 (1988) 365.
- 24 S. Mori and M. Mouri, *Anal. Chem.*, 61 (1989) 2171.
- 25 S. Mori, in H. G. Barth (Editor), *Proceedings of the First International Symposium Polymer Analysis and Characterization, Toronto, 1988*; *J. Appl. Polym. Sci., Appl. Polym. Symp. Ed.*, 43 (1989) 65.
- 26 G. Glöckner, M. Stickler and W. Wunderlich, *Fresenius Z. Anal. Chem.*, 328 (1987) 76.
- 27 G. Glöckner, in H. G. Barth (Editor), *Proceedings of the First International Symposium Analysis and Characterization, Toronto, 1988*; *J. Appl. Polym. Sci. Appl. Polym. Symp. Ed.*, 43 (1989) 39.
- 28 M. A. Quarry, M. A. Stadius, T. H. Mourey and L. R. Snyder, *J. Chromatogr.*, 358 (1986) 1.
- 29 M. A. Stadius, M. A. Quarry, T. H. Mourey and L. R. Snyder, *J. Chromatogr.*, 358 (1986) 17.
- 30 R. E. Boehm and D. E. Martire, *Anal. Chem.*, 61 (1989) 471.
- 31 G. Glöckner, *J. Chromatogr.*, 403 (1987) 280.
- 32 G. Glöckner, M. Stickler and W. Wunderlich, *Fresenius Z. Anal. Chem.*, 330 (1988) 46.
- 33 R. Bhikhabhai, H. Lindblom, I. Kallman and L. Fagerstam, *Am. Lab.*, 21, No. 5 (1989) 76.

CHROM. 21 707

## EFFECT OF OPERATING PARAMETERS ON POLYMER MOLECULAR WEIGHT ACCURACY WITH TIME-DELAY, EXPONENTIAL-DECAY THERMAL FIELD FLOW FRACTIONATION

J. J. KIRKLAND\* and W. W. YAU

*E. I. DuPont de Nemours and Co., Central Research and Development Department, Experimental Station, B-228, P.O. Box 80228, Wilmington, DE 19880-0228 (U.S.A.)*

---

### SUMMARY

Previous studies have demonstrated the advantages of determining polymer molecular weight distributions (MWD) by time-delay, exponential-decay thermal field flow fractionation (TDE-TFFF). The method is especially promising for characterizing the MWD of fragile, ultra-high-molecular-weight (MW) polymers. With this method, high-resolution separations are carried out by imposing a thermal gradient across a flowing mobile liquid phase in a thin channel formed with parallel plates. The TDE-TFFF technique permits highly reproducible MW measurements to be made without frequent recalibration. This study examines the effect of important operating parameters, flow-rate and time-delay/decay time constant  $\tau$  values, on the accuracy of MW measurements by TDE-TFFF. Separation resolution and molecular-weight accuracy are increased in TDE-TFFF by operating at longer  $\tau$  values and higher flow-rates. Nomographs are given that allow the selection of optimum operating parameters using results from a preliminary separation.

---

### INTRODUCTION

A wide range of organic-soluble polymers<sup>1-5</sup> and certain water-soluble polymers<sup>6</sup> can be characterized by thermal field flow fractionation (TFFF). This method uses a temperature gradient across a thin, open channel formed by parallel plates to separate materials on the basis of molecular weight (MW) differences<sup>7,8</sup>. As result of the temperature difference between the two plates, sample components are pushed against an accumulation wall. Higher MW components that are pushed closer to this wall are intercepted by slower flowstreams of the essentially laminar flow profile formed between the two plates, and elute after the lower MW components that are carried away by faster flowstreams. Compared to the widely used method of polymer characterization by size-exclusion chromatography (SEC), TFFF provides higher resolution for better MW accuracy and superior capability for characterizing ultra-high MW polymers<sup>5</sup>.

A useful technique for characterizing polymers by TFFF involves programming a temperature gradient ( $\Delta T$ ) decrease during the separation, so that a wide MW

range can be covered during a single experiment. A convenient programming method involves maintaining a constant temperature differential  $\Delta T$  for a time  $\tau$  after injecting the sample, after which  $\Delta T$  is exponentially decreased, also with a time constant  $\tau$ . This approach, called time-delay, exponential-decay TFFF (or TDE-TFFF), results in a linear plot of log MW versus retention time  $t_R$  that provides convenient and accurate calibrations over a wide MW range<sup>4</sup>. Previous studies have demonstrated that the TDE-TFFF method is capable of reproducing number- and weight-average MW values for polymers within 3% (1  $\sigma$ ) without the need for frequent recalibration<sup>5</sup>. This method also has been used with a continuous viscosity detector to produce unique intrinsic viscosity distributions that closely correlate with polymer end-use and solution properties<sup>9</sup>.

The object of this study was to determine the effect of major operating variables on the accuracy of MW values that are measured by TDE-TFFF. Such information should assist in defining experimental conditions for conveniently determining accurate molecular weight distribution (MWD) values for polymer samples.

#### THEORY

The basis for solute retention in TFFF has previously been established<sup>1,7</sup>. With TDE-TFFF, the MW-retention relationship can be expressed as<sup>4</sup>:

$$\ln M = (1/\alpha) \ln \{(2.2 b \tau F)/[D_T V_0 (\Delta T)_0]\} + (t_R/\alpha\tau) \quad (1)$$

where  $M$  is the molecular weight (g/mol),  $\alpha$  (a constant describing polymer conformation) is  $\approx 0.6$  for random-coil polymers,  $b$  is a channel constant,  $\tau$  is the exponential delay/decay time constant,  $F$  is the flow-rate (ml/min),  $D_T$  is the thermal diffusion coefficient (apparently independent of polymer molecular weight  $M$ ),  $V_0$  is the channel dead volume (ml),  $(\Delta T)_0$  is the initial temperature difference between the hot and cold plates ( $^{\circ}\text{C}$ ), and  $t_R$  is the retention time (min) of the solute. Eqn. 1 predicts that sample analysis time is primarily controlled by  $\tau$ . Flow-rate exhibits less influence on retention, as does  $(\Delta T)_0$ . The level of the latter often is dictated by the retention needed to separate the lowest MW component in the sample from the channel dead-volume peak at  $V_0$ . As a result,  $(\Delta T)_0$  often is not an experimental variable used in optimizing a particular TDE-TFFF measurement.

Resolution and the ultimate MW accuracy of the measurement are also functions of the operating variables in a separation, as predicted by<sup>10</sup>,

$$R_{sp} = 0.58 \alpha\tau/\sigma \quad (2)$$

$$M_w^* = e^{\frac{1}{2}(\sigma/\alpha\tau)^2} - 1 \quad (3a)$$

$$M_n^* = e^{-\frac{1}{2}(\sigma/\alpha\tau)^2} - 1 \quad (3b)$$

where, the specific resolution value  $R_{sp}$  represents the usual chromatographic resolution for a pair of bands having a decade of MW difference, and the band standard deviation  $\sigma$  is the square root of the band variance contribution resulting from instrumental band broadening. The MW accuracy parameters  $M_w^*$  and  $M_n^*$  describe

the expected errors in the calculated  $M_w$  and  $M_n$  values as the result of instrumental band broadening.

Eqns. 2 and 3 describe the influence of the exponential time delay/decay  $\tau$  value and flow-rate on band broadening, and their resultant effect on MW accuracy<sup>10</sup>. Therefore, information on the level of effect of these variables in experimental situations is needed to anticipate errors in MW measurements that can be expected under particular operating conditions.

The effect of operating variables on TDE-TFFF retention can be predicted from the relationship in eqn. 1. The change in retention time with change in  $\tau$  is described by,

$$\Delta t_R = t_{R1}[(\tau_2/\tau_1) - 1] - \tau_2 \ln(\tau_2/\tau_1) \quad (4)$$

where  $\Delta t_R = (t_{R2} - t_{R1})$  is the change in retention time,  $t_{R1}$  is the retention time of the initial experiment,  $t_{R2}$  is the retention time of the proposed experiment,  $\tau_1$  is the exponential time delay/decay constant for the initial experiment, and  $\tau_2$  is the exponential time delay/decay constant for the proposed experiment. This expression is useful in application studies to determine the change in time of a separation when the  $\tau$  value is varied, or conversely, after a preliminary separation with an initial  $\tau_1$  value, to predict the  $\tau_2$  value that will result in desired separation time. For example, if a TDE-TFFF separation was carried out with an initial  $\tau_1$  value of 20.0 min and showed an initial retention time  $t_{R1}$  of 60 min, eqn. 4 predicts that if a new value  $\tau_2$  of 25.0 min is used, the change in the retention time of the peak would be,

$$\Delta t_R = 60[(25/20) - 1] - 25 \ln(25/20) = 9.4 \text{ min}$$

Thus, the new retention time for the larger  $\tau$  value would be  $60 + 9.4 = 69.4$  min.

Similarly, the effect of a flow-rate change on TDE-TFFF retention is predicted by,

$$\Delta t_R = -\tau \ln(F_2/F_1) \quad (5)$$

or in another form,

$$F_2 = F_1 e^{-\Delta t_R/\tau} \quad (5a)$$

Fig. 1 shows a nomograph that can be used to predict the separation time change for a desired flow-rate change, or the flow-rate change required for a particular separation time change. This nomograph relates the change in analysis time to the initial/proposed flow-rate ratio for a range of exponential delay/decay  $\tau$  values. For example, this nomograph can be used to predict the change in TDE-TFFF analysis time with flow-rate change. If the flow-rate in a  $\tau = 20$  min separation is changed from ( $F_1$ ) 0.15 ml/min to ( $F_2$ ) 0.67 ml/min, the resulting  $F_1/F_2$  ratio (0.22) in the Fig. 1 nomograph indicates a 30-min decrease in analysis time (as illustrated by the black circle in the figure).

An analogous relationship exists for the effect of changing the initial channel

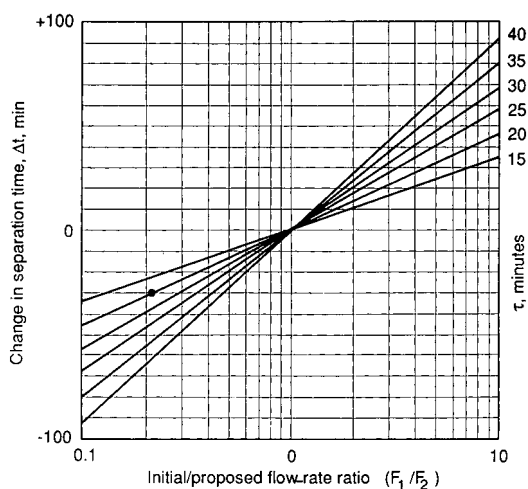


Fig. 1. Nomograph for variation in TDE-TFFF analysis time for change in the initial/proposed flow-rate ratio.

block temperature difference  $(\Delta T)_0$  on solute retention time in TDE-TFFF. This relationship can be expressed as,

$$\Delta t_R = -\tau \ln[(\Delta T_0)_1/(\Delta T_0)_2] \quad (6)$$

or, alternatively,

$$(\Delta T_0)_2 = (\Delta T_0)_1 e^{\Delta t_R/\tau} \quad (6a)$$

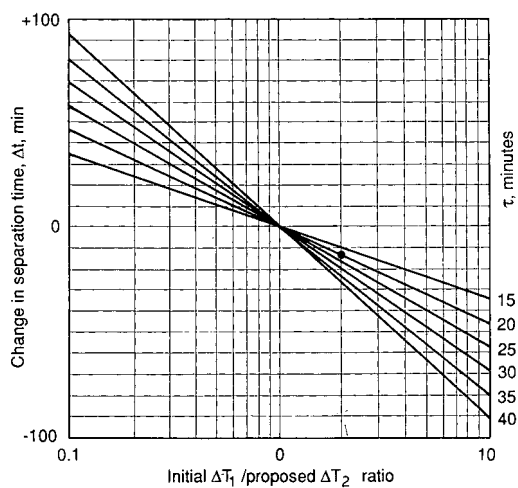


Fig. 2. Nomograph for variation in TDE-TFFF analysis time for change in the initial  $(\Delta T)_0$ /proposed  $(\Delta T)_0$  ratio.

Shown in Fig. 2 is a nomograph describing the effect of varying  $(\Delta T)_0$  to produce a change in TDE-TFFF separation time. For example, when the initial temperature difference  $(\Delta T_0)_1$  of  $80^\circ\text{C}$  is changed to a proposed temperature  $(\Delta T_0)_2$  of  $40.0^\circ\text{C}$  (ratio = 2.00), the nomograph in Fig. 2 indicates a decrease in analysis time of 13.9 min (as indicated by the black circle in the figure).

#### EXPERIMENTAL

The apparatus used in this study has been previously described<sup>4-6</sup>. TDE-TFFF separations were performed using the following conditions: channel thickness,  $132\ \mu\text{m}$ ; initial hot block temperature,  $90^\circ\text{C}$ ; cold block temperature,  $20^\circ\text{C}$ ; mobile phase, dioxane; sample,  $25\ \mu\text{l}$ , 1 mg/ml of each standard; UV detector, 260 nm. HPLC-grade dioxane was from American Burdick and Jackson (Muskegon, MI, U.S.A.). Polymer standards were obtained from Polymer Labs. (Amherst, MA, U.S.A.).

Peak analysis measurements were conducted with a new software program called THEOPS written in Fortran 77 on a Hewlett-Packard 1000 Series computer<sup>11</sup>. Separation data were collected on a Hewlett-Packard LAS data handling system. Polymer MW calculations were carried out with the software previously described<sup>5</sup>.

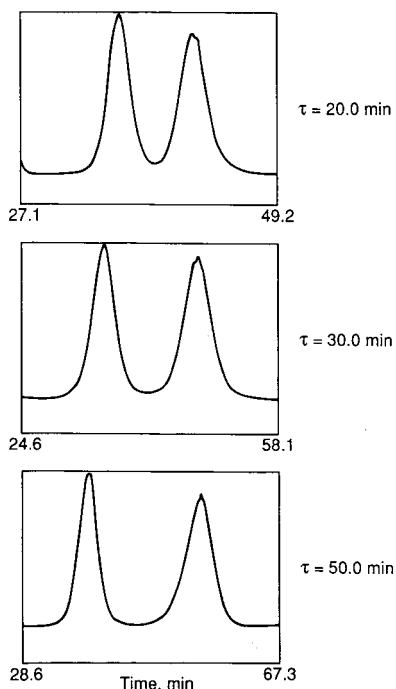


Fig. 3. Effect of exponential time-delay, time-decay  $\tau$  values on separation resolution. Narrow MW polystyrene standards; initial hot block temperature,  $90^\circ\text{C}$ ; cold block temperature,  $20^\circ\text{C}$ ; exponential time-delay, time-decay constant,  $\tau$ , as shown; dioxane carrier flow-rate, 0.15 ml/min; sample,  $25\ \mu\text{l}$ , 1 mg/ml each; UV detector, 260 nm.

## RESULTS AND DISCUSSION

*Effect of  $\tau$* 

Eqn. 2 predicts that separation resolution should increase as the  $\tau$  value used for the TDE-TFFF separation is increased. Therefore, the effect of increasing  $\tau$  should be to increase the accuracy of MW measurements as a result of decreasing the effects of instrumental band broadening. Fig. 3 shows the increasing resolution for MW 194 000 and 1 000 000 polystyrene standards with increasing  $\tau$  values.

However, peak width or the variance of the peak can also be affected by the extent that individual components making up the polymer standard are resolved by the separation method. Since TFFF is a high-resolution method, capable of higher resolution than SEC<sup>4,5</sup>, the end effect is that apparent band broadening can be mainly a method-resolution effect, rather than instrumental band-broadening effects. If this

TABLE I  
EFFECT OF  $\tau$  VALUES ON PEAK VARIANCE AND SHAPE

<i>Polystyrene standards</i>								
$\tau$ (min)	194K		515K		1000K		1850K	
	Variance <sup>a</sup>	Skew <sup>b</sup>	Variance	Skew	Variance	Skew	Variance	Skew
20	7.45	0.03	8.41	-0.42	11.42	0.50	9.55	0.24
25	9.76	0.06	9.39	-0.12	14.79	0.56	14.13	-0.30
Repeat	9.66	0.09	-	-	12.79	0.27	-	-
Repeat	9.62	0.14	-	-	13.58	0.43	-	-
30	11.85	-0.10	14.22	0.60	15.51	-0.19	17.70	-0.04
40	18.57	-0.20	18.82	-0.26	22.98	-0.40	29.55	-0.21
50	18.93	-0.19	24.13	-0.17	35.79	-0.71	40.00	-0.25

<sup>a</sup>Variance in min<sup>2</sup>.

<sup>b</sup>Mathematical peak skew from ref. 11.

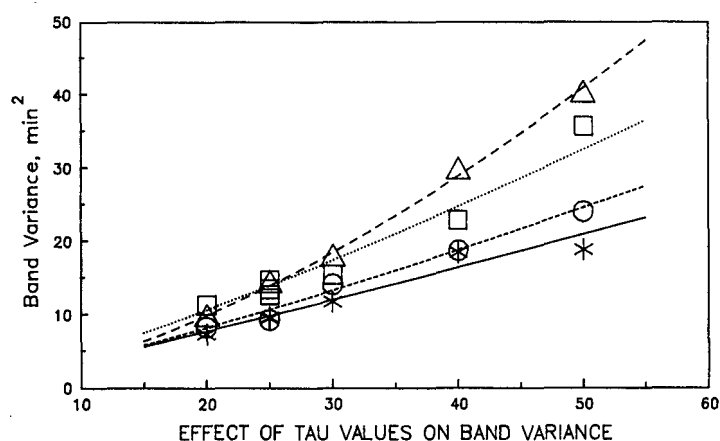


Fig. 4. Effect of exponential time-delay, time-decay  $\tau$  values on band variance. Conditions as in Fig. 3 (\* ) 194K; (○) 515K; (□) 1000K; (△) 1850K.



is the case, it would be expected that as resolution is increased by increasing  $\tau$  values, the variance of the bands actually should increase (rather than the intuitively expected decrease) as larger  $\tau$  values are used in the separation. This trend is borne out by the data in Table I with narrow MW polystyrene standards.

As the separation  $\tau$  value is increased, the measured peak variance values also increase as a result of greater resolution of the individual constituents in the polystyrene standards. This trend is graphically shown in Fig. 4, where the increase in band variance with increasing  $\tau$  values is almost linear, with plots for the higher MW components showing a steeper slope. This latter trend could be due to the higher resolution that TDE-TFFF exhibits for higher MW (more strongly retained) components (smaller impact of instrumental band broadening.) A less likely explanation is the larger polydispersity of the higher MW standards, resulting in broader bands because of larger resolution of the individual components as resolution is increased (larger  $\tau$  values).

The effect of increasing resolution by increasing the  $\tau$  values is also illustrated by the data for band skew in Table I. The general trend is a decrease of the mathematical band skew values as resolution is increased (increase in  $\tau$ ). The tendency of the data to slightly negative values (slight frontal band skew) with  $\tau$  increase could be due to the natural MW distribution of the sample towards the low MW end—as resolution increases, the instrumental band broadening is decreased so that the true MWD is now more apparent.

The effect of increasing the separation  $\tau$  values on measured molecular weights is also shown in Table II, which contains calculated MW values for four narrow MW polystyrene standards. As the separation  $\tau$  value was increased (increased resolution), calculated  $M_w$  values generally decreased, indicating increased accuracy due to the decreased effects of instrumental band broadening. Note that instrumental band broadening generally tends to increase measured  $M_w$  values as a result of the positive bias that is given to the features of the distribution curve from which values are calculated<sup>5</sup>.

Because of the bias of the level of resolution on measured  $M_w$  values, the influence of  $\tau$  values is especially reflected in calculated polydispersity values  $d$ , as shown in Table II. As  $\tau$  is increased (increased resolution), the calculated polydispersity values decrease. The “true” polydispersity values for these standards probably still are not approached by the conditions of these experiments. Other TFFF studies have shown that these ionic-polymerized polymers have polydispersities of  $< 1.01$  (ref. 12).

#### *Flow-rate effects*

Eqn. 1 predicts that a plot of log MW versus retention time  $t_R$  obtained with a particular  $\tau$  value should produce a straight-line (except at  $t_R$  values approaching the channel dead volume  $V_0$ ). Also predicted by eqn. 1 is that a change in flow-rate should result in a change in the intercept of this straight-line plot, but no change in its slope. This effect was verified in previous work<sup>4</sup>, and is further confirmed by the data in Fig. 5. Here, as the flow-rate is increased from 0.1 to 0.4 ml/min, the intercept increases and the absolute level of MW accessible during the experiment also increases, as predicted by Eqn. 4. For example, at 0.4 ml/min it can be anticipated that polystyrenes in the  $5 \cdot 10^4$ – $3 \cdot 10^6$  MW range could be accessed and measured under these particular operating conditions.

TABLE II  
EFFECT OF  $\tau$  ON MOLECULAR WEIGHT

*Polystyrene standards*

$\tau$	194K			515K			1000K			1850K		
	$M_w^a$	$M_n^b$	$d^c$	$M_w$	$M_n$	$d$	$M_w$	$M_n$	$d$	$M_w$	$M_n$	$d$
20	199 000	189 000	1.05	513 000	491 000	1.08	1 060 000	977 000	1.09	1 910 000	1 770 000	1.08
25	196 000	184 000	1.06	550 000	479 000	1.15	1 020 000	964 000	1.07	1 940 000	1 830 000	1.06
Repeat	205 000	191 000	1.07	549 000	517 000	1.06	1 070 000	976 000	1.10	1 860 000	1 770 000	1.05
30	200 000	188 000	1.06	552 000	520 000	1.06	991 000	941 000	1.05	1 820 000	1 710 000	1.06
40	195 000	184 000	1.06	537 000	507 000	1.06	997 000	945 000	1.03	1 860 000	1 770 000	1.06
50	190 000	181 000	1.05	522 000	504 000	1.04	973 000	927 000	1.05	1 807 000	1 770 000	1.06

<sup>a</sup> $M_w$  = weight-average molecular weight.

<sup>b</sup> $M_n$  = number-average molecular weight.

<sup>c</sup> $d$  = polydispersity,  $M_w/M_n$ .

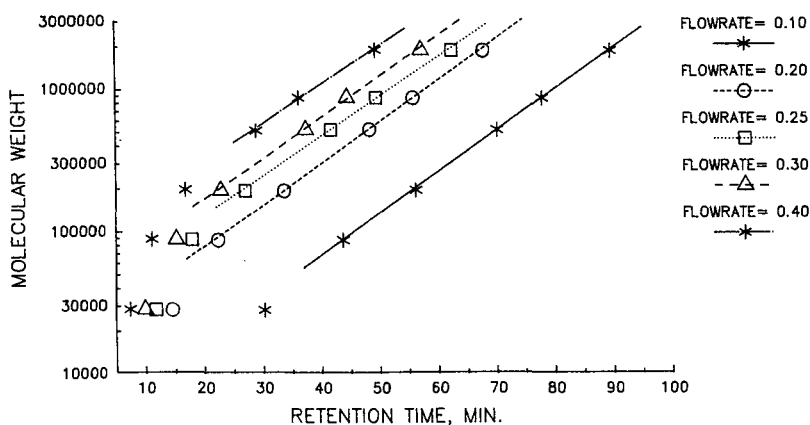


Fig. 5. Effect of flow-rate on TDE-TFFF calibration plots. Conditions as in Fig. 3, except flow-rates as shown.

Flow-rate and the initial temperature differential  $(\Delta T)_0$  both can influence separation resolution and significantly affect the accuracy of molecular weights determined by TDE-TFFF. Flow-rate is often of more concern, since the level of  $(\Delta T)_0$  usually is dictated by the range of molecular weights in the sample, and normally is not a parameter that is changed after the desired resolution from the channel dead-time peak is established. Intuitively, one would expect that increasing the flow-rate,  $F$ ,

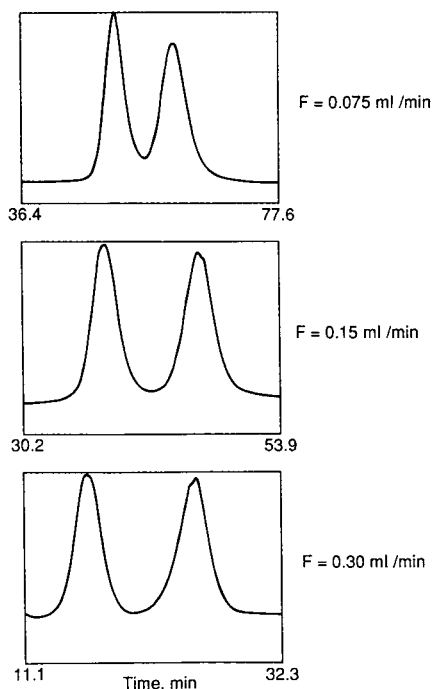


Fig. 6. Effect of flow-rate on separation resolution in TDE-TFFF. Conditions as in Fig. 3, except flow-rates as shown;  $\tau = 25.0 \text{ min}$ .

TABLE III  
EFFECT OF FLOW-RATE ON BAND VARIANCE AND SHAPE

Polystyrene standards		194K			515K			1000K			1850K		
Flow-rate (ml/min)	$\sigma_t^a$	$\sigma_v^b$	Skew	$\sigma_t$	$\sigma_v$	Skew	$\sigma_t$	$\sigma_v$	Skew	$\sigma_t$	$\sigma_v$	Skew	
0.075	3.57	0.268	0.39	3.25	0.244	0.44	4.73	0.355	0.54	4.22	0.316	-0.34	
0.10	3.24	0.324	0.19	3.49	0.349	0.43	3.99	0.399	0.00	4.30	0.430	0.40	
0.15	3.10	0.466	0.09	3.06	0.459	0.12	3.49	0.523	0.27	3.76	0.564	-0.30	
Repeat	3.10	0.465	0.14	—	—	—	3.69	0.553	0.43	—	—	—	
0.20	3.23	0.645	-0.30	3.04	0.609	-0.07	3.17	0.633	0.09	3.53	0.704	0.23	
0.30	2.94	0.882	-0.26	3.71	1.11	-0.91	3.66	1.10	-0.94	3.46	1.04	0.24	
0.40	2.41	0.963	-0.05	3.93	1.57	-0.27	4.00	1.60	-0.89	3.63	1.45	0.00	

<sup>a</sup>Standard deviation, min.

<sup>b</sup>Standard deviation, ml.

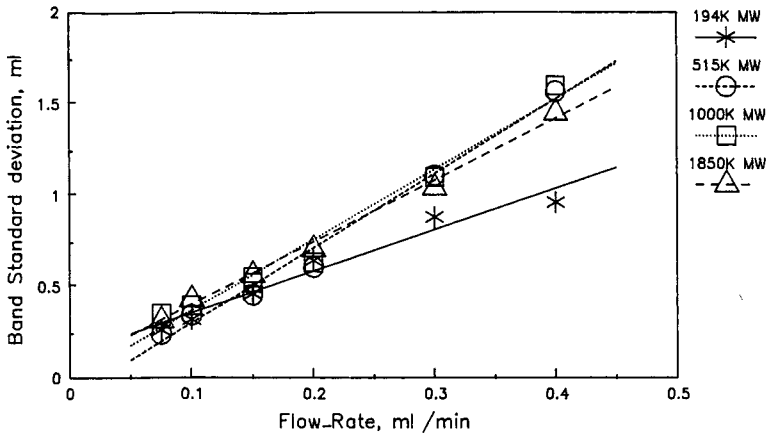


Fig. 7. Effect of flow-rate on band volume standard deviation. Conditions as in Fig. 3, except  $\tau = 25.0$  min, flow-rates as shown.

would decrease resolution because of added band broadening caused by resistance to mass transfer effects. However, as illustrated in Fig. 6, increasing  $F$  (constant  $\tau$ ) actually increases resolution in TDE-TFFF. The reason for this is that at higher flow-rates, solutes under a higher thermal-gradient field elute earlier from the channel, staying closer, on average, to the accumulation wall. This results in shorter distances for diffusion-limited mass-transfer contributions to band broadening within the channel; less-than-expected band broadening at higher flow-rates is observed, and higher resolution results. This same effect has been predicted and experimentally observed in exponential time-delay, time-decay sedimentation FFF<sup>13</sup>.

The unique increase in resolution in TDE-TFFF with increased flow-rate is also shown by the data in Table III. As illustrated by the plot in Fig. 7, the standard deviation of the bands in volume units show the usual increase with increased flow-rate because of resistance to mass transfer effects, as previously described<sup>8</sup>. The in-

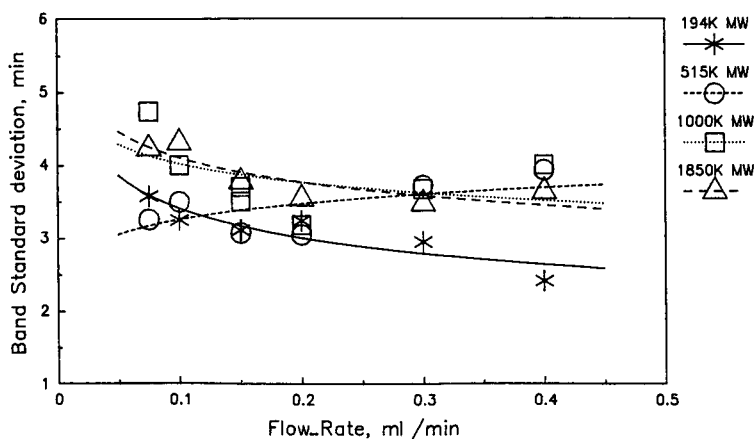


Fig. 8. Effect of flow-rate on band time standard deviation. Conditions as in Fig. 3, except  $\tau = 25.0$  min, flow-rates as shown.

TABLE IV  
EFFECT OF FLOW-RATE ON MOLECULAR WEIGHT

Flow-rate (ml/min)	1000K				515K				1850K			
	$M_w^a$	$M_n^b$	$d^c$	$M_w$	$M_n$	$d$	$M_w$	$M_n$	$d$	$M_w$	$M_n$	$d$
0.075	213 000	195 000	1.09	536 000	494 000	1.09	1 260 000	1 010 000	1.24	2 220 000	1 860 000	1.19
0.10	194 000	190 000	1.02	564 000	502 000	1.13	1 000 000	919 000	1.09	1 980 000	1 830 000	1.09
0.15	196 000	184 000	1.06	550 000	479 000	1.15	1 020 000	964 000	1.07	1 940 000	1 830 000	1.06
Repeat	205 000	191 000	1.07	549 000	517 000	1.06	1 070 000	976 000	1.10	1 860 000	1 770 000	1.05
Repeat	212 000	200 000	1.06	—	—	—	1 060 000	1 000 000	1.07	—	—	—
0.20	199 000	183 000	1.09	559 000	512 000	1.09	998 000	949 000	1.05	1 960 000	1 810 000	1.08
0.30	191 000	179 000	1.07	511 000	475 000	1.08	953 000	908 000	1.05	1 940 000	1 800 000	1.08
0.40	196 000	177 000	1.11	540 000	482 000	1.12	940 000	885 000	1.06	1 910 000	1 750 000	1.09

<sup>a</sup>  $M_w$  = weight-average molecular weight.

<sup>b</sup>  $M_n$  = number-average molecular weight.

<sup>c</sup>  $d$  = polydispersity,  $M_w/M_n$ .

crease in band volume is somewhat less for the smaller MW 194 000 polystyrene standard because of the larger solute diffusion coefficient. The increased band volumes for the higher MW components in Fig. 7 is a combination of poorer diffusion (poorer mass transfer) and larger sample polydispersity effects. On the other hand, as shown in Fig. 8, the band standard deviation in time units decreases with increasing flow-rate, verifying the increased time-based resolution seen in Fig. 6.

The effect of flow-rate on band skew shown in Table III is variable, and no significant trend is apparent.

The effect of flow-rate on the calculated molecular weights for polystyrene standards is shown in Table IV. The data indicate that satisfactorily accurate MW values for polymers can be obtained over a wide range of flow-rates. However, as discussed earlier, separations performed by TDE-TFFF at higher flow-rates provide somewhat higher resolution and more accurate MW measurements. Note that the concentration of eluting species is decreased at higher flow-rates because of increased band volumes (Fig. 8); increasing the flow-rate reduces the detector/background noise ratio and decreases the precision of the MW measurement. Therefore, a compromise of flow-rate and other operating parameters often is indicated.

As expected, polydispersity values at higher flow-rates are generally smaller as a result of better resolution and reduced instrumental band broadening.

## CONCLUSIONS

Nomographs relating retention to the exponential time-delay, time-decay constant  $\tau$  values and flow-rate levels are useful in arriving at practical operating conditions for MW measurements by TDE-TFFF. Most-accurate MW and polydispersity measurements are obtained with conditions for highest resolution with TDE-TFFF: large  $\tau$  values and high flow-rates. However, in most practical situations, a compromise is often in order, since large  $\tau$  values mean long analysis times. With the channel thickness and apparatus used in this study, it appears that a flow-rate of 0.15–0.2 ml/min and a  $\tau$  value of about 25 min represent a reasonable compromise between MW accuracy, precision and sample detectability. However, other studies<sup>12</sup> suggest that thinner channels will permit higher resolution, improved sample detectability and faster analyses by using smaller  $\tau$  values.

## ACKNOWLEDGEMENT

We thank V. E. Burton for carrying out the experiments in this study.

## REFERENCES

- 1 M. N. Myers, K. D. Caldwell and J. C. Giddings, *Sep. Sci.*, 9 (1974) 47.
- 2 J. C. Giddings, M. Martin and M. N. Myers, *J. Chromatogr.*, 158 (1978) 419.
- 3 J. C. Giddings, M. N. Myers and J. Janca, *J. Chromatogr.*, 186 (1979) 37.
- 4 J. J. Kirkland and W. W. Yau, *Macromolecules*, 18 (1985) 2305.
- 5 J. J. Kirkland, S. W. Rementer and W. W. Yau, *Anal. Chem.*, 60 (1988) 610.
- 6 J. J. Kirkland and W. W. Yau, *J. Chromatogr.*, 353 (1986) 95.
- 7 G. H. Thompson, M. N. Myers and J. C. Giddings, *Anal. Chem.*, 41 (1969) 1219.
- 8 M. E. Hovings, G. H. Thompson and J. C. Giddings, *Anal. Chem.*, 42 (1970) 195.

- 9 J. J. Kirkland, S. W. Rementer and W. W. Yau, *J. Polym. Sci.*, in press.
- 10 W. W. Yau, J. J. Kirkland, D. D. Bly and H. J. Stoklosa, *J. Chromatogr.*, 125 (1976) 219.
- 11 W. W. Yau, J. J. Kirkland and S. W. Rementer, in preparation.
- 12 M. E. Schimpf, M. N. Myers and J. C. Giddings, *J. Appl. Polym. Sci.*, 33 (1987) 117.
- 13 W. W. Yau and J. J. Kirkland, *Sep. Sci. Technol.*, 16 (1981) 577.



CHROMSYMP. 1675

## ION CHROMATOGRAPHY OF TRANSITION METALS ON AN IMINO-DIACETIC ACID BONDED STATIONARY PHASE

G. BONN\* and S. REIFFENSTUHL

*Institute of Radiochemistry, University of Innsbruck, Innrain 52a, A-6020 Innsbruck (Austria)*

and

P. JANDIK

*Waters Chromatography, Millipore Corporation, 34 Maple Street, Milford, MA 01757 (U.S.A.)*

---

### SUMMARY

A stationary phase synthesized by covalent binding of iminodiacetic acid to a porous silica support was investigated for the separation of transition metals by ion chromatography. Eluents containing carboxylic acids either alone or in combination with stronger complexing agents were studied in order to examine the elution mechanisms of alkali, alkaline earth and transition metal ions. It was found that both complexation reactions and ion-exchange mechanisms occurred, their rate being governed by the stability of metal complexes. These investigations were used to find optimum conditions for the determination of transition metal ions in alkali and alkaline earth metal-rich matrices, *e.g.*, sea water.

---

### INTRODUCTION

The need for rapid and convenient methods for the determination of heavy metals in environmental and biological samples has induced a great deal of research work in the field of cation chromatography<sup>1–3</sup>. This method allows the separation and subsequent detection of a large number of bivalent transition metals in liquid samples without tedious sample cleanup procedures<sup>4–6</sup>. Short analysis times, simple handling and low cost of equipment and maintenance are assets that make ion chromatography (IC) very attractive for the screening and routine analysis of metal ions.

Stationary phases generally applied to the ion-chromatographic determination of transition metals are low-capacity cation-exchange materials with sulfonic acid functional groups<sup>1,7</sup>. These packing materials give good results if aqueous standard solutions are analysed, but frequently fail as soon as more complex real samples are injected. One problem often encountered during IC of environmental or biological samples is interference from other ionic constituents. For instance, in samples such as sea water the large system peak produced by the predominant ions  $\text{Na}^+$  and  $\text{Mg}^{2+}$  impedes the determination of trace levels of heavy metals. This shows that new stationary phases with higher selectivities for transition metal ions are required. Dicarboxylic acids show high affinities toward transition metals<sup>8–10</sup>, especially if a nitrogen atom is part of the chelating center<sup>9,11,12</sup>.

Iminodiacetic acid (IDA) gels have found extensive application as powerful chelating agents for the preconcentration of heavy metal ions from complex matrices<sup>13-17</sup>. In this study, a newly synthesized, pressure-stable, silica-based material with IDA functions covalently coupled to its surface was examined for use in cation chromatography.

## EXPERIMENTAL

### *Chromatographic conditions*

Analyses were performed on an HPLC system consisting of a Model 501 pump (Waters Assoc., Milford, MA, U.S.A.), a Model 7010 injection valve (Rheodyne (Cotati, CA, U.S.A.), equipped with a 100- $\mu$ l loop, and a Model 430 conductivity detector (Waters Assoc.). The peaks were integrated by a CR-2A integration system (Shimadzu, Kyoto, Japan). The column temperature was maintained at 25°C.

### *Column*

The stationary phase was a 7- $\mu$ m silica-based material with an average pore size of 300 Å (Nucleosil 300-7; Macherey Nagel & Co., Düren, F.R.G.). The silica was derivatized with  $\gamma$ -glycidoxypropyltrimethoxysilane. IDA was covalently coupled to the epoxy activated surface<sup>18,19</sup>. The stationary phase in a methanol slurry was packed into a 100  $\times$  4.6 mm I.D. stainless-steel column.

### *Materials*

The mobile phases were prepared by dissolving analytical-reagent grade L(+)-tartaric acid, citric acid monohydrate, ethylenediamine (EDA) and pyridine-2,6-dicarboxylic acid (Merck, Darmstadt, F.R.G.) in deionized water. In some instances the pH was adjusted by addition of 1 M hydrochloric acid. Metal ion solutions were prepared from analytical-reagent grade chlorides or nitrates (Sigma, St. Louis, MO, U.S.A. and Fluka, Buchs, Switzerland). The stock solutions (1000 mg/l) were adjusted to pH 1 with nitric acid.

## RESULTS AND DISCUSSION

IDA exhibits a strong complexing ability for transition metal ions, which can be attributed to the carboxylic groups and the nitrogen atom. Free carboxylate groups act as ion-exchange sites, especially with ions that have low tendencies to form complexes, such as alkali or alkaline earth metal ions.

### *Chromatography of alkaline earth metal ions with an ethylenediamine-citric acid eluent*

The behavior of IDA columns as a normal cation exchanger was investigated for alkaline earth metal ions using an ethylenediamine-citric acid eluent system. In order to optimize the composition of the mobile phase, both the citric acid and the ethylenediamine concentrations were varied independently.

The (ethylenediammonium)<sup>2+</sup> concentration has a strong influence on retention time. Addition of citric acid increases the retention of cations owing to the decrease in pH caused by the acid dissociation (Fig. 1). This means that the complexation ability of the citrate ions is mainly governed by pH.

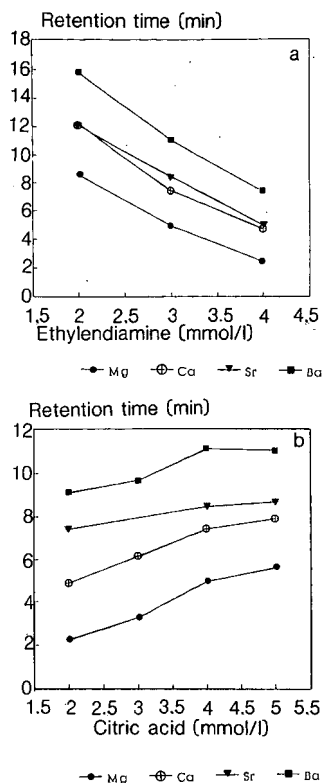


Fig. 1. Influence of ethylenediamine and citric acid concentration on retention times. (a) 4.0 mmol/l citric acid; (b) 3.0 mmol/l ethylenediamine. Stationary phase, 7- $\mu$ m porous silica coupled with iminodiacetic acid (IDA-silica); flow-rate, 1.0 ml/min; samples, 1 ppm of each ion; detection, conductivity. ●, Mg<sup>2+</sup>; ○, Ca<sup>2+</sup>; ▼, Sr<sup>2+</sup>; ■, Ba<sup>2+</sup>.

Fig. 2. Separation of alkaline earth metals. Stationary phase, IDA-silica; mobile phase, 3.0 mmol/l ethylenediamine-4.0 mmol/l citric acid; flow-rate, 1.0 ml/min; detection, conductivity. Sample concentration: (1) 1.5 ppm Mg<sup>2+</sup>; (2) 5 ppm Ca<sup>2+</sup>; (3) 10 ppm Sr<sup>2+</sup>; (4) 20 ppm Ba<sup>2+</sup>.

The chromatogram of a standard mixture of Mg<sup>2+</sup>, Ca<sup>2+</sup>, Sr<sup>2+</sup> and Ba<sup>2+</sup>, as depicted in Fig. 2, was obtained under optimized conditions, using an eluent consisting of 3.0 mmol/l EDA and 4.0 mmol/l citric acid.

#### *Chromatography of alkali, alkaline earth and transition metals with organic acid eluents*

Different organic acids were screened for their ability to elute alkali, transition and alkaline earth metals from the IDA column. Citric acid and tartaric acid showed very similar elution behavior, but the retention times achieved with citric acid were slightly longer owing to its lower degree of dissociation.

Retention times of alkali, alkaline earth and transition metal ions are plotted against the tartaric acid concentration in Fig. 3. The eluent concentration affects the retention of bivalent ions more markedly than that of monovalent ions. Although in the pH range investigated (2.5–3.0) there is evidence for ion-exchange processes taking place additionally (also between transition metals and partially protonated IDA

functions), the elution order reflects the affinity of metal ions to iminodiacetic acid as a complexing ligand. Alkali metal ions, which obviously do not form IDA complexes, are eluted first, followed by alkaline earth metal ions (plus  $Mn^{2+}$  and  $Fe^{2+}$ ), then by the transition metals  $Cd^{2+}$ ,  $Co^{2+}$  and  $Zn^{2+}$ . Ions that form IDA complexes of higher stability, such as  $Cu^{2+}$  and  $Ni^{2+}$ , remain on the column under these conditions. This fact and the long retention times of transition metals observed with citric or tartaric acid justified further efforts to find more efficient eluents for the IDA column.

One complexing agent that proved particularly useful for this purpose was pyridine-2,6-dicarboxylic acid (dipicolinic acid, DPA). Both DPA and IDA have three centers involved in complexation (Fig. 4), *i.e.*, the two carboxylate groups and the nitrogen atom, which are apparently very similarly arranged within the molecules.

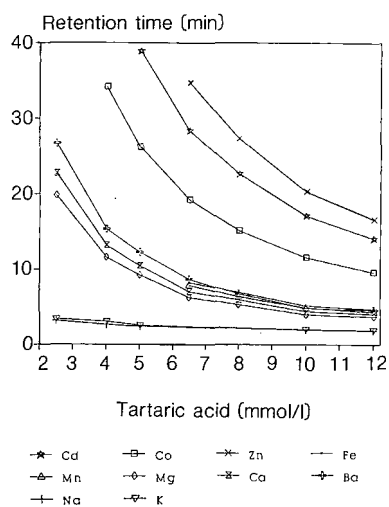


Fig. 3. Influence of tartaric acid concentration on retention times. Stationary phase, IDA-silica; mobile phase, tartaric acid (2.5–12.0 mmol/l); flow-rate, 1.0 ml/min; detection, conductivity.

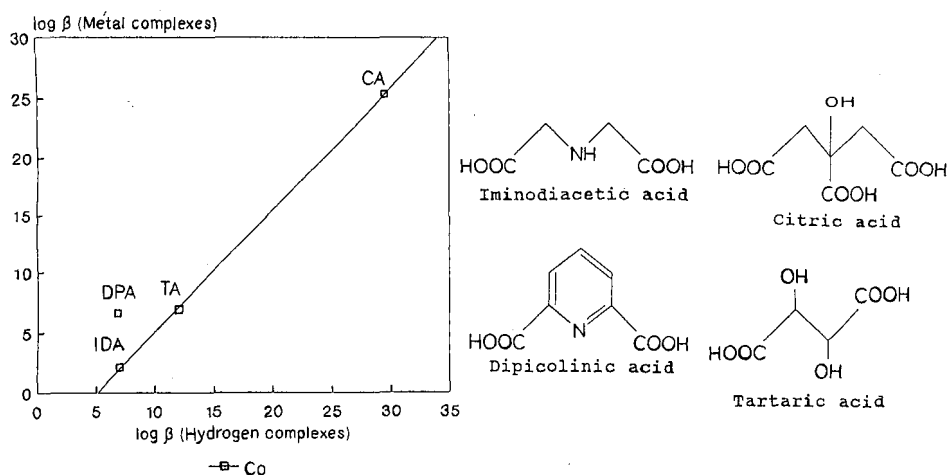


Fig. 4. Correlation between basicity and stability of  $Co^{2+}$  complexes. DPA = dipicolinic acid; TA = tartaric acid; IDA = iminodiacetic acid; CA = citric acid.

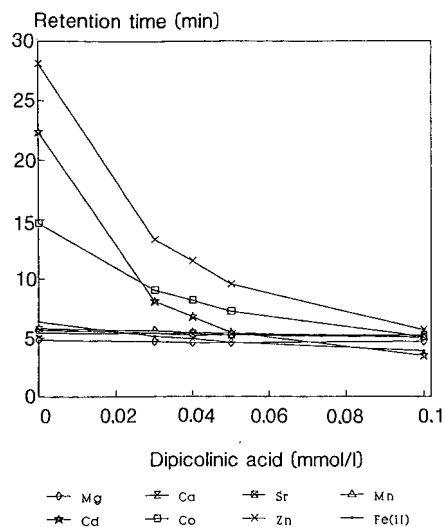


Fig. 5. Addition of DPA to 10.0 mmol/l citric acid. Stationary phase, IDA-silica; mobile phase, citric acid (10.0 mmol/l)-DPA (0-0.10 mmol/l); flow-rate, 1.0 ml/min; detection, conductivity; sample concentration, 5 ppm each.

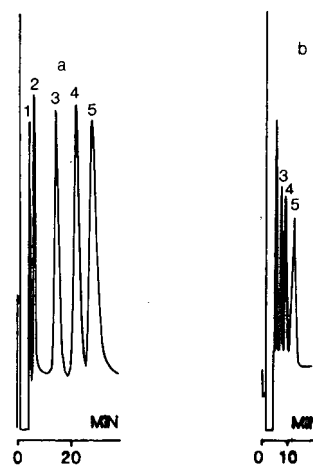


Fig. 6. Separation of transition metals. Stationary phase, IDA-silica; mobile phase, (a) 10.0 mmol/l citric acid, (b) 10 mmol/l citric acid-0.04 mmol/l DPA; flow-rate, 1.0 ml/min; detection, conductivity. Sample: standard solution containing (1) 1 ppm  $Mg^{2+}$ ; (2) 3 ppm  $Fe^{2+}$ ; (3) 5 ppm  $Co^{2+}$ ; (4) 10 ppm  $Cd^{2+}$ ; (5) 10 ppm  $Zn^{2+}$ .

Nevertheless, the IDA molecule has a flexible structure, whereas the nitrogen atom of DPA is part of an aromatic system, which rigidly holds the two carboxylate groups in a position coplanar to the pyridine ring, thus favoring complex formation.

Normally the tendency of the ligand to bind a proton parallels its complexation ability. In Fig. 4 the stability constants of cobalt complexes are plotted against the protonation constants of the corresponding acids. If a double-logarithmic scale is employed, the values for IDA, tartaric acid and citric acid lie on a straight line, showing that the stability of metal complexes is in direct proportion to the affinity of the ligand for protons. The dipicolinic acid anion, on the other hand, shows a chelating ability higher than would be expected from its basicity. This is due to the steric effect discussed above. The uniquely high degree of complexation of DPA is especially advantageous in acidic solutions. In this investigation, the complexing ability of DPA in acidic solution was monitored. An eluent consisting of 10.0 mmol/l citric acid was modified by addition of up to 0.10 mmol/l DPA which caused a slight decrease in pH from 2.58 to 2.50. The retention times achieved with these eluents are depicted in Fig. 5. A concentration of 0.03 mmol/l DPA, added to the citric acid eluent, halves the retention times of transition metals, whereas the elution of alkaline earth metal ions and manganese is not significantly influenced by the DPA concentration. The small decrease in retention time observed for the latter is rather caused by the pH changes. This indicates that in the pH range investigated DPA acts as a strong complexing agent for transition metals but has little affinity for alkaline earth metal ions (Fig. 6). If the log  $k'$  values are plotted against the logarithm of DPA concentration,

straight lines with slopes proportional to the stability constants of the metal–DPA complexes are obtained. Owing to the high affinity of the ligand for cadmium, the elution of this ion is speeded up most, and this causes the observed cross-over of  $\text{Cd}^{2+}$  and  $\text{Co}^{2+}$  (Fig. 5).

In order to investigate the equilibrium between complexation of DPA and iminodiacetic acid, further experiments were carried out in a simpler system. Hydrochloric acid was used instead of citric acid for pH adjustment to eliminate any complexation reactions apart from those involving DPA and IDA (Fig. 7). The retention of  $\text{Na}^+$  and  $\text{Mg}^{2+}$  showed a strong dependence on pH but was not significantly influenced by the amount of DPA in the eluent.

Transition metals, on the other hand, exhibit a strong dependence on both DPA concentration and pH. The order of affinity towards DPA is  $\text{Cd} < \text{Co} < \text{Zn} < \text{Cu}$ . At low DPA concentrations (Fig. 7, 0.04 mmol/l) even transition metals of high complex stability, such as  $\text{Cu}^{2+}$  or  $\text{Co}^{2+}$ , exhibit a retention behavior similar to that

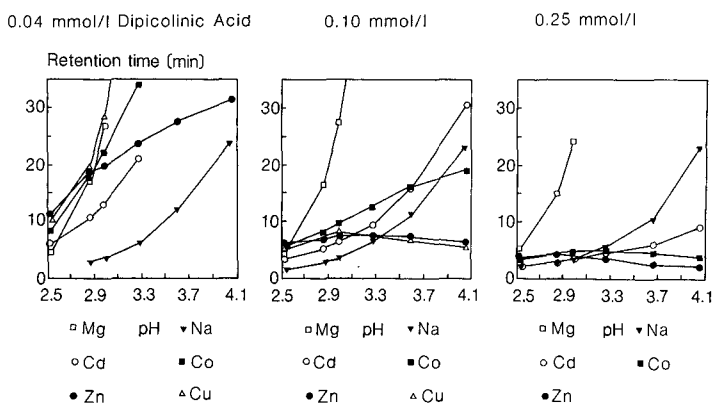


Fig. 7. Influence of pH of DPA eluents on the retention of alkali, alkaline earth and transition metals. Stationary phase, IDA–silica; mobile phase, dipicolinic acid (0.04, 0.10 and 0.25 mmol/l), pH adjusted with 1 M HCl; flow-rate, 1.0 ml/min; sample, 5 ppm of each ion.

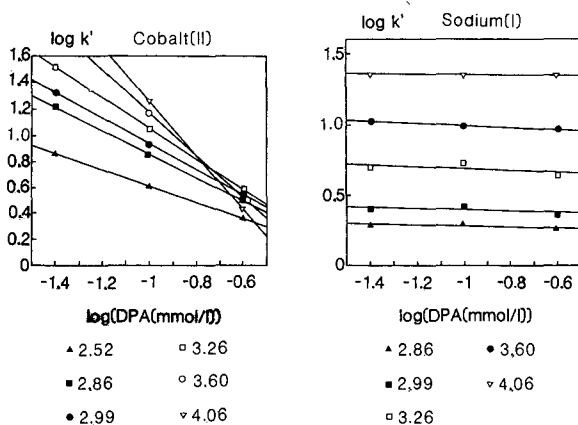


Fig. 8. Influence of complexing agent concentration and pH on the retention of metal ions. Chromatographic conditions as in Fig. 7.

of other bivalent ions, such as  $Mg^{2+}$ . Under these conditions elution is governed mainly by ion-exchange mechanisms. If higher levels of DPA are incorporated in the eluent, the graphs for metal ions with a high affinity towards DPA change their shape, indicating that complexation processes are favored. This causes lower retention times at higher pH (see  $Zn^{2+}$  and  $Co^{2+}$  in Fig. 7; 0.10 and 0.25 mmol/l DPA).

In Fig. 8 the  $\log k'$  for two representative ions ( $Co^{2+}$  and  $Na^+$ ) are plotted against the logarithm of the DPA concentration. The different lines of the graph correspond to different pH values.

$Co^{2+}$  shows the behavior typical of transition metals, with a linear relationship between  $\log k'$  and the logarithm of DPA concentration. The slopes of these regression curves increase with increasing pH, reflecting the increasing dissociation and complexing ability of the ligand.

Sodium is representative of ions with a low tendency to form chelates. The regression curves have a slope of zero, indicating that the amount of DPA present in the eluent has no influence on elution. One must bear in mind, however, that two complexation reactions take place under these conditions. The metal ions form chelates with either the IDA groups immobilized on the stationary phase or with DPA incorporated in the eluent. Changes in pH influence the complexing ability of both agents. By careful choice of the experimental conditions, either complexation by an eluent ion or complexation by the stationary phase can be favored.

Conditional stability constants<sup>9</sup> were calculated from the original stability constants to account for the loss of chelating properties due to protonation of the ligand. These conditional constants were plotted against pH. Fig. 9a shows the conditional stability constants of  $Mg^{2+}$ , a cation with a generally low tendency toward complex formation. The conditional constants for IDA are negative throughout the pH range studied, indicating that  $Mg^{2+}$  reacts with IDA only by ion exchange under acidic conditions. Tartaric acid and DPA show higher affinities to  $Mg^{2+}$ , but their complexation ability can also be neglected at  $pH < 3$ . pH alone is the determining factor in eluting metals of low complexation tendency.

$Co^{2+}$  (Fig. 9b) behaves differently. The conditional stability constants are positive, which means that all three of the acids are capable of forming cobalt chelates. The stability of cobalt-DPA complexes is high throughout the pH range studied, confirming the ability of this complexing agent to accelerate the elution of transition metal ions under acidic conditions.

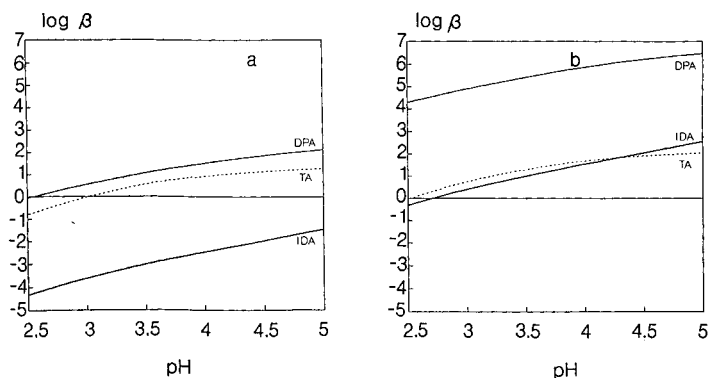


Fig. 9. Conditional stability constants of  $Mg^{2+}$  and  $Co^{2+}$  complexes with change in pH. IDA = iminodiacetic acid; TA = tartaric acid; DPA = dipicolinic acid.

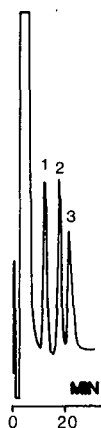


Fig. 10. Separation of transition metals in sea water. Stationary phase, IDA-silica; mobile phase, 10 mmol/l tartaric acid (pH 2.54); flow-rate, 1.0 ml/min; detection, conductivity; integration, attenuation 8. Sample: sea water spiked with (1) 5 ppm  $\text{Co}^{2+}$ , (2) 5 ppm  $\text{Zn}^{2+}$  and (3) 10 ppm  $\text{Cd}^{2+}$ .

The affinity of the IDA stationary phase towards transition metal ions is a great advantage for the determination of trace metals in samples containing high levels of alkali and alkaline earth metal ions, such as sea water, which contains large amounts of  $\text{Na}^+$  and  $\text{Mg}^{2+}$ , among other ionic constituents. In order to investigate the influence of high concentrations of alkali metal ions on the determination of transition metals, solutions containing up to 10% of  $\text{Na}^{2+}$  and  $\text{Mg}^{2+}$  were chromatographed. These ions were well separated from the transition metal peaks and did not exert any significant influence on either retention times or signal strength. This means that transition metals can be determined in alkali and alkali earth metal-rich matrices. Fig. 10 shows a chromatogram of sea water spiked with transition metals in the range 5–10 ppm.

In subsequent work, these investigations at ambient temperatures will be extended to include the influence of higher temperatures on separations.

#### REFERENCES

- 1 J. S. Fritz, D. T. Gjerde and C. Pohlandt, *Ion Chromatography*, Hüthig, Heidelberg, 1982.
- 2 G. Schmuckler, *J. Chromatogr.*, 313 (1984) 47.
- 3 G. O. Franklin, *Int. Lab.*, 1985, 56.
- 4 J. S. Fritz, *Anal. Chem.*, 59 (1987) 335A.
- 5 J. S. Fritz, *J. Chromatogr.*, 439 (1988) 3.
- 6 D. R. Yan, E. Stumpp and G. Schwedt, *Fresenius Z. Anal. Chem.*, 322 (1985) 474.
- 7 G. Schmuckler, *J. Liq. Chromatogr.*, 10 (1987) 1887.
- 8 G. J. Sevenich and J. S. Fritz, *Anal. Chem.*, 55 (1983) 12.
- 9 J. Inczédy, *Analytical Applications of Complex Equilibria*, Wiley, New York, 1976.
- 10 A. E. Martell and M. R. Smith, *Critical Stability Constants*, Vol. 3, Plenum Press, New York, 1977.
- 11 S. K. Sahni and J. Reedijk, *Coord. Chem. Rev.*, (1984) 1.
- 12 G. Anderegg, *Helv. Chim. Acta*, 43 (1960) 414.
- 13 D. E. Leyden and W. Wegscheider, *Anal. Chem.*, 53 (1981) 1059A.
- 14 L. Rasmussen, *Anal. Chim. Acta*, 125 (1981) 117.
- 15 R. R. Greenberg and H. M. Kingston, *J. Radioanal. Chem.*, 71 (1982) 147.
- 16 R. R. Greenberg and H. M. Kingston, *Anal. Chem.*, 55 (1983) 1160.
- 17 A. J. Paulson, *Anal. Chem.*, 58 (1986) 183.
- 18 J. Porath, B. Olin and B. Graustrand, *Arch. Biochem. Biophys.*, 225 (1983) 543.
- 19 Z. El Rassi and Cs. Horváth, *J. Chromatogr.*, 359 (1986) 241.



CHROMSYMP. 1642

## Note

---

### Calculation of column performance in nitrate removal from water supplies by anion exchange

RONG-JIN LEU, YNG-LONG HWANG and FRIEDRICH G. HELFFERICH\*

*Department of Chemical Engineering, The Pennsylvania State University, University Park, PA 16802 (U.S.A.)*

Contamination of drinking water supplies by nitrate from agricultural run-off is a serious environmental problem and health hazard. Anion exchange suggests itself as an effective means of nitrate removal and has been studied by several investigators<sup>1–3</sup>. The present communication addresses calculation of column performance in such operations on the basis of independently determined parameters.

In practice, nitrate removal by anion exchange is a multicomponent problem because the water usually also contains chloride, sulfate, and carbonate in comparable concentrations. Moreover, in most cases, the stepwise dissociation equilibrium of carbonic acid and, if weak-base resins are used, the association equilibrium of the fixed ionogenic groups, must be accounted for.

The most detailed previous study has been by Clifford and Weber<sup>1,4</sup>. A promising procedure was found to be a two-column operation. The water is acidified in a cation-exchange column in H<sup>+</sup> form, and is then passed through an anion-exchange column in free-base form. Breakthrough occurs in the sequence of increasing affinity of the anions for the ion exchanger: carbonate, chloride, nitrate, sulfate. The column is run to nitrate breakthrough. Best economics are obtained with weak-base resins because they can be regenerated with carbonate.

Clifford<sup>4</sup> was able to account for much of the effluent history by using independently determined separation factors of the anions and the Helfferich–Klein theory of multicomponent chromatography<sup>5</sup>. This theory does not include dissociation–association equilibria and so cannot predict early column behavior involving pH variation from alkaline to acidic and protonation of carbonate and fixed weak-base groups. However, from chloride breakthrough onward, the acidity of the feed guarantees complete protonation of the fixed groups and thus approximately constant pH and carbonate association. This allows the remainder of the effluent history to be calculated in good approximation, beginning with chloride breakthrough.

The present communication demonstrates calculation of the entire effluent history, based on a recent extension<sup>6</sup> of the original theory. The theory as presented postulates local equilibrium and absence of dispersive effects and so gives no information on the sharpness of the breakthrough waves.

## THEORY

The multicomponent theory of Helfferich and Klein<sup>5</sup> operates with the concept of “coherence” of waves (concentration variations). Coherence is an asymptotically stable state in which the waves of all species present at the respective location and time travel at the same velocity and so do not separate from one another. In the case at hand, with an acidic feed entering a column with anion exchanger in free-base form, all waves are shocks, *i.e.* would be concentration discontinuities under conditions of local equilibrium and absence of dispersive effects. For systems without reactions, the velocity  $v_{\Delta x_i}$  of a concentration discontinuity  $\Delta x_i$  (shock) of a species  $i$  can be related to the concentration variations across the shock by a material balance argument (notation follows ref. 6):

$$v_{\Delta x_i} = v^0/[1 + \gamma(\Delta y_i/\Delta x_i)] \quad (1)$$

For the shock to be coherent, this velocity must be the same for all species present, *i.e.*,

$$\Delta y_i/\Delta x_i = A \quad \text{for all } i \text{ present} \quad (2)$$

where  $A$  has the same value for all species.

The extended theory allowing for reactions<sup>6</sup> views the system as composed of “moieties”, which are conserved with respect to the reactions. For example, the species  $\text{CO}_3^{2-}$ ,  $\text{HCO}_3^-$ ,  $\text{H}_2\text{CO}_3$ , and  $\text{H}^+$  are considered as composed of the moieties  $\text{CO}_3$  and  $\text{H}$  in different proportions. Eqns. 1 and 2 remain formally valid for moieties even if reactions occur. The normalized concentrations of moieties ( $s_k$  and  $q_k$ ) and species are interrelated as follows:

$$s_k = \sum_i \mu_{ki} x_i \quad q_k = \sum_i \bar{\mu}_{ki} y_i \quad (3)$$

where  $\mu_{ki}$  and  $\bar{\mu}_{ki}$  are reaction-coupling factors of species  $i$  with respect to moieties  $k$  in the solution and ion exchanger, respectively. Combination of these factors and the stoichiometric coefficients of the reactions leads to a reaction matrix for each phase as a compact representation of the reactions. For the system considered here, the reaction matrices are listed in Table I. As these matrices show, sulfate is assumed to be entirely in the form of  $\text{SO}_4^{2-}$  ion and its association is disregarded as in the work of Clifford and Weber<sup>1,4</sup>. The calculation here will focus on the early effluent history involving the protonation of carbonate and fixed weak-base groups of the resin.

Required in addition are equations describing ion-exchange equilibria of the species. Here, binary separation factors  $\alpha_{ij}$  are assumed to be constant:

$$y_i x_j / y_j x_i \equiv \alpha_{ij} = \text{constant} \quad (4)$$

Such a set of equilibrium equations in terms of  $\{x_i\}$  and  $\{y_i\}$  can be converted to a set of relations between  $\{s_k\}$  and  $\{q_k\}$  with eqns. 3, the reaction matrices, the equilibrium constants of the reactions and the electroneutrality conditions.

In the case at hand, a “frontal analysis” pattern<sup>1,4,7</sup> is known to develop:

TABLE I  
SPECIES, REACTIONS, MOIETIES AND REACTION MATRICES OF NITRATE REMOVAL SYSTEM

Moiety/reaction	Species <sup>a</sup>									
	Cl <sup>-</sup>	NO <sub>3</sub> <sup>-</sup>	SO <sub>4</sub> <sup>2-</sup>	CO <sub>3</sub> <sup>2-</sup>	HCO <sub>3</sub> <sup>-</sup>	H <sub>2</sub> CO <sub>3</sub>	OH <sup>-</sup>	H <sup>+</sup>	-B	-BH <sup>+</sup>
<i>Solution phase</i>										
Cl	1	0	0	0	0	0	0	0	0	0
NO <sub>3</sub>	0	1	0	0	0	0	0	0	0	0
SO <sub>4</sub>	0	0	1	0	0	0	0	0	0	0
CO <sub>3</sub>	0	0	0	1	1	1	0	0	0	0
H	0	0	0	0	1	2	-1	1	0	0
H <sub>2</sub> O ↔ H <sup>+</sup> + OH <sup>-</sup>	0	0	0	0	0	0	1	1	0	0
H <sub>2</sub> CO <sub>3</sub> ↔ H <sup>+</sup> + HCO <sub>3</sub> <sup>-</sup>	0	0	0	0	1	-1	0	1	0	0
HCO <sub>3</sub> <sup>-</sup> ↔ H <sup>+</sup> + CO <sub>3</sub> <sup>2-</sup>	0	0	0	1	-1	0	0	1	0	0
HSO <sub>4</sub> <sup>-</sup> ↔ H <sup>+</sup> + SO <sub>4</sub> <sup>2-</sup>	0	0	1	0	0	0	0	1	0	0
<i>Exchanger phase</i>										
Cl	1	0	0	0	0	0	0	0	0	0
NO <sub>3</sub>	0	1	0	0	0	0	0	0	0	0
SO <sub>4</sub>	0	0	1	0	0	0	0	0	0	0
CO <sub>3</sub>	0	0	0	1	1	1	0	0	0	0
H	0	0	0	0	1	2	-1	1	0	1
B	0	0	0	0	0	0	0	0	1	1
H <sub>2</sub> O ↔ H <sup>+</sup> + OH <sup>-</sup>	0	0	0	0	0	0	1	1	0	0
H <sub>2</sub> CO <sub>3</sub> ↔ H <sup>+</sup> + HCO <sub>3</sub> <sup>-</sup>	0	0	0	0	1	-1	0	1	0	0
HCO <sub>3</sub> <sup>-</sup> ↔ H <sup>+</sup> + CO <sub>3</sub> <sup>2-</sup>	0	0	0	1	-1	0	0	1	0	0
-BH <sup>+</sup> ↔ -B + H <sup>+</sup>	0	0	0	0	0	0	0	1	1	-1

<sup>a</sup> Species -B and -BH<sup>+</sup> denote the fixed base group and its ionic conjugate, respectively.

traversing the column in the direction of flow, an observer sees one moiety disappear at each successive wave; specifically, of the moieties left, each time that with highest affinity for the ion exchanger disappears. This makes it possible to calculate the velocities of the shock waves one by one, starting with the slowest, the sulfate front, at which the SO<sub>4</sub> moiety disappears. Upstream of that wave the column is in equilibrium with the feed, and downstream of it no SO<sub>4</sub> in any form is present. Accordingly, for this moiety, the concentration differences  $\Delta s_{SO_4}$  and  $\Delta q_{SO_4}$  across the wave equal the feed concentration  $s_{SO_4^0}$  and exchanger concentration  $q_{SO_4^0}$  in equilibrium with feed, respectively. With these substitutions, the value of  $A$  is obtained from eqn. 2 and the velocity of the sulfate front can then be calculated from eqn. 1. Now, the concentrations of the other species in the plateau zone downstream of the front can be calculated from eqn. 2 and the equilibrium equations. The procedure is then repeated for the other waves in succession, first for the nitrate front, at which sulfate is entirely absent and NO<sub>3</sub> now is the moiety with highest affinity for the exchanger; then for the chloride front, etc. From the column inlet to the chloride front the fixed weak-base groups of the resin can be assumed to be completely protonated, so their deprotonation reaction can be disregarded in the calculations. That reaction, however, becomes essential in the calculation of the carbonate front (that of the CO<sub>3</sub> moiety), across which the resin is converted from its initial free-base to its ionic form.

## CALCULATIONS

For demonstration, the calculation of column performance in one of the experiments by Clifford and Weber<sup>1</sup> is presented. Their run No. 10 was selected because of its low flow-rate, ensuring a reasonably close approximation to local equilibrium as evident from its relatively sharp waves. Data on the ion exchanger, column, flow-rate, and feed composition are summarized in Table II. The total normality of the solution and the ion-exchange capacity of the resin are chosen as reference concentrations for the purpose of normalization.

The values of the separation factors and reaction equilibrium constants are shown in Tables III and IV. As far as available, values independently determined by Clifford<sup>4</sup> were used. In addition, the fractional water content and the  $\text{Cl}^-/\text{HCO}_3^-$  separation factor was assumed to be the same as for the similar anion exchanger Amberlite IRA-93 (ref. 8); the  $\text{HCO}_3^-/\text{OH}^-$  separation factor was taken to be 1.00 as ideal Donnan equilibrium would demand. The column void volume, not reported by Clifford, was estimated from his calculated effluent history for another run<sup>4</sup> with the same resin. The dissociation constants in solution were taken from the literature<sup>9</sup> and converted to the concentration scale used here (normalized molarity). The dissociation constants in the resin were assumed to have the same values as in solution if expressed in terms of molalities; the values in Table IV are those after conversion to the normalized-molarity scale.

## RESULTS

Fig. 1 shows a comparison of the measured and calculated effluent concentration histories. The agreement is quite good, except for the lack of ideal sharpness of

TABLE II  
DATA FOR EXPERIMENT OF NITRATE REMOVAL

Weak-base resin (Duolite ES-368)	$\text{p}K_b$	6.2
	Exchange capacity (equiv./l)	1.54
	Fractional water content	0.57 <sup>a</sup>
Ion-exchange bed	Length (cm)	61
	Diameter (cm)	2.54
	Flow-rate (ml/min)	100
	Fractional void volume	0.57 <sup>b</sup>
Simulated water supply	$\text{NO}_3^-$ (mequiv./l)	1.5
	$\text{Cl}^-$ (mequiv./l)	1.5
	$\text{SO}_4^{2-}$ (mequiv./l)	1.5
	$\text{HCO}_3^-$ (mequiv./l)	1.0 <sup>c</sup>
	pH	6.5
	Total normality (mequiv./l)	5.5 <sup>d</sup>

<sup>a</sup> Value from ref. 8 for Amerlite IRA-93 is used here for Duolite ES-368 because of similar resin characteristics.

<sup>b</sup> Estimated from calculated effluent history (using the original Helfferich-Klein theory) in ref. 4 for another run with the same resin.

<sup>c</sup> Total carbonate ( $\text{CO}_3$  moiety) expressed in terms of the normality of  $\text{HCO}_3^-$  ion<sup>1,4</sup>.

<sup>d</sup> Total normality of simulated water supply containing calcium, magnesium, and iron.

TABLE III  
SEPARATION FACTORS OF NITRATE REMOVAL SYSTEM

Counterion pair $ij$	Separation factor $\alpha_{ij}$
$\text{SO}_4^{2-}/\text{NO}_3^-$	2.83
$\text{NO}_3^-/\text{Cl}^-$	3.87
$\text{Cl}^-/\text{HCO}_3^-$	4.00 <sup>a</sup>
$\text{HCO}_3^-/\text{OH}^-$	1.00 <sup>b</sup>

<sup>a</sup> Value from ref. 8 for Amberlite IRA-93 is used here for Duolite ES-368 because of similar resin characteristics.

<sup>b</sup> Based on ideal Donnan equilibrium.

TABLE IV  
REACTION CONSTANTS OF NITRATE REMOVAL SYSTEM

Reaction	Normalized equilibrium constant
<i>Solution</i>	
$\text{H}_2\text{O} \leftrightarrow \text{H}^+ + \text{OH}^-$	$3.31 \cdot 10^{-10}$
$\text{H}_2\text{CO}_3 \leftrightarrow \text{H}^+ + \text{HCO}_3^-$	$8.36 \cdot 10^{-5}$
$\text{HCO}_3^- \leftrightarrow \text{H}^+ + \text{CO}_3^{2-}$	$8.00 \cdot 10^{-9}$
<i>Exchanger</i>	
$\text{H}_2\text{O} \leftrightarrow \text{H}^+ + \text{OH}^-$	$1.37 \cdot 10^{-15}$
$\text{H}_2\text{CO}_3 \leftrightarrow \text{H} + \text{HCO}_3^-$	$1.70 \cdot 10^{-7}$
$\text{HCO}_3^- \leftrightarrow \text{H}^+ + \text{CO}_3^{2-}$	$1.63 \cdot 10^{-11}$
$-\text{BH}^+ \leftrightarrow -\text{B} + \text{H}^+$	$5.87 \cdot 10^{-9}$

the observed waves and slight discrepancies in the carbonate breakthrough and nitrate concentration after its breakthrough. Specifically, the breakthroughs of the various fronts and the compositions of the intermediate plateau zones match the observations satisfactorily.

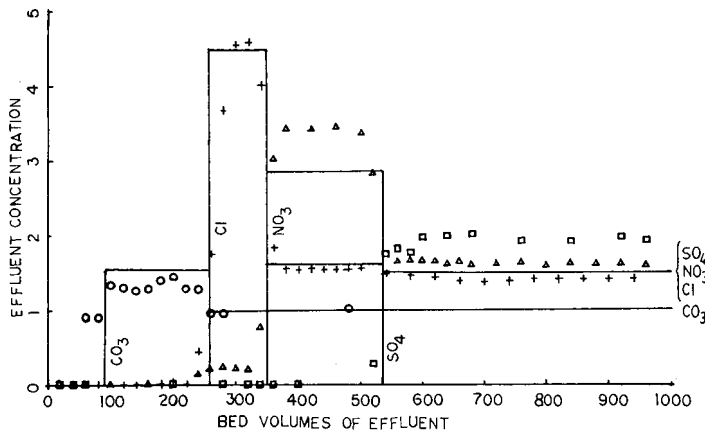


Fig. 1. Comparison of observed and calculated effluent concentration histories (observed histories are from Clifford and Weber<sup>1</sup>; following them, total sulfate and total carbonate are presented in terms of the normalities of  $\text{SO}_4^{2-}$  and  $\text{HCO}_3^-$  ions, respectively). — = Predicted;  $\circ$  =  $\text{HCO}_3^-$ ;  $+$  =  $\text{Cl}^-$ ;  $\Delta$  =  $\text{NO}_3^-$ ;  $\square$  =  $\text{SO}_4^{2-}$ . Effluent concentration is in mequiv./l.

## DISCUSSION

It is to be noted that the calculation was carried out with best available input data and without any adjustment of parameters. It is possible that the use of  $\text{Cl}^-/\text{HCO}_3^-$  and  $\text{HCO}_3^-/\text{OH}^-$  separation factors experimentally determined for the ion exchanger used and of more accurate values for the fractional water content and column void volume might improve the agreement between observed and calculated effluent histories. Moreover, since  $\text{SO}_4^{2-}$  is divalent, a selectivity coefficient rather than the separation factor measured by Clifford should be used for the  $\text{SO}_4^{2-}/\text{NO}_3^-$  exchange equilibrium.

For practical purposes, an accurate prediction of the point of breakthrough of first traces of nitrate will require the relaxation of the premise of local equilibrium, to account for the lack of ideal sharpness of the waves. However, this need be done only for the nitrate front and can be applied as a correction after the approximate effluent history with ideally sharp shocks has been calculated with the premise of local equilibrium.

## SYMBOLS

$q_k$	=	normalized concentration <sup>a</sup> of moiety $k$ in exchanger
$s_k$	=	normalized concentration <sup>a</sup> of moiety $k$ in solution
$v^0$	=	linear velocity of bulk flow of solution
$v_{\Delta x_i}$	=	wave velocity of shock $\Delta x_i$
$x_i$	=	normalized concentration <sup>a</sup> of species $i$ in solution
$y_i$	=	normalized concentration <sup>a</sup> of species $i$ in exchanger
$\alpha_{ij}$	=	separation factor of counterion $i$ to counterion $j$
$\gamma$	=	$\frac{\text{(fractional exchanger volume)} \text{ (exchanger capacity)}}{\text{(fractional column void volume)} \text{ (total normality of solution)}}$
$A$	=	eigenvalue of coherent shocks
$\mu_{ki}$	=	reaction-coupling factor of species $i$ with respect to moiety $k$ in solution
$\bar{\mu}_{ki}$	=	reaction-coupling factor of species $i$ with respect to moiety $k$ in exchanger

## ACKNOWLEDGEMENT

The financial support by the National Science Foundation under Grant CBT-8511956 is gratefully acknowledged.

## REFERENCES

- 1 D. A. Clifford and W. J. Weber, Jr., *Report EPA-600/2-78-052*, U.S. Environmental Protection Agency, Cincinnati, OH, 1978.
- 2 R. P. Lauch and G. A. Guter, *J. Am. Water Works Assoc.*, 5 (1986) 83.
- 3 M. Cox and D. Murgatroyd, in P. A. Williams and M. J. Hudson (Editors), *Recent Developments in Ion Exchange*, Elsevier Applied Science, London, New York, 1987.

<sup>a</sup> "Normalized concentration" is defined as the ratio of the respective molarity to the total normality in the solution phase, or to the exchanger capacity (normality) in the exchanger phase.

- 4 D. A. Clifford, *Ind. Eng. Chem. Fundam.*, 21 (1982) 141.
- 5 F. G. Helfferich and G. Klein, *Multicomponent Chromatography—Theory of Interference*, Marcel Dekker, New York, 1970.
- 6 Y.-L. Hwang, F. G. Helfferich and R.-J. Leu, *AIChE J.*, 34 (1988) 1615.
- 7 S. Claesson, *Ark. Kemi Mineral. Geol.*, A20 (1945) No. 3.
- 8 D. A. Skoog and D. M. West, *Fundamentals of Analytical Chemistry*, Holt, Rinehart and Winston, NC, New York, NY, 1969.





CHROM. 21 708

## DETERMINATION OF INORGANIC ANIONS BY FLOW INJECTION ANALYSIS AND HIGH-PERFORMANCE LIQUID CHROMATOGRAPHY COMBINED WITH PHOTOLYTIC-ELECTROCHEMICAL DETECTION

L. DOU and I. S. KRULL\*

*Department of Chemistry, The Barnett Institute (341 MU), Northeastern University, 360 Huntington Avenue, Boston, MA 02115 (U.S.A.)*

---

### SUMMARY

Post-column, on-line photolytic derivatization in liquid chromatography with electrochemical detection for some inorganic anions is described. Flow injection analysis and ion-pair reversed-phase chromatography followed by photolysis and electrochemical detection were used for the determinations of anions. Several operation conditions, such as mobile phase, lamp used for the photolysis, flow-rate, and applied potential, have been optimized for the determinations. Analytical figures of merit were determined. Method validation was carried out by the analysis of single blind, spiked samples. Inherent from the advantages of electrochemical detection in liquid chromatography, the method is of high sensitivity and selectivity for anion analysis.

---

### INTRODUCTION

The powerful separation ability of high-performance liquid chromatography (HPLC) has been widely employed for the analysis of organic and biochemical mixtures. The availability of many chromatographic methods, based on the different models of separation, provides very sensitive and selective determination of many organic and biochemical species. The analysis of inorganic ions by HPLC, however, has not been as well developed. The reasons for this, in brief, may be two: (1) the poor retention of inorganic ions on the most commonly used reversed- and normal-phase columns; and (2) the poor detectability of most inorganic ions by the most commonly used ultraviolet (UV) (254 nm) and fluorescence (FL) detectors. Ion-exchange or ion-suppression chromatography (single or dual column), are the most commonly used methods for the analysis of ionizable compounds. Newly developed polymeric resins for ion chromatography column packings can be used within a wide range of pH and under high pressure with good reproducibility and high column efficiency. It provides a means for sensitive and selective determinations of inorganic ions. Another chromatographic method for ionizable compound separation is ion-pair chromatography<sup>1</sup>. Operated in the normal or reversed-phase modes, it also provides an efficient technique for the analysis of many ionogenic substances. With suitable detection

methods, ion-pair chromatography can be used easily for inorganic anion analysis. At present, the detection techniques available for inorganic anion analysis using ion-pair HPLC need to be improved.

Post-column, on-line, continuous photochemical irradiation has been shown to be an excellent derivatization approach for improved detection of many classes of organics by liquid chromatography–electrochemical detection (LC–ED)<sup>2–8</sup>. More recently, we have shown that a photoreduction process can occur in an aqueous methanol mobile phase, whereby nitrate can be efficiently converted into nitrite<sup>9</sup>. The nitrite was then detected at a variety of oxidative working potentials using thin layer amperometry with glassy carbon (GC) electrodes (dual parallel) to detect the original nitrate injected. Ion-pair chromatography was used together with photolytic-ED (hv-ED) in order to first separate nitrate from nitrite. It was clear that HPLC/flow injection analysis (FIA)–hv-ED could be immediately applicable to various inorganic, oxidized species, wherein these did not possess inherent oxidative ED properties.

This paper shows that it is possible to develop optimized HPLC and FIA–hv-ED analytical procedures to photoreduce and then sensitively detect inorganic anions under mild oxidative potentials with a GC electrode. It is likely that many other related inorganic species will prove suitable analytes for this basic analytical protocol. We describe in this paper the basic approach, instrumentation, optimized operational conditions, analytical figures of merit, and typical chromatograms using dual electrode detection. Qualitative and quantitative results will be presented for single blind, spiked sample determinations using ion-pair HPLC–hv-ED methods.

## EXPERIMENTAL

### *Apparatus*

The design of LC–hv-ED instrumentation has been described in detail<sup>2</sup>. Basically, the instrumentation consisted of an HPLC system, an irradiation apparatus, and an amperometric electrochemical detector. The HPLC system was composed of a Model 590 solvent delivery system (Waters, Milford, MA, U.S.A.), a LiChroma-Damp III pulse dampener (Handy and Harmon Tube Co., Norristown, PA, U.S.A.), a Rheodyne Model 7010 injector with a 20- or 50- $\mu$ l sample loop (Rheodyne, Cotati, CA, U.S.A.), and a 10- $\mu$ m LiChrospher C<sub>18</sub> reversed-phase column (E. Merck, Darmstadt, F.R.G.). Mobile phase conditions will be given in the Discussion section. All mobile phases were filtered and degassed using a 0.45- $\mu$ m solvent filtration kit (Millipore, Milford, MA, U.S.A.). Electrochemical detection was performed using dual amperometric controllers (Model LC-4B), a dual glassy carbon working electrode cell half operated at potentials of +1.15 V (all potentials were vs. Ag/AgCl reference electrode) and +1.00 V (dichromate and chromate ions, see figure captions for other anions) in parallel, a stainless-steel auxiliary electrode cell half, and a Ag/AgCl reference electrode (RE-1B), all obtained from Bioanalytical Systems (West Lafayette, IN, U.S.A.). The photolysis apparatus included a Photronix Model 816 UV batch irradiator (Photronix, Medway, MA, U.S.A.) with a quartz tube coil of 1.8 ml in volume. A zinc lamp (main irradiation line at 214 nm) and accompanying power supply obtained from BHK (Monrovia, CA, U.S.A.) were used as the UV light source for the irradiation of the samples. Also a photolytic reactor consisted of a knitted open tubular (KOT) reactor coil, constructed from 0.5 mm I.D. PTFE tubing (Rainin

Instruments, Woburn, MA, U.S.A.) and wound about a low pressure, mercury arc discharge lamp, was used for the photolysis of the analytes. The irradiation apparatus was maintained at 0–5°C using an ice–water bath. Upchurch fingertight fittings (Alltech Associates, Deerfield, IL, U.S.A.) were used to connect the column, irradiation unit, and electrochemical detector. The data were collected on an OmniScribe dual pen, strip chart recorder (Houston Instrument Co., Houston, TX, U.S.A.).

#### *Chemicals, reagents and solvents*

Inorganic standards were obtained in the highest available purity as follows: potassium dichromate, sodium thiocyanate and sodium perchlorate from Aldrich (Milwaukee, WI, U.S.A.), sodium chromate from J. T. Baker (Phillipsburg, NJ, U.S.A.), and potassium periodate from Fisher Scientific (Fairlawn, NJ, U.S.A.). Reagent grade sodium hydrogenphosphates (monobasic and dibasic) and sodium chloride were also obtained from Fisher Scientific. Ion-pair reagents, tetrabutylammonium hydrogensulfate (TBAHS) and tetraethylammonium hydrogensulfate (TEAHS), were bought from Fluka (Ronkonkoma, NY, U.S.A.), and tetrabutylammonium phosphate (TBAP) (IPC A) from Alltech Assoc. Methanol, the organic solvent used for preparing the mobile phase, was obtained from EM Science (Cherry Hill, NJ, U.S.A.) as their Omnisolv grade. Deionized water was prepared in our laboratory using a Barnstead water purification system (Sybron, Boston, MA, U.S.A.).

#### *Procedures*

Flow injection analysis (FIA)–photolysis (hv)–ED was carried out for the analytes before ion-pair HPLC–hv–ED was performed. Hydrodynamic voltammetry (HDV) was carried out using the FIA–hv–ED method. It was not necessary for this study to be carried out with an HPLC column on-line. The potential range for HDV studies was from +0.1 to +1.2 V. The hydrodynamic voltammograms were obtained in the conventional manner, by plotting ED response *vs.* applied potential.

The optimization of residence time of analytes in the photolytic reactor was performed by measuring the change in ED response with the change of flow-rate. The flow-rates used for this study were from 0.4 to 2.0 ml/min. The plot of peak height *vs.* flow-rate gave the optimal flow-rate condition for subsequent determinations.

The optimization of ion-pair HPLC–hv–ED detection involved the choice of proper mobile phase, including the ion-pair reagent, the electrolyte, pH and composition of the organic solvent in the mobile phase. Several mobile phases were tested for optimization of the mobile phase conditions. Details will be discussed below (Results and Discussion). Studies of linearity, reproducibility of the determinations, and determinations of spiked samples, were carried out under optimal mobile phase and flow-rate conditions using different concentrations of samples, all dissolved in the mobile phase. Calibration plots used for all quantitative determinations were obtained conventionally, by plotting peak height *vs.* concentration of samples.

## RESULTS AND DISCUSSION

*Determination for dichromate and chromate ions*

Both dichromate and chromate ions are oxidized species which have no inherent oxidative ED properties. Direct ED after HPLC for these anions is difficult. However, it is known by photochemists that both anions have a photoreduction ability<sup>10-14</sup>. Although there is still some disagreement on the final photoreduction products, the photoderivatization of anions can be taken advantage of for the sensitive and selective detection of these anions combined with ion-pair reversed-phase chromatography. In Fig. 1, chromatograms are shown for dichromate ion, under both lamp on and lamp off conditions. When the lamp was off, there was no irradiation of the analyte, and the anion showed no ED response. However, it did show a sensitive ED response when the lamp was on. The same results were obtained for chromate ion. Since very little difference exists between the structures of dichromate and chromate ion, and in solution, both structures can be converted into hydrochromate ion,  $\text{HCrO}_4^-$  (refs. 15

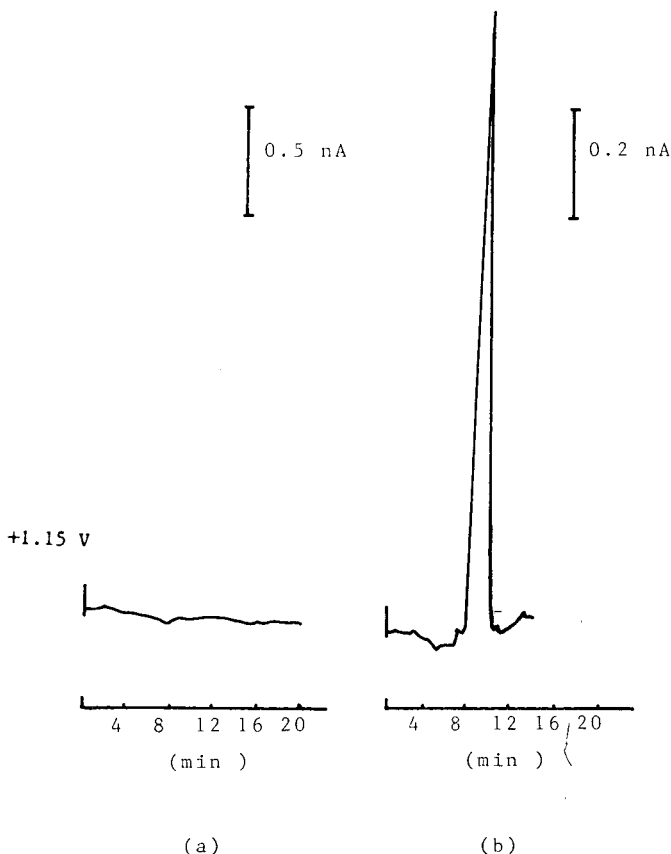


Fig. 1. Ion-pair RPLC-hv-ED chromatograms of 20 ppm dichromate ion (potassium salt). (a) Lamp off; (b) lamp on.  $\text{C}_{18}$  reversed-phase column, 250 mm  $\times$  4.0 mm I.D., mobile phase, methanol- $\text{Na}_2\text{HPO}_4$  and  $\text{NaH}_2\text{PO}_4$  (0.0070 and 0.0072 M) (30:70) (pH 6.8) with 0.0030 M TBAHS, flow-rate, 0.8 ml/min, injection volume, 50  $\mu\text{l}$ . ED at +1.15 V, glassy carbon working electrode, Ag/AgCl reference electrode.

and 16), they were never separated chromatographically. There are apparently no literature reports of the HPLC separation of dichromate and chromate ions, under any conditions<sup>17</sup>, perhaps due to the fast equilibria in solution. Thus, a quantitative determination of either species actually represented a combination of the mixtures, at least at a pH of 6.8. We have compared different pH conditions in FIA-hv-ED, and sensitivity of detection did not change greatly from pH 3.0 to 7.5, a range determined by the silica based RP column. This also indicated that FIA/HPLC-hv-ED methods for the detection of dichromate and chromate were actually the detection of total amounts of  $\text{Cr}^{6+}$  in solution.

#### Characterization of photolysis-ED for dichromate and chromate ions

Initially, as part of the optimization for both anion's detection, hydrodynamic voltammetry (HDV) and the peak height change vs. flow-rate were performed using FIA-hv-ED. In Fig. 2, the HDV for potassium dichromate is shown. ED did not have a good response (lamp on) until the applied potential reached +0.6 V. A good linear relationship existed between ED response and applied potential between +0.6 and +1.15 V, suggesting that diffusion controlled ED was taking place. There were diffusion limited responses at  $E_{\text{app}} \geq +1.20$  V ( $E_{1/2} = +0.91$  V). The optimal potential for detection should be above +1.20 V. Considering the maximum possible potential of a GC working electrode (+1.25 V), working potentials for the determination of dichromate and chromate ions were chosen to be +1.15 V vs. Ag/AgCl. In Fig. 3, the plot of FIA-hv-ED responses vs. flow-rate for chromate is shown. Two factors can affect the final response under FIA/HPLC-hv-ED conditions when the flow-rate is changed. One is flow-rate itself, and another is residence time of the analyte in the irradiation tubing (photolytic reactor). According to the hydrodynamic equations for laminar flow, an amperometric response is dependent on the cube root of the linear velocity of a flowing solution (without irradiation)<sup>18</sup>, *i.e.*, the ED amperometric response should increase with the increase of flow-rate. However, as shown in Fig. 3, the lower flow-rates (longer residence times) gave much better

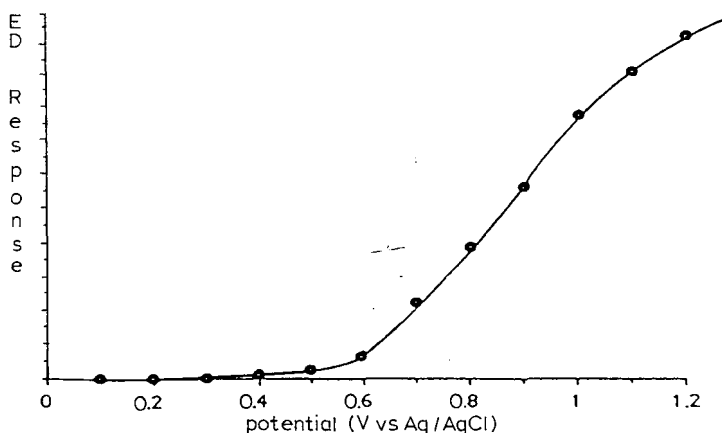


Fig. 2. Hydrodynamic voltammogram of irradiated dichromate ion (potassium salt) obtained using on-line photolysis with FIA-hv-ED. Mobile phase as in Fig. 1; flow-rate, 1.0 ml/min, injection volume, 50  $\mu\text{l}$ . ED: glassy carbon working electrode, Ag/AgCl reference electrode.

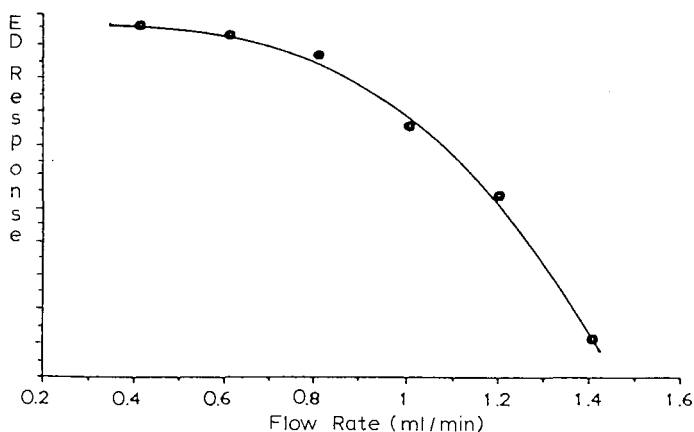


Fig. 3. Flow-rate optimization for the determination of chromate ion (sodium salt).  $C_{18}$  reversed-phase column, 250 mm  $\times$  4.0 mm I.D.; mobile phase as in Fig. 1; injection volume, 50  $\mu$ l. ED, glassy carbon working electrode at +1.15 V, Ag/AgCl reference electrode.

responses. This simply indicated that the residence time of the anions in the irradiator played a more important role than flow-rate itself. However, at very low flow-rates (<0.7 ml/min), the peak broadening problem became more serious. From a practical point of view, a flow-rate of 0.7–1.0 ml/min was chosen.

#### Optimization of ion-pair HPLC-hv-ED

On-line, post-column photolysis-ED combined with ion-pair reversed-phase liquid chromatography for dichromate and chromate ions was initiated by using methanol–1 M NaCl (2:98, v/v) solution with TBAP ion-pair reagent (5 mM) as mobile phase. Later tetrabutylammonium hydrogensulfate (TBAHS) (5 mM) was used with the same methanol–NaCl solution instead of TBAP as ion-pair reagent. Finally, a  $\text{Na}_2\text{HPO}_4$ – $\text{NaH}_2\text{PO}_4$  buffer solution was used instead of NaCl as the electrolyte. The reason for changing the mobile phase was to reduce the background current so as to improve the sensitivity of detection. Commercial TBAP ion-pair reagent was found to have a large background current when used with hv-ED. Also, chloride ion contributed to the background current, especially at potentials > +1.10 V.

However, by using  $\text{Na}_2\text{HPO}_4$ – $\text{NaH}_2\text{PO}_4$  buffer (0.0070 and 0.0072 M) as the electrolyte and TBAHS (0.0030 M) as the ion-pair reagent, the background current was lowered to a few nA. Several mobile phases with different compositions of methanol– $\text{Na}_2\text{HPO}_4$  and  $\text{NaH}_2\text{PO}_4$  buffer (10:90, 20:80, 30:70, v/v), all used with ion-pair reagent, were checked for the optimization of mobile phase conditions. Although mobile phases with 10 and 20% methanol gave longer retention times, the hv-ED response was significantly increased with a mobile phase containing 30% methanol. It seemed that methanol could help the photoreduction of dichromate or chromate ions or stabilize the photolytic products that were electrochemically active<sup>1,2</sup>. Finally, the optimal mobile phase for both ion-pair reversed-phase chromatographic retention and hv-ED was found to be methanol– $\text{Na}_2\text{HPO}_4$  and  $\text{NaH}_2\text{PO}_4$  buffer (0.0070 and 0.0072 M) (30:70, v/v) (pH 6.8) with 0.0030 M TBAHS ion-pair reagent. All the following experiments were carried out using this optimal mobile phase.

Both the zinc lamp (with quartz coil) and mercury lamp [with a PTFE knitted open tubular (KOT) reactor] were used as light sources for the study of their effect on the photolytic responses. With the zinc lamp, maximum emission line at 214 nm, and a quartz coil used as the light source, under optimal mobile phase conditions, detection limits were in the sub-ppm range. However, significant band broadening resulted from the quartz coil (the zinc lamp can only be used with a quartz coil) and prevented any improvement of detection limits. However, there was no hv-ED response when the mercury lamp was used (with KOT). The energy of the main emission line of Hg (254 nm) was probably not high enough for dichromate ion to be photoreduced. Dichromate ion absorbs UV three times more strongly at 214 than at 254 nm, thus there is absorption at 254 nm, but the lower absorption and decreased intensity of irradiation may not be enough to promote photoreduction.

The linearity of the determinations for both dichromate and chromate ions are shown in Table I. A good linearity was observed within the working concentration range (2–100 ppm extended to detection limit, 0.5 ppm). The  $r^2$  term was 0.9993 for dichromate and 0.9997 for chromate ion. The fact that relative standard deviations (R.S.D.s) ( $n = 3$ ) for all data points were within 4% suggested that run-to-run reproducibility was excellent (dichromate standard as analyte). There is no comparison of slopes between dichromate and chromate ions due to the difference of absolute amount of total  $\text{Cr}^{6+}$  of the same concentrations of dichromate and chromate ions (in ppm) as well as the poor day-to-day reproducibility of the electrode surface.

In Table II, the mean, standard deviation (S.D.) and R.S.D. of three determinations are given for four single blind, spiked dichromate samples. Determinations were carried out by using a calibration curve. All determinations were performed in the same day as the calibration curve data were obtained. A comparison is made of the determined concentrations of dichromate samples with the actual spiked levels. The relative errors were within 5%.

Table III shows the three determinations, mean, S.D., and R.S.D. for four spiked chromate samples. The determinations shown were performed in 3 days with one determination per day. Each determination used a calibration curve obtained on

TABLE I  
LINEARITY STUDY OF THE DETERMINATIONS

$Y = AX + B$ ,  $Y$  was the ED response and  $X$  was the concentration of the analyte in ppm. See Table V for linear response ranges. Chromatographic conditions: see Table II, Fig. 5 and text.

Analyte	Potential I <sup>a</sup>			Potential II <sup>b</sup>		
	A	B	$r^2$	A	B	$r^2$
Dichromate	0.993	3.339	0.9993	0.369	3.643	0.9971
Chromate	0.651	-0.241	0.9997	0.220	0.197	0.9995
Perchlorate	0.906	-1.025	0.9994	0.459	-2.211	0.9947
Thiocyanate	11.586	47.01	0.9973	1.833	12.109	0.9965

<sup>a</sup> Potential I for dichromate was +1.15 V, chromate +1.15 V, perchlorate +1.10 V, and thiocyanate +1.05 V.

<sup>b</sup> Potential II for dichromate was +1.00 V, chromate +1.00 V, perchlorate +0.90 V, and thiocyanate +0.90 V.

TABLE II

SUMMARY OF THE DETERMINATION OF CONCENTRATIONS OF SPIKED DICHROMATE SAMPLES<sup>a</sup>

Chromatographic conditions, C<sub>18</sub> reversed-phase column, 250 mm × 4.0 mm I.D.; mobile phase, methanol-Na<sub>2</sub>HPO<sub>4</sub> and NaH<sub>2</sub>PO<sub>4</sub> (0.0070 and 0.0072 M) (30:70) with 0.003 M TBAHS; flow-rate, 0.8 ml/min; injection volume, 50 μl. ED, dual glassy carbon working electrode at +1.15 V and +1.00 V; Ag/AgCl reference electrode.

Spiked sample <sup>b</sup>	Determinations (ppm)			Mean (ppm)	S.D.	R.S.D. (%)
	I	II	III			
1	4.3	4.0	3.9	4.1	0.2	5.1
2	39.5	38.4	40.3	39.4	1.0	2.4
3	96.6	95.0	94.4	95.3	1.1	1.2
4	24.1	24.0	24.0	24.0	0.1	0.2

<sup>a</sup> At a potential of +1.15 V.

<sup>b</sup> Spiked in the mobile phase.

that day. Although these determinations were performed on different days, the R.S.D.s for these three determinations (four spiked samples) were less than 6%, and the relative errors between determined concentrations and actual spiked levels were within 4%. However, good agreement of the three different day's results did not mean good day-to-day reproducibility. Each determination used its own calibration curve, which was different from day-to-day. In fact, good agreement between different day's determinations was a direct result of good run-to-run reproducibility. The error was very small if both spiked sample determinations and calibration curve were obtained within a day. This is not surprising if we consider the fact, in general, of short term reproducibility for all ED, especially in flowing solutions.

In Table IV, the dual electrode response ratios are listed for both anions (obtained separately) with the S.D. and R.S.D. of measurements. The dual electrode response ratios for different sample concentrations were obtained by monitoring the samples at two different potentials (+1.15 V/+1.00 V) and taking the ratio of these

TABLE III

## SUMMARY OF THE DETERMINATION OF CONCENTRATIONS OF SPIKED CHROMATE SAMPLES

At a potential of +1.15 V. Chromatographic conditions and ED as in Table II.

Spiked sample <sup>a</sup>	Determinations (ppm)			Mean (ppm)	S.D.	R.S.D. (%)
	I	II	III			
1	41.9	38.4	39.0	39.8	1.9	4.8
2	97.4	95.5	95.0	96.0	1.3	1.4
3	0.0	0.0	0.0	0.0	0.0	—
4	3.7	3.9	4.0	3.9	0.2	5.1

<sup>a</sup> Spiked in the mobile phase.



responses (peak heights). In general, there is good reproducibility of response ratios at all concentration levels. However, the response ratios changed slightly with the concentration change for both anions and also the response ratios for dichromate and chromate were a little different. The reason may again be the short term reproducibility of the electrode surface (these data were obtained on different days). In fact, we measured some of these response ratios again (only at some concentrations) on the same day, and found the same number for these ratios. This indicated that the dual electrode response ratio did not change with the concentration, and that they were the same for both dichromate and chromate ions, if the data were obtained on the same day.

*Ion-pair HPLC-hv-ED for thiocyanate, perchlorate, and periodate ions*

Besides dichromate and chromate ions, a number of inorganic anions have been evaluated for ED activity, with and without photolysis<sup>19</sup>. The results indicated that other anions, including perchlorate, periodate and thiocyanate, had oxidative responses photolytically induced, although they showed no ED responses under normal conditions (no irradiation). These anions were also evaluated for their detection using ion-pair HPLC-hv-ED. Perchlorate and periodate ions had no inherent ED responses because of their high oxidation states, but both were ED active after proper irradiation. In Fig. 4, the ED responses of periodate are shown with irradiation (lamp on) and without irradiation (lamp off). Thiocyanate ion had an ED signal with both lamp on and lamp off at higher applied potentials, *i.e.*,  $> +1.00$  V. However, improved detection sensitivity was obtained for this anion after irradiation. We have discussed other instances where organic compounds having native oxidative ED properties showed improved detection sensitivity following irradiation<sup>6</sup>.

FIA was used to optimize the applied potential and residence time of each analyte in the photoreactor. As shown in Fig. 5, the HDV of perchlorate ion indicated that a higher applied potential could give higher responses. However, the GC working electrode could only tolerate potentials less than  $+1.25$  V. Meanwhile, the back-

TABLE IV

SUMMARY OF DUAL ELECTRODE RESPONSE RATIOS,  $i_1/i_2$ 

Chromatographic conditions and ED as in Table II.

Concentration (ppm)	Dichromate ion <sup>a</sup>		Chromate ion <sup>b</sup>	
	$i_1/i_2^c$	R.S.D. (%)	$i_1/i_2^c$	R.S.D. (%)
0.5	—	—	$2.00 \pm 0.20$	10.0
1.0	—	—	$2.20 \pm 0.26$	11.6
5.0	$1.87 \pm 0.05$	2.8	$2.64 \pm 0.06$	2.2
10.0	$1.96 \pm 0.09$	4.5	—	—
25.0	$2.11 \pm 0.04$	2.0	$2.60 \pm 0.06$	2.5
50.0	$2.33 \pm 0.01$	0.3	$2.78 \pm 0.01$	0.2
100.0	$2.56 \pm 0.03$	1.0	$2.96 \pm 0.02$	0.6

<sup>a</sup> As potassium dichromate.

<sup>b</sup> As sodium chromate.

<sup>c</sup>  $i_1$  was the ED response at potential of  $+1.15$  V, and  $i_2$  was the ED response at potential of  $+1.00$  V.

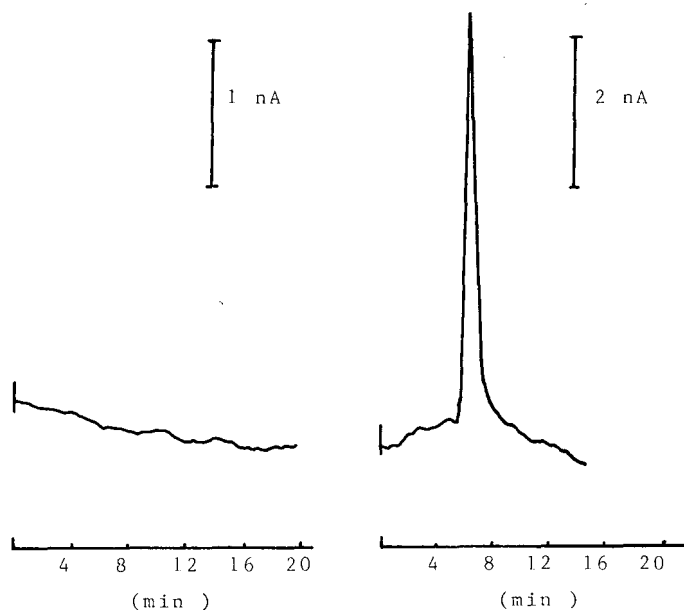


Fig. 4. Ion-pair RPLC-hv-ED chromatograms of periodate ion (potassium salt). (a) Lamp off, 40 ppm; (b) lamp on, 10 ppm.  $C_{18}$  reversed-phase column, 250 mm  $\times$  4.0 mm I.D.; mobile phase, methanol- $Na_2HPO_4$  and  $NaH_2PO_4$  (0.0140 and 0.0144 M) (10:90) (pH 6.7) with 0.0060 M TBAHS; flow-rate, 0.8 ml/min; injection volume, 20  $\mu$ l. ED at +1.00 V, glassy carbon working electrode, Ag/AgCl reference electrode.

ground currents at potentials higher than +1.15 V became too large. The final applied potential was selected as +1.10 V for perchlorate detection. For thiocyanate ion, the HDV was also obtained, and the final applied potential was selected as +1.05 V.

Flow-rate optimization was also carried out by FIA for these anions. The lower

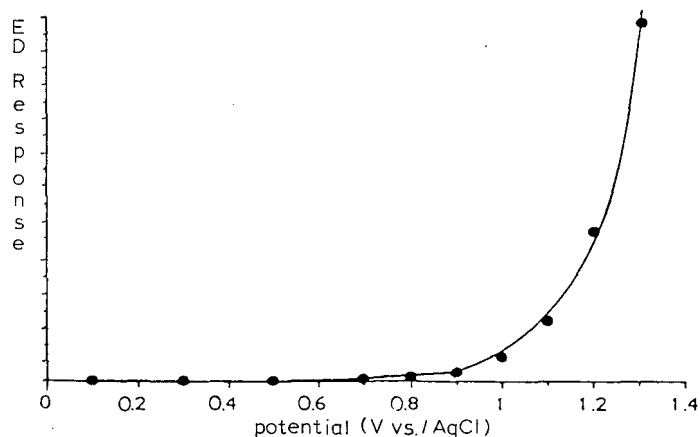


Fig. 5. Hydrodynamic voltammogram of irradiated perchlorate ion (sodium salt) obtained using on-line photolysis with FIA-hv-ED. Mobile phase, methanol- $Na_2HPO_4$  and  $NaH_2PO_4$  (0.0070 and 0.0072 M) (20:80) (pH 6.8) with 0.0050 M TBAHS; flow-rate, 0.8 ml/min; injection volume, 20  $\mu$ l. ED, glassy carbon working electrode, Ag/AgCl reference electrode.

the flow-rates, the larger the responses. As in the case of chromate/dichromate ions, too low flow-rates gave greatly broadened peaks. The optimal flow-rates were determined to be 0.7 and 0.8 ml/min for thiocyanate ion and perchlorate ion, respectively.

Both thiocyanate and perchlorate ions were well retained on the ion-pair RP-HPLC column with TBAHS. However, when tetraethylammonium hydrogen-sulfate (TEAHS) was used, both ions showed no retention even when the concentration of methanol in the mobile phase was as low as 2%. This was understood because of the shorter carbon chain of TEAHS. After trying several mobile phases (different methanol concentrations), the final mobile phase compositions for both ions were methanol-phosphate buffer (20:80) (thiocyanate) and methanol-phosphate buffer (18:82) (perchlorate). The separation of anions under study by ion-pair reversed-phase chromatography followed by photolysis-ED was carried out and the chromatograms obtained under both lamp on and lamp off are shown in Fig. 6. The mixture of periodate, perchlorate and thiocyanate could be well separated within 15 min. The ED

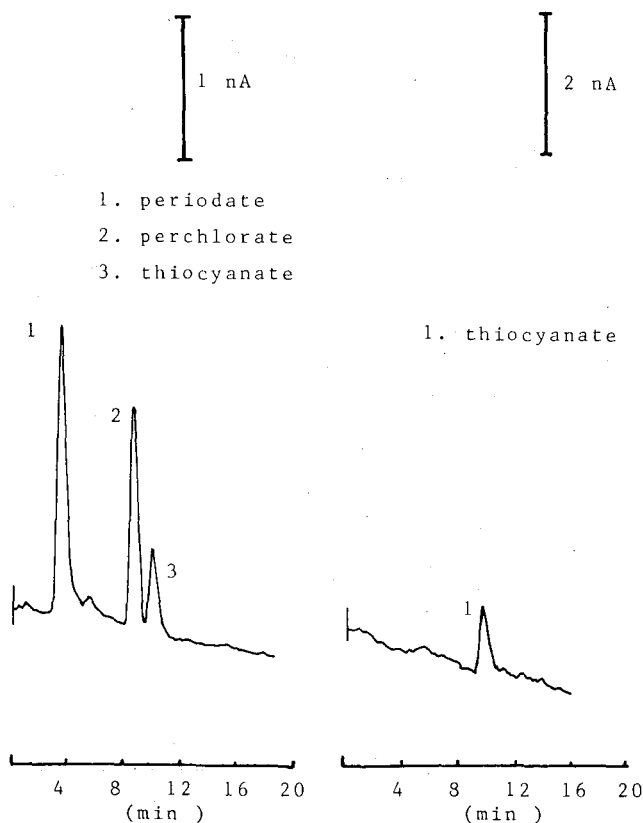


Fig. 6. Ion-pair RPLC-hv-ED chromatograms of anions. (a) Lamp on; (b) lamp off. Sample concentration: 10 ppm periodate, 25 ppm perchlorate, 1 ppm thiocyanate.  $C_{18}$  reversed-phase column, 100 mm  $\times$  4.0 mm I.D.; mobile phase, methanol- $\text{Na}_2\text{HPO}_4$  and  $\text{NaH}_2\text{PO}_4$  (0.0140 and 0.0144 M) (15:85) (pH 6.7) with 0.001 M TBAHS; flow-rate, 0.8 ml/min; injection volume, 20  $\mu\text{l}$ . ED at +1.10 V, glassy carbon working electrode, Ag/AgCl reference electrode.

TABLE V

SUMMARY OF LINEARITY RANGES AND LIMITS OF DETECTION FOR INORGANIC ANIONS USING ION-PAIR RPLC-hv-ED

See Table II, Fig. 5 and text for chromatographic and ED conditions.

Anion	Limit of detection <sup>a</sup> (ppb)	Linearity range <sup>b</sup> (ppm)
Dichromate	300	100
Chromate	500	100
Perchlorate	300	200
Thiocyanate	70	200

<sup>a</sup> Obtained experimentally at signal-to-noise (S/N) equal to 3.<sup>b</sup> Listed are only the maximum concentrations which were within the linear response ranges.

response differences between lamp on and lamp off offered another potential of selectivity in addition to the selectivity provided by the selection of working potential applied. For example, if another anion with inherent oxidative ED properties has the same retention time as perchlorate, the quantitative determination of this anion is possible under lamp off conditions, because there is no ED response for perchlorate. The peak obtained under lamp on conditions (containing two components) can be used to determine quantitatively the concentration of perchlorate (subtracting the peak area or peak height contributed from the first anion from the total peak area or peak height).

The linear response ranges for perchlorate and thiocyanate ions were measured, Table V, from the detection limits to 200 ppm. The data for the linearity study for these ions were given in Table I. The linear equation fitting the responses vs. concentrations gave  $r^2$  values of 0.9973 and 0.9994 for thiocyanate and perchlorate. Detection limits (Table V) were 70 and 300 ppb ( $\mu\text{g/l}$ ), respectively.

Periodate ion was not well retained on the RP column even with higher concentrations of ion-pair reagent. However, Fig. 4, periodate was very sensitive to hv-ED. 40 ppm potassium periodate was injected under lamp off conditions and nothing could be detected. On the other hand, 10 ppm of the same sample gave an off-scale response with the lamp on. The detection limit for this anion may also be several hundred ppb, though it was not physically determined.

## ACKNOWLEDGEMENTS

This research was supported, in part, by an unrestricted grant and materials donations to Northeastern University from Bioanalytical Systems, through the generosity and assistance of P. T. Kissinger. Additional funding was provided, in part, by an NIH Biomedical Research Support Grant to Northeastern University (RR07143), Department of Health and Human Resources (DHHS). Funding was also provided, in part, by an unrestricted grant from Pfizer (Groton, CT, U.S.A.). We are very grateful to these and other sponsors of our research in the areas of improved ED in HPLC. Some of the initial studies in the determination of inorganic anions using HPLC-hv-ED were successfully performed by C. M. Selavka and X.-D. Ding at NU

and M. Lookabaugh at the U.S. Food & Drug Administration Laboratories of the Winchester Engineering and Analytical Center (WEAC). Helpful and constructive discussions were provided by numerous colleagues, especially: J. Mazzeo, A. Bourque, H. H. Stuting, and C.-X. Gao.

This is contribution number 398 from The Barnett Institute of Chemical Analysis and Materials Science at Northeastern University.

#### REFERENCES

- 1 M. T. W. Hearn (Editor), *Ion-Pair Chromatography*, (Chromatographic Science Series, Vol. 31), Marcel Dekker, New York, 1985.
- 2 C. M. Selavka and I. S. Krull, *Anal. Chem.*, 59 (1987) 2699.
- 3 C. M. Selavka and I. S. Krull, *Anal. Chem.*, 59 (1987) 2704.
- 4 C. M. Selavka, K. S. Jiao, I. S. Krull, P. Sheih, W. Yu and M. Wolf, *Anal. Chem.*, 60 (1988) 250.
- 5 C. M. Selavka, I. S. Krull and I. S. Lurie, *J. Chromatogr. Sci.*, 23 (1985) 499.
- 6 C. M. Selavka, I. S. Krull and I. S. Lurie, *Forensic Sci. Int.*, 31 (1986) 103.
- 7 I. S. Krull and W. R. LaCourse, in I.S. Krull (Editor), *Reaction Detection in Liquid Chromatography* (Chromatographic Science Series, Vol. 34), Marcel Dekker, New York, 1986, p. 303.
- 8 W. J. Bachman and J. T. Stewart, *LC · GC Int.*, 7 (1989) 38.
- 9 M. Lookabaugh and I. S. Krull, *J. Chromatogr.*, 452 (1988) 295.
- 10 J. Plotnikow, *Allgemeine Photochemie*, Walter de Gruyter, Berlin, 1936.
- 11 P. Muller, *Chimia*, 31 (1977) 209.
- 12 D. Rehorek and R. Wagener, *Inorg. Chim. Acta*, 33 (1979) 129.
- 13 U. Klaning, *Acta Chem. Scand.*, 12 (1958) 807.
- 14 U. Klaning and M. C. R. Symons, *Proc. Chem. Soc.*, 95 (1958).
- 15 J. D. Neuss and W. Riemann, *J. Am. Chem. Soc.*, 56 (1934) 2238.
- 16 J. Y. Tong and E. L. King, *J. Am. Chem. Soc.*, 75 (1953) 6180.
- 17 I. S. Krull, K. W. Panaro and L. L. Gershman, *J. Chromatogr. Sci.*, 21 (1983) 460.
- 18 P. T. Kissinger, in P. T. Kissinger and W. R. Heineman (Editors), *Laboratory Techniques in Electroanalytical Chemistry*, Marcel Dekker, New York, 1984, p. 619.
- 19 I. S. Krull, X. D. Ding, C. M. Selavka and R. Nelson, *LC, Mag. Liq. Chromatogr., HPLC*, 2 (1984) 214.



CHROMSYMP. 1654

## KINETICS OF CYSTEINE OXIDATION IN IMMOBILIZED pH GRADIENT GELS

MARCELLA CHIARI, CLAUDIA CHIESA and PIER GIORGIO RIGHETTI\*

*Department of Biomedical Sciences and Technologies, University of Milano, Via Celoria 2, Milan 20133 (Italy)*

MICHELE CORTI

*Institute of Animal Husbandry, Faculty of Agriculture, University of Milano, Via Celoria 2, Milan 20133 (Italy)*

and

TIKAM JAIN and ROBERT SHORR

*AT Biochem, 74 Great Valley Parkway, Malvern, PA 19355 (U.S.A.)*

---

### SUMMARY

It was recently found that, during the gel polymerization step, persulphate could oxidize the alkaline Immobiline species (acryloyl weak bases used for producing immobilized pH gradients, IPG) by forming N-oxides. When focusing proteins in alkaline pH ranges, free SH groups were oxidized to –S–S– bonds, generating artefactual, higher *pI* bands. The kinetics of this phenomenon were investigated in a model system consisting in incubating free Cys with a crushed IPG gel auto-buffered at pH 9.0 under aerobic or anaerobic conditions. After appropriate incubation periods, any excess free SH was blocked with acrylonitrile. After dansylation, Cys and its oxidized derivatives were separated and quantified by high-performance liquid chromatography in a C<sub>18</sub> column. Under anaerobic conditions, control Cys (incubated in the absence of IPG gel) showed 30% oxidation after a period of 12 h, whereas Cys incubated with a pH 9.0 crushed IPG gel was 100% oxidized to cystine. When the same experiment was repeated under aerobic conditions, the oxidation process was accelerated by a factor of 3–4. Successful focusing of alkaline proteins can still be achieved if (a) the IPG gel is washed in 100 mM ascorbic acid, prior to the run, for elimination of N-oxides from the matrix, (b) the IPG gel is run anaerobically and (c) the focusing time is kept to a minimum (*e.g.*, 4 h vs. the standard overnight run).

---

### INTRODUCTION

Recently, when focusing recombinant or urine-purified urokinase [a 50 000-dalton glycoprotein consisting of two chains of 20 000 and 30 000 dalton, connected by a disulphide bridge, containing an unusually high level of Cys residues (a total of 24)], used in human therapy as a fibrinolytic agent, we detected an extreme charge heterogeneity (at least ten major and ten minor bands in the pH range 7–10)<sup>1</sup>. This

protein, extensively purified by immunoaffinity and ion-exchange chromatography<sup>2</sup>, gave in sodium dodecyl sulphate polyacrylamide gel electrophoresis (SDS-PAGE) a single, size-homogeneous zone and was classified as a therapeutic-grade product, already distributed by Lepetit (Gerenzano, Italy) for human use as a thrombolytic agent in acute myocardial infarction. The finding of this extensive heterogeneity was therefore a cause of great concern. In an extensive investigation<sup>1</sup>, we could eliminate glycosylation, isoelectric focusing (IEF) artefacts [*e.g.*, binding to carrier ampholytes, (CA)] or carbamylation as potential sources of this polydispersity. Finally, a great part of this heterogeneity could be traced back to the existence of a multitude of protein molecules containing Cys residues at different oxidation levels (SH, -S-S-, possibly even cysteic acid). The cause of these different redox states of Cys in urokinase was not apparent, although part of it might be attributed to spontaneous oxidation by atmospheric oxygen, owing to the relatively high *pI* of native urokinase (*ca.* 9.5–9.8 by conventional IEF).

We subsequently discovered that, to a large extent, this oxidation power was inherent to the Immobiline matrix because, during the polymerization step, at appropriate pH values, the persulphate could oxidize, to different extents, all four alkaline Immobilines (the *pK* 6.2, 7.0, 8.5 and 9.3 species) used as buffers for focusing in basic pH regions<sup>3</sup>. It was hypothesized that, on exposure to ammonium persulphate, there would be addition of oxygen to the tertiary amino group of deprotonated alkaline Immobilines, producing amine oxides ( $R_3-N^+O^-$ ). This reaction is facile and usually occurs readily at room temperature in water, alcohol or benzene solvents in the presence of even dilute solutions of organic peracids<sup>4</sup>. Hence the assumption that, on washing, or electrophoretically pre-running an immobilized pH gradient (IPG) matrix, the latter would be devoid of any oxidizing power, as harmful persulphate would be washed away or be discharged at the anode, proved to be fallacious because these "oxidizing units" were indeed anchored to the gel matrix in the form of N-oxides ( $R_3N^+O^-$ ). As the redox potential in reactions involving nitrogens is of the order of +0.5 V, whereas that of similar reactions involving sulphur is of the order of -0.5 V, it was apparent that the N-oxides anchored to the IPG matrix would act as oxidizing agents on free SH groups (possibly even on -S-S- bridges) of proteins migrating through the gel, producing species of higher oxidation level. Hence the alkaline Immobiline themselves (oxidized by persulphate during polymerization) would act as electron acceptors in this redox process. During the IPG run, two reactive Cys residues in a protein would release two protons and two electrons which would be captured by an oxygen atom bound to the tertiary amine, thus reducing the latter and forming a water molecule. This phenomenon was verified when focusing human  $\alpha$ -globin chains<sup>3</sup> and its suppression could be achieved by simply reducing the matrix, *e.g.*, by a washing step in 100 mM ascorbic acid at pH 4.5.

More recently, the same phenomenon could be observed even in conventional IEF, in presence of CA buffers<sup>5</sup>; when polymerizing the gel at low ammonium persulphate (AP) levels (0.025%), the  $\alpha_{ox}/\alpha_{red}$  ratio was only 15:85; at the normal AP levels (0.04%) this ratio was increased to 35:65, whereas at high AP levels (*e.g.*, 0.2%) the oxidized  $\alpha$ -chain was clearly predominant ( $\alpha_{ox}/\alpha_{red} = 80:20$ ). Here also a remedy could be found by polymerizing an "empty" gel, washing, drying it and reswelling in the presence of the desired CA interval.

In this work, we have devised an experimental model for studying the kinetics



of this oxidation process: free Cys is incubated, at pH 9.0, in presence of a crushed IPG gel and its reaction products are analysed and quantified, after blocking of free SH groups with acrylonitrile and dansylation, by high-performance liquid chromatography (HPLC) on a C<sub>18</sub> column. The process was studied both under anaerobic and aerobic conditions and guidelines are given for the successful fractionation of alkaline proteins.

#### EXPERIMENTAL

Cysteine, cystine, cysteic acid, acrylonitrile and spectrophotometric-grade solvents [trifluoroacetic acid (TFA) and acetone] were obtained from Merck (Darmstadt, F.R.G.) and Ellman's reagent (5,5'-dithiobis-2-nitrobenzoate, DTNB) from Serva (Heidelberg, F.R.G.). The HPLC apparatus was equipped with a Model 655 A-12 pump, a Model D-2000 integrator, a Model 655A variable-wavelength detector and a Model L-5000 gradient programmer (all from Merck-Hitachi). Detection of dansylated compounds was by UV absorption at 254 nm.

#### *Thin-layer chromatography (TLC)*

TLC analyses were carried out on silica gel 60F<sub>254</sub> plates (Merck), developed for 10 min with ethanol-2.5% ammonia solution (7:3). The plates were stained either with iodine vapours or by spraying with ninhydrin and incubating at 90°C for 20 min.

#### *Titration of free SH groups with DTNB*

A 10 mM solution of DTNB in 300 mM Tris-HCl (pH 8.0) was prepared in the dark just prior to use. For the assay, 100  $\mu$ l of DTNB and 10  $\mu$ l of sample solutions are added to 890  $\mu$ l of the above buffer. The absorbance at 410 nm is measured after 10 min against blank tubes. The calibration graph is constructed using standards of cysteine (0-12 mmol). The molar absorption coefficient of reduced DTNB is taken as 13 600, according to Ellman<sup>6</sup>.

#### *Preparation of dansyl derivatives*

A stock solution (100 mg in 2 ml) of dansyl chloride is prepared in spectroscopic-grade acetone. Prior to use, it is diluted 1:10 in acetone. Mix 350  $\mu$ l of 0.1 M hydrogencarbonate buffer (pH 9.5) with 20  $\mu$ l of a 2.5 mM sample solution (Cys and oxidation products thereof) and with 100  $\mu$ l of freshly diluted stock dansyl chloride. Incubate at 37°C for 60 min; the reaction is stopped by adding 750  $\mu$ l of 25 mM TFA.

#### *Synthesis of S-cyanoethylcysteine*

The S-cyanoethyl Cys standard is prepared according to Friedman *et al.*<sup>7</sup> as follows. A solution of 6.7 g (0.056 mole) of Cys in 15 ml of water is titrated to pH 8.1 with dilute ammonia. The solution is diluted to 60 ml, transferred into a 100-ml reaction flask and stirred with nitrogen flushing. A 0.057-mol (3.7-ml) amount of acrylonitrile is added and the reaction is continued with stirring for 4 h. The solution is evaporated to dryness under vacuum at 30-33°C and the residue is recrystallized first from 75% ethanol and then from 80% ethanol. At 5°C, white crystals are formed (80% yield). The IR spectrum of the product shows a nitrile signal at 2240 cm<sup>-1</sup>. <sup>1</sup>H NMR spectrum (in deuterated TFA):  $\delta$  4.7 ppm [1H, CH(NH<sub>3</sub>)COOH]; 3.53 ppm (2H, CH<sub>2</sub>CN); 3 ppm [4H, (CH)<sub>2</sub>S].

#### *Incubation of Cys with an IPG granulated matrix*

The IPG gel contains 10%T, 8%C<sup>a</sup> and 10 mM pK 6.2, 10 mM pK 7.0, 5 mM pK 8.5 and 5 mM pK 9.3 Immobilines titrated to a single pH value of 9.0 with the pK 3.6 species. After polymerization<sup>8</sup> and standard washing procedures<sup>9</sup>, the gel is crushed through a 100 mesh/in.<sup>2</sup> sieve and placed (a total of 5.5 g wet weight of gel) in a 100-ml reaction flask equipped with a mechanical stirrer and flushed with nitrogen. A 10 mM Cys solution is prepared in 100 mM borate buffer (pH 9.0), 10 ml of this solution are added to the flask containing the crushed IPG gel and the reaction is followed by harvesting and analysing aliquots after 4 and 12 h of incubation. In parallel, the same stock Cys solution is incubated in another flask in the absence of IPG matrix and under a nitrogen atmosphere, as above. At the appropriate time intervals, (a) duplicate aliquots are taken for immediate titration of free SH groups with Ellman's reagent, and (b) additional aliquots are harvested and acrylonitrile (10  $\mu$ l of a 0.15 M solution, pH 8.1) is added in order to block unreacted free SH groups (this will prevent further reaction during the subsequent manipulation steps prior to HPLC analyses). After completion of reaction the pH is increased to 11.5 by addition of 6 M sodium hydroxide solution (this solubilizes cystine, which tends to precipitate at lower pH) and finally the reaction products are dansylated for HPLC analysis.

#### *HPLC analysis*

After acrylonitrile and dansyl derivatization, the samples, freed from gel particles, are injected into the column (300  $\times$  4 mm I.D. microparticle reverse-phase Hypersil C<sub>18</sub> from Gynkoteck, München, F.R.G.) of an HPLC apparatus. Gradient elution (flow-rate 1.0 ml/min) is performed with two solutions, (A) acetonitrile–25 mM sodium trifluoroacetate buffer, pH 7.2 (10:90) and (B) sodium trifluoroacetate buffer, pH 7.2–acetonitrile (30:70), with the following gradient composition at the times indicated: 0–4 min, 96% A–4% B; 12 min, 70% A–30% B; 16 and 19 min, 30% A–70% B; 21 min 96% A–4% B. The column and sample temperature was 40°C. For calculating the percentage oxidation with time, calibration graphs were constructed with standards (2.5 mmol) of S-cyanoethyl dansylcysteine and of dansylcysteine injected into the HPLC column.

#### RESULTS

When standards of Cys are incubated in the presence of IPG particles containing all the four alkaline Immobilines, titrated to a constant pH of 9.0 (the approximate *pI* value of  $\alpha$ -globin chains in an IPG gel) and analysed by TLC, it is clearly seen that there is substantial conversion to at least the oxidized cystine stage (possibly also to other oxidation products, as an additional spot is clearly visible at 5 and 10 h just below the Cys zone; see Fig. 1A). After 10 h of incubation, it is seen that no free Cys remains, most of it being converted to cystine (Cys<sub>2</sub>) and to the unknown product below the Cys band. Conversely, when the same experiment is repeated in the presence of IPG particles which had been reduced in 100 mM ascorbate (pH 4.5), prior to the incubation, it is seen (Fig. 1B) that substantial amounts of Cys remain even after 10 h of incubation (in both instances the experiments were performed in atmospheric

<sup>a</sup> C = g Bis/%T; T = (g acrylamide + g Bis)/100 ml solution.

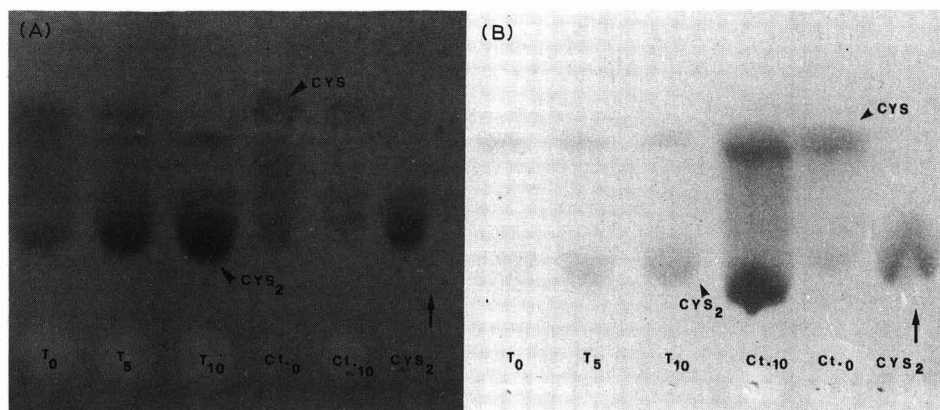


Fig. 1. Kinetics of Cys oxidation in the presence of IPG particles as monitored by TLC. 10 mM Cys solutions were incubated with (A) unreacted and (B) reduced IPG gel particles (pH 9.0) under aerobic conditions for 0, 5 or 10 h ( $T_0$ ,  $T_5$  and  $T_{10}$ , respectively). Ct. = Control incubations, in the absence of IPG particles;  $Cys_2$  = standard of cystine. The vertical arrow indicates the direction of migration. The TLC plate was developed with a ninhydrin spray.

oxygen). However, it was found to be impossible to obtain reliable kinetic data by spot integration and densitometry. This system was therefore abandoned in favour of HPLC fractionation and analysis.

In HPLC, although analysis of Cys has already been reported<sup>10</sup>, we still found the system to suffer from many practical problems. First, the reproducibility was very poor, and this was related to the time lag between the end of the reaction (incubation in the presence or absence of IPG particles) and the injection time. During the dansylation step, in fact, additional oxidation by atmospheric oxygen could take place. This problem was solved by reacting, at the end of the incubation period and prior to HPLC analysis, the excess free SH group with acrylonitrile, thus producing a stable S-cyanoethyl-Cys. In addition, it was found that the peaks of cystine were highly irreproducible, and often absent, even though we could follow the disappearance of the Cys peak in the chromatogram and the decrement of free SH groups by the Ellman reaction. This loss of cystine was traced back to its insolubility at the pH prevailing during the incubation step with IPG particles (pH 9.0). Hence the system had to be extracted at pH 11.5. When all these precautions were taken, highly reproducible results could be obtained.

The HPLC gradient utilized was selected for its ability to separate the most common conversion products of Cys, *i.e.*, cystine and the fully oxidized cysteic acid, as we suspected that the terminal product of oxidation in presence of an IPG gel could be this latter compound. Fig. 2 shows that the HPLC method adopted can indeed separate Cys,  $Cys_2$  and cysteic acid, in addition to the blocked derivative, S-cyanoethyl-Cys. Fig. 3A demonstrates the oxidation progress of Cys to  $-S-S-$  bonds in a control incubation during a 12-h period in the absence of IPG particles and under anaerobic conditions. It is seen that, even in this controlled environment, auto-oxidation (presumably due to traces of oxygen still present) takes place up to a level of 29% at the end of the 12-h period. However, when the same experiment is

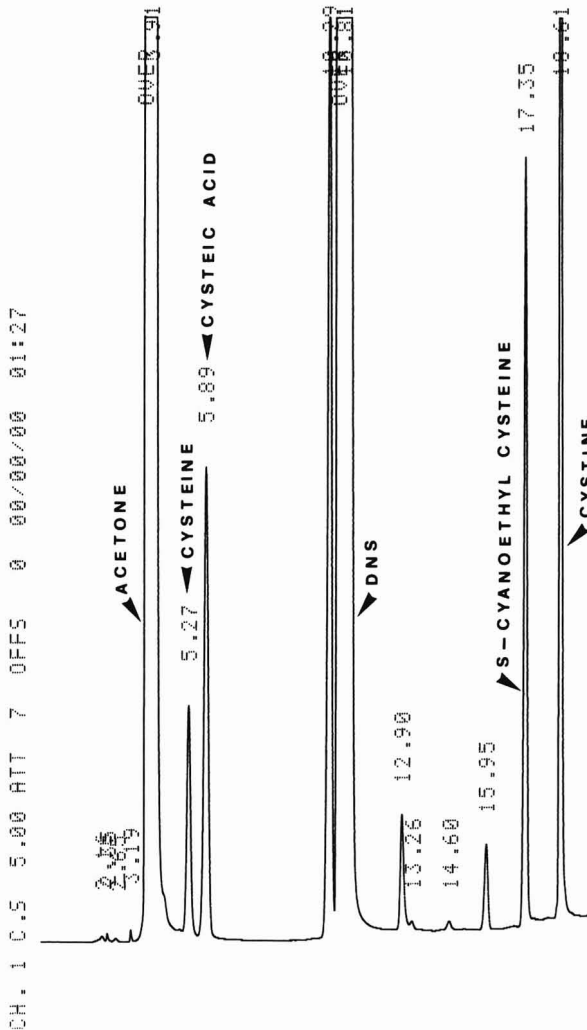


Fig. 2. HPLC fractionation of Cys derivatives. The gradient utilized (see Experimental) allows the separation of cysteic acid, cysteine, cystine and S-cyanoethylcysteine [the two other major peaks are acetone and excess dansyl (DNS)].

repeated in the presence of the pH 9.0 IPG particles (containing all four alkaline Immobiline species; Fig. 3B), at the end of this 12-h period 100% oxidation has taken place and the Cys peak has completely disappeared (in agreement with Fig. 1A).

When the two experiments are repeated under aerobic conditions, the conversion rate is accelerated by a factor of 3–4. As seen in Fig. 4A, in the control 30% oxidation has already taken place in only 4 h, whereas in the presence of IPG particles 100% oxidation has already occurred in the same time period (Fig. 4B; *cf.*, only 18% under anaerobic conditions, Fig. 3B). The kinetics of both phenomena are summarized in Fig. 5. The left-hand side shows the oxidation kinetics (under aerobic and anaerobic conditions) of control incubates and in presence of unreduced IPG parti-

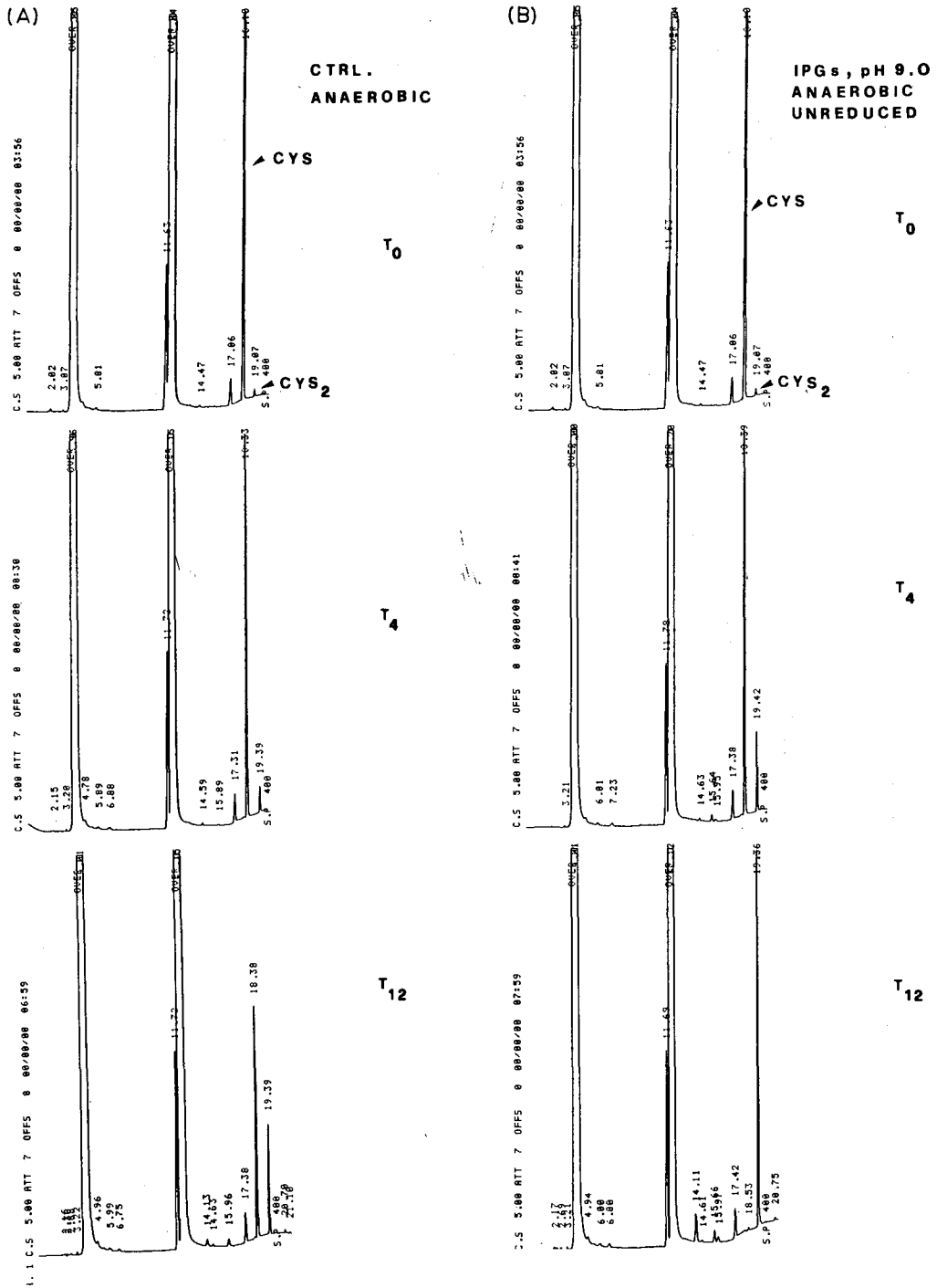


Fig. 3. Kinetics of Cys oxidation as followed by HPLC analysis. (A) Control incubations in the absence of IPG particles at 0, 4 and 12 h ( $T_0$ ,  $T_4$  and  $T_{12}$ , respectively); (B) incubations in the presence of unreduced IPG gel particles titrated to pH 9.0 at the same time intervals. In all instances the incubations were done under a nitrogen atmosphere. Cys = Cysteine; Cys<sub>2</sub> = cystine. Note that, in the presence of the IPG matrix, an unknown oxidation peak with a retention time of 14.11–14.47 min appears, the chemical nature of which is unknown.

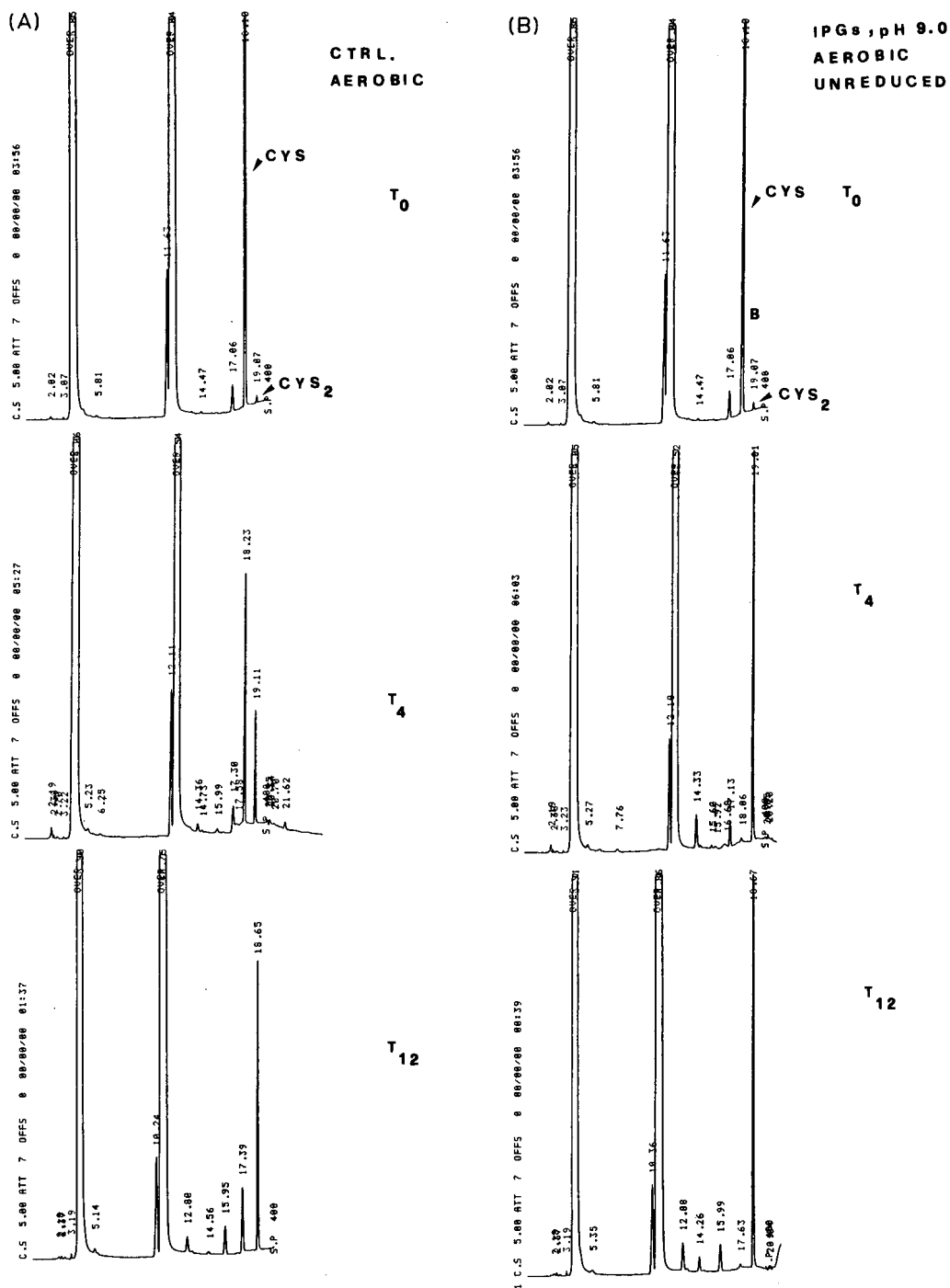


Fig. 4. Kinetics of Cys oxidation as followed by HPLC analysis. (A) Control incubations in the absence of IPG particles at 0, 4 and 12 h ( $T_0$ ,  $T_4$  and  $T_{12}$ , respectively); (B) incubations in the presence of unreduced IPG gel particles titrated to pH 9.0 at the same time intervals. In all instances the incubations were done under aerobic conditions. Cys = Cysteine; Cys<sub>2</sub> = cystine. Note that, in presence of the IPG matrix, an unknown oxidation peak with a retention time of 14.11–14.47 min appears, the chemical nature of which is unknown. Note also the much accelerated oxidation kinetics in presence of atmospheric oxygen.

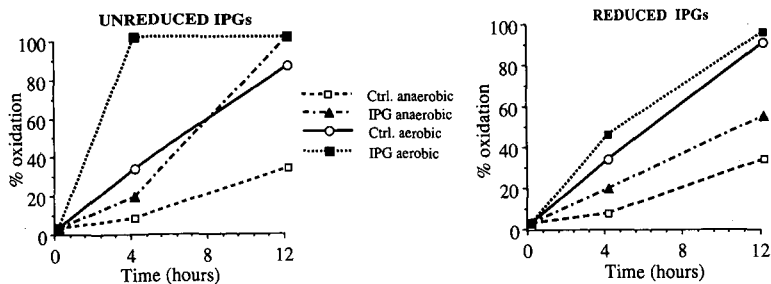


Fig. 5. Kinetics of Cys oxidation as followed by HPLC analysis. The data are presented as percentage cysteine oxidation as measured by peak integration in the HPLC traces in Figs. 3 and 4. The values reported refer to both aerobic and anaerobic conditions. Left, unreduced IPG particles; right, reduced IPG matrix. □ = Control, anaerobic; ▲ = IPG, anaerobic; ○ = control, aerobic; ■ = IPG, aerobic.

cles. On the right, the same values are reported but in the presence of a reduced IPG matrix (*i.e.*, treated with 100 mM ascorbate, pH 4.5). It is seen that, under anaerobic and reducing conditions, oxidation of Cys is greatly reduced. Fig. 6 gives the same data obtained by monitoring in parallel the incubates with the DTNB reaction (Ellman's reagent); even though, in this last instance, only the disappearance of free SH groups could be quantified, the two sets of data (HPLC fractionation and direct chemical analysis) agree fairly well.

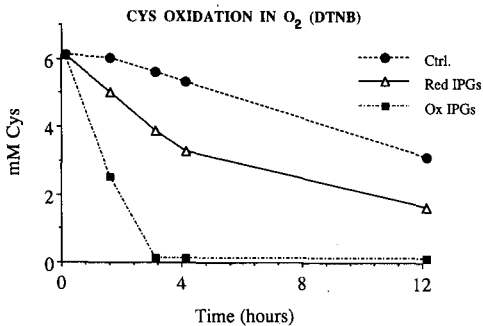


Fig. 6. Kinetics of Cys oxidation as followed with Ellman's reagent. A 6 mM Cys solution was incubated at pH 9.0 either as such (●, control) or in the presence of (■) unreduced or (△) reduced IPG particles. All data points refer to aerobic conditions. The disappearance of free SH groups is followed by the DTNB reaction.

DISCUSSION

A vast literature exists on the oxidation of thiols in aliphatic and aromatic compounds (for a review, see Capozzi and Modena<sup>11</sup>). Whereas in protein chemistry courses, we are used to dealing with only three oxidation states (free thiols, disulphides and, in extreme cases, cysteic acid), in reality thiols are oxidized by a variety of reagents to a whole series of higher oxidation products, depending on the specific reaction conditions (see Fig. 7). There are therefore two main oxidation chains, with a number of interconversions, which could occur via the hydrolytic products shown on the right-hand side of Fig. 7. In principle, all these intermediate reaction products

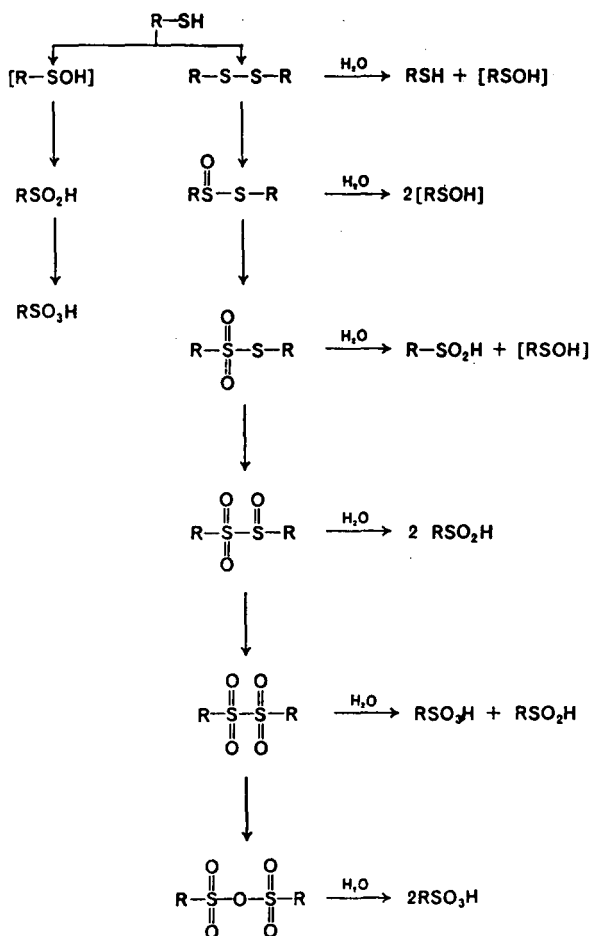


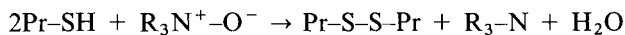
Fig. 7. Scheme of possible oxidation pathways of Cys. Note that several sulphone intermediate products of Cys<sub>2</sub> exist as stable compounds, in addition to the well known Cys<sub>2</sub> and cysteic acid terminal products. (From ref. 11.)

could exist in a thiol compound, except for the very labile sulphenic acid (shown in brackets), the isolation of which is virtually impossible. Perhaps the most popular oxidation pathway for thiols is via molecular oxygen. The ease of oxidation of thiols on exposure to air is well known, as is the sensitivity of this reaction to catalysts, such as metal ions, UV light and other initiators of radical reactions<sup>12</sup>. It is also reported that auto-oxidation of thiols is accelerated by bases. Of great concern to protein chemists dealing with electrophoresis in polyacrylamide gels is the chemical oxidation of thiols by peroxidic compounds. The oxidation of thiols by hydrogen peroxide, alkyl hydroperoxides and peroxy acids is a well known reaction<sup>13</sup>: the initially formed product is the corresponding disulphide in most instances, which can easily be further oxidized by excess of oxidant. As polyacrylamide gels are routinely prepared by radical reactions in the presence of persulphate ions, it is in general recommended to deplete this strong oxidant electrophoretically by discharging it at the anode during a



short prerun. With this precaution, electrophoresis of native proteins has always been considered to be a safe procedure, as no residual oxidizing activity is left in the gel matrix after passage of the persulphate boundary (*i.e.*, the pendant amido groups are not oxidized by persulphate).

With our recent findings, it became clear that in IPG gels, all the alkaline Immobilines (except for the quaternary titrant, QAE-arylamide) can be oxidized, at appropriate pH, to N-oxides<sup>3</sup> of the type  $R_3N^+-O^-$ , and that in CA-IEF gels, the carrier ampholyte buffers are oxidized forming primary to tertiary amine oxides<sup>5</sup>. Hence in an IEF experiment, the idea of prerunning the gel to discharge harmful persulphate has proved to be fallacious, as neither the CA buffers nor the Immobilines can leave the gel. The former will migrate at different velocities to their *pI* position until a steady state is reached; the latter are anchored to the gel matrix and therefore can only oscillate about their bond in a strong electric field. We have contended that these N-oxides could act as "oxidizing units" on thiol groups of proteins according to the following scheme:



where Pr-SH represents a protein macroion with a reactive thiol and  $R_3-N^+-O^-$  is an oxidized alkaline Immobiline (see Chiari *et al.*<sup>14,15</sup> for their formulae and properties) or an oxidized carrier ampholyte buffer (see Righetti<sup>16</sup> for an extensive review on these chemicals). In fact, we have proved that in an IPG run, human  $\alpha$ -globin chains (*pI*  $\approx$  9.2) were at least 50% oxidized in an overnight run, whereas if the IPG matrix were reduced in ascorbic acid prior to the run, full protection of globin chains would ensue<sup>3</sup>. The same was true in a CA-IEF gel: depending on the initial level of persulphate used, as much as 80% oxidation of  $\alpha$ -chains could be elicited in only 4 h<sup>5</sup>.

As we are dealing here with IPG gels, can in reality our presumptive  $R_3N^+-O^-$  species oxidize thiols? In addition to the data presented here, there is ample evidence in the literature for such a mechanism. Thus, it is known that nitroso and nitro compounds can indeed oxidize thiols. In basic media, thiols are oxidized to disulphides by nitrobenzene or nitrosobenzene<sup>17</sup>, which are in turn reduced mainly to azoxy- and azobenzene. Among the oxidizing species reported, 4-nitropyridine N-oxide (a weakly basic compound which could mimic grafted Immobilines) seems to be among the most reactive species<sup>18</sup>.

Another aspect we should consider is the kinetics of the phenomenon: when incubated in the presence of oxidized IPG particles under aerobic conditions, full oxidation of Cys to cystine is seen to occur in 4 h. There are examples in the literature of even faster reactions. Thus, 2-propene-1-thiol is 90% oxidized by diethyl azodicarboxylate at room temperature in only 30 min<sup>19</sup>; 2-mercaptobenzothiazole is converted into the disulphide by the same reagent with 95% yield in 30 min at the refluxing temperature of benzene. We should, however, distinguish between oxidation kinetics under anaerobic or aerobic conditions. In the former instance, the kinetics are slowed by a factor of *ca.* 3 (full oxidation in 12 h anaerobically *vs.* 4 aerobically). Hence the presence of both oxidized IPG particles and atmospheric oxygen has a synergistic effect on the reaction. We also emphasize that in proteins Cys oxidation does not necessarily occur at the rate we have demonstrated here for free Cys. In fact (see Fig. 10 in ref. 3), under anaerobic conditions and with a reduced IPG

matrix, oxidation of Cys in  $\alpha$ -globin chains is fully inhibited in an overnight run. Probably the protein moiety shields the Cys group and thus considerably slows the oxidation process.

Can a higher oxidation level be obtained in the presence of oxidized IPGs or CAs? At present we have only been able to see the conversion SH to  $-S-S-$ , whereas Jacobs<sup>20</sup> has reported oxidation to cysteic acid. Although in our HPLC system we cannot see any cysteic acid (which is well separated by our system; see Fig. 2), we cannot exclude the presence of other oxidation intermediates, as the TLC plate (see Fig. 1) gave a clear hint of two oxidized spots. Jacobs<sup>20</sup> reported oxidation of cysteine to cysteic acid in alkaline proteins, such as ribonuclease, after CA-IEF. As his data were based on total hydrolysis of ribonuclease isoforms, followed by chromatography with an amino acid autoanalyser, traces of CAs present in the protein during hydrolysis could have catalysed full oxidation to the cysteic acid form. It is known, in fact, that weak thiols can be partially transformed into their conjugated base by amines. As the anion oxidation proceeds much faster than on the undissociated thiol, this could account for Jacobs' data.

We conclude with the following guidelines for performing successful IPG fractionations of proteins:

- (a) reduce the IPG gel by a washing step in 100 mM ascorbate (pH 4.5);
- (b) run the IPG gel anaerobically (either submerged under paraffin oil or sandwiched between two plates);
- (c) try to minimize the focusing time (4–5 h, instead of an overnight run).

#### ACKNOWLEDGEMENTS

This work was supported in part by a grant from the Consiglio Nazionale delle Ricerche (CNR, Rome), Progetto Finalizzato "Biotecnologie e Biosensori". This work is part of the Ph.D. Thesis of C. C. We thank Dr. O. Brenna (Department of Food Science and Technology, University of Milan) for stimulating discussions and criticism.

#### REFERENCES

- 1 P. G. Righetti, B. Barzaghi, E. Sarubbi, A. Soffientini and G. Cassani, *J. Chromatogr.*, 470 (1989) 337–350.
- 2 A. Corti, M. L. Nollì, A. Soffientini and G. Cassani, *Thromb. Haemostas.*, 56 (1986) 219–224.
- 3 P. G. Righetti, M. Chiari, E. Casale and C. Chiesa, *Appl. Theor. Electrophoresis*, 1 (1989) 115–121.
- 4 B. C. Challis and A. R. Butler, in S. Patai (Editor), *The Chemistry of the Amino Group*, Wiley-Interscience, New York, 1972, pp. 326–327.
- 5 G. Cossu, M. G. Pirastru, M. Satta, M. Chiari, C. Chiesa and P. G. Righetti, *J. Chromatogr.*, 475 (1989) 283–292.
- 6 G. L. Ellman, *Arch. Biochem. Biophys.*, 82 (1959) 70–77.
- 7 M. Friedman, J. F. Cavins and J. S. Wall, *J. Am. Chem. Soc.*, 87 (1965) 3672–3682.
- 8 P. G. Righetti, K. Ek and B. Bjellqvist, *J. Chromatogr.*, 291 (1984) 31–42.
- 9 P. G. Righetti, *J. Chromatogr.*, 300 (1984) 271–321.
- 10 Y. Yapuhi, N. T. Miller and B. L. Karger, *J. Chromatogr.*, 205 (1981) 325–337.
- 11 G. Capozzi and G. Modena, in S. Patai (Editor), *The Chemistry of the Thiol Group, Part 2*, Wiley, New York, 1974, pp. 785–835.
- 12 E. E. Reid, *Organic Chemistry of Bivalent Sulphur*, Vol. 1, Chem. Publ. Co., New York, 1958.

- 13 D. S. Tarbell, in N. Kharash (Editor), *Organic Sulphur Compounds*, Vol. 1, Pergamon Press, New York, 1961, Ch. 10, pp. 97–102.
- 14 M. Chiari, E. Casale, E. Santaniello and P. G. Righetti, *Appl. Theor. Electrophoresis*, 1 (1989) 99–102.
- 15 M. Chiari, E. Casale, E. Santaniello and P. G. Righetti, *Appl. Theor. Electrophoresis*, 1 (1989) 103–107.
- 16 P. G. Righetti, *Isoelectric Focusing: Theory, Methodology and Applications*, Elsevier, Amsterdam, 1983.
- 17 F. J. Smentowski, *J. Am. Chem. Soc.*, 85 (1963) 3036–3040.
- 18 T. J. Wallace, J. M. Miller, H. Probner and A. Schriesheim, *Proc. R. Soc. London*, 43 (1962) 384–390.
- 19 F. Yoneda, K. Suzuki and Y. Nitta, *J. Org. Chem.*, 32 (1967) 727–732.
- 20 S. Jacobs, *Analyst (London)*, 98 (1973) 25–33.



CHROMSYMP. 1639

## CAPILLARY ELECTROPHORESIS WITH INDIRECT AMPEROMETRIC DETECTION

TERESA M. OLEFIROWICZ and ANDREW G. EWING\*

*Department of Chemistry, Penn State University, University Park, PA 16802 (U.S.A.)*

---

### SUMMARY

The use of indirect amperometric detection with capillary electrophoresis is demonstrated. The system consists of a porous glass coupler which allows amperometric detection at a carbon fiber electrode placed in the end of the capillary. 3,4-Dihydroxybenzylamine is added to the buffer system as a continuously eluting electrophore. Indirect amperometric detection in 9- $\mu\text{m}$  I.D. capillaries provides detection limits as low as 380 attomole for the amino acid arginine. Finally, both direct and indirect amperometric detection can be accomplished simultaneously.

---

### INTRODUCTION

Capillary electrophoresis (CE) is a highly efficient, small-volume separation technique that can be used to separate a wide range of biological compounds<sup>1–4</sup>. However, many biological compounds do not inherently possess the necessary characteristics for sensitive detection. Laser fluorescence and amperometric detection both provide subattomole detection limits and are among the most sensitive detectors available for CE<sup>2,4–9</sup>. Although these detection methods are very sensitive, selectivity is limited to those species which possess native fluorescence or are easily oxidized.

An area of great interest in CE is its use for separation and detection of substances removed from biological microenvironments. A microinjector<sup>10</sup> has been used to acquire samples from the cytoplasm of single nerve cells<sup>4,8</sup>. An important aspect of this experiment is the use of amperometry for sensitive detection of underivatized substances. We have developed a system which uses a porous glass coupler to allow electrophoresis in a “separation” capillary and an off-column amperometric detector in a “detection” capillary<sup>7</sup>. This system can provide subattomole detection limits for the easily oxidized catechols and indoles<sup>9</sup>; however, many solutes of interest are not easily oxidized and are, therefore, not detectable via this method.

Detectability can be provided by sample derivatization<sup>1,2,5,6</sup>, but there are several drawbacks to this approach. The derivatization procedure can result in multiple products for peptides, derivatization is difficult with very small volume samples, and detection by this method is still far from universal. Indirect detection provides an alternative scheme that promises to be more universal. This detection

scheme has been demonstrated with CE for the detection of bromide and several organic acids by indirect UV absorbance<sup>11</sup> and for native amino acids, nucleotides and nucleosides by indirect fluorescence<sup>12,13</sup>. In these experiments, a lower limit of detection of 50 amol was obtained for several native amino acids.

Previous reports of indirect detection in CE have centered on the detection of anions by use of UV absorbance or laser fluorescence<sup>11-13</sup>. In this paper, we demonstrate the use of indirect amperometry for the detection of several cationic amino acids and dipeptides. The advantages of indirect amperometric detection include sensitivity and instrumental simplicity while providing, in concept, detection of all ionic solutes.

## EXPERIMENTAL

### *CE apparatus*

The system used for electrochemical detection has been described by Wallingford and Ewing<sup>7</sup>. In this work, 5- $\mu\text{m}$  and 10- $\mu\text{m}$  diameter carbon fibers (Amoco Performance Products, Greenville, SC, U.S.A.) with an exposed length of 200–250  $\mu\text{m}$  were used as the working electrodes for electrochemical detection. Detection was performed in the amperometric mode with a two-electrode configuration. The reference electrode was a sodium-saturated calomel electrode (SSCE). The low currents measured required that the detection end of the system be housed in a Faraday cage in order to minimize the effects of external noise sources. Untreated fused-silica capillaries having internal diameters of 26 and 9  $\mu\text{m}$  and outer diameters of 260 and 370  $\mu\text{m}$ , respectively, were obtained from Polymicro Technologies (Phoenix, AZ, U.S.A.). Injections were performed by electromigration<sup>14</sup>.

### *Chemicals*

2-Morpholinoethanesulfonic acid (MES) and 3,4-dihydroxybenzylamine (DHBA) were obtained from Sigma (St. Louis, MO, U.S.A.). All solutions were adjusted to the appropriate pH using dilute sodium hydroxide. Lysine (Lys), arginine (Arg), histidine (His), lysylphenylalanine (Lys-Phe), histidylphenylalanine (His-Phe), arginylleucine (Arg-Leu), histidylglycine (His-Gly), dopamine, norepinephrine, and epinephrine were used as received from Sigma.

## RESULTS AND DISCUSSION

### *Indirect detection of amino acids*

Indirect detection involves the addition of a detectable ionic component to the electrophoretic buffer. Zones of non-detectable analyte ions displace the added ions during zone migration. For analytes with the same charge as the detectable component, displacement of the detectable ions results in a lower level of the detector-active component, and negative peaks result. A schematic diagram outlining this process is shown in Fig. 1. Although this is a simplification and it is likely that many processes are occurring simultaneously, detectability is based on the properties of the detector-active component which results in a universal detection scheme.

Indirect electrochemical detection has been accomplished by addition of a cationic electrophore, DHBA, to the electrophoretic buffer. When the working

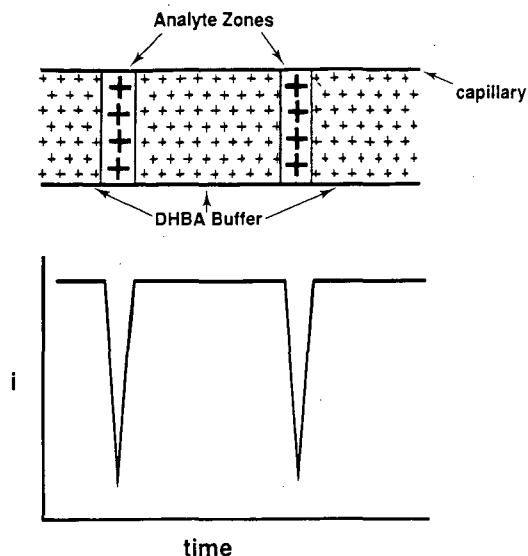
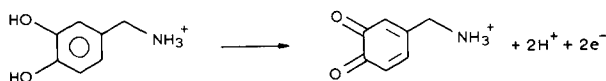


Fig. 1. Schematic diagram of cation displacement by migrating zones of cationic solutes.

electrode is held at a constant potential of +0.7 V *versus* the SSCE, the DHBA undergoes a two-electron two-proton transfer to give the corresponding orthoquinone as follows:



Continuous oxidation of this species, as it passes through the detector region, produces a constant background current. Due to the need to preserve charge neutrality, the cationic DHBA in the buffer is displaced by cationic analyte zones. As these cationic zones pass through the detector region, a lower level of oxidizable species is observed in these zones and the background current decreases. As a result, negative peaks are expected in the detection of cations.

Detection of several cationic native amino acids by indirect amperometry is demonstrated in Fig. 2. The electropherogram shows the separation of three non-electroactive amino acids obtained in a 26- $\mu\text{m}$  I.D. capillary. Ethanol was added to the electrophoretic buffer in an attempt to change the zeta potential at the capillary surface and thus change the electroosmotic flow-rate. This, however, did not significantly enhance the resolution, although the peak tailing was decreased relative to a separation obtained without ethanol (not shown).

The first peak in the electropherogram represents a zone in which the DHBA is virtually absent. This displacement peak is present since all samples were prepared in buffer without the DHBA. A system peak, labelled S, is observed at a migration time corresponding to the rate of electroosmotic flow. The injected amounts of amino acids were 160, 160, and 150 fmol, respectively, for peaks A, B and C in an injection volume

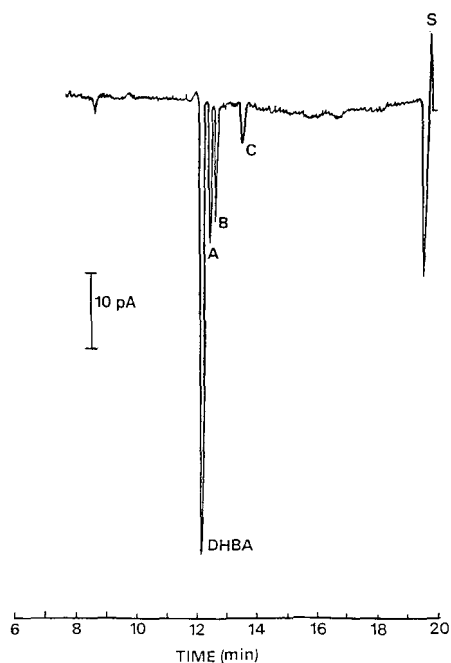


Fig. 2. Electropherogram of amino acids with indirect amperometric detection on a 26- $\mu\text{m}$  I.D. capillary: buffer, 0.1 mM DHBA–0.025 M MES (pH 5.50)–10% (v/v) ethanol; 72.1-cm-long separation capillary; 0.6-cm detection capillary; injection by electromigration, 3 s at 15 kV; separation voltage, 15 kV; electrode potential, 0.7 V vs. SSCE. Peaks: A = Lys; B = Arg; C = His; S = system peak (electroosmotic flow velocity).

of 1 nl (based on the electroosmotic flow-rate). This corresponds to detection limits ranging from 14 to 43 fmol. To calculate the detection limit we used two times the peak-to-peak noise measured over a period of baseline equal to ten peak widths at half height<sup>15</sup>. Thus, detection limits reported are twice those that would be calculated using three times the root-mean-square noise.

#### *Detection in narrow-bore capillaries*

An important parameter in indirect detection is the dynamic reserve (DR)<sup>16</sup>. This dimensionless parameter is defined as the ratio of the background signal to the noise on that signal. Using indirect amperometric detection, we have found DR values ranging from 50 to 300. This wide range of DR values appears to be the result of differences in electrode response between detectors. These differences are believed to be due mainly to varying electrode area, but could be caused by cracks in the carbon fiber. Variations in the procedure used to seal the small electrodes with epoxy could also increase the surface area of the electrode. Electrochemical noise is thought to be governed, in part, by the exposed electrode area. The DR can be used to determine the minimum concentration ( $C_{\text{lim}}$ ) that should theoretically be detectable under a given set of conditions.  $C_{\text{lim}}$  is defined as

$$C_{\text{lim}} = \frac{C_m}{(\text{DR})(R)}$$



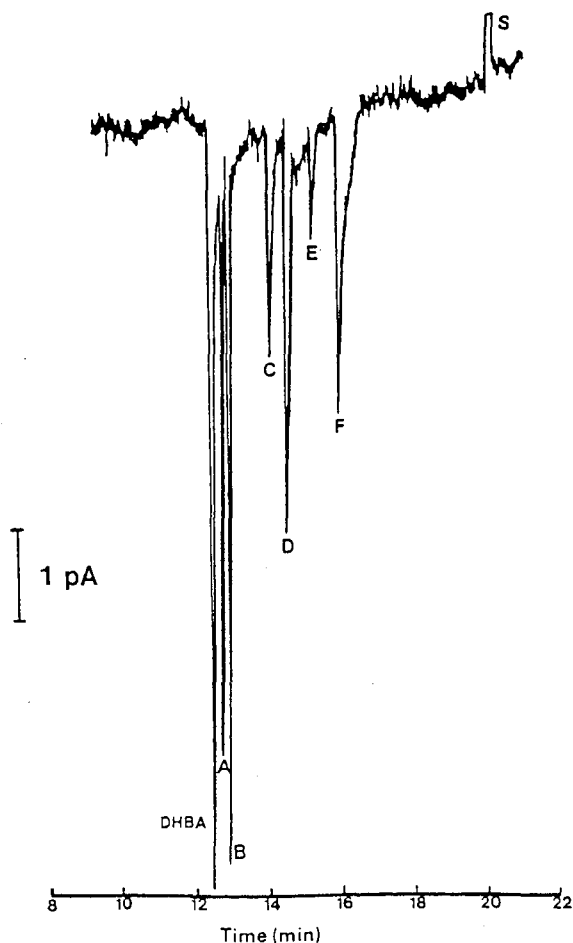


Fig. 3. Electropherogram of amino acids and peptides with indirect amperometric detection on a 9- $\mu\text{m}$  I.D. capillary: buffer, 0.01  $mM$  DHBA–0.025  $M$  MES (pH 5.65); 97-cm separation capillary; 1.0-cm detection capillary; injection, 1 s at 20 kV; separation voltage, 20 kV. Peaks: A = 8.5 fmol Lys; B = 8.2 fmol Arg; C = 7.4 fmol His; D = 7.0 fmol Arg-Leu; E = 6.4 fmol His-Gly; F = 5.8 fmol His-Phe; S = system peak.

where  $C_m$  is the concentration of the electrophore and  $R$  is the displacement ratio, which takes into account the net charges of the electrophore and analyte ions<sup>17</sup>. Although the displacement ratio can only be roughly estimated for zone electrophoresis, this equation is useful because it predicts that lowering the electrophore concentration will lead to lower detection limits. Fig. 3 shows an electropherogram obtained for the separation of three non-electroactive amino acids and three non-electroactive dipeptides by using an electrophore concentration only one-tenth that used for the data shown in Fig. 2. In this separation, the numbers of theoretical plates for each peak were calculated from the peak half-widths and were found to be 355 000 for Lys, 169 000 for Arg, 69 000 for His, 161 000 for Arg-Leu, 228 000 for His-Gly, and 71 000 for His-Phe. The amount of each substance injected ranged from 8.5 fmol for Lys to 5.8 fmol for His-Phe in an injection volume of 52  $\mu\text{l}$ . The detection

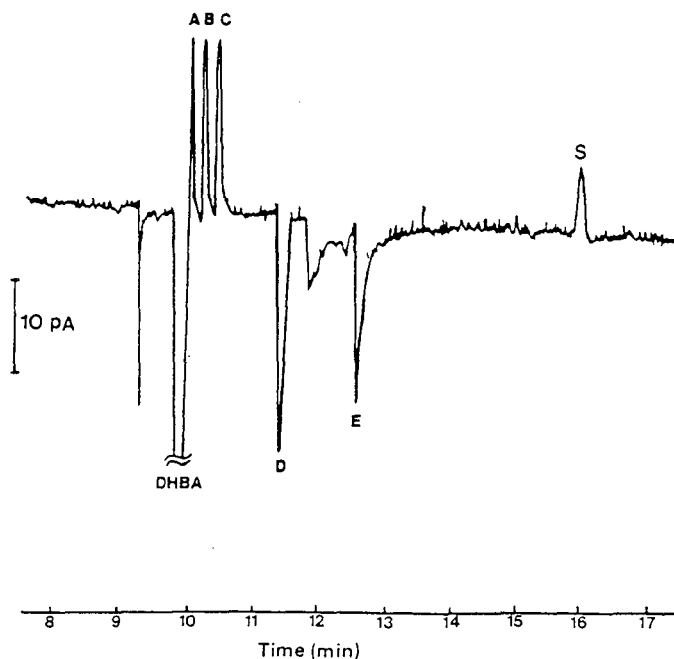


Fig. 4. Electropherogram of catecholamines and peptides with combined direct and indirect amperometric detection in a 9- $\mu\text{m}$  I.D. capillary. Conditions are the same as for Fig. 3, except as follows: injection, 5 s at 25 kV; separation voltage, 25 kV. Peaks: A = dopamine; B = norepinephrine; C = epinephrine; D = Lys-Phe; E = His-Phe. The broad peak between peaks D and E is an unknown impurity in the Lys-Phe.

limit for Arg was 530 amol injected. Detection limits as low as 380 amol have been obtained for Arg with this system (not shown).

#### *Simultaneous direct and indirect amperometric detection*

An advantage of indirect amperometric detection is the ability to determine both electroactive and non-electroactive species simultaneously. Fig. 4 shows the separation of three easily oxidized catecholamines and two non-electroactive dipeptides in a 9- $\mu\text{m}$  I.D. capillary. In this case, the detector is responding directly to the oxidation of separated catecholamines, and via the indirect mode for detection of the dipeptides. Total injections are 500 amol for each of the catecholamines, which corresponds to a detection limit of 74 amol when operated under these conditions. The amounts of dipeptides injected are 45 fmol for Lys-Phe and 37 fmol for His-Phe with corresponding detection limits of 5.2 and 5.5 fmol.

#### CONCLUSIONS

The results presented here demonstrate the utility of indirect amperometric detection with narrow-bore capillary electrophoresis. Separation efficiencies in the range from 69 000 to 355 000 theoretical plates are maintained with this method for the separation of relatively small molecules. A detection limit as low as 380 amol of Arg

has been achieved, and further buffer optimization could reduce this to the level of a few attomoles. In addition, amperometric detection has a distinct advantage over most other detectors in that it can easily be used in both the direct and indirect mode simultaneously. Combination of sensitive detection, instrumental simplicity and a universal nature make this a powerful approach to detection in capillary electrophoresis.

#### ACKNOWLEDGEMENTS

This material is based on work supported by the National Institutes of Health under Grant No. GM37621-03 and by Shell Development, Beckman Instruments, Sterling Research Group, Monsanto Company and Lilly Research. Andrew G. Ewing is the recipient of a Presidential Young Investigator Award (CHE-8657193) and is an Alfred P. Sloan Research Fellow.

#### REFERENCES

- 1 J. W. Jorgenson and K. D. Lukacs, *Science (Washington, D.C.)*, 222 (1983) 266.
- 2 M. J. Gordon, X. Huang, S. L. Pentoney and R. N. Zare, *Science (Washington, D.C.)*, 242 (1988) 224.
- 3 A. S. Cohen and B. L. Karger, *J. Chromatogr.*, 397 (1987) 409.
- 4 A. G. Ewing, R. A. Wallingford and T. M. Olefirowicz, *Anal. Chem.*, 61 (1989) 292A.
- 5 S. L. Pentoney, X. Huang, D. S. Burgi and R. N. Zare, *Anal. Chem.*, 60 (1988) 2625.
- 6 Y.-F. Cheng and N. J. Dovichi, *Science (Washington, D.C.)*, 242 (1988) 562.
- 7 R. A. Wallingford and A. G. Ewing, *Anal. Chem.*, 60 (1988) 258.
- 8 R. A. Wallingford and A. G. Ewing, *Anal. Chem.*, 60 (1988) 1972.
- 9 R. A. Wallingford and A. G. Ewing, *Anal. Chem.*, 61 (1989) 98.
- 10 R. A. Wallingford and A. G. Ewing, *Anal. Chem.*, 59 (1987) 678.
- 11 S. Hjertén, K. Elenbring, F. Kilar, J.-L. Liao, A. J. C. Chen, C. J. Siebert and M.-D. Zhu, *J. Chromatogr.*, 403 (1987) 47.
- 12 W. G. Kuhr and E. S. Yeung, *Anal. Chem.*, 60 (1988) 1832.
- 13 W. G. Kuhr and E. S. Yeung, *Anal. Chem.*, 60 (1988) 2642.
- 14 J. W. Jorgenson and K. D. Lukacs, *J. Chromatogr.*, 218 (1981) 209.
- 15 J. E. Knoll, *J. Chromatogr. Sci.*, 23 (1985) 422.
- 16 S. Mho and E. S. Yeung, *Anal. Chem.*, 57 (1985) 2253.
- 17 W. D. Pfeffer, T. Takeuchi and E. S. Yeung, *Chromatographia*, 24 (1987) 123.



CHROM. 21 859

## HIGH-EFFICIENCY LIQUID EXTRACTOR FOR ISOLATION OF A DESIRED MATERIAL FROM COMPLEX ORGANIC MIXTURES<sup>a</sup>

MAX BRENNER\*

*Institute of Organic Chemistry, University of Basle, St. Johannis-Ring 19, CH-4056 Basle (Switzerland)*  
and

CLAUDE MOIRANDAT and RONALD SCHLIMME

*SM Elektronik AG, Basle (Switzerland)*

---

### SUMMARY

A novel counter flow liquid extraction system is described that offers major potential advantages for the purification of fine chemicals and biochemicals. This system utilizes the flexibility of liquid extraction to provide a much more effective operating mode than is possible in elution chromatography. It is based on a novel contactor design which provides highly effective mass transfer, and is operated via a control system which facilitates process optimization.

The apparatus is a multi-stage liquid extractor with provision for independent control of each stream rate and also the feed schedule. It can therefore be operated in a wide variety of processing modes, including both transient and steady-state operation. One particularly useful mode for the batch purification of complex mixtures is described in detail. A transient feed to the centre of the column is combined with a stream rate ratio which reduces the migration velocity of the desired product to zero. All other species then pass out at one or other end of the column and operation is continued until dispersion begins to result in leakage of the desired material. It is shown by an extension of the plate theory of Martin and Synge that such an operation is much more efficient than that used in elution chromatography, and that its advantage increases with increasing difficulty of the separation. The column design is also an important feature in providing much higher resolution than conventional liquid extractors. Another important feature is a computer-controlled valving system which simplifies optimization and control of stream flows. The accessibility of sampling ports over the entire length of the extractor greatly facilitates control of the separation process.

---

### INTRODUCTION

The increasing need for the purification of complex chemical species not amenable to crystallization has led to increasing interest in chromatographic

---

<sup>a</sup> Presented at *AICHE Biotechnology Conference, New York, November 15-17, 1987, Session No. 165.*

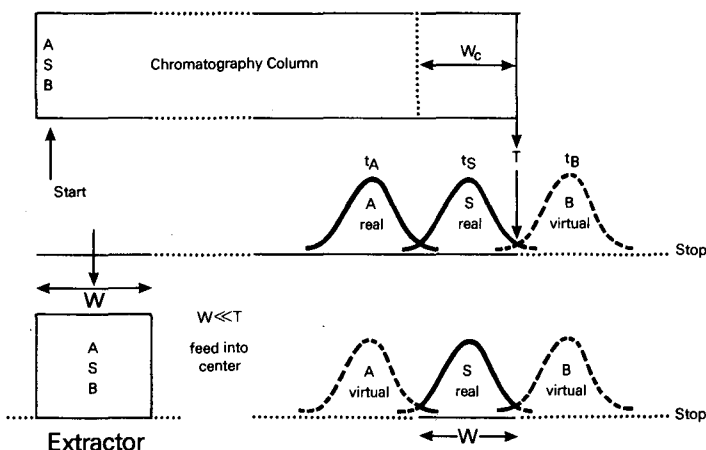


Fig. 1. Qualitative comparison of conventional elution chromatography with the proposed counterflow extraction system. Shown is the end of separation of a 1:1:1 mixture of closely related species A, S and B: Typically, the chromatographic peak width  $W_c$ , *i.e.*, the column length occupied by the wanted species S, is much smaller than the total column length  $T$  but similar to the total length of the extractor. Ideally, the extractor length and extractive peak width  $W$  are identical. The evident saving of equilibrium stages, expressed by  $W \ll T$ , reflects the superiority of dual- over single-flow operation.

techniques. These can achieve a very high resolution, but column packings are expensive, and the chromatographic mode does not use these packings efficiently. Column inefficiency arises in large part from the need to keep the solid phase stationary. In liquid extraction, this restriction can be relaxed in such a way as to reduce the required number of stages substantially. This point is illustrated in Fig. 1, where the separation of a 1:1:1 mixture A–S–B by conventional elution chromatography up to the beginning of elution of S is compared with the same separation by a transient counter-flow liquid extraction process.

We begin by contrasting these two processes qualitatively. To do this, we consider a chromatographic column and an extractor in which “plates” and “stages” are drawn to the same scale (*cf.*, Fig. 1). In normal elution chromatography, a narrow band of mixed solutes migrates from the feed end of the column and gradually separates into the partially overlapping bands at peak positions  $t_A$ ,  $t_S$  and  $t_B$  (imaginary), shown at the upper right section. In the process, the entire column volume is used at one time or another, but at all times most of it is essentially solute free and contributes nothing to the separation. The total number of plates required for this separation is  $T$ , but the maximum portion of the column occupied at any instant by S is the much smaller number of plates  $W_c$ .

In the extraction process, performed with  $W$  stages, the feed mixture is introduced to the central region of the separator, and the centre of mass of the desired solute, S, is stationary. Unwanted solutes, A and B, are discharged from the two ends of the column as indicated in the lower right section, and all stages of the extractor are helping to effect the separation, except at the very early stages. Operation is now continued until product leakage begins. To a first approximation, valid under the usual conditions of chromatographic separation, the total number of stages  $W$  required is now approximately  $W_c$ , the same number as those occupied in the chromatograph at

the end of the separation. The difference  $N = T - W_c$  may be considered the number of non-working plates in the chromatographic column.

Later we provide mathematical descriptions for these two processes, which provide the basis for quantitative comparison, and we show that the advantage of the proposed extraction mode increases with increasing difficulty of the separation. This is basically because the number of non-working plates  $N$  increases in proportion to the time required for separation while the number of working plates  $W$  increases only with the square root of time. First, however, we point out that a large number of stages,  $W$ , is required even for the extractor and therefore that there is a need to provide multi-stage operation at low capital cost. The solution we recommend for this purpose is the apparatus described in Figs. 2 and 3. We also note in this introductory section that an effective control system is needed for transient operations of this type. The approach that we use for this purpose is described under Apparatus.

#### ANALYSIS

We need a means of describing the migration of the centre of mass of each species and its spatial distribution about this centre. Here we provide such a description in the context of the apparatus shown in Figs. 2 and 3, and we introduce approximations to simplify the description and emphasize the key features of the system behaviour.

The column consists of two or more rotating cylinders (Fig. 3), each divided into a number of discrete stages by partitions perpendicular to the column axis (Fig. 2). Each stage has a total volume,  $v$ , of which a portion  $v_L$  is occupied by the lower phase L, and a portion  $v_U$  by the upper phase U. Each stage is totally liquid filled so that

$$v = v_L + v_U \quad (1)$$

and we define the hold-up ratio by

$$r = v_U/v_L \quad (2)$$

The upper phase is taken as moving to the right and the lower phase to the left. Rates of flow are defined by  ${}^0V_U$ ,  ${}^0V_L$  = volume of upper and lower phase, respectively, fed to the column per unit time. These volumetric flow-rates will be assumed to be constant over position and time during the analysis, neglecting volume changes accompanying the redistribution of solutes. In practice, however, the flow-rates will be manipulated during operation to establish the stationarity of the desired peak.

Analysis will be made in terms of *ideal* stages, defined as producing thermodynamic equilibrium between the two streams leaving each stage, but it is recognized that the physical stages in Figs. 2 and 3 may not be as effective as ideal stages. Therefore, we define a stage efficiency factor  $f$  by the relation

$$W_{\text{real}} = W_{\text{ideal}}/f \quad (3)^a$$

<sup>a</sup> The same ratio  $f$  exists between the final volumes of the respective product solutions, and between the amounts of solvents required in the ideal and the real processes that effect the same resolution; cf., footnote to eqn. 11. Depending on the operating conditions, the observed values of  $f$  range from 0.3 to 0.8.

where  $W_{\text{real}} =$  the number of real extractor segments needed to perform the same resolution as  $W_{\text{ideal}}$  ideal stages (*cf.*, *Extractor and column lengths*).

It will be assumed that  $f$  is a constant, but in reality it is expected to depend on the flow-rates of the streams and other operating conditions. In general,  $f$  may be significantly different for each species, but we will not consider such a refinement here. Ideal operation corresponds to assuming complete mixing and equilibrium within each stage but no mixing between stages.

Solutes injected into the centre of the column are subject to transport by the flowing phases. Their migration rates depend only on the volumetric stream rates and their ratio,

$$R = {}^0V_U/{}^0V_L \quad (4)$$

the hold up ratio,  $r$  (eqn. 2), and the respective partition coefficients,  $K_X$  of solute X is defined by

$$K_X = [X]_U/[X]_L \quad (5)$$

the brackets and subscripts denoting equilibrium concentrations of X in the upper and the lower phase, respectively<sup>a</sup>.

We describe the migration rates as displacements  $\Delta$  (in terms of stage numbers) of the centre of mass produced on feeding volumes  $V_U$  and  $V_L$  of the upper and lower phases, respectively:

$$\Delta_X = \Delta_{U,X} - \Delta_{L,X} \quad (6)$$

where

$$\Delta_{U,X} = (V_U/v_U)(1 - Q_X); \quad \Delta_{L,X} = (V_L/v_L)Q_X \quad (7)$$

and the probability of residence of X in the lower phase is

$$Q_X = 1/(1 + K_X r) \quad (8)$$

The concentration ratio  $K_X$ , which depends on the physical properties of solute X and the phases involved in the distribution of X, shares its impact on that distribution with the volume ratio  $r$  of the said phases within the system (hold-up ratio) (*cf.*, eqns. 2 and 8). The mass distribution of X between the phases is thus a function of the product  $K_X r$ , the reciprocal of which in partition chromatography is termed "capacity factor", and denoted by  $k'_X$ .

Considering the equal weights of  $K$  and  $r$  in eqn. 8, and the increase in descriptive

<sup>a</sup> In partition chromatography,  $K_X$  is defined by the ratio of concentrations of X in the moving (numerator) and in the stationary (denominator) phase, whereas in adsorption chromatography  $K_X$  would be related to the reciprocal of the adsorption coefficient. For convenience it is assumed that  $K_X$  is independent of the overall concentration. Clearly, partition coefficients in liquid-liquid and in liquid-solid systems depend on different mechanisms and generally cannot be expected to be of the same order.



and experimental range covered by their product, we adopt

$$K_X r = 1/k'_X \quad (9)$$

as the operating variable actually governing the overall behaviour of X in the distribution process. Treating  $K_X$  as the variable would unduly reduce the role of  $r$  to that of a parameter and unnecessarily complicate the following discussion.

It must be emphasized in this context that the hold-up ratio  $r$  is to some extent, depending on the type of apparatus, amenable to choice by the operator. Thus, within the constraints defined by physical realities (stage geometry, flow mechanics, bulk phase mixing), there exists an important degree of freedom with respect to optimization of the numerical value of  $k'_X$ .

Dispersion of solutes about the centre of mass for an idealized system can be obtained very simply by extending the concept of equilibrium stages introduced by Martin and Synge<sup>1</sup> to motion of both phases. This is because the Poisson distribution of a solute X derived for the motion of a single phase is determined completely by the variance  $\sigma_X^2$ , which in turn is just equal to the net displacement of X. Since variances due to individual disturbances in a linear system are additive, one may then write for any solute X that the variance for motion of both phases is just the sum of those for the individual motions:

$$\sigma_{X,\text{ideal}}^2 = \Delta_{U,X} + \Delta_{L,X} \quad (10)$$

with

$$\sigma_{X,\text{real}}^2 = \sigma_{X,\text{ideal}}^2/f \quad (11)^a$$

where it should be noted that both contributions  $\Delta$  are now positive. Note that both  $\Delta_{U,X}$  and  $\Delta_{L,X}$ , the magnitudes of migrations resulting from the motions of X by the individual phases in terms of numbers of ideal stages, are dimensionless, as is  $\sigma_X^2$ .

The description of the solute distributions may be simplified by noting that Poisson distributions can be adequately approximated by the normalized Gaussian probability distribution function

$$\varphi(u)\Delta u = (2\pi)^{-1/2} \exp[-u^2/2]\Delta u \quad (12)$$

with

$$u = w_X/\sigma_X \quad (12a)$$

$$\Delta u = (1/\sigma_X)\Delta w_X \quad (12b)$$

where  $w_X$  = distance, on either side, from the maximum of peak X, in terms of the respective number of plates, where  $\varphi(u)$ , the probability density for a deviation between  $u$  and  $u + \Delta u$  from the maximum, is to be determined;  $\sigma_X$  = standard deviation of the Poisson distribution; *cf.*, eqn. 10;  $\Delta w_X = 1$  (width of one plate).

<sup>a</sup> Eqn. 11 reflects the ratio  $\sqrt{f}$  of the widths of calculated and observed mass distributions in ideal and real systems that are effected by throughput of the same amounts of solvents; *cf.*, footnote to eqn. 3.

Eqn. 12a provides a convenient means of defining the width of a solute band in a chromatographic column or an extractor. Thus, the width of the S peak in Fig. 7 may be denoted by

$$W = 2u\sigma_S \quad (13)$$

where  $u$  is the number of standard deviations on either side of the peak considered to comprise a major fraction of the solute band. Numerically, the respective fraction corresponds to the area  $A$  enclosed by the curve  $\varphi(u)$  and the abscissa within  $u = \pm u$ , and is given by

$$A = 2 \int_0^u \varphi(u) du \quad (14)$$

Values of  $A$  are tabulated in any treatise on statistics: limits  $u = 2$  or  $2.33$  define areas representing 95.45 or 99% of the total peak area, which is defined by the limit  $u = \infty$ .

We shall show (*cf.*, eqn. 20a), for a desired solute S, that the displacement  $\Delta_S$  becomes zero when the flow ratio  $R$  (*cf.*, eqn. 4), is set to

$$R = 1/K_S \quad (15)^a$$

Assume that we have a stationary peak, formed under this condition, finally extending over the whole length of the extractor. Assume that length corresponds to  $u = 2$  or  $2.33$  standard deviations on each side of the peak centre. On the basis of the notions above, we conclude that the mass of S represented by this peak corresponds to 95 or 99% of the total S distributed in the operation. We can therefore quantitatively express S recoveries from distributions, observing that missing material is not lost, but recoverable from the eluates collected during the operation.

Assume we have (Fig. 7) an extractor containing sufficient plates to accommodate the stationary S peak assumed above and, in addition, the migrating peaks A and B, emerging from peak S, on the grounds of the presence of contaminants A and B, where  $K_B > K_S > K_A$ , and the respective weights are  $m_A = m_S = m_B$ . The separation of species S from contaminant B is readily observed as a distance between peak centres S and B,  $\Delta_B - \Delta_S$ , which can be expressed as a multiple  $u$  of the sum  $\sigma_B + \sigma_S$ . Thus,

$$\Delta_B - \Delta_S = u(\sigma_B + \sigma_S) \quad (16)$$

When  $u = 2$  or  $3$ , we speak of 4- or 6- $\sigma$  separations between S and B. On the basis of the notions above, the 4- $\sigma$  separation, followed for example by stagewise withdrawal and pooling of the extractor contents from extractor stage 0 (centre of S peak) up to stage  $+2\sigma_S$  (approximate site of the S peak front), corresponding to that half of the S peak facing the B peak, would provide a recovery of an S fraction representing 47.5% of all

<sup>a</sup> The formalism of diffusion leads to the same general conclusion, verified by experiment<sup>2</sup>.

S originally present, with an S content of 95% and a B content of 5%. The opposite half of the peak would obviously provide an S fraction with an S content of 100%.

The number  $u$ , characteristic of the degree of a given separation (recovery, purity), will be denoted as the "separation parameter".

An approximate estimation of peak widths in terms of standard deviations is possible in practice by concentration measurements at various distances from the peak centre, considering that the concentration in the extractor of solute X at  $u = 2$  or 3 is about 10 or 100 times smaller than at  $u = 0$  [cf., the respective ordinates  $\phi(u)$  of the Gaussian probability distribution function].

## APPARATUS

### *Separation unit*

The extractor consists essentially of two or more serially connected horizontal cylinders of the kind shown schematically in Figs. 2 and 3. They rotate about their axes, and each is divided into a large number of narrow segments, which act as the separation stages. To provide these segments the cylinder is coaxially partitioned by tightly fitting circular discs, held in place by PTFE gaskets. A small opening at the periphery of each disc provides for inter-segment communication. Aligning these openings yields a channel for flow of liquid throughout the entire cylinder. Each cylinder end bears a cover perforated at its centre to accommodate a non-rotating piping system. It provides separate access to the lower and upper section of the adjacent segment (Fig. 2).

Neighbouring cylinder ends are connected by means of their respective piping. The piping at the outer cylinder ends serve for throughput of U, *e.g.*, from left to right, and for throughput of L in the opposite direction, assuming the separation unit is completely filled with a partially miscible solvent pair. Clearly, such throughput requires the channels of serial cylinders to be aligned and to be immersed in the same particular phase which is going to be transferred. Phase throughput is timed by the cylinders' rotation and, consequently, pulsed.

The upper section of Fig. 3 shows a transient position of the communicating holes above the phase boundary, allowing for throughput of a pulse of upper phase U. The opposite situation, allowing for throughput of a pulse of lower phase L, is pictured in the lower section. Onset and shutdown of the pulses are programmable as a function of periodically attained angular positions of the communicating holes<sup>3</sup>. Fig. 3 shows

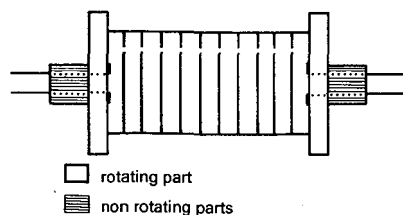


Fig. 2. Separation cylinder (schematic) with inlets and outlets for the flowing phases, and holes in the partitioning walls which provide for interchamber communication. Not shown are additional holes in the cylinder wall which allow samples to be drawn. At least two such cylinders are aligned to form the basic element of the extractor (*cf.*, Fig. 3).

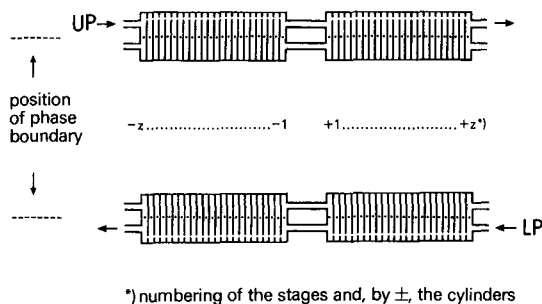


Fig. 3. Phase transfer coupled to cylinder rotation: periodic passage of the communicating holes through space occupied by UP and LP, respectively, allows for alternate pulsed throughput of solvent streams coming from opposite ends of the system, and thus effects a quasi-continuous counterflow.

also the serial numbering of the elements  $\pm 1, \pm 2, \dots, \pm z$ , the numbers and the cylinders left or right from the centre bearing a negative or positive sign, respectively. The centre of the system coincides with the location of the feed (*cf.*, Fig. 4).

Owing to differing surface tensions, the walls of the segments (glass, PTFE or stainless steel) become unequally wetted by U and L. The better wetting phase tends to form a film which, on rotation, is drawn through the lesser wetting phase. Back in its mother phase this film is replenished. This concept was introduced by Signer<sup>4</sup>.

The film and its immediate surroundings represent a mixing zone, and the bulk phases constitute the conjugate settling zone. No additional stirring is required to promote solute transport between the phases. Such transport is admittedly slower than in a dispersion of droplets, but this is partly compensated for by the system's insensitivity to the presence of emulsifiers.

Permissible rates of rotation must still be determined by practical experience, but satisfactory operation has generally been obtained over a range of 0.3–2 rad/s ( $\approx 3$ –20 rpm). Mixing between phases becomes a problem at too low a speed, and film detachment (with excessive formation of droplets) when the system is rotating too fast. Some of the segments, equidistant from each other, are equipped with sampling holes (ports) drilled into the cylinder wall.

This design offers important advantages. The horizontal orientation of the column makes it possible to stop the operation for sampling purposes and solves many of the problems associated with flooding. Together with the valve controls discussed below, it makes possible the accurate control of phase ratios. The gentle motion of the rotating disk surface minimizes emulsification and at the same time provides good bulk mixing within each compartment.

#### *Valve and piping systems*

Computer-controlled on-off valves are provided for each inlet and outlet stream, as indicated in Fig. 4. These valves permit the input and output flows of both solvents and feed streams to be controlled. They can be used for withdrawal of product from the central region of the extractor after a transient separation process, and to compensate for flow ratio changes between the right and left extractor sections, relative to the feed point, in the case of repeated feeds.

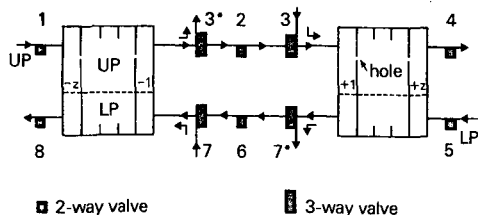


Fig. 4. The inner valving system. Valve functions and respective valve conditions are summarized in Table I.

Pumps P1 and P5 in Fig. 5 operate continuously on the U and L reservoirs shown, to pump liquid from the reservoirs to valves 1A and 5A. These valves then provide either input or circulation of the phases (valve 1A, upper phase; valve 5A, lower phase). Valves 1L and 5L are used to readjust the phase boundary levels as needed. Thus, if the boundary in stage  $-z$  (Fig. 5) is too low it can be raised by energizing valves 5A, 5, 6, 1 and 1L, which is a single programmable operation (*cf.*, Table I).

Figs. 4 and 5 show the valve positions and functions needed for column operation. It must be recognized that there are two types of valves used: (1) two-way valves, indicated by a single black square can only provide straight-through flow and are either open (energized, +) or closed (de-energized, -); (2) three-way valves, shown as black oblongs, can provide flow in either of two directions, as indicated by arrows. When not energized (-) they provide what shows as straight-through flow in the figure. When energized (+) they provide the branched flow indicated.

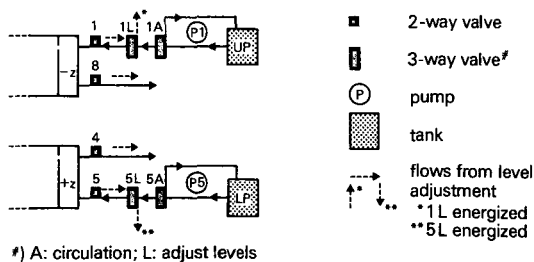
The various valve positions needed for extractor operation are summarized in Table I.

*Control unit*

The complex sequence of valve sequences needed for operation of this apparatus is automated by an electronic control unit which performs the following functions:

- (1) All of the valve positions listed in Table I are automatically synchronized.
- (2) Operation is based on a master cycle which corresponds to one rotation of the cylinders, and the time periods for each set of valve positions are determined by the

**Solvent Supply/Level Adjustment**



\*) A: circulation; L: adjust levels

Fig. 5. The outer valving system: see caption to Fig. 4.

TABLE I  
VALVE CONDITIONS FOR EXTRACTOR OPERATION

Function	Valve conditions (+ or -)													
	1	2	3	3*	4	5	6	7	7*	8	1A	1L	5A	5L
Throughput of U	+	+	-	-	+	-	-	-	-	-	+	-	-	-
Throughput of L	-	-	-	-	-	+	+	-	-	+	-	-	+	-
Input of feed in U <sup>a</sup>	-	-	+	-	+	-	-	-	-	-	-	-	-	-
Input of feed in L <sup>a</sup>	-	-	-	-	-	-	-	+	-	+	-	-	-	-
Output of product in U <sup>b</sup>	+	-	-	+	-	-	-	-	-	-	+	-	-	-
Output of product in L <sup>b</sup>	-	-	-	-	-	+	-	-	+	-	-	-	+	-
Pressure build up (U input)	+	+	-	-	-	-	-	-	-	-	+	-	-	-
Pressure release (U output)	-	+	-	-	+	-	-	-	-	-	-	-	-	-
Pressure build up (L input)	-	-	-	-	-	+	+	-	-	-	-	-	+	-
Pressure release (L output)	-	-	-	-	-	-	+	-	-	+	-	-	-	-
Increase of $r$ in stage $-z^c$	+	-	-	-	-	-	-	-	-	+	+	-	-	-
Decrease of $r$ in stage $-1, -z^c$	+	-	-	-	-	+	+	-	-	-	-	+	+	-
Increase of $r$ in stage $-1, -z^c$	+	-	-	-	-	+	+	-	-	-	+	-	-	+
Decrease of $r$ in stage $+1, +z^c$	+	+	-	-	-	+	-	-	-	-	-	+	+	-
Increase of $r$ in stage $+z, +1^c$	+	+	-	-	-	+	-	-	-	-	+	-	-	+
Decrease of $r$ in stage $+z^c$	-	-	-	-	+	+	-	-	-	-	-	-	+	-
All flows stopped	-	-	-	-	-	-	-	-	-	-	-	-	-	-

<sup>a</sup> By gravity; transient and continuous process.

<sup>b</sup> Transient process.

<sup>c</sup> See Figs. 3, 4 and 5 for numbers and locations of stages.

angular positions of the communicating holes in the discs. Both the initiation and duration of each setting are programmable to specify:

- (i) throughput of the upper and lower phases;
- (ii) input of feed, which may be dissolved in either solvent (batch or continuous operation);
- (iii) withdrawal of product, again from either phase (only batch operation);
- (iv) withdrawal of upper or lower phase (reflux, in case of continuous operation);
- (v) input of upper or lower solvent without concomitant output (pressure adjustment);
- (vi) output of upper or lower phase without concomitant input (pressure adjustment);
- (vii) reversal of sense of rotation (to eliminate any propeller effect, no valves are affected);
- (viii) vacant: all flows stopped.

The present controller can produce any desired combination of program steps (up to 80) within any one program cycle. The "zero" point (beginning) of the master cycle is programmable and must be set to coincide with the crossing of the communicating holes from the lower to the upper phase.

## SAMPLE CALCULATIONS

*Extractive mode*

We now illustrate operation of the extractor by showing how one may isolate a desired species S from a solution contaminated with closely related species A and B, using the extractive mode described briefly above.

*Operating principle*

We start the separation by dissolving as much as possible of the mixture A-S-B in the phase which is the better solvent, avoiding, however, viscosities that prevent easy flow through the piping and valves which lead the solution into the stage assembly. The volume of the feed solution should not exceed one tenth of the extractor volume. The equilibrated extractor is set in rotation, and phase throughput is initiated at a flow ratio  $R = 1$  or, if  $K_S$  is approximately known,  $R \approx 1/K_S$ .

The extractor is now ready for input of the feed. This input is pulsed, the feed pulses replacing totally or partly the pulses of the respective phase throughput (*cf.*, Fig. 3). Any desired sequence of the two sorts of pulses can be programmed. This program is changed to replace feed pulses by solvent pulses when the feed solution is used up. The operation is then continued until the distribution of S broadens to the point of noticeable leakage of S from the ends of the extractor.

Clearly, replacement of ideal (= instantaneous) by gradual feed input as described above is not without effect on the mass profile of the final solute distribution. However, calculations and practice show that the distortion of the ideal Poisson profiles is moderate enough to be neglected in the prediction and control of experimental separations.

We do not need an exact knowledge of  $K_S$  and its dependence on solution composition. Instead, we can find the required flow ratio  $R$  by trial and error, *i.e.*, by monitoring the evolution of the S distribution through the sample ports and making heuristic adjustments of the solvent streams as the separation proceeds. We do this by making a series of semi-quantitative measurements of relative concentrations of S along the entire length of the extractor.

This is indicated in Fig. 6, which refers to an actual example, the isolation of a cyclosporin derivative from 200 g of raw material in an extractor composed of 200 segments containing a total volume of 20 l. Shown here are spots on three thin-layer chromatograms obtained from samples drawn at three different states of the operation, defined by the respective *total* solvent throughputs  $V_1, V_2, V_3$  where  $V_i = (V_U + V_L)_i$ , and *overall* flow ratios  $R_1, R_2, R_3$  where  $R_i = (V_U/V_L)_i$ :

State defined by:	Samples drawn from segments:
$V_1 = 0.297$ l; $R_1 = 1.16$	– 12 to + 15 yielded spots (top) which reveal a complex distribution of a largely unresolved mixture centered around the feed point
$V_2 = 16.915$ l; $R_2 = 1.23$	– 100 to + 100 yielded spots (centre) now revealing an advanced state of purification, with the centre of mass of the cyclosporin peak almost ideally located

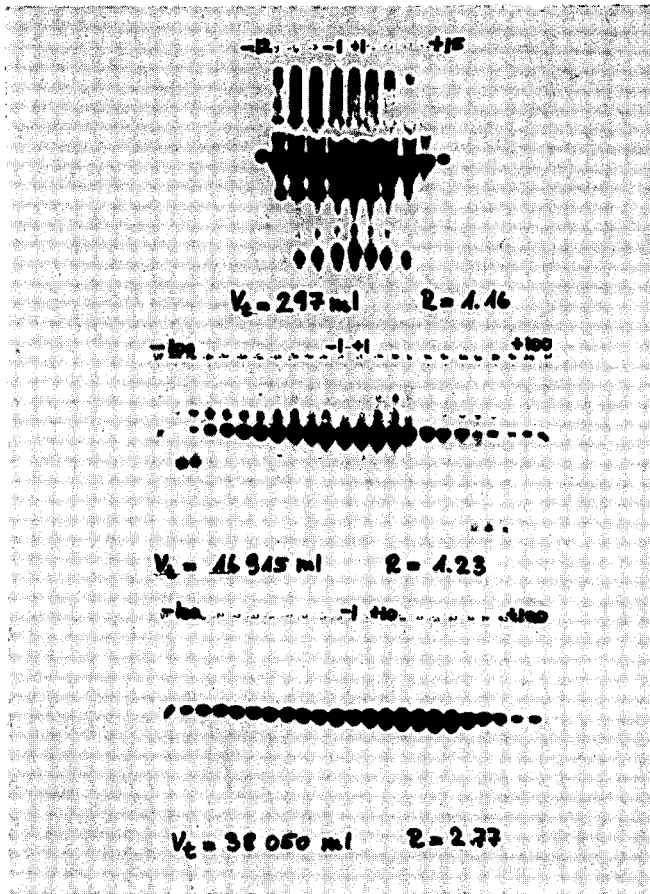


Fig. 6. Example of thin-layer chromatographic monitoring of the evolution of an extractor separation, and of heuristic manipulation thereof.

$V_3 = 38.050$  l;  $R_3 = 2.77$  — 100 to +100 yielded spots (bottom) revealing a pure cyclosporin peak, asymmetric owing to the more difficult elimination of material eluted to the left by the lower phase.

Note the continuing increase in  $R$ , first necessary to keep the wanted peak centred in the extractor, and later necessary to avoid product loss with outgoing lower phase<sup>a</sup>.

#### *Stage requirements*

We now show how such an extractor may be designed by considering some representative hypothetical situations: we assume mixtures of equal amounts of A,

<sup>a</sup> Evidently, all manipulations that involve monitoring distributions and adjustment of solvent streams are amenable to full automation<sup>5</sup>.



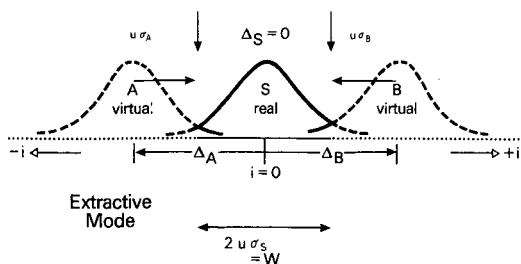


Fig. 7. Extractive mode. Ternary A-S-B (1:1:1) separated up to incipient loss of S. Shown are the elements of calculation used in the long column approximation assuming the separating system to extend beyond the actual extractor boundaries. The virtual peaks are imaginary.  $\pm i$  = serial stage number;  $i = 0$ , location of the feed point.  $u$  = number of standard deviations  $\sigma$  providing a desired recovery and purity of species S. Vertical arrows point to actual extractor boundaries. The figure corresponds to  $\sigma_{AS} = \sigma_{SB}$  and  $k' = 1$ , producing a symmetrical distribution with respect to the feed point:  $\Delta_A = -u(\sigma_A + \sigma_S)$ ;  $\Delta_B = +u(\sigma_S + \sigma_B)$ . The drawing shows a resolution such that  $u = 2$  on both sides of the S peak.

S and B; we consider conditions such that  $K_A < K_S < K_B$ , and for convenience we shall assume that

$$K_B/K_S = K_S/K_A = \alpha \quad (17)$$

where  $\alpha$  is the separation factor; and we note that the extractor operates best with holdup ratios (eqn. 2), between 1/4 and 4, and we therefore choose as representative examples  $r = 1/4, 1$  and 3.

Our purpose is to determine the number of ideal stages  $W_{ideal}$  needed for a given degree of purification in terms of the fractional removal of contaminants A and B from a ternary A-S-B mixture subjected to extraction. The number of ideal stages  $W_{ideal}$  for the separation is that which will just hold species S within the extractor at the end of the separation operation. To find that number, we first shall consider 4- $\sigma$  separations of S from binaries A-S and S-B as examples. The extension to corresponding 6- $\sigma$  separations will then be quite obvious.

*Binaries A-S and S-B.* We base calculations on the mathematical assumption that the extractor is infinitely long, as suggested in Fig. 7. Then the calculated required length of the actual extractor needed, in terms of the number of chambers, is given by eqn. 13, with the proviso that  $\sigma_x^2$  (cf., eqn. 10), is known, which by eqn. 7 calls for a knowledge of the turnover numbers  $V_U/v_U$  and  $V_L/v_L$ . These are interrelated by the holdup and volume ratios  $r$  and  $R$ , and related to the sums  $V = V_U + V_L$  (the total volume throughput) and  $v = v_U + v_L$  (the total plate volume) in the following manner:

$$V_U/v_U = (V/v)[(R/(1+R))[(1+r)/r]] \quad (18)$$

$$V_L/v_L = (V/v)[(1+r)/(1+R)] \quad (19a)$$

For convenience,  $V_L/v_L$  as expressed by eqn. 19a, is termed the "volume factor",

$$V_L/v_L = \Phi \quad (19b)$$

Now note (Fig. 7 and eqn. 6), that

$$\Delta_S = \Delta_{U,S} - \Delta_{L,S} = 0$$

or, from eqns. 2, 7, 15, 19a and 19b

$$= \Phi_S(K_S R - 1)Q_S \quad (20a)$$

$$= [\text{volume factor}][\text{mobility factor}]$$

where  $\Phi_S$  so far is indeterminate, but (eqn. 15),  $K_S R = 1$  and (eqns. 8 and 9),

$$Q_S = k'/(1 + k') \quad (21a)$$

where, for convenience,  $k'$  is an abbreviation defined by

$$k' = k'_S \quad (22)$$

Note further (eqn. 10), that

$$\begin{aligned} \sigma_S^2 &= \Delta_{U,S} + \Delta_{L,S} \\ &= \Phi_S(K_S R + 1)Q_S \end{aligned} \quad (23a)$$

while (eqns. 15 and 17),

$$\Delta_A = \Phi_A[(1/\alpha) - 1]Q_A < 0 \quad (20b)$$

and

$$\sigma_A^2 = \Phi_A[(1/\alpha) + 1]Q_A \quad (23b)$$

where (eqns. 8, 9, 17 and 22)

$$Q_A = \alpha k'/(1 + \alpha k') \quad (21b)$$

and

$$\Delta_B = \Phi_B(\alpha - 1)Q_B > 0 \quad (20c)$$

$$\sigma_B^2 = \Phi_B(\alpha + 1)Q_B \quad (23c)$$

with

$$Q_B = k'/(a + k') \quad (21c)$$

where all  $\Phi$ s are still indeterminate. However, as may be seen from Fig. 7,

$$\Delta_A = \Delta_{AS} = -u(\sigma_A + \sigma_S) \quad (24a)$$

determining a simultaneous value  $\Phi_{AS}$  for  $\Phi_A$  and  $\Phi_S$ ;

$$\Delta_B = \Delta_{SB} = +u(\sigma_S + \sigma_B) \quad (24b)$$

determining a simultaneous value  $\Phi_{SB}$  for  $\Phi_B$  and  $\Phi_S$ .

On the basis of these equations, especially remembering the condition expressed by eqn. 15, we derive expressions for the volume factors  $\Phi_{AS}$ ,  $\Phi_{SB}$  (*cf.*, Appendix, eqns. 40 and 41) and for  $V_{AS}$ ,  $V_{SB}$  in eqns. 19a and 19b, and hence arrive at the following approximations for  $W$ :

Case 1: separation A-S:

$$W = W_{AS} = 2u\sigma_{AS}$$

(*cf.*, eqn. 13), which from eqns. 15 and 23a

$$\begin{aligned} &= 2u(\Phi_{AS} \cdot 2Q_S)^{0.5} \\ &= W_{AS}(u^2, \alpha, k') \end{aligned} \quad (25)$$

(*cf.*, Appendix, eqn. 25a, and Fig. 8).

Case 2: separation S-B:

$$\begin{aligned} W &= W_{SB} = 2u\sigma_{SB} \\ &= 2u(\Phi_{SB} \cdot 2Q_S)^{0.5} \\ &= W_{SB}(u^2, \alpha, k') \end{aligned} \quad (26)$$

(*cf.*, Appendix, eqn. 26a, and Fig. 8).

When  $k' = 1$ , then eqns. 25 and 26 reduce to

$$W_{AS} = W_{SB} = 4u^2 \cdot \frac{\alpha + 1}{\alpha - 1} \quad (27)$$

Eqn. 27 represents a useful approximation of eqns. 25 and 26 because, within the accessible range, the  $k'$  dependence of  $W$  is moderate.

*Ternaries A-S-B.* Assuming equal amounts of the components A, S and B, and using eqns. 25 and 26, one must choose the larger of the two values to obtain the desired separation of S with respect to neighbouring A or B. The separation of S from the opposite neighbour B or A is then better than estimated from the value of  $u$ . Thus, the plate requirement for the separation of a 1:1:1 ternary with separation factors  $\alpha_{AS} = \alpha_{SB}$  is conveniently read from graphs of the type shown in Fig. 9, which is derived

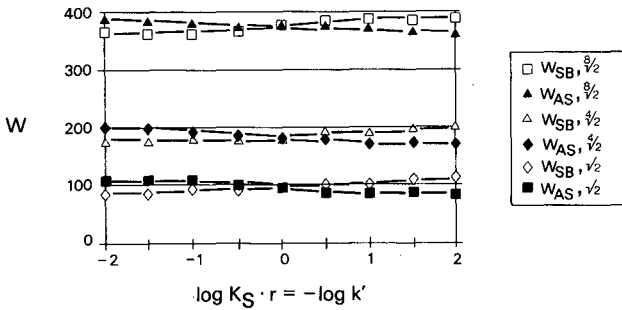


Fig. 8. Extractive mode: binaries. Stage number requirements,  $W_{AS}$  and  $W_{SB}$ , for desired separations ( $4\sigma$ ) of binaries A-S or S-B (1:1), retaining S and eluting A by LP, or B by UP. Data based on separation factors  $\alpha_{AS} = \alpha_{SB} = 2^{1/2}, 2^{1/4}, 2^{1/8}$ .

from data in Fig. 8. If the separation factors for the two binary pairs A-S and S-B are different, then the above calculation of  $W$  may tentatively be made only for the smaller factor. Caution is indicated.

Evaluation of the separation of ternaries composed of unequal weights of A, S and B can also be based on eqn. 14. However, overlaps cannot be estimated in terms of overlapping peak areas, with the  $u$ -scale on the abscissa, unless the individual peaks of A, S and B are drawn on individual ordinate scales  $\varphi(u)$  that are proportional to the underlying masses  $m_A, m_S$  and  $m_B$ .

*Separating power of a given set of  $W$  stages.* In practice, the separation power of an extractor is fixed by the number  $W$  of its stages. Suppose  $W = 120$ , and a binary A-S distributed until S appears in the effluents from stages  $-60$  and  $+60$ . What is then the degree of separation of S from A in terms of  $u = u'$ , when  $\alpha = \sqrt{2}$  and  $k' = 10^{1.5}$ ?

One way to find the answer comes from inspection of the algebraic form of eqn.

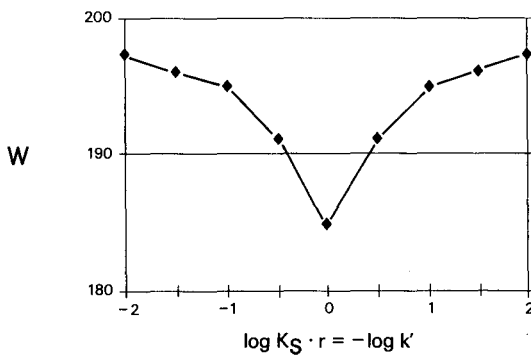


Fig. 9. Extractive mode: ternaries. Stage number requirements,  $W$ , for desired separations ( $4\sigma$ ) of ternaries A-S-B (1:1:1), retaining S and eluting A by LP, and B by UP. Data based on separation factors  $\alpha_{AS} = \alpha_{SB} = 2^{1/4}$ , and taken from  $W$ s for binaries in Fig. 8, selecting the larger value within each pair  $W_{AS}, W_{SB}$  as explained in the text.

25, using calculated values of  $W_{AS}$ . Accordingly, 105 stages would provide a  $4\text{-}\sigma$  separation, *i.e.*,  $u = 2$ . Therefore, with 120 stages available,

$$(u')^2 = 2^2(120/105)$$

and  $u' = 2.14$ .

#### Recoveries and purity

The boundaries of the extractor affect the system behaviour, because solutes cannot be returned to the system by non-existent streams. The error introduced into the calculation of the distribution of S by assuming an infinite extractor is small, because loss of S is negligible. The errors for A and B, however, are significant, but proper allowance for them is difficult mathematically<sup>6</sup>. We therefore content ourselves here by noting that the long-column approximation overestimates the contamination of S by A and B, and therefore provides a conservative estimate.

#### Chromatographic mode

We now turn our attention to the extraction analogue of elution chromatography, to justify the comparison already shown in Fig. 1.

#### Operation principle

Note that the extractor described above can be operated in a chromatographic mode and then provides a system which simulates partition chromatography; we just shift the feed point to the stage next to the inlet of either of the phases, the upper phase for example, and then suppress the flow of the lower phase. Accordingly, stage numbering  $t$  becomes unidirectional and begins at the feed point. Finally, using chromatographic language, stages become plates (*cf.*, Figs. 1 and 10).

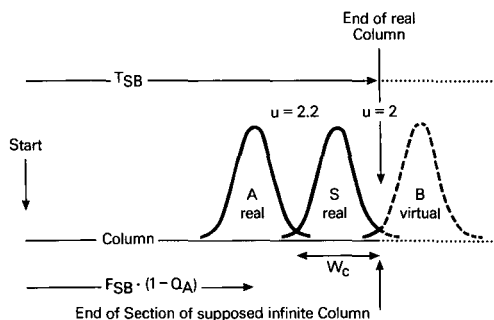


Fig. 10. Extractor in chromatographic mode. Ternary A-S-B (1:1:1) separated up to incipient loss of S. Shown are the elements of calculation used in the long column approximation, assuming the column to extend beyond its actual length,  $T_{SB}$ , in terms of ideal plates. The virtual peak is imaginary.  $u = 2$ , number of standard deviations  $\sigma_S$  and  $\sigma_B$  providing the desired resolution between species S and B;  $u = 2.2$ , measure of the resulting resolution A-S, due to inherent distribution asymmetry;  $W_c$ , width of the S peak;  $F_{SB}$ , turnover number of the mobile phase per plate which brings the front of the S peak up to  $T_{SB}$ ;  $F_{SB}(1 - Q_A)$  is the concomitant displacement  $\Delta_A$ . The figure corresponds to  $\alpha_{AS} = \alpha_{SB} = 2^{1/2}$  and  $k' = 1$ .

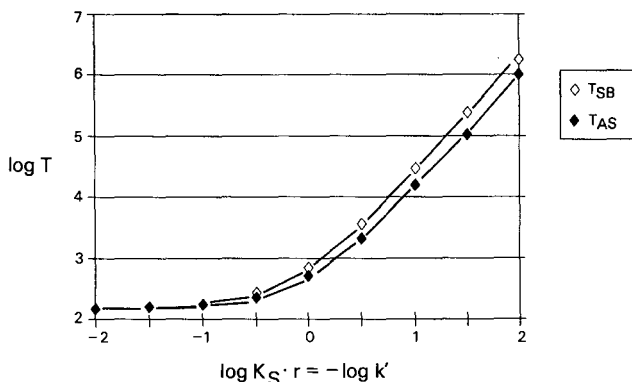


Fig. 11. Chromatographic mode: binaries. Stage number requirements  $T_{AS}$  and  $T_{SB}$  for desired separations ( $4\sigma$ ) of binaries A-S or S-B (1:1), retaining A and eluting S, or retaining S and eluting B. Data based on separation factors  $\alpha_{AS} = \alpha_{SB} = 2^{1/2}$ .

#### Plate requirements

We base the discussion on Fig. 10, in which the situation at the end of the chromatographic process in a column with  $T_{SB}$  plates is shown; peak B would be present in a hypothetical column of infinite length. The column length, in terms of its number of plates  $T$  needed for the separation of binaries, can be derived in the manner used above by combinations of displacements  $\Delta_c$  from the origin and standard deviations  $\sigma_c = \sqrt{\Delta_c}$ , the suffix  $c$  referring to the chromatographic mode. The procedure, familiar to chromatographers, is outlined in the Appendix (*cf.*, eqns. 27a-34).

*Binaries A-S and S-B.* The column length needed for the separation of A from S (not shown in Fig. 10), or S from B (*cf.*, Fig. 10) is described by eqn. 32 or 33. The peak width of S after removal of B<sup>a</sup> is given by eqn. 34.

Graphs of eqns. 32-34, when  $\alpha_{AS} = \alpha_{SB}$ , are shown in Figs. 11 and 12.  $T_{AS}$  is always slightly smaller than  $T_{SB}$ . It may be recalled at this point that there was no such fixed relation between  $W_{AS}$  and  $W_{SB}$ . Both  $T_{SB}$  and  $W_{SB}$  represent column lengths required for S-B separations with retention of S and removal of B. There is no such symmetry between  $T_{AS}$  and  $W_{AS}$ : the former refers to removal of S with retention of A, the latter to removal of A with retention of S.

*Ternaries A-S-B.* Assuming equal amounts of A, S and B in a ternary, and  $\alpha_{AS} = \alpha_{SB}$ , the stage requirement for separation in the extractive mode was defined by the larger of the two numbers  $W_{AS}$ ,  $W_{SB}$ . That number equalled the width of the S peak. Now, adopting the same assumptions with respect to the properties of the ternary, we define the plate requirement for separation in the chromatographic mode by the larger number  $T_{SB}$ . The separation S-B to be expected is then characterized by the value of the parameter  $u$  which was used in calculating  $T_{SB}$  by eqn. 33. How good is the separation A-S at this stage of the process (Fig. 10)? It must be better (characterized, for example, by  $u = 2.2$ ), since the A-S separation could have been achieved with a shorter column (*cf.*, Fig. 11).

<sup>a</sup> Driving B beyond the plate with serial number  $T_{SB}$  in the infinitely long column is considered as an equivalent to elution from the last plate ( $T_{SB}$ ) of a finite column.

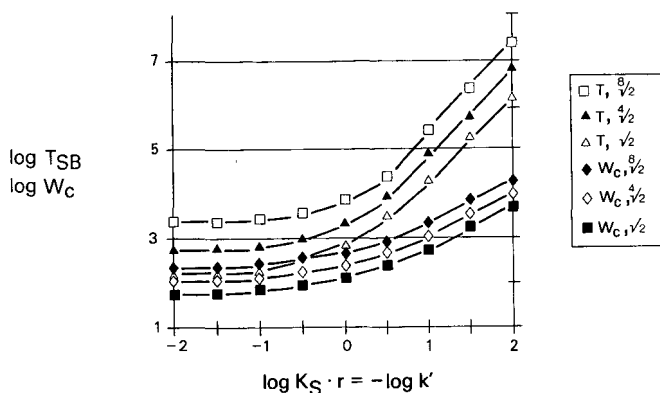


Fig. 12. Chromatographic mode: binaries. Stage number requirements,  $T_{SB}$ , and space requirement,  $W_c$ , for desired separations ( $4\alpha$ ) of binaries S-B (1:1), retaining S and eluting B (cf. Fig. 1). Data based on separation factors  $\alpha_{AS} = \alpha_{SB} = 2^{1/2}, 2^{1/4}, 2^{1/8}$ .

#### EXTRACTIVE VERSUS CHROMATOGRAPHIC MODE

##### Stage and plate requirements for binary separations S-B, with retention of S

For comparison, calculated stage and plate number requirements for the separation of S from binaries A-S and S-B, and from the ternary A-S-B by the extractive and the chromatographic modes are presented in Figs. 8, 9, 11, 12 and 13 as functions of the variable  $K_{Sr} = 1/k'$ , with separation factors  $\alpha = 2^{1/2}, 2^{1/4}$  and  $2^{1/8}$  as parameters. The lower groups of curves in Figs. 12 and 13 furnish a further comparison of corresponding peak widths  $W_c$  and  $W_{SB}$ .

All data refer to  $4\sigma$  separations, *i.e.*, to a numerical value of 2 for the separation parameter  $u$ , corresponding to about 95% recovery of S from a supposed symmetrically distributed 1:1:1 ternary. Multiplication of these data by 1.36 or 2.25 yields plate numbers theoretically required for 99 and 99.7% recoveries, respectively. Recall in this context the slight distribution asymmetry due to  $W_{AS} \neq W_{SB}$ , and  $T_{SB} \neq T_{AS}$ , and the section on *Recovery and purity*. The range of  $K_{Sr}$ , chosen from 0.01 up to 100, is broader than is accessible in practice. It is assumed to illustrate trends. Also,  $\alpha = 2^{1/8}$  presents a lower limit to feasibility in the extractor.

##### Extractor and column lengths

A straightforward comparison is based on  $W (= W_{SB})$  and  $T_{SB}$  (cf., Fig. 13). Clearly, there is a stage-saving effect of dual flow, and it becomes increasingly attractive with increasing difficulty of the separation. Extractors with several hundred real stages, with a stage efficiency<sup>a</sup> of about 50%, may well match separation by chromatography, especially when the demand on yields is lessened: minor elution (cf., Fig. 7) of S from either or both of its peak ends in order to wash out contaminating peak tails of A and/or B is equivalent to an increase in extractor length. A yield-saving alternative is offered by repetition of a run after recovery and concentration of the

<sup>a</sup> See footnote to eqn. 3.

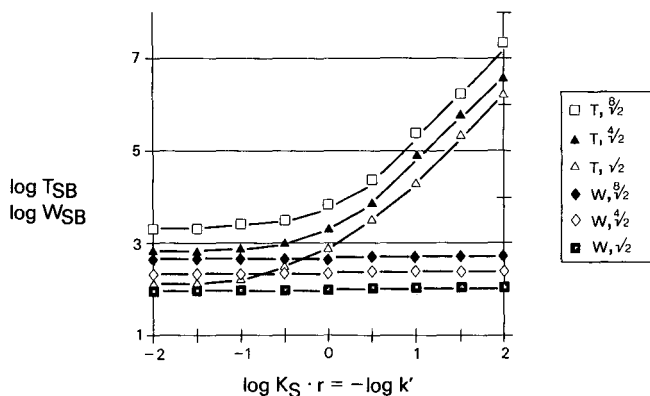


Fig. 13. Extractive versus chromatographic mode: binaries. Stages  $W_{SB}$  and plates  $T_{SB}$  required for desired separations ( $4\sigma$ ) of binaries S-B (1:1), retaining S, eluting B. Data based on separation factors  $\alpha_{AS} = \alpha_{SB} = 2^{1/2}, 2^{1/4}, 2^{1/8}$ .

reactor contents. In fact, with each repetition the mass of contaminants A and B in the tails of the outgoing peaks will drop in geometrical progression.

#### Space requirements of retained S

In the Introduction, the number of extractor stages  $W \approx (W_{SB})$  accommodating S was said to be expected to be of the same order as the number of column plates  $W_c$  occupied by S after elution of B (Fig. 1). In fact, this holds only when  $k' \approx 1$ . The deviations from expectation as shown by Figs. 12 and 13 appear as a consequence of the impact on peak widths of the migration mechanism. The displacement  $\Delta$  of a peak and its standard deviation  $\sigma$  (or peak width), when effected by uni- or bidirectional flow, are based on mobility probabilities which are characteristically different.

In the chromatographic mode (*cf.*, Appendix, eqns. 27a and b and 28a and b), the standard deviation  $\sigma_x = \sqrt{[F(1 - Q_x)]}$  depends, apart from the volume factor  $F$ , exclusively on the probability  $(1 - Q_x)$  for residence of X in the mobile phase.

In the extractive mode (eqns. 23a-c),

$$\sigma_x = \sqrt{[\Phi(K_x R + 1)/(K_x r + 1)]} = \sqrt{[\Phi([R/r]K_x r + 1)/(K_x r + 1)]} \quad (23d)$$

depends, apart from the volume factor  $\Phi$ , on both  $(1 - Q_x)$  and  $Q_x$ , the probabilities for residence of X in UP and in LP, but with weight  $R/r$  for  $1 - Q_x$  and weight 1 for  $Q_x$ . Therefore, the extractive peak widths  $W$  are similar at all values of  $k'$ , whereas the chromatographic peak widths  $W_c$  change rapidly with small shifts in  $k'$ , even within the chromatographically preferred range of  $k' = 3-10$ .

#### Solvent consumption

The feasibility of a separation process depends on the equipment and on the solvent consumption. Comparison from this aspect of the extractive and the chromatographic modes must be done under comparable situations. For example, operations may be considered to start with a solvent-charged extractor and a conditioned column, and to end with the extractor and column ready for a restart. It



may further be considered that these conditions are met by draining the final product solution off the extractor, followed by recharging with fresh solvent on the one hand, and by total non-gradient elution of all materials from the column on the other.

It appears convenient to state solvent consumption in terms of multiples of the total volume of an extractor stage or a column plate. Of course, these multiples are related to the turnover numbers  $\Phi$  and  $F$ .

#### Extractive mode

For the extractive separation of a ternary A-S-B, the so-defined solvent consumption is derived from the volume factor  $\Phi$  (*cf.*, eqns. 19a and b and Appendix, eqns. 40 and 41) belonging to the larger value  $W_{AS}$  or  $W_{SB}$  (Figs. 8 and 9) used to perform the separation. Hence, the total relative volume  $V_{et}/v$  required in the extractive mode is given by (eqns. 19a and b, 25 and 26)

$$V_{et, AS}/v = V_{AS}/v + W_{AS} = \Phi_{AS}[(1 + R)/(1 + r)] + W_{AS} \quad (35a)$$

or by

$$V_{et, SB}/v = \Phi_{SB}(1 + R)/(1 + r) + W_{SB} \quad (35b)$$

Recall that  $V_{et}$  is biphasic, being composed of UP and LP. Note the explicit dependence of  $V_{et}$  on the holdup ratio  $r$ . It adds to an implicit dependence which via  $k'$  is hidden in  $\Phi$ . There is no comparable dependence on the flow ratio  $R$  because the latter is a parameter fixed by the relationship given in eqn. 15.

Graphs combined from the functions 35a and 35b, by choice of the larger ordinate  $V_{et, AS}/v$  or  $V_{et, SB}/v$  at each abscissa, are shown in Fig. 14 with holdup ratios  $r = 0.25, 1$  and  $3$  as parameters. It must be noted that the choice of  $r$  fixes the point on the abscissa corresponding to  $\log K_S r$  when  $K_S$  is fixed by the nature of the feed and the solvent.

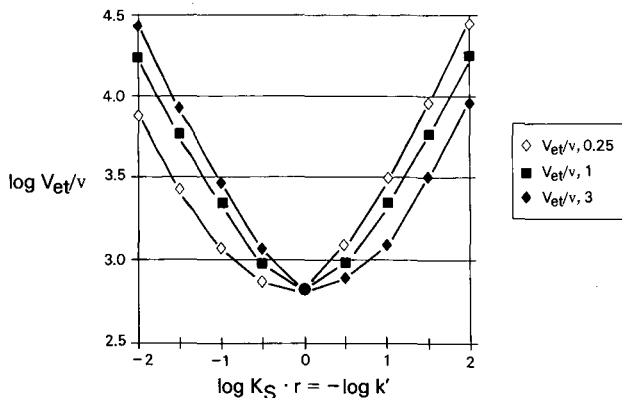


Fig. 14. Extractive mode: solvent consumption. Desired separations ( $4\sigma$ ) of ternaries A-S-B (1:1:1), based on  $W$  stages, where  $W$  is the larger value selected from the pair  $W_{SB}, W_{AS}$  (*cf.*, Figs. 8 and 9), require a total solvent volume  $V_{et}$  as defined in the text. This figure shows relative volumes  $V_{et}/v$  at holdup ratios  $r = 0.25, 1$  and  $3$ , when  $\alpha_{AS} = \alpha_{SB} = 2^{1/2}$ .

Minimizing the solvent consumption is seen to involve just a shift via  $r$  of the product  $K_{S^r}$  as close to 1 as is physically possible in view of the hydrodynamics of the system. This shift will be accompanied by another advantage, *i.e.*, a slight simultaneous decrease in the stage number requirement (*cf.*, Fig. 9). Adaptable holdup ratios thus prove to be a valuable feature of the equipment presented in this paper.

#### Chromatographic mode

Turning to the chromatographic mode, proceeding up to complete elution of the slowest moving species A (at least  $3\sigma$  with respect to the tailing half of the peak), we must remember that it is always eqn. 33 which determines the column length (separation of S with respect to neighbouring B). Complete elution of A from a column of  $T_{SB}$  plates requires at least the volume

$$V_{ct} = V_{R,A} + 3V_{R,A}/\sqrt{T_{SB}} \quad (36)$$

where

$$V_{R,A} = T_{SB}v[r/(1+r)]/(1-Q_A) \quad (37)$$

is the retention volume of A, and

$$\sigma_{V,A} = V_{R,A}/\sqrt{T_{SB}} \quad (38)$$

is the standard deviation about  $V_{R,A}$ . Hence (eqn. 21b),

$$V_{ct}/v = (r/1+r)(1+\alpha k')(T_{SB} + 3\sqrt{T_{SB}}) \quad (39)$$

Recall that  $V_{ct}$  is monophasic. Note again the explicit dependence on the phase ratio  $r$ .

Graphs of the function 39 are shown in Fig. 15 with holdup ratios  $r = 0.25$ , 1 and 3 as parameters. Note the differences when compared with Fig. 14: there is no

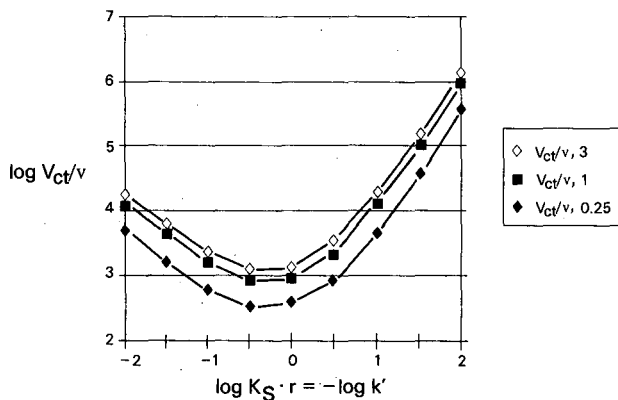


Fig. 15. Chromatographic mode: solvent consumption. Desired separations ( $4\sigma$ ) of ternaries A-S-B (1:1:1), based on  $T_{SB}$  plates (*cf.*, Fig. 12), require a total solvent volume  $V_{ct}$  as defined in the text. This figure shows relative volumes  $V_{ct}/v$  at holdup ratios  $r = 0.25$ , 1 and 3, when  $\alpha_{AS} = \alpha_{SB} = 2^{1/2}$ .

curve crossing, and the minima are displaced to  $\log K_{S'} < 0$ . However, the remarks with respect to the evaluation of Fig. 14 apply, and the minimization rule remains valid.

*Extractive versus chromatographic mode*

With the proviso of identical holdup ratios in the extractor and the chromatographic column, we deduce from Figs. 14 and 15 that the latter, within the range of  $k'$  accessible to chromatography, offers a slight advantage with respect to solvent consumption. However, the adaptability of the holdup ratio, characteristic of the extractor, is largely non-existent with columns, and the estimate of  $V_{ct}/v$  according to the previous section is highly conservative.

#### HARDWARE AND APPLICATIONS

Several units of the type described above have been built and put into operation. The smallest, shown in Fig. 16 (Mechanische Werkstätte Max Kohler, Basle, Switzerland) consists of two glass cylinders, each 15.26 m  $\times$  5 cm I.D. Each consists of 282 stages and five interdispersed sampling chambers. The former (latter) have a width of 0.4 (1) cm and contain about 7.7 (19) ml of liquid. The cylinders are arranged parallel to each other, with U-turns for the flows and a feed port in each line. The unit is equipped with a motor and a controller, located near stages  $\pm 1$ , with two solvent reservoirs, two receiving flasks and two ceramic pumps, located near stages  $\pm 282$ . The supporting bench is movable.

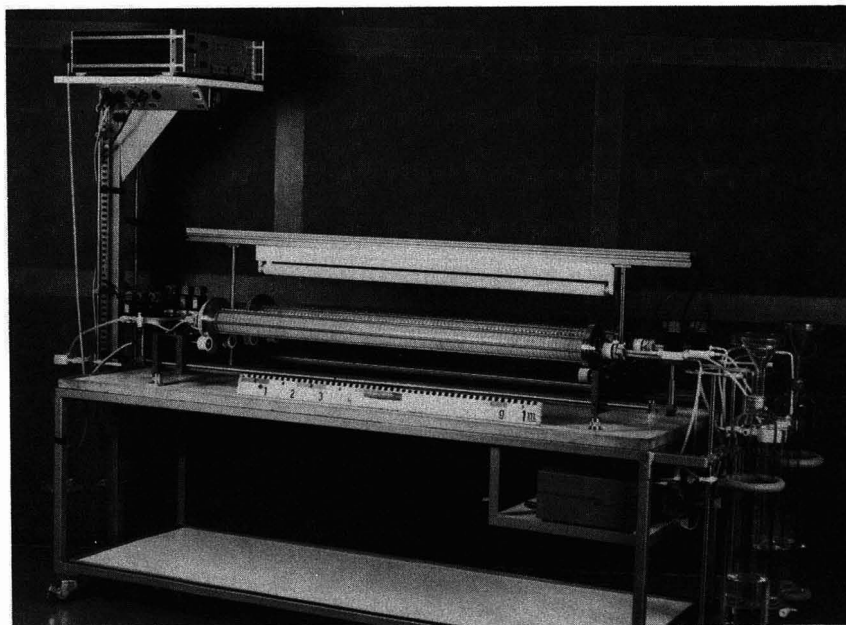


Fig. 16. Laboratory-scale extractor. Volume, 4.5 l; feed  $\leq$  450 ml; motor and controller near feed point, pumps, solvent reservoirs and receiving flasks at opposite end, movable bench.

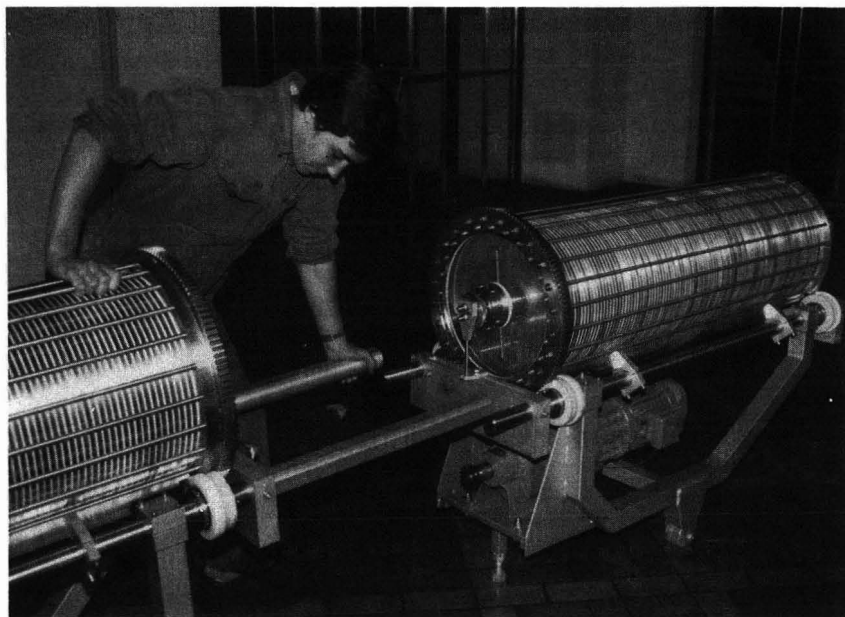


Fig. 17. Assembling two cylinders, pilot-scale extractor. Volume, 250 l; feed  $\leq 25$  l; explosion-proof motor underneath, other accessories located in a separate room; movable.

The larger, shown in Fig. 17 (Mechanische Werkstätte Max Kohler), is intended for pilot-scale operation and has an I.D. of 40 cm. It consists of two cylinders (stainless steel) mounted end to end, each with 100 inner stages of width 1 cm and two outer stages with terminating glass walls. Each inner stage is accessible through a sampling hole.

Results obtained on peptide purifications with the smaller unit were reported by a group from Smith Kline and French Laboratories<sup>7</sup>. A more detailed discussion of that work will be provided in a forthcoming paper.

#### SYMBOLS

$A$	area defined by the normalized Gaussian probability distribution function; eqn. 14
$A$	contaminant of S, with smaller affinity to upper phase than S
$A'$	contaminant of S, with smaller affinity to upper phase than A
$\alpha_{ij}$	separation factor $K_S/K_A$ or $K_B/K_S$ ; $\alpha_{ij} = K_i/K_j > 1$
$B$	contaminant of S, with greater affinity to upper phase than S
$B'$	contaminant of S, with greater affinity to upper phase than B
$\Delta_X$	total displacement from the origin of the centre of mass of the migrating species X
$\Delta_{L,X}$	displacement from the origin of the centre of mass of the migrating species X, effected by flow only of LP
$\Delta_{U,X}$	displacement from the origin of the centre of mass of the migrating species X, effected by flow only of UP

$f$	an empirical efficiency factor, relating for a given degree of resolution, $W_{\text{real}}$ to $W_{\text{ideal}}$ ; <i>cf.</i> , eqn. 3; for a given throughput of solvent, by $\sqrt{f}$ , real (= observed) and ideal (= theoretical) peak widths; <i>cf.</i> , eqn. 11
$\varphi(u)$	ordinates in the normalized Gaussian probability distribution function
$F_{ij}$	volume factor (chromatographic mode); eqns. 28 and 29
$\Phi_{ij}$	volume factor (extractive mode); eqn. 19b
$\pm i$	serial numbering of reactor stages; <i>cf.</i> , Figs. 3–5
$k'$	chromatographic capacity factor for species S, synonym of $1/K_S r$
$K_X$	partition coefficient of species X; eqn. 5
L, LP	lower phase
$m_X$	mass of species X present in a mixture or, after separation, represented by the respective peak in a distribution profile
$N$	non-working plates in a chromatographic column
$Q_X$	probability of residence of solute X in the lower phase; eqns. 21a–c
$r$	holdup ratio $v_U/v_L$ , <i>i.e.</i> , ratio of volumes of light (upper) and heavy (lower) phase present in a plate or stage; eqn. 2
$R$	flow ratio, <i>i.e.</i> , ratio of volumetric stream rates ${}^0V_L$ and ${}^0V_U$ passing through an extractor; eqn. 4
S	species to be separated from contaminants A and B present in a ternary A–S–B
$\sigma_X$	standard deviation about $\Delta_X$
$\sigma_X^2$	variance about $\Delta_X$ ; eqn. 10
$\sigma_{ij}$	standard deviation about displacement $\Delta$ of species $i$ or $j$ after a separation process involving $i$ and $j$ ; eqns. 25 and 26
$\sigma_{v,x}$	standard deviation about $V_{r,x}$ ; eqn. 38
$t$	serial numbering of plates in a chromatographic column; <i>cf.</i> , Fig. 1
$t_X$	position of peak X in a chromatographic column; <i>cf.</i> , Fig. 1
$T$	total number of plates in a chromatographic column; <i>cf.</i> , Fig. 1
$T_{ij}$	$T$ required for separation of species $i$ and $j$ by elution of the faster moving one; Fig. 13, eqns. 27a and b and 28a and b
$u$	variable in the normalized Gaussian probability distribution function; eqns. 12 and 14
$u$	separation parameter, a measure of resolution defined by eqn. 16, or a preset value of the variable $u$ providing a desired resolution; eqns. 25, 26, 32 and 33
$u'$	resolution to be expected by a given number $W$ of stages
U, UP	upper phase
$v$	total volume of liquid present in a plate or stage; eqn. 1
$V$	sum of $V_L + V_U =$ total solvent volume used during an extractive separation
$V_{ij}$	$V$ needed for the separation of species $i$ and $j$
${}^0V_L$	volumetric stream rate of LP
${}^0V_U$	volumetric stream rate of UP
$V_{\text{et}}, V_{\text{ct}}$	total solvent volumes required for extractive and chromatographic separations of a ternary, with complete recovery of the feed

$V_{m,ij}$	effluent volume of mobile phase (driving the faster component of a binary beyond a certain plate of an infinitely long chromatographic column); eqns. 28 and 29
$V_{R,X}$	retention volume of species X in elution chromatography; eqn. 37
$v_L, v_U$	volumes of LP and UP present in a stage or plate
$V_L, V_U$	total volumes of LP and UP used during an extractive separation process
$W$	number of extractor stages
$W_{ideal}$	number of ideal extractor stages required to store a wanted species S being separated from A and/or B
$W_{real}$	$= W_{ideal}/f$ which is the real number of extractor stages required to store S; eqn. 3
$W_{ij}$	$W_{ideal}$ required to separate species $i$ and $j$ by retention of either and elution of the other one; eqns. 25 and 26
$W_c$	peak width of species S at impending elution from a chromatographic column
$[X]$	concentration of species X in a solution
$\pm z$	ultimate serial stage numbers in reactor cylinders (+) and (-); <i>cf.</i> , Figs. 3-5

## APPENDIX

*Stage requirements*

From eqns. 20b, 21a and b and 24a

$$(\Phi_{AS})^{1/2} = u \cdot \frac{[(\alpha k' + 1)/k']^{1/2} \{(\alpha + 1)^{1/2} + [2(\alpha k' + 1)/(k' + 1)]^{1/2}\}}{\alpha - 1} \quad (40)$$

From eqns. 20c, 21a and c and 24b

$$(\Phi_{SB})^{1/2} = u \cdot \frac{[(\alpha + k')/k']^{1/2} \{(\alpha + 1)^{1/2} + [2(\alpha + k')/(k' + 1)]^{1/2}\}}{\alpha - 1} \quad (41)$$

From eqns. 25 and 40

$$W_{AS} = u^2 \cdot \frac{2\{2(\alpha k' + 1)/(k' + 1) + [2(\alpha + 1)(\alpha k' + 1)/(k' + 1)]^{1/2}\}}{\alpha - 1} \quad (25a)$$

From eqns. 26 and 41

$$W_{SB} = u^2 \cdot \frac{\alpha\{2(\alpha + k')/(k' + 1) + [2(\alpha + 1)(\alpha + k')/(k' + 1)]^{1/2}\}}{\alpha - 1} \quad (26a)$$

*Plate requirements*

For the binary A-S separation we have (*cf.*, Fig. 10)

$$T_{AS} = \Delta_{cS} - u\sigma_{cS} = F_{AS}(1 - Q_S) - u[F_{AS}(1 - Q_S)]^{0.5} \quad (27a)$$

$$= \Delta_{cA} + u\sigma_{cA} = F_{AS}(1 - Q_A) + u[F_{AS}(1 - Q_A)]^{0.5} \quad (27b)$$

where

$$F_{AS} = (V_{m,AS}/v)[(1+r)/r] \quad (28)$$

$F_{AS}$  is the "volume factor" separating A-S, and has the dimension of a total turnover number of the mobile phase present in a plate;

$(1 - Q_X)$  = probability of residence of X in the mobile phase (UP); it represents in this context the "mobility factor" of species X.  $Q_S = Q_S(k')$ ,  $Q_A = Q_A(\alpha, k')$  (cf., eqns. 9 and 21a and b);

$V_{m,AS}$  = effluent volume of mobile phase needed for the separation of A-S;

$vr/(1+r)$  = fraction of the plate volume occupied by mobile phase.

For the binary S-B separation we have (cf., Fig. 10)

$$T_{SB} = \Delta_{cB} - u\sigma_{cB} = F_{SB}(1 - Q_B) - u[F_{SB}(1 - Q_B)]^{0.5} \quad (28a)$$

$$= \Delta_{cS} + u\sigma_{cS} = F_{SB}(1 - Q_S) + u[F_{SB}(1 - Q_S)]^{0.5} \quad (28b)$$

where

$$F_{SB} = (V_{m,SB}/v)[(1+r)/r] \quad (29)$$

$F_{SB}$  is the "volume factor", separating A-S;  $F_{SB} \neq F_{AS}$ , because  $V_{m,SB} \neq V_{m,AS}$ ;

$1 - Q_X$ ; see comment on eqns. 27a and b;  $Q_B = Q_B(\alpha, k')$  (cf., eqn. 21c);  $Q_S = Q_S(k')$  (cf., eqn. 21b).

Each of the pairs of eqns. 27a and b and 28a and b can now be solved to obtain

$$(F_{AS})^{1/2} = \frac{u}{[1/(k' + 1)]^{1/2} - [1/(\alpha k' + 1)]^{1/2}} \quad (30)$$

and

$$(F_{SB})^{1/2} = \frac{u}{[\alpha/(k' + \alpha)]^{1/2} - [1/(k' + 1)]^{1/2}} \quad (31)$$

and these are used to determine the column lengths.

From eqns. 27b and 30

$$T_{AS} = u^2 \cdot \frac{[(\alpha k' + 1)/(1 + k')]^{1/2}}{\{[(\alpha k' + 1)/(1 + k')]^{1/2} - 1\}^2} \quad (32)$$

From eqns. 28b and 31

$$T_{SB} = u^2 \cdot \frac{[\alpha(k' + 1)/(k' + \alpha)]^{1/2}}{\{[\alpha(k' + 1)/(k' + \alpha)]^{1/2} - 1\}^2} \quad (33)$$

From eqn. 28b we deduce for the peak width  $W_c$  of species S

$$W_c = 2u[F_{SB}(1 - Q_S)]^{0.5} \quad (34a)$$

which from eqn. 29 becomes

$$W_c = u^2 \cdot \frac{2}{[\alpha(k' + 1)/(k' + \alpha)]^{1/2} - 1} \quad (34)$$

#### ACKNOWLEDGEMENT

We thank Professor E. N. Lightfoot, Department of Chemical Engineering, University of Madison, WI, U.S.A., for his encouraging and enthusiastic help in the preparation of the manuscript.

#### REFERENCES

- 1 A. J. P. Martin and R. L. M. Synge, *Biochem. J.*, 35 (1941) 1358.
- 2 R. E. Cornish, R. C. Archibald, A. E. Murphy and M. H. Evans, *Ind. Eng. Chem.*, 26 (1934) 397.
- 3 F. G. Müller, *U.S. Pat.*, 3 782 624, 1974.
- 4 R. Signer, in E. Müller (Editor), *Houben Weyl, Methoden der Organischen Chemie*, Georg Thieme Verlag, Stuttgart, Vol. 1/1, 1958, p. 332.
- 5 M. Brenner, *U.S. Pat.*, 4 698 159, 1987.
- 6 A. M. Lenhoff and E. N. Lightfoot, *Chem. Eng. Sci.*, 41 (1986) 2795.
- 7 J. L. Hughes, D. Stevenson, M. Edelstein and K. Tubman, *American Institute of Chemical Engineers, 1987 Annual Meeting, with Biotechnology Conference, New York*, extended abstracts, No. 165K.



CHROM. 21 709

## GAS CHROMATOGRAPHIC STUDY OF THE SOLUTION THERMODYNAMICS OF ORGANIC SOLUTES IN TETRAALKYLAMMONIUM ALKANESULFONATE AND PERFLUOROALKANESULFONATE SOLVENTS

RENA M. POMAVILLE and COLIN F. POOLE\*

*Department of Chemistry, Wayne State University, Detroit, MI 48202 (U.S.A.)*

---

### SUMMARY

The partial molar Gibbs free energy, enthalpy, and entropy of solution for a number of test solutes are determined in five pairs of tetraalkylammonium alkanesulfonate and perfluoroalkanesulfonate salts that are liquid at 121°C. The presence of fluorine is shown to reduce retention due to dispersive interactions, to have little influence on orientation and electron-donor interactions, and to have a large influence on proton-donor interactions. These properties are correlated with the weak dispersive interactions characteristic of highly fluorinated solvents and the inductive effect of fluorine which affects the electron density on the sulfonate group.

---

### INTRODUCTION

Highly fluorinated stationary phases have been used in gas chromatography (GC) for the separation of chemically reactive compounds such as metal halides, interhalogen compounds, and the halides of hydrogen, sulphur, and phosphorus<sup>1</sup>. Fluorinated stationary phases also show unique selectivity for the separation of fluorocarbon homologues and freons. They have not been accepted, however, for general use in GC due to their poor support coating characteristics manifesting themselves in low column efficiencies and poor film stability at moderate to high temperatures. Fluorocarbon groups also exhibit weak support deactivating properties resulting in columns of high activity exhibiting poor peak shape for polar molecules. The film stability, column efficiency and support deactivating properties of highly fluorinated solvents can be dramatically enhanced by incorporating polar anchor groups into the solvent structure using poly(perfluoroalkyl ethers)<sup>1–3</sup>, fluorocarbon surfactants containing polar functional groups<sup>4,5</sup> and tetraalkylammonium perfluoroalkanesulfonate salts<sup>6</sup>. The organic salt phases have low melting points, upper column operating temperature limits in the range 160–220°C, and acceptable chromatographic properties towards a wide range of polar solutes<sup>6</sup>. The alkanesulfonate analogues of the fluorinated salts are easily prepared and provide a convenient model system to study the influence of replacing alkane chains by perfluoroalkane chains on retention. In an earlier study it was shown that retention changes were significant and could be qualitatively explained by two types of behavior;

weak intermolecular interactions with the perfluorocarbon chain tending to diminish retention in a non-specific manner and selective retention of proton-donor solutes resulting from the high electronegativity of fluorine and its inductive effect<sup>6</sup>. In this paper a quantitative interpretation of solute-solvent interactions in the perfluoroalkanesulfonate salts is attempted to better explain the above observations using chemical thermodynamics.

## EXPERIMENTAL

The synthesis, physical and spectroscopic properties of tetra-*n*-butylammonium methanesulfonate (QBA MS), tetra-*n*-butylammonium trifluoromethanesulfonate (QBA FMS), tetra-*n*-butylammonium butanesulfonate (QBA BuS), tetra-*n*-butylammonium perfluorobutanesulfonate (QBA FBuS), tetra-*n*-butylammonium octanesulfonate (QBA OS), tetra-*n*-butylammonium perfluorooctanesulfonate (QBA FOS), tri-*n*-butylmethylammonium butanesulfonate (TBMA BuS), tri-*n*-butylmethylammonium perfluorobutane sulfonate (TBMA FBuS), tri-*n*-butylmethylammonium octanesulfonate (TBMA OS), and tri-*n*-butylmethylammonium perfluorooctanesulfonate (TBMA FOS) are described elsewhere<sup>6</sup>. Chromosorb W AW (40–60 mesh) and Gas Chrom Q (60–80 mesh) were purchased from Anspec Co. (Ann Arbor, MI, U.S.A.). All other chemicals and reagents were analytical or reagent grade in the highest purity available.

For column evaluation a Varian 3700 gas chromatograph (Walnut Creek, CA, U.S.A.) was used and modified to permit the measurement of the inlet pressure with a mercury manometer ( $\pm 1$  mmHg) and the average column temperature with a National Bureau of Standards certified thermometer ( $\pm 0.2^\circ\text{C}$ ). Nitrogen was used as the carrier gas at an accurately known flow-rate of approximately 20 ml/min determined with a thermostated soap-film bubble meter. Column packings were prepared by the rotary evaporator technique using standard procedures<sup>6,7</sup>. Accurate phase loadings were determined by exhaustive Soxhlet extraction, 20–30 h, with acetonitrile<sup>6,8</sup>. Samples were injected as headspace vapors to approximate the conditions for infinite dilution/zero surface coverage. All sample peaks were symmetrical and retention volumes were independent of sample size in the measurement region.

The net retention volume was determined using eqn. 1

$$V_N = 3/2[(P^2 - 1)/(P^3 - 1)][(t_R - t_m)F_a][T_c/T_a][1 - (P_w/P_a)] \quad (1)$$

where  $P$  is  $P_i/P_a$ ,  $P_i$  the column inlet pressure,  $P_a$  the column outlet pressure,  $t_R$  the retention time,  $t_m$  the gas holdup time (assumed to be equal to the retention time of methane at  $T_c$ ),  $F_a$  the column flow-rate measured at  $P_a$  and  $T_a$ ,  $T_c$  the column temperature (K),  $T_a$  the ambient temperature, and  $P_w$  the vapor pressure of water at  $T_a$ . Since retention was known to occur by a combination of gas-liquid partitioning and interfacial adsorption<sup>6</sup>, the gas-liquid partition coefficients independent of interfacial adsorption were determined from plots of  $V_N^*/V_L$  vs.  $1/V_L$  using eqn. 2<sup>9-13</sup>

$$V_N^*/V_L = K_L + (A_{GL}K_{GL} + A_{LS}K_{GLS})(1/V_L) \quad (2)$$

where  $V_N^*$  is the net retention volume per gram of packing,  $V_L$  the volume of liquid phase per gram of packing,  $K_L$  the gas-liquid partition coefficient,  $A_{GL}$  the gas-liquid interfacial area,  $K_{GL}$  the coefficient for adsorption at the gas-liquid interface,  $A_{LS}$  the gas-support interfacial area, and  $K_{GLS}$  the coefficient for adsorption at the support surface. The  $K_L$  value for each test solute at a fixed temperature were obtained by linear extrapolation of the data for four columns with phase loadings between 7 and 18% (w/w). The gas-liquid partition coefficients were determined at five temperatures in the range 110–140°C and the data fitted to eqn. 3<sup>12</sup>

$$\log K_L = A - B(T_c) \quad (3)$$

where  $A$  and  $B$  are constants determined by linear regression and  $T_c$  is the column temperature (K). The correlation coefficients,  $r^2$ , were generally better than 0.998 except for butylbenzene (0.991), nitropentane (0.997), nitrobenzene (0.997), 2-methyl-2-pentanol (0.997), nonanone (0.995), dihexyl ether (0.996), and benzodioxane (0.983) on QBA BuS; tetradecane (0.996), butylbenzene (0.990), nitropentane (0.988), nitrobenzene (0.995), nonanone (0.994), and dihexyl ether (0.993) on QBA FBU S; dodecane (0.997), butylbenzene (0.996) on QBA FOS; dodecane (0.990) on TBMA FBU S; and butylbenzene (0.993), nitropentane (0.996), and 2-methyl-2-pentanol (0.987) on TBMA FOS.

The liquid organic salt densities used to convert phase loadings into  $V_L$  values were taken from ref. 6.

The polarity of the liquid organic salts was determined by the solvent strength parameter (the partial molar Gibbs free energy of solution for a methylene group per unit solvent volume) using eqn. 4<sup>14-16</sup>

$$SSP = \Delta G_k^\circ(\text{CH}_2)/\rho_c \quad (4)$$

where  $\Delta G_k^\circ(\text{CH}_2)$  is the partial molar Gibbs free energy of solution for a methylene group and  $\rho_c$  the stationary phase density at the column temperature, Table I. The

TABLE I

SOLVENT STRENGTH PARAMETERS FOR TETRAALKYLAMMONIUM ALKANESULFONATE AND PERFLUOROALKANESULFONATE SALTS AT 121°C

Phase	$\Delta G_k^\circ(\text{CH}_2)$ (cal/mol)	SSP (eqn. 4)
QBA MS	-384	-403
QBA FMS	-371	-358
QBA BuS	-403	-432
QBA FBU S	-374	-337
QBA OS	-446	-469
QBA FOS	-385	-293
TBMA Bus	-374	-395
TBMA FBU S	-360	-300
TBMA OS	-426	-459
TBMA FOS	-371	-278

partial molar Gibbs free energy of solution for each test solute was calculated according to eqn. 5<sup>17-20</sup>:

$$\Delta G_k^\circ(X) = -2.3 RT_c \log K_L^X \quad (5)$$

The partial molar enthalpy of solution for solute X was calculated according to eqn. 6<sup>20</sup>

$$\Delta H_k^\circ(X) = 2.3 RT_c^2 B \quad (6)$$

where  $\Delta H_k^\circ(X)$  is the partial molar enthalpy of solution for solute X and  $B$  the regression coefficient defined in eqn. 3. The partial molar entropy of solution for solute X,  $\Delta S_k^\circ(X)$ , was calculated by difference according to eqn. 7:

$$\Delta S_k^\circ(X) = [\Delta H_k^\circ(X) - \Delta G_k^\circ(X)]/T_c \quad (7)$$

## RESULTS AND DISCUSSION

An established property of fluorocarbon solvents is the large positive deviations from Raoult's law for their mixtures with alkane solvents that in some cases are so large as to cause limited miscibility<sup>21</sup>. It is also well known that derivatives formed with fluorocarbon-containing reagents are less retained on most non-fluorinated stationary phases than their hydrocarbon analogues when retention occurs exclusively by gas-liquid partitioning and selective interactions are absent<sup>22,23</sup>.

In support of the above arguments the solubility of *n*-alkanes in the tetraalkylammonium alkanesulfonate salts is more favorable than for the perfluoroalkanesulfonate salts. The partial molar Gibbs free energy of solution for a methylene group is in all cases more positive for the fluoroalkanesulfonate salts than for their alkanesulfonate analogues, Table I. Likewise, the partial molar Gibbs free energy of solution for tetradecane in the tetraalkylammonium salts, Table II, is more positive for the fluoroalkanesulfonate salts than their analogous alkanesulfonate salts. These differences in properties are due to enthalpy differences as demonstrated by Fig. 1. From the figure it can be seen that entropy changes accompanying solution of the *n*-alkanes are adequately accounted for by the changes in freedom of migration associated with the differences in strength of the solute-solvent enthalpic interactions (enthalpy-entropy compensation). The differences in slope for QBA BuS and QBA FOS compared to the other salts indicates that the capacity of the salts for solute-solvent interactions may also depend on solvent structure. There is no thorough knowledge of the structure of liquid organic salts but most studies indicate that the salts are at least partially ordered and held together by the strong Coulombic fields between ions, and in some cases, by additional ion-ion molecular interactions to form ion aggregates<sup>12,24-26</sup>. For QBA BuS and QBA FOS we might infer that differences in the melt structure exist compared to the other salts which influence the solubility of the *n*-alkanes but since the *n*-alkanes can only interact by dispersive and inductive forces there is no change in the selectivity of these interactions due to changes in solvent structure. Confirmation of this observation comes from plotting either the enthalpy or Gibbs free energy of solution for tetradecane in the fluoroalkanesulfonate salts against

TABLE II

SOLUTION THERMODYNAMICS OF TEST SOLUTES IN THE TETRAALKYLAMMONIUM SULFONATE SALTS AT 121°C

Stationary phase	Test solute	$-\Delta G_k^\circ$ (kcal/mol)	$-\Delta H_k^\circ$ (kcal/mol)	$-\Delta S_k^\circ$ (cal/mol · K)
QBA MS	Tetradecane	$4.24 \pm 0.03$	$12.7 \pm 0.3$	$21.4 \pm 0.8$
QBA FMS		$4.18 \pm 0.03$	$11.5 \pm 0.3$	$18.6 \pm 0.8$
QBA BuS		$4.50 \pm 0.03$	$13.2 \pm 0.7$	$22.1 \pm 1.8$
QBA FBuS		$4.28 \pm 0.05$	$10.8 \pm 0.7$	$16.7 \pm 2.0$
QBA OS		$5.08 \pm 0.04$	$12.5 \pm 0.4$	$18.9 \pm 0.9$
QBA FOS		$4.50 \pm 0.03$	$11.7 \pm 0.2$	$18.3 \pm 0.4$
TBMA Bus		$4.60 \pm 0.03$	$12.4 \pm 0.3$	$19.7 \pm 0.8$
TBMA FBuS		$4.44 \pm 0.03$	$10.5 \pm 0.2$	$15.4 \pm 0.4$
TBMA OS		$4.89 \pm 0.03$	$11.8 \pm 0.2$	$17.5 \pm 0.4$
TBMA FOS		$4.29 \pm 0.03$	$11.1 \pm 0.2$	$17.2 \pm 0.5$
QBA MS	<i>n</i> -Butylbenzene	$4.04 \pm 0.04$	$10.4 \pm 0.3$	$16.2 \pm 0.7$
QBA FMS		$4.08 \pm 0.03$	$9.9 \pm 0.4$	$14.8 \pm 0.9$
QBA BuS		$4.02 \pm 0.03$	$11.7 \pm 0.5$	$19.4 \pm 1.0$
QBA FBuS		$3.85 \pm 0.05$	$9.4 \pm 1.2$	$14.0 \pm 2.0$
QBA OS		$4.35 \pm 0.02$	$9.7 \pm 0.2$	$13.5 \pm 0.5$
QBA FOS		$3.93 \pm 0.03$	$10.9 \pm 0.5$	$17.6 \pm 1.2$
TBMA BuS		$4.17 \pm 0.03$	$9.9 \pm 0.2$	$14.6 \pm 0.5$
TBMA FBuS		$4.21 \pm 0.03$	$9.9 \pm 0.7$	$14.4 \pm 1.8$
TBMA OS		$4.22 \pm 0.06$	$9.6 \pm 0.3$	$13.7 \pm 0.8$
TBMA FOS		$3.71 \pm 0.03$	$9.5 \pm 0.8$	$14.6 \pm 2.0$
QBA MS	1-Nitropentane	$4.87 \pm 0.03$	$10.7 \pm 0.1$	$14.7 \pm 0.3$
QBA FMS		$4.76 \pm 0.03$	$9.7 \pm 0.2$	$12.5 \pm 0.5$
QBA BuS		$4.79 \pm 0.02$	$11.6 \pm 0.6$	$17.2 \pm 1.5$
QBA FBuS		$4.51 \pm 0.03$	$7.2 \pm 0.1$	$6.7 \pm 0.1$
QBA OS		$5.13 \pm 0.10$	$10.0 \pm 2$	$12.0 \pm 6$
QBA FOS		$4.42 \pm 0.02$	$9.6 \pm 0.1$	$13.2 \pm 0.3$
TBMA BuS		$4.94 \pm 0.03$	$10.5 \pm 0.5$	$14.2 \pm 1.2$
TBMA FBuS		$4.89 \pm 0.03$	$8.8 \pm 0.2$	$10.0 \pm 0.4$
TBMA OS		$4.71 \pm 0.03$	$9.4 \pm 0.2$	$11.8 \pm 0.4$
TBMA FOS		$4.35 \pm 0.03$	$8.5 \pm 0.5$	$10.6 \pm 1.3$
QBA MS	Nitrobenzene	$6.06 \pm 0.03$	$12.0 \pm 0.1$	$15.1 \pm 0.3$
QBA FMS		$5.78 \pm 0.03$	$10.7 \pm 0.4$	$12.6 \pm 1.0$
QBA BuS		$6.19 \pm 0.03$	$12.7 \pm 0.7$	$16.5 \pm 1.7$
QBA FBuS		$5.44 \pm 0.03$	$9.3 \pm 0.7$	$9.8 \pm 1.7$
QBA OS		$5.94 \pm 0.04$	$10.9 \pm 0.4$	$12.6 \pm 0.9$
QBA FOS		$5.27 \pm 0.03$	$9.9 \pm 0.3$	$11.8 \pm 0.6$
TBMA BuS		$6.11 \pm 0.03$	$11.9 \pm 0.5$	$14.7 \pm 1.3$
TBMA FBuS		$5.76 \pm 0.03$	$9.5 \pm 0.2$	$9.6 \pm 0.4$
TBMA OS		$5.80 \pm 0.03$	$10.5 \pm 0.2$	$12.0 \pm 0.4$
TBMA FOS		$5.16 \pm 0.03$	$9.8 \pm 0.3$	$11.7 \pm 0.8$
QBA MS	2-Methyl-2-pentanol	$4.27 \pm 0.03$	$12.2 \pm 0.1$	$20.1 \pm 0.1$
QBA FMS		$3.45 \pm 0.03$	$9.8 \pm 0.1$	$16.1 \pm 0.2$
QBA BuS		$4.26 \pm 0.07$	$13.2 \pm 0.7$	$22.7 \pm 1.8$
QBA FBuS		$3.33 \pm 0.02$	$9.9 \pm 0.4$	$16.8 \pm 1.0$
QBA OS		$4.36 \pm 0.05$	$11.7 \pm 0.3$	$18.7 \pm 0.7$
QBA FOS		$3.22 \pm 0.02$	$10.5 \pm 0.4$	$18.4 \pm 0.9$
TBMA BuS		$4.54 \pm 0.03$	$12.3 \pm 0.4$	$19.6 \pm 1.0$

(Continued on p. 754)

TABLE II (continued)

Stationary phase	Test solute	$-\Delta G_k^\circ$ (kcal/mol)	$-\Delta H_k^\circ$ (kcal/mol)	$-\Delta S_k^\circ$ (cal/mol · K)
TBMA FBU S		3.63 ± 0.03	8.7 ± 0.4	12.7 ± 1.1
TBMA OS		4.23 ± 0.03	10.8 ± 0.2	16.6 ± 0.6
TBMA FOS		3.19 ± 0.04	10.8 ± 1.2	19.2 ± 3.2
QBA MS	Nonanone	4.57 ± 0.03	11.2 ± 0.1	16.9 ± 0.2
QBA FMS		4.71 ± 0.03	10.7 ± 0.3	15.1 ± 0.7
QBA BuS		4.57 ± 0.03	12.4 ± 0.9	20.0 ± 2.3
QBA FBU S		4.56 ± 0.01	9.8 ± 0.8	13.4 ± 2.0
QBA OS		4.81 ± 0.04	10.8 ± 0.4	15.2 ± 0.9
QBA FOS		4.64 ± 0.03	10.8 ± 0.4	15.6 ± 1.0
TBMA BuS		4.68 ± 0.02	11.2 ± 0.5	16.5 ± 1.3
TBMA FBU S		4.98 ± 0.03	9.7 ± 0.1	11.9 ± 0.3
TBMA OS		4.65 ± 0.03	10.1 ± 0.2	13.9 ± 0.4
TBMA FOS		4.48 ± 0.04	10.2 ± 0.2	14.4 ± 0.6
QBA MS	Dihexyl ether	4.03 ± 0.03	11.7 ± 0.2	19.6 ± 0.5
QBA FMS		4.07 ± 0.04	10.9 ± 0.3	17.3 ± 0.7
QBA BuS		4.50 ± 0.01	11.4 ± 0.1	17.5 ± 0.2
QBA FBU S		4.08 ± 0.04	10.6 ± 0.9	16.6 ± 2.3
QBA OS		4.67 ± 0.03	11.8 ± 0.3	18.2 ± 1.0
QBA FOS		4.24 ± 0.04	11.2 ± 0.3	17.8 ± 0.8
TBMA BuS		4.22 ± 0.03	11.2 ± 0.4	18.9 ± 1.1
TBMA FBU S		4.33 ± 0.02	10.1 ± 0.2	14.7 ± 0.4
TBMA OS		4.53 ± 0.03	11.0 ± 0.4	16.5 ± 1.1
TBMA FOS		4.04 ± 0.03	10.5 ± 0.2	16.5 ± 0.7
QBA MS	Benzodioxane	6.02 ± 0.03	12.6 ± 0.1	16.7 ± 0.2
QBA FMS		5.76 ± 0.03	11.3 ± 0.3	14.1 ± 0.8
QBA BuS		5.84 ± 0.02	16.0 ± 2.1	25.8 ± 5
QBA FBU S		5.40 ± 0.03	10.0 ± 0.1	11.7 ± 0.3
QBA OS		5.96 ± 0.01	11.5 ± 0.1	14.0 ± 0.4
QBA FOS		5.21 ± 0.03	10.5 ± 0.2	13.4 ± 0.6
TBMA BuS		5.69 ± 0.03	11.9 ± 0.7	15.8 ± 1.8
TBMA FBU S		5.74 ± 0.03	10.4 ± 0.4	11.8 ± 1.0
TBMA OS		5.83 ± 0.03	11.0 ± 0.1	13.2 ± 0.3
TBMA FOS		5.12 ± 0.03	10.6 ± 0.3	13.9 ± 0.7

the analogous alkanesulfonate salts which line up into two groups with parallel slopes that depend only on the identity of the cation (QBA or TBMA).

The solvent strength parameter (SSP) has been suggested as a single parameter to evaluate solvent polarity<sup>14,16</sup>. It is equivalent to the partial molar Gibbs free energy of solution for a methylene group per unit solvent volume and, unlike the free energy itself, has been demonstrated to show linear relationships with changes in solvent composition for homologous solvents. For the salts studied in Table I the SSP parameter shows a linear correlation for both series of salts with increasing number of methylene groups or carbon difluoride groups in the alkane- and perfluoroalkane-sulfonate anions. With increasing chain length the SSP value decreases by approximately 23 cal · cm<sup>3</sup>/g.mol for each carbon unit when a carbon difluoride group replaces a methylene group in the alkanesulfonate chain. This value encompasses two trends. An increase in the magnitude of the SSP value for the alkanesulfonate anion with

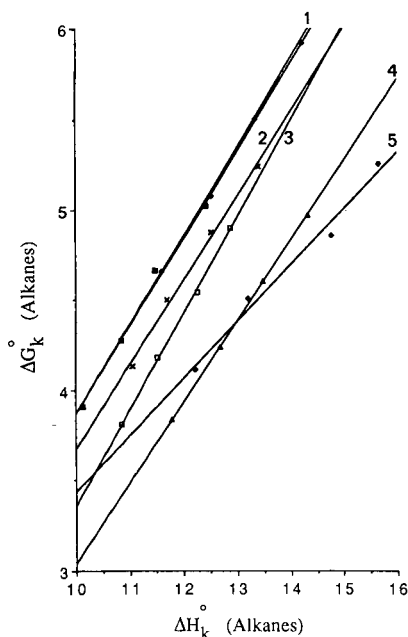


Fig. 1. A plot of  $\Delta G_k^\circ$  against  $\Delta H_k^\circ$  for the  $C_{13}$ - $C_{16}$  *n*-alkanes on the tetra-*n*-butylammonium sulfonate salts. Identification: 1, QBA FBuS and QBA OS; 2, QBA FOS; 3, QBA FMS; 4, QBA MS; 5, QBA BuS. Numerical values for axes are negative.

increasing chain length and a decrease in magnitude of the SSP value for the perfluoroalkanesulfonate anion with increasing chain length.

The aromatic test solute *n*-butylbenzene and dodecyne, Table III, were selected as examples of non-polar test solutes that are readily polarized and might be expected to show different solution behavior to the *n*-alkanes due to the presence of strong Coulombic fields in the liquid organic salts. Dodecane and dodecyne have similar boiling points (difference is 1.2°C at atmospheric pressure) and have similar molecular sizes. They should, therefore, have similar cavity terms and differences in their solution properties must be due largely to selective interactions of a dipolar nature. Differences in the free energy of solution for dodecane and dodecyne in the analogous alkanesulfonate and fluoroalkanesulfonate salts are substantial being greatest for the methanesulfonates (1.11 kcal/mol) and least for the octanesulfonates. If the dispersive interactions of dodecane and dodecyne are assumed to be of similar magnitude then there is a small but significant difference between the free energy of solution for the solutes in analogous alkane- and fluoroalkanesulfonate salts. The selective interaction for dodecyne, then, is primarily due to the presence of strong Coulombic fields between ions which are modified to a small extent by the inductive effect of fluorine which lowers the electron density on the sulfonate group compared to the analogous alkanesulfonate anion. Similar behavior is seen for *n*-butylbenzene except that compared to dodecyne the differences in free energy and enthalpy of solution for the alkanesulfonate and perfluoroalkanesulfonate salts are much smaller.

1-Nitropentane and nitrobenzene, were selected as test solutes expected to have

TABLE III

SOLUTION THERMODYNAMICS FOR DODECANE AND DODECYNE IN TETRAALKYL-AMMONIUM ALKANESULFONATES AND PERFLUOROALKANESULFONATES AT 121°C

Average uncertainty in  $\Delta G_k^\circ$  is 0.03 kcal/mol,  $\Delta H_k^\circ$  0.35 kcal/mol, and  $\Delta S_k^\circ$  0.7 cal/mol·K.

Stationary phase	Dodecane			Dodecyne		
	$-\Delta G_k^\circ$ (kcal/mol)	$-\Delta H_k^\circ$ (kcal/mol)	$-\Delta S_k^\circ$ (cal/mol·K)	$-\Delta G_k^\circ$ (kcal/mol)	$-\Delta H_k^\circ$ (kcal/mol)	$-\Delta S_k^\circ$ (cal/mol·K)
QBA MS	3.43	11.0	19.2	4.54	12.9	21.2
QBA FMS	3.32	10.2	17.5	4.30	11.5	18.1
QBA BuS	3.72	11.0	18.5	4.51	16.3	29.9
QBA FBU S	3.49	9.3	14.8	4.09	11.7	19.2
QBA OS	4.15	10.8	16.8	4.97	12.5	19.2
QBA FOS	3.73	10.2	16.4	4.24	11.5	18.4
TBMA BuS	3.55	10.9	18.5	4.70	12.6	20.1
TBMA OS	3.93	10.2	15.8	4.83	11.7	17.5
TBMA FOS	3.61	9.4	18.6	4.07	11.0	17.5

a large contribution from orientation interactions to their retention (dipole moments 3.52 and 3.97 respectively<sup>14</sup>). In all cases the free energy and enthalpy of solution are less for the fluoroalkanesulfonate than for the analogous alkanesulfonate salts. From a plot of  $\Delta G_k^\circ$  vs.  $\Delta H_k^\circ$ , shown for nitrobenzene in Fig. 2, there is a reasonable grouping of points around a central line for all salts except those containing a perfluoro-

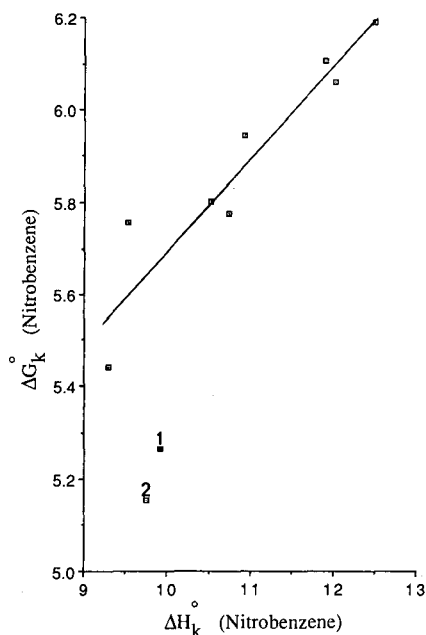


Fig. 2. Plot of  $\Delta G_k^\circ$  against  $\Delta H_k^\circ$  for nitrobenzene in the sulfonate salts illustrating the anomalous behavior of the perfluorooctanesulfonate salts. Identification: 1, tri-*n*-butylmethylammonium and 2, tetra-*n*-butylammonium perfluorooctanesulfonates. Numerical values for axes are negative.



octanesulfonate group (this behavior is typical of 1-nitropentane as well). The octanesulfonate chain is fairly flexible and can be packed into the ordered structure of the liquid organic salts. The covalent radius of fluorine (0.67 Å) is somewhat larger than that of hydrogen (0.37 Å) reducing the flexibility of the perfluorooctane chain which does not pack as easily into the salt structure. The Coulombic fields between ions is changed to accommodate the stiffer perfluorooctanesulfonate anions compared to the octanesulfonate anions which in turn influences the strength of orientation interactions. The difference in solution enthalpy and entropy between the alkanesulfonate and fluoroalkanesulfonate salts is significantly greater for the methanesulfonates and butanesulfonates than for the octanesulfonate salts suggesting an increase in enthalpy (and decrease in entropy) associated with solution of the dipolar solutes in the perfluorooctanesulfonate salts.

2-Methyl-2-pentanol, dihexyl ether, nonanone, and benzodioxane were selected as test solutes to evaluate proton donor-acceptor interactions. The sulfonate group is the most likely proton-acceptor center in the sulfonate salts and 2-methyl-2-pentanol should be the most sensitive test solute for observing changes resulting from the inductive effect of fluorine on the electron density on the sulfonate group. In all cases the free energy and enthalpy of solution are less favorable for solution of 2-methyl-2-pentanol in the fluoroalkanesulfonate salts than for the analogous alkanesulfonate salts. The differences in free energy and enthalpy of solution for the alcohol in the alkanesulfonate and fluoroalkanesulfonate salts are large by comparison to the other test solutes. This difference is largest for the methanesulfonate salts and then increases only shallowly as the length of the alkyl chain is increased. The differences in solution

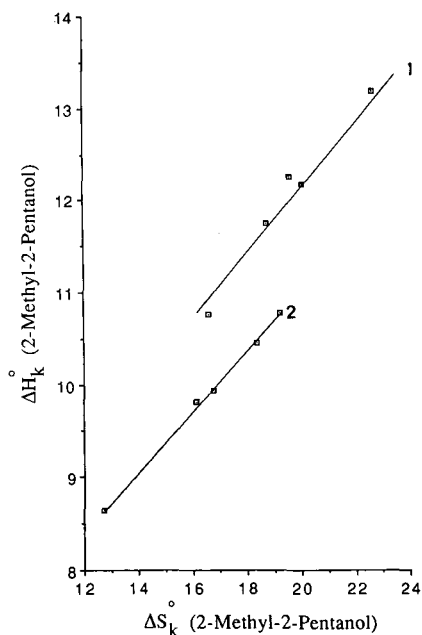


Fig. 3. Plot of  $\Delta H_k^\circ$  against  $\Delta S_k^\circ$  for 2-methyl-2-pentanol in the sulfonate salts indicating the difference in behavior for 1, alkanesulfonates and 2, perfluoroalkanesulfonates. Numerical values for axes are negative.

enthalpy increase from the methanesulfonates to the butanesulfonates and then decline significantly to the octanesulfonates. A plot of  $\Delta H_k^\circ$  against  $\Delta S_k^\circ$  for 2-methyl-2-pentanol in the sulfonate salts, Fig. 3, divides the salts into two essentially linear groups depending upon whether the anion contains fluorine or not. Enthalpy-entropy compensation is similar for both groups (slope of the line) indicating that the difference between the two groups depends primarily on enthalpy differences. The fluoroalkanesulfonate salts exhibit lower enthalpic interactions compared to their alkanesulfonate analogues due to the inductive effect of fluorine which reduces the electron density on the sulfonate group and is reinforced by weaker dispersive interactions for the perfluorocarbon chains compared to the analogous hydrocarbon chains. It is well established that in aqueous solution the perfluoroalkanesulfonic acids are very strong acids, much stronger than the alkanesulfonic acids, which has been explained in terms of the inductive effect of fluorine<sup>27</sup>. The first carbon difluoride group adjacent to the sulfonic acid moiety is most responsible for the acid strength and the addition of further carbon difluoride groups has only a small effect. This picture is entirely consistent with the interpretation of the thermodynamic solution data for 2-methyl-2-pentanol in the alkanesulfonate and fluoroalkanesulfonate salts.

For nonanone and dihexyl ether the differences in free energy and enthalpy of solution between the alkanesulphonates and fluoroalkanesulphonates are generally small indicating a specific interaction between the electron-donor solutes and the fluoroalkanesulfonate salts that must occur in opposition to the general reduction in dispersive interactions. In a few cases, particularly for the methanesulfonates, the free energy of solution for the test solutes is more favorable for the fluoroalkanesulfonates than the alkanesulfonates. Either the sulfonate group or the carbon backbone of the fluoroalkanesulfonate group could act as electron-donor acceptor sites as their electron density are both influenced by the inductive influence of fluorine. The magnitude of the observed differences is not so large as to suggest that electron-donor interactions for fluoroalkanesulfonate salts are strong selective interactions, particularly when compared to the differences observed for proton-donor solutes. There are of course two possible explanations for this. Either the observed interactions are not very selective compared to those for the alcohols or dihexyl ether, nonanone, and benzodioxane are much weaker electron-donor test solutes than the alcohols are examples of proton-donor test solutes. This question cannot be answered adequately at present but there is reasonable evidence to suggest that the conventional selection of ethers and ketones as electron-donor solutes in schemes designed to evaluate stationary phase selectivity in GC may have to be revised<sup>14,16,18</sup>.

The model solvent systems studied here permit a quantitative evaluation of the influence of replacing the alkyl chains by perfluoroalkyl chains in sulfonate anions on the solvent properties of tetraalkylammonium alkanesulfonate solvents used as stationary phases for GC. The general influence of fluorine is to diminish dispersive interactions and to selectively reduce proton-donor interactions through the inductive removal of electron density from the sulfonate group. The inductive effect of fluorine does not seem to have a large influence on the strength of the Coulombic fields between ions which dominate orientation interactions. The stiffness of the perfluorooctane chain may influence orientation interactions compared to the analogous alkanesulfonate salts by changing the ion separation distances in the ordered structure of the liquid salts. The Coulombic fields also influence the solubility of easily polarizable molecules

such as aromatic and unsaturated alkanes which are retained much longer than their saturated analogues of similar volatility.

#### ACKNOWLEDGEMENT

Acknowledgement is made to the donors of the Petroleum Research Fund administered by the American Chemical Society for support of this research.

#### REFERENCES

- 1 R. M. Pomaville and C. F. Poole, *Anal. Chim. Acta*, 200 (1987) 151.
- 2 S. C. Dhanesar and C. F. Poole, *J. Chromatogr.*, 267 (1983) 388.
- 3 S. C. Dhanesar and C. F. Poole, *Anal. Chem.*, 55 (1983) 1462.
- 4 W. W. Blaser and W. R. Kracht, *J. Chromatogr. Sci.*, 16 (1978) 111.
- 5 S. C. Dhanesar and C. F. Poole, *Anal. Chem.*, 55 (1983) 2148.
- 6 R. M. Pomaville and C. F. Poole, *J. Chromatogr.*, 468 (1989) 261.
- 7 C. F. Poole and S. A. Schuette, *Contemporary Practice of Chromatography*, Elsevier, Amsterdam, 1984, p. 60.
- 8 E. F. Sanchez, J. A. G. Dominguez, J. G. Munoz and M. J. Molera, *J. Chromatogr.*, 299 (1984) 151.
- 9 C. F. Poole, K. G. Furton, R. M. Pomaville, S. K. Poole and B. R. Kersten, in G. Lovering and R. D. Gale (Editors), *Molten Salt Techniques*, Vol. 4, Plenum, New York, 1989, in press.
- 10 B. R. Kersten and C. F. Poole, *J. Chromatogr.*, 399 (1987) 1.
- 11 R. M. Pomaville and C. F. Poole, *Anal. Chem.*, 60 (1988) 1103.
- 12 S. K. Poole, P. H. Shetty and C. F. Poole, *Anal. Chim. Acta*, 218 (1989) 241.
- 13 C. F. Poole and S. K. Poole, *Chem. Rev.*, 89 (1989) 377.
- 14 B. R. Kersten, S. K. Poole and C. F. Poole, *J. Chromatogr.*, 468 (1989) 235.
- 15 C. F. Poole, R. M. Pomaville and T. A. Dean, *Anal. Chim. Acta*, (1989) in press.
- 16 S. K. Poole and C. F. Poole, *J. Chromatogr.*, 500 (1990) 329.
- 17 S. K. Poole, B. R. Kersten and C. F. Poole, *J. Chromatogr.*, 471 (1989) 91.
- 18 B. R. Kersten and C. F. Poole, *J. Chromatogr.*, 452 (1988) 191.
- 19 B. R. Kersten, C. F. Poole and K. G. Furton, *J. Chromatogr.*, 411 (1987) 43.
- 20 R. C. Castells, *J. Chromatogr.*, 350 (1985) 339.
- 21 C. R. Patrick, in R. E. Banks (Editor), *Preparation, Properties, and Industrial Applications of Organofluorine Compounds*, Ellis Horwood, Chichester, 1982, p. 323.
- 22 S. H. Langer, R. J. Sheehan and J.-C. Huang, *J. Phys. Chem.*, 86 (1982) 4605.
- 23 C. F. Poole and S. K. Poole, *J. Chromatogr. Sci.*, 25 (1987) 434.
- 24 C. F. Poole, K. G. Furton and B. R. Kersten, *J. Chromatogr. Sci.*, 24 (1986) 400.
- 25 C. L. Hussey, *Adv. Molten Salt Chem.*, 5 (1983) 185.
- 26 J. E. Lind, *Adv. Molten Salt Chem.*, 2 (1973) 1.
- 27 G. A. Olah, G. K. Surya Prakash and J. Sommer, *Superacids*, Wiley, New York, 1985, p. 36.



## Author Index

- Ahuja, S.  
Optimization of selectivity, detectability and analysis time in high-performance liquid chromatography 489
- Albert, K., see Buszewski, B. 305
- Allam, K.  
—, Saha, M. and Giese, R. W.  
Preparation of electrophoric derivatives of N7-(2-hydroxyethyl)guanine, an ethylene oxide DNA adduct 571
- Alpert, A. J.  
Hydrophilic-interaction chromatography for the separation of peptides, nucleic acids and other polar compounds 177
- Anspach, F. B.  
—, Johnston, A., Wirth, H.-J., Unger, K. K. and Hearn, M. T. W.  
High-performance liquid chromatography of amino acids, peptides and proteins. XCV. Thermodynamic and kinetic investigations on rigid and soft affinity gels with varying particle and pore sizes: comparison of thermodynamic parameters and the adsorption behaviour of proteins evaluated from bath and frontal analysis experiments 103
- Appelt, G., see Engelhardt, H. 165
- Armstrong, D. W., see Stalcup, A. M. 627
- Asai, M., see Takeuchi, T. 549
- Atamna, I. Z.  
—, Muschik, G. M. and Issaq, H. J.  
Effect of alcohol chain length, concentration and polarity on separations in high-performance liquid chromatography using bonded cyclodextrin columns 477
- Bacolod, M. D., see El Rassi, Z. 141
- Barth, H. G., see Glöckner, G. 645
- Bartha, A.  
—, Vigh, G. and Varga-Puchony, Z.  
Basis of the rational selection of the hydrophobicity and concentration of the ion-pairing reagent in reversed-phase ion-pair high-performance liquid chromatography 423
- , see Strasters, J. K. 523
- Basa, L. J.  
— and Spellman, M. W.  
Analysis of glycoprotein-derived oligosaccharides by high-pH anion-exchange chromatography 205
- Bassler, B. J., see Kaliszan, R. 333
- Bayer, E., see Buszewski, B. 305
- Beale, S. C.  
—, Hsieh, Y.-Z., Wiesler, D. and Novotny, M.  
Application of 3-(2-furoyl)quinoline-2-carbaldehyde as a fluorogenic reagent for the analysis of primary amines by liquid chromatography with laser-induced fluorescence detection 579
- Benedek, P.  
— and Jankó, T.  
Investigation and improvement of the Horváth-Lin equation of state 463
- Berg, J. H. M. van den, see Lammers, N. G. F. M. 541
- Berkel-Geldof, O. van, see Van Berkel-Geldof, O. 345
- Billiet, H. A. H., see Strasters, J. K. 499, 523
- Bonn, G.  
—, Reiffenstuhl, S. and Jandik, P.  
Ion chromatography of transition metals on an iminodiacetic acid bonded stationary phase 669
- Bowers, L. D., see Pedigo, S. 279
- Brenner, M.  
—, Moirandat, C. and Schlimme, R.  
High-efficiency liquid extractor for isolation of a desired material from complex organic mixtures 721
- Brinkman, U. A. Th., see Irth, H. 617
- Brown, P. R., see Turcotte, J. G. 55
- Buszewski, B.  
—, Suprynowicz, Z., Staszczuk, P., Albert, K., Pfeleiderer, B. and Bayer, E.  
Effect of coverage density on the retention mechanism in reversed-phase high-performance liquid chromatography 305
- Cardinali, F.  
—, Ziggliotti, A. and Viscomi, G. C.  
Scaling-up procedure from the range of milligrams to grams for the purification of amino acid derivatives in displacement chromatography 37
- Carr, P. W., see Cheong, W. J. 373
- Carr, P. W., see Rigney, M. P. 291
- Caude, M., see Veuthey, J. L. 637
- Cheong, W. J.  
— and Carr, P. W.  
Study of partition models in reversed-phase liquid chromatography based on measured mobile phase solute activity coefficients 373

- Chiari, M.  
 —, Chiesa, C., Righetti, P. G., Corti, M., Jain, T. and Shorr, R.  
 Kinetics of cysteine oxidation in immobilized pH gradient gels 699
- Chiesa, C., see Chiari, M. 699
- Chloupek, R., see Sievert, H.-J. P. 221
- Coolsaet, F., see Strasters, J. K. 523
- Corti, M., see Chiari, M. 699
- Cserháti, T., see Valko, K. 361
- Dallenbach-Toelke, K., see Nyiredy, S. 453
- De Galan, L., see Strasters, J. K. 499, 523
- De Jong, G. J., see Irth, H. 617
- Dellafera, S. S., see Wong, S. H. Y. 601
- De Ocampo, L. F., see El Rassi, Z. 141
- Derguini, F., see Stalcup, A. M. 627
- Dewaele, C., see Lammers, N. G. F. M. 541
- DiBussolo, J. M., see Miller, N. T. 317
- Dong, M. W.  
 — and Tran, A. D.  
 Factors influencing the performance of peptide mapping by reversed-phase high-performance liquid chromatography 125
- Dorsey, J. G., see Michels, J. J. 435
- Dou, L.  
 — and Krull, I. S.  
 Determination of inorganic anions by flow injection analysis and high-performance liquid chromatography combined with photolytic-electrochemical detection 685
- El Rassi, Z.  
 —, De Ocampo, L. F. and Bacolod, M. D.  
 Binary and ternary salt gradients in hydrophobic-interaction chromatography of proteins 141
- Engelhardt, H.  
 —, Appelt, G. and Schweinheim, E.  
 Unexpected elution behaviour of peptides with various reversed-phase columns 165
- Ewing, A. G., see Olefirowicz, T. M. 713
- Fernandes, R., see Wong, S. H. Y. 601
- Frei, R. W., see Irth, H. 617
- Frenz, J., see Jacobson, J. M. 5
- Funkenbusch, E. F., see Rigney, M. P. 291
- Fürst, P.  
 —, Pollack, L., Graser, T. A., Godel, H. and Stehle, P.  
 Appraisal of four pre-column derivatization methods for the high-performance liquid chromatographic determination of free amino acids in biological materials 557
- Galan, L. de, see Strasters, J. K. 499, 523
- Gangoda, M. E., see Varughese, P. 469
- Giese, R. W., see Allam, K. 571
- Gilpin, R. K., see Varughese, P. 469
- Glöckner, G.  
 — and Barth, H. G.  
 Use of high-performance liquid chromatography for the characterization of synthetic copolymers 645
- Godel, H., see Fürst, P. 557
- Graser, T. A., see Fürst, P. 557
- Guiochon, G., see Katti, A. M. 21
- Hancock, W. S., see Sievert, H.-J. P. 221
- Haraguchi, H., see Takeuchi, T. 549
- Hartwick, R. A., see Kaliszan, R. 333
- Hearn, M. T. W., see Anspach, F. B. 103
- Helfferich, F. G., see Leu, R.-J. 677
- Henderson, D. E.  
 — and Mello, J. A.  
 Physicochemical studies of biologically active peptides by low-temperature reversed-phase high-performance liquid chromatography 79
- Hjertén, S., see Lindeberg, J. 153
- Holzhauser-Rieger, K.  
 —, Zhou, W. and Schügerl, K.  
 On-line high-performance liquid chromatography for the determination of cephalosporin C and by-products in complex fermentation broths 609
- Hsieh, Y.-Z., see Beale, S. C. 579
- Hurtubise, R. J., see Mohseni, R. M. 395
- Hwang, Y.-L., see Leu, R.-J. 677
- Irth, H.  
 —, Lamoree, M., De Jong, G. J., Brinkman, U. A. Th., Frei, R. W., Kornfeldt, R. A. and Persson, L.  
 Determination of *D*-*myo*-1,2,6-inositol trisphosphate by ion-pair reversed-phase liquid chromatography with post-column ligand exchange and fluorescence detection 617
- Ishii, D., see Takeuchi, T. 549
- Issaq, H. J., see Atamna, I. Z. 477
- Jacobson, J. M.  
 — and Frenz, J.  
 Determination of competitive adsorption isotherms for modeling large-scale separations in liquid chromatography 5
- Jain, T., see Chiari, M. 699
- Jandik, P., see Bonn, G. 669
- Jang, N.-I., see Turcotte, J. G. 55
- Janicot, J. L., see Veuthey, J. L. 637
- Jankó, T., see Benedek, P. 463
- Jin, H. L., see Stalcup, A. M. 627
- Johnston, A., see Anspach, F. B. 103
- Jong, G. J. de, see Irth, H. 617
- Kalász, H.  
 —, Kerecsen, L., Knoll, J. and Pucsok, J.  
 Chromatographic studies on the binding, action and metabolism of (–)-deprenyl 589

- Kalghatgi, K.  
Micropellicular stationary phases for rapid protein analysis by high-performance liquid chromatography 267
- Kaliszan, R.  
—, Ośmiałowski, K., Bassler, B. J. and Hartwick, R. A.  
Mechanism of retention in high-performance liquid chromatography on porous graphitic carbon as revealed by principal component analysis of structural descriptors of solutes 333
- Karger, B. L., see Lin, S. 89
- Katti, A. M.  
— and Guiochon, G.  
Quantitative comparison between the experimental band profiles of binary mixtures in overloaded elution chromatography and their profiles predicted by the semi-ideal model 21
- Kerecsen, L., see Kalász, H. 589
- Kirkland, J. J.  
— and Yau, W. W.  
Effect of operating parameters on polymer molecular weight accuracy with time-delay, exponential-decay thermal field flow fractionation 655
- Knoll, J., see Kalász, H. 589
- Kornfeldt, R. A., see Irth, H. 617
- Kraak, J. C., see Van Berkel-Geldof, O. 345
- Kranzler, H., see Wong, S. H. Y. 601
- Krull, I. S., see Dou, L. 685
- Lammers, N. G. F. M.  
—, Van den Berg, J. H. M., Verzele, M. and Dewaele, C.  
Performance of micro-liquid chromatographic columns in an industrial environment: a case history 541
- Lamoree, M., see Irth, H. 617
- László, E., see Szepesy, L. 197
- Leu, R.-J.  
—, Hwang, Y.-L. and Helfferich, F. G.  
Calculation of column performance in nitrate removal from water supplies by anion exchange 677
- Lin, S.  
— and Karger, B. L.  
Reversed-phase chromatographic behavior of proteins in different unfolded states 89
- Lindeberg, J.  
—, Srichaiyo, T. and Hjertén, S.  
High-performance adsorption chromatography of transfer ribonucleic acids and proteins on 2- $\mu$ m spherical beads of hydroxyapatite. Influence of sodium chloride and magnesium ions on the resolution 153
- Macbride, D., see Turcotte, J. G. 55
- Mazsaroff, I.  
—, Várady, L., Mouchawar, G. A. and Regnier, F. E.  
Thermodynamic model for electrostatic-interaction chromatography of proteins 63
- Mazur, P., see Stalcup, A. M. 627
- Mello, J. A., see Henderson, D. E. 79
- Michels, J. J.  
— and Dorsey, J. G.  
Estimation of the reversed-phase liquid chromatographic lipophilicity parameter  $\log k'_w$  using ET-30 solvatochromism 435
- Miller, N. T.  
— and DiBussolo, J. M.  
Studies on the stability of *n*-alkyl-bonded silica gels under basic pH conditions 317
- Mohseni, R. M.  
— and Hurtubise, R. J.  
Retention characteristics of several compound classes in reversed-phase liquid chromatography with  $\beta$ -cyclodextrin as a mobile phase modifier 395
- Moirandat, C., see Brenner, M. 721
- Mouchawar, G. A., see Mazsaroff, I. 63
- Muschik, G. M., see Atamna, I. Z. 477
- Nakanishi, K., see Stalcup, A. M. 627
- Novotny, M., see Beale, S. C. 579
- Nyiredy, S.  
—, Dallenbach-Toelke, K., Zogg, G. C. and Sticher, O.  
Strategies of mobile phase transfer from thin-layer to medium-pressure liquid chromatography with silica as the stationary phase 453
- Ocampo, L. F. De, see El Rassi, Z. 141
- Olajos, S., see Valko, K. 361
- Olefirowicz, T. M.  
— and Ewing, A. G.  
Capillary electrophoresis with indirect amperometric detection 713
- Oscarsson, S.  
— and Porath, J.  
Protein chromatography with pyridine- and alkyl-thioether-based agarose adsorbents 235
- Ośmiałowski, K., see Kaliszán, R. 333
- Pedigo, S.  
— and Bowers, L. D.  
Comparison of retention behavior on polymeric resins and an alkyl-bonded silica phase in reversed-phase high-performance liquid chromatography 279
- Persson, L., see Irth, H. 617
- Peterson, E. A., see Torres, A. R. 47
- Pfleiderer, B., see Buszewski, B. 305
- Pivarnik, P. E., see Turcotte, J. G. 55
- Pohl, C. A., see Stillian, J. R. 249
- Pollack, L., see Fürst, P. 557

- Pomaville, R. M.  
 — and Poole, C. F.  
 Gas chromatographic study of the solution thermodynamics of organic solutes in tetraalkylammonium alkanesulfonate and perfluoroalkanesulfonate solvents 749
- Poole, C. F., see Pomaville, R. M. 749
- Poppe, H., see Van Berkel-Geldof, O. 345
- Porath, J., see Oscarsson, S. 235
- Pucso, J., see Kalász, H. 589
- Rassi, Z. El, see El Rassi, Z. 141
- Regnier, F. E., see Mazsaroff, I. 63
- Reiffenstuh, S., see Bonn, G. 669
- Righetti, P. G., see Chiari, M. 699
- Rigney, M. P.  
 —, Funkenbusch, E. F. and Carr, P. W.  
 Physical and chemical characterization of microporous zirconia 291
- Rosset, R., see Veuthey, J. L. 637
- Saha, M., see Allam, K. 571
- Schlimme, R., see Brenner, M. 721
- Schügerl, K., see Holzhauser-Rieger, K. 609
- Schweinheim, E., see Engelhardt, H. 165
- Sehgal, R. K., see Turcotte, J. G. 55
- Shirali, S. S., see Turcotte, J. G. 55
- Shorr, R., see Chiari, M. 699
- Sievert, H.-J. P.  
 —, Wu, S.-L., Chloupek, R. and Hancock, W. S.  
 Automated evaluation of tryptic digest from recombinant human growth hormone using ultraviolet spectra and numeric peak information 221
- Singh, H. K., see Turcotte, J. G. 55
- Spellman, M. W., see Basa, L. J. 205
- Srichaiyo, T., see Lindeberg, J. 153
- Stalcup, A. M.  
 —, Jin, H. L., Armstrong, D. W., Mazur, P., Derguini, F. and Nakanishi, K.  
 Separation of carotenes on cyclodextrin-bonded phases 627
- Staszczuk, P., see Buszewski, B. 305
- Stefansson, M.  
 — and Westerlund, D.  
 Reversed-phase ion-pair liquid chromatography of glucuronides 411
- Stehle, P., see Fürst, P. 557
- Sticher, O., see Nyiredy, S. 453
- Stillian, J. R.  
 — and Pohl, C. A.  
 New latex-bonded pellicular anion exchangers with multi-phase selectivity for high-performance chromatographic separations 249
- Strasters, J. K.  
 —, Billiet, H. A. H., De Galan, L. and Vandeginste, B. G. M.  
 Strategy for peak tracking in liquid chromatography on the basis of a multivariate analysis of spectral data 499
- Strasters, J. K.  
 —, Coolsaet, F., Bartha, A., Billiet, H. A. H. and De Galan, L.  
 Peak tracking and subsequent choice of optimization parameters for the separation of a mixture of local anaesthetics by high-performance liquid chromatography 523
- Suprynowicz, Z., see Buszewski, B. 305
- Szepesy, L.  
 —, Vida, L., Tóth, M. and László, E.  
 Investigation of some  $\alpha$ -amylases by high-performance hydrophobic-interaction chromatography 197
- Takeuchi, T.  
 —, Asai, M., Haraguchi, H. and Ishii, D.  
 Direct coupling of capillary liquid chromatography with conventional high-performance liquid chromatography 549
- Torres, A. R.  
 — and Peterson, E. A.  
 Purification of monoclonal antibodies by complex-displacement chromatography on CM-cellulose 47
- Tóth, M., see Szepesy, L. 197
- Tran, A. D., see Dong, M. W. 125
- Turcotte, J. G.  
 —, Pivarnik, P. E., Shirali, S. S., Singh, H. K., Sehgal, R. K., Macbride, D., Jang, N.-I. and Brown, P. R.  
 Preparative-scale high-performance liquid chromatographic separation and purification of 3'-azido-3'-deoxythymidine-5'-phosphate 55
- Unger, K. K., see Anspach, F. B. 103
- Valko, K.  
 —, Olajos, S. and Cserháti, T.  
 Prediction of the high-performance liquid chromatographic retention behaviour of some benzodiazepine derivatives by thin-layer chromatography 361
- Van den Berg, J. H. M., see Lammers, N. G. F. M. 541
- Van Berkel-Geldof, O.  
 —, Kraak, J. C. and Poppe, H.  
 Preparation of silicone-coated 5–25- $\mu$ m I.D. fused-silica capillary columns for open-tubular liquid chromatography 345
- Vandeginste, B. G. M., see Strasters, J. K. 499
- Várady, L., see Mazsaroff, I. 63
- Varga-Puchony, Z., see Bartha, A. 423



- Varughese, P.  
—, Gangoda, M. E. and Gilpin, R. K.  
Reversed-phase liquid chromatographic studies of non-ionic surfactants and related solutes 469
- Verzele, M., see Lammers, N. G. F. M. 541
- Veuthey, J. L.  
—, Janicot, J. L., Caude, M. and Rosset, R.  
Comparitive supercritical-fluid chromatographic properties of carbon dioxide and sulphur hexafluoride-ammonia mixtures with packed columns 637
- Vida, L., see Szepesy, L. 197
- Vigh, G., see Bartha, A. 423
- Viscomi, G. C., see Cardinali, F. 37
- Westerlund, D., see Stefansson, M. 411
- Wiesler, D., see Beale, S. C. 579
- Wirth, H.-J., see Anspach, F. B. 103
- Wong, S. H. Y.  
—, Dellafera, S. S., Fernandes, R. and Kranzler, H.  
Determination of fluoxetine and norfluoxetine by high-performance liquid chromatography 601
- Wu, S.-L., see Sievert, H.-J. P. 221
- Yau, W. W., see Kirkland, J. J. 655
- Zhou, W., see Holzhauer-Rieger, K. 609
- Ziggiotti, A., see Cardinali, F. 37
- Zogg, G. C., see Nyiredy, S. 453



## PUBLICATION SCHEDULE FOR 1990

*Journal of Chromatography and Journal of Chromatography, Biomedical Applications*

MONTH	J	F	M	
Journal of Chromatography	498/1 498/2 499	500 502/1	502/2 503/1 503/2	The publication schedule for further issues will be published later
Cumulative Indexes, Vols. 451-500		501		
Bibliography Section		524/1		
Biomedical Applications	525/1	525/2	526/1	

### INFORMATION FOR AUTHORS

(Detailed *Instructions to Authors* were published in Vol. 478, pp. 453-456. A free reprint can be obtained by application to the publisher, Elsevier Science Publishers B.V., P.O. Box 330, 1000 AH Amsterdam, The Netherlands.)

**Types of Contributions.** The following types of papers are published in the *Journal of Chromatography* and the section on *Biomedical Applications*: Regular research papers (Full-length papers), Notes, Review articles and Letters to the Editor. Notes are usually descriptions of short investigations and reflect the same quality of research as Full-length papers, but should preferably not exceed six printed pages. Letters to the Editor can comment on (parts of) previously published articles, or they can report minor technical improvements of previously published procedures; they should preferably not exceed two printed pages. For review articles, see inside front cover under Submission of Papers.

**Submission.** Every paper must be accompanied by a letter from the senior author, stating that he is submitting the paper for publication in the *Journal of Chromatography*. Please do not send a letter signed by the director of the institute or the professor unless he is one of the authors.

**Manuscripts.** Manuscripts should be typed in double spacing on consecutively numbered pages of uniform size. The manuscript should be preceded by a sheet of manuscript paper carrying the title of the paper and the name and full postal address of the person to whom the proofs are to be sent. Authors of papers in French or German are requested to supply an English translation of the title of the paper. As a rule, papers should be divided into sections, headed by a caption (*e.g.*, Summary, Introduction, Experimental, Results, Discussion, etc.). All illustrations, photographs, tables, etc., should be on separate sheets.

**Introduction.** Every paper must have a concise introduction mentioning what has been done before on the topic described, and stating clearly what is new in the paper now submitted.

**Summary.** Full-length papers and Review articles should have a summary of 50-100 words which clearly and briefly indicates what is new, different and significant. In the case of French or German articles an additional summary in English, headed by an English translation of the title, should also be provided. (Notes and Letters to the Editor are published without a summary.)

**Illustrations.** The figures should be submitted in a form suitable for reproduction, drawn in Indian ink on drawing or tracing paper. Each illustration should have a legend, all the legends being typed (with double spacing) together on a *separate sheet*. If structures are given in the text, the original drawings should be supplied. Coloured illustrations are reproduced at the author's expense, the cost being determined by the number of pages and by the number of colours needed. The written permission of the author and publisher must be obtained for the use of any figure already published. Its source must be indicated in the legend.

**References.** References should be numbered in the order in which they are cited in the text, and listed in numerical sequence on a separate sheet at the end of the article. Please check a recent issue for the layout of the reference list. Abbreviations for the titles of journals should follow the system used by *Chemical Abstracts*. Articles not yet published should be given as "in press" (journal should be specified), "submitted for publication" (journal should be specified), "in preparation" or "personal communication".

**Dispatch.** Before sending the manuscript to the Editor please check that the envelope contains three copies of the paper complete with references, legends and figures. One of the sets of figures must be the originals suitable for direct reproduction. Please also ensure that permission to publish has been obtained from your institute.

**Proofs.** One set of proofs will be sent to the author to be carefully checked for printer's errors. Corrections must be restricted to instances in which the proof is at variance with the manuscript. "Extra corrections" will be inserted at the author's expense.

**Reprints.** Fifty reprints of Full-length papers, Notes and Letters to the Editor will be supplied free of charge. Additional reprints can be ordered by the authors. An order form containing price quotations will be sent to the authors together with the proofs of their article.

**Advertisements.** Advertisement rates are available from the publisher on request. The Editors of the journal accept no responsibility for the contents of the advertisements.

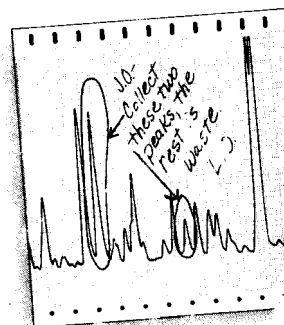
Discover new solutions

## Foxy 200:

# the new expert fraction collector for prep LC

Now it's easier than ever before to collect the right fractions —Foxy<sup>®</sup> 200 sizes and sorts them exactly the way you want.

- Easy-to-follow menus. Setup is quick and intuitive for any HPLC or prep LC protocol.
- Collect only the peaks you want. Peak detection by slope, height, and/or time windows is built in.
- Change LC scale easily from drops to liters/min. Collect in anything from microcentrifuge tubes to off-deck containers.



**Ask today for details.**

Isco, Inc., Box 5347,  
Lincoln NE 68505, U.S.A.  
Tel. (800)228-4250

Isco Europe AG, Brüschr. 17  
CH8708 Männedorf, Switzerland  
Fax (41-1)920 62 08



**Distributors** • Austria: INULA • Belgium: SA HVL NV • Denmark: Mikrolab Aarhus • Finland: ETEK OY • France: Ets. Roucaire, S.A. • Germany: Colora Messtechnik GmbH • Hungary: Lasis Handelsges. mbH • Italy: Gio. de Vita e C. s.r.l. • The Netherlands: Beun-de Ronde B.V. • Norway: Dipl. Ing. Houm A.S. • Spain: CHEMICONTRON, S.L. • Sweden: SAVEN AB • Switzerland: IG Instrumenten-Gesellschaft AG • U.K.: Life Science Laboratorie